

http://researchcommons.waikato.ac.nz/

Research Commons at the University of Waikato

Copyright Statement:

The digital copy of this thesis is protected by the Copyright Act 1994 (New Zealand).

The thesis may be consulted by you, provided you comply with the provisions of the Act and the following conditions of use:

- Any use you make of these documents or images must be for research or private study purposes only, and you may not make them available to any other person.
- Authors control the copyright of their thesis. You will recognise the author's right to be identified as the author of the thesis, and due acknowledgement will be made to the author where appropriate.
- You will obtain the author's permission before publishing any material from the thesis.

NEARSHORE AND INNER SHELF SEDIMENTATION ON THE EAST COROMANDEL COAST, NEW ZEALAND

A thesis
submitted in fulfilment
of the requirements for the Degree
of
Doctor of Philosophy in Earth Sciences
at the
University of Waikato
by

Barry Edward Bradshaw BSc (Hons) (Sydney)

University of Waikato
New Zealand
1991



To Sarah, Matthew, and Katrina, thank you for waiting so patiently for Uncle Barry to finish playing with his beaches in New Zealand.

ABSTRACT

The east Coromandel coastline on the northeast coast of New Zealand has been characterised by localised erosion problems since its commercial subdivision. Increasing pressures have also arisen in recent years for possible use of the adjacent continental shelf as a repository for dredge and mining tailings, and extraction of commercial aggregate and mineral deposits. This has raised the question of dynamic links between the continental shelf and local beach systems, and resulting impacts on the coastline from such activities. The east Coromandel shelf study was therefore undertaken to investigate the modern and past shelf sedimentation processes, and relate these findings to local resource management issues. The results also contribute to the present international understanding of inner shelf sedimentation processes in 'storm-dominated' shelf environments.

Surficial sedimentation patterns have been examined by a variety of methods, including: the use of sea-bed drifters and Aanderaa current meters to determine the shelf hydrodynamics; the collection of 563 samples to determine surface sediment textural patterns; a detailed examination of morphological features on the sea floor through a series of 3 side-scan sonar surveys in which 620 km of sonograph and echosounding trace have been obtained; diver surveys using depth of activity rods to provide information on the mobility of surface sediments under different sea conditions; the collection of 174 km of continuous sub-bottom seismic profiles which have been used to determine sub-surface stratigraphic patterns; and an examination of the provenance of shelf sediments through a detailed examination of their light and heavy mineralogy.

The east Coromandel coast is located on an active plate margin, resulting in the presence of a steep and rocky coastline fronted by a relatively narrow continental shelf (20 to 30 km wide), and a local geology dominated by Tertiary volcanics covered by a thin veneer of more recent volcanic air fall deposits. It is also located on a lee shelf in a mid-latitude zone of dominant westerly winds, with these prevailing weather patterns disrupted by high speed east to northeasterly winds associated with the infrequent passage of subtropical low pressure systems, occluded fronts, or more infrequent decaying tropical cyclones. This physiographic setting results in spatially and temporally highly variable sedimentation patterns, with sediment transport primarily controlled by the interaction of wave oscillatory and wind-generated currents during storm conditions. However, characteristics of tide- and oceanic current-dominated conditions also occur in some areas, and conditions generally vary along the coast from being higher energy (current-dominated) on the southern exposed coast, to lower energy (wave- or current-dominated) on the northern embayed coastline. Shelf sedimentation is inferred to occur under three different scale events of fair weather, storm, and extreme storm conditions. The model proposed involves extreme storm conditions transporting large quantities of fine nearshore sands seawards onto the inner shelf surface, where they are slowly reworked along the shelf during annual storm events, and back onshore during fair weather conditions. This latter onshore return of fine sands is proposed to

result from an enhanced shear stress effect of long-period swell waves over coarse megarippled inner shelf sands.

Shelf sedimentation patterns within the study area are inferred to have been primarily established by processes occurring at about the time sea level stabilised 6500 years B.P. At this stage, transgressive shelf sediments were reworked into equilibrium with the regional oceanographic conditions by the winnowing of fine sand from coarser material during storms, with the fine sands subsequently transported onshore by wave-induced currents during calm periods. Depending on the volume of sediments incorporated into transgressive sand bodies and the local shelf gradients, each embayment then developed into either an integral part of the shelf transport system (usually off large estuary systems), with fine shelf sands moving onshore and forming wide barrier spits, or a closed sedimentary system unaffected by shelf sedimentation patterns (pocket embayments). Shelf equilibrium was evidently attained by the fine sands forming a steep seaward dipping concave-up nearshore profile, and coarse sands developing a flatter inner shelf profile.

An autochthonous mode of shelf sedimentation characterised the east Coromandel coast in early Holocene times, and is still evident under present conditions in most areas by the cyclical reworking of fine sands between the lower nearshore and inner shelf surfaces. Most east Coromandel embayments are, however, presently characterised by varying degrees of an allochthonous mode of shelf sedimentation. This involves the deposition of very fine grained, volcanic glass-enriched terrigenous sands, which are derived from either local catchments or Bay of Plenty river systems. The east Coromandel coast generally differs from most allochthonous shelf environments because the supply of terrigenous sediments has not as yet been sufficient to blanket the lower nearshore and inner shelf surfaces on the open ocean coastlines. Two separate modes of shelf sedimentation occur at present, with a nearshore inner shelf recycling of fine allochthonous shelf sands, and an open exchange of terrestrial autochthonous deposits from the upper nearshore surface to the mid shelf plain.

The results of the study suggest that coastal erosion problems can largely be resolved by establishing stable incipient and frontal dune systems along the coast, and encouraging accretion by renourishment from adjacent infilling harbour deposits. The study has also shown that the dispersion of dredged sediments provides potential benefits to the coast in terms of promoting beach accretion, and that sand and mineral extraction can proceed without adverse coastal erosion effects, provided the extraction does not interfere with the natural shelf sedimentation system.

ACKNOWLEDGEMENTS

This study has been carried out over a period of seven years, and involved important contributions from many different people, all of whom I will do my best to acknowledge. My most sincere thanks go to my Chief Supervisor, Prof Terry Healy, for his contribution in initiating this study, helping to obtain funds for research costs, and his invaluable comments on the contents of this dissertation. Also for their inputs into this study, I would like to thank: Mr Paul Dell and Mr Tony Colby for obtaining much of the original data, particularly Paul for taking the time to explain his original approaches to this study; Dr Willem de Lange who has been invaluable in both writing many of the computer programs and editing many sections of the text; Prof Cam Nelson for his incisive editorial comments on this dissertation; Dr Peter Roy for his original encouragement to take up this study, and for his numerous ideas which have been an important contribution.

For their technical expertise in both the field and laboratory, I would like to thank: the Earth Science technicians, Mr Mike Dravitzki, Mr Laurie Gaylor, Mr Mike Vennard, Dr Hugh Grenfell, Mr Renat Radosinsky, and Mr Rob Langridge; the university photographer Mr Ross Clayton; the university draughtsman Mr Frank Bailey; Mr Dudley Bell of the Biological Sciences Dept.; Mr Max Oulton of the Geography Dept.; Mr Peter Hill of the New Zealand Oceanographic Institute; and Mr Rodney Jones of the Hauraki Catchment Board. For their assistance with computer software and programming, I would like to thank: Dr Bill Bolstad, Mr Tony Fenton; Ms Susan Brown; Mr Craig Lynchbloss, and Mr Darryl Gillgren. A special thanks also to the Earth Science Dept. secretaries Sydney and Elaine for their assistance in a variety of areas.

This study would not have been possible without funding from several important sources, namely: the Hauraki Catchment Board; the New Zealand Vice Chancellor's Committee; and the University of Waikato. Equipment and vessels have been obtained from numerous sources, including: the New Zealand Oceanographic Institute; the Royal New Zealand Navy; the University of Otago; Mr David Moncur (M.V. Enterprise); and Mr Lou Jones (M.V. Te Ra). For allowing instruments to be deployed on private property at important sites along the coast, I would like to thank Mr Ray Williams of the Bowentown Boat Club; and Mr Geoff Williams of the Whiritoa Surf Club. Field data could not have been obtained without the valuable (and free) services of several personnel, including Miss Angela Sheffield, Mr Greg Foster, Mr Vance Fulton, and Mr David Hay.

On a personal note, I would like to thank all of the great friends I've made here in New Zealand, especially Ella, Greg (and family), Tim, Rob, Brent, John, Leonie, Wayne, Claire, "Wigs", Vance, Glen B., Grant, Francis, Red (and all the other members of Ham.Star Cricket Club), and the

Sheffields, as well as my other great friends across the Tasman (especially Hoges, Phil the "Greek", Lesley the "Thistle Head", and Robyn), and all the flatmates who have help keep me fed and sane over the years. Finally, I am greatly indebted to my family who have continued to encourage my work in New Zealand while waiting patiently for my return, and Angela Sheffield for being such a great buddy and helping me through the final few traumatic weeks of this study.

CONTENTS

		Page
ABSTRACT		II
ACKNOWLEDGEMNTS		IV
CONTENTS		VI
LIST OF TABLES		XI
LIST OF FIGURES		XII
1	**INTRODUCTION**	
	1.0 Research background	1
	1.1 Research objectives	4
	1.2 Thesis outline	5
	1.3 Terminology	8
2	**REGIONAL SETTING**	
	2.0 Introduction	9
	2.1 Regional geology	10
	2.2 Climate	15
	2.3 Oceanographic setting	17
	2.3.1 Offshore currents	17
	2.3.2 Surface gravity waves and storm surges	19
	2.4 Coastal geomorphology	23
	2.4.1 Estuaries	23
	2.4.2 Barrier systems	25
	2.4.3 Beaches	30
	2.4.4 Continental shelf	36
	2.5 Summary	40
3	**REVIEW OF SHELF SEDIMENTATION PROCESSES**	
	3.0 Introduction	45
	3.1 Sedimentation processes on storm-dominated shelves	46
	3.1.1 Wave-induced flows	46
	3.1.2 Wind-forced currents	49

3.1.3 Combined wave-current flows 54
3.2 Continental shelf zones 55
3.3 Examples from different storm-dominated shelf settings 57
3.3.1 North America 58
3.3.2. East Australia 63
3.3.3. New Zealand 69
3.4 Summary 76

4 REGIONAL OCEANOGRAPHIC PATTERNS

4.0 Introduction 79
4.1 Methods 79
4.1.1 Sea-bed drifters 79
4.1.2 Aanderaa current meters 81
4.2 Sea-bed drifter results 82
4.2.1 Retrieval rates and interpretations 82
4.2.2 Sea-bed drifter experiments 83
4.2.3 Residual current patterns 91
4.3 Onemana Aanderaa current meter results 93
4.3.1 Current meter and anemograph records 93
4.3.2 Current flow patterns during storm events 96
4.3.3 Forcing mechanisms of current flows 98
4.3.4 Mean circulation and potential net sediment transport 101
4.4 Model for east Coromandel shelf flows 105
4.5 Additional current measurements 109
4.5.1 Opito Bay-Whangapoua 109
4.5.2 Waihi-Whiritoa 117
4.6 Conclusions 121

5 SURFICIAL SEDIMENT TEXTURAL PATTERNS

5.0 Introduction 123
5.1 Sample collection 123
5.2 Textural analysis 129
5.2.1 Hydraulic equivalence textural properties 129
5.2.2 Surface texture of grains 130
5.2.3 Carbonate 131
5.3 Textural characteristics of shelf sediments 131
5.3.1 Southern coastline 131
5.3.2 Northern coastline 144

5.4 Beach and dune texture 153
5.5 Fluvial sediment texture 159
5.6 Statistical classification of textural data 165
5.6.1 Entropy program 165
5.6.2 Textural classification results 166
5.6.3 Entropy class descriptions and interpretations 170
5.7 Conclusions 182

6 SHELF MORPHOLOGICAL SURVEYS

6.0 Introduction 187
6.1 Method 188
6.1.1 Side-scan sonar 188
6.1.2 Bathymetric data 189
6.1.3 Ripple and megaripple observations 189
6.2 Side-scan sonar data 190
6.2.1 Side-scan sonar operation and sonograph interpretations 190
6.2.2 Regional side-scan and bathymetric surveys 194
6.2.3 Implications of sonograph and bedform patterns for shelf erosion and transport pathways 248
6.3 Ripple and megaripple observations 259
6.3.1 Ripple and megaripple morphology 259
6.4 Conclusions 274

7 SHELF MORPHODYNAMICS

7.0 Introduction 285
7.1 Hydrodynamic interpretations of wave-generated bedforms 285
7.1.1 Theoretical background 285
7.1.2 Interpretations of wave conditions from ripple and megaripple observations 290
7.2 Depth of activity rod surveys 298
7.2.1 Method 298
7.2.2 Survey results 300
7.2.3 Significance of results to empirical estimations for wave flow characteristics 310
7.3 Morphodynamic interpretations of shelf sand ridges 316

7.4 Significance of wave refraction patterns to shelf sedimentation 322
7.4.1 Wave refraction processes 322
7.4.2 Wave refraction results 324
7.4.3 Significance of wave refraction patterns to coarse megaripple band formation 332
7.5 Conclusions 335

8 SHALLOW SUB-BOTTOM SHELF STRATIGRAPHY

8.0 Introduction 339
8.1 Methods 339
8.2 Seismic stratigraphy 345
8.2.1 Principles of seismic stratigraphic analysis 345
8.2.2 Seismic units 347
8.2.3 Regional seismic stratigraphic patterns 360
8.3 Box core data 401
8.4 Radiocarbon dates 405
8.5 Conclusions 407

9 SEDIMENT COMPOSITION

9.0 Introduction 413
9.1 Methods 413
9.2 Results of mineralogical analysis 417
9.2.1 Characteristics of major minerals identified 417
9.2.2 River sand mineralogy 422
9.2.3 Barrier sand mineralogy 425
9.2.4 Beach sand mineralogy 428
9.2.5 Shelf sand mineralogy 433
9.3 Clay composition 438
9.4 Statistical classification of mineralogical data 438
9.4.1 Entropy class descriptions and interpretations 439
9.5 Provenence for east Coromandel coastal and shelf sediments 450
9.6 Conclusions 459

10 CONCEPTUAL MODELS FOR SHELF SEDIMENTATION AND EVOLUTION

10.0 Introduction 461
10.1 East Coromandel shelf lithofacies 461

10.1.1 Delineation of shelf lithofacies 461
10.1.2 Lithofacies distribution on the southern shelf 462
10.1.3 Lithofacies distribution on the northern coast 469
10.1.4 Interpretations of shelf lithofacies distributions 474
10.2 Nearshore and inner shelf sedimentation 476
10.2.1 Regional sediment transport pathways 476
10.2.2 Nearshore and inner shelf sedimentation processes 479
10.3 Diabathic beach-shelf interactions 489
10.3.1 Pocket beach systems 489
10.3.2 Barrier spit beach systems 493
10.3.3 Summary of beach-shelf interactions 498
10.4 Holocene evolution 499
10.4.1 Last glacial lowstand 500
10.4.2 Holocene marine transgression 502
10.4.3 Holocene stillstand 502
10.5 Conclusions 512

11 IMPLICATIONS AND CONCLUSIONS OF STUDY

11.0 Introduction 517
11.1 Implications for coastal resource management 517
11.1.1 Beach and dune erosion 517
11.1.2 Disposal of dredge and mining tailings on the shelf 527
11.1.3 Potential offshore aggregate and mineral resources 529
11.2 Future research 538
11.4 Summary of major findings in the east Coromandel shelf study 541

REFERENCES 545

APPENDICIES
1 Current measurement information A-1
2 Sediment sample locations A-17
3 Sediment texture results A-27
4 Side-scan sonar and sub-bottom fix positions A-71
5 Bedform surveys A-87
6 Box core data A-101
7 Radiocarbon dates A-109
8 Mineralogy results A-113
9 Entropy Program Results A-121

LIST OF TABLES

		PAGE
Table 2.1.	Summary of Coromandel Peninsula regional geology.	12
Table 2.2.	Holocene sedimentation rates for east Coromandel estuaries.	24
Table 3.3.	Comparison of east Coromandel with other storm-dominated shelves.	78
Table 4.1.	Details of the release and retrieval of sea-bed drifters.	81
Table 4.2.	Results from the four sea-bed drifter experiments.	84
Table 5.1.	Quantification of sedimentary grain size parameters.	132
Table 5.2.	Summary of textual data for east Coromandel beaches.	154
Table 5.3.	Summary of textural data for east Coromandel dune systems.	160
Table 5.4.	Summary of textual properties for east Coromandel river samples.	162
Table 5.5.	Summary of mean textural properties for 7 entropy classes.	171
Table 6.1.	Morphological definition of various bedforms identifies in this study.	187
Table 6.2.	Summary of the dominant shelf morphological characteristics.	276
Table 7.1.	Wave heights required to initiate sediment transport.	294
Table 7.2.	Regional variations in sand ridge spacing.	316
Table 8.1.	Inferred seismic stratigraphic units and relative ages.	349
Table 8.2.	Radiocarbon ages and approximate sedimentation rates.	406
Table 9.1.	Summary of distribution of mineralogical entropy classes.	441
Table 9.2.	Characteristic lithology of various east Coromandel volcanic lithologies.	455
Table 9.3.	Mineral assemblages of Coromandel Group volcanics.	457
Table 9.4.	Mineral assemblages for Whitianga Group volcanics.	457
Table 9.5.	Mineralogy of late Quaternary tephras.	458
Table 9.6.	Comparison between Waikato River and east Coromandel sand mineralogy.	458
Table 10.1.	Characteristic features of east Coromandel lithofacies.	463
Table 11.1.	Textural characteristics of Whiritoa Beach and east Coromandel inner shelf deposits.	530

LIST OF FIGURES

Page

CHAPTER 1

Figure 1.1. Location map of east Coromandel study area. 2

Figure 1.2. Erosion accretion trends for beach systems along east Coromandel. 3

Figure 1.3. Organisational structure of the east Coromandel shelf study. 6

CHAPTER 2

Figure 2.1. Generalised geology of the Coromandel volcanic zone. 11

Figure 2.2. Structural and tectonic map of the Coromandel Volcanic Zone. 13

Figure 2.3. Local patterns in wind, rainfall, and temperature. 16

Figure 2.4. General direction and speed for flood and ebb tidal currents in ocean waters. 18

Figure 2.5. Ocean current circulations found around the New Zealand land mass. 18

Figure 2.6. Wave observation from the northeast coast of New Zealand. 21

Figure 2.7. Waverider buoy data from Tauranga Harbour. 22

Figure 2.8. The partially infilled Tairua Harbour system. 26

Figure 2.9. Pleistocene inner barrier deposits at Orokawa Bay. 27

Figure 2.10. Holocene barrier types along east Coromandel coast. 28

Figure 2.11. The WRIGHT and SHORT (1984) beach classification model. 32

Figure 2.12. Ridge and runnel system at Whiritoa Beach. 33

Figure 2.13. Transverse bar and rip morphology at Whiritoa Beach. 33

Figure 2.14. Possible range of beach types on the central Netherlands coast. 34

Figure 2.15. Waihi Beach under moderate wave conditions. 35

Figure 2.16. Shelf bathymetry between the Bay of Plenty and Tairua. 37

Figure 2.17. Bathymetric contours between between Mercury Bay and the Kuaotunu Peninsula. 38

Figure 2.18. Structural map of seismic basement for the Coromandel region. 39

Figure 2.19. Nearshore and inner shelf sediment distribution off Onemana Beach 41

Figure 2.20. Grain size distributions of beach and shelf sands at Whiritoa. 41

Figure 2.21. Surface sediment textural patterns off Whiritoa Beach. 42

Figure 2.22. Surface sediment textual patterns within Mercury Bay. 42

CHAPTER 3

Figure 3.1. Conditions for which different wave theories are most applicable. 48

Figure 3.2. Conceptual diagram showing sediment entrainment under amplitude-modulated waves. 48

Figure 3.3. Wind-induced Ekman flow for the northern hemisphere. 50

Figure 3.3. The three main dynamic layers within the coastal boundary zone. 50

Figure 3.5. Dynamic zones of the coastal ocean. 52

Figure 3.6. Characteristic current flow patterns within the coastal boundary zone. 52

Figure 3.7. Schematic current circulation patterns under different orientations of the wind relative to the coastline. 53

Figure 3.8. Morphological components which characterise the coastal boundary zone. 56

Figure 3.9. Bedform sequences over the nearshore and inner shelf zones. 56

Figure 3.10. Schematic sediment budget for a landward migrating barrier on the mid-Atlantic shelf. 60

Figure 3.11. Sediment inputs to coastal barrier systems of the Mississippi Delta. 62

Figure 3.12. Seasonal sedimentation regime for the Oregon shelf. 64

Figure 3.13. Schematic models for late Quaternary deposition in New South Wales. 67

Figure 3.14. Shelf sediment lithofacies on the New South Wales coast. 68

Figure 3.15. Schematic diagram showing shelf sand body morphology and offshore transport system on New South Wales coast. 68

Figure 3.16. Conceptual model for barrier formation on the New South Wales shelf. 70

Figure 3.17. Distribution of main sediment types on the New Zealand shelf. 71

Figure 3.18. Conceptual model for shelf sediment transport on the Pakiri coast. 73

Figure 3.19. Sediment facies distribution and hydrodynamic processes at Tauranga. 73

Figure 3.20. Holocene sand wedge off the Otago coast. 75

CHAPTER 4

Figure 4.1. Location map of Aanderaa current meter and wind recording stations. 80

Figure 4.2. Drifter dispersal patterns from experiment No. 1. 85

Figure 4.3. Drifter dispersal patterns from experiment No. 2. 87

Figure 4.4. Drifter dispersal patterns from experiment No. 3. 89

Figure 4.5. Drifter dispersal patterns from experiment No. 4. 90

Figure 4.6. Relationship between drifter dispersal patterns and wind climate. 92

Figure 4.7. Time series plots of current and wind data from Onemana. 95

Figure 4.8. Hourly current and wind speed plots during major storm events, Onemana. 97

Figure 4.9. Spectral analysis of current and wind data from Onemana. 100

Figure 4.10. Current roses from hourly observations at Onemana. 103

Figure 4.11. Progressive vector plots for Onemana current data. 104

Figure 4.12. Probability of exceedance for various wind speeds over 18 month period. 106

Figure 4.13. Seasonal wind frequency and speed over 18 month period. 106

Figure 4.14. Conceptual models for inner shelf dynamics and sediment transport. 107

Figure 4.15. Progressive vector plots for Opito Bay and Whangapoua current data. 110

Figure 4.16. Opito Bay current meter data. 111

Figure 4.17. Hourly wind data at Matarangi Beach. 112

Figure 4.18. Time series plots of Whangapoua current data. 114

Figure 4.19. Inferred current flow patterns off northern east Coromandel coast. 116

Figure 4.20. Time series plots of Whiritoa current data. 118

Figure 4.21. Hourly wind data from Whiritoa and Waihi Beach. 119

Figure 4.22. Time series plots of Waihi Beach wind data. 120

CHAPTER 5

Figure 5.1. Location map of surface sediment samples on the southern coastline. 125

Figure 5.2. Location map of surface sediment samples on the northern coastline. 127

Figure 5.3. Distribution of mean grain size for shelf deposits on the southern coastline. 133

Figure 5.4. Distribution of sediment sorting for shelf deposits on the southern coastline. 135

Figure 5.5. Cross-shelf variations in sediment textural properties from southern coast. 137

Figure 5.6. Occurrence of mud in selected east Coromandel sediment samples. 140

Figure 5.7. Distribution of mean grain size for shelf deposits on the northern coastline. 145

Figure 5.8. Distribution of sediment sorting for shelf deposits on the northern coastline. 147

Figure 5.9. Cross-shelf variations in sediment textural properties from northern coast. 149

Figure 5.10. Variations in textural properties of beach deposits. 155

Figure 5.11. Comparisons of grain size distribution curves between beach, dune, surfzone and nearshore deposits. 157

Figure 5.12. Variations in textural properties of dune deposits. 161

Figure 5.13. Comparisons between grain size distributions of river, barrier spit beach, and nearshore sands. 163

Figure 5.14. Plot showing the different number of entropy classes into which textural data can be classified. 167

Figure 5.15. Grain size frequency distribution histograms of 7 entropy classes. 168

Figure 5.16. Plot of mean grain size vs. sediment sorting for 7 entropy classes. 169

Figure 5.16. Plot of mean grain size vs. skewness sorting for 7 entropy classes. 169

Figure 5.17. Macro- and micro-photographs of 7 entropy classes. 172

Figure 5.18. Distributions of entropy classes on the southern coastline. 175

Figure 5.19. Distributions of entropy classes on the northern coastline. 177

Figure 5.21. Relationship between textural parameters within each entropy class for barrier dune samples. 179

Figure 5.22. Relationship between textural parameters within each entropy class for beach samples. 180

CHAPTER 6

Figure 6.1. Sonograph off Whangamata Beach showing fine featureless, coarse megarippled and bedrock pattern. 192

Figure 6.2. Sonograph off Whangamata Beach showing blebby pattern. 192

Figure 6.3. Sonograph off Whangapoua Harbour showing mottled pattern. 193

Figure 6.4. Sonograph off Opoutere Beach showing isolated strong reflectors. 193

Figure 6.5. Wavy sonograph pattern off Waihi Beach. 195

Figure 6.6. Fizzy sonograph pattern off Onemana. 195

Figure 6.7. Location of side-scan sonar track lines on southern coast. 197

Figure 6.8. Location of side-scan sonar track lines on northern coast. 199

Figure 6.9. Waihi Beach side-scan sonograph map from the Mar-84 survey. 202

Figure 6.10. Waihi Beach side-scan sonograph map from the Jun-90 survey. 203

Figure 6.11. Echosounding profiles from Waihi Beach. 204

Figure 6.12. Sonograph offshore from Waihi Beach over sand ridges in Mar-84. 206

Figure 6.13. Sonograph offshore from Waihi Beach over sand ridges in Jun-90. 206

Figure 6.14. Sonograph offshore from Waihi Beach in Jun-90 showing coarse megarippled sands over the southeastern flank of a prominent rock pinnacle. 207

Figure 6.15. Whiritoa-Mataora side-scan sonograph map from the Mar-84 survey. 209

Figure 6.16. Whiritoa-Mataora side-scan sonograph map from the Jun-90 survey. 210

Figure 6.17. Echosounding profiles from Mataora and Whiritoa. 211

Figure 6.18. Sonograph offshore from Whiritoa Beach in Mar-84 showing coarse megaripples sands and hummock of fine sand. 213

Figure 6.19. Sonograph offshore from Whiritoa Beach in Jun-90 showing narrow coarse megarippled sand band. 213

Figure 6.20. Whangamata side-scan sonograph map from the Mar-84 survey. 216

Figure 6.21. Whangamata side-scan sonograph map from the Mar-85 survey. 217

Figure 6.22. Whangamata side-scan sonograph map from the Jun-90 survey. 218

Figure 6.23. Echosounding profiles from Whangamata. 219

Figure 6.24. Three-dimensional image of the nearshore surface where a coarse megarippled band occurs, off Te Ananui Headland, Whangamata. 221

Figure 6.25. Sonograph from Whangamata in Jun-90 showing shore parallel bands of coarse megarippled sands where extensive field had previously occurred. 222

Figure 6.26. Sonograph from the base of the inner shelf zone at Whangamata, Mar-84, showing patches of coarse and fine sand associated with hummocks. 222

Figure 6.27. Onemana side-scan sonograph map from the Mar-84 survey. 224

Figure 6.28. Onemana side-scan sonograph map from the Mar-85 survey. 225

Figure 6.29. Onemana side-scan sonograph map from the Jun-90 survey. 226

Figure 6.30. Echosounding profiles from Onemana. 227

Figure 6.31. Opoutere side-scan sonograph map from the Mar-84 survey. 230

Figure 6.32. Echosounding profiles from Opoutere Beach. 231

Figure 6.33. Sonograph of shore-normal orientated coarse megaripple bands on the nearshore surface, Opoutere, Mar-84. 232

Figure 6.34. Pauanui-Tairua side-scan sonograph map from the Mar-84 survey. 233

Figure 6.35. Echosounding profiles from Pauanui and Tairua Beach. 234

Figure 6.36. Sonograph off Pauanui Beach in Mar-84, showing presence of an apparent offshore bar in 5 m water depth. 235

Figure 6.37. Hotwater Beach side-scan sonograph map from the Mar-84 survey. 237

Figure 6.38. Echosounding profile from Hotwater Beach. 238

Figure 6.39. Sonograph off Hotwater Beach in Mar-84, showing presence of a small hummock of fine sand over coarse inner shelf sands. 239

Figure 6.40. Mercury Bay side-scan sonograph map from the Mar-84 survey. 241

Figure 6.41. Mercury Bay side-scan sonograph map from the Jun-90 survey. 242

Figure 6.42. Echosounding profiles from Mercury Bay. 243

Figure 6.43. Sonograph from Mercury Bay in Jun-90 showing sand waves off the southern end on Wharekaho Harbour. 243

Figure 6.44. Sonograph from Mercury Bay in Jun-90 showing small fingers offshore from Waitaia Beach. 244

Figure 6.45. Sonograph from Mercury Bay in Jun-90 showing small sand waves coinciding with fingers offshore from Waitaia Beach. 244

Figure 6.46. Otama-Whangapoua side-scan sonograph map from the Mar-84 survey. 246

Figure 6.47. Echosounding profiles from Otama and Whangapoua. 247

Figure 6.48. Occurrence of coarse megarippled sand, bedrock, and fine featureless sand on the southern coast. 249

Figure 6.49. Inferred sediment transport pathways on the southern coast. 251

Figure 6.50. Occurrence of coarse megarippled sand, bedrock, and fine featureless sand on the northern coast. 255

Figure 6.51. inferred sediment transport pathways on the northern coast. 257

Figure 6.52. Plot of oscillation ripple size along the east Coromandel coast. 261

Figure 6.53. Wave-generated bedforms recorded along the southern coast. 263

Figure 6.54. Flat featureless lower nearshore surface off Whiritoa. 265

Figure 6.55. Large, low relief ripples on the lower nearshore off Whangamata. 265

Figure 6.56. Megaripples on the inner shelf off Waihi Beach. 267

Figure 6.57. Wave-generated bedforms recorded along the northern coast. 269

Figure 6.58. Megaripple bedforms in the nearshore zone off Hahei. 271

Figure 6.59. Small ripples in the nearshore zone off Hahei. 271

Figure 6.60. Large ripples in the nearshore zone off Otama. 273

Figure 6.61. Flat featureless sea-bed on the Otama inner shelf. 273

Figure 6.62. Small ripples on the Whangapoua nearshore zone. 275

Figure 6.63. Flat featureless sea floor on the Whangapoua inner shelf. 275

Figure 6.64. Summary diagram of the major morphological components off east Coromandel embayments. 278

Figure 6.65. Summary diagram of the changes in shelf morphology on the southern following Cyclone Bola in Mar-88. 282

CHAPTER 7

Figure 7.1. Velocity threshold curves for grain movement and sheet flow of quartz sand in water. 287

Figure 7.2 Plot of ripple to grain size against ratio of orbital diameter to grain size. 287

Figure 7.3. Representative wave parameters fro the east Coromandel coast. 291

Figure 7.4. Dimensions of ripples observed by divers along the east Coromandel coast. 293

Figure 7.5. Combinations of wave height and water depth that will generate sheet flow conditions under waves of different periods. 297

Figure 7.6. Location map for depth of activity rod survey sites. 299

Figure 7.7. Changes in the sea-bed observed from depth of activity rod surveys at Whiritoa. 301

Figure 7.8. Surveyed changes in bedform morphology on the inner shelf at Whiritoa. 302

Figure 7.9. Wave conditions necessary to generate the surveyed bedforms at Whiritoa. 303

Figure 7.10. Changes in the sea-bed observed from depth of activity rod surveys at Whangamata. 305

Figure 7.11. Surveyed changes in bedform morphology on the inner shelf at Whangamata. 307

Figure 7.12. Cross-sectional profile of megaripples at Whangamata. 308

Figure 7.13. Wave conditions necessary to generate the surveyed bedforms at Whangamata. 309

Figure 7.14. Changes in the sea-bed observed from depth of activity rod surveys at Onemana. 311

Figure 7.15. Cross-sectional profile of megaripples at Onemana. 312

Figure 7.16. Wave conditions necessary to generate the surveyed bedforms at Onemana. 313

Figure 7.17. Map showing distribution and orientation of sand ridge crests on the southern coast. 317

Figure 7.18. Plot of sand ridge relief on the east Coromandel coast based on sonograph and echosounding traces. 319

Figure 7.19. Wave refraction patterns and association with coarse megaripple bands off Whiritoa Beach. 326

Figure 7.20. Wave refraction patterns and association with coarse megaripple bands off Whangamata and Onemana Beach. 328

Figure 7.21. Wave refraction patterns and association with coarse megaripple bands off Opoutere and Pauanui Beach. 330

Figure 7.22. Wave refraction patterns and association with coarse megaripple bands off Cooks Beach. 333

CHAPTER 8

Figure 8.1. Location of box cores and seismic track lines from the southern exposed coastline. 341

Figure 8.2. Location of box cores and seismic track lines from the northern embayed coastline. 343

Figure 8.3. Seismic reflection termination patterns used in delineating unconformities apparent truncations. 346

Figure 8.4. Association of seismic units with late Quaternary sea level oscillations. 351

Figure 8.5. Seismic reflection profile off mid Waihi Beach. 353

Figure 8.6. Seismic reflection profile off Bowentown, Waihi Beach. 355

Figure 8.7. Seismic reflection profile off Mataora Beach. 357

Figure 8.8. Surface distribution of seismic stratigraphic units off Waihi Beach. 361

Figure 8.9. Seismic reflection profile off northern Waihi Beach. 363

Figure 8.10. Seismic reflection profile off mid Waihi Beach. 367

Figure 8.11. Seismic reflection profile along shore-parallel track off Orokawa Bay. 369

Figure 8.12. Surface distribution of seismic stratigraphic units off Whiritoa and Mataora. 371

Figure 8.13. Seismic reflection profile off Whiritoa Beach. 373

Figure 8.14. Seismic reflection profile off Whiritoa Beach. 375

Figure 8.15. Seismic reflection profile along shore-parallel track off Whiritoa Beach. 377

Figure 8.16. Surface distribution of seismic stratigraphic units off Whangamata Beach. 381

Figure 8.17. Seismic reflection profile off Otahu Harbour. 383

Figure 8.18. Seismic reflection profile off Whangamata Beach. 385

Figure 8.19. Seismic reflection profile along shore-parallel track off Whangamata. 387

Figure 8.20. Seismic reflection profile along shore-parallel track off Onemana. 389

Figure 8.21. Seismic reflection profile between Otahu and Whangamata. 391

Figure 8.22. Surface distribution of seismic stratigraphic units in Mercury Bay. 393

Figure 8.23. Seismic reflection profile off Buffalo Beach. 395

Figure 8.24. Seismic reflection profile off Waitaia Beach. 397

Figure 8.25. Seismic reflection profile along shore-parallel track in Mercury Bay. 399

Figure 8.26. Photographs of representative box cores. 403

Figure 8.27. Inferred environmental conditions present on the east Coromandel coast during a lower interstadial sea level event. 411

CHAPTER 9

Figure 9.1. Location sites for samples used in mineralogical analysis on the southern coast. 414

Figure 9.2. Location sites for samples used in mineralogical analysis on the northern coast. 415

Figure 9.3. CL photo-micrograph of feldspar, quartz and lithic fragments. 419

Figure 9.4. CL photomicrograph of feldspar, lithics, and volcanic glass. 420

Figure 9.5. Photo-micrograph of hypersthene, cummingtonite, green hornblende, and opaques. 421

Figure 9.6. Photo-micrograph of hypersthene, cummingtonite, opaques and zircon. 421

Figure 9.7. Mineralogy of the 2 to 4 ϕ sand fraction of river sands. 423

Figure 9.8. Heavy mineralogy of river sands. 424

Figure 9.9. Mineralogy of the 2 to 4 ϕ sand fraction of barrier sands. 426

Figure 9.10. Heavy mineralogy of barrier sands. 427

Figure 9.11. Mineralogy of the 2 to 4 ϕ sand fraction of beach sands. 429

Figure 9.12. Heavy mineralogy of beach sands. 430

Figure 9.13. Mineralogy of the 2 to 4 ϕ sand fraction of shelf sands. 434

Figure 9.14. Heavy mineralogy of shelf sands. 436

Figure 9.15. Number of entropy classes into which mineralogical data is classified. 440

Figure 9.16. Plots of the average occurrence of minerals within entropy classes. 443

Figure 9.17. Distribution of mineralogical entropy classes on the southern shelf. 445

Figure 9.18. Distribution of mineralogical entropy classes on the northern shelf. 447

Figure 9.19. F:Q ratios of barrier deposits along the east Coromandel coast. 451

Figure 9.20. F:Q ratios of beach deposits along the east Coromandel coast. 453

CHAPTER 10

Figure 10.1. Distribution of shelf lithofacies along the southern coast. 465

Figure 10.2. Distribution of east Coromandel shelf lithofacies across shelf morphological provinces on the southern coast. 467

Figure 10.3. Distribution of shelf lithofacies along the northern coast. 471

Figure 10.4. Distribution of east Coromandel shelf lithofacies across shelf morphological provinces on the northern coast. 473

Figure 10.5. Conceptual model for along-shelf, northerly-directed, and smaller southerly-directed transport pathways on the east Coromandel shelf. 477

Figure 10.6. Predicted suspended sediment concentrations of shelf sediments under different wave conditions. 480

Figure 10.7. Shelf transport processes occurring during fair weather conditions. 483

Figure 10.8. Shelf transport processes occurring during annual storm events. 485

Figure 10.9. Shelf transport processes occurring during extreme storm events. 487

Figure 10.10. Conceptual model showing the response of pocket beach systems to calm and storm conditions. 490

Figure 10.11. Typical response of a pocket beach system during storm wave conditions. 492

Figure 10.12. Conceptual model showing the response of barrier spit beach systems to calm and storm conditions. 494

Figure 10.13. Waihi Beach during fair weather conditions. 495

Figure 10.14. Matarangi Beach during fair weather conditions. 497

Figure 10.15. Matarangi Beach during storm wave conditions. 497

Figure 10.16. Inferred coastal physiography during the Last Glacial Period. 501

Figure 10.17. Inferred coastal physiography during the Holocene marine transgression. 503

Figure 10.18. Evolutionary model for barrier spit systems during the Holocene stillstand. 506

Figure 10.19. Evolutionary model for pocket beach systems during the Holocene stillstand. 510

CHAPTER 11

Figure 11.1. Example of a beach system in its natural state of integrity, Orokawa Bay. 518

Figure 11.2. Stable frontal dune system at Matarangi Beach. 518

Figure 11.3. Unstable dune blowouts threatening property at Tairua Beach. 520

Figure 11.4. Example of requirements for an adequate buffer zone. 520

Figure 11.5.	Example of a developed barrier system at Pauanui with an adequate buffer zone present.	522
Figure 11.6.	Successful dune stabilisation at Hotwater Beach.	522
Figure 11.7.	Problem experienced with coastal flooding at Buffalo Beach.	524
Figure 11.8.	Example of an ineffective management strategy at Buffalo Beach.	524
Figure 11.9.	Example of a revetment designed in harmony with the natural beach dynamics.	526
Figure 11.10.	Important offshore zones for shelf resource management.	526
Figure 11.11.	The proposal by Max resources N.Z. Ltd. which has caused considerable controversy.	533
Figure 11.12.	Proposed exploration region by Max Resources N.Z. Ltd.	534
Figure 11.13.	Potential sites for placer mineral exploration in shelf deposits.	535
Figure 11.14.	Heavy mineral concentrations in bulk sediment samples.	536
Figure 11.15.	Heavy mineral seams in dune deposits at Whiritoa Beach.	537
Figure 11.16.	Heavy mineral concentrations in the 2 to 4 ϕ sand fraction.	539

CHAPTER ONE

INTRODUCTION

1.0. RESEARCH BACKGROUND

The east Coromandel coastline on the northeast coast of New Zealand (Figure 1.1) is an outstanding scenic attraction. With the growth in wealth and improvement of population mobility, the Coromandel coastline had by the 1970s become popular with the urban dwellers of the surrounding Auckland, Waikato and Bay of Plenty region. Increasing pressure through subsequent development of the coast has led to localised erosion problems since the 1970s. The vulnerability of properties to coastal erosion was particularly evident in July 1978, when a severe storm coincided with high spring tides to cause extensive property damage along the Bay of Plenty and Coromandel coastlines, particularly at Cooks Beach and Hahei (HEALY and DELL, 1987).

As a result of increasing pressures for more coastal subdivisions and erosional episodes on some sectors of the coast at Waihi Beach, Cooks Beach, Whangamata, Whiritoa and Pauanui, the Department of Earth Sciences, University of Waikato and Hauraki Catchment Board combined resources to study the major sandy beach systems of the east Coromandel coast (HEALY *et al.*, 1981; HEALY and DELL, 1982). These surveys provided baseline information of general textural and compositional characteristics of the dune, beach and nearshore sediments at 27 beach localities along the coastline, as well as a reconnaissance assessment of the erosion/accretion state of each beach system.

The erosion-accretion analysis (Figure 1.2) showed no clear regional trends, although embayed low-energy fine-grained beach systems (Wharekaho, Buffalo, and Kennedy) tended to show the most marked erosion, possibly the result of the focussing of wave energy during storms, while paradoxically relatively high-energy coarse-grained pocket beach systems (Whiritoa, Onemana, Otama, Rings, Kuaotunu West and Whangapoua) did not appear to have suffered marked dune recession, but instead were susceptible to episodic cut and fill (HEALY and DELL, 1987). Also, a number of bayhead beaches (Matarangi, Cooks, Pauanui and Whangamata) showed accretion at the point where the ebb-tidal delta welds onto the beach, whereas the basal ends typically eroded as sediment migrated over time from the beach toward the ebb-tide delta system (HEALY and DELL, 1987).

One of the important questions raised in these earlier surveys was the relationship of the sand on the beaches to that on the continental shelf. Geomorphically, many beaches on the eastern Coromandel Peninsula have the appearance of pocket systems, implying that they are isolated sedimentary systems (HEALY *et al.* , 1981). This was strongly indicated for Whiritoa and the neighbouring Mataora Beach by HEALY (1981), based on the textural and mineralogical properties of beach sands from these locations. He concluded that the major source of beach sediments for the Mataora Beach system since the Holocene marine transgression was erosion of the adjacent cliffs, with minor quantities of sand contributed also from the Mataora Stream. Sands from the continental shelf and littoral drift were not considered to be contributing much sediment to Mataora Beach.

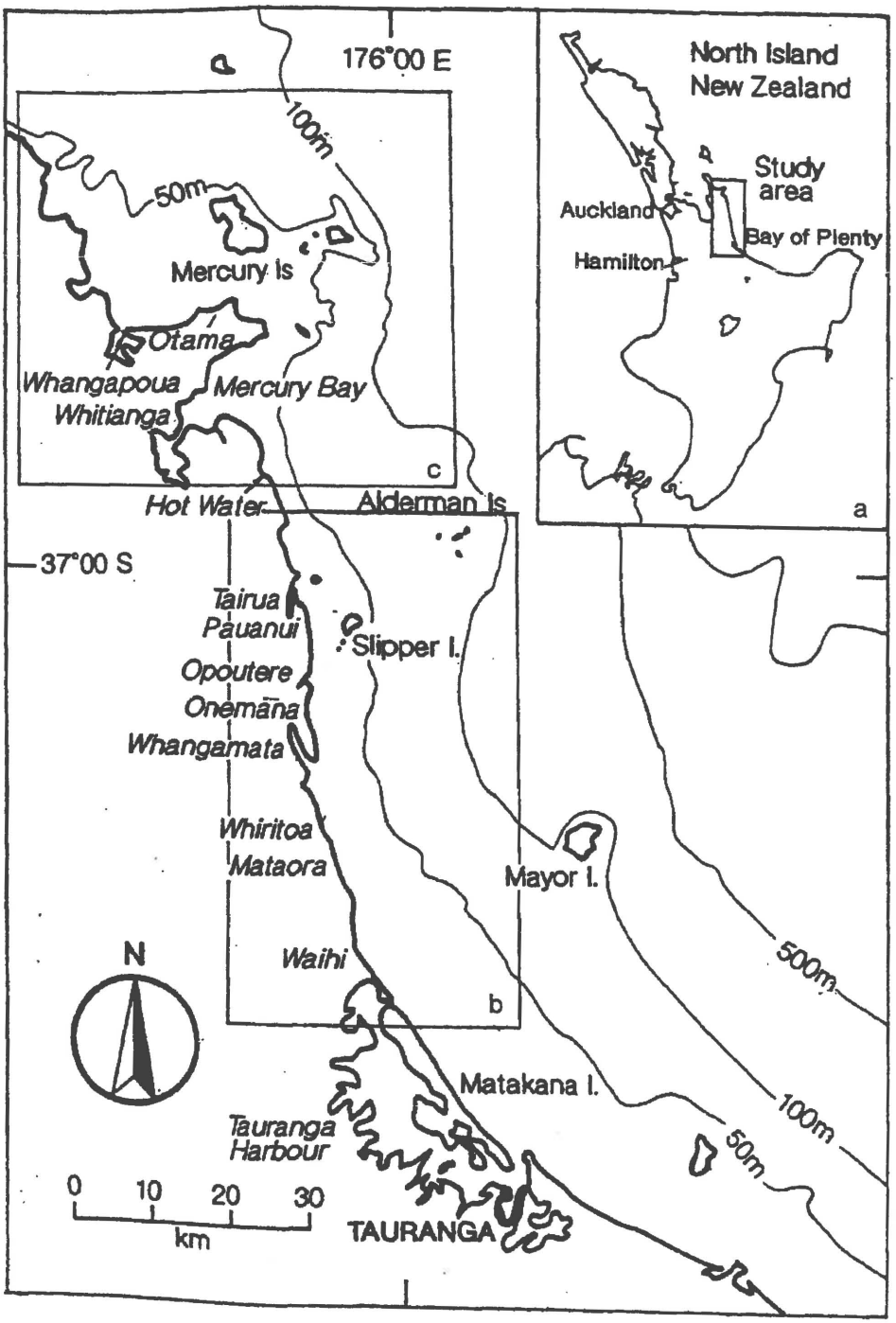

Figure 1.1. Location map (a) of the east Coromandel study area. Outlined regions in the enlarged map show the southern exposed (b) and northern embayed (c) sections into which the study area has been divided to aid in data presentation.

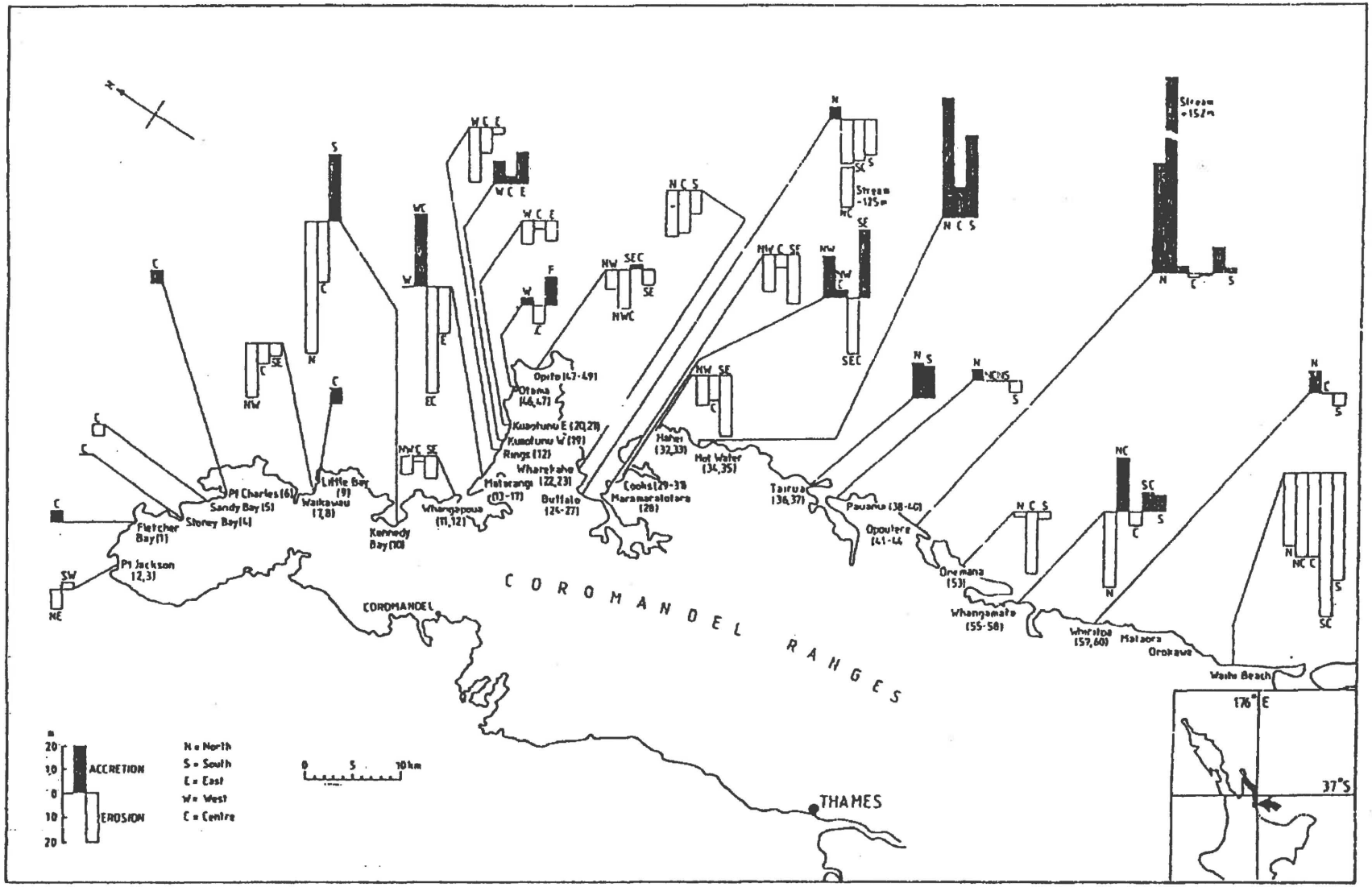

Figure 1.2. Erosion-accretion trends of the frontal dunes in beach systems along the east Coromandel coast, as recorded by HEALY *et al.* (1981) from aerial photograph analysis for the period 1944-1978.

From the results of these baseline studies of the coast, HEALY and DELL (1987, p. 2) raised the important question :

" are all other beaches on the eastern Coromandel Peninsula likewise closed sedimentary systems, or is there a potential interchange of sand from one beach to another via a nearshore littoral drift system? "

" alternatively, is there an exchange of beach material with the inner continental shelf ? "

These questions have important implications for resource development along the Coromandel Coast in that they relate to the contentious issue of episodic beach erosion, continuous shoreline retreat, implementation of building set back in coastal sub-division and commercial extraction of sand from the coastal sedimentary systems.

In light of the results of these background studies, the East Coromandel Shelf Study (E.C.S.S.) was initiated by Paul Dell in 1984 to investigate the open questions of the relationship between beach and continental shelf sediments and the potential for across-shelf sand migration to nourish the beach systems of the east Coromandel coast. This involved extensive dredge and box sampling, scuba observations, bottom photography, and side-scan sonar mapping. In addition, a similar investigation was initiated in 1984 by Tony Colby off the Kuaotunu Peninsula, and later incorporated into the E.C.S.S. The original investigation was curtailed by Paul Dell in 1987, but continued by this author between 1988 and 1991, with additional interest on the response of the shelf to a major storm event (Cyclone Bola) in 1988. In view of the practical background to the E.C.S.S., the investigation has focussed on shelf regions adjacent to coastal areas of active development, especially Waihi-Onemana, Mercury Bay and Otama-Whangapoua.

In addition to the practical application of the results of the investigation, it is also believed that the E.C.S.S. will make an important scientific contribution to the modern understanding of nearshore and inner shelf sedimentation processes. This was noted by WRIGHT (1987) as a frontier zone of contemporary coastal sedimentary research, particularly regarding the problem of diabathic (i.e. shore-normal) sediment exchanges between the beach and shelf systems. As WRIGHT (1987, p. 26) states:

"the state of the art regarding shoreface transport processes, particularly in the diabathic dimension, and shoreface-surfzone coupling mechanisms is still in its infancy."

1.1. RESEARCH OBJECTIVES.

The specific aims of the E.C.S.S. are to:

1. Determine the nearshore and inner shelf sedimentation patterns along the east Coromandel coast, and the past and present processes responsible for these. To achieve these aims, data have been collected on the nature of shelf currents, wave-induced transport, sediment lithology (texture and mineralogy), morphology, morphodynamics and stratigraphy, as well as similar though less detailed information from the local beach-barrier systems. Through integrating these data, a number of conceptual models are presented which describe the response of shelf sediments to different oceanographic conditions, the diabathic coupling between local beach and shelf sediments, and the Holocene evolution of shelf and coastal deposits.

2. Compare and contrast the findings from the E.C.S.S. to some overseas investigations in which nearshore and inner shelf sedimentation processes have been extensively modelled, and thus improve our presently inadequate knowledge of such processes.

3. Apply these results to local coastal management issues, specifically those relating to the protection of properties presently at risk from coastal erosion, as well as the potential of the east Coromandel continental shelf as a repository for dredge spoil and mine tailings, or as a possible source for aggregate and mineral deposits.

1.2. THESIS OUTLINE.

In this investigation, data presentation has been organised in such a way that the information from each chapter can be integrated to achieve the main objectives of the E.C.S.S. The thesis structure is shown in detail in Figure 1.3, and briefly outlined below.

Chapter 2 describes the physical setting of the east Coromandel coastline by reviewing previous studies of the local coastal geomorphology, geology, climate, and oceanographic setting.

In Chapter 3, the present international understanding of nearshore and inner shelf sedimentation processes is reviewed, with particular attention to previous studies from North America, eastern Australia and elsewhere in New Zealand. This information can then be both applied and evaluated with results from the E.C.S.S. in subsequent chapters.

In Chapter 4, the regional current patterns are investigated through data obtained from sea-bed drifter experiments and Aanderaa current meters deployed along the shelf. Particular emphasis is on the current patterns most likely to erode and transport the shelf sediments.

Chapter 5 investigates the textural character of surficial shelf sediments collected along the coast, and statistically classifies the data to provide an initial grouping of deposits which can latter be integrated with other information to define shelf lithofacies and active transport pathways.

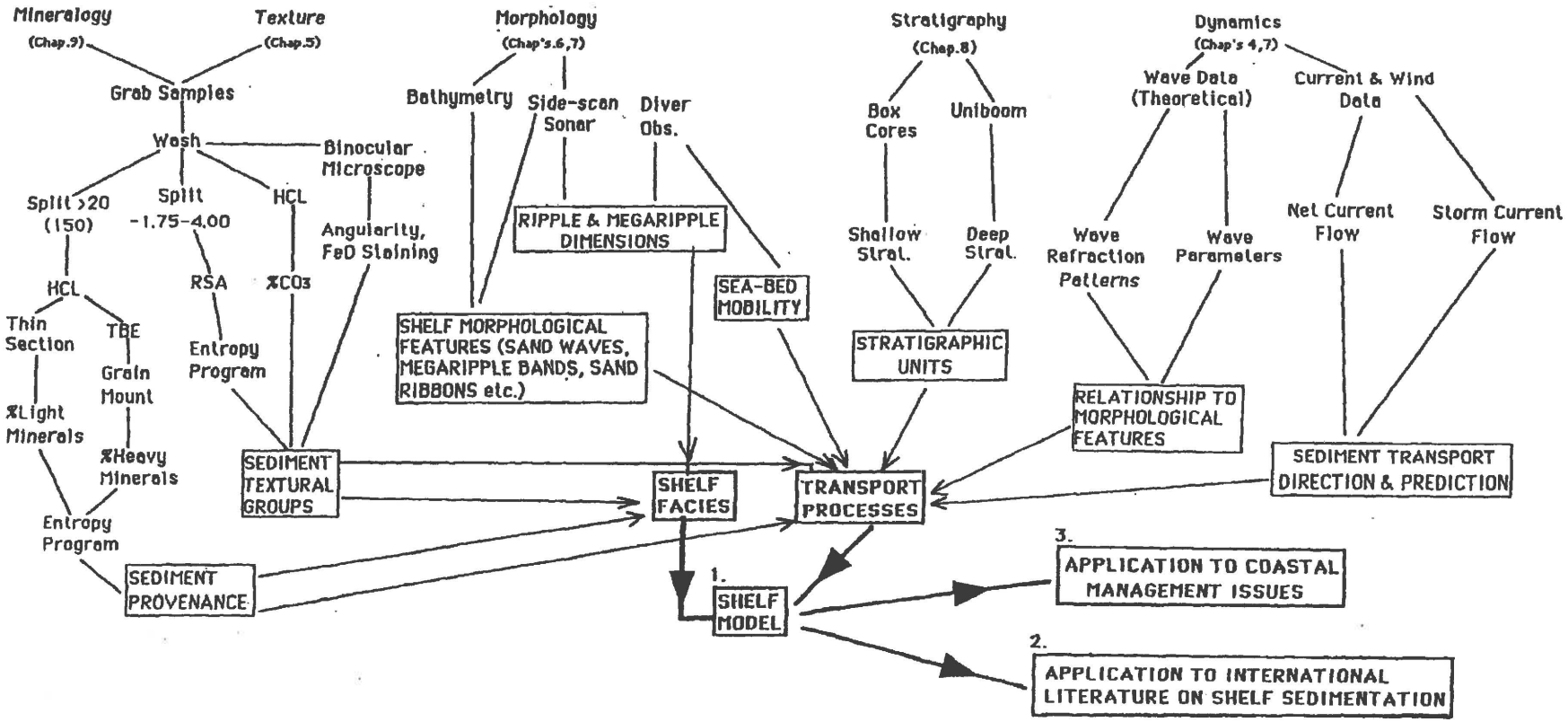

Figure 1.3. Organisational structure of the E.C.S.S., showing the data presented and the anticipated results from each chapter, thus enabling the major objectives of this investigation (1, 2, and 3) to be achieved.

Chapter 6 investigates the shelf morphology with a series of detailed side-scan sonar and scuba surveys. This information is used to infer areas of shelf erosion and deposition, the response of shelf sediments to different oceanographic conditions, and to define shelf morphological provinces .

In Chapter 7, the interaction between morphological features and shelf hydrodynamics is investigated to determine the mobility of different shelf deposits, and the various hydrodynamic processes responsible for present nearshore and inner shelf sedimentation patterns.

Chapter 8 makes a preliminary assessment of the shelf stratigraphic patterns through combining the results of both shallow box core and deeper continuous sub-bottom seismic profile data.

Chapter 9 presents the mineralogical composition of selected shelf, beach, barrier and river samples, to determine the degree of interaction between these different sedimentary environments and the provenance of coastal sediments.

In Chapter 10 data presented in previous chapters on shelf lithofacies, sediment transport pathways, and hydrodynamic processes occurring along the coast, is integrated to present a series of conceptual models which account for the present nearshore and inner shelf sedimentation patterns, and diabathic links between the shelf and local beach systems.

Chapter 11 concludes the study by applying the results to local management issues regarding coastal erosion and use of the shelf as either a commercial source or repository for sediments.

A problem encountered during the investigation, is that both the length of coastline covered (100 km) and the large number of embayments (10 major ones) has made presentation of data difficult. The approach adopted has been to divide the study area up into two separate physiographic sections (see Figure 1.1): a southern exposed coastline extending from Waihi-Tairua which is open to the regional oceanographic climate; and a northern embayed coastline between Hotwater Beach and Kennedy Bay, which is generally sheltered from open ocean conditions. The data are then presented on fold-out maps for each section of coast, and more detailed descriptions of individual embayments are provided in the text only where absolutely necessary.

Some preliminary results of the E.C.S.S. have been published in the course on the investigation, with information on the general background of the study found in DELL *et al.* (1985), results from the regional current pattern analysis (Chapter 4) published in BRADSHAW *et al.* (1991), and applications to shelf resource management found in BRADSHAW *et al.* (in press).

1.3. TERMINOLOGY

Before presenting results of this investigation, it is considered pertinent to briefly clarify a few terms which are frequently used in subsequent chapters. The following terms are used as defined in GARY *et al.* (1972):

Nearshore - 'extending seawards or lakewards an indefinite but generally short distance from the shoreline, specifically said of the indefinite zone extending from the low-water shoreline well beyond the breaker zone, and defining the area of nearshore circulation, and including the inshore zone and part of the offshore zone.' (GARY *et al.*, 1972, p. 475).

Shoreface - 'the narrow, rather steeply sloping zone seaward or lakeward from the low-water shoreline permanently covered by water and over which beach sands and gravels actively oscillate with changing water conditions. The zone lies between the seaward limit of the shore, and the more nearly horizontal surface of the offshore zone.' (GARY *et al.*, 1972, p. 654-655).

As both of these terms appear to be analogous in definition, the term 'nearshore zone' is used throughout subsequent chapters in the same sense that the term 'the shoreface zone' has been applied by other researchers (e.g. SWIFT, 1976; NIEDORODA *et al.*, 1985; WRIGHT *et al.*, 1991).

Also, the term 'lithofacies' is frequently used, and defined as:

Lithofacies - 'a lateral mappable subdivision of a designated stratigraphic unit of any kind (or an arbitrarily limited body of sedimentary deposits) distinguished from other adjacent subdivisions on the basis of noteworthy lithological characteristics, including all physical and chemical (mineralogical and petrographical) characteristics, and those biological (paleontologic) characteristics that influence the appearance, composition, or texture of the rock (or sediments).' (GARY *et al.*, 1972, p. 412).

CHAPTER TWO

REGIONAL SETTING

2.0. INTRODUCTION

The Coromandel Peninsula occurs on the northeast coast of the North Island of New Zealand. It is located about 100 km from Auckland and Hamilton cities, and extends for approximately 80 km from the township of Thames on the west coast to Cape Colville at the northern tip of the peninsula. The present study area is located on the eastern coast and shelf of the Coromandel Peninsula, and is part of a tectonically active plate margin found on the boundary between the Australian and Pacific Plates, with physical aspects typical of a collision coast in the classification scheme of INMAN and NORDSTROM (1971).

Physiographically, the Coromandel Peninsula is an uplifted horst block that is tilted to the east. The Coromandel and Moehau Ranges run the length of the peninsula making much of the interior steep and inaccessible (EASDALE and JACOMB, 1982). The steep and rugged topography reaches altitudes of 600 to 800 m along the main axis (HUME and DAHM, 1991), and has been incised by deep river valleys during lower sea level events in Late Cenozoic times to produce embayments of variable sizes and orientation, characterised by irregular dendritic outlines (ABRAHAMSON, 1987). Catchment areas are highly variable along the coast, some of the largest being 280 km^2 at Tairua (GIBB and ABURN, 1986) and 441 km^2 at Whitianga (SMITH, 1980).

The east Coromandel coastline has been described by McLEAN (1979) as a headland-bay coast, comprised of a succession of steep rocky headlands separated by narrow shallow bays. Further south, wide sandy plains characterise the Bay of Plenty coastline, while north of the study area the coastline becomes increasingly rocky and is mainly without sandy beaches (HARRIS, 1985). Most east Coromandel beaches are sheltered from prevailing mid-latitude westerly winds and thus the high energy wave climate of the Tasman Sea. However, they are exposed to episodic storms from the north and east, which are primarily responsible for local beach erosion (HEALY and DELL, 1987).

High, episodic, orographically-induced rainfall characterises the eastern Coromandel Peninsula, which results in significant runoffs within local catchments (HEALY *et al.*, 1981; HUME and DAHM, 1991). The peninsula has a deeply weathered regolith, which has been destabilised since European settlement by mining and forestry activities, and thus such extreme rainfall events often lead to widespread erosion in the form debris avalanches and deep earth slips (VINE, 1981), and high quantities of sediment runoff into coastal embayments.

The forementioned physical characteristics of the study area project the essential elements for coastal instability, viz. a variable sediment supply, and variable and sometimes extreme wave, wind and tidal patterns, these latter possibly being influenced by offshore islands (HEALY *et al.*, 1981).

2.1. REGIONAL GEOLOGY

The Coromandel Peninsula forms the eastern-most part of the Hauraki Volcanic centre, the largest and longest active area of andesite-dacite volcanism in New Zealand (SKINNER, 1986). Rocks within the Coromandel Volcanic Zone consist of a series of Tertiary volcanics overlying an indurated Jurassic sedimentary basement (SKINNER, 1976; Figure 2.1; Table 2.1). Upper Jurassic sedimentary rock outcrops are found mainly on the northern Coromandel Peninsula, and are divided into two conformable formations (Moehau and Takatea Hill) within the Manaia Hill Group. The older Moehau Formation is characterised by a lithic greywacke and sub-greywacke suite, whereas the younger Takatea Hill Formation is a feldspathic greywacke suite (SKINNER, 1976). Isolated occurrences of younger sedimentary rocks are also found, with Te Kuiti Group siltstones and limestones on the western side of the peninsula, and fluviatile and lacustrine carbonaceous sediments of the Waitemata Group resting unconformably upon Moehau Formation near Otama (SKINNER, 1976).

Tertiary volcanic rocks unconformably overlie the sedimentary basement and dominate the present Coromandel Peninsula topography. They include a wide range of igneous rock compositions from basalt to rhyolite, as well as sub-volcanic hypabyssal and plutonic rock complexes. The oldest Coromandel Group volcanics (including Beesons Island Volcanics) range in composition from basic andesite to rhyodacites, and were erupted in late Miocene times, younging in a southwards direction (SKINNER, 1986). The overlying Whitianga Group rhyolites have a wide range of compositions, and are subdivided into Minden Rhyolite and Coroglen Ignimbrite; these were erupted from the late Miocene to early Pleistocene. Accompanying the Whitianga Group volcanism were significant areas of hydrothermal alteration and base metal mineralisation, resulting in some of the largest underground goldmines and fossil geothermal fields in New Zealand (SKINNER, 1986). Mercury Basalts consist of basalts and basaltic andesite, and lie on a 15 km long submarine plateau around and including the Mercury Islands group, with small areas also found on the adjacent mainland (SKINNER, 1986).

Pleistocene and late Quaternary tephra deposits thinly mantle extensive areas of the Coromandel Peninsula. Major constituents of the ash sequence include the Hamilton Ash beds, Rotoehu Ash, Tuhua Tephra Formation,Taupo Ash, and Kaharoa Ash (HOGG and McCRAW, 1983). Most of these are calcalkaline deposits which originated from Central North Island eruptions, and have thus formed a northward thinning sequence over the peninsula. However, the Tuhua Tephra was erupted from Mayor Island and is a peralkaline deposit with thickest occurrence at Whangamata (HOGG an McCRAW, 1983).

The regional fault pattern is consistently one of north-northwest and northeasterly trends (Figure 2.2). These are inherited from, and controlled by, pre-existing faults formed in the Jurassic basement rocks during the early Cretaceous Rangitata Orogeny (SKINNER, 1967, 1976).

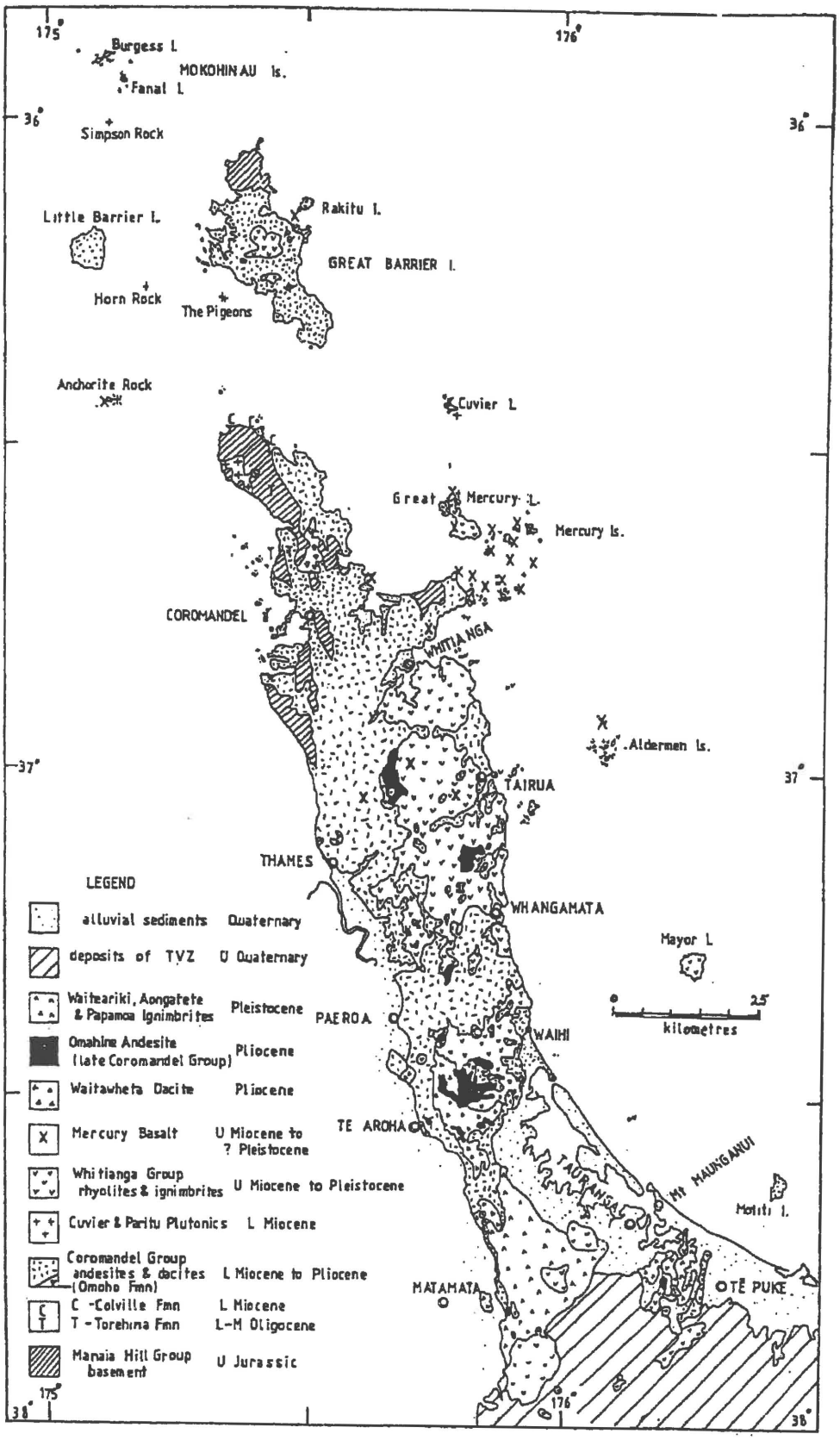

Figure 2.1. Generalised geology of the Coromandel Volcanic Zone (from SKINNER, 1986).

Group	Sub Group	Formations	Age	Comments
Whakamarama		Waitewhariki Ignimbrite Aongatete Ignimbrite	mid Pleistocene	Houghton (in prep): dacitic; only in Kaimai Range; young Papamoa Ignimbrite near Te Puke is also dacitic.
	"Waitawheta Dacite"	informal	Plio-Pleistocene	Informal 'bag' unit south of Waihi; includes andesite and ignimbrite.
Kerikeri Volcanic	Mercury Basalts	several centres	late Upper Miocene and/or younger	Known only in north Coromandel particularly in Mercury Islands; bimodal association with Whitianga Group; basalt and basaltic andesite.
Whitianga	Minden Rhyolite Coroglen (ignimbrite)	5 formal units + many informal centres Several flow sheets + 7 formal units	Late Miocene to Pliocene Late Miocene to Early Pleistocene	Group includes all pre TVZ rhyolitic rocks; Minden are rhyolite dome complexes and flows; Coroglen are ignimbrites, pumice breccias, airfall tuffs and breccias, and epiclastic sediments; associated in the north with caldera formation and collapse;
Coromandel	Omahine Kaimai Kiwitahi Waiwawa Kuaotunu	1 formal + few informal units 3 formal units several centres 3 formal units 16 formal units Paritu and Cuvier Plutonics	Late Miocene-Pliocene Late Miocene-Pliocene Mid to Late Miocene Early late Miocene Early to mid Miocene Late early Miocene	Group includes all predominantly 'andesitic' rocks of HVR; compositions range up to dacite and even rhyodacite; Omahine (ex Omahia) includes all post Whitianga Group andesites but in Kaimai. Range may be indistinguishable from Kaimai Subgroup; Kaimai Subgroup (Houghton in press) in south only; Waiwawa and Kuaotunu are central to north only, separated by regional erosional unconformity; plutonics are sub volcanic intrusive complexes in north only; Kiwitahi applies only to west of Hauraki Graben.
Waitemata	Kawau and Warkworth	Colville	Early lower Miocene	Conformable below earliest exposed andesite.
Te Kuiti		Torchina	Mid to upper Oligocene	Predates all volcanic activity.
Manaia Hill		Several formal units	Late Jurassic	Basement to region

Table 2.1. Summary of Coromandel Peninsula regional geology (from SKINNER, 1986).

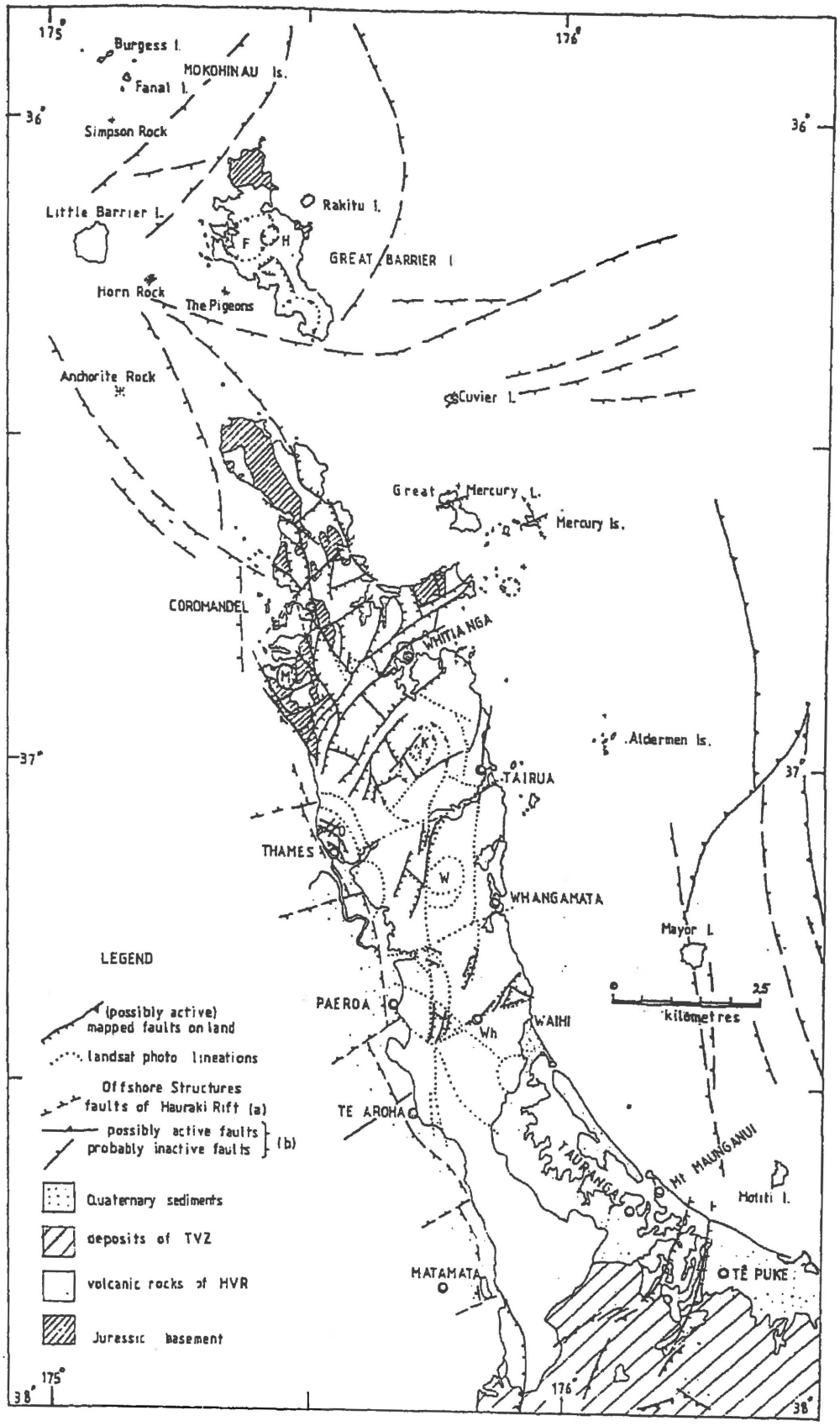

Figure 2.2. Structural and tectonic map of the Coromandel Volcanic Zone (from SKINNER, 1986).

SKINNER (1986) concluded that the elongate Great Barrier Island-Coromandel Peninsula high is not in itself a north-northeast trending volcanic arc, but a product of Neogene volcanism over a basement horst structure on which both the volcanism and Neogene tectonics have been superimposed. Almost all of the northeasterly trending faults have been downthrown to the south, progressively lowering the Jurassic basement in that direction and preserving a thickening sequence of Neogene volcanics towards the Taupo Volcanic Zone (SKINNER, 1986). Three physiographic sub-regions exist; the Moehau Ranges, Coromandel Ranges, and Kuaotunu Peninsula. The latter is predominantly controlled by northeast and north-northwest trending faults, and by the greywacke 'inlier' of Waitaia Ridge (SKINNER, 1967). Offshore faults are possibly active near the erupted active Quaternary volcano of Mayor Island, and link onland with faults mapped between Tauranga and Te Puke (SKINNER, 1986).

Faulting has been suggested by SKINNER (1986) as having continued through Pliocene and Quaternary times along previous east-northeast and northwest trends. Recent faulting has had an important impact on Quaternary sedimentation within the Tauranga Basin, which has formed by the northeast tilting of a large fault block and subsequent infilling by volcanic air fall deposits, as well as terrestrial and marine sediments (HARMSWORTH, 1983). Faulting has also had an important impact on offshore sedimentation within tectonically formed basins on the continental shelf (see later section on continental shelf sedimentation). A late Quaternary downstepping of the peninsula to the south along northeast trending faults is supported by results of ABRAHAMSON (1987), based on the boundaries of Pleistocene coastal sediments and presence of Rotoehu Ash along the east coast, at a calculated average rate of 0.04 $mm.y^{-1}$ for the last 125 000 years.

Since the cessation of volcanism, extensive erosion has modified the topography of the Coromandel Peninsula, with deep valleys eroded by eastward flowing streams during periods of lower sea level. In Quaternary times, eroded volcanic debris has infilled these valleys and low-lying areas with alluvium and provided a source of sediment, in addition to erosion of basement rocks, for coastal sedimentation (ABRAHAMSON, 1987).

ABRAHAMSON (1987) identified two main sediment compositions along the east Coromandel coast; a 'marine' and 'fluvial' sand suite. 'Marine' sands occupy the beach-dune coastal zone, and are dominated by quartz (25 to 45%), feldspar (30 to 45%), and significant proportions of volcanic glass (10%), rocks and shell fragments, and minor heavy minerals (<10%, mainly hypersthene, hornblende and opaques). 'Fluvial' sediments are composed primarily of feldspar (>40%), and significant proportions of volcanic glass (10%), heavy minerals (~ 10%), eroded rock fragments and minor quartz (<15%). The 'marine' sands are generally texturally mature, and occur as the result of marine and aeolian reworking in the coastal zone. 'Fluvial' sediments include angular gravels, sands, and muds, which have been transported by rivers from the hinterland and trapped within estuarine sinks. A dominant feature of the mineralogy of east Coromandel coastal sands is a high feldspar content, usually >50% (SCHOFIELD, 1970). The mineralogy shows an affinity of quartz-rich beach sands associated with large catchment areas

of Minden rhyolite rocks, and feldspar-rich sands associated with hinterland catchments of Coromandel Volcanics, mainly andesitic rocks (HEALY and DELL, 1982, 1987).

Based on these broad mineralogical trends, ABRAHAMSON (1987) proposes that the Tertiary volcanics are probably the major source of east Coromandel coastal deposits, with secondary contributions also probably derived from deposits within the Central Volcanic Region, and a direct contribution from airfall tephras erupted mainly from the Central North Island. However, in only a few previous studies has it been possible to positively determine the transport pathways and provenance of coastal sands (e.g. HARRAY and HEALY, 1978; HEALY, 1981), due to the general absence of local tracer minerals.

2.2. CLIMATE

The east Coromandel coast is subject to a temperate climate, conditions being generally warm and humid, with an average rainfall of 1800 to 2000 $mm.y^{-1}$ (HUME and DAHM, 1991; Figure 2.3). Winds along the east coast are predominantly low speed west and southwesterlies associated with the passage of mid-latitude high pressure systems. High speed onshore-directed east and northeasterly winds occur during less frequent storm events, and cause torrential orographically-induced rainfall on the Coromandel Ranges, making many of the streams along the coast prone to flooding (DELL and HEALY, 1982).

The study area is a lee shelf setting in a mid-latitude zone of dominant westerly winds, and thus coastal sedimentation processes should be most significantly influenced by storm events producing winds with an onshore-directed component. Three main types of weather systems have been found to cause such storm conditions; occluded cyclones, Tasman Depressions, and tropical cyclones (HARRIS, 1985). Occluded cyclones develop from troughs between easterly migrating mid-latitude high pressure systems, whilst Tasman Depressions are episodically generated in the subtropics on the western side of the Tasman Sea. Tropical cyclones and hurricanes arise between latitudes of 5 to 20° S in the southwest Pacific, and follow trajectories of east to southeast, occasionally impinging on New Zealand waters (2 to 3 each year; HARRIS, 1985), usually between November and April (e.g. Cyclone Bola, March 1988).

The frequency of occurrence for different scale storm events has been extensively studied on the Bay of Plenty coastline just south of the study area by HAY (1991) for the period between 1873 and 1990. This has shown that most storm events occur from an easterly quadrant (74%), with moderate scale events of Force 7 Beaufort Scale winds (13.9 to 17.1 $m.s^{-1}$) occurring on average once every 0.71 years, and extreme winds of Force 8 and 9 Beaufort Scale (17.2 to 20.7 $m.s^{-1}$ and 20.8 to 24.4 $m.s^{-1}$) every 14 and 30 years respectively. These storm events are usually of limited duration, ranging from 6 to 39 hours, with an extreme value of 92 hours.

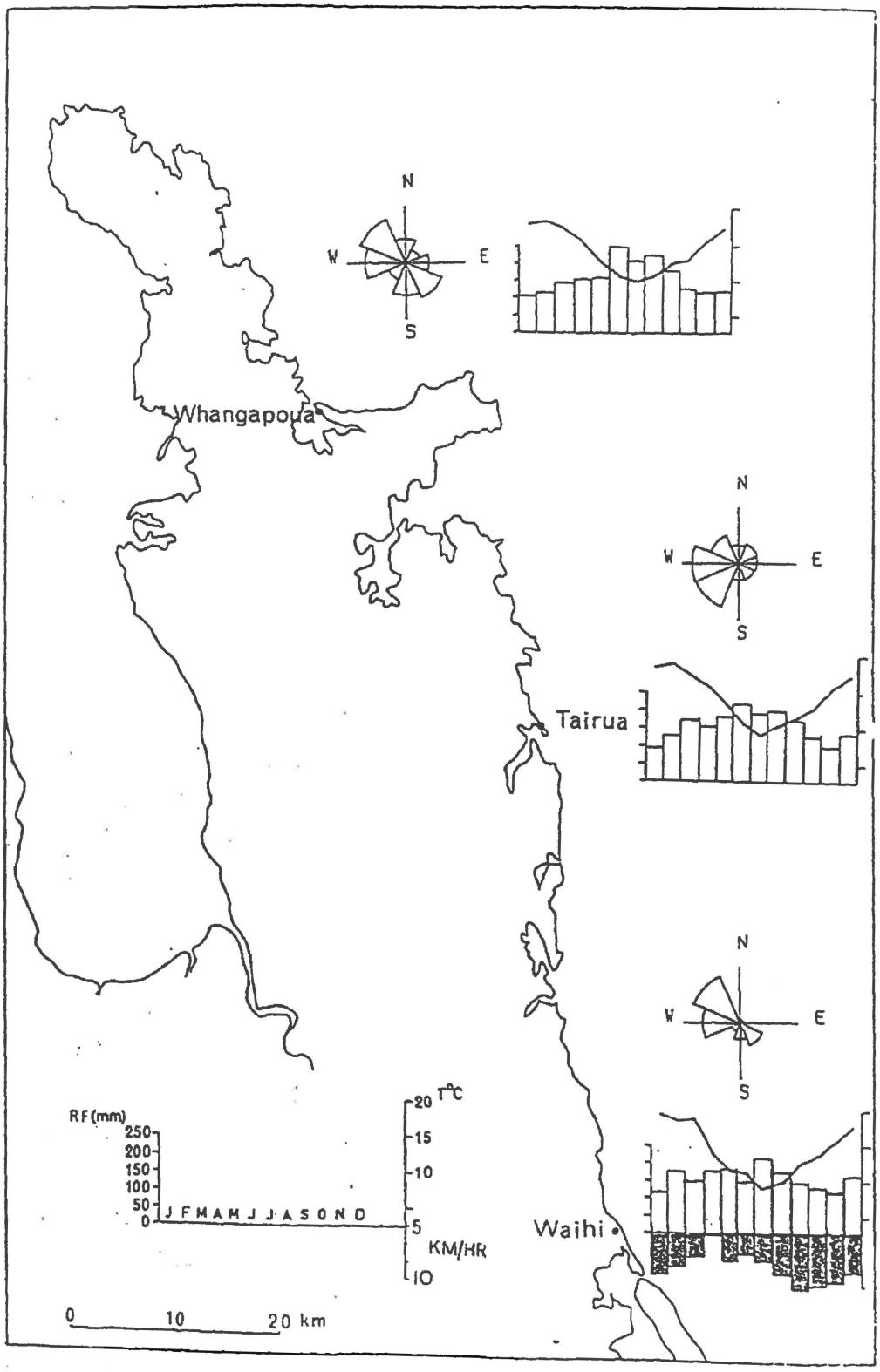

Figure 2.3. Local patterns in wind, rainfall and temperature along the east Coromandel coast (from ABRAHAMSON, 1987).

2.3. OCEANOGRAPHIC SETTING

2.3.1. Offshore Currents

Currents along the east Coromandel continental shelf capable of influencing sedimentation patterns include tidal flows associated with the semi-diurnal or diurnal tidal wave, regional oceanographic currents, and local wind-generated flows.

Tides along the east Coromandel Coast are essentially semi-diurnal, though small diurnal variations in height do occur (HARRIS, 1985). Spring tidal ranges vary from 1.5 m on the open coast (Slipper Island) to 1.62 m in Mercury Bay (SMITH, 1980), thus making this a microtidal coastline.

Along open shelf waters on the northeast coast of New Zealand, the tidal stream direction is northeast on the flood tide and southeast on the ebb tide, with tidal vectors directed into and out of the Hauraki Gulf from the tip of the Coromandel Peninsula to Cape Brett (Figure 2.4; HARRIS, 1985). Current velocities in the open ocean on the spring tides are in the order of a knot (0.5 $m.s^{-1}$) off East and North Cape, but along the east Coromandel coast are low (0.13 $m.s^{-1}$), thus making shelf sediment transport by tidal currents alone unlikely.

Tidal currents do however have an important impact on sediment transport at the entrance to some harbours and inlets, as shown by DELL (1983) at Tairua Harbour. Here, southerly directed ebb tide currents exiting from the inlet mouth are of sufficient speed (0.5 $m.s^{-1}$) to transport ebb tidal delta deposits for about 1600 m, where they are then deposited as speeds drop to < 0.1 $m.s^{-1}$. This has an important effect on erosion-accretion trends for the adjacent Pauanui Beach system, with the northern distal end slowly accreting but the southern basal end showing signs of episodic erosion (GIBB and ABURN, 1986).

Tidal current patterns are also significantly modified by the presence of deep indentations in the coastline, as shown at Mercury Bay by SMITH (1980). Here, near-surface currents during tidal flows form a clockwise circulation gyre, with oceanic waters entering the southern side of the bay then mixing with Whitianga Harbour waters before exiting along the northern headland. SMITH (1980) observed that this results in a significant increase in temperature and decrease in salinity of adjacent coastal waters. Tidal currents at the entrance to Whitianga Harbour are also strong enough to transport sediments, usually occurring at speeds of 1.0 $m.s^{-1}$, but observed at speeds of 3.8 $m.s^{-1}$ during catchment flooding on an ebbing storm surge.

Investigations of ocean waters on the northeast coast by BRODIE (1960) and BARKER and KIBBLEWHITE (1965) have shown the presence of a southward-directed geostrophic flow, the East Auckland Current (Figure 2.5). This current represents part of the easterly flow of the

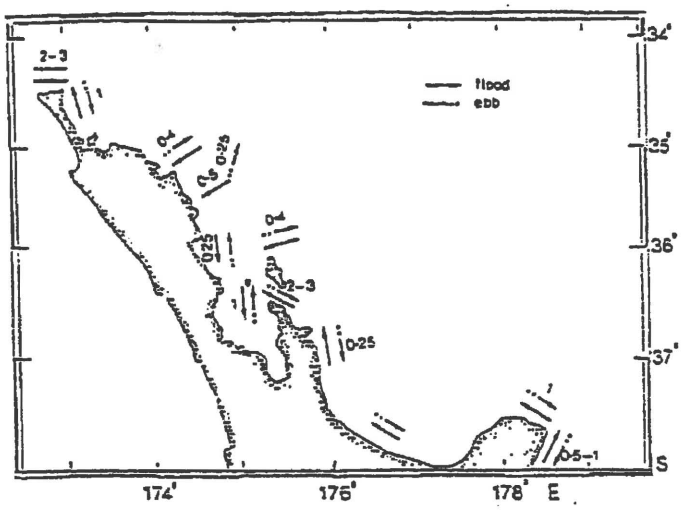

Figure 2.4. General directions and speed (knots) for flood (solid arrow) and ebb tidal currents (dashed arrow) in ocean waters. The chart is schematic with neither the length of arrows or their distance from the shore of any particular significance (from HARRIS, 1985).

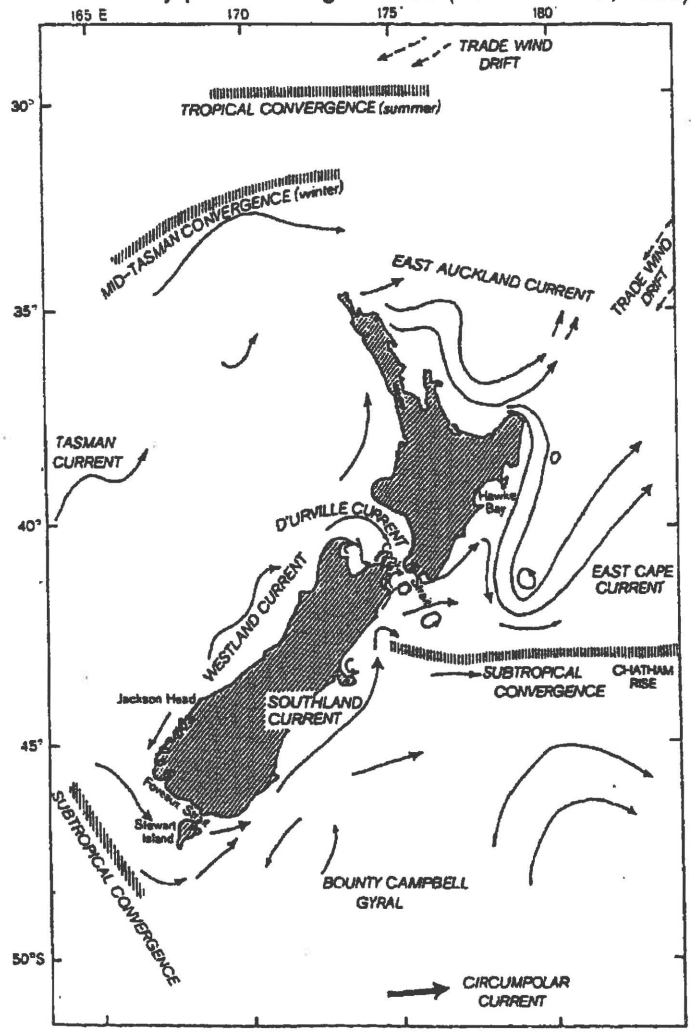

Figure 2.5. Oceanic current circulations found around the New Zealand land mass (from CARTER and HEATH, 1975). Of importance to this study is the East Auckland Current off the northeast coast of the North Island.

South Pacific Gyre, and is fed by the Tasman Front which is ultimately derived from the East Australian Current (STANTON, 1981; HEATH, 1985). After being deflected around the northern tip of New Zealand, the current flows southeast along the continental slope and around the Bay of Plenty. Surveys of the current by DENHAM *et al.* (1984) have shown it to be highly variable, both spatially and temporally. Evidence to date suggests that the East Auckland Current flows along the east Coromandel and Bay of Plenty shelf as a series of vorticies (HARRIS, 1985), which may be partly responsible for its variable nature. Along the continental shelf, the current has been reported at speeds of between 0.18 and 0.30 $m.s^{-1}$ by HEATH (1980), and 0.18 $m.s^{-1}$ and 0.25 $m.s^{-1}$ off East Cape and Great Barrier Island respectively by SANDERSON (1979). This current is responsible for the intrusion of relatively warm (15 to 16° C) and saline (35.7 °/oo) waters onto the east coast (HARRIS, 1985).

The East Auckland Current appears to have some influence on shallower coastal water circulations, as shown by regional studies of inner shelf current patterns. North of the Coromandel Peninsula at Pakiri, HILTON (1990) found a weak residual southeasterly flow (0.06 $m.s^{-1}$) during periods of dominant offshore westerly winds, that was superimposed over stronger bi-directional currents (< 0.16 $m.s^{-1}$) associated with the semi-diurnal tidal wave. Offshore from Tauranga Harbour, HARMS (1989) likewise found a weak southerly flow (< 0.10 $m.s^{-1}$) during periods of offshore westerly winds, which he inferred to be either associated with offshore flows of the East Auckland Current, or part of a local upwelling circulation pattern.

The role of currents associated with local wind stress has not been previously determined for the northeast coast. However, data from Tauranga by HARMS (1989) indicate that downwelling current patterns may play an important role in the transport of shelf sediments, as shown by the presence of a high speed northwesterly directed flow (up to 0.40 $m.s^{-1}$) during periods of strong onshore winds (15 $m.s^{-1}$). Upwelling current patterns may also occur in shallow water depths, as found by HARRIS (1985) on the east coast between 1982-83. Here, an unusual period of persistent offshore westerly winds caused an upwelling of cold nutrient-rich waters, and resulted in the blooming of a plankton species, which subsequently decayed and reduced oxygen levels near the sea bed, resulting in high fish mortalities. However, currents associated with such offshore wind patterns have not previously been measured at sufficient speeds to transport shelf sediments.

2.3.2. Surface Gravity Waves and Storm Surges

Wave energy on the northeast coast of New Zealand is lower and more variable than on other exposed coastlines around New Zealand, being sheltered from persistent waves and swells generated by winds from the west and southwest blowing across long fetches in the Tasman Sea (HARRIS, 1985; HILTON, 1990). Instead, local storm events are the dominant influence, with winds blowing from an easterly quadrant over only short distances resulting in fetch-limited conditions, and the mobile nature of these storms also causing duration-limited conditions

(HARRIS, 1985). PICKRILL and MITCHELL (1979) describe the northeast coast as a mixed storm and swell wave environment, swell conditions generated by subtropical disturbances north of New Zealand, and shorter period seas generated by local weather patterns.

Some concept of the northeast coast wave climate comes from various wave recording data between East Cape and North Cape (Figure 2.6 a). This includes waverider buoy data at Bream Bay (PEEK, 1979), Hobbs Bay (DELFT HYDRAULICS LABORATORY, 1976), Great Barrier Island (EWANS and COUP, 1982 a & b), and off Hicks Bay (PICKRILL and MITCHELL, 1979; HARRIS *et al.*, 1983). Shoaling and breaking wave observations have also been made at Tauranga by DAVIES-COLLEY and HEALY (1978). However, HARRIS (1985) notes that only the Hicks Bay and Great Barrier Island data are taken from quasi-deep water locations and can therefore be considered representative of regional conditions, with other shallower sites representing local specialised conditions.

The approach direction for waves ranges from north through east, with a dominant wave direction from the northeast (Figure 2.6 b; PICKRILL and MITCHELL, 1979). Average significant wave heights (H_s) have been reported in open waters to range from 1.0 m (HARRIS, 1985) to 1.44 m (PICKRILL and MITCHILL, 1979), with wave height at Hicks Bay only rarely falling below 0.5 m (< 2% of the time; Figure 2.6 c). A maximum H_s of 5.2 m was recorded by HARRIS *et al.* (1983) at Hicks Bay, resulting from the action of a merged Tasman Depression and weak tropical cyclone. More extreme storm wave conditions have been recorded at Bream Bay by PEEK (1979), where from 18 to 21 July 1978 a subtropical cyclone brought near hurricane force winds (30 $m.s^{-1}$) from the northeast to southwest, resulting in a maximum observed wave height of 9.0 m and period of 12 s. These exceptional wave conditions probably resulted from the combination of distant swell, locally generated seas, and waves generated at intermediate distances (HILTON, 1990). However, HARRIS *et al.* (1983) found that waves greater than 3 m in height never persisted longer than 36 hours, and above 4 m for no longer than 12 hours duration. In contrast, low wave heights less than 1.5 m could persist for as long as 300 hours. Wave periods (T) in open waters average about 6.5 s, and range from 4 to 9 s most of the time (Figure 2.6 d). Longer period swell waves of T= 8 to 12 s tend to arrive from the north, and most likely originate from major depressions north or northeast of New Zealand (PICKRILL and MITCHELL, 1979; HAY, 1991).

Local wave conditions may differ from those typically found on the northeast coast, as Harbour Pilot observations reported by DAVIES-COLLEY and HEALY (1978) at Tauranga Harbour record mean H_s= 1.5 m and T= 11 s, the latter ranging from 5 to 15 s. Also, recent waverider recordings at the same location (W. DeLANGE, pers.comm.) have found similar long period swell conditions prevailing, with H_s= 0.91 to 1.73 m and T= 8.3 to 13.0 s, these mainly arriving from the northeast (Figure 2.7). PICKRILL and MITCHELL (1979) noted that in shallower water locations such as the Bay of Plenty, wave period may lengthen due to shoaling wave transformations. However, they may also result from unusual weather patterns at the time of

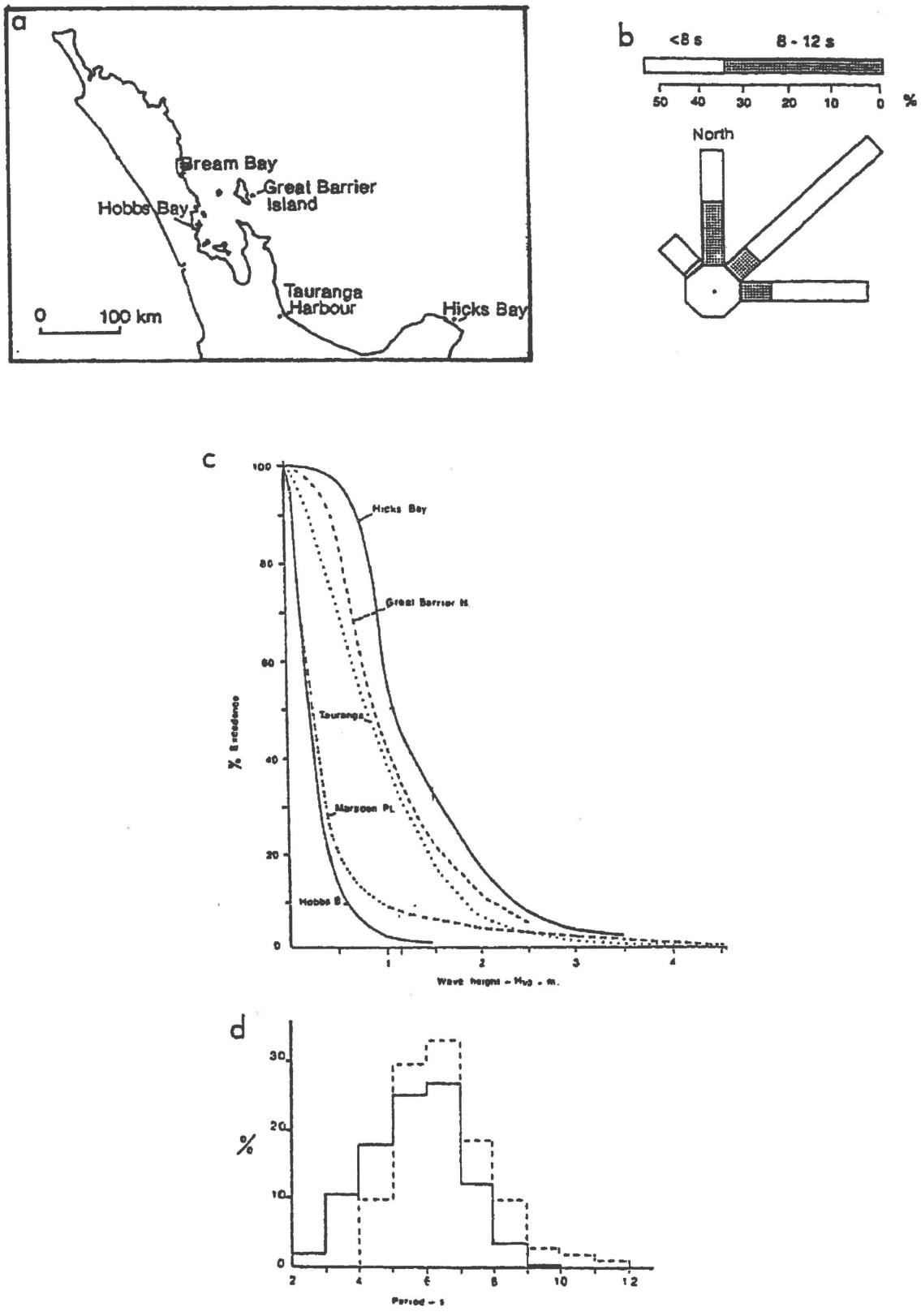

Figure 2.6. a) Location of wave observation stations on the northeast coast; b) frequency of wave directions (PICKRILL and MITCHELL, 1979); c) significant wave height exceedence curves (HARRIS, 1985); d) frequency of occurrence of zero crossing periods at Great Barrier Island for August to October 1980 (solid line) and Hicks Bay from March to November 1979 (dashed line; HARRIS, 1985).

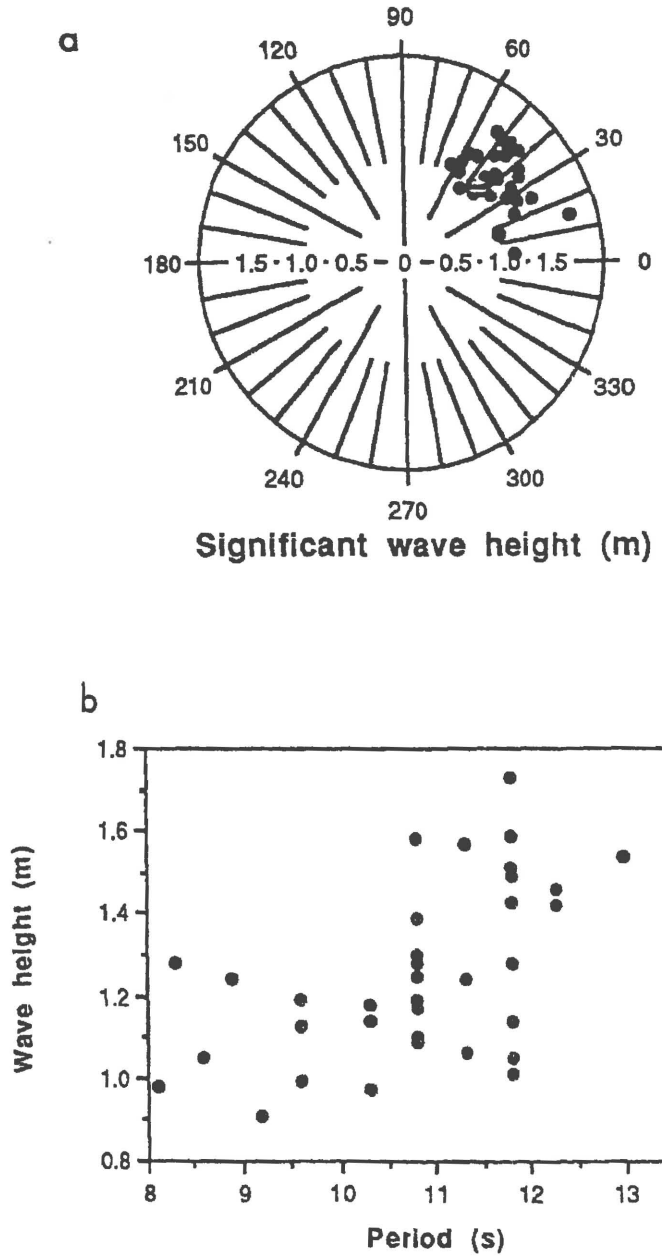

Figure 2.7. Waverider buoy data from off the ebb tidal delta of Tauranga Harbour between 2- and 7-May-91 showing; a) direction and height of waves b) wave height vs. period (data courtesy of Dr.W. De LANGE).

these wave observations, and require further investigation to determine how representative such conditions are of the east Coromandel coastline. Most periods of high wave energy on the east Coromandel coast will be generated by the various storm weather patterns outlined previously, i.e. occluded cyclones, Tasman Depressions, and tropical cyclones. Studies of local storm wave conditions on the Bay of Plenty coastline by HAY (1991) have shown that heights range from 1.01 m to 5.00 m, with a mean storm wave height of 2.97 m, and periods from 4.34 s to 10.42 s, with a mean of 7.65 s.

Associated with these cyclonic storm events are storm surges formed by the interaction of large reductions in atmospheric pressure with locally high wind stresses and waves. Such storm surges have caused extensive flooding and coastal erosion problems along the east Coromandel coast. For example, during the July 1978 storms described above, strong northeasterly winds combined with low barometric pressures (982 mb), a heavy northeasterly swell, spring tides, and very high catchment discharges to produce a 0.8 m high storm surge in Mercury Bay, which subsequently caused extensive coastal flooding, erosion, and property damage (SMITH, 1980).

2.4. COASTAL GEOMORPHOLOGY AND SEDIMENTATION

2.4.1. Estuaries

East Coromandel estuaries are generally relatively small features, ranging in area from 4 to 25 km^2, and are also very shallow (< 5 m) and characterised by narrow tidal inlets (average 250 m wide; ABRAHAMSON, 1987). Estuary systems along the east Coromandel coast initially formed in drowned river valleys behind marine sand bodies when sea level rose during the Holocene marine transgression (i.e. the period between oxygen isotope stages 1 to 2, BLACK *et al.*, 1988), and have been infilling with sediments over the past 6500 years. Infilling presently occurs near the estuary mouth with marine sands incorporated into small tidal deltas which prograde over sandy muds, and at river mouths with fluvial deltaic deposits over muddy estuary basins (ABRAHAMSON, 1987).

Investigations of estuary sedimentation (HUME and GIBB, 1987; HUME and DAHM, 1991; SHEFFIELD, 1991) have shown variable rates of deposition throughout the Holocene stillstand, with significant increases occurring following human settlement and subsequent disruption of the natural vegetation cover (Table 2.2). At Wangapoua, HUME and DAHM (1991) found a 25 to 45 x increase in background sedimentation rates following European settlement of the catchment area, as well as an increase in the sandiness of estuary deposits (originally 10 to 46% sand, now 59-66%). These changes are attributed to an increase in deep seated erosion of catchment deposits as a consequence of land use practises, particularly the establishment of exotic forests since 1950, although HUME and DAHM (1991) note that the evidence is generally inconclusive. Increased sedimentation rates appear to have caused a significant shallowing of estuary systems,

Table 2.2. Holocene sedimentation rates for east Coromandel estuaries.

Location	Time Interval	Sedimentation Rate	Reference
Whangamata			
causeway	1940-1990 AD	11.0 $mm.y^{-1}$	SHEFFIELD (1991)
	1140 BP-1940 AD	0.28 $mm.y^{-1}$	
	6710-1140 BP	0.06 $mm.y^{-1}$	
sand flats	1940-1990 AD	9.60 $mm.y^{-1}$	
	1300 BP-1940 AD	0.31 $mm.y^{-1}$	
	3000-1300 BP	0.35 $mm.y^{-1}$	
Tairua			
mid harbour	1933-1984 AD	6.0 $mm.y^{-1}$	HUME & GIBB (1987)
Whangapoua			
upper harbour	1960-1988 AD	0.89 $mm.y^{-1}$	HUME & DAHM (1991)
	1850-1960 AD	1.30 $mm.y^{-1}$	
	700 BP-1850 AD	0.13 $mm.y^{-1}$	
	5890-4000 BP	0.03 $mm.y^{-1}$	
	6500-5890 BP	0.50 $mm.y^{-1}$	
upper harbour	1950-1988 AD	1.33 $mm.y^{-1}$	
	1850-1950 AD	1.50 $mm.y^{-1}$	
	700 BP-1850 AD	0.12 $mm.y^{-1}$	
	1060-700 BP	0.08 $mm.y^{-1}$	
	4000-1060 BP	0.13 $mm.y^{-1}$	

as evidenced by the previous use of inlets as harbours for shipping prior to the 1930s (HEALY and DELL, 1987).

Continued infilling of estuaries causes channels to bifurcate around broad sandy bars and shoals, and fluvial silts and colonising vegetation to aggrade over estuarine basins (Figure 2.8). Estuaries which have been totally infilled (e.g. at Hotwater Beach) have their tidal prisms confined to river channels by flood plain deposits (ABRAHAMSON, 1987). Some infilled or partially infilled estuary systems appear to have been an important source for adjacent nearshore and barrier deposits, as shown by GIBB (1983) at Tairua Harbour, where during floods tidal reach sand banks migrate towards the harbour mouth, and most if not all of the ebb tidal delta is washed out to sea. However, tidal inlets also seem to infill with beach sediments during calm weather periods (SHEFFIELD, 1991). Estuarine sedimentation patterns therefore have the potential to influence offshore sedimentation trends, either by supplying fluvial sands to the beach and nearshore system during catchment flooding events, or drawing marine sands into their inlet mouths during calm weather periods.

2.4.2. Barrier Systems

Barrier deposits along the east Coromandel coast are generally composed of quartzo-feldspathic sands which are inferred to have been derived mainly from the continental shelf (HARRAY and HEALY, 1978; ABRAHAMSON, 1987). Deposits along the east Coromandel coast include 'inner barriers' formed during the Pleistocene Last Interglacial Period (i.e. corresponding to oxygen isotope stage 5 about 125 000 y. B.P., BLACK *et al.*, 1988), and Holocene sands (from oxygen isotope stage 1) formed under present sea level conditions (HEALY and KIRK, 1982). The Pleistocene 'inner barrier' deposits have been identified to varying degrees within most embayments (Figure 2.9), their absence in some areas probably being due to fluvial erosion during the Last Glacial Period 18 000 to 30 000 y. B.P. (oxygen isotope stages 2 and 3), and indicate that east Coromandel embayments have been an important sink for marine sands throughout late Quaternary times.

The morphology of Holocene barrier deposits can be generally divided into barrier spit systems which are attached to the mainland at their basal ends and enclose relatively large infilling estuary systems, and pocket barriers which occur in small embayments on steep rocky sections of coast (Figure 2.8). Holocene barriers have also been classified by ABRAHAMSON (1987) according to the scheme presented for eastern Australia by THOM (1984), and includes prograded, stationary, and receding barrier types (Figure 2.10). The main controlling factors of barrier morphology are suggested by ABRAHAMSON (1987) to be sediment supply, embayment and shelf geometry, and the local wind and wave regime.

Barrier spit systems are generally prograded barriers (except at Opoutere) which contain evidence of extensive progradation, suggesting a local abundant sediment supply. The morphology



Figure 2.8. The partially infilled Tairua Harbour system, characterised by the presence of numerous intertidal sand flats (1) and mid channel shoals (2). During catchment flooding, these deposits migrate towards the harbour mouth, and ebb tide delta sands (3) are washed out to sea (GIBB, 1983). The harbour is enclosed by the extensive prograded barrier spit system of Pauanui (4). Further north, the stationary pocket barrier system of Tairua (5) forms a Tombolo like feature, and is associated with extensive Pleistocene inner barrier deposits (6).



Figure 2.9. Pleistocene inner barrier deposits at Orokawa Bay, just north of Waihi Beach. These features typically consist of a veneer of Rotoehu Ash (age 50 000 y. B.P.) over older aeolian and marine sands (ABRHAMSON, 1987).

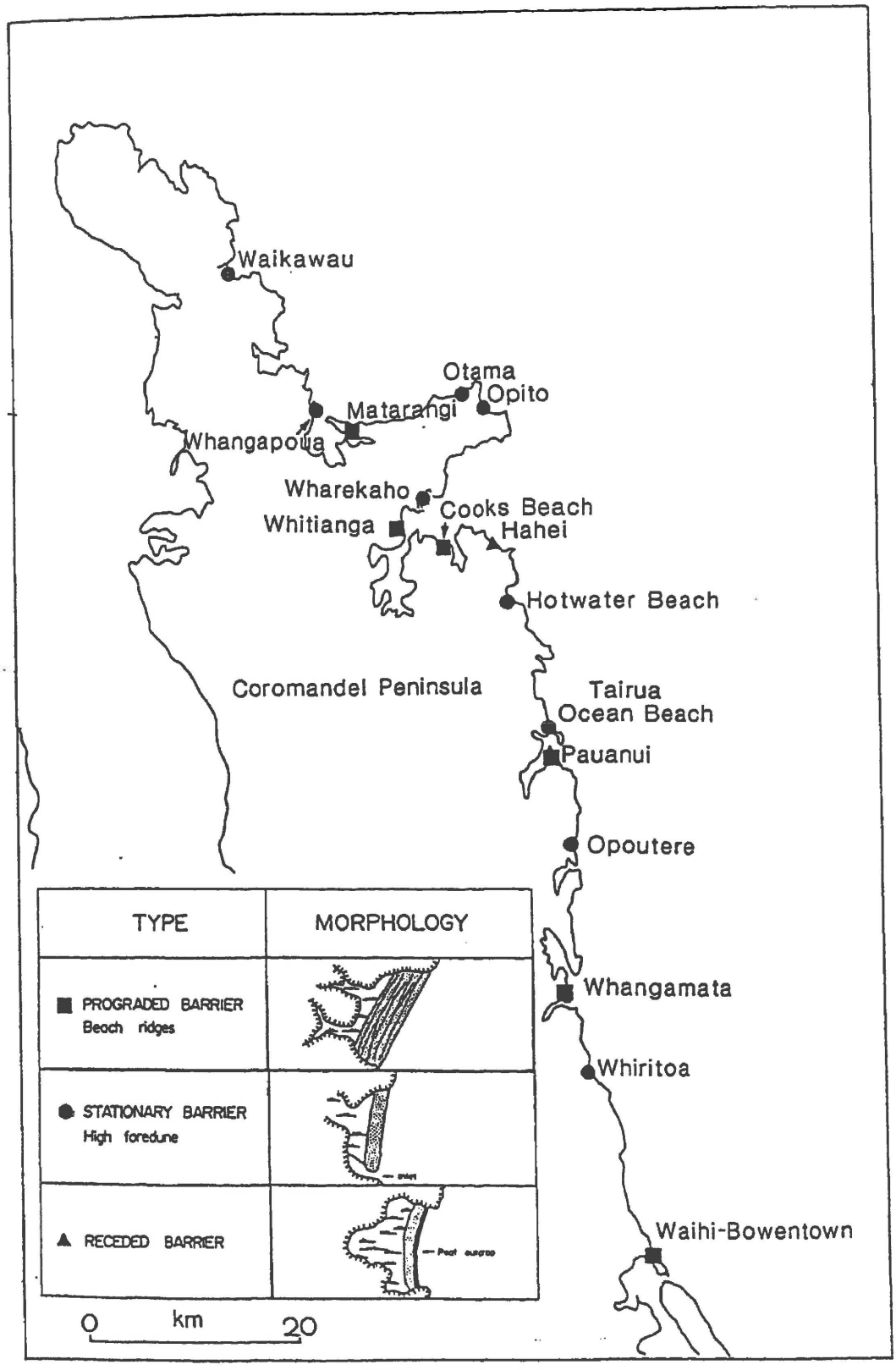

Figure 2.10. Holocene barrier types identified by ABRAHAMSON (1987) along the east Coromandel coast.

is characterised by a series of parallel dune ridges approximately 2 to 3 m high, separated by 10-20 m wide low-lying swales. The most extensive prograded barrier system occurs at Whitianga, where a series of over 30 dune ridges has formed. Other embayments in which prograded barrier systems occur include Cooks, Matarangi, Pauanui, Whangamata, and Bowentown Beaches (ABRAHAMSON, 1987). These locations are all found at the mouths of the major harbour systems along the coast, and are generally characterised by comparatively low shelf gradients. ABRAHAMSON (1987) therefore concluded that they form from an abundant sand supply originally derived from their local extensive hinterlands, and relatively low wave energy conditions.

Stationary morphologies generally characterise pocket barrier systems, and are characterised by limited dune ridge progradation, forming an often high relief vegetated sand body extending no more than 150 m inland. A striking feature of their morphology is the presence of only a few dune ridges attaining comparatively higher elevations than the prograded systems (average 10 m), these often characterised by a hummocky topography induced by sand blowouts and transgressive sand movement. Stationary barrier morphology has been further subdivided by ABRAHAMSON (1987) into high dune ridge systems (up to 30 m in elevation) at Waikawau, Otama, Opito, Hotwater and Opoutere Beaches, and less commonly occurring low foredune types at Whangapoua, Whiritoa, Onemana, and Wharekaho. Tairua Beach is seen as a Tombolo type stationary system formed by the interaction of offshore islands with Pacific swells and littoral drift (HEALY and DELL, 1987). Stationary barrier systems are attributed by ABRAHAMSON (1987) to have formed by comparatively higher wave conditions than prograded systems, due to steeper shelf gradients. They are not generally associated with large harbour systems, and so probably have a lower supply of sediments compared to the prograded systems. One exception occurs at Opoutere, which ABRAHAMSON (1987) attributes to the locally very steep offshore gradients found here (1:80).

Receded barrier systems are rare along the east Coromandel coast, with only the one example found at Hahei Beach, due to very limited volumes of sand within the local beach system (HEALY *et al.*, 1981; ABRAHAMSON, 1987).

The late Quaternary evolution of barrier deposits has been conceptually modelled by ABRAHAMSON (1987), based on stratigraphy and data from tephra chronology and radio carbon dates. The main controlling factor for barrier formation was envisaged to be late Quaternary variations in sea level. The source of most sediments along the coast was attributed by ABRAHAMSON (1987) to be primarily from shelf deposits ultimately derived from weathered Coromandel volcanic lithologies. However, at Waihi Beach HARRAY and HEALY (1978) have shown that the magnetic mineral assemblages of barrier deposits indicates these were ultimately derived from rivers draining the extensive Taupo Volcanic Zone.

In ABRAHAMSON's (1987) model, barriers formed similar morphological features during the Last Interglacial Period to those presently found, and also impounded infilling embayments as shown by

the presence of Pleistocene estuarine deposits beneath palaeo-beach and -dune features at Otama. In the Last Glacial Period, rivers eroded and cut down into the Coromandel Peninsula volcanic terrain, thus supplying greater volumes of fluviatile sand to the coast, and also eroded into the Pleistocene barrier (and offshore) deposits, in some cases almost completely removing these from embayments (e.g. Whangamata; SHEFFIELD, 1991). During the Holocene marine transgression, inner shelf sands were mobilised and flooded into coastal embayments, where they were then available for coastal progradation. Barrier systems formed as nearshore deposits adjusted to equilibrium with stable sea level conditions about 6500 y. B.P. Equilibrium was established at different times within each embayment. For example, at Opoutere the presence of Tuhua Tephra deposits (6200 y. B.P.) shows that landward migrating dune systems formed at the head of transgressive marine deposits, thus initiating stationary barrier formation. At Pauanui, barrier progradation appears to have occurred rapidly within the first 4000 years (0.4 $m.y^{-1}$), after which rates significantly declined as the barrier approached a condition of dynamic equilibrium (GIBB and ABURN, 1986). However, at Whitianga over half of the barrier system has prograded in the past 2000 years (ABRAHAMSON, 1987), indicating locally abundant fluvial inputs into the barrier system. Stationary barrier deposits show evidence of several dune phases in later Holocene times from the presence of Taupo Pumice layers, with emplacement occurring at 2000 to 1500 y. B.P., 900 to 600 y. B.P., and 500 y. B.P. However, ABRAHAMSON (1987) believes older barrier sequences are probably buried beneath these younger onlapping deposits. In most open ocean embayments, a set of high frontal dune ridges is presently found, which represent a recent phase of dune instability (ABRAHAMSON, 1987), as exemplified at Bowentown where transgressive dune deposits lie seawards of older Holocene palaeo-dune ridges (HARRAY and HEALY, 1978).

Barrier deposits along the east Coromandel coast therefore show a range of variable morphologies, reflecting the influences of local sediment supplies and wave conditions. Previous studies of these deposits, particularly by ABRAHAMSON (1987), suggest that diabathic coupling between the shelf and local embayments has been an important factor in barrier formation during late Quaternary times, and may thus still be responsible for local phases of barrier erosion and accretion.

2.4.3. Beaches

The morphodynamic behaviour of beach systems along the east Coromandel has until recently been poorly understood. However, this is now being studied in some detail by FULTON (in prep) at the University of Waikato, and some initial results are presented here and later integrated with diabathic coupling processes to the continental shelf in Chapter 10.3.

For the steep-faced medium to coarse grained pocket beach systems described by HEALY and DELL (1987; e.g. Whiritoa, Tairua, Hotwater and Rings), the beach morphology is characteristic of intermediate beach types in the east Australian WRIGHT and SHORT (1984) beach model (Figure 2.11). At Whiritoa, these range from a low tide terrace-ridge runnel system after prolonged low wave conditions (Figure 2.12), to transverse bar and rip under more moderate to high wave energy conditions (Figure 2.13). At Tairua and Hotwater Beach, the morphology shows higher energy transverse bar and rip to rhythmic bar and beach morphologies.

It is interesting that such relatively moderate-high energy beach types from eastern Australia exist on the east Coromandel, despite the coarse nature of their beach sediments and comparatively lower wave energy conditions. However, SHORT and WRIGHT (1984) have related the different beach morphologies formed to DEAN's (1973) parameter :

$$W = H_b/W_sT$$

where H_b = breaking wave height and W_s is the sediment fall velocity. For eastern Australian beaches, larger W values result in higher energy beach systems. Thus, the presence of relatively high energy pocket beach systems on the east Coromandel coast for the given low wave heights and coarse sands could be a result of the lower period modal wave conditions which appear to occur here.

The longer fine to medium grained barrier spit beaches tend to have a far greater complexity to their morphology, presumably a result of their finer and thus more dynamic beach sands, showing aspects similar to the recent central Netherlands beach model of SHORT (in press; Figure 2.14). These are usually characterised by the presence of at least 2 to 3 offshore bars, the morphology of these ranging from ridge-runnels, to transverse bar and rips, and longshore bars and troughs. However, during calm conditions only the inner bar was observed to be actively interacting with incident waves, with the outer bars essentially antecedent features. On the open ocean barrier spit beaches (e.g. Waihi, Opoutere and Pauanui), the inner bar is characterised by small rip channels during calm weather conditions at high tide, which then become exposed as ridge-runnel systems as the tide falls (Figure 2.15). On more embayed barrier spit beaches (Buffalo and Matarangi), calm conditions are characterised by a low tide terrace feature across the length of the beach. During storm conditions, the offshore bars become active causing these beach systems to adopt a more dissipative character (see Chapter 10 for more details).

The morphodynamics of east Coromandel beaches is thus very complex, which should result in variable processes of diabathic exchange between these and the continental shelf along the coast.

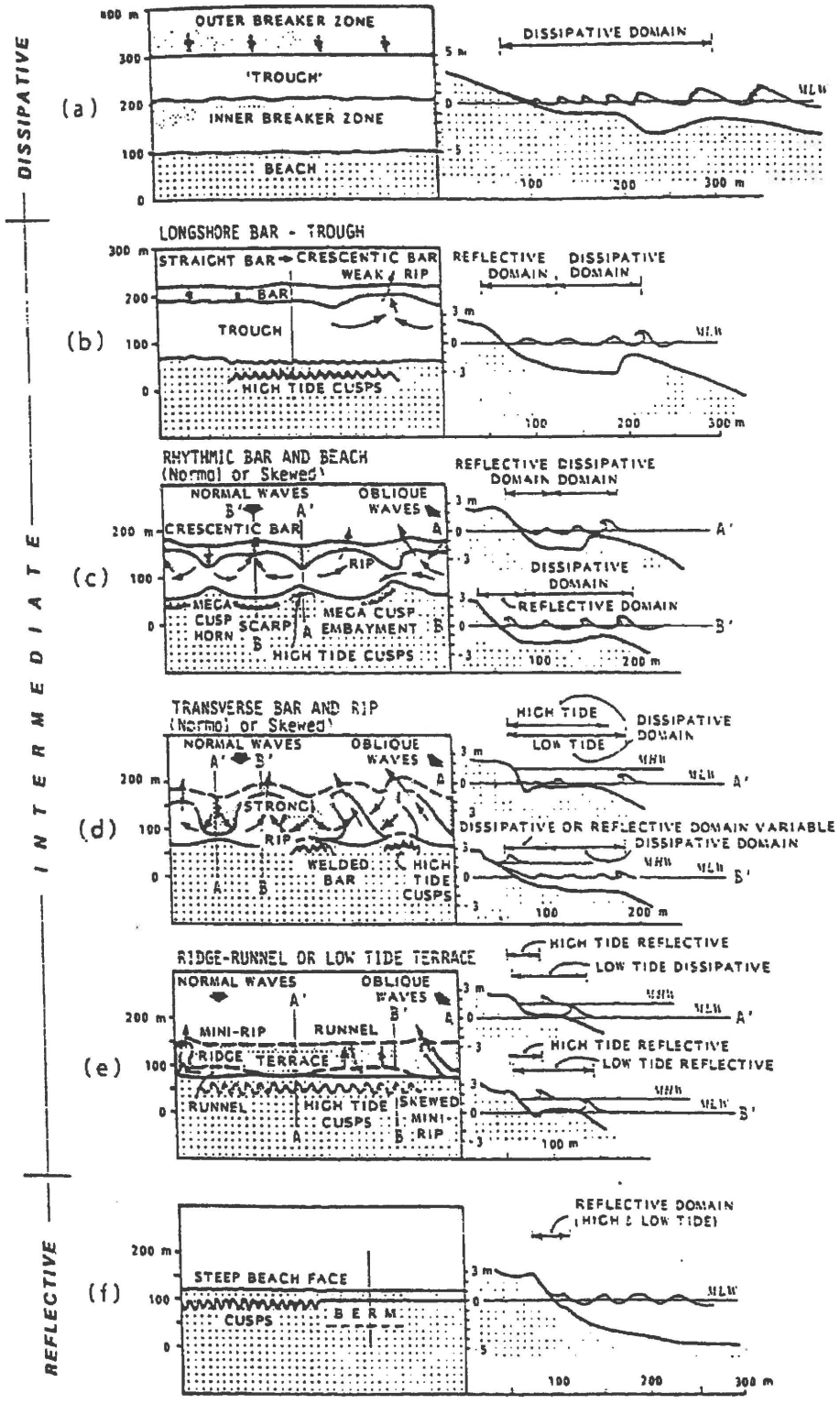

Figure 2.11. The WRIGHT and SHORT (1984) model for classification of Australian microtidal beach systems.



Figure 2.12. Ridge and runnel beach morphology observed during low tide at Whiritoa Beach following a period of prolonged calm weather conditions along the coast (10-May-89). Note the exposed small rip channel near the boat and associated runnel along beach face.



Figure 2.13. Transverse bar and rip beach morphology observed at Whiritoa Beach under moderate wave conditions (4-Sep-89). Photo taken at low tide as transverse bars become exposed.

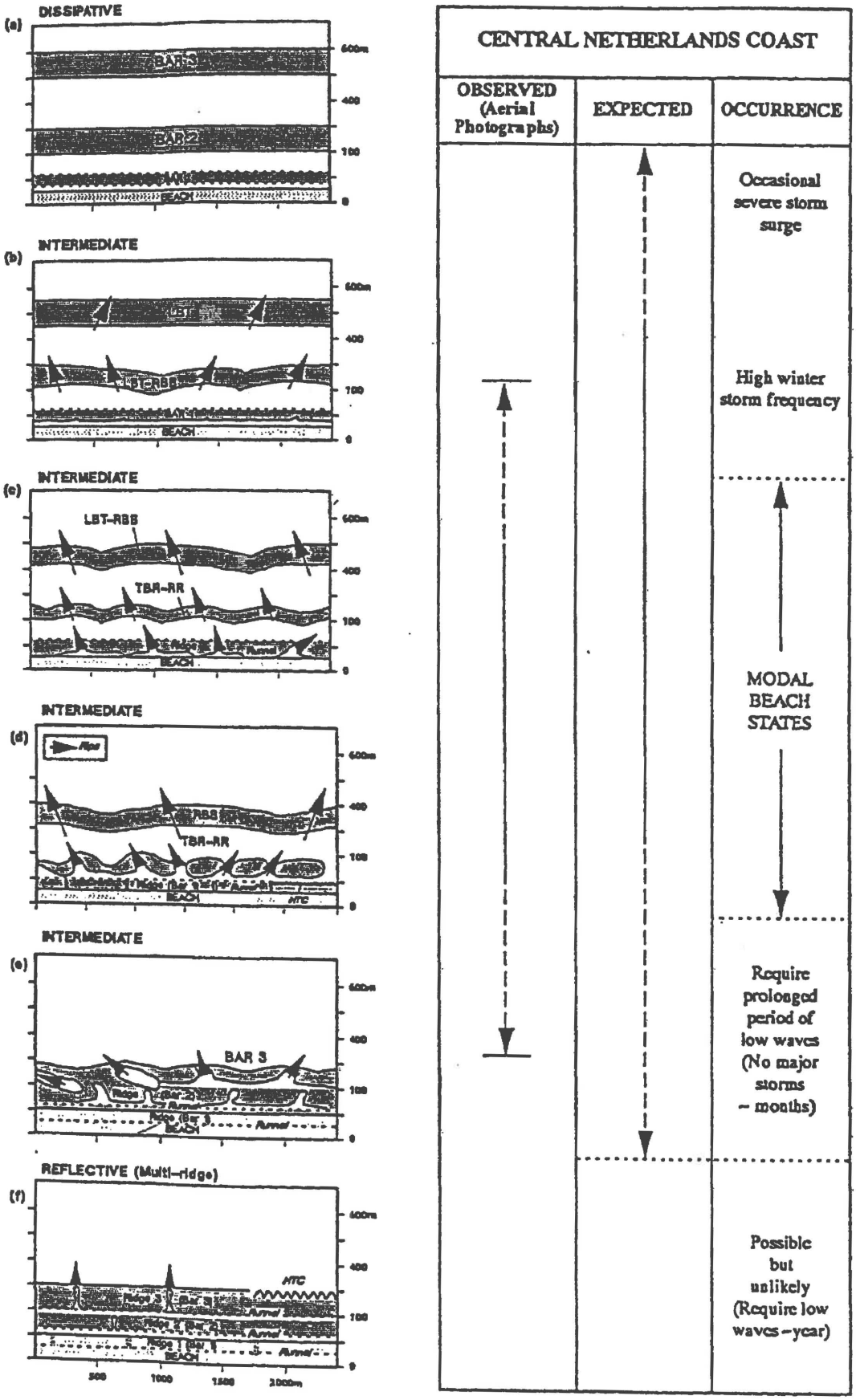

Figure 2.14. Possible range of beach types on the central Netherlands coast (from SHORT in press), which also appear to characterise the morphology of fine to medium grained barrier spit beaches on the east Coromandel coast.



Figure 2.15. Waihi Beach under moderate wave conditions at high tide (5-Nov-89). Note the rip currents with offshore bars occurring in their channels, similar to the central Netherlands 'type E' morphology in Figure 2.14.

2.4.4. Continental Shelf

Some broad-scale data have previously been obtained from the continental shelf off the east Coromandel Peninsula, mainly in the form of bathymetric charts published for the shelf region along Bay of Plenty to Tairua by WRIGHT (1989), and Mercury Bay to Kuaotunu Peninsula by the ROYAL NEW ZEALAND NAVY (1975). Some broad-scale information on shelf stratigraphy has also been previously collected by THRASHER (1986), and on surface sediments by DOYLE *et al.* (1979).

The shelf morphology offshore from Waihi Beach appears similar to that along much of the Bay of Plenty coastline further south (Figure 2.16). This is characterised by a relatively broad continental shelf, extending for 29 km offshore to the shelf break at 125 m water depth at a gradient of 1:232. Prominent irregularities in isobaths are evident in this region, and extend on bathymetric charts from 20 to 80 m water depth, these possibly representing sand ridges on the shelf surface. Further north towards Whangamata, the coastline changes from a northwest-southeast to more north-south orientation. Offshore the shelf narrows considerably to 20 km in width and slopes at a comparatively steeper gradient of 1:133, this change occurring just north of Mayor Island where an embayment like feature is apparent on the shelf break. The isobath irregularities seem to disappear in this vicinity, and so the change in shelf physiography here may cause a significant modification in shelf transport processes.

North of the Alderman Islands, the shelf break extends further offshore (32 km) into 200 m water depth, resulting in a slight flattening of the shelf surface to 1:160 (Figure 2.17). Further north between Mercury Bay and the Kuaotunu Peninsula, the shelf continues to broaden out to 42 km and 80 km offshore, with gradients of 1:210 and 1:400 respectively. The coastal and shelf physiography in this region appears to represent two semi-enclosed embayments which are partly connected by the Hole in the Wall channel between Opito Bay and the Mercury Island group. Isobath irregularities again appear to be present offshore of the Kuaotunu Peninsula in 50 m water depth, these possibly representing active transport pathways extending to or from the Colville Channel further north.

Seismic sub-bottom data collected from the east Coromandel shelf by THRASHER (1986) largely account for these observed broad-scale shelf morphological trends (Figure 2.18). Sediments extending to sub-surface depths of up to 1200 m occupy fault-angle basins offshore from Tauranga Harbour, just south of Waihi Beach. Further north offshore from Whangamata, smaller basins have formed landwards of two downthrown faults, which may account for the reduced width and increased steepness of the shelf surface here. Sediments within basins from both regions have been divided by THRASHER (1986) into two distinct depositional sequences: a lower Pliocene to Pleistocene age unit of semi-lithified sediments deposited in a high energy environment, as shown by their variable dip, foreset bedding and strong but discontinuous reflectors; and an upper late Quaternary unit of soft shelf and upper slope sediments. North of the Alderman Islands

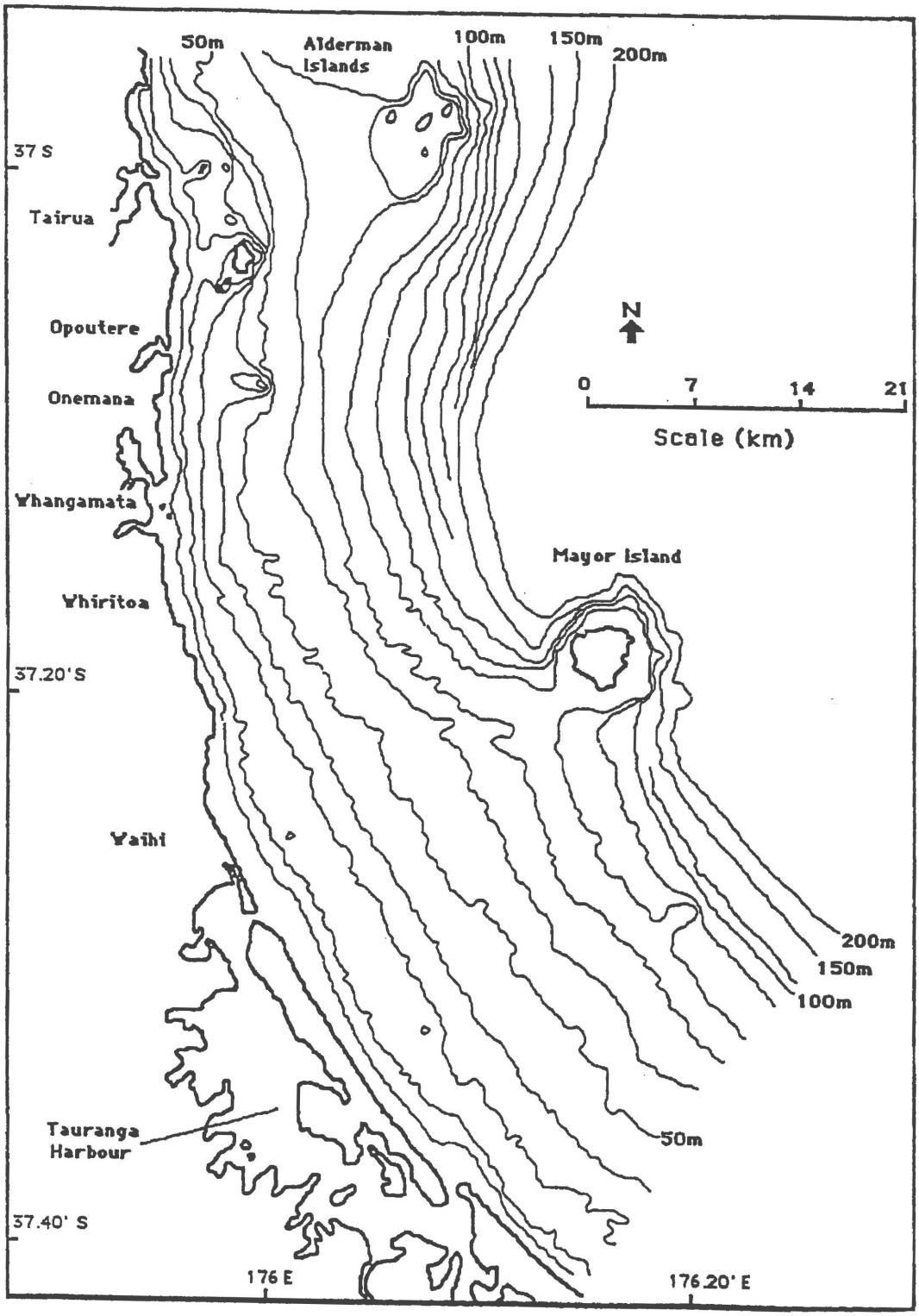

Figure 2.16. Bathymetric contours across the continental shelf for the region extending between the northern Bay of Plenty to just north of Tairua (from WRIGHT 1989).

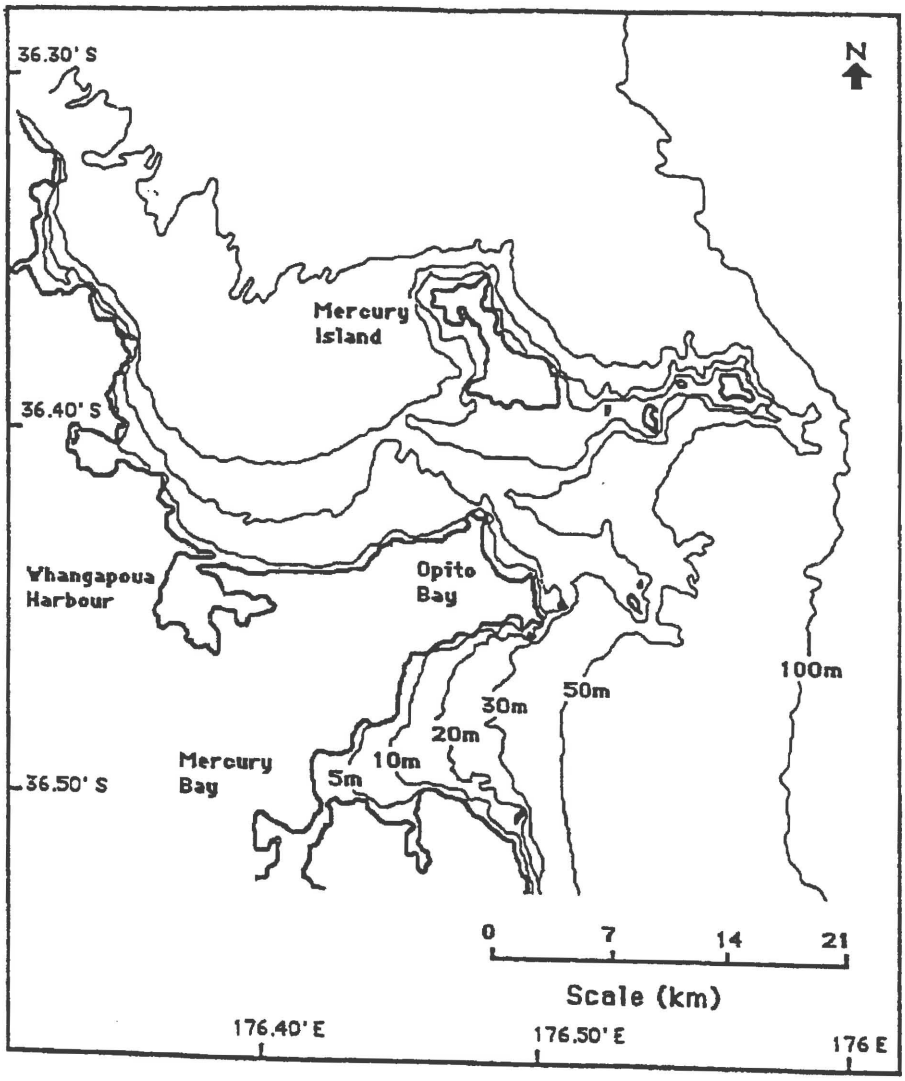

Figure 2.17. Shelf bathymetry between Mercury Bay and the Kuaotunu Peninsula (from Royal New Zealand Navy Hydrographic Chart No. NZ531).

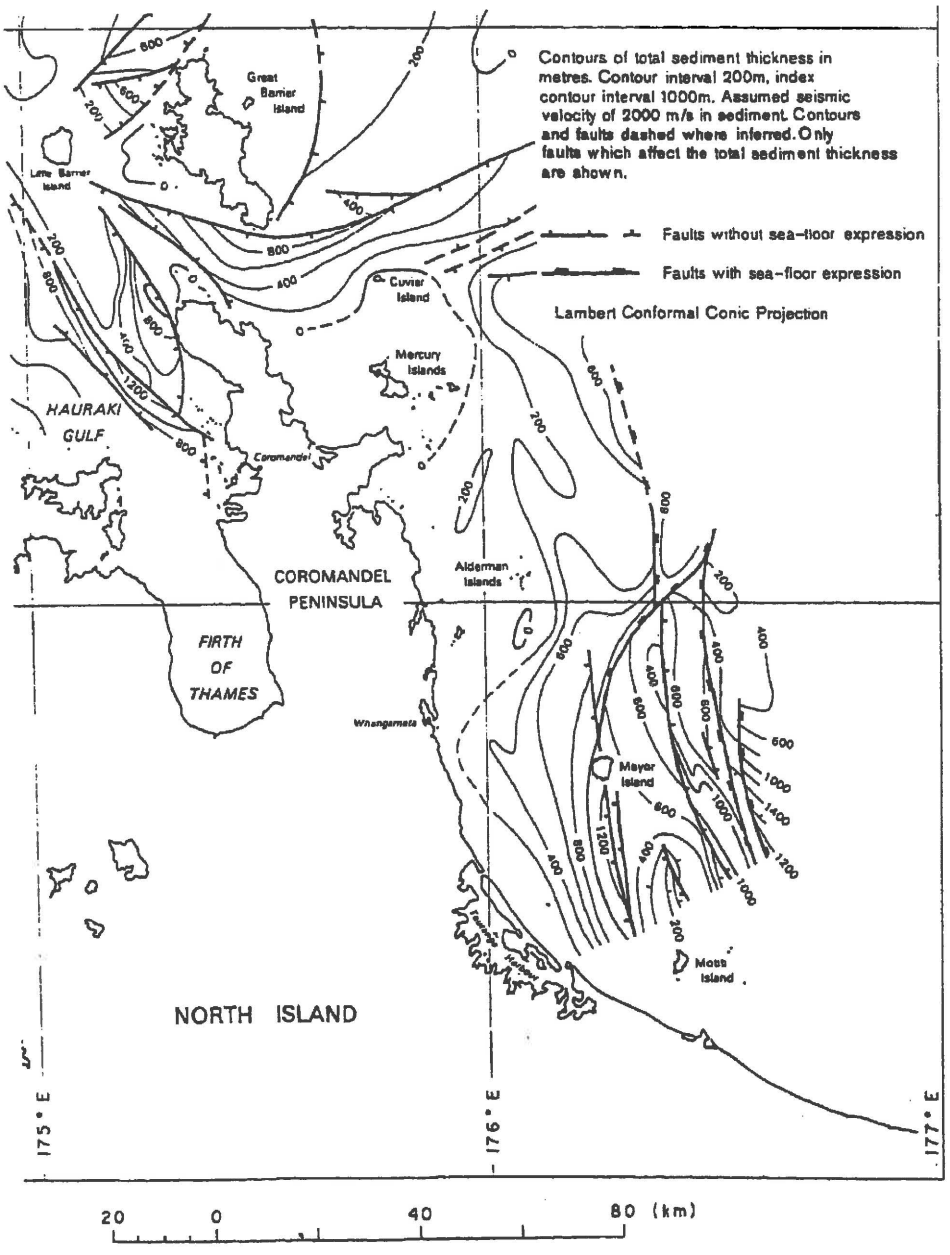

Figure 2.18. Structural map of seismic basement (in metres) for the Coromandel region (from THRASHER, 1986). Note the deep seismic basins present off Tauranga Harbour and to a lesser extent off Whangamata, but only an igneous platform mantled by a thin sediment veneer extending across the shelf north of here.

however, only a thin surficial cover of the upper late Quaternary sediments was identified by THRASHER (1986), with the shelf morphology controlled by an igneous platform extending from the Coromandel Peninsula.

Broad-scale surficial shelf sediment patterns were originally mapped by DOYLE *et al.* (1979), which show deposits within the 50 m isobath of dominantly sandy texture, with patches of calc-gravels offshore from Waihi Beach and Mataora, and silty sands and muds dominating the shelf surface further offshore. DELL *et al.* (1985) have presented some initial findings on surficial sediment patterns from the E.C.S.S. (Figure 2.19), in which they found deposits between Waihi Beach and Hotwater Beach to be dominated by fine to very fine rippled sands within 20 m, medium to coarse megarippled sands within 20 to 40 m (although patches of fine sand are also found here), and featureless muddy very fine sands commencing beyond 40 to 50 m water depth. Based on sediment textural data and theoretical considerations of wave climate from Whiritoa (Figure 2.20), they concluded that during onshore swell conditions in the presence of a superimposed shore-normal unidirectional current, the offshore medium to coarse grained megaripple sands can migrate shorewards to depths of at least 20 m, and possibly shallower onto the beach face.

Smaller scale local studies of surficial sediment patterns have also been conducted in a few sites along the coast. Deposits offshore from Whiritoa Beach were investigated by McCLEAN (1979) and WILLOUGHBY (1981), and showed bands of medium sand within 5 m and beyond 30 m water depth, with fine to very fine sand on the intervening shelf surface (Figure 2.21). Additional studies at Whiritoa and Mataora by HEALY (1981) have shown a sharp textural and mineralogical boundary between surface deposits at about 8 m water depth, which suggests no exchange between surfzone and shelf deposits. Surface deposits have also been studied within the inner bay area at Mercury Bay by SMITH (1980), who found very fine sand dominating the bay bed out to at least 15 m water depth (Figure 2.22), these often containing significant amounts of mud (up to 50 %).

2.5. SUMMARY

This review of the east Coromandel regional setting shows a highly variable physical background for processes of nearshore and inner shelf sedimentation to occur within. Important aspects of the setting include:

1. Location of the study area on an active plate margin, which has produced a regional geology dominated by Tertiary volcanic rocks (mainly rhyolites and andesites), overlain by a thin veneer of Quaternary tephra deposits. These in turn have been extensively weathered to produce a deep regolith, which has become destabilised by removal of the natural vegetation canopy since European settlement. The active plate setting also results in the presence of active faults on the Coromandel Peninsula, which have been slowly downwarping coastal sediments throughout late

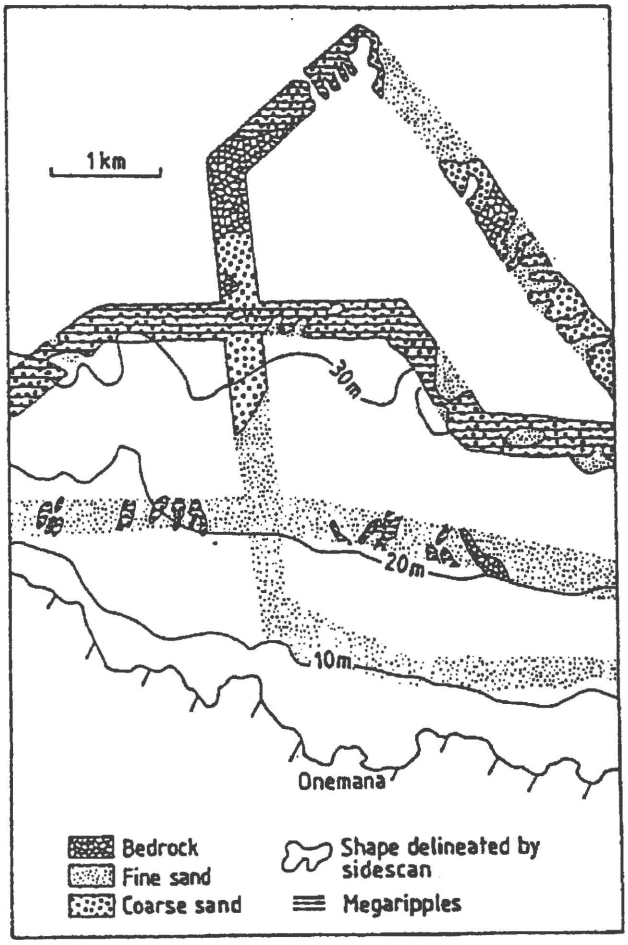

Figure 2.19. Nearshore and inner shelf sediment distribution off Onemana Beach, based on initial side-scan sonar and surface sediment sampling results (from DELL *et al.*, 1985).

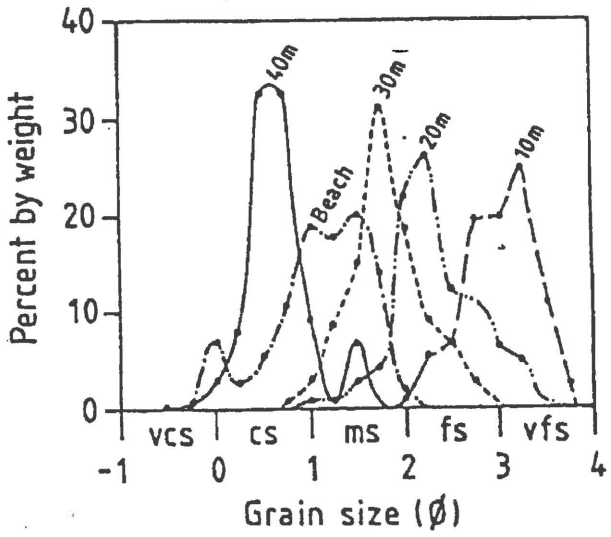

Figure 2.20. Grain size distributions of beach and shelf sands at Whiritoa. Vcs, cs, fs and vfs refer to very coarse, coarse, medium, fine and very fine sand respectively (from DELL *et al.*, 1985).

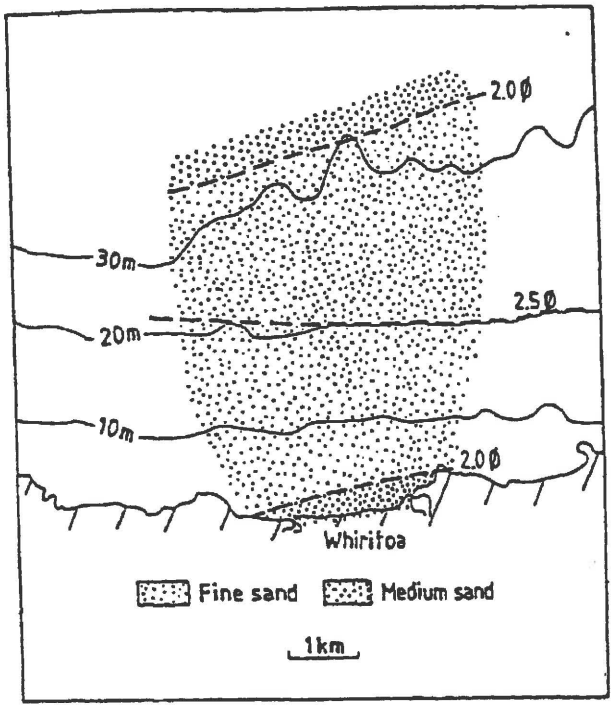

Figure 2.21. Surface sediment textural patterns offshore from Whiritoa Beach, showing bands of medium sand in 0 to 5 m and > 30 m water depth, and fine to very fine sand at intermediate depths (from McCLEAN, 1979; WILLOUGHBY, 1981).

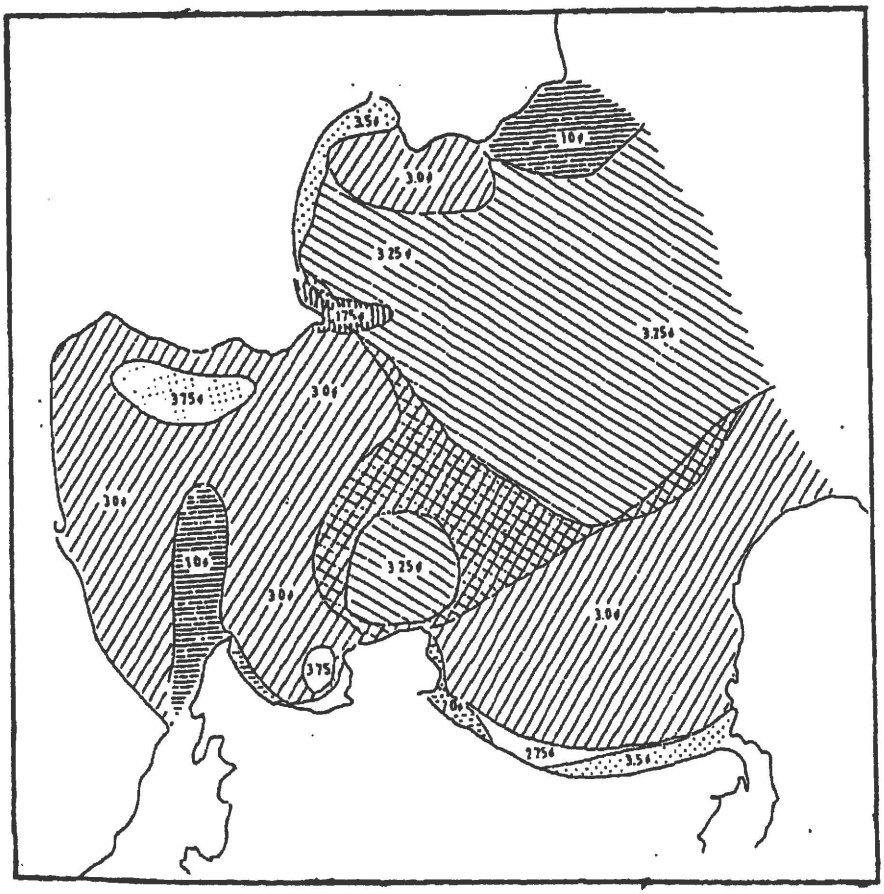

Figure 2.22. Surface sediment textural patterns identified within Mercury Bay by SMITH (1980), showing extensive areas of very fine sand.

Quaternary times, and have also formed several deep basins for shelf and coastal sedimentation to occur within, particularly at and offshore of Tauranga Harbour.

2. Location of the study area on a lee shelf in a mid-latitude zone of dominant westerly winds, with these dominant weather patterns occasionally disrupted by storm conditions associated with occluded mid latitude cyclones, sub-tropical Tasman Depressions, and decaying tropical cyclones, to produce periods of torrential rainfall and catchments flooding, and high speed onshore winds.

3. A microtidal coastal setting with tidal currents generally too low in speed on the shelf to entrain and transport sediments, thus restricting their influence to local harbours and inlets. Oceanic flows associated with the regional East Auckland Current likewise appear to be too low in speed for transport of shelf sediments. However, local wind-generated currents may be more important, as occurs on the Tauranga inner shelf further south.

4. A mixed storm and swell wave environment, characterised by either low wave (H_s= 1 to 1.5 m, T= 4 to 9 s) or longer period swell waves conditions (H_s= 0.91 to 1.73 m, T= 8.3 to 13 s) during fair weather periods, with higher waves produced during storms (H_s= 1.0 to 5.0 m, T= 4 to 10 s), and rare extreme storm conditions of up to H_s= 9.0 m and T= 12 s.

5. Local estuary systems dominantly semi- to infilled by terrestrial and marine sands, with sedimentation rates dramatically increased since European settlement, and estuaries presently providing a source for offshore deposits during periods of catchment flooding, as well as a sink for these at inlet mouths during calm weather periods.

6. Barrier systems of both Holocene and Pleistocene age found along the coast, deposits within these appearing to have been derived mainly from the continental shelf during marine transgressions, but ultimately from weathered volcanic rocks along the Coromandel Peninsula. The morphology of Holocene barriers is very complex, with either prograded barrier spits or stationary pocket barriers generally found, their morphology dependant on local sediment supply, wave energy, and shelf and embayment geometry.

7. Two dominant beach morphologies found along the coast, with coarse grained pocket systems usually characterised by one offshore bar transected by numerous rip channels, and medium to fine beaches associated with barrier spits characterised by the presence of numerous offshore bars (2 to 3) and a range of different rips and ridge runnel systems.

8. A narrow but morphologically variable continental shelf, tending to be comparatively wider and flatter to the north and south, but narrower and steeper in the central part of the study area. Deposits over the shelf surface tend to show broad trends, with fine rippled sands in < 20 m water depth, medium and coarse megarippled sands in 20 to 40 m, and featureless muddy sands in deeper waters.

CHAPTER THREE

REVIEW OF SHELF SEDIMENTATION PROCESSES

3.0. INTRODUCTION

Continental shelves are gently sloping features (typically 1°) which extend from the shoreline out to a shelf break and a steeper dipping shelf slope (typically 4°). Shelf width varies according to the tectonic setting, tending to be narrower on collision coasts such as the east Coromandel, compared to passive plate settings (SHEPARD, 1973). The continental shelf is one of the most complicated geological environments to study, as late Cenozoic glacio-eustatic sea levels have oscillated across its surface resulting in numerous phases of erosion and deposition through a variety of different terrestrial and marine environments (ROY, 1989).

Interpretations of shelf sedimentation essential began with JOHNSON's (1919) early concept of the 'graded shelf' profile of equilibrium, in which the slope and grain size distribution were believed to progressively decrease across the shelf surface in response to a presumed seaward decrease in wave energy. The 'graded shelf' concept was eventually abandoned when field evidence showed very patchy and irregular grain size distributions in shelf deposits throughout the world (SHEPARD, 1932). Instead, sediment patterns were interpreted to represent relict deposits from older fluvial or glacial environments lying seawards of a thin band of modern detrital sands presently supplied by rivers, coastal erosion, and aeolian or glacial activity (EMERY, 1952, 1968). Later studies by SWIFT *et al.* (1971) distinguished true relict shelf sediments, which are not in equilibrium with modern shelf hydrodynamics, and palimpsest deposits, which were originally of relict origin but have since been reworked by modern shelf processes. SWIFT (1976a) also distinguished autochthonous shelf deposits, essentially derived from the onshore reworking of older shelf deposits during marine transgressions, from allochthonous sediments derived from modern onshore sources.

Continental shelves have been classified by SWIFT *et al.* (1971) according to their principal hydrodynamic processes of sedimentation into three broad groups: tide-dominated shelves; oceanic current-dominated shelves; and storm-dominated shelves.

Tide-dominated shelves usually occur where currents generated by tidal forcing exceed velocities of between 0.50 and 1.0 ms^{-1} over the shelf surface (BOGGS, 1987). These currents are typically bi-directional but asymmetrical with respect to velocity, resulting in a net sediment transport in one direction. Morphological features commonly generated by tidal currents include large sand waves, tidal sand ridges or sand ribbons, and sand and gravel sheets. Tide-dominated shelves occur throughout about 17% of modern settings, and the North Sea is a classic example of such a shelf type (BOGGS, 1987). However, for the east Coromandel coast where tidal current velocities are mainly < 0.10 ms^{-1} (Figure 2.4 from Chapter 2), this influence on shelf sedimentation is expected to generally play only a small role.

Continental shelves where oceanic currents intrude from the ocean basins and cause a significant transport of sediments are relatively rare, affecting only about 3% of the world's coastlines. In

such areas, shelf sediments are mainly relict and commonly reworked to form large sand waves, sand ribbons, and coarse sand and gravel deposits (BOGGS, 1987). The southeast African coastline is a classic example of this shelf type (FLEMMING, 1978, 1980). The presence of the East Auckland Current off the east Coromandel coast shows some potential for this type of shelf setting (see Figure 2.5). However, the measured velocities of < 0.3 ms^{-1} in deep ocean water (see Chapter 2.3.1.), and the presence of muddy shelf deposits beyond 50 m water depth make it unlikely to dominate shelf sedimentation.

Storm-dominated shelves were first suggested following observations of HAYES (1967) on the effects of Hurricane Carla and Cindy on the Texas continental shelf. These are regions in which sediment transport is mainly controlled by surface gravity waves and wind-forced flows, and presently affects about 80% of the world's coastlines (BOGGS, 1987). Because storm events are the dominant forcing mechanisms of shelf flows, sediment entrainment and transport in such settings tends to be episodic. In regions where relict and palimpsest sands dominate (e.g. North American Atlantic coast), these have often been reworked into shore retreat massifs, linear sand ridges, and smaller sandwaves, megaripples and ripples (BOGGS, 1987). Storm-dominated shelves where the input of modern terrestrial sediment overwhelms relict deposits are characterised by generally low relief surfaces of finer grained sediments, often showing exposed windows of relict coarse sands and gravels. The oceanographic setting of the east Coromandel coast shows the characteristic features of a storm-dominated shelf setting. Therefore, it is important to elaborate on the nature of their hydrodynamic processes and morphological features before attempting to present and interpret results from the E.C.S.S.

3.1. SEDIMENTATION PROCESSES ON STORM-DOMINATED SHELVES

Until recently, marine geologists, oceanographers, and coastal engineers throughout the world have primarily been concerned with understanding and modelling the extreme onshore and offshore boundaries of the continental shelf, i.e. the beach system and outer continental shelf. Consequently, a fuller understanding of transport processes within the intermediate depths of the coastal boundary zone (i.e. the nearshore and inner shelf), particularly regarding the interaction between beach systems with these intermediate shelf waters, is only now emerging (WRIGHT, 1987). Processes which have to date been recognised as important for the transport of sediments within this important part of the continental shelf are briefly reviewed here in the context of storm-dominated settings.

3.1.1. Wave-Induced Flows

Surface gravity waves in the ocean occur in a wide range of shapes that propagate as apparently regular undulations (NIEDORODA *et al.*, 1985a). Gravity waves are not significantly influenced by the bottom as they begin to pass over the continental shelf, and thus retain a sinusoidal wave motion with no mass transport of water or associated net movement of

sediments. The physical behaviour of waves at these depths, particularly their orbital diameters and maximum velocities, can be very simply modelled by Airy or linear wave theory (Figure 3.1 KOMAR, 1976).

As the waves enter shallower shelf waters within the coastal boundary zone (usually depths of between 0.5 to 0.25 x their wavelength), their form changes such that the crests become increasingly narrow and peaked, and the troughs broad and flat. Associated with this shoaling of waves is an asymmetry in the flow of water particles, such that a short but strong onshore component develops beneath the crest, and a longer but weaker offshore component beneath the trough. This in turn gives rise to a residual flow towards the shore. Such non-linear behaviour of waves is more complex to model, and is usually done by applying Stokes second and higher order theories (Figure 3.1; KOMAR, 1976). At depths equivalent to about 0.05 x their wavelength, the wave propagation speed is exceeded by orbital velocities of water particles, resulting in an oversteepening of wave crests and thence wave breaking. Water motion is nearly horizontal throughout the water column, and is modelled using Cnoidal and Solitary wave theories (Figure 3.1; KOMAR, 1976).

The velocity asymmetries and mass transport current associated with shoaling waves has been widely regarded as the primary mechanism responsible for cross-shore transport of sediments at intermediate shelf depths. Hypotheses to date recognise the potential of velocity asymmetries to initiate sediment entrainment and transport, however, there is little subsequent agreement on the nature of transport directions or sorting of sediments (HILTON, 1990). Theories proposed have largely been presented in an attempt to account for the commonly observed tendency for shelf sediments to decrease in grainsize offshore over a steep seaward dipping concave-up surface at their landward margin (often referred to as the shoreface). Early studies by CORNISH (1898) proposed that the higher onshore velocities of short duration will move both large and small particles in an onshore direction, while lower but longer offshore velocities will result in a net offshore movement of finer material. Subsequent studies proposed the null-point hypothesis, in which shoreward increases in orbital asymmetry should be balanced by shoreward increases in bed slope (e.g. EAGLESON and DEAN, 1961). This theory suffers, however, as it assumes that negligible contributions are made by flows other than oscillatory flows of waves, while more recent studies have shown that other both wave- and non wave-induced flows are important in the cross-shore movement of shelf sediments (WRIGHT *et al.*, 1991).

Rip currents generated onshore by breaking waves have been proposed by COOK and GORSLINE (1972) as a more likely cause of seaward-fining textural gradients through rip-current fallout on the shelf surface. These are probably important in transporting sands seaward of the surfzone, but are unlikely to affect shelf sedimentation patterns more than a few hundred metres beyond the outer breaker zone (WRIGHT, 1987).

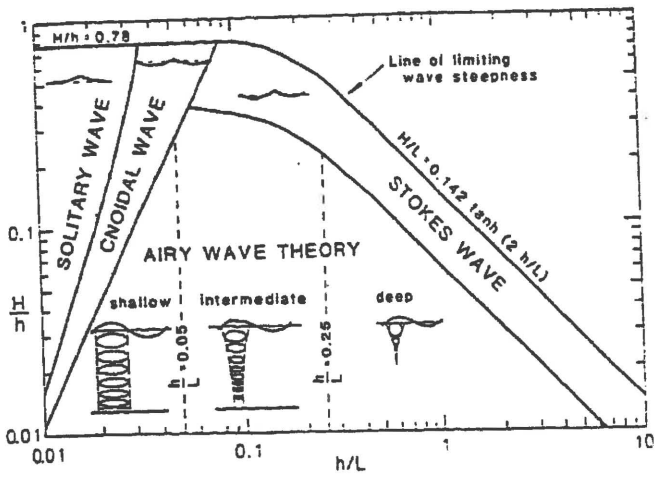

Figure 3.1. Conditions of wavelength (L), wave height (H), and water depth (h) for which different wave theories are most applicable (from KOMAR, 1976). Appropriate theoretical wave forms are shown within each field.

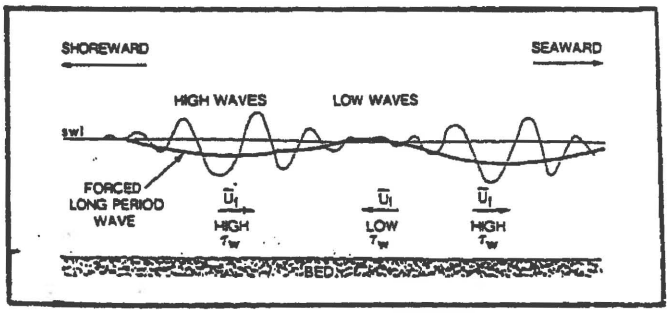

Figure 3.2. Conceptual diagram showing the notion of sediment entrainment by groups of large waves and advection by low frequency velocities associated with amplitude-modulated waves (from WRIGHT *et al.*, 1991).

An important recent observation is that mass transport currents associated with shoaling waves are not necessarily directed onshore, and in many cases may flow offshore. In particular, amplitude modulated waves associated with groupy long period swell wave conditions have been proposed by SHI and LARSEN (1984) as an important forcing mechanism for offshore sediment transport by waves (Figure 3.2). When such groupy wave conditions occur (i.e. the waves travel in pockets of high and low amplitudes), they yield a long period wave whose trough coincides with groups of high waves, and crest in low wave groups. As with other shoreward propagating gravity waves, the onshore directed current occurs under the crests and offshore directed flows beneath the troughs. However, since the large waves will entrain more sand into suspension than the low waves, a net seaward movement of sediment will occur (WRIGHT *et al.*, 1991). Also, where oscillatory flows occur over rippled bedforms, they can cause a significant phase angle between instantaneous velocity yielding a sediment flux in an opposite direction to the net mass transport (NIELSON, 1979).

Previous observations by DELL *et al.* (1985) that ripple and megaripple bedforms occur on the shallow shelf surface along the east Coromandel coast (out to at least 45 m), indicate that in most places the bottom boundary layer is controlled by wave orbital motions. Surface gravity waves must therefore be an important component to the shelf transport system within the study area.

3.1.2. Wind-Forced Currents

Outside of the surfzone, oceanic water circulations on storm-dominated shelves are largely controlled by the action of wind-driven currents (WRIGHT, 1987). As a wind blows over the shelf, it will directly transfer energy to the water surface which is subsequently transferred and reduced throughout the water column within an upper boundary layer (or surface Ekman layer). As the water begins to move, a surface current is formed which is immediately affected by the Earth's rotation (Coriolis effect), causing a layer averaged turning of 90° to the right in the northern hemisphere or to the left in the southern hemisphere (Figure 3.3; PICKARD and EMERY, 1984). This surface current may then either flow towards or away from the coastline, leading to a set-up or set-down of the sea level (Figure 3.4; NIEDORODA *et al.*, 1985a). A pressure gradient force develops, and is directed away from surface elevations. The entire water column responds to the force and experiences the Coriolis effect, causing it to veer either right or left for northern and southern hemisphere waters respectively (SWIFT *et al.*, 1985). The resulting flow is known as a geostrophic (Earth turning) current. At the sea-bed, a bottom stress is exerted on the water column causing current velocities to decrease towards the bed. However, this decelerating flow is also subjected to the Coriolis effect and is rotated about 45° to the left of the geostrophic current flow in the northern hemisphere, or to the right in the southern hemisphere (POND and PICKARD, 1983), to form a lower boundary (or Ekman) layer (Figure 3.4).

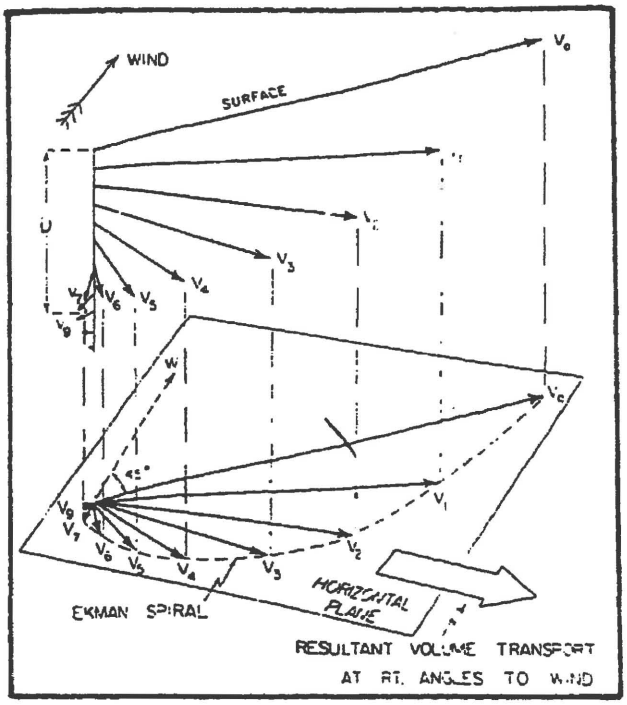

Figure 3.3. Wind-induced Ekman flow for the northern hemisphere, with water velocity decreasing and rotating at increasing water depths. The net resultant flow is at right angles to the right of wind direction in the northern hemisphere, and to the left in the southern hemisphere (from PICKARD and EMERY, 1984).

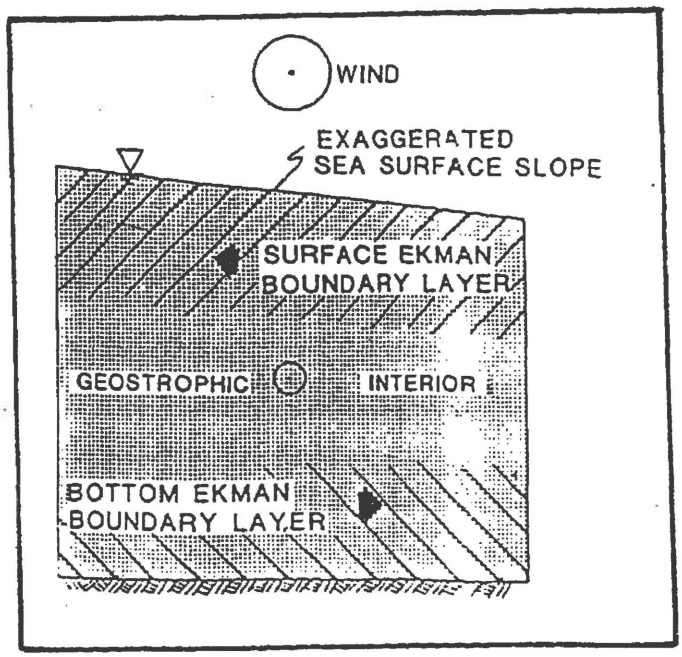

Figure 3.4. The three main dynamic layers within the coastal boundary zone, formed by the action of wind on the sea surface (from NIEDORODA *et al.*, 1985a).

In modelling wind-driven current patterns on storm-dominated continental shelves, coastal waters are often broken down into distinct dynamic zones (Figure 3.5; NIEDORODA *et al.*, 1985a; SWIFT *et al.*, 1985). The innermost surfzone is intimately coupled to the beach system, and is dominated by processes associated with breaking waves. Seaward of this is the friction-dominated zone, where wave orbital currents are intense and interact with mean flows to greatly increase the bottom stress (SWIFT *et al.*, 1985). As a consequence of extreme turbulence within this zone, the eddy viscosity is relatively high and the Coriolis effect on current flows reduced, so that surface currents tend to flow parallel to the wind stress and bottom currents move down the horizontal pressure gradients (SWIFT *et al.*, 1985), thus producing either an upwelling or downwelling circulation (Figure 3.6). Outer margins of the friction-dominated zone grade smoothly into the geostrophic zone, where waters are sufficiently deep that the surface and bottom boundary layers are separated by an interior region of geostrophic flow, directed perpendicular to the causative forces (SWIFT *et al.*, 1985). NIEDORODA *et al.* (1985a) report that under typical ocean conditions, the geostrophic zone seldom extends shorewards of depths ranging between 20 and 40 m.

These shelf zones are defined by dynamical considerations, and thus their shore-normal length scales vary according to the intensity of the forcing mechanisms. The complexity of flows within the dynamic zones varies according to the orientation of wind stress relative to the shoreline, some resulting in relatively smooth transitions (Figure 3.7 a, b), while others develop currents with opposite direction components within each zone, resulting in alongshore counter currents and shore-normal divergences and convergences (Figure 3.7 c; NIEDORODA *et al.*, 1985a; SWIFT *et al.*, 1985). As the east Coromandel coast varies significantly in terms of coastal orientation and wind patterns, wind-generated current flows along the shelf are likely to show complex regional patterns.

Current flow patterns may be further complicated by density stratification and the presence of a pycnocline surface within the water column. This pycnocline surface will respond similarly to wind stresses as the water surface. However, it will tend to be depressed in areas of surface water elevation, and thus produce pressure gradient forces (baroclinic flows) which tend to oppose those driven by sea surface slopes (barotropic flows). The pycnocline surface usually intersects the sea floor within the transition zone (it is absent within the friction zone due to high mixing), and can thus significantly reduce bottom stresses within the geostrophic zone (SWIFT *et al.*, 1985). Modification of current flows by density stratification may be important in the context of the east Coromandel coast, as HARRIS (1985) found coastal waters within the study area to be significantly cooler than adjacent shelf waters during winter, which he presumed resulted from the intrusion of cool fluvial waters derived further south from the Taupo Volcanic Zone.

Wind-generated currents also vary in characteristics according to the weather systems responsible for their generation (SWIFT and NUMMEDAL, 1987). Tropical cyclones and

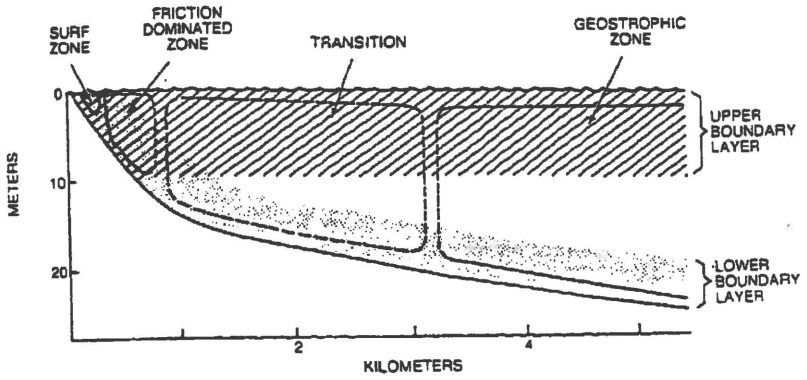

Figure 3.5. Dynamic zones of the coastal ocean. Thickness of the two boundary layers and positions of the zone boundaries vary with intensity of the flows (from SWIFT *et al.*, 1985).

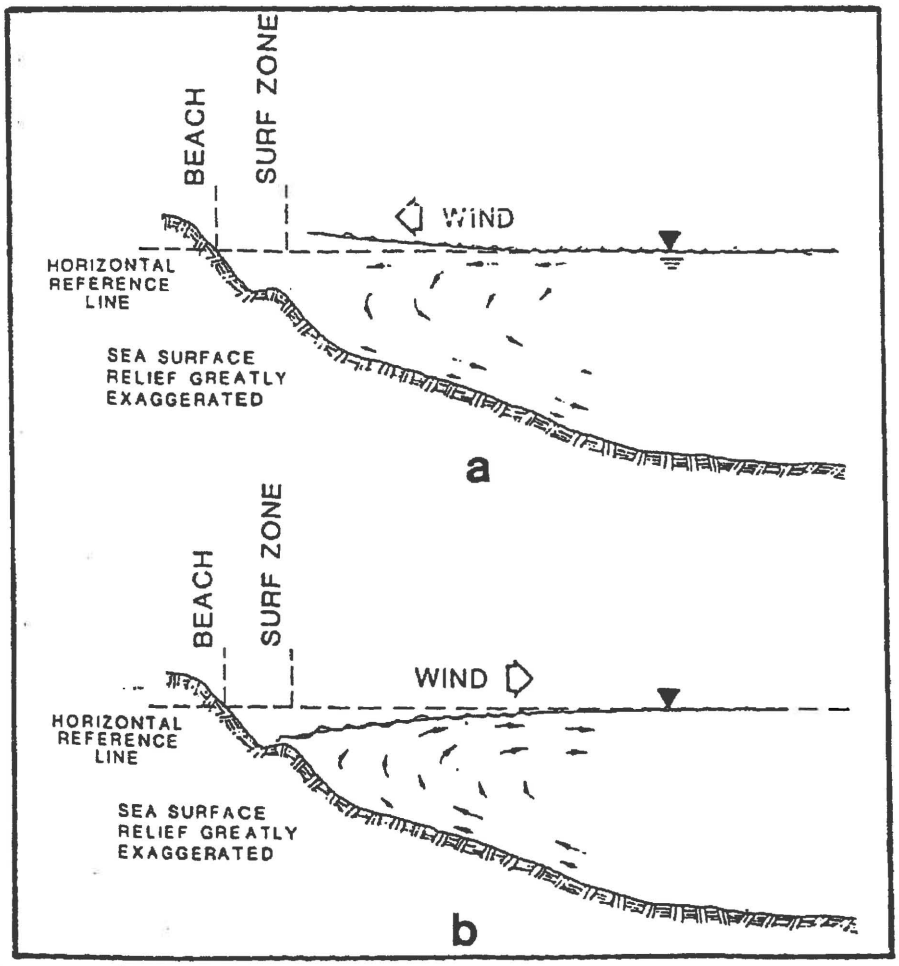

Figure 3.6. Characteristic current flow patterns within the coastal boundary zone associated with: a) onshore winds and downwelling circulation; b) offshore winds and upwelling circulation (from NIEDORODA *et al.*, 1985a).

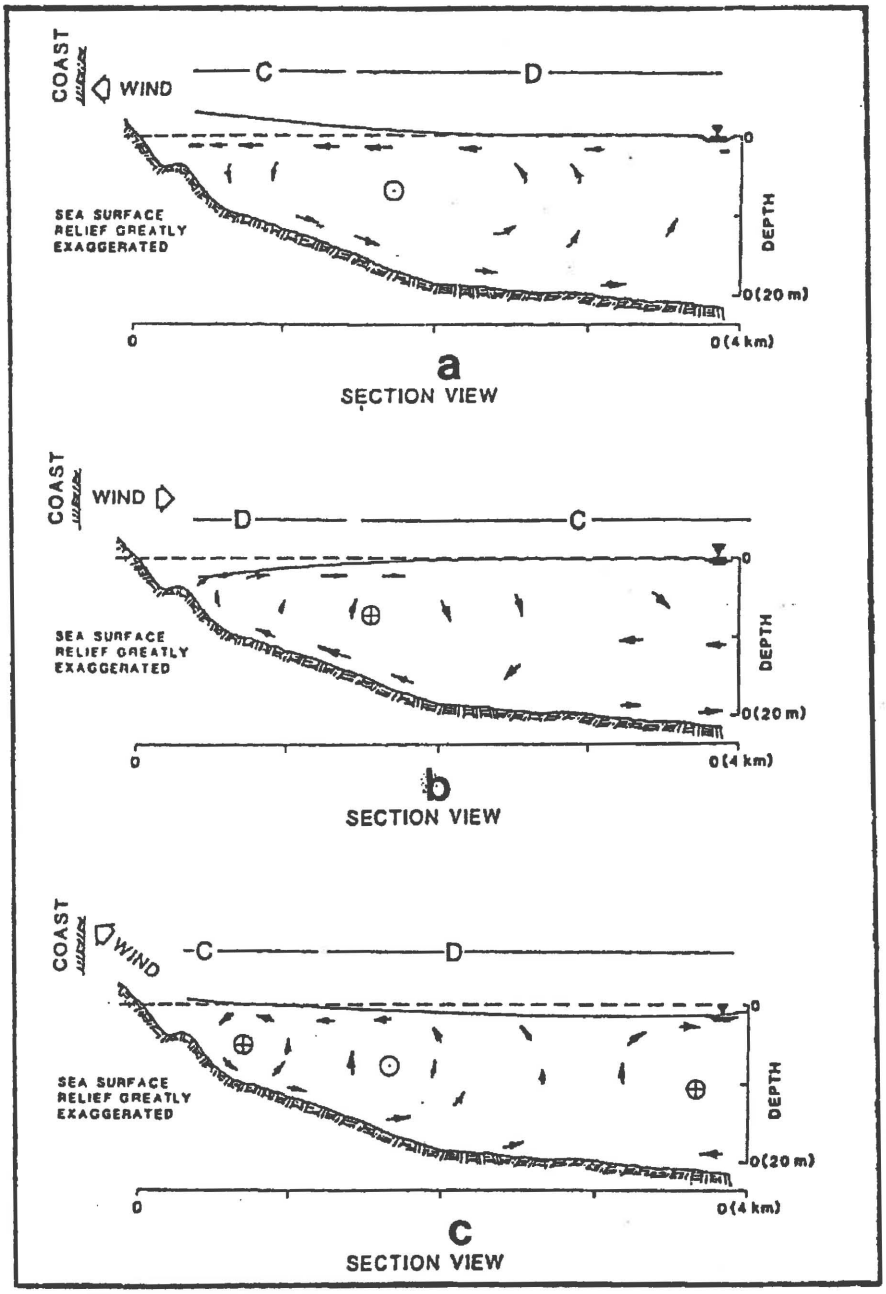

Figure 3.7. Schematic circulation patterns under different orientations of the wind relative to the coastline in the northern hemisphere: a) onshore winds forcing a simple downwelling circulation pattern; b) offshore winds forcing a simple downwelling circulation pattern; c) shore-oblique onshore winds creating a complex downwelling pattern with alongshore counter flows and shore-normal divergences and convergences (from NIEDORODA *et al.*, 1985a, based on observations from Long Island, North America).

hurricanes cause high storm surges (i.e. set-up of sea level) over a relatively small length of coast, and drive very strong unidirectional geostrophic currents along the shelf (up to 1.6 ms^{-1} on the Florida coast; MURRAY, 1970), which will extend beyond the perimeter of the hurricane itself. Mid-latitude storm currents are also driven by along-shelf geostrophic flows. The coastal set-up associated with these less intense storms is not as extreme, but extends for greater distances along the coast. Geostrophic currents associated with these storm events on the mid-Atlantic coast, North America, typically attain speeds on the order of 0.40 ms^{-1} (SWIFT and NUMMEDAL, 1987). As both mid-latitude storms and decaying tropical cyclones affect the east Coromandel coast, each of these storm current types may influence shelf sedimentation patterns within the study area.

An important kind of mid-latitude storm is the 'scale-matching' type, where the storm dimensions match that of the continental shelf. This results in a 'slab-like' response in the shelf water column, with a coherent along-shelf geostrophic flow along large sections of coastline. A second type is where a storm piles water up against the coastline, and then moves on (SWIFT and NUMMEDAL, 1987). This stranded storm surge does not simply run out to sea, but instead propagates itself as a long period, low amplitude shelf wave along the coast, with the Coriolis effect continually pushing the wave against the coastline. Such waves are referred to as 'coastally trapped topographic waves', and the geostrophic flows associated with them are amongst the most intense experienced on storm-dominated shelves (SWIFT and NUMMEDAL, 1987). This type of geostrophic flow may be generated along the east Coromandel coast, as occluded cyclones and Tasman Depressions are usually quite mobile and produce strong winds of limited duration, while more persistent winds form less frequently when these weather systems become blocked to the east by a stationary anticyclone. HEATH (1979, 1982) has previously suggested that similar edge waves occur on the new Zealand east coast continental shelf in the form of oscillations within adjacent harbours, and are generated by meteorological disturbances.

In summary, it appears that the strongest components to shelf flows within the coastal boundary zone are isobath-parallel geostrophic currents. However, the comparatively moderate diabathic flows associated with downwelling and upwelling circulations are also important, and are an additional possible cause of the seaward fining trend commonly observed on storm-dominated shelves, which has traditionally been solely attributed to the action of wave orbital currents (WRIGHT, 1987).

3.1.3. Combined Wave-Current Flows

Although wave-induced flows associated with orbital asymmetry are an effective mechanism of sediment transport within shallow water depths (usually 10 to 15 m; SWIFT *et al.*, 1985), the interaction of wave orbital currents with slow-varying wind-driven flows plays a very important role in the transport of sediments within the coastal boundary zone. GRANT and MADSEN (1979) have modelled the effects of non-linear wave-current interactions in the lower boundary layer, and

found that they lead to an enhancement of both the stress and apparent roughness experienced by the mean current. In this model, a wave boundary layer is present in the immediate vicinity of the sea-bed where the shear stress is dependent on a non-linear combination of both the wave- and current-induced stress, and a roughness associated with the physical bottom roughness. Above the wave boundary layer, stress is associated with the physical bottom roughness. However, the highly dissipative turbulent flow in the wave boundary layer extracts energy from the flow above, causing an enhanced mean shear stress in this region. Effectively, the shear stress enhancement is equivalent to an enhanced or apparent roughness length for the flow in the outer region, this roughness length being dependent both on the true bottom roughness and the wave boundary layer characteristics (LYNE *et al.*, 1990a).

Therefore, in studies of sediment transport on storm-dominated shelves, it is usually assumed that high frequency wave orbital motions agitate bottom sediments, whereas superimposed steady currents produce the net sediment advection of which purely oscillatory flows alone are incapable (COWELL and NIELSON, 1984). This leads to the simple 'rule of thumb' that waves determine when, and currents determine where, sediment is transported. Thus, the dominant effects of storm conditions in the coastal boundary zone are usually to cause a significant shore-parallel bedload transport, with an important shore-normal secondary component (VINCENT *et al.*, 1981). However, the complex nature of wave-current interactions must always be considered, as depending on factors such as bed roughness and the horizontal angle between wave incidence and the mean current, the vector resultant of sediment flux may be opposite to the current and need not parallel either wave incident angle or the mean current (WRIGHT, 1987).

3.2. CONTINENTAL SHELF ZONES

From consideration of its cross sectional form, the continental shelf surface has traditionally been divided into a regular succession of morphological provinces, each associated with a distinctive zone of hydraulic activity (Figure 3.8; SWIFT 1976). The outermost part of the continental shelf is referred to as the 'outer shelf' zone, which is thought to be dominated by frontal processes developed at the interface between contrasting ocean and shelf water masses. The 'mid shelf' zone is characterised by a low gradient shelf plain where surface features and sediments are either relict or consist of actively accumulating mud deposits, and in which weak boundary layers enable the dominating flows to be reasonably geostrophic (COWELL and NIELSON, 1984). Further landwards, the shelf surface begins to rise steeply and forms a coastal boundary zone to shelf flows. This inner portion of the continental shelf comprises the 'inner shelf and nearshore zones', which are the main focus of this study. These are an important part of the continental shelf along unconsolidated coasts, as collectively they couple the sediment transport systems of the beach and surfzones with the deeper mid and outer shelf zones.

The nearshore zone (i.e. the 'shoreface') has been defined morphologically as extending from the base of the surfzone as a steep concave-up surface (gradients typically in the order of 1:100), and

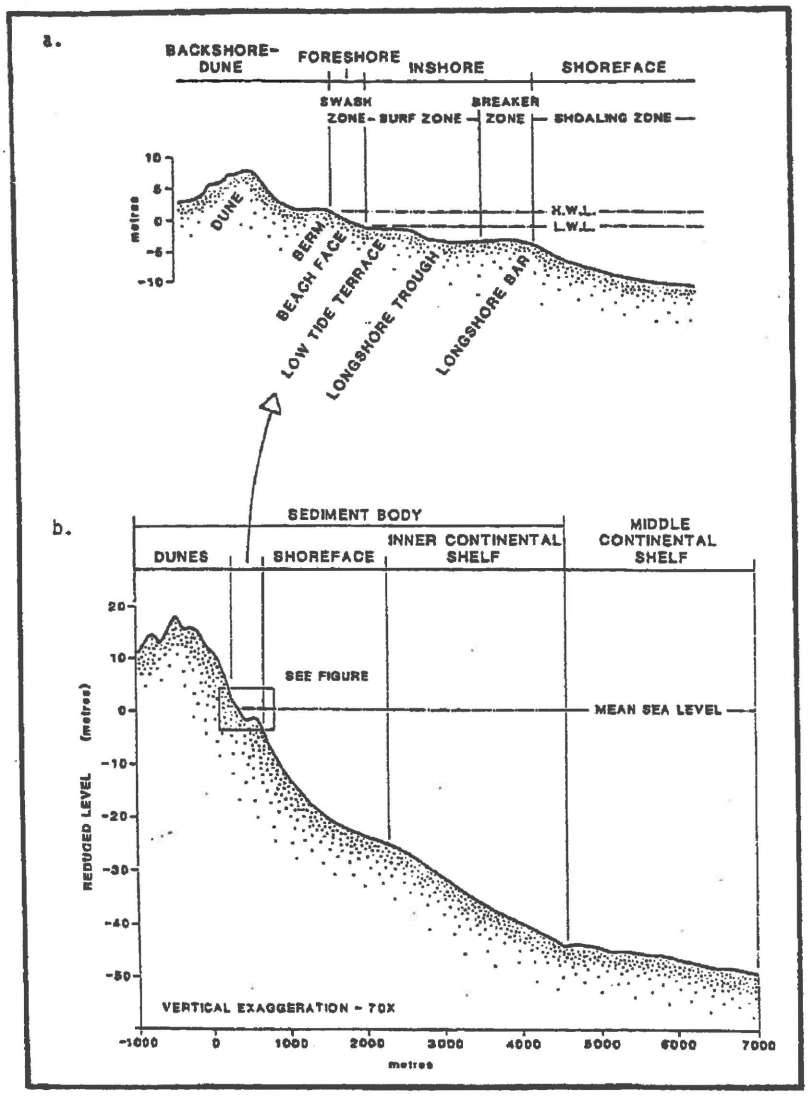

Figure 3.8. Morphological components which commonly characterise the inner surface of continental shelves, based on the Pakiri coast, north of the Coromandel Peninsula (from HILTON, 1990). Note that the term 'nearshore' is used in the same context in this study as 'shoreface' in the figure.

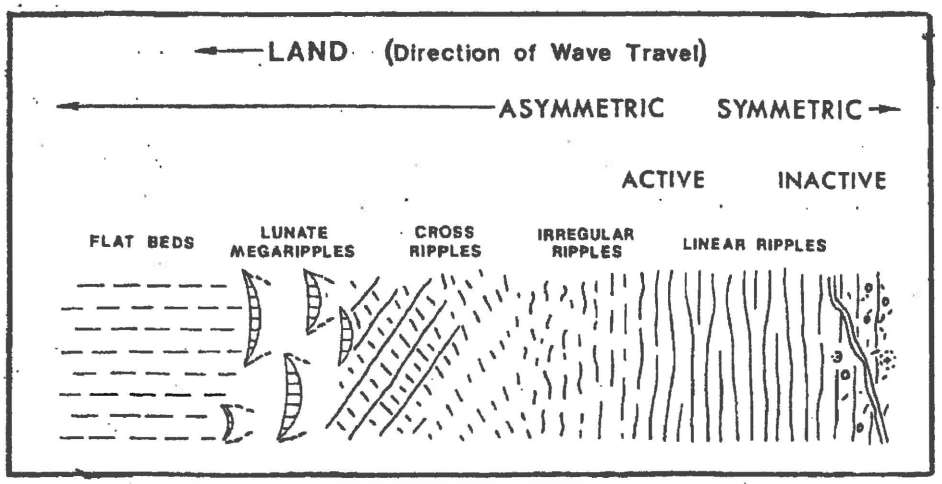

Figure 3.9. Bedform sequences over the nearshore and inner shelf zones, associated with increasing wave orbital asymmetry towards the shore (from CLIFTON, 1976).

is usually divided into an upper and lower section (NIEDORODA *et al.*, 1985a). On the mid-Atlantic shelf, North America, this zone extends to depths of between 10 to 20 m, where either an abrupt or gentle change to a flatter inner shelf surface occurs (SWIFT 1976). The overall character of the nearshore and inner shelf zones will ultimately be determined by the rate of relative sea level rise, rate and character of sediment supplied, and the rate of fluid power expenditure (SWIFT *et al.*, 1985). The exact nature of surface deposits within the nearshore and inner shelf zones will therefore vary with different coastal settings. However, sediments generally fine seawards across the nearshore zone, and will then either coarsen, or form a veneer of muds over coarser inner shelf sands, in autochthonous and allochthonous settings respectively (SWIFT, 1976a; NIEDORODA *et al.*, 1985a).

Processes which operate over the nearshore and inner shelf zones are seen to be a transition from the breaking wave environment of the surfzone, to the larger scale geostrophic flows of the mid shelf (WRIGHT *et al.*, 1991). Attempts have been made to relate these essentially morphological zones to the previously described dynamic zones of the coastal boundary zone, with observations that the length scales of the dynamic zones during peak flow conditions tend to coincide with the morphological zones of the nearshore and inner shelf (SWIFT *et al.*, 1985). Thus, the upper nearshore is seen as the hydraulic zone of friction-dominated flows associated with shoaling waves, whereas the lower nearshore and inner shelf are a transition zone also affected by shoaling waves, but where the sea floor is increasingly influenced by the dominant isobath-parallel flows driven by winds (SWIFT, 1976b). This is reflected in the bedforms found in surface deposits, with megaripples, long-crested ripples, and hummocky bedforms dominating the lower nearshore and inner shelf surface, and irregular crested ripples, cross ripples, lunate ripples, and flat beds becoming increasingly dominant shorewards across the upper nearshore surface as wave orbitals become increasingly asymmetrical (Figure 3.9; CLIFTON, 1976)

However, NIEDORODA *et al.* (1985a) note that the nearshore and inner shelf boundaries are hard to define on this basis, as these dynamic zones are highly variable and will expand or contract depending on the prevailing conditions. Consequently, problems exist in matching dynamic length and time scales to the morphological scales, which raises the question of whether morphological zones are 'tuned' to either average wave conditions, storm conditions, or extreme storm conditions (NIEDORODA *et al.*, 1985a).

3.3. EXAMPLES FROM DIFFERENT STORM-DOMINATED SHELF SETTINGS

The nature of nearshore and inner shelf deposits on storm-dominated shelves varies significantly throughout the world depending on local environmental conditions, specifically the nature of relative sea level oscillations, the degree of modern versus relict sediment inputs into the shelf transport system, and the oceanographic climate. In order to gain a thorough background on nearshore and inner shelf sedimentation processes, it is considered pertinent to briefly review studies from different storm-dominated shelf settings.

3.3.1. North America

Our present understanding of sedimentation processes within storm-dominated shelves is based largely on numerous studies undertaken in North America. In particular, the east Atlantic coastline has been the focus of much important research. This is a region in which sea level has been rising sufficiently rapidly throughout the Holocene that most of the coastline is retreating at rates of 0.1 to 3.0 $m.y^{-1}$, with barrier spits and islands transgressing landwards and estuaries forming sinks for river and littoral sands (NIEDORODA *et al.*, 1985b). Thus, the Atlantic shelf generally represents an autochthonous sediment regime, in which deposits are essentially of 'in situ origin' (SWIFT, 1976). The North American Atlantic shelf is a broad gently sloping feature associated with a passive plate setting, with nearshore slopes initially steep (1:200), but flattening out over the inner shelf to gradients of 1:2000.

Sedimentation processes on the Atlantic shelf show important variations between calm and storm weather conditions. During periods of calm weather, sands can move onshore and deposit on the upper nearshore and beach systems, in response to the action of asymmetrical wave orbital currents (NIEDORODA *et al.*, 1984, 1985a) and fall out from offshore flowing rip currents (COOK and GORSLINE, 1972). More recent studies by WRIGHT *et al.* (1991) have shown that during windless swell conditions, wave-induced near-bottom return flows may significantly counter this shoreward transport generated by incident waves. They also found that onshore and offshore directed tidal current flows may be important for fair weather sediment transport. On the lower nearshore and inner shelf surface, observations by NIEDORODA *et al.* (1985b) indicate that wave orbital velocities interact with weak tidal and wind-driven currents to move sand landwards in a similar manner, though at much lower rates, to the landward sand flux in the upper nearshore zone.

Under storm conditions, the rate of sediment transport is intensified greatly, with more sediment moving offshore during a few hours of a moderate northeasterly storm than can move onshore in two or more days (WRGHT *et al.*, 1991). During storm events, very high near-bottom sediment resuspension occurs by wave agitation, which is subsequently advected primarily southwest along the shelf by intense 'jet like' flows, with a subordinate but important offshore flux of sands by downwelling flows (SWIFT and FREELAND, 1978; NIEDORODA *et al.*, 1985b; LYNE *et al.*, 1990b; WRIGHT *et al.*, 1991). Under these high resuspension rates, hyperpycnal plumes of sufficient thickness and suspended sediment concentration may develop, resulting in pressure gradients which drive a down-slope gravity flow (WRIGHT *et al.*, 1991). Over longer geological time scales on the Atlantic shelf, there is a net export of sand from the nearshore zone onto the inner shelf floor, due to more sand moving offshore during storm events than is subsequently reworked back onshore in calm weather conditions.

Three important bedform types have been observed on the Atlantic shelf, namely megaripples, sand waves, and sand ridges. Megaripples are flow transverse bedforms with spacings in the order of 2 to 3 m, and often have either a 'hummocky' appearance, or occur as sharp-crested features. Both types appear to be responses to combined flow regimes of storms, with hummocky megaripples formed on fine to very fine sand when the flow components are of subequal value, and sharp crested features favoured in coarse sand where the wave orbital current component is weak relative to the mean flow component (SWIFT *et al.*, 1983; NIEDORODA *et al.*, 1985a). Large-scale low amplitude sand waves are found on the lower nearshore and inner shelf surface (1 m high, 100 m apart), and have their crests opening to the shoreline at an angle of about 80°. Sand ridges rise up to 10 m above the surrounding sea floor, and have crestlines which may be traced for distances of up to 10 km into depths as shallow as 2 m, and usually make angles of 10° to 45° with the coastline (SWIFT and FREELAND, 1978; SWIFT and FIELD, 1981). The ridges typically have steeper down-current slopes, and show a textural phase lag, with coarser grained sediments occurring on the down-current flanks. These ridges appear to migrate slowly offshore and down the coast in the storm current direction as the shoreline retreats (NIEDORODA *et al.*, 1985b).

Erosional retreat has left a characteristic textural imprint, with fine grained sands forming a seaward fining blanket over the upper nearshore surface to a depth of about 10 m. Here, it thins to a feather edge over coarser lag sands which mantle earlier Holocene and Pleistocene sediments (NIEDORODA *et al.*, 1985b). Further seawards over the lower nearshore and inner shelf, bottom grain sizes vary according to the sand ridge topography, as outlined above. Shoreline retreat occurs by the transitory seaward thinning veneer of upper nearshore sands being entirely stripped off during major storms, which are subsequently either incorporated into the shelf transport system (i.e. the sand waves and sand ridge field), or into backbarrier deposits by processes of aeolian, washover, and tidal delta formation (NIEDORODA *et al.*, 1985b). This then exposes older backbarrier deposits, which are released by nearshore erosion and recycled back through the system (Figure 3.10). New deposits are input into the sediment budget by either tidal inlets eroding into the underlying Pleistocene substrate, or erosion of adjacent headlands (LEATHERMAN, 1985; NIEDORODA *et al.*, 1985b).

South of the Atlantic North American coast is the east Texas-Louisiana shelf within the Gulf of Mexico. This is an example of an allochthonous shelf environment, in which sediment is supplied into the shelf transport system through fluvial deltas. Sea level is presently rising along the coast due to the compaction of deltaic deposits, with subsidence varying according to the age and thickness of deposits. The shoreline is therefore retreating in many locations, with rates of shoreline retreat for abandoned delta complexes varying from 1.0 to over 15 $m.y^{-1}$, with extreme rates of 50 $m.y^{-1}$ (BOYD and PENLAND, 1984).

The Gulf of Mexico represents a low energy microtidal shelf environment, with a modal wave height of 1.0 m and wave periods ranging from 5 to 6 s (BOYD and PENLAND, 1984). Fair weather conditions dominate, in which generally low speed southerly winds are unable to

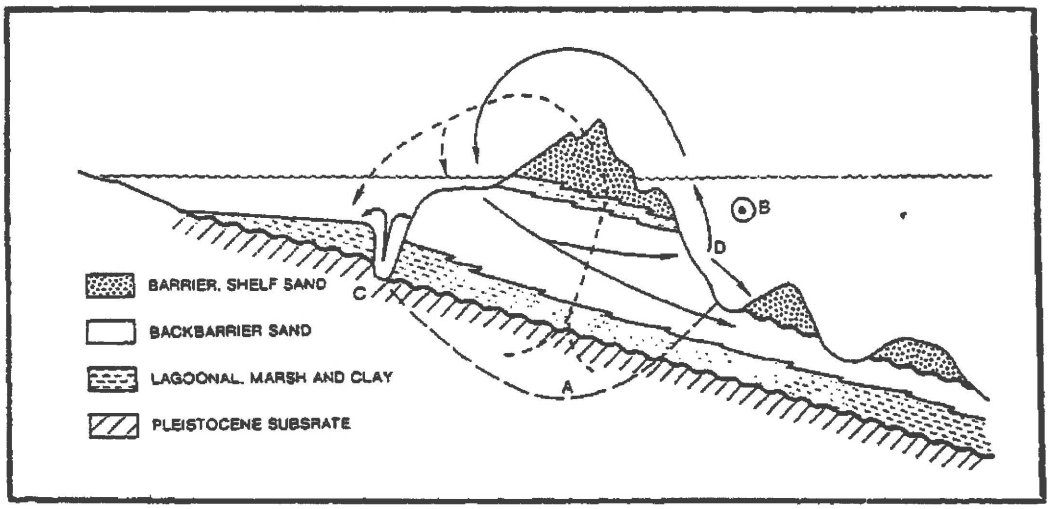

Figure 3.10. Schematic sediment budget for a landward migrating barrier on the middle Atlantic shelf. A= Sand eroded from an inlet throat (ultimate source) is deposited in flood tidal delta; mud eroded from inlet is deposited on lagoon floor. B= Sand eroded from Pleistocene headland (ultimate source) is supplied to system via littoral drift. C= Sand and mud is also eroded by tidal channel in lagoon (ultimate source). D= Sand eroded from the nearshore (ultimate source) moves onto beach or toward shelf sand sheet (from NIEDORODA *et al.*, 1985b).

generate waves or current flows of sufficient strength to rework sediments beyond 10 m water depth (SNEDDEN *et al.*, 1988). However, storm events associated with the passage of cold fronts in winter, or hurricanes and tropical storms in summer, are accompanied by strong onshore or along-shore winds. SNEDDEN *et al.* (1988) have found from current meter arrays that these conditions produce a three-layered flow in the geostrophic zone, with an onshore directed surface current, a strong along-shelf interior flow to the southwest, and an obliquely offshore directed bottom boundary flow. During hurricane events, geostrophic currents have been measured at speeds of up to 1.0 ms^{-1}, and the combined wave-current flows generated can transport sediments as far as 65 km from the shoreline (MAZZULLO, 1986).

Deposits on the east Louisiana-Texas shelf form a complex mosaic of fine and very fine sand, silt and clay of late Quaternary age, formed over a very low gradient (1: 3000) surface (BOYD and PENLAND, 1984; MAZZULLO, 1986). Shelf deposits were once thought to have been transported from the major river systems of the Colorado, Brazos and Mississippi, although smaller river systems within the Texas and Louisiana coastal plains are now also recognised as important sources of shelf deposits (MAZZULLO, 1986). Off the Louisiana coast, mean grain size varies from 2.6 ϕ on the shoreline to 3.9 ϕ at the base of the nearshore zone, with prodelta muds dominating further offshore (BOYD and PENLAND, 1984). On the Texas coast, modern shelf sediments consist of thin discrete beds (1 to 10 cm thick) of very fine sand and silt in an otherwise clay-rich section. These discrete beds appear to have been ultimately derived from onshore sources, and are deposited by combined wave-current transport processes occurring during storm events (SNEDDEN *et al.*, 1988).

Shelf and barrier deposition on the Louisiana coast presently occurs through a well defined three-stage cycle (Figure 3.11; PENLAND *et al.*, 1981). Distributary mouth sands are initially reworked into flanking spits and barrier islands. Following upstream diversion, the delta complex becomes abandoned and ongoing subsidence induces a sea-level transgression, thus forming an intra-deltaic lagoon behind a barrier island arc. With continued transgression and loss of the deltaic sand source, barrier migration cannot keep pace with the subsidence and lagoon shoreline retreat. Barrier deposits are then reworked offshore below the base of the nearshore zone, resulting in the formation of a subaqueous inner shelf shoal (BOYD and PENLAND, 1984).

Another important region in North America is the Oregon-Washington continental shelf, located on the west Pacific Ocean coast. This is a leading edge coast fronted by only a narrow and steep continental shelf (17 to 74 km wide, 145 to 183 m deep at its outer edge), but is characterised by well developed beaches and a large sediment prism within the coastal and nearshore zone (DAVIS and HAYES 1984). The Oregon-Washington shelf is a low macrotidal coastal setting (tidal ranges up to 4 m), however, the coastal morphology is distinctly wave-dominated with shore-parallel spits developed across estuary mouths and an absence of ebb tide deltas (DAVIS and HAYES, 1984). The shelf is characterised by an allochthonous sediment regime, with terrestrial sediments mainly derived from the Columbia River However, unlike the Texas-Louisiana coast, large fluvial delta

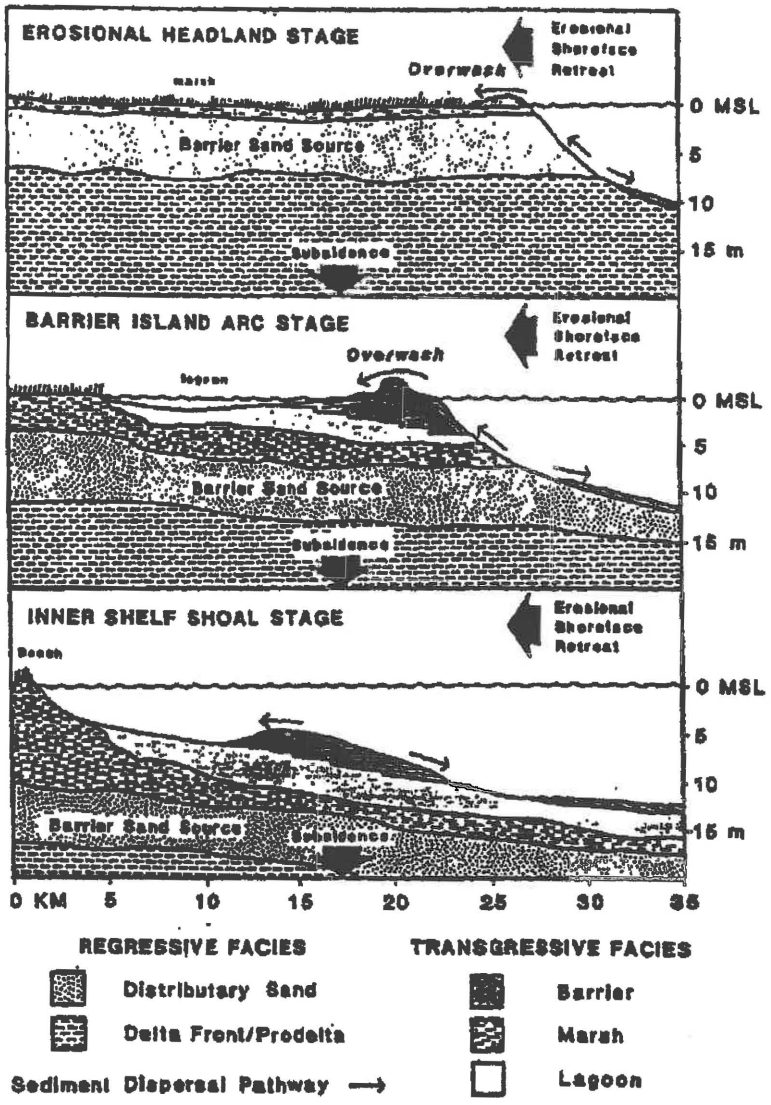

Figure 3.11. Sediment inputs to coastal barrier systems of the Mississippi Delta are controlled by the process of subsidence and erosional shoreface retreat. The original sand source lies in distributary and pre-existing barrier deposits. During transgressions, this source is reworked to form new barrier deposits by erosional shoreface retreat until ongoing compactional subsidence removes the sand source below the base of the shoreface, resulting in eventual barrier submergence. (BOYD and PENLAND, 1984).

systems are not present, as drowned river valleys act as a sink for both terrestrial and marine bedload material, and allow only very fine sand and finer sediments to filter through into the shelf transport system during periods of high river discharge (KULM *et al*, 1975).

The Pacific coast of North America is characterised by a high energy swell environment, with strong seasonal fluctuations. Lower wave conditions occur during spring and summer, with observations of H= 2 m and T= 15 s on the Californian coast further south (SEYMOUR *et al.*, 1982). The most severe wave conditions occur in fall and winter, when winds associated with low pressure systems reach speeds of 40 knots or more, and waves of between H= 3 to 6 m are maintained for long durations (KULM *et al.*, 1975). Water circulations are characterised by the southward-directed California Current in ocean waters, and seasonal northerly and southerly flows in winter and summer respectively over the continental shelf (KULM *et al.*, 1975).

Sedimentation patterns on the Oregon-Washington shelf have been conceptually presented by KULM *et al.* (1975). Basal sands and gravels found over much of the shelf were deposited during the Holocene marine transgression which terminated here about 5000 to 7000 y.B.P. Since then, modern terrestrial sands and muds have been transported to the shelf in turbid layers at the surface and mid water depths (associated with the seasonal and permanent thermocline respectively), and a bottom layer generated by rippling and wave and current resuspension on the sea floor (Figure 3.12). During periods of moderate wave conditions, clays and silts are deposited and immediately mixed with underlying basal sands by benthic organisms to form a mixed mud and sand facies. In areas of high sediment supply offshore from the major river systems, mud accumulates more rapidly, and the zone of benthic reworking shifts upwards away from the basal sand to form a mud facies over a smooth mid shelf surface. The extent of this mud facies is limited onshore by wave stirring, and offshore by shelf edge turbulence and sediment by-passing. The mud facies develops slowly, as surface waves periodically resuspend silts and clays, particularly during winter, and transport them seawards. Substantial portions of the inner shelf are mantled by modern very fine sands, particularly where river discharge and sediment input are highest. In regions of low sediment supply, particularly on the central Oregon coast, little mud or very fine sand accumulates, and relict sand and gravel form a rough shelf surface.

3.3.2. East Australia

The east Australian coast is another storm-dominated region which has been the subject of several important shelf investigations, particularly on the New South Wales (N.S.W.) coastline. This region has been characterised by relatively stable sea level conditions for the past 6500 y (THOM and ROY, 1984), and forms a microtidal coastal setting. The continental shelf is very narrow and steep, and is more comparable to the active Pacific American coast than the Atlantic passive coast, with inner shelf gradients of 1: 100 found off Sydney (FIELD and ROY, 1984; GORDON and HOFFMAN, 1986). This results in a high wave energy coastline, with dissipation of only 4% of deep water incident wave energy, compared to 48% to 84% on the North American

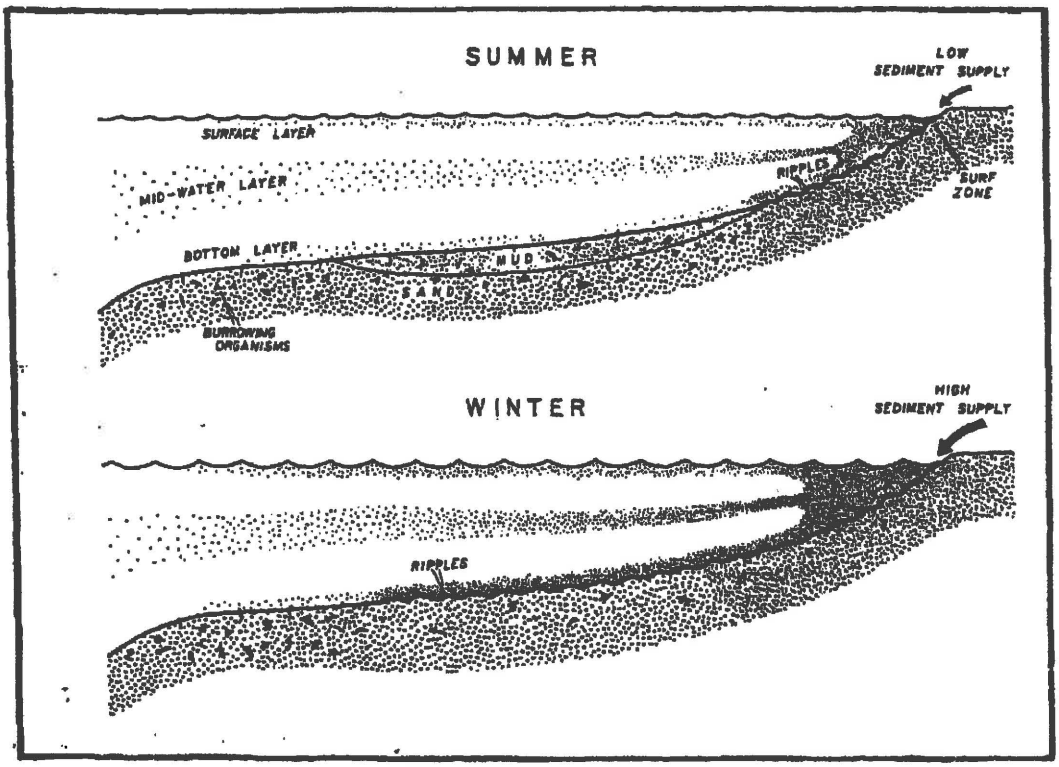

Figure 3.12. Seasonal sedimentation regime for the Oregon shelf. Sediment rippling and turbid layer transport are enhanced during the winter due to high sediment input from coastal streams and long period waves that ripple the bottom sediments in water depths of at least 125 m. Turbid layer transport, especially in the surface and mid-water layers, is greatest during late spring off the Columbia River (from KULM *et al.*, 1975).

mid Atlantic coast, and 58% in the Gulf of Mexico (WRIGHT, 1976). Modal wave conditions are characterised by persistent swell waves from the south and southeast (H= 1.5 m, T= 10 s; SHORT, 1987), with winter storms producing waves observed as high as H= 10 to 12 m and T= 14 to 16 s (GORDON and HOFFMAN, 1986). Studies of sediment transport on the Sydney continental shelf by COWELL and NIELSON (1984) and GORDON and HOFFMAN (1986) have shown that whilst the dominant steady current direction is to the south, bedload transport occurs mainly during episodic storm events which generate northerly downwelling currents and high energy wave conditions, resulting in a net movement of shelf sediments to the north.

Embayments on the N.S.W. coast are characterised by bay barriers composed of dune ridge sequences or larger dune complexes, seawards of drowned river valleys which trap fluvial sands in upper estuary margins (ROY *et al.*, 1980). The highly compartmentalised nature of the coast inhibits longshore sediment transport between embayments, and a lack of modern terrigenous supply of sediments to the coast from river systems (except the Shoalhaven River) has resulted in an autochthonous offshore source of coastal sediments from the continental shelf (ROY and THOM, 1981). Along the N.S.W. coastline, several important variations in morphology occur from south to north. These include a general broadening of the continental shelf, and an increase in the size, age and complexity of coastal deposits. Although barrier deposits of Holocene age are found along the entire N.S.W. coast, deposits of Pleistocene age (inner barrier deposits) are restricted to the section of coast north of Newcastle (latitude 33°S).

To account for these variations in coastal morphology, ROY and THOM (1981) proposed that the dominant southerly wave climate of the southeast Australian coast provides the potential for sediment to be eroded from the southern N.S.W. shelf and deposited on the northern shelf. This process would mainly have occurred during glacial events throughout the Quaternary period, when the shoreline was located away from the present highly embayed coastline, and on the relatively flatter present outer shelf region. A detailed mineralogical study of marine sands along the N.S.W. coast by HUDSON (1985) suggests a southerly source for marine sediments on the Sydney inner shelf, and thus gives evidence in support of the model proposed by ROY and THOM (1981).

In addition, ROY and THOM (1981) propose two different responses to marine transgressions for the northern and southern regions. On the northern N.S.W. coast, marine transgressions in both Holocene and Pleistocene times have resulted in the onshore reworking of shelf sediments to form subaerial barrier deposits (Figure 3.13 A). On the southern N.S.W. coast, marine transgressions over a relatively steeper continental shelf have resulted in the offshore reworking of marine sediments (Figure 3.13 B). It was only during the Holocene marine transgression that subaerial barriers formed on the southern coastline, from the reworking of sand deposits stranded high on the inner shelf during the last Pleistocene Interglacial Period.

Shelf deposits show two basic patterns on the N.S.W. coast. Offshore from most embayments, three main sediment facies are usually found: nearshore sand; inner shelf sand; and mid shelf

muddy sand (Figure 3.14; ROY and STEPHENS, 1980). Sedimentation is believed to be presently active in the nearshore and mid shelf zones, but inner shelf sands are of a palimpsest nature. Nearshore sands occupy a concave-up surface extending to depths of 15 to 30 m. They show a seaward fining trend from medium to fine sands in upper nearshore depths (4 to 12 m), but are relatively uniform fine sands on the lower nearshore surface. Bedforms range from small ripples and large symmetrical sandwaves on upper nearshore sands, to small symmetrical wave-formed ripples on the lower nearshore surface. Inner shelf sands occur to depths of 50 to 60 m, and are characterised by extensively iron stained medium to coarse, and in places gravelly sands. Inner shelf deposits are generally poorly sorted due to their polymodal character, and are often reworked by waves into megaripple bedforms. The abrupt change in grain size between outer nearshore and inner shelf sands suggests that the latter do not significantly contribute to the modern coastal sediment budget. Mid shelf sediments occur seawards of the 50 to 60 m isobath, and are fine to very fine grained muddy sands. The occurrence of fine sediments in this region suggests a 'low energy window' between the wave-dominated inner shelf and current-dominated outer shelf zones.

Off many steep rocky sections of the N.S.W. coast, the shelf is characterised by a relatively thick, convex-up, inner shelf 'sand body' (Figure 3.15). These features have been extensively studied on the Sydney inner shelf, where they form 10 to 30 m thick deposits, extending from depths of 30 to 70 m for at least 30 km along the coast (FIELD and ROY, 1984). Shelf deposits across these 'sand bodies' differ from those on other parts of the N.S.W. coast, in showing a relatively uniform distribution of medium to fine sands across their surfaces, with no apparent distinction between nearshore and inner shelf sands, but a distinct offshore boundary with mid shelf deposits (COWELL and NIELSON, 1984). Detailed morphological investigations have shown the 'sand bodies' along-shelf surfaces resembles a large scale (non-mobile) sand wave field, with numerous seaward widening (50 to 100 m wide) coarse megarippled sand channels occurring on the southern flanks of large sand body lobes (COWELL and NIELSON, 1984; FIELD and ROY, 1984). This shows that they are modified by northerly storm-generated currents. However, there is extensive morphological and stratigraphic evidence that they have formed from the offshore reworking of pre-Holocene dunes fronting the present day marine cliffs by storm-generated downwelling currents (Figure 3.15; FIELD and ROY, 1984; ROY, 1985). Coarse megarippled channels appear to be the main conduits for the offshore movement of fine sand, with the megaripple bedforms causing a preferential mobility of fine sand in the channels due to their higher surface roughness and hence higher shear stress (COWELL and NIELSON, 1984).

Coastal barrier genesis in N.S.W. began when sea level stabilised ~ 6500 y. B.P., with sediments derived from the adjacent continental shelf. Stratigraphic and radiocarbon dates show that barrier formation in most embayments was complete by about 3000 y. B.P., and have since either remained stable or eroded (THOM *et al.*, 1978). The initial onshore movement of shelf sediments began when landward rates of shoreline translation during the Holocene marine transgression exceeded the capabilities of onshore sediment transfer, resulting in an over-steepened

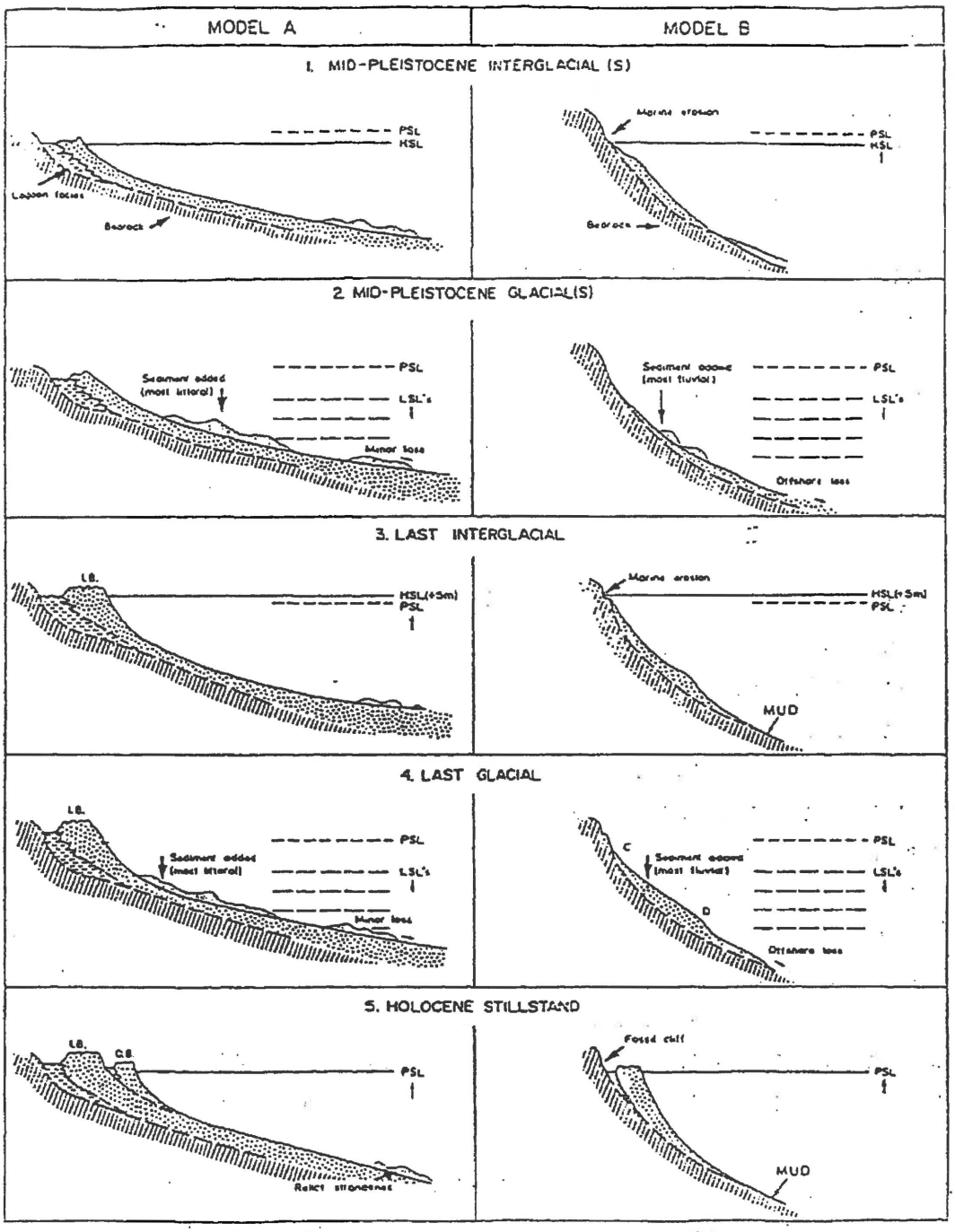

Figure 3.13. Schematic models for late Quaternary deposition along the A) northern N.S.W. and B) southern N.S.W. coast during sea level oscillations, as proposed by ROY and THOM (1981).

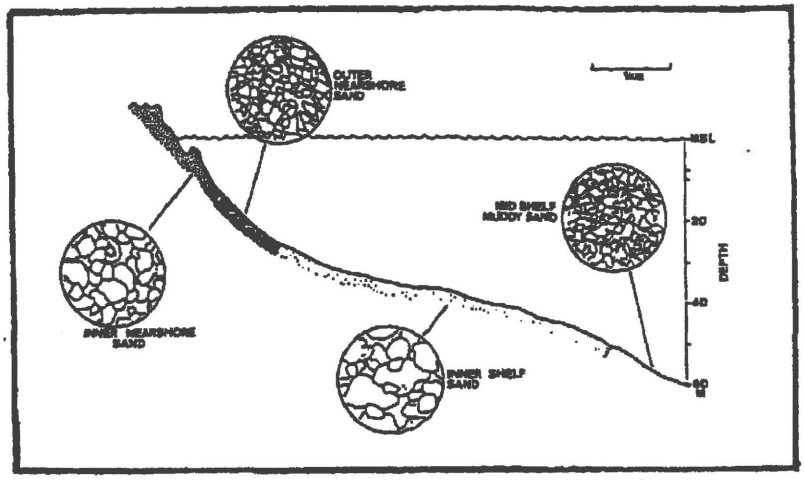

Figure 3.14. Shelf sediment lithofacies recognised on the N.S.W. coast by ROY and STEPHENS (1980), with illustrated grain sizes and shapes as seen in photomicrographs.

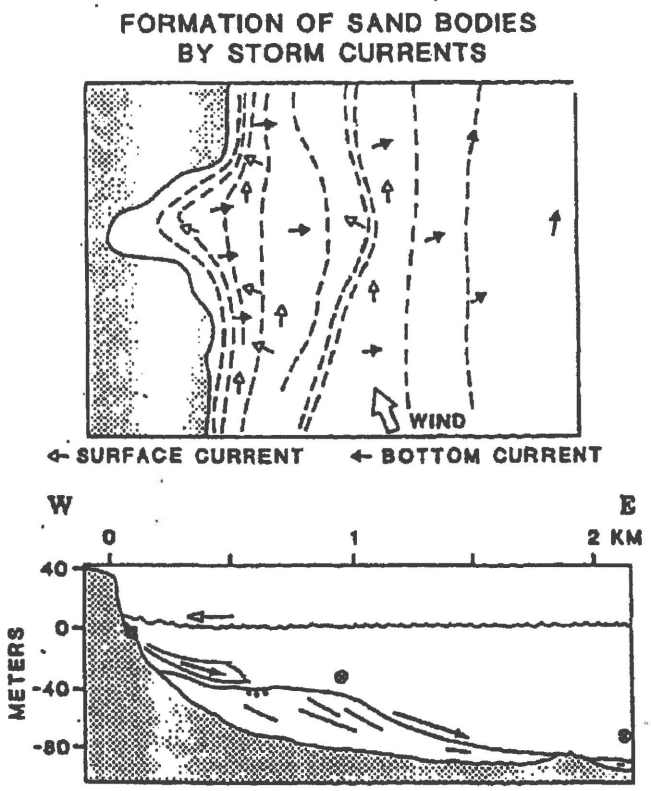

Figure 3.15. Schematic diagram showing shelf 'sand body' morphology and hypothesised offshore transport system off the Sydney coast (FIELD and ROY; 1984). Southerly winds on the N.S.W. coast force water onshore and result in downwelling and seaward returning bottom flows. Further offshore these flows become parallel to the coast under the influence of Coriolis forces and wind-generated coastal currents.

disequilibrium offshore profile (BOYD and PENLAND, 1984). When sea level stabilised at it's present position, equilibrium is inferred to have been established by the action of asymmetrical wave orbital currents reworking sediments onshore from either a shallower inner shelf surface, or a convex bulge of nearshore sediments (Figure 3.16; ROY and THOM, 1981). Barrier growth was initially rapid due to this large onshore flux of sediments, but has since halted as shelf deposits have equilibrated.

3.3.3. New Zealand

CARTER and HEATH (1975) have described New Zealand continental shelves as generally dominated by the effects of storm-generated flows. Shelf tidal currents are considered to be dominant only in the Cook and Foveaux Straits and around North and East Capes. However, along most of the remaining New Zealand coastline, researchers such as HEATH (1978) and KIBBLEWHITE *et al.* (1982) have found wind-generated currents dominating inner shelf flow patterns. Sea level conditions in New Zealand appear to have been very similar to those in east Australia, with an initial rapid rise (10 to 15 $mm.y^{-1}$) during the Holocene marine transgression from 12 000 to 6500 y. B.P., since when sea level has remained essentially at its present position (GIBB, 1986). However, radiocarbon dates and seismic evidence from the east South Island by CARTER *et al.* (1985) indicate that the Holocene marine transgression was punctuated by sea level stillstands often accompanied by the construction of seaward thinning sediment wedges.

Shelf deposits around New Zealand are comprised of modern and relict terrigenous and biogenic sediments with a range of grain sizes (Figure 3.17; CARTER and HEATH, 1975). Modern terrigenous sediments dominate the Westland and Wairarapa-Hawkes Bay shelf, as well as the nearshore zones of other regions. Modern nearshore sediments are usually medium to fine sands, whereas muds dominate mid and outer shelf deposits. Relict clastic sediments are mainly fine to medium grained sands and gravels, and usually occur in mid and outer shelf deposits, particularly off the Otago-Canterbury and Southland coast. Calcareous biogenic sediments are common where modern terrigenous sediments are low, such as the mid and outer shelf of Southland, Otago and Northland.

One of the most intensively studied shelf regions of the New Zealand coast is on the northeastern coast of the North Island. Numerous workers have described from various locations the presence of an offshore belt of medium-coarse grained sand, and a finer nearshore sand facies, including: Pakiri (HILTON, 1990), Omaha (SCHOFIELD, 1978, 1985; RILEY *et al.*, 1985), Whangarei Harbour (BLACK and HEALY, 1983, 1988), and Tauranga Harbour (DAHM and HEALY, 1980, HARMS, 1989). These coastlines appear to consist predominantly of sands of autochthonous shelf origin which were reworked onshore during the Holocene marine transgression, with no major input of modern terrigenous sands as yet identified.

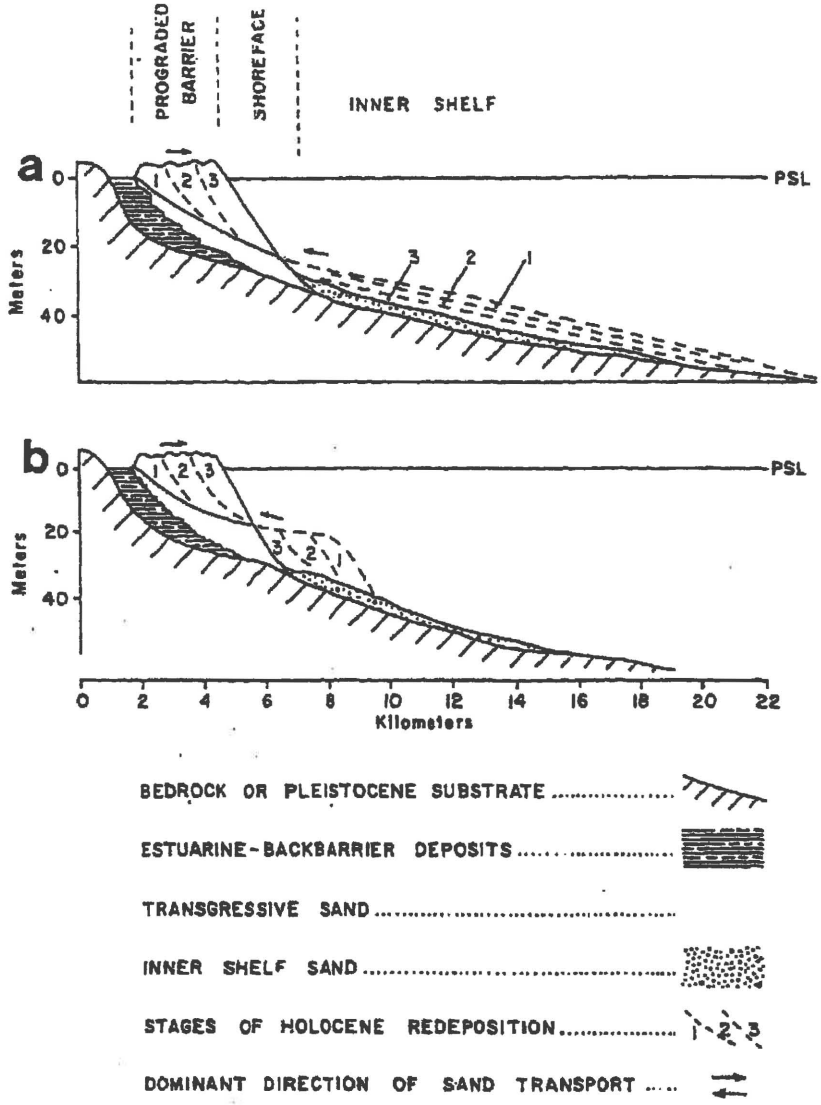

Figure 3.16. A conceptual model for barrier formation on the N.S.W. coast as proposed by ROY and THOM (1981) with either a) onshore reworking of an elevated shelf surface, or b) onshore reworking of a convex bulge of nearshore sediments.

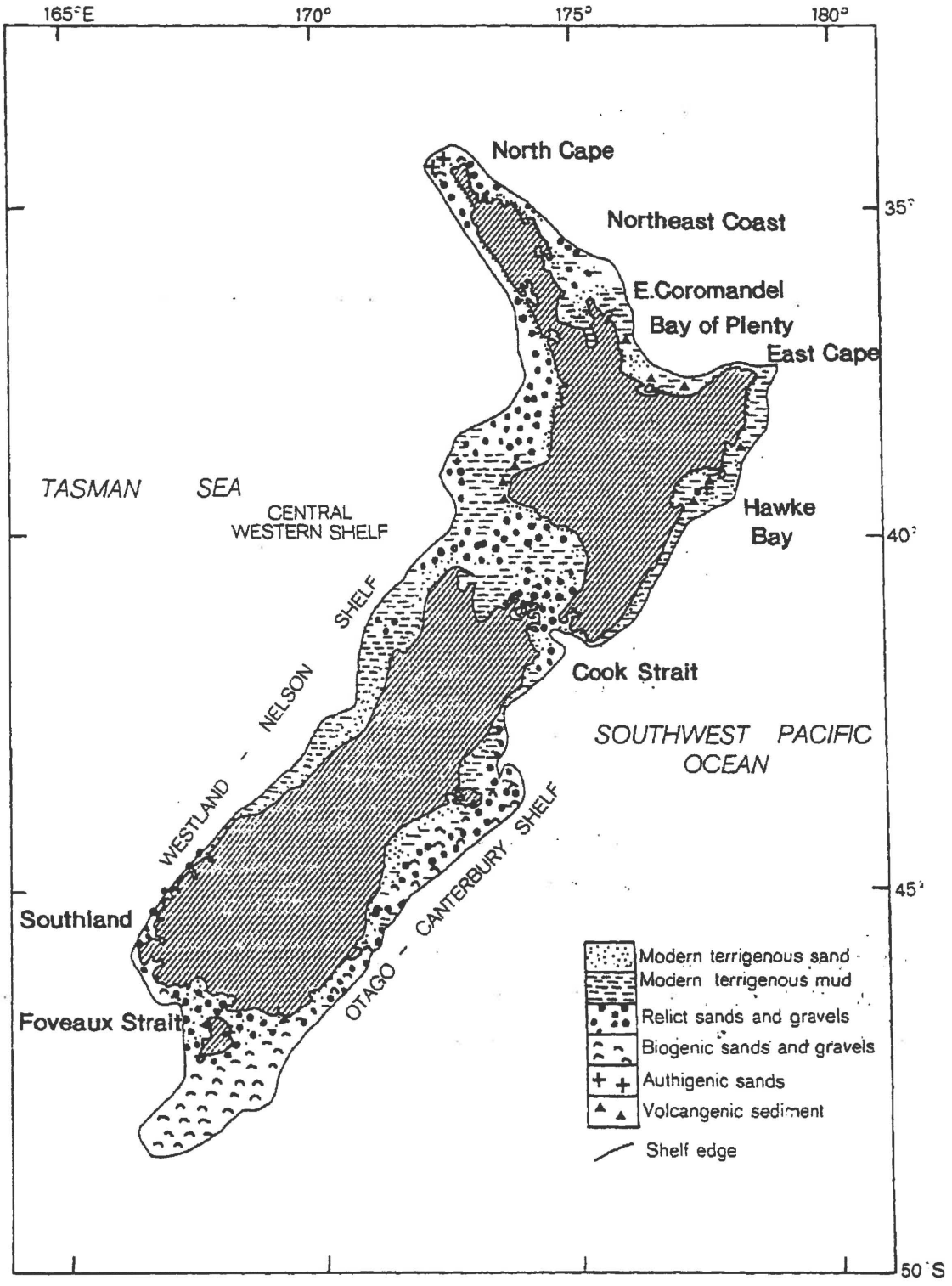

Figure 3.17. Distribution of main sediment types on the New Zealand continental shelf (from CARTER and HEATH, 1975).

Omaha Bay is located on the moderately protected outer limits of the Hauraki Gulf, just north of Auckland. SCHOFIELD (1978) studied the sea floor within Omaha Bay, and found it to consist of three main offshore zones:

1. A concave-up upper nearshore surface consisting of seaward fining sands.

2. A convex-up lower nearshore surface characterised by an abrupt increase in grain size to medium sands.

3. An abrupt change in slope to the relatively flatter inner shelf, consisting of silty fine sands.

Based on shallow core and radiocarbon data, SCHOFIELD (1978) proposed that sedimentation in Omaha Bay has ultimately been controlled by changes in sea level, the seaward fining sands being deposited in second-order sea level transgressions, and the coarser shelly lags formed during second-order sea level regressions. That is, as sea level fell the tendency would be for a winnowing action of the sea floor sediments, with a consequent removal of the finer sand fraction (RILEY *et al.*, 1985).

Subsequent studies on the Pakiri coast just north of Omaha by HILTON (1990), and at Tauranga Harbour by DAHM and HEALY (1980) and HARMS (1989), have identified similar offshore facies, with fine, medium-coarse, and muddy very fine sands associated with the shelf morphological components of the nearshore, inner shelf and mid shelf respectively. However, HILTON (1990) related these sediment patterns to the modern shelf hydraulic regime rather than sea level shifts, with a landward transport of fine nearshore sands occurring during calm weather periods by the shoaling action of surface currents, and a similar onshore transport of mid and inner shelf sands by storm waves, with a counter wind-generated downwelling offshore flow of sands on the nearshore surface (Figure 3.18). Other investigations have also identified that coarse grained shelf sands can form under the modern shelf hydraulic regime, such as by refraction and focussing of wave rays at Whangarei Harbour (BLACK and HEALY, 1988), and by combined storm wave-current flows at Tauranga Harbour (HARMS, 1989). This latter study also gives supporting evidence to HILTON's (1990) hypothesis that shoaling waves are important for the onshore transport of nearshore and inner shelf sands, as shown by the observed landward movement of sediments from dredge mounds on the inner shelf (Figure 3.19).

The western Cook Strait shelf region on the southwest coast of the North Island has been studied by LEWIS (1979). In contrast to the northeast coast, this is constantly exposed to the west coast swell wave climate, with modal conditions of H= 1.2 m and T= 6 to 9s, and storm waves observed as much as H= 12 m and T= 9s (PICKRILL and MITCHELL, 1979; LEWIS, 1979). Two distinct sediments occur along the coast, a black augite and hornblende rich sand derived from littoral drift of laharic deposits near Mount Egmont, and fine felsic sands from rivers draining the Wanganui Basin and Central North Island volcanic region. Much of the river-borne material reaches the coast

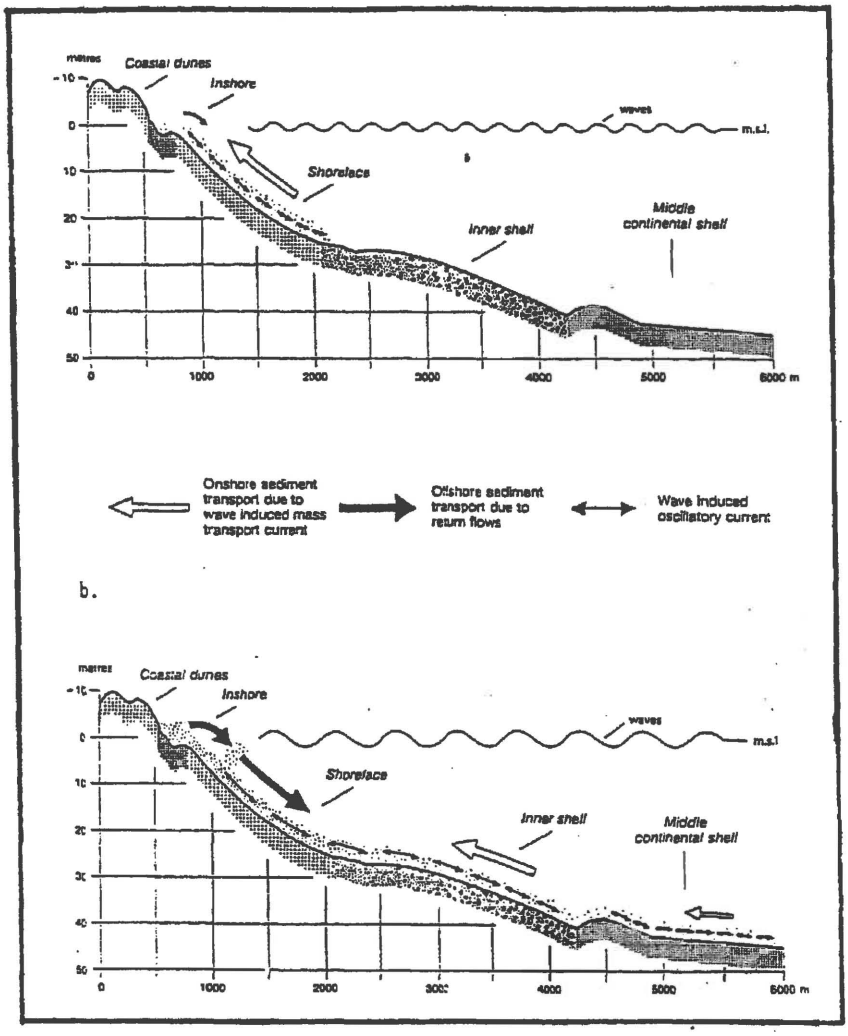

Figure 3.18. Conceptual model for sediment transport on the nearshore and inner shelf zones a Pakiri by HILTON (1990): a) calm conditions with net onshore movement over the nearshore surface; b) storm conditions with offshore movement of nearshore sands by downwelling currents and onshore movement of inner and mid shelf sands due to mass transport currents associated with storm waves.

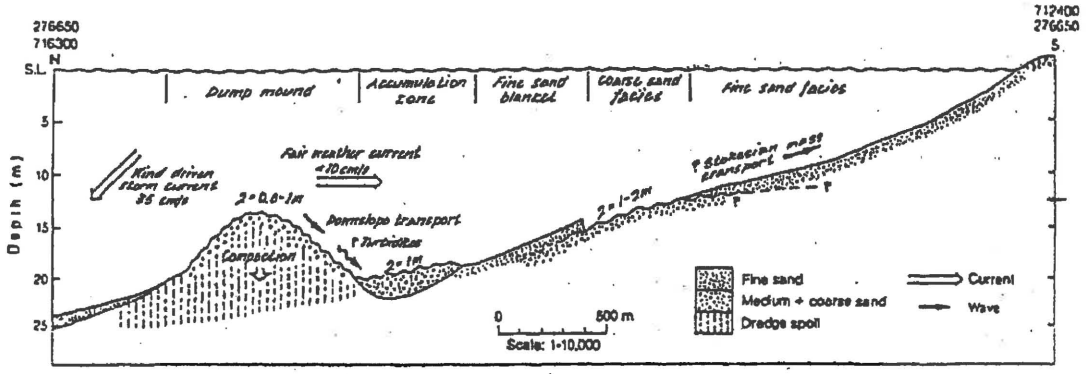

Figure 3.19. North-south orientated offshore beach profile at Tauranga showing the sediment facies distribution and hydrodynamic processes responsible for dispersion of offshore dredge spoil (from HARMS, 1989).

during peak flow conditions, where it subsequently by-passes the surfzone to deposit on the inner and mid shelf surfaces. The shelf is characterised by large sand ridges (4 to 12 m high, several 100 m's wide and km's long), which are aligned sub-parallel to the coast. The ridges are composed of the black mafic sands, and are not presently connected to the nearshore zone, indicating that they were formed under lower sea level conditions when these black sands were transported onto the shelf. Fine felsic sands form smaller ribbons within the ridge troughs, and appear to respond to the modern hydraulic regime of combined storm wave-current transport to the southeast. These fine sand ribbons represent a feather edge of a seaward migrating nearshore wedge of modern sediments.

The Otago-Canterbury shelf on the east coast of the South Island is also one in which modern terrestrial sediments are an important part of the shelf transport system. Sediments are transported to the northeast along the shelf by the modern hydraulic regime which comprises of a southerly swell, the Southland Current, strong tidal flows, and storm-induced currents (CARTER and HEATH, 1975). Modal waves along the Otago-Canterbury coast are characterised by H= 1.8 m and T= 7.4 s, and sand appears to be transported across the inner shelf on a daily basis even under fair weather conditions (CARTER and CARTER, 1986).

Shelf sediments on the central Otago shelf consist of four main facies which occur in distinct shore-parallel belts (Figure 3.20; CARTER *et al.*, 1985). Relict gravels and palimpsest sands characterise mid shelf deposits, while a biogenic carbonate facies of modern and relict origin occurs on the outer shelf. Of most significance is a modern sediment wedge which extends across the nearshore and inner shelf zones, and consists of fine grained sands up to 34 m in thickness, derived mainly from the Clutha River. This appears to have evolved in two main stages, with a lower wedge formed in an earlier stillstand period during the Holocene marine transgression about 9600 to 8800 y. B.P. when the shore stood between 27 to 24 m lower than present, and an upper wedge formed under present sea level conditions over the last 6500 y. (CARTER and CARTER, 1986).

The Canterbury coast has a similar input of modern river sediments and northeasterly transport of shelf sediments (CARTER 1986). Here however, modern inputs are much greater, with sediments presently accumulating at a rate of 1 to 3 m/1000 y. on the inner shelf in 60 m depth. These are mainly derived from gravels and sands within local river systems, 95% of which is ground up in the beach and surfzone to produce mud. Offshore, very fine sand rapidly settles out onto the inner shelf in depths of < 30 m where it is transported as bedload, while muds tend to remain in suspension (GIBB and ADAMS, 1982). However, a modern sand wedge has not been able to develop here as at Otago, as the sediments are entrained into a northeasterly transport system from the river mouths (CARTER, 1986).

New Zealand continental shelves therefore show a variety of different sedimentation regimes, with autochthonous sediments appearing to dominate the northeast coast of the North Island (in which the study area is located), but modern terrigenous sediments being of greater significance

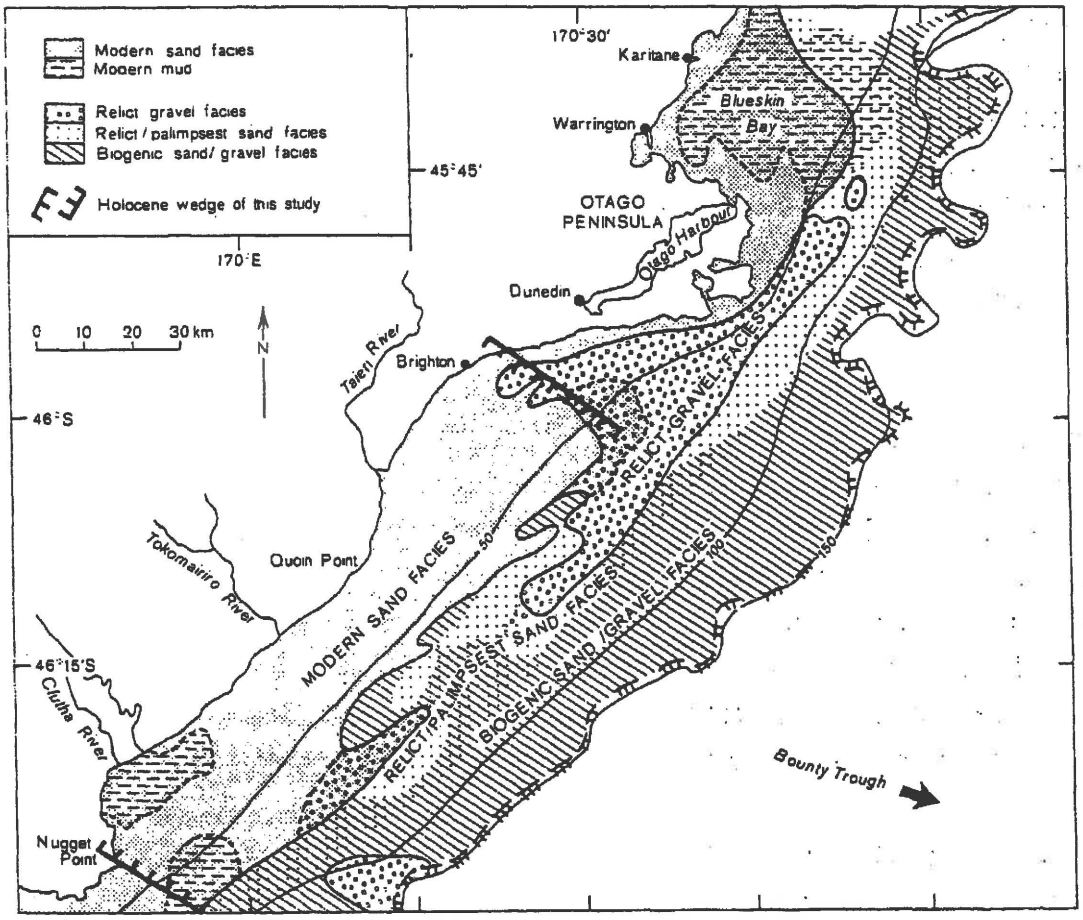

Figure 3.20. Holocene sand wedge with its modern sand mantle on the Otago continental shelf, as determined from surface sediment samples, and associated sediment facies (from CARTER and CARTER, 1986).

along the western Cook Strait and Otago-Canterbury coastlines producing allochthonous nearshore and inner shelf sedimentation systems.

3.4 SUMMARY

This review of some of the literature about nearshore and inner shelf sedimentation processes on modern continental shelves provides a background for the subsequent interpretations and conceptual modelling of the E.C.S.S. data. Important concepts which require further consideration in this study include:

1. Continental shelves are amongst the most complex modern environments to study, in that sedimentation patterns may reflect both modern and past phases of deposition or erosion from a variety of marine and terrestrial processes. However, they can generally be broken down into autochthonous settings in which modern shelf sediments were derived from older relict or in situ sources, and allochthonous settings where shelf sediments are presently derived from terrestrial sources.

2. Continental shelves can be grouped into three broad categories depending on their dominant hydrodynamic processes of sedimentation, including tide-dominated, oceanographic current-dominated, and storm-dominated shelves. From the background oceanographic data presented in Chapter 2, the east Coromandel shelf would fit into the latter storm-dominated category.

3. Processes of sedimentation of most importance to storm-dominated shelf settings are those associated with waves and wind-generated currents. Wave-induced flows of importance are mainly those associated with asymmetrical orbital flows in shallow water, which lead to an onshore sediment transport. However, reverse offshore directed transport can also result from either amplitude-modulated waves associated with groupy wave conditions, or the complex interaction of wave orbital currents with bedforms. Wind-generated currents usually take the form of a cross-shore directed upwelling or downwelling flow, and an associated alongshore geostrophic flow. However, the strength and complexity of wind-forced circulations depend on factors such as the strength, duration and orientation of the wind with respect to the coastline, and the nature of weather systems associated with the winds. Sedimentation processes on storm-generated shelves are inevitably linked to the interaction of both wave- and wind-generated flows, which leads to the simplified 'rule of thumb' that waves determine when, and currents determine where, sediments will be transported.

4. Continental shelves are commonly divided up into discrete morphological provinces or zones, including the surfzone, nearshore (or shoreface), inner shelf, mid shelf, and outer shelf. The nearshore and inner shelf zones are the primary subject of this study, the former defined as the steep seaward dipping, usually concave-up surface which extends from the offshore bar to a point

of noticeable decrease in slope, where the inner shelf surface then extends seawards to the flat mid shelf plain. These morphological zones are often linked to dynamic zones within coastal waters, with the friction-dominated zone, transition zone, and geostrophic zone, coinciding with the nearshore, inner shelf, and mid shelf zones respectively. However, the dynamic zones are highly variable depending on the prevailing conditions, whereas shelf morphological zones are more fixed. It is thus difficult to determine whether the morphological zones are a response to average, storm, or extreme storm conditions.

5. Previous studies of storm-dominated shelves from different environmental settings around the world provide further insight into the processes which influence nearshore and inner shelf sedimentation. The similarities and differences between different regions, and thus between the east Coromandel coast and other locations, is mainly dependant on their Holocene sea level history, the degree of relict versus modern sediment sources (i.e. autochthonous vs. allochthonous sedimentation patterns), on shelf slope, and linked to this, their oceanographic climate. Comparisons between these characteristics on the east Coromandel coast and other storm-dominated regions are shown in Table 3.1.

Table 3.1. Comparisons between environmental setting of the east Coromandel coastline with other storm-dominated shelves.

Location	1 Wave Climate	2 Sea Level	3 Sediment Source	4 Shelf Morphology
East Coromandel	Low energy storm-dominant	Stable	Reworked shelf, modern fluvial ?	Very steep 1:130-1:400
Mid Atlantic U.S.A.	Low energy storm-dominant	Rising	Pleistocene & shelf sands	Low gradient 1:2000
Texas-Louisiana	Low energy storm-dominant	Rising	Fluvial deltas	Low gradient 1:3000
Oregon-Washington	High energy swell-dominant	Stable	Relict shelf & modern fluvial	Very steep 1:117-1:400
East Australia	High energy swell-dominant	Stable	Reworked shelf sands	Very steep 1:100
Northeast New Zealand	Low energy storm-dominant	Stable	Reworked shelf sands	Steep 1:400
West Cook Strait	High energy swell-dominant	Stable	Relict shelf & modern fluvial	Steep 1:600
Otago-Canterbury	High energy storm-dominant	Stable	Relict shelf & modern fluvial	Steep 1:400

CHAPTER FOUR

REGIONAL OCEANOGRAPHIC PATTERNS

4.0. INTRODUCTION

As one aspect of the investigation into the sediment transport processes operating on the east Coromandel coast, a study of the offshore current patterns was carried out between June 1985 and September 1990, concentrating on the segments of coast from Waihi to Onemana, and Opito Bay to Whangapoua (Figure 4.1).

A detailed assessment of shelf current patterns was initially undertaken in the E.C.S.S., with sea-bed drifters and Aanderaa current meters deployed by Paul Dell. Sea-bed drifter experiments were conducted over an 18 month period to obtain an overview of the regional current patterns. Aanderaa current meters then provided detailed measurements at a specific site (Onemana) over the first 6 months of the sea-bed drifter experiment. To investigate the possibility of a local wind-forced origin for these currents, an anemograph was set-up on the frontal dune at Whiritoa and operated throughout the duration of these experiments. Results were subsequently integrated into a conceptual model of east Coromandel current flow patterns by the present author.

In the latter stages of this study, the present author obtained additional current meter and wind data from adjacent areas from Waihi to Whiritoa, and from Opito Bay to Whangapoua (Figure 4.1). Although these latter recordings were limited to only 6 weeks duration, they helped to show regional similarities and variations in current patterns.

4.1 METHODS

4.1.1. Sea-bed Drifters

Sea-bed drifters were chosen in this investigation as they have proved to be a reliable and inexpensive means of determining residual bottom current patterns in numerous studies (e.g. PHILLIPS, 1970; BARTOLINI and PRANZINI, 1977; GREGORY, 1979). HAMMOND and WALLACE (1982) point out, however, that interpretations from sea-bed drifters are limited to the assumption that the path travelled is in a straight line from the release to recovery point, and problems also arise in relating the drifter speed to that of the current (PHILLIPS, 1970).

Sea-bed drifters used in this study were similar to those originally designed by WOODHEAD and LEE (1960). They consisted of an orange polythene saucer, 19 cm in diameter, to which is attached a 54 cm long solid polyvinyl stem with a copper weight at its lower end (see Appendix 1A).

A total of 1000 drifters were released in four experiments between June 1985 and November 1986 by divers on the sea floor. Details of the release and recovery of drifters is given in Table 4.1. During the first two experiments in June and July 1985, drifters were released at Whiritoa, Whangamata, and Onemana in depths ranging from 10 to 33 m. The third and fourth experiments

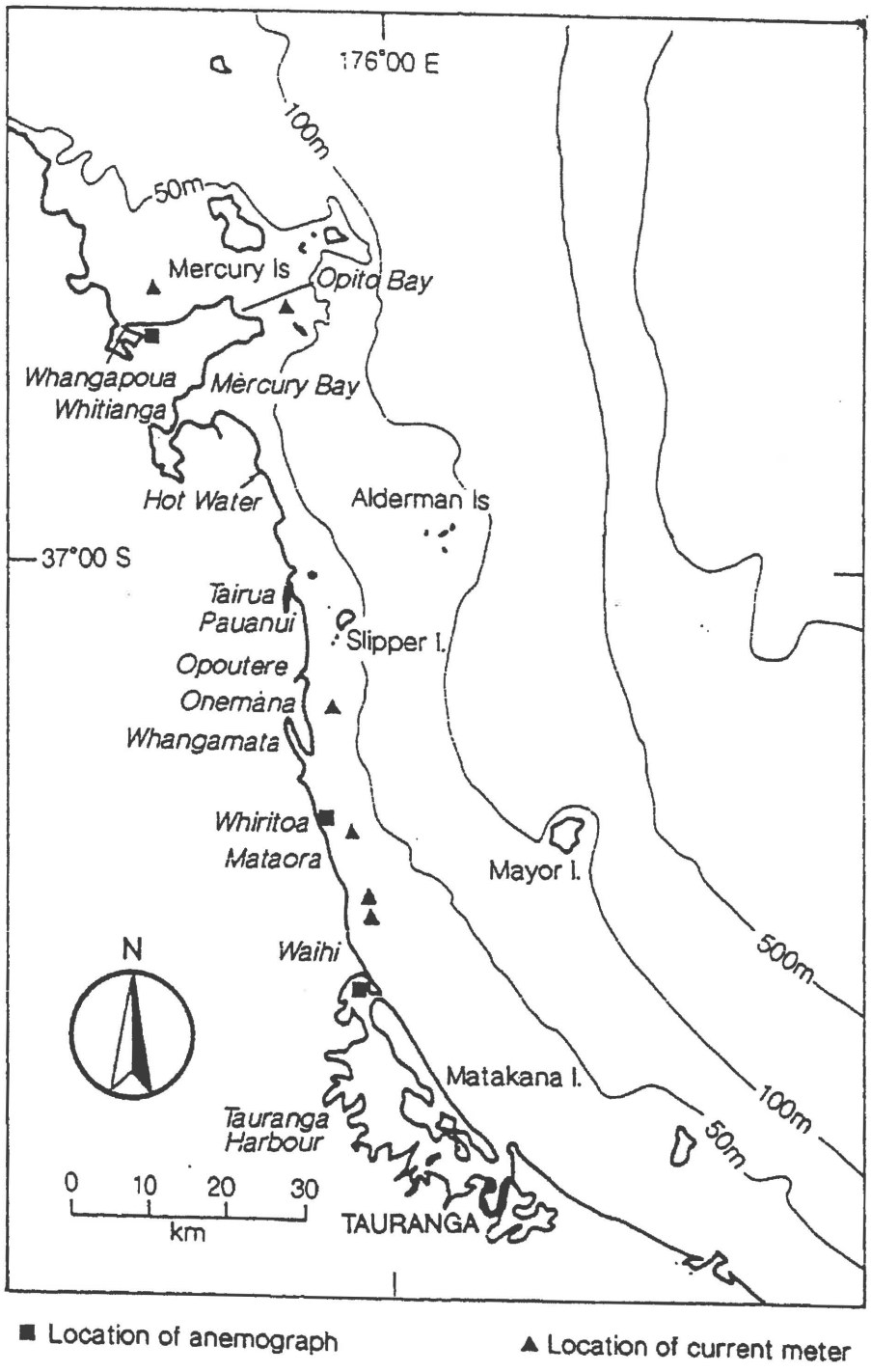

Figure 4.1. Location map of Aanderaa current meter and wind recording stations.

were conducted one year later in July and November 1986, drifters only being released at Whangamata in 17, 22 and 27 m water depth.

Table 4.1. Details of the release and retrieval of sea bed drifters.

EXPT NO	RELEASE DATE	LOCATION	DEPTH (M)	NO. RELEASED	NO. RETRIEVED	RETRIEVAL (%)	AVE. DAYS TO RETRIEVE
	6/6/85	ONEMANA	10-12	50	8	16	28
1	6/6/85	WHANGAMATA	10-12	50	27	54	8
	6/6/85	WHIRITOA	10-12	50	13	26	16
	6/7/85	ONEMANA	12	50	12	24	32
	6/7/85	ONEMANA	15	50	15	30	21
2	6/7/85	WHANGAMATA	33	50	9	18	47
	6/7/85	WHANGAMATA	15	50	11	22	42
	6/7/85	WHIRITOA	30	50	7	14	63
	6/7/85	WHIRITOA	22-24	50	10	20	67
	27/7/86	WHANGAMATA	27	100	29	29	29
3	27/7/86	WHANGAMATA	22	100	20	20	27
	27/7/86	WHANGAMATA	17	100	27	27	27
	29/11/86	WHANGAMATA	27	100	15	15	56
4	29/11/86	WHANGAMATA	22	100	20	20	61
	29/11/86	WHANGAMATA	17	50	14	28	48

Retrieval was by the general public, with the finder asked to complete a numbered card attached to the drifter giving details as to the exact time and location of retrieval, and requesting the finder to return the card upon completion.

4.1.2. Aanderaa Current Meter

The required detailed near-bottom current data for this study was gathered through use of a standard Aanderaa RCM-4 Eulerian continuous recording current meter (Appendix 1A). With this type of current meter, speed is measured by a savonious rotor and interval averaged every 15 minutes to ± 0.01 m.s^{-1} resolution. Direction is measured instantaneously with a magnetic compass to $\pm 5^{o}$, adjustments being made for magnetic variance. The current meter can also record water temperature to $\pm 0.2^{o}$ C and conductivity (salinity) to ± 0.1 $^{o}/_{oo}$.

As only a standard RCM-4 current meter was used, the main source of error in the current measurements arises from the effects of wave-induced currents (wave pumping), which can cause overspeeding of the Savonious rotor and a lagged response of the vane to flow direction changes (LYNE *et al.*, 1990a). BELL *et al.* (1988) have found that for shallow coastal waters in New Zealand (< 40 m), this type of current meter can give inaccurate speed recordings during storm wave conditions. However, VINCENT *et al.* (1981) on the Long Island shelf in North America found wave pumping only caused significant errors in shallow waters at low mean current speeds of 0.10

$m.s^{-1}$. Also, LYNE *et al.* (1990 a) established that when the mean current speed exceeds that of the wave orbital current, as is usually the situation during storm conditions, errors in speed recordings are reduced to < 10%. This source of error was further reduced by using shrouded current meters in the latter experiments, and locating the current meters in reasonably deep water (17 to 35 m). Another possible source of error is from bio-fouling of the savonious rotor and conductivity sensors, particularly after periods of about 6 weeks, which will cause inaccurate speed and salinity measurements (HEALY *et al.*, 1987; see Appendix 1A).

Due to limited resources, only one site could be used initially. This was located offshore from Onemana at a depth of 26 m. Onemana was considered the best location for the current meter as the inner shelf here appears representative of the southern exposed east Coromandel coast, with no major harbours or offshore islands to modify open shelf current flows. Two current meters were deployed (both unshrouded meters), the first (No.69236) from 6-Jun-85 to 8-Sep-85, which was then replaced by another meter (No.72046) that operated until 11-Dec-85. The meters were first calibrated by the New Zealand Oceanographic Institute (N.Z.O.I.), and later lowered on site from the ship deck and deployed at 1 m above the sea floor. At 1 m above the sea floor the occurrence of mooring motions on the current records during waves will be small, leaving just the rotor pumping and bio-fouling as the main error sources.

Later in the study, shrouded current meter systems were deployed at Opito Bay (27 m) and Whangapoua (35 m) between 19-Oct-89 and 14-Dec-89, then Waihi (17 m, 20 m; shrouded systems) and Whiritoa (30 m; unshrouded system) between 10-Sep-90 and 1-Nov-90.

Throughout these current meter recordings, a Woeffler Anemograph was used to gather continuous information on wind direction and speed (see Appendix 1A). For the various experiments outlined above, these were located at Whiritoa, Whangapoua, and Waihi respectively, at approximately 10 m above sea level. During the last experiment, a computerised Starlog recording system was also used at Whiritoa to help identify differences in wind patterns between here and Waihi (see Appendix 1A).

4.2. SEA-BED DRIFTER RESULTS

4.2.1. Retrieval Rates and Interpretations

Retrieval rates of the sea-bed drifters are shown in Table 4.1. These are generally good compared to similar studies by BARTOLINI and PRANZINI (1977) and MARSDEN (1979), ranging from 14% to 54% and averaging 24% of drifters released. However, factors affecting retrieval rates of drifters need to be briefly considered to determine how well the dispersal patterns reflect regional current patterns.

BARTOLINI and PRANZINI (1977) and MARSDEN (1979) have described factors affecting the retrieval rates of drifters as including population along the coastline, distance travelled from release site, time at sea, and prevailing sea conditions.

In this study, public access to the coastline was found to influence retrieval rates. Remote locations such as offshore islands showed lower returns and longer times to retrieve drifters. However, as much of the east Coromandel coast is regularly visited by the public for recreation, this factor should not have severely hindered or biased the results.

Distance travelled by the drifters seems to be an important factor. Retrieval rates decreased over progressively greater distances travelled, particularly within the first 10 km. This is probably because of the high number of drifters that were moved short distances onshore by wave action from their release sites.

Time at sea appears to affect retrieval rates. In general, the longer drifters remained at sea the lower was the likelihood of recovering them. This would seem reasonable as the longer they remain at sea, the greater the chance of them being lost offshore into deep water, onshore into estuaries, through sediment burial and kelp snagging on the shelf, or from arrival at a remote location.

Prevailing sea conditions did not seem to directly affect the recovery of drifters, although it would have influenced the distance travelled and time at sea. An additional factor noted in this study was the release depth of drifters. This can be seen in Table 4.1 with shallower release sites in general associated with higher retrieval rates. Again, this trend probably results from drifters released in shallower waters being moved directly onshore by wave action.

4.2.2. Sea-bed Drifter Experiments

Results from the four drifter experiments are listed in Table 4.2. This shows information on the major near-bottom current patterns based on the direction drifters were displaced, and on the relative strengths of these currents from the drifters average distance travelled and their net speeds (calculated by distance and time at sea).

Maps summarising the drifter dispersal patterns for each experiment are shown in Figures 4.2 to 4.5. The average number of days and total number of drifters found at each embayment are shown in brackets on these maps. This information allow some deductions to be drawn on the duration and direction of offshore currents during each experiment, and indicates the possibility of onshore sediment movement at certain locations.

Insets within each map show information on the wind run and direction of drifter displacement in each experiment. This allows deductions to be drawn on the degree to which winds are affecting the drifter dispersal patterns.

Table 4.2. Results from the four sea-bed drifter experiments.

EXP	DIRECTION DRIFTERS MOVED			AVE DIST TRAVELLED(KM)			AVE NET SPEED (KM/DAY)		
NO	NORTH	SOUTH	ONSHORE	MEAN	NORTH	SOUTH	MEAN	NORTH	SOUTH
1	35%	33%	32%	7.7	17.6	3.3	0.45	0.65	0.24
2	57%	30.6%	12.4%	23.5	26.9	10.7	0.52	0.47	0.29
3	35.6%	21.2%	43.2%	8.9	11.8	15.7	0.32	0.39	0.49
4	93.7%	0%	6.3%	12.6	13.0	0	0.24	0.24	0.00

Experiment No. 1 (6-Jun-85)

In the first experiment, sea-bed drifters were released in shallow water (10 to 12 m) offshore from Onemana, Whangamata and Whiritoa. During the experiment, approximately the same number of drifters was displaced either north, south or onshore, migrating on average 7.7 km from the release site and travelling at an average minimum net speed of 0.45 km.day^{-1}. However, the northward migrating drifters were displaced over a much greater distance and speed than the southward migrating ones. Most of the southerly migrating drifters were retrieved within 15 days, and the northerly migrating ones within 20 to 35 days.

During the first experiment, drifters were retrieved from only a relatively small range of locations, extending from Mataora to Tairua (Figure 4.2). Most were retrieved at Whangamata (55%), with significant numbers also at Mataora (17%), Opoutere (6.4%), Pauanui (6.4%) and Tairua (6.4%). Of the drifters retrieved at Whangamata, most of these moved directly onshore within the first 10 days. However, some also travelled north from Whiritoa. None were found to have migrated directly onshore at either Onemana or Whiritoa.

The initial southward drifter displacement pattern followed a short period of offshore winds from the west and southwest (Figure 4.2 inset). The latter change to a northerly displacement pattern followed a period of strong (up to 10 m.s^{-1}) onshore winds from the east and northeast.

The results show that a relatively weak southerly-directed current was most likely to have been present on the inner shelf during the first 20 days of this experiment. This was followed by a relatively stronger northerly directed current which was associated with high speed onshore winds (10 m.s^{-1}) from the east and northeast. Onshore currents are indicated within the 10 to 12 m depth range at Whangamata throughout the experiment, but appear to have been absent within

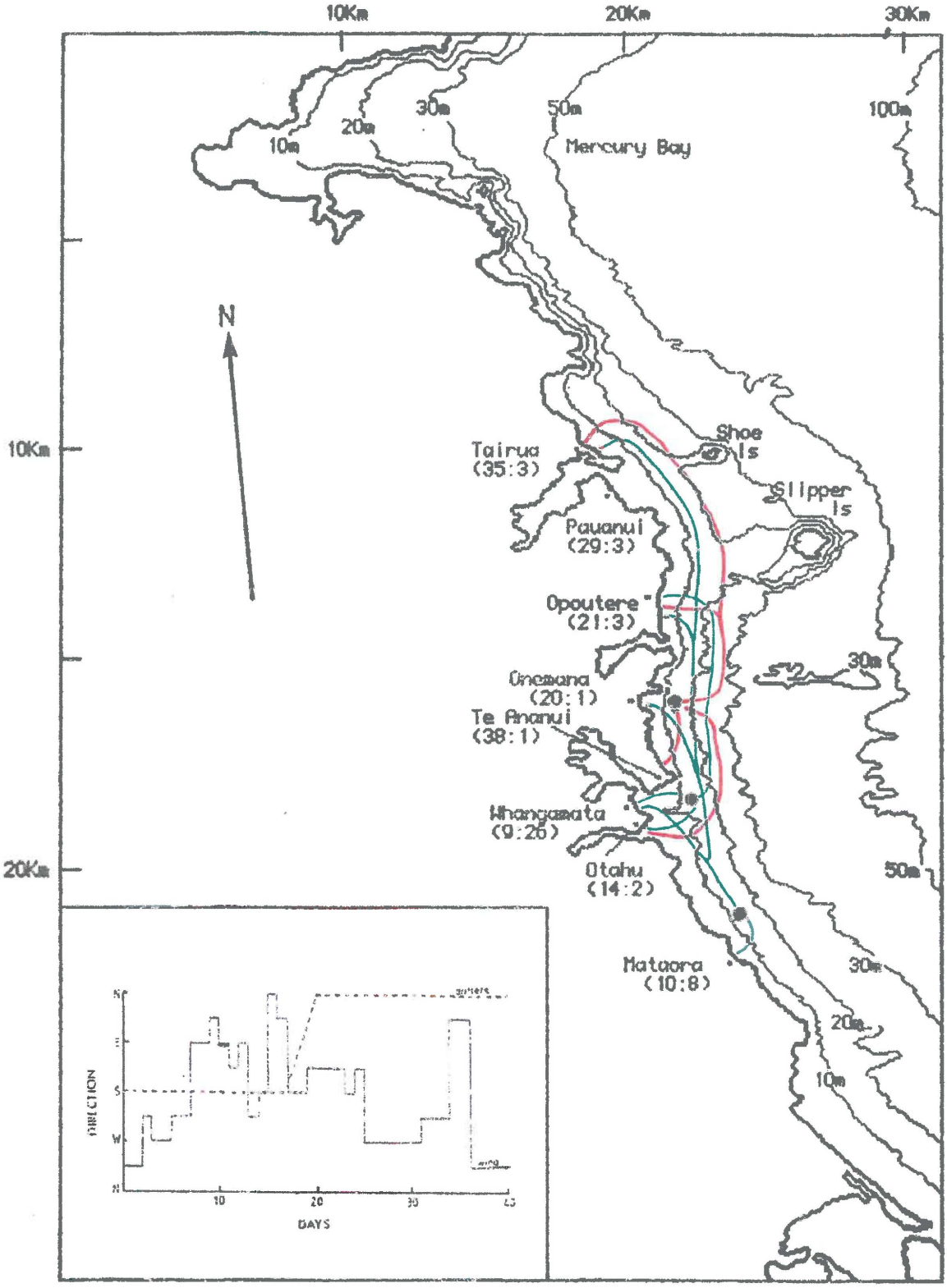

Figure 4.2. Drifter dispersal patterns from experiment No.1 (6-Jun-85). Coloured lines denote inferred transport pathways for drifters from Onemana (red), Whangamata (blue), and Whiritoa (green). Bracketed numbers denote average number of days to retrieve and number of drifters found at each location. Inset shows wind direction during the experiment from Tauranga, with bold lines indicating periods in which wind speed exceeded 7 $m.s^{-1}$. Also shown are the drifter migration directions (dashed line) during these wind measurements.

the depth range at Onemana. The high number of drifters retrieved at Mataora Beach, adjacent to Whiritoa, suggests that onshore currents with a slight southerly component may have been present here.

Experiment No.2 (6-Jul-85)

In the second experiment, drifters were released from two deeper sites off the previous locations. During the experiment, the majority of drifters were displaced to the north (57%), with approximately the same percentage displaced to the south as before (30.6%), and only a small number moving onshore (12.4%). Overall, drifters were displaced approximately three times greater distance than in the previous experiment (23.5 km), northerly displaced ones moving the furthest. However, the net minimum speed of the drifters (0.52 km.day^{-1}) did not increase significantly due to the longer period of time to retrieve them (30 to 80 days in most locations). Again, the northward displaced drifters showed the highest apparent speeds.

In this second drifter experiment, the location of retrievals tended to be more widespread, locations ranging from Matakana Island in the south to Otama in the north (Figure 4.3). Several were also retrieved by offshore trawlers near the Alderman Islands and on the western shore of Slipper Island. Again, the majority of drifters were retrieved at Whangamata (23%), some moving directly onshore, but most having moved south from Onemana. Several were also retrieved at Pauanui (15%). Small numbers of drifters at Onemana and Whangamata moved directly onshore from shallower water (15 m), but none at Whiritoa.

Although no clear pattern in displacement directions are evident, from the wind data (Figure 4.3 inset) the northerly displaced drifters appear to follow periods of onshore winds from the east and northeast, at times reaching up to 15 m.s^{-1}. The southerly displaced drifters occur in a period dominated by offshore winds blowing from the southwest.

These results indicate that during the second drifter experiment, strong currents flowing both north and south were present for a period of about 50 days. Significant numbers of drifters may have moved into deeper waters around the Alderman Islands from the action of offshore directed currents, but as these were retrieved by fishing trawlers it is also possible they were dragged offshore from shallower water by the trawlers. The high magnitude current patterns observed appear to have resulted from the presence of very strong onshore winds which dominated throughout the experiment.

Experiment No.3 (27-Jul-86)

In the third experiment, drifters were released at three depth locations offshore from Whangamata. The majority of drifters were displaced onshore and to the north at an average distance of 8.9 km and a net minimum speed of 0.32 km.day^{-1}. The southward displaced drifters tended to move

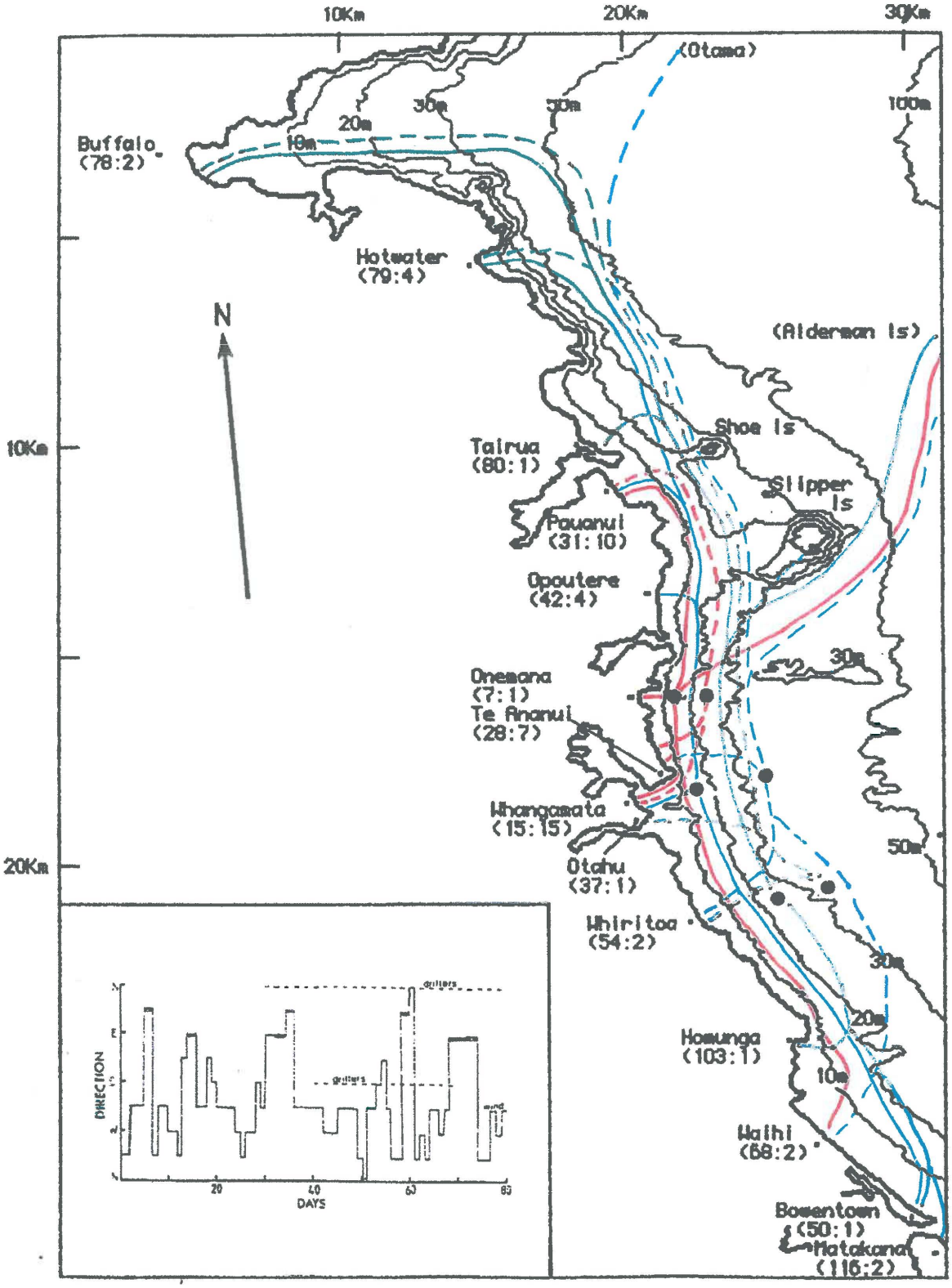

Figure 4.3. Drifter dispersal patterns from experiment No.2 (6-Jul-85). Coloured lines denote inferred transport pathways for drifters from Onemana (red), Whangamata (blue), and Whiritoa (green). Bracketed numbers denote average number of days to retrieve and number of drifters found at each location. Inset shows wind direction during the experiment from Whiritoa, with bold lines indicating periods in which wind speed exceeded 7 $m.s^{-1}$. Also shown are the drifter migration directions (dashed line) during these wind measurements.

slightly further and faster than those to the north. Most of the northerly displaced drifters were recovered within the first 27 days and the southerly ones within 23 to 57 days. Drifters at Whangamata were retrieved on average within 26 days, indicating that these were first moved northwards before returning south and migrating onshore. However, those released in shallow water (17 m) were mainly recovered within 10 to 15 days, indicating some initial direct onshore movement.

During the third experiment, a wide range of retrieval sites occurred along the coast, ranging from Matakana Island in the south to Pauanui in the north (Figure 4.4). Whangamata had the highest retrievals (38%), with Whiritoa (11%), Onemana (11%), and Pauanui (9.7%) showing significant returns. A drifter was also recovered on the southern shore of Slipper Island, offshore from Opoutere.

The northward movement of drifters again followed a period of onshore winds blowing from the east and northeast (Figure 4.4 inset), these winds occasionally reaching up to 12 $m.s^{-1}$ in speed. The following change to a southerly displacement direction accompanied a 30 day period in which offshore winds blew from the west and southwest.

Results from the third experiment indicate that a northerly bottom current was present along the inner shelf during the first 25 days, followed by a current reversal to the south which then dominated for the next 35 days. Local winds again appear to have been mainly responsible for the drifter dispersal patterns.

Experiment No.4 (29-Nov-86)

In the fourth and final experiment, drifters were released from the same previous sites but 6 months later in order to determine any seasonal variations in the regional current patterns. Nearly all of the drifters were displaced to the north, with only a few moving onshore and none to the south. The average net displacement of drifters increased slightly (12.6 km) due to the lower amounts moving onshore, and the average minimum net speed decreased (0.24 $km.day^{-1}$) due to the longer time to retrieve them (30 to 60 days). Of the drifters that moved onshore at Whangamata, all were from the two shallower release sites and most did so within the first 15 days. It is therefore likely that these moved directly onshore.

In contrast to the previous experiment, there was only a small range of retrieval sites, extending from Whangamata to Tairua (Figure 4.5). The majority of drifters were retrieved at Opoutere (59%) and Onemana (12%). Three were also retrieved by trawlers south of Slipper Island.

The northerly movement of drifters followed a period of about 40 days in which winds blew mainly from the southeast, east and northeast (Figure 4.5 inset), these winds reaching up to 7.5 $m.s^{-1}$ in

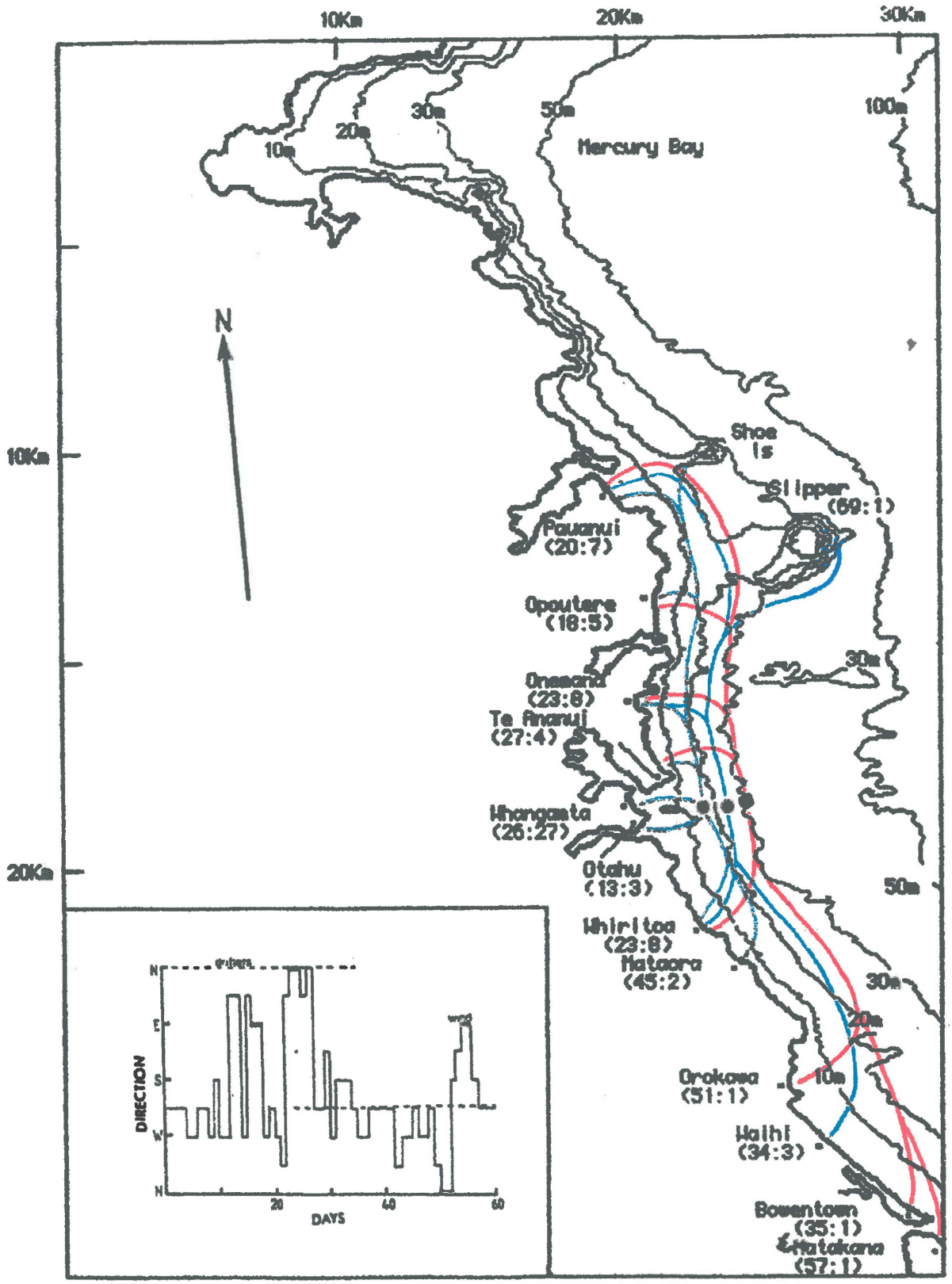

Figure 4.4. Drifter dispersal patterns from experiment No.3 (6-Jul-86). Coloured lines denote inferred transport pathways for drifters from Whangamata at water depths of 17 m (green), 22 m (blue), and 27 m (red). Bracketed numbers denote average number of days to retrieve and number of drifters found at each location. Inset shows wind direction during the experiment from Whiritoa, with bold lines indicating periods in which wind speed exceeded 7 $m.s^{-1}$. Also shown are the drifter migration directions (dashed line) during these wind measurements.

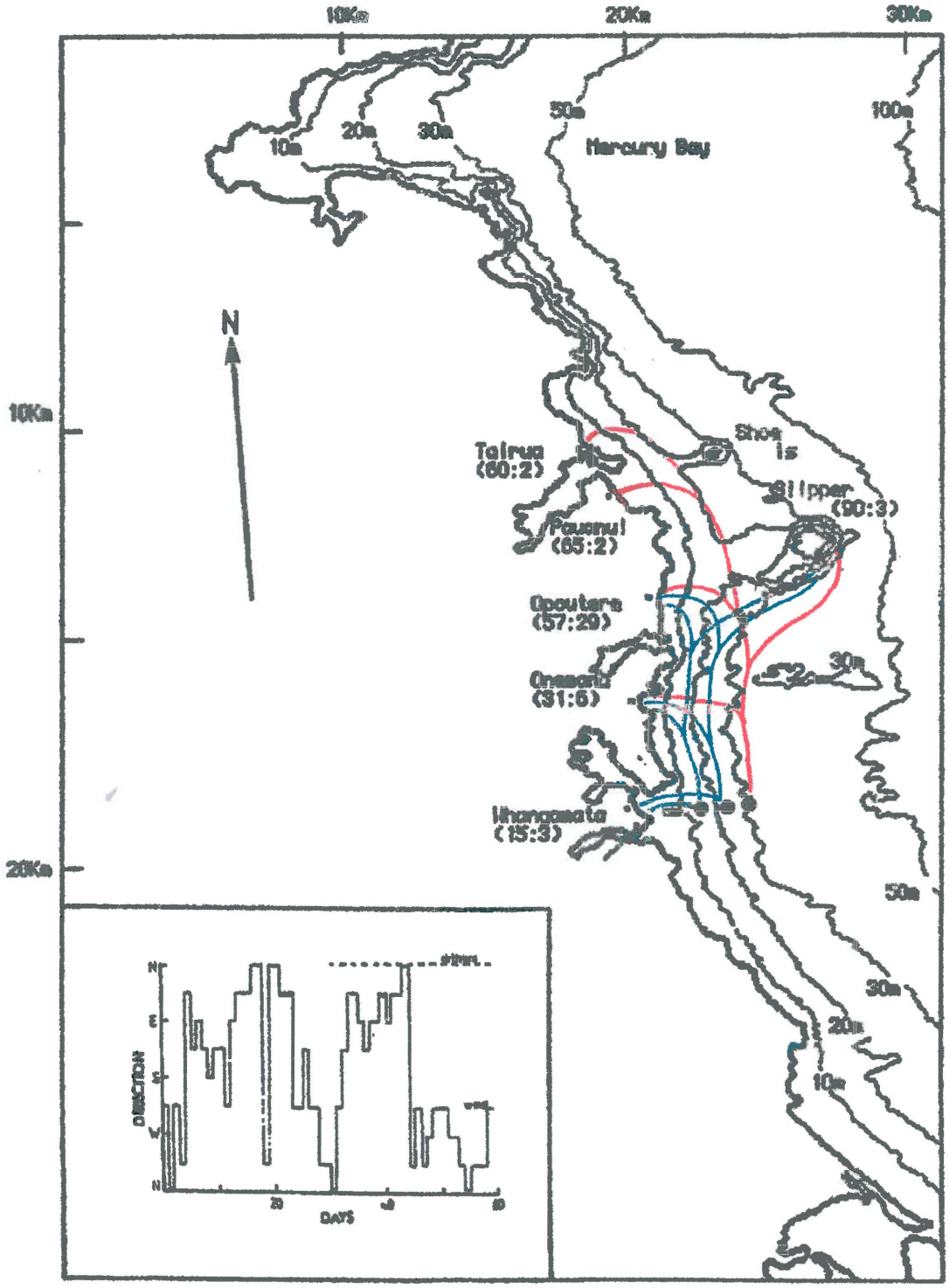

Figure 4.5. Drifter dispersal patterns from experiment No.4 (29-Nov-86). Coloured lines denote inferred transport pathways for drifters from Whangamata at water depths of 17 m (green), 22 m (blue), and 27 m (red). Bracketed numbers denote average number of days to retrieve and number of drifters found at each location. Inset shows wind direction during the experiment from Whitianga, with bold lines indicating periods in which wind speed exceeded 7 $m.s^{-1}$. Also shown are the drifter migration directions (dashed line) during these wind measurements.

speed. Offshore winds were then present for the next 15 days, however no southward movement of drifters was observed.

Results from the fourth and final experiment indicate that a persistent northerly current was present for at least 60 days. A smaller but significant branch of this current also appears to have flowed around the southern margin of Slipper Island. The northerly-directed current seems to have resulted from the presence of persistent onshore winds. Despite the presence of offshore winds, no southerly flowing currents were observed.

4.2.2. Residual Current Patterns

Results from the four sea-bed drifter experiments allow some initial deductions to be made regarding the nature of regional current flow patterns. The overall direction of drifter movement was both north and south in the first three experiments, and dominantly to the north in the fourth experiment. Some drifters were found to move directly onshore from shallower release sites (10 to 22 m), particularly at Whangamata in the first and third experiments. This is presumably due to the effects of non-linear wave orbital motions at these depths. However, the major current patterns, particularly on the inner shelf, appear to be shore-parallel northerly and southerly flowing currents (northerly flowing meaning a current flowing to the north and southerly to the south). A third minor current branching off the main northerly flowing one just south of Slipper Island may also be present, although the evidence for this comes largely from retrievals of drifters from the southern waters of Slipper Island by fishing trawlers.

From observations of the number of days to retrieve drifters along the coast, it appears that when either the northerly or southerly flowing currents were present, they would dominate for periods of between 10 to 15 days before reversing in direction. The trend was usually for a progressive increase in the number of days for retrieval either north or south, indicating a steady dominant current in one direction.

Of the two alongshore flow directions, the northerly one seems to have been the strongest, based on the consistently higher speed and displacement values shown in each experiment. The southerly flow was only present in the first three experiments, and appeared to be significantly weaker than its northerly flowing counterpart.

Some seasonality in the drifter retrieval patterns was apparent, stronger northerly and southerly flows dominating in winter, but only a relatively weaker northerly flow observed in summer. A relationship between wind and dispersal patterns was observable which is summarised in Figure 4.6.

The strongest association occurs between the northerly flow and high speed onshore winds (> 7 $m.s^{-1}$) from the east and northeast (Figure 4.6 a). It is possible that the observed trend of a

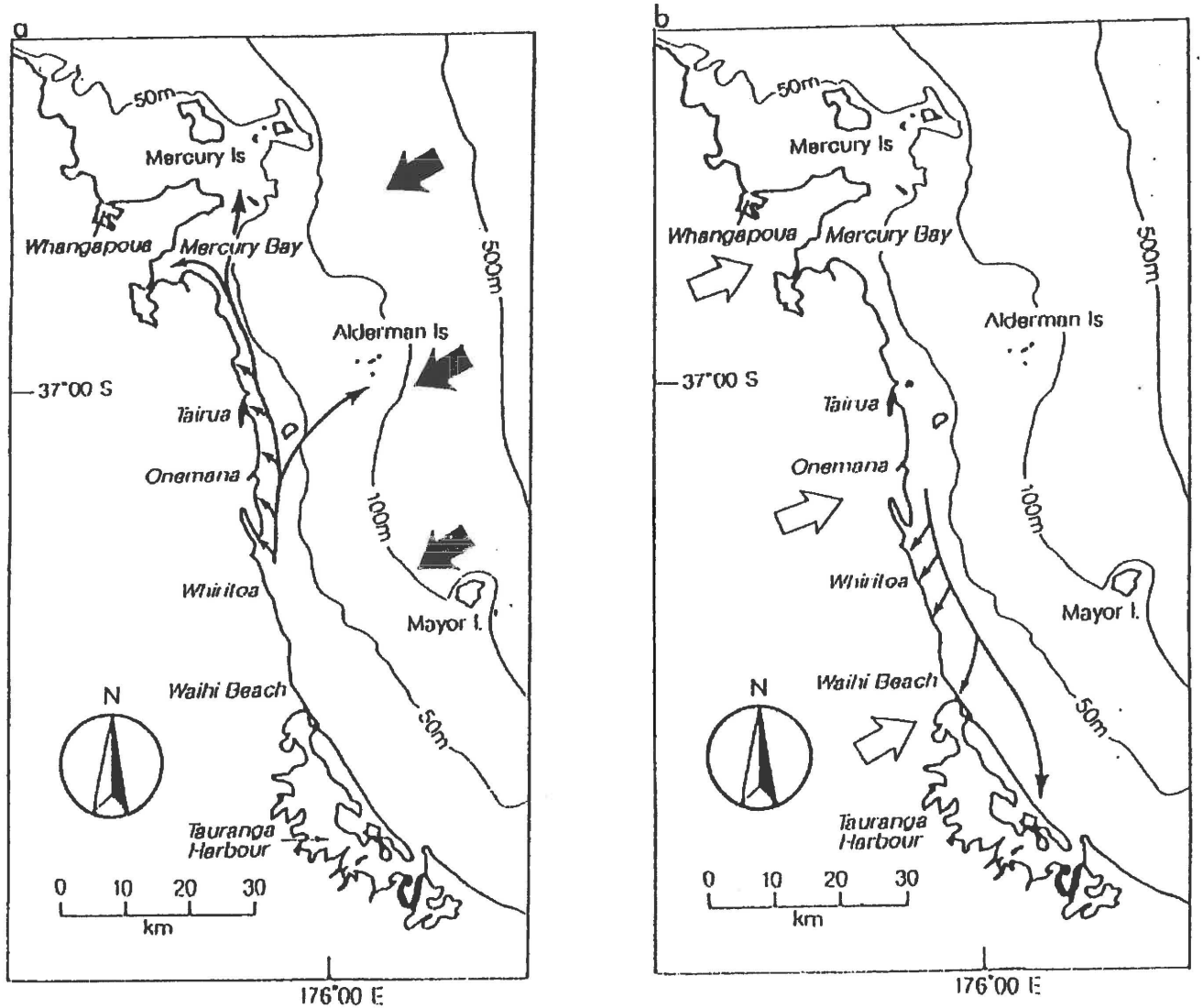

Figure 4.6. Observed relationship between drifter dispersal patterns (small arrows) and the local wind climate (large arrows): a) northward movement associated with strong easterly winds; b) southward movement associated with weak westerly winds.

stronger northerly flow in winter and spring coincides with the onshore winds reaching their maximum speeds during these periods.

Although there seems to be some relationship between low speed offshore winds from the west and southwest and the southerly flow (Figure 4.6 b), the apparent absence of a southerly flow during the fourth experiment, despite the presence of these offshore winds, suggests local meteorological conditions may not be entirely responsible for its generation.

From observations of the number of drifters retrieved at each location during the four experiments, the beaches that consistently showed the highest overall returns of drifters are Whangamata (30.5%), Opoutere (19.6%), and Pauanui (8.8%). This is an important observation as it indicates that conditions within these embayments are consistently favourable for the ultimate onshore movement of drifters. These locations are all on beaches adjacent to major estuary systems along the coastline, and the pattern may therefore be due to either the influence of tidal currents in shallow waters adjacent to tidal inlets, or from shore-parallel currents diverging into the embayments associated with these harbours where wave-induced currents could then transport them onshore. Sections of the above beaches were observed by HEALY and DELL (1987) to be presently accreting, and it is therefore possible that shelf sediments are being transported onshore in these locations.

4.3. ONEMANA AANDERAA CURRENT METER RESULTS

Current meter records obtained offshore from Onemana Beach over a 6 month period provided the most detailed account of local flow patterns. The current meter was located just south of a coarse megaripple band in 26 m water depth. It was hoped that by obtaining records over such a long time period that a representative model for east Coromandel current flow patterns could be determined.

4.3.1. Current Meter and Anemograph Records

Examinations of the Aanderaa current records show no obvious semi-diurnal variations in current meter records (see Appendix 1B), and so it is assumed that tidal currents are of minor importance to the mean inner shelf circulation of the study area. Therefore, only the low frequency current and wind oscillations (i.e.> 24 hours) are evaluated. For this, daily averages from the raw hourly Aanderaa current meter and Anemograph records are obtained by breaking the data into 45^0 quadrants (i.e. N, NE, E, etc.) and then calculating the resultant current or wind components in both the west-east (R_x) and south-north (R_y) directions, according to the formula given by PANOFSKY and BRIER (1968):

$$R_x = \frac{SW - SE + 0.707(SSW + SNW) - 0.707(SSE + SNE)}{n} \qquad (4.1)$$

$$R_y = \frac{SS - SW + 0.707(SSW + SSE) - 0.707(SNE + SNW)}{n} \qquad (4.2)$$

where "n" in the denominator is the number of observations and the capitals stand for the speed of each directional component. Resultant speed is determined by taking the square root of $Rx^2 + Ry^2$, and resultant direction from the tangent of Rx/Ry. Results from both deployment periods are plotted in Figure 4.7. Note that current data are in 'direction to' and wind data in 'direction from'.

Resultant bottom current directions are dominantly to the north and south throughout, oscillations in direction occurring every 2 to 14 days (Figure 4.7 a). Wind records show a similar pattern, with winds from both easterly and westerly quadrants dominating for periods ranging from 2 to 12 days (Figure 4.7 b). There appears to be some association between the wind and current directions, the strongest being between winds blowing from the east or northeast and a current flowing to the north.

Resultant current speeds vary considerably, ranging from a minimum of 0.05 $m.s^{-1}$ to a maximum of 0.32 $m.s^{-1}$ (Figure 4.7c), and reaching a maximum hourly observation of 0.44 $m.s^{-1}$ on 26-Jun-85. Three major high magnitude current events are apparent in the records, on the 26-Jun-85, 22-Jul-85, and 15- to 20-Sep-85. These high speed current events all coincide with periods of northerly flowing currents. Data obtained from both current meters show anomalously low speeds after a period of 45 to 60 days. This is most likely due to bio-fouling of the savonious rotor on the current meter.

Oscillations in resultant wind speed range from 0.4 to 14.9 $m.s^{-1}$ and coincide with the current speed oscillations (Figure 4.7c). The unreliable nature of current speed data after 45 to 60 days is quite evident when compared with wind speed records in Figure 4.7 c. High speed wind events are associated with resultant easterly and northeasterly wind directions. Therefore, the resultant current and wind data confirm the sea-bed drifter observation of high speed easterly winds associated with a strong shore-parallel inner shelf current flowing to the north.

Temperature and salinity records obtained from the current meters are shown in Figure 4.7 d. Although the temperature data appear accurate throughout both deployment periods, the salinity records seem inaccurate at the change over of current meters as shown by a measured 3 $^{o}/_{oo}$ increase in salinity, this being most likely due to bio-fouling of the conductivity sensors on the current meter. An important observation from the temperature and salinity records is the tendency for both to decrease sharply when the high speed northerly currents are present. Similar observations on the east Coromandel coast have been made by HARRIS (1985), which he

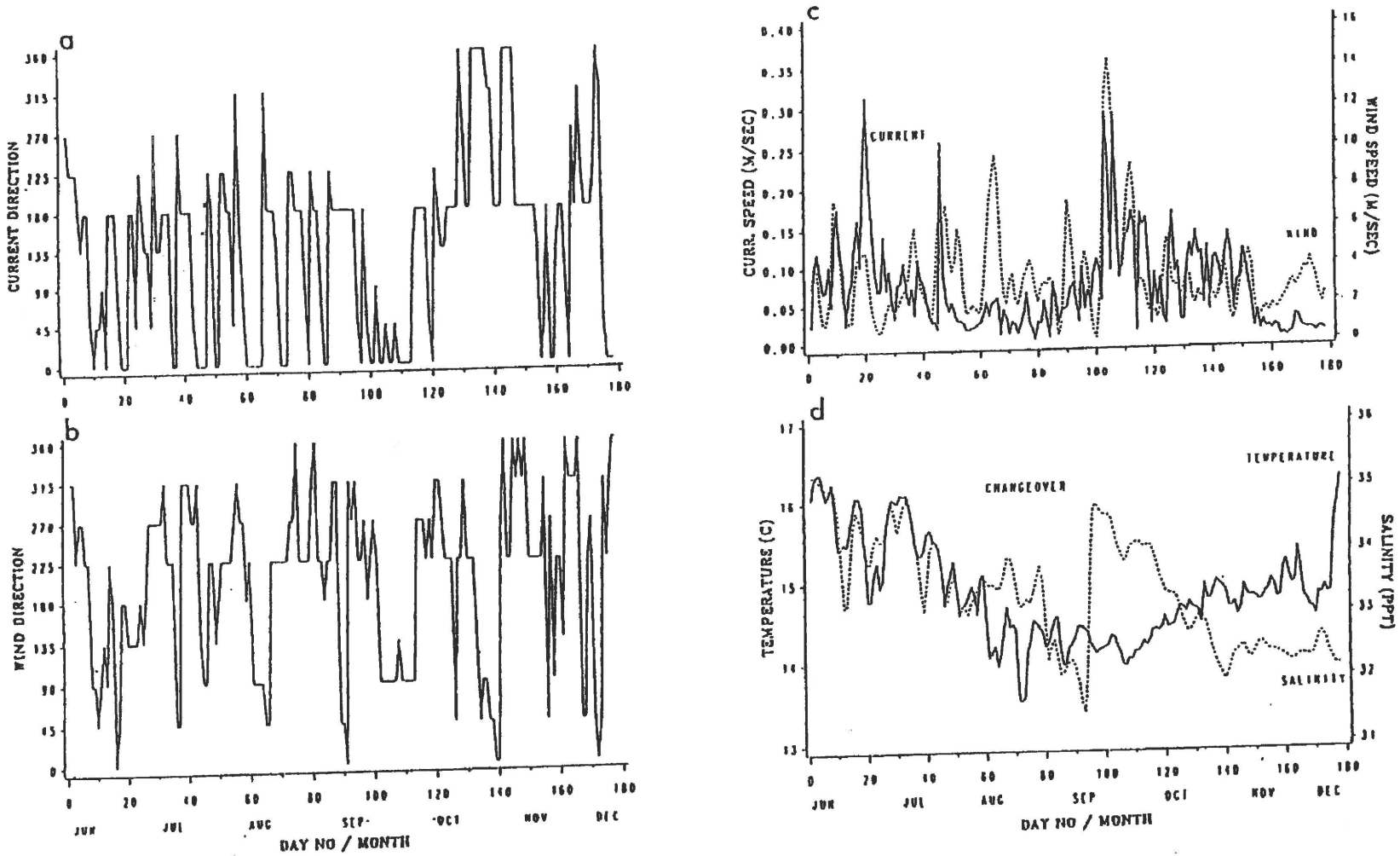

Figure 4.7. Time series plots of current and wind data from Onemana: a) resultant current direction (direction to); b) resultant wind direction (direction from); c) resultant current and wind speed; d) mean water temperature and salinity (note the apparent increase in salinity at the change over of current meters).

proposed was associated with discharges of cold water from Bay of Plenty river systems further south. However, at Onemana it may be due to local outflows of estuarine waters onto the shelf from Whangamata Harbour as a result of heavy rains associated with the easterly winds.

4.3.2. Current Flow Patterns During Storm Events

The resultant current and wind plots show some relationship exists between these parameters during high magnitude wind speed events. To further examine the extent to which winds may be generating the near bottom inner shelf currents, hourly current and wind records are examined during storm events. Major events observed during portions of applicable wind and current records are shown in Figure 4.8. Note that the major current event on 26-Jun-85 could not be examined as only Tauranga wind records were available in Jun-85, which have been shown by DELL (1983) to have a good directional but poor speed correlation with the study area.

In the first event from 11- to 14-Jul-85 (Figure 4.8 a), a southeasterly tracking low pressure system migrated over the North Island and produced northeasterly winds exceeding 7 $m.s^{-1}$ for 30 hours and 12 $m.s^{-1}$ for 5 hours. An observable response in the current meter records occurred 20 hours later when speed increased by 0.05 $m.s^{-1}$ to a maximum of 0.18 $m.s^{-1}$. Current direction at this time oscillated considerably from north to south, indicating that the winds were not strong enough to overwhelm the antecedent current conditions and cause a steady flow to the north. Six days later, a depression formed in the Tasman Sea and subsequently passed over New Zealand, producing winds from the east-southeast in excess of 7 $m.s^{-1}$ for 30 hours and 12 $m.s^{-1}$ for 10 hours. A steady high speed current to the north of up to 0.39 $m.s^{-1}$ was indicated in the current meter records within 10 hours, and remained high for about 30 hours. Wind direction remained constant for 40 hours, however the northerly current remained steady for 72 hours. It therefore appears that the time scale of current motion exceeded the inertial wind period.

Although no wave data are available during the current meter experiment, the significance of wave pumping affecting the current records was assessed through theoretical considerations. For the above wind conditions, a significant wave height of 1.74 m and period of 6.1 s is predicted, which will mean deep water wave conditions were present and therefore Airy wave theory is applicable. This predicts a maximum horizontal wave orbital velocity of 0.095 $m.s^{-1}$, which is at least three times less than the speed observed on the current records. Thus, it is assumed that any errors resulting from wave pumping are minimal.

From 15- to 29-Sep-85, a depression and associated cold front formed in the Tasman Sea, which upon migrating east became blocked over New Zealand by a stationary anticyclone to the east. Gale force easterly winds developed which exceeded 7 $m.s^{-1}$ for 110 hours and 12 $m.s^{-1}$ for 65 hours (Figure 4.8 b). A steady northerly current up to 0.35 $m.s^{-1}$ in speed was generated within 5 hours and persisted for about 100 hours. Wind speed then dropped and changed direction, oscillating from both the southeast and east. Current speed also decreased, however the steady

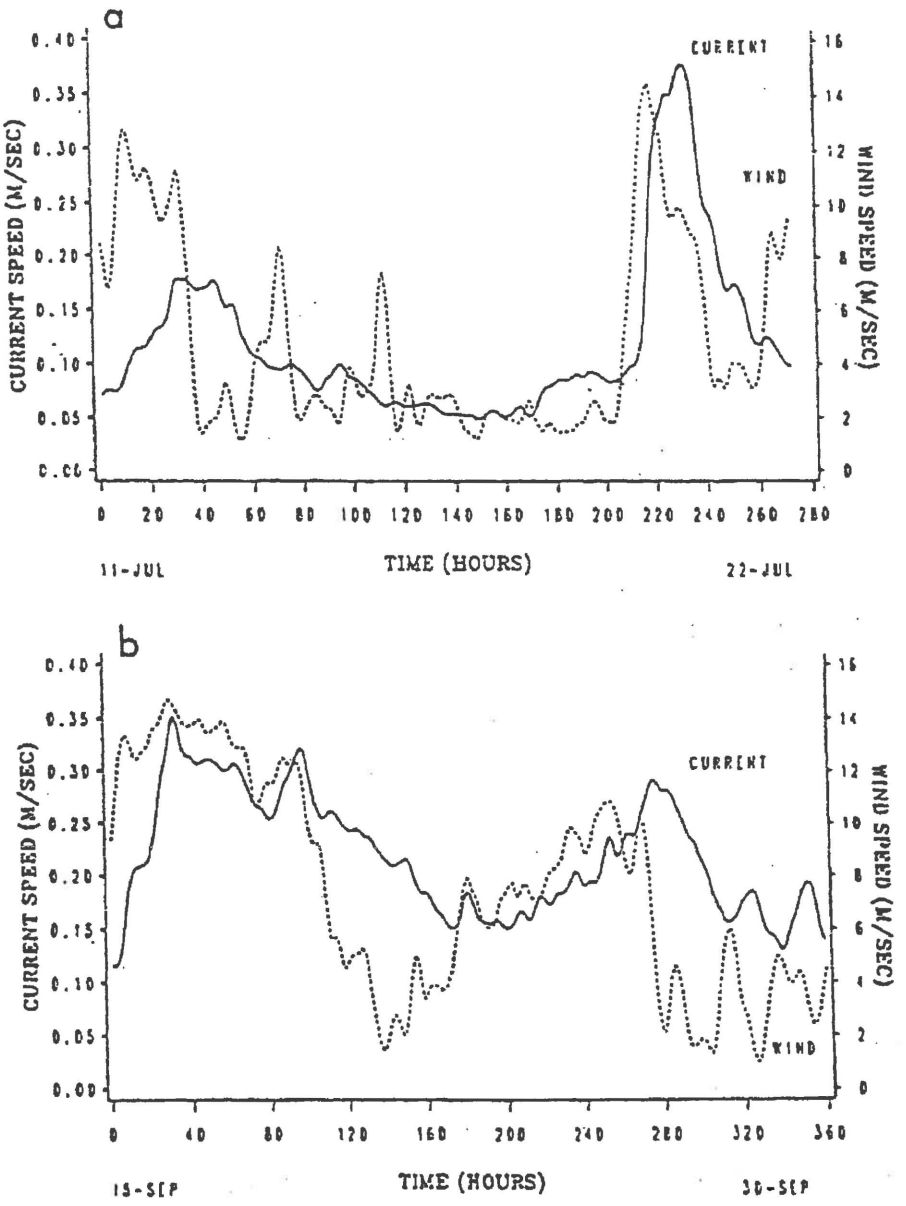

Figure 4.8. Hourly current and wind speed plots from Onemana during major storm events: a) 11- to 12-Jul-85; b) 15- to 30-Sep-85.

northerly current persisted. Wind speed increased again on the 23-Sep-85 when another depression became blocked by the same stationary anticyclone off the east coast, and remained above 7 $m.s^{-1}$ for 80 hours. The steady northerly current responded about 30 hours later by increasing in speed to a maximum of 0.31 $m.s^{-1}$. Again, it appears that the duration of the northerly current exceeded the inertial wind period.

For these conditions, a significant wave height of 1.86 m and period of 6.0 s is predicted to have occurred. This again means deep water wave conditions and that Airy wave theory applies, yielding a horizontal wave orbital velocity of 0.097 $m.s^{-1}$ at the current meter mooring. As the highest speed registered on current meter records was 0.36 $m.s^{-1}$, the affects of wave pumping again appear to have been minimal.

The above results provide some generalisations concerning the wind conditions necessary to generate inner shelf currents in the study area. From theoretical considerations, it appears that onshore directed winds exceeding 7 $m.s^{-1}$ are required to cause an increase in current speed, but for a steady current (i.e. one of constant direction) to form, winds in excess of 12 $m.s^{-1}$ are required for at least 5 hours duration. This is consistent with findings on the east coast by HARRIS (1985), who proposed that steady winds of 5 to 10 hours duration are required for wind-generated currents to fully develop. As reported by NIEDORODA *et al.* (1985a), specific response times are required for the current to adjust to changes in the local winds, weak or rapidly changing forces result in incoherent current patterns whereas strongly forced flows of significant duration produce more coherent current patterns. However, antecedent current conditions are also an important factor, as shown on 23-Sep-85, when a steady high speed current persisted under low wind speed conditions due to the presence of a strong current 3 days prior. This may indicate that inertial currents play a significant role in flow patterns along the east Coromandel coast, particularly following periods of strong onshore winds.

4.3.3. Forcing Mechanisms of Current Flows

Further information on the forcing mechanisms of inner shelf currents at Onemana is obtained by undertaking spectral analysis of the current and wind data. For this the 'SAS SPECTRA' program is utilised. As any wind-driven currents present should be represented as low frequency (> 24 hours) oscillations, the filtered resultant current and wind data are used again in this analysis.

Portions of the raw Aanderaa record indicating very low current speeds at the end of the deployment period which do not correlate with the wind records are considered suspect and thus omitted from the analysis. The current data are separated into north and south components, using the convention that the northerly component equals the current if it flows to the north and zero if it is to the south, and likewise for the southerly component. The east-west wind data is broken down into an east and west component in a similar manner. This is done to allow the two current directions to have different causes.

Spectral density plots in Figures 4.9 a and 4.9 b show most of the energy of the long-shelf currents and cross-shore winds occurs at low frequencies with broad peaks at periods of about 10 and 15 days duration.

Coherency squared plots between current and wind data are shown in Figure 4.9 c. For the number of observations used in this analysis, published data in KOOPMANS (1974) show the critical value for the test of the hypothesis $r=0$ vs. $r\neq0$ is 0.44. Coherency squared values above this critical value are judged to be statistically different from zero, whereas lower values are statistically indistinguishable from zero in this study. This does not mean they are equal to zero, but rather that they are small compared to the variability in the data. Thus a strong linear association exists between currents to the north and winds from the east (60%) at frequencies equivalent to 15 and 3 days duration, but a much weaker association exists between the southerly-directed current and offshore winds (< 40%) over all frequencies.

Phase plots in Figure 4.9 d show the average lead time of winds over the currents at each frequency of the currents. The northerly current and easterly winds appear to be in phase at all but the highest frequencies, where the currents then tend to lag behind the winds. The southerly current and westerly winds in contrast are out of phase at relatively lower frequencies, the current continually lagging behind the wind.

Spectral density, explained spectral density (coherency squared times spectral density), and unexplained spectral density (one minus coherency squared times spectral density) are illustrated for both current patterns in Figures 4.9 e and 4.9 f. Figure 4.9 e shows that most of the power of the northerly current can be explained by a linear relationship with the easterly wind. Figure 4.9 f however shows that most of the power of the southerly current cannot be explained by a linear relationship with the westerly wind.

Results of the spectral analysis suggest that both of the major inner shelf bottom currents on the east Coromandel coast oscillate in direction and speed about every 10 or 15 days. They also indicate a possible wind-generated origin for the northerly currents by the local easterly winds.This is shown by the high proportion of spectral density over the frequency range that contains most of the power that can be explained by a linear regression on the easterly winds. The phase plot over this range shows that a line with a very small negative slope would give a good fit. This indicates that there is only a slight delay in the onset of the current following the occurrence of the easterly winds. However, the results seem to indicate a remotely forced origin for the southerly current. This is shown by the low proportion of spectral density over the frequency range containing most of the power that can be explained by a linear regression on the westerly winds.

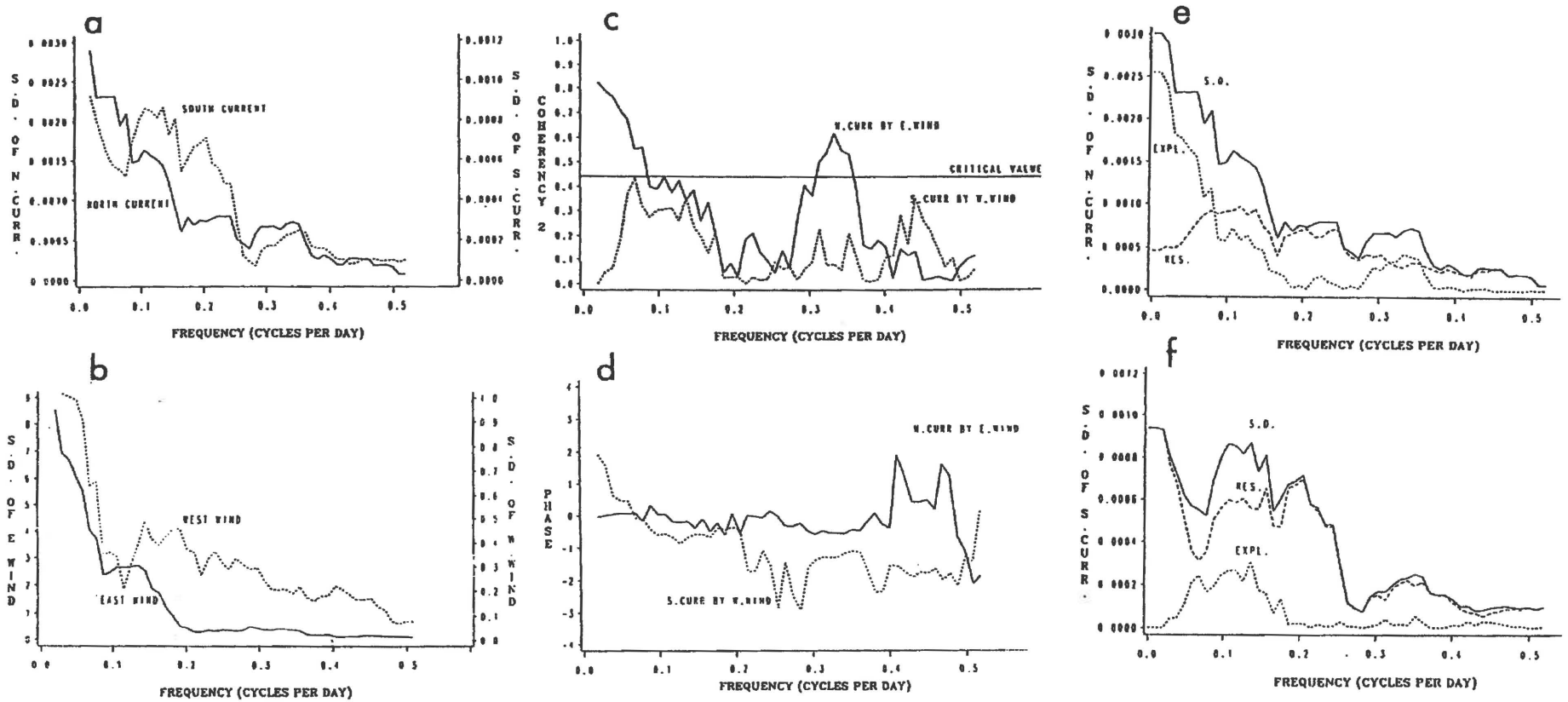

Figure 4.9. Spectral analysis plots of current and wind data from Onemana: a) spectral density (S.D.) of north and south currents; b) spectral density of east and west winds; c) coherency squared plots of north currents by east winds and south currents by west winds, showing critical value for the hypothesis r=0 and r≠0; d) phase plots of north current by east wind and south current by west wind in units π; spectral density (S.D.), explained spectral density (EXPL.) and unexplained spectral density (RES.) plots for e) northerly- and f) southerly-directed currents.

4.3.4. Mean Circulation and Potential Net Sediment Transport

To determine the mean inner shelf current circulation and directions of potential net sediment transport, the frequency of each current direction at three speed ranges was determined. A suitable sediment transport threshold value for the action of currents only was first calculated by using the method outlined by BLACK (1983) which accounts for the surface roughness of the sea-bed.

The method involves firstly calculating the critical skin friction velocity ($\bar{u}_{*cr}$) from the YALIN (1977) threshold curve. For fine sand this corresponds to a value of $\bar{u}_{*cr}$=0.0128 m.s^{-1}.

Surface roughness (z_0) over 2-dimensional bedforms is calculated by

$$z_0 = \frac{\eta^2}{2\lambda} \qquad (4.3)$$

where η=height and λ=wavelength. For the Onemana shelf where the current meter was moored, rippled bedforms were observed of height 0.03 m and wavelength 0.13 m, giving a z_0 value of 0.0035.

The critical form drag friction factor c" is then determined from

$$\frac{c''}{8} = 3.3 \log_{10} \qquad \frac{c''}{\sqrt{8}} = 3.3 \log_{10}\left(\frac{h}{2z_0}\right) - 2.3 \qquad (4.4)$$

where h=water depth (26 m) giving a value of c"=26.8.

Critical friction velocity u_{*cr} is given by

$$u_{*cr} = \frac{\bar{u}_{*cr}}{\left\{1-\left[\frac{5.75}{c''}\log_{10}\left(\frac{0.37h}{z_0}\right)\right]^2\right\}^{1/2}} \qquad (4.5)$$

=0.019 m.s^{-1}

and related to critical threshold velocity at 1 m above the sea floor (u_{1cr})

$$u_{1cr} = 5.75\, u_{*cr} \log_{10}\left(\frac{1}{z_0}\right) \qquad (4.6)$$

=0.26 m.s^{-1}

However, this method does not account for the important effect wave-induced currents will have on the threshold speed for sediment movement. GRANT and MADSEN (1979) determined that wave-current interactions in the bottom boundary layer enhance both the shear stress and apparent roughness experienced by the mean current. They also enhance the instantaneous stress felt by sediment particles at the bed, and suspended sediment concentrations within and above the wave boundary layer. However, calculation of the resulting velocity profiles, bottom stress and

apparent roughness require data on the mean current velocity, wave orbital velocity and period, relative angle between wave and current, and bottom roughness. As only the first and last parameters were measured directly in this study, the GRANT and MASDEN (1979) method could not be applied. However, VINCENT *et al.* (1981) also deduced that large waves during storm events cause much lower than the current threshold speed to be exceeded for a fraction of each wave period at suitable water depths. Following on from the results of GADD *et al*. (1978) at Long Island in North America, they used a range of threshold values between 0.15 to 0.20 $m.s^{-1}$. From the the presence of wave-generated bedforms on the sea-bed at the current mooring, it is obvious that wave oscillatory currents interact with the sea floor, thus warranting use of a second threshold value, which was estimated from the results of GADD *et al.* (1978) as 0.18 $m.s^{-1}$.

Frequencies for each velocity range are plotted as current rose diagrams in Figures 4.10 a and 4.10 b. Care was taken to include only data from the accurate portions of the current meter records. During the first deployment period (Figure 4.10 a), the most frequent current directions are to the south (24.2%), southwest (17.6%), north (16%), southeast (15.1%), and northeast (10.6%). Threshold speeds were exceeded 24.3% for the 0.18 $m.s^{-1}$ value, and 13.5% for the 0.26 $m.s^{-1}$ value in all directions. However, the most significant directions for exceedence are to the north (7.4%, 5.2%) and northeast (4.8%, 2.5%).

Results from the second deployment period (Figure 4.10 b) showed two current directions dominating throughout, to the south (32.6%) and north (28.8%). In comparison, other current directions are relatively insignificant. Currents exceeding threshold speeds occurred 18.7% and 8.6% for the 0.18 $m.s^{-1}$ and 0.26 $m.s^{-1}$ values respectively. Again, the most significant directions are to the north (7.4%, 3.6%) and northeast (4.2%, 2.2%).

Aanderaa current records from both deployment periods were further analysed using the University of Waikato's computer progressive vector analysis program, 'RESIDUAL', employing the same current threshold speeds. Plots are shown in Figures 4.11 a to e. During the first deployment period, the overall residual current direction is to the southeast (Figure 4.11 a), however the residual direction for currents greater than both threshold speeds (Figures 4.11 b, c) are overwhelmingly to the north. Results from the second deployment period show an overall northerly residual current direction (Figure 4.11 d), and a northerly direction of potential inner shelf sediment transport again at both threshold values (Figure 4.11 e to f).

It therefore appears that on the east Coromandel inner shelf, while the mean current flow may be directed to the south during calm weather periods, the direction of potential sediment transport will be to the north during episodic storm events, regardless of whether or not wave oscillatory currents interact with the steady current flows. Also, as noted on the Long Island coast by NIEDORODA *et al.* (1984), the same strong onshore winds that generate the steady northerly currents will also generate high waves, thus intensifying rates of sediment transport to the north

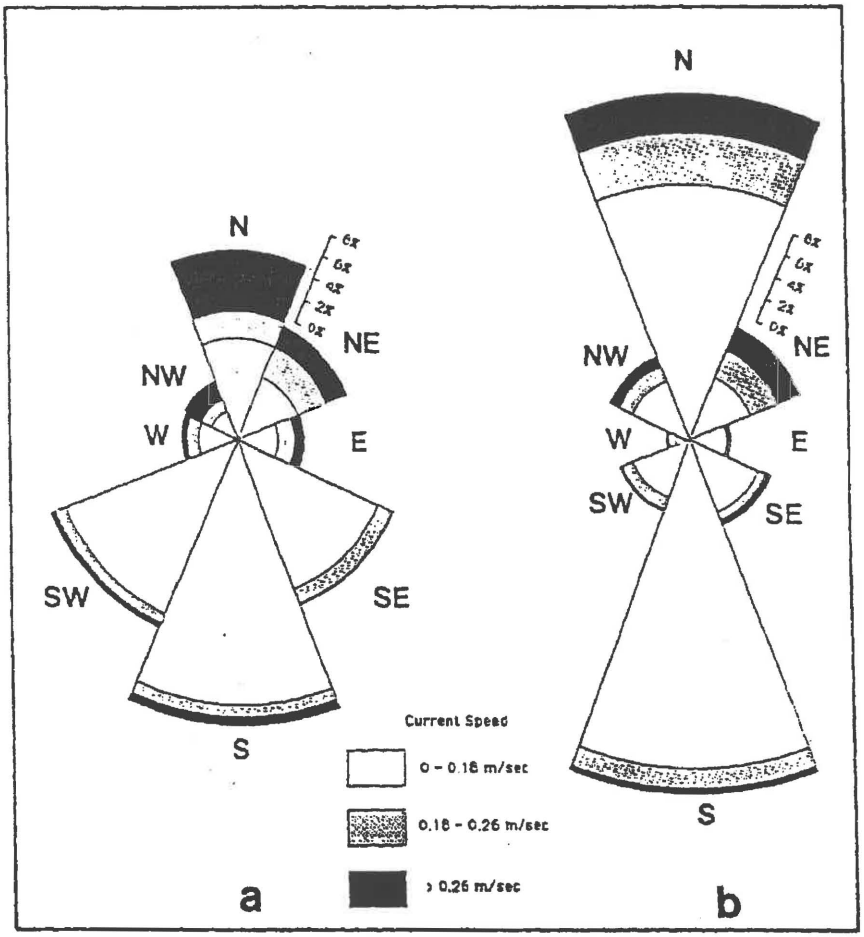

Figure 4.10. Current roses for both threshold speed values from hourly observations at Onemana between: a) 6-Jun- to 30-Jul-85; b) 8-Sep- to 1-Nov-85.

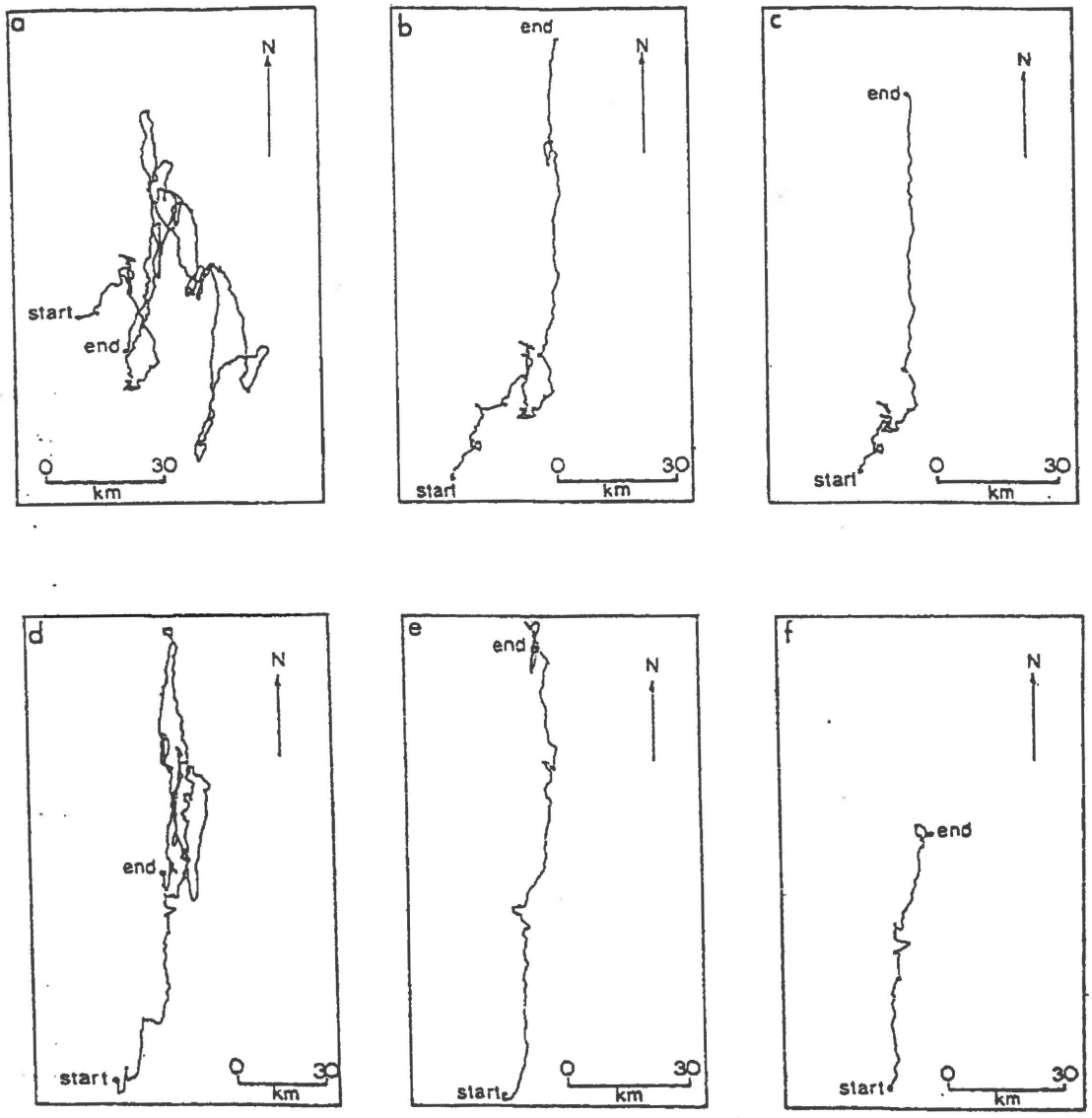

Figure 4.11. Progressive vector plots for threshold speed values of o $m.s^{-1}$, 0.18 $m.s^{-1}$, and 0.26 $m.s^{-1}$ from Onemana for the periods: 6-Jun- to 30-Jul-85 (a, b, and c); and 8-Sep- to 1-Nov-85 (d, e, and f).

during these storm events.

In order to determine some idea of the average annual frequency of sediment transport on the east Coromandel coast, the probability of exceedence of various wind speeds was calculated from the 18 months of wind records at Whiritoa, and is shown in Figure 4.12. Winds exceeding 7 $m.s^{-1}$ and capable of generating a current response are found to occur 6% of the time. However, winds exceeding 12 $m.s^{-1}$ and most likely to generate a steady current of sufficient speed to transport inner shelf sediments are found to occur only 0.5% of the time. These high magnitude wind events are mainly from the east or northeast, and most frequent between June and October (winter and spring; Figure 4.13).

As no published longer term wind records are available from the study area, it is difficult to determine the long term frequency of potential sediment transport. However, annual summaries of maximum wind run values obtained from the New Zealand Meteorological Service for the period 1969 to 1986, show the maximum wind run observed at Whiritoa in September 1985 of 518 km is only slightly below the published average maximum value of 580 km. From this longer term data, it also seems that high speed wind events occur most frequently in September and October each year. Therefore, conclusions drawn from the Whiritoa wind data appear to be fairly representative of mean conditions.

4.4. MODEL FOR EAST COROMANDEL SHELF FLOWS

The east Coromandel regional shelf current pattern is dominated by two mutually exclusive shore-parallel bottom currents which flow to the north and south. Conceptual models of current dynamics and sediment transport for each current pattern are illustrated in Figures 4.14 a and 4.14 b.

Frequent periods of fair weather conditions are characterised by the presence of a southerly flowing current (Figure 4.14 a), which typically ranges in speed from 0.10 to 0.20 $m.s^{-1}$. As the current does not exceed sediment threshold speeds, and as significantly high waves will not be generated by the offshore winds to interact with the steady current, no along-shelf sediment transport is inferred to occur during these fair weather periods. From diver observations taken during such calm conditions, a slight to and fro movement of sand by wave oscillatory currents occurs at depths ranging from 12 to 24 m, but sediment transport is evident only at shallower depths where a net onshore movement of sand occurs (see Chapter 6.3.).

Although the southerly-directed current tends to be associated with the presence of local offshore west and southwesterly winds, it does not appear to be directly generated by these. One possible origin for this flow is from the southward-directed East Auckland Current (see Figure 2.5). As the core of the East Auckland Current is located over the continental slope (DENHAM *et al.*, 1984), it is possible that the southerly flowing current is formed by an incursion of this onto the continental shelf.

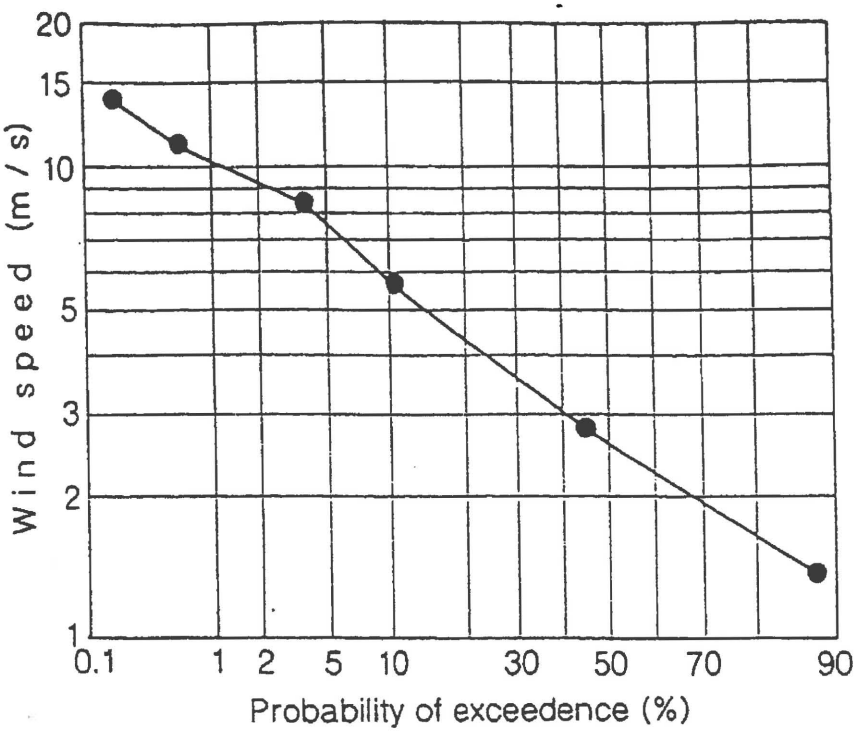

Figure 4.12. Probability of exceedence for various wind speeds from 18 months of wind records (3-Jul-85 to 26-Jan-87) obtained from Whiritoa.

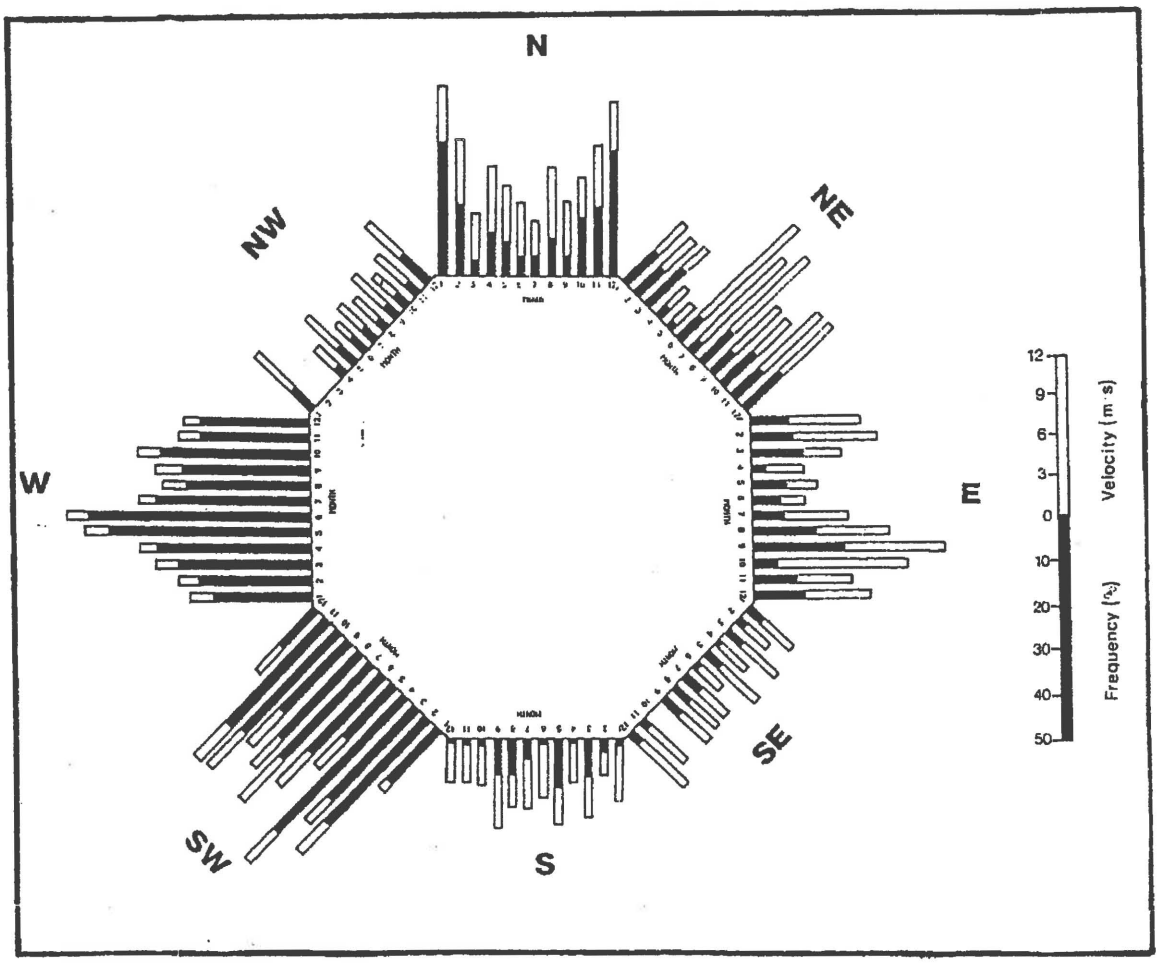

Figure 4.13. Seasonal wind frequency and speed data for Whiritoa wind records (3-Jul-85 to 26-Jan-87).

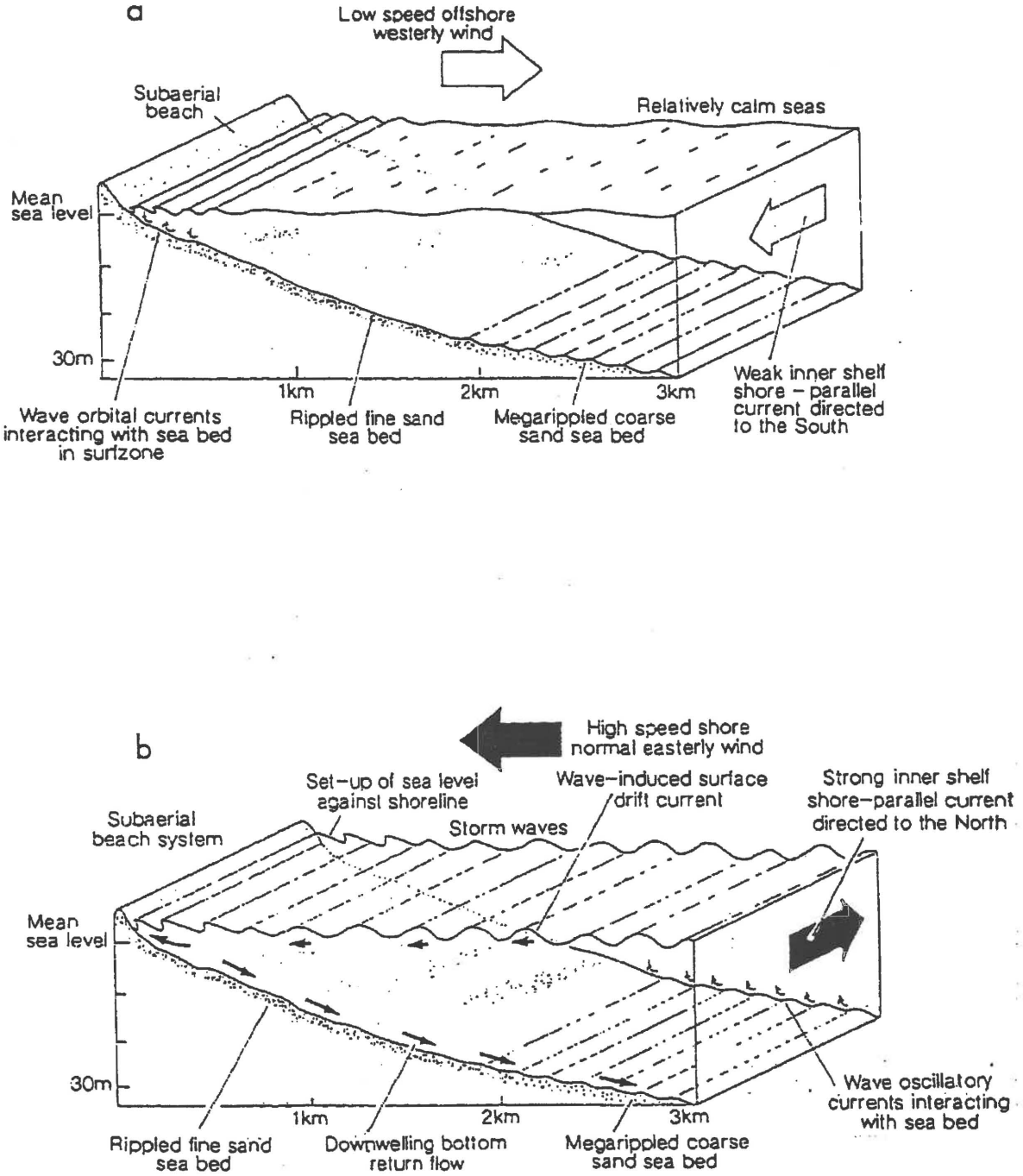

Figure 4.14. Conceptual models for inner shelf dynamics and sediment transport during: (a) calm weather periods characterised by a weak southerly flowing current and transport restricted to the surfzone; (b) episodic stormy periods dominated by downwelling conditions and a strong shore-parallel current resulting in along-shelf sediment transport to the north. Wave oscillatory currents interact with the sea floor, as shown by the presence of megaripples, and will combine with the mean current flow to increase the shear stress excerted on sediments, thus reducing the current speed required to erode and transport these.

Evidence supporting this hypothesis includes:

(i) similar water temperatures and salinities of the southerly flowing current with those reported for the East Auckland Current by BARKER and KIBBLEWHITE (1965);

(ii) Open ocean East Auckland Current velocities reported by HEATH (1980) of between 0.18 to 0.30 $m.s^{-1}$ are slightly greater than those observed for the southerly flowing current, as would be expected due to bottom friction over the continental slope and shelf;

(iii) the absence of a southerly flowing current in one sea-bed drifter experiment conducted in summer, a period in which the East Auckland Current has been observed by DENHAM *et al.* (1984) to migrate further offshore; and

(iv) similar observations in eastern Australia, where eddies from the East Australian Current, which ultimately feeds the East Auckland Current, frequently penetrate the continental shelf (GORDON and HOFFMAN, 1986).

The infrequent intrusion of cyclonic depressions from the Tasman Sea into the study area results in the presence of strong onshore winds and the formation of a northerly flowing bottom current, measured at speeds up to 0.40 $m.s^{-1}$ (Figure 4.14 b). This is very similar to values reported by SWIFT and NUMMEDAL (1987) for regions affected by mid-latitude storms on the North American coast. The current alone is capable of transporting inner shelf sediments, however the presence of storm-generated waves should act to intensify the rates of sediment movement to the north.

As this northerly-directed current appears to be generated by local onshore winds, the most obvious interpretation for the flow is that it represents part of a more complex 3-dimensional downwelling circulation as described in other storm-dominated shelf settings from North America by NIEDORODA *et al.* (1985a) and SNEDDEN *et al.* (1988), and in eastern Australia by FIELD and ROY (1984) and GORDON and HOFFMAN (1986). The interpretation is that onshore winds acting over a limited fetch, in combination with storm surge and inverse barometric effects, cause a set-up of water against the shore. A cross-shelf pressure gradient would then develop causing a bottom return or downwelling flow. The shore-parallel northerly current maintains a geostrophic balance with pressure gradient and Coriolis forces, as indicated by the tendency for the duration of the current to exceed inertial wind periods.

High rainfalls produced by the Tasman Depressions cause sharp changes in water temperature and salinity, and may therefore produce density stratification and strong pressure gradients, resulting in a baroclinic component to the northerly flow. However, turbulence during these storm events is probably quite high and may cause complete mixing of the water column.

Another factor that must be considered is that the variable coastal topography in the study area, and mobile nature of weather systems which generate the strong onshore winds, may lead to the generation of coastally trapped topographic waves, as described in Chapter 3.1.2. However, the presence of such current flows cannot be identified from the present spatially limited data analysis.

4.5. ADDITIONAL CURRENT MEASUREMENTS

4.5.1. Opito Bay-Whangapoua

Two current meters were located on the inner shelf offshore from Opito Bay and Whangapoua Harbour in the northern part of the study area. As the records were obtained during relatively calm weather conditions, and were of limited duration, it was not possible to analyse in detail the current flow patterns in this region. However an initial understanding of these flow patterns is possible.

Throughout the observation period, currents off Opito Bay show a residual flow to the northeast (Figure 4.15 a). However this varies considerably over different time scales. Daily records show strong semi-diurnal variations in current direction from northwest to northeast, resulting in a northerly residual current flow. These semi-diurnal changes in direction occur with the onset of both the flood and ebb tides, with the direction of these tidal components varying between different days (Appendix 1B). Over longer periods of about 5 days, residual current direction changes from north to southeast (Figure 4.15, 4.16 a). In two instances on 22-Oct-89 and 5- to 7-Sep-89, both current directions appear to have overwhelmed the semi-diurnal tidal component (Figure 4.15), indicating the development of relatively strong local wind-generated currents. Wind data collected at Matarangi Beach show a north-northwesterly wind associated with the northerly current on 22-Oct-89, and a northeast wind for the southerly currents on 29- to 30-Oct-89 and 5-Nov-89 (Figure 4.17 a). Elsewhere, winds appear to have been mainly from the south and west.

Current speed off Opito Bay generally ranges between 0.10 to 0.20 $m.s^{-1}$. However, records appear to have been affected by bio-fouling after 20 days as shown by a decreasing trend in speed values (Figure 4.16 b). For the sea-bed conditions present at Opito, a u_{1cr} threshold speed value of 0.32 $m.s^{-1}$ for sediment transport is calculated from Eq.4.6. The only time currents were found to exceed this speed was during the northerly flowing current on 22-Oct-89, when these reached up to 0.38 $m.s^{-1}$. This event was associated with a subtropical cyclonic depression which moved over the coast and produced north-northwesterly winds up to 11 $m.s^{-1}$ for a limited duration (< 3 hours.; Figure 4.17 b). These results are in general accord with findings from Onemana, as the current did not develop into a steady flow, and winds were below the minimum speed and duration (< 12 $m.s^{-1}$, 5 hours.) for such a response to occur. Strong semi-diurnal variations in current speed generally occur, maximum values occurring a few hours before low water on the ebb tide, and minimum speeds on the flood tide (Appendix 1B).

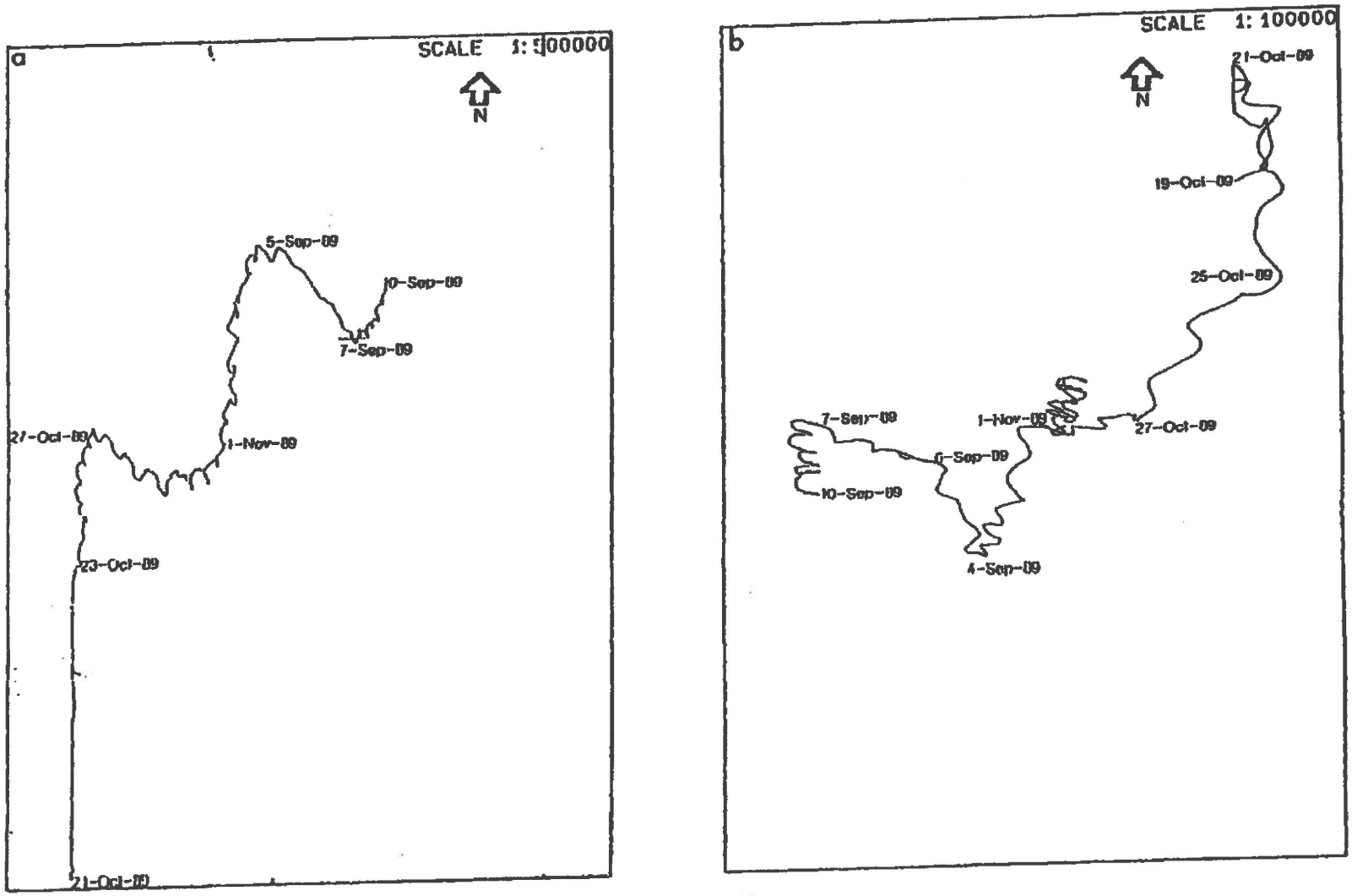

Figure 4.15. Progressive vector plots of current data obtained from: a) Opito Bay; b) Whangapoua.

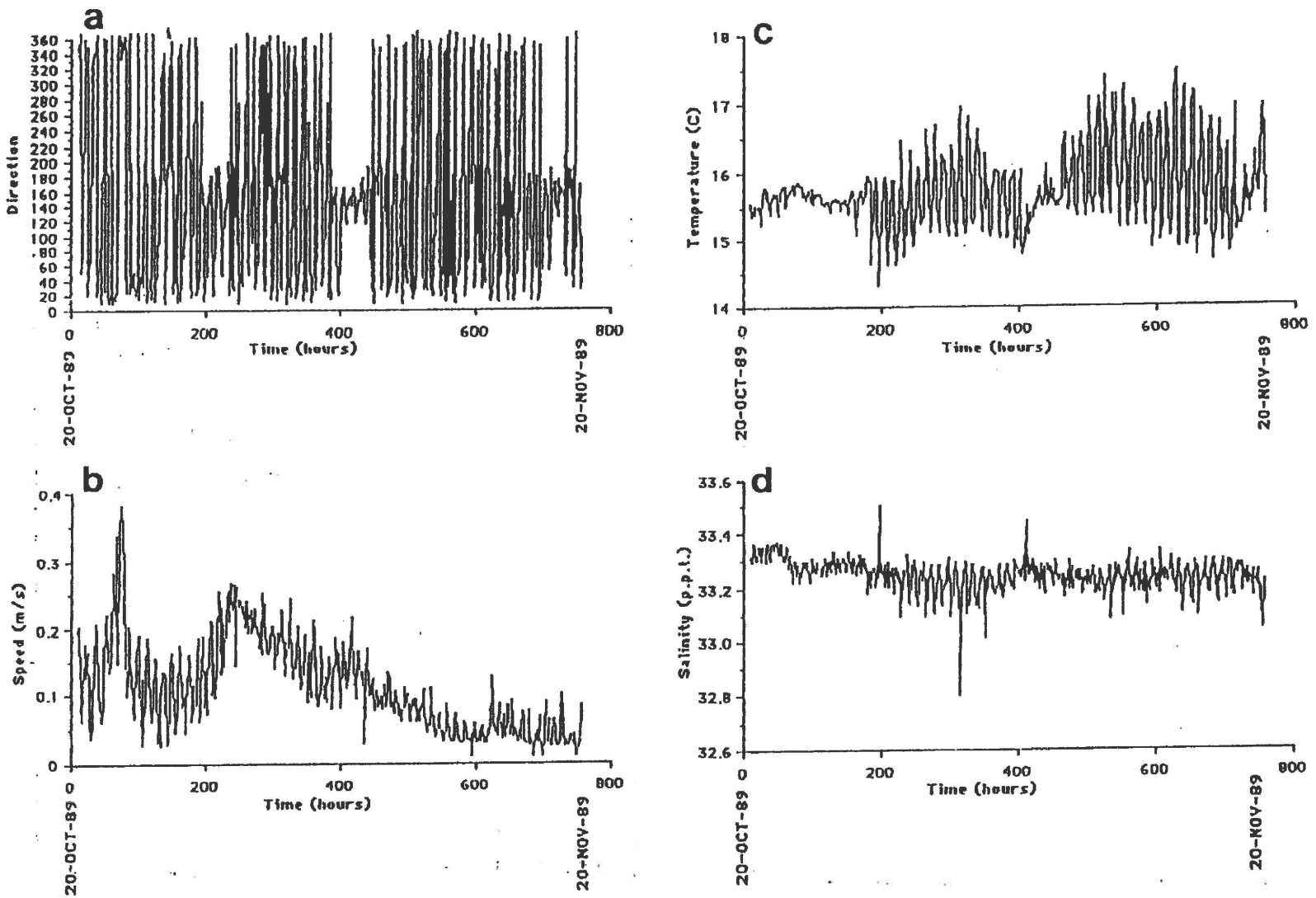

Figure 4.16. Time series plots of hourly current meter data from Opito Bay: a) current direction; b) current speed; c) water temperature; d) water salinity.

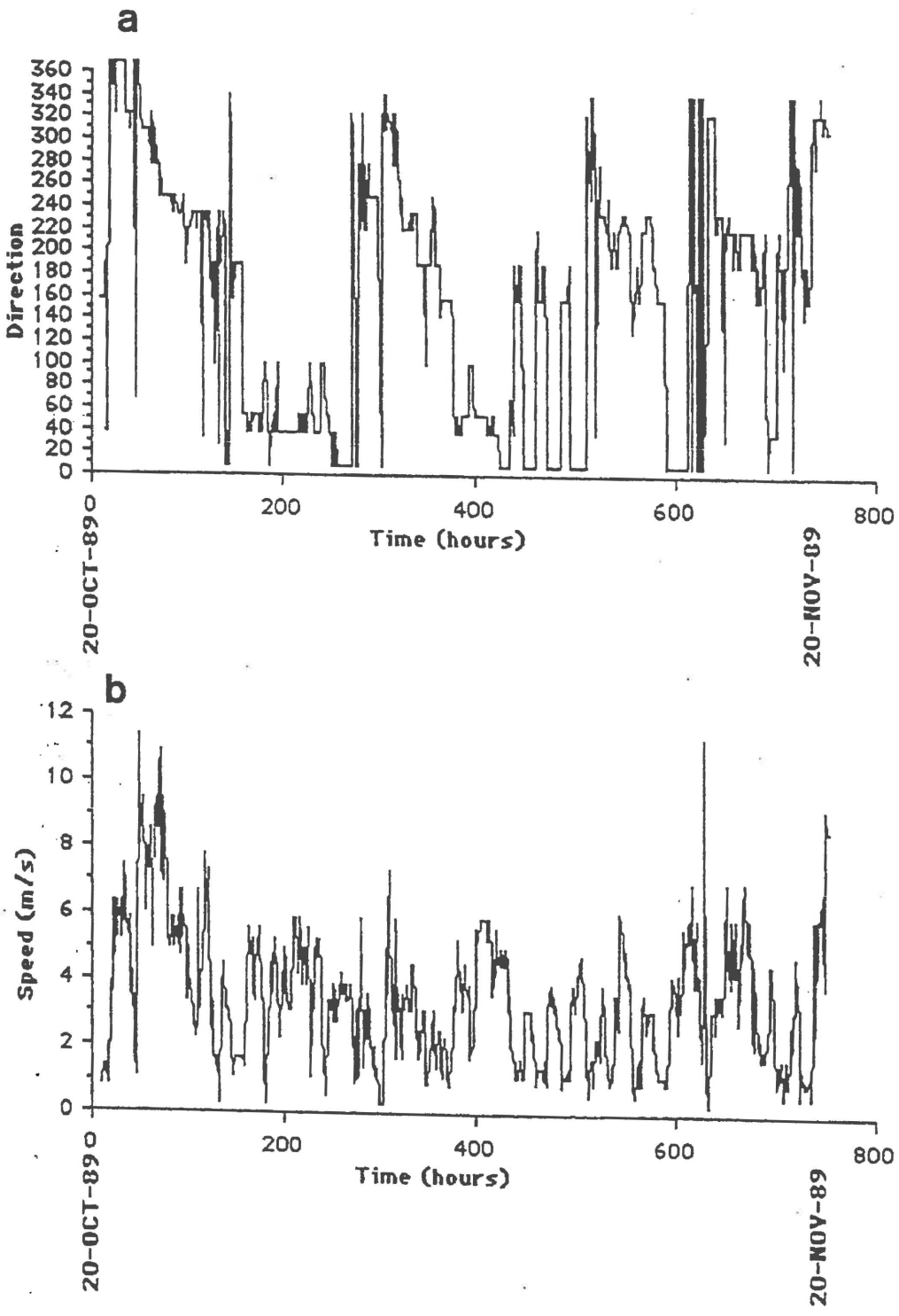

Figure 4.17. Hourly wind data at Matarangi Beach: a) wind direction; b) wind speed.

Water temperature at Opito Bay generally ranges from 15 to 17° C (Figure 4.16 c). The main obvious trend is the presence of strong diurnal fluctuations in water temperature (up to 2.5° C) throughout most of the records, but more uniform temperatures present between 20- to 27-Oct-89 and 5-Nov-89. The semi-diurnal variations appear to be associated with tidal currents, with maximum temperatures occurring at low water and minimum values at high water (Appendix 1B). SMITH (1980) has reported warmer and less saline waters within Mercury Bay than in the open ocean, which flow out of Whitianga Harbour during the ebb tide jet and clockwise along the northern bay area. Thus the temperature fluctuations at Opito Bay may be associated with a northerly extension of the Mercury Bay current flow patterns (Figure 4.19). Periods of constant temperature values coincide with the two periods when wind-generated currents overwhelmed tidal flows.

Water salinity appears to be relatively constant off Opito Bay, values generally ranging from 33.1 to 33 °/oo (Figure 4.16 d). However, a similar trend to water temperature in salinity values occurs, with semi-diurnal fluctuations generally present at periods when tidal currents dominated offshore flows, lowest salinity values being found during flood tides (Appendix 1B). This again possibly results from a northerly extension of Mercury Bay water masses.

Currents measured off Whangapoua Harbour show a southwesterly residual flow over the observation period (Figure 4.15 b). However, current direction varies through time. Over daily time scales, strong semi-diurnal variations occur, with northeast and west to northwest currents present initially, but west to southwest and east to southeast directions dominating most days (Figure 4.18 a, Appendix 1 B). Periods of dominant northerly currents at Opito Bay (22- to 27-Oct-89, 1- to 4-Nov-89) are characterised here by south to southwesterly-directed currents, and likewise intervals when southeasterly currents dominate the former area (27- to 31-Oct-89, 5- to 7-Sep-89) are characterised by north to northwesterly currents at Whangapoua. Thus both tidal- and wind-forced currents appear to flow in opposite directions between the two areas. This must relate to the different orientations of respective coastlines, from southeast to northwest at Opito, and east to west at Whangapoua, which presumably causes alterations in current flows between both areas.

Current speed off Whangapoua is much lower than Opito, generally ranging from 0.025 to 0.1 $m.s^{-1}$, with no obvious peak flows occurring (Figure 4.18 b). Relatively strong semi-diurnal fluctuations do appear to be present, with maximum speeds occurring either just before low water on the ebbing tide, or at mid tide (Appendix 1B).

Water temperature at Whangapoua generally ranges from 15.4 to 15.6° C, but shows a sudden increases of up to 1° C during the periods of northerly flowing wind-generated currents (Figure 4.18 c). This may result from warmer estuarine waters in Whangapoua Harbour flowing offshore during catchment flooding associated with local heavy rainfalls. Water temperature off Whangapoua does not show the same strong semi-diurnal variations as Opito Bay, with only slight decreases and

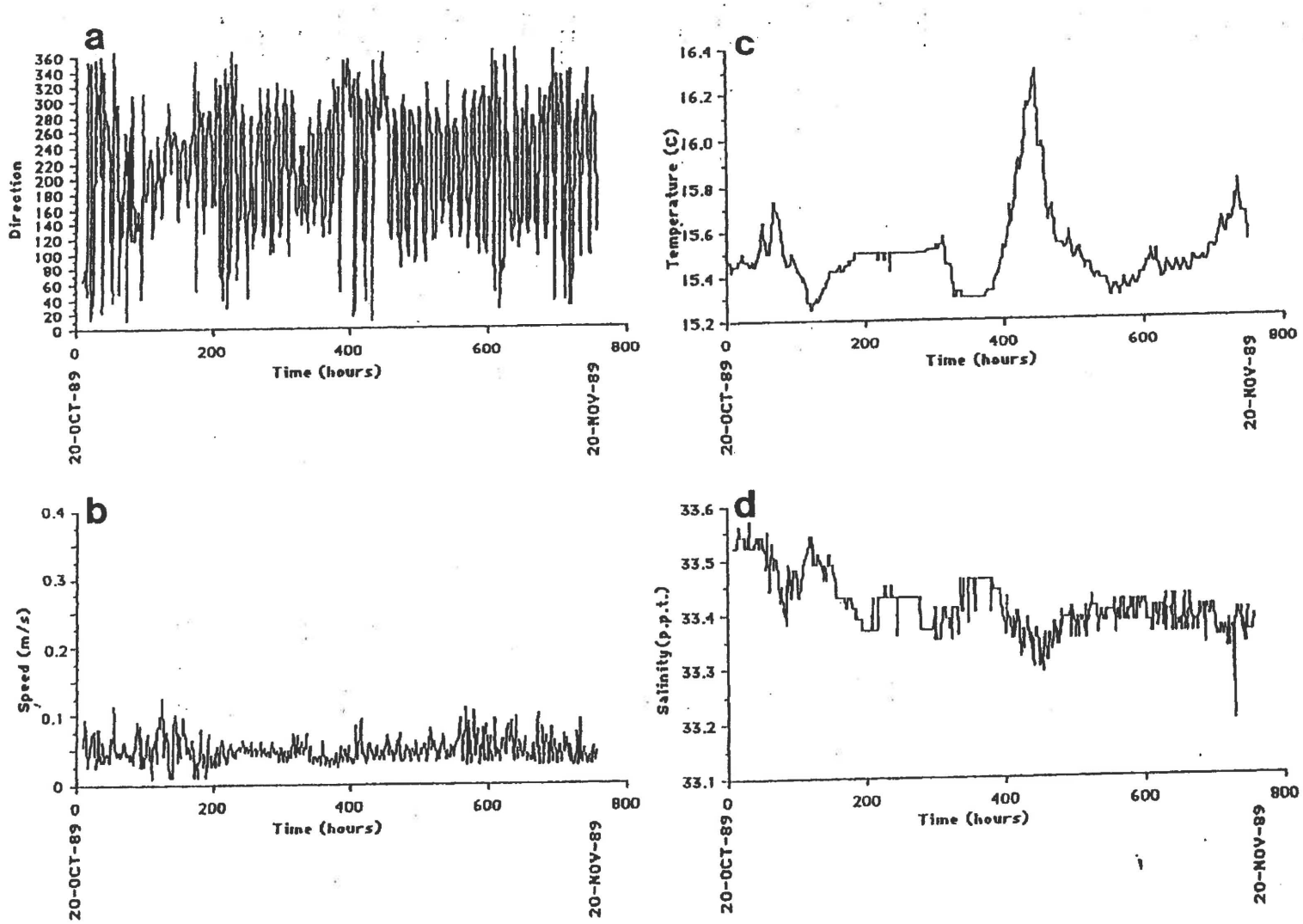

Figure 4.18. Time series plots of hourly current meter data from Whangapoua: a) current direction; b) current speed; c) water temperature; d) water salinity.

increases occurring on the respective ebb and flood tides (Appendix 1B). Thus, the influence of Mercury Bay water masses does not appear to extend beyond Opito Bay.

Water salinity seems to follow a similar trend to temperature at Whangapoua, being generally stable at 33.4 to 33.6 °/oo, but decreasing by 1°/oo during the northerly flows (Figure 4.18 d). This tends to support the observed changing water mass characteristics as resulting from catchment flooding and penetration of warmer less saline harbour waters onto the shelf. This differs slightly from observations in winter at Onemana, where temperature decreased during flooding. However, such seasonal changes in the influence of harbour waters on adjacent deeper coastal waters is quite common around New Zealand (HEATH, 1985). Salinity also shows only weak semi-diurnal variations at Whangapoua, with sharp changes at mid tide and more stable values at high and low tide (Appendix 1B).

Current measurements from the northern part of the study area are important in understanding the sediment transport processes that should occur here. Clearly, the semi-diurnal M_2 tidal wave forms an important part of current flows in this region, particularly off Opito Bay. These currents were too low in speed off Opito to transport sediments, although they may occasionally reach threshold speeds during spring tides. Local wind-generated currents in this region are directed both north and south. However, the only current strong enough to transport shelf sediments is to the north at Opito Bay. Thus, both tidal- and wind-generated currents could be important components to sediment transport processes around Opito Bay.

The characteristics of current flows off Whangapoua differs significantly to Opito, with opposite flow directions and lower current speeds consistently found, and also less variable water temperatures and salinities. This suggests that the Whangapoua offshore region forms a semi-enclosed embayment, with only restricted current circulation occurring through the channel off Opito Bay. As the tidal-forced currents are of opposite direction and flowing onshore, it is possible that a separation current develops around the Kuaotunu Peninsula and forms a small eddy off Whangapoua Harbour (Figure 4.19). Such a phenomena has been observed by HARRIS (1985) north of the study area on the Whangaparoa Peninsula. The circulation patterns developed here may result in some onshore movement of shelf sands in shallower waters. However, sediment transport by currents will generally be insignificant, and is probably associated with relatively rare high speed wind events and wave-induced near bottom currents.

The northern part of the study area therefore shows some similarities with the model presented in Figure 4.14, as sediment transport here is mainly associated with wind-generated northerly currents. However, it also shows some important differences, namely the presence of a strong tidal component, and the apparent absence of the southward-directed East Auckland Current during calm weather periods. This variation from the model may be due to the different physiography here, with the Mercury Island group offshore from Opito Bay and the Kuaotunu Peninsula deflecting the East Auckland Current flow away from the coast, and thus allowing tidal

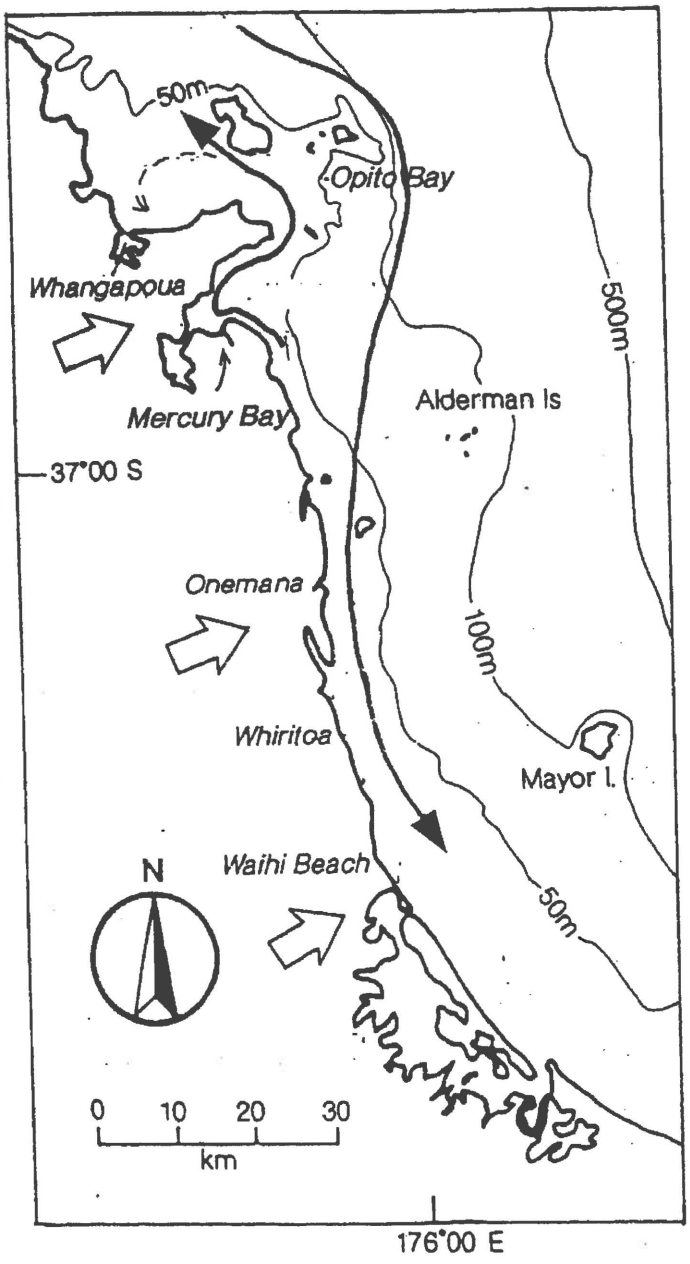

Figure 4.19. Inferred current flow patterns off the northern east Coromandel coast during fair weather periods. Here, the the East Auckland Current is deflected away from the coast between Whangapoua and Opito Bay by the Mercury Islands. This allows the semi-diurnal tidal stream to extend northwards from Mercury Bay to Opito. Offshore of Whangapoua, the tidal stream is deflected by the Kuaotunu Peninsula to develop a weak eddy.

currents to dominate during calm weather periods (Figure 4.19). These local physiographic effects also result in very restricted current flows off Whangapoua, which are more characteristic of a semi-enclosed embayment than open coastal waters. Also, the higher flows at Opito may result from tidal currents being constricted by these islands and thus accelerating through the Hole in the Wall channel.

4.4.2. Waihi-Whiritoa

Three current meters were deployed in the southern part of the study area in Sep-89. Two of these were located on a sand ridge off northern Waihi Beach, one in the trough (7204) and one on the crest of this feature (7200). The third current meter was located on the Whiritoa inner shelf. It had originally been hoped that this experiment would produce some major findings regarding the nature of flows over the sand ridges, and regional differences in current flow patterns between Waihi and Whiritoa. Unfortunately, no direction data were obtained as the compasses were affected on all the current meters by magnetic fields from the batteries used. In addition, the water salinity records appear unreliable, as shown by large regional differences between Waihi and Whiritoa (2.5‰), and the absence of these records at the second Waihi site (7204). Despite this, some useful information was obtained from the current speed records.

The highest current speeds were measured on the inner shelf off Whiritoa, these generally ranging from 0.10 to 0.20 $m.s^{-1}$ (Figure 4.20 a). No semi-diurnal variations in the data are apparent, either here or at Waihi (Appendix 1B). Three high speed current events are noted, on the 18-Sep-90 (0.28 $m.s^{-1}$), 30-Sep-89 (0.26 $m.s^{-1}$) and 7-Oct-89 (0.28 $m.s^{-1}$), all associated with moderate south to southwesterly winds (7-9 $m.s^{-1}$; Figure 4.20 a, b). During these higher speed current events, there is a noticeable decrease in water temperature and salinity in the first two cases, but an increase in salinity in the latter (Figure 4.20 c). This is an important observation, as the Onemana data show that the southerly flowing currents associated with the East Auckland Current have high water temperatures and salinities, and that wind-generated northerly currents are marked by a sudden decrease in these properties. Although the direction data were not directly usable, they do show a sharp clockwise rotation to the north in the first two events. Thus, the high speed current events are probably wind-generated flows of limited duration.

Records obtained offshore from Waihi Beach show currents of significantly lower speed than at Whiritoa, generally ranging from 0.05 to 0.10 $m.s^{-1}$, and tending to be higher over the sand ridge crest (Figure 4.21 a) compared to the trough (Figure 4.21 b). Thus, differences in flow intensities occur on both a regional and local scale. Peaks in current speed tend to occur at the same time as those from Whiritoa, however only on the 18-Sep-90 did these significantly exceed mean flow speeds (17 $m.s^{-1}$ and 13 $m.s^{-1}$ for the crest and trough respectively). Wind data from Waihi show west to southwest winds dominating during the deployment period (Figure 4.20 c, d), which tend to be of higher speed than the dominant southerly winds at Whiritoa (up to 12 $m.s^{-1}$). The salinity and

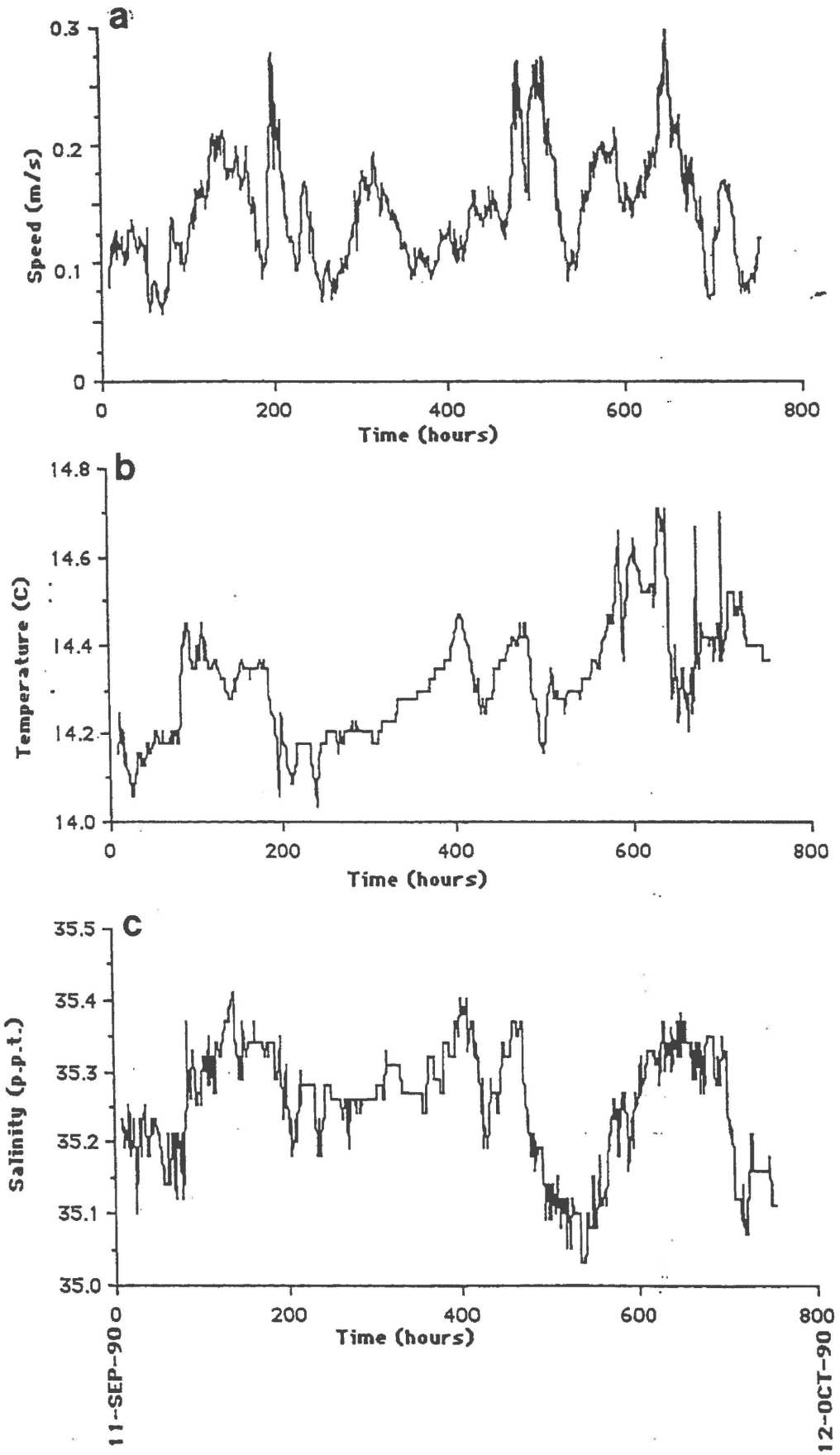

Figure 4.20. Time series plots of hourly current meter data from Whiritoa: a) current speed water temperature; c) water salinity.

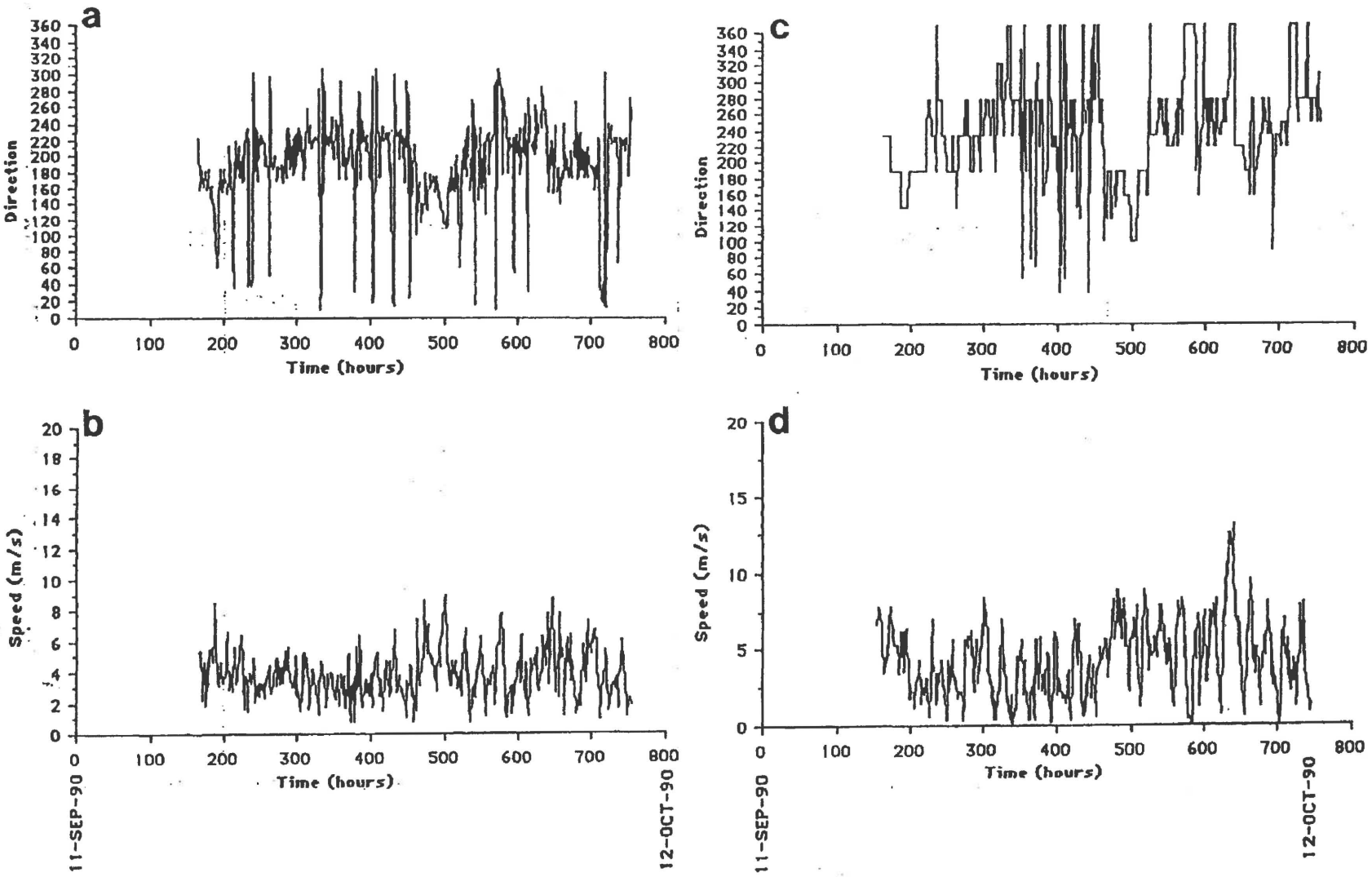

Figure 4.21. Hourly wind data obtained from :Whiritoa Beach, a) wind direction, b) wind speed; and Waihi Beach, c) wind direction, d) wind speed.

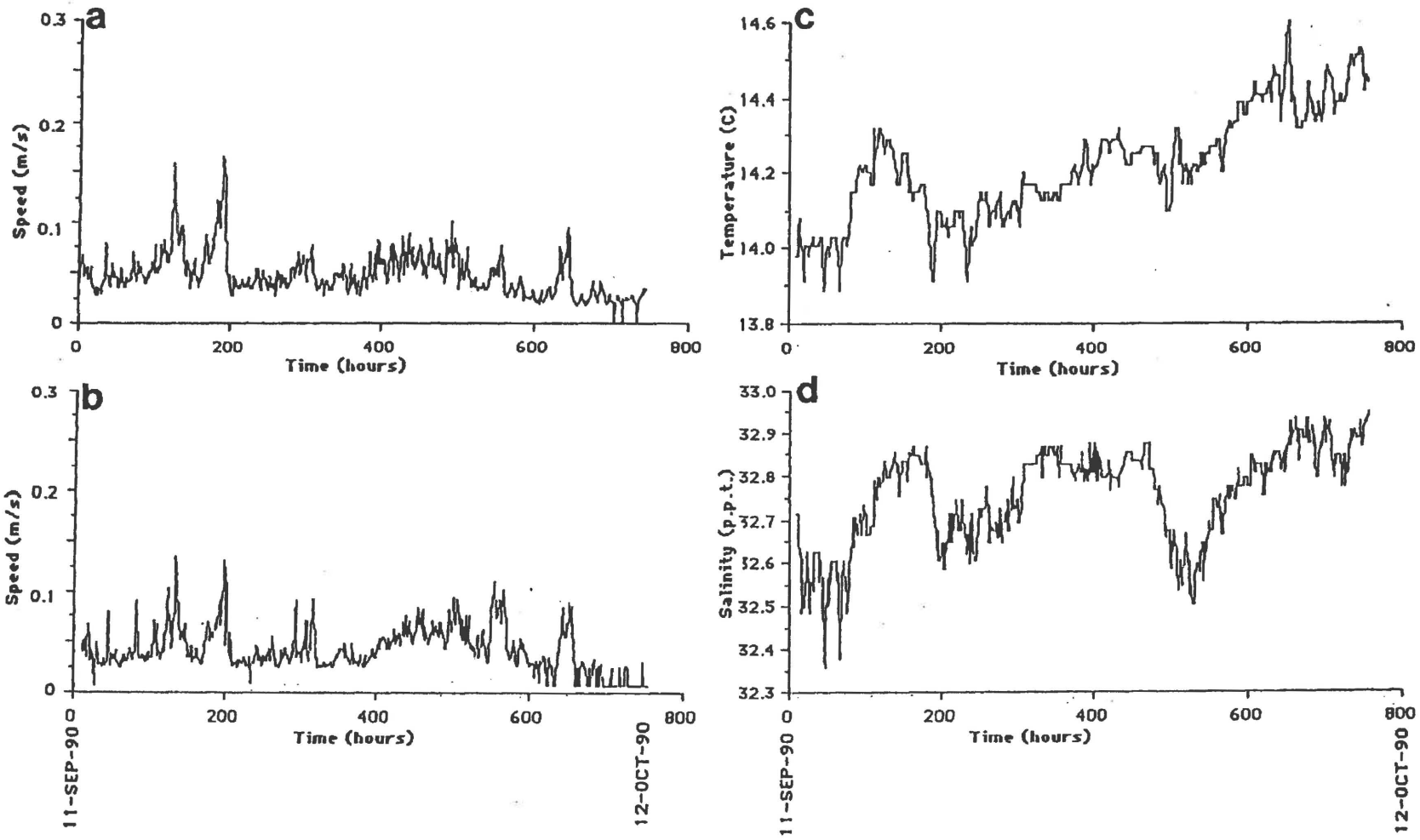

Figure 4.22. Time series plots of hourly current meter data from Waihi: a) current speed over sand ridge crest; b) current speed over sand ridge trough; c) water temperature; d) water salinity.

temperature data at Waihi show similar trends to Whiritoa (Figure 4.21c, d), therefore both areas were probably affected by the same water masses and thus current flows.

This limited data presented from the southern part of the study area indicates that similar current flows probably extend along the coast from Waihi to Whiritoa. However, they vary significantly in intensity, both between these two regions, and over bathymetric features present offshore. As the current records were obtained during dominantly fair weather periods, the results may be showing a difference in intensity of the southerly-directed current along the coast. This is supported by similar ranges in speed at Whiritoa to the southerly current recorded from Onemana, and comparable trends in water temperature and salinity during calm and stormy weather periods. The differences in current intensities may also result from the regional variations in wind climate found along the coast, as the southerly winds at Whiritoa would blow parallel to the coastline here, whereas the southwesterly winds at Waihi would blow offshore. Current speed variations may, however, result from the different depth locations, and thus be showing offshore variations in current speed rather than regional variations. A fourth possibility may be the records reflecting instrumental errors, as the Waihi current meters were shrouded to reduce the effects of wave pumping, whereas the Whiritoa current meter was an older non-shrouded system. However, the experimental period was dominated by offshore winds and thus calm sea conditions, and it is unlikely that wave-orbital motions interacted with the sea-bed in 30 m water depth at Whiritoa. Clearly, further analysis of current patterns within the southern part of the study area is necessary to obtain a more thorough understanding of regional current flow patterns.

4.6. CONCLUSIONS

An initial account of the east Coromandel offshore current patterns has been possible through collecting detailed current measurements, and integrating these with the regional current patterns obtained from extensive sea-bed drifter experiments. From this approach, a conceptual model for the study area has been presented which shows it to be dominated by two mutually exclusive shore-parallel near-bottom current flows.

Throughout much of the year, particularly in summer and autumn, fair weather periods prevail along the east Coromandel as mid-latitude anticyclones dominate the local weather patterns. Associated with these fair weather periods is a relatively weak southerly flowing current, which was of insufficient speed to transport inner shelf sediments. The southerly flow appears to be remotely forced, and is possibly associated with the regional East Auckland Current flow.

The episodic generation of low pressure systems in the Tasman Sea and their subsequent passage over the study area causes the local formation of strong onshore easterly winds. A northerly-directed current is generated by these onshore winds. An important finding is that this wind-generated current will only develop a steady, coherent flow pattern if the winds are of sufficient speed and duration (> 12 $m.s^{-1}$ speed and 5 hours duration), although antecedent current conditions

are also important. This northerly-directed current has sufficient speeds (up to 0.40 $m.s^{-1}$) to transport inner shelf sediments, with waves formed by the same onshore winds likely to intensify rates of sediment transport. As the weather patterns observed during the study seem representative of average conditions, it is likely that inner shelf sediments are being transported northwards along parts of the east Coromandel coast.

However, subsequent current measurements from both the northern and southern limits of the study area show that important variations from this basic model do occur. Between Opito Bay and Whangapoua, northerly- and westerly-directed tidal currents are a significant component of fair weather flows, probably as a result of the absence of the southerly flowing current. A northerly directed flow capable of transporting shelf sediments is still present at Opito during storm events. Regional variations in flow direction and intensity occur between these areas during both calm and stormy periods, with higher speed currents (0.1 to 0.2 $m.s^{-1}$) at Opito Bay, and lower intensity (< 0.1 $m.s^{-1}$) reverse direction flows off Whangapoua . Thus, current-induced sediment transport rates are likewise expected to vary from high to low between these two areas.

Results from the region extending between Whiritoa and Waihi are less conclusive, due to an absence of direction data in the current records. However, it is apparent that current flows during calm periods vary in intensity from higher in the former area (up to 0.28 $m.s^{-1}$), to very low in the latter (< 0.1 $m.s^{-1}$). Thus, regional variations in current patterns seem to occur between these two areas. This might relate to the narrower and steeper shelf surface off Whiritoa allowing greater incursions of the East Auckland Current than on the much broader and flatter shelf at Waihi.

CHAPTER FIVE

SURFICIAL SEDIMENT TEXTURAL PATTERNS

5.0. INTRODUCTION

A major aim of the E.C.S.S. was to investigate the surface sediment textural patterns on the shelf and associated beach-barrier systems. Initial observations were reported by DELL *et al.* (1985) and are examined here in much greater detail by investigating the hydraulic and physical properties of the sediments, as well as their biogenic (carbonate) constituents, and by attempting to define texturally-based sediment groups from the statistical analysis of textural data. The procedure represents the first step in defining various shelf lithofacies along the east Coromandel coast, and for determining transport pathways of the shelf sediments.

5.1. SAMPLE COLLECTION

A total of 563 sediment samples were collected for the E.C.S.S. from the shelf, beach-barrier systems, and local rivers. Locations of samples on the southern and northern coastlines are shown in Figures 5.1. and 5.2. respectively (for more detailed locations see Appendix 2). The rationale behind sample collection was to focus on the areas of most concentrated coastal development. Initially samples were collected at random locations over the shelf floor inshore of 50 m water depth to observe the overall textural trends, but in later surveys samples were gathered along side-scan sonar traces to assist interpretations of sonograph patterns (see Chapter 6).

Collection of such a large number of samples has spanned a period of 7 years and involved the efforts of several people. Offshore samples were collected from various vessels, including the H.M.N.Z.S. TUI, and using techniques ranging from diver grabs, pipe dredge, grab sampler, and box corer, the latter obtaining samples from up to 0.3 m below the surface. Position of samples was determined by ship radar and/or sextants.

Paul Dell commenced sample collection in February 1984 and continued until July 1986. He obtained 293 samples from 5 to 50 m water depth, mainly within the region extending between Waihi Beach and Whangamata. Tony Colby also collected 190 samples in the offshore region between Otama and Whangapoua in April 1984, mainly in water depths of 0 to 30 m. The remaining onshore samples were collected by the present author between September 1988 and November 1990, with beach samples gathered from the high tide swash (to about 0.1 m surface depth) and barrier samples from about 1 m below the surface. Bed samples were also collected by hand from all the major river systems along the coast and analysed for textural properties. However, these did not form an important part of the textural analysis but rather were collected for their mineralogical characteristics (see Chapter 9).

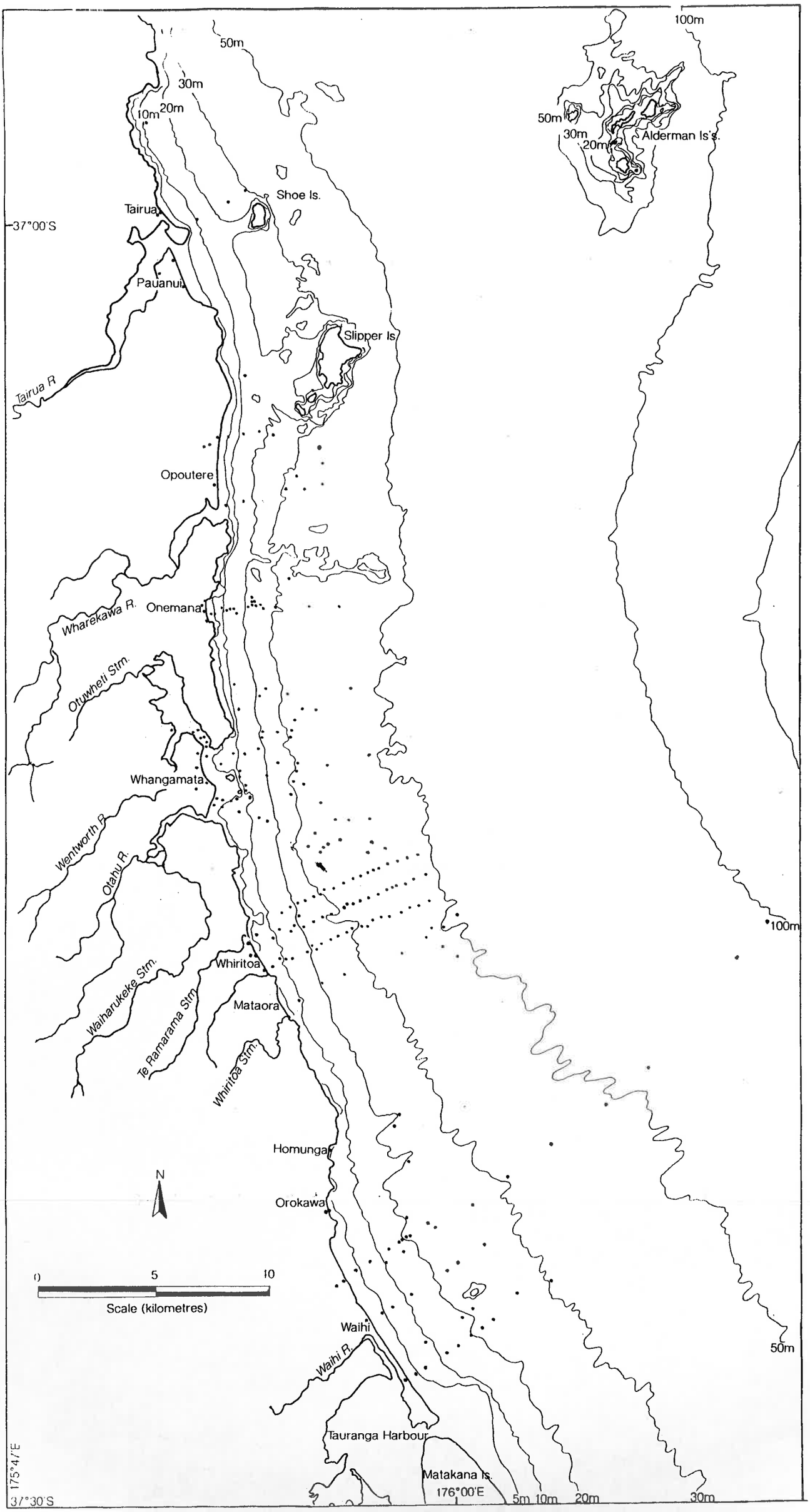

Figure 5.1. Location map of E.C.S.S. surface sediment samples on the southern coastline (note that more detailed location maps with sample numbers are presented in Appendix 2).

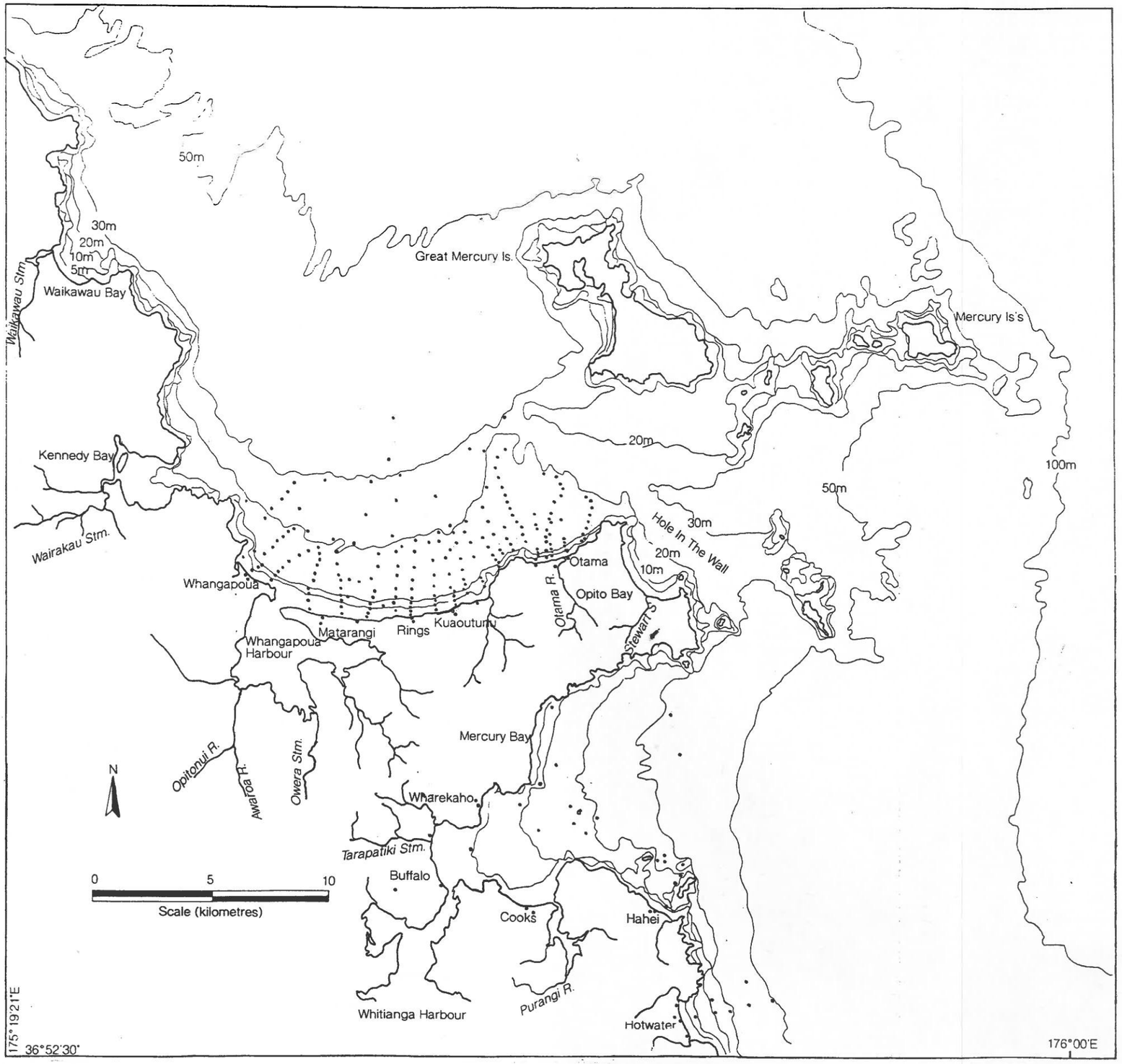

Figure 5.2. Location map of E.C.S.S. surface samples on the northern coastline (note that more detailed location maps with sample numbers are presented in Appendix 2).

5.2. TEXTURAL ANALYSIS

Textural analysis of samples involved three main steps. Firstly the hydraulic property of samples was determined, then the surface texture of grains examined, and finally the nature and content of the carbonate fraction were analysed. Results are listed in Appendix 3A.

5.2.1. Hydraulic Equivalence Textural Properties

Analysis of the hydraulic equivalence textural properties of samples (mean, sorting, skewness) were made using the University of Waikato's Rapid Sediment Analyser (R.S.A.). Samples were first washed through -1.75 and 4.0 ϕ sieves to remove coarse granules (coarser than 1.75 ϕ) and any silts and clays (finer than 4 ϕ). This generally resulted in only minor amounts of coarse shell fragments and muds being discarded from the analysis. The samples were then released into the settling tube, where the rate of grain accumulation on a balance plate at the bottom of the tube was measured by computer. Further details about the operation of the R.S.A. are available in the theses of McCABE (1985) and HARMS (1989) .

Advantages of using the R.S.A over standard mechanical sieves for measuring textural properties are that it provides data based on the hydraulic equivalent behaviour of sediments. In this analysis, the generally applied density of 2650 $kg.m^{-3}$ for quartz was used. While this is considered to be generally representative of east Coromandel shelf sediments, the presence of shell fragments, titanomagnetite, and volcanic glass shards in large quantities for some samples may be a potential source of experimental error. However, for a study such as this concentrating on the hydraulic behaviour of shelf deposits, the R.S.A. method is considered superior to standard dry sieving techniques.

Results from the R.S.A. are output as normal frequency distribution and cumulative frequency curves, with particle size results given for both graphical and moment method parameters. Although both techniques are equally accurate for textural analysis, the moment method parameters were used in this study as they are generally considered more sensitive to environmental processes than the graphic method (FRIEDMAN and SANDERS, 1978).

Mean grain size is perhaps the most important textural parameter to measure, as it is a simple comparative indicator of the weight force that must be balanced by an applied stress before transport by water or wind is possible (LEEDER, 1982). Mean grain size will also reflect the availability of different pre-existing sediments and the resistance of particles to weathering and physical abrasion (FRIEDMAN and SANDERS, 1978). Another important size parameter is the modal grain size, as sediment populations with a bimodal or polymodal size distribution will indicate two or more different sources for the sample.

Sorting refers to the spread of values or standard deviation about the mean for a sample. This is a useful measure in sedimentology as it indicates the degree of uniformity in grain transport and deposition (LEEDER, 1982), and thus reflects the general competency of the flow.

Skewness shows the deviation from symmetry of a sediment population, and reflects the presence or absence of fine and coarse material in a sediment sample (FRIEDMAN and SANDERS, 1978). The skewness of sediments has often been found to be a sensitive measure of the environment of deposition (FRIEDMAN and SANDERS, 1978).

Although kurtosis values were provided for each sample, these were not analysed as they appear to have been of limited use in most sedimentological studies.

An additional textural parameter obtained for some samples was their percent of mud (i.e. silt and clay size material). This was simply determined by removing the muddy fraction through a 4 ϕ wet sieve, and then measuring the dry weight of mud vs. coarser sized material. However, mud analysis was of limited use in this study, as in most of Paul Dell's original samples the mud had already been discarded.

5.2.2. Surface Texture of Grains

Information on the surface properties of individual grains in samples was obtained by taking a representative split and examining it under a binocular microscope. Properties observed were the roundness of grains through comparison with photograph plates published in LEEDER (1982), and the proportion of grains with iron oxide coatings.

The degree of roundness or angularity of the surface of grains is a general indicator of the extent of physical abrasion a sediment has undergone, with predominantly rounded sediment populations being considered to be texturally mature (in the geological sense of having undergone a number of cycles of subaerial and subaqueous weathering) compared to more angular grains. However, important effects such as increasing angularity with decreasing grain size, and selective sorting of rounded grains from more angular ones, need to be kept in mind when interpreting the roundness data.

The presence of iron oxide coatings on grain surfaces was considered an important textural property of shelf sediments, as oxidation of grain surfaces will not occur in anaerobic conditions, or environments where sediments are being continually agitated. Thus, sediment populations with abundant iron oxide stained grains most likely indicate the intermittent reworking of these deposits by wave and/or current action. Alternatively, they may represent deposits eroded from older relict sediments which were once exposed to subaerial weathering, or deposits recently derived from a terrestrial source. The percent staining in sediment populations was determined by making

a visual estimate of the number of grains with iron oxide coatings using the comparison charts in LEWIS (1984).

5.2.3. Carbonate

Although the amount and types of biogenic carbonate material present are primarily a biological characteristic of the sediments, its importance as a textural parameter must be considered for several reasons. Firstly, in areas of low clastic sedimentation carbonate material will act as the primary source of sediment and so can be used as a general indicator of sedimentation rates. Secondly, carbonate material may affect other textural parameters as a result of its unusual grain shape. MEHTA *et al.* (1980) found that shell fragments with platey shapes tend to settle in a relatively unstable mode compared to more spherically shaped clastic fragments, and therefore have higher drag coefficients. Thus shell fragments may appear coarse, but have a fine hydraulic equivalence due to lower settling velocity than equivalently sized but more spherical clastic grains. Finally, the shell species themselves will favour different physical environments and can thus be used as an indicator of hydraulic conditions on the sea floor.

Analysis of the percent calcium carbonate in samples was made by taking a 10 to 20 g split and measuring its weight loss when treated with HCl acid. Macrofaunal species were identified from published data in POWELL (1979), with Dr. Hamish Spencer assisting in the identification of molluscan fauna, and Abby Smith with the bryozoan species. The microfaunal population was also observed under a binocular microscope and important foraminiferal species identified using BARKER (1960).

5.3. TEXTURAL CHARACTERISTICS OF SHELF SEDIMENTS

Results from the textural analysis of nearshore and inner shelf surface samples are now presented for the southern and northern coastlines respectively. More detailed information on the original textural data is presented in Appendix 3. To assist in the presentation of data, a textural comparison key is presented in Table 5.1. which quantifies the various mean grain size, sorting, and skewness terms.

5.3.1. Southern Coastline

Textural data for the southern exposed east Coromandel coastline are shown as maps of mean and sorting in Figures 5.3 and 5.4 respectively, and cross-shelf variations in these and other textural parameters (carbonate, iron oxide staining, roundness) off the major beach sites shown in Figure 5.5. The amount of mud found in selected samples is also plotted in Figure 5.6. for both the southern and northern coastlines. The most striking observation from these various plots is the lack of consistency in textural patterns off different embayments along the southern coast.

Table 5.1. Quantification of sedimentary grain size parameters used in textural analysis (from LEWIS, 1984).

Textural Parameter	Numerical Range	Verbal Scale	Abbreviatio
Mean	-1.0 to 0.0 ϕ	Very Coarse Sand	V.C.S.
	0.0 to 1.0 ϕ	Coarse Sand	C.S.
	1.0 to 2.0 ϕ	Medium Sand	M.S.
	2.0 to 3.0 ϕ	Fine Sand	F.S.
	3.0 to 4.0 ϕ	Very Fine Sand	V.F.S.
Sorting	<0.35 ϕ	Very Well Sorted	V.W.Sor.
	0.35 to 0.50 ϕ	Well Sorted	W.Sor.
	0.50 to 0.71 ϕ	Moderately Well Sorted	M.W.Sor.
	0.71 to 1.0 ϕ	Moderately Sorted	M.Sor.
	1.0 to 2.0 ϕ	Poorly Sorted	P.Sor.
Skewness	+1.0 to +0.3	Very Fine Skewed	V.F.Sk.
	+0.3 to +0.1	Fine Skewed	F.Sk.
	+0.1 to -0.1	Near Symmetrical	N.S.
	-0.1 to -0.3	Coarse Skewed	C.Sk.
	-0.3 to -1.0	Very Coarse Skewed	V.C.Sk.

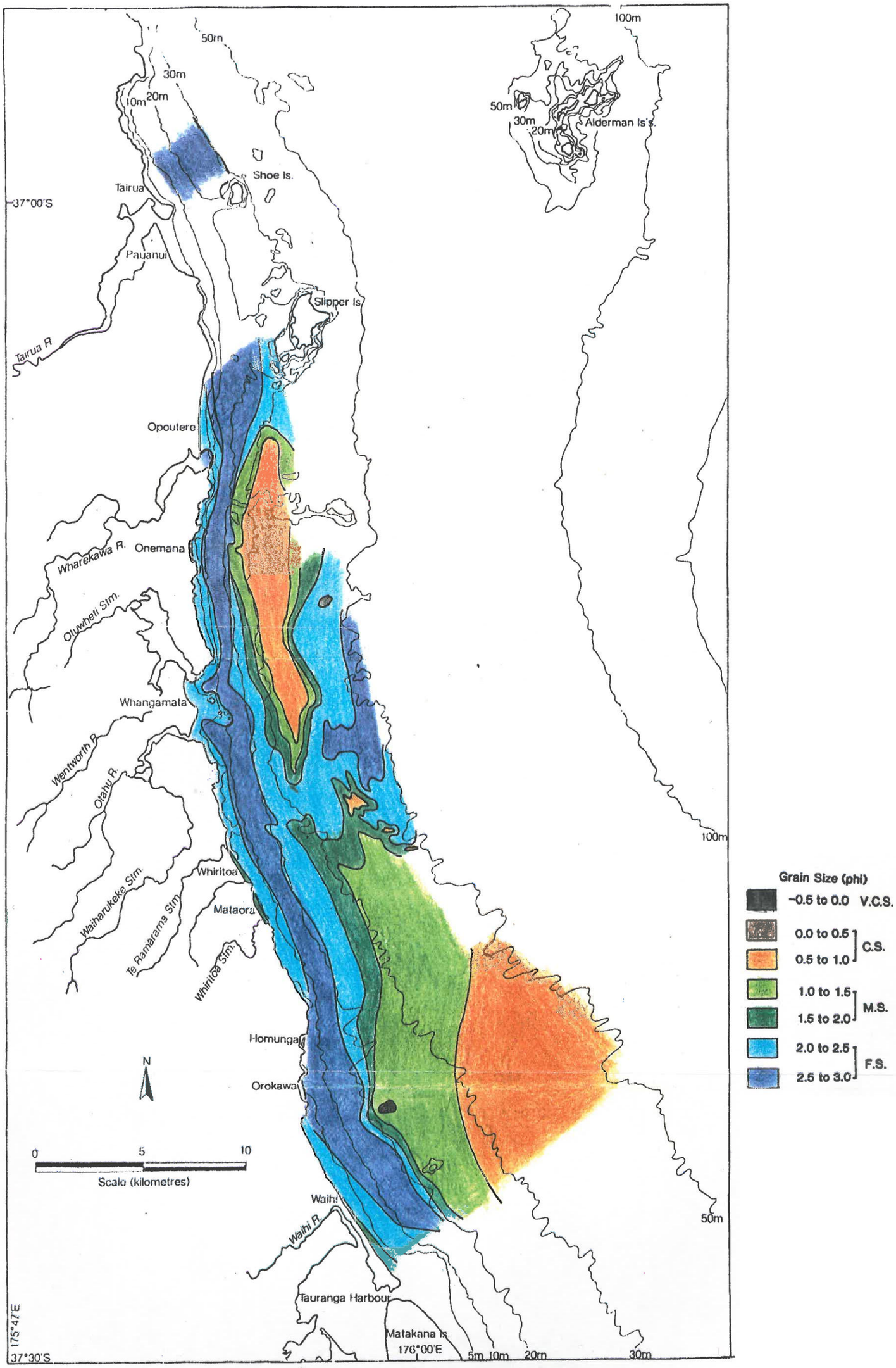

Figure 5.3. Distribution of mean grain size for shelf deposits on the southern coastline (note that more detailed maps of mean grain size for each major location are found in Appendix 3B).

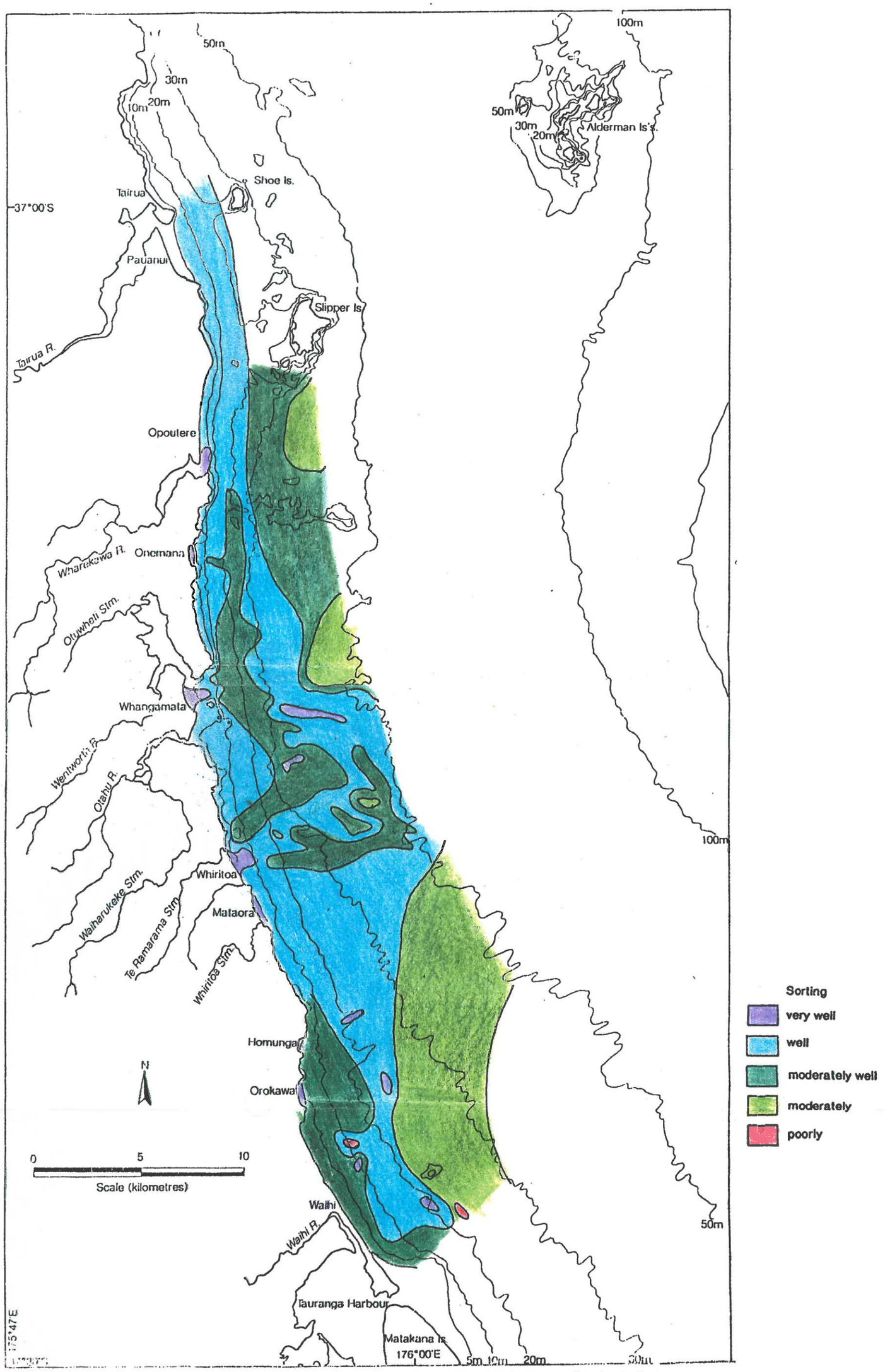

Figure 5.4. Distribution of sediment sorting for shelf deposits on the southern coastline (note that more detailed maps of sediment sorting for each major location are found in Appendix 3C).

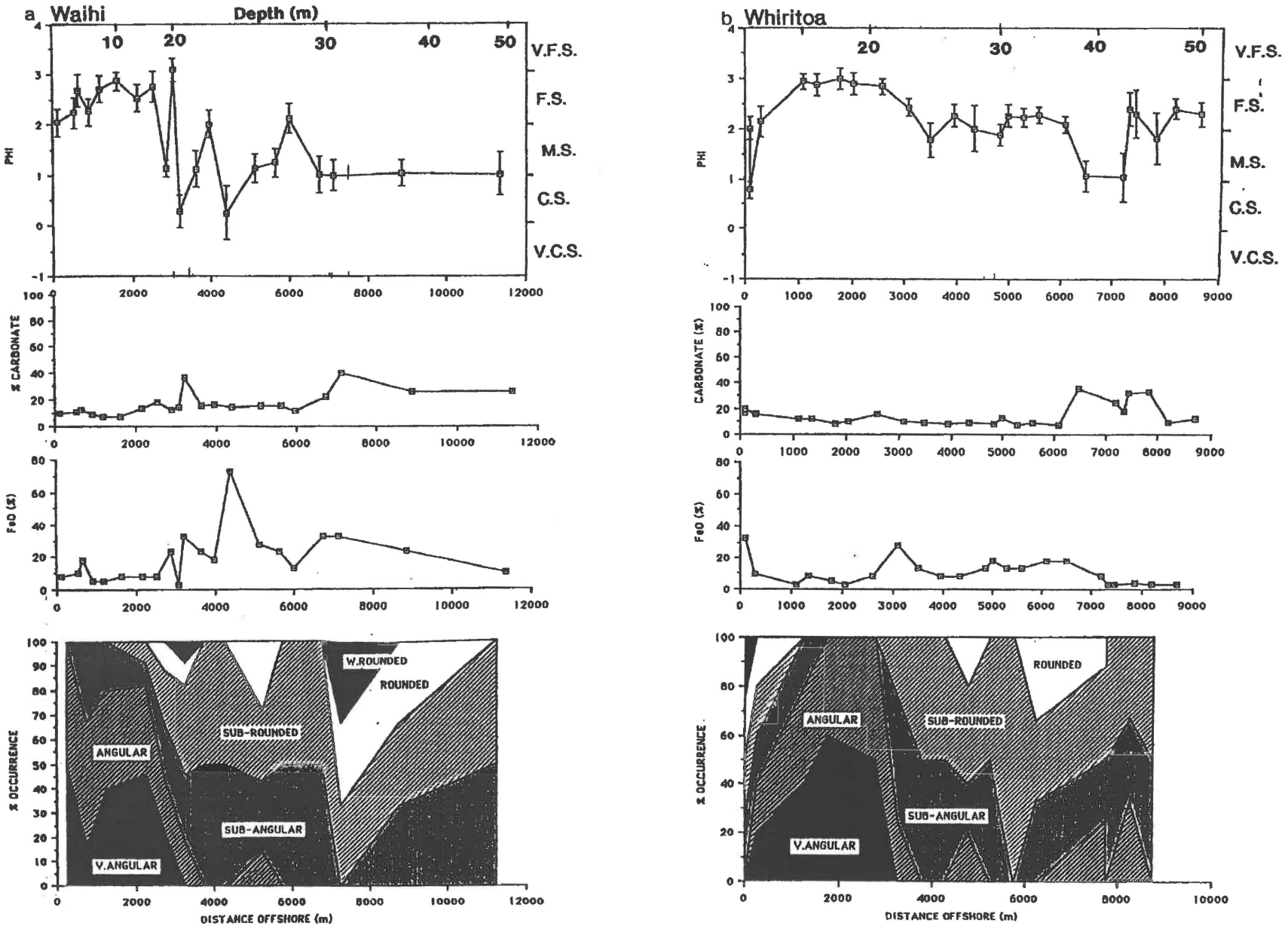

Figure 5.5. Cross-shelf variations in sediment textural properties offshore from southern coastal embayments: a) Waihi Beach; b) Whiritoa; c) Whangamata; d) Onemana; e) Opoutere (Note that the vertical bars on grain size graphs indicate the standard deviation or sorting of sediments).

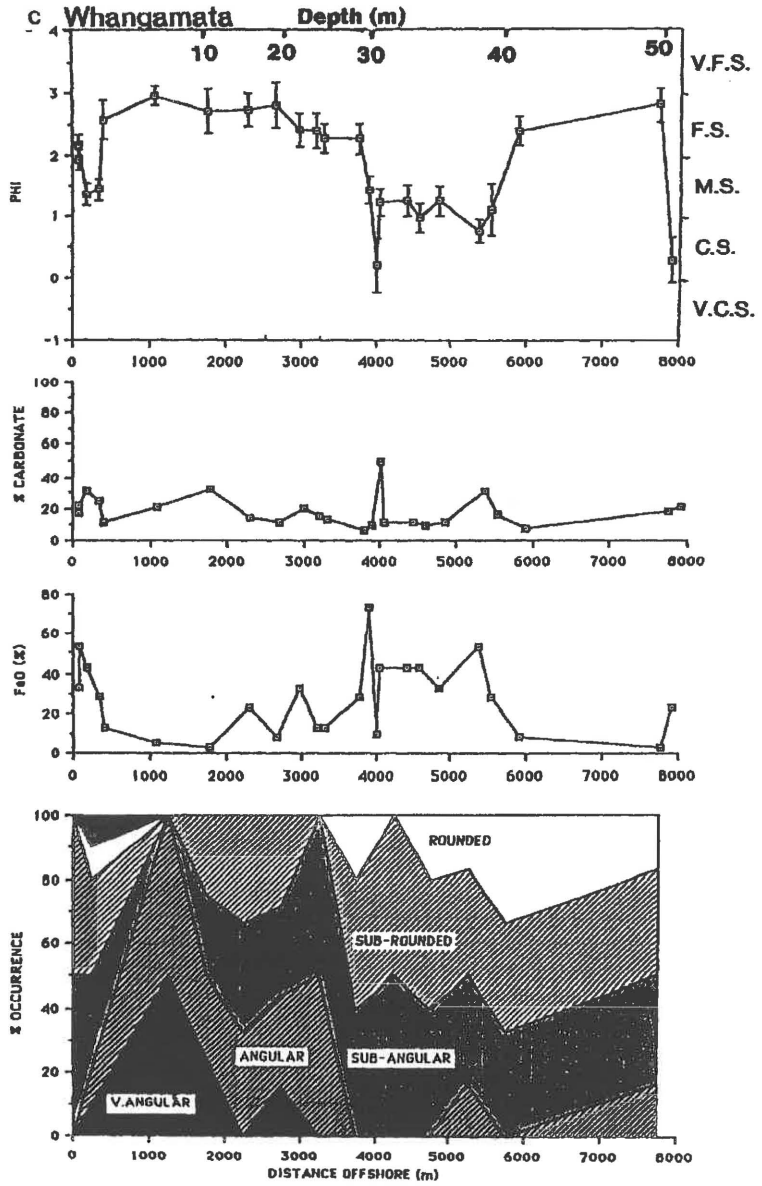

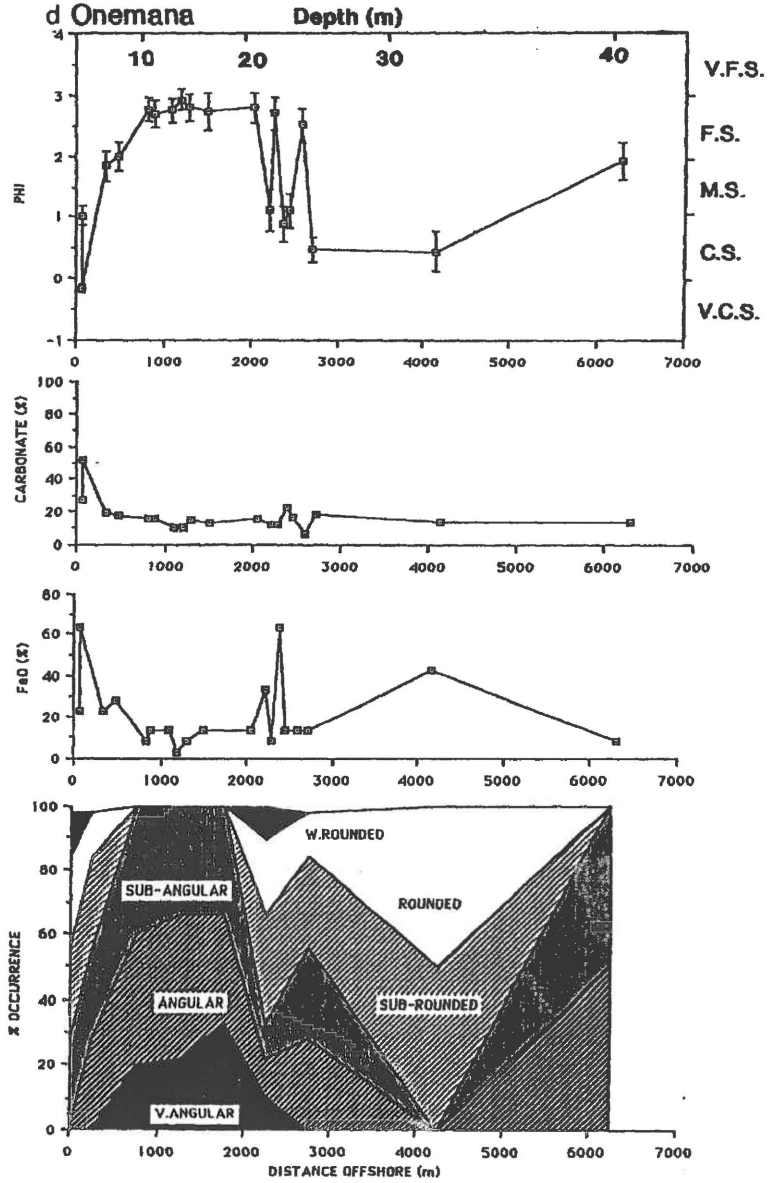

Figure 5.5 (continued).

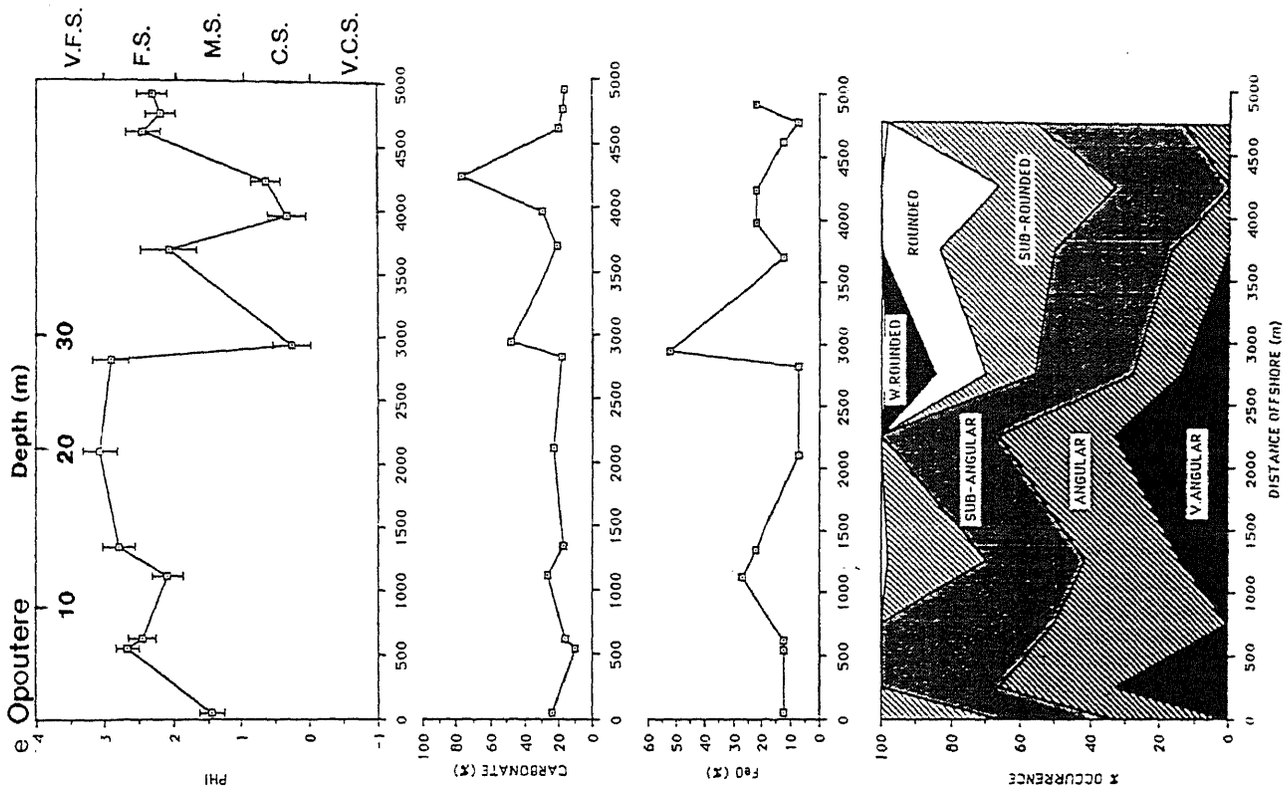

Figure 5.5. (continued).

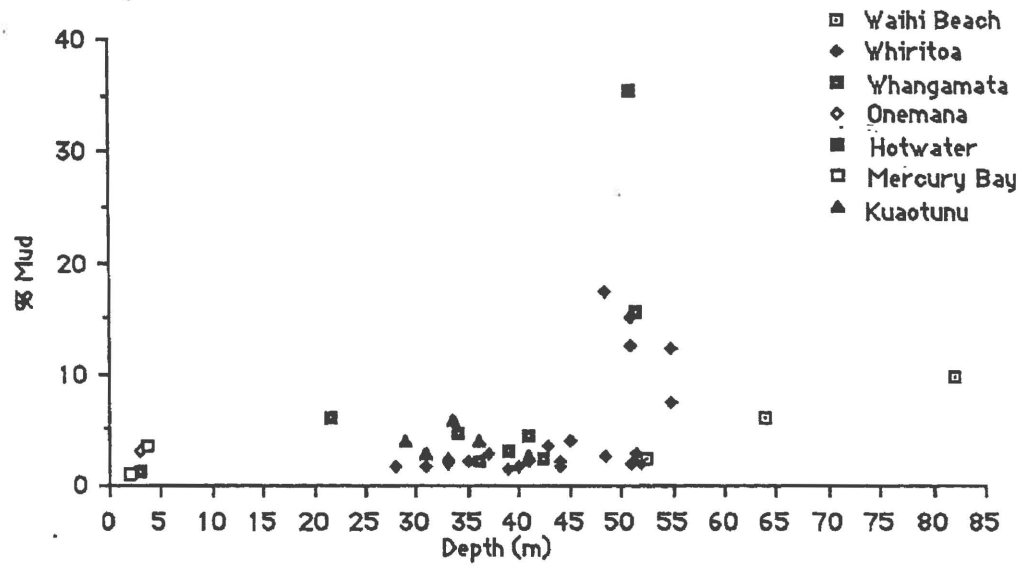

Figure 5.6. Occurrence of mud (finer than 4 ϕ) in selected east Coromandel sediment samples (for southern and northern coastlines). Note the substantial increase in mud for samples in 50 m water depth, indicating the presence of mid shelf samples.

One of the most highly variable textural properties is the mean grain size of surface samples over the shelf (Figure 5.3). Some uniformity is apparent in shallower deposits, with either fine or medium sands present in 5 to 10 m water depth, which decrease in size offshore to fine to very fine sands. The latter appear to extend into shallow depths (5 m) near inlet mouths at Otahu, Whangamata and Opoutere, which may indicate an onshore source for these fine sediments from the local estuary systems and associated catchments. Their offshore extent is generally restricted to a depth of 20 m along the coast, although this tends to increase northwards to 25 m and 30 m at Opoutere and Tairua respectively. The uniformity in distribution of these fine to very fine sands along the coast, together with their offshore fining trend, suggests that currents generated by surface gravity waves are primarily responsible for their deposition. This is consistent with the characteristic features of the upper nearshore surface as described in Chapter 3.2., and so the fine to very fine sands are tentatively termed 'upper nearshore' sands. Tidal currents may also be important for the reworking of these deposits close to harbour inlets, as indicated at Waihi Beach where they increase in size southwards to fine and medium sands where a large ebb tide delta extends offshore from Tauranga Harbour.

Further offshore, mean grain size patterns are highly variable. At Waihi Beach, there is an abrupt increase in grain size at 20 m depth to medium and coarse sands, with a noticeable patch of very coarse sands off northern Waihi Beach in 25 m water depth. Coarse sands dominate out to 50 m water depth, where medium grained muddy sands (5% to 10% mud) then occur, possibly marking the inner-mid shelf boundary. At Whiritoa, grain size increases only slightly at 20 m water depth, with fine sands dominating surface deposits out to at least 50 m. However, grain size distribution at Whiritoa is very patchy at depths of 40 to 50 m, where coarse and fine to very fine muddy sands (up to 14% mud) occur between lobes of fine sand. Textural patterns at Whangamata show an offshore coarsening trend from fine to very fine upper nearshore sands in 20 m, to fine, medium, and coarse grained sands between 20 and 30 m depth. Coarse sands dominate out to 40 m, where deposits then begin to fine again offshore to fine to very fine muddy sands (15 % mud) in 50 m water depth. A similar textural pattern occurs off Onemana Beach, although grain size increases more suddenly here from the fine to very fine upper nearshore sands, to medium and coarse grained sands in 24 m water depth. Off Opoutere Beach, grain size varies from coarse sands in the south, to fine sands further north in 30 m water depth.

Mean grain size patterns are therefore highly variable along the southern coastline in depths greater than 20 m. In general, there appears to be a band of fine sand in 20 to 30 m water depth, which may represent a lower nearshore deposit. Beyond this, grain size increases abruptly to medium and coarse sands which extend seawards to depths of 40 to 50 m. This would appear to correspond to the coarse grained inner shelf facies defined in previous studies of the northeast continental shelf (see Chapter 3.3.3.). Mid shelf deposits then occur in depths greater than 45 to 50 m, as shown by a sudden decrease in grain size to fine to very fine grained muddy sands. However, the fine grained lower nearshore sands appear to be absent at Waihi Beach and Onemana, whereas similar sized deposits are more extensive in deeper water at Whiritoa and

Opoutere. This suggests that nearshore deposits are eroding at Waihi and Onemana, and depositing further north.

Data presented in Chapter 4.4. showed that wind-generated currents are capable of eroding and advecting fine sands to the north, and so this textural pattern is consistent with wind-generated currents dominating sediment transport beyond 20 m water depth. The extensive deposition of fine sands at Whiritoa and Opoutere must therefore be due to some change in either the intensity or direction of these along-shelf flows. At Whiritoa, current measurements show that fair weather flows are more intense on the inner shelf than they are off Waihi Beach, and so a decrease in current intensity would seem unlikely. Deposition must therefore result from the presence of complex current flows, due to either the change in orientation of the coastline with respect to local wind patterns, or the deep indentation in the continental shelf which occurs further offshore. At Opoutere, flow intensity may decrease due to Slipper Island either retarding this northerly flow in 30 m water depth, or creating a wave shadow zone and thus decreasing the shear stress exerted on shelf deposits by combined wave-current flows.

Another important variation in textural patterns which requires consideration is the contrast in grain size of mid shelf deposits between Waihi and areas further north. The dearth of fine sediments at Waihi may be due to the absence of a nearby source for such deposits, although this would seem unlikely due to the presence of large river systems in the Bay of Plenty region further south. Alternatively, it may indicate higher energy conditions on the mid shelf here than for regions further north.

The patterns of sorting for shelf sediments along the southern coast are highly variable, particularly off Whiritoa Beach (Figure 5.4). However, some generalisations to the patterns can be discerned. The fine to very fine grained upper nearshore sands are generally well sorted, which supports earlier deductions that these are primarily reworked and deposited by the currents associated with surface gravity waves. However, off Waihi Beach they tend to be only moderately well sorted deposits. As ebb tidal delta deposits at the southern Bowentown end of Waihi Beach are moderately sorted sands, then it is possible that the comparatively poorer sorting of Waihi Beach upper nearshore sands results from large inputs of recent terrestrial deposits out of Tauranga Harbour. The fine grained lower nearshore sands tend to be only moderately well sorted deposits, which may reflect a transition from wave- to current-dominated flow conditions between the shallow upper nearshore and deeper inner shelf zones. Inner shelf deposits are highly variable, but are mainly well or moderately well sorted sands, with some isolated patches of very well and poorly sorted sediments also present. The cause of this variability is uncertain. However, it may indicate varying intensities of flow conditions both along and across the inner shelf, the presence of recently exposed relict sediments in some areas, or the mixing of modern shell fragments with older clastic grains. Mid shelf deposits appear to be mainly moderately sorted sediments, which reflects the decrease in intensity of hydrodynamic

conditions in deeper waters, as is also evidenced by the presence of significant quantities of mud in these deposits.

The amount of carbonate or biogenic material in sediments does show some more consistent trends (Figure 5.5). The upper and lower nearshore sands are generally low in carbonate (< 20%), with higher concentrations then found in the coarser grained inner shelf sediments (20 to 40%), before decreasing again in mid shelf deposits. This is consistent with observations made by HILTON (1990) at Pakiri further north, who noted that this was contrary to the modern production of biogenic material, with the greatest infaunal productivity occurring on the nearshore surface, but highest modern shell concentrations found on the inner shelf surface. HILTON (1990) attributes this to the inner shelf material forming a lag deposit from which the non-biogenic fraction has been largely removed, and the nearshore carbonate diluted by high rates of clastic sedimentation. Exceptions to this general pattern occur near reefs and offshore islands where shell hash deposits of enriched carbonate material (50 to 80%) are often found, and also at Onemana where carbonate is consistently low away from the beach face. The former will result from the abundant amounts of epifauna which live on these rocky substrates and are thus incorporated into sediments. However, the low carbonate content in Onemana shelf samples is surprising in view of the extensive occurrences of rock reefs in this area. This may result from the reef epifauna being swept away by the strong wind-generated currents which occur in this area, to be deposited further north at Opoutere where carbonate concentrations are much higher.

The content of iron oxide stained grains in sediment populations is consistently low in the upper nearshore and mid shelf sands (< 20%), but higher in lower nearshore and inner shelf deposits (20 to 80%; Figure 5.5). The increase which occurs offshore across the nearshore and inner shelf is inferred to reflect the increasing dominance of intermittent sediment transport during storm conditions in deeper waters, while onshore decreases in upper nearshore sediments result from the frequent agitation of these which prevents oxidation from occurring. The lack of iron staining in mid shelf deposits will be due to anaerobic conditions dominating in this low energy environment.

Trends in the relative roundness or angularity of sediment populations are also fairly consistent (Figure 5.5). The upper nearshore sands are dominated by very angular grains, while grains become more rounded in the lower nearshore and inner shelf deposits, before increasing in angularity again in mid shelf deposits. This pattern is not in accord with the variations in hydrodynamic conditions inferred from other textural properties, as the upper nearshore sands appear to be more frequently agitated than lower nearshore and inner shelf sediments, and so should be subject to greater attrition. Two possible reasons for this pattern in surface texture can be offered. It may indicate that they are texturally immature terrestrially derived sediments which have only undergone a limited amount of subaerial and subaqueous weathering. Alternatively, the very fine size of upper nearshore deposits will result in a dominant suspended sediment mode of transport, thus preventing grain to grain contacts from frequently occurring

The higher degree of roundness in lower nearshore and inner shelf sands indicates that they are probably much older extensively reworked shelf deposits.

5.3.2. Northern Coastline

Surface sediment textural patterns from the northern embayed coast are shown as maps of mean grain size and sorting in Figures 5.7 and 5.8, and cross-shelf patterns for these and other textural parameters are given in Figure 5.9. The most striking feature of these textural patterns is that variations in sediment texture tend to be more dramatic between adjacent embayments than across the shelf surface. Therefore, it is not possible to make generalisations about the textural patterns for the northern region. Instead, trends within each of the four major beach locations (Hotwater, Mercury Bay, Otama, and Whangapoua) are described individually.

At Hotwater Beach, shelf samples show an initial fining offshore pattern from medium grained sands within 10 m water depth, to fine sands out to 20 m depth (Figures 5.7 and 5.9 a). Grain size then increases to medium sands from 20 to 30 m depth, and coarse sands out to 50 m water depth, where a sudden decrease to very fine grained muddy sands (35% mud) occurs. This offshore variation in grain size is consistent with that observed on the southern shelf, and the deposits are thus similarly labelled upper nearshore, lower nearshore, inner shelf, and mid shelf sands, for the fine, medium, coarse, and very fine muddy sands respectively. However, Hotwater Beach differs from the southern coastal embayments in that nearshore deposits are much coarser, and mid shelf deposits much finer and muddier. This may indicate that a higher wave energy coastline is present here due to the narrower and steeper inner and nearshore surfaces (see Chapter 6.2.2. for details of shelf morphology), which prevents fine material from depositing in depths shallower than 50 m. However, it may also result from the absence of a local source for fine sediments to be deposited on the nearshore surface.

Hotwater Beach shelf samples are comparatively better sorted than those found off southern embayments, with well to very well sorted nearshore and inner shelf deposits dominating, and moderately well sorted mid shelf deposits occurring further seawards (Figures 5.8 and 5.9 a). This shows that a high degree of sediment reworking occurs here, which adds support to the hypothesis that wave energy may be higher in this shelf region. Carbonate concentrations are consistently high in the shelf samples (15 to 30%), reaching a maximum of 55 to 80% between 20 and 30 m water depth (Figure 5.9 a). This may result from local high inputs of biogenic material from epifauna growing on the extensive reefs around Hotwater Beach, as well as a lack of clastic material from nearby catchments. Iron oxide staining on grains is also consistently high, ranging from 30 to 70% out to the mid shelf break, where no iron staining is then found on sand grains (Figure 5.9 a). This high staining of sediments at Hotwater may be due to their mineralogy, or from local hydrothermal alteration dominating over the effects of intermittent sediment transport (e.g. SCHOFIELD, 1970). The surface texture of grains shows a consistent pattern of

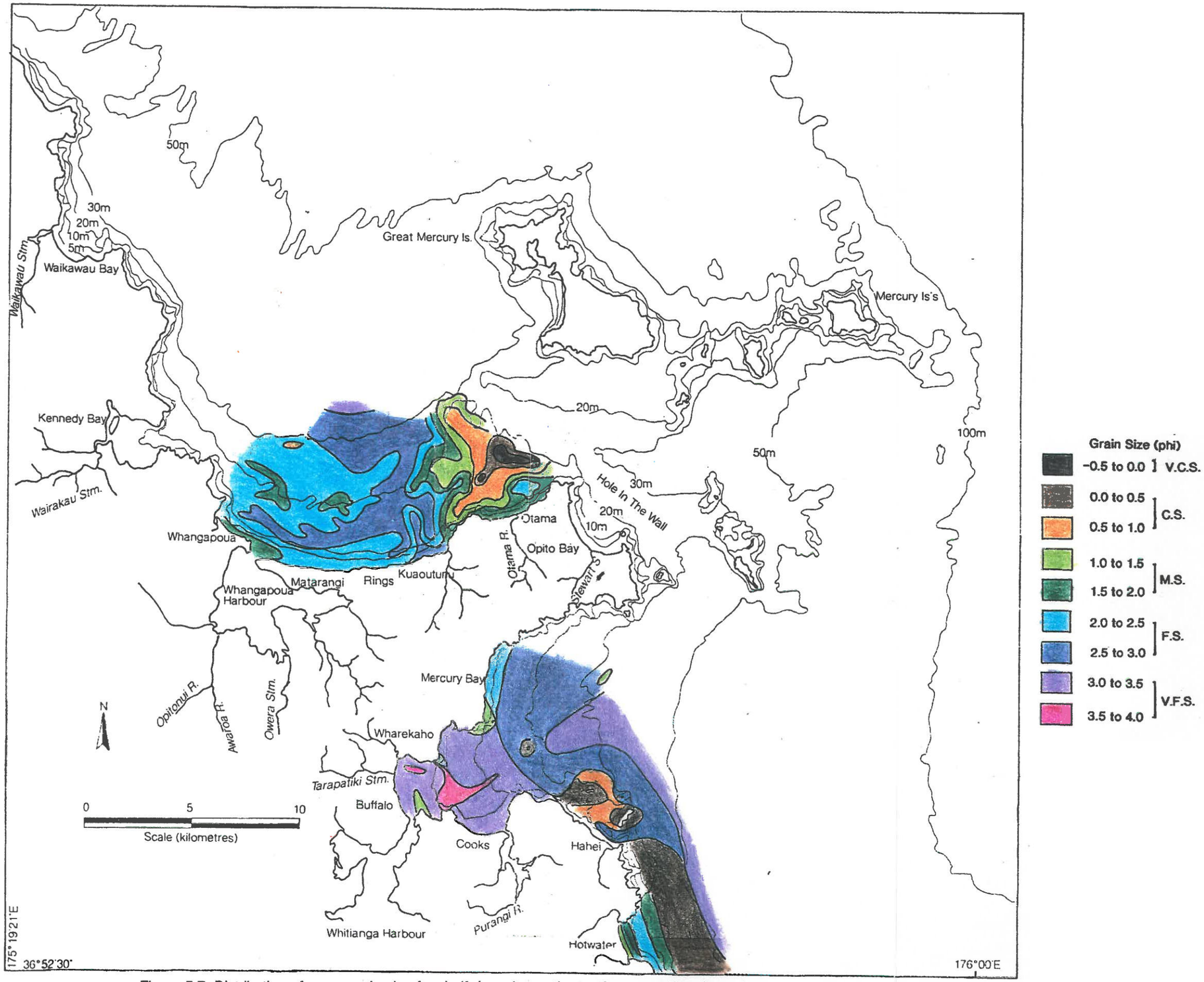

Figure 5.7. Distribution of mean grain size for shelf deposits on the northern coastline (note that more detailed maps of mean grain size for each major location are found in Appendix 3B).

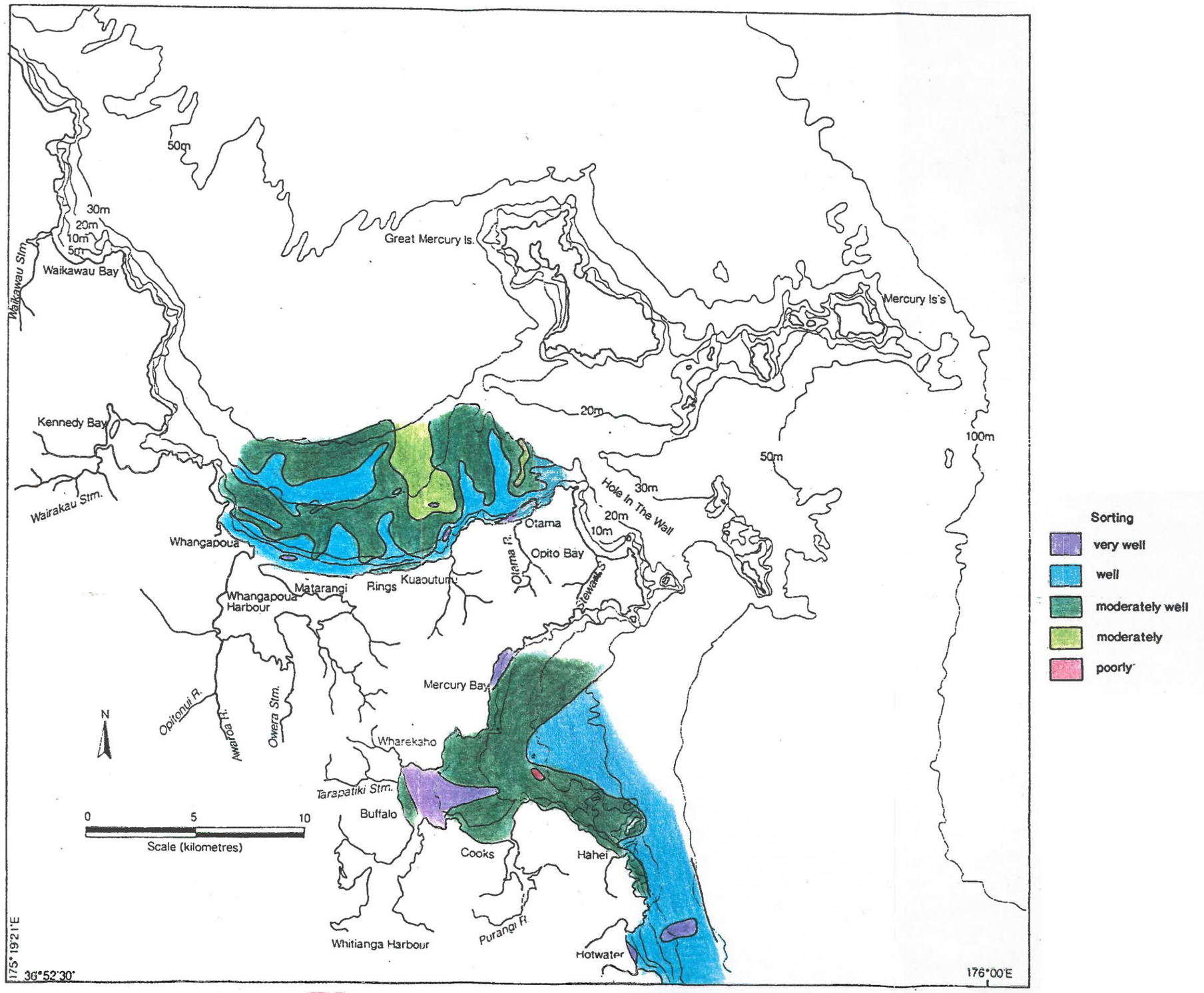

Figure 5.8. Distribution of sediment sorting for shelf deposits on the northern coastline (note that more detailed maps of sediment sorting for each major location are found in Appendix 3C).

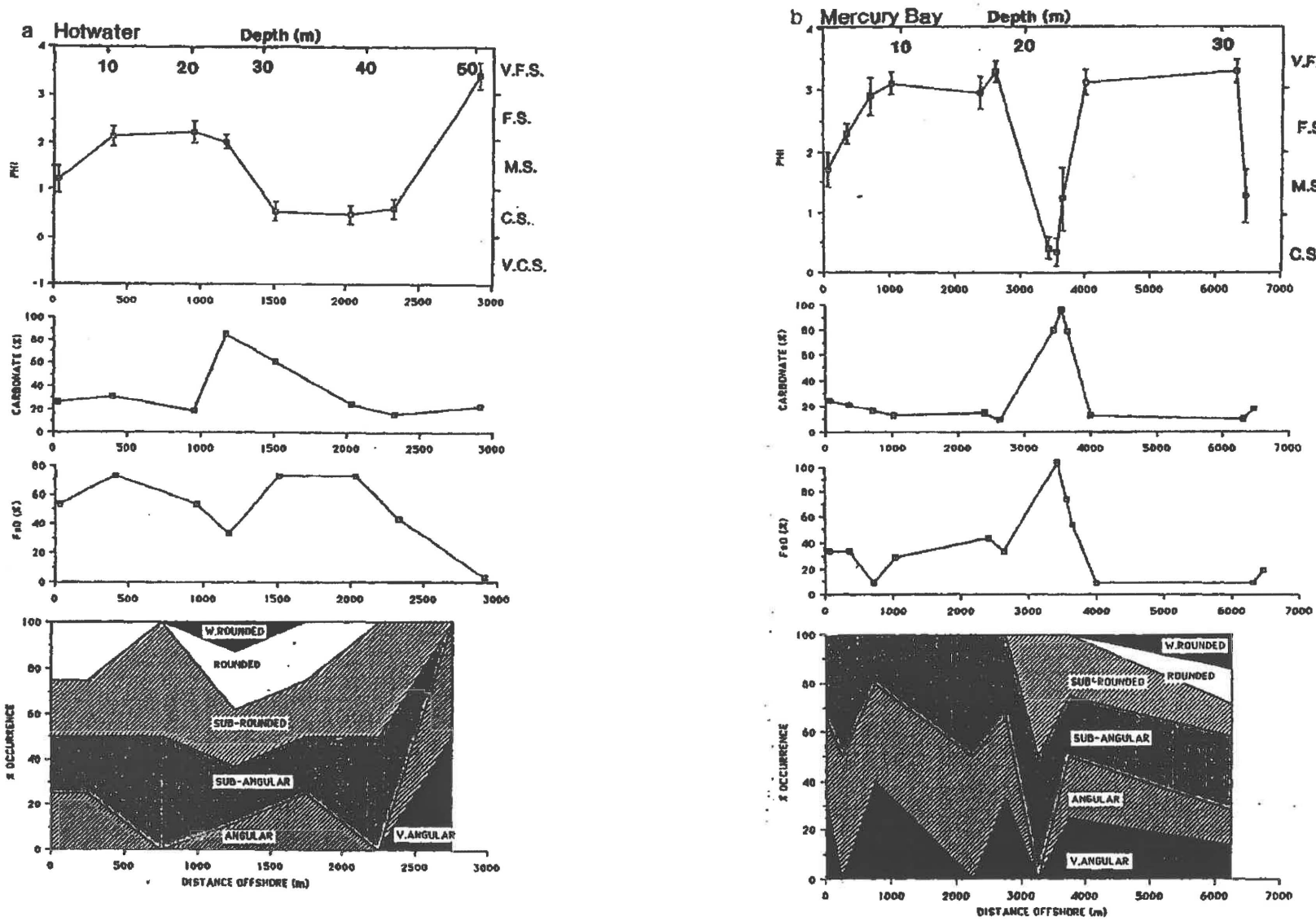

Figure 5.9. Cross-shelf variations in sediment textural properties offshore from northern coastal embayments: a) Hotwater Beach; b) Mercury Bay; c) Otama; d) Whangapoua (Note that the vertical bars on grain size graphs indicate the standard deviation or sorting of sediments).

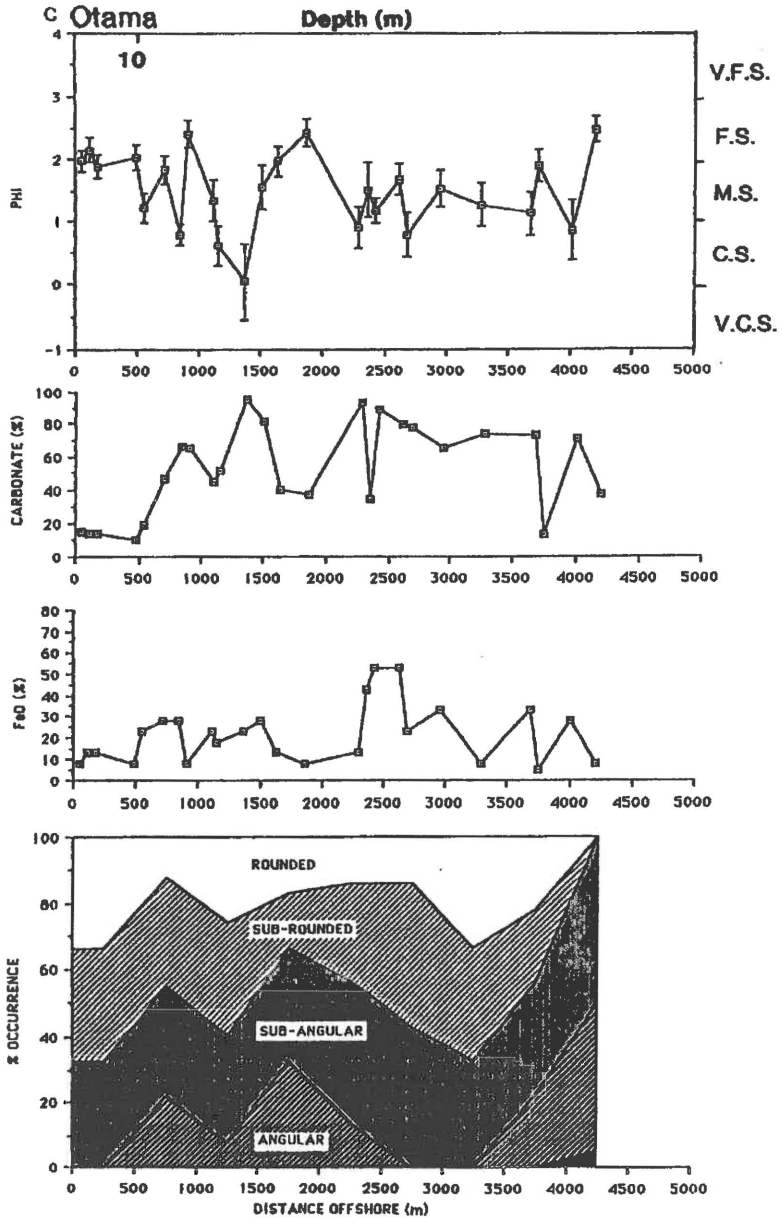

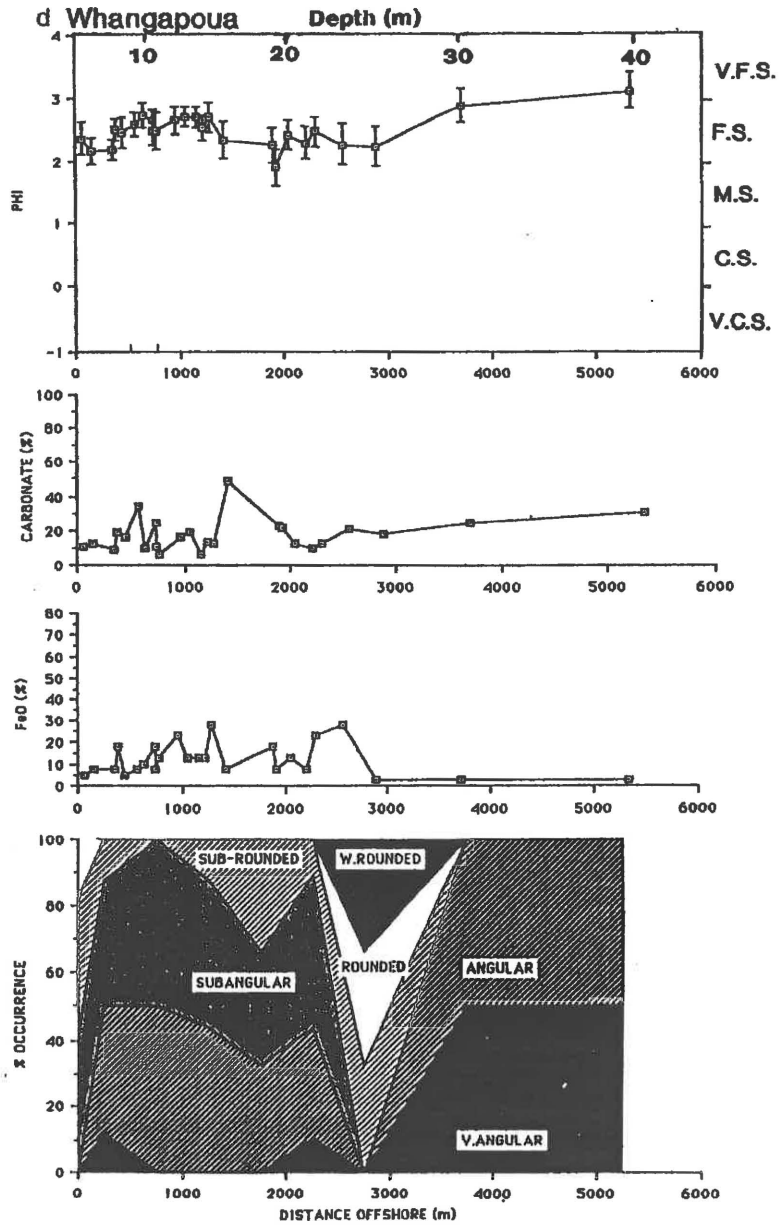

Figure 5.9. (continued).

angular to rounded grains dominating from the beach to the inner shelf-mid shelf break, where very angular non-iron stained grains then occur (Figure 5.9 a). The absence of very angular upper nearshore sands at Hotwater Beach, in contrast to areas further south, shows that a lack of recent sediment inputs is probably an important factor, along with high wave energy for the unique textural patterns.

Sediment textural patterns within Mercury Bay contrast with those at Hotwater Beach in being dominated by very fine rather than coarse deposits (Figures 5.7 and 5.8 b). The inner semi-enclosed part of Mercury Bay (< 10 m water depth) is dominated by very fine sand on the bay bed, which ranges in mud content from < 5% over the southern part of the inner bay, to 10% off the southern end of Wharekaho Beach, and up to 50% off the northern end of Buffalo Beach (SMITH, 1980). Areas of coarser medium grained sediments were shown by SMITH (1980) to be limited to higher energy areas, namely the ebb tidal delta off Whitianga Harbour, the northern end of Maramaratotara Beach, and the adjacent northern headland. Further offshore in the more exposed part of Mercury Bay, coarse shell hash deposits were found in this study between Mahurangi and Motueka Islands offshore from Hahei, and just south of Motukorure Island in Mercury Bay. A medium grained sand deposit was also found in deeper waters (33 m) from the northern part of Mercury Bay, but elsewhere fine to very fine grained sand dominates. The abundant occurrence of fine sediments in Mercury Bay suggests that energy conditions in the bay are relatively low, and that a local source for very fine sand and mud is present. As similar fine deposits on the southern coast appear to be derived from local catchments, their most obvious source here is from Whitianga Harbour. Very fine sands and muds within Mercury Bay could also be the source of mid shelf deposits at Hotwater Beach, which would account for their finer grain size than mid shelf deposits further south.

Sorting ranges from very well sorted very fine sands on the inner bay bed (< 10 m), to moderately well to well sorted fine sands in deeper water, and well to poorly sorted coarse sands around the offshore islands (Figures 5.8 and 5.9 b). This high degree of sorting in Mercury Bay sediments suggests that a significant reworking of deposits occurs. This is inconsistent with low energy conditions dominating, and thus leaves high terrestrial sediment inputs as a major cause for the extensive occurrence of very fine grained shelf sands within Mercury Bay. Carbonate content is generally low within the inner bay (< 20%; Figure 5.9 b), although SMITH (1980) found higher concentrations (50%) around the previously mentioned medium sand deposits. In the outer bay, values up to 90% are found around the offshore islands, but elsewhere remain low. This is again consistent with a high influx of fine sands from the local catchments of Mercury Bay, with shell hash deposits only forming around offshore islands where large numbers of epifauna live. Iron oxide staining is relatively high on inner bay sands (25 to 40%), and very high on the coarse shell hash deposits (up to 100%), but on deeper shelf sands (30 m) iron staining is quite low (<15%; Figure 5.9 b). This trend could be explained by freshly weathered terrestrial sands depositing on the inner bay surface, being subsequently reworked offshore, the attrition removing their iron oxide coatings.The presence of low staining in deeper deposits may also indicate anaerobic

conditions and thus very limited sediment reworking. Surface texture of grains is very angular to angular for deposits within the inner bay, but increasingly higher amounts of rounded grains are found offshore in the outer part of Mercury Bay (Figure 5.9 b). This adds support to the hypothesis that terrestrial sands are being reworked offshore from the inner bay surface. Alternatively, the deeper shelf sediments may be palimpsest sands, while the inner bay deposits are dominated by modern terrigenous sediments.

The area offshore from Otama Beach shows a very erratic and patchy textural distribution (Figures 5.7 and 5.9 c). Off the eastern end of the beach, a small patch of fine sand is present from 10 to 14 m, although further offshore in 17 to 20 m water depth a patch of very coarse to coarse sand is found. Medium grained sands tend to dominate the shelf region west of Otama out to 20 m water depth, however fine to very fine sands become increasingly dominant further west. This unusual textural pattern may relate to the presence of the Mercury Island Group offshore of Otama and Opito Bay, which appear to cause constriction and hence acceleration of tidal and wind-generated flows in this area (see Chapter 4.5.1.). High speed currents such as these flowing across Otama, in combination with the wave shadow zone caused by offshore islands, would explain the along-shore rather than offshore textural trends observed on the shelf.

Otama was the only location on the east Coromandel where significant occurrences of bimodal sands are found (9 samples in total). Two main groups of bimodal sands occur. The first occur in 4 samples from just west of Otama in 7 to 19 m depth, and show modal peaks in the fine sand and fine to very fine sand fraction. This may indicate a mixing of Otama shelf samples with finer deposits to the west in the Whangapoua shelf region. The second group shows modal peaks in the very coarse and coarse sand fractions, and is found in some carbonate-rich deposits (> 40%) to the east. This probably results from a mixing of relatively fresh coarse shell fragments with in situ coarse clastic grains.

Sediment sorting patterns show well to moderately sorted shelf deposits alternating in a shore-normal pattern (Figure 5.8). This pattern is consistent with an alongshore dominated reworking of shelf sediments. Another distinguishing feature of the Otama shelf is the generally high carbonate component to the sediments, with values ranging from 30 to 90% on the shelf, and only becoming low (< 20%) in surfzone deposits (Figure 5.9 c). This indicates that modern clastic inputs into this region are very low (which is consistent with the lack of a large local catchment area), and that biological productivity is very high, particularly epifauna growing on the extensive reef outcrops around the Mercury Islands and within the Hole in the Wall channel. Iron oxide staining also tends to be low (< 10%) in surfzone deposits, then becomes more variable offshore ranging from 10 to 50% (Figure 5.9 c). These high values probably reflect the dominant intermittent reworking of shelf deposits by tidal and wind-generated flows. The surface texture of sand grains is fairly consistent over most of Otama, grains ranging from angular to rounded, except in the deepest samples where they tend to be more angular (Figure 5.9 c). The high biogenic component to Otama sands, and the absence of very angular nearshore sands, also indicate that very little

modern clastic sedimentation occurs in this area. Most recent deposition would thus seem to result from modern shell fragments mixing with older (possibly relict) clastic grains.

For the shelf region offshore of Whangapoua Harbour, textural patterns contrast to Otama as they are generally more uniform, with fine to very fine sand dominating most parts, and only a few isolated patches of medium to fine grained sands (Figures 5.7 and 5.9 d). Samples from 28 to 40 m water depth are very fine muddy sands (2 to 5% mud), which suggests the presence of mid shelf deposits. However, it is impossible to distinguish nearshore and inner shelf deposits due to the uniform nature of grain sizes. What patterns are present offshore tend to occur in shore parallel bands, which indicates that sediments are dominantly reworked by shore-normal currents associated with waves, rather than shore-parallel wind-generated flows. This is consistent with current measurements from Whangapoua, which showed no strong wind- or tide-generated flows present in this shelf region (see Chapter 4.5.1.)

Sediment sorting at Whangapoua ranges from well sorted surfzone deposits, to well to moderately well sorted sands over the nearshore and inner shelf, and only moderately sorted mid shelf deposits (Figures 5.8 and 5.9 d). This offshore trend in sediment sorting is again consistent with a wave-dominated reworking of shelf sediments. Carbonate content in Whangapoua samples is generally relatively low (< 20%), with only a few high carbonate samples (40%) found in nearshore and inner shelf deposits (Figure 5.9 d). Iron oxide staining is also generally low (5 to 20%) in nearshore and inner shelf sands, and absent in the deeper shelf deposits (Figure 5.9 d). This is again consistent with a lack of current reworking of shelf deposits. The surface texture of samples shows angular to subangular grains dominating most nearshore and inner shelf sediments, with more angular to very angular grains occurring in deeper water. This high occurrence of fine grained, low carbonate, angular sands on the Whangapoua shelf indicates high sedimentation occurring here, possibly from either sediments transported out of Whangapoua Harbour, or fine sands winnowed from the coarser Otama shelf sediments.

5.4. BEACH AND DUNE SEDIMENT TEXTURE

The textural characteristics of east Coromandel beach and dune deposits have previously been examined by HEALY and DELL (1982). However, the E.C.S.S. provides additional information on the hydraulic properties of these sediments (as HEALY and DELL used dry sieving to determine size and sorting), as well as their carbonate content and grain surface textures. As beach sediments usually coarsen adjacent to tidal inlets (HEALY and DELL, 1982), this analysis concentrates on samples (one from each location) collected from mid-beach locations away from the influence of inlets and ebb tide deltas.

Textural data have already been shown for individual beach locations in Figures 5.5 and 5.9, but are integrated here into Table 5.2 and Figure 5.10. In general, the mean grain size of east Coromandel beaches shows two broad patterns, with pocket beach systems composed of coarse

Table 5.2. Summary of textural data for east Coromandel beaches.

Location	Type	Mean (ϕ)	Sorting (ϕ)	CO_3 (%)	FeO (%)	Roundness
Waihi	Barrier Spit	1.95	0.42	6	5	A-SA
Orokawa	Pocket	1.04	0.48	23	5	SA-R
Homunga	Pocket	0.81	0.55	27	5	SA-R
Whiritoa	Pocket	1.07	0.24	8	5	SR-WR
Whanga.	Barrier Spit	2.06	0.35	18	60	A-R
Onemana	Pocket	0.94	0.31	24	20	SA-WR
Opoutere	Barrier Spit	1.83	0.44	12	10	A-SA
Pauanui	Barrier Spit	1.82	0.48	6	15	A-SA
Tairua	Pocket	1.00	0.40	26	20	SA-R
Hotwater	Pocket	1.12	0.58	22	50	A-R
Hahei	Pocket	1.96	0.53	25	5	A-SA
Cooks	Barrier Spit	2.29	0.69	14	0	VA-SA
Buffalo	Barrier Spit	2.35	0.49	6	20	A-SR
Wharekaho	Pocket	1.27	0.52	21	15	SA-R
Opito	Pocket	1.62	0.42	22	20	A-SR
Otama	Pocket	1.64	0.30	5	2	SR
Kuaotunu	Pocket	2.03	0.38	11	5	SA-R
Rings	Pocket	0.93	0.60	35	5	SR-WR
Matarangi	Barrier Spit	2.24	0.49	7	2	SA-SR
Whangap.	Pocket	2.20	0.37	5	5	A-SR

(VA= very angular; A= angular; SA= subangular; SR= subrounded; R= rounded; WR= rounded).

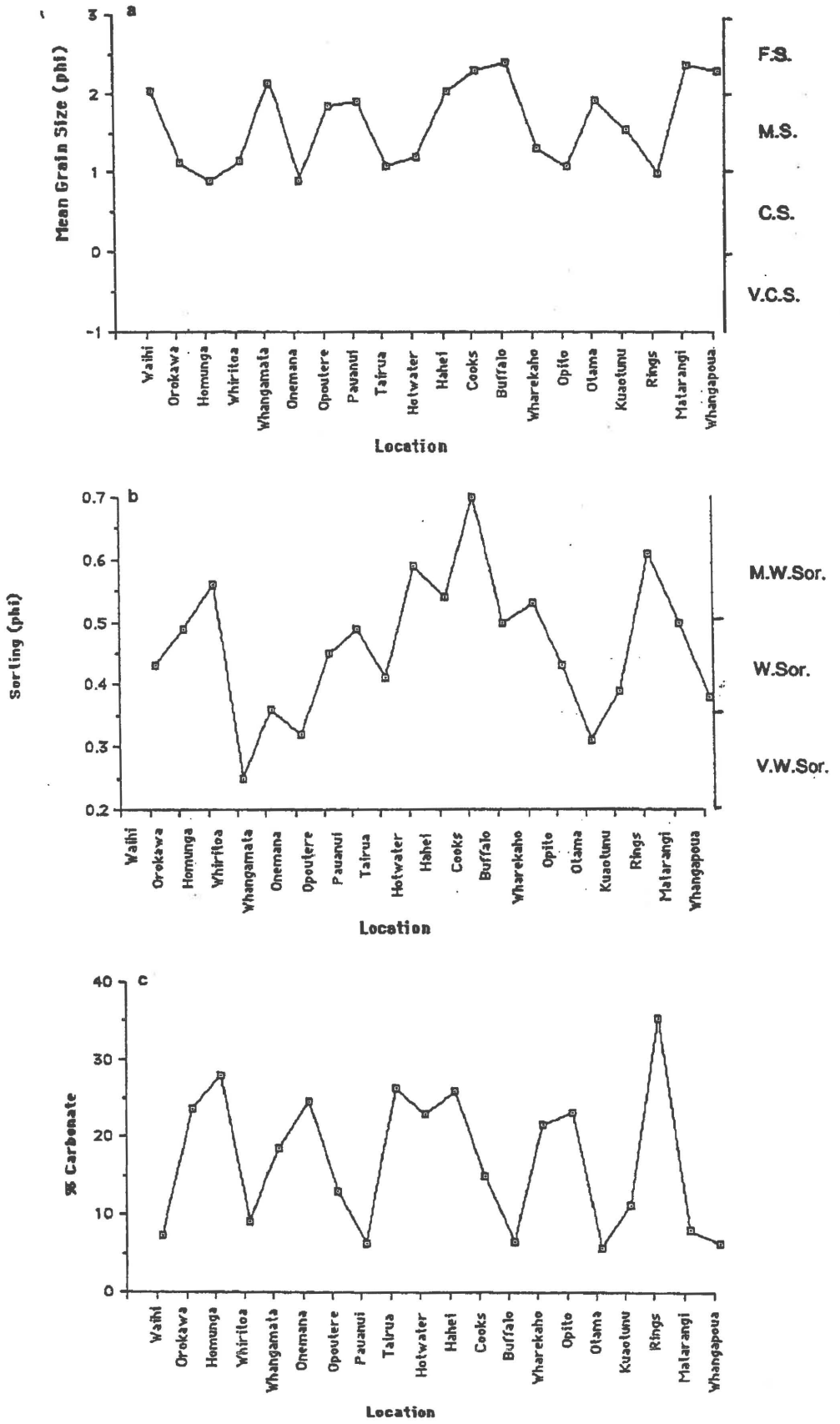

Figure 5.10. Variations in textural properties of beach deposits along the east Coromandel coast: a) mean grain size; b) sediment sorting; c) carbonate content.

to medium grained sands, and barrier spit beaches (which enclose large estuary systems) composed of fine sand sized deposits. However, both beach types (i.e. pocket and barrier spit) tend to be coarser grained on the southern coast than on the northern embayed coastline. This may indicate different incident wave energy conditions for both sections of coastline, with the northern coast more sheltered by offshore islands and shallow, broad embayments, whereas the southern coast will be more exposed to open ocean waves. This is also reflected in the sorting of beach sediments, with southern beach deposits generally ranging from very well sorted to moderately well sorted sands, but northern beaches tending to be less well sorted than southern beaches.

The amount of carbonate within beach sands is generally only low to moderate (5 to 20%), although some beaches have much higher concentrations (20 to 35%). There does not appear to be any obvious trends in the carbonate concentrations, except that very low values tend to occur on barrier spit beaches (Waihi, Pauanui, Buffalo, Pauanui and Wharekaho), and high values in regions where either offshore islands or extensive reefs are found close to the beach (Whangamata, Onemana, Tairua, Hotwater, Hahei, Opito).

Iron oxide staining on beach sands tends to be low in most locations (< 20 %), which reflects the active reworking of these deposits. However, some higher values are found at Whangamata (60%) and Hotwater Beach (50%), which must indicate some input of extensively weathered grains from either the shelf, local cliffs, or local catchments.

The surface texture of beach sands tends to reflect the different beach types, with pocket beach systems generally composed of subangular to rounded grains, whereas the barrier spit beaches are composed of more angular to subrounded grains. This pattern, along with those observed in the mean grain size and carbonate content of beach deposits, may indicate different sources for each embayment type along the east Coromandel coast.

The interaction of beach deposits with nearshore sediments is briefly examined here by comparing the normal frequency distribution histograms of dune, beach, surfzone, and nearshore sands from four pocket beach and barrier spit beach systems on the southern and northern coasts (Figure 5.11). This shows that deposits within pocket beaches on the southern coast (Whiritoa and Onemana) do not texturally overlap with nearshore sands, and therefore most likely form closed sedimentary systems in which no interaction occurs with the adjacent nearshore zone. However, some overlap occurs in the surfzone sample (5 m depth) from Onemana, which may indicate this is the landward limit of onshore shelf sand transport. Similar conclusions have previously been reached by HEALY (1981) at Whiritoa Beach, based largely on mineralogical considerations. However, pocket beaches on the northern coast (Hotwater, Otama), and barrier spit beaches on both coastlines (Waihi, Whangamata Opoutere, Buffalo, Matarangi) generally show a very strong textural overlap with nearshore deposits, and it is therefore possible that they form more open systems in which sands are actively exchanged between the beach and nearshore zone.

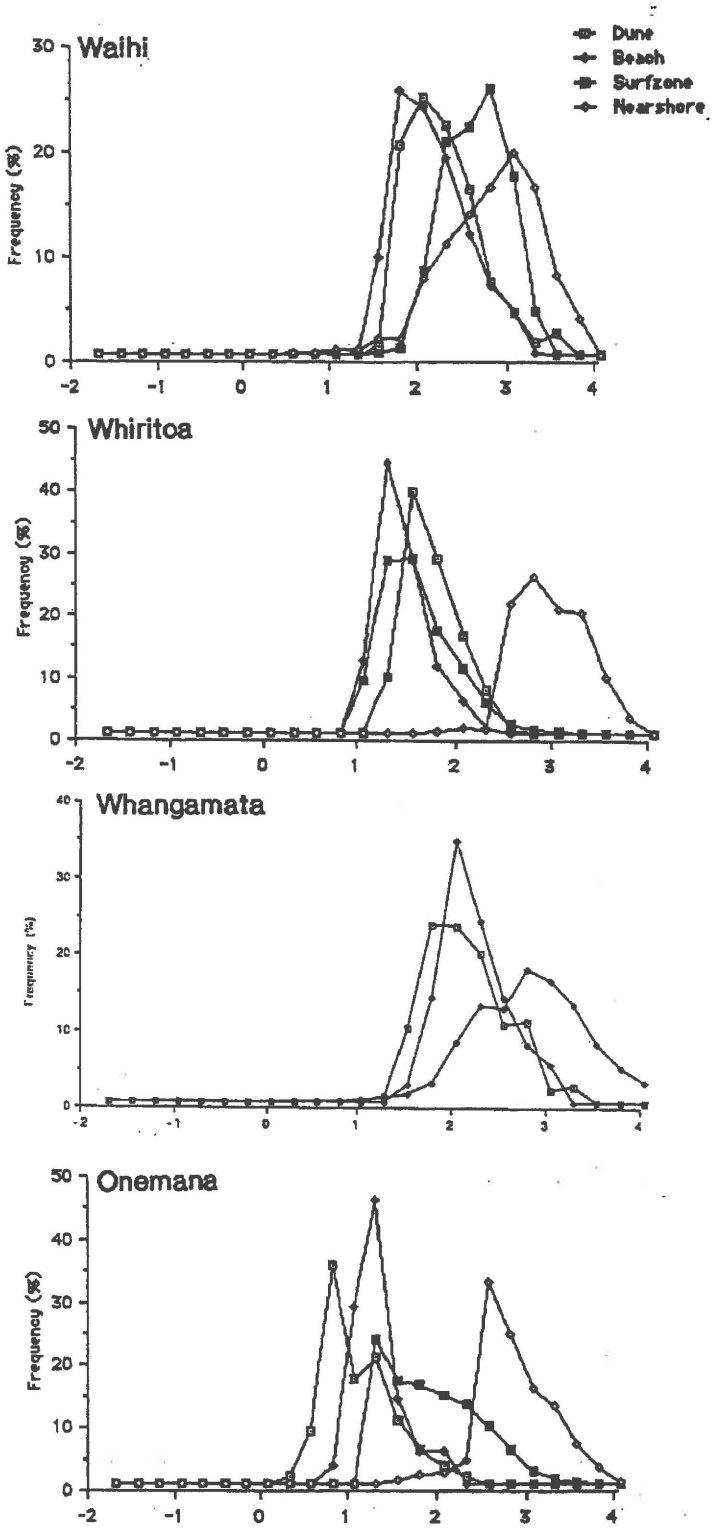

Figure 5.11. Comparison of grain size distribution curves between dune, beach, surfzone, and nearshore deposits in different embayments along the east Coromandel coast. Note the poor overlap between beach and nearshore deposits at Whiritoa and Onemana, which indicates no sediment exchange occurring between these beaches and the shelf. Other beach systems appear to be interacting with the shelf, however, as shown by the good overlap between beach, surfzone, and nearshore deposits.

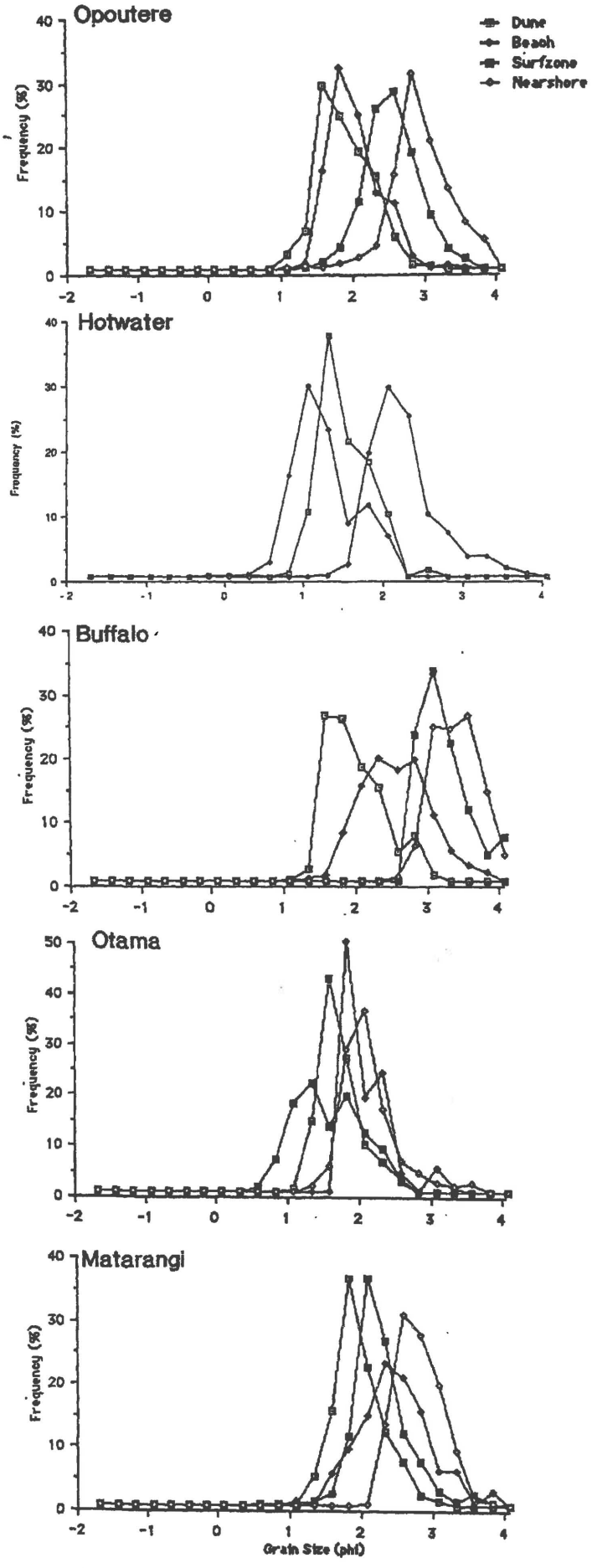

Figure 5.11. (continued).

The textural characteristics of east Coromandel dune deposits is summarised in Table 5.3. and illustrated in Figure 5.12. No information on carbonate or iron staining is given as both properties are affected by leaching in dune deposits. The grain size of dune deposits is fairly consistent along the coast, with most embayments characterised by medium to fine grained sands. However, pocket beaches on the southern coast tend to have coarser grained dune deposits than barrier spit beaches on both coasts, or pocket beaches on the northern coast. This may indicate a different source of barrier deposits for the southern pocket beaches than other embayments. In comparison to modern beach sediments, dune deposits tend to be finer grained in the pocket beach systems, but coarser grained on the barrier spit beaches. As the aeolian processes which form dune deposits will preferentially remove fine sand from beach deposits, this trend may indicate a change in source for modern barrier spit beach deposits, possibly from the large estuaries they presently enclose, as proposed by GIBB and ABURN (1986) at Pauanui.

Dune deposits are generally well to very well sorted, with only one moderately well sorted sample, at Wharekaho Beach. Within most embayments, dune deposits are better sorted than modern beach sands, which is expected in the light of their original source from older beach deposits. However, dune deposits from embayments on the southern coast are generally better sorted than those on the northern coast, which again may relate to the different incident wave energy along both coastlines, or alternatively their different exposure to onshore winds, with some northern embayments being more sheltered from east and northeasterly winds.

The grain surface textures in dune deposits are generally subangular to rounded, with pocket beach dune sands tending to be slightly more rounded than in barrier spit systems. Dune sands on barrier spits also tend to be more rounded than their modern beach sands, which again may indicate a change in source to finer and more angular terrestrial sands from harbours in modern beach deposits, or alternatively indicate a selective sorting process by winds.

5.5. FLUVIAL SEDIMENT TEXTURE

The sediment texture of fluvial sediments is not of primary concern to the E.C.S.S. However, as the textural properties of some shelf and beach deposits suggest a possible modern terrigenous source, it is necessary to briefly summarise the textural characteristics of fluvial sediments (Table 5.4). In most areas, river sediments are characterised by coarse to medium grained sands. This is coarser than the beach and shelf deposits which are inferred to be of terrestrial origin. However, the relatively poor sorting of these fluvial deposits (moderately well to poorly sorted) means that fine and very fine sand fractions may be preferentially transported by flood waters and deposited in coastal waters. This possibility was examined by also overlapping the grain size distribution of river bed samples and some modern barrier spit and nearshore sand deposits (Figure 5.13). In most barrier spit embayments, there is a very strong overlap of grain size distribution between beach and river sands, which adds support to the hypothesis that modern

Table 5.3. Summary of textural data for east Coromandel dune systems.

Location	Type	Mean (ϕ)	Sorting (ϕ)	Round.
Waihi	Barrier Spit	2.04	0.44	A-SR
Orokawa	Pocket	1.27	0.34	SA-R
Whiritoa	Pocket	1.57	0.29	SR-WR
Whanga.	Barrier Spit	1.98	0.42	SA-SR
Onemana	Pocket	0.91	0.40	SA-R
Opoutere	Barrier Spit	1.95	0.38	A-SR
Pauanui	Barrier Spit	1.76	0.37	SA-SR
Tairua	Pocket	1.09	0.37	SA-WR
Hotwater	Pocket	1.31	0.43	SA-R
Hahei	Pocket	1.46	0.42	SA-WR
Cooks	Barrier Spit	1.66	0.41	A-SR
Buffalo	Barrier Spit	1.77	0.41	A-SR
Wharekaho	Pocket	1.69	0.57	SA-R
Opito	Pocket	2.06	0.49	SA-SR
Otama	Pocket	1.50	0.29	SR-R
Kuaotunu	Pocket	1.74	0.45	SA-R
Rings	Pocket	1.39	0.45	SA-R
Matarangi	Barrier Spit	1.75	0.42	SA-SR
Whangap.	Pocket	1.53	0.46	SA-R

(VA= very angular; A= angular; SA= subangular; SR= subrounded; R= rounded; WI rounded).

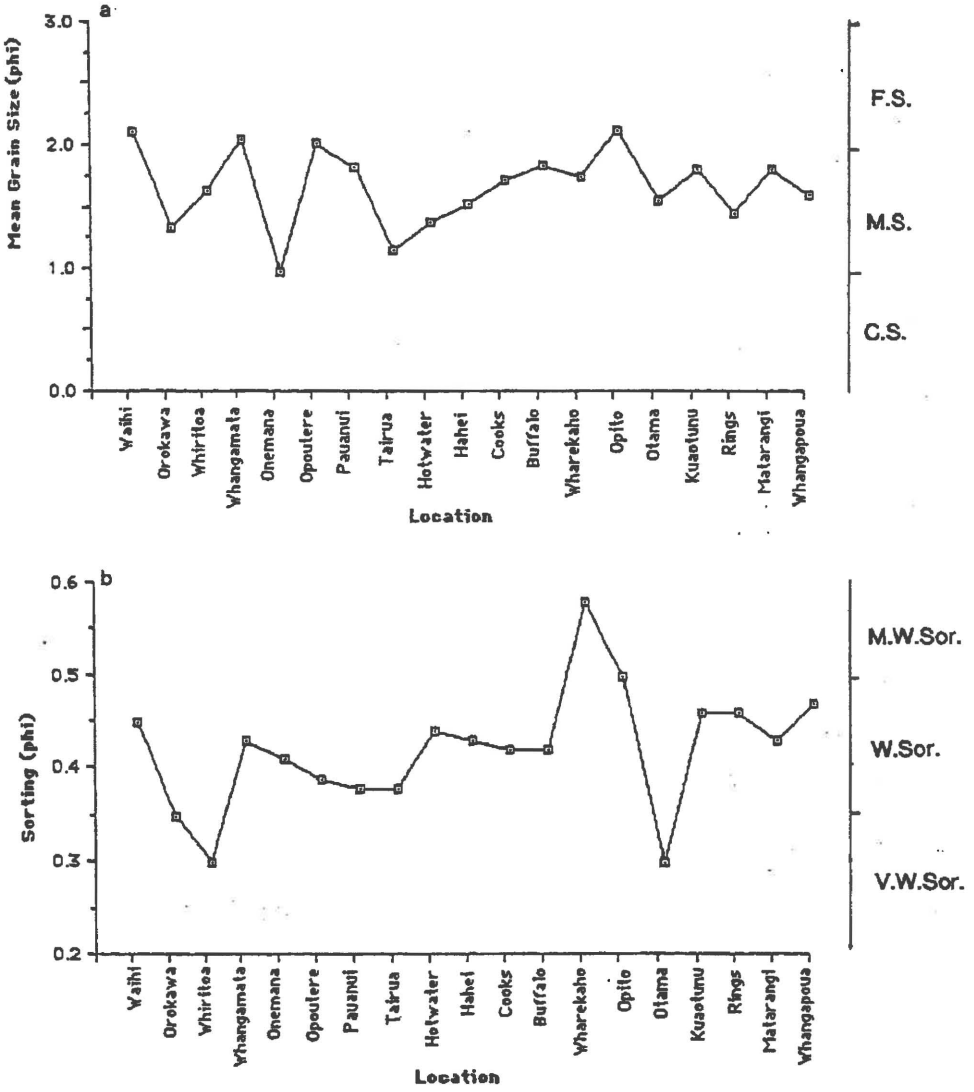

Figure 5.12. Variations in sediment textural properties of dune deposits along the east Coromandel coast: a) mean grain size; b) sediment sorting.

Table 5.4. Summary of textural properties for river bed samples associated with Coromandel embayments.

Location	Mean (ϕ)	Sorting (ϕ)	FeO (%)	Roundness
Waihi	1.24	0.64	10	A-SR
Whiritoa	0.84	0.99	20	A-SR
Otahu	1.20	0.92	50	A-SA
Whangamata	1.42	0.84	50	VA-SA
Opoutere	1.87	0.53	30	VA-SA
Tairua	1.62	0.56	50	VA-SA
Hotwater	1.58	0.56	30	VA-R
Mercury Bay	1.78	0.84	30	A-SA
Opito	0.53	0.86	50	A-SA
*Otama	1.65	0.59	5	SA-R
Matarangi	1.35	0.53	50	A-SA

*= possibly contaminated with beach sands as collected in intertidal waters.

(VA= very angular; A= angular; SA= subangular; SR= subrounded; R= rounded; WF rounded).

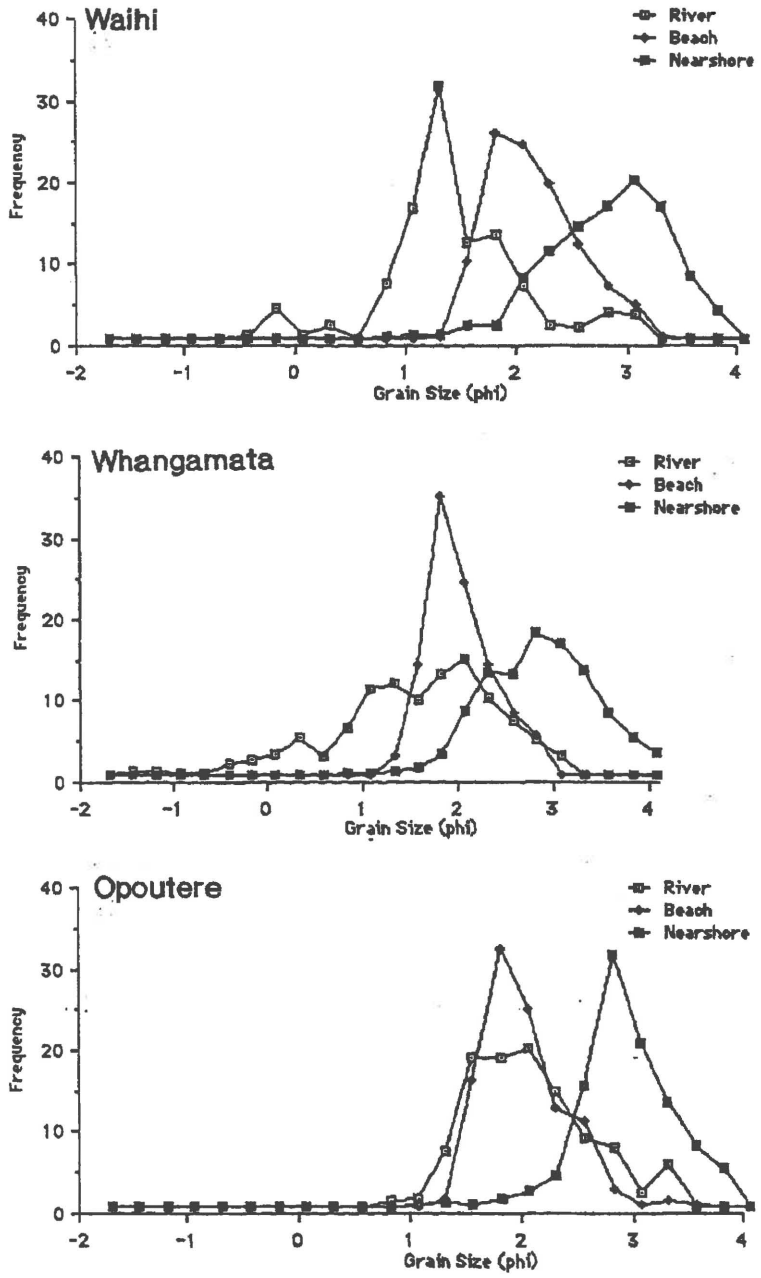

Figure 5.13. Comparison between grain size distribution curves of river bed, barrier spit beach, and upper nearshore sands along the east Coromandel coast. Note the very strong overlap between river and beach sands, particularly at Opoutere, which supports the hypothesis that modern beach sands on barrier spits are mainly derived from the local catchments. As the upper nearshore deposits only partly overlap with river bed sediments, they must be derived from either finer grained fluvial deposits in floodplains and deltas, or from outside of the study area.

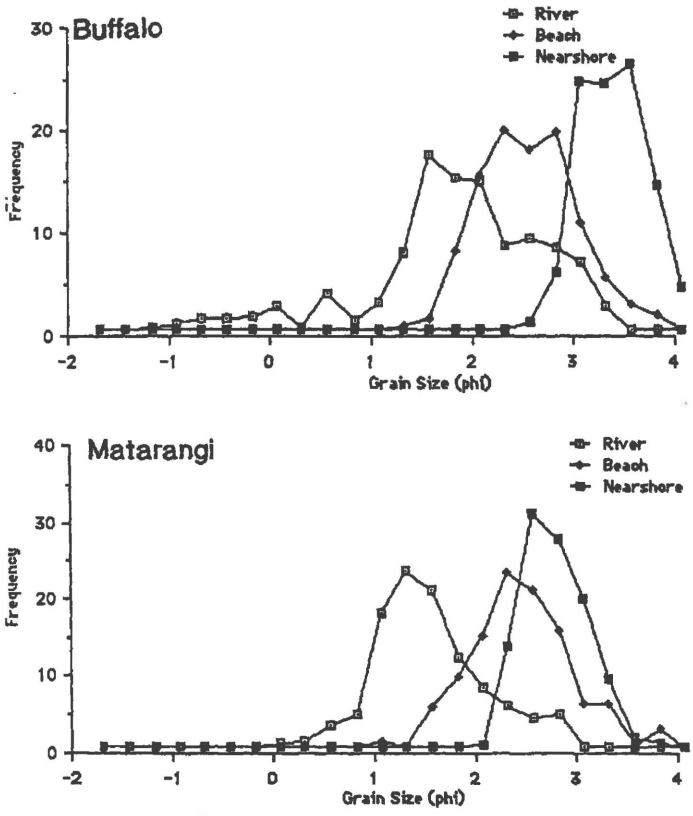

Figure 5.13. (continued).

modern barrier spit beach sands are derived from their local catchments. Nearshore sands, however, show only partial overlap, with the fluvial deposits usually lacking the very fine sand fraction (> 3ϕ) which dominates the grain size distribution of nearshore deposits. This may be due to either nearshore sands being derived from sources outside of the local catchments, specifically from the extensive coastal plains of the Bay of Plenty region further south, or because they are derived from lower energy fluvial environments within the local catchments, specifically from flood plains or fluvial deltas in harbours.

The fluvial sands are also very angular and extensively iron stained, due to their recent source from catchment weathering. These are similar characteristics to barrier spit beach and upper nearshore deposits. Thus, the textural characteristics of fluvial deposits are compatible with a modern terrestrial origin of shelf and barrier spit beach deposits in several east Coromandel embayments.

5.6. STATISTICAL CLASSIFICATION OF TEXTURAL DATA

As a final part of the textural analysis within the E.C.S.S., it was decided to attempt a statistical grouping of the data. This was undertaken for two main reasons. Firstly, overlapping of textural data has already proven to be a successful method in this study for determining the extent to which upper nearshore sands are interacting with local beach system. A similar approach for all shelf and beach/barrier deposits may therefore help identify the present and past diabathic links between east Coromandel shelf and beach/barrier deposits. However, due to the large quantity of samples collected, a simple comparison of grain size distribution histograms would be awkward to apply over the entire study area. Statistical analysis of this same information though can help define different textural groups and thus allow regional comparisons of shelf and beach/barrier samples to be made. Secondly, grouping of textual data is the first step towards defining the various shelf lithofacies which occur along the east Coromandel coast.

5.6.1. Entropy Program

For statistical analysis of textural data, an information statistics program, ENTROPY, was obtained from the Geography Department at the University of Sydney, and modified by Dr. Willem de Lange, Earth Sciences Department, University of Waikato, to handle a larger data matrix and re-programmed to the University's VAX computer system. Details of the original computer alogarithm are published in JOHNSTONE and SEMPLE (1983). Unfortunately, even with the modified program, only 250 observations can be analysed and so samples had to be selected from those considered in the previous regional observations to be representative locations. Examples of the application of the ENTROPY program to textural and mineralogical data from the southeast Australian coast are found in HUDSON (1985).

The program calculates an entropy statistic (entropy meaning a measure of the disorder of a system, or in this case variations in the textural data) for each sample through the formula:

$$H(Y) = \sum_{i=1}^{M} y_i \log_z (1/y_i)$$

where: y_i =the proportion of the ith component in the distribution

M =the number of variables into which the distribution is divided

H(Y)=entropy measure for sample Y.

The program then identifies the best classification of N samples into n classes by maximising the between class entropy across M variables. The optimum classification is recognised when the between class entropy (i.e. variation) begins to increase at a decreasing rate with the addition of each new class. At the completion of the classification procedure, Z statistics are calculated which compare class means for each variable against the mean for each variable in the total matrix. The Z statistics are not used in the actual classification procedure, but only serve to highlight the source of variability in each class relative to the entire matrix.

5.6.2. Textural Classification Results

Textural data were entered into the ENTROPY program by placing interval frequency values obtained from the R.S.A. results for each 1/4 phi interval from -2.0 to 4.0 phi. Results of the program are illustrated in Figure 5.14, from which a classification of 7 groups (termed 'entropy classes') explaining 78.55% of the matrix variability was obtained. From the mean values of each entropy class, the interval frequency data were then run through the R.S.A. program to obtain normal frequency distribution curves and values of mean, sorting, and skewness for each class. These graphs are shown in Figure 5.15. The mean, sorting, and skewness values for each sample from these classes were then plotted against each other to better define these and to determine the degree of overlap of each entropy class.

Plots of mean against sorting in Figure 5.16 show that the different entropy class are defined mainly by their mean grain size, with class 1 comprised of coarse grained samples, and mean grain size then decreasing with each successive group to the fine to very fine grained class 7 sediments. However, each entropy class also shows different ranges in sorting, with classes 1, 2, and 4 tending to be well to poorly sorted samples, classes 6 and 7 very well to moderately sorted, and classes 3 and 5 very well to moderately well sorted deposits. Plots of mean grain size against skewness for each entropy class in Figure 5.17 show important variations in skewness between several of these, with 1, 2, and 3 comprised almost entirely of fine skewed sediments, class 4 containing some coarse skewed samples, and values then decreasing noticeably with classes 6 and 7 containing mainly coarse skewed sediments.

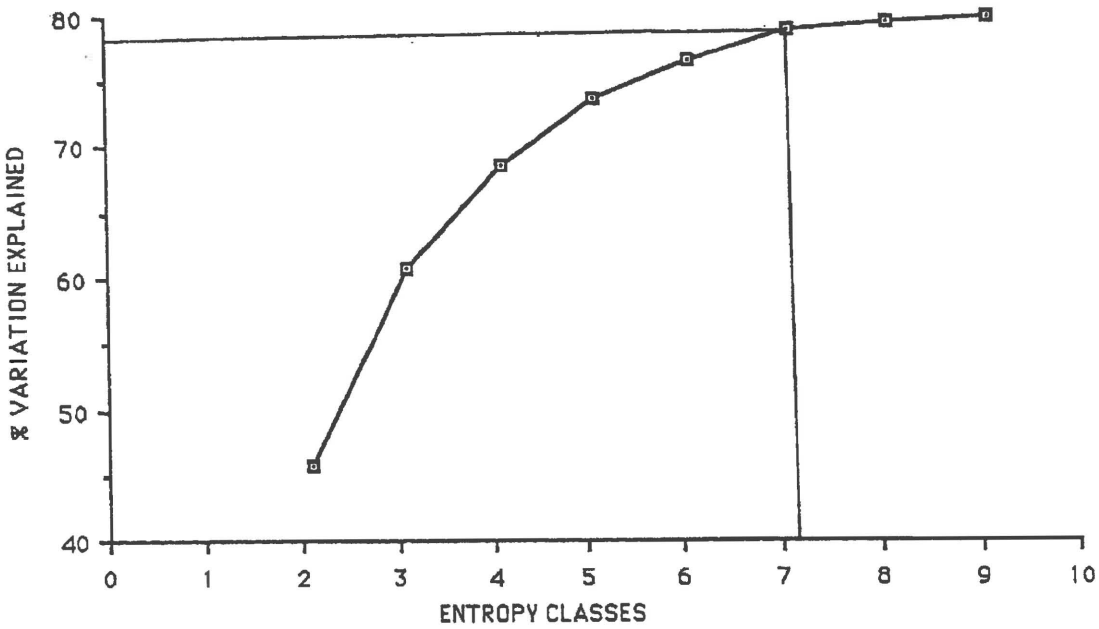

Figure 5.14. Plot showing the different number of entropy classes into which the textural data can be classified, and the amount of variation in the data matrix that each classification will explain. For this study, a 7 entropy class classification was used, as this is the point on the graph where additional entropy classes do not result in any significant increase in the amount of data variation that is explained.

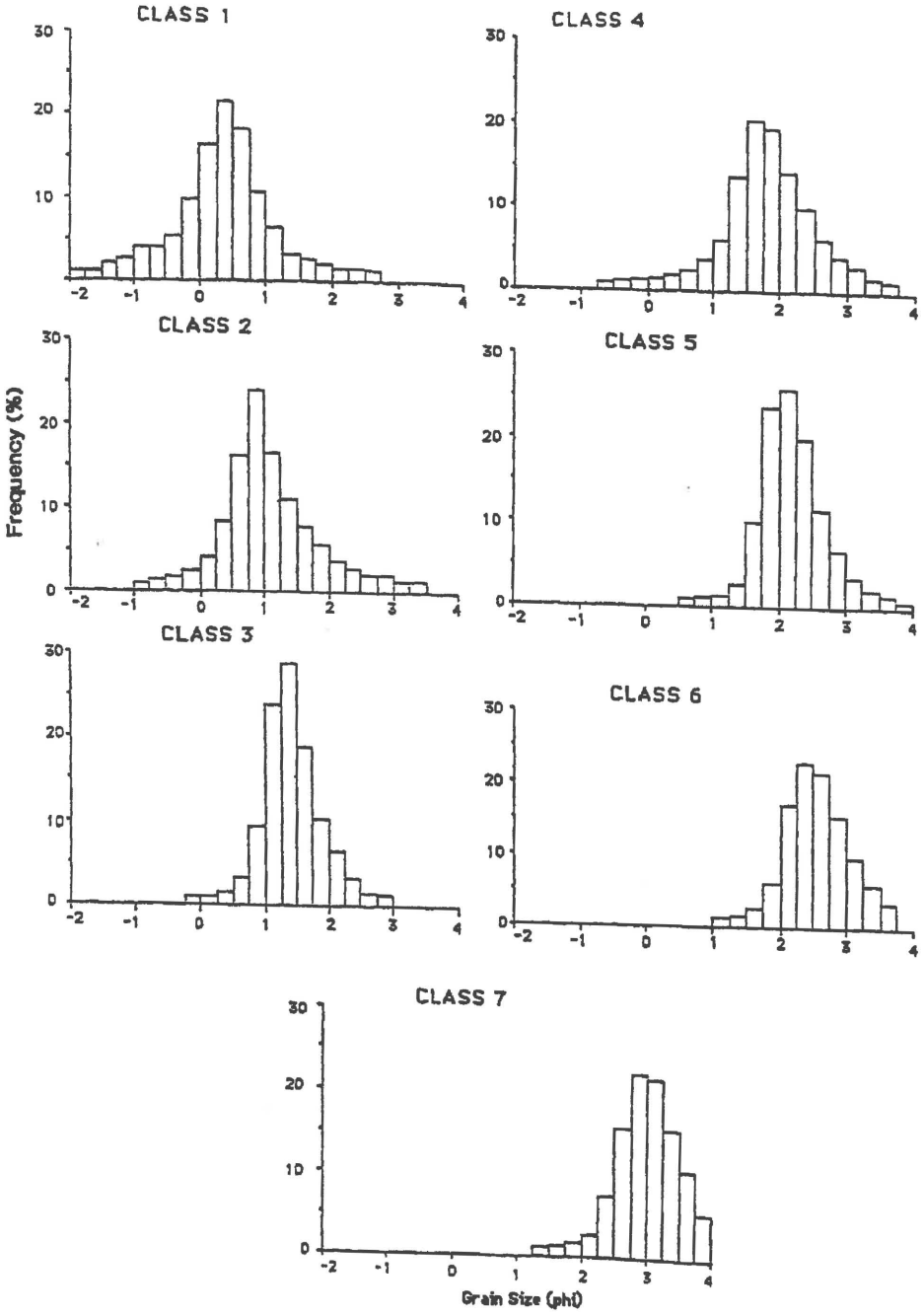

Figure 5.15. Grain size frequency distribution histograms for each of the 7 different er classes.

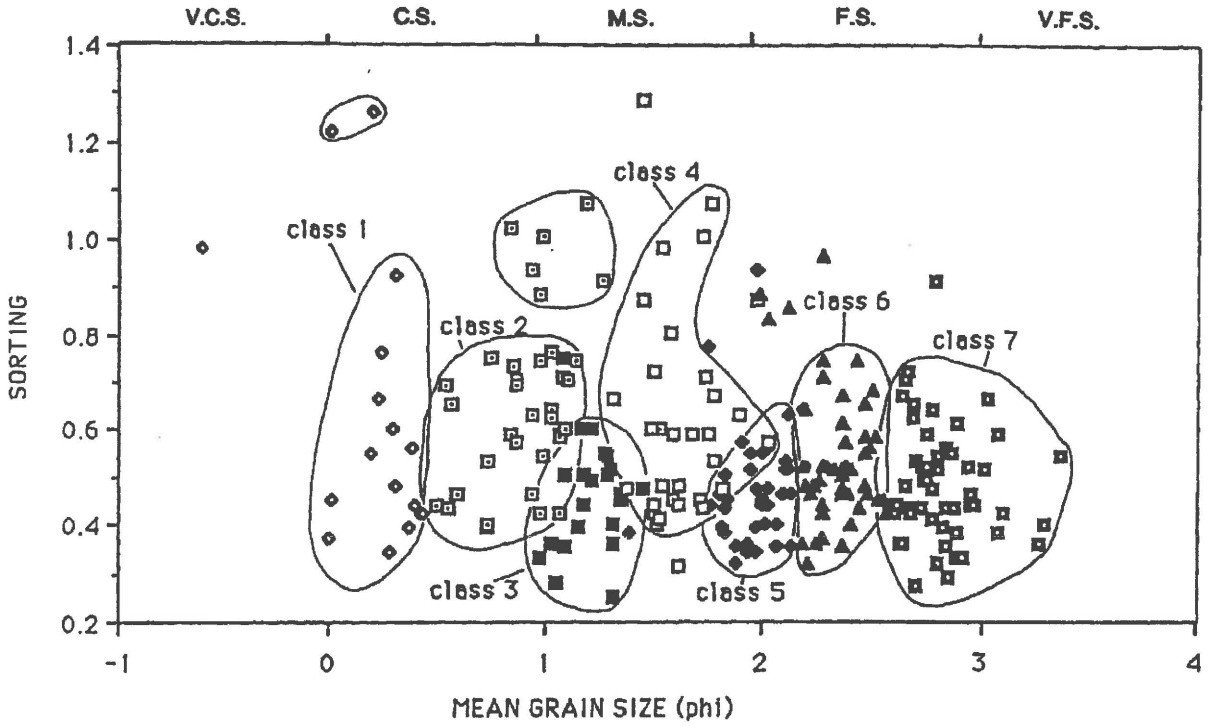

Figure 5.16. Plot of mean grain size vs. sediment sorting for each of the 7 entropy classes. This shows that the classification is based mainly on mean grain size, with sediment sorting an important secondary factor. This is particularly so with classes 5 and 6, which are very well to well sorted sediments whose mean grain size strongly overlaps with adjacent entropy classes.

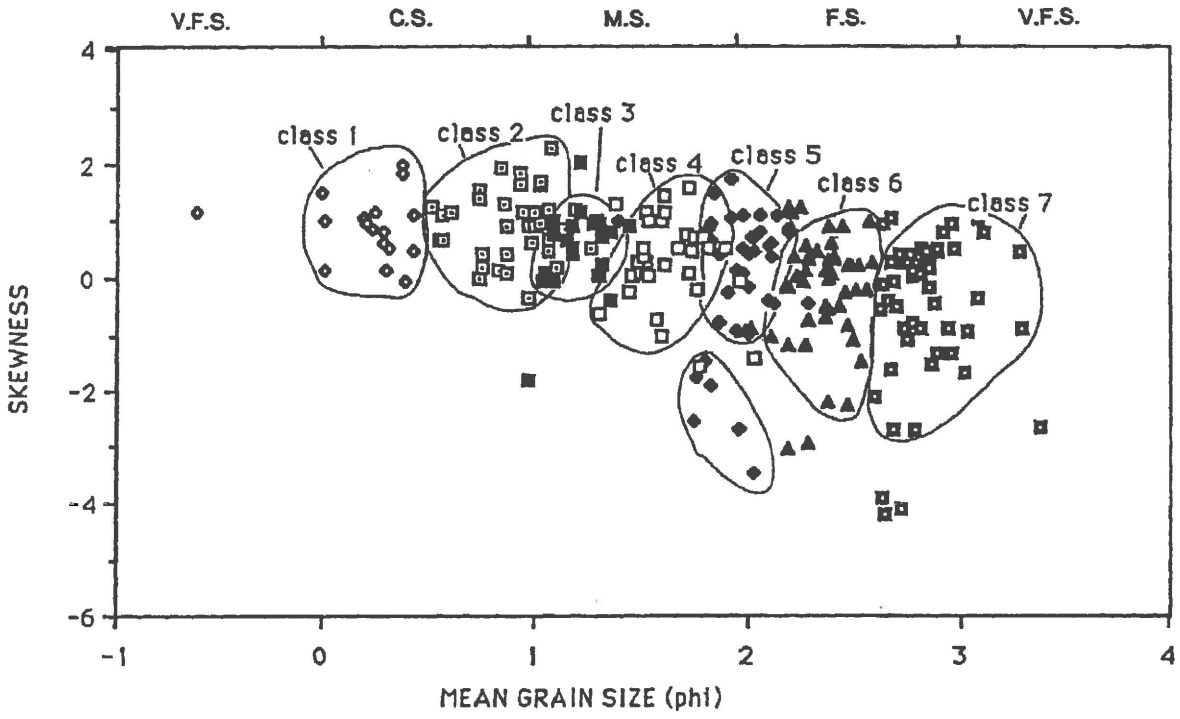

Figure 5.17. Plot of mean grain size vs. sediment skewness for each of the 7 entropy classes. This shows that skewness is also an important secondary factor in the classification, with sediments becoming increasingly coarser skewed in the finer grained classes, particularly classes 6 and 7.

From these textural plots, remaining samples not included in the original ENTROPY program were placed into the 7 various entropy classes. Other textural data which are independent of the ENTROPY program classification (carbonate content, iron oxide staining, and roundness) were then incorporated into each group and their mean values determined. Results of this analysis are tabulated in Appendix 9, along with maps showing the regional distribution of entropy classes. Information on the characteristics of each entropy class is listed in Table 5.5, and type examples of each class shown as colour plates in Figure 5.18. Distributions of the 7 entropy classes on the shelf from both the southern and northern coastlines are shown in Figures 5.19. and 5.20., and the characteristics of these within the different beach and barrier types along the coast are plotted in Figures 5.21. and 5.22. Note that the degree of overlap in textural data and percent of variability unexplained in the ENTROPY program means that some variation of data occurs within each entropy class. Thus, the following descriptions are generalisations aimed at simplifying the data matrix so that regional comparisons can be made and conclusions drawn relating to interactions between, and sources of, east Coromandel coastal deposits.

5.6.3. Entropy Class Descriptions and Interpretations.

Class 1 (Figure 5.18 A): Entropy class 1 deposits are generally coarse grained, moderately well sorted carbonate-rich sands. The coarse nature of these sediments suggests they may form a lag deposit in a relatively high energy environment. However, the extensive iron staining present on grains indicates that such high energy conditions only occur intermittently, and thus are most likely associated with storm wave and current flows. This is strongly supported by their occurrence in depths of 30 to 50 m along the shelf, which corresponds to the inner shelf zone of storm-dominated shelves (see Chapter 3.2.). This class may represent palimpsest deposits reworked from older pre-existing Pleistocene sands, as the high degree of roundness found on some grains would be more effectively produced by subaerial exposure to wind action rather than abrasion by aqueous transport (SELLEY, 1982). However, much of the carbonate material within these sands is probably derived from outside their present site of deposition, as the *Tawera spissa* shells which tend to dominate their macrofauna live preferentially in finer substrates within lower nearshore water depths (20 to 30 m; see Chapter 8.3; and HILTON, 1990). Class 1 sands do not occur in any local beach or barrier systems, and are therefore not a direct source for these deposits.

Class 2 (Figure 5.18 B): Deposits from entropy class 2 show textural similarities with those of class 1, the slight differences in size, roundness, and sorting in the former being in part due to an overall lower carbonate content. They therefore appear to represent similar coarse grained storm lag deposits to the entropy class 1 sediments, and occur in the same inner shelf water depths of 30 to 50 m. As with the class 1 deposits, the macrofaunal species which characterise class 2 are probably derived from shallower sources. Class 2 sands are also found in some southern coastline

Table 5.5. Summary of the mean textural properties for each of the 7 entropy classes. Note that only mean grain size, sediment sorting, and skewness are dependent variables in the classification, with other textural values calculated independently from mean values of samples occurring within each entropy class.

Class	Mean	Sorting	Skew.	CO_3 (%)	FeO (%)	Round.	Shells	Forams
1	v.c.s.-c.s.	m.w.sor.	v.f.	44	40	SA-R	1, 2, 3, 10,	a.
2	c.s.-m.s.	m.w.sor.	v.f.	30	25	SA-R	1, 3, 5, 2, 4, 10.	a, b.
3	m.s.	w.sor.	v.f.	18	30	SA-R	1, 2, 3, 5, 6, 10.	a, b, c.
4	m.s-f.s.	m.w.sor.	f.	22	16	A-SR	1, 2, 5, 6, 8, 9.	a, b, c.
5	f.s.	w.sor.	c.	13	17	A-SR	1, 2, 3, 6, 7, 8.	a, b, c.
6.	f.s.	m.w.sor	v.c.	15	13	A-SR	1, 6, 8.	a, b, c, d
7.	f.s.-v.f.s.	w.sor.	v.c.	14	9	VA-SA	1, 3, 5, 8.	a, b, c, d, e.

Symbol key:

Shell species - 1= *Tawera spissa*, 2= *Nucula nitidula*, 3= *Sigapatella scalpellum*, 4= *Chlamys gemmulata*, 5= *Venericardia purpurata*, 6= *Scalpomactra scalpellum*, 7= *Myadora striata*, 8= unknown juvenile bivalves, 9= unknown brachiopod, 10= *Flabellum rubrum*

Foraminifera species - a= *Quinqueloculina*, b= *Elphidium*, c= *Anomaiina*, d= *Cibicides*, e= *Lenticulina.*

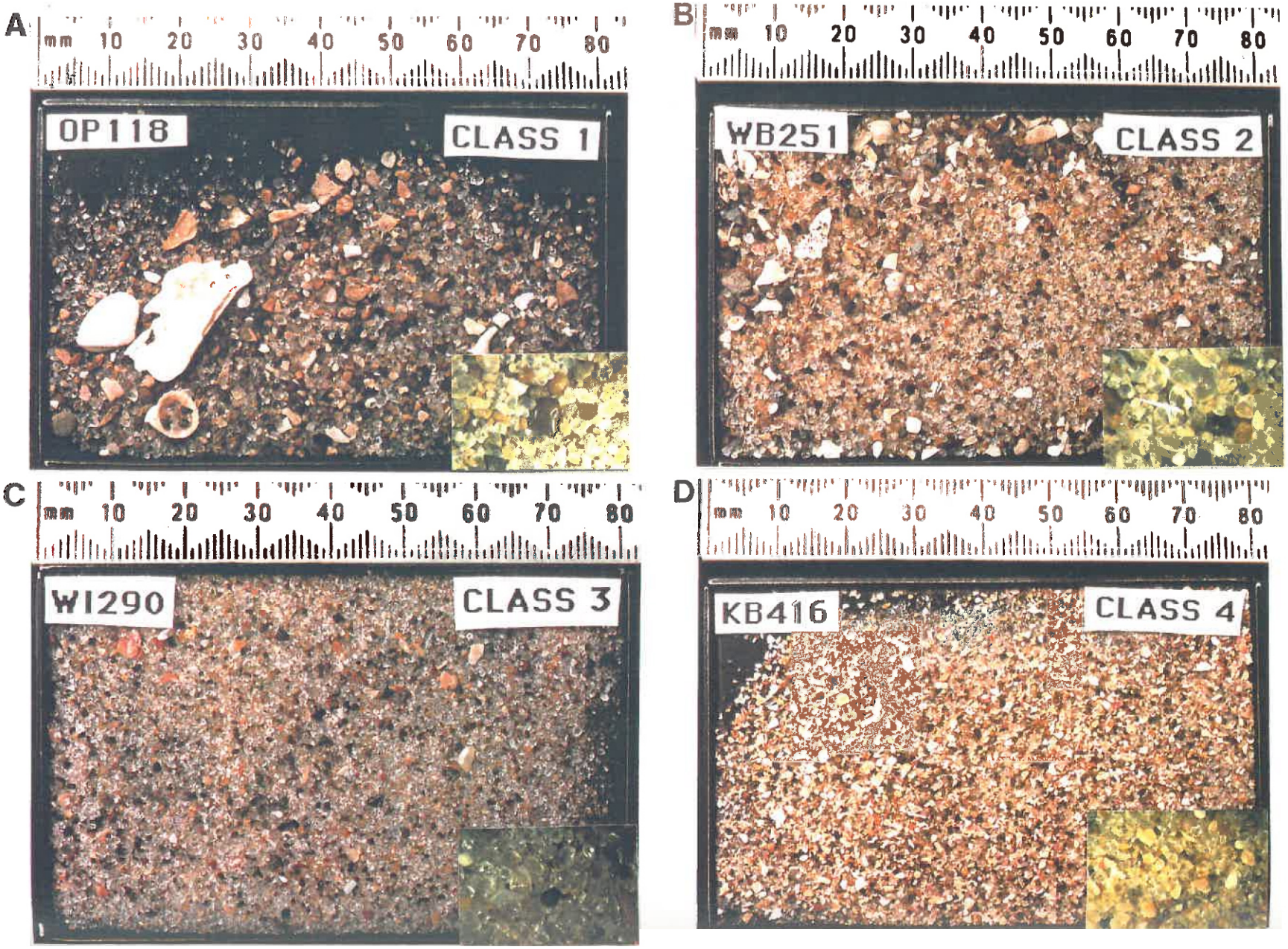
A
mm 10 20 30 40 50 60 70 80
OP118
CLASS 1
B
mm 10 20 30 40 50 60 70 80
WB251
CLASS 2
C
mm 10 20 30 40 50 60 70 80
WI290
CLASS 3
D
mm 10 20 30 40 50 60 70 80
KB416
CLASS 4

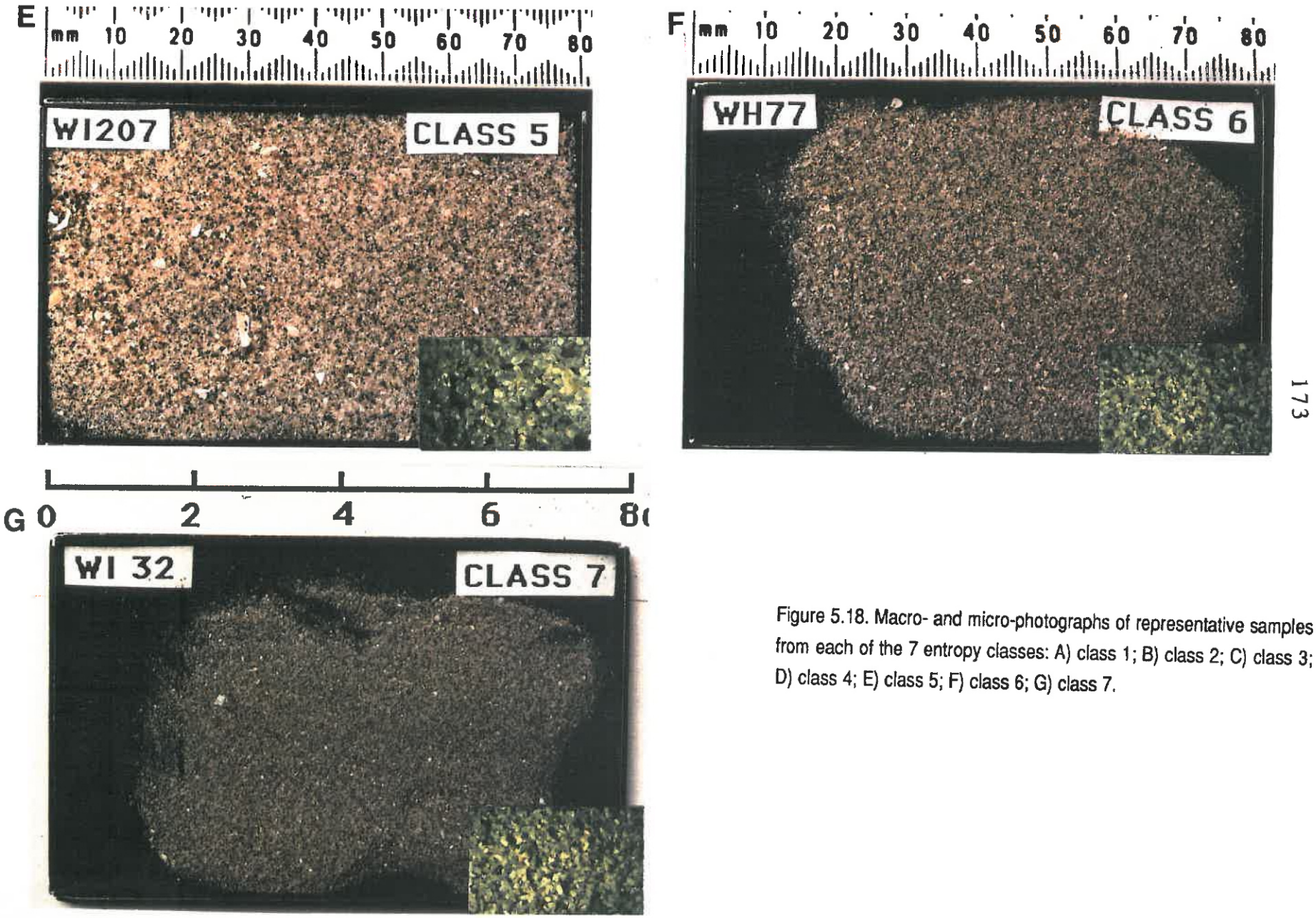

Figure 5.18. Macro- and micro-photographs of representative samples from each of the 7 entropy classes: A) class 1; B) class 2; C) class 3; D) class 4; E) class 5; F) class 6; G) class 7.

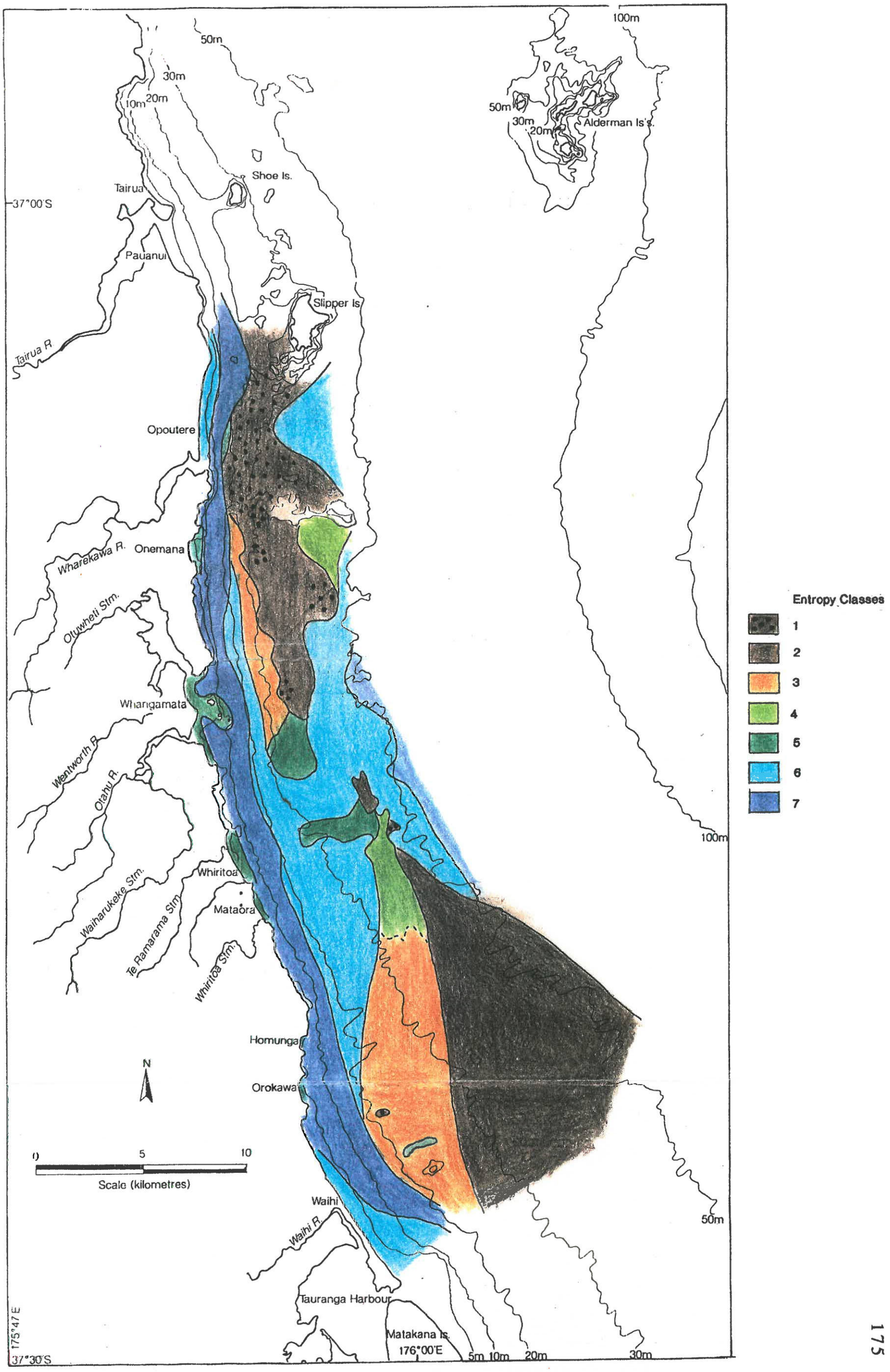

Figure 5.19. Distributions of the various entropy classes over the continental shelf on the southern coastline.

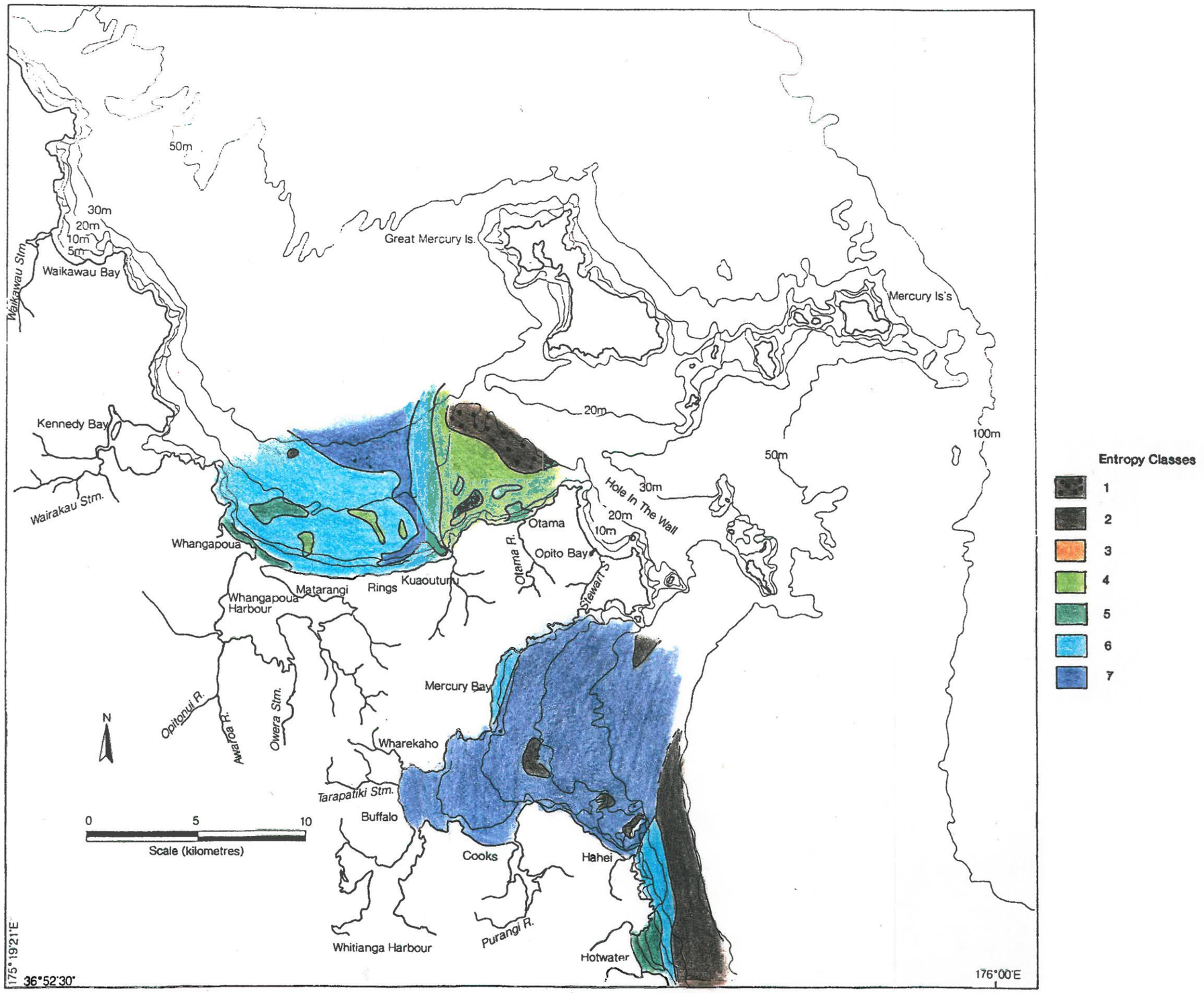

Figure 5.20. Distributions of the various entropy classes over the continental shelf on the northern coastline.

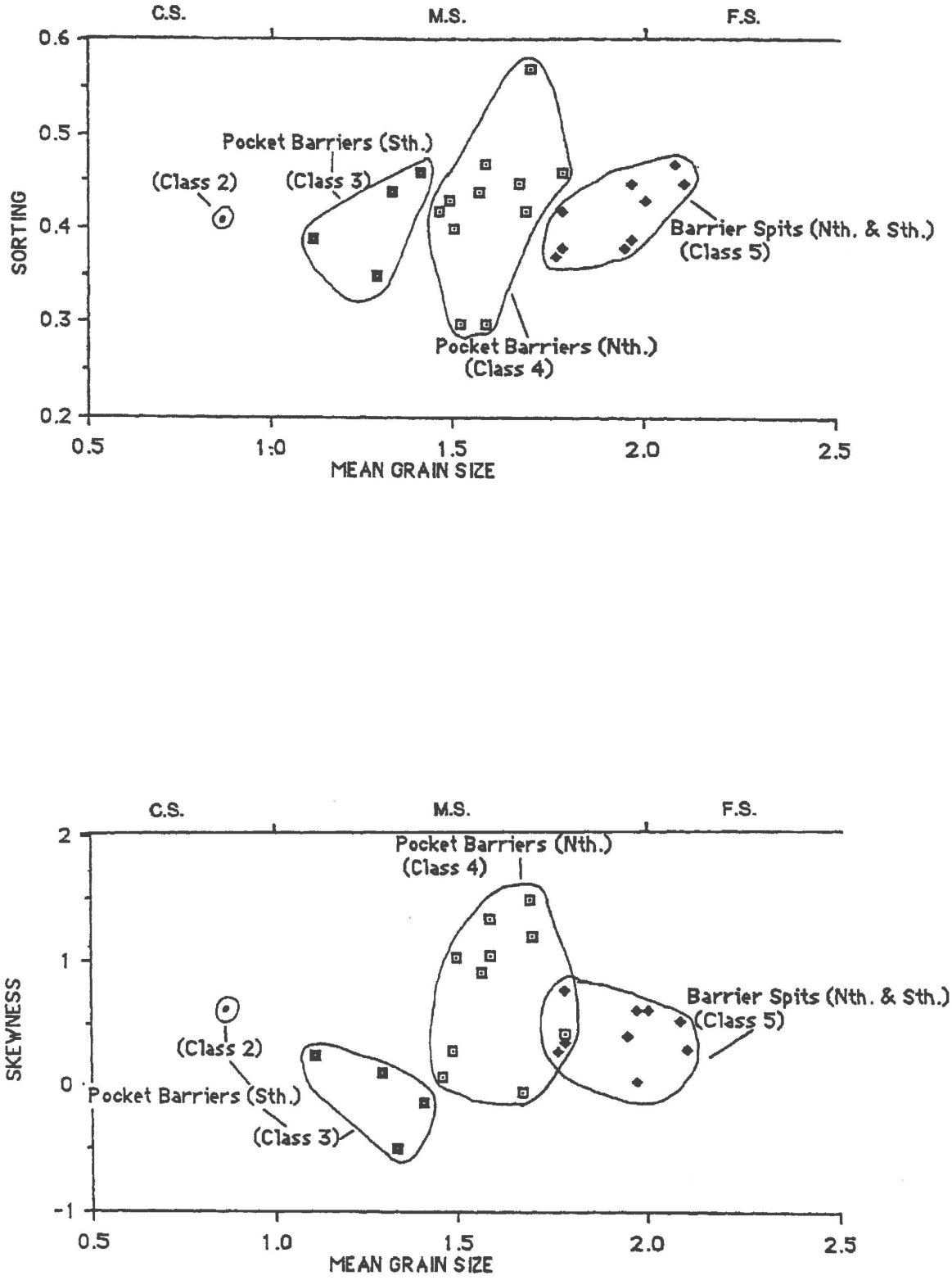

Figure 5.21. Relationship between textural parameters within each entropy class for barrier dune samples along the east Coromandel coast: a) mean grain size vs. sorting; b) mean grain size vs. skewness. Note the trend of decreasing grain size from pocket barrier sediments on the southern coast, to those on the northern embayed coast, and barrier spit deposits on both northern and southern coastlines.

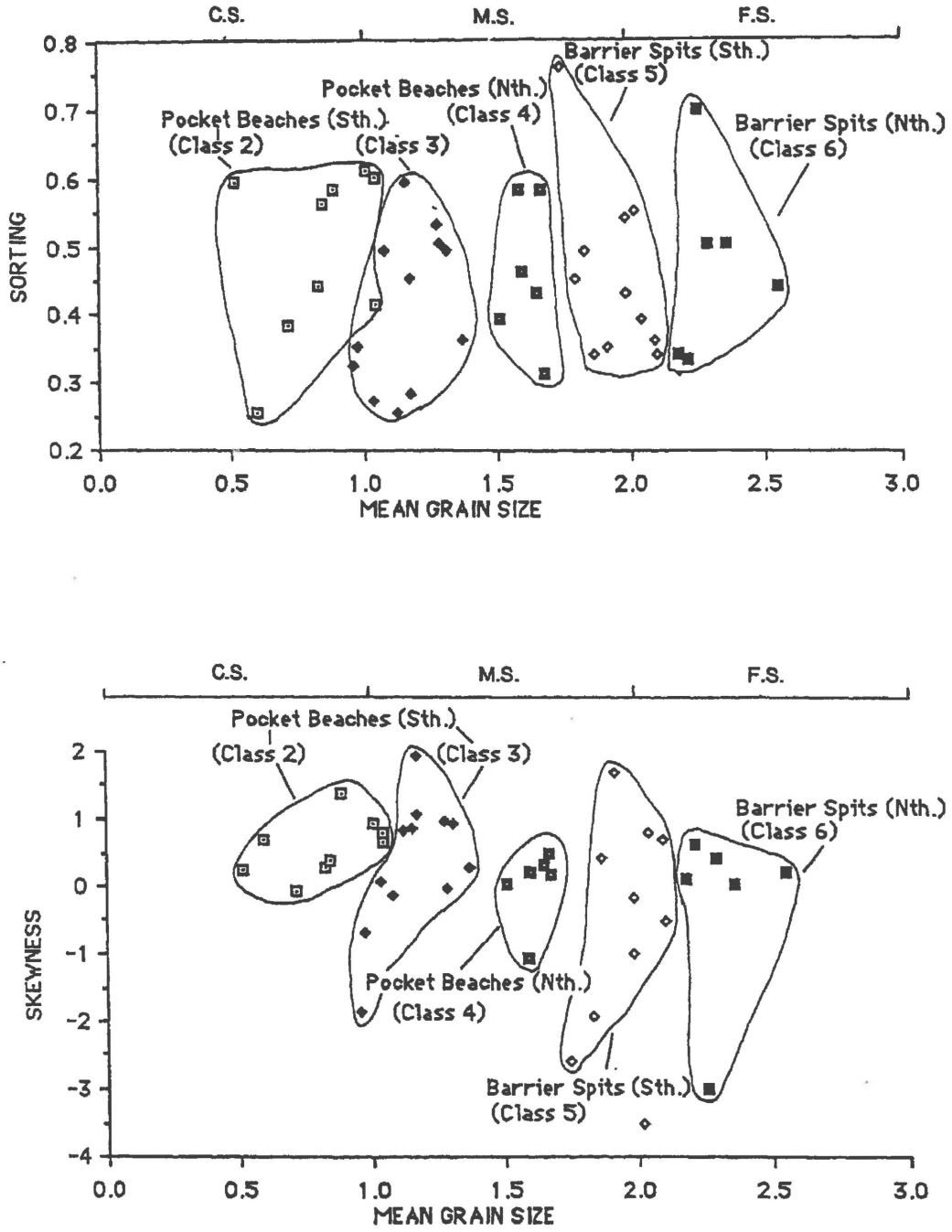

Figure 5.22. Relationship between textural parameters within each entropy class for beach samples along the east Coromandel coast: a) mean grain size vs. sorting; b) mean grain size vs. skewness. Note the trend of decreasing grain size from pocket beach sediments on the southern coast, to those on the northern embayed coast, and then for barrier spit deposits on the southern and northern coastlines respectively. This trend, along with those for barrier deposits in Figure 5.21, are inferred to indicate different sources for both pocket and barrier spit systems, and differences in incident wave energy for the southern exposed and northern embayed coastlines.

pocket beach and barrier deposits, which suggests the coarse grained inner shelf deposits may have been a source for these pocket beach systems along the southern coast.

Class 3 (Figure 5.18 C): The medium grained, well sorted sands from entropy class 3 show some important similarities to classes 1 and 2 in terms of size, skewness, iron oxide staining and roundness. Class 3 deposits are almost exclusive to the southern shelf, where they tend to occur landwards of the coarser and less well sorted classes 1 and 2 in depths of 20 to 30 m. This suggests that they represent extensively reworked, and hence very well sorted medium grained sands, derived from these less extensively reworked erosional coarse lag deposits. They are also found in pocket beach and barrier sands along the southern coastline, which may indicate that deposits within these embayments were derived from either the coarse grained offshore sands (i.e. entropy classes 1, 2 and 3), or at least from reworking of similar textured pre-existing Pleistocene deposits. Evidence supporting the latter possibility is shown at Orokawa Bay where class 3 sands are found in Pleistocene barrier deposits behind the modern beach.

Class 4 (Figure 5.18 D):The medium to fine grained class 4 deposits are relatively rare in shelf deposits on the southern coastline. However, they are more common further north offshore from Otama Beach, where they dominate the shelf surface away from the Hole in the Wall channel. It is the high carbonate content of the shelf sands from this area which makes this one of the most poorly sorted of the 7 classes. Unlike the coarser classes 1, 2 and 3, the macrofauna which form these high carbonate sands are probably largely in situ deposits. The same class of sediments also dominates pocket beach and barrier deposits from the northern embayed coastline, but are much better sorted than the same class of shelf sediments. As Pleistocene barrier deposits at Otama are composed of class 4 deposits, it is possible that northern pocket beach and barrier deposits were also originally derived from reworking of older pre-existing Pleistocene sediments.

Class 5 (Figure 5.18 E): The fine grained and well sorted entropy class 5 deposits occur in only small isolated patches on the shelf surface. However, they are very extensive in barrier spit dune deposits from both the southern and northern coastlines, and in barrier spit beach deposits on the southern coast. As sediments with similar textural properties do not occur on the shelf, no direct offshore source for these sands can be positively determined. However, it is possible that these barrier spit sands were derived from winnowing of coarser, less well sorted sediments, as may be present in the form of class 1 and 2 deposits on both the southern and northern shelf.

Class 6 (Figure 5.18 F): Fine grained moderately well sorted deposits from entropy class 6 form the most abundant group of sediments in the study area. They are particularly abundant in the shelf deposits from 20 to 50 m at Whiritoa, and from 0 to 30 m at Whangapoua. Elsewhere, they commonly form a lower nearshore deposit from 20 to 30 m water depth. Unlike the coarse lag deposits of classes 1 and 2, the macrofauna which characterise these deposits are in situ, but of lower concentration, presumably due to higher sedimentation rates (HILTON, 1990). Unlike the coarser entropy classes, microfauna form a significant component in these sands (about 5%),

particularly at Whangapoua, with four commonly occurring species of benthic foraminifera. This is presumed to indicate a relatively low energy environment of deposition. The coarse skewness of class 6 deposits suggests they may have been derived from winnowing of coarser, less well sorted class 1, 2 and 3 deposits which occur adjacent to them on the southern shelf. Further north at Whangapoua, they may have been derived from winnowing of the medium grained class 4 deposits at Otama, or alternatively be presently derived from sediments within Whangapoua Harbour during catchment flooding. As these are texturally very similar to class 5 deposits, it is possible that both classes of sediments are genetically related and thus formed together, with the better sorted class 5 deposits reworked onshore by wave and aeolian processes to form large barrier spits, and the slightly finer and less well sorted class 6 sands remaining offshore to form a fine grained lower nearshore and inner shelf deposit. Class 6 deposits are also found in barrier spit beach sands on the northern coastline, where they may be of modern terrigenous origin.

Class 7 (Figure 5.18 g): The very angular and fine grained nature of class 7 deposits suggests they may represent a fairly recently derived group of terrigenous sediments in the study area. On the southern shelf, they are found in a continuous band in upper nearshore water depths of 5 to 20 m, and in mid shelf depths of 50 m off Whiritoa and Whangamata. On the northern embayed coast, they occur very extensively over the shelf in Mercury Bay, and are also found on the mid shelf at Hotwater Beach and Whangapoua. As class 7 deposits are so extensive within Mercury Bay, it is possible that the Hotwater Beach and Whangapoua mid shelf deposits have been derived from this large source area. The common occurrence of class 7 deposits within deep mid shelf waters is reflected in the abundant microfossil assemblages which characterise them, with five species of benthic foraminifera very commonly forming up to 5% of the sediments. Class 7 deposits are not found in any east Coromandel beach or barrier sediments, presumably because the environmental energy levels would be too high for such fine grained sediments to accumulate.

5.7. CONCLUSIONS

A very distinctive feature of the east Coromandel shelf surface sediments is the highly variable nature of their textural patterns, particularly the hydraulic textural properties of mean grain size and sediment sorting. This is inferred to indicate the presence of variable hydrodynamic conditions along the coast, especially current energy and flow patterns, as was indicated to some degree from current measurements (see Chapter 4.6.)

Along the relatively open southern coastline, textural patterns vary significantly between embayments, although some generalisations can be made:

1. Fine to very fine grained, well sorted, low carbonate, low iron stained, very angular sands occur in a continuous band along the coast in 5 to 20 m water depth. These textural properties suggest this is a modern terrestrially-derived sediment which is being actively reworked by waves along the coast. It is tentatively labelled an 'upper nearshore' very fine grained sand.

2. A fine grained, well to moderately well sorted, low carbonate, moderate to extensively iron stained, angular to subrounded group of sediments, forms a very patchy distribution from 20 to 50 m water depth, but appear to occur more commonly in a more continuous band from 20 to 30 m water depth. The textural properties indicate less extensive reworking under modern hydraulic conditions than the upper nearshore sands, and so they are probably reworked and deposited by less frequent storm waves and currents. These sediments are labelled as 'lower nearshore and inner shelf' fine sands.

3. Medium to coarse grained, well to moderately well sorted, high carbonate, extensively iron stained, rounded sands which consistently occur in depths ranging from 20 to 50 m. The textural properties suggest a coarse lag or palimpsest deposit which is intermittently reworked by storm waves and currents, and is defined as an 'inner shelf coarse lag' deposit.

4. Fine to very fine grained, moderately sorted, low carbonate, non-iron stained, very angular, muddy sands occur in depths > 50 m at Whiritoa and Whangamata. Their textural properties are consistent with a low energy environment of deposition, and so they are termed 'mid shelf' muddy sands. Similar muddy deposits are also present off Waihi Beach to the south, although here they are medium grained deposits and thus possibly formed under higher current energy conditions.

Further north at Hotwater Beach, similar bands of fine nearshore, coarse inner shelf , and very fine muddy mid shelf sands occur. However, they differ in lacking a very fine grained upper nearshore band of sands, and are generally coarser grained and better sorted than shelf sediments from the southern coastline. This is inferred to indicate higher wave energy conditions on the steeper and narrower shelf surface at this locality, and the absence of an onshore source for very fine upper nearshore sands.

North of Hotwater Beach, the presence of broad shallow embayments, and numerous offshore islands produces a very haphazard textural pattern on a regional scale, in which either coarse or fine sediments tend to dominate the shelf surface in different locations. Thus it is not possible to associate textural patterns with the different sediment lithofacies that are generally found in various shelf zones (see Chapter 3.2.). At Mercury Bay and Whangapoua, very fine and fine grained sands dominate respectively, which indicate conditions of high sedimentation from local catchments, and possibly also from adjacent shelf sediments at Whangapoua. At Otama Beach, coarse carbonate-enriched sands dominate the shelf surface, but grade to finer sands towards Whangapoua in the west. This is interpreted as indicating wind- and tidal-generated flows dominating sediment transport in this region, a deduction supported by current measurements at Opito Bay (Chapter 4.5.1.).

In comparison to other storm-dominated shelf settings reviewed in Chapter 3, the coastline from Waihi to Hotwater Beach shows similar aspects to several of these. In particular, the presence of

fine nearshore, coarse inner shelf, and very fine muddy mid shelf sands has previously been described in eastern Australia by ROY and STEPHENS (1980), and at Pakiri on the northeast New Zealand coast by HILTON (1990). Therefore, similar hydrodynamic conditions may be present on much of the east Coromandel coastline as occurs in these two regions. However, the very fine upper nearshore sands are more characteristic of allochthonous shelf settings such as the Oregon-Washington coast in North America, and the Otago Canterbury shelf in New Zealand (see Table 3.1). Also the very patchy distribution of fine sands along the southern coast is similar to the North American Atlantic shelf. However, the east Coromandel coast differs from this latter region in tending to show a seaward coarsening trend in grain size. Therefore, an understanding of the sedimentation processes on the southern east Coromandel coast will require integrating different ideas and models from these various shelf settings. One previously studied area which does show a similar shelf textural pattern is on the Tauranga coast, just south of the study area (DAHM and HEALY, 1980; HARMS, 1989). Sedimentation conditions on the southern east Coromandel coast may therefore extend some distance to the southeast along the Bay of Plenty coastline.

Sediment textural patterns occurring along the northern coastline between Mercury Bay and Whangapoua are not commonly encountered in other storm-dominated shelf settings. They therefore represent unique local conditions associated with a deeply embayed shelf setting, in which current and wave energy conditions and modern sediment inputs are highly variable.

In terms of beach-shelf sediment interactions, the textural data provide some evidence that many of the beaches along the east Coromandel coast are actively interacting with nearshore deposits. Exceptions appear to occur in the pocket beach systems of the southern coastline, as shown by the lack of overlap in textural properties between beach and nearshore deposits. The textural data also show some evidence that modern beach deposits on barrier spit systems are supplied by terrestrial sediments from local catchments, as indicated by their finer grain size than older barrier deposits, and textural overlap with fluvial sediments. Variations in the mean grain size and sorting of beach deposits from different sections of the coast show evidence of higher incident wave energy on the southern coastline from Waihi to Hotwater, than on the deeply embayed northern coastline from Mercury Bay to Whangapoua. This difference in energy conditions is consistent with a greater exposure of the southern coastline to open ocean waves, while the presence of numerous offshore islands and broad embayments to the north dissipates much of the incident wave energy here.

Statistical grouping of textural data provides some information on the potential sources of different shelf and beach/barrier deposits. This has categorised east Coromandel sediments into 7 classes. For shelf deposits, there are 3 classes of coarse lag deposits inferred to represent palimpsest sands (classes 1, 2 and 3), two classes of actively depositing fine sands (classes 6 and 7), and one class of possibly mixed palimpsest and actively depositing biogenic sediments at Otama (class 4). From the textural data, it is inferred that the actively depositing class 6

sediments were mainly derived from reworking of the coarse palimpsest sands (although at Whangapoua they may also have a modern terrestrial origin), and that the class 7 deposits have a modern terrigenous source. On the beach and barrier systems, the coarse grained textural classes 2 and 3 mainly occur on southern pocket beach systems, which indicates they may have been derived from either an onshore transport of the coarse palimpsest shelf sands, or from a similar source material such as the Pleistocene barrier deposits found within many of these pocket embayments. Pocket beaches on the northern coastline are characterised by the finer grained class 4 deposits, which also show textural similarities with older Pleistocene barrier sands, and thus may have been derived from reworking of these deposits. Barrier spits along both coastlines are characterised by class 5 deposits, which is inferred to indicate a possible origin for these larger barrier systems from the onshore transport of the fine grained class 6 shelf sediments. Confirmation of the sources for different shelf and beach/barrier deposits can only be made following a detailed examination of their mineralogy, which is addressed later in Chapter 9.

CHAPTER SIX

SHELF MORPHOLOGICAL SURVEYS

6.0. INTRODUCTION

Results so far have indicate rather variable sedimentation conditions exist across the east Coromandel shelf surface. In particular, the variable nature of sediment textural patterns and current recordings along the coast are inferred to indicate changeable hydrodynamic conditions, particularly in regions of altering coastal and shelf physiography. Additionally, the presence of different textural patterns across the shelf on the southern exposed coastline is inferred to indicate varying hydrodynamic conditions, with wave-dominated sediment transport occurring in depths of < 20 m, changing to more current-dominated flows in depths of 20 to 50 m, and only low transport conditions in deeper waters. Thus, sediments across the shelf have been tentatively divided into upper nearshore, lower nearshore, inner shelf, and mid shelf deposits (see Chapter 5.7.). However, the evidence to date does not fully identify the hydrodynamic processes responsible for the shelf sedimentation patterns, or indicate the transport pathways for these sediments.

Such information has been obtained in previous studies by mapping the nature and distribution of morphological features, or bedforms, on the sea floor, and their relationship with different surface sediments (e.g. SWIFT and FREELAND, 1978; SWIFT and FIELD, 1981; MORANG and McMASTER, 1980; NELSON and HEALY, 1982; TWICHELL, 1983; BLACK and HEALY, 1983, 1988; HUNTER *et al.*, 1988; GORDON and HOFFMAN, 1986; HARMS, 1989). Morphological features of interest to the east Coromandel coast will be those typically found on similar storm-dominated shelf settings (see Chapter 3.2.), which include in order of decreasing size: sand ridges; sand waves; megaripples; and ripples. Definitions of these bedforms as used in this study are shown in Table 6.1., with ripples, megaripples, and sand waves differentiated according to the scheme of HARMS *et al.* (1975) and modified by BOOTHROYD (1978), and sand ridges defined on the basis of characteristic features shown by North American (SWIFT and FREELAND, 1978; SWIFT and FIELD, 1981; NIEDORODA *et al.*, 1985 b) and western Cook Strait in New Zealand (LEWIS, 1979) examples.

Table 6.1. Morphological definition of various bedforms identified in this study (*= based on scheme by BOOTHROYD, (1978); #= based on various North American and New Zealand studies).

	*Ripples	*Megaripples	*Sandwaves	#Sandridges
Spacing	< 0.6 m	0.6 to 6.0 m	> 6 m	> 100 m
Height vs Spacing	variable	relatively large	relatively small	very small
Geometry	highly variable	sinuous to highly 3-dimensional, prominent scour pits in troughs	straight to sinuous, uniform scour in troughs	long crested, scour concentrated on up-current flanks
Detection	Divers	Divers & Sonographs	Divers & Sonographs	Sonographs & Echosounder

The recognition, description, and mapping of bedforms over relatively wide areas is commonly achieved by obtaining plan views of the shelf surface from side-scan sonograph images, along with more generally available information from echosounding profiles and diver observations (BELDERSON *et al.*, 1982). This chapter presents results from such morphological surveys of the east Coromandel shelf, and makes some initial interpretations of sedimentation patterns and transport pathways along the coast by integrating this information with the current patterns and sediment textural data from previous chapters. However, a more detailed analysis of hydrodynamic conditions responsible for the generation of bedforms is attempted later in Chapter 7.

6.1 METHODS

6.1.1. Side-Scan Sonar

Side-scan sonar data used in the E.C.S.S. were collected in three separate surveys between 1984 and 1990. In Mar-84 and -85 Paul Dell collected the initial side-scan sonar data aboard the M.V.Tuhua, using personnel from the University of Waikato, Hauraki Catchment Board, and New Zealand Oceanographic Institute. The first survey was conducted between 7- and 20-Mar-84, in which 385 km of sea floor was scanned by both shore-parallel and shore-normal runs from Waihi Beach to Whangapoua. The second survey occurred from the 12- to 13-Mar-85, and covered 59 km of the shelf with a series of shore-parallel runs between Whangamata and Onemana. For these initial surveys, the side-scan sonar equipment used was a 100 kHz EG&G dual channel system provided by the New Zealand Oceanographic Institute, utilising a scanning range of 300 m during the first survey, and 200 m for the second. The change in scanning range was made as 200 m provided a more detailed resolution of bedforms such as megaripples, which could then be measured for their wavelength and height. Sonographs were recorded using wet chemically-based traces. Position-fixing for these initial surveys was made by taking bearings with sextant and monocular compass from prominent features on land.

The third survey was undertaken by the present author between 25- and 28-Jun-1990 aboard the M.V. Enterprise, using personnel from the University of Waikato and New Zealand Oceanographic Institute. This side-scan survey was run simultaneously with a sub-bottom profiling system, which placed limits on the amount of data that could be collected and the location of survey lines. However, where possible it was attempted to overlap previous side-scan sonar tracks to determine any significant changes in the sea-bed, in particular to assess the effects of an extreme storm event (Cyclone Bola) in 1988. A total of 174 km of shelf was surveyed between Waihi and Onemana, and within Mercury Bay, along both shore-parallel and shore-normal lines. A Klein 100 kHz dual channel system was used in this survey, with sonographs recorded on dry thermal paper, using a 200 m lateral range. The boat position was determined primarily by a Magellan GPS NAV 1000 satellite navigation system, and backed up by on-board radar when this system was inoperative due to incomplete satellite coverage.

In all the surveys undertaken, the side-scan fish was towed at a constant speed of 5 knots approximately 20 m behind the ship. This separation between the boat and fish was taken into account when compiling sonograph maps. Ideally, the fish was kept about 5 m above the sea-bed as this provided the best resolution. However, as only 50 m of cable was available this was not possible in waters deeper than ~ 30 m. Also, where reefs were present on the sea floor, the fish had to be kept at a higher elevation to avoid damage to the equipment.

6.1.2. Bathymetric Data

Bathymetric data were collected simultaneously with the side-scan sonographs so that sediment textural patterns could be related to morphological features on the sea-bed. In the first two surveys carried out by Paul Dell (Mar-84 and -85), a Koden SR 658 echosounder was used. However in the Jun-90 survey by the present author, a Ratheon DE 719B system was utilised, as this gave an increased vertical exaggeration of the sea-bed, and thus provided a better resolution of bathymetric features. Positioning of the bathymetric soundings in each survey was as outlined above for the sonograph surveys.

6.1.3. Ripple and Megaripple Observations

Observations of ripple and megaripple bedforms were initially undertaken by divers as part of the sediment sampling program in Feb- and Nov-84 by Paul Dell, and Apr-85 by Tony Colby. Measurements were taken by placing a board calibrated at 2.5 cm intervals into the bedforms, and then measuring the spacing of consecutive crests (wavelength = λ) and distance from trough to crest (height = η). In most cases, the orientation of the crests was determined by using an underwater compass, and a visual interpretation of the bedform patterns and degree of symmetry made by the diver. Representative surface samples were collected by the divers to relate bedform configurations to sediment texture. At several sites underwater photographs were taken of the bedforms, and are presented where appropriate in the text.

Direct measurements of bedforms could only be made by divers to a maximum depth of 34 m. Beyond this, indirect measurements had to be made from the side-scan sonograph records. On sonographs traces, λ is relatively easy to measure where a clear resolution of bedforms appears by simply dividing the number of acoustic shadows indicating bedform crests by the distance shown on the sonograph. To determine heights from sonographs, a technique described by BLACK and HEALY (1983) was used. This involves determining the side-scan fish height from the sea-bed (z), acoustic shadow length of the object (s), and horizontal distance of the object from the fish (l). Simple trigonometry then determines the height of the object from the relationship: $h = z.s/l$. This could only be accurately resolved on the sonographs in which a 200 m scanning range was used, and where bedforms produced shadows at least 1 mm wide on the trace. The main short-coming in using sonographs for such small-scale bedform analysis is that only a relative idea of the sediment

texture associated with the bedform is provided. Measurements from sonographs were therefore avoided when data on mean grain size were required in subsequent analyses.

6.2. SIDE-SCAN SONAR DATA

6.2.1. Side-Scan Sonar Operation and Sonograph Interpretations

Side-scan sonar has proved to be a popular tool for the mapping of the shelf surface in recent years, as it provides a relatively quick and inexpensive means of determining broad textural patterns and morphological features over a continuous and relatively wide range (D'OLIER, 1979). Sonographs can resolve a range of features including megaripples, sandwaves, sand patches, and sand ribbons, and thus indicate potential sediment transport pathways (D'OLIER, 1979; BLACK and HEALY, 1983).

The side-scan sonar system works by emitting a fan-shaped sonic beam from a sonar 'fish', which is scattered from the sea floor and detected by a transducer pointing sideways from the vessel, then processed and presented as a plan image on an appropriate graphical device (D'OLIER, 1979). The 100 kHz systems used were able to produce distinguishable resolution of features greater than $\lambda = 0.66$ m during the first survey, and $\lambda = 0.5$ m in the subsequent ones.

Details regarding the interpretation of side-scan sonographs have been reviewed elsewhere (e.g. BELDERSON *et al.*, 1972; D'OLIER, 1979) and will only be briefly discussed here. Side-scan sonar works by recording the intensity of the returning acoustic signal from the sea-bed. This may be displayed as tonal variations on recording paper. The sediment texture of the sea-bed affects the strength of echoes: mud and fine sand causing little back-scattering; whereas shells, gravel, and coarser sediment reflect more acoustic energy. These variations then show up as different shades or tones on the trace, the former producing a relatively light tone, and the latter a darker shade. Morphological features of significant relief will also be detected by the acoustic shadow they produce. Positive relief features facing the transmitter will have a high reflectivity and thus be recorded as dark bands, whilst those facing away will be in an acoustic shadow and recorded as white bands. This is how side-scan sonographs provide lateral images of sediment textural types and morphological features.

Sonographs collected in this study showed six commonly recurring patterns. Previous workers involved in interpreting sonographs have often classified recurring patterns as side-scan sonar 'facies' (HARMS, 1989; RYAN, 1989). However, this term has been avoided in keeping with its true geological definition as a description of a particular suite of grain types, sediment sizes, sedimentary structures, and sediment geometry (LEEDER, 1982). Sonograph patterns observed in this study include:

1. Fine Featureless Pattern. Very common pattern characterised by a light tone on sonograph records (Figure 6.1). This was interpreted as a fine sand deposit. No indication of bedforms were found on sonographs where this pattern occurred. However, as the side-scan equipment could not resolve features < λ= 0.5 to 0.6 m, it is possible that ripples are present on the fine sand (later confirmed to be present in most areas by divers).

2. Coarse Megarippled Pattern. Common pattern characterised by a dark or coarse tone on sonographs (Figure 6.1). This is interpreted as indicating a medium or coarse grained sand deposit. Crenulated features indicating the presence of bedforms were usually found associated with this pattern along shore-parallel sonograph traces, but were generally absent on shore-normal runs. Similar observations were made by BLACK and HEALY (1983) at Whangarei Harbour, which they accounted for as due to the anisotropy of straight-crested bedforms, causing a better reproduction of bedforms if the sonar fish travels along their crests rather than across them. The term megaripples is used to describe these features, although it should be noted that where a 200 m scanning range was used, features between λ= 0.5 and 0.6 m could be present, which are below the HARMS *et al.* (1975) ripple-megaripple boundary of λ= 0.6 m. The presence of megaripples is indicative of active bedload transport occurring over the coarse sand deposits. Coarse Megaripple Patterns (CMR) were found in a variety of features, ranging in terms of increasing size, from elongate bands (usually shore-normal and < 100 m wide), to wider patches and extensive fields.

3. Bedrock Pattern. Common pattern characterised by its strong reflectivity and rough texture (Figure 6.1), consistent with bedrock sonograph patterns described by BELDERSON *et al.* (1972). Simultaneous echo sounding traces also indicate this pattern is associated with reefs on the sea-bed.

4. Blebby Pattern. Pattern sometimes found with a Fine Featureless background, characterised by discrete closely spaced 'blebs' giving a pock marked appearance to the trace (Figure 6.2). Similar features have been described for sonographs from Tauranga by HARMS (1989), and were identified by diver observations in this study as upstanding colonies of the horse mussels *Atrina novaezelandica*. Horse mussels produce this 'Blebby' appearance because sponges and other marine organisms colonising their shells provide large surfaces for reflection of the sonar (W.de LANGE, pers.comm.).

5. Mottled Pattern. Pattern only found abundantly in the area offshore from Whangapoua, characterised by a mottled texture of strong reflectors (Figure 6.3). The mottled texture occurs randomly in patches and is often dissected by linear features interpreted as dredge marks. Thus, this pattern may indicate areas of live scallop and other shellfish beds on the sea floor.

6. Isolated Strong Reflectors. Pattern shows a coarse granular texture which is strongly reflective (Figure 6.4). Appearance is one of clusters of small rounded features, interpreted as possibly

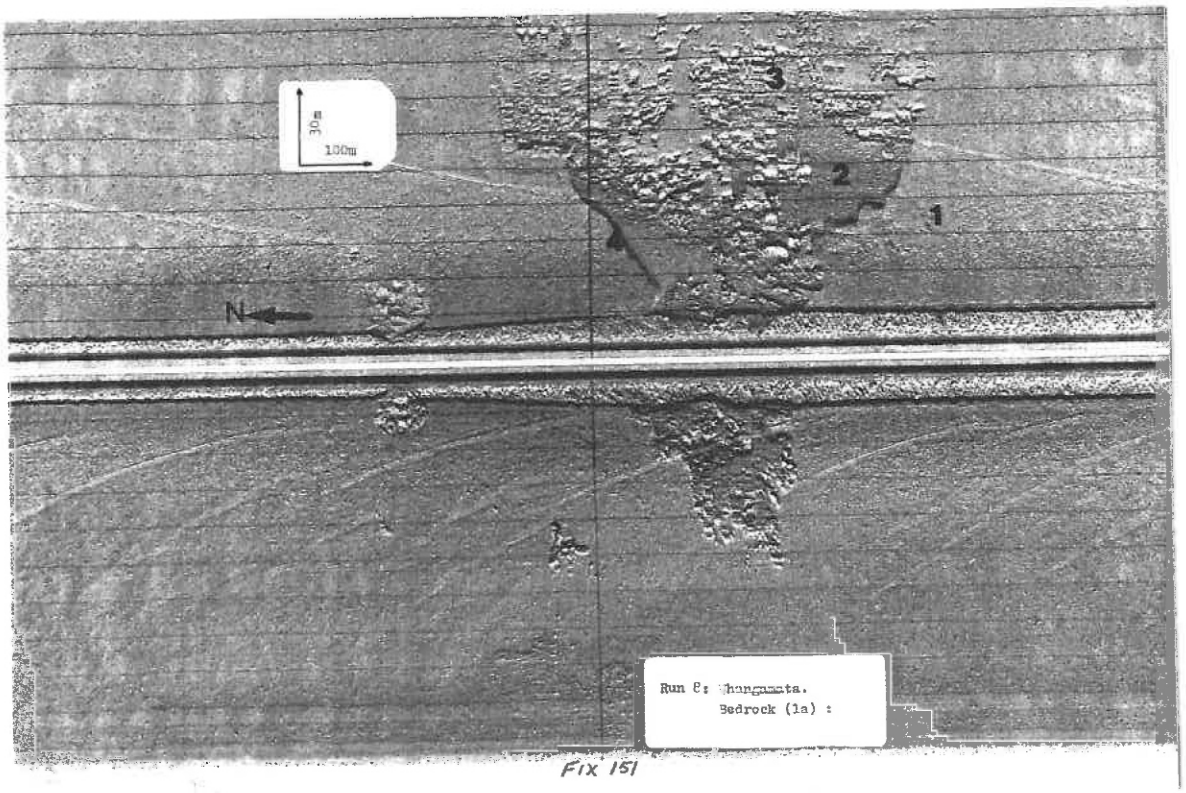

Figure 6.1. Sonograph off Whangamata Beach (10 m water depth), showing examples of: 1. Fine Featureless sediments; 2. Coarse Megarippled (CMR) sediments; 3. Bedrock; 4. sharp contact between Fine Featureless and CMR sediments.

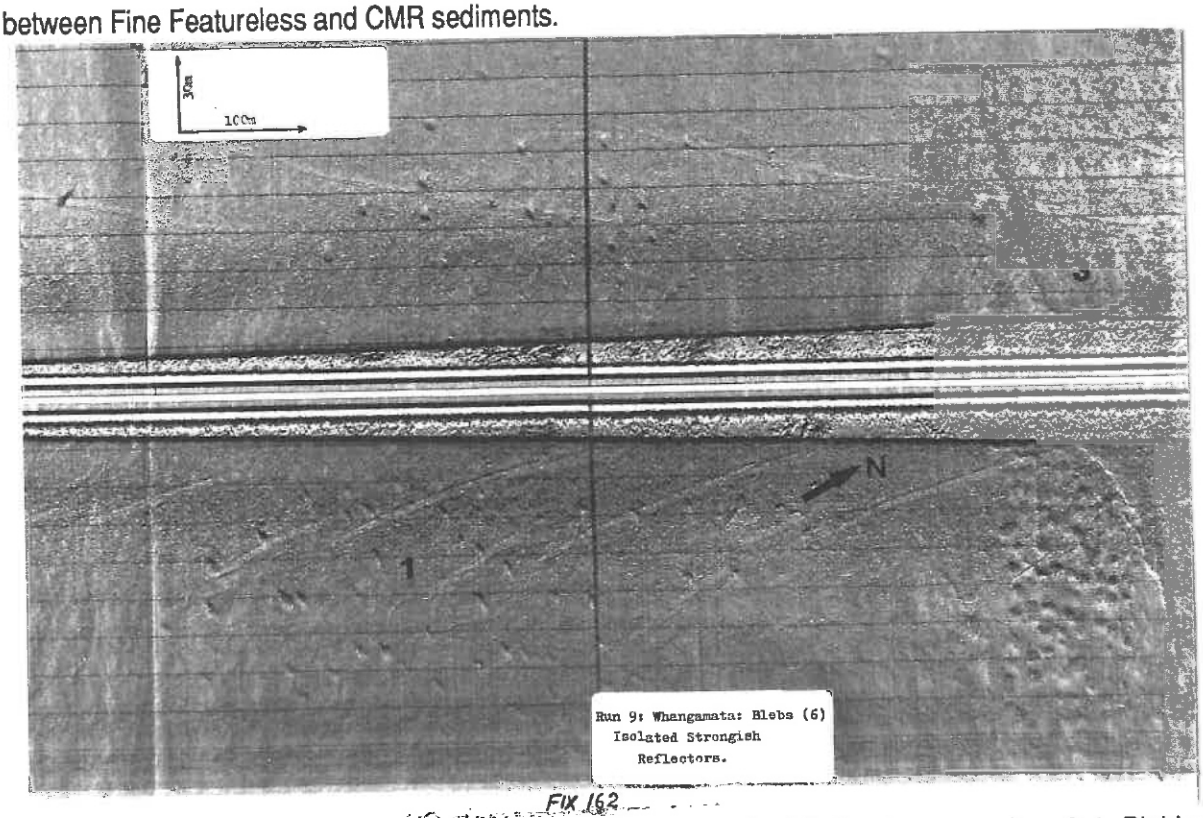

Figure 6.2. Sonograph off Whangamata Beach (20 m water depth) showing examples of: 1. Blebby Pattern indicating horse mussel colonies; 2. sharp contact between Fine Featureless and CMR sediments; 3. gradational contact between CMR and Fine Featureless sediments.

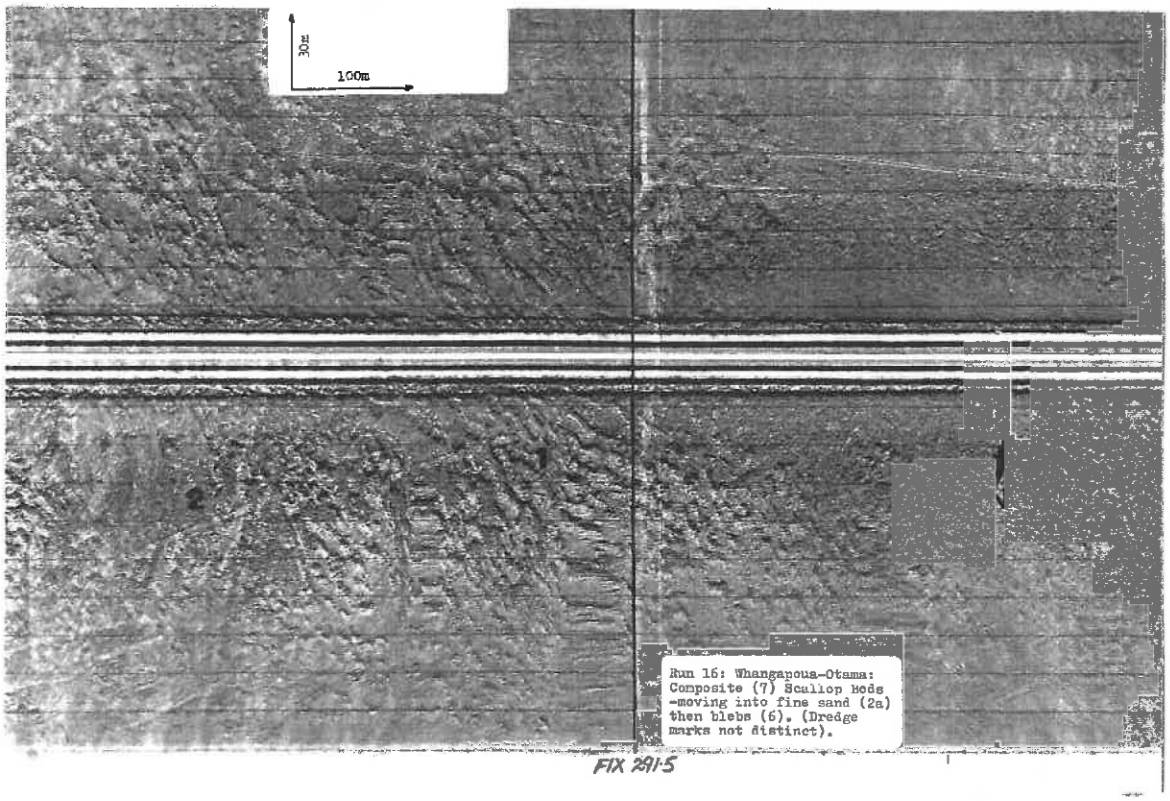

Figure 6.3. Sonograph offshore from Whangapoua Harbour (12 m water depth), showing example of Mottled Pattern (1) indicative of live shell fish beds, with linear dredge marks (2) apparent on the surface.

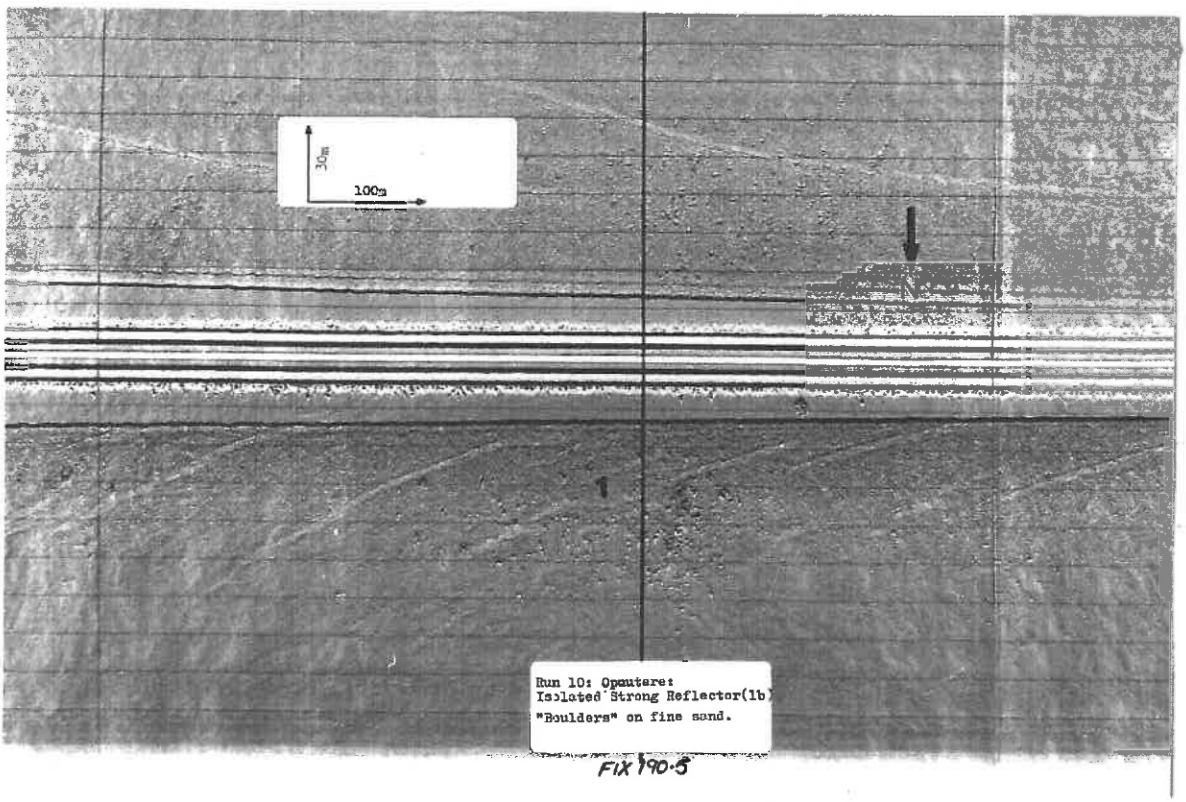

Figure 6.4. Sonograph offshore from Opoutere Beach (25 m water depth) showing example of Isolated Strong Reflectors (1) due to scattered boulders on the sea-bed. Note that the 'swoop marks' (2) on this and other sonographs are simply creases on the trace paper.

representing scattered areas of small boulders on fine sand. This interpretation has been confirmed by diver observations off Opoutere and Kuaotunu Beaches.

The sonographs also enable the nature of boundaries between different patterns to be defined, particularly between patterns 1, 2, and 3. In some cases a very sudden boundary or contact between sonograph patterns occurs (Figure 6.1), and in other areas one pattern simply appears to grade into another (Figure 6.2). This may indicate the sonar fish was passing over a topographic feature, the slopes facing the fish giving a strong reflection and those away producing a weaker reflection (D'OLIER, 1979). Alternatively, it may be showing a sudden change in textural boundaries associated with erosion, as opposed to gradational changes in texture indicative of deposition. The latter case was usually the most likely scenario, as indicated by the consistent occurrence of the identical boundary type for the same features from different approach angles. Thus the nature of boundaries is shown on sonograph maps and used to make some deductions about transport pathways.

Other side-scan sonograph patterns were also identified, but were considered to be due to reflections from sources other than the sea-bed. Side-scan runs in shallow waters (< 10 m) often showed a 'wavy' pattern, parallel to the trace (Figure 6.5). This is possibly related to reflection from the sea surface producing a Lloyd's Mirror Effect, as described by BELDERSON *et al.* (1972) and D'OLIER (1979). Such patterns have previously been misinterpreted by some workers, such as MORANG and McMASTER (1980), as sand wave features on the sea-bed, but can be distinguished due to their blurred appearance (WERNER, 1981). Another interference pattern which often showed up on sonographs was a 'fizzy' wavy appearance, interpreted as reflection from the boat wake (Figure 6.6). In one instance fish shoals gave a 'Blebby' type pattern, but were distinguished by interference marks present in the water column. In the Jun-90 survey, dark symmetrical elongate patches similar in appearance to coarse sand were found on sonographs, but were interpreted as objects in the water (probably dolphins observed following the vessel) because of the presence of acoustic shadows some distance behind the images.

6.2.2. Regional Side-Scan and Bathymetric Surveys

From the above side-scan sonograph interpretations, regional maps have been compiled for each major coastal sector from Waihi Beach to Whangapoua. These data are presented in the text as sonograph maps showing the side-scan traces and patterns observed over the scanning range used, and reproductions of appropriate bathymetric features from the simultaneous echosounding traces. Also where appropriate, representative photographs of sonographs are presented in each regional description. The side-scan sonar tracks used in all three surveys are shown for the southern and northern coastlines in Figures 6.7 and 6.8 respectively. More detailed information on the survey tracks and fix positions are presented in Appendix 4. In the following regional descriptions, only the broad textural patterns and large-scale morphological features (i.e. sand waves and sand ridges)

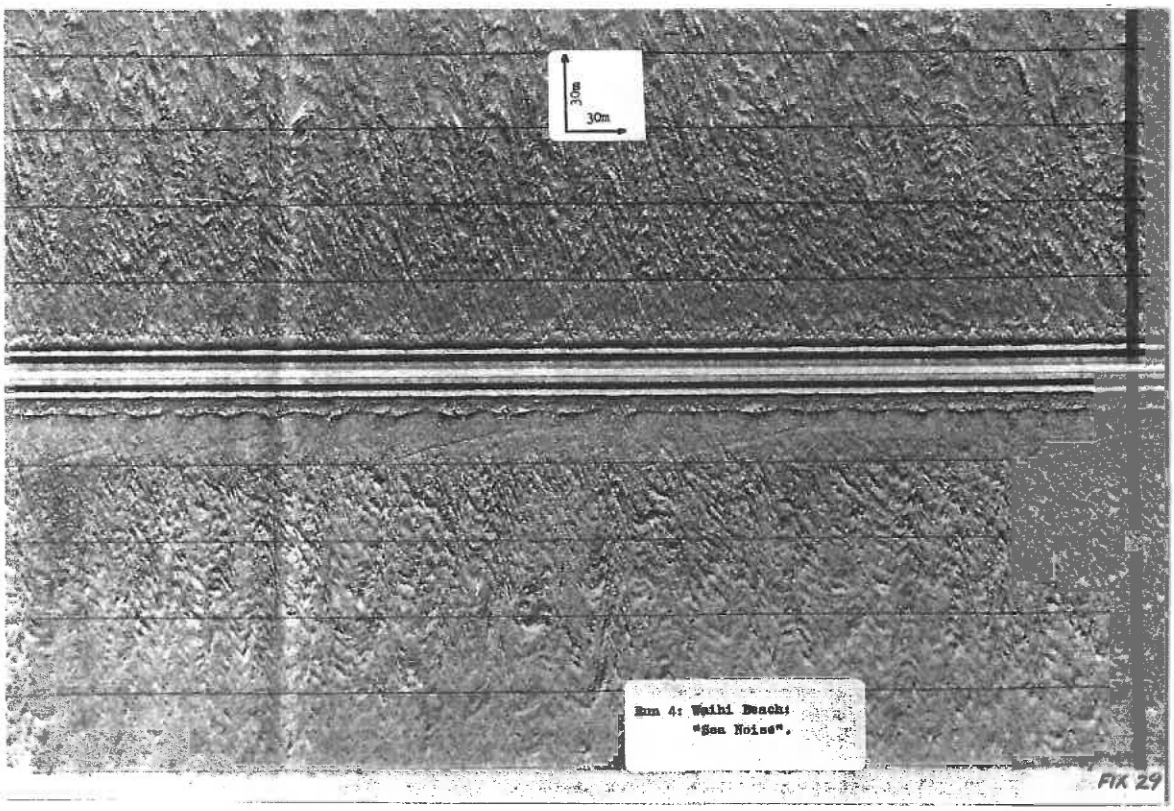

Figure 6.5. Wavy sonograph pattern off Waihi Beach (5 m), interpreted as a Lloyd's Mirror Effect due to reflection from sea surface.

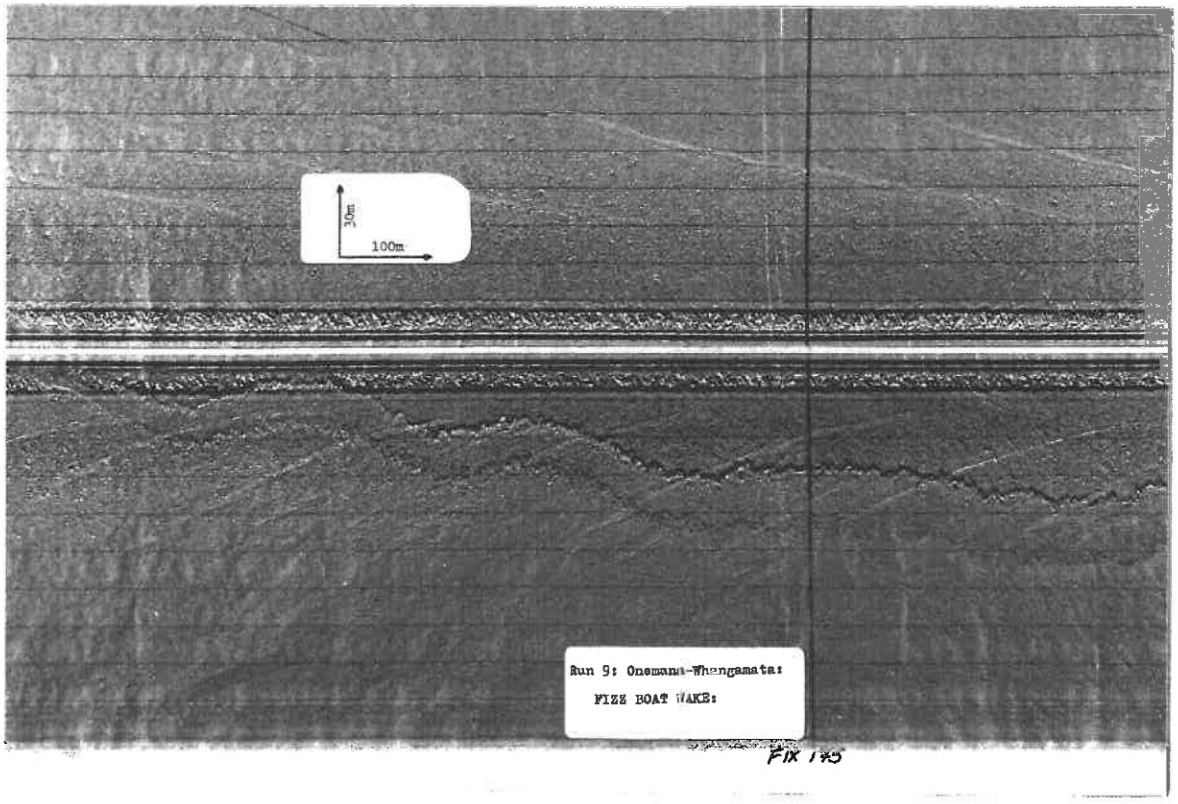

Figure 6.6. Fizzy sonograph pattern at Onemana (10 m) due to reflection from boat wake.

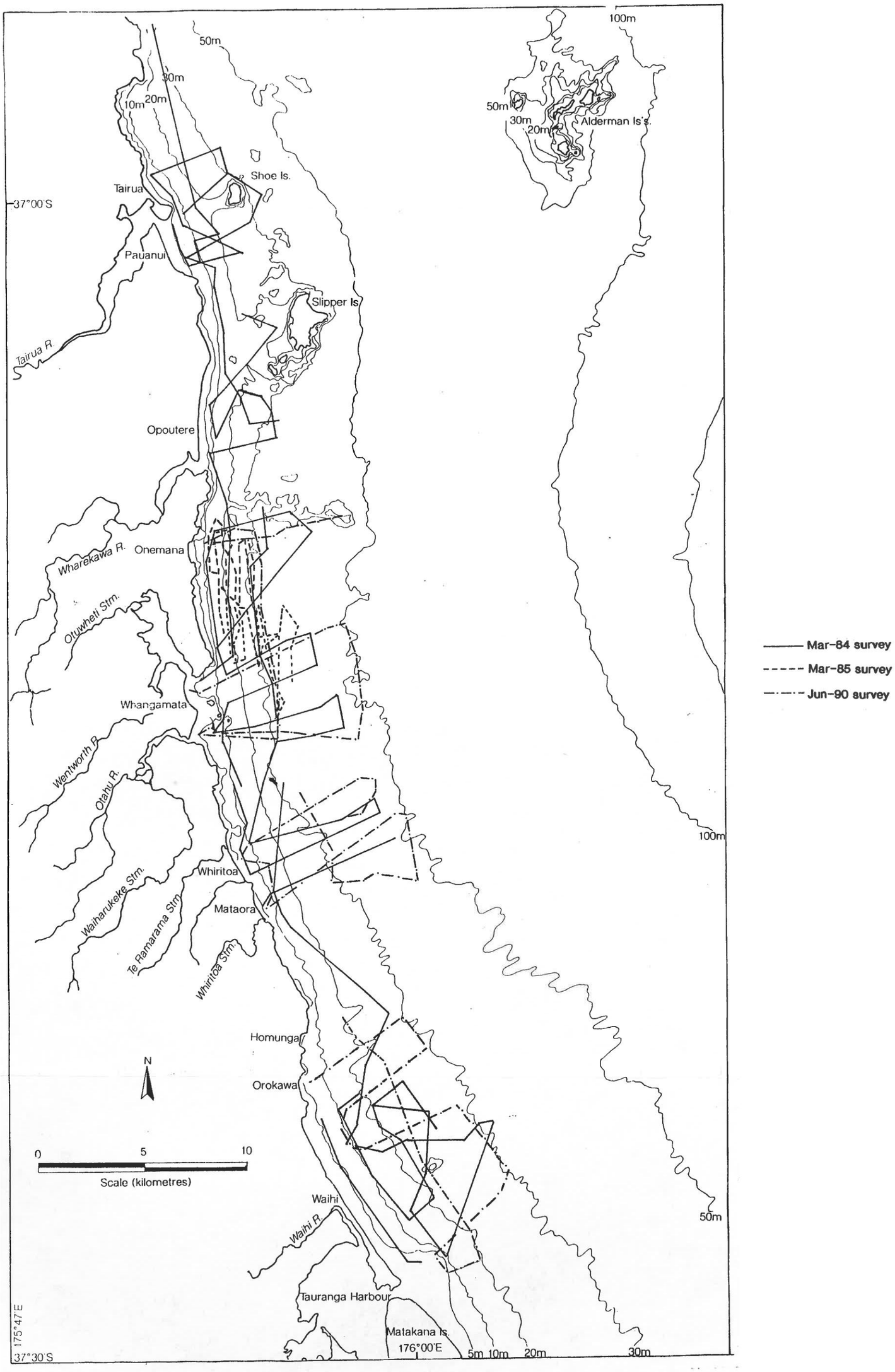

Figure 6.7. Location of side-scan sonar track lines from the three separate surveys on the southern coastline (see Appendix 4 for more details on fix positions).

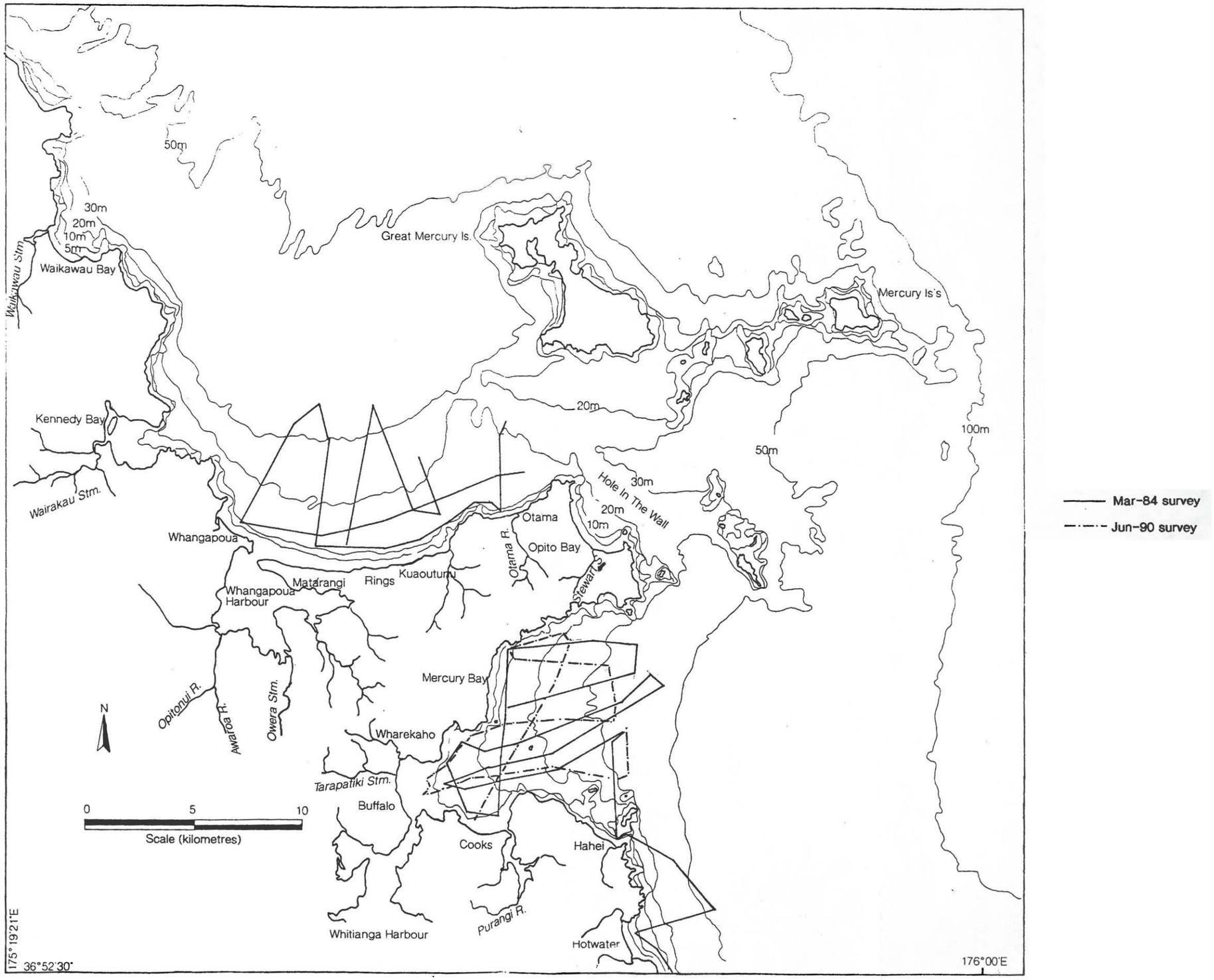

Figure 6.8. Location of side-scan sonar track lines from the two separate surveys on the northern coastline (see Appendix 4 for more details on fix positions)

are described, as the smaller ripple and megaripple bedform patterns are analysed later from diver observations.

Waihi Beach

The region offshore from Waihi Beach was subject to two separate side-scan surveys, the first on 10-Mar-84 and 20-Mar-84 in which 66 km of sea floor was scanned, and the second 6 years later on 26-Jun-90 in which 46 km was scanned. Results from both surveys are plotted in Figures 6.9 and 6.10.

The Waihi surveys show the same broad pattern of sediment texture described in Chapter 5.3., with relatively fine sediments dominating surface deposits in depths of 5 to 22 m, after which coarser deposits dominate to at least 30 m water depth. Shore-normal echosounding profiles from mid-Waihi Beach (Figure 6.11 a) show that fine sediments occur across a steeply dipping (1:180) concave-up surface, and the change to coarser sediments at 22 m depth coincides with a much flatter (1:1000) convex-up feature. This is consistent with the broad morphological features of the nearshore and inner shelf zones as described in Chapter 3.2., and thus gives evidence supporting the presence of distinct nearshore and inner shelf sediments, as suggested in Chapter 5.7. from the textural data.

However, the side-scan sonar surveys provide greater detail of the distribution of the broad textural patterns. Firstly, while fine sediments dominate the nearshore zone, shore-normal elongate bands of coarse megarippled (CMR) sands are also found in depths of 10 to 20 m, but were presumably too sparse to be detected by surface sediment sampling. In the first survey, these features were found in three locations off the northern, middle, and southern end of Waihi Beach, where they range in width from 50 to 100 m. In the second survey, bands were located in different locations off Orokawa Bay, and northern and southern Waihi Beach, where they formed much narrower features, only 5 to 50 m wide. In both surveys, the bands consistently show sharp southeastern and gradational northwestern contacts with Fine Featureless sediments, but do not coincide with any significant bathymetric features in echosounding profiles. The lack of current-generated bedforms within the CMR bands suggests that no significant sediment transport is associated with them, and that they possibly represent isolated areas of wave or current scouring.

Further offshore over the lower gradient inner shelf surface, an along-shore variation in the occurrence of fine and coarse sand was evident in both surveys. From north Waihi Beach to Homunga Bay, relatively large patches of CMR sediments occur (600 to 800 m in width), which show similar sharp southeastern and gradational northwestern contacts with Fine Featureless sediments as the narrower CMR bands on the nearshore surface. Here however, the CMR patches are associated with bathymetric features, as they consistently occur on the southeastern flanks of a series of four sand ridges. These ridges range in width (λ) from 600 to 1100 m, and height (η) = 3.2 to 7.4 m, and show asymmetry in their form in being skewed south (Figure 6.11 b). The same

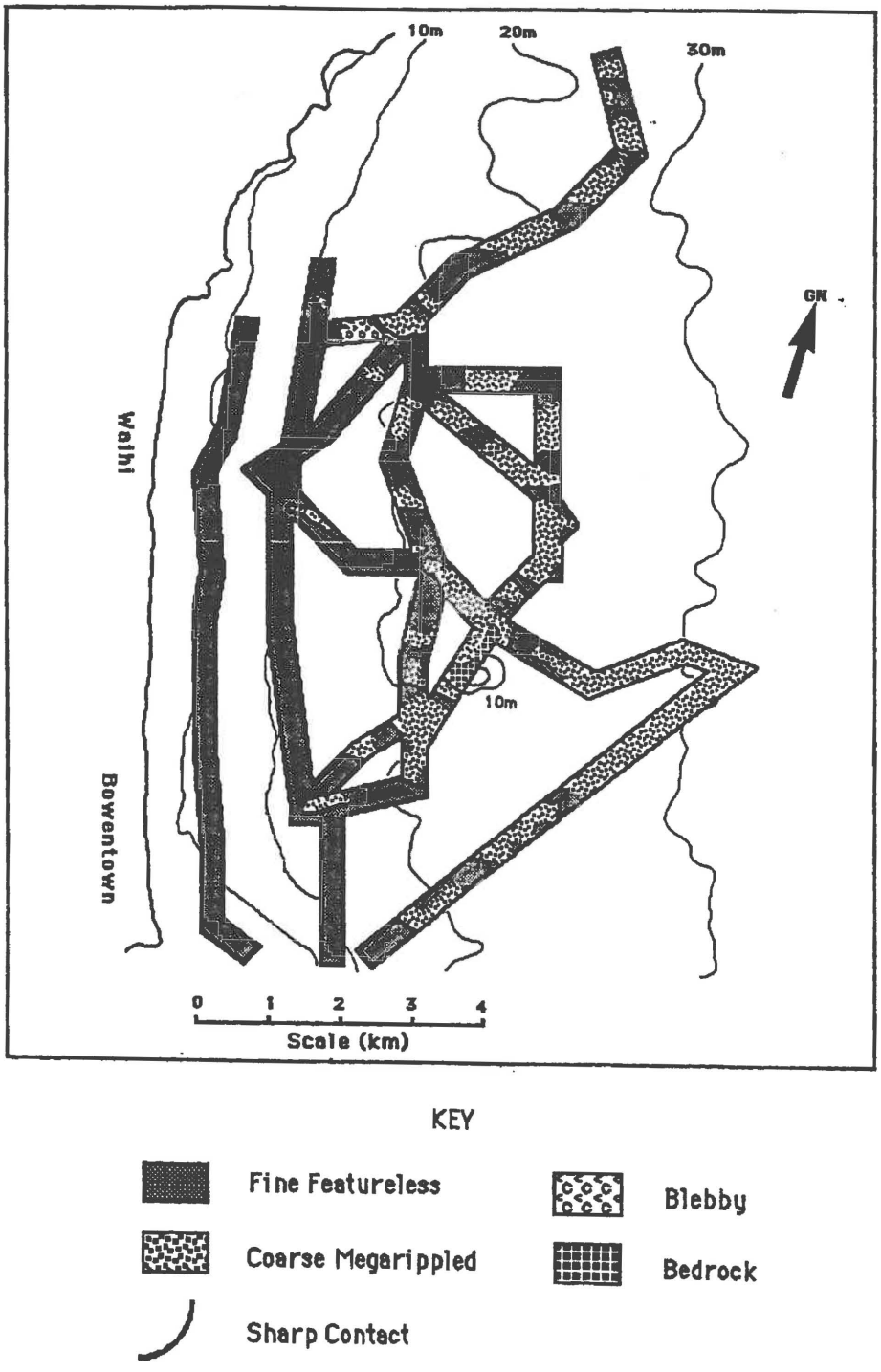

Figure 6.9. Waihi Beach side-scan sonograph map from the Mar-84 survey.

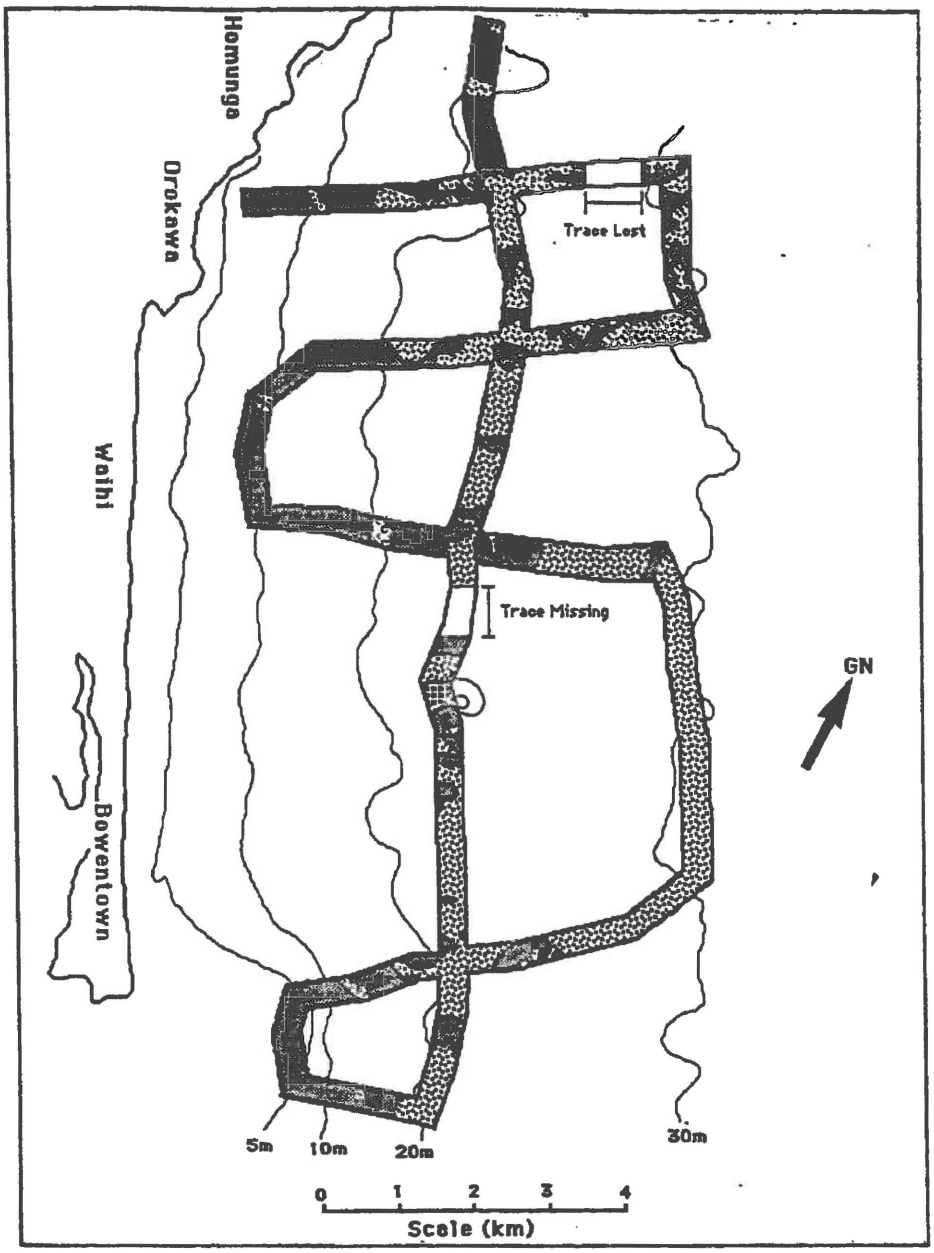

Figure 6.10. Waihi Beach side-scan sonograph map from the Jun-90 survey.

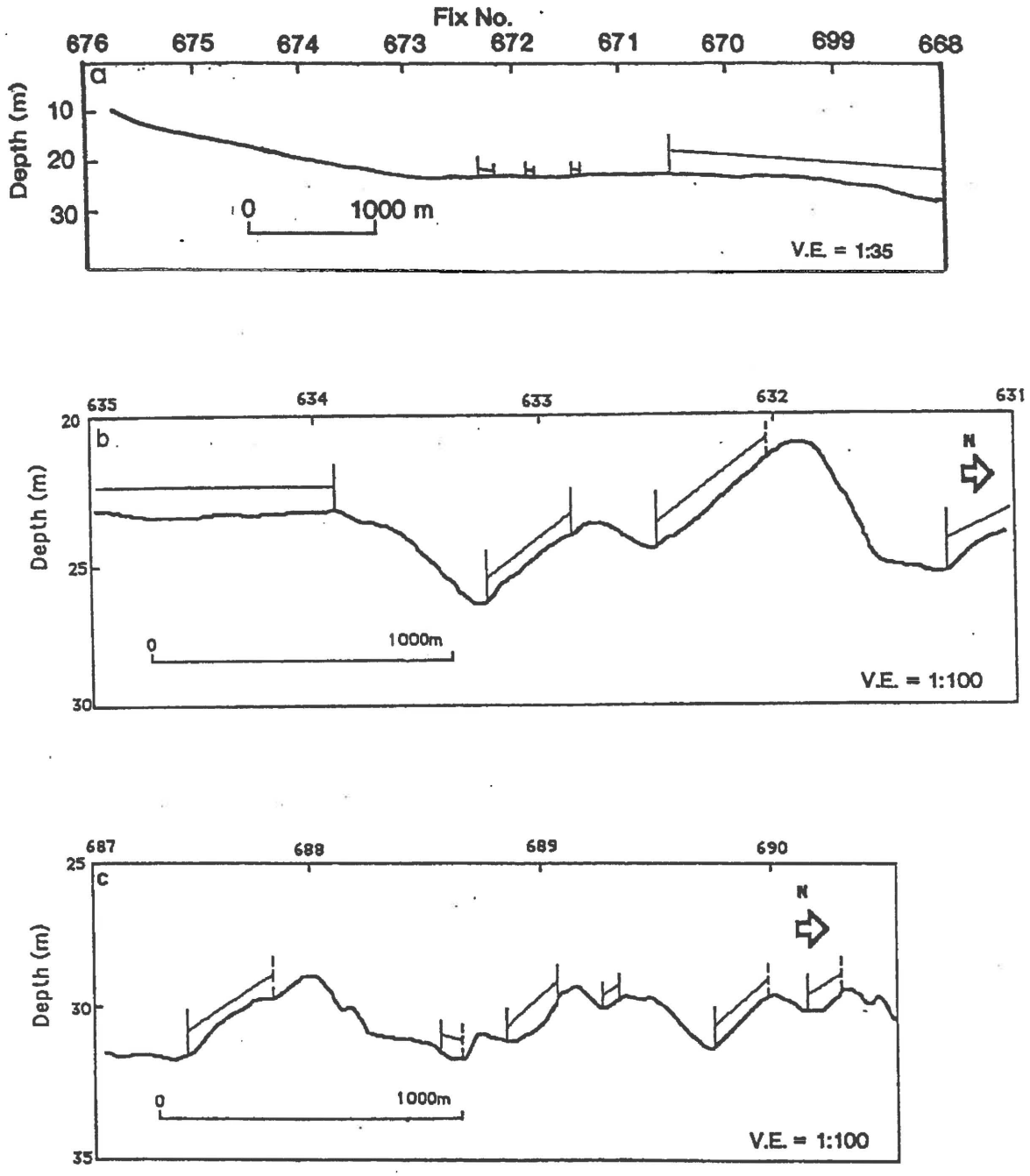

Figure 6.11. Echosounding profiles from Waihi Beach. Bracketed areas indicate coarse megarippled (CMR) sands, with boldened line showing sharp contact, and brokened line indicating gradational contact: a) offshore from mid Waihi Beach (Jun-90); b) sand ridge field from north of Waihi Beach in 20 to 25 m water depth (Jun-90). Note the textural phase lag with CMR sands on the southwestern up-current flanks; c) same sand ridge field as (b) but in 30 m water depth (Jun-90). Note the presence of more irregular features, with small sand ridges superimposed on surface of larger ridges.

'phase lag' in sediment texture over sand ridges (i.e. coarse sands on one flank and fine sediments on the other) has also been observed on the mid-Atlantic shelf in North America by SWIFT and FREELAND (1981), and is indicative of unidirectional current transport over the coarse grained flank. At Waihi Beach, this indicates active sediment transport on the inner shelf from southeast to northwest. Active sediment transport over the southeastern flanks of the sand ridges is further indicated by the occurrence of tongues of Fine Featureless sediments over CMR deposits in sonographs from both surveys. In the first side-scan sonar survey, the tongues of fine sediment were fairly sparse and parallel to the ridge crests, suggesting the presence of small sand waves (Figure 6.12). However in the second survey, tongues of fine sediment were more abundant and tended to change in orientation from transverse to parallel features from the ridge trough to crest (Figure 6.13). This suggests that both sand ribbons (i.e. flow parallel bedforms) and sand waves are present over the southeastern ridge flanks, and that an increase in the deposition of fine sediments over the ridges may have occurred between surveys.

Further offshore (30 to 35 m depth), sand ridges are still present in the northern Waihi shelf area, and are of similar wavelength (λ= 840 to 1000 m), but form lower relief (η= 1.8 to 2.7 m), more irregular, hummocky features (Figure 6.11 c). The hummocky features superimposed on their surfaces appear to be accumulations of fine sediments in small sand ridges (λ= 150 to 270 m, η= 1 to 2 m high), with CMR patches present on their intervening troughs and southern flanks. The higher abundance of fine sediments in sand ridges further offshore, indicates that either an increase in supply of fine sands or a decrease in flow intensities occurs across the inner shelf .

Further south, sand ridges are only present in depths of 20 to 25 m, where they form similar width but smaller amplitude features (η= 1 to 2 m high), and show the same textural phase lag as described for the northern bedforms. This indicates that a northwesterly directed transport of shelf sediments also occurs in the southern shelf region, which is further supported by the occurrence of CMR deposits over the southeastern flanks of a prominent offshore reef (Figure 6.14). However, in depths of 25 to 30 m, sand ridges are absent and CMR deposits occur in extensive fields across a very flat inner shelf surface. This pattern contrasts to that found further north, as here fine sediments decrease in occurrence across the inner shelf. A change in sedimentation conditions therefore occurs both offshore and along-shore on the Waihi Beach inner shelf. This appears to involve the erosion of inner shelf sediments from the south and deposition in large sand ridges further north off Waihi Beach, which may indicate a decrease in current energy from south to north. Sediments may also deposit in these ridges from eroded beach and nearshore sands at the northern end of Waihi Beach. Thus, the higher occurrence of fine sands over the southeastern flanks of ridges following Cyclone Bola in 1988 could be accounted for by erosion of fine sands from either the adjacent inner shelf or nearshore zone during this extreme storm event.

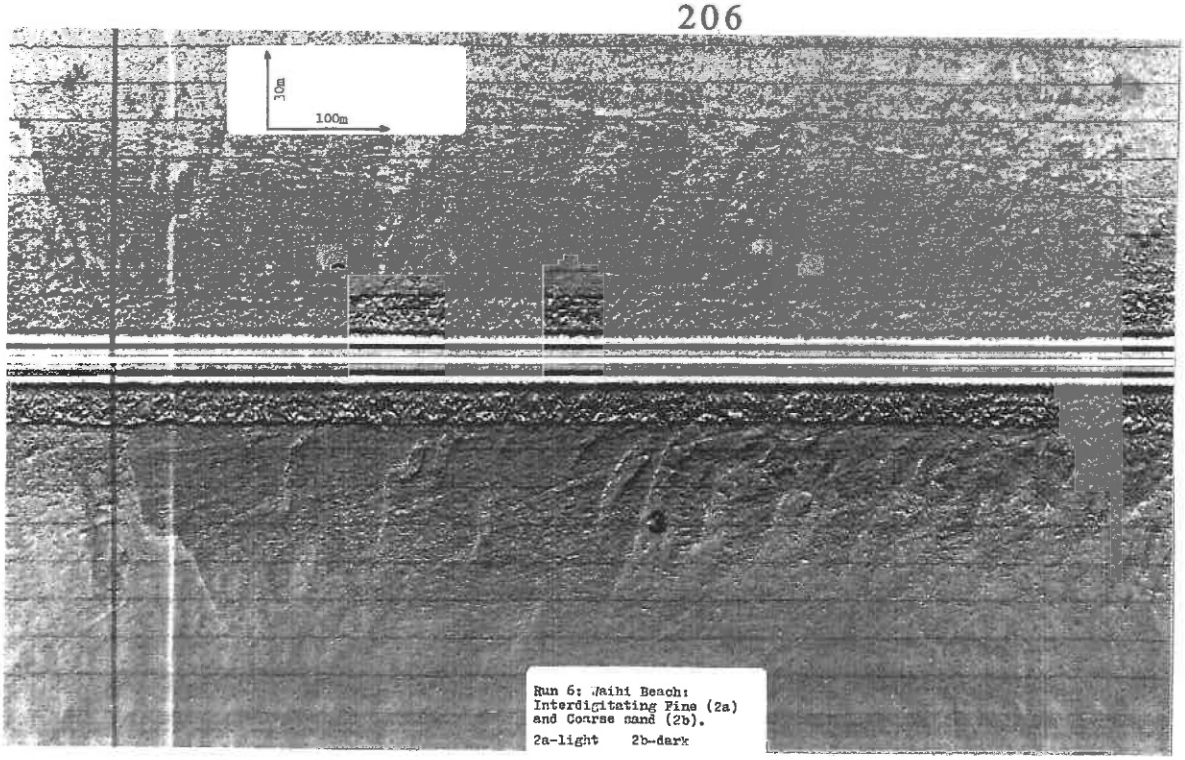

Figure 6.12. Sonograph offshore from Waihi Beach (20 m; Mar-84), showing a sharp change from Fine Featureless sediments in the trough of the sand ridge (1), to CMR sands over the southwestern flank (2), and an increasing occurrence of fine sand waves over the crest (3). This is consistent with the active erosion of fine sands in the sand ridge troughs, and their subsequent transport by wind-generated currents to the northwest.

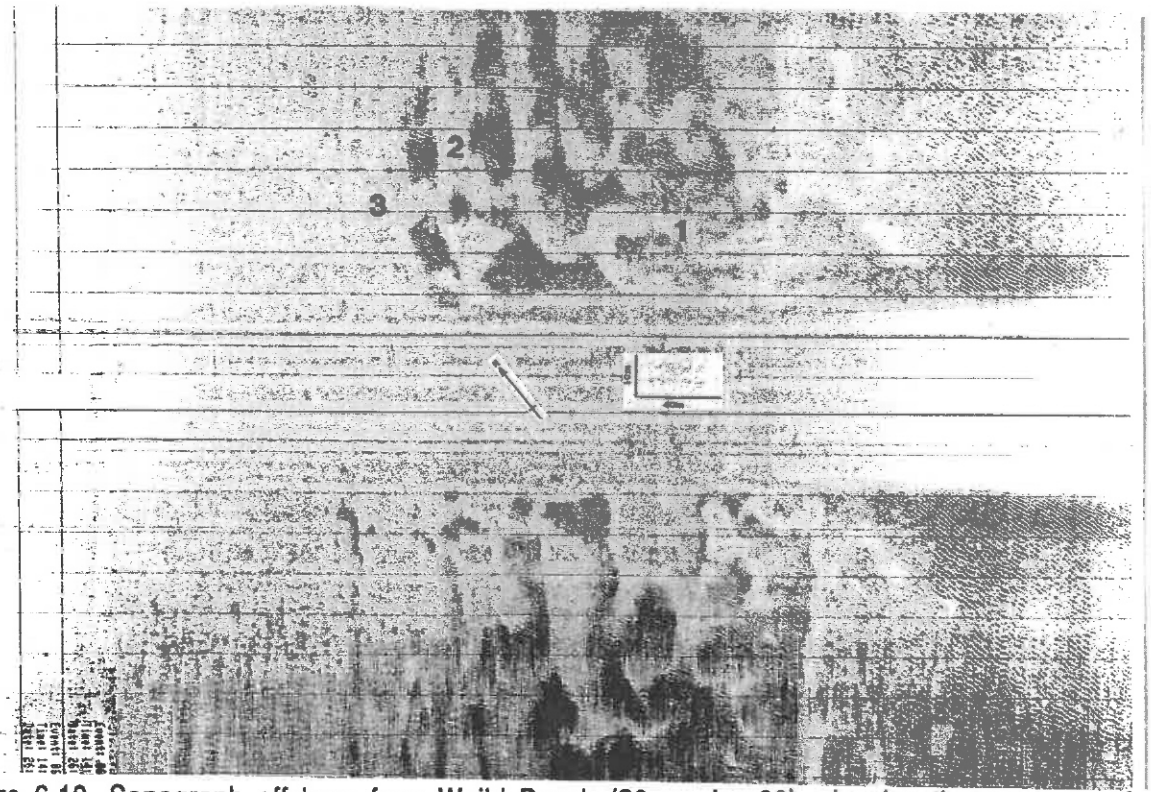

Figure 6.13. Sonograph offshore from Waihi Beach (20 m; Jun-90), showing the presence of extensive fine sand ribbons (1) and sand waves (2) over the ridge flank, and Fine Featureless sediments dominating over their ridge crest (3). The increase in occurrence of fine sediments since Mar-84 (Figure 6.12) may indicate the extensive deposition of eroded nearshore and inner shelf sands following Cyclone Bola.

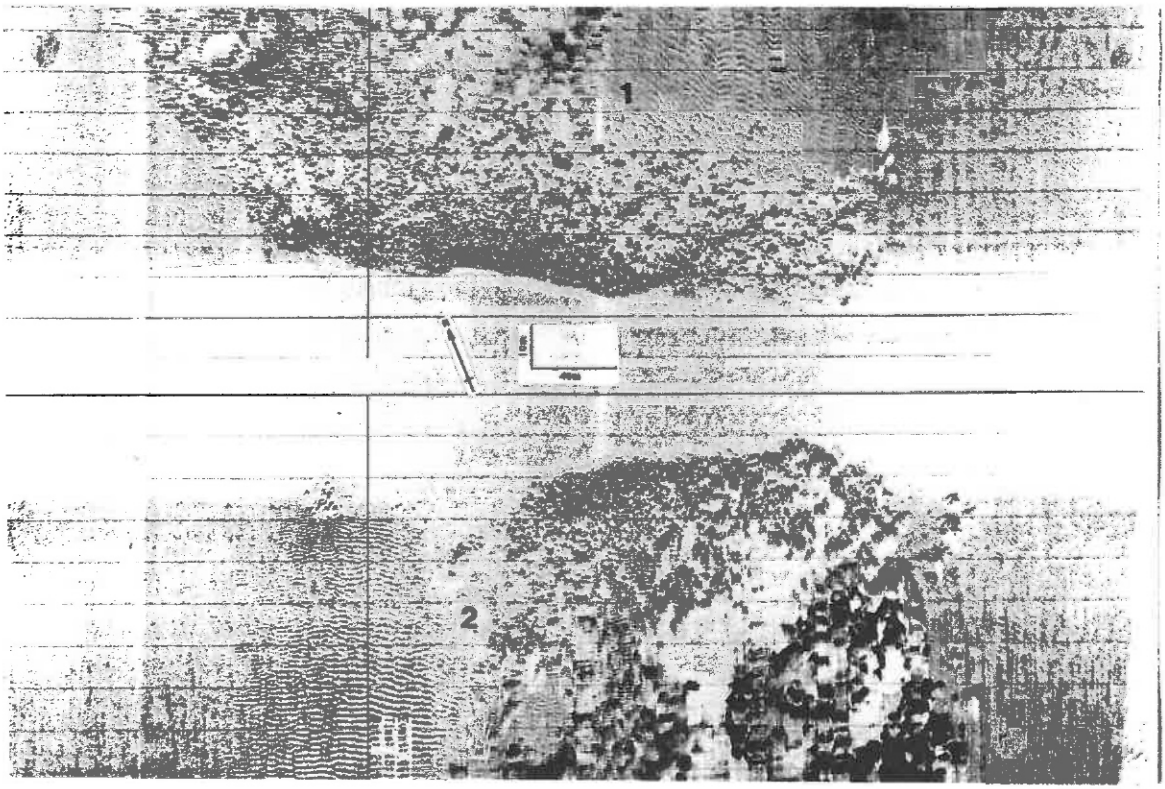

Figure 6.14. Sonograph off Waihi Beach (20 m; Jun-90), with CMR deposits mantling the southeastern flank of a prominent rock pinnacle (1), and occurring at the base of its northwestern side (2). This gives supporting evidence for a northwesterly-directed transport of shelf sediments by wind-generated currents during storms.

Whiritoa-Mataora Beaches

The region offshore from Whiritoa and Mataora Beaches was subject to two side-scan surveys. The first of these occurred on 11- and 19-Mar-84 in which 42 km of sea-bed was scanned, and the second on the 26-Jun-90 in which 38 km was scanned. Results from both surveys are shown in Figures 6.15 and 6.16.

Both side-scan surveys from Whiritoa and Mataora show similar patterns to the textural observations in Chapter 5.3., with fine grained sediments dominating over the shelf surface. Offshore profiles from Mataora and Whiritoa Beaches (Figures 6.17 a and b) show both regions are characterised by an initial steep convex-up profile (gradients 1:100 to 1:125) from depths of 10 to 20 m, with fine surface deposits. This is inferred to be the upper nearshore surface in which very fine grained sands occur (Chapter 5.3.) Further offshore, both the surface morphology and sediment types are variable, but an initial concave-up surface which possibly corresponds to the lower nearshore zone extends to 30 m water depth, where a flatter (1:200) and more convex-up inner shelf surface then continues offshore to 45 to 50 m. However, the lower nearshore and inner shelf surfaces appear to have changed in elevation between surveys off both beaches, with the former tending to be about 1 m lower and the latter several metres higher in the second survey. This may indicate that lower nearshore deposits were eroded and deposited further offshore during Cyclone Bola. However, the evidence supporting this is inconclusive due to the poor overlap of survey lines, particularly across the inner shelf (Figure 6.7).

Small elongate bands of CMR sand (12 to 100 m in width) aligned at a high angle to the coastline were found in both surveys across the nearshore zone. These tend to be concentrated in depths of 10 to 30 m, and generally show sharp southern and gradational northern contacts with Fine Featureless deposits. The bands appear to be associated with the southern flanks of sand ridges, which range in size from η= 1 to 4 m in depths of 10 to 25 m respectively. This indicates that nearshore sediments at Whiritoa and Mataora are probably being transported northwards. However, the length and asymmetry of these ridges could not be determined as profiles were taken at a high angle across their surfaces. Also commonly found on the nearshore surface in sonographs were extensive colonies of horse mussels (*Atrina novaezelandica*), demonstrating this is a biologically productive part of the shelf. An important observation from the sonographs was the occurrence of a relatively large patch of CMR sand off Whiritoa Beach in 20 m water depth during the second survey, in the same area where Fine Featureless deposits were present during the first (Figure 6.16). This patch coincides with the area of decreased nearshore surface elevation in Figure 6.17 b, and thus supports deductions that erosion of lower nearshore deposits occurred during Cyclone Bola.

Across the inner shelf surface, sonograph patterns vary significantly between the two surveys. Off Whiritoa Beach, the first survey showed extensive patches of CMR deposits between 30 and 40 m water depth, which usually coincided with the offshore flanks of relative large hummocky

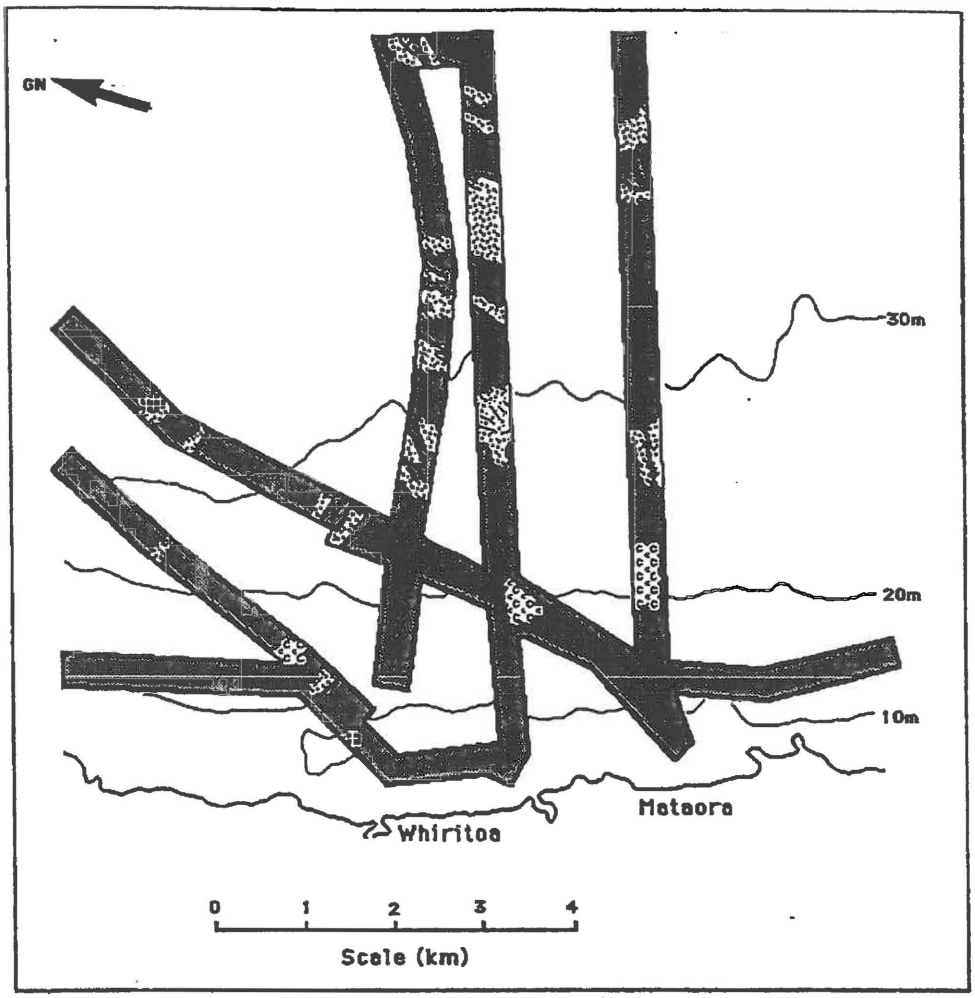

KEY

Fine Featureless

Bedrock

Coarse Megarippled

Blebby

Sharp Contact

Figure 6.15. Whiritoa-Mataora side-scan sonograph map from the Mar-84 survey.

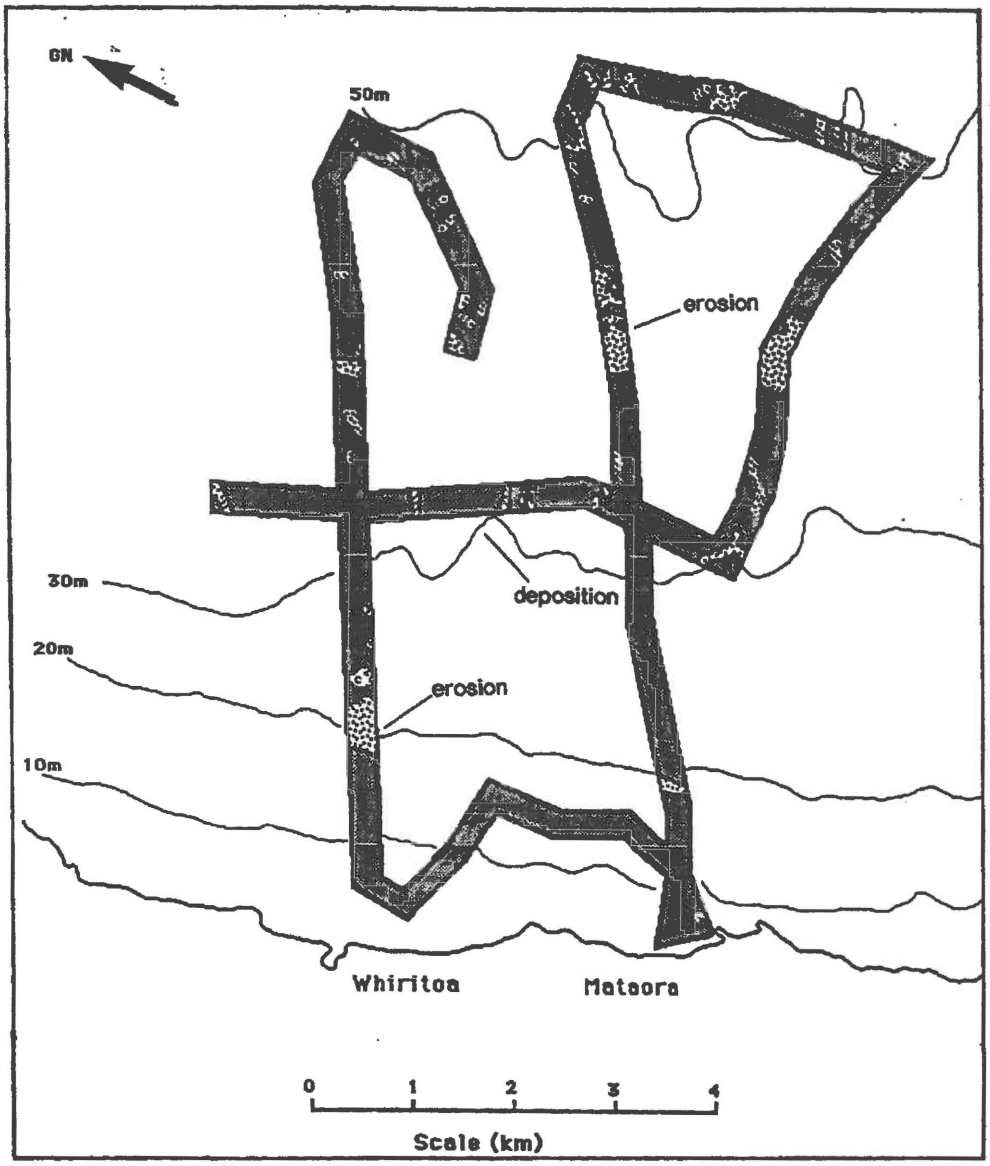

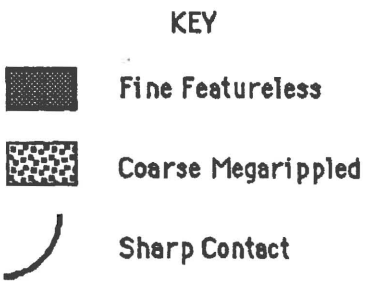

Figure 6.16. Whiritoa-Mataora side-scan sonograph map from the Jun-90 survey. Note the apparent erosion in 20 and 40 m water depth, but increased deposition of fine sediments at 30 m.

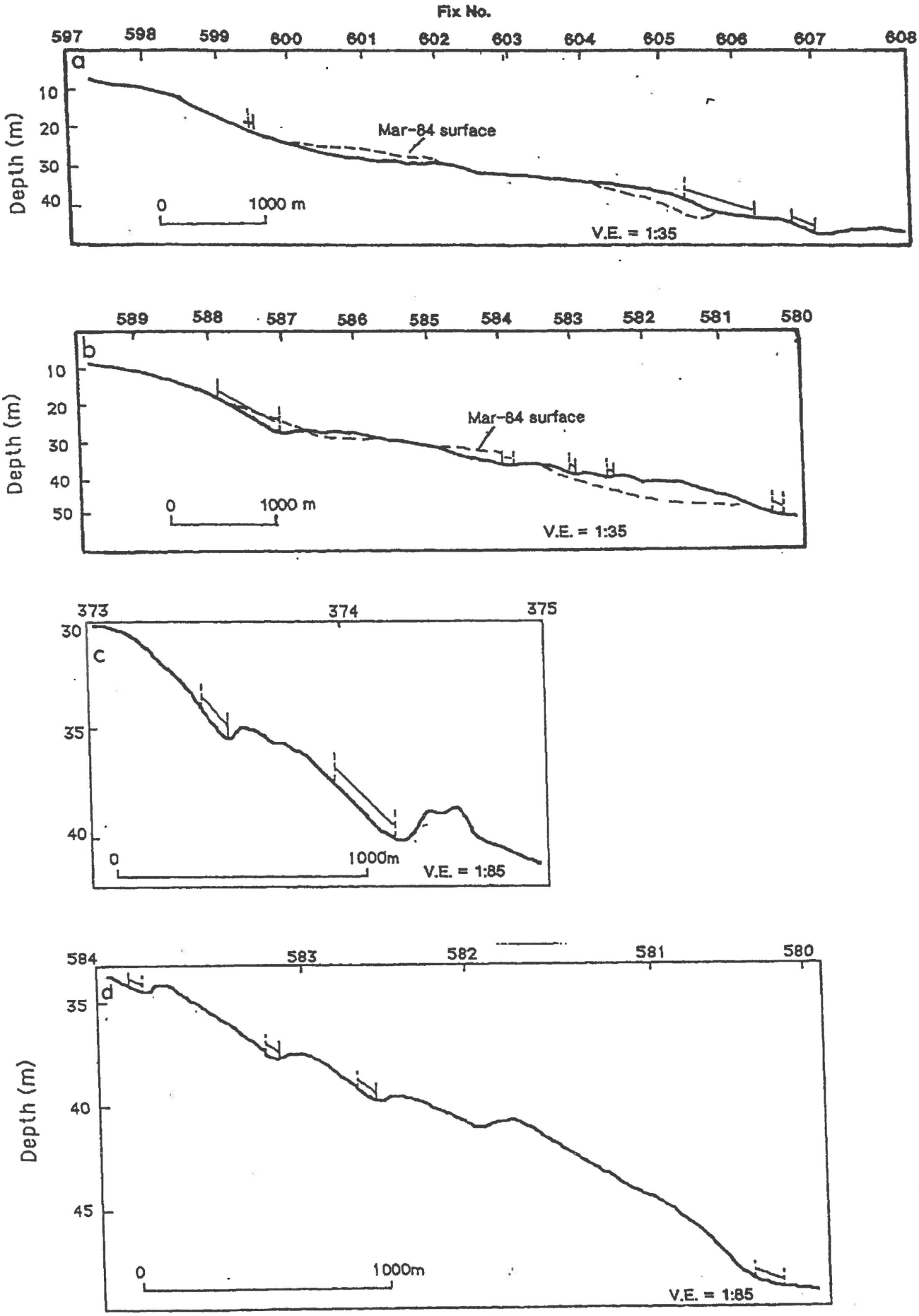
Fix No.
597 598 599 600 601 602 603 604 605 606 607 608
a
Depth (m)
10
20
30
40
Mar-84 surface
0 1000 m
V.E. = 1:35
589 588 587 586 585 584 583 582 581 580
b
Depth (m)
10
20
30
40
50
Mar-84 surface
0 1000 m
V.E. = 1:35
373 374 375
30
c
35
40
0 1000m
V.E. = 1:85
584 583 582 581 580
d
Depth (m)
35
40
45
0 1000m
V.E. = 1:85

Figure 6.17.

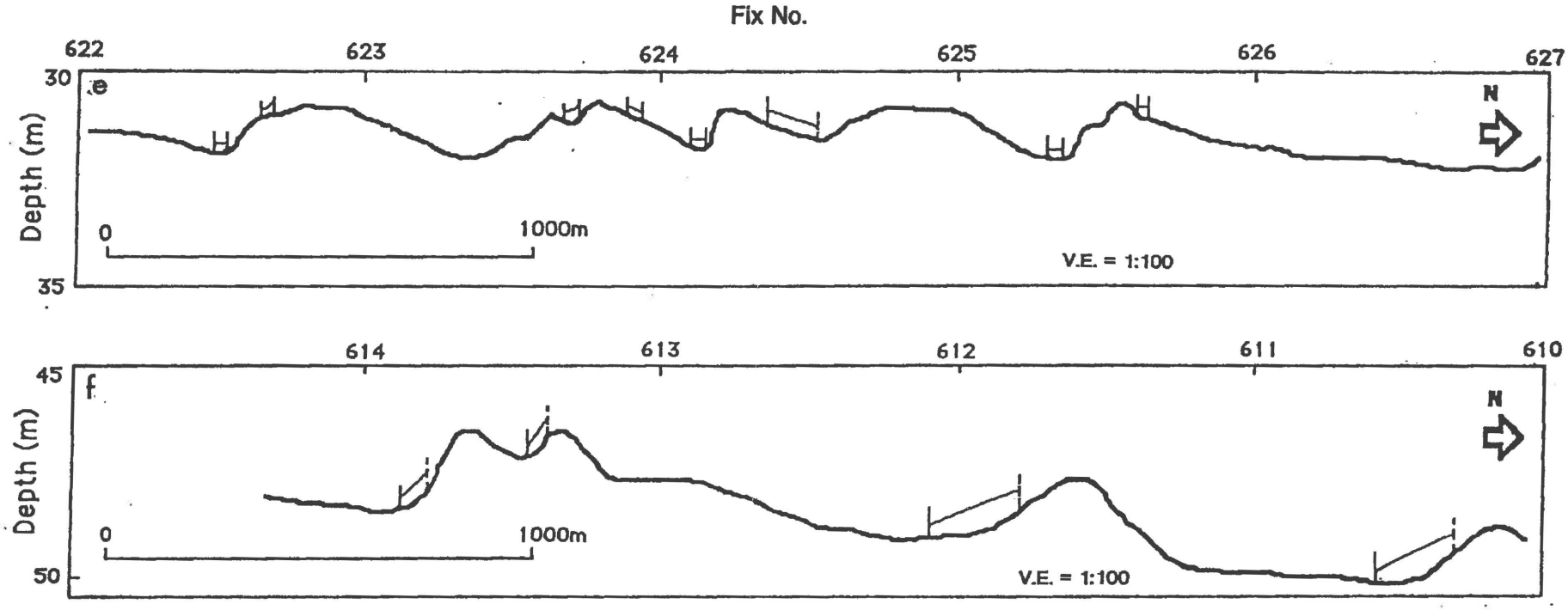

Figure 6.17. Echosounding traces from Mataora and Whiritoa. Bracketed areas indicate CMR sands, with bolded line showing sharp contact, and brokened line indicating gradational contact: a) Offshore from Mataora Beach in Jun-90, and changes since the Mar-84 survey; b) Offshore from Whiritoa Beach in Jun-90, and changes since the Mar-84 survey; c) Pronounced hummocky features found on the inner shelf during Mar-84; d) Lower relief hummocks on inner shelf surface in Jun-90; e) Sand ridges found in shore-parallel traces along the inner shelf. Note the skewness of ridges to the north, and CMR bands on their northern flanks. This is inferred to indicate a southerly-directed transport of sediments by wind-generated currents. f) Sand ridges identified in shore-parallel tracks along the mid shelf surface. Note the presence of CMR bands on their southern flanks, indicating a northerly-directed transport of sediments further offshore.

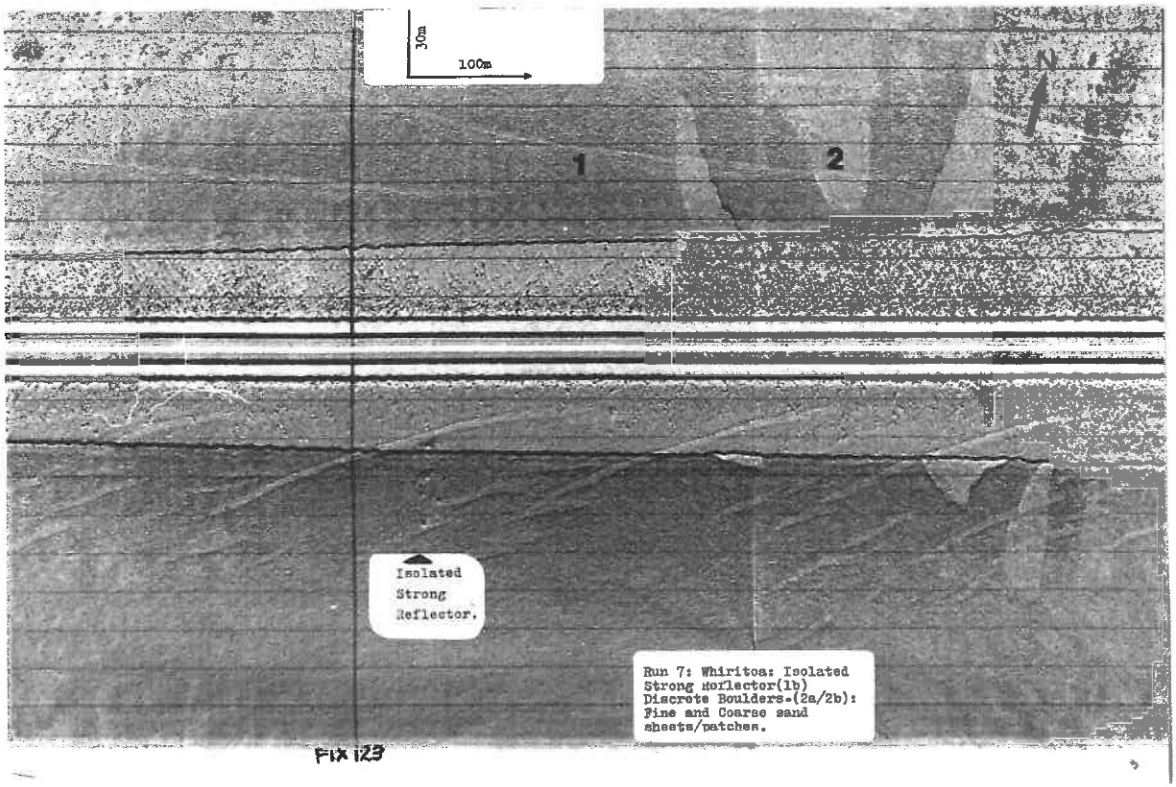

Figure 6.18. Sonograph offshore from Whiritoa Beach (40 m water depth) in Mar-84, showing extensive area of CMR sand (1), and hummocks of fine-featureless sediments (2).

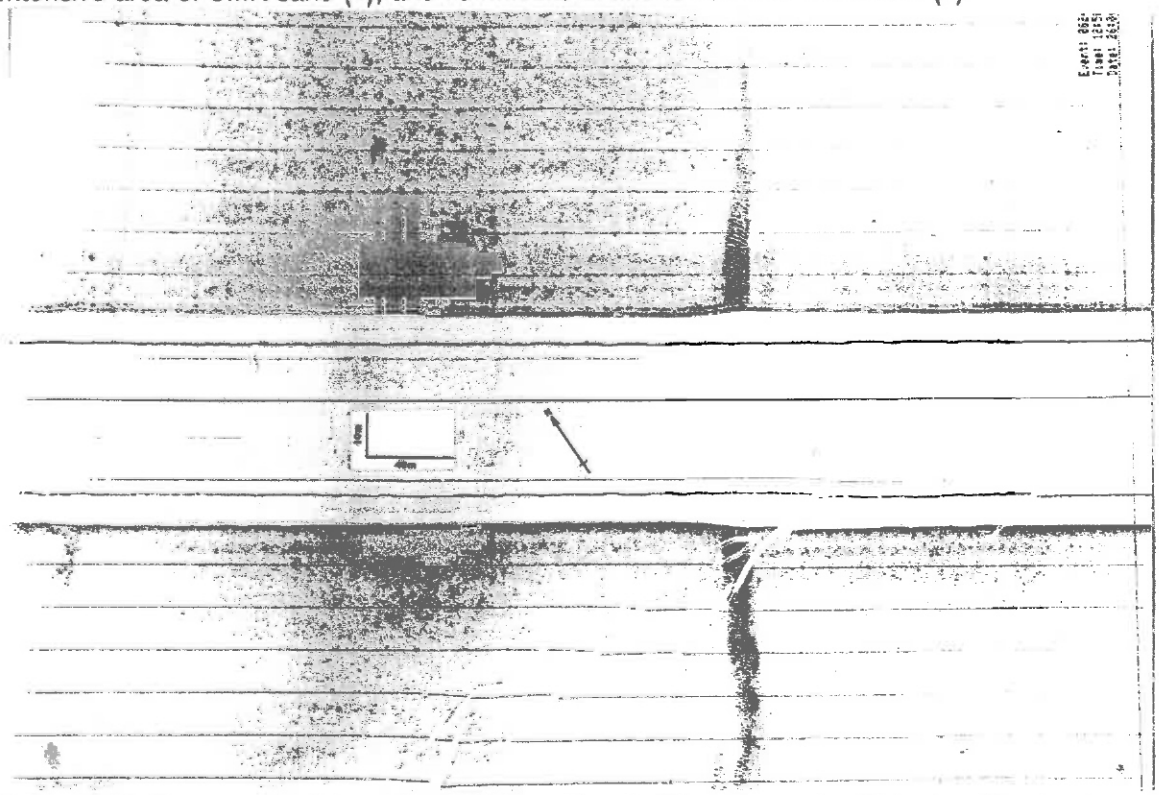

Figure 6.19. Sonograph offshore from Whiritoa Beach (30 m water depth) in Jun-90, showing very narrow, shore-normal oriented CMR band and extensive fine sediments, in an area where more extensive CMR deposits occurred during Mar-84. The CMR band occurs on the northern flank of an inner shelf sand ridge, and is associated with a southerly-directed transport of sediments.

features on the sea-bed (Figures 6.17 c and 6.18). Similar features have been previously identified at Pakiri by HILTON (1990), which he inferred as indicating the onshore transport of fine sands from the lower inner shelf surface. In the second side-scan sonar survey, these feature were still present but tended to be broader and lower in relief (Figure 6.17 d). During the second survey, the previously extensive patches of CMR sand also appear to have been replaced by smaller shore-normal elongate bands of CMR deposits in water depths of 30 m (Figures 6.16, 6.19). This is further evidence that fine sands were eroded from the nearshore zone during Cyclone Bola and deposited on the inner shelf. However, offshore from Mataora Beach in 40 m water depth, CMR deposits appeared to increase in their extent. Thus, erosion of lower inner shelf deposits may have occurred during this extreme storm event.

Shore-parallel profiles across the inner shelf zone during the second survey showed a series of relatively small sand ridges, ranging in size from λ= 270 to 600 m, and η= 1 m (Figure 6.17 e). They are significantly lower in amplitude than the sand ridge observed on the lower nearshore surface (4 m high), which may indicate reduced current flow conditions on the inner shelf. The asymmetry of these features is skewed to the north, which suggests a southward-directed transport of sediments over their surfaces. The narrow elongate CMR bands observed on sonographs (Figure 6.19) tend to occur on the northern flanks and within troughs of sand ridges, which supports a southerly directed transport of sediments. Thus, a reversal in sediment transport direction from that observed off Waihi Beach to the south, appears to occur on the Whiritoa inner shelf. Sand ridges tend to coincide with the hummocky bedforms in shore-normal profiles, and are of similar dimensions, which suggests the hummocks are cross-shelf expressions of the shore-normal oriented sand ridges.

Further offshore on the mid shelf surface (45 to 50 m depth), narrow shore-normal elongate bands of CMR deposits (~ 100 m wide) were observed in both side-scan surveys, and tend to show sharp southern and gradational northern boundaries with Fine Featureless deposits. These CMR bands are found on the southern flanks of sand ridges, which range in size from λ= 1000 to 1250 m, and η= 1.6 to 2 m (Figure 6.17 f). This indicates that mid shelf deposits are mobile off Whiritoa and Mataora, and are presently being transported to the north. It also shows that current flow conditions vary considerably across the nearshore, inner shelf and mid shelf zones in this region, which may be linked to the unusual extensive occurrence of fine grained sands across the inner shelf surface at Whiritoa (see Chapter 5.3.).

Whangamata Beach

The region offshore from Whangamata Beach was the subject of three separate side-scan surveys. The first of these was undertaken on 11-,12- and 18-Mar-84 in which 45 km of sea-bed was scanned; the second on 12- and 13-Mar-85 in which 29 km was scanned; and the third on 25-Jun-90 in which 37 km of sea floor was scanned. Sonograph maps from each survey are illustrated in Figures 6.20, 6.21 and 6.22.

The Whangamata side-scan surveys generally confirm textural patterns identified in Chapter 5.3., as they show fine sands extending offshore to a depth of about 30 m, where an extensive field of CMR sand then dominates to 37 m water depth. Fine sands continue further seawards with some coarse sand also present. These textural patterns tend to coincide with broad morphological features on the offshore profiles from both Otahu and Whangamata Beach (Figures 6.23 a and b), with fine sands initially extending across a relatively steep (1:120) convex- to concave-up nearshore surface, and CMR sands then occurring where the morphology changes to a flatter (1:200) more convex-up inner shelf surface. However, the offshore morphology did show some very noticeable changes between the first and third surveys, with the nearshore surface lowered and the inner shelf surface elevated by ~ 2 to 4 m in the latter survey. This again suggests that Cyclone Bola in 1988 caused extensive erosion of the nearshore surface and deposition of fine sediments over the inner shelf. Evidence from Whangamata is more conclusive however, as the offshore profiles from Whangamata Beach (Figure 6.23 b) were taken along very similar runs between each survey.

Sonographs from the nearshore zone show consistent patterns between each survey, with Fine Featureless sand dominating, and isolated bands of narrow (width 15 to 30 m) CMR deposits found at various locations in depths of 10 to 30 m. These are generally shore-normal features, although some shore-parallel bands are also found, and usually show sharp southern and gradational northern boundaries with fine deposits. One of the most intensively studied CMR bands was off the northern Te Ananui Headland at Whangamata (Figure 6.2). This was examined over a 12 month period in both the first and second side-scan surveys, during which time the band consistently showed the same outline. The CMR band was traced offshore over a series of 5 shore-parallel runs in the second survey, which showed that it extends seawards from 15 to 30 m water depth over a length of 1400 m to the inner shelf boundary. The sea floor morphology associated with this CMR band varied from a flat surface in 15 m water depth, to a sharp 2.5 m rise further offshore, suggesting the presence of a small sand ridge (Figure 6.24). This indicates that the band is probably associated with localised wave or current scouring of the sea floor in 15 m water depth, but is increasingly associated with current transport further offshore. As the band occurs on the southern flank of this ridge and shows a sharp southern contact with fine sand, it is consistent with a northerly-directed transport of nearshore sediments at Whangamata.

In contrast to the nearshore zone, inner shelf deposits at Whangamata show highly variable patterns between surveys. In the first survey, the CMR field was only found off Whangamata Beach in depths of 30 to 37 m, while the area further south off Otahu was dominated by fine sand out to 35 m water depth, with only a series of narrow CMR bands occurring in 30 m (Figure 6.20). In the second survey, the nearshore-inner shelf boundary still occurred at 30 m water depth off Whangamata Beach. However, the CMR field appeared to extend further south, and the offshore contact with fine sediments had migrated ~ 750 m onshore to a depth of 35 m (Figure 6.21). Several moderate scale annual storm events had occurred between the two surveys, and so it is possible

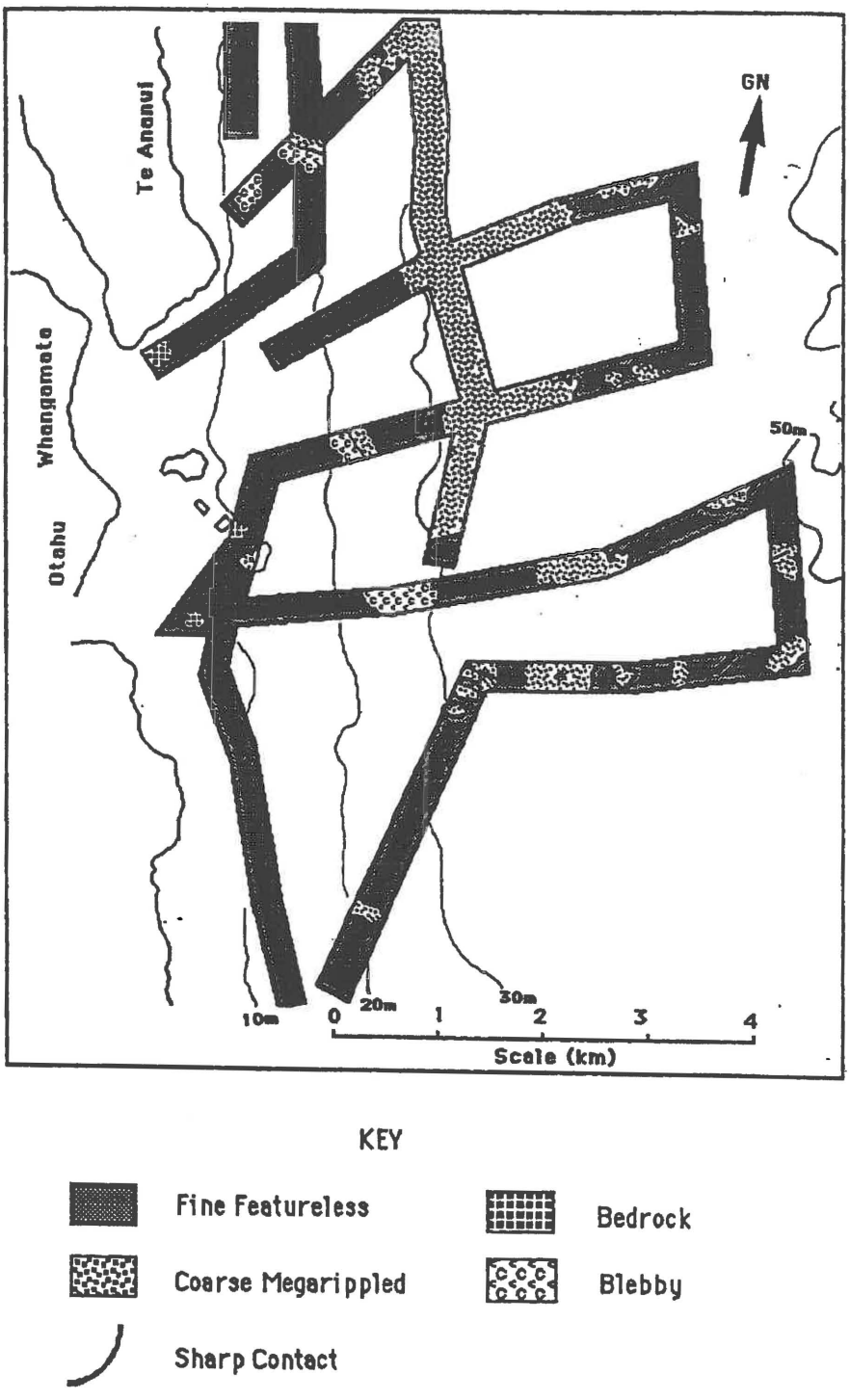

Figure 6.20. Whangamata side-scan sonograph map from the Mar-84 survey.

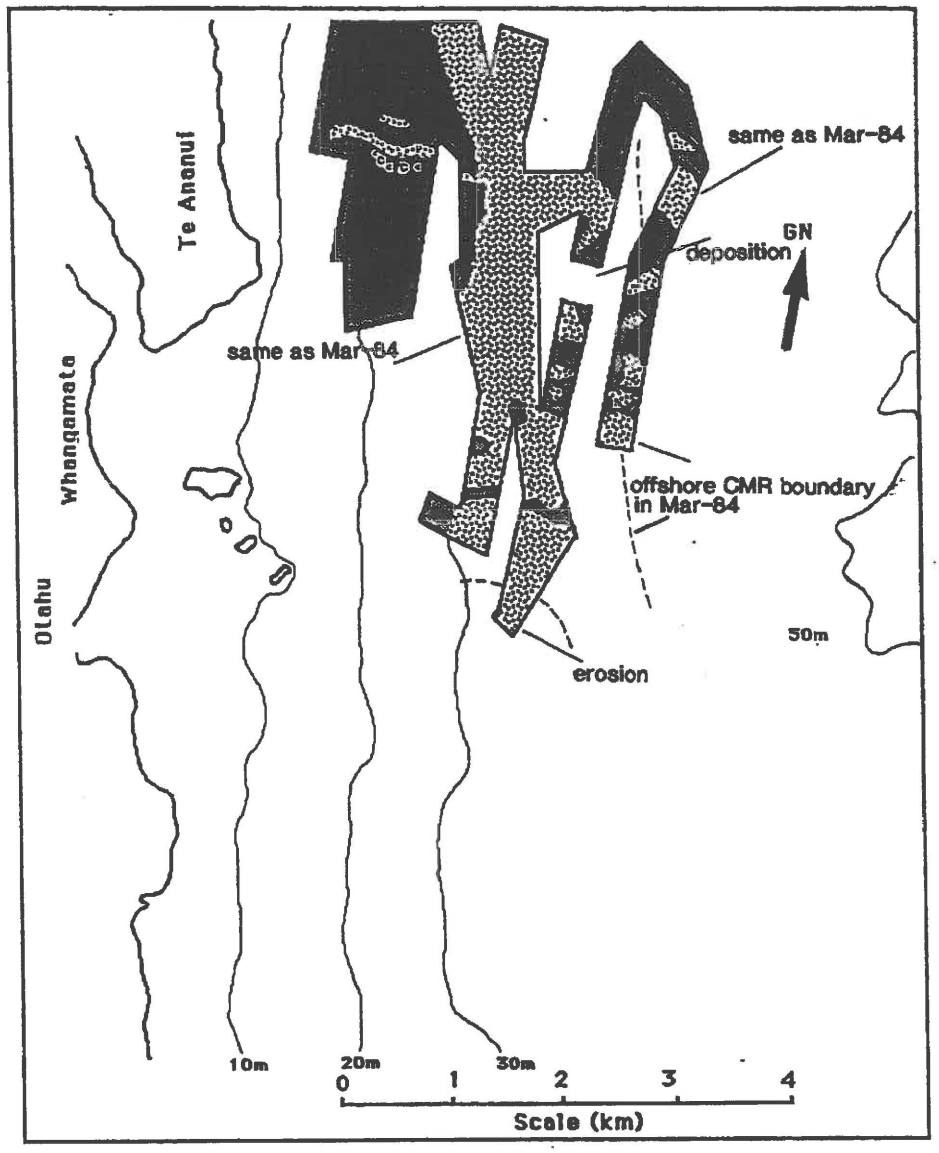

Figure 6.21. Whangamata side-scan sonograph map from the Mar-85 survey.

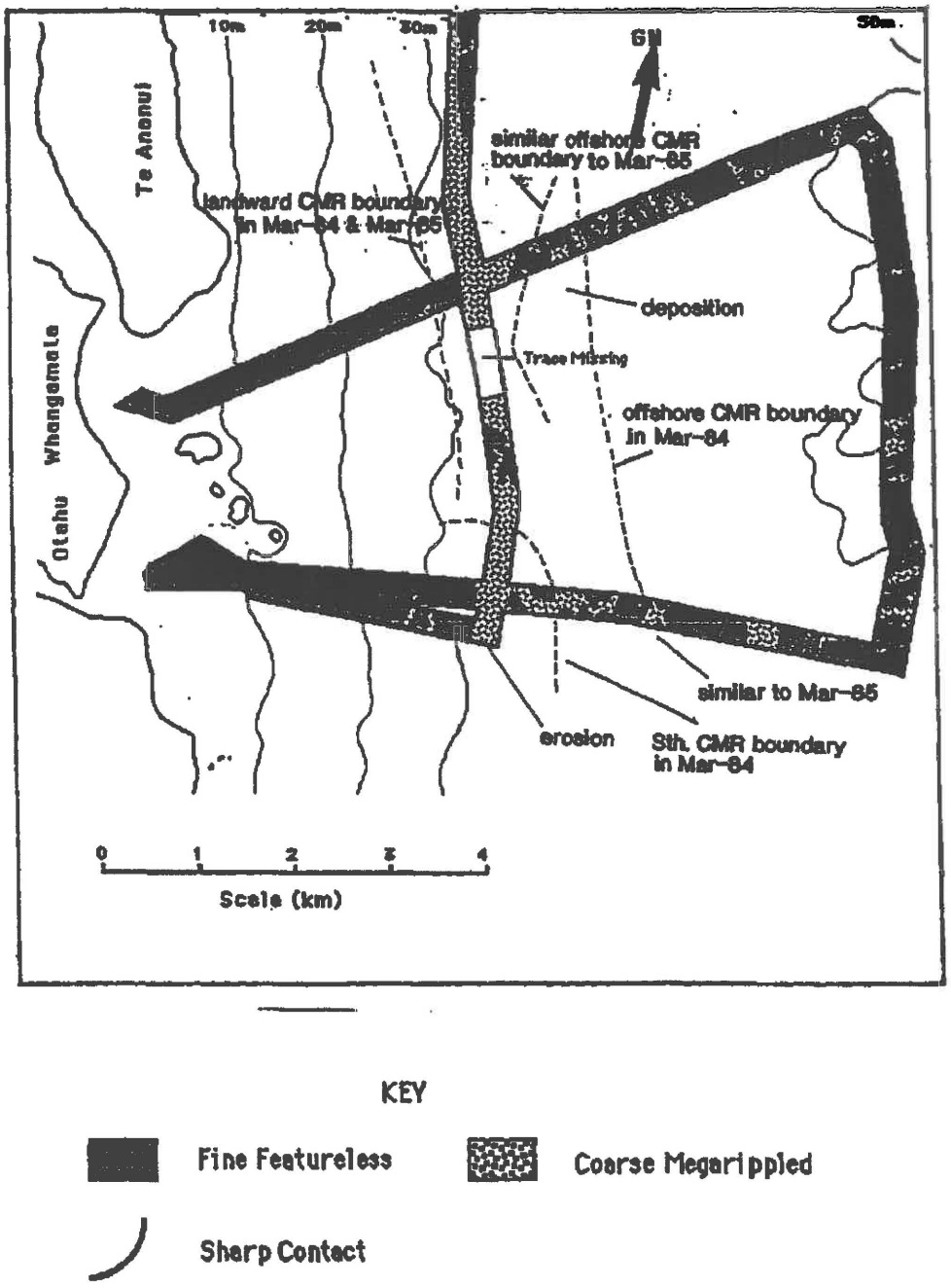

Figure 6.22. Whangamata side-scan sonograph map from the Jun-90 survey.

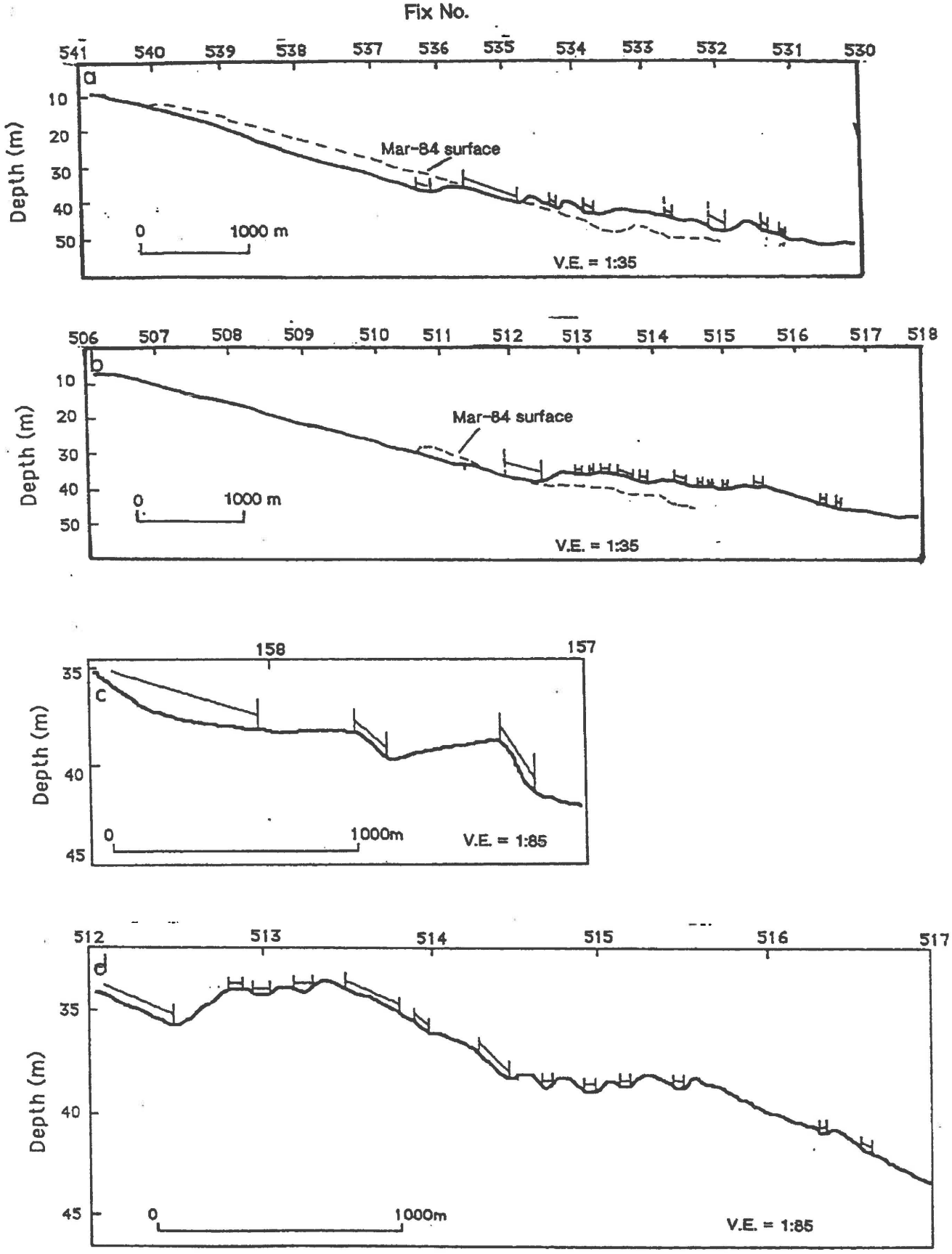
Fix No.
541 540 539 538 537 536 535 534 533 532 531 530
a
Depth (m)
10
20
30
40
50
Mar-84 surface
0
1000 m
V.E. = 1:35
506 507 508 509 510 511 512 513 514 515 516 517 518
b
Depth (m)
10
20
30
40
50
Mar-84 surface
0
1000 m
V.E. = 1:35
158
157
c
Depth (m)
35
40
45
0
1000m
V.E. = 1:85
512 513 514 515 516 517
d
Depth (m)
35
40
45
0
1000m
V.E. = 1:85

Figure 6.23.

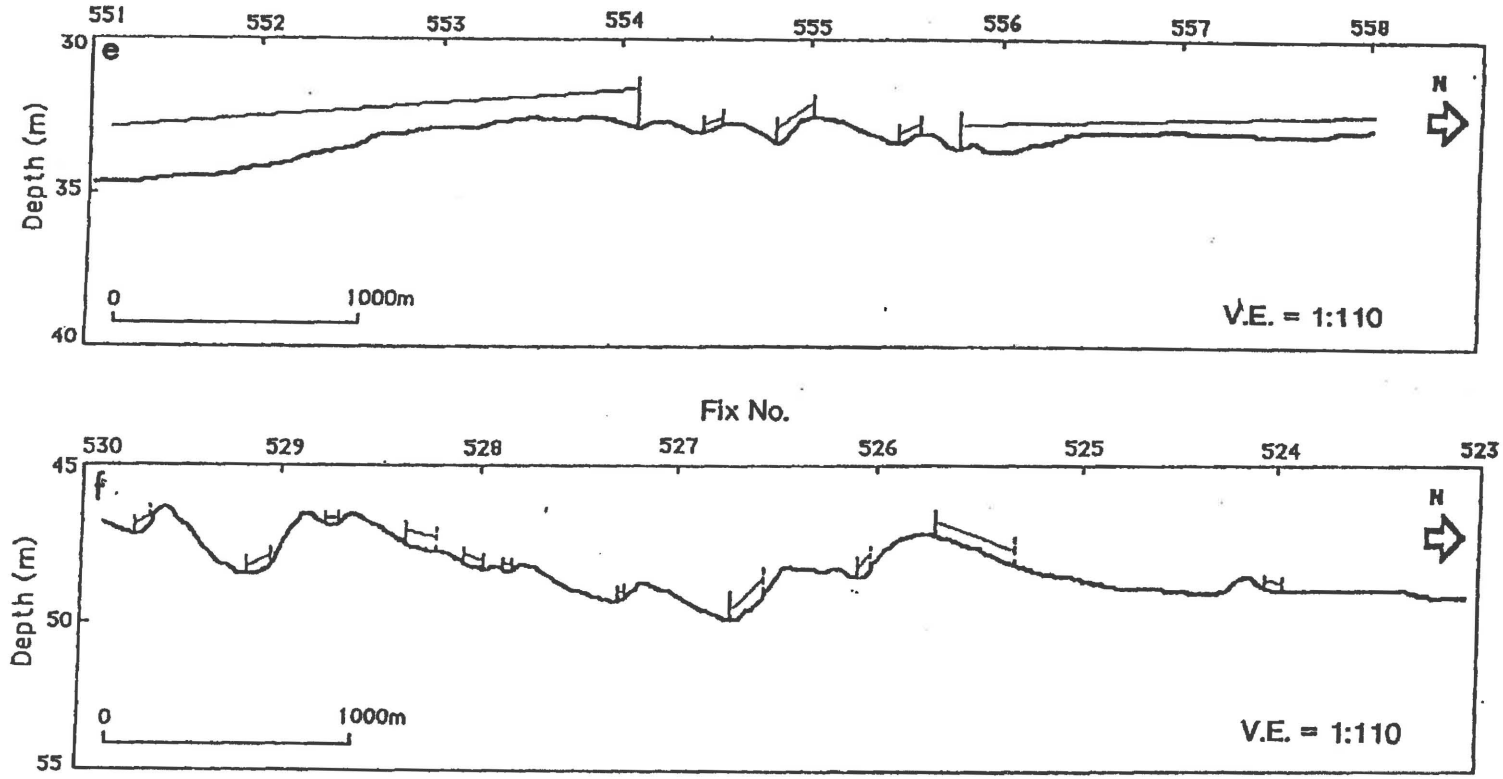

Figure 6.23. Bathymetric surveys from Whangamata. Bracketed areas indicate CMR sands, with bolded line showing sharp contact, and brokened line indicating gradational contact: a) Offshore from Otahu Beach in Jun-90, also showing the original Mar-84 surface. Note lowering of the nearshore and increased elevation of inner shelf surface. b) Offshore from Whangamata Beach in Jun-90, also showing the original Mar-84 surface. Note the prominent lobe of fine sand at the base of the nearshore zone in Mar-84, which appears to have been eroded and reworked offshore onto the inner shelf surface in Jun-90. c) Hummocky features found on inner shelf surface off Whangamata Beach in Mar-84. d) Same shelf area as (c) in Jun-90, showing both large and small hummocks now present, as inner shelf surface has aggraded through deposition of fine sands. e) Shore-parallel transect across the inner shelf surface in Jun-90, showing a mainly relatively flat sea-bed, with small sand ridges. The presence of CMR bands on the southern flanks of the ridges appears to indicate a northerly-directed transport for inner shelf sediments at Whangamata. f) Shore-parallel transect on the mid shelf surface, showing sand ridges skewed to the north, indicating a possible southerly-directed transport of mid shelf sediments.

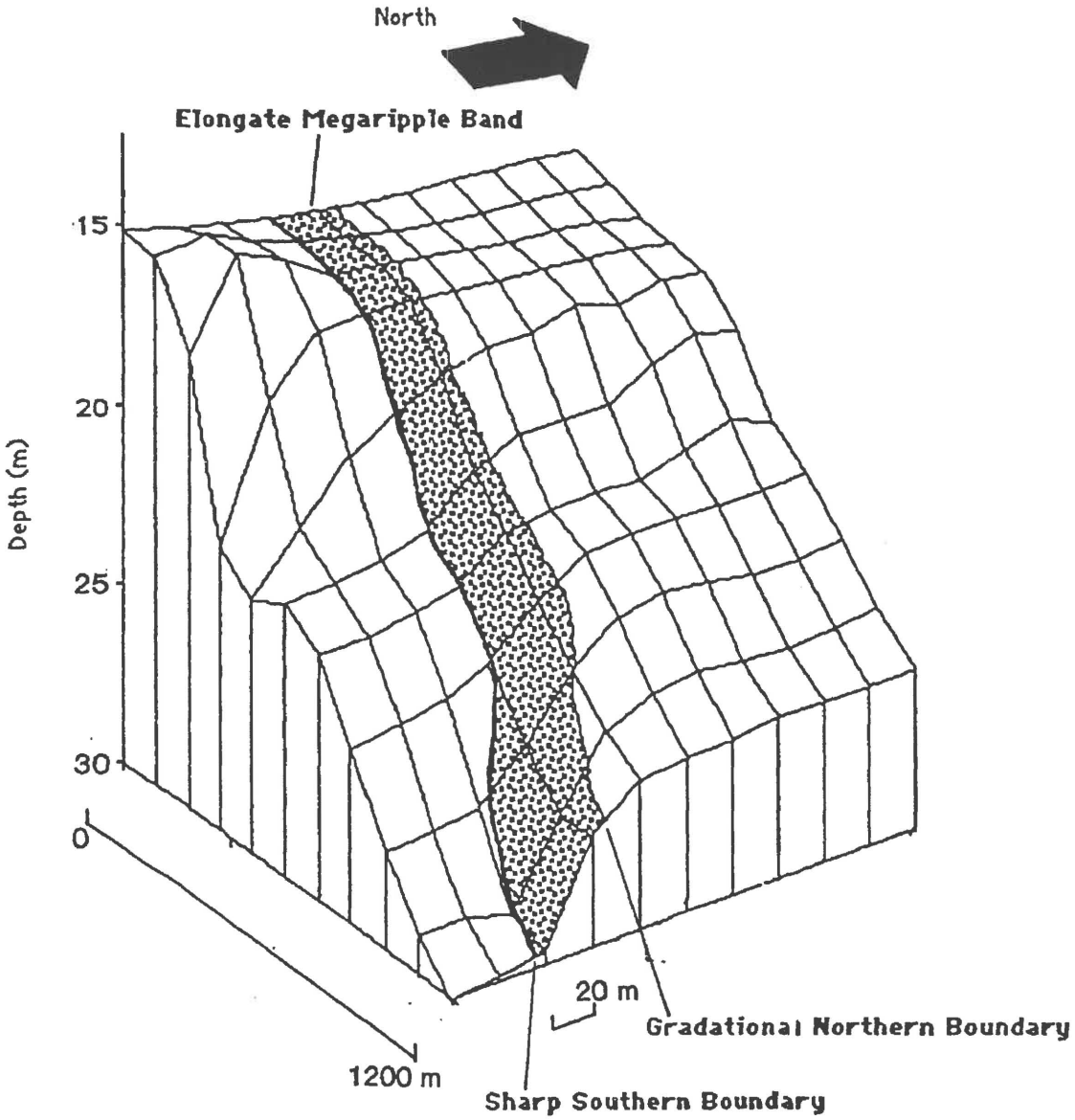

Figure 6.24. Three-dimensional image of the nearshore surface where a CMR band occurs off the northern Te Ananui Headland at Whangamata (based on echosounding traces from Mar-85 survey). This shows the band occurs on a flat surface in 15 m water depth, but further offshore is associated with a sharp rise in the sea-bed, inferred to represent the southern flank of a small sand ridge.

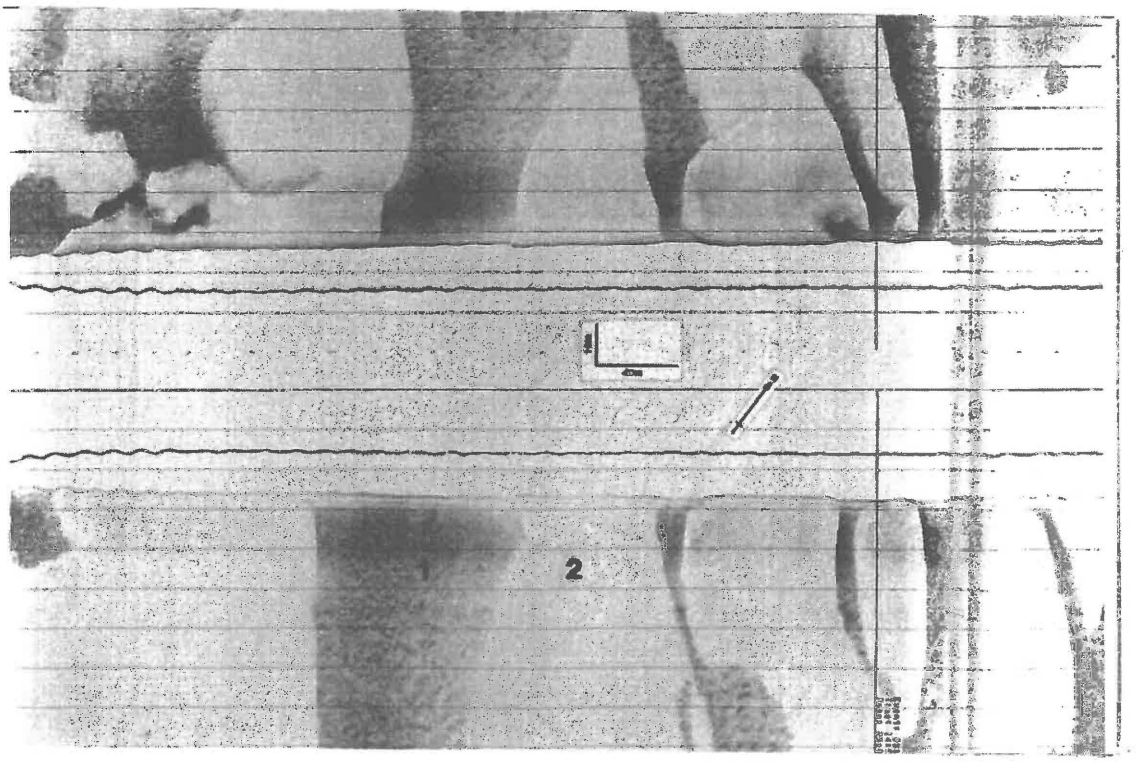

Figure 6.25. Sonograph from Whangamata in Jun-90 (37 m water depth), showing shore-parallel bands of CMR sand (1) and hummocks of fine sand (2) in an area where an extensive CMR field had been in the Mar-84 survey.

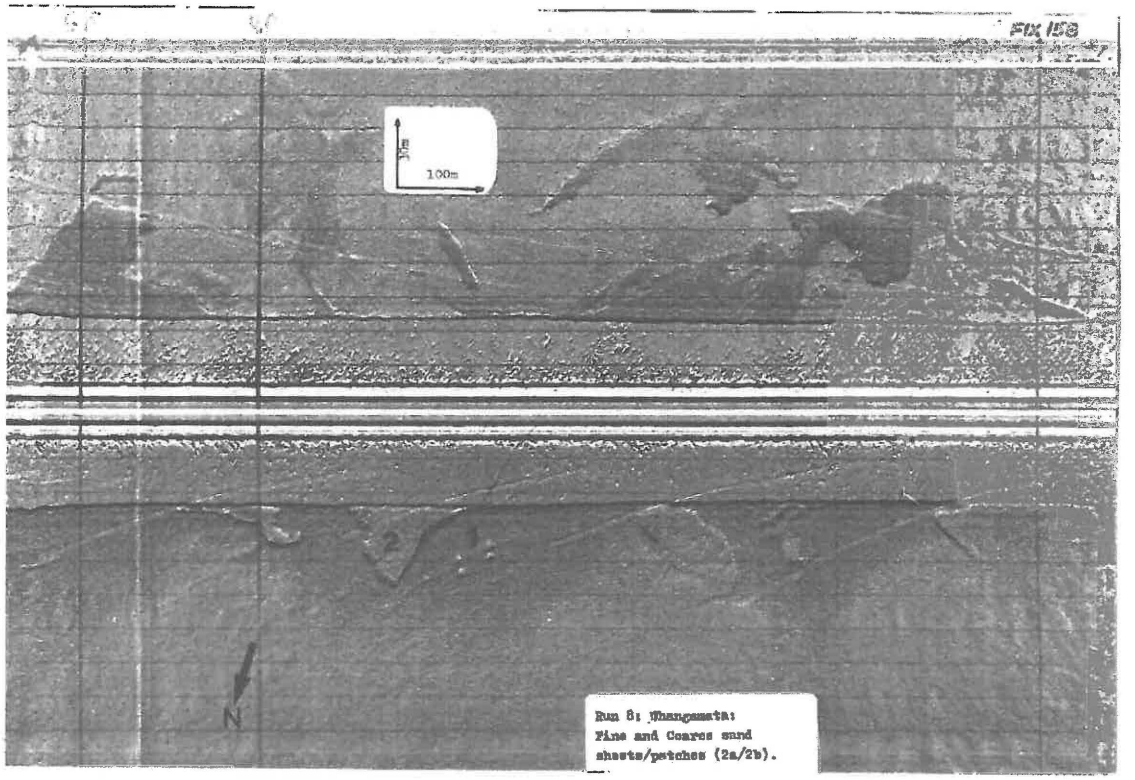

Figure 6.26. Sonograph from the base of the inner shelf zone (40 m water depth) at Whangamata in Mar-84, showing patches of CMR sand (1) associated with hummocks of fine sand (2).

that fine sediments were eroded from the southern boundary of the CMR field, and deposited further north on its seaward margin. In the third side-scan sonar survey following Cyclone Bola, the inner shelf pattern was in complete contrast to the first survey, with the field commencing ~ 250 m further offshore in 32 m water depth, and only continuing to 35 m depth, where a series of narrow shore-parallel oriented CMR bands then occur over a dominantly Fine Featureless sea-bed (Figures 6.22 and 6.25). Offshore from Otahu, the inner shelf shows a similar pattern to Whangamata in the third survey. However, the CMR field extended at least 1500 m further south since the original 1984 survey. Thus, shelf erosion during both annual storms and Cyclone Bola appear to be most extensive on the southern nearshore and inner shelf region off Otahu, and deposition most concentrated on the inner shelf off Whangamata Beach. This trend is supported by observations from offshore profiles in Figures 6.23 a and b.

Hummocky bedforms are also present on the inner shelf surface at Whangamata and Otahu, which show the consistent occurrence of CMR bands on their steep offshore flanks (Figures 6.23 c,d and 6.26). These features again coincide with the presence of small sand ridges on the inner shelf surface, which at Whangamata range in size from λ= 250 to 500 m; and η= 0.5 to 1.0 m. The sand ridges appear to be associated with a northerly-directed transport of sediments, as shown by the presence of CMR bands on their southern flanks (Figure 6.23 e). However, over most of the inner shelf a relatively flat and featureless CMR surface dominates.

Further offshore on the mid shelf surface (45 to 50 m depth), Fine Featureless sediments dominate sonograph records, with patches of CMR sand also quite common. These CMR patches are associated with sand ridges on the mid shelf, which range in size from λ= 500 to 1500 m, and η= 0.5 to 1.0 m (Figure 6.23 f). The asymmetry of these features appears to be skewed northwards, indicating a likely southward-directed transport of fine sand. However, where CMR patches are found, they occur both on the northern and southern flanks of these ridges, and tend to show sharp southern and gradational northern boundaries. Thus both north- and southward-directed transport may occur under different flow conditions in this mid shelf region, although the present net movement appears to be to the south.

Onemana Beach

The region offshore from Onemana Beach was the subject of three separate side-scan surveys. The first of these was undertaken on 11-,12- and 18-Mar-84 with 31 km of sea floor scanned; the second from 12- to 13-Mar-85 with 30 km scanned; and the third survey on 25-Jun-90 in which 13 km of sea floor was scanned. Maps showing sonograph patterns from each survey are presented in Figures 6.27, 6.28 and 6.29.

Side-scan surveys of the Onemana offshore region show a more complex pattern than the sediment texture results in Chapter 5.3., due to the greater area of sea floor examined by sonographs. Fine sediments dominate out to depths of 22 to 27 m across a steeply dipping (1:110)

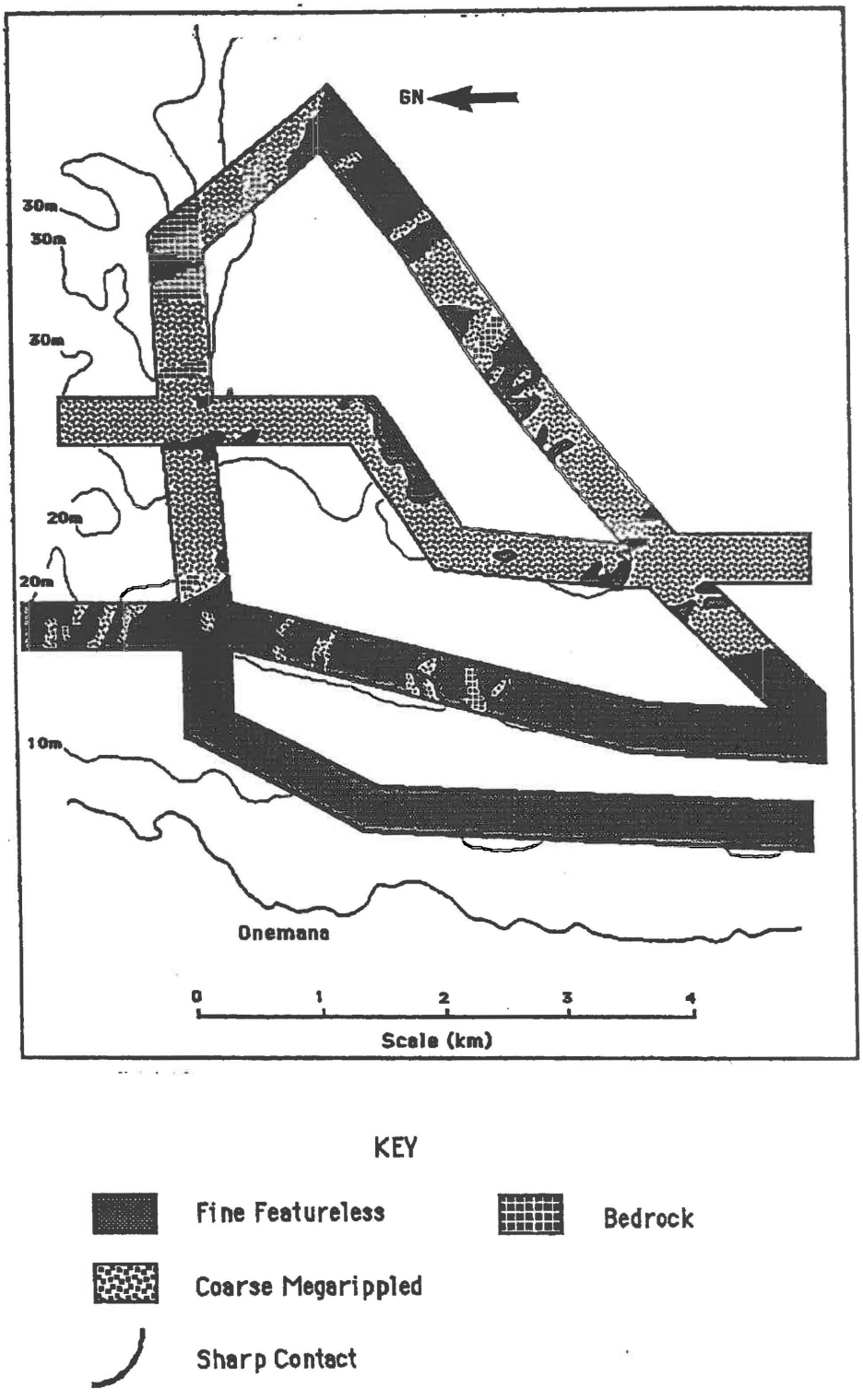

Figure 6.27. Onemana side-scan sonograph map from the Mar-84 survey.

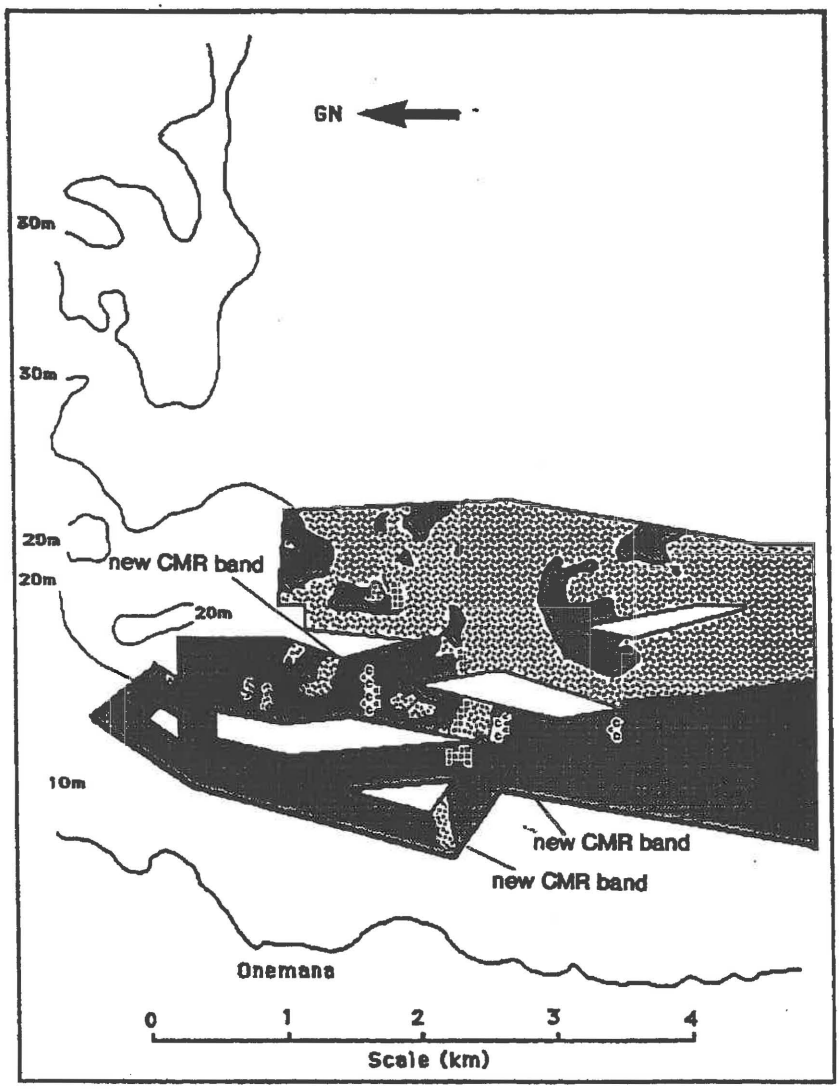

KEY

Fine Featureless

Bedrock

Coarse Megarippled

Blebby

Sharp Contact

Figure 6.28. Onemana side-scan sonograph map from the Mar-85 survey. Note evidence of some nearshore erosion with several new CMR bands present compared to Figure 6.27.

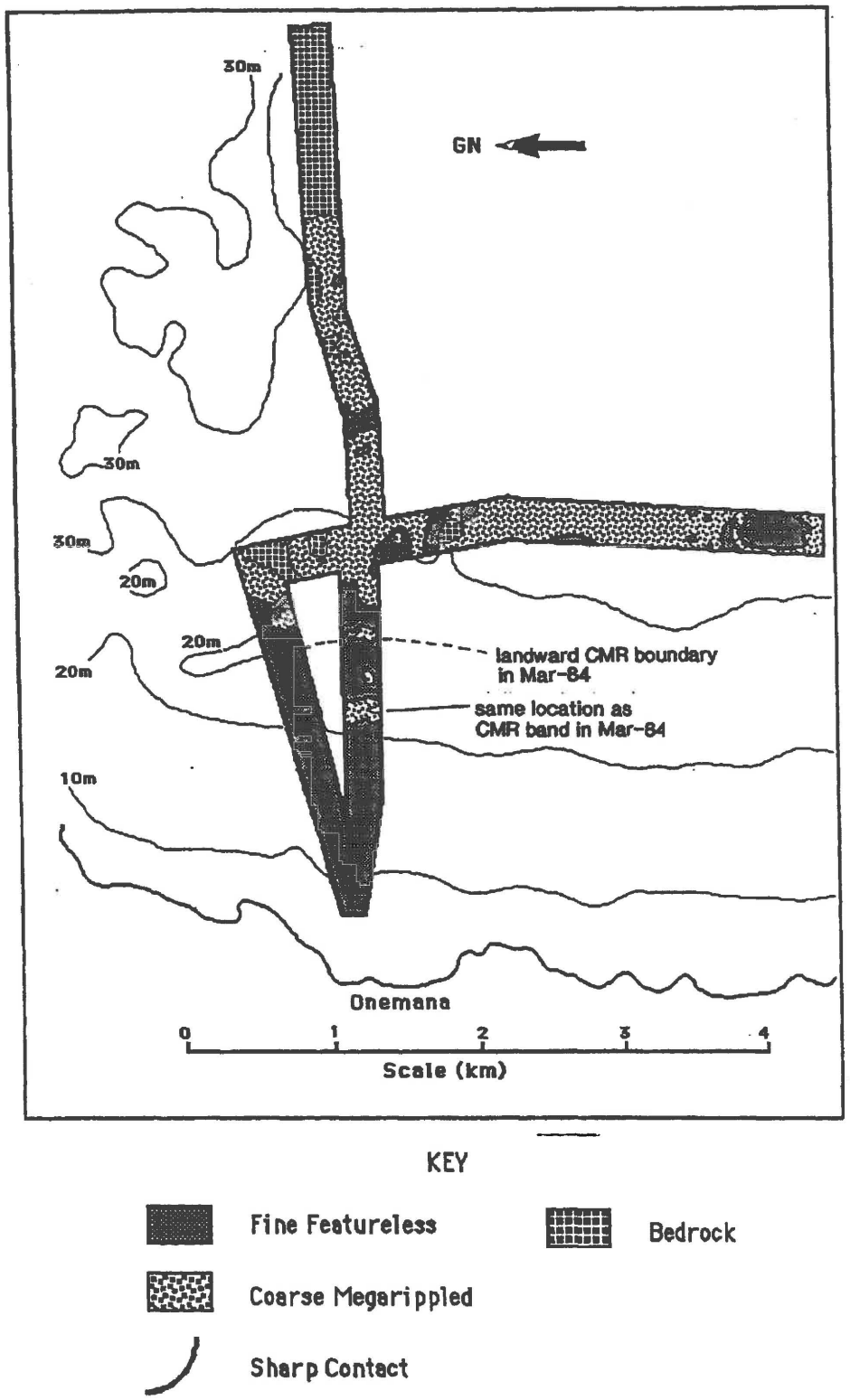

Figure 6.29. Onemana side-scan sonograph map from the Jun-90 survey. Note the seaward extension of nearshore-inner shelf boundary compared to Figure 6.28, indicating deposition of fine sands over the inner shelf surface.

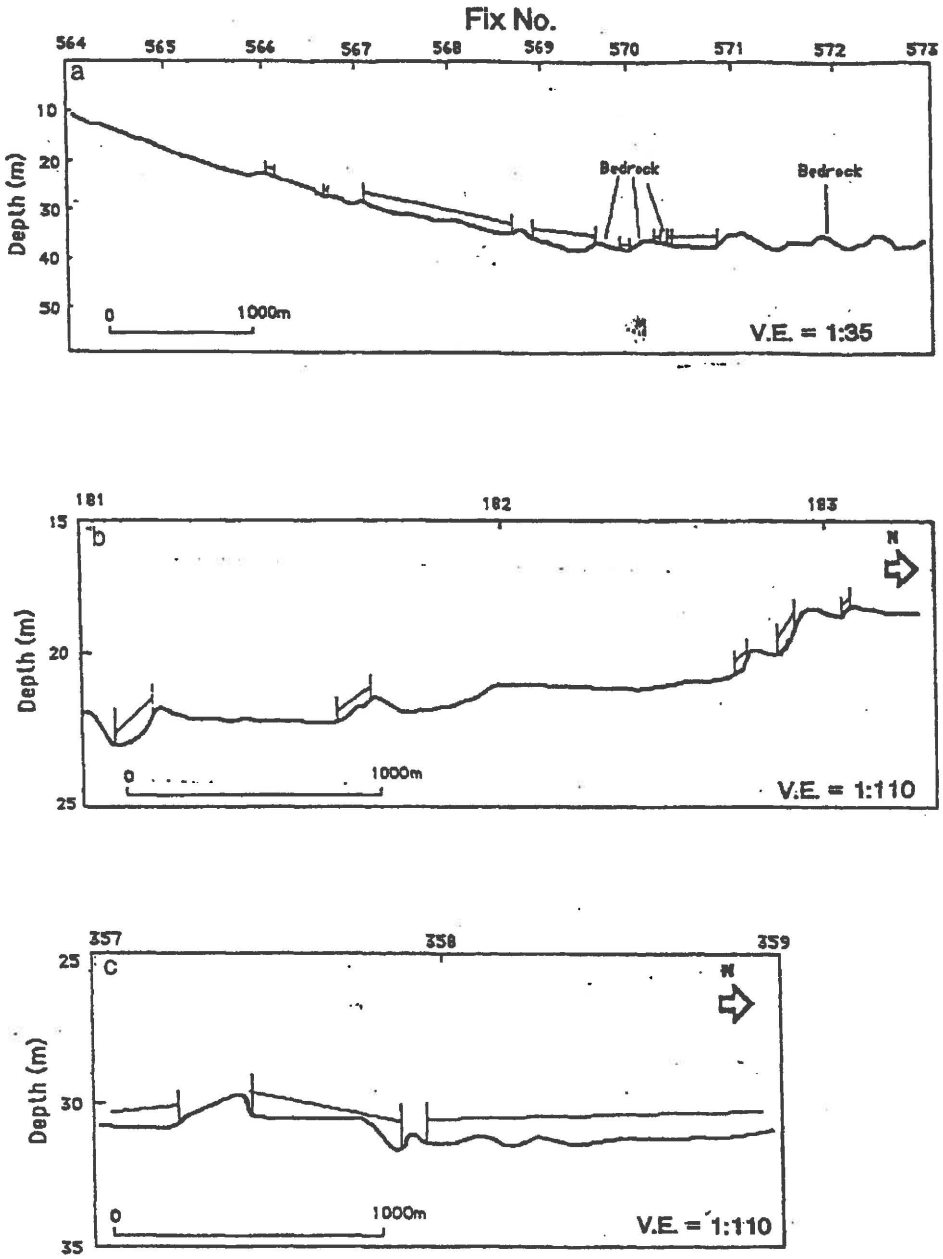

Figure 6.30. Bathymetric survey off Onemana Beach. Bracketed areas indicate CMR sands, with bolded line showing sharp contact, and brokened line indicating gradational contact: a) Offshore profile from Onemana Beach in Jun-90; b) Shore-parallel track across the nearshore surface, showing CMR bands occurring on the southern flanks of small sand ridges. This indicates a northerly transport of nearshore sediments at Onemana; c) Shore parallel transect across the inner shelf, showing a relatively flat sea-bed in areas of CMR sands, and small ridges of fine sediments.

concave-up nearshore surface. CMR deposits then continue out to depths of 42 m across a much flatter (1:350), but very irregular inner shelf surface caused by the presence of numerous rock pinnacles (Figure 6.30 a).

Although the nearshore zone is dominated by fine sediments, elongate bands of CMR sands are a very common feature, particularly in 20 to 25 m water depth. These bands show very similar characteristics to those described from other regions, in that they are narrow (width 40 to 100 m), shore-normal oriented features, which often have a sharp southern and gradational northern contact with Fine Featureless deposits. Also in common with other regions, the bands occur on the southern flanks of small sand ridges (λ= 245 m, η= 1.0 to 1.5 m; Figure 6.30 b), which indicates that they are associated with a northerly-directed transport of sediments by currents. This is supported by the long-term current meter observations at Onemana (see Chapter 4.3.) which were taken from just south of a CMR band, and showed a strong northerly wind-generated current present during storms, sufficiently fast to erode and transport fine sands. Repeated side-scan surveys of the CMR bands between Mar-84 and Mar-85 show that most of the bands occurred in the same locations but tended to change their configurations (Figure 6.28), although some did retain their original shape between surveys. In a few instances, new CMR bands were also evident between surveys (Figure 6.28). Thus, the CMR bands appear to be dynamic features associated with localised erosion of the lower nearshore surface during annual storm events.

Across the Onemana inner shelf, the CMR field described to the south at Whangamata continues into this region. However, Fine Featureless deposits occur here in large patches rather than as narrow elongate bands. The fine sand patches occur as either small ridges (η= 1 m, λ= 300 m; Figure 6.30 c) or in slight depressions of the sea floor. The general absence of sand ridges on the inner shelf may indicate a decrease in intensity of sediment transport along the CMR field from Whangamata to Onemana. The CMR field continues out to 42 m water depth, where fine sand and bedrock then become more dominant, the latter possibly indicating only a thin veneer of sediment occurs on the Onemana inner shelf. Boundaries between adjacent fine and coarse sands are usually quite sharp in all directions on the inner shelf. However, CMR sands were observed in sonographs to mantle the southern face of a large offshore reef (Figure 6.27), which shows that a northward transport of inner shelf sediments continues to occur along the CMR field.

Surveys of the nearshore-inner shelf boundary at Onemana indicate some definite changes occurring following Cyclone Bola in 1988, with this boundary found ~ 350 m further offshore in the Jun-90 survey (Figure 6.29). This is consistent with the trends of nearshore erosion and inner shelf deposition of fine sands recorded at Whangamata and Whiritoa. However, as offshore profiles from Onemana Beach did not overlap between each survey, it can not be conclusively shown that the nearshore surface was eroded here.

Opoutere Beach

The area offshore from Opoutere Beach was the subject of only one side-scan survey on the 12- and 18-Mar-84, in which 31 km of sea-bed was scanned (Figure 6.31). This survey showed similar offshore and along-shore variations in textural patterns as was found in surface sediment samples. Off the southern end of Opoutere Beach, fine sands extend to depths of 25 m across a very steeply dipping convex-up nearshore surface (1:70), where CMR sands then occur over a flatter (1:170) convex-up inner shelf surface to 35 m water depth (Figure 6.32 a). Elongate, shore-normal bands of CMR deposits occur extensively in depths as shallow as 10 m over the nearshore surface off the southern end of Opoutere (Figure 6.33). These bands are very similar in appearance to those described from Onemana, and are likewise associated with the southern flanks of small (η= 1 m high) ridges on the sea-bed, thus indicating a northerly transport of nearshore sediments off Opoutere. The large patch of CMR sands which occurs further offshore on the inner shelf extends ~ 1 km along the coast, and is possibly part of the CMR field identified at Whangamata and Onemana to the south. Further north, these deposits begin to break up into smaller elongate shore-normal CMR bands, which are associated with small hummocks of fine sand (λ= 150 m, η= 1 m high) on the inner shelf surface (Figure 6.32 b). Fine Featureless sands then dominate both the nearshore and inner shelf surface offshore from northern Opoutere Beach, with scattered occurrences of boulders also a significant feature on the sea floor (Figure 6.4).

These variations in the textural nature of nearshore and inner shelf deposits off Opoutere Beach seem to indicate higher energy conditions and thus erosion occurring to the south, and lower energy conditions and deposition to the north. Such variations in hydrodynamic conditions may result from Slipper Island shadowing the northern area from northeasterly storm waves, and focussing wave energy through refraction around the island onto the southern Opoutere shelf area.

On the shelf surface between Slipper Island and the mainland just north of Opoutere Beach, CMR deposits are a dominant feature in depths of 10 to 20 m, with only occasional small patches of Fine Featureless sand and rock outcrops. The CMR deposits often occur on the southwestern faces of large 'ridge like' features (λ= 700 m, η= 3.5 m; Figure 6.32 c), but it is uncertain whether these represent true sand ridges or CMR sands piled up against rock reefs. However, they do indicate that sediment transport occurs to the northeast behind Slipper Island. The extensive occurrence of CMR deposits may thus be due to currents being confined and therefore accelerated through this shallow shelf region. Alternatively, it may result from the refraction and focussing of northeasterly storm waves around the northern tip of Slipper Island.

Pauanui-Tairua Beaches

The area offshore from Pauanui and Tairua Beaches was examined in one side-scan survey on the 12-, 13-, 17- and 18-Mar-84, in which 37 km of sea floor was scanned (Figure 6.34). Sonograph observations off Pauanui and Tairua are important as insufficient samples were collected in this

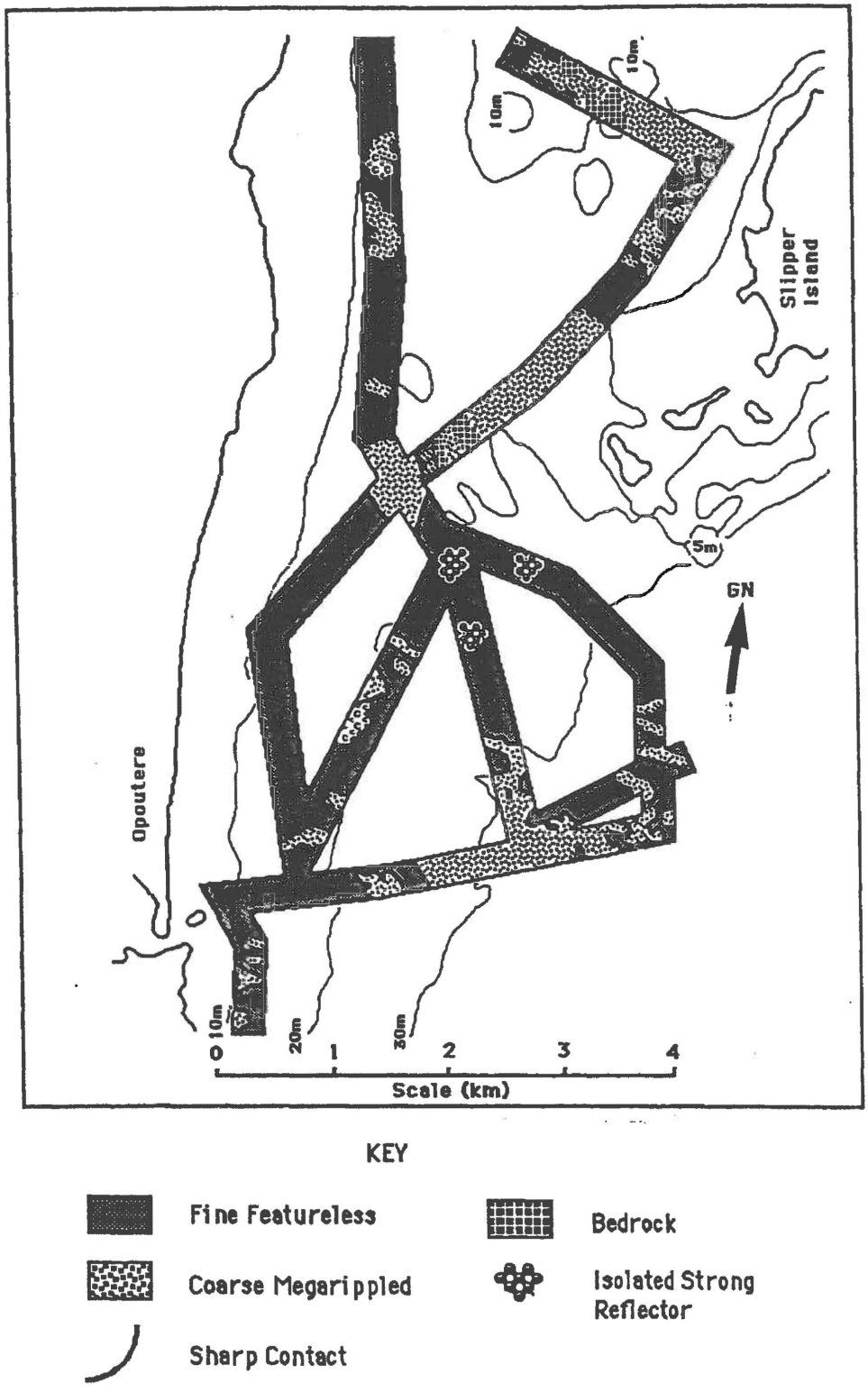

Figure 6.31. Opoutere side-scan sonograph map from the Mar-84 survey.

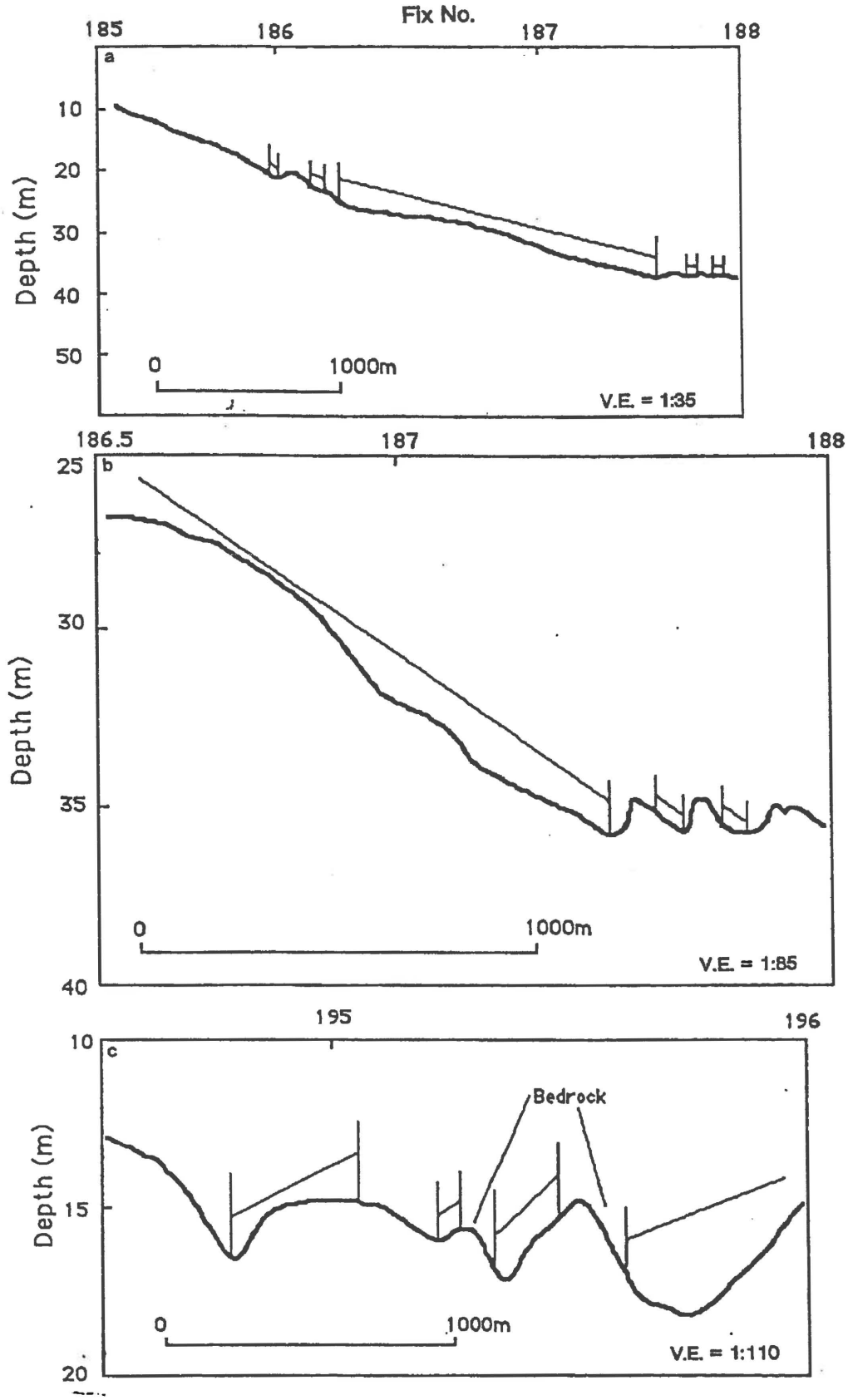

Figure 6.32. Bathymetric profiles from Opoutere Beach. Bracketed areas indicate CMR sands, with bolded line showing sharp contact, and brokened line indicating gradational contact: a) Offshore profile from southern Opoutere Beach; b) Small hummocks of fine sand found on the inner shelf surface off southern Opoutere; c) Shore-parallel trace behind Slipper Island showing CMR bands on the southwestern flanks of sand ridges and rock pinnacles, indicating a northeasterly-directed transport of sediments.

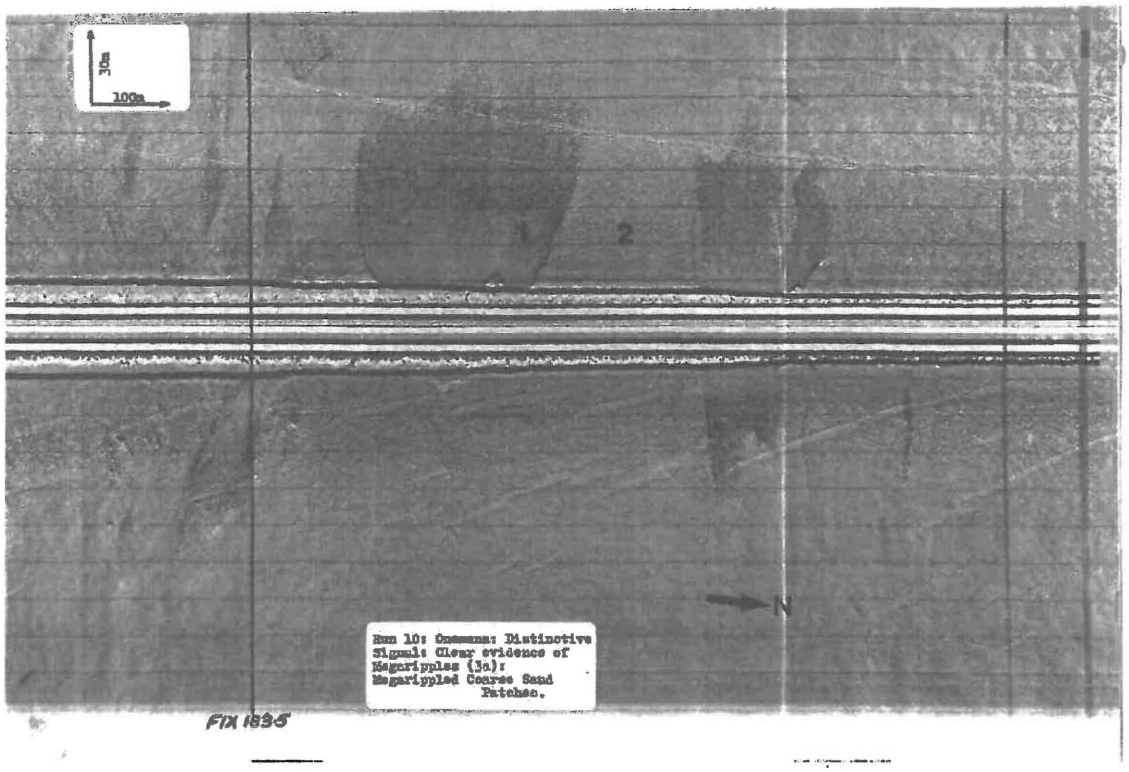

Figure 6.33. Sonograph from the nearshore surface (10 m water depth) at Opoutere in Mar-84, showing the extensive occurrence of shore-normal CMR bands (1). These are associated with the southern flanks of small sand ridges (2), and indicate a northerly-directed transport of nearshore sediments.

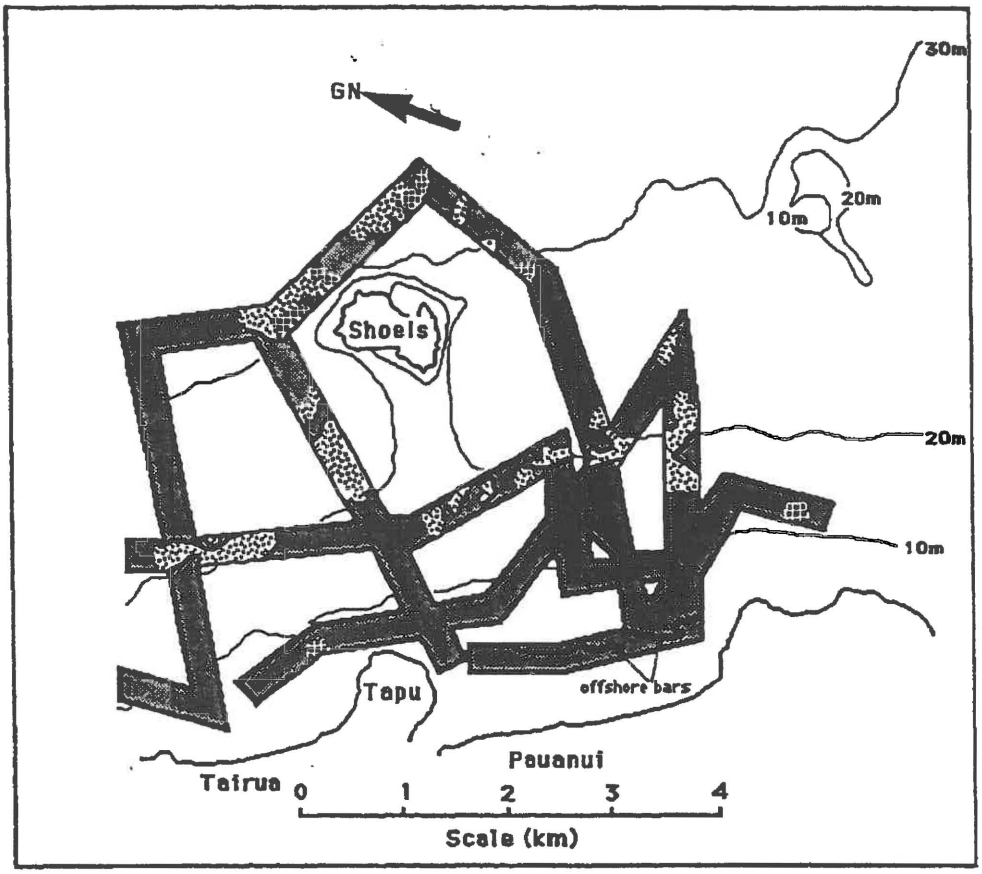

KEY

Fine Featureless

Bedrock

Coarse Megarippled

Sharp Contact

Figure 6.34. Pauanui-Tairua side-scan sonograph map from the Mar-84 survey.

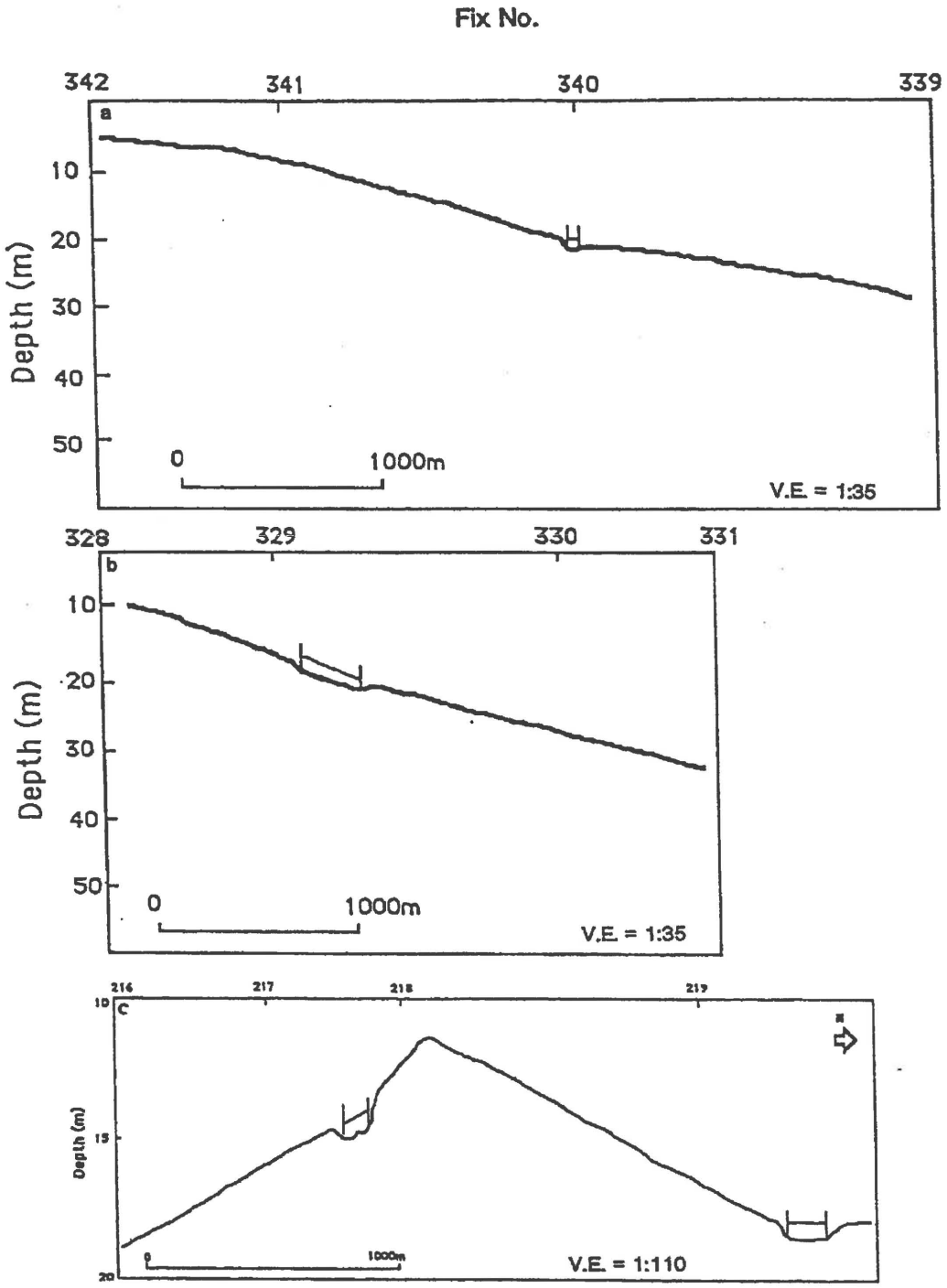

Figure 6.35. Bathymetric profiles from Pauanui-Tairua. Bracketed areas indicate CMR sands, with bolded line showing sharp contact, and brokened line indicating gradational contact: a) Offshore profile from Pauanui Beach in Mar-84; b) Offshore profile from Tairua Beach in Mar-84; c) Shore-parallel transect across Pauanui and Tairua Beach, showing a sharp rise in the sea floor behind Shoe Island, and CMR bands occurring in small surface depressions. The latter indicates that shelf erosion here is probably associated with localised scouring by waves.

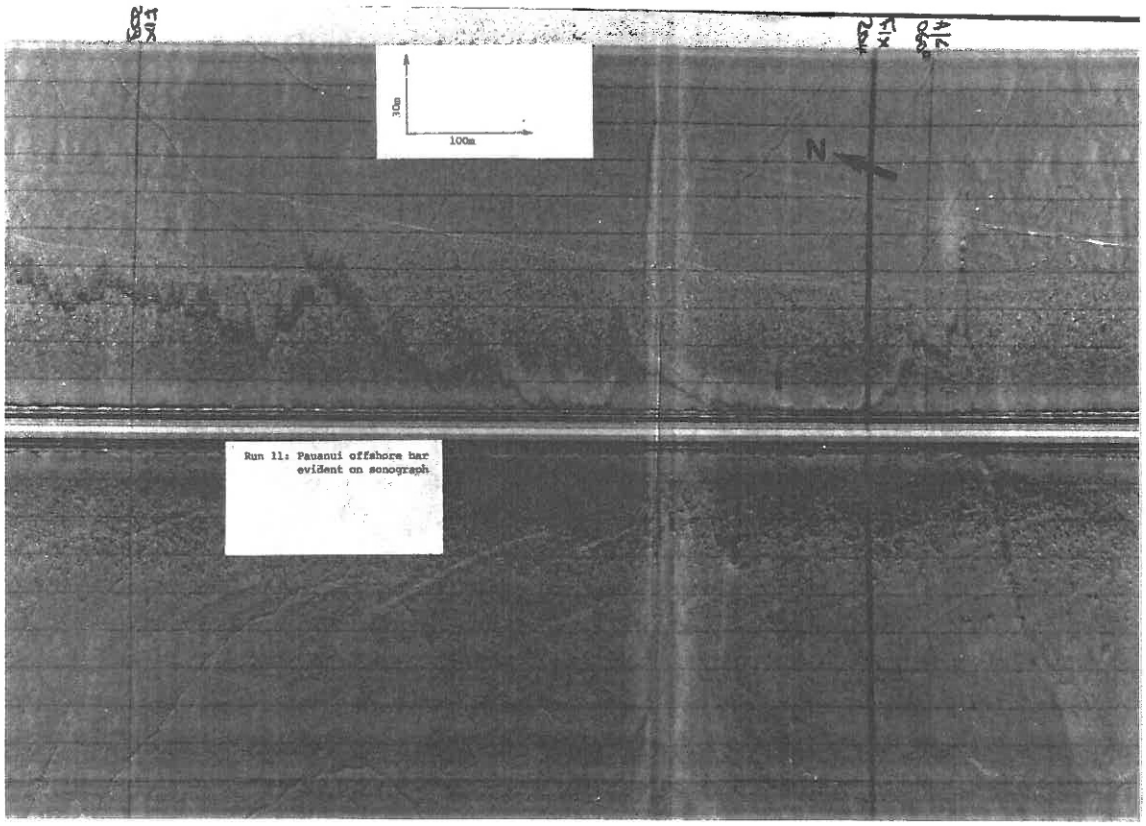

Figure 6.36. Sonograph from the nearshore zone (5 m) off Pauanui Beach, showing the presence of an inferred offshore bar (1). This indicates that the surf zone extends at least 500 m offshore to the nearshore surface during storms.

region for sediment textural patterns to be deduced. Off Pauanui Beach, Fine Featureless sediments extend across a steeply dipping convex-up nearshore surface (1:140) to 22 m water depth, where a change in slope to a flatter convex-up inner shelf surface (1:280) occurs (Figure 6.35 a). Sonographs from the nearshore zone at Pauanui are dominated by Fine Featureless sands. An important feature found in this region is the presence of offshore bars in 5 m water depth (Figure 6.36), which indicate the surfzone extends up to 500 m offshore onto the upper nearshore surface during storm conditions. The nearshore-inner shelf boundary at Pauanui is characterised by extensive elongate bands of CMR deposits, which are generally 50 m in width and oriented either parallel or normal to the coast. Further offshore, Fine Featureless sand dominates the inner shelf surface.

Offshore from Tairua Beach, the nearshore and inner shelf zones are difficult to differentiate based on broad shelf morphology, as the surface slopes fairly constantly at a gradient of 1:130 to at least 30 m water depth (Figure 6.35 b). However, CMR patches are very extensive beyond 20 m depth, particularly near Shoe Island, which may indicate the presence of inner shelf sediments.

The CMR deposits which occur off both Pauanui and Tairua Beaches do not coincide with any bedforms on the sea-bed, as was commonly found for regions further south, but rather occur within small depressions on the sea floor (0.5 m deep; Figure 6.35 c). Therefore, they may represent areas of intense scouring due to wave focussing around Shoe Island. Evidence supporting this comes from the extensive occurrence of CMR bands and patches around Shoe Island, particularly on its northeastern side offshore from Tairua.

Hotwater Beach

The sea-bed offshore from Hotwater Beach was only subject to limited scanning due to the small shelf area and limited coastal development in this region. This was undertaken on 13-Mar-84 with 17 km of trace collected along one shore-parallel and one shore-normal line (Figure 6.37). Sonographs from Hotwater Beach show the same pattern as the limited textural analysis from this area, with Fine Featureless deposits extending offshore to 28 m water depth across a very steeply dipping convex-up nearshore surface (1:75). CMR deposits then occur on a very steep concave-up inner shelf surface (1:90) out to the mid shelf boundary in 50 m water depth (Figure 6.38 a). A small hummock of fine sand is present on the inner shelf surface in a depth of 37 m (Figures 6.38 b, 6.39), which may indicate the presence of a sand ridge bedform on the sea floor. Sonographs also provide some information on the offshore region south of Hotwater Beach. This is dominated by extensive rock reefs and interspersed CMR sand patches. The latter occur within depressions in the rocky sub-strate, but do not appear to flank their surfaces. Thus, there appears to be very little current-induced transport of sediments in this region. These sonograph observations from Hotwater Beach support deductions made from textural data in Chapter 5, in that this is an area of high wave erosion, and limited deposition of clastic sediments.

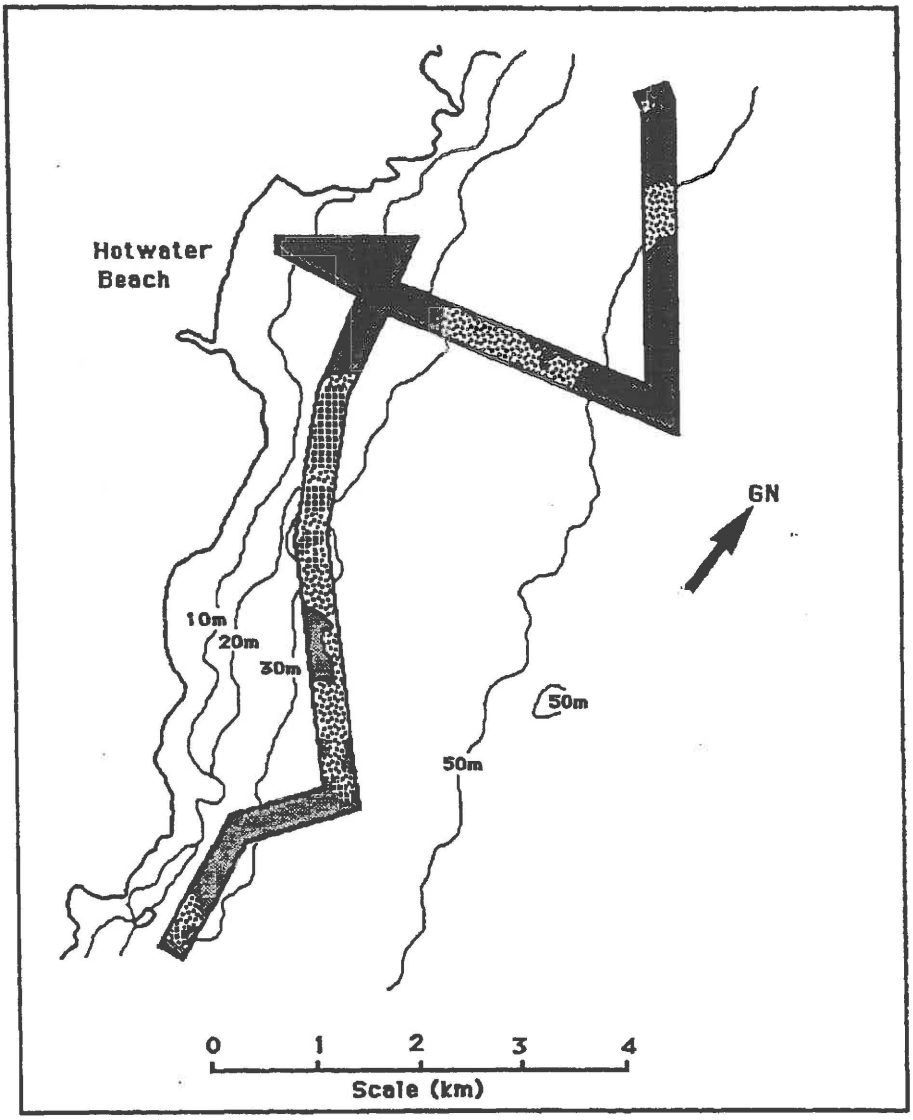

KEY

Fine Featureless

Bedrock

Coarse Megarippled

Sharp Contact

Figure 6.37. Hotwater Beach side-scan sonograph map from the Mar-84 survey.

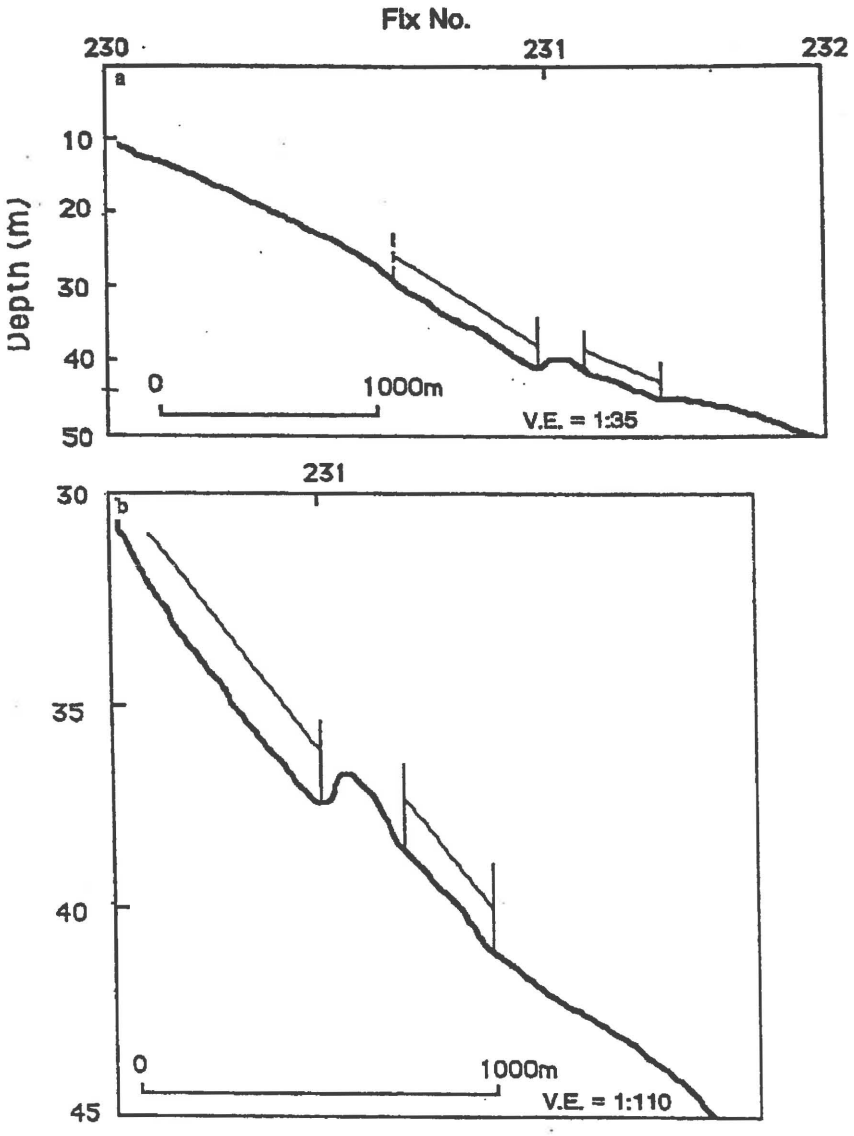

Figure 6.38. Bathymetric profiles from Hotwater Beach. Bracketed areas indicate CMR sands, with bolded line showing sharp contact, and brokened line indicating gradational contact: a) Offshore profile from Hotwater Beach; b) Small hummock of fine sand on the inner shelf surface off Hotwater Beach.

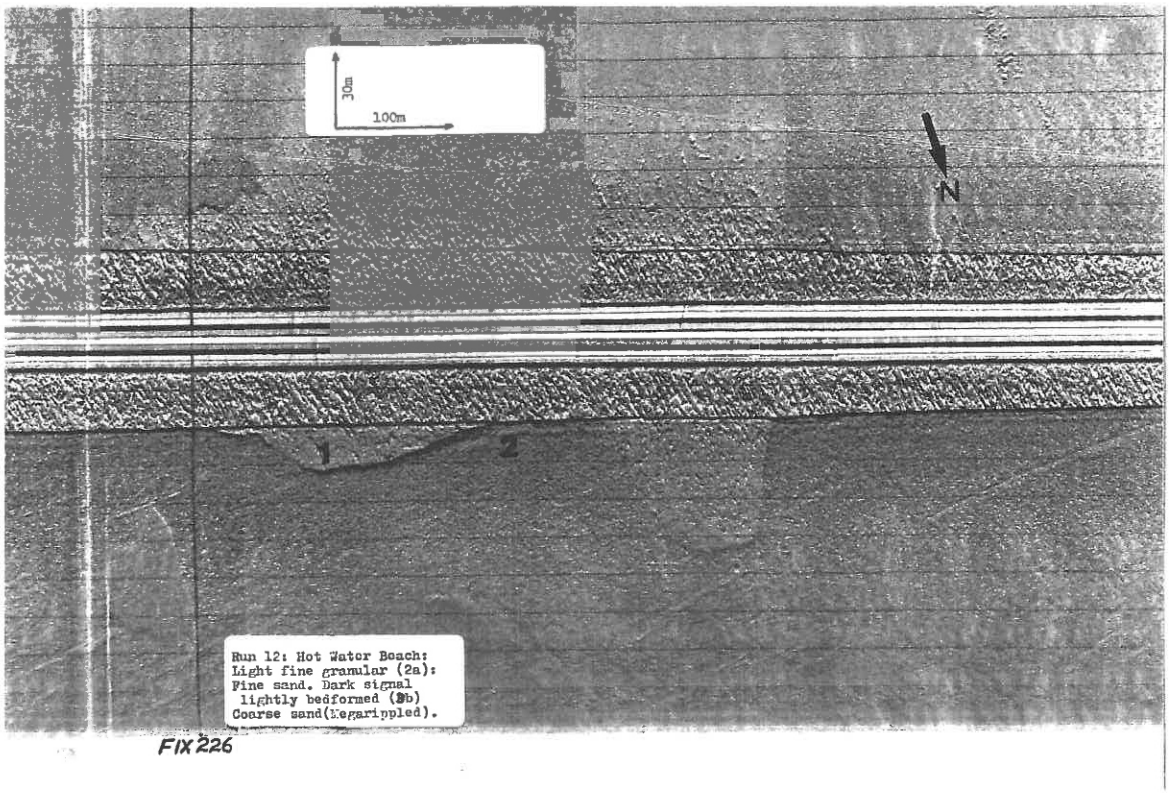

Figure 6.39. Sonograph from the inner shelf (40 m water depth) at Hotwater Beach, showing a fine sand hummock (1) occurring over a dominantly CMR surface (2).

Mercury Bay

The sea-bed within Mercury Bay was extensively examined during two side-scan surveys. The first occurred on the 13- and 14-Mar-84 in which 61 km of sea floor was scanned, and the second on the 28-Jun-90 when 40 km was scanned. Sonograph maps from each survey are illustrated in Figures 6.40 and 6.41.

Both side-scan sonar surveys from Mercury Bay indicate that fine sand dominates most of the sea floor over a relatively gently sloping shelf surface (1:290). Differentiation of the nearshore and inner shelf morphological components is therefore difficult in Mercury Bay, but is inferred to occur in 20 m water depth where the surface changes from a convex-up outline to a more concave-up surface (Figure 6.42). This inflection point is also marked by the presence of extensive CMR deposits on the inferred inner shelf surface.

Although Fine Featureless sand dominates in most of the sonograph records, significant areas of CMR deposits are also found in various regions. Within the inner bay area (< 10 m water depth) shore-normal elongate CMR bands (50 to 160 m in width) are found south of Wharekaho Beach, in a similar region to where SMITH (1980) identified medium grained sands in surface samples. These bands do not coincide with any significant bathymetric features in echosounding records, although sand wave bedforms are apparent on their surface in sonographs (Figure 6.43), with crests striking normal to the coast and spaced ~13 m apart. As these sand waves were only identified in the second survey, their presence may indicate that intense currents were generated on the northern side of the inner bay area during Cyclone Bola.

The outer part of Mercury Bay is also dominated by fine deposits, but is characterised by much more extensive CMR sands than found in the sediment textural analysis. Patches and bands of CMR sand are particularly concentrated on the nearshore surface along the southern and northern margins of Mercury Bay. This includes the areas offshore from Hahei, Cooks and Waitaia Beaches. Off Cooks Beach, the nearshore surface is characterised by the presence of three shore-normal elongate CMR bands in the first survey, but during the Jun-90 survey appeared to be replaced by a more extensive patch of CMR deposits (Figure 6.41). This may indicate that increased erosion of nearshore deposits occurred off Cooks Beach during Cyclone Bola. At Waitaia Beach, numerous CMR bands were found in both surveys, these striking perpendicular to the beach and ranging in width from 3 to 100 m. The CMR bands off Waitaia are characterised by sharp southern and gradational northern contacts with fine sediments, but do not coincide with any significant bathymetric features. However, a series of very small bands (3 to 6 m in width) are found in depths of 10 to 20 m, which coincide with the presence of small (λ= 6 m, η= 0.2 m) sand wave bedforms on the sonographs (Figures 6.44, 6.45). As narrow elongate CMR bands were found in the same region during the first survey, the sand waves are probably a common feature on the outer bay surface. This indicates that some current-induced sediment transport occurs on the nearshore surface around the margins of Mercury Bay, which off Waitaia Beach appears to be directed

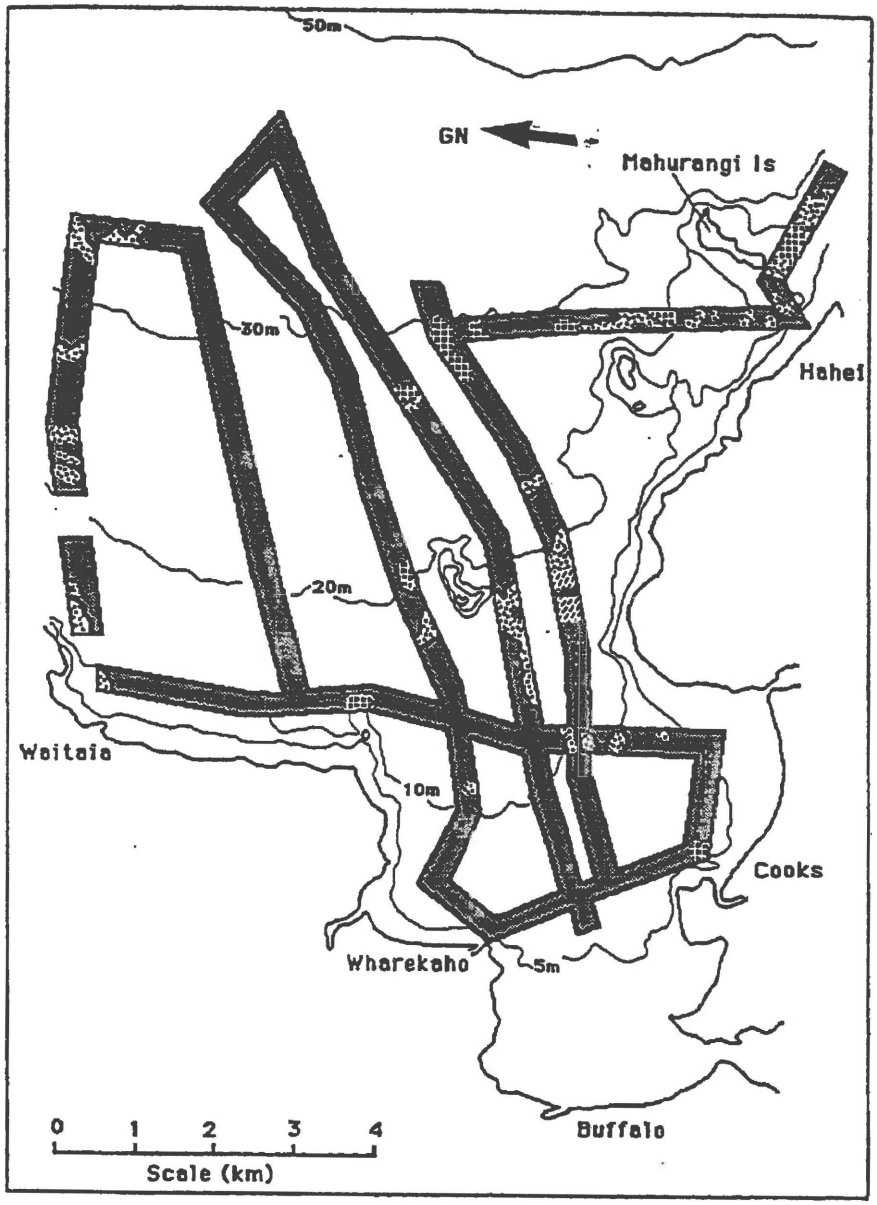

KEY

Fine Featureless

Bedrock

Coarse Megarippled

Mottled

Sharp Contact

Figure 6.40. Mercury Bay side-scan sonograph map from the Mar-84 survey.

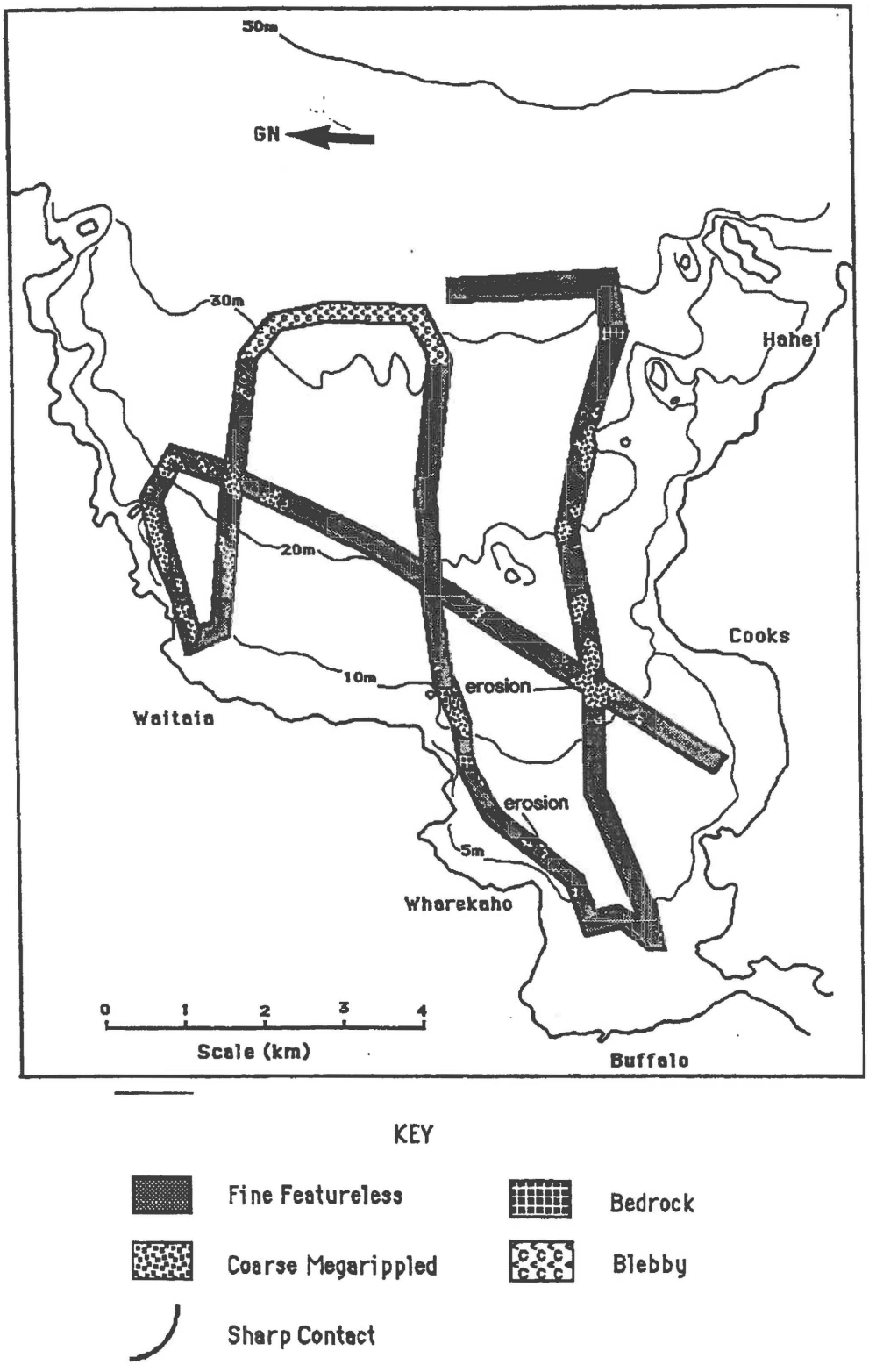

Figure 6.41. Mercury Bay side-scan sonograph map from the Jun-90 survey.

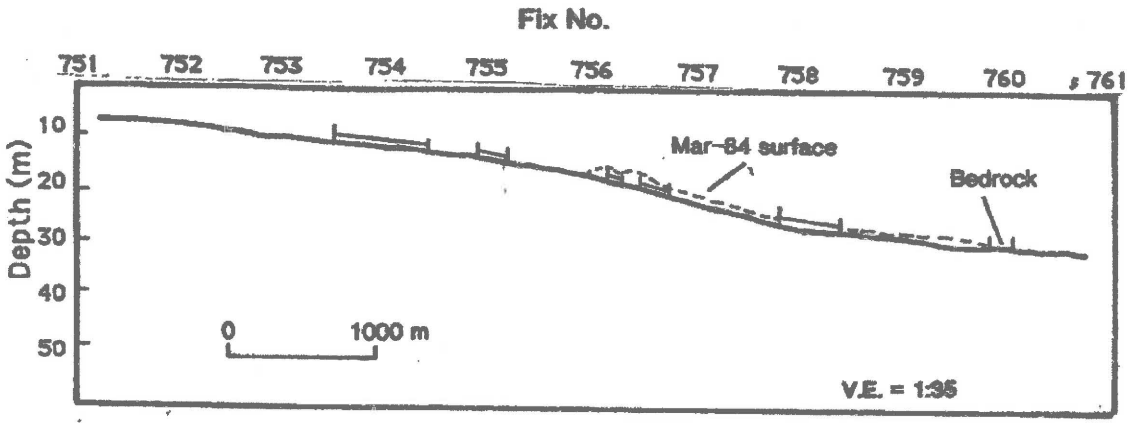

Figure 6.42. Offshore profile from Buffalo Beach in Jun-90, also showing the original Mar-84 surface. Bracketed areas indicate CMR sands, with bolded line showing sharp contact, and brokened line indicating gradational contact. Note very similar shelf surfaces present during both surveys in Mercury Bay.

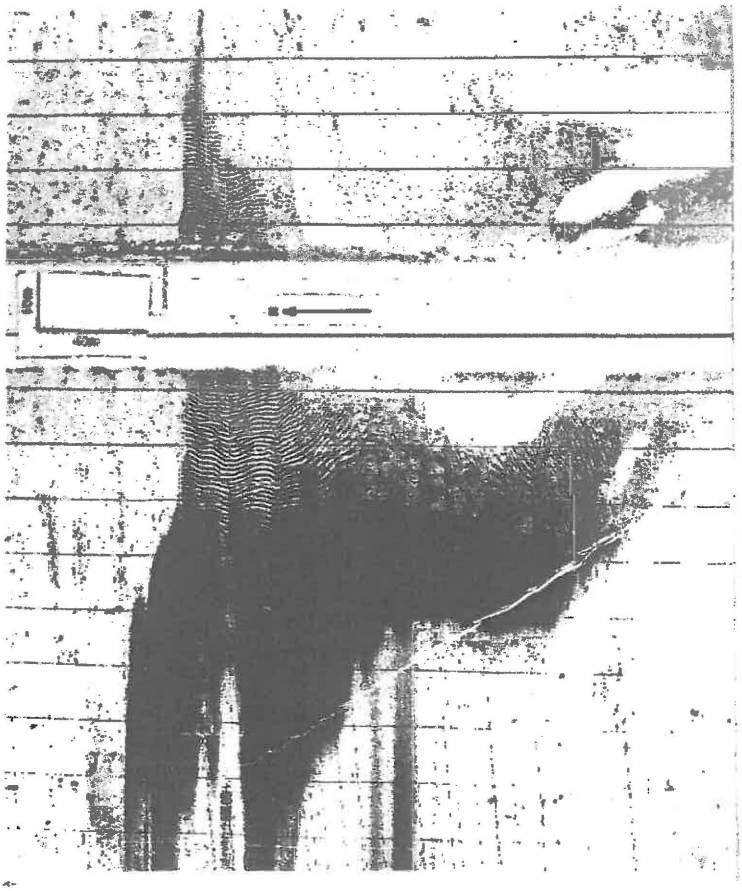

Figure 6.43. Sonograph from inner bay surface (7 m water depth) just south of Wharekaho Beach in Mercury Bay (Jun-90), showing patch of CMR sand with small megaripples occurring over larger crenulated features, interpreted as representing sand waves. This feature was not present in Mar-84 in the same area, and may have formed from scouring by strong downwelling currents during Cyclone Bola.

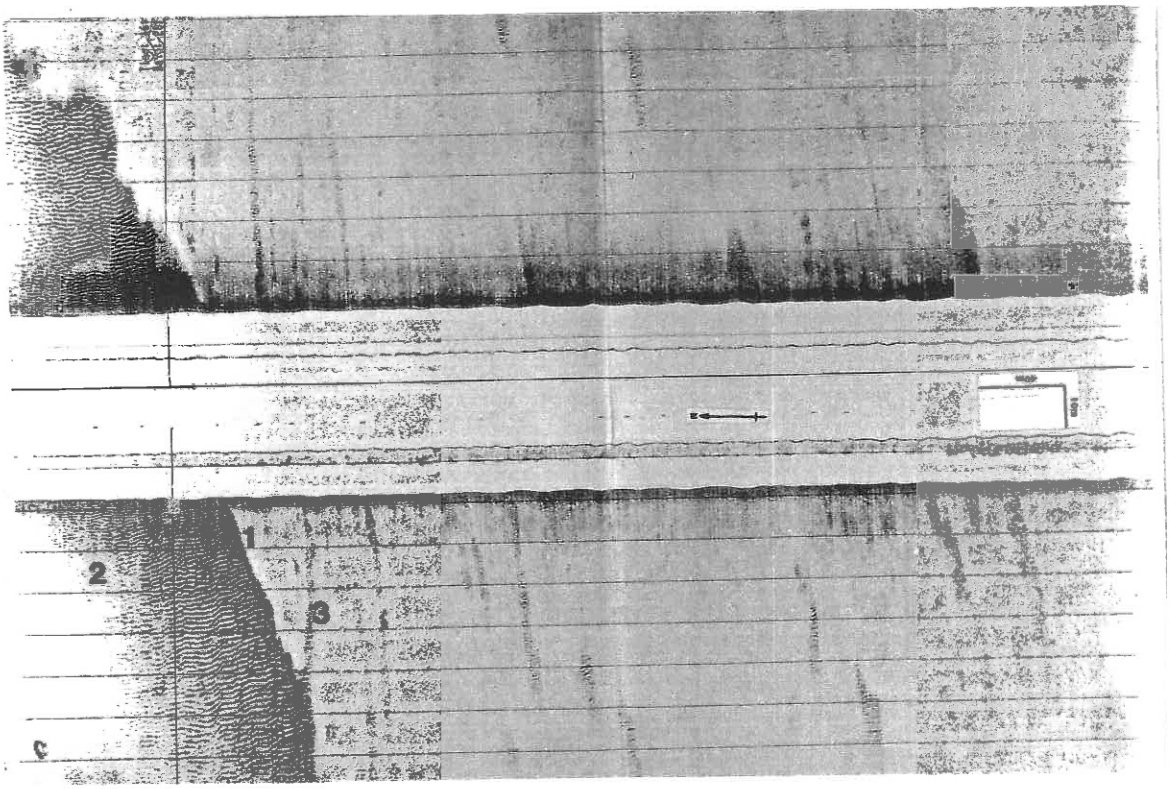

Figure 6.44. Sonograph of the nearshore surface (22 m) offshore from Waitaia Beach in Jun-90, showing a large CMR patch with a sharp southern (1) and gradational (2) northern boundary, and numerous very narrow bands oriented perpendicularly to the shore (3).

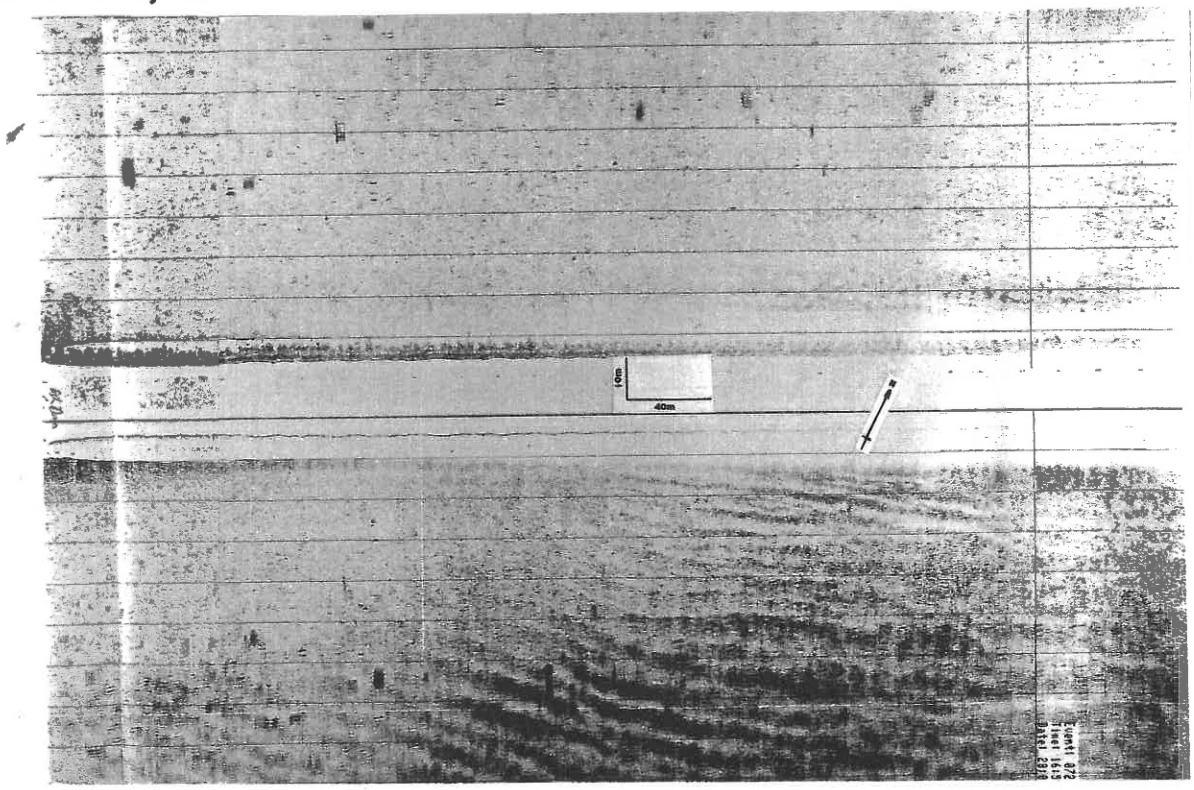

Figure 6.45. Sonograph from the same shelf area as Figure 6.44 on a shore-normal track, showing small sand waves (1) where the narrow elongate CMR bands are found in the shore-parallel track.

towards the north. However, transport by currents within Mercury Bay appears to be less intense than on the southern exposed coastline, as shown by the much smaller size of current-generated bedforms.

Deposits of CMR sands are also relatively abundant near offshore islands, particularly around Motukorure Island in the middle of the bay. This indicates that wave focussing through refraction of storm waves around offshore islands may also be an important process in the formation of CMR deposits within parts of Mercury Bay.

Additional important information indicated in the sonograph records from Mercury Bay was the extensive occurrence of shell fish beds over the bay surface, particularly horse mussels on the inner shelf surface (30 m water depth) during the second survey. This indicates favourable conditions for the growth of these organisms, which may be either the very fine sandy sub-strate which occurs here, or the presence of relatively low current energy conditions.

Otama-Whangapoua Beaches

The offshore region extending along the Kuaotunu Peninsula from Otama to Whangapoua Beach was studied in only one side-scan survey on the 15- and 16-Mar-84, in which 55 km of sea-bed was examined (Figure 6.46). The results confirm observations made of sediment textural patterns in Chapter 5.3. This includes the dominant occurrence of a coarse textured sonograph pattern off Otama Beach, these coarse deposits occurring across a steep (1:180) concave-up nearshore surface to 15 m water depth, and then across a very flat (1:440) convex-up inner shelf surface (Figure 6.47 a). However, coarse deposits at Otama lack the characteristic megarippling usually found on this sonograph pattern. The absence of megaripple features here supports deductions made in Chapter 5.3. that sediments off Otama Beach are frequently reworked by tidal- and wind-generated currents, but only experience limited wave reworking due to the shadowing effect of the Mercury Islands to the northeast. This is further supported by the presence of large sand ridges in bathymetric records, which range in size from λ= 235 to 1250 m, and η= 1.5 to 6.5 m (Figure 6.47 b).

Sonographs also show fine sand dominating most of the shelf area from Kuaotunu to Whangapoua, with numerous shell fish beds occurring over these fine deposits (Figure 6.3). Offshore profiles in this region show a relatively flat (1:200) concave-up nearshore surface present to 20 m water depth, and a similar low gradient (1:250) and more convex-up inner shelf surface extending seawards to 33 m. Further offshore, a flatter mid shelf surface then appears to be present (Figure 6.47 c). The shell fish beds which dominate sonograph patterns off the Kuaotunu Peninsula occur mainly in depths of 10 to 22 m. As at Mercury Bay, this may indicate favourable conditions for infaunal shell production, with a fine grained, relatively stable sandy sub-strate present in a relatively low current energy environment. Coarse sediments in this region are very limited in sonograph records, and restricted mainly to the area offshore of Whangapoua Beach. These observations again

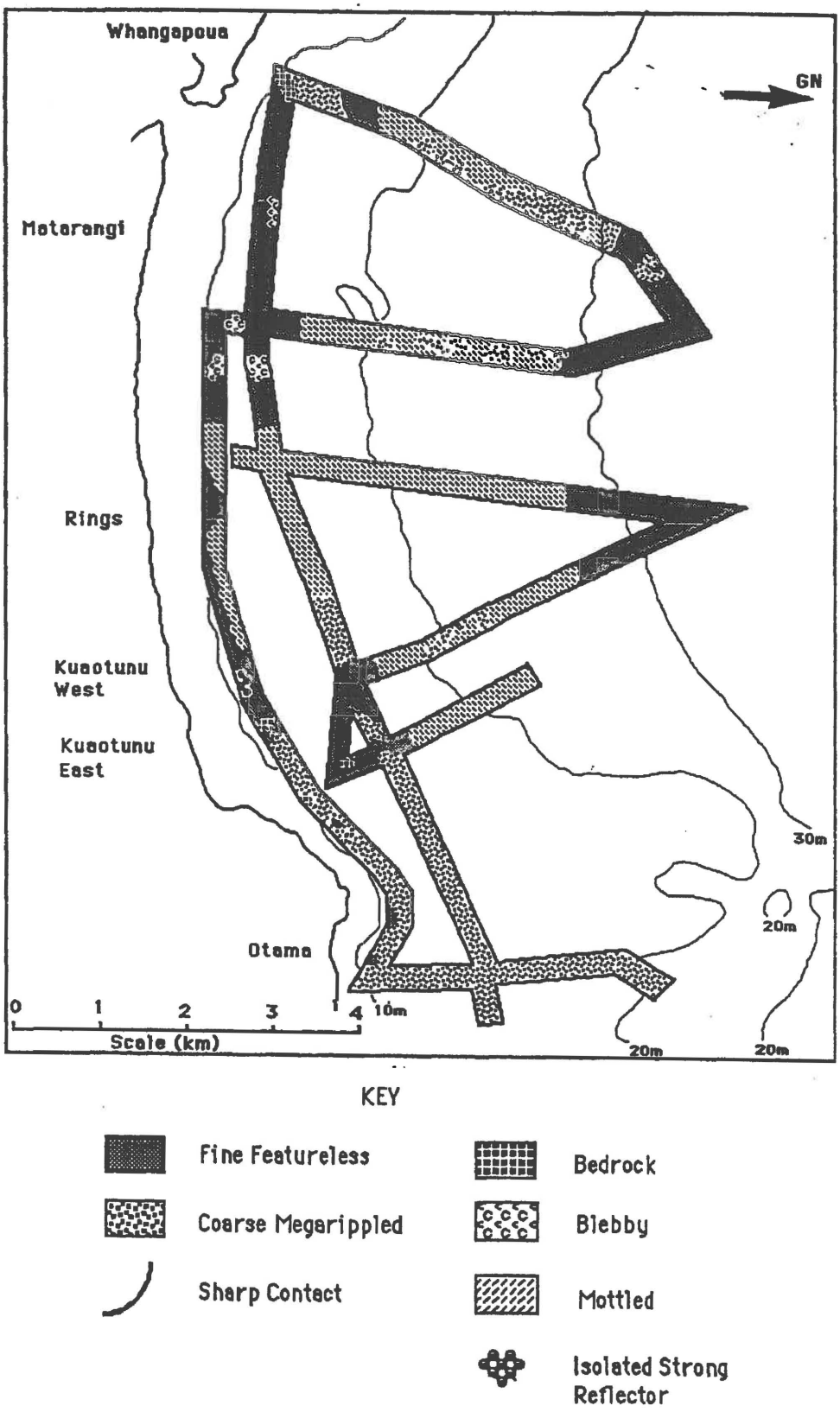

Figure 6.46. Otama-Whangapoua side-scan sonograph map from the Mar-84 survey.

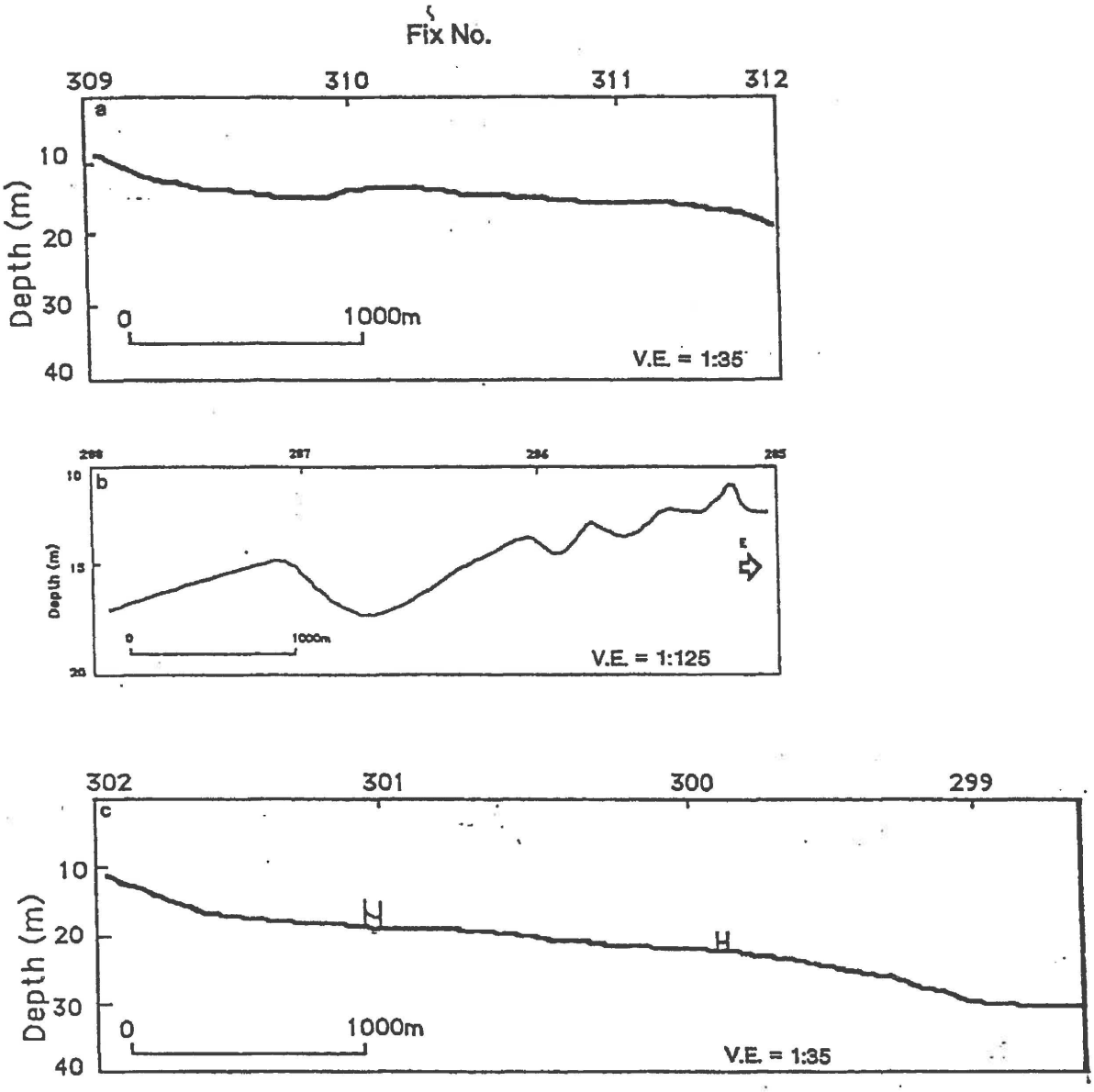

Figure 6.47. Bathymetric profiles from the Otama-Whangapoua survey. Bracketed areas indicate CMR sands, with bolded line showing sharp contact, and brokened line indicating gradational contact: a) Offshore profile from Otama Beach in Mar-84; b) Shore-parallel transect off Otama Beach in Mar-84, showing both large and small sand ridges present; c) Offshore profile from Matarangi Beach in Mar-84.

support deductions made in Chapter 5, that the offshore environment from Kuaotunu to Whangapoua Beach is an area of low energy conditions, and high clastic sedimentation.

6.2.3. Implications of Sonograph and Bedform Patterns for Shelf Erosion and Transport Pathways

The information gained from sonograph surveys provides important information about the areas of erosion or deposition on the shelf, and the transport pathways for sediments along the shelf. Areas of shelf erosion are inferred to coincide with the areas of CMR sands, as this sonograph pattern matches those locations in which medium and coarse grained storm-lag deposits were identified in the previous sediment textural analysis (Chapter 5.3.). Sediment transport pathways are deduced from the morphology of the sand ridges and sand waves identified in sonographs and bathymetric traces, and the phase-lag relationship of CMR sands with their flanks. This information is integrated on a regional scale for the southern and northern coastlines separately.

Southern Coastline

On the southern exposed coastline, the distribution of CMR sands and hence shelf erosion varies considerably both along the coast and across the shelf surface (Figure 6.48). These variations coincide with the presence of morphological features on the sea-bed (Figure 6.49), which tends to support deductions made in Chapter 5 that the variable nature of shelf deposits indicates changeable hydrodynamic conditions along the coast.

Off Waihi Beach, shelf erosion occurs in small isolated bands across the nearshore surface from depths of 10 to 20 m. As these do not coincide with any morphological features on the sea-bed, they are possibly areas of isolated scouring due to wave focussing, as proposed for similar features at Whangarei Harbour by BLACK and HEALY (1988). However, the inner shelf surface out to at least 30 m water depth is an area of very extensive erosion, as shown by a field of CMR sand deposits which extends along the coast for 5 km. The erosion of inner shelf deposits appears to be more disrupted north of Waihi Beach, where CMR deposits occur in shore-normal oriented bands on the southeastern flanks of sand ridges. The shelf morphology in this area is consistent with a northwesterly shore-parallel transport of fine sands, these being eroded from the inner shelf in the southeast and deposited in the sand ridge field to the northwest. This may indicate a decrease in the intensity of wind-generated current flows in this area, possibly associated with the very sudden increase of inner shelf gradients from 1:1000 to 1:200.

The area north of Waihi Beach off Mataora and Whiritoa Beaches is characterised by the extensive deposition of fine sands. Shelf erosion is generally limited to small isolated bands on the nearshore, inner shelf and mid shelf, although one more extensive area of erosion is found on the lower inner shelf surface (40 m water depth). The predominant deposition of fine sands in this area may be a continuation of the trend found north of Waihi Beach off Orokawa and Homunga Bays. However, the sea-bed morphology here indicates complex transport pathways and hence current

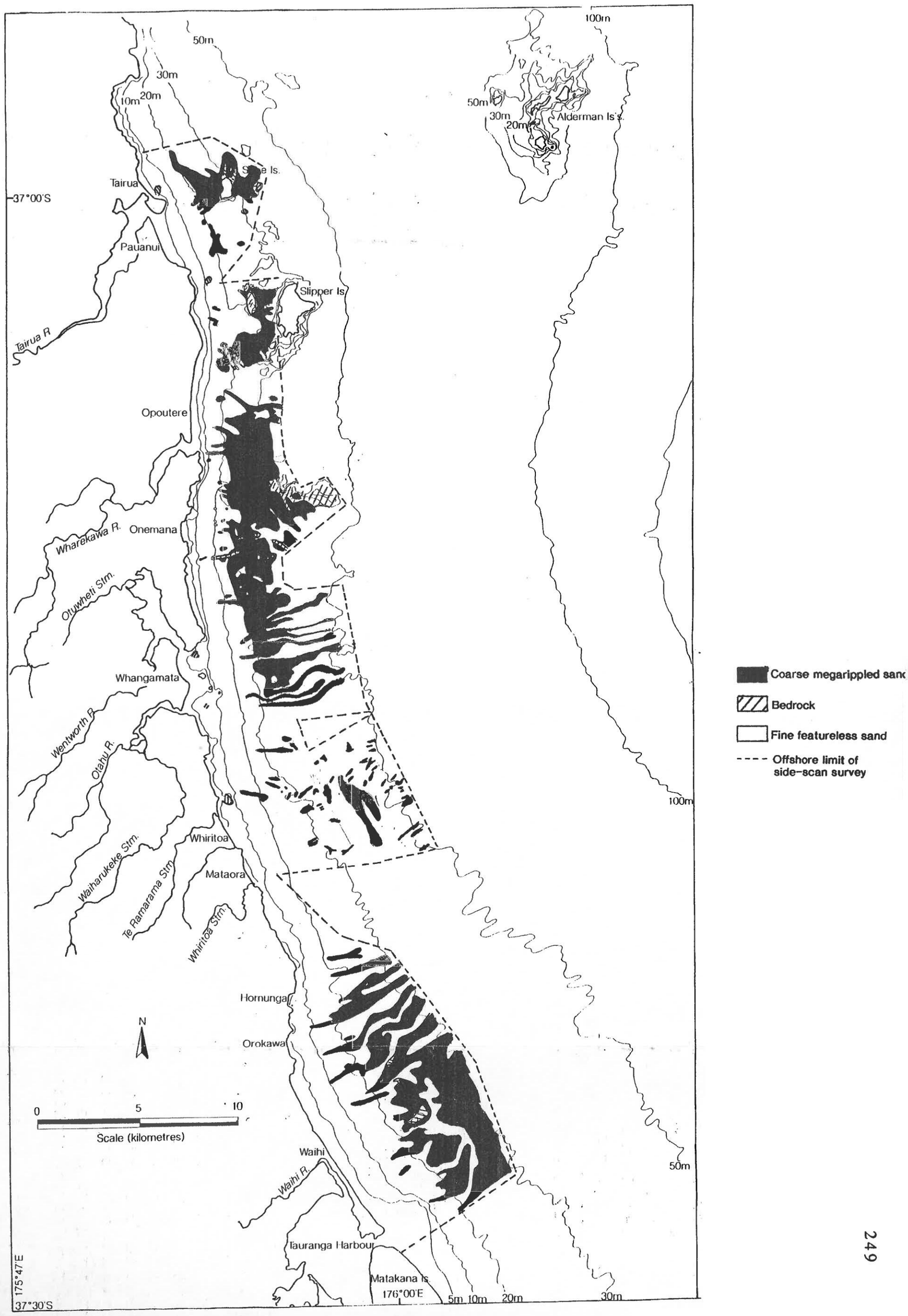

Figure 6.48. Occurrence of CMR sands, bedrock and Fine Featureless sediments on the southern coast, as shown from sonograph surveys. The CMR deposits and bedrock are inferred to indicate areas of shelf erosion, whereas the fine sediments are inferred to represent areas of shelf sedimentation.

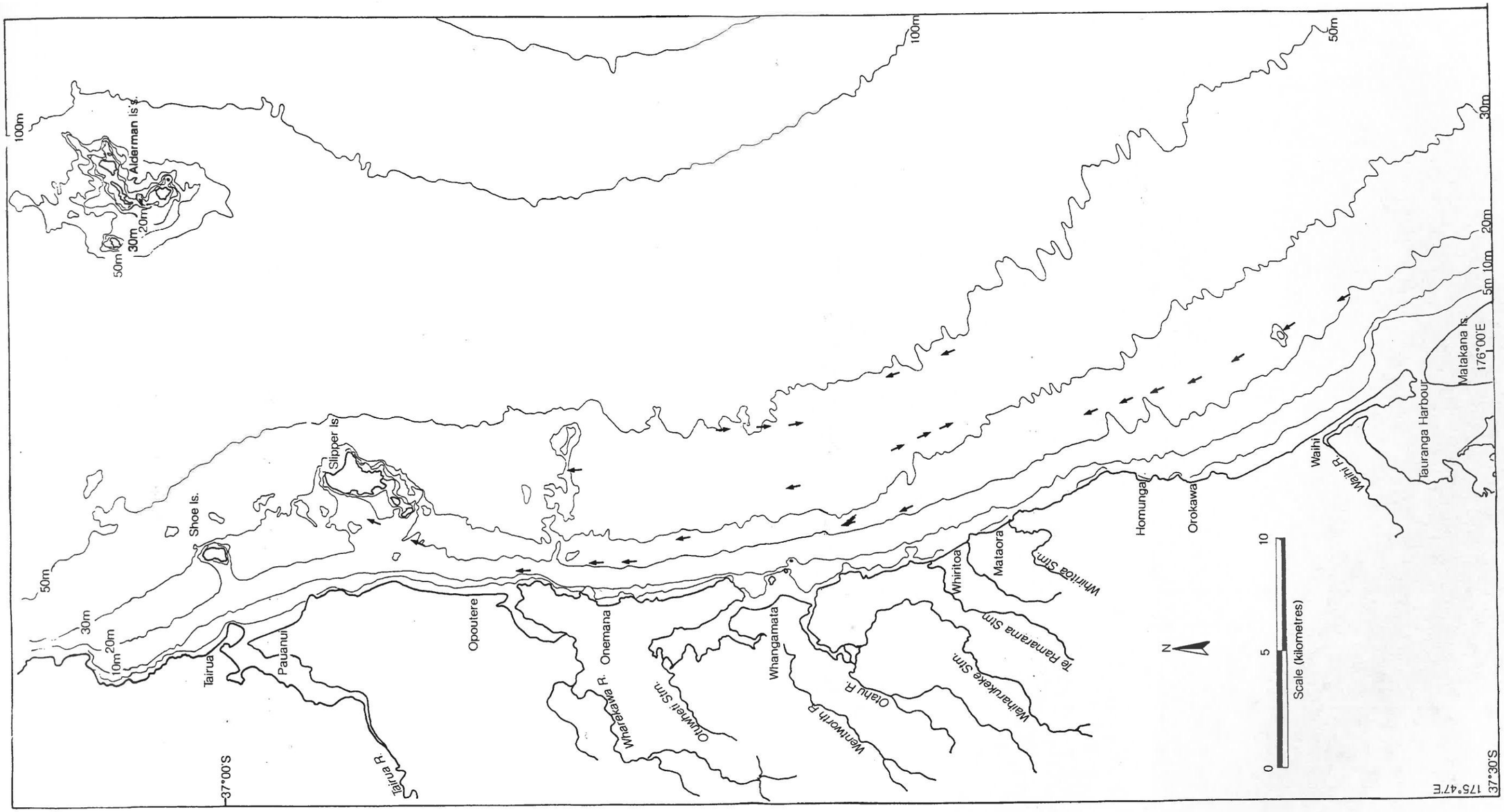

Figure 6.49. Inferred net-sediment transport pathways on the southern coast, based on the morphological association of CMR deposits with sand ridges and rock pinnacles.

flows occurring offshore, with a northerly-directed transport of sediments apparent on the nearshore and mid shelf, but a reverse southerly direction of transport on the inner shelf surface.

A major area of erosion occurs north of Whiritoa, on the inner shelf surface extending from Whangamata to Opoutere Beach (15 km). This varies in offshore extent (during the Mar-84 survey) from 30 to 37 m water depth at Whangamata Beach, to depths of 25 to 35 m off Onemana and Opoutere Beaches. Shelf erosion therefore appears to extend onshore towards the north, resulting in the extensive erosion of nearshore deposits at Onemana and Opoutere (as shown by the numerous CMR bands in shallow water depths). Shelf erosion between Whangamata and Opoutere seems to be associated with wind-generated currents, as shown by the presence of numerous sand ridges on the sea-bed. Along the nearshore and inner shelf surface, sediment transport appears to be directed to the north. However, sand ridges found on the mid shelf surface indicate a possible southerly direction of transport for these sediments. Thus, the increase in shelf sedimentation towards the south appears to be associated with a reverse in sediment transport direction from the inner shelf to mid shelf surface, which may be linked to the complex transport patterns which occur off Whiritoa.

The area of extensive shelf deposition off Whiritoa and Mataora Beaches therefore appears to result from a convergence of fine sediments transported by wind-generated currents, from the inner shelf south at Waihi Beach, and the mid shelf-inner shelf surface just north between Whangamata and Whiritoa. Shelf erosion between Whangamata and Opoutere may thus result from a divergence in the transport of fine sands both north and south. Alternatively, it may result from an increase in current intensity as the flow patterns become more uniform away from the shelf area between Whangamata and Whiritoa.

Other areas of extensive shelf erosion on the southern coast are associated with offshore islands at Opoutere and Tairua Beaches. In both cases, CMR deposits are concentrated in the area between the mainland and the lee side of the islands, and at Tairua also around the northeastern side of Shoe Island. Behind Slipper Island off Opoutere Beach, the erosion appears to be associated with an intensified northerly-directed current flow, as shown by the sand ridge morphology in this area. However, at Shoe Island no current-generated bedforms were identified from either the sonographs or echosounding traces, which suggests that erosion may be associated with the refraction and focussing of northeasterly storm waves around the island. This may also be an additional important factor in shelf erosion associated with Slipper Island. Evidence supporting this comes from the extensive deposition of fine sediments on the shelf surface to the south of both islands, which would be in a wave-shadow zone from northeasterly waves. However, the possibility of wave-focussing affecting shelf sedimentation in these and other areas is more fully investigated from theoretical considerations in Chapter 7.

Northern Coastline

On the northern embayed coastline, areas of extensive erosion or deposition tend to be very localised (Figure 6.50), and do not generally coincide with the presence of sand ridges or sand waves in sonograph and echosounding traces (Figure 6.51).

An extensive area of shelf erosion occurs on the inner shelf surface at Hotwater Beach. However, there is very little evidence for any current-induced transport of shelf sands in this area. Therefore, inner shelf erosion at Hotwater Beach probably results from the presence of high energy wave conditions due to reduced frictional dissipation across a very narrow and steep inner shelf surface (1:90). Further north where the shelf surface begins to widen, current-induced transport and erosion may be more significant, as shown by the presence of shore-parallel patches of CMR and fine sand.

Within Mercury Bay, areas of extensive erosion are confined mainly to the southern and northern margins of the embayment and around offshore islands. Most of the bay surface, however, represents an extensive area for accretion of very fine grained sediments. There is little morphological evidence of the sediment transport directions within Mercury Bay, which indicates that current-induced sediment transport is significantly less active here than on the southern exposed coastline. A low current energy environment within Mercury Bay is further indicated by the extensive occurrence of shell fish beds on the inner shelf surface. Small sand waves off Wharekaho and Waitaia Beaches do indicate that some cross-shelf transport occurs on the inner bay, and along-shelf transport on the outer bay surface. Current measurements from Mercury Bay by SMITH (1980) are indicative of a clockwise circulation pattern within the bay during semi-diurnal tidal flows, which is incapable of entraining and transporting sediments. However, if downwelling currents generated during storm conditions were to form a similar circulation pattern, then sediment transport would follow a shore-parallel path around the edges of the bay towards the north. Such a flow pattern is consistent with the occurrence of CMR bands around the periphery of Mercury Bay, particularly with the shelf morphology in sonographs offshore from Waitaia on the northern bay margin.

North of Mercury Bay, a large area of erosion occurs on the shelf region offshore from Otama Beach. This is consistent with observations in Chapter 5.3. of the presence of coarse grained carbonate rich sands present off Otama, which indicate high energy conditions and very limited deposition of modern clastic material. Across the nearshore and inner shelf west of Otama, these sediments gradually become finer. This pattern, along with the presence of large sand ridges and lack of CMR bedforms at Otama, indicates that erosion here is due to the presence of intense currents which flow through the Hole in the Wall channel further east, and then veer westwards across Otama. This is supported by current measurements from Opito Bay in Chapter 4.5.1., which showed a relatively strong northward-directed current during flows associated with both tidal- and wind-generated currents.

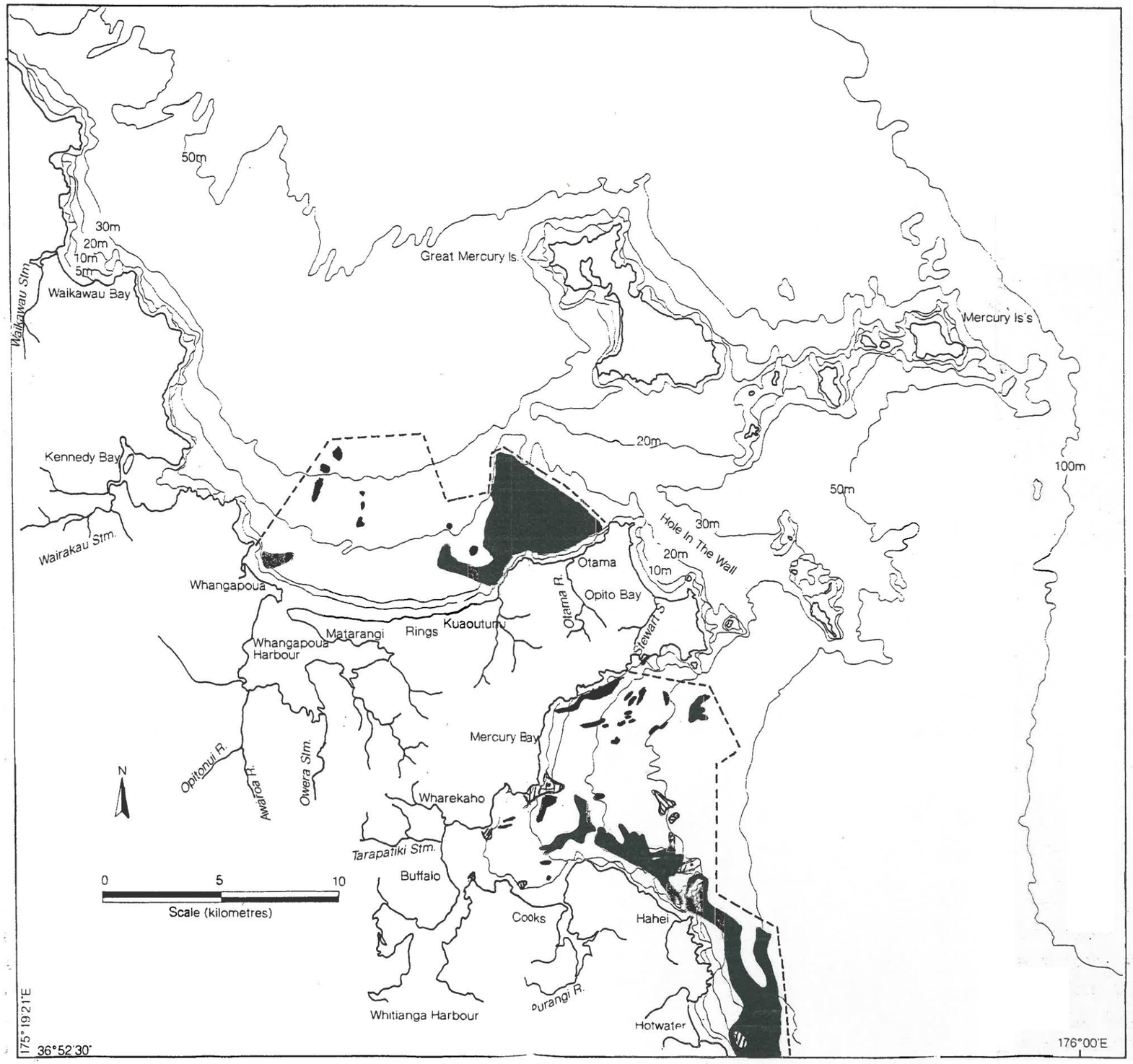

Figure 6.50. Occurrence of CMR sands, bedrock and Coarse Megarippled sediments on the northern coast, as shown from sonograph surveys. The CMR deposits and bedrock are inferred to indicate areas of shelf erosion, whereas the fine sediments are inferred to represent areas of shelf sedimentation.

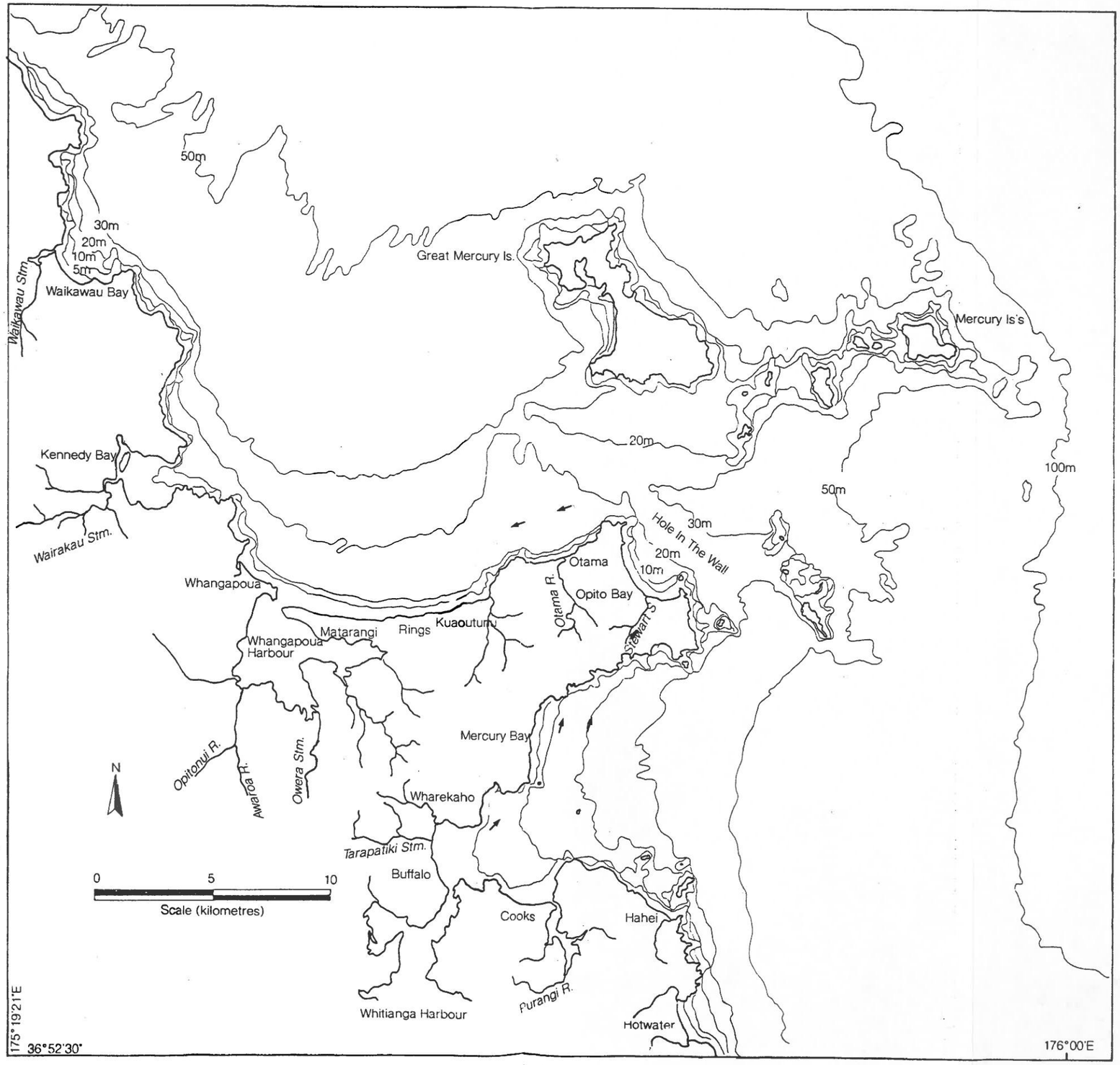

Figure 6.51. Inferred net-sediment transport pathways on the northern coast, based on the morphological association of CMR deposits with sand ridges and rock pinnacles.

Offshore from Whangapoua Harbour just west of Otama Beach, areas of shelf erosion are extremely limited, and are only significant on the nearshore and inner shelf surface adjacent to Whangapoua Beach. This indicates that low current energy conditions and extensive shelf sedimentation characterises this region. Support for this comes from current measurements at Whangapoua in Chapter 4.5.1., which are of very low speed (< 0.10 $m.s^{-1}$). The extensive occurrence of live shell fish beds over the inner shelf surface also indicates that low energy conditions prevail. The small area of erosion which occurs offshore from Whangapoua Beach is probably associated with focussing of northeasterly storm waves around Great Mercury Island.

6.3. RIPPLE AND MEGARIPPLE BEDFORM OBSERVATIONS

Analysis of sonographs and echosounding traces indicates that wind-generated currents are an important component of shelf sedimentation processes on the east Coromandel shelf, and that changes in these current patterns can largely account for variations in sedimentation patterns along the coast. However, in most storm-dominated shelf settings such as the east Coromandel, sedimentation processes are usually linked to the interaction of wave- and current-generated flows (see Chapter 3.1.3.). As no detailed information on the east Coromandel wave climate has previously been obtained, and as the textural patterns of shelf and beach/barrier deposits seem to indicate variable wave conditions along the coast, an analysis of wave-formed morphological features on the sea floor is important for a thorough understanding of shelf sedimentation patterns and processes.

The bedforms that are usually generated by flows associated with surface gravity waves are oscillation ripples. The configuration of oscillation ripples is generally determined by the flow characteristics and composition of the bed (texture and mineralogy). Accordingly, their size and shape can be used to interpret the wave conditions likely to have generated them (CLIFTON and DINGLER, 1984). In this section, the morphological attributes of oscillation ripples are examined along the east Coromandel coast from both direct diver measurements and sonograph observation (refer to Appendix 5 for more detailed information on bedform measurements from each location). However, more detailed interpretations of wave conditions likely to have generated these bedforms are reserved until Chapter 7.

6.3.1. Ripple and Megaripple Morphology

The morphology of oscillation ripples on the east Coromandel shelf has been divided into two classes, ripples and megaripples, based on the BOOTHROYD (1978) classification scheme (Table 6.1). Such a designation of different oscillation ripple types has been criticised by some workers (e.g. BELDERSON *et al.*, 1982; FORBES and BOYD, 1987), as the cut-off value of λ= 0.60 m is quite arbitrary and does not necessarily indicate changes in the nature of wave flow conditions, although it may in some cases reflect variations in the intensity of these flows. This division of oscillation ripples is however useful in the context of this study, in that features of about megaripple size are

detectable in side-scan sonograph images, whereas ripples generally show as a featureless sea floor. Thus the terms 'ripples' and 'megaripples' are used here in a strictly morphological sense, and do not imply different wave flow conditions in their formation.

Most oscillation ripples on the east Coromandel coast fall into two size groups, small ripples which range from λ= 0.05 to 0.25 m, and large ripples and megaripples which range from λ= 0.5 to 1.3 m (Figure 6.52). Small ripples are generally observed from depths of ~ 5 m (landward of which conditions are usually too turbulent for orbital ripples to form) to the outer limit of diver observations in ~ 35 m water, and probably extend further offshore. Megaripples are found in depths as shallow as 6 m, and extend offshore to at least mid shelf depths of 50 m. Thus, along most parts of the east Coromandel coast, flows associated with wave orbital currents are important in the reworking of surface sediments across the nearshore, inner shelf, and mid shelf surfaces. Important patterns to the occurrence of ripples and megaripples are apparent, however, both across the shelf surface, and along the coast.

Southern Coast

Along the southern exposed coastline (Figure 6.53), the upper nearshore surface (5 to 20 m depth) is characterised by the extensive occurrence of small ripples (λ= 0.05 to 0.25 m). At the time of observation by divers, these bedforms were seen to actively respond to the prevailing wave conditions (H~ 1.5 m, T~ 6 s), and were oriented at 135° to a northeasterly direction of approach for these waves. As these wave conditions correspond to those which generally prevail on the northeast coast of New Zealand during calm sea conditions, it is inferred that upper nearshore sediments on the southern coast are consistently reworked by waves. This supports deductions made in Chapter 5, that the well sorted nature of upper nearshore sands is due to their extensive reworking by wave-orbital currents. The morphology of small ripple crests is indicative of current flow asymmetry, as they are often discontinuous crested, hummocky or cross-hatched features, as have been observed to form under asymmetrical flow conditions in other studies (CLIFTON, 1976; see Figure 3.9). Thus, a net-onshore transport of fine to very fine grained upper nearshore sands probably occurs under fair weather conditions, associated with asymmetrical onshore currents formed under shoaling wave conditions.

On the lower nearshore surface at Whiritoa and Whangamata (20 to 30 m depth), the sea-bed was characterised by either a flat featureless surface (Figure 6.54), or relatively long and low relief ripples (λ= 0.2 to 0.5 m, η=0.04 m; Figure 6.55). The flat featureless bed is inferred to have formed either from previous intense wave conditions resulting in sheet flow conditions, or from the degradation of smaller pre-existing ripples. Where ripples are present, their crest patterns vary from long-crested to irregular crested forms, indicating both symmetrical and asymmetrical flow conditions associated with their formation. At the time of observation by divers, these bedforms were not observed to respond to the prevailing wave conditions, although they were oriented at 135° to a northeasterly wave direction. Therefore, these are inferred to represent features formed

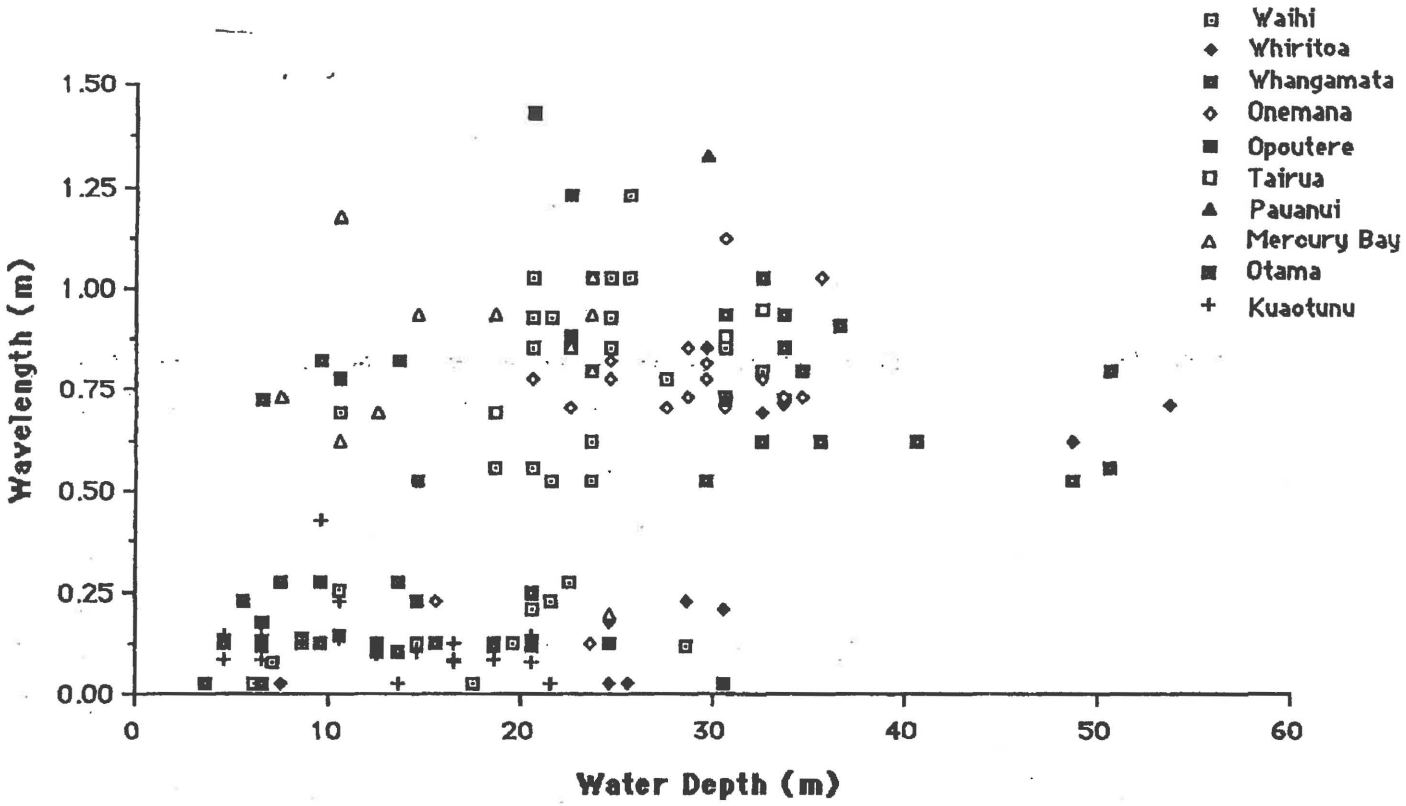

Figure 6.52. Plot of oscillation ripple sizes along the east Coromandel coast, based on both diver and sonograph observations. Note how these fall into two distinct size groups, with small ripples ($\lambda <$ 0.25 m) from 5 to 30 m water depth, and large ripples and megaripples (λ = 0.5 to 1.3 m) from 7 to 50 m water depth. Note that small ripples may be present in deeper waters beyond the outer limit of diver observation.

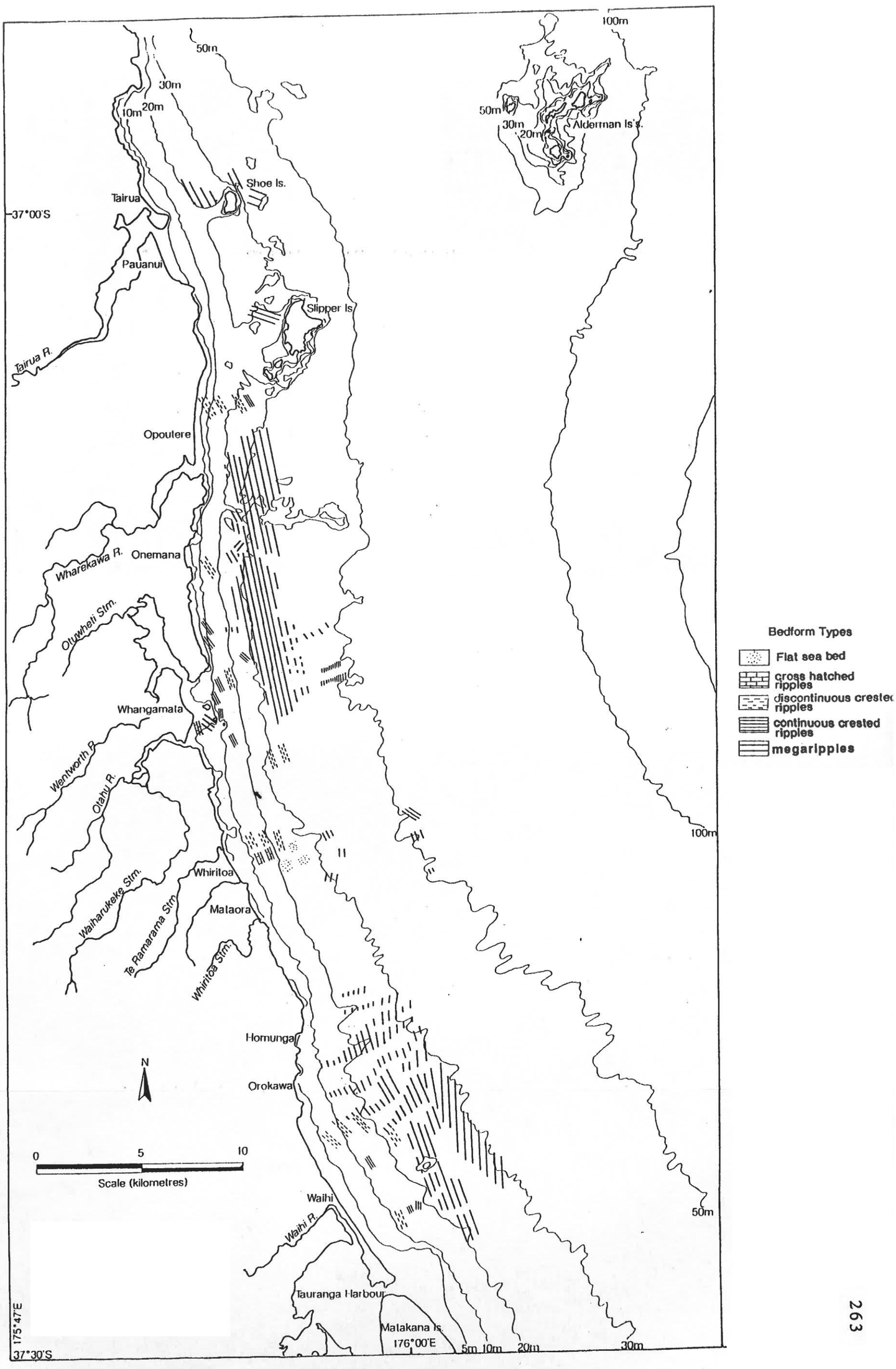

Figure 6.53. Wave-generated bedforms recorded along the southern coastline, showing ripple types, crest pattern, and crest orientation.

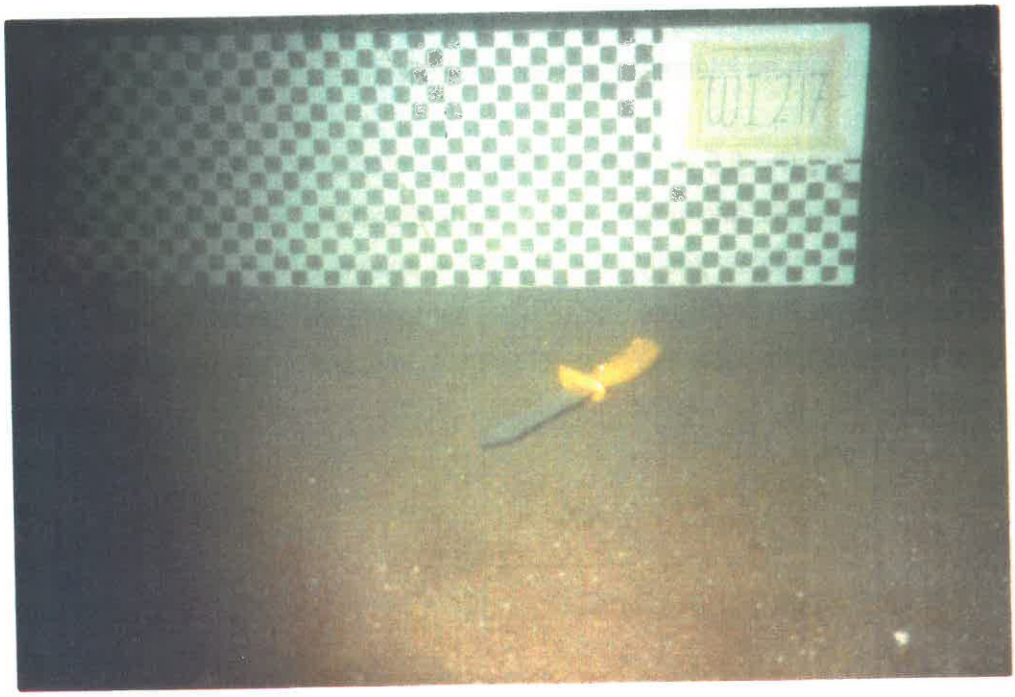

Figure 6.54. Flat featureless lower nearshore surface at Whiritoa (25 m water depth), formed on fine grained sediments (Mz= 2.20 ϕ). This indicates that either intense sheet flow conditions have occurred during previous storm conditions, or that small ripples have been degraded during calm conditions (note that the board shown in the photo is 1 m long).



Figure 6.55. Large, low relief ripples (λ= 0.5 m, η= 0.04 m) on the lower nearshore surface at Whangamata (29 m water depth) formed on medium grained sand (Mz= 1.11 ϕ). These are interpreted to have formed under antecedent storm wave conditions (note that the board shown in the photo is 1 m long).

under antecedent conditions associated with intense wave flows during annual storm events. This interpretation is again consistent with results from the textural analysis, which showed lower nearshore deposits to be moderately well sorted and extensively iron stained sands, such characteristics consistent with an intermittent reworking of sediments.

Bedforms of megaripple size (λ= 0.6 to 1.0 m) on the southern coast occur in narrow bands on the nearshore and mid shelf surface, and in most areas tend to dominate the inner shelf surface. They are usually characterised by coarser shelly sediments in the troughs than on their crests, and have a rounded symmetrical appearance (Figure 6.56). This is consistent with bedforms which have been observed in other studies to form under the action of storm waves, and subsequently degrade under calmer flow conditions (GILLIE, 1979). The megaripples usually occur as long continuous crested features in sonographs with a distinct sinuous or serpentine outline, a morphology supported by diver observations. This is characteristic of bedforms which form on coarse sands under the combined flow conditions of both oscillatory wave and mean flow conditions (NIEDORODA *et al.*, 1985b; LEE YOUNG and SLEATH, 1990). Thus, megarippled bedforms on the southern coastline are most likely formed by the combined flow conditions of relatively large storm waves and strong wind-generated currents. Evidence supporting this comes from their common occurrence in coarse deposits on the down-current flanks of larger-scale sand ridge bedforms. Thus, the oscillatory currents associated with storm waves appear to play an important role in the along-shelf transport of sediments, this role most likely being to entrain fine sands into suspension on the down-current flanks of sand ridges, where they are subsequently transported by wind-generated mean flows to the north or south.

Megaripple crests on the southern shelf are generally shore-parallel features striking at an angle of 180 to 135°, thus orienting them with an east to northeast wave direction. However, the orientation does vary in some areas, with nearshore and inner shelf bedforms generally oriented at a different angle to those on the mid shelf, thus indicating the latter form under different, probably more extreme wave conditions than the inner shelf megaripples. Also, the orientation of nearshore and inner shelf megaripples often shows high variation in areas associated with offshore islands and reefs (Onemana, Opoutere, Tairua), which indicates that wave refraction and hence wave focussing could be an important process in the formation of these coarse grained megaripple deposits. Evidence of wave focussing is particularly strong from bedform observations at Opoutere, where very large megaripples are present on coarse sands both north and south of Slipper Island (λ= 1.2 to 1.4 m), and very small ripples on fine nearshore sands behind Slipper Island (λ < 0.1 m)

It is not completely certain what bedforms exist in fine sands on the inner and mid shelf surfaces. Where these were observed by divers on the shallower parts of the inner shelf, small ripples with irregular crests were usually found. In other studies, hummocky megaripples are often observed on fine to very fine grained inner shelf deposits where combined wave and current flow conditions occur (NIEDORODA *et al.*, 1985 b; SWIFT and NUMMEDAL, 1987). However, no evidence for the existence of similar deposits was found from sonographs in this study. Previous investigations of

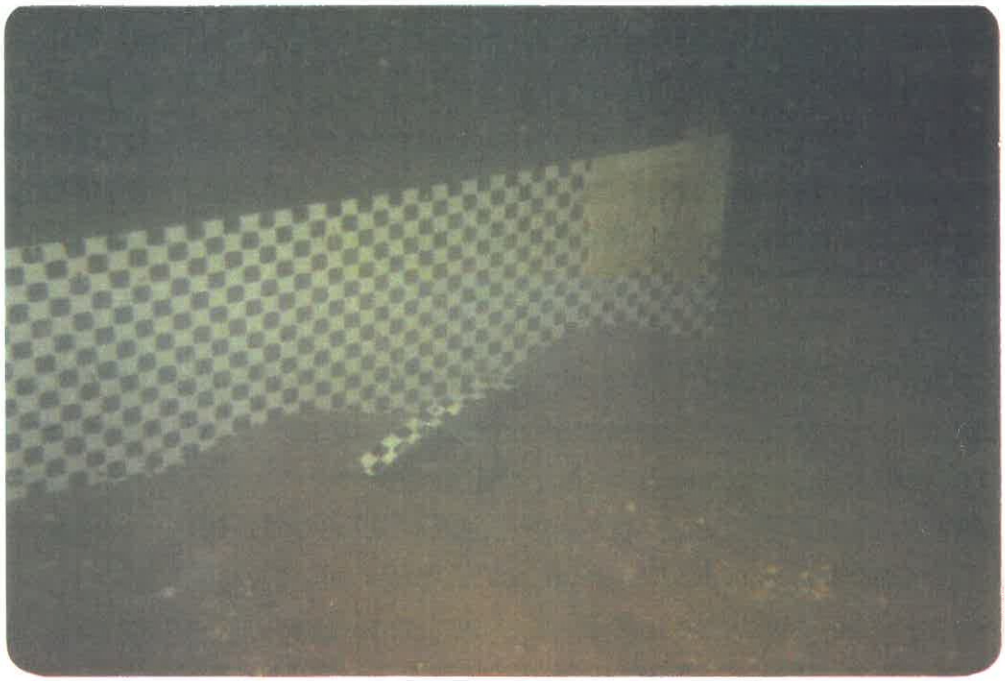

Figure 6.56. Megaripples (λ= 0.6 m, η= 0.07 m) on the inner shelf at Waihi Beach (23 m water depth) in medium sands (M_z= 1.02 ϕ). Note the coarse shelly sediments in the troughs, and the rounded nature of the megaripples. This is inferred to indicate that they formed under storm wave conditions, and have subsequently degraded during calm weather periods (note the board shown in the photograph is 1 m long).

mid shelf deposits on the northeast New Zealand coast by HILTON (1990) have shown that fine grained mid shelf deposits which occur adjacent to coarser megaripple sands are usually characterised by a flat featureless bed, with extensive evidence of bioturbation on their surface. As the textural characteristics of mid shelf deposits on the east Coromandel coast are very similar to Pakiri, it is likely that a flat and featureless surface dominates over fine mid shelf sediments in the study area.

Northern Coastline

The morphology of orbital ripples on the northern embayed coastline varies between embayments (Figure 6.57). Some of the largest bedforms are found in coarse sands on the nearshore and inner shelf between Hotwater and Hahei Beaches, with megaripples measuring up to λ= 1.3 to 1.15 m at respective locations (Figure 6.58). This gives some supporting evidence to the Hotwater Beach region as being one of the highest wave energy shelves in the study area. Megaripples here have the same morphology of those found on the southern coast, and are likewise interpreted as having formed under intense storm wave conditions, which from the strike of their crests (180 to 135°) would appear to be from east and northeasterly directions.

Fine grained nearshore sands off Hahei Beach are characterised by only small ripples (λ= 0.17 m; Figure 6.59). These occur adjacent to the coarse megaripple deposits, but have a different strike of 180° to an easterly wave approach. Therefore, each bedform would appear to have formed under different wave conditions. The small ripples are probably active under calm wave conditions, as shown by their similar asymmetrical crest pattern to ripples on the upper nearshore surface off southern coastal embayments. However, divers at the time of observation did not notice ripples at Hahei responding to the prevailing wave conditions.

Within Mercury Bay, no diver observations were made of the sea-bed and so it is uncertain what bedforms occur on the fine sand sub-strate. However, sonographs show that areas of coarse sand are characterised by megaripples (λ= 0.67 to 1.0 m) across depths of at least 7 to 30 m. Thus, sediments within Mercury Bay are reworked by wave orbital currents during storm conditions. As bedforms associated with wind-generated currents are only poorly developed within Mercury Bay, it is likely that waves are primarily responsible for sediment reworking, and that wind-generated currents play a more secondary role. The orientation of megaripple crests varies from northeast on the southern side of the bay, to more easterly in the northern bay area. This pattern probably shows the refraction pattern of wave rays as they enter Mercury Bay from the east during storm conditions.

Off Otama Beach, small to large ripples are the dominant bedforms on medium grained nearshore sands (λ= 0.06 to 0.5 m; Figure 6.60), with larger megaripples only being comparatively rare features. This supports earlier deductions that the Otama Beach shelf is an area of relatively low wave energy. The ripples observed by divers often have a trochoidal appearance, with sharp

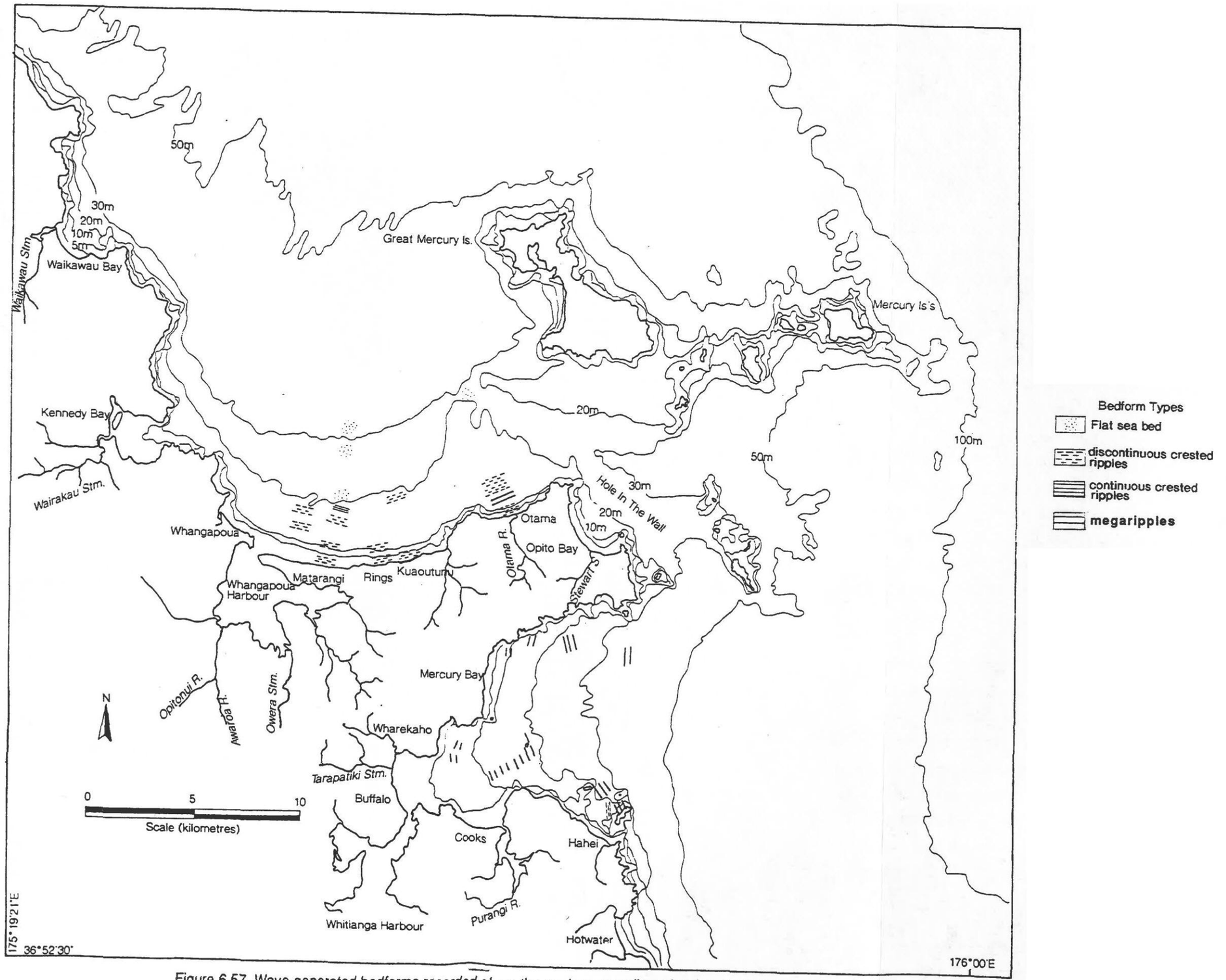

Figure 6.57. Wave-generated bedforms recorded along the northern coastline, showing, ripple types, crest pattern, and crest orientation.

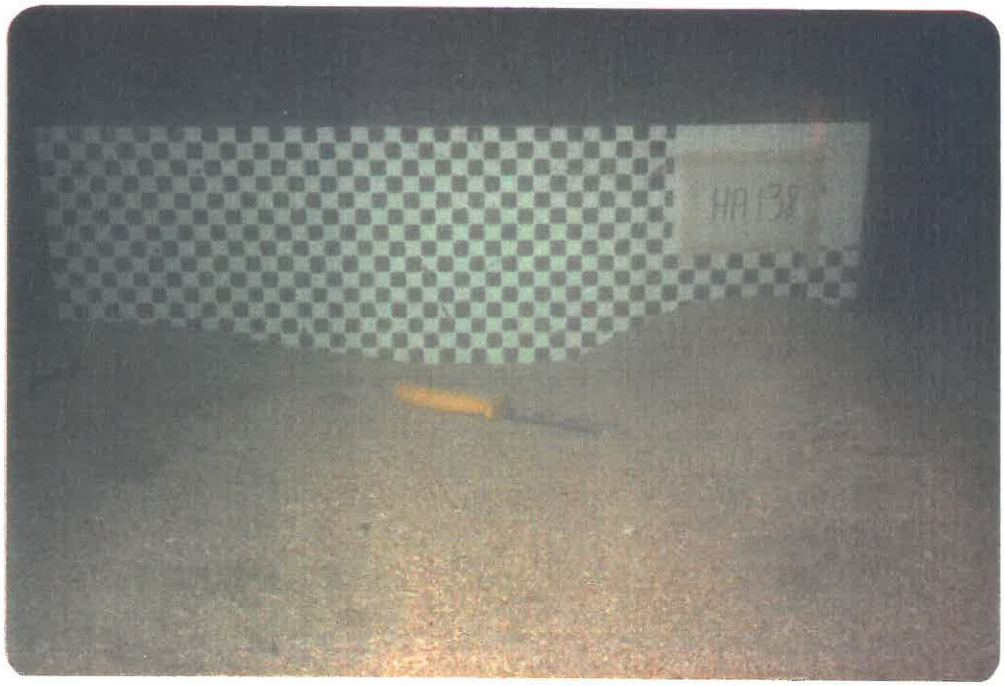

Figure 6.58. Megaripple bedforms (λ= 1.1.5 m, η= 0.20 m) in the nearshore zone (12 m water depth) at Hahei on coarse sand (Mz= 0.79 ϕ). Note the coarse shelly sediments in the trough, inferred to have formed by intense scouring under storm wave conditions (note the board shown in the photograph is 1 m long).

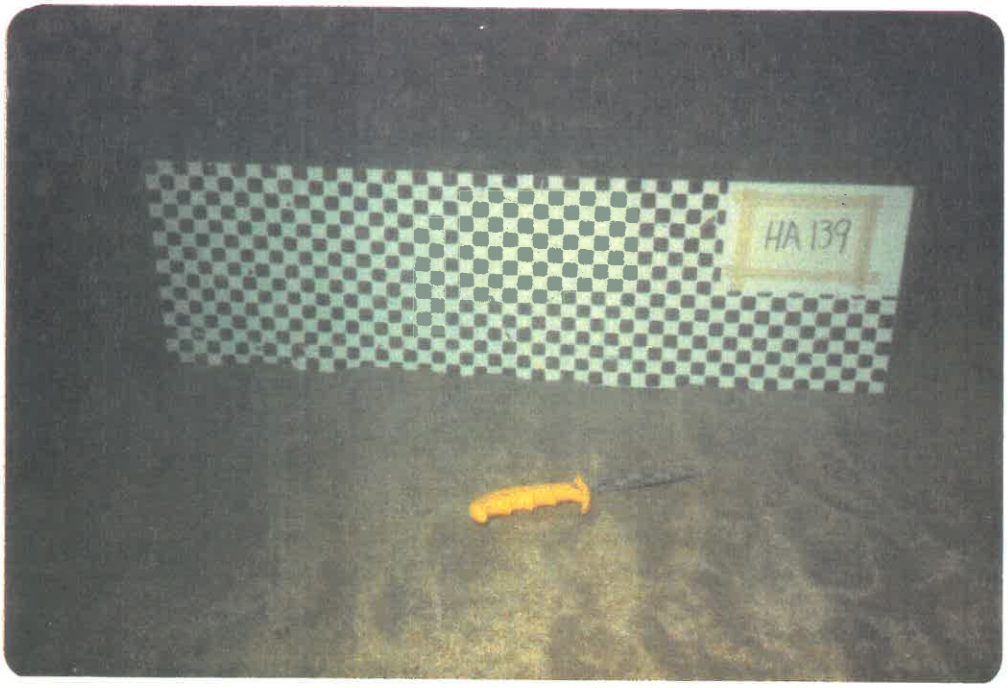

Figure 6.59. Small ripples (λ= 0.17 m, η= 0.02 m) in the nearshore zone (13 m water depth) at Hahei, formed on fine sand (Mz= 2.73 ϕ). These occur adjacent to the megaripples in Figure 6.58, but appear to have formed under calm wave conditions as shown by their discontinuous crest pattern and different orientation to the megaripple crests (note the board shown in the photograph is 1 m long).

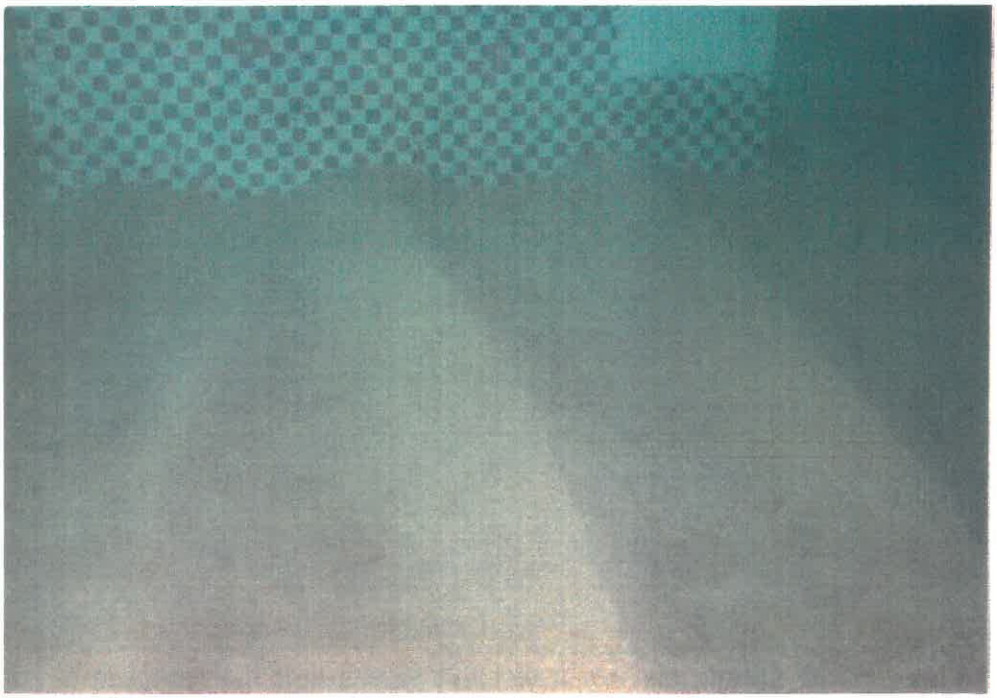

Figure 6.60. Large ripples (λ= 0.5 m, η= 0.06 m) in the nearshore zone (14 m water depth) at Otama, formed on medium sand (Mz= 1.25 ϕ). Note the trochoidal pattern of ripples, with sharp crests and relatively flat trough, suggesting that they are fairly recently developed bedforms (note the board shown in the photograph is 1 m long).

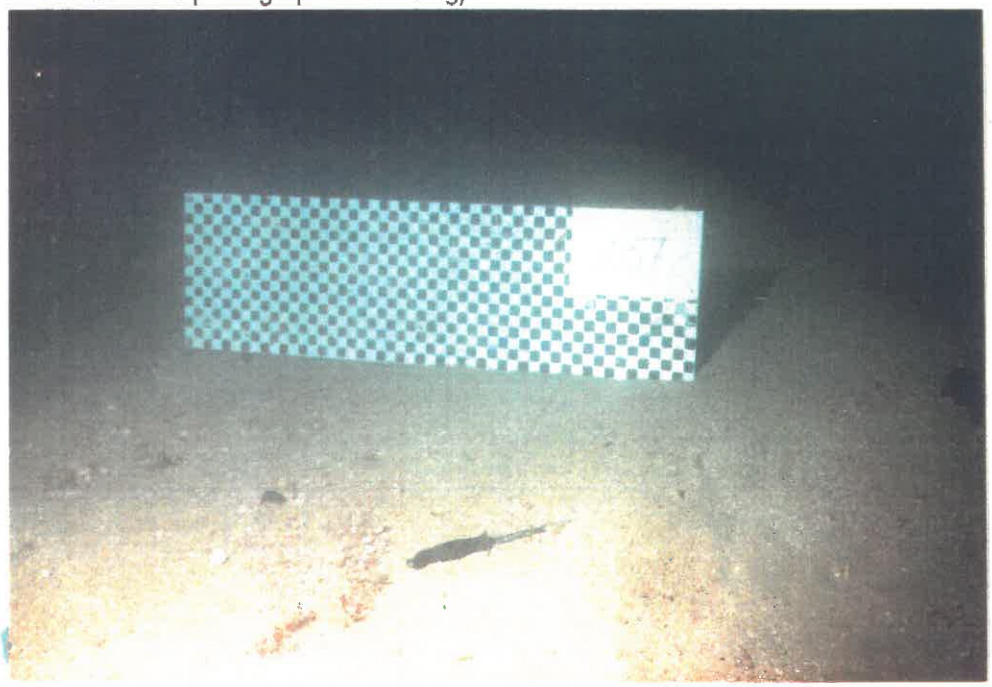

Figure 6.62. Flat featureless sea-bed on the Otama inner shelf (30 m water depth) on medium sand (Mz= 1.82 ϕ). This occurs just offshore from the Hole in the Wall channel, and is inferred to indicate the presence of intense tidal- and wind-generated flows (note the board shown in the photograph is 1 m long).

crests and flat troughs, which indicates that these were recently formed features at the time of observation (GILLIE, 1979). Ripple crests strike at an angle of 45°, orienting them to a northwest wave direction, which shows they are probably formed by waves refracted around Great Mercury Island from either a north or northeasterly direction. In deeper waters on the inner shelf (30 m), a flat featureless bed is found over similar medium grained sands (Figure 6.61). Thus, wave reworking appears to be confined to the nearshore surface, with either no wave interaction on the inner shelf, or any bedforms generated subsequently obliterated by tidal- and wind-generated currents through the Hole in the Wall channel.

Offshore from Whangapoua Harbour small ripples dominate the fine grained nearshore sands (λ= 0.05 to 0.2 m; Figure 6.62). These are usually discontinuous crested features, and were found to be active at the time of observation to depths of 14 m, with an onshore movement of sand occurring in depths of < 10 m. Thus the ripples indicate a net-onshore transport of fine sands occurring at Whangapoua under calm weather conditions. The strike of ripple crests varies from 45° off Rings and Kuaotunu Beaches, to 135° off Matarangi Beach, which is consistent with the pattern observed further east off Otama, and again probably results from the refraction of north and northeasterly waves around Great Mercury Island. Over the inner and mid shelf surfaces in depths > 20 m, only a flat featureless surface was observed by divers (Figure 6.63), which is often extensively colonised by live shell fish such as horse mussels and *Tawera spissa*. This indicates that only nearshore sands are frequently reworked by waves offshore from Whangapoua Harbour, with inner and mid shelf sands probably reworked by less frequent storm waves from the north and northeast.

6.4. CONCLUSIONS.

Analysis of the sea floor morphological features along the east Coromandel continental shelf indicates that variable sedimentation patterns, both across the shelf and along the coast, result from variations in the nature of modern hydrodynamic processes. Similar conclusions were reached following a detailed analysis of textural properties for surface sediments in Chapter 5.7. This showed that distinct textural properties occur at various water depths across the shelf surface between Waihi and Hotwater Beaches, but relatively uniform textural properties characterise the deeply embayed coastlines at Mercury Bay, Otama and Whangapoua. A detailed morphological analysis in this chapter has shown more conclusive evidence of the various hydrodynamic processes which cause these variations.

The major shelf morphological components off each embayment along the coast are illustrated in Figure 6.64, and their characteristic bedforms summarised in Table 6.2. An important observation is that off embayments between Waihi Beach and Opoutere, a distinct change in the cross-shelf morphological characteristics occurs at the same depth ranges that different sediment textural properties were identified in Chapter 5. These distinct morphological characteristics can be summarised as follows:

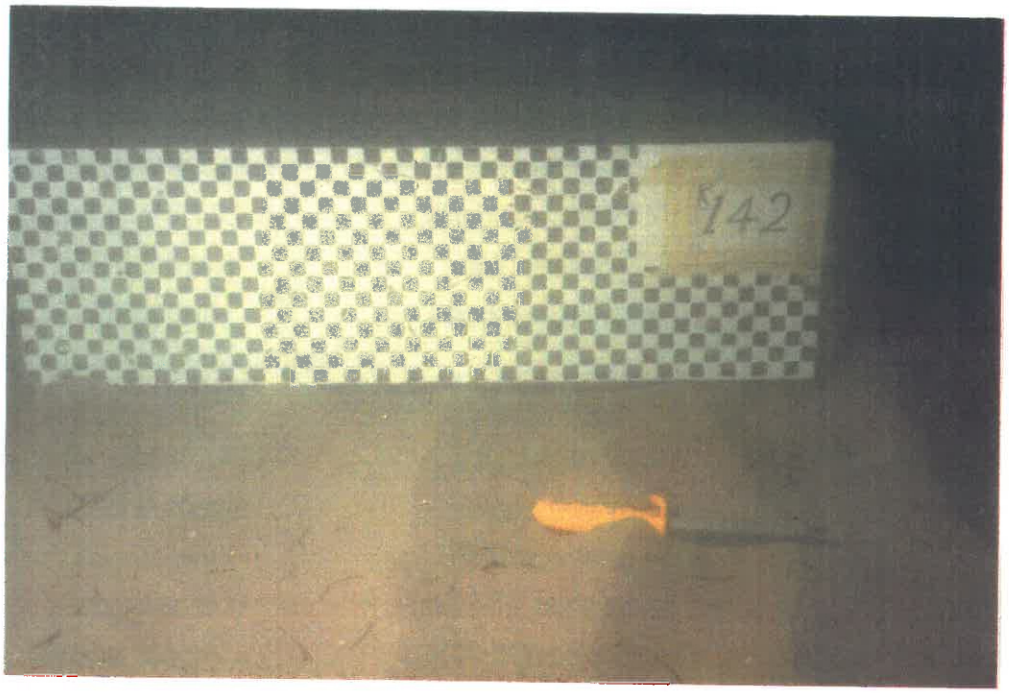

Figure 6.62. Small ripples (λ= 0.2 m, η= 0.04 m) in the Whangapoua nearshore zone (10 m) formed on fine sand (M_z= 2.41 ϕ). These were observed by divers to actively respond to the prevailing calm wave conditions (H= 1.5 m; T= 6 s), and indicate an onshore transport of fine sands in the nearshore zone (note the board shown in the photograph is 1 m long).



Figure 6.63. Flat featureless sea-bed in the Whangapoua inner shelf zone (21 m) formed on fine sands (M_z= 2.28 ϕ). This pattern continues out across the inner and mid shelf surface, and is inferred to indicate very low energy conditions beyond the nearshore zone. Evidence supporting this comes from the extensive live shell fish beds on the inner shelf, evident in the photograph (note the board shown in the photograph is 1 m long).

Table 6.2. Summary of the dominant morphological characteristics observed in this study for the shelf surface at each major embayment along the east Coromandel coast.

Location	Nearshore Morphology	Inner Shelf Morphology
Waihi Beach	< 20 m water depth, gradient 1:180, active small ripples.	> 20 m water depth, gradient 1:1000, megaripples, sand ribbons, waves and ridges.
Whiritoa Beach	< 30 m water depth, gradient 1:125, active small ripples (5-20 m), flat sea-bed (20-30 m), sand ridges (10-30 m).	20-45 m water depth, gradient 1:200, megaripples, sand ridges.
Whangamata Beach	< 30 m water depth, gradient 1:120, active small ripples (5-20 m), large ripples (20-30 m), sand ridges (20-30 m).	30-45 m water depth, gradient 1:200, megaripples, sand ridges.
Onemana Beach	< 27 m water depth, gradient 1:110, small ripples, sand ridges (20-27 m).	>27 m water depth, gradient 1:350, megaripples.
Opoutere Beach	< 25 m water depth, gradient 1:70, small active ripples, sand ridges (10-25 m).	> 25 m water depth, gradient 1:170, megaripples.
Pauanui Beach	< 22 m water depth, gradient 1:140, sand bars (5 m depth).	>22 m water depth, gradient 1:280, megaripples.
Tairua Beach	< 20 m water depth, gradient 1:130.	> 20 m water depth, gradient 1:130, megaripples.

Table 6.2. continued

Location	Nearshore Morphology	Inner Shelf Morphology
Hotwater-Hahei Beaches	< 28 m water depth, gradient 1:75, small ripples, megaripples.	> 28 m water depth, gradient 1:90, megaripples.
Mercury Bay	< 20 m water depth, gradient 1:290, megaripples, sand waves.	> 20 m water depth, gradient 1:290, megaripples.
Otama Beach	< 15 m water depth, gradient 1:180, small & large ripples.	> 15 m water depth, gradient 1:440, flat bed, sand ridges.
Whangapoua	< 20 m water depth, gradient 1:200, small ripples (active < 10 m).	20-33 m water depth, gradient 1:250, flat bed.

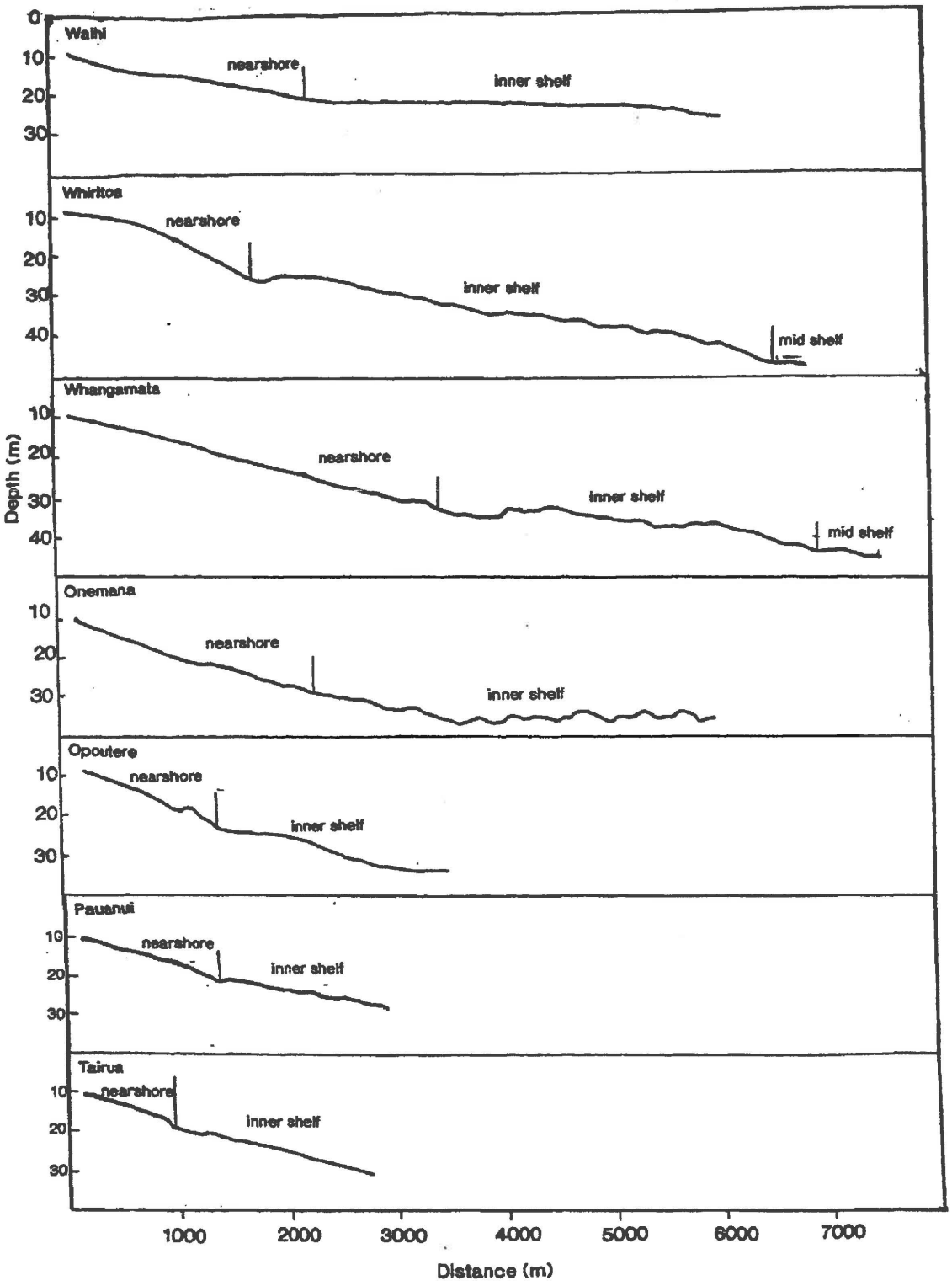

Figure 6.64. Summary diagram of the major shelf morphological components off each east Coromandel embayment, based on soundings obtained in this investigation.

Figure 6.64. (continued).

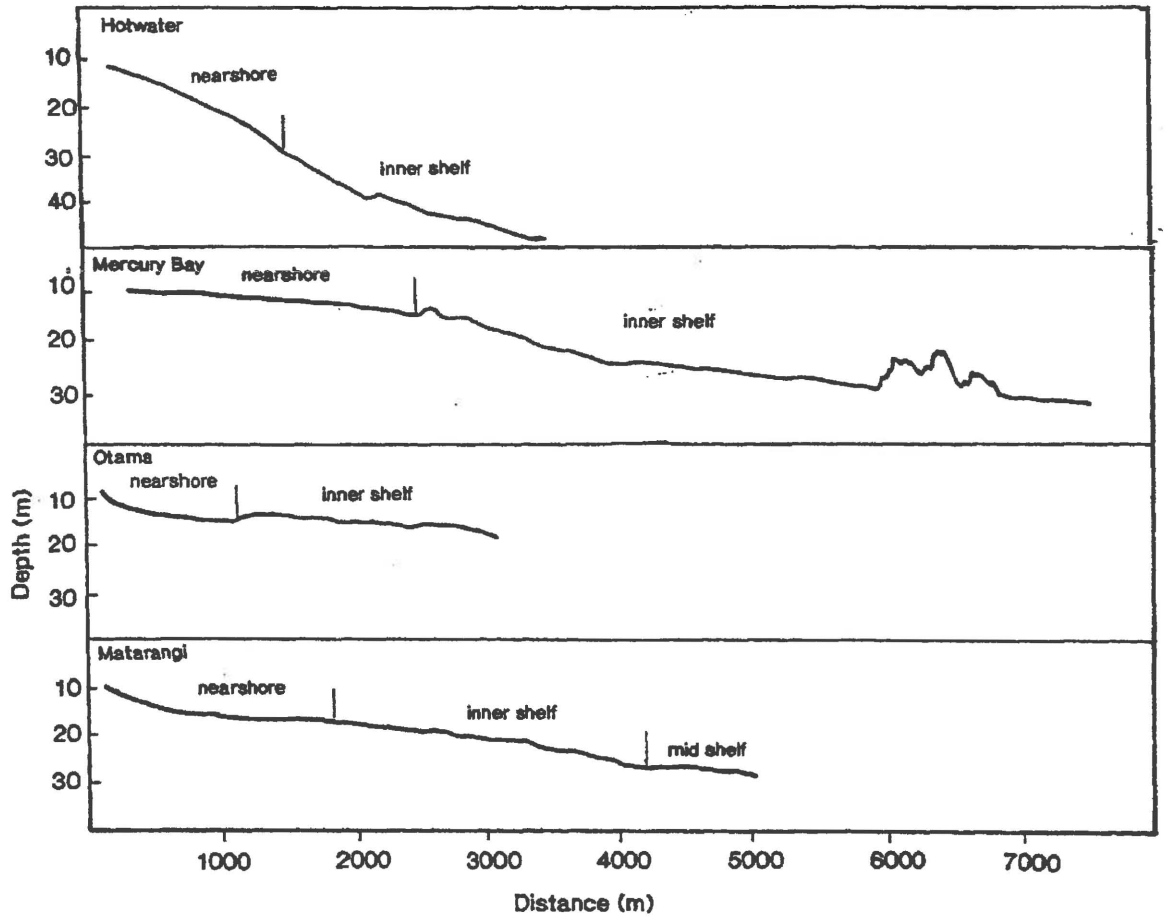

1. A steeply dipping upper nearshore surface (~ 1:150) from depths of 5 to 20 m, which varies in outline from a concave- to convex-up curvilinear surface. This is dominated by the occurrence of fine sediments that are actively reworked into small ripples by waves. However, some transport by wind-generated currents to the north is also evident from the occurrence of small sand ridges (η= 1.0 to 1.5 m) in locations such as Whiritoa and Opoutere. Thus, wind-generated currents may form a secondary mode of transport for upper nearshore sands during storm conditions.

2. A similar steeply dipping, but more concave-up curvilinear lower nearshore surface in most locations (except Waihi Beach) from depths of 20 to 25-30 m, which is also dominated by fine sediments. These are however reworked into either a flat sea-bed or large ripples by less frequent, but more intense, storm waves. Bands of CMR sands oriented perpendicular to the coast are also common on this lower nearshore surface, and are associated with the presence of relatively large sand ridges (η= 1.5 to 7.4 m). Thus, lower nearshore sands appear to be reworked by wind-generated currents to the north during episodic storm conditions.

3. A noticeably flatter and slightly convex-up inner shelf surface from depths of 22 m at Waihi, and 25 to 30 m between Whiritoa and Opoutere. This is characterised by varying degrees of both coarse and fine sediments at different locations. Sinuous crested megaripples are the characteristic bedform developed over coarse inner shelf sediments, and are inferred to form by orbital currents associated with intermittent storm waves. However, wind-generated currents appear to be very important in the transport of inner shelf sediments, as shown by the presence of numerous sand ridges, which vary in relief from η= 0.5 to 2.5 m. Variations in the direction of currents appears to occur over the inner shelf surface. These are inferred to be largely responsible for the differences in sedimentation patterns which occur along the coast. Areas of extensive erosion at Waihi Beach and from Whangamata to Opoutere, are characterised by fields of CMR deposits over a relatively flat and featureless inner shelf surface, and may result from either intense current flows or a divergence in the transport of fine sediments by wind-generated currents. Areas of more extensive deposition for fine sediments at Mataora and Whiritoa are often associated with sand ridges of varying orientation, and are inferred to result from either a decrease in intensity or change of direction of current flows. Areas of localised erosion and deposition on the inner shelf at Opoutere may also result from the refraction and focussing of storm waves around Slipper Island.

4. A flatter mid shelf surface seawards of ~ 45 m water depth at Whiritoa and Whangamata, which is characterised by both wave-generated megaripples (on coarse deposits) and current-generated sand ridges. The mid shelf zone is therefore a more dynamic environment than indicated by the sediment textural analysis. Conditions which mobilise mid shelf deposits probably occur less frequently than for shallower shelf sediments, as shown by the different orientation of megaripples here than on the inner shelf and nearshore surfaces. The sediment transport direction of mid shelf deposits also appears to change between Whiritoa and Whangamata, which may further influence the extensive deposition of fine sediments off Whiritoa.

North of Opoutere Beach, offshore variations in broad shelf morphology tend to be less distinct, particularly between the nearshore and inner shelf. However, variations between each embayment are more noticeable. This is inferred to partly result from a decreasing influence of wind-induced currents, and increasing influence of wave-induced currents off most embayments, as shown by a general lack of current-generated bedforms.

At Hotwater Beach, a very steep shelf surface is present out to 50 m water depth. The nearshore surface is distinguished here by having a steeper convex-up outline, and in being composed of fine sediments, whereas the inner shelf is slightly flatter and dominated by Coarse Megarippled sediments. However, there is no evidence of changing hydrodynamic conditions from wave- to current-dominated transport across these morphological zones.

Within Mercury Bay, the shelf is relatively flat and dominated by fine sediments from 5 to 30 m water depth. The nearshore zone can be distinguished by its convex-up curvilinear surface, whereas the inner shelf has a more concave-up outline. The presence of megaripples in isolated areas of coarse sediments across the shelf indicates that storm waves are important for the intermittent reworking of both nearshore and inner shelf sediments. However, some reworking of sediments by currents also appears to occur (though less intense than on the southern coast), as shown by the presence of small shore-normal oriented sand waves at Wharekaho and Waitaia Beaches. These appear to be concentrated in shallow waters (5 to 20 m) around the periphery of Mercury Bay, and are possibly associated with a clockwise downwelling circulation pattern.

The shelf off Otama Beach is dominated by coarse sediments, however it does show a distinct change from a steep concave-up curvilinear nearshore surface, to a much flatter convex-up inner shelf. As with embayments south of Opoutere, this distinct change in shelf morphology appears to be associated with variations in hydrodynamic conditions, from wave-dominated on the nearshore surface (as shown by the presence of ripples), to current-dominated conditions on the inner shelf (as shown by the absence of wave-generated bedforms, and presence of sand ridges).

West of Otama at Matarangi Beach, the shelf shows a more consistent morphology, with a relatively flat surface dominated by fine sediments. The nearshore and inner shelf zones are distinguished by an offshore change from a concave-up to more convex-up surface. A flatter mid shelf surface also appears to be present in 30 m water depth, where slightly muddy sediments are indicated from the textural analysis. Nearshore sediments appear to be consistently reworked by shoaling waves, as shown by the presence of small bedforms. However, both inner and mid shelf sediments appear to be relatively inactive, as shown by the absence of wave- or current-generated bedforms, and extensive occurrences of live shell fish colonies.

An important aspect of the sonograph surveys is the evident change in shelf sedimentation patterns and morphology following the extreme storm event of Cyclone Bola in March 1988. The most dramatic response occurred on the shelf surface between Whiritoa and Onemana. Here,

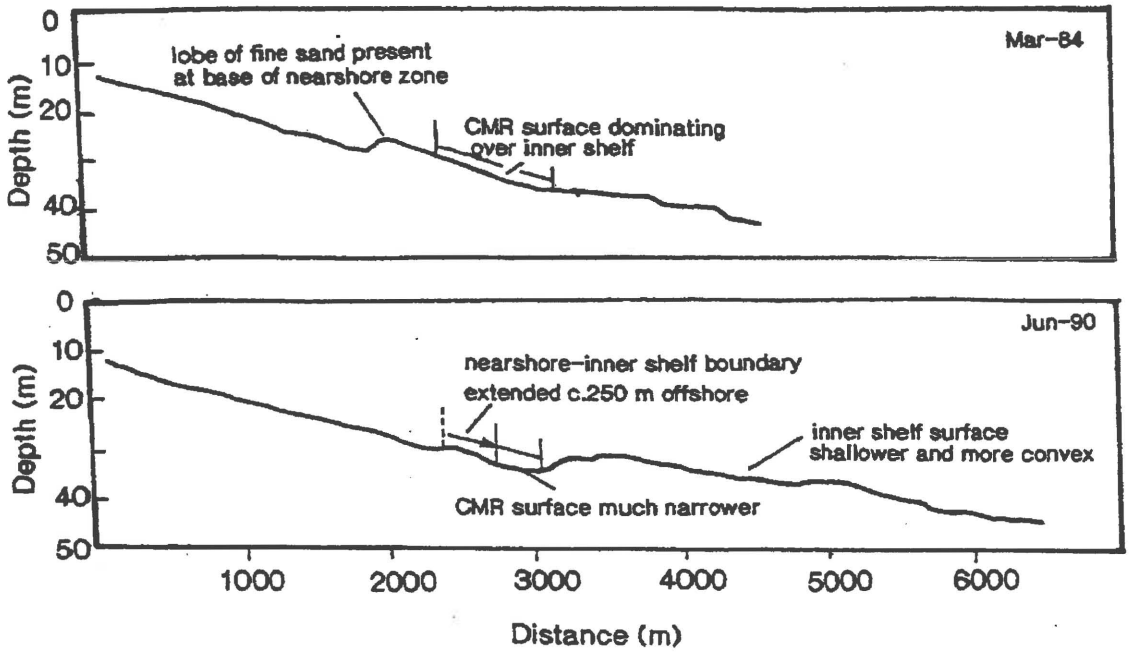

Figure 6.65. Summary diagram of the changes in shelf morphology on the southern exposed coast following Cyclone Bola in Mar-88, based on surveys off Whangamata. Note the accretion of fine sands at the base of lower nearshore surface in Mar-84, and subsequent erosion and redeposition over CMR deposits on the inner shelf in Jun-90.

sonographs typically showed a seaward increase in the occurrence of fine sediments over previous CMR deposits on the inner shelf. Offshore bathymetric profiles, particularly off Whangamata Beach, indicate that these changes were associated with a reduction in the level of the lower nearshore surface in the order of 1 to 4 m, and a similar scale increase in the elevation of the inner shelf surface (Figure 6.65). Changes in offshore sedimentation patterns also appear to have occurred at Waihi, where an increase in the occurrence of fine sediments in sand waves and ribbons over the flanks of sand ridges was observed on sonographs. Thus the surveys provide good evidence that along the southern exposed coastline, extreme storm events such as Cyclone Bola cause extensive erosion of the lower nearshore surface, and deposition of these fine sediments further offshore over the inner shelf surface.

Within Mercury Bay, very few significant changes in the offshore sedimentation patterns were identified after Cyclone Bola. Small changes may have occurred with the formation of a larger patch of CMR sand off Cooks Beach, where only smaller elongate CMR bands had been previously present. Thus, Cyclone Bola may have caused an increased scouring of the shelf surface in this area, which could be important in the light of the erosion problems the northern end of Cooks Beach has experienced during past extreme storm events. One possible explanation for this is that scouring of the sea floor here is associated with wave refraction and focussing around Motukorure Island, which may also cause higher waves to impact on the northern end of Cooks Beach, a possibility investigated in the study of wave refraction patterns in Chapter 7.4. Another apparent response to Cyclone Bola is the formation of sand waves east of Wharekaho Beach by relatively strong downwelling currents. However, in general the deeply embayed shelf within Mercury Bay appears to have been either insignificantly affected by Cyclone Bola, or had fully recovered from any erosional effects within the two years following its occurrence. This may reflect the lower current energy environment within Mercury Bay compared to the exposed southern coastline, and the more extensive deposition of modern terrigenous sediments which is inferred to occur within Mercury Bay.

CHAPTER SEVEN

SHELF MORPHODYNAMICS

7.0. INTRODUCTION

In the preceding chapter on nearshore and inner shelf morphology, some broad interpretations were made about the various hydrodynamic conditions operating along the coast and across the shelf, based on bedform character and distribution. In this chapter a more detailed assessment of the hydrodynamic conditions forming the bedforms is made, based largely on theoretical considerations of wave and current dynamics. Some field data are also presented on the dynamics of the smaller scale morphological features (ripples and megaripples) from depth of activity rod surveys. The chapter aims to interpret the morphodynamics of the east Coromandel shelf, by examining the causal links by which different hydrodynamic conditions interact to generate and modify the nearshore and inner shelf morphological features (WRIGHT and THOM, 1977).

7.1. HYDRODYNAMIC INTERPRETATIONS OF WAVE-GENERATED BEDFORMS

In Chapter 6 the morphology of wave-generated bedforms (ripples and megaripples) was described in detail. Hydrodynamic interpretations were restricted to inferences about whether calm or storm wave conditions were likely to have generated these features. However other studies, such as that by CLIFTON and DINGLER (1984), have shown that wave-generated bedforms are diagnostic of the wave conditions which generate them, and that they reflect not only the velocity and direction of wave-orbital currents, but also the length of the horizontal component of orbital motion and the presence of velocity asymmetry in the flow. Thus, the morphology of ripples and megaripples can be related via standard wave theories to different kinds of wave conditions that generate the features.

7.1.1. Theoretical Background

CLIFTON and DINGLER (1984) have outlined an approach that allows aspects of the wave climate to be reconstructed from theoretical considerations of bedform geometry and existing wave theories. The procedure first involves inferring wave flow parameters from oscillation ripple configuration. Two important parameters are determined, the maximum orbital velocity (U_m) and the wave orbital diameter (d_o), based on existing laboratory and field investigations of bedform responses to different wave conditions. The method is only suitable for bedforms generated by symmetrical orbital flows, as little is presently known about the degree of velocity asymmetry required to form asymmetrical ripples.

Estimates of orbital velocity are based on threshold criteria for grain movement and sheet flow. Under the influence of wave-orbital currents, ripples form quickly upon the initiation of grain movement (DINGLER, 1974). Ocean wave conditions that result in the initial movement of sediments have been examined by KOMAR and MILLER (1973), and found to be dependent on both grain diameter (D) and wave period (T). Two relationships exist for grain sizes, whether less or greater than 0.5 mm, the difference due to the breakaway from laminar to turbulent near-

flow conditions (RIGLER and COLLINS, 1984). DINGLER (1979), in a separate experimental study, found that motion for grain sizes between 0.18 and 1.454 mm (i.e. 2.5 to 0.5 ϕ) commenced when:

$$U_m = 52.4\ (TD)^{1/2}\ cm.s^{-1} \qquad -7.1.$$

for quartz sand in water. Threshold curves from both KOMAR and MILLER (1975) and DINGLER (1979) are shown in Figure 7.1. These indicate that for any particular grain size, a longer period wave requires a higher orbital velocity to initiate grain movement than a comparatively shorter one. In this study, Eq. 7.1 has been applied as it covers the range of grain sizes present along most of the east Coromandel shelf.

Threshold velocities for the onset of sheet flow conditions have been calculated for quartz sand by DINGLER and INMAN (1977) as:

$$U_m = 19.9\ (gD)^{1/2} \qquad -7.2$$

where g is the acceleration of gravity. However, CLIFTON and DINGLER (1984) warn that this is based on a rather narrow range of grain sizes (D = 0.128 to 0.158 mm, or 2.5 to 3.0 ϕ), and that extrapolation beyond this range must be treated with caution.

It should be noted that these relationships are based on sediment movement on a flat bed by the action of wave-orbital currents alone, whereas natural conditions on the east Coromandel have been shown in Chapter 6.3. to involve a pre-existing rippled or megarippled surface, and the presence of combined wave and current flows. Both of these effects have been observed in experimental studies to significantly lower the threshold velocity required for sediment movement (BAGNOLD, 1963; SOUTHARD and DINGLER, 1971). Consequently, Eq. 7.1 and 7.2 probably represent an oversimplification of natural flow conditions.

Estimates of orbital diameter are derived from the relationship between ripple spacing and grain size. CLIFTON (1976) subdivided oscillation ripples into three broad types, based on plots of λ/D and d_o/D for data obtained from numerous laboratory and field observations (Figure 7.2). Orbital ripples have wavelengths that are directly proportional to the orbital diameters of the associated shoaling waves. MILLER and KOMAR (1980b) found this relationship can be approximated by

$$\lambda = 0.75.d_o \qquad -7.3$$

These generally form in shallow water under the influence of short period waves. Suborbital ripples form under longer period waves, and their spacing is a function of both orbital diameter and grain size, with λ tending to decrease as d_o increases (CLIFTON and DINGLER, 1984). MILLER and KOMAR (1980a) suggest that ripple growth ceases where :

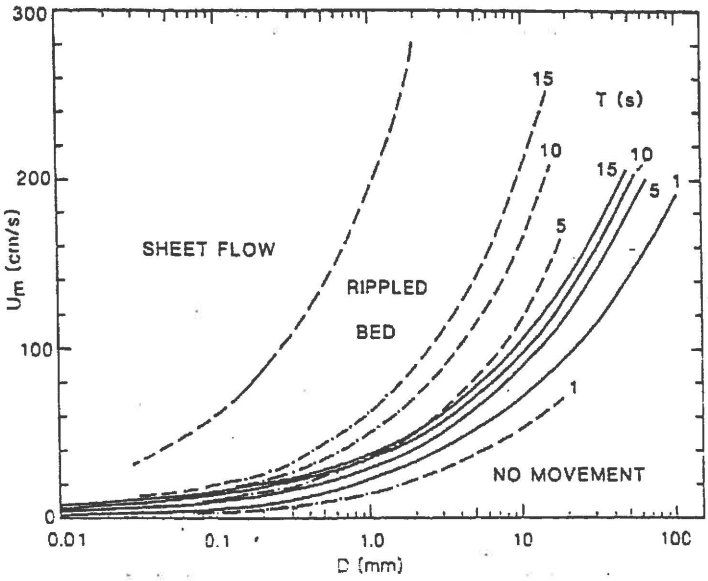

Figure 7.1. Velocity thresholds for grain movement and sheet flow of quartz sand in water. Solid lines are threshold curves of KOMAR and MILLER (1975). Dashed lines connected by dots are threshold curves of DINGLER (1979) in the range of experimental evidence; dots are absent where curves are extrapolated. Threshold curve for sheet flow, from DINGLER and INMAN (1977), is solid in the range of experimental evidence, and dashed where extrapolated (from CLIFTON and DINGLER, 1984).

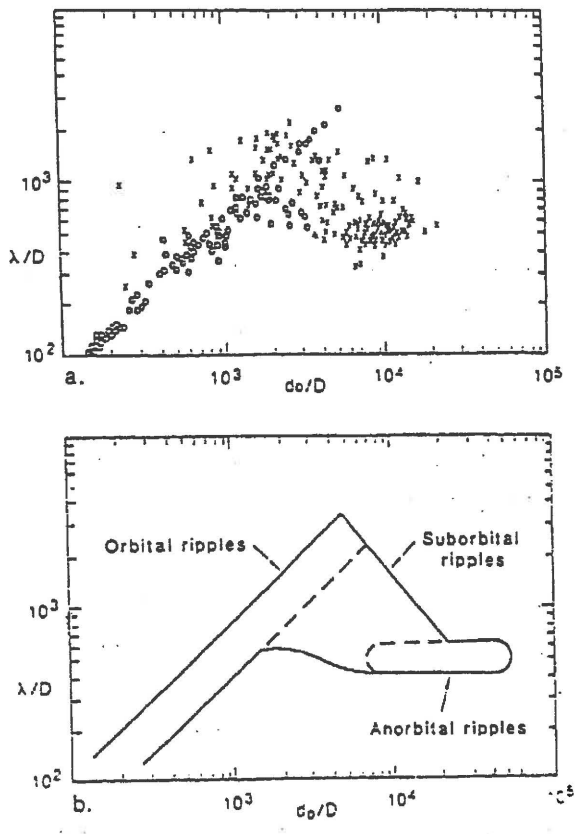

Figure 7.2. a) Plot of ripple spacing to grain size against ratio of orbital diameter to grain size (x = field observations, o = experimental); b) classification of ripples based on the distribution shown in a) (from CLIFTON and DINGLER, 1984).

$$\lambda = 14.7\ D^{1.68} \times 10^3 \qquad -7.4$$

with λ and D both measured in units of cm. Anorbital ripples form where orbital diameters are very large, and their spacing is dependent solely on grain diameter. They are most commonly generated on fine sand and have wavelengths of λ= 0.05 to 0.10 m (CLIFTON and DINGLER, 1984).

Another descriptive scheme for wave-formed ripples is based on the ratio of ripple steepness (λ/η) and grain size (CLIFTON and DINGLER, 1984). This includes vortex ripples and post-vortex ripples. Vortex ripples form at the onset of sediment movement by wave action, and are characterised by relatively constant steepness values of about 0.15, and a range of about 0.12 to 0.22, with both ripple height and wavelength changing together under increasing wave intensity (DINGLER and INMAN, 1977). This continues until very strong flows occur, where steepness then decreases as sand is stripped from the ripple crests to form post-vortex ripples. While this scheme also presents an empirical relationship between bed ripple morphology and orbital diameter, it is generally avoided as the dependence on ripple height will cause inaccuracies where this has been altered by faunal activity, compaction, or post-depositional processes (CLIFTON and DINGLER, 1984).

KOS'YAN (1988) proposes that many wave-generated bedforms are passive ripple marks, which form just before a storm begins to abate and tangential stresses on the sea-bed become too small to move individual grains. At this point, the ripple dimensions will remain stable. Thus KOS'YAN (1988) concluded that parameters of λ and η can only be used to determine wave conditions towards the end of an individual storm event, and will never show the peak storm conditions. He also found several relationships between parameters of ripple height (η), spacing (λ), and grain diameter (D):

$$\lambda = (83.5 \pm 2)\ D^{1.08 \pm 0.03} \qquad -7.5$$

$$\eta = (17.3 \pm 0.5)\ D^{1.22 \pm 0.03} \qquad -7.6$$

$$\lambda/\eta = 0.207\ D^{0.14} \qquad -7.7$$

Plots of ripple size against grain diameter can thus be used to establish whether bedforms are dependent or independent of wave orbital diameter, and thus whether Eq. 7.3 is applicable.

Once flow parameters (U_m and d_o) have been estimated from the bed configuration, these can be related to wave height and period by applying an appropriate wave theory (Airy, Stokes, Cnoidal, or Solitary). Although each wave theory is most applicable under a specific set of conditions of

wave height, wave period, and water depth (see Figure 3.1), CLIFTON and DINGLER (1984) apply Airy wave theory, as Le MEHAUTE *et al.* (1969) have shown that it provides a reasonable approximation to measured orbital diameters and near-bottom maximum velocities for finite amplitude waves in shallow water. Various equations for calculating wave flow parameters in Airy wave theory are extensively discussed in KOMAR (1976), and only presented where appropriate to the discussion.

In Airy wave theory, the orbital diameter (d_o) at the sea floor is calculated by:

$$d_o = \frac{H}{\sinh(kh)} \qquad -7.8$$

where H = the wave height, k is the wave number ($2\pi/L$), and h = the water depth. The maximum orbital velocity (U_m) under the wave crest at the sea-bed is calculated by:

$$U_m = \frac{\pi H}{\sinh(kh)} \qquad -7.9$$

Rearranging Eq. 7.8 and 7.9 such that:

$$H = d_o \sinh(kh) \quad = \frac{U_m T \sinh(kh)}{\pi} \qquad -7.10$$

allows wave height to be calculated for a selected series of water depths under waves of different periods, using the variables of d_o and U_m derived from the wave-generated bedforms. These calculations require the surface gravity wavelength (L) to be determined, which for deep water ($h/L_\infty > 0.25$) conditions:

$$L_\infty = \frac{g T^2}{2\pi} \qquad -7.11$$

and in shallow water ($h/L_\infty < 0.05$) conditions:

$$L_s = T (gh)^{1/2} \qquad -7.12$$

However, for intermediate water conditions ($0.05 < h/L_\infty < 0.25$), wave length is more complex to calculate as it involves an unknown variable (L) on both sides of the equation:

$$L = \frac{g T^2}{2\pi} \tanh \frac{2\pi h}{L} \quad = L_\infty \tanh(kh) \qquad -7.13$$

The problem is resolved by dividing both sides of Eq. 7.13 by the water depth (h) and rearranging such that:

$$\frac{h}{L_\infty} = \frac{h}{L}\tanh(kh) \qquad \text{- 7.14}$$

This expression has been solved by WIEGEL (1954) and presented in tabular form in the Shore Protection Manual (U.S. Coastal Engineering Research Centre, 1973). These tables can then be used to compute wave height for various combinations of wave period, wave length, and water depth using Eq. 7.10. Limitations on the size of waves at any water depth are a useful constraint to the combination of solutions possible from the wave equations. In coastal waters outside of the surfzone, wave size is limited under breaking conditions where $H > L_\infty/7$ (MICHE, 1944).

Thus, oscillatory ripples can be used to indirectly determine the range of wave sizes that could generate their morphology, provided it can be established that these wave conditions exceeded sediment threshold velocities, and that ripple spacing is only dependent on wave orbital diameter.

7.1.2. Interpretation of Wave Conditions from Ripple and Megaripple Observations

Possible wave conditions responsible for the generation of the ripple and megaripple bedforms are analysed by applying the CLIFTON and DINGLER (1984) method. The first step is to determine what range of representative wave periods to use in the analysis. Despite the fact that no direct measurements of wave conditions have been obtained from the east Coromandel coast, observations from other studies on the northeast coast (see Chapter 2.3.2.) indicate that wave periods of T = 6 to 13 s probably occur under conditions ranging from fair weather to extreme storms. To gain the most representative range of values for the east Coromandel coast during the bedform surveys, wind data collected for current analysis (Chapter 4.3.) were used to hindcast wave conditions during storm events. This was undertaken using the University of Waikato, Earth Science Department program WAVES. The JONSWAP method was applied, as the study area should represent a fetch- and often duration-limited situation when wave-generating cyclonic depressions migrate over the east coast (HARRIS, 1985). From the results output by the program, the component wave heights are calculated using the equation

$$H_c = (8S(f)Df)^{1/2} \text{ (de LANGE, 1988)} \qquad \text{- 7.15}$$

where Df = frequency interval and S(f) = spectral energy for a given period. Also obtained from the program output is the significant wave heights and periods for each event. Results are plotted in Figures 7.3 a and b, and show a range of wave conditions from T = 4 to 10 s, and H = 1.0 to 3.0 m. Findings by HAY (1991) for storm wave conditions over a 27 year period on the Bay of Plenty coast are also presented in Figure 7.3 c, and show a similar range of wave conditions to

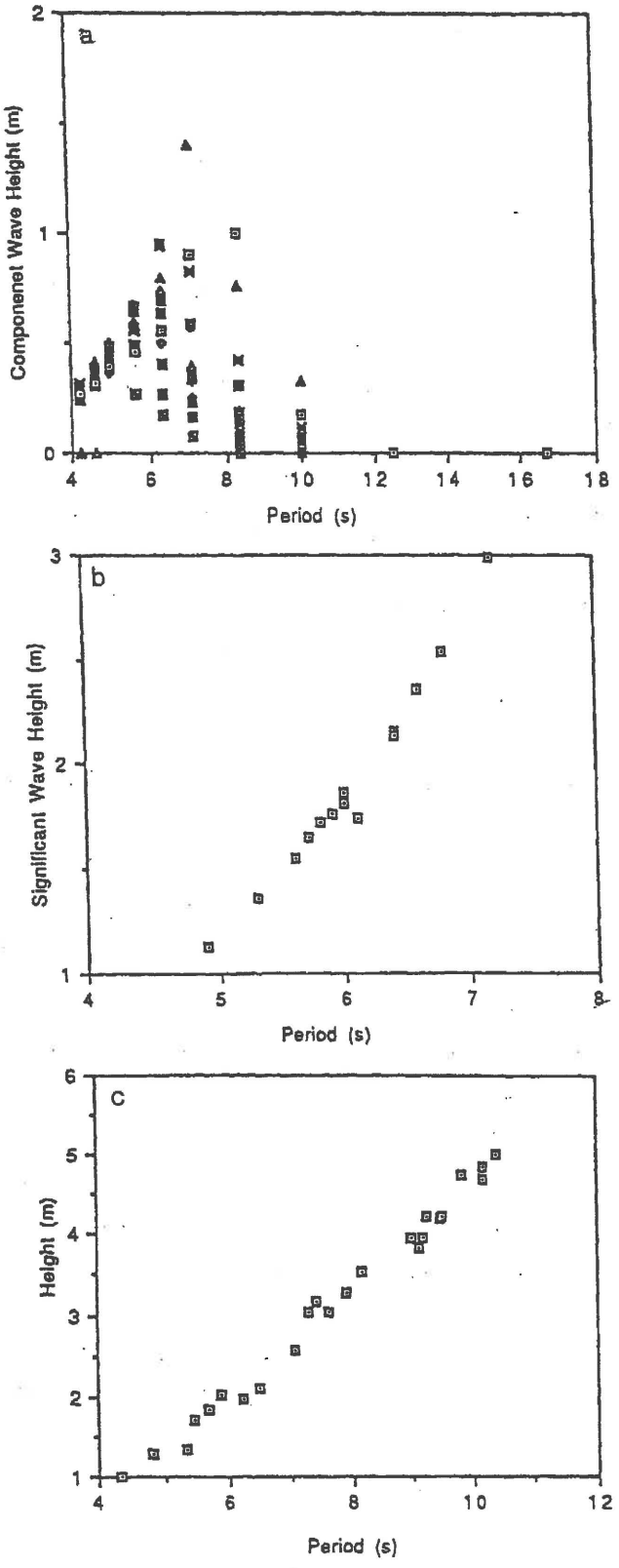

Figure 7.3. Representative wave parameters for the east Coromandel coast: a) Component wave parameters hindcast from wind data obtained between Jun-85 and Jan-87 at Whiritoa; b) significant wave height and period from the same source as (a); and also from media observations c) along the western Bay of Plenty coast reported by HAY (1991).

the hindcast values in this study (T = 4 to 10 s, H = 1.0 to 5.0 m). For this analysis, it was therefore decided to concentrate on wave periods of 6, 8, 10, and 12 s, and to also include periods of 14 and 16 s to allow for the influence of relatively rare extreme storm wave conditions.

Bedform Analysis

Before applying the CLIFTON and DINGLER (1984) technique, it is necessary to establish whether the bedforms observed are dependent for their ripple spacing on the orbital diameter of waves. This was determined by plotting ripple dimensions (λ, η) observed by divers against the mean grain diameter of samples collected from the bedforms (Figures 7.4 a, b). The wavelength of the bedforms appears to be dependent on grain size, and follows a similar trend to Eq. 7.5 for D < 0.4 mm and λ < 0.50 m. However, above these values ripple spacing seems to be independent of grain size (Figure 7.4 a). Plots of bedform heights (Figure 7.4 b) also show these to be dependent on grain diameter for D < 0.4 mm, and independent for higher values. Therefore, it is concluded that bedforms present on sediments coarser than 0.4 mm, with ripple spacings of λ > 0.5 m, are orbital ripples. As their size is dependent on wave orbital diameter, they can be used to interpret possible wave-generating conditions. Bedforms outside of this range, however, are either suborbital or anorbital (Figure 7.2 b), and can not be applied to hydrodynamic interpretations.

Bedforms of large ripple and megaripple size (λ > 0.5 m) are therefore applied to calculate wave flow parameters of orbital diameter (d_o) and maximum orbital velocity (U_m). The spacing of bedforms used in the analysis is based on Figure 6.52 (Chapter 6), with average values of: λ = 0.8 m in 10, 20, and 30 m water depth; λ = 0.6 m in 40 m depth; and λ = 0.5 m in 50 m water. As most large ripples and megaripples occur on medium to coarse grained sand (Figure 7.4 a), an average grain size of D = 0.5 mm was used in the analysis. The spacings of these wave-generated bedforms were then used to calculate wave height (H) from Eq. 7.10, using the range of wave periods outlined above. Results of the analysis are shown in Table 7.1.

Wave heights necessary for megaripple generation under low period wave conditions (T = 6 s) are generally inconsistent with those observed on the northeast coast, except in shallow water depths of 10 m where only low waves (H = 0.83 m) are required. Thus, megaripples on the upper nearshore surface are possibly active under fair weather conditions.

Megaripple bedforms observed in depths of 10 to 30 m could be generated by conditions associated with annual storm events (T = 8 s), with moderate to high storm wave heights of H = 1.26 to 3.62 m being required. In depths of 40 and 50 m, the necessary wave heights (H = 5.02 to 8.4 m) are much larger than those observed to occur under moderate storm conditions.

For wave periods of 10 s, the megaripples in depths of 10 m to 20 m could be generated by relatively low swell waves (H = 0.93 to 1.45 m), similar to those observed offshore from Tauranga Harbour (see Figure 2.7). The bedforms in depths of 30 and 40 m may be generated

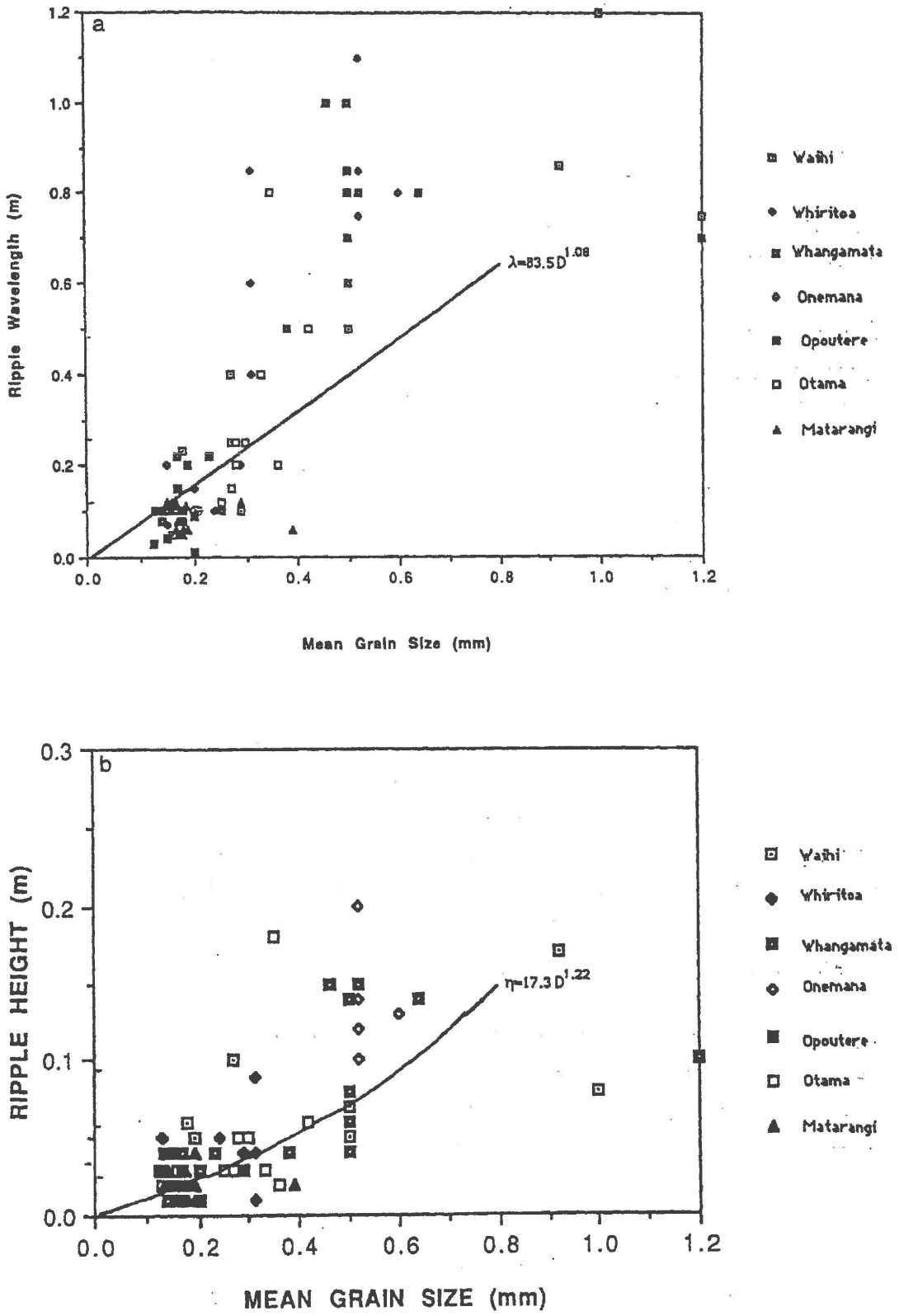

Figure 7.4. Dimensions of ripples observed by divers along the east Coromandel coast, plotted against associated mean grain size: a) Ripple spacing vs. grain size, and association with theoretically expectable curve from Eq. 7.5; b) Ripple height vs. mean grain, and association with theoretically expectable curve from Eq. 7.6.

Table 7.1. Calculation of wave heights (H) required to initiate sediment transport and to generate bedforms, at various combinations of water depth (h) and period (T), using Airy wave theory (note: d_o = wave orbital diameter required to generate bedforms; H^1 = wave height required to initiate sediment transport; H^2 = wave height required to generate bedform; U_m = threshold velocity for sediment transport).

h (m)	do (m)	H1 (m)	H2 (m)
T = 6 s		U_m = 0.29 m.s^{-1}	
10	1.23	0.83	1.85
20	1.23	2.5	5.5
30	1.23	7.5	16.7
40	0.92	22.6	37.5
50	0.77	67.8	94.2
T = 8 s		U_m = 0.33 m.s^{-1}	
10	1.23	0.86	1.26
20	1.23	1.75	2.56
30	1.23	2.47	3.62
40	0.92	4.59	5.02
50	0.77	8.40	7.7
T = 10 s		U_m = 0.37 m.s^{-1}	
10	1.23	0.89	0.93
20	1.23	1.38	1.45
30	1.23	2.51	2.62
40	0.92	2.80	2.19
50	0.77	4.27	2.79
T = 12 s		U_m = 0.41 m.s^{-1}	
10	1.23	1.0	0.78
20	1.23	1.39	1.09
30	1.23	1.60	1.54
40	0.92	2.36	1.59
50	0.77	3.33	1.73
T = 14 s		U_m = 0.44 m.s^{-1}	
10	1.23	1.02	0.64
20	1.23	1.25	0.78
30	1.23	2.01	1.26
40	0.92	2.30	1.08
50	0.77	2.30	0.90
T = 16 s		U_m = 0.47 m.s^{-1}	
10	1.23	0.98	0.5
20	1.23	1.52	0.78
30	1.23	2.06	1.06
40	0.92	2.67	1.03
50	0.77	2.81	0.90

under these longer period conditions by storm waves with H = 2.19 to 2.62 m. However, mid shelf bedforms show a significant disparity between the wave conditions necessary for threshold sediment transport and large ripple formation (H = 4.27 m vs H = 2.79 m). This may indicate an error in the calculations for mid shelf bedforms, with either the grain size or ripple size being incorrect. Each of these alternatives is possible, as very few mid shelf deposits were collected to determine the size of coarse deposits, and it was only possible to measure ripple size from side-scan sonographs, which may have underestimated their size (particularly as the sonar fish was high above the bed in these deep mid shelf waters).

For longer period waves (T = 12 to 16 s), the disparity between conditions required for threshold sediment transport and bedform generation is significant over all water depths. Thus, it is unlikely that bedforms observed during this study were generated by such extreme wave conditions.

Sheet Flow Analysis

Necessary wave conditions for initiation of sheet flow to occur (i.e. the transport of sand grains as a continuous film over a relatively flat surface) is also examined over the above range of wave periods. This analysis is restricted to sediments between fine and very fine sand size, in keeping with the limits in accuracy of Eq. 7.2. As surface sediments vary considerably in grain size, both along the coast and across the shelf, three different grain sizes are analysed: 0.25 mm (2.0 ϕ); 0.18 mm (2.5 ϕ); and 0.12 mm (3.0 ϕ). Each of these correspond respectively to: lower nearshore and inner shelf deposits on the southern coast and at Whangapoua; nearshore and mid shelf deposits on the southern coast and Whangapoua; and surface deposits across Mercury Bay. The various wave conditions required to generate sheet flow conditions over each of these grain sizes are shown as wave height vs. water depth plots in Figure 7.5.

Fine grained sands on the lower nearshore surface (Figure 7.5 a) will occasionally be subject to sheet flow conditions under the influence of relatively large storm waves, in which T = 10 to 16 s, and H = 4 to 3 m. However, fine sands on the inner shelf surface are unlikely to experience sheet flow conditions, except under very extreme wave conditions (T = 12 to 16 s, H = 7 to 4 m). Hence the flat sea floor observed by divers on the Whangapoua inner shelf is unlikely to be generated by sheet flow conditions during storms, and probably indicates that low wave energy conditions prevail here.

Fine to very fine grained sands on the upper nearshore surface (5 to 20 m water depth) are predicted to experience sheet flow conditions relatively frequently (Figure 7.5 b), with only moderate storm waves (T = 6 to 8 s, H = 2.0 m), or small long period swell waves (T = 10 to 16 s, H = 2.0 to 1.5 m) required. However, the same size deposits on the mid shelf surface will only be reworked by sheet flow conditions under very large waves during extreme storms (T = 14 to 16 s, H = 5.0 to 4.0 m).

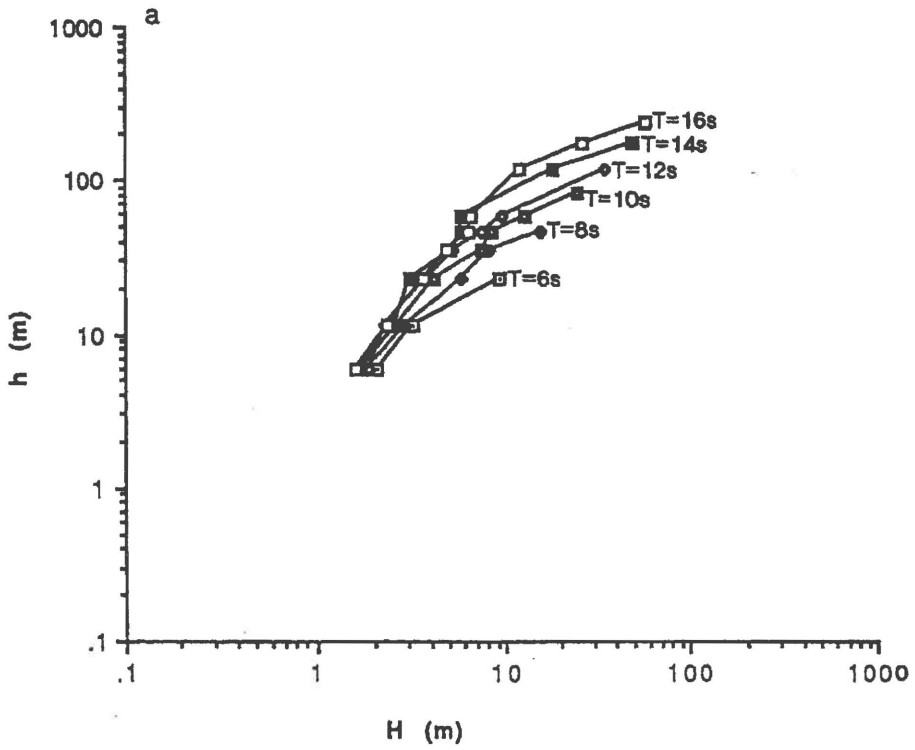
a
1000
100
10
1
.1
h (m)
.1
1
10
100
1000
H (m)
T=16s
T=14s
T=12s
T=10s
T=8s
T=6s

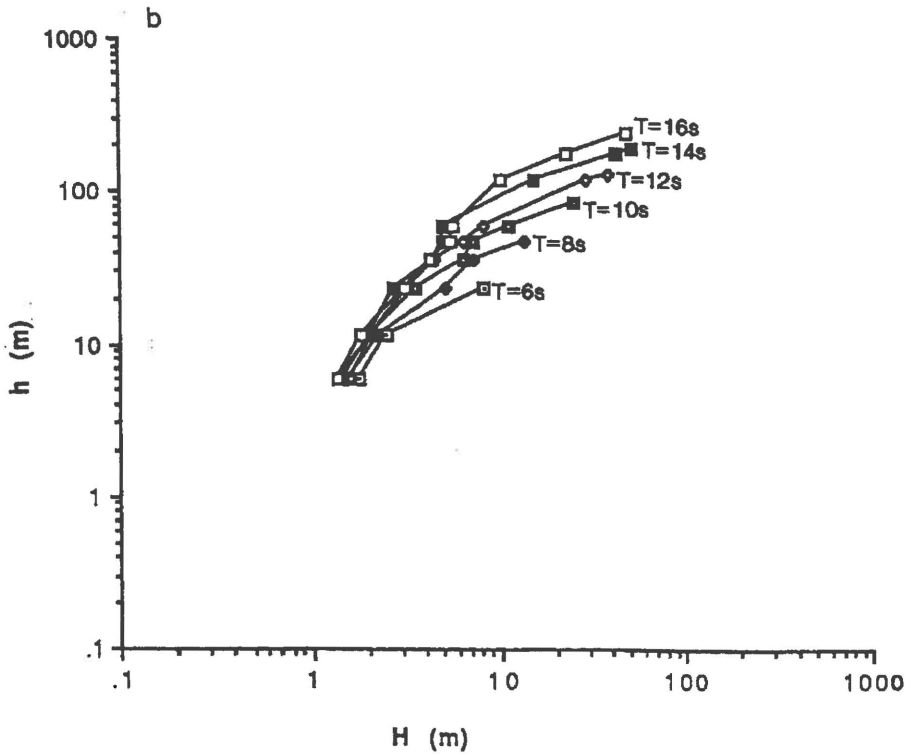
b
1000
100
10
1
.1
h (m)
.1
1
10
100
1000
H (m)
T=16s
T=14s
T=12s
T=10s
T=8s
T=6s

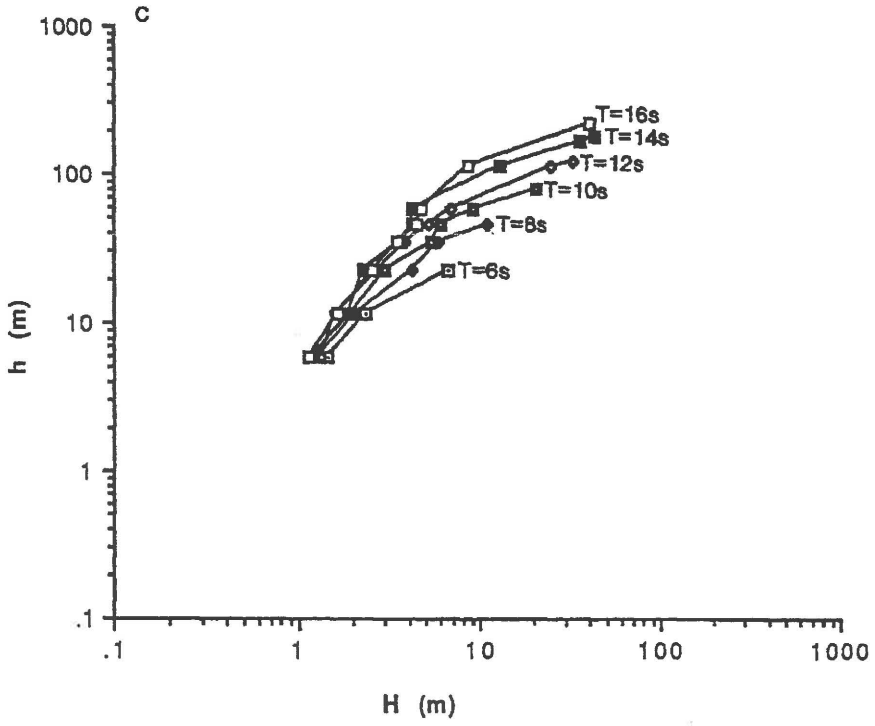

Figure 7.5. Combinations of wave height (H) and water depth (h) that will generate sheet flow conditions under waves of different period, for quartz sand of different grain sizes: a) D = 0.25 mm; b) D = 0.18 mm; c) D = 0.12 mm.

The very fine grained sands which dominate Mercury Bay surface sediments are potentially more susceptible to sheet flow conditions than other east Coromandel shelf regions (Figure 7.5 c). On the shallow inner bay surface (< 10 m depth), sheet flow will occur under relatively calm wave conditions (T = 6 to 16 s, H = 2.02 to 1.46 m). Nearshore deposits require relatively high storm waves (T = 10 to 16 s, 2.20 to 2.60 m), while inner shelf deposits will only experience sheet flow under extreme wave conditions (T = 10 to 16 s, H = 4.75 to 3.0 m).

7.2. DEPTH OF ACTIVITY ROD SURVEYS

7.2.1. Methods

As a final part of the hydrodynamic interpretations of wave-generated bedforms, detailed surveys of the sea-bed were undertaken to determine the response of morphological features to different wave conditions, and thus test the accuracy of the above empirical deductions. This was undertaken through depth of activity rod survey sites on the sea floor at six main locations, on the nearshore and inner shelf off Whiritoa, Whangamata, and Onemana. After a period of twelve months, three new moorings were also established at Whangamata in 17, 22, and 27 m water depth. Locations of each survey site are shown in Figure 7.6. The nearshore survey sites were established on fine sand to determine any changes in bed levels which may be associated with sheet flow conditions. Deeper inner shelf sites were located on coarse megaripple sand deposits to see how they respond and change to different wave flow conditions.

At each site, 1- to 2-m long depth-of-activity rods were hammered into the bed, and about 0.2 m left exposed. Changes in bed level associated with erosion or accretion could then be determined by taking measurements from the top of the rod to the sea-bed. In the latter part of these surveys, metal washers were placed over the rods, and their changing levels measured to determine the maximum depth of sediment reactivation. SALLENGER and RICHMOND (1984) used the same method to measure high frequency sediment level oscillations in a swash zone system. These authors found the method accurate to within 2 to 5 mm, any errors usually being caused by the rods sinking into the sediment or by divers disturbing the sea-bed when standing too close to the rods. Errors could also be caused by the rods concentrating wave or current energy and causing scouring of the sea floor immediately beneath them. Problems encountered in the east Coromandel surveys were usually associated with either storms or trawlers shifting the moorings which marked the survey site positions, so making their relocation impossible. Also, in some cases the rods proved to be too short, and were toppled during storm events. Where this occurred they were subsequently replaced by 4 m-long rods.

The first six survey sites were established between June and July 1985, and subsequently re-examined at about one month intervals, until either the rods or moorings were lost. The later Whangamata sites were established in July 1986 and remained until December 1986. Over the experimental period, the previously described sea-bed drifter and Onemana current meter

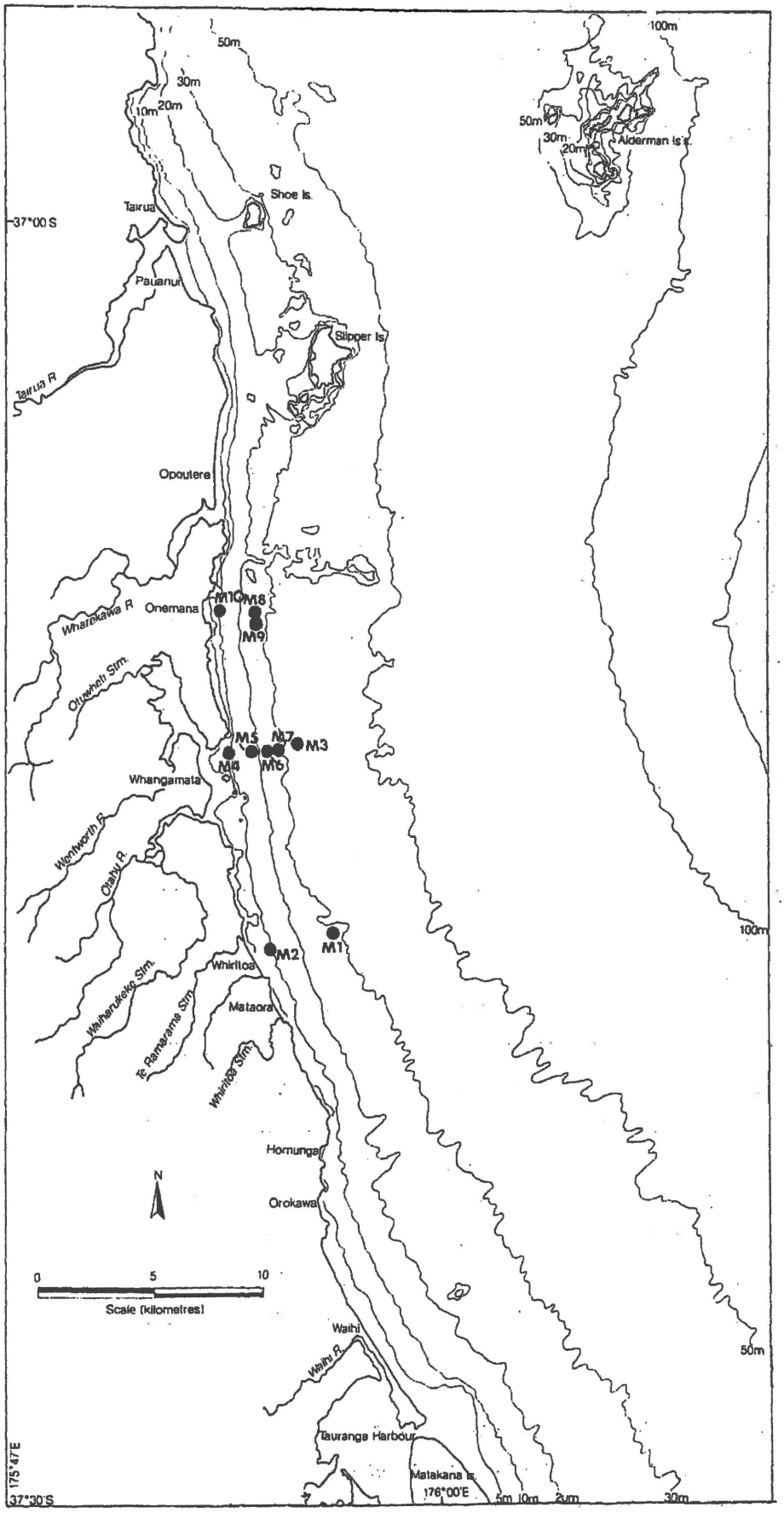

Figure 7.6. Location map for depth of activity rod survey sites at Whioitoa (M.1 and M.2), Whangamata (M.3, M.4, M.5, M.6, M.7) and Onemana (M.8, M.9, M.10).

experiments were also undertaken. Wind data obtained from Whiritoa in this 18 month period were used to hindcast the wave conditions likely to have been present between each diver observation.

One shortcoming was that no sediment samples were collected from the bedforms during each survey. In retrospect, such data would have been very useful for determining whether the change in morphology of bedforms was associated with similar changes in sediment texture.

7.2.2. Survey Results

Whiritoa

Surveys offshore from Whiritoa Beach were made on fine upper nearshore deposits (10 m), and coarse inner shelf sediments (30 m). The inner shelf survey area appeared to experience little change in net-bed levels (Figure 7.7 a). However, the morphology of bedforms varied noticeably (Figure 7.8). The most dramatic change in morphology occurred between 7-Jul- and 17-Aug-85 when bedforms grew from large ripples (λ=0.4 m, η=0.04 m) to megaripples (λ=0.85 m, η=0.1 m). Wave conditions necessary to generate these bedforms are plotted against hindcast wave parameters in Figure 7.9. This indicates that the hindcast wave conditions are lower than those predicted by Eq. 7.3, particularly for the changes observed on 17-Aug-85. This may indicate inaccuracies in the CLIFTON and DINGLER (1984) method for predicting wave flow conditions. For instance, high speed current flows (> 0.2 $m.s^{-1}$) were observed between each survey, which may have interacted with the wave orbital currents to increase the shear stress exerted on the sea floor. Also, the presence of antecedent bedforms may have reduced the wave orbital diameter necessary for megaripple development by enhancing the shear stress exerted by these wave flows.

Changes in bed level were relatively high on the upper nearshore zone (Figure 7.7 b), with up to 0.20 m of erosion occurring between 6-Jun- and 7-Jul-85, resulting in toppling of all but two of the original 2 m long rods. The presence of sheet flow conditions would be expected by the wave conditions experienced during the experimental period, and appears to be indicated by the observation of washers 0.12 m beneath the sea-bed on the 5-Oct-85 survey.

Whangamata

Surveys offshore from Whangamata Beach were initially made in 10 and 34 m water depth in 1985, then later examined in 17, 22, and 27 m water depth in 1986.

Megaripples on the inner shelf (34 m) were examined in two adjacent areas to determine if observed bed level changes are similar along the shelf surface. The results show accretion occurring at one site, and slight deposition just to the north (Figure 7.10 a). Washers were observed at one site to be about 0.07 m below the sea-bed, but as this corresponds to the height

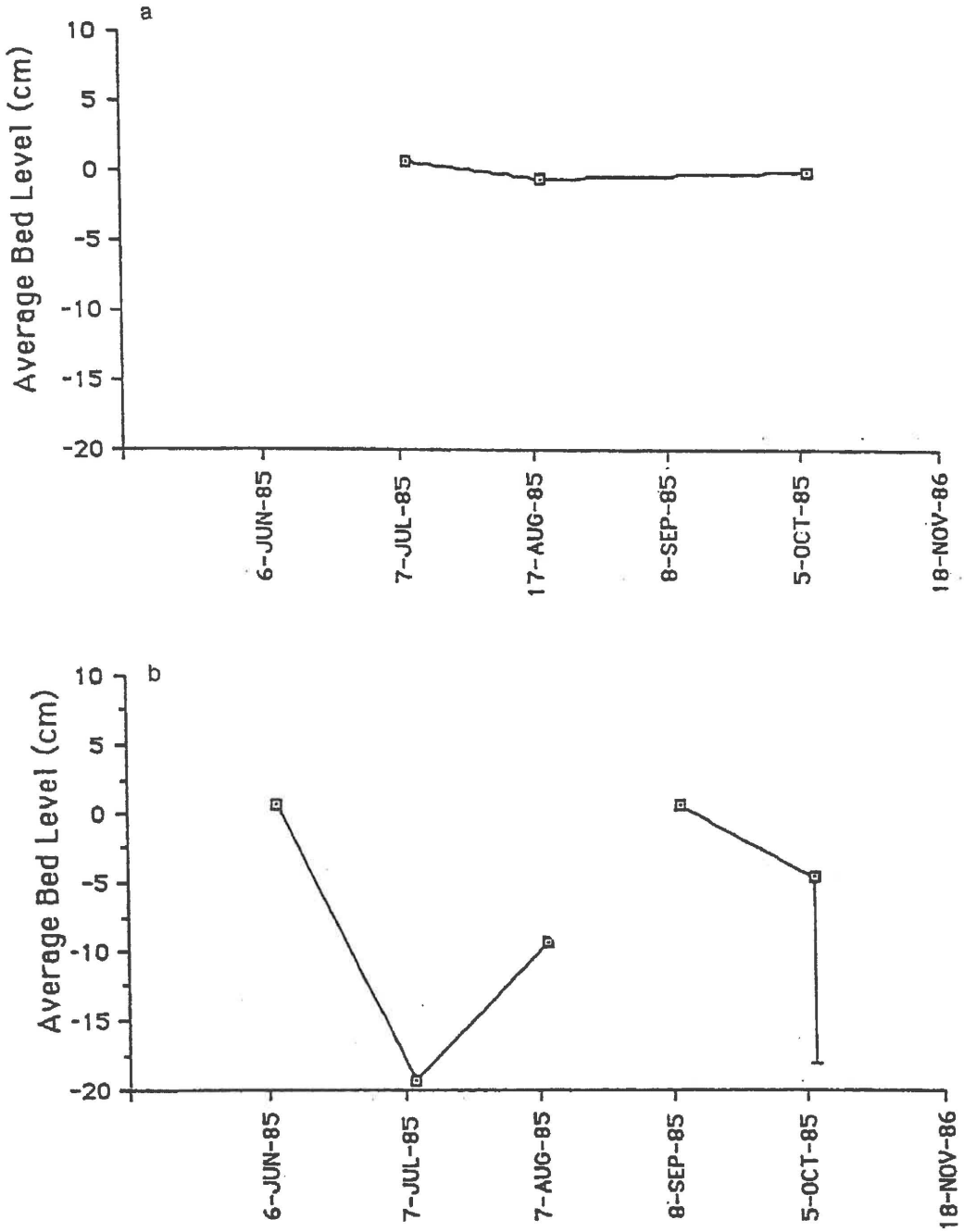

Figure 7.7. Changes in sea-bed level observed from depth of activity rod surveys at Whiritoa: a) inner shelf survey site in 30 m water depth (M.1.); b) upper nearshore survey site in 10 m water depth (M.2). Note that the vertical bar on 5-Oct-85 in (b) indicates the sub-surface depth at which washers were observed by divers.

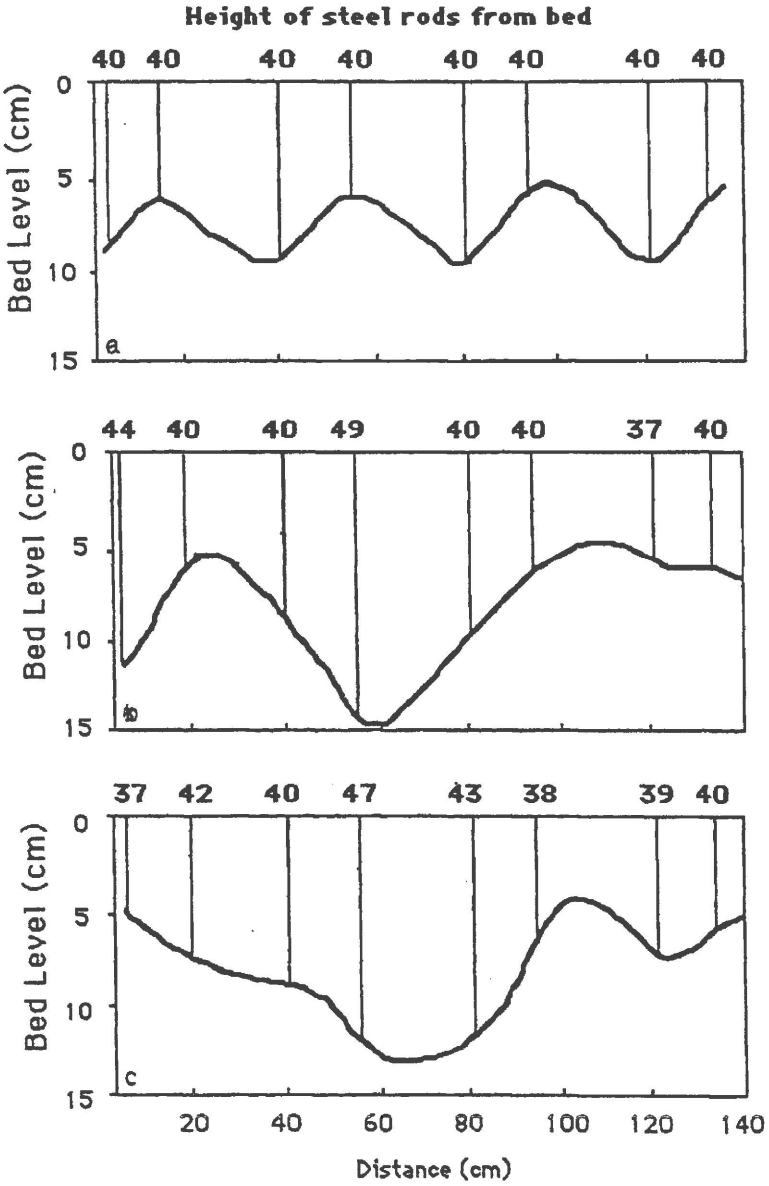

Figure 7.8. Surveyed changes in bedform morphology on the inner shelf at Whiritoa (M.1): a) 7-Jul-85; b) 17-Aug-85; c) 5-Oct-85.

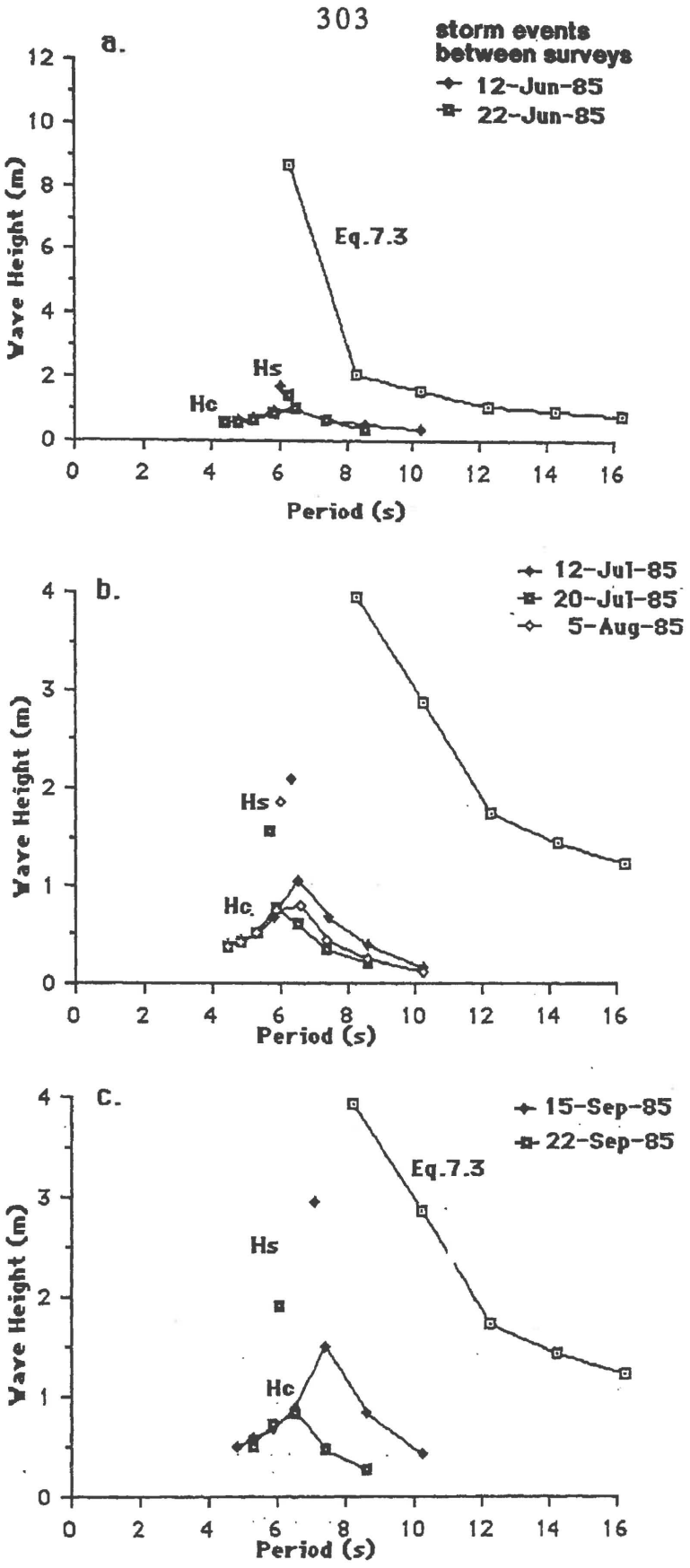

Figure 7.9. Wave conditions necessary to generate bedforms at Whiritoa as surveyed on: a) 7-Jul-85; b) 17-Aug-85; b) 5-Oct-85. Also shown are comparisons to hindcast component (H_c) and significant wave height (H_s) parameters from storm events which occurred between each survey.

of megaripples observed from this survey area, it most likely indicates that a megaripple crest had migrated over a previous trough between surveys. This is supported by the bedform profiles from each survey in Figure 7.11, which indicate only slight increases in the size of the megaripples during the surveys (λ=0.7 to 1.0 m, η = 0.04 to 0.1 m), but the continual migration of crest and trough positions.

A more detailed survey line through the megaripples by divers (Figure 7.12) reveals the complex morphology of these bedforms, with the megaripple wavelength and height varying significantly over a short distance (λ = 0.8 to 1.2 m, η = 0.06 to 0.1 m). This in part results from smaller bedforms emerging in the troughs of larger megaripples, and is inferred to indicate either increased wave flows generating anorbital ripples, or decreased flows causing orbital ripples to reduce in size. As no sediment samples were collected at the time of observation, the ripple growth cut-off point (Eq. 7.4; MILLER and KOMAR. 1980a) cannot be accurately determined. However, similar sized megaripples at this water depth off Whangamata are characterised by grains with D = 0.5 mm, which produces a maximum wavelength of λ = 0.96 m. Hence, it is quite possible that the smaller features emerging in megaripple troughs represent anorbital ripples.

Plots of hindcast wave conditions against those necessary for the generation of the surveyed megaripples (Figure 7.13) show that wave flow conditions were insufficient to generate these features. Thus it would appear that the megaripple morphology here is also influenced by factors other than wave orbital diameter, specifically the presence of strong wind-generated currents and the shear stress enhancement effect of antecedent bedforms.

Bed level changes observed on fine sediments varied considerably over the different depths surveyed. On the upper nearshore surface (10 m) changes in bed level were large, with up to 0.10 m of erosion observed (Figure 7.10 b). Washers were also found up to 0.13 m beneath the surface, which is inferred to indicate the presence of sheet flow conditions. However, these changes are not as large as those observed at Whiritoa during the same period of time, and so a difference in the depth of sediment reworking may exist between the two regions. The three deeper moorings used in 1986 recorded relatively insignificant changes in bed levels, and no evidence for the presence of sheet flow conditions (Figure 7.10 c, d and e). This supports deductions made from empirical considerations of sheet flow conditions, that fine sands over the lower nearshore and inner shelf are only subject to sheet flow during extreme wave conditions.

Onemana

The region offshore from Onemana Beach was mainly surveyed on the elongate megaripple band observed in sonograph traces in Mar-84 and Mar-85. This feature showed the same basic outline on sonographs over a 12 month period, and so it was of interest to compare the relative mobility of associated coarse grained sediments and adjacent fine sands. The surveys showed dramatic changes in the bed level of coarse deposits within the band (0.34 m; Figure 7.14 a), indicative of

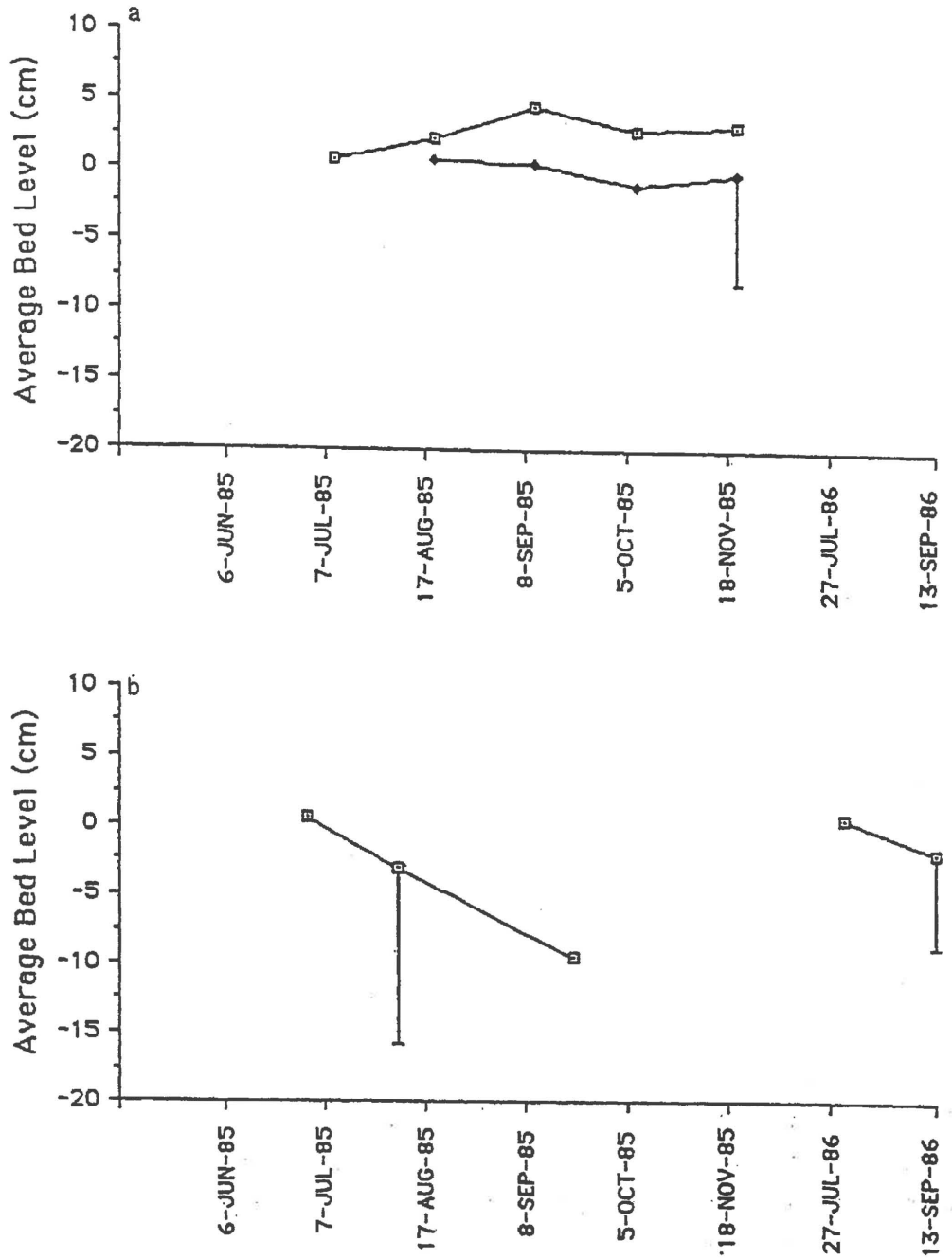

Figure 7.10. Changes in sea-bed level observed from depth of activity rod surveys at Whangamata: a) Inner shelf sites in 34 m water depth (M.3); b) Upper nearshore site in 10 m water depth (M.4); c) Upper nearshore site in 17 m water depth (M.5); d) Lower nearshore site in 22 m water depth (M.6); e) Lower nearshore site in 27 m water depth (M.7.). Note that the vertical bars indicate the sub-surface depth at which washers were observed by divers.

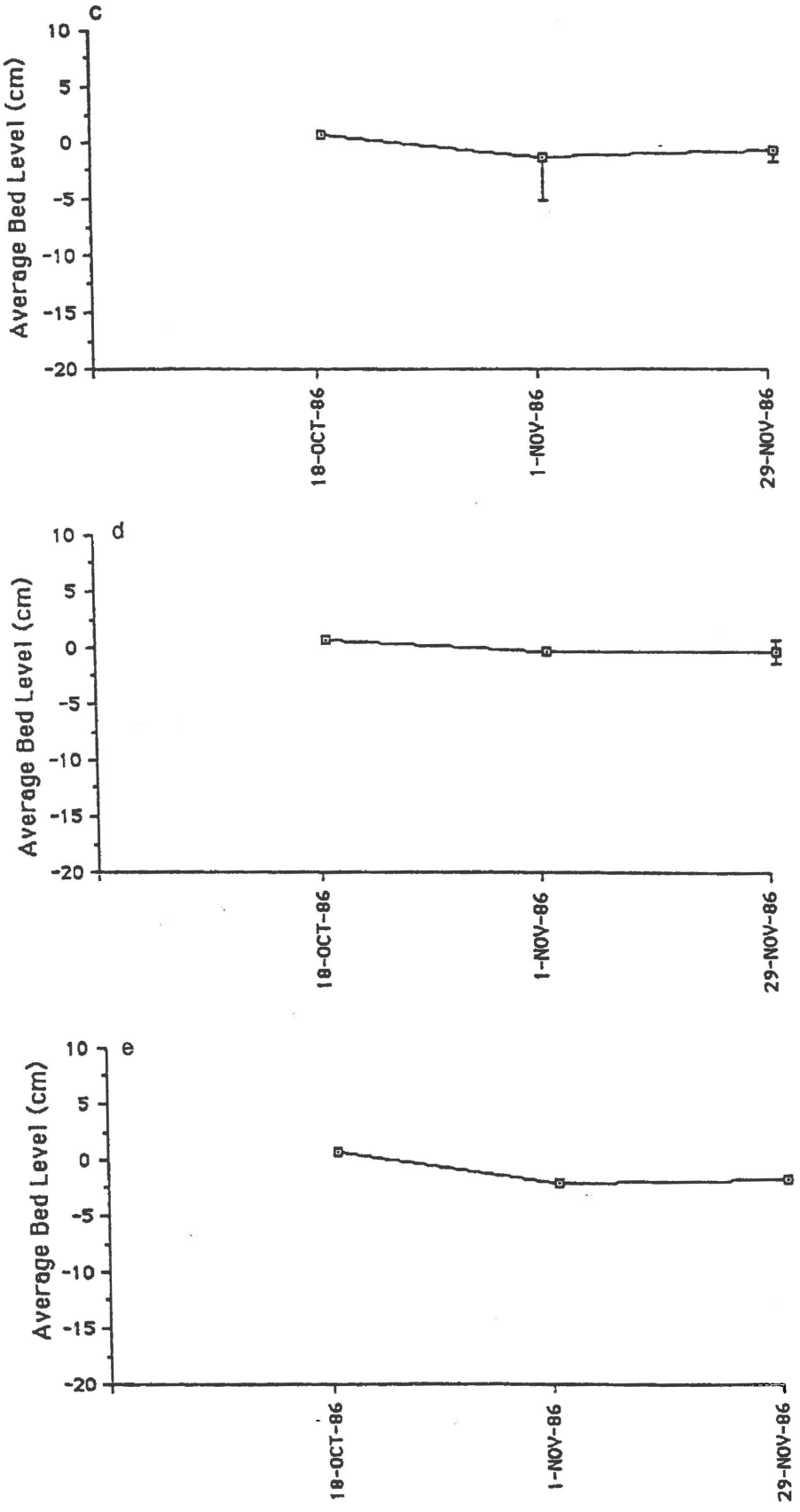

Figure 7.10 (continued).

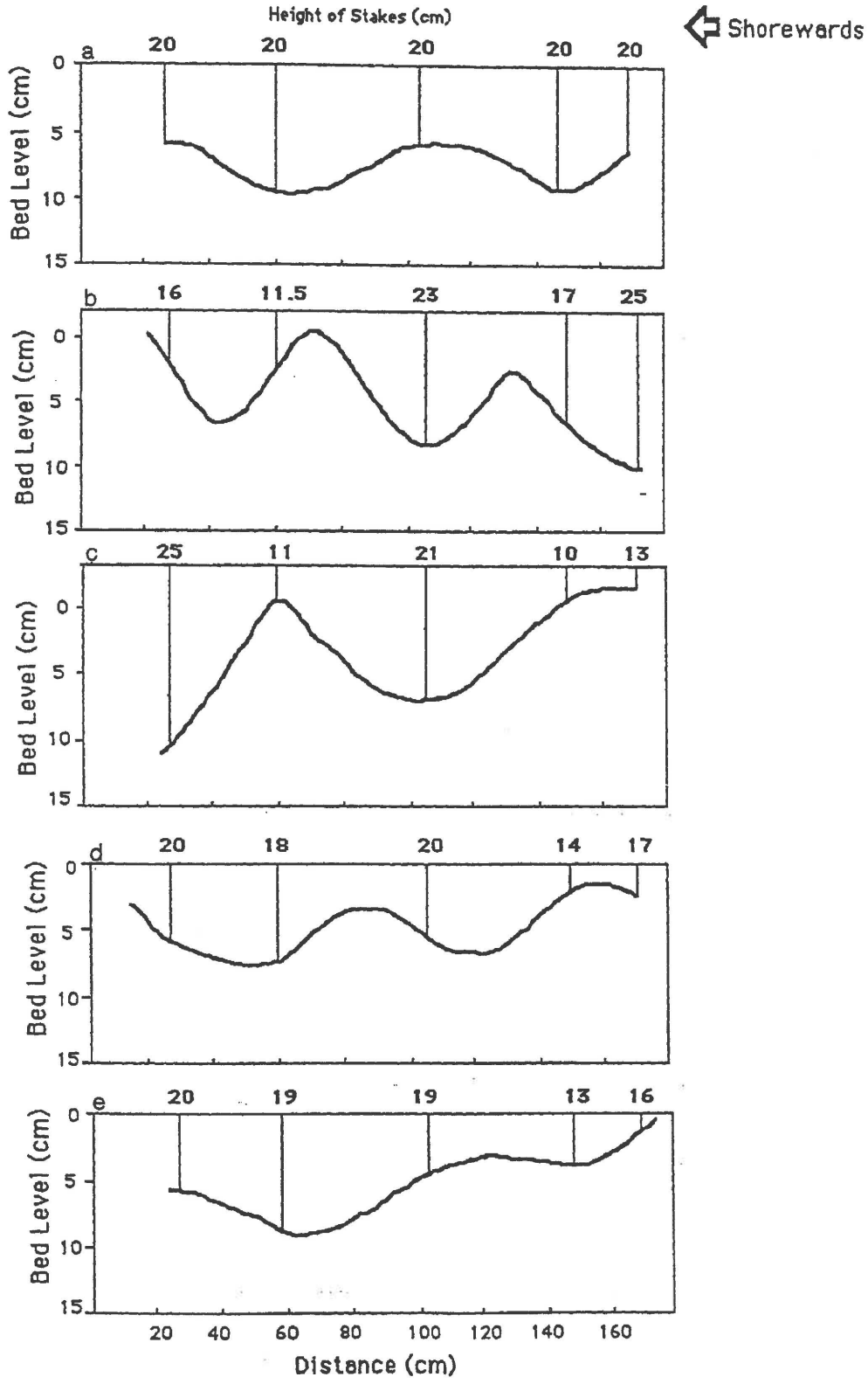

Figure 7.11. Observed changes in bedform configuration at the Whangamata inner shelf survey site (M.3): a) 7-Jul-85; b) 17-Aug-85; C) 8-Sep-85; d) 5-Oct-85; e) 18-Nov-85.

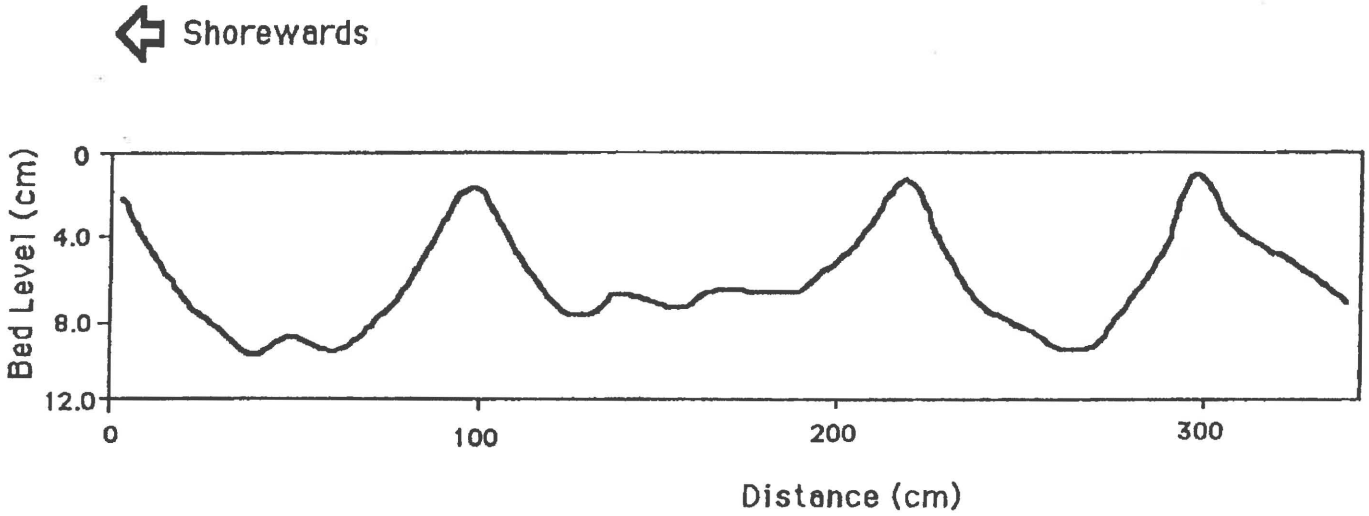

Figure 7.12. Cross-sectional profile of megaripples measured by divers from Whangamata (M.3) 5-Oct-85

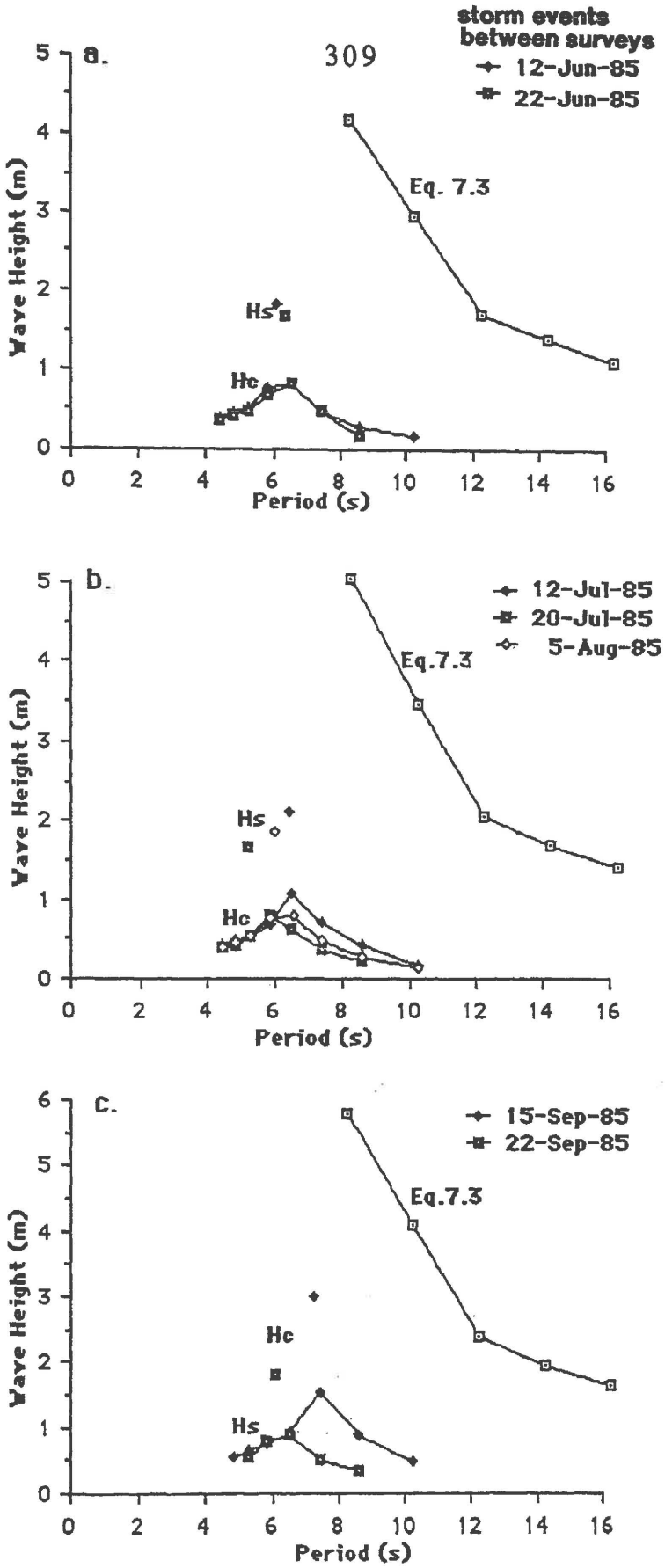

Figure 7.13. Wave conditions necessary to generate bedforms at Whangamata as surveyed on: a) 7-Jul-85; b) 17-Aug-85; b) 5-Oct-85. Also shown are comparisons to hindcast component (H_c) and significant wave height (H_s) parameters from storm events which occurred between each survey.

significant erosion. However, adjacent areas of fine sand just south of the band experienced relatively insignificant changes in bed level (Figure 7.14 b). Thus, the band would appear to be an area of strong flow conditions, possibly resulting from intensified current flows over the sand ridge associated with the band, or due to a convergence of wave rays by refraction further offshore. Megaripples within the band increased in dimensions initially from λ=0.77 to 1.1 m and η=0.1 to 0.2 m between 7-Jul- and 5-Oct-85, then decreased to λ= 0.8 m and η=0.09 m on 15-Feb-86. Survey lines taken through the bedforms by divers indicate the latter changes are very clearly associated with the growth of smaller features within the troughs of larger megaripples (Figure 7.15). As wave conditions appear to have been relatively calm between these latter two surveys, this change is most likely associated with the decay of large orbital ripples to smaller orbital ripples under lower wave flows.

Plots of hindcast wave conditions against those necessary for megaripple generation are shown in Figure 7.16, and indicate that wave conditions were again lower than those required for megaripple formation, although close on 15-Sep-85. Aanderaa current measurements (Chapter 4.3.) from adjacent to this megaripple band showed strong wind-generated currents present between the surveys. Hence, the very high level of erosion observed within the megaripple band was possibly associated with intense combined wave-current flows.

Surveys from the upper nearshore surface at Onemana (10 m) show significant erosion (0.07 m; Figure 7.14 c) and sheet flow conditions occurred, as indicated by washers 0.1 m beneath the surface. As at Whangamata, bed level changes are not as severe as observed at Whiritoa. Thus, a significant reduction in the depth of sediment reworking appears to extend between Whangamata and Onemana.

7.2.3. Significance of Survey Results to Empirical Estimations for Wave Flow Conditions

Results from the depth of activity rod surveys allow the degree of certainty in the wave flow estimates by the CLIFTON and DINGLER (1984) method to be tested. In general, the surveys show the wave conditions and water depths in which sheet flow appear to occur to be consistent with those predicted by Eq. 7.2. However, the hindcast wave conditions which are associated with reworking of megaripples are much lower than those predicted from Eq. 7.3. Several factors may explain these inconsistencies between predicted and observed responses:

1. The method only considers influences from wave orbital flows, with no allowance made for the increased shear stress of combined wave- and wind-generated current flows. GRANT and MADSEN (1979) found that such combined wave-current flows enhance the shear stress felt by sediments on the sea-bed, and increase suspended sediment concentrations. As strong wind-generated currents were measured from Onemana under storm conditions during these sea-bed surveys, such shear stress enhancement by combined flows is likely to occur. However, combined

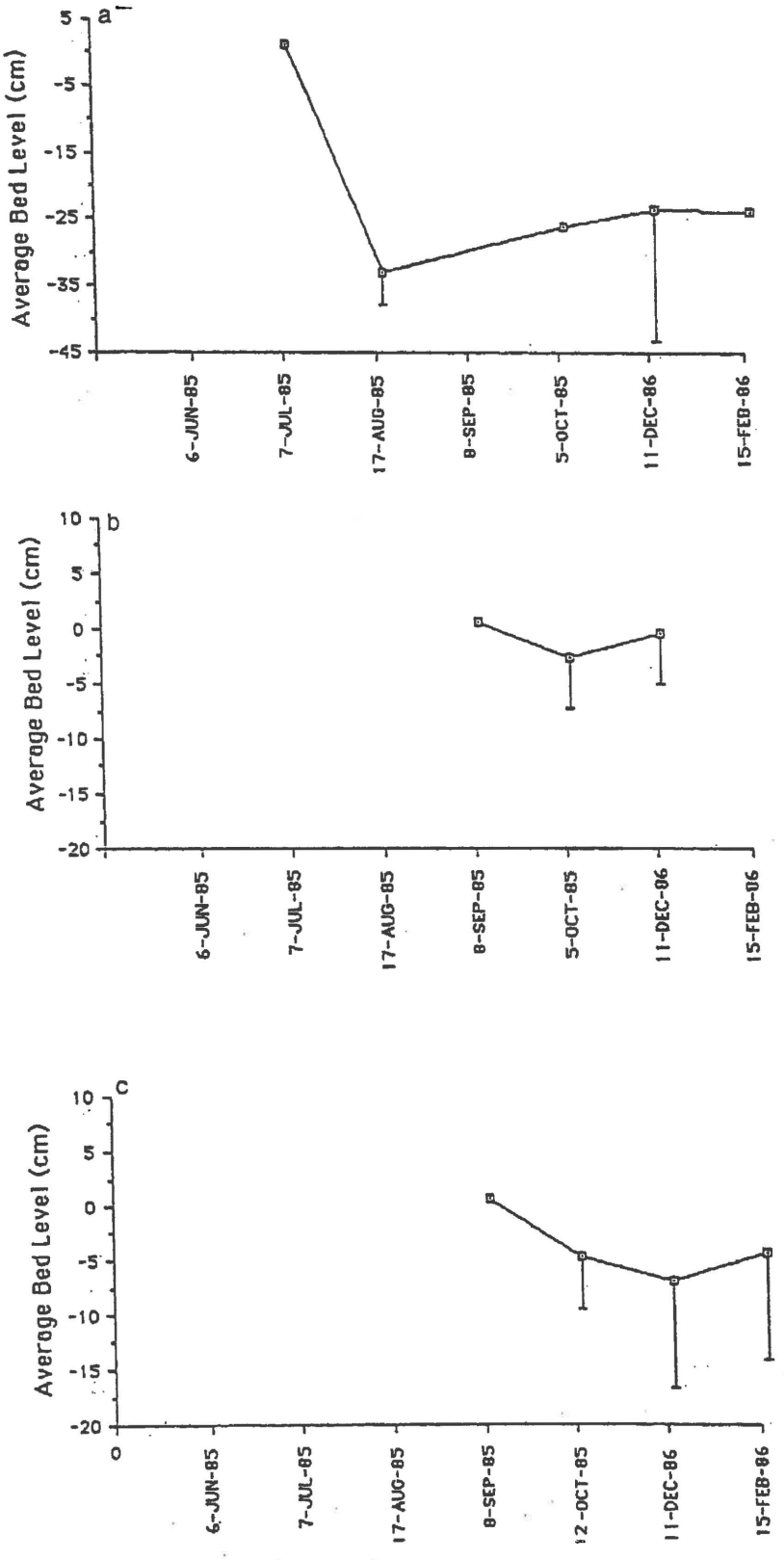

Figure 7.14. Changes in sea-bed level observed from depth of activity rod surveys at Onemana: a) lower nearshore CMR band (M.8); b) lower nearshore fine sand (M.9); c) upper nearshore site (M.10). The vertical bars indicate the sub-surface depth at which washers were observed by divers.

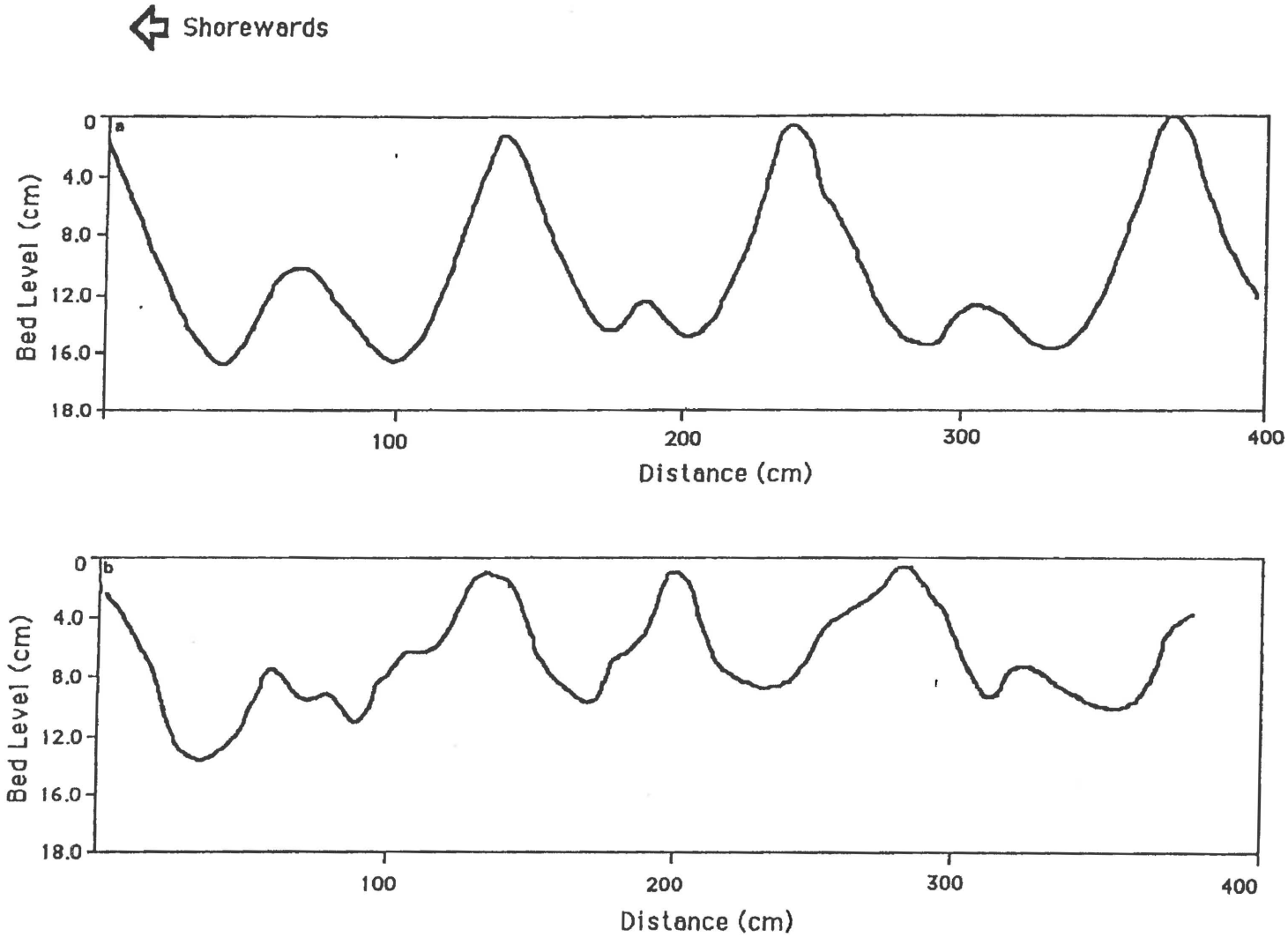

Figure 7.15. Cross-sectional profile of surveyed megaripples measured by divers within the Onemana CMR band: a) 5-Oct-85; b) 15-Feb-86. Note the degraded nature of megaripples in B) and emergence of smaller bedforms in troughs of larger features.

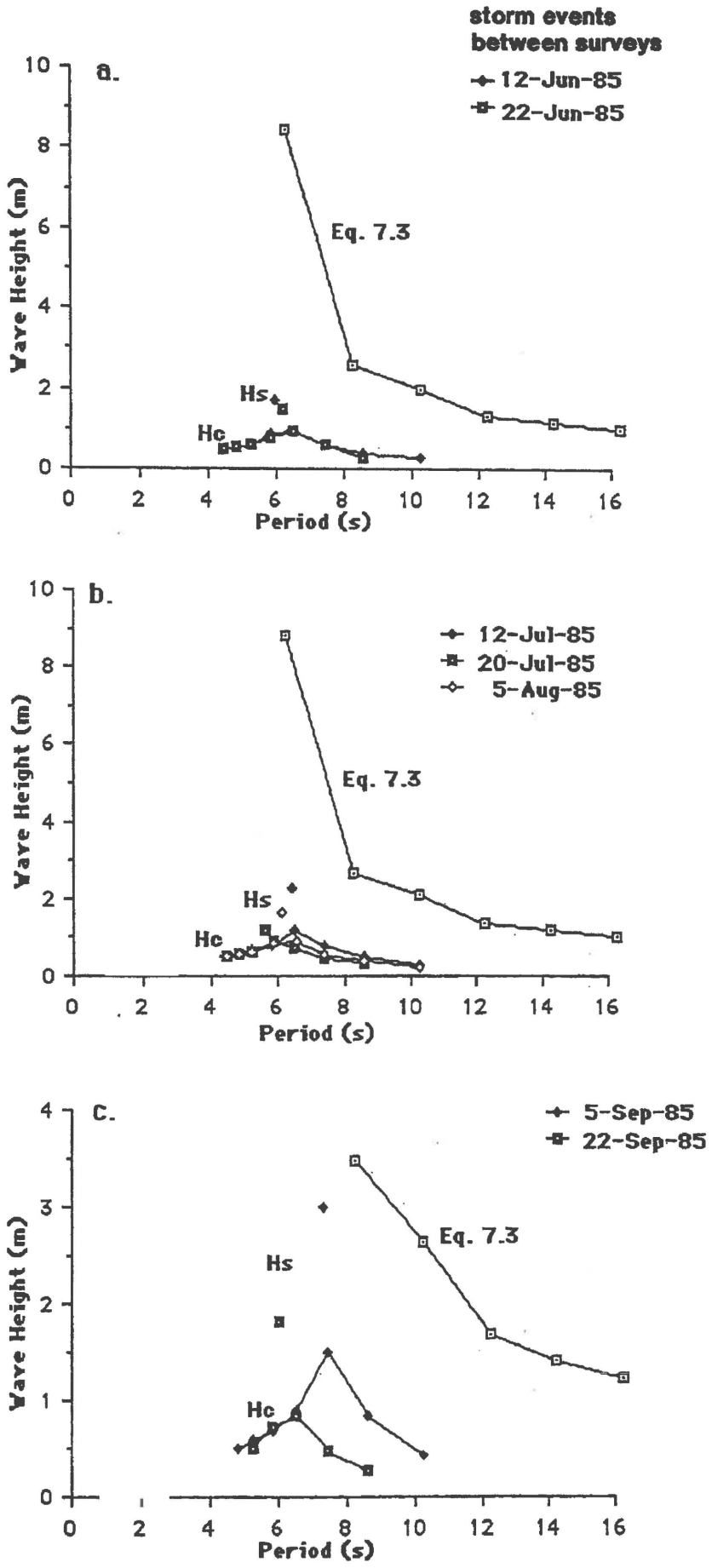
storm events
between surveys
a.
12-Jun-85
22-Jun-85
Eq. 7.3
Hs
Hc
Wave Height (m)
Period (s)
b.
12-Jul-85
20-Jul-85
5-Aug-85
Eq. 7.3
Hs
Hc
Wave Height (m)
Period (s)
c.
5-Sep-85
22-Sep-85
Eq. 7.3
Hs
Hc
Wave Height (m)
Period (s)

Figure 7.16.

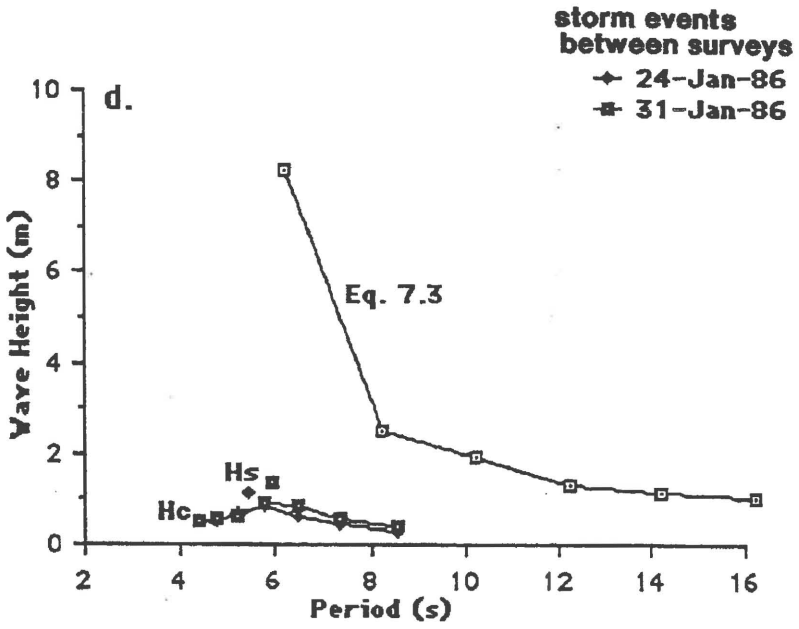

Figure 7.16. Wave conditions necessary to generate bedforms at Onemana as surveyed on: a) 7-Jul-85; b) 17-Aug-85; c) 5-Oct-85; d) 15-Feb-85. Also shown are comparisons with hindcast component (H_c) and significant wave height (H_s) parameters from storm events which occurred between each survey.

flows did not cause deviations from predicted sheet flow (or non-sheet flow) conditions on fine sediments, and is likely to be only a relatively minor cause of the disparities.

2. The method assumes wave flows over uniform sized, well sorted grains. For the fine rippled sands this assumption may be valid, as diver observations (Chapter 6.3.) generally showed these to be composed of relatively uniform-sized material. However, the megaripples are generally composed of coarse shelly sediments in their troughs, and finer clastic grains on their crests. Diver surveys from Onemana indicate small bedforms emerge in the troughs of larger megaripples when low wave conditions prevail. This probably occurs as the finer crest deposits would require a lower threshold transport velocity than the coarser trough deposits. They may therefore be reworked under these low wave flow conditions into the megaripple troughs, and develop a bedform which is more in equilibrium with the prevailing wave conditions. During more intense flows, these finer deposits would be eroded out of the troughs and deposited back on the megaripple crests. Evidence that this occurs is shown by the extreme changes in megaripple morphology observed at Whiritoa and Onemana on 17-Aug-85, and at Onemana between 5-Oct-85 and 15-Feb-86.

3. The method assumes wave flow over an initially flat sea-bed. For the fine sediments in which sheet flow conditions were examined this assumption is probably valid, as only small ripples are developed on their surface during low wave flow conditions, which would be planed off into a flat bed relatively quickly under storm wave conditions. However, coarse sediments were consistently found to be characterised by either large ripples or megaripples. CLIFTON and DINGLER (1984) note that it is usually impossible to establish in the field if bedforms are responding to on-going processes without prior influence. This is because the bedforms may have developed under more energetic conditions than those at the time of observation, and retained their shape under less intense processes. Also, the bedforms themselves may influence the flows in such a way as to retain their original character. Several other studies have shown the form drag created by bedforms will cause an enhanced shear stress on the sea floor, and thus reduce the threshold velocity required for sediment entrainment (GRANT and MADSEN, 1979; COWELL and NIELSON, 1984; KAPDASLI and DYER 1986; VINCENT *et al.*, 1991). Thus, once megaripples have been generated on coarse sediments, they will tend to maintain their form through their morphodynamic interactions with the prevailing hydrodynamic conditions.

4. It is possible that the hindcast wave values are underestimates of natural conditions, with longer period swells also being present in the storm wave field. However, the hindcast values are consistent with previous records from wave-rider buoys (Chapter 2.3.2.).

In summary, results from this study show that the method outlined by CLIFTON and DINGLER (1984) for interpreting wave conditions responsible for ripple and megaripple generation is generally invalid, and will usually overestimate the wave conditions associated with their formation. This is because of several oversimplifying assumptions in their interpretations, particularly the inference of uniform-sized sediments and initial flat bed conditions. These

assumptions seem to be more valid for sheet flow conditions on fine grained nearshore and inner sediments.

7.3. MORPHODYNAMIC INTERPRETATIONS OF SHELF SAND RIDGES

Sand ridges have been identified on various parts of the east Coromandel shelf from sonograph and echosounding traces (see Chapter 6.2.2.). The morphology of ridges indicates that they respond to the modern shelf hydrodynamic conditions, their surfaces being reworked by storm waves and shore-parallel wind-generated currents. However, the morphology of these features varies considerably along the coast, which is inferred to reflect regional changes in hydrodynamic conditions. These variations in sand ridge morphology can be summarised as:

1. An extensive field of sand ridges occurs along the southern coast between Waihi Beach and Opoutere (~ 60 in total; Figure 7.17), but is generally absent further north (except off Otama Beach). Observations in this study, and from published bathymetric charts (WRIGHT, 1989), show that these are shore-normal oriented features which occur in depths of 10 to 80 m, and have crests ranging in length from 500 to 6000 m.

2. Relatively low relief ridges (η = 1 to 2 m) tend to occur on the upper nearshore, inner shelf, and mid shelf surfaces, but much higher features are found on the lower nearshore surface in depths of 20 to 30 m (Figure 7.18). Ridge height on the lower nearshore surface also varies significantly along the coast, from up to η = 7.4 m high just north of Waihi Beach, to η = 1.5 m high at Onemana.

3. The width of sand ridges varies systematically along the coast in lower nearshore and inner shelf water depths (20 to 40 m), from λ = 600 to 1100 m wide at Waihi Beach, to λ = 250 m wide at Onemana (Table 7.2). Sand ridge width also varies across the shelf, with wider features (λ = 500 to 1500 m) occurring on the mid shelf surface at Whangamata and Whiritoa.

Table 7.2. Regional variations in sand ridge spacing.

Location	Ridge Spacing (h=20m-30m)	Ridge Spacing (h=50 m)
Waihi	600-1100 m	-
Whiritoa	270-600 m	1000-1250 m
Whangamata	250-500 m	500-1500 m
Onemana	245-300 m	-
Otama	235-1250 m	-

4. Sand ridges only occur in areas of relatively abundant fine sand (except at Otama). Although they respond to modern hydrodynamic processes, it was not possible in this study to determine whether the ridges are stationary or are currently being reworked along the shelf.

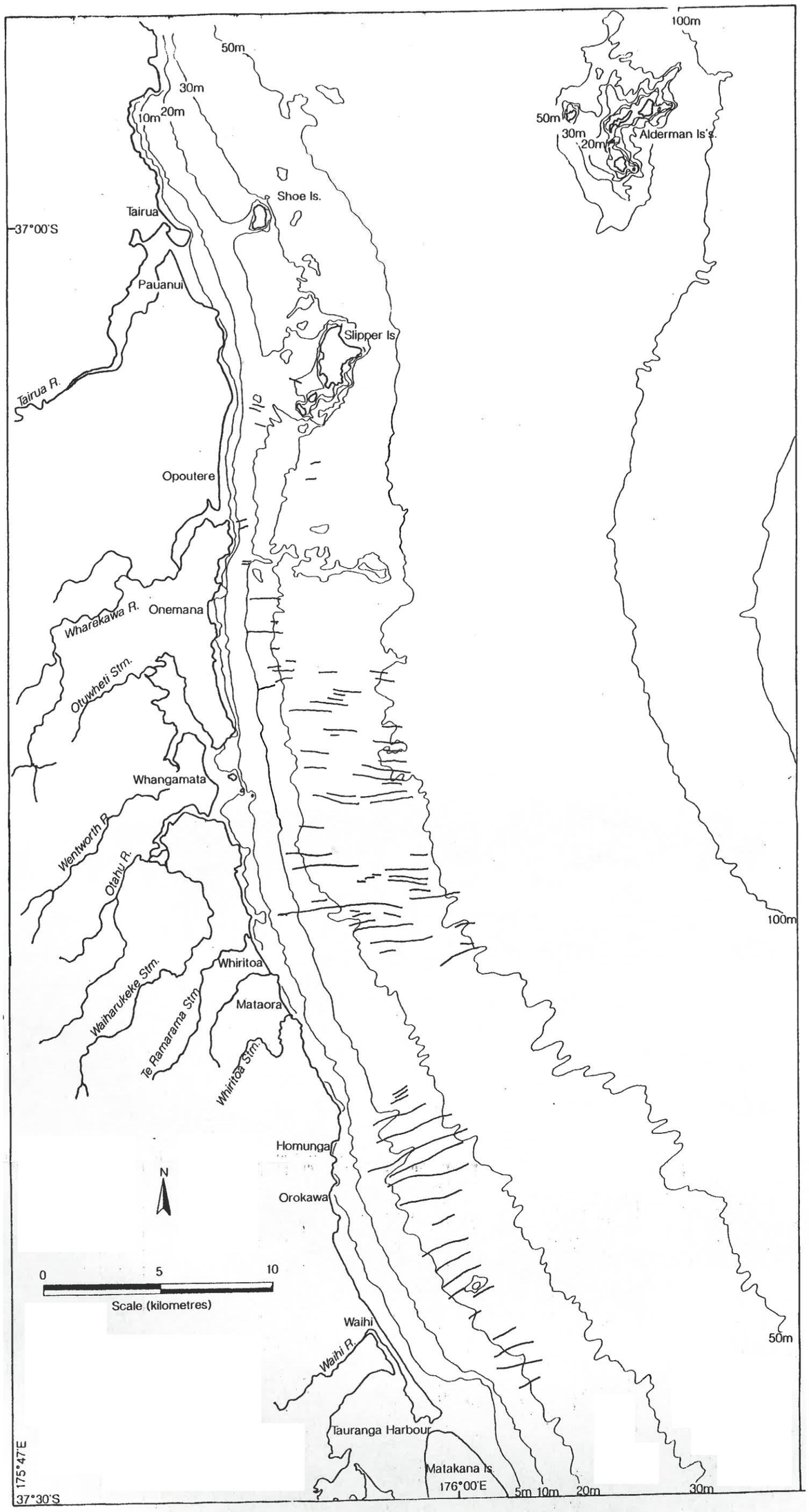

Figure 7.17. Map showing distribution and orientation of sand ridge crests along the southern east Coromandel coast, based on sonographs and echosounding traces (Chapter 6.2.2.).

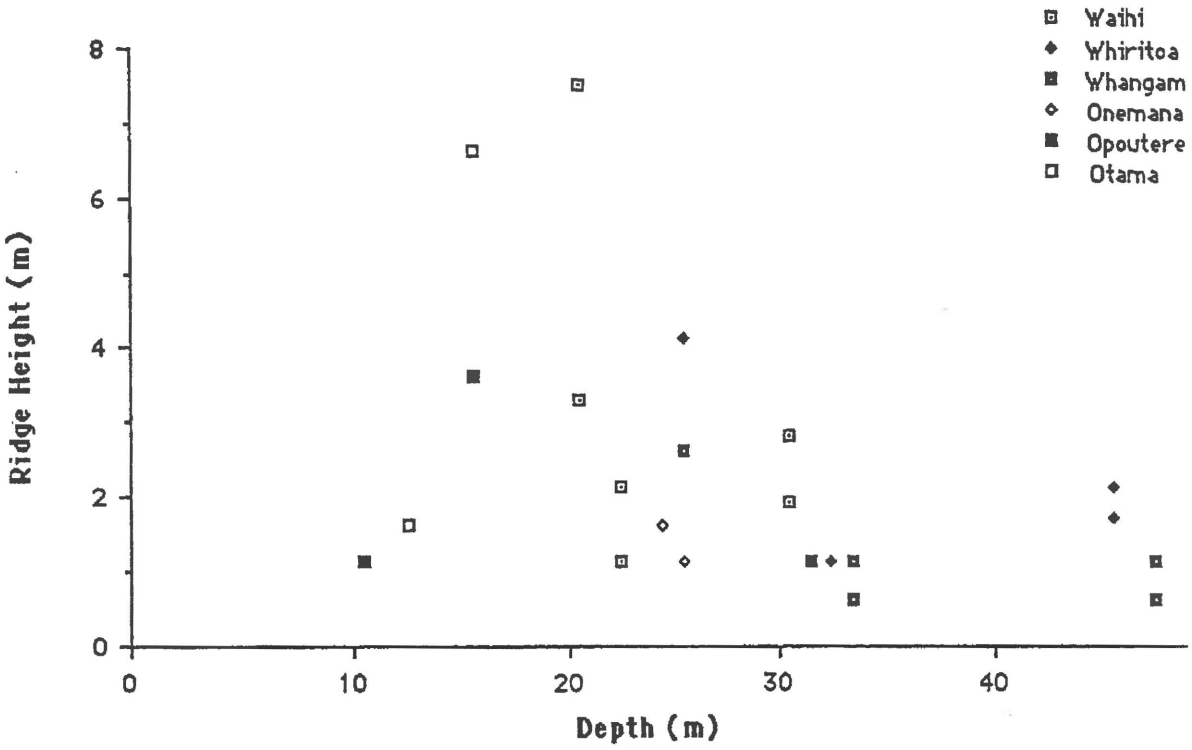

Figure 7.18. Plot of sand ridge relief on the east Coromandel coast based on sonograph and echosounding traces. Note the largest features are developed in 20 m water depth, particularly off Waihi Beach and Otama.

Sand ridges of similar morphology are a common feature on storm-dominated shelves, and have been extensively studied for their modes of formation. Early investigations on the North American mid-Atlantic shelf (McKINNEY *et al.*, 1974; SWIFT and FREELAND, 1978; SWIFT and FIELD, 1981) found sand ridges are actively forming in the nearshore zone under modern hydrodynamic processes, and slowly migrating offshore and down the coast in the storm current direction. In New Zealand, LEWIS (1979) identified extensive sand ridges in the Western Cook Strait. These occur in depths > 30 m, and are inferred to represent relict features formed during the Holocene marine transgression, but presently modified by storm-generated flows.

More recent investigations on the Nova Scotia shelf by BOCZAR-KARAKIEWICZ *et al.* (1990; 1991) have found that sand ridge formation may relate to the interaction of two processes:

1. Spatially periodic sediment fluxes associated with either infragravity waves (T = 0.5 to 5 min.) or internal tidal waves, which determines the spacing and orientation of their crests and troughs.

2. Mobilisation of sediments by waves and currents, which provides sufficient material for sand ridges to form, and for subsequent modifications of their morphology.

BOCZAR-KARAKIEWICZ *et al.* (1991) also note that ridge morphology is strongly influenced by shelf slope and water depth, with both the number of ridge crests and their spacing tending to decrease as shelf slope increases, and the spacing of ridge crests tending to increase with increasing water depth. This is consistent with the observations of sand ridge morphology along the east Coromandel coast, outlined above. The influence of shelf slope seems to be particularly important on the east Coromandel coast, as large ridges occur on the lower nearshore surface just north of Waihi Beach and off Whiritoa Beach, and are associated with major changes in shelf morphology. At Waihi Beach, this involves a sudden decrease in shelf width between the 20 and 50 m isobaths from 12 to 5 km wide, and at Whiritoa a decrease in the lower nearshore width (20 to 30 m isobaths) from 2.5 to 1.0 km wide. Also, the gradual disappearance of ridges from Waihi Beach to Opoutere coincides with an increase in continental shelf slope from 1:232 to 1:133, and a decrease in width from 29 to 20 km. Hence, shelf morphology appears to influence the hydrodynamic processes which generate sand ridges.

Hydrodynamic processes responsible for the generation of east Coromandel sand ridges are probably similar to those proposed by BOCZAR-KARAKIEWICZ *et al.* (1990; 1991) for the Nova Scotia shelf, i.e. infragravity waves. As the ridges are consistently oriented perpendicular to the coastline, such infragravity flows would propagate along the shelf. Without more detailed current data, the exact nature of these flows can only be speculated upon. However, it is possible that over the broader shelf surface off Waihi Beach, and south in the Bay of Plenty, coastally-trapped topographic waves are generated by cyclonic depressions passing over the east coast, and then propagate northwards along the east Coromandel coast. This would be consistent with

observations by HEATH (1979, 1982) of edge waves generated on the east coast of New Zealand by meteorological disturbances. Their generation would be favoured here by the mechanism of non-scale matching between the storm and shelf, as described in Chapter 3.1.2. (SWIFT and NUMMEDAL, 1987). Since these are long-period and low-amplitude infragravity waves, their form will undergo similar transformations in areas of changing shelf morphology as do shorter period surface gravity waves (BOCZAR-KARAKIEWICZ *et al.*, 1990). Thus, the narrower spacing and higher relief of ridge crests on the lower nearshore surface may result from a shoaling transformation of these infragravity waves in shallower shelf waters. As coastally-trapped topographic waves are maintained by Coriolis forces continually pushing these waves against the coastline (SWIFT and NUMMEDAL, 1987), the gradual disappearance of sand ridges to the north could be accounted for by this process breaking down on the steeper and narrower shelf surface north of Waihi Beach.

Thus, coastally-trapped topographic waves generated during cyclonic storm events is a possible process responsible for sand ridge genesis along the east Coromandel coast. Processes which subsequently modify the ridge morphology would include storm waves and intense northerly-directed geostrophic flows, also formed by these cyclonic depressions. However, at Whiritoa and Whangamata, ridge morphology appears to be modified by southerly-directed current flows. This is a region in which a relatively sharp and narrow indent in the continental shelf occurs. Topographic variations in the shelf surface such as this have commonly been found in other studies to form a coastal counter current on the inshore side of an oceanic current (BOWDEN, 1983). As the southerly-directed East Auckland Current was detected in current recordings from Onemana, it is possible that this forms eddies on the very narrow and steep shelf offshore from Whiritoa and Whangamata, which are sufficiently intense to entrain and transport inner shelf and mid shelf sediments. Some evidence supporting this comes from the current recordings at Whiritoa, which showed relatively strong currents present (up to 0.28 $m.s^{-1}$) during calm conditions, at the same time that only low current speeds (< 0.10 $m.s^{-1}$) were recorded off Waihi Beach.

Changes in sand ridge morphology along the east Coromandel coast may therefore result from the variable shelf physiography, which favours the generation of northerly-propagating infragravity waves on the broad and flat shelf region to the south, and their subsequent dissipation on the narrower and steeper shelf north of Waihi Beach. Variations in shelf physiography may also affect sand ridge morphology by influencing the hydrodynamic processes which modify their form once generated by these infragravity flows. As sand ridges were found to be associated with areas of both extensive shelf deposition and erosion (Chapter 6.2.3.), these variations in hydrodynamic processes are probably important to the changes in sedimentation patterns which occur along the coast.

7.4. SIGNIFICANCE OF WAVE REFRACTION PATTERNS TO SHELF SEDIMENTATION

The morphology of narrow, elongate, shore-normal oriented CMR bands was examined in Chapter 6.2.2. In depths of 20 to 50 m from areas south of Opoutere Beach, these bands usually occur on the down-current flanks of sand ridges, thus indicating a likely current-generated origin. However, in depths of < 10 m south of Opoutere, and in deeper northern waters, CMR bands are usually associated with either small depressions in the sea floor, or a relatively flat surface. BLACK and HEALY (1988) studied similar bands in shallow nearshore waters at Whangarei Harbour, and from combined wave refraction studies, numerical modelling, and field measurements, found that these are wave-generated features. The process by which the bands are generated was concluded by BLACK and HEALY (1988) to result from refraction of surface gravity waves along a distended zone across the ebb tide delta, which created a band of wave height- and thus wave energy-reinforcement in the band locations.

The presence of relatively high relief sand ridges, rock pinnacles, and numerous offshore islands along the east Coromandel coast provides the potential for the refraction of ocean waves to influence shelf sedimentation patterns, particularly from sea floor scouring in localised areas of significant wave height-reinforcement, and so it was originally intended to include a comprehensive study of local wave refraction patterns as a major part of this investigation. However, the detailed nature of investigations into other aspects of shelf sedimentation has not allowed sufficient time for a thorough analysis. Only some initial attempts to relate wave refraction patterns to the occurrence of CMR bands are made here based on applications of the REFRACTION Program of BLACK and HEALY (1981), as modified by Dr Willem de Lange (1991), in various unpublished coastal erosion studies from the Marine Geosciences Group of the Earth Science Department, University of Waikato.

7.4.1. Wave Refraction Processes

The principles of wave refraction have been extensively described in KOMAR (1976), and are summarised where appropriate here. Under general shelf conditions with an irregular sea floor and waves travelling in various directions, the direction of wave travel changes due to refraction, so that wave crests parallel the depth contours. The refraction of wave rays is analogous to the bending of light rays, so that changes in direction (α) may be related to changes in wave phase velocity (C) through Snell's law:

$$\frac{\sin\alpha_1}{C_1} = \frac{\sin\alpha_2}{C_2} = \text{constant} \qquad -7.16$$

For the simple case of a straight shoreline with parallel contours, the angle at any water depth can be related to deep water wave angle approach α_∞ by:

$$\sin\alpha = \frac{C}{C_\infty} \sin\alpha_\infty \qquad -7.17$$

Since C decreases from deep to shallow water, it follows that α also decreases. Wave refraction also affects wave energy, and hence wave height, with increases occurring in areas of converging wave rays, and decreases in wave divergence zones. Given an arbitrary spacing between orthogonals (s), the energy flux along wave crests between orthogonal is defined as:

$$P = ECns \qquad -7.18$$

where E is the total wave energy density, and n is the ratio of wave group velocity to wave phase velocity. Since this flux should remain constant, any change in the orthogonal spacing will cause a change in at least one of the other terms. Assuming that group velocity remains constant, changes in energy are related to changes in wave spacing. This change is indicated by a refraction coefficient (K_r), which is defined as:

$$K_r = (s_\infty/s)^{1/2} \qquad -7.19$$

where s_∞ is the orthogonal spacing in deep water.

Using the refraction coefficient, it is possible to evaluate the change in wave height of a shoaling wave undergoing refraction as:

$$\frac{H}{H_\infty} = K_r \sqrt{\frac{C_\infty}{2nC}} \qquad -7.20$$

These equations are derived for a plane sloping beach with parallel isobaths. The real solution is more complex than this, and these equations are not suitable for deriving a solution over more complex bathymetries, such as those occurring over the east Coromandel continental shelf.

BLACK and HEALY (1981) developed a computer program, REFRACTION, which uses wave-ray tracking to solve problems of refraction over complex bathymetries. The program starts by using Snell's law to define initial values for the wave parameters, and assumes an initial dimensionless spacing between wave orthogonal of 1 unit. The wave ray is then propagated onshore, and using geometrics optics theory, the governing differential equations for the wave ray path and wave heights (NODA, 1972) are solved with a Runge Kutta algorithm. Phase celerities (c) are obtained from the dispersion relation for sinusoidal waves by:

$$c = \frac{\sigma}{k} \qquad -7.21$$

with:

$$\sigma^2 = gk \tanh(kh) \qquad -7.22$$

In addition, the program also derives a number of other wave-related parameters, including the maximum orbital velocity, and the competence of the maximum velocity.

The wave tracking procedure used in the REFRACTION program has several important limitations. In particular, singularities known as caustics arise when the orthogonal spacing decreases to zero ($s_2 = 0$). This involves an infinitely large concentration of energy (and hence an infinitely large wave), which is artificially prevented from occurring by wave breaking criteria. However, the results can be misleading, especially in intermediate and deeper waters (BLACK and HEALY, 1988). The program also considers wave heights over individual rays rather than as an average of the incoming wave energies. Thus the program can show unrealistically large variations in wave height between neighbouring rays. Finally, as the water depths are digitised from bathymetric maps over a square grid system, the accuracy of refraction analysis will depend on how finely spaced these grids are. The maximum grid spacing allowed in the program must be at least half the deep water wavelength. The latter problem was the main limitation in this refraction analysis, as the bathymetry in digitised maps was in some instances significantly different to those used as base maps for sonograph interpretations, making accurate comparisons between the two data sets difficult.

7.4.2. Wave Refraction Results

Due to time restrictions, the wave refraction results presented here have by necessity been obtained from other non-related studies along the east Coromandel coast. As the data input into these analysis have been designed to obtain different information (i.e. information on breaking wave heights and beach erosion), some limitations are placed on their applicability to this analysis of relationships between CMR bands and wave convergence zones. In particular, the wave parameters used in these analyses are often design conditions based on hindcasting from extreme storm events, and so the results should be treated with some caution.

In all of the wave refraction analyses, approach directions for wave rays was first determined by employing a reverse wave tracking function in the REFRACTION program. The wave ray fans in most instances show offshore wave orthogonal approach angles of between 135° and 210° true (northeast to southeast). Only northeast to east directions were analysed though, as these are the most common storm wave approach angles on the east Coromandel coast.

Mataora-Whiritoa

Wave refraction patterns off Whiritoa and Mataora Beaches were originally analysed by Miss Helen Neil, as part of an unpublished beach erosion study within the Department of Earth Sciences, University of Waikato. Waves were run on an 11 by 14 km grid, with a 550 m offshore grid spacing. Design waves in the analysis were H = 9.8 m and T = 13.2 s, based on hindcasting

from Cyclone Bola in March 1988, during which wind speeds of up to 40 knots over a 12 hour duration were reported by media sources.

Results from this analysis are shown in Figure 7.19 for orthogonal approach angles of 135°, 155°, and 180°. Waves from a northeasterly direction (Figure 7.19 a) show areas of intense wave ray convergence to the north and south of Whiritoa Beach, and off Mataora Beach.These convergence zones are associated with refraction over inner shelf sand ridge crests. The latter area off Mataora Beach is the most extensive convergence zone, extending out to depths of ~.33 m. It is also the only wave convergence zone from this wave angle associated with CMR bands, with three separate bands in depths of 10, 20, and 30 m identified in the Jun-90 survey. Wave rays from a more east-northeasterly approach (Figure 7.19 b) show an important zone of intense wave convergence, and hence height- and energy-reinforcement off the northern end of Whiritoa Beach. This is the same area where extensive nearshore erosion appeared to occur during Cyclone Bola, as shown in the side-scan sonar and echosounding surveys. Waves run from an easterly approach form three main zones of intense wave convergence out to 40 m water depth, in areas both north and south of Whiritoa Beach, and south of Mataora Beach (Figure 7.19 c). The convergence zones off Whiritoa Beach coincide with areas in which CMR bands were identified on the lower nearshore and inner shelf surface during both the Mar-84 and Jun-90 side-scan sonar surveys.

Thus, off Whiritoa and Mataora Beaches, zones of intense wave ray convergence associated with refraction of very large storm waves over sand ridge crests, may be an important process in the formation of CMR bands. Wave refraction may also have been important in causing the extensive erosion of nearshore deposits observed following Cyclone Bola (see Chapter 6.4.).

Whangamata-Onemana

Wave refraction patterns on the coastline between Whangamata and Onemana Beaches have been analysed as part of a tidal inlet study at Whangamata estuary by SHEFFIELD (1991). Waves were run on a grid of 11 by 7 km, with a 350 m offshore grid spacing. The design waves used by SHEFFIELD (1991) were representative of relatively extreme storm conditions, with H = 4.2 m and T = 9.5 s.

Results from the analysis are shown in Figure 7.20, for approach angles of 140°, 150°, and 170°. Waves from a northeasterly approach form distinct areas of wave ray convergence north and south of Whangamata (Figure 7.20 a). The southern convergence zone off Otahu estuary is associated with refraction over a mid shelf sand ridge crest, and appears to concentrate wave energy on the inner shelf where several small CMR bands were identified in the Mar-84 side-scan sonar survey. The northern convergence zone off Te Ananui Headland is associated with refraction around reefs offshore from Onemana Beach, but does not coincide with any CMR bands on the sea floor. However, waves from a more east-northeast approach cause this latter

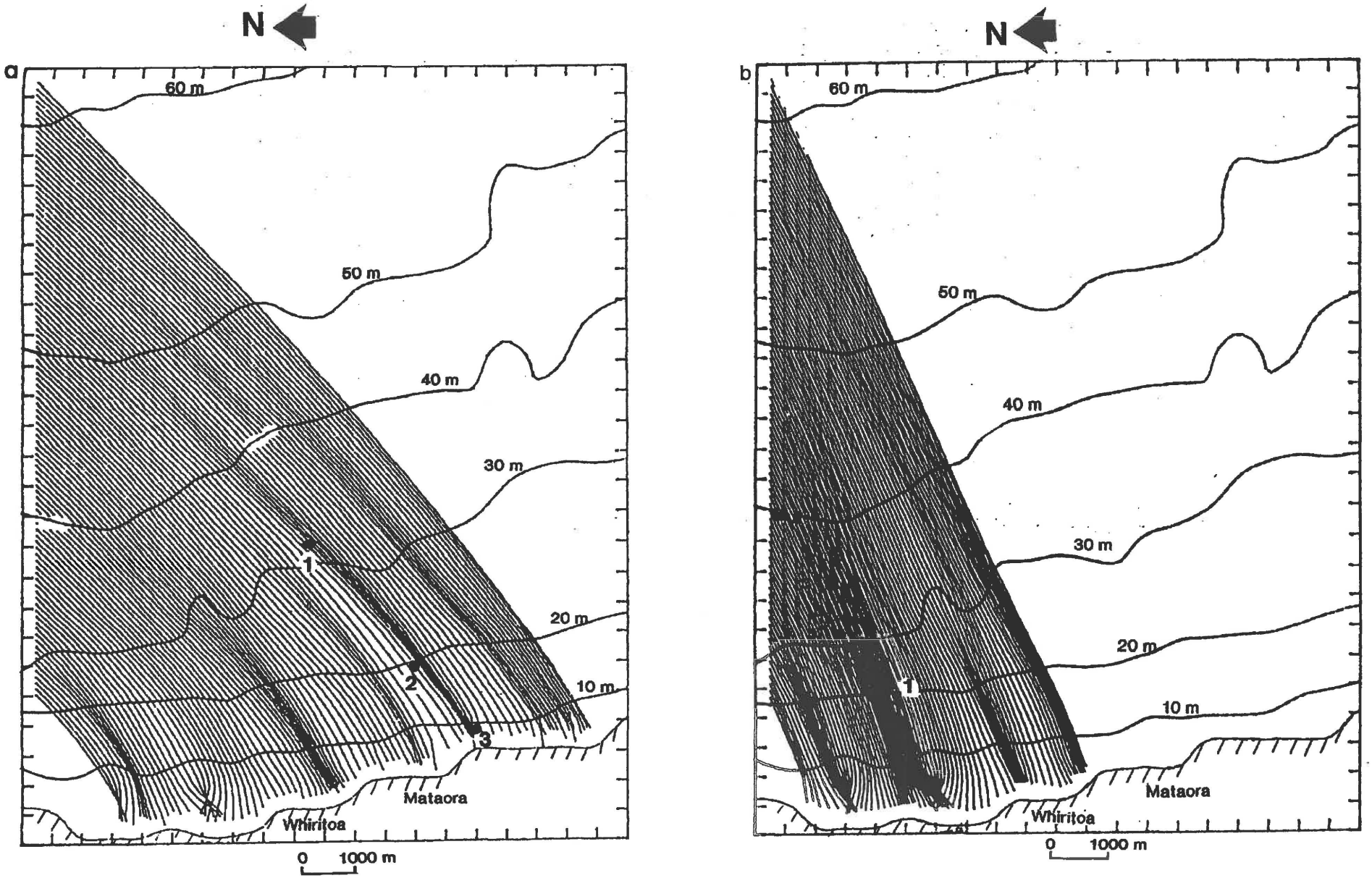
a
N
60 m
50 m
40 m
30 m
20 m
10 m
1
2
3
Whiritoa
Mataora
0 1000 m
b
N
60 m
50 m
40 m
30 m
20 m
10 m
1
Whiritoa
Mataora
0 1000 m

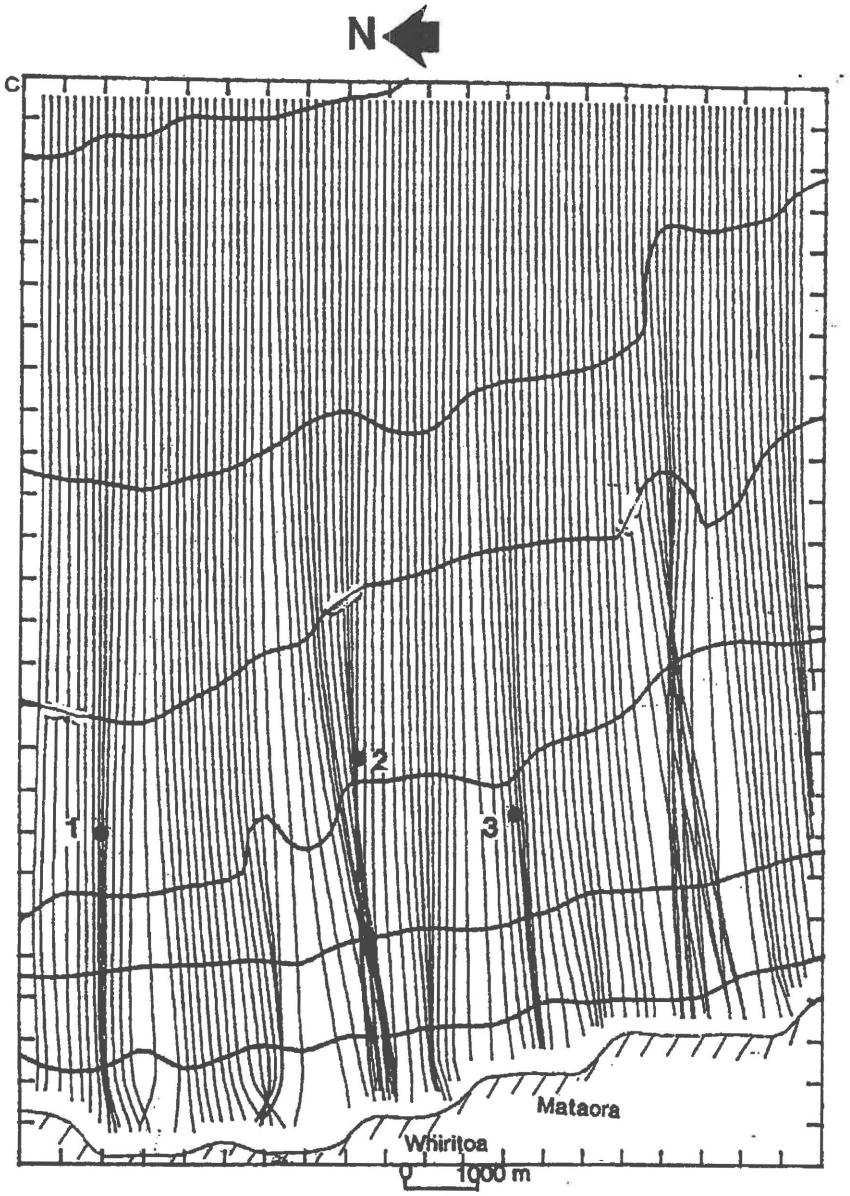

Figure 7.19. Wave refraction patterns and association with CMR bands off Whiritoa and Mataora Beaches, using a design storm wave of H= 9.98 m, T= 13.2 s, and orthogonal wave approach angles of: a) 135°; b) 155°; c) 180° (results obtained from Helen Neil, Earth Science Department, University of Waikato). CMR band locations are shown on diagrams as numbered dots: a) 1; b) 1; c) 1, 2, 3.

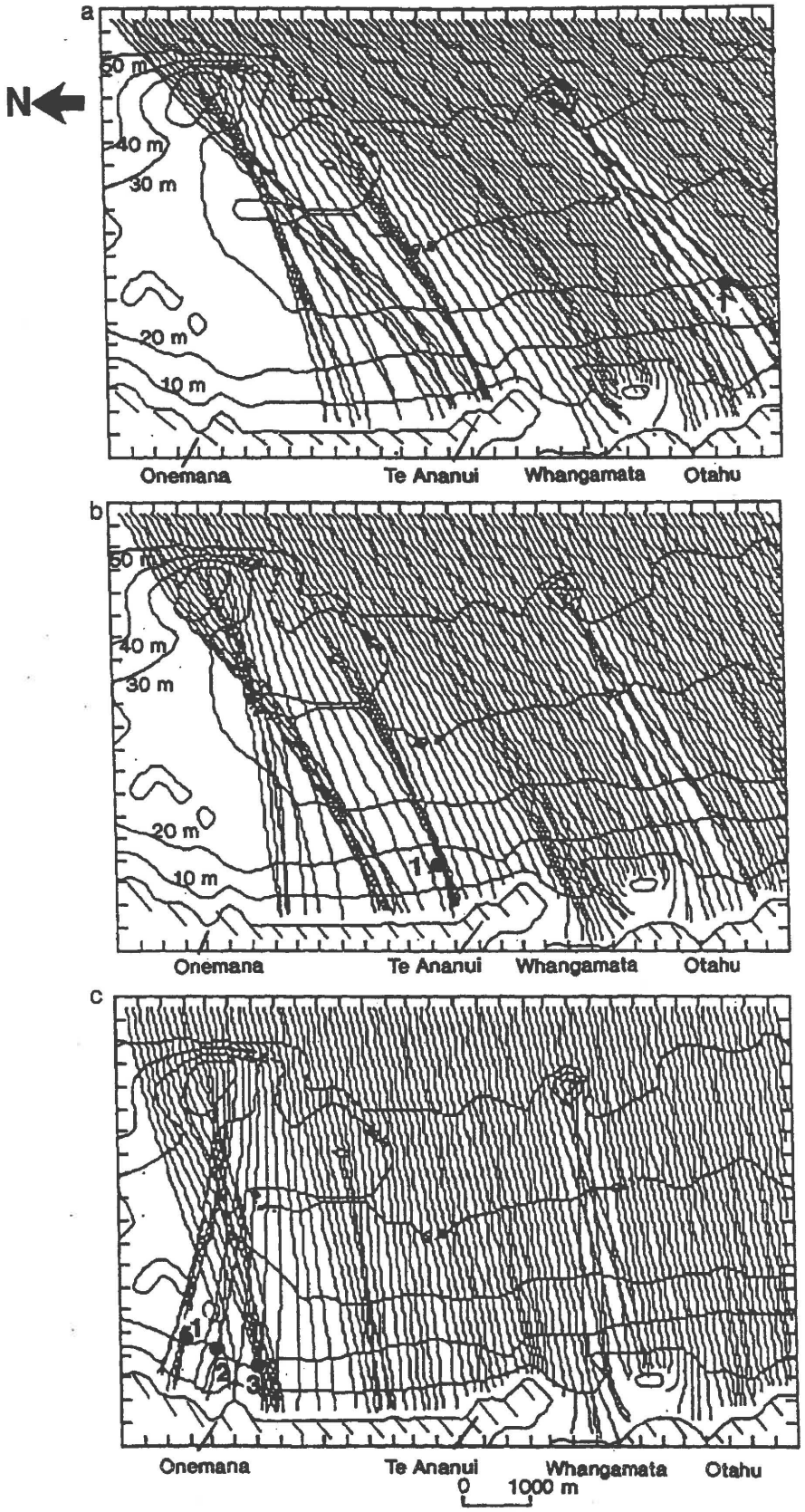

Figure 7.20. Wave refraction patterns and association with CMR bands off Whangamata and Onemana Beaches, using a design storm wave of H= 4.2 m, T= 9.5 s, and orthogonal wave approach angles of: a) 140°; b) 150°; c) 170° (from SHEFFIELD, 1991). CMR band locations are shown on diagrams as numbered dots: a) 1; b) 1; c) 1, 2, 3.

convergence zone to shift northwards (Figure 7.20 b), and coincide with the extensively examined CMR band from the Mar-84 and Mar-85 side-scan sonar surveys (see Figure 6.24). Waves from an easterly approach refract over this same offshore reef to produce important wave convergence zones off Onemana Beach (Figure 7.20 c). This causes wave height-reinforcement on the lower nearshore surface in the same areas that extensive CMR bands were identified in the Mar-84 and Mar-85 side-scan surveys. The approach angles of these refracted wave rays vary from northeast to southeast, which is consistent with observations of megaripple crest orientations in the CMR bands (see Figure 6.53).

It appears that refraction of wave rays over mid shelf sand ridge crests and inner shelf reefs is an important process in the generation of CMR bands at Whangamata and Onemana. Variations in CMR band morphology between side-scan sonar surveys may also be accounted for by these refraction patterns. For example, storm waves from a northeasterly approach favour wave height-reinforcement to occur on the nearshore and inner shelf surface, both north and south of Whangamata. However, storm waves from a more easterly approach do not produce significant zones of wave focussing at Whangamata, but instead cause extensive convergence zones to develop off Onemana. The relative stability of the Te Ananui CMR band north of Whangamata, and the dynamic nature of Onemana CMR bands between the Mar-84 and Mar-85 surveys, may therefore be due to easterly storm waves dominating through this 12 month period.

Opoutere-Tairua

Wave refraction patterns on the coastline between Opoutere and Tairua Beaches were originally studied by Mr. Greg Foster as part of an unpublished coastal erosion study of Pauanui Beach.Wave tracking was run over a 22 by 15 km area, with a 750 m offshore grid spacing. The design storm waves used in this analysis were based on conditions hindcast from the major storm event in July 1978, with H = 8.94 m and T = 14.9 s.

Results of the wave refraction analysis are shown in Figure 7.21, with orthogonal approach angles of 140°, 160°, and 170°. Waves from a northeasterly approach form a distinct zone of wave convergence on the northern side of Shoe Island, arising from the refraction of waves over offshore reefs to the northeast (Figure 7.21 a). This is an area in which extensive CMR patches were found in the side-scan sonar surveys. Waves from an east-northeast approach show several important wave convergence zones off both Tairua and Opoutere Beaches (Figure 7.21 b). At Tairua, convergence zones are again associated with refraction around offshore reefs, and are concentrated on the northern and southeastern sides of Shoe Island, and on the lower nearshore-inner shelf boundary off mid Tairua Beach. These are all areas in which extensive CMR patches were evident on sonographs. At Opoutere, east-northeast waves refract around Slipper Island, causing convergence of wave rays onto the lee areas both south and north of the island. This may therefore be a contributing factor to the presence of extensive CMR deposits in the lee shelf area. Important zones of both wave divergence and convergence also occur south of Slipper Island, in

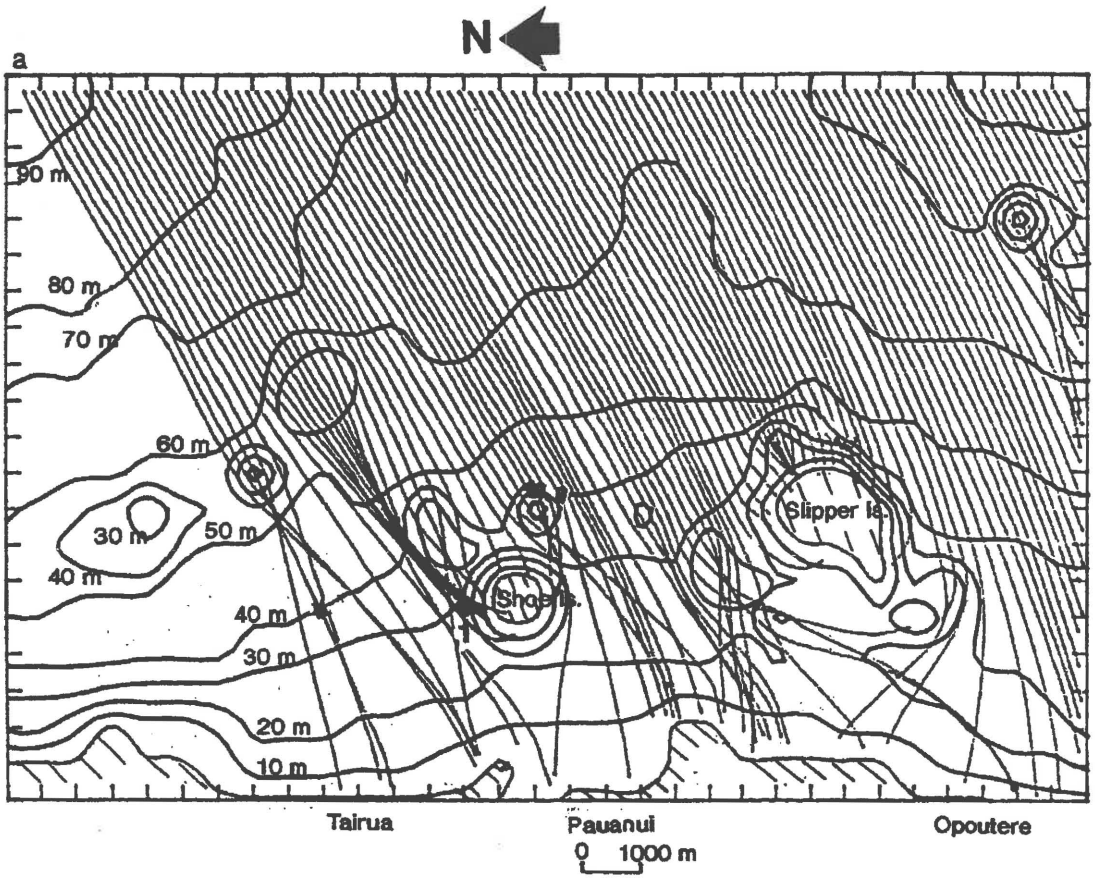
a
N
90 m
80 m
70 m
60 m
30 m
50 m
40 m
40 m
30 m
20 m
10 m
Shoe Is.
Slipper Is.
1
0
Tairua
Pauanui
Opoutere
0 1000 m

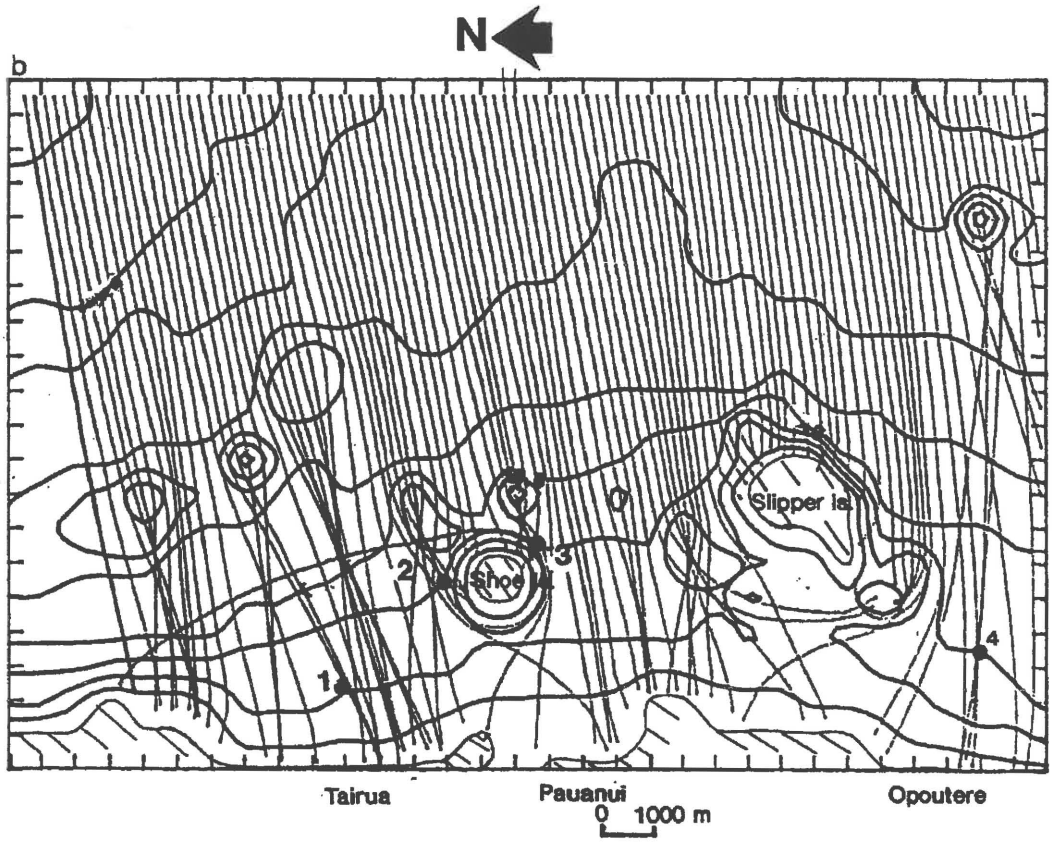
b
N
Slipper Is.
Shoe Is.
0
1
2
3
4
Tairua
Pauanui
Opoutere
0 1000 m

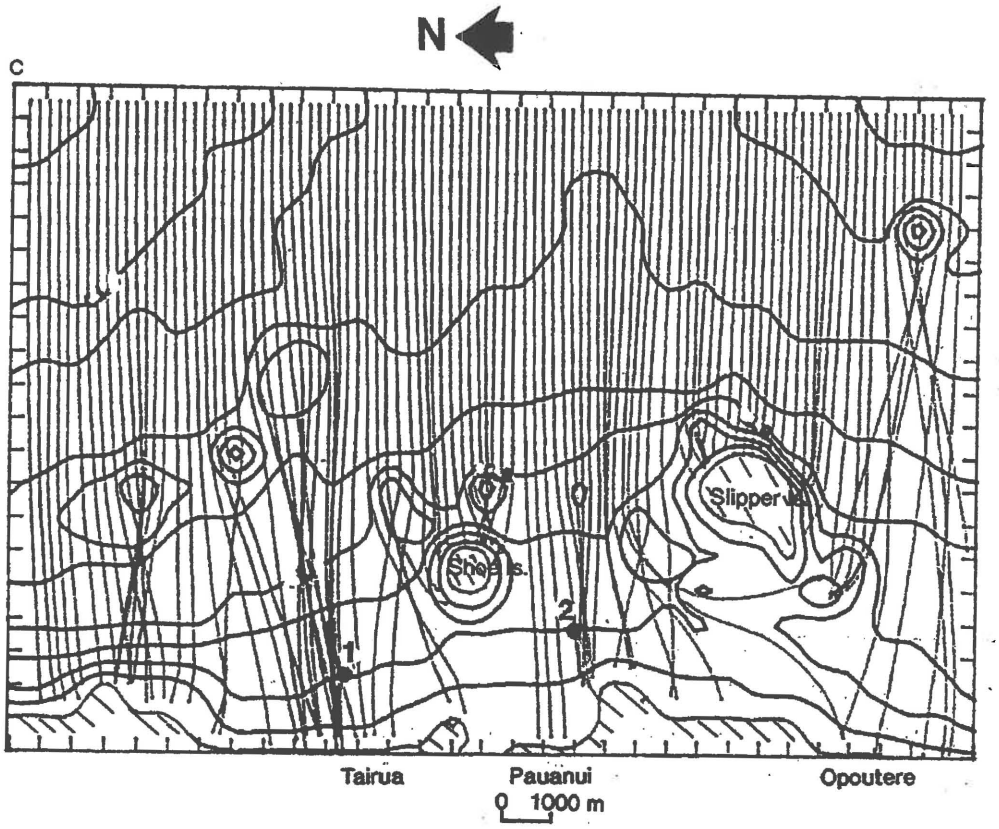

Figure 7.21. Wave refraction patterns and association with CMR bands off Opoutere, Pauanui and Tairua Beaches, using a design storm wave of H= 8.94 m, T= 14.9 s, and orthogonal wave approach angles of: a) 140°; b) 160°; c) 170° (results obtained from Greg Foster, Earth Science Department, University of Waikato). CMR band locations are shown on diagrams as numbered dots: a) 1; b) 1, 2, 3, 4; c) 1, 2.

the same shelf vicinities where extensive fine grained and CMR deposits occur. Easterly storm waves produce similar wave convergence zones, but also result in an area of wave convergence off Pauanui Beach, in the same location where extensive CMR bands occur on sonographs (Figure 7.21 c).

Again, analysis of wave refraction patterns on the coastline between Opoutere and Tairua Beaches support deductions made from the morphological analysis in Chapter 6, namely that CMR bands and patches in these areas result from the refraction of storm waves around offshore islands and reefs. In addition, this analysis indicates that the most extensive areas of CMR deposits (i.e. mid Tairua Beach, Shoe Island and Slipper Island) consistently coincide with wave convergence zones from northeast to easterly wave approaches, whereas the less extensive CMR bands off Pauanui Beach only coincide with convergence zones from easterly storm waves.

Mercury Bay

Wave refraction patterns within Mercury Bay were analysed by Mr Grant Kensington as part of an unpublished coastal erosion study of Cooks Beach. Wave rays were run over a 11 by 11 km grid, with a 90 m offshore grid spacing. Design waves in this analysis were also based on the July 1978 storm, but hindcast slightly lower wave conditions of H = 7.1 m and T = 12 s.

Results are shown in Figure 7.22, with an orthogonal approach angle of 132° (note that a wider range of approach angles was not used in this analysis, as ray back tracking showed that only waves from a northeasterly direction were significant for erosion at Cooks Beach). This indicates that the refraction of storm waves around Motukorure Island in the middle of Mercury Bay produces zones of significant wave convergence, in areas just south of the island, and in 10 m water depth off Cooks Beach. These are both areas in which extensive CMR patches and bands occur on sonographs. The latter convergence zone also coincides with the area in which shelf erosion appeared to occur during Cyclone Bola. Thus, wave refraction analysis off Cooks Beach supports deductions made from the morphological analysis in Chapter 6, that CMR deposits adjacent to offshore islands in Mercury Bay are associated with the refraction and convergence of storm waves around these islands.

7.4.3. Significance of Wave Refraction to CMR Band Formation

Analysis of wave refraction patterns along the east Coromandel coast allows some important deductions to be made regarding the role of surface gravity waves in the formation of isolated bands and patches of shelf erosion. It must be again emphasised though, that limitations in the accuracy of the analysis mean the results are strongly suggestive rather than conclusive.

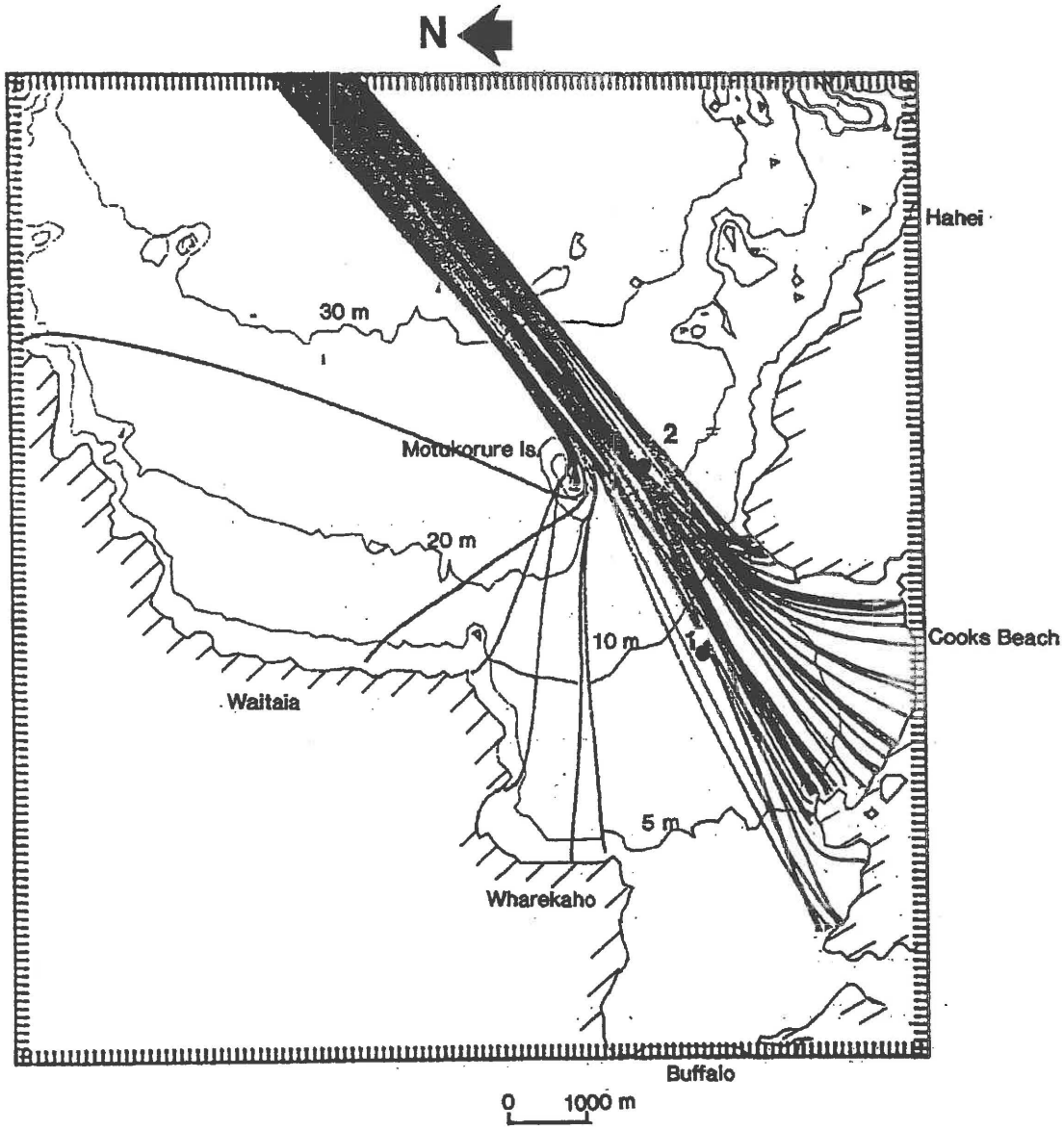

Figure 7.22. Wave refraction patterns and association with CMR bands off Cooks Beach, using a design storm wave of H= 7.1 m, T= 12.0 s, and an orthogonal wave approach angles of: 132° (results obtained from Grant Kensington, Earth Science Department, University of Waikato). CMR band locations are shown on diagram as numbered dots: 1, 2.

In general, the refraction of very large storm waves around bathymetric features (i.e. sand ridges, rock pinnacles, and offshore islands) results in the development of distinct wave ray convergence zones, where wave height- and thus wave-energy reinforcement will occur. In many (but not all) instances, these zones of wave convergence tend to coincide with areas in which CMR bands and patches are identified on the side-scan sonographs. Hence there is strong supportive evidence that wave refraction may play an important role in the formation of these CMR bands, as determined at Whangarei Harbour by BLACK and HEALY (1988). Alternative generating mechanisms suggested in other studies include:

- strong offshore flowing rip currents (MORANG and McMASTER, 1980; COOK, 1982);

- offshore flowing downwelling currents (CACCHIONE *et al.*, 1984);

- shore-parallel wind-generated currents (SWIFT and FREELAND, 1978).

The first possibility is considered unlikely, as the bands are generally found too far offshore to be influenced by rip currents. Downwelling currents may generate CMR bands in areas where topographic features are present to concentrate such flows, such as along the northern margins of Mercury Bay (see Chapter 62.2.). However, along more open coastlines, downwelling currents should develop a relatively uniform offshore flow, and thus not produce isolated areas of intense scouring. Shore-parallel wind-generated currents do, however, appear to be an important mechanism in the generation of many CMR bands, as shown by their association with the down-current flanks of sand ridges. Therefore, only in areas where no sand ridges are associated with the CMR bands (i.e. Pauanui, Tairua, Cooks Beach) can wave refraction be considered the primary mechanism of their formation.

As CMR bands are often formed on sand ridges, or associated with the refraction pattern of storm waves over sand ridge crests (e.g. Whiritoa and Whangamata), it is possible that bands are generated by the complex morphodynamic interactions between along-shelf propagating infragravity waves, intense wind-generated currents, and storm wave convergence zones. In shelf regions dominated by sand ridges (Waihi Beach to Whangamata), the first two processes would be the primary ridge- and thus band-generating processes. Subsequent interactions with storm waves would cause these to refract and thus converge along their crests, resulting in a band of wave-height reinforcement, which possibly extend further landwards beyond the influence of wind-generated currents. This process could explain the occasional occurrence of CMR bands on sand ridge crests in lower nearshore water depths (20 to 30 m), but over a relatively flat sea floor in shallower waters (5 to 10 m; see Figure 6.24). In areas where offshore reefs and islands influence wave refraction patterns, and CMR bands are associated with sand ridges (Onemana and Opoutere), the position of these bands and ridges may be primarily determined by wave convergence zones. In this case, a zone of intense combined wave-current flows would develop due

to wave height-reinforcement, thus resulting in the generation of a sand ridge and associated CMR band.

Accordingly, this analysis of wave refraction patterns suggests that along many parts of the east Coromandel coast the presence of isolated areas of shelf erosion, as indicated by CMR bands and patches, may be associated with the refraction patterns of storm waves. However, this is based on analysis of a limited range of very extreme wave conditions. More detailed investigations would need to be undertaken in future to more accurately determine the precise role of wave refraction in CMR band generation.

7.5. CONCLUSIONS

Analysis of the morphodynamic characteristics of the east Coromandel shelf allows some deductions to be drawn regarding the mobility of shelf sediments under different hyrodynamic conditions, and possible causes of regional variations in these hydrodynamic processes.

Theoretical considerations of sea-bed mobility using the method outlined by CLIFTON and DINGLER (1984), tend to be consistent with broad deductions made in Chapters 5 and 6 from analysis of sediment textural properties and shelf morphological features. These include:

1. Upper nearshore sediments should be actively reworked, with the dominantly fine to very fine grained sands subject to sheet flow conditions under either moderate storm waves (T = 6 to 8 s, H = 2.2 to 2.0 m), or long period swell waves (T = 10 s, H = 1.8 m). The less extensive coarse deposits should also form megaripples under relatively low wave conditions (T = 6 s, H = 1.8 m).

2. Lower nearshore deposits are less frequently reworked, fine deposits only being subject to sheet flow during very high storm wave conditions (T = 10 s, H = 4 m), and coarse deposits forming megaripples under either storm waves (T = 8 s, H = 2.6 m), or relatively low but long period swell waves (T = 10 s, H = 1.4 m).

3. Inner shelf deposits are only intermittently reworked, with sheet flow on fine sands expected under extreme conditions (T = 12 to 16 s, H = 7 to 4 m), and megaripples formed on coarse sediments during relatively large storm wave conditions (T = 8 to 10 s, H = 3.6 to 2.6 m).

4. Mid shelf deposits are infrequently reworked by waves, with sheet flow conditions on very fine grained sands being almost impossible under the observed wave conditions for the northeast coast, and megaripples only forming on coarse sediments under large storm waves (T = 10 s, H = 2.8 m).

5. Very fine grained nearshore and inner shelf sediments in Mercury Bay are potentially more mobile than deposits from the same depth range both south and north, due to their much finer texture.

Data obtained from depth of activity rod surveys give supporting evidence for deductions of the wave conditions associated with sheet flow of fine sands. However, these data also indicate significant inaccuracies in the method of interpreting wave conditions associated with ripple and megaripple generation, with the CLIFTON and DINGLER (1984) technique consistently overestimating these conditions. This is thought to result from several oversimplifying assumptions made in the technique. Firstly, it does not account for the increased shear stress associated with combined wave-current flows. However, this is probably not a major cause of inaccuracies, as it had no apparent effect on estimates of sheet flow conditions for adjacent fine sands. Secondly, the technique does not account for the varying grain size of crest and trough deposits in megaripples, with the finer crest sediments appearing to deposit in troughs under calm conditions, and reworked back onto the crests during storms, thus causing very sudden changes in megaripple dimensions. Thirdly, it does not account for the very important effect of the high surface roughness produced by megaripples, which will significantly reduce the wave (and current) conditions required to rework deposits, and possibly modify the orbital diameter of wave flows.

Similarly complex morphodynamic interactions appear to be associated with the larger scale sand ridge bedforms which extend along the shelf from Waihi Beach to Opoutere. It is proposed that infragravity waves associated with coastally-trapped topographic waves determine the spacing and position of ridges, although their formation and morphological characteristics are largely determined by shore-parallel shelf currents. In most cases, these appear to be the intense northerly-directed wind-generated currents formed during easterly storms. However, at Whiritoa and Whangamata, it is possible that strong eddies branch off the east Auckland Current flow over the steep and narrow indentation in the shelf here, and are of sufficient strength to entrain and transport sediments over sand ridges to the south. This would account for the change in morphology of sand ridges on the inner shelf and mid shelf at Whiritoa and Whangamata respectively, and thus explain the extensive deposition of fine sands across the shelf at Whiritoa. Sand ridge morphology also appears to be influenced by the effects of surface gravity waves, as shown by the presence of bands and patches of CMR sands on their down-current flanks.

Thus, sand ridges probably form under the complex morphodynamic interactions occurring during storm conditions. This involves infragravity waves generated to the south in the Bay of Plenty causing spatially periodic sediment fluxes along the shelf, and storm waves entraining fine sands into suspension, which are then transported by wind-generated currents to form the sand ridges. Subsequent morphodynamic interactions may then occur, with storm waves refracting over sand ridge crests to produce a zone of wave height-reinforcement, and thus localised scouring of the sea floor. This may be the process by which CMR bands form on the coast where sand ridges are a significant shelf morphological feature. In locations north of Whangamata where sand ridges are of

decreasing influence, areas of shelf erosion and deposition appear to be associated with the refraction patterns of storm waves around offshore islands and reefs. Thus, CMR bands in these areas are primarily formed by zones of wave-height reinforcement, with wind-generated currents playing a secondary role in some locations (Onemana, Opoutere).

CHAPTER EIGHT

SHALLOW SUB-BOTTOM SHELF STRATIGRAPHY

8.0. INTRODUCTION

In preceding chapters, the variable nature of nearshore and inner shelf sedimentation patterns along the east Coromandel coast has been described in detail. These sedimentation patterns have so far been accounted for by observations and theoretical considerations of the variable nature of present day hydrodynamic conditions, both along the coast and across the shelf surface. However, so far no consideration has been given to the possible association of modern sedimentation patterns with shallow sub-bottom patterns, and the possible controls on the former by past environments of deposition. Accordingly, this chapter seeks to:

1. Ascertain the thickness of modern (Holocene) sand bodies on the east Coromandel shelf, and thus determine whether present sedimentation patterns represent either a thin veneer of deposits associated with long-term erosion or non-deposition, or whether they form relatively thick stratigraphic units suggestive of long-term shelf deposition;

2. Attempt to identify the depth of reworking of modern shelf deposits;

3. Attempt to identify stratigraphic units that may indicate past environments of deposition, and determine what influence these (may) have had on the present shelf physiography and sedimentation patterns.

Interpretations of shallow shelf stratigraphy are determined primarily through high resolution, continuous sub-bottom seismic reflection profile data, with some additional shallow subsurface information provided by box cores. Limitations in time and resources did not allow a thorough investigation of the shelf stratigraphy, only five areas being surveyed, and no deeper core data collected. However, a preliminary interpretation of stratigraphic patterns has been possible.

8.1. METHODS

Stratigraphic data were initially obtained by Paul Dell between 12 and 16-Nov-84, 52 box cores being collected from various sites at Waihi, Whiritoa, Whangamata, Onemana, and Whangapoua. This was done using equipment provided by the New Zealand Oceanographic Institute, and aboard the H.M.N.Z.S. "TUI". Locations of box cores are shown in Figures 8.1 and 8.2. The data were of limited use, however, as penetration was restricted to a maximum depth of 0.40 m, allowing only the surficial nature of stratigraphic units to be determined. Once the cores had been obtained, they were immediately photographed and a P.V.C. tube inserted to obtain a representative sample for subsequent analysis and archiving. Unfortunately, no peels were taken from the cores to help identify sedimentary structures, and the samples were not sealed and have subsequently dried out and lost their original integrity. This has limited analysis of the box core data to the original observations made by Paul Dell (see Appendix 6).

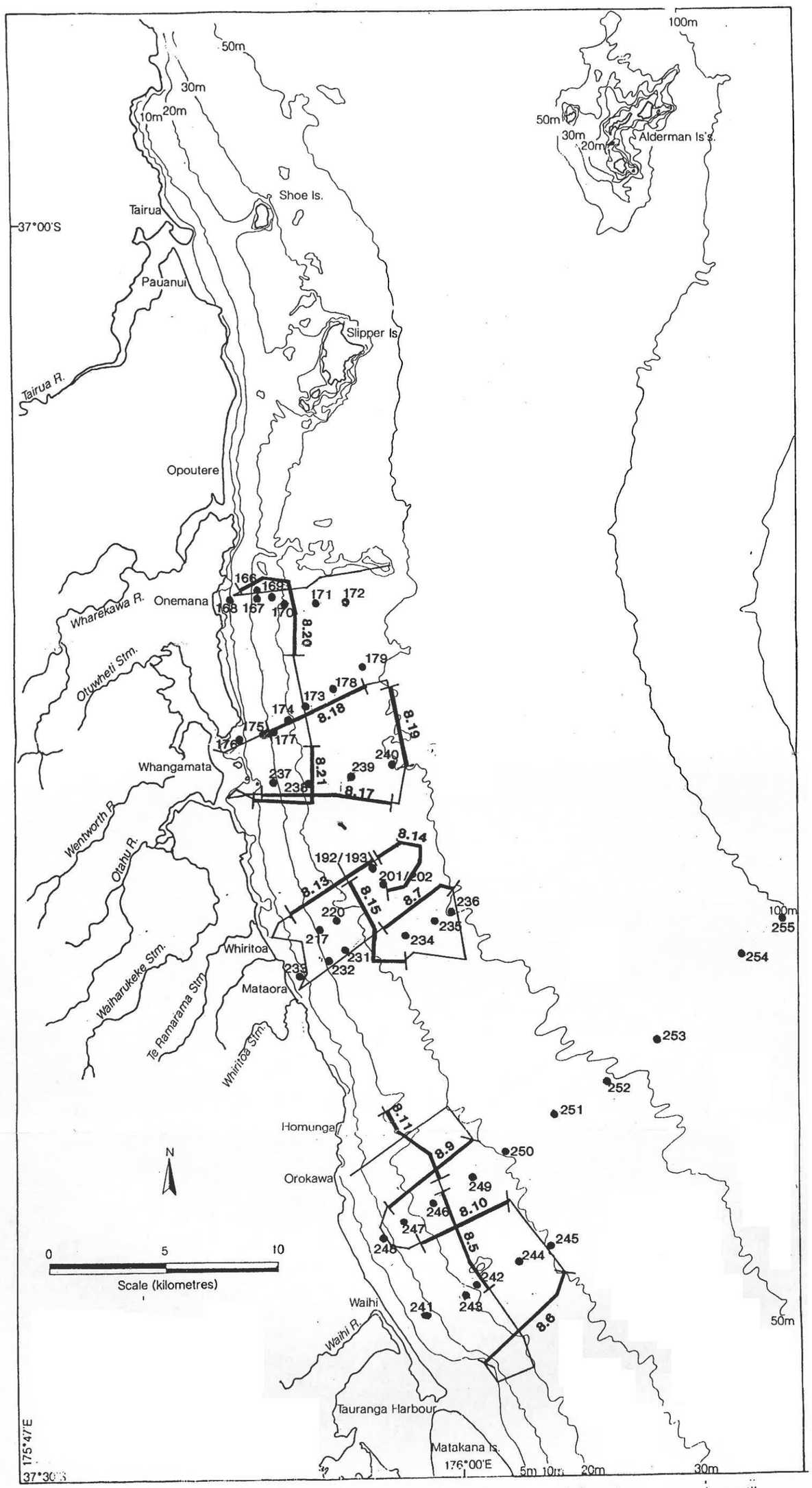

Figure 8.1. Location of box cores and seismic track lines from the southern exposed coastline. Highlighted tracklines indicate seismic profiles illustrated in the text (bold numbers = figure number), and numbered dots are box core sample numbers.

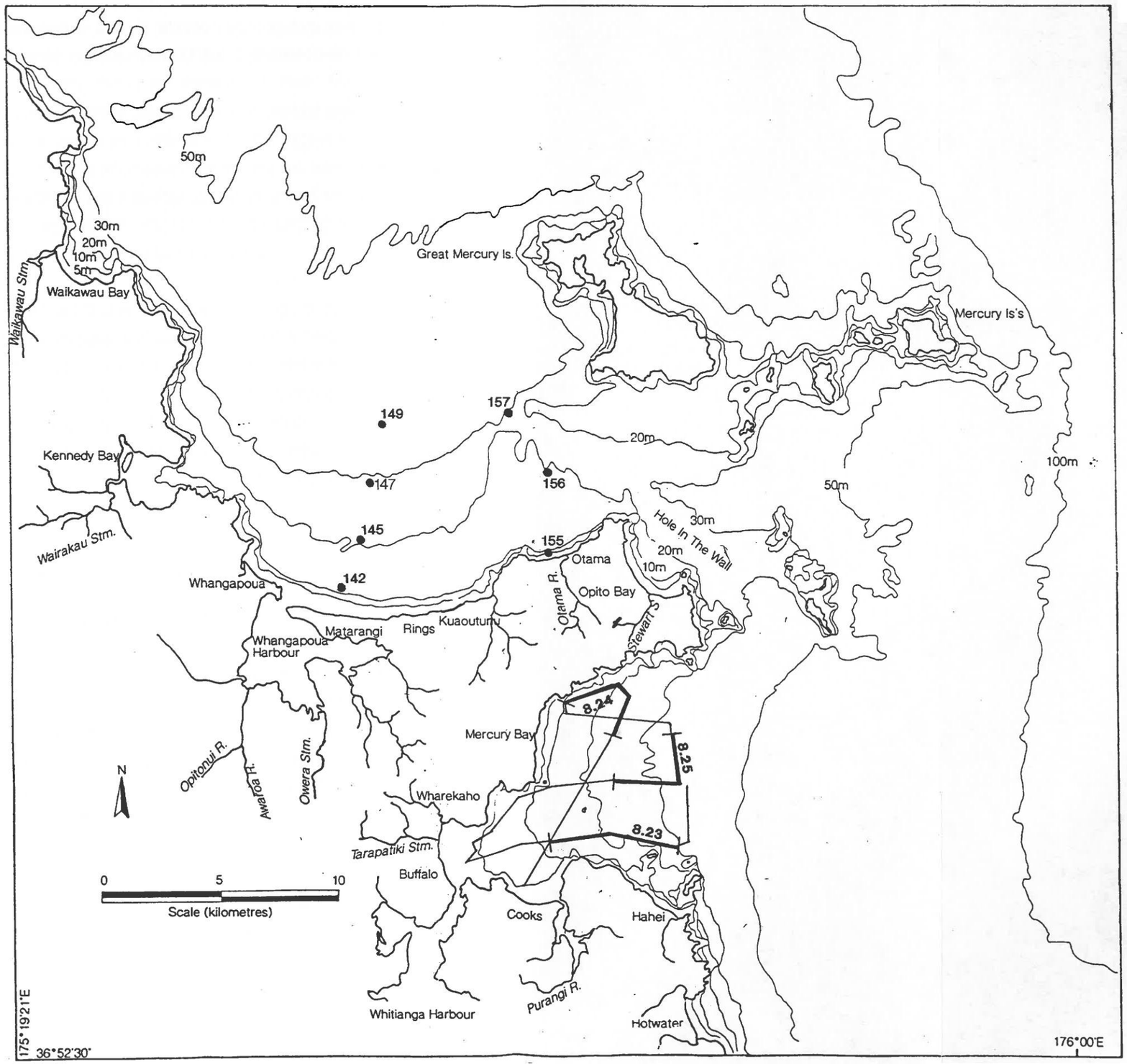

Figure 8.2. Location of box cores and seismic track lines from the northern embayed coastline. Highlighted tracklines indicate seismic profiles illustrated in the text (bold numbers = figure number), and numbered dots are box core sample numbers.

More detailed stratigraphic information was collected by this author between the 25 and 28-Jun-90, when high resolution continuous sub-bottom seismic reflection profiling data were obtained. An earlier attempt had been made in Nov-89, but was cancelled due to problems with equipment and poor sea conditions. Surveys were ultimately carried out offshore from Waihi, Mataora, Whiritoa, Whangamata, Onemana, and Mercury Bay, with a total of 174 km of sea-bed profiled in 10 to 50 m water depth. It had been hoped to include the area offshore from Whangapoua in this survey, but poor sea conditions prevented this at the time when equipment and vessels were made available. Profiles were taken simultaneously with the third side-scan survey, described in Chapter 6, which allows the sub-bottom data to be integrated with information on the textural nature of surface deposits where ever surface expressions of seismic units are apparent.

The seismic equipment used was an EG and G Uniboom (model 230-1) high resolution system, hired from the New Zealand Oceanographic Institute, and operated by their technician, Mr Peter Hill. According to the manufacturers, this model is capable of penetrating sediments to a depth of 50 m, and provides a resolution of 0.15 m. In this investigation, a penetration of 30 to 50 m was generally obtained, multiple reflectors distorting the image in shallow water. The track lines were pre-determined and plotted using the same system described for the side-scan survey in Chapter 6.1.1. The sub-bottom survey track lines are illustrated in Figures 8.1 and 8.2, and fix numbers shown in Appendix 4.

8.2. SEISMIC STRATIGRAPHY

8.2.1. Principles of Seismic Stratigraphic Analysis

Stratigraphic interpretations in this study are primarily dependent on analysis from seismic profiles, and correlation with other information from side-scan sonographs and box cores. Accurate geophysical modelling requires absolute dating of subsurface deposits, and information on their lithology from long cores (SHIPP *et al.*, 1991). However, until such information becomes available, seismic stratigraphy provides the best constraint on the nature and depositional history of subsurface deposits on the east Coromandel coast.

A fundamental assumption in seismic stratigraphic analysis is that seismic reflectors represent time lines (VAIL, 1987). Sequence stratigraphy is a recent method of subdividing, correlating and mapping sediments, based on interpretations of seismic reflectors (VAIL *et al.*, 1977). Sequence stratigraphy involves delineating seismic data into depositional sequences. Each sequence corresponds to a chronostratigraphically constrained genetic depositional interval, developed through a cycle of global eustatic sea level oscillation (VAIL, 1987). Sequence boundaries are defined based on the presence of stratigraphic unconformities, as expressed in geometric patterns of stratal onlap and offlap (Figure 8.3; CHRISTIE-BLICK, 1991). Once a depositional sequence has been defined, seismic facies may then be interpreted based on the internal configuration and types

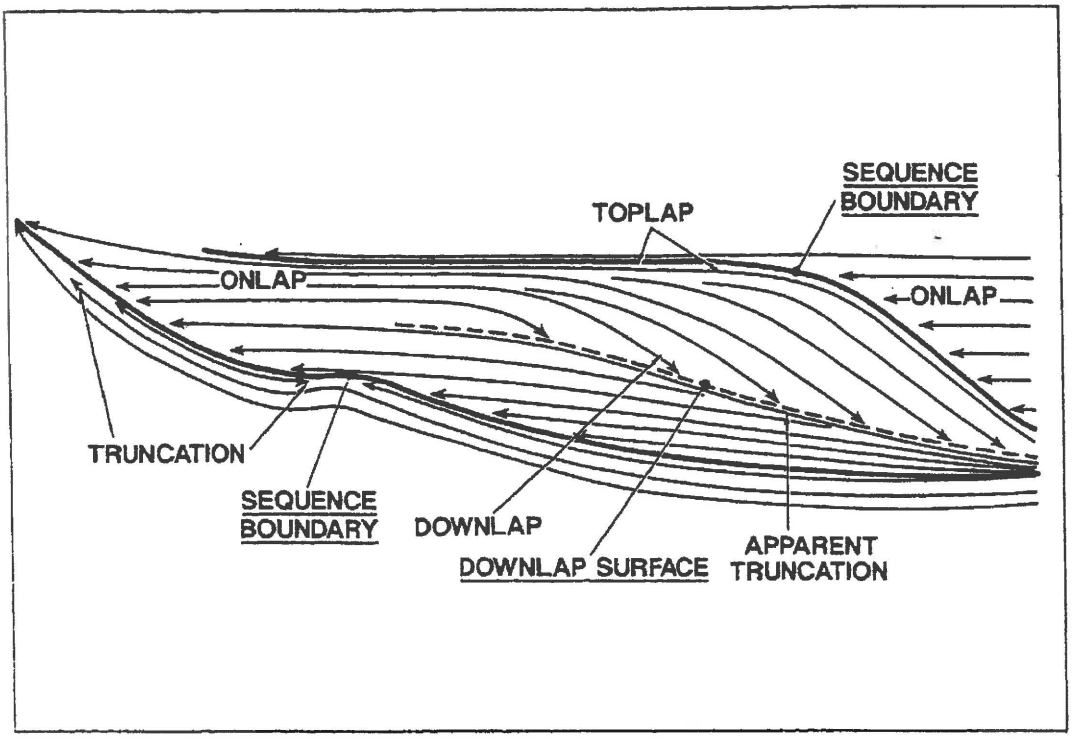

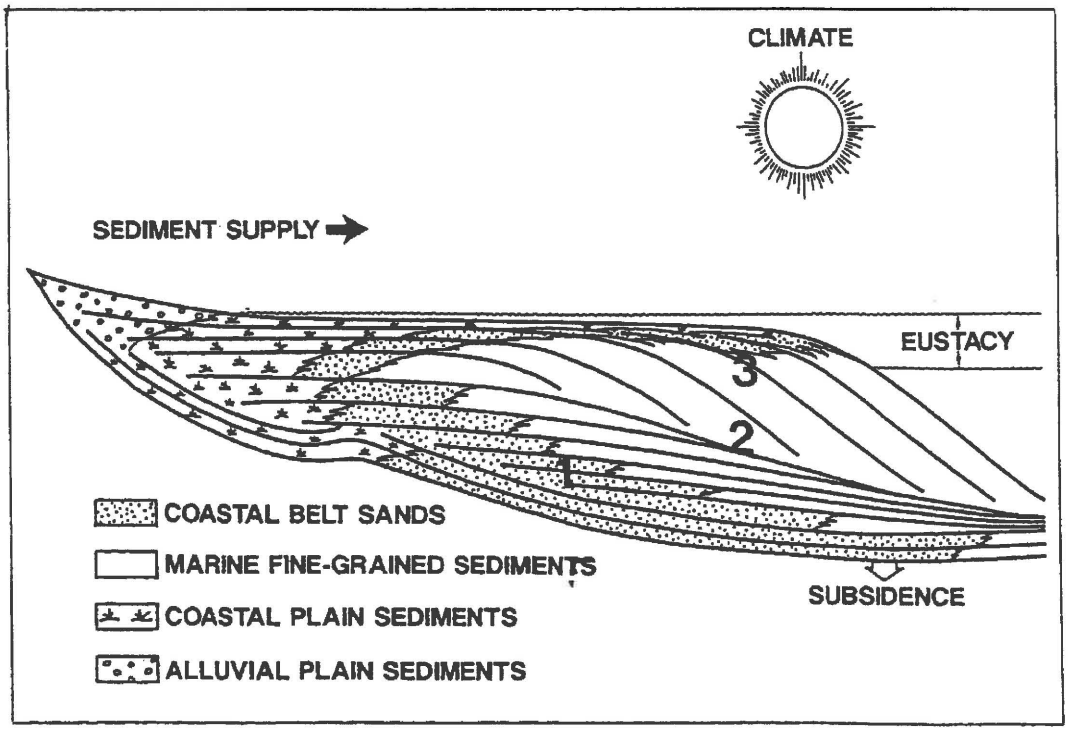

Figure 8.3. a) Seismic reflection termination patterns used in delineating unconformities (truncation surfaces) from apparent truncations; b) Various seismic reflections and associated lithofacies found in a typical sequence. Here, a lower transgressive systems tract (1) has formed over a marine truncation surface (2), followed by a high stand systems tract of aggraded and prograded coastal and shelf sands (3). Also shown are the major variables affecting stratigraphy (from VAIL, 1987).

of seismic reflection characteristics. However, these should if possible be calibrated to lithological and depositional facies interpretations from well logs (VAIL, 1987).

Numerous geological and seismic observations have shown that within each depositional sequence, a predictable succession of systems tracts will be generated by each stage of a global eustatic sea level oscillation (POSAMENTIER, 1988). These include high stand, low stand, transgressive, and shelf margin system tracts. A particular set of depositional processes, and hence environments and lithofacies, are associated with each systems tract (VAIL, 1987). A common sequence found from Pleistocene times and back, is one consisting of a well developed low stand system tract, followed by a transgressive system tract, and finally ending with a truncated high stand systems tract (Figure 8.3 b; VAN WAGONER *et al.*, 1990). However, such a sequence will only be preserved in the stratigraphic record where a relatively abundant supply of terrigenous sands are present, and space for sediment accumulation (accommodation) is available, usually through the presence of a subsiding basin (CHRISTIE-BLICK, 1991).

According to VAN WAGONER *et al.* (1990), a low stand systems tract forms during falls in eustatic sea levels, when subaerial exposure of sediments leads to valley incision of underlying strata by river channels. During sea level rises, these incised valleys infill with alluvial sediments, and are subsequently truncated by a marine flooding (transgressive) surface. A transgressive systems tract then develops over the marine flooding surface, in which a veneer of transgressive sands is deposited. These form an onlapping relationship with underlying low stand deposits, and have a back-stepping upper surface characterised by lag deposits of coarse sands derived from shoreface erosion. A hiatus or period of non-deposition will then occur, possibly resulting in the development of an apparent truncation surface. A high stand systems tract is then emplaced, in which coastal and shelf deposits accrete and prograde seawards, forming a downlapping relationship with transgressive deposits.

These principles of seismic and sequence stratigraphic analysis are utilised in this study to assist in the interpretation of high resolution, continuous sub-bottom seismic profiles, particularly regarding the interpretations of past depositional environments formed in response to oscillations in late Quaternary eustatic sea levels.

8.2.2. Seismic Units

Seismic profiles were interpreted assuming a speed of sound through water of 1500 ms^{-1}, and 1800 ms^{-1} in sediments (McQUILLIN and ARDOS, 1977). In analysing the records, the above mentioned principles were followed, with seismic sequences delineated by the presence of major unconformities. Various systems tracts were then identified, based on the internal configuration and types of seismic reflection characteristics. In this analysis, care was taken not to misinterpret secondary reflections with the above primary ones. The main secondary events looked for were multiple reflectors. These are indicated in seismic records by their identical configuration to the

sea-bed, and their occurrence below the sea floor at intervals equivalent to the water depth. In general, multiple reflections only present problems of analysis in shallow water depths (<10 m), where they rise close to the sea floor.

Four main unconformities are identified in the seismic profiles, and are referred to as R_1, R_2, R_3 and R_4. The latter three are inferred to represent erosional surfaces and hiatuses in the deposition of sediments, associated with late Quaternary oscillations in eustatic sea levels. Relative dates for these surfaces have been inferred by associating them with marine transgressions and regressions, produced by the late Quaternary sea level curves of CHAPPELL (1983). Results are shown in Figure 8.4 and Table 8.1, and can be summarised as follows: R_1 = seismic basement surface; R_2 = fluvial incision and marine planation surface, inferred to have formed during the fall in sea level following the last interglacial period (isotope stage 5 to 4); R_3 = fluvial incision surface, inferred to have formed during the maximum fall in sea level during the Last Glacial Period (isotope stages 3 to 2); R_4 = marine planation surface that probably formed during the Holocene marine transgression (isotope stages 2 to 1).

These unconformities separate 5 major seismic stratigraphic units, each with distinct internal configurations and reflection characteristics. Examples of each seismic unit are shown in Figures 8.5, 8.6, and 8.7, and their inferred association with global eustatic oscillations in sea level summarised in Figure 8.4 and Table 8.1. These units include:

Unit 1 (Basement Rock; Figure 8.5.) - characterised by a very intensely reflective surface, with no distinct internal reflection surfaces. Surface expressions of this unit coincide with reefs on sonographs and echo sounder, and so it is inferred to represent basement rock. Geophysical studies by THRASHER (1986) have found a similar seismic basement rock on the east Coromandel to be associated with high frequency magnetic anomalies, which indicates a probable Tertiary igneous basement. The upper boundary is defined as unconformity R_1.

Unit 2 (Undifferentiated Pleistocene; Figures 8.5, 8.6, and 8.7) - characterised by intense, continuous, parallel to chaotic internal reflectors. The upper surface is bounded by unconformities R_2, R_3, and/or R_4 in various locations, and appears to link-up onshore with subaerial Pleistocene inner barrier deposits. The upper section of this unit often shows strong, parallel, relatively continuous reflectors, possibly representing marine deposits, with more chaotic reflectors in lower sections probably indicating old alluvial deposits. Thus, this unit has probably formed through several minor oscillations in sea level, as characterised the period spanning isotope stage 5 (Figure 8.4 a). The lithology of this unit is uncertain due to its limited surface expressions, although it appears to crop out on the sea floor and comprises coarse shelf sands off Whiritoa Beach.

Unit 3 (Figures 8.5 and 8.6) - is divided into two sub-units based on different geometrical associations and reflective characteristics. Unit 3A (Pleistocene Transgressive Deposits) is

Table 8.1. Inferred seismic stratigraphic units and relative ages for east Coromandel shelf deposits, as determined from high resolution continuous seismic reflection profile data.

Seismic Unit	Unconformity	Stratigraphic Unit	Isotope Stage	Inferred Age (ky.B.P.)
Unit 5E		Nearshore Accretionary Wedge		
Unit 5D		Fine Surficial Sands		
Unit 5C		Mid Shelf Muddy Sands	1	0 to 12
Unit 5B		Transgressive Sand Sheet		
Unit 5A		Hummocky Transgressive Sands		
	R4		2 to 1 transition	16 to 12
Unit 4		Pleistocene Alluvial	2	20 to 16
	R3		3 to 2 transition	28 to 20
Unit 3B		Pleistocene Progradational	3	60 to 28
Unit 3A		Pleistocene Transgressive	4 to 3 transition	70 to 60
	R2		5 to 4 transition	80 to 70
Unit 2		Undifferentiated Pleistocene	5	140 to 80
	R1		6 or older	
Unit 1		Basement Rock		Tertiary

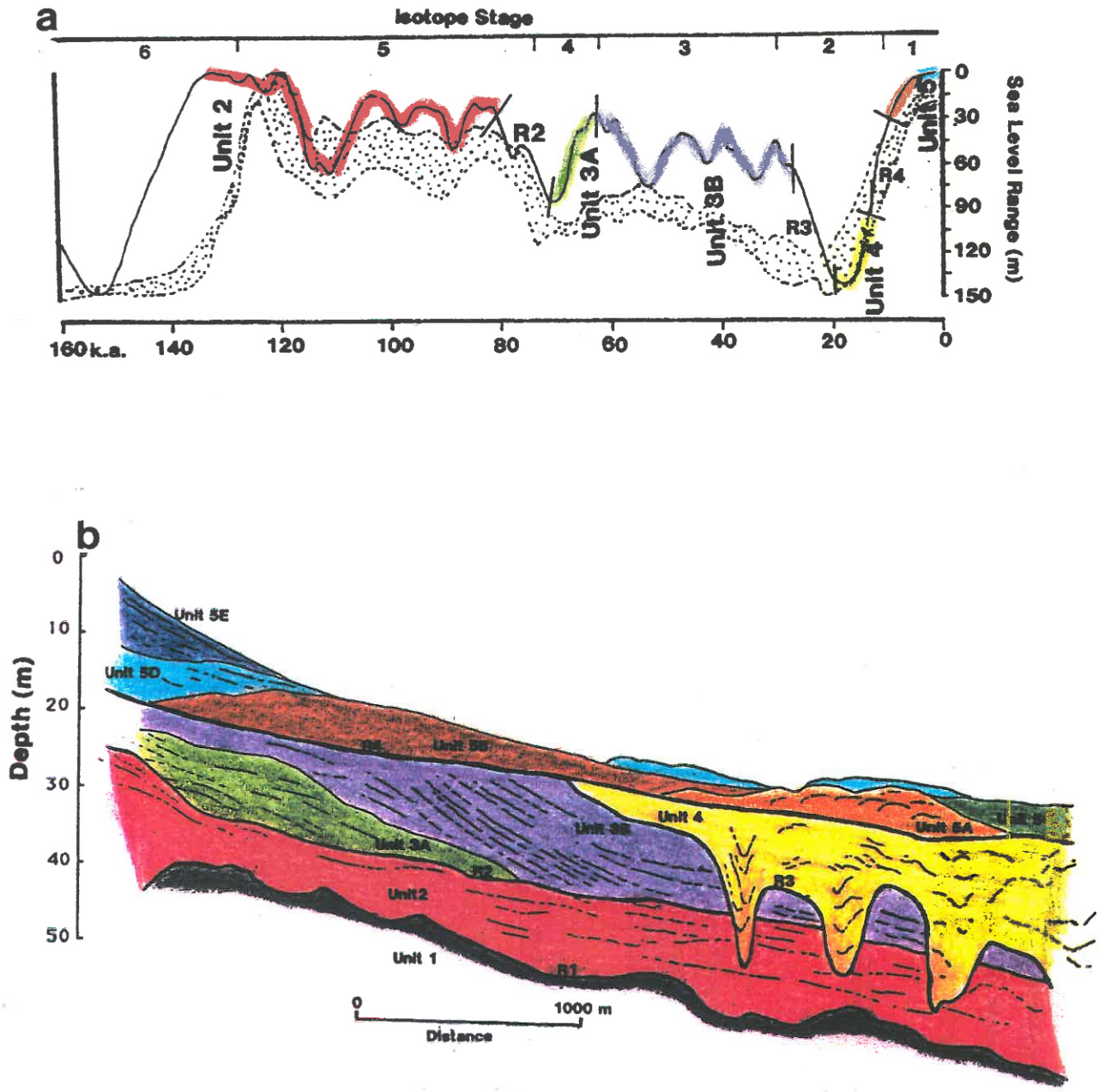

Figure 8.4. a) Late Quaternary sea level curve based on raised coral terraces on the Huon Peninsula, Papua New Guinea (CHAPPELL, 1983). Also shown are the various oxygen isotope stages and envelope of isotopic records (dotted curves) from SHACKLETON and OPDYKE (1973) and HAYES *et al.* (1976), and the inferred ages for emplacement of various east Coromandel unconformities and seismic units. b) Schematic diagram showing inferred emplacement of various seismic units, and development of major unconformities during late Quaternary sea level oscillations. Unit thickness and geometry are conceptual, and not based on a particular seismic profile.

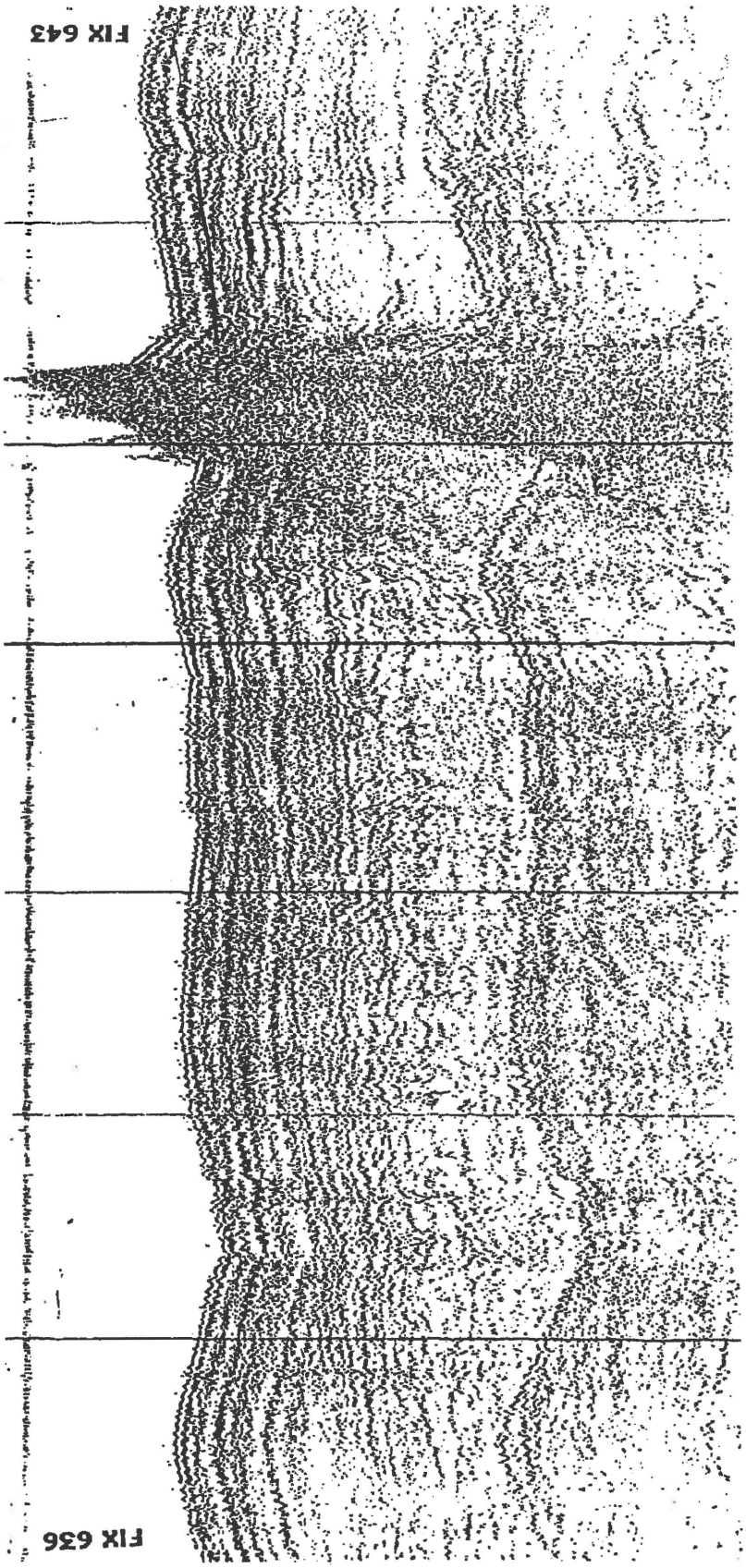

Figure 8.5 a. Raw seismic profile record off mid-Waihi Beach.

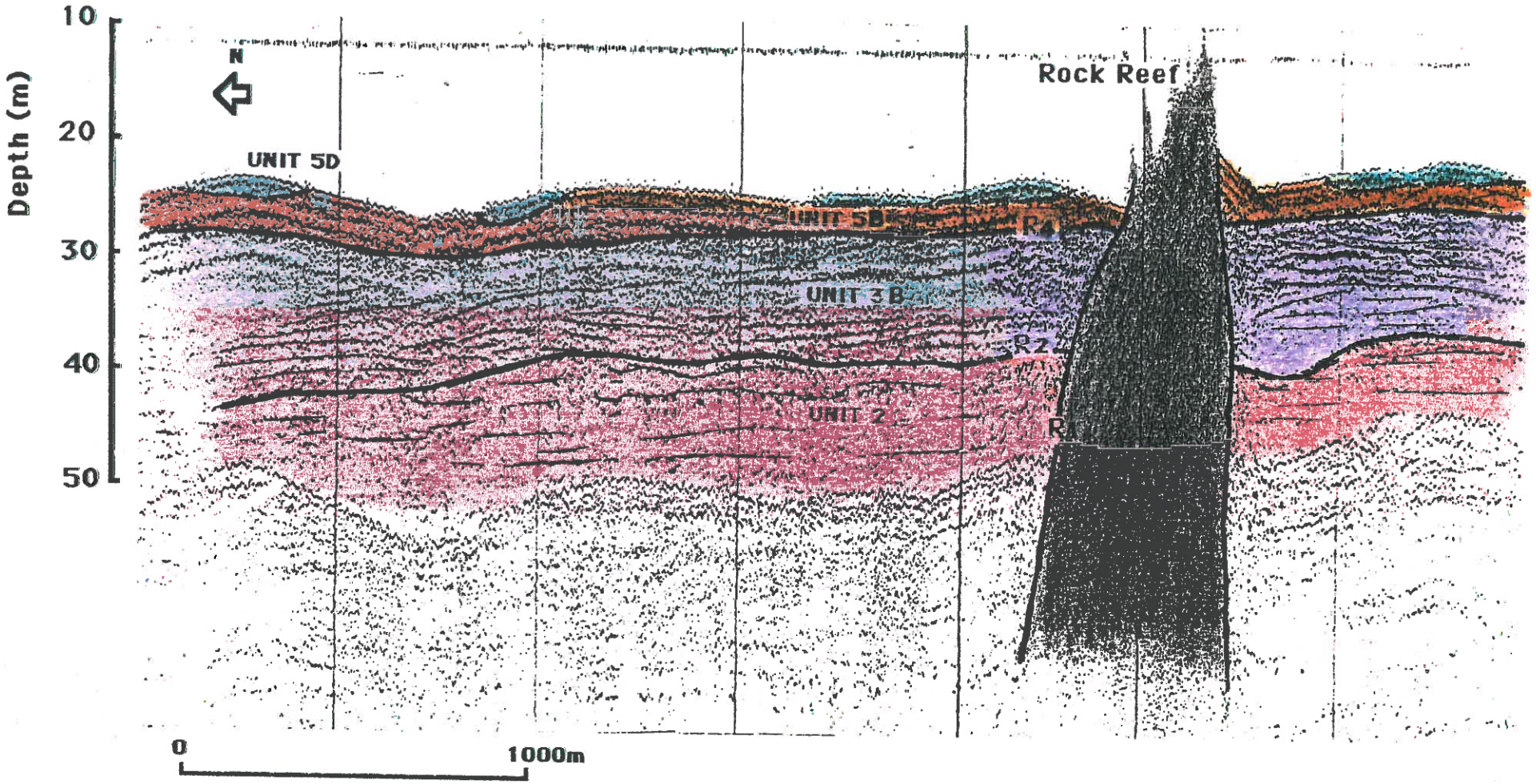

Figure 8.5 b. Inferred seismic stratigraphy along a shore-parallel transect offshore from mid Waihi Beach. This shows lenses of surficial fine sands (Unit 5D), and transgressive sediments (Unit 5B) forming a ramp over the southern face of a basement rock outcrop (Unit 1). Subsurface deposits are thick Pleistocene prograded (Unit 3B), and Undifferentiated Pleistocene (Unit 2) seismic units. Note that in this and subsequent seismic profiles, only the water depth scale is shown, as this is very similar to the sediment thickness scale at these shallow sub-bottom depths. Also, seismic interpretations are only attempted to the subsurface depth where the first major multiple reflector occurs.

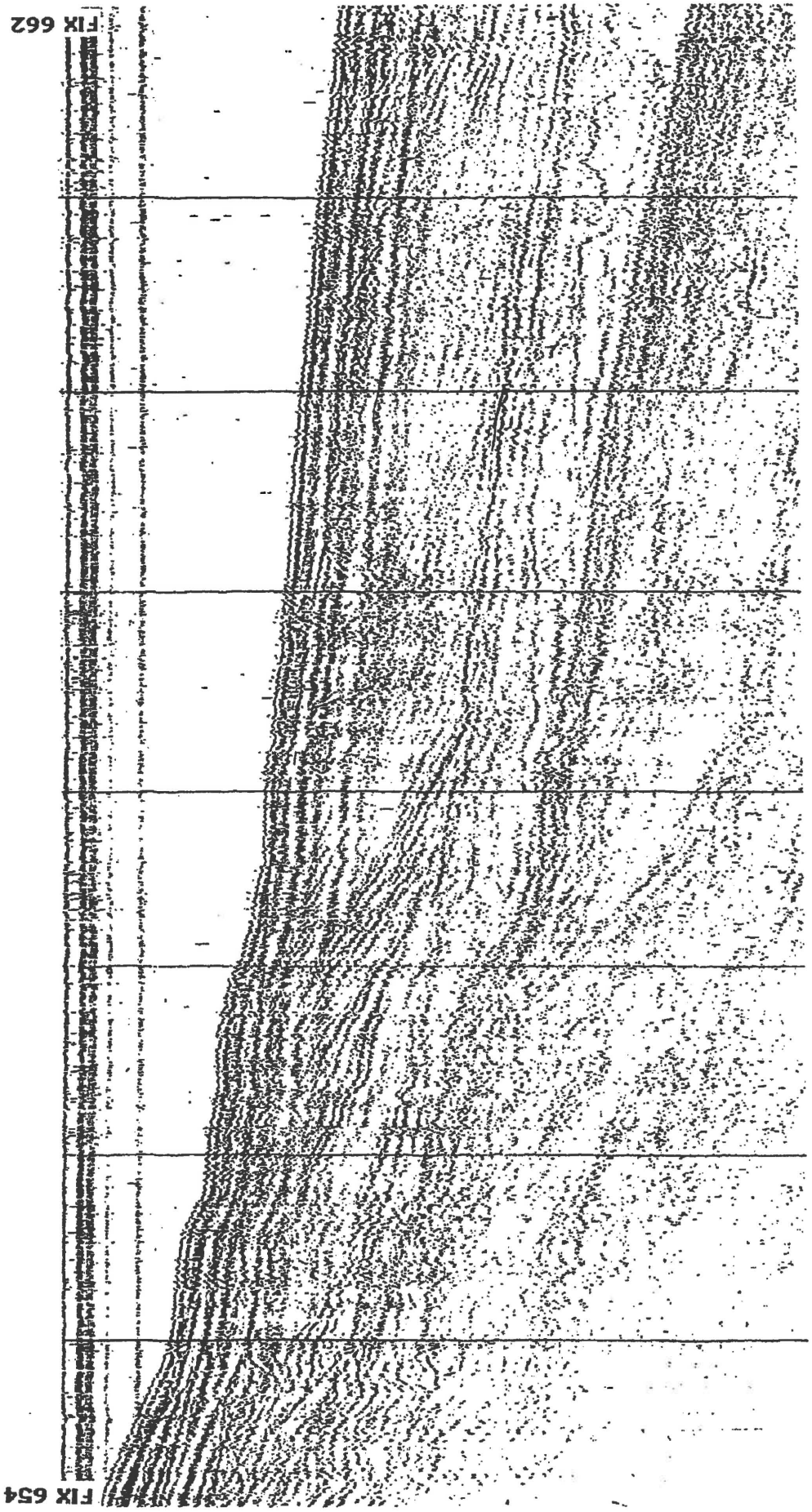

Figure 8.6 a. Raw seismic profile record off Bowentown.

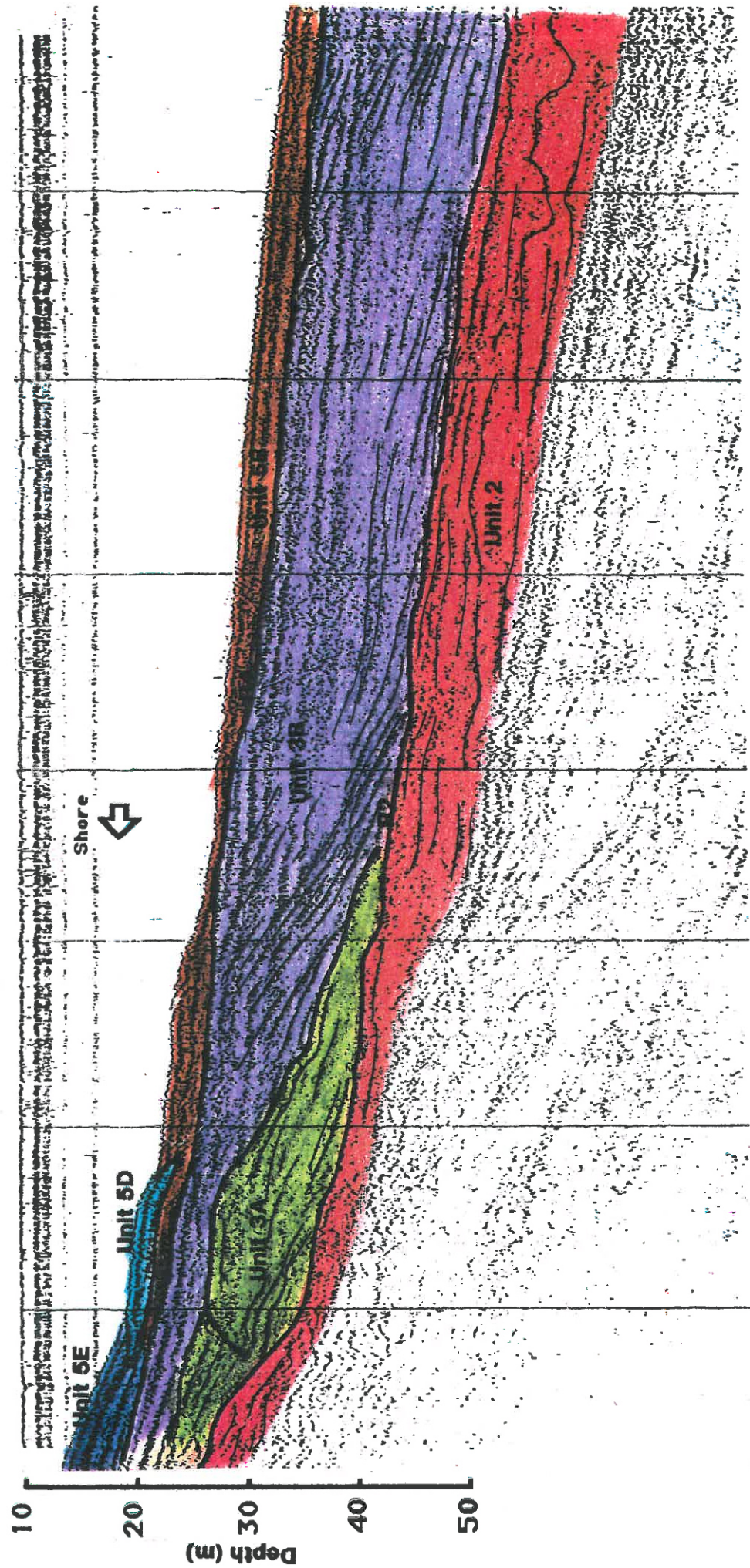

Figure 8.6 b. Inferred seismic stratigraphy offshore from Bowentown. The nearshore accretionary wedge is particularly well developed in this region (Unit 5E), and appears to extend seawards over Holocene transgressive sands (Unit 5B). Pleistocene transgressive and progradational sediments (Units 3A and 3B) form a thick sequence close to the modern sea-bed, the latter showing distinct seaward dipping clinoforms. Beneath this sequence occurs a Undifferentiated Pleistocene (Unit 2), which rises steeply landwards and probably links-up onshore with Pleistocene inner barrier deposits.

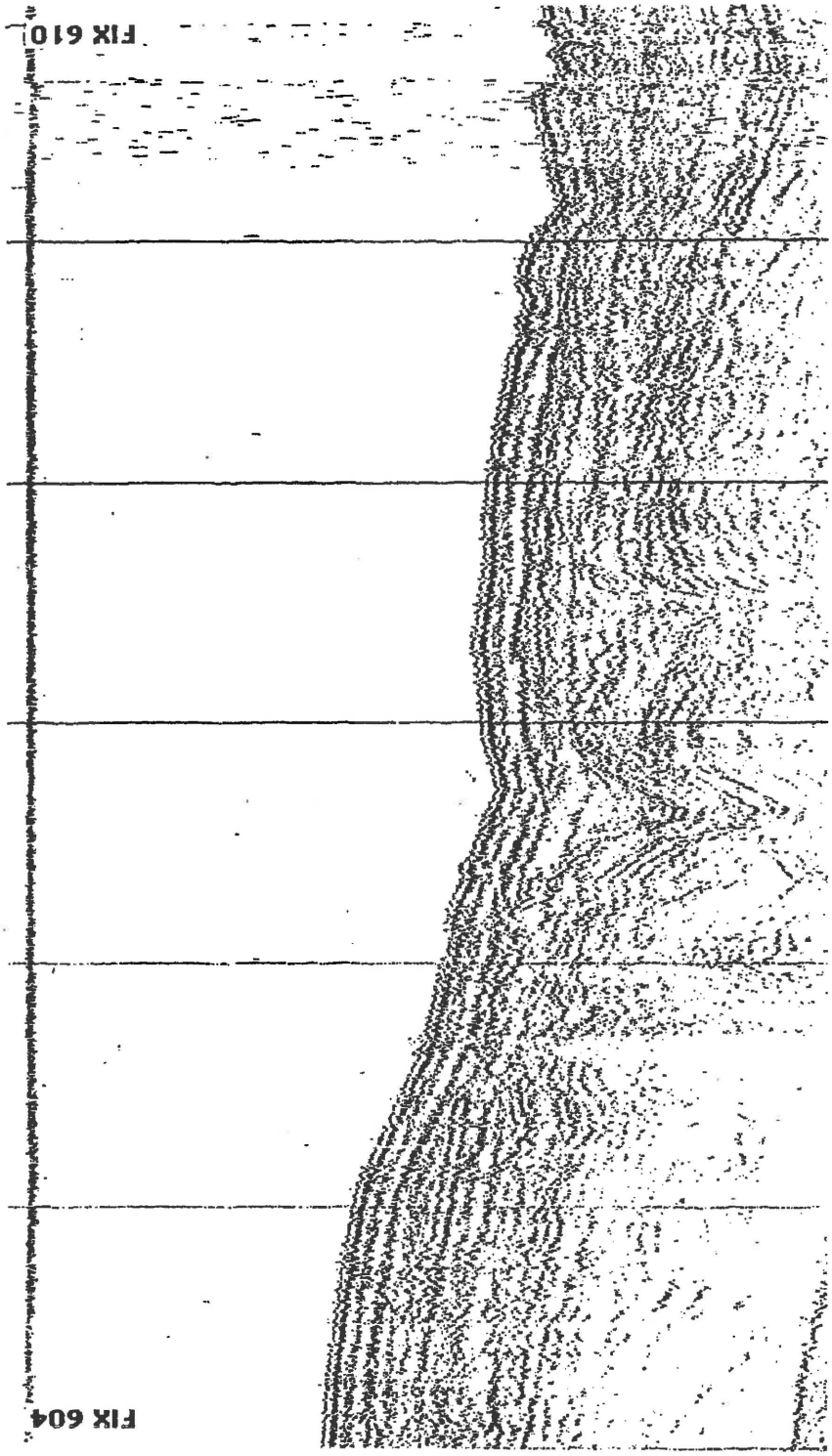

Figure 8.7 a. Raw seismic profile record off Mataora Beach.



Figure 8.7 b. Inferred seismic stratigraphy offshore from Mataora Beach. Fine grained surficial sands (Unit 5D) occur continuously over older Holocene transgressive and mid shelf deposits (Units 5A, 5B, 5C), and the Undifferentiated Pleistocene (Unit 2). The latter has been incised by deep river channels, and infilled with inferred alluvial deposits (Unit 4).

characterised by moderate to strong chaotic reflectors, with 'white-out' occurring in some areas (suggesting the presence of gas in sediments). This sub-unit occurs as a landward-thickenning, back-stepping wedge over both fluvial incision and marine planation surfaces, associated with unconformity R_2. Thus, it is inferred to represent a transgressive systems tract emplaced during a marine transgression between isotope stages 4 and 3 (Figure 8.4 a). Unit 3B (Pleistocene Progradational Deposits) is characterised by intense, seaward dipping clinoform reflectors, which have a downlapping relationship with Units 3A and 2. This pattern is consistent with a high stand systems tract, and indicates a phase of significant aggradation and progradation of coastal and shelf sediments (CHIN *et al.*, 1988). The unit is inferred to have formed during a stillstand (interstadial event) during isotope stage 3 (Figure 8.4 a). This subunit has very limited surface expression, which coincides with areas in which coarse sands occur in surface deposits off Waihi Beach. The upper surface of Unit 3B is terminated by unconformities associated with both fluvial incision (R_3) and marine planation (R_4) surfaces.

Unit 4 (Pleistocene Alluvium; Figure 8.7) - is characterised by subdued, chaotic reflectors, which have an unconformable association with Units 1, 2, and 3. The unit occurs within fluvial incision features associated with unconformity R_3, and is consistent with a low stand systems tract. The unit is inferred to represent fluvial sediments deposited within river channels, incised into underlying sediments (and basement rock) during the maximum low sea level stand in the Last Glacial Period. The lithology is uncertain, although limited areas of surface expression off Waihi Beach are associated with a patch of very coarse surface sediments on the shelf floor. The upper surface of Unit 4 is truncated by a marine planation surface, defined as unconformity R_4.

Unit 5 (Figures 8.4, 8.5 and 8.6) - is divided into 5 subunits based on different geometrical associations and reflective characteristics. Unit 5A (Hummocky Transgressive Deposits) is characterised by subdued, hummocky internal reflectors, which onlap units occurring beneath the Holocene marine planation surface (R_4). This subunit forms a wedge of limited extent beneath the present inner shelf surface, and is inferred to represent a transgressive systems tract formed during an early phase of the Holocene marine transgression. Limited surface expressions off Whangamata are associated with coarse sands in sonographs.

Unit 5B (Transgressive Sheet) is characterised by subdued reflection properties, with no internal reflecting surfaces. This generally occurs as a continuous sheet over the marine planation surface, and beneath modern nearshore and inner shelf deposits, and appears to downlap over the surface of Unit 5A. Thus, it is also inferred to represent a transgressive systems tract, deposited shortly after Unit 5A. This unit has numerous sea floor surface expressions, which correspond to the coarse grained, shelly, inner shelf storm lag deposits (see Chapter 5.7.). Limited radio-carbon dates of surface shell deposits confirm an early Holocene age for the emplacement of this unit (see section 8.3.).

Unit 5C (Mid Shelf Muddy Sediments) is characterised by subdued reflection properties, with internal reflectors either absent or slightly chaotic. This unit is only found beneath deep mid shelf waters, where it onlaps pre-Holocene units beneath the marine planation surface (R_4). It is inferred to represent a highstand systems tract of aggrading mid shelf deposits. Surface expressions of this sub-unit coincide with muddy, fine grained mid shelf sands.

Unit 5D (Fine Grained Surficial Sediments) has a characteristically subdued reflection, with internal reflectors ranging in character from chaotic on sand ridges, to discontinuous parallel or absent where it occurs as a more extensive inner shelf blanket or lower nearshore wedge. This unit downlaps over 5A, 5B, and 5C, and is inferred to represent a presently aggrading highstand systems tract. Surface expressions show this sub-unit is associated with fine grained nearshore and inner shelf sands in surface deposits.

Unit 5E (Nearshore Accretionary Wedge) is characterised by subdued, continuous parallel, slightly seaward dipping reflectors. This occurs beneath the upper nearshore surface, where it forms a seaward thinning wedge which downlaps over units 5B and 5D. It is therefore inferred to represent a recently formed high stand systems tract, which is presently aggrading and prograding seawards. Surface expressions coincide with the very fine grained upper nearshore sands, inferred to be of modern terrigenous origin (see Chapter 5.7.).

8.2.3. Regional Seismic Stratigraphic Patterns

Variations in the character and extent of these inferred seismic units are now described for each of the major surveyed shelf locations. The data are presented as maps showing the inferred surface distribution of the seismic stratigraphic units, and as selected seismic profiles from each location. For the latter, both the raw seismic profile, and an interpreted profile are presented, their locations being sown in Figures 8.1 and 8.2.

Waihi Beach

Seismic profiles off Waihi Beach show late Quaternary deposits extending to subsurface depths of at least 30 m, with no indication of geological basement beneath these. As studies at Tauranga to the south by HARMSWORTH (1983) have shown up to 240 m of Quaternary sediments within the Tauranga Basin, it is likely that shelf deposits off Waihi Beach also extend much deeper into the subsurface.

Holocene sediments occur across most of the shelf, with some Pleistocene sediments exposed on the lower nearshore surface off northern Waihi Beach and Orokawa Bay (Figures 8.8 and 8.9). In depths shallower than 20 m, the nearshore accretionary wedge (Unit 5E) dominates subsurface deposits, particularly offshore from the Bowentown ebb tide delta. The unit thickens landwards, to

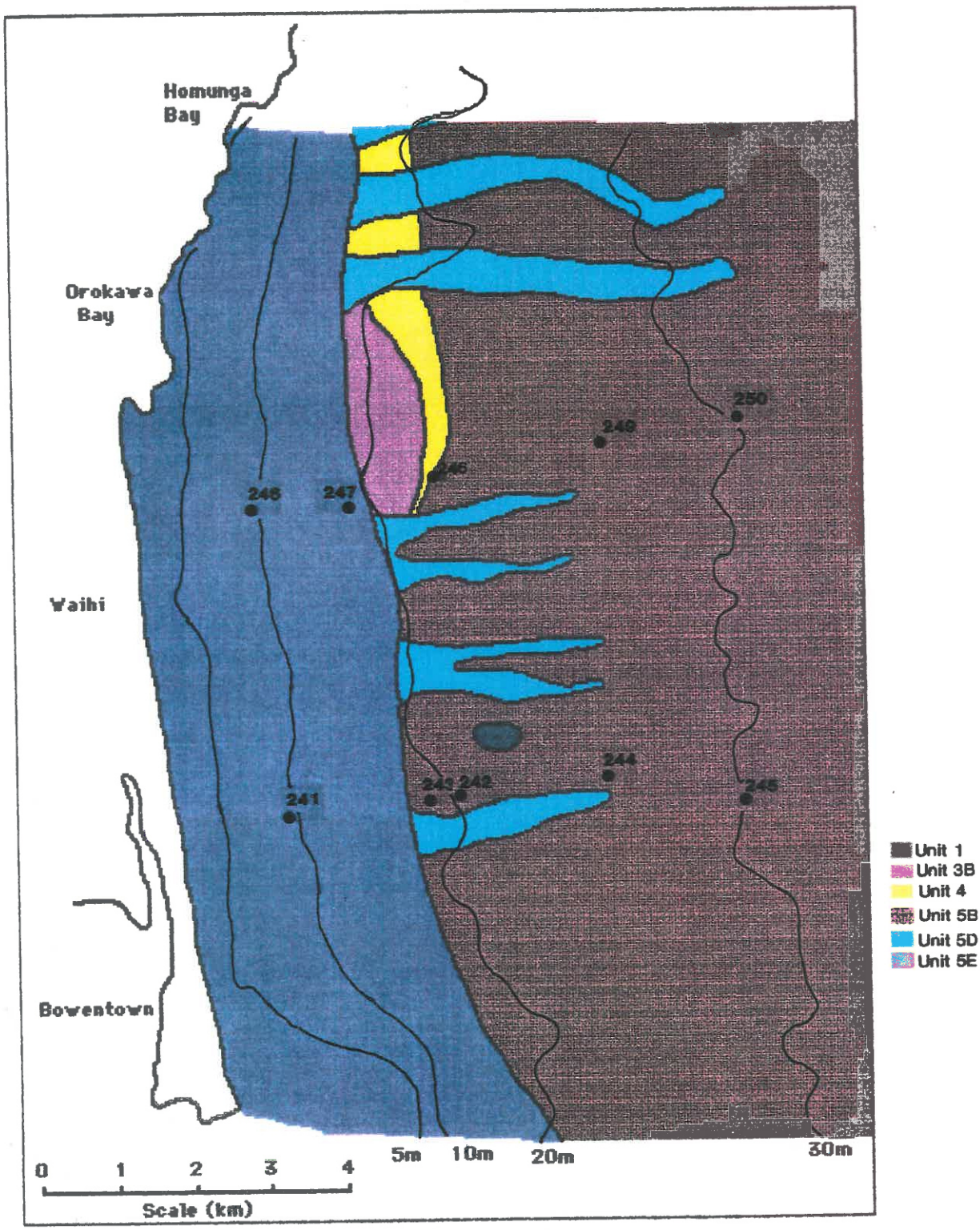

Figure 8.8. Surface distribution of seismic stratigraphic units offshore from Waihi Beach. Also shown are box core locations.



Figure 8.9 a. Raw seismic profile record off northern Waihi Beach.



Figure 8.9 b. Interpreted seismic stratigraphy offshore from northern Waihi Beach. This shows Pleistocene alluvial (Unit 4) and Pleistocene progradational sediments (unit 3B) exposed on the sea-bed, with rather thin and spatially limited Holocene deposits (Units 5B and 5E).

10 m thick in about 5 m water depth, and generally downlaps over the Holocene transgressive sheet (Unit 5B) or older Pleistocene deposits (Units 4 and 3B; Figures 8.6 and 8.10). This stratigraphic relationship provides an origin for the numerous CMR bands found in 10 to 20 m water depth along Waihi Beach, the bands representing localised scouring along wave convergence zones (see Chapter 7.4.3.) of the outer nearshore accretionary wedge and exposure of underlying coarse grained Units 5B or 3B.

Across most of the inner shelf off Waihi Beach, the Holocene transgressive sands (unit 5B) dominate subsurface deposits, generally forming a 5 m-thick veneer over older Pleistocene sediments (Units 3B and 4; Figures 8.5, 8.6, 8.9, 8.10, and 8.11). In the area offshore from mid Waihi Beach, seismic profiles show evidence for these sediments being transported northwards by shore-parallel currents, where they form a distinct ramp against the southern face of a protruding rock pinnacle on the sea-bed (Figure 8.5). Fine grained surficial sediments (Unit 5D) are relatively insignificant in this region. However, they do appear to form relatively thick (5 m) deposits beneath sand ridges in the shelf area north of Waihi Beach (Figure 8.11). This supports deductions from earlier chapters, that the sand ridges are modern depositional features which respond to the present oceanographic climate.

The Waihi Beach offshore region therefore appears to be an area presently dominated by shelf erosion, and accounts for the extensive exposure of both Holocene transgressive deposits and Pleistocene sediments on the inner shelf surface. Accretion of fine grained sands appears to be presently limited to the nearshore zone. However, tongues of fine surficial sand extending across the inner shelf as sand ridges may be derived from the erosion of these nearshore sediments, and their subsequent transport and deposition by wind-generated currents further offshore.

Pleistocene sediments form a significant component of the subsurface stratigraphy off Waihi Beach. The dominant Pleistocene sediments identified in seismic profiles are the Pleistocene progradational deposits (Unit 3B). These generally form a 20 m-thick unit beneath the Holocene sediments, although they do appear to have surface expression on the northern inner shelf surface (Figure 8.9). Their upper surface tends to be relatively flat in seismic profiles (Figures 8.5, 8.6 and 8.10), and may thus have influenced the presently very broad and flat nature of the Waihi Beach inner shelf surface. The unit has probably further contributed to the present shelf character, through its surface being reworked during the Holocene marine transgression and incorporated into the transgressive sand sheet (Unit 5B).

The Undifferentiated Pleistocene deposits (Unit 2) found beneath this younger Pleistocene sequence also forms a relatively thick (at least 15 m) and extensive subsurface unit. However, its surface is too deep to have influenced the present offshore morphology. Closer to shore, the surface does rise steeply, and possibly links-up with Pleistocene inner barrier deposits behind Waihi Beach (ABRAHAMSON, 1987).

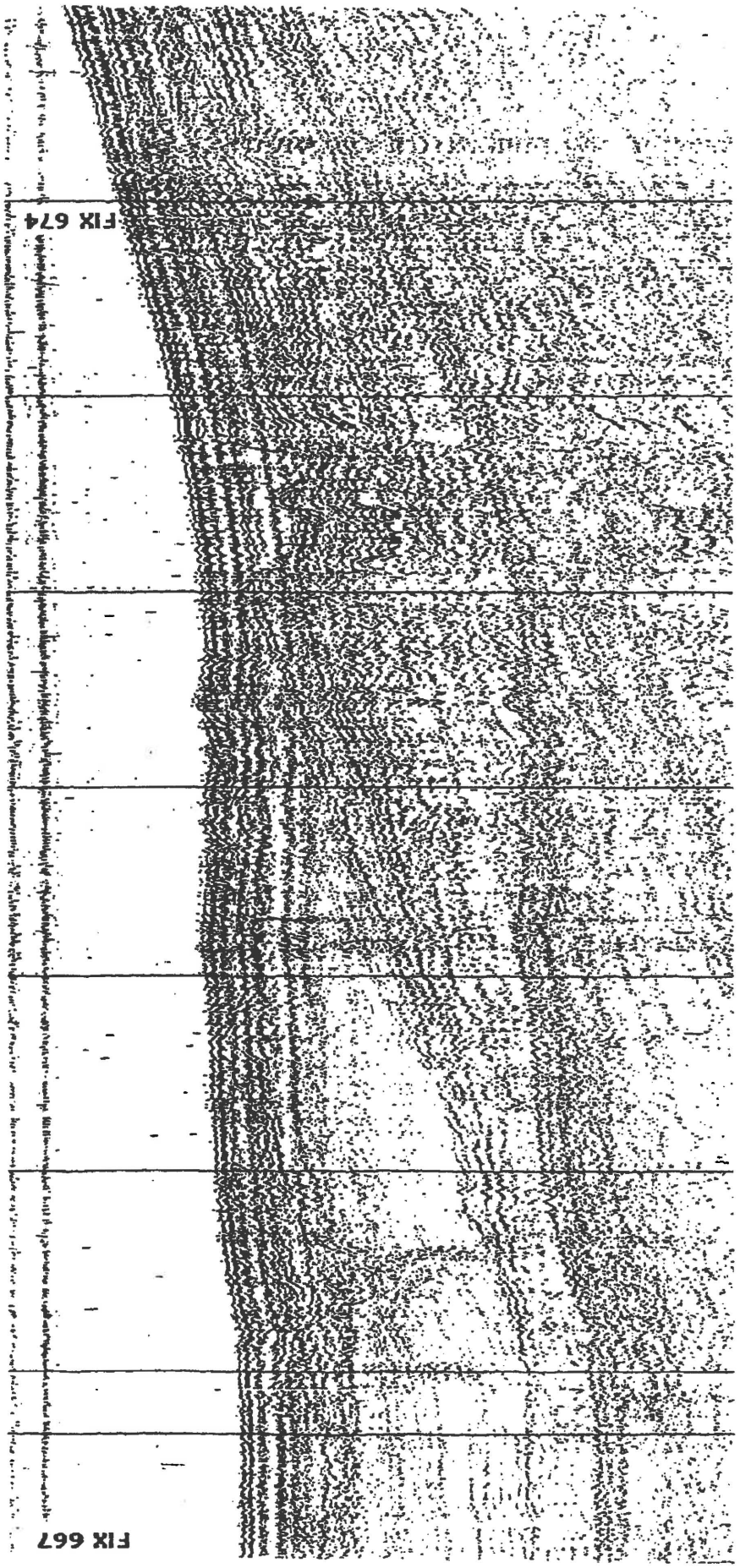

Figure 8.10 a. Raw seismic profile record from mid Waihi Beach.

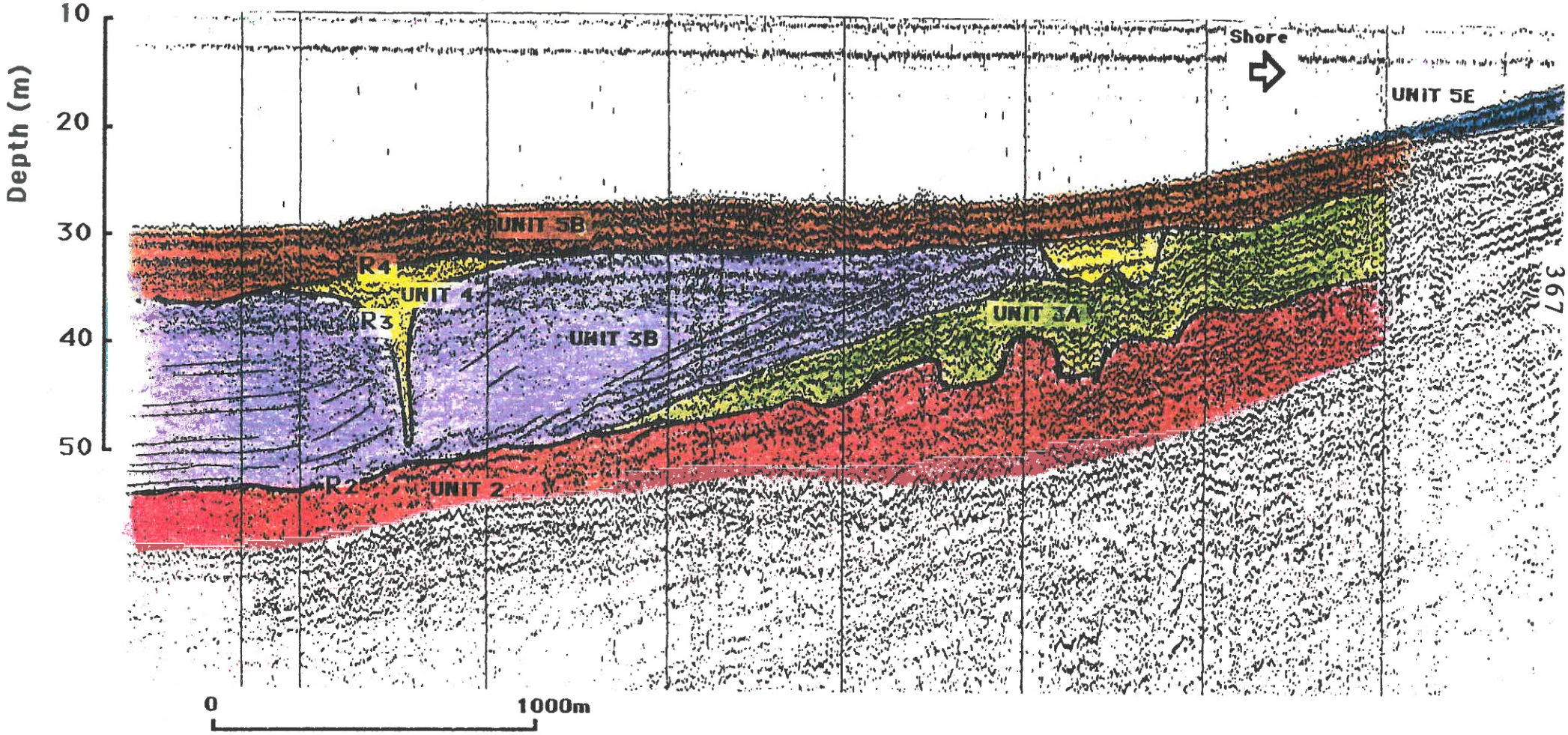

Figure 8.10 b. Interpreted seismic stratigraphy offshore from mid Waihi Beach. A thin sheet of Holocene transgressive sands (Unit 5B) overlies relatively thick Pleistocene sediments (Units 3A and 3B).

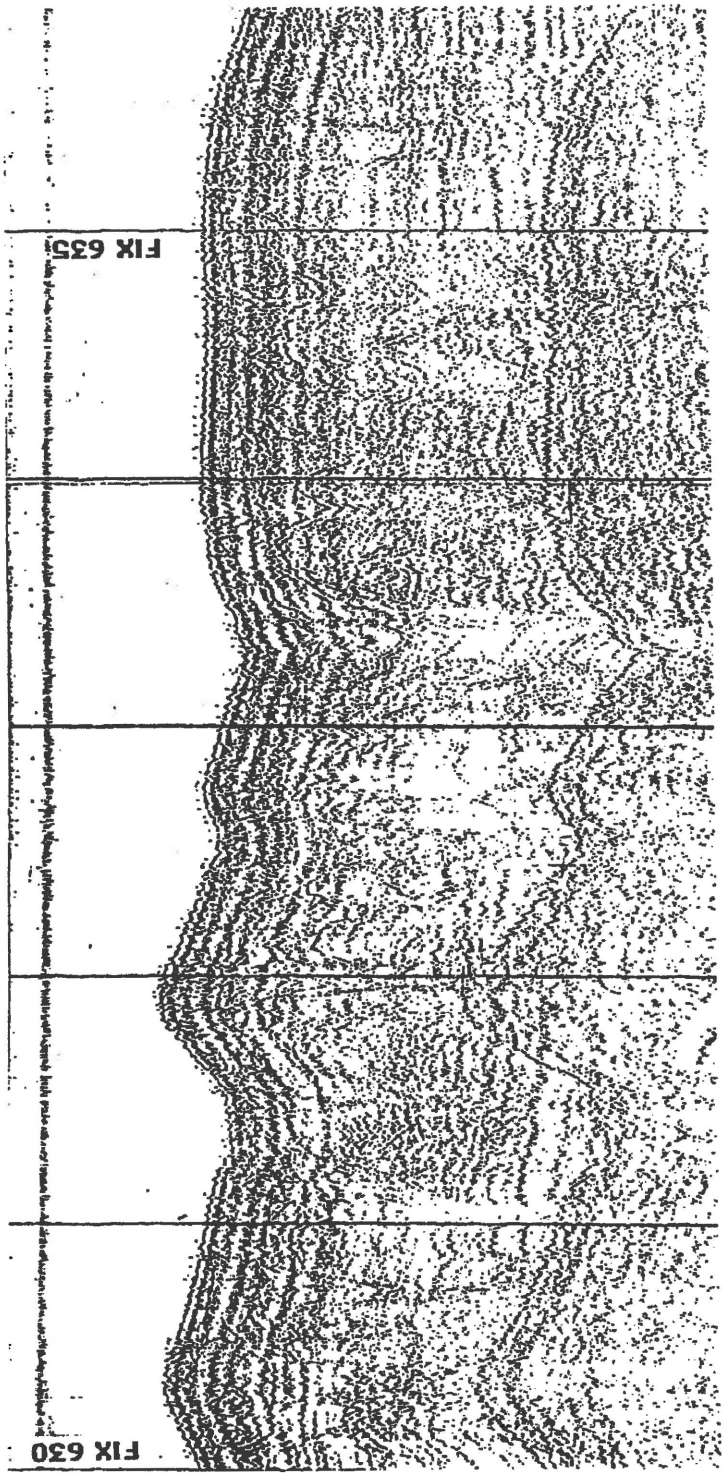

Figure 8.11 a. Raw seismic profile record off Orokawa Bay.

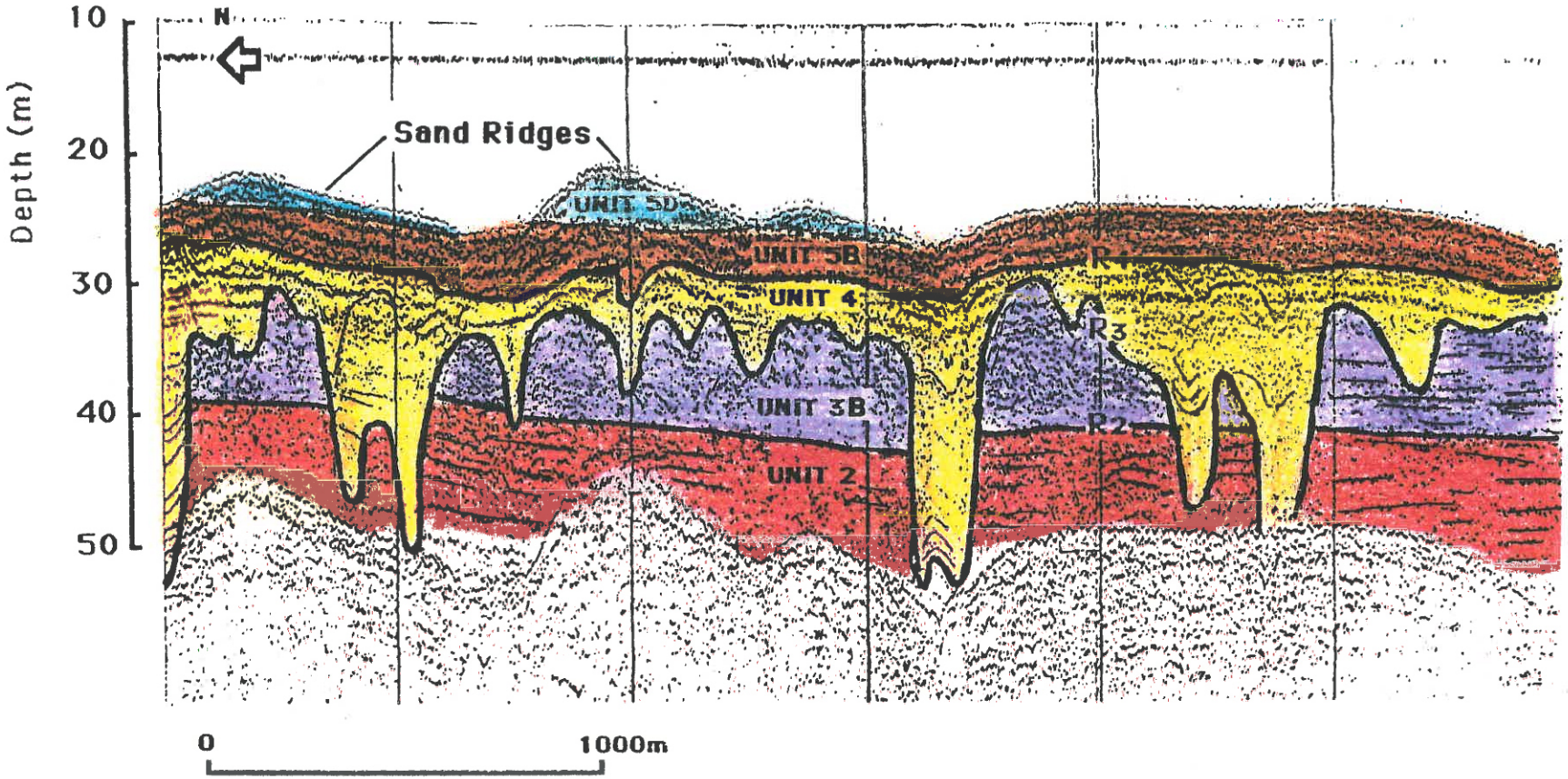

Figure 8.11 b. Interpreted seismic stratigraphy along a shore-parallel track off Orokawa Bay, with Holocene surficial fine sands (Unit 5D) occurring within relatively large sand ridges. Subsurface deposits show extensive alluvial deposits (Unit 4) formed within channels incised into older Pleistocene sediments (Units 2 and 3B).

Both Pleistocene surfaces have been extensively incised by fluvial channels to the north, probably by rivers draining eastwards from Orokawa Bay during the low sea level stand in the Last Glacial Period (Figures 8.9 and 8.11). The alluvial deposits which infill these channels (Unit 4) have surface expression offshore of northern Waihi Beach and Orokawa Bay, and may have been another important source for Holocene transgressive sands in this area.

Whiritoa Beach

Sub-bottom profiles in the region offshore from Whiritoa and Mataora Beaches show sediments extending at least 60 m beneath the surface, with no basement rock apparent. Of the major seismic units identified along the east Coromandel, only Units 2 and 5 are found in abundance here.

Holocene deposits form an extensive blanket over most of the offshore region surveyed (Figure 8.12). In depths of < 20 m, the nearshore accretionary wedge (Unit 5E) dominates surface deposits, reaching a maximum thickness of 10 m in 5 m water depth. This seems to extend further seawards and form a thicker unit offshore at Mataora Beach compared to Whiritoa Beach (Figure 8.12).

Fine grained surficial sediments (Unit 5D) underlie the nearshore accretionary wedge, and then extend across the inner shelf and mid shelf zones as a relatively continuous blanket (Figures 8.7, 8.13, 8.14, and 8.15). These fine surficial sediments are generally 5 m-thick, and indicative of modern accretion occurring on the shelf. Internal seismic reflectors with seaward dipping surfaces are occasionally present, and further offshore large wedges of this unit overlie mid shelf deposits (Unit 5C; Figures 8.7, 8.13, and 8.14). This pattern may indicate layers of fine sand accumulating on the inner shelf, and subsequently moving offshore onto the mid shelf surface. Across the inner shelf, similar reflectors are found dipping southwards beneath sand ridge crests, and are inferred to indicate a long-term southward transport of the fine sands (Figure 8.15).

The Holocene transgressive sand sheet (Unit 5B) extends from below the mid-inner shelf, to the nearshore-inner shelf boundary, forming a veneer of relatively constant thickness (5 m). Although it is usually buried beneath the surficial sediment blanket, surface exposures occur on the sea-bed in a few limited areas of scouring, at the nearshore-inner shelf and inner shelf-mid shelf boundaries (Figures 8.12, 8.13, and 8.14). These areas of exposure coincide with extensive zones of megarippling found during the associated side-scan sonar survey. The transgressive sand sheet appears to taper out offshore, where the hummocky transgressive unit then onlaps over its surface (Unit 5A; Figure 8.14). This relationship suggests that the hummocky unit perhaps represents a transgressive deposit formed in an early stillstand event during the Holocene marine transgression, as proposed for similar features on the Otago continental shelf by CARTER and CARTER (1986).

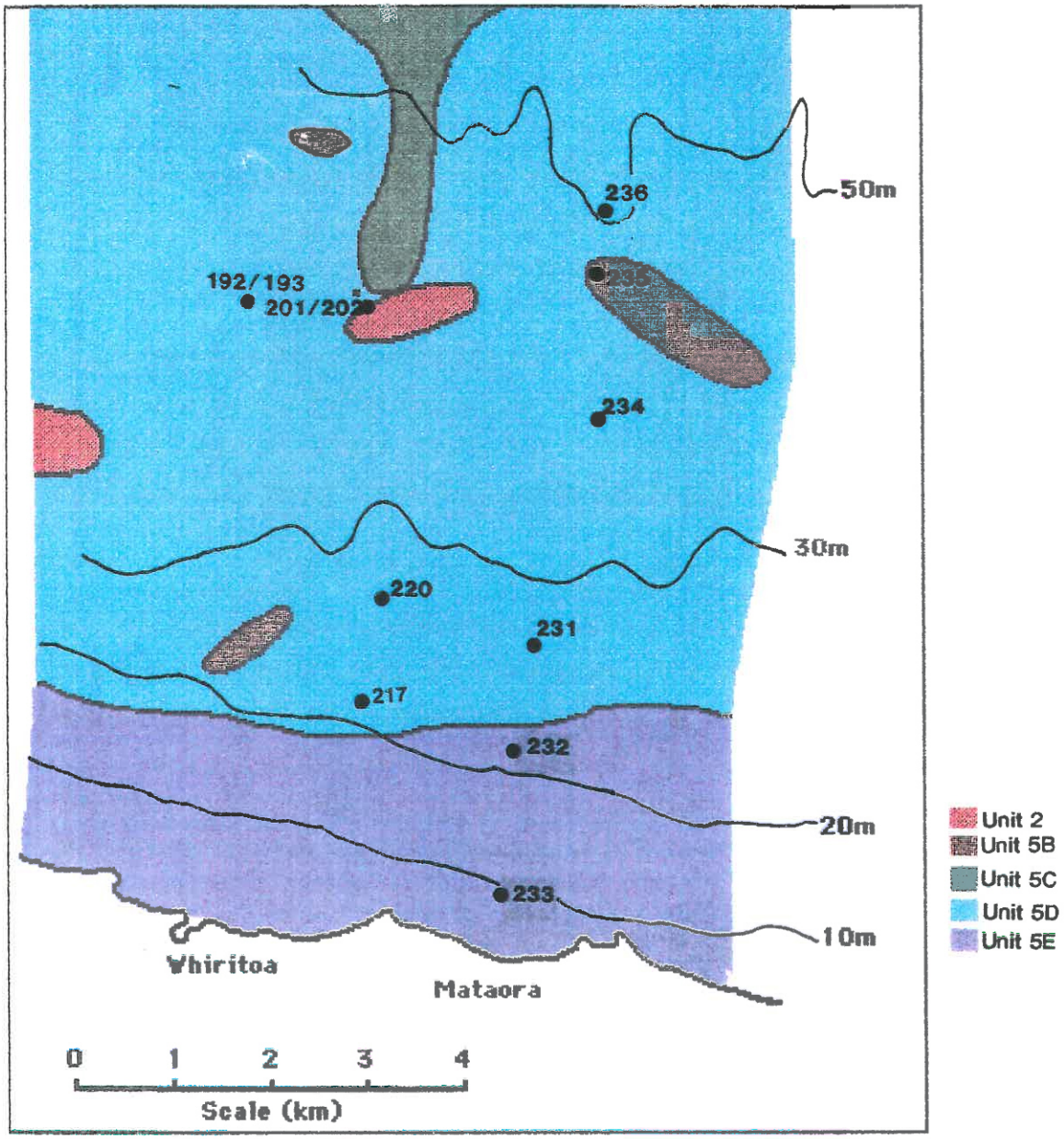

Figure 8.12. Surface distribution of seismic stratigraphic units offshore from Whiritoa and Mataora Beaches. Also shown are box core locations.

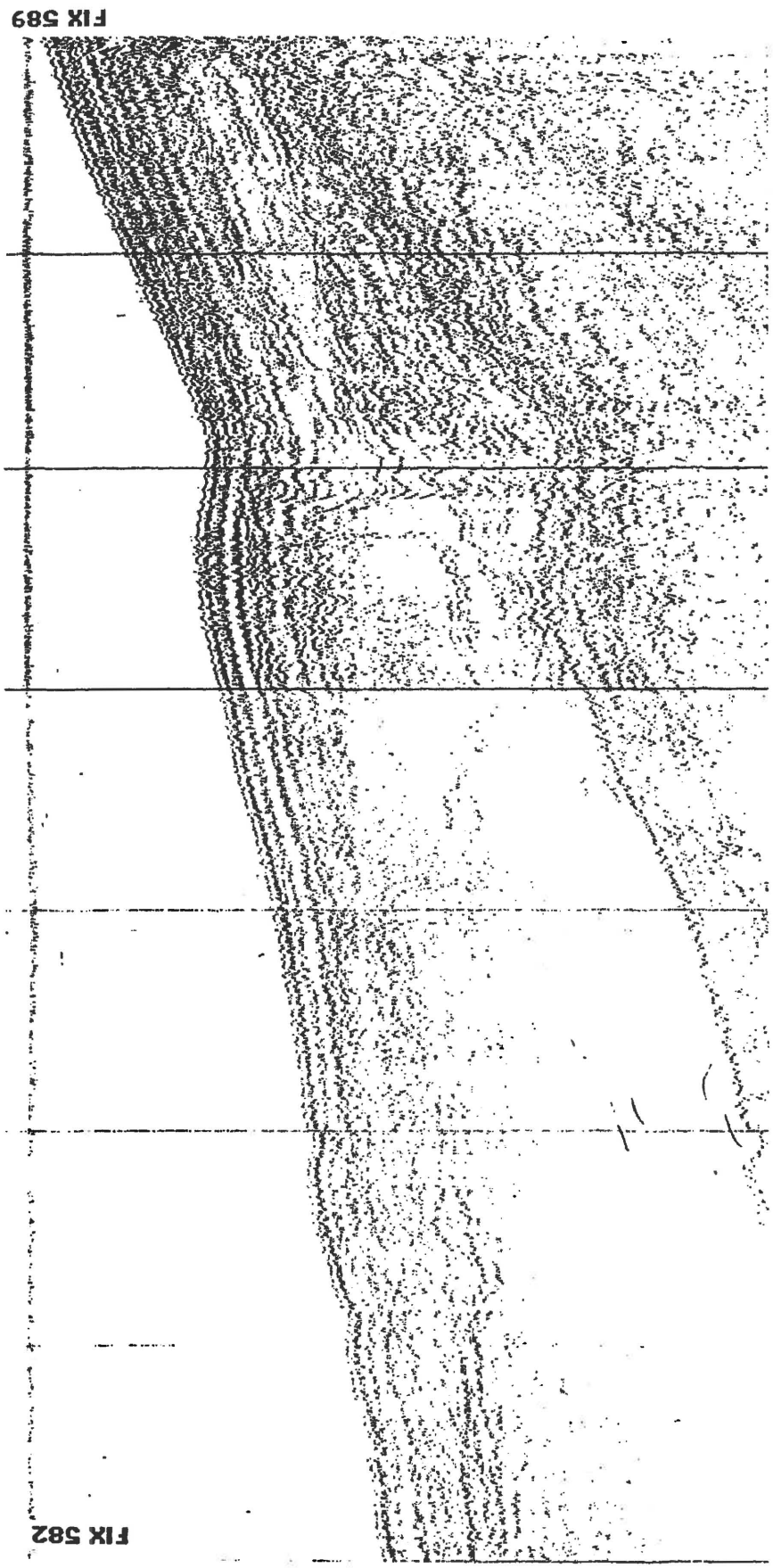

Figure 8.13 a. Raw seismic profile record off Whiritoa Beach.

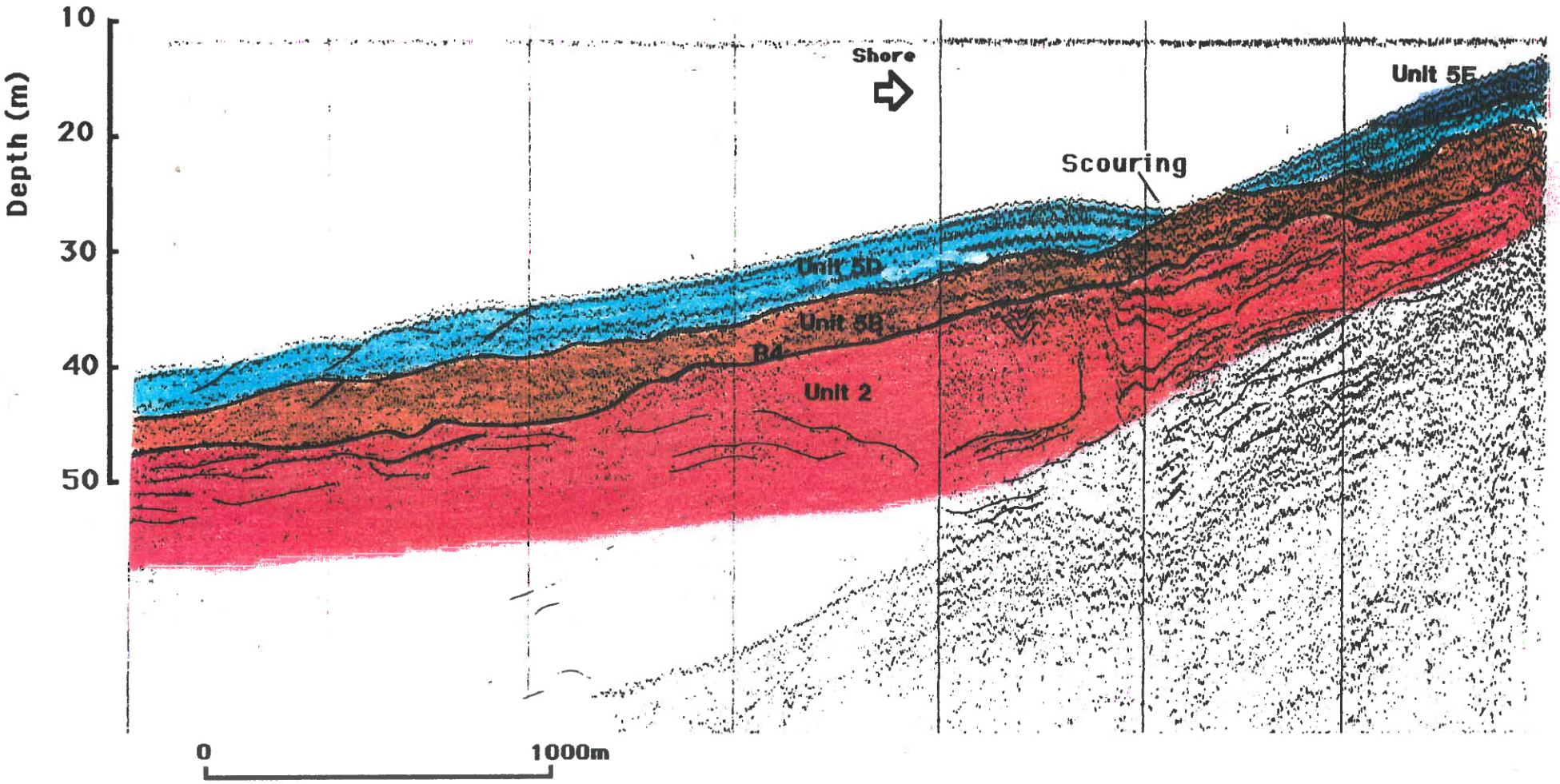

Figure 8.13 b. Interpreted seismic stratigraphy offshore from Whiritoa Beach. This shows the Holocene fine grained nearshore accretionary (Unit 5E) and surficial sediments (Unit 5D) blanketing most of the shelf surface. Holocene basal transgressive sands (Unit 5B) form thick deposits beneath these, and have been exposed on the lower nearshore surface through erosion. Undifferentiated Pleistocene deposits (Unit 2) occur beneath Holocene sediments, their upper surface sloping relatively steeply seawards.

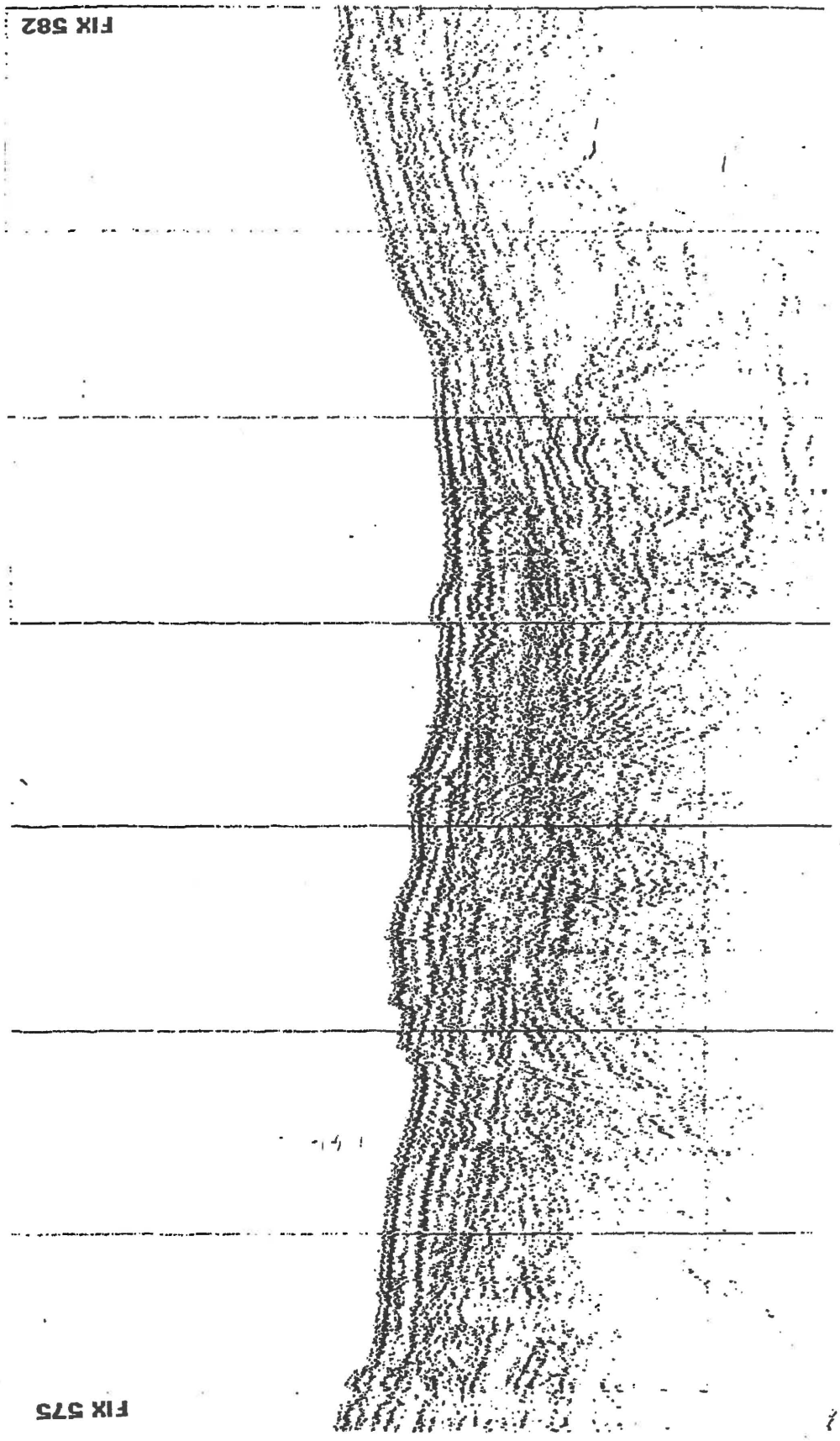

Figure 8.14 a. Raw seismic profile record off Whiritoa Beach.

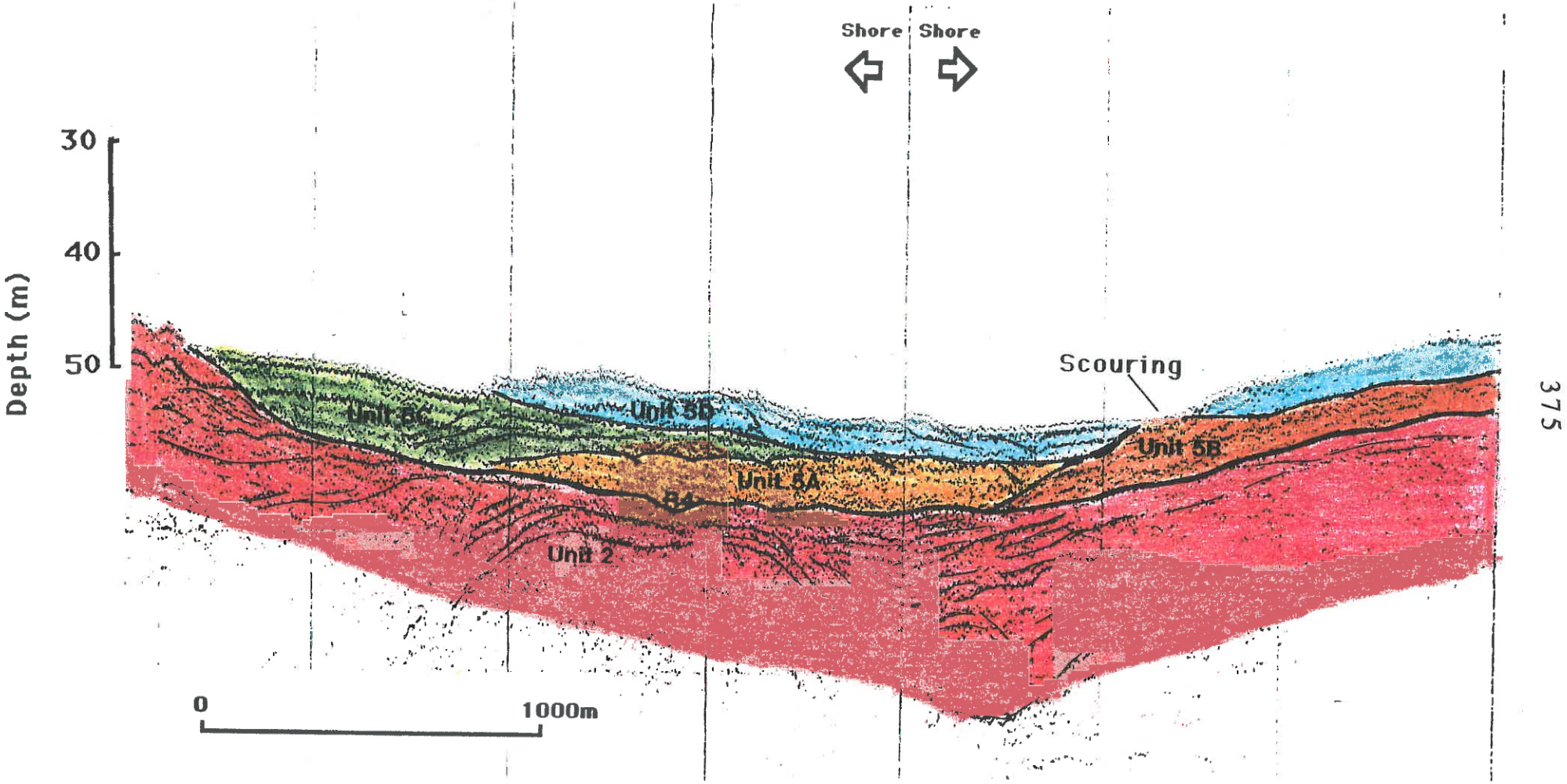

Figure 8.14 b. Interpreted seismic stratigraphy offshore from Whiritoa Beach. Thick wedges of Holocene fine grained surficial sands (Unit 5D) have formed over mid shelf deposits (Unit 5C) and transgressive (Units 5A and 5B) deposits. The exposure of several older Holocene and Pleistocene units (Units 5B and 2) on the sea-bed indicates areas of isolated shelf erosion.

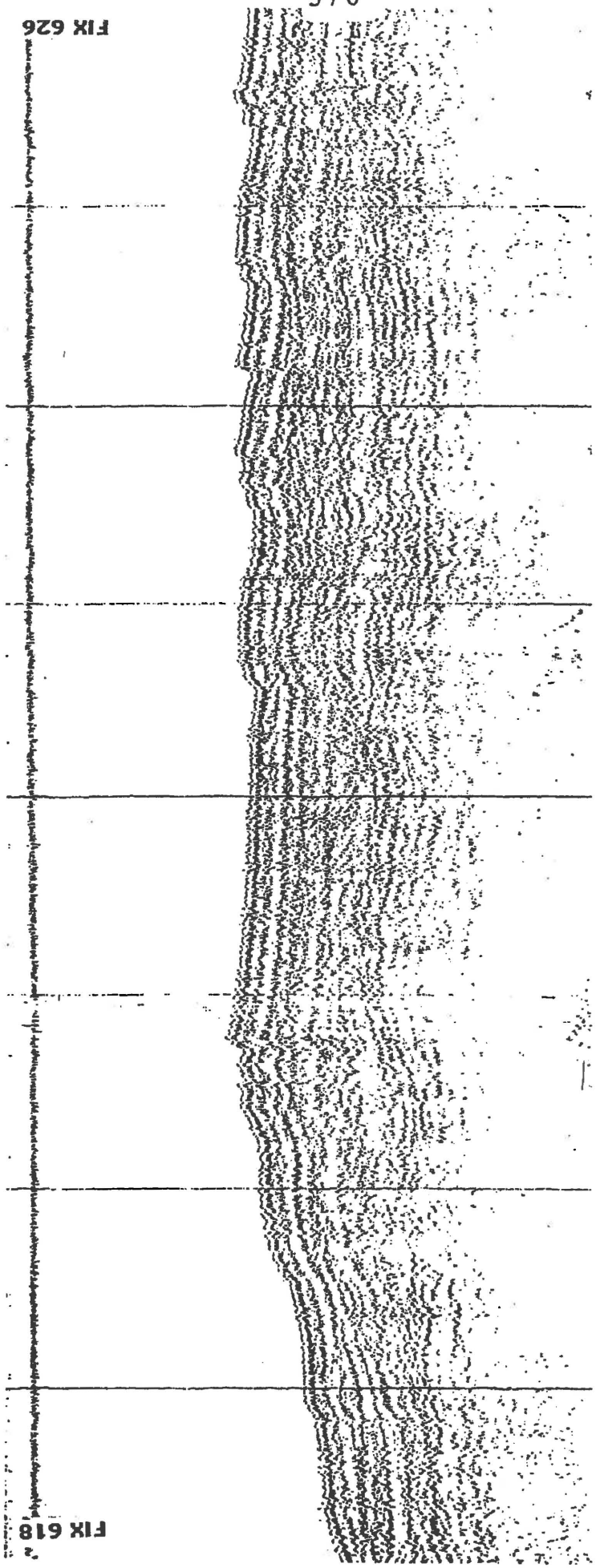

Figure 8.15 a. Raw seismic profile record between Mataora and Whiritoa Beaches.

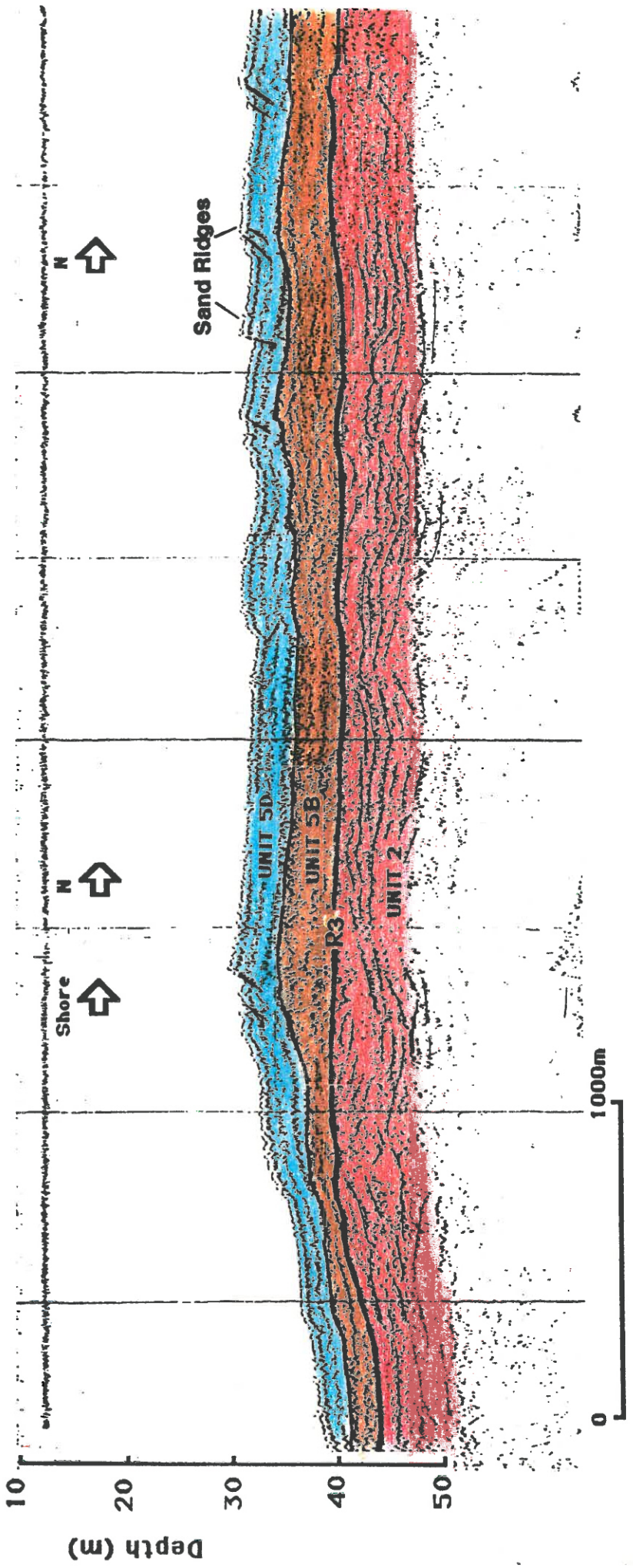

Figure 8.15 b. Interpreted shore-parallel inner shelf seismic stratigraphy between Mataora and Whiritoa Beaches. The Holocene fine grained surficial sediments (Unit 5D) occur continuously here over basal transgressive sands (Unit 5B). Further north, the Undifferentiated Pleistocene (Unit 2) rises sharply and is exposed at the sea-bed.

Mid shelf deposits (Unit 5C) are generally restricted to the subsurface in depths > 50 m. They range in thickness from 7 to 8 m, are usually overlain by fine surficial sands, and onlap the hummocky transgressive deposits (Figure 8.14). However, in one location they are exposed at the sea-bed in 45 to 50 m water depth, this exposure coinciding with the only offshore area at Whiritoa where significant occurrences of muddy sands (15%) are found in < 50 m water depth (Figures 8.12 and 8.14).

Subsurface occurrences of units older than Holocene age are mainly restricted to the Undifferentiated Pleistocene deposits (Unit 2). These reach up to 45 m in thickness, possibly greater, and are continuously present in seismic profiles. The surface rises quite sharply in some offshore areas, and is exposed at the sea-bed on the inner shelf off Whiritoa, this coinciding with an extensive patch of coarse sand found in surface samples (Figures 8.12 and 8.14). This protruding surface does not appear to be associated with any fluvial incision features, and so may represent the remains of a subaerial dune surface. The Undifferentiated Pleistocene also rises quite sharply landwards, and slopes offshore at a similar gradient to the present shelf (1:200; Figure 8.13). This unit appears to extend landwards beyond the nearshore zone, and may thus be associated with the sharp change in gradient and sediment texture at the surf zone, and presence of Pleistocene inner barrier deposits behind Whiritoa Beach.

Stratigraphic patterns offshore from Whiritoa and Mataora Beaches therefore indicate a region of active shelf sedimentation, with offshore zones presently appearing to expand seawards. Areas of significant erosion are minimal, restricted mainly to the nearshore-inner shelf boundary off Whiritoa Beach, and across parts of the lower inner shelf zone in 40 to 45 m water depth. An underlying Undifferentiated Pleistocene is important for the present shelf morphology, with its upper surface strongly influencing the present offshore gradients found here, and surface outcrops producing significant areas of coarse sands.

Whangamata-Onemana Beaches

Surveys of the region offshore from both Whangamata and Onemana are described together, due to the limited coverage of the latter area. Seismic profiles show a sequence of sediments off Whangamata > 55 m-thick, including seismic units 2, 4, and 5. However, off Onemana Beach, seismic basement occurs in about 30 m water depth.

Holocene deposits dominate exposed stratigraphic units in both offshore regions, with the only non-Holocene unit exposed being Tertiary basement rock (unit 1) off Onemana. The nearshore accretionary wedge varies in thickness and extent along the coast. Off Otahu Harbour, this unit reaches up to 11 m in thickness, extending offshore to 25 m water depth, and decreases to a maximum of 8 m thickness in 18 m water depth off Onemana (Figure 8.16).

The fine grained surficial sediments (Unit 5D) commence in all offshore areas beneath the nearshore accretionary wedge. They also vary in thickness and extent, from 5 to 7 m-thickness and 32 m water depth off Otahu and Whangamata, to 3 m thickness and 24 m water depth off Onemana. The fine grained surficial sediments then taper out beyond the lower nearshore boundary, where they occur as relatively thin (2 to 3 m) and discontinuous lobes, or lenses over sand ridges, on the inner and mid shelf surfaces (Figures 8.17, 8.18, 8.19, and 8.20). Off Whangamata Beach, sub-bottom profiles show a lobe of fine sand overlying transgressive deposits in the same location where bathymetric and side-scan sonar surveys indicated the erosion and offshore transport of fine lower nearshore sands during Cyclone Bola (Figure 8.18). The transgressive sand sheet surface beneath these fine sands has the same outline as the Mar-84 inner shelf surface, and thus supports previous deductions of lower nearshore erosion and inner shelf deposition of fine sands during extreme storm events.

The transgressive sand sheet (Unit 5B) extends continuously across the inner shelf at Whangamata from about 45 m water depth, before thinning out beneath the surficial sediment blanket on the lower nearshore zone (Figures 8.17, 8.18, and 8.21). Across the inner shelf, it reaches up to 10 m in thickness, and is often exposed at the sea-bed between lenses of fine sand. The units presence here coincides with an offshore area of coarse grained surface samples and a megaripple field. The thin nature of surficial fine sediments at the lower nearshore boundary, particularly at Onemana, suggests that the CMR bands here are associated with exposure of the transgressive sand sheet from erosion of these lower nearshore deposits. Off Whangamata Beach, the offshore boundary of the transgressive sand sheet onlaps hummocky transgressive deposits (Unit 5A; Figure 8.18). These hummocky deposits are about 5 m-thick, and show surface exposure in one small area on the inner shelf. At Onemana, transgressive sands form only a relatively thin veneer (1 to 3 m-thick), and are very discontinuous over the inner shelf surface (Figure 8.20).

Mid shelf deposits commence as a downlapping unit over the transgressive deposits in 45 m water depth (Figure 8.19). The unit is generally 7 to 8 m-thick, and occurs extensively on the sea-bed where muddy surface samples are found (15% mud). In some areas, lenses of fine sediments occur in sand ridges formed over the surface of this unit (Figure 8.20). Boundaries between the two units often show as CMR on sonograph records, which are inferred to form from either reworking of shells growing on the sea-bed, or coarser deposits within the muddy mid shelf unit.

Pleistocene units form the most extensive sub-bottom deposits off Whangamata, but are not exposed on the sea-bed. Alluvial channel deposits are very widespread (Unit 4). These have formed in large incised channels close to shore (25 m deep, 1000 m wide; Figures 8.17, 8.18, and 8.21), but in much broader features further offshore (10 m deep, 4000 m wide; Figure 8.19). Thus,

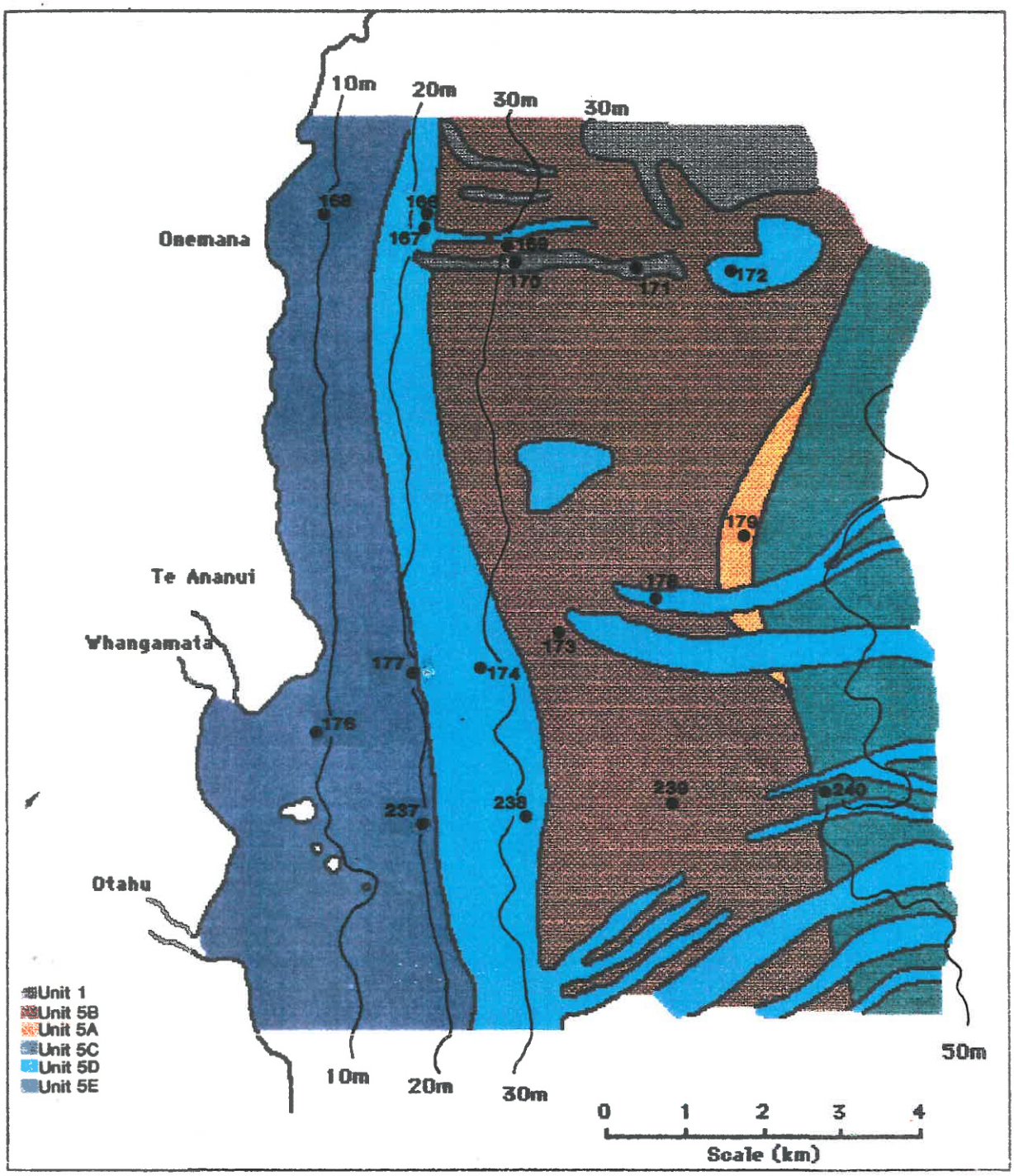

Figure 8.16. Surface distribution of seismic stratigraphic units offshore from Whangamata and Onemana Beaches. Also shown are box core locations.

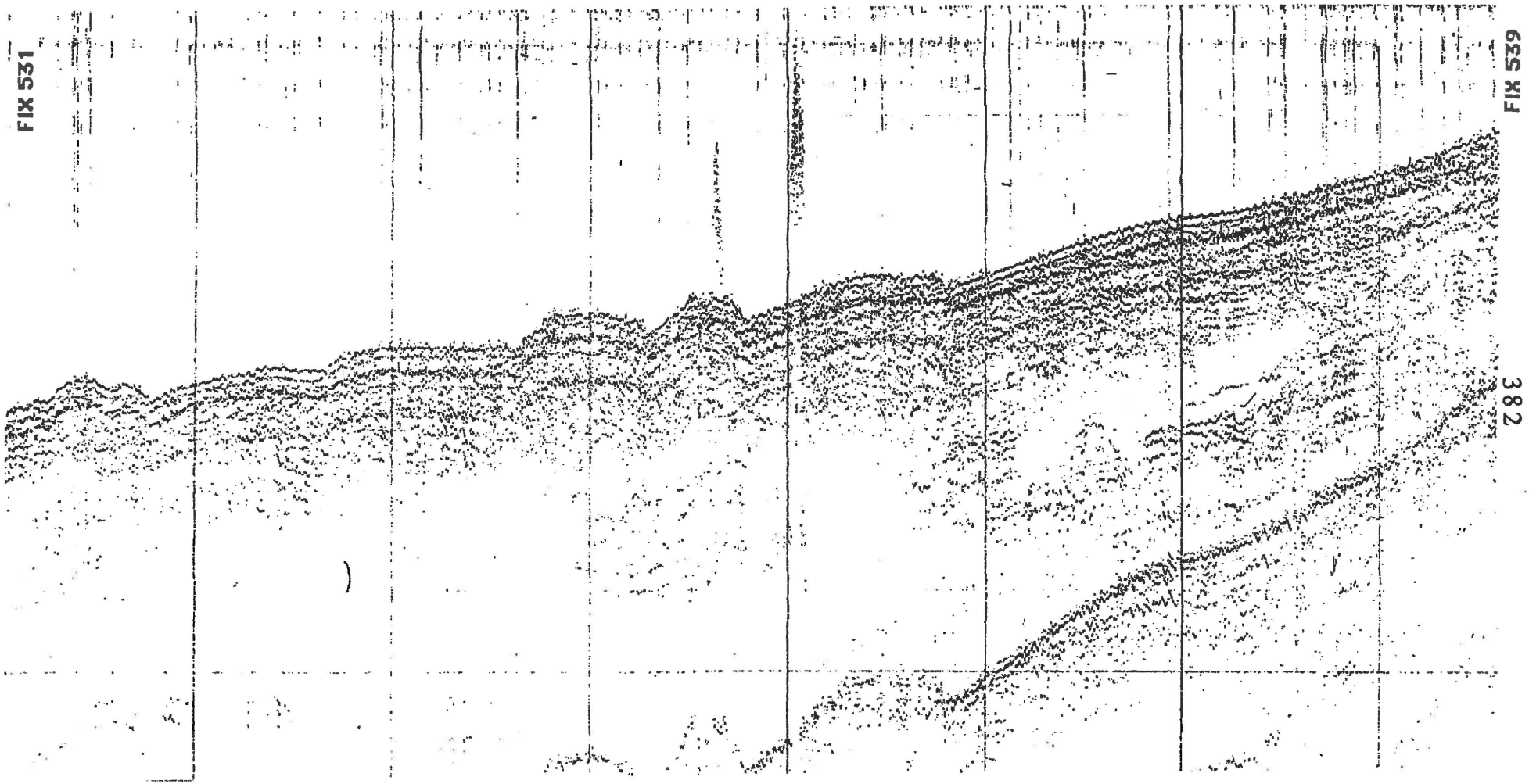

Figure 8.17 a. Raw seismic profile record off Otahu.

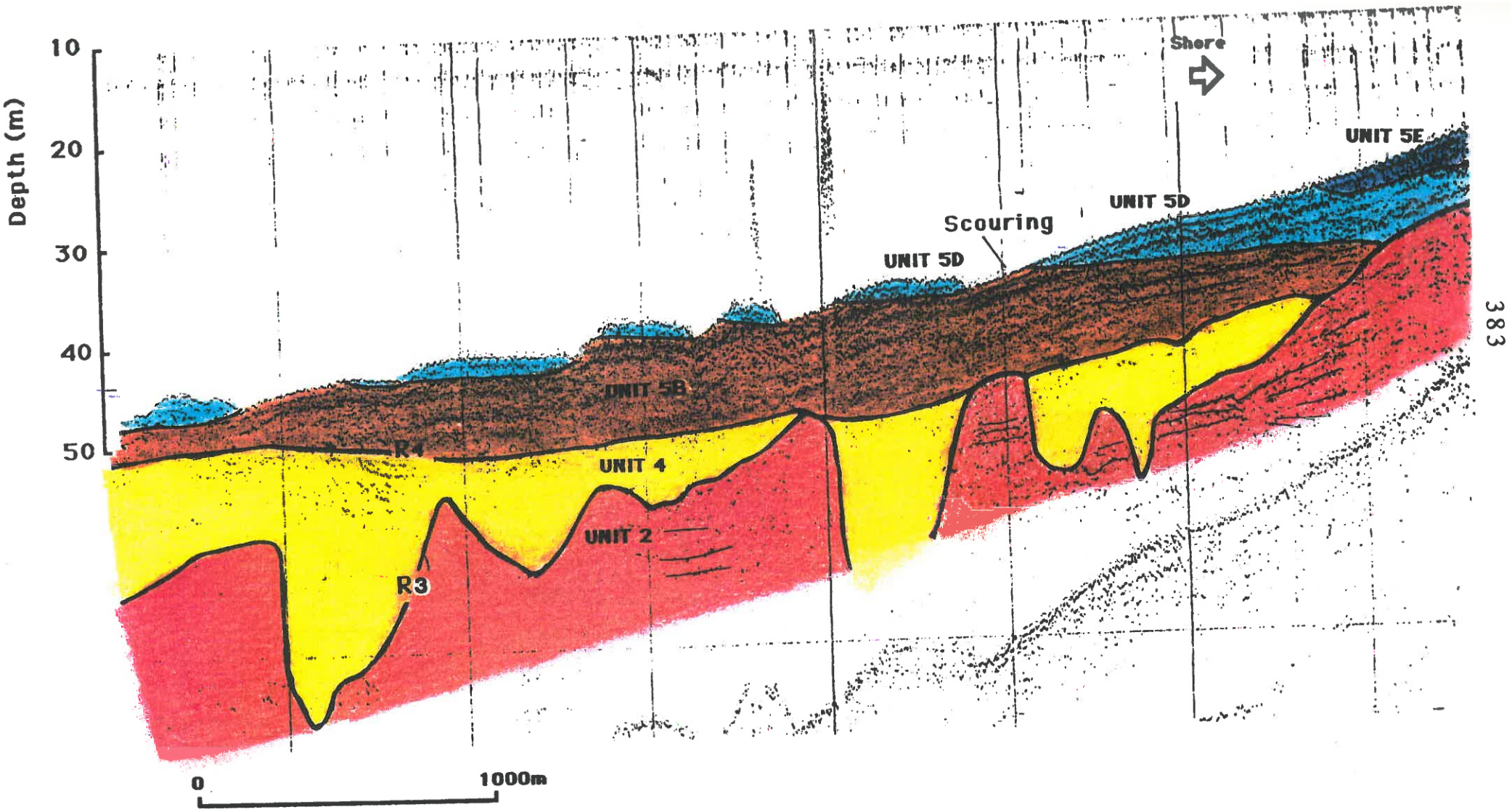

Figure 8.17 b. Interpreted seismic stratigraphy offshore from Otahu. Holocene fine grained surficial sands (Unit 5D) occur discontinuously as relatively thin hummocks (sand ridges) over thick basal transgressive deposits (Unit 5B). Beneath these, the Undifferentiated Pleistocene (Unit 2) has been extensively incised by deep fluvial channels, and infilled with thick alluvial deposits (Unit 4).

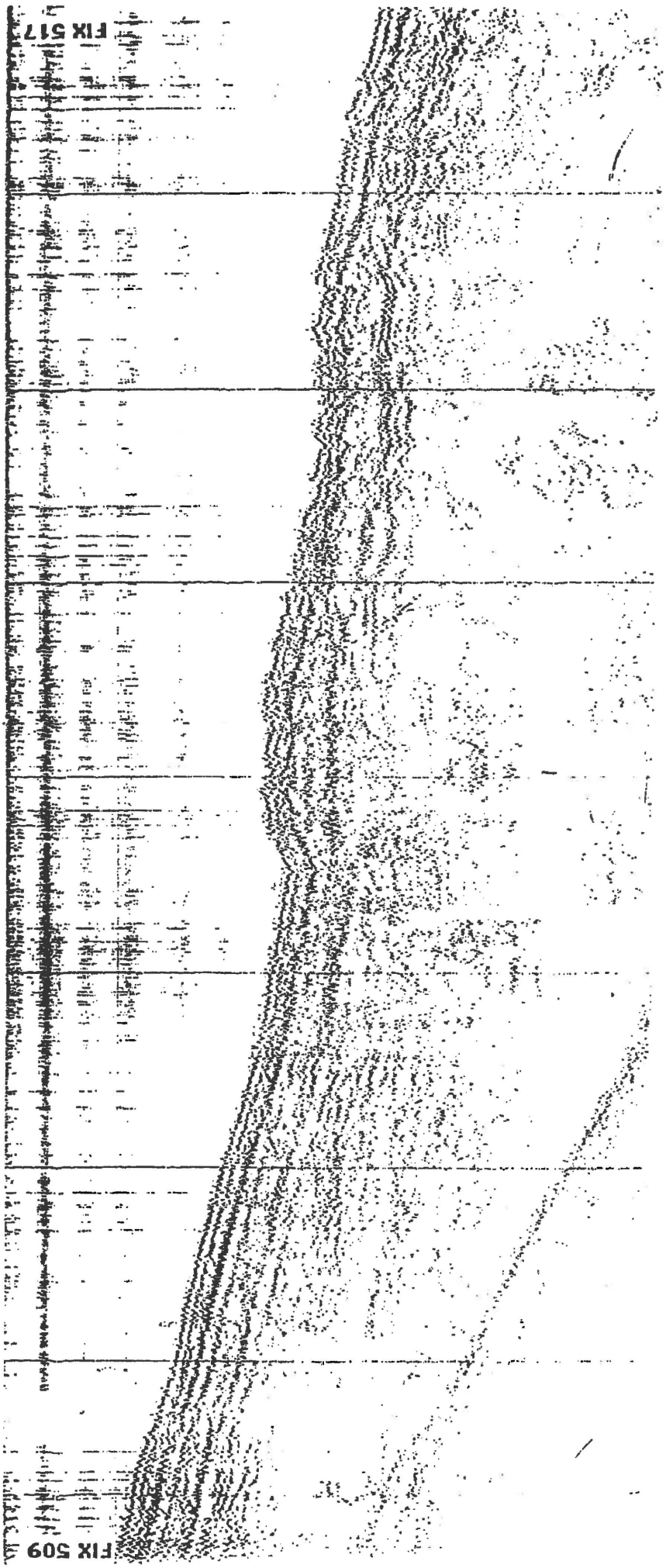

Figure 8.18 a. Raw seismic profile data off Whangamata Beach.

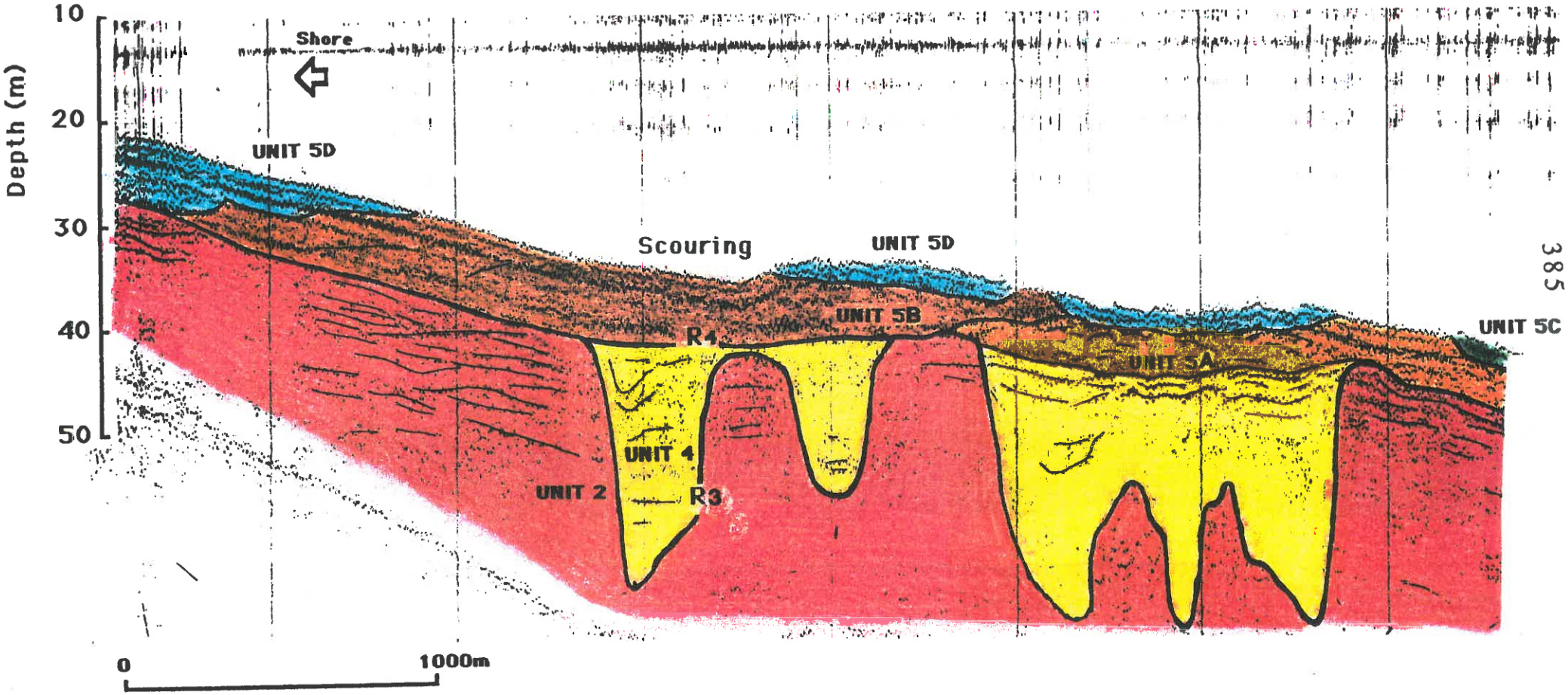

Figure 8.18 b. Interpreted seismic stratigraphy offshore from Whangamata Beach. Holocene fine grained surficial sands (Unit 5D) form a relatively thick wedge on the lower nearshore zone, but occur as only thin lenses over transgressive deposits (Units 5A and 5B) on the inner shelf. These lenses have only formed recently during Cyclone Bola in Mar-88, and the original Mar-84 sea-bed can still be detected beneath these deposits. The Undifferentiated Pleistocene (Unit 2) has been eroded by several large channels and infilled with younger alluvial deposits (Unit 4).

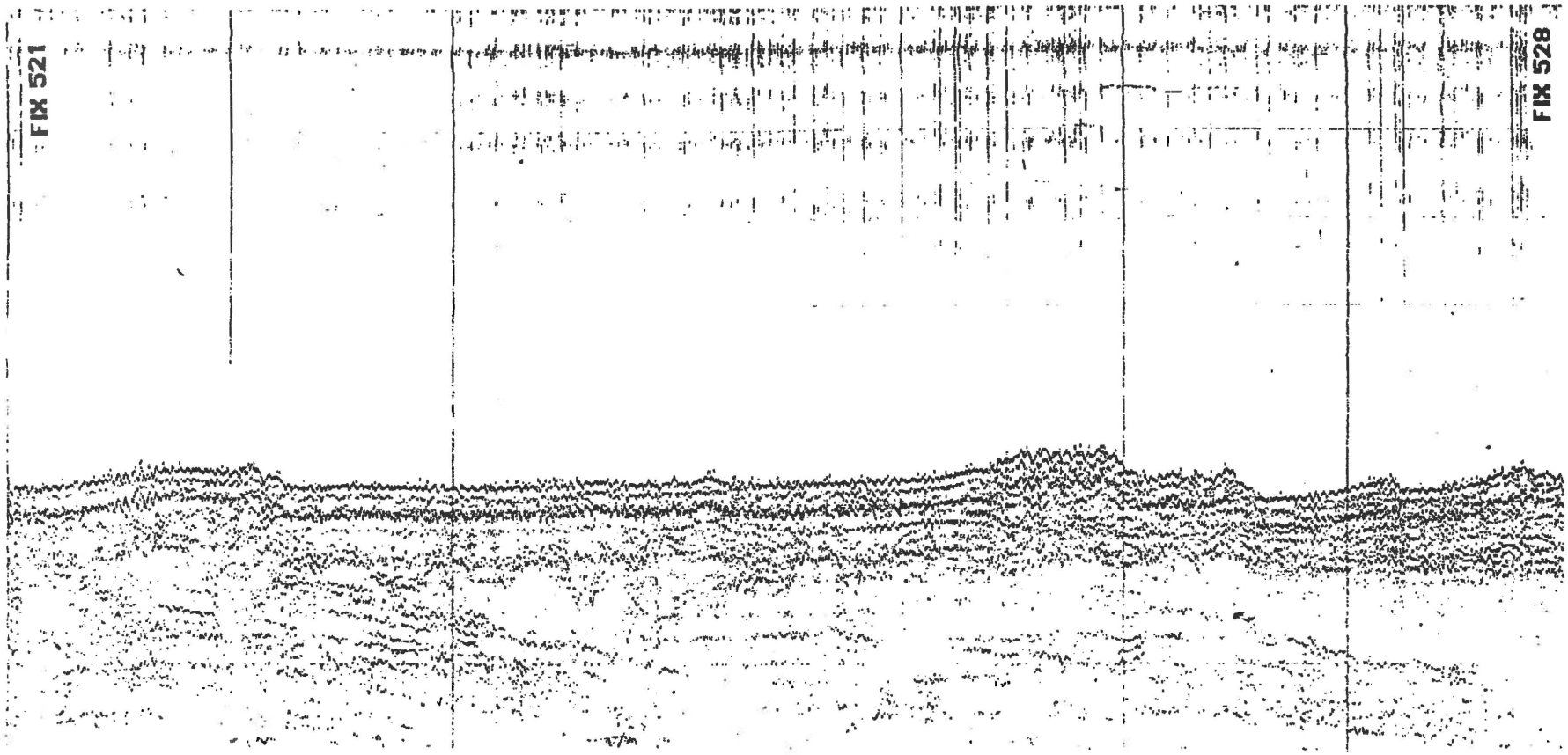

Figure 8.19 a. Raw seismic profile data from the mid shelf between Whangamata and Otahu.

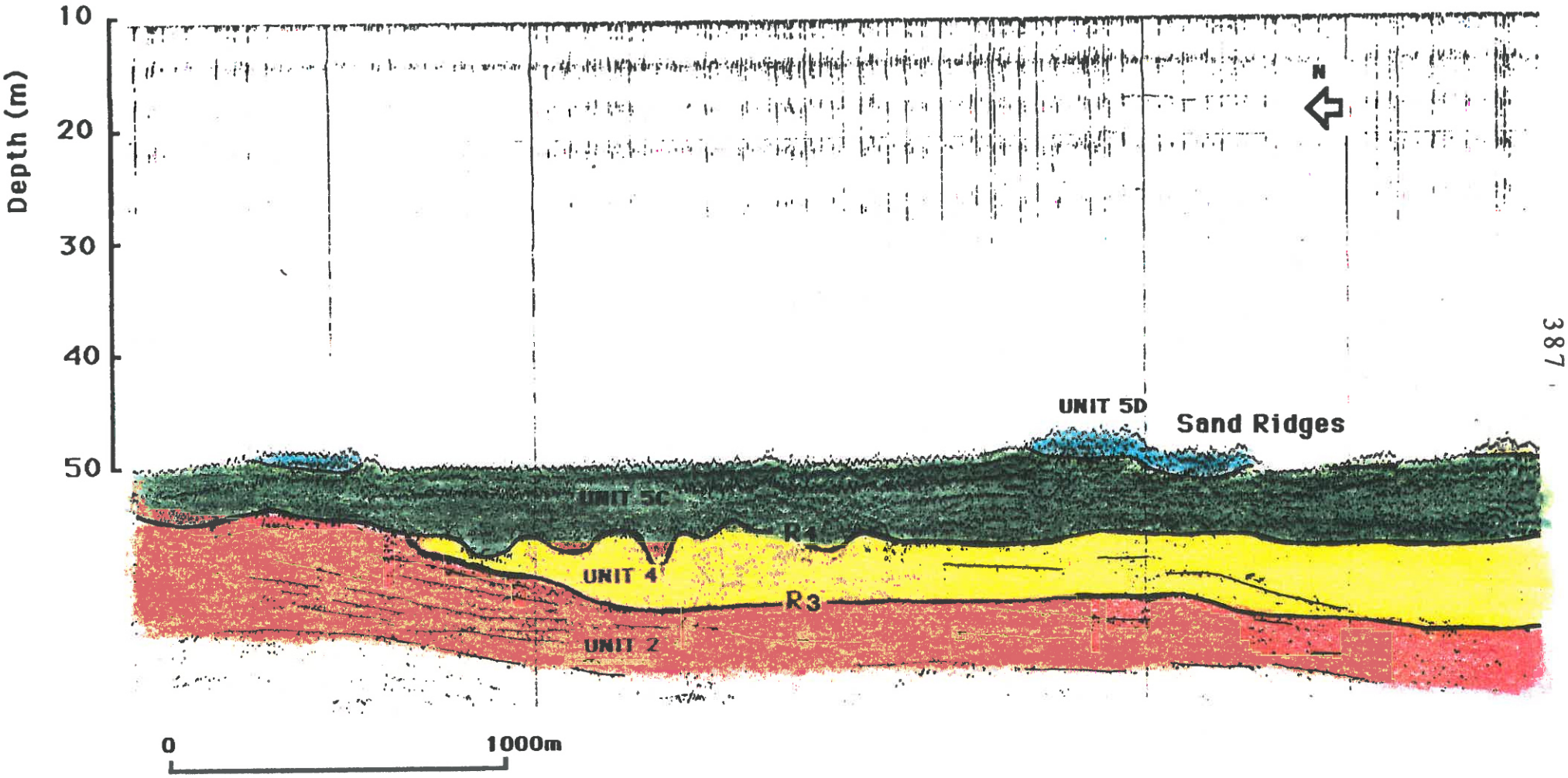

Figure 8.19 b. Interpreted shore-parallel mid shelf seismic stratigraphy between Whangamata and Otahu. Small lenses of Holocene surficial fine sands (Unit 5D) form sand ridges over thick mid shelf muddy deposits (Unit 5C). The Undifferentiated Pleistocene (Unit 2) shows southward dipping reflectors, and was eroded to form a very broad alluvial plain, before accumulation of fluvial deposits comprising Unit 4.

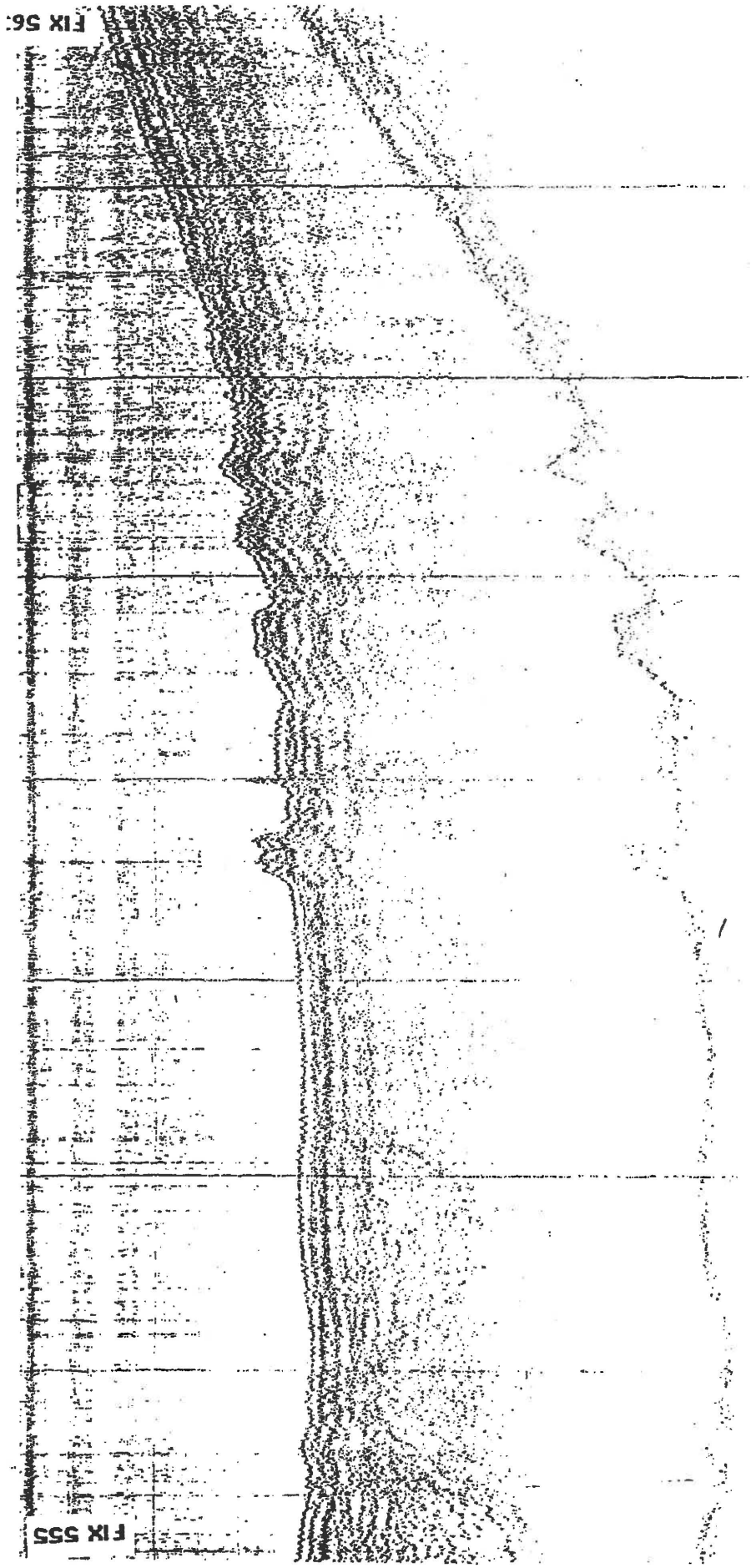

Figure 8.20 a. Raw seismic profile data from the inner shelf between Whangamata and Onemana.

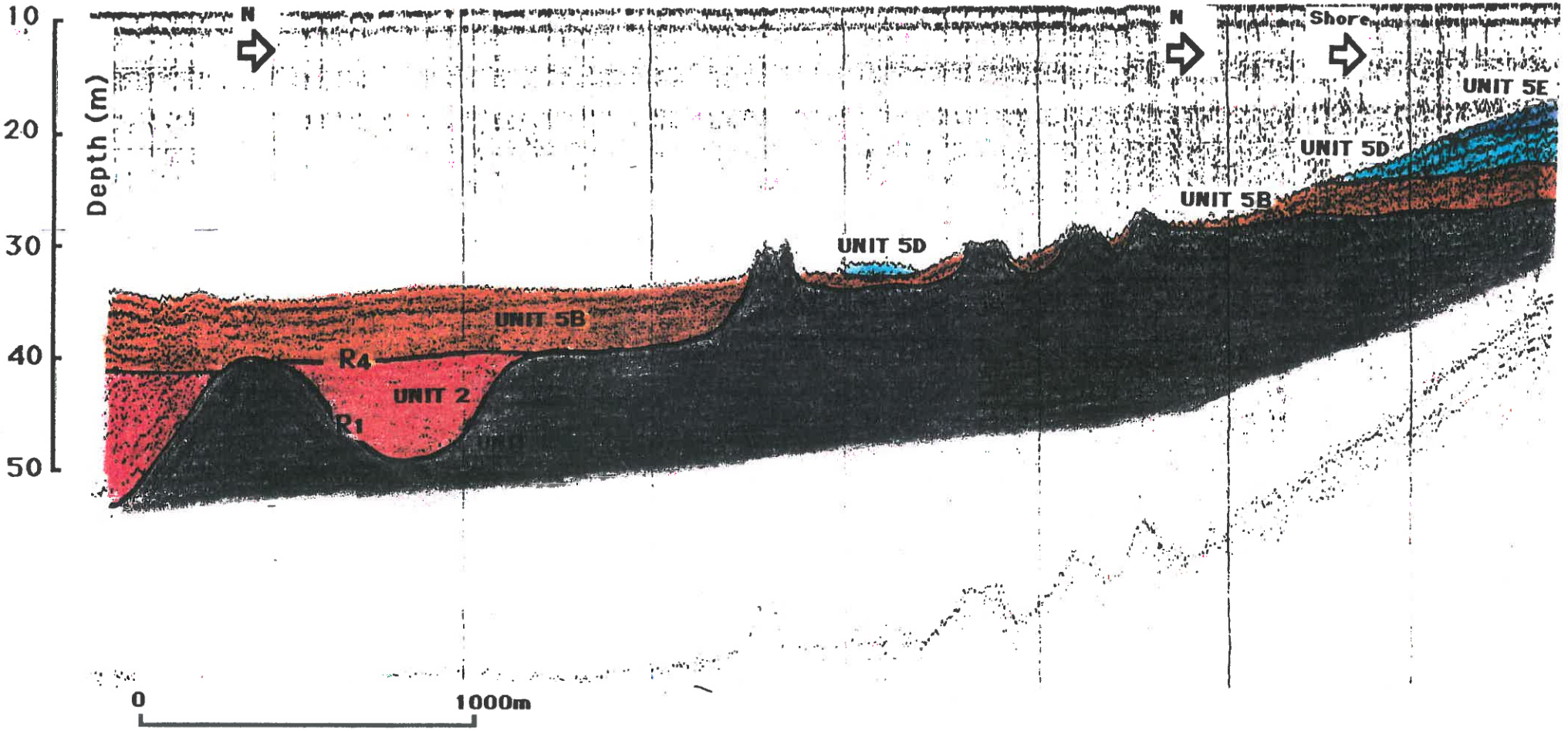

Figure 8.20 b. Interpreted shore-parallel seismic inner shelf stratigraphy between Whangamata and Onemana. Here, basement rock (Unit 1) rises sharply north of Whangamata, and is exposed extensively over the inner shelf surface. Thick sediment sequences are restricted to Holocene deposits (Units 5B, 5D, 5E) in the nearshore zone, with only a very thin veneer of these occurring over the basement rock on the inner shelf.

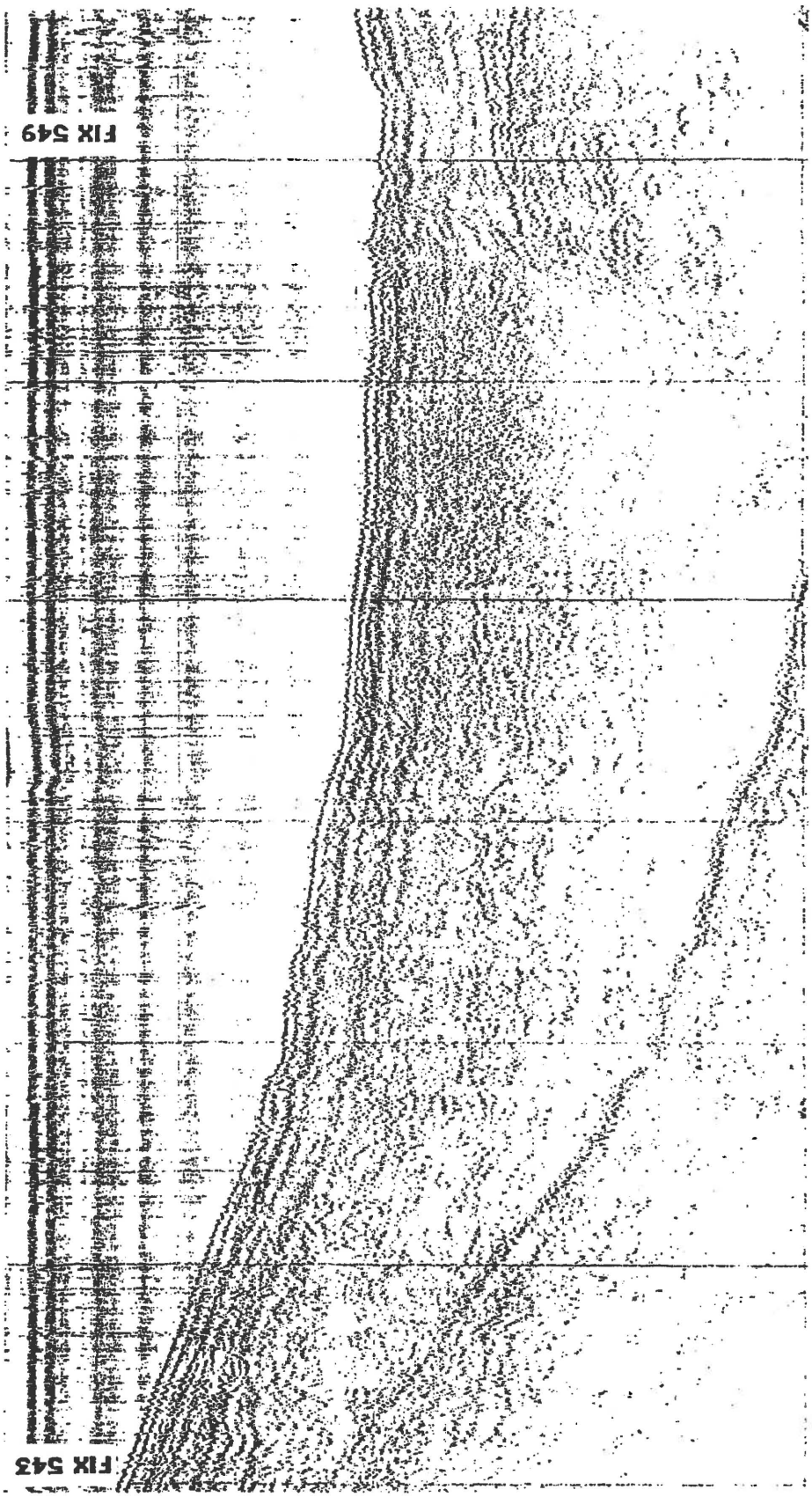

Figure 8.21 a. Raw seismic profile data from the inner shelf between Otahu and Whangamata.

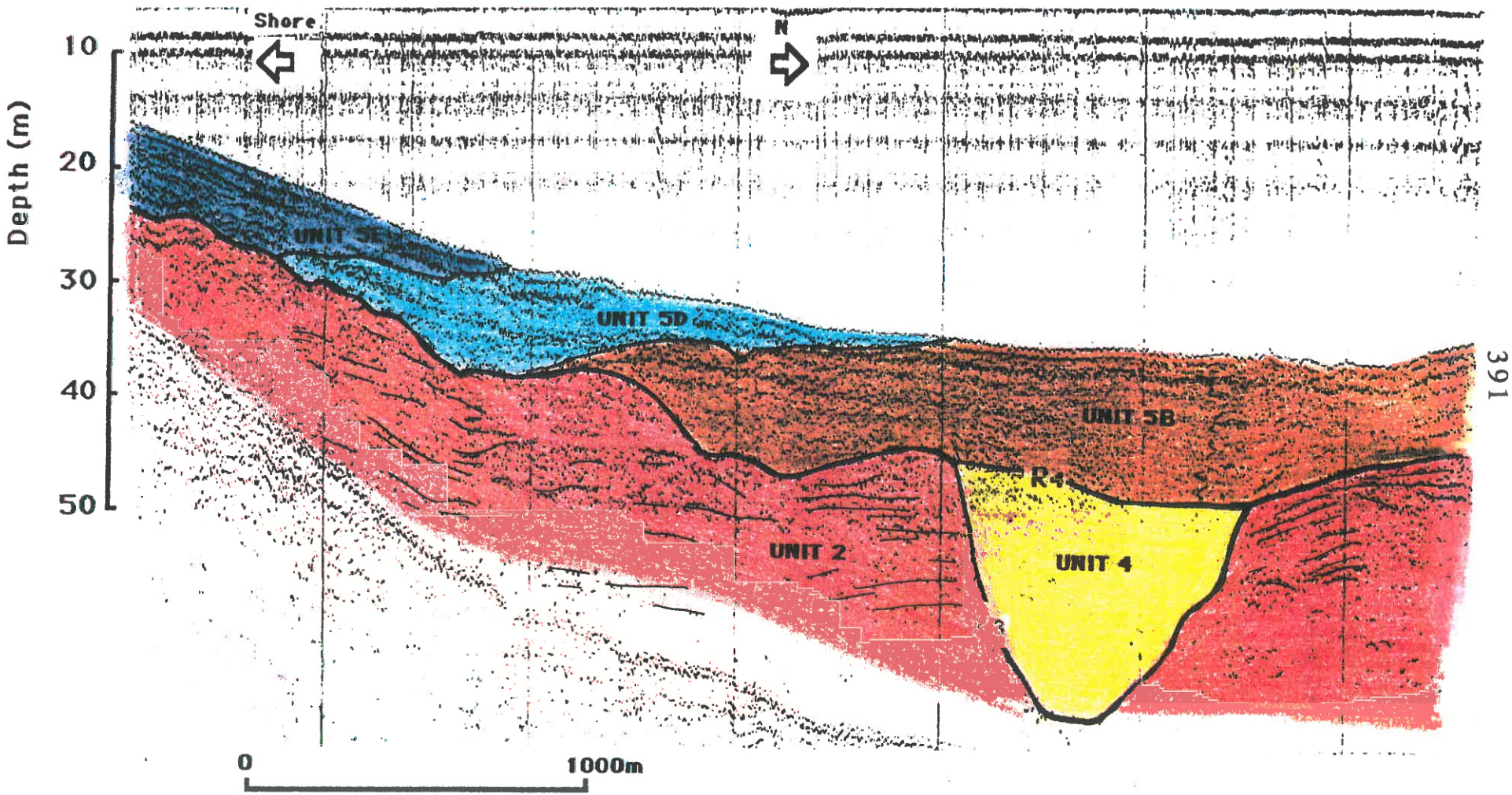

Figure 8.21 b. Interpreted shore-parallel inner shelf seismic stratigraphy between Otahu and Whangamata. Thick wedges of Holocene nearshore sand (Units 5D and 5E) can be seen extending off Otahu over older Holocene transgressive and Undifferentiated Pleistocene deposits (Units 5B and 2). The transgressive sands then form thick deposits on the inner shelf over older alluvial and Undifferentiated Pleistocene sediments (Unit 4).

rivers probably extended from the present Otahu and Whangamata Harbours during the Last Glacial Period, and merged further offshore into a larger braided system. This is consistent with models of low stand system tract environments, as described by VAN-WAGONER *et al.* (1990). The large quantities of alluvial material available would have formed a major source of Holocene transgressive sands during the Holocene marine transgression.

Undifferentiated Pleistocene deposits (Unit 2) also occur extensively off Whangamata Beach. Seismic reflectors show a similar pattern here to the other regions, although they have been more disrupted by extensive river valley incision. In one shore-parallel profile, reflectors within this unit were observed to dip southwards at an angle of 0.5^{o} (Figure 8.19). The unconformity separating Pleistocene units from the Holocene deposits slopes at a similar gradient to the present offshore profiles (1:200), and hence has probably been an important control on the broad shelf morphology.

Pleistocene units appear to be absent from the subsurface stratigraphy off Onemana Beach, with basement rock (Unit 1) rising sharply to the surface north of the Te Ananui Headland (Figure 8.20). This also appears to affect the shelf morphology here, with the relatively flat bedrock platform resulting in a broad and irregular inner shelf surface.

Stratigraphic patterns therefore show significant variation within the short distance between Whangamata and Onemana Beaches. Whangamata is an area generally characterised by modern accretionary stratigraphic patterns in the nearshore and mid shelf zones. However, the inner shelf patterns are more indicative of long term erosion, with only isolated areas of deposition present. The poor development of accretionary units at Onemana (i.e. Units 5D and 5E), and the presence of only a thin veneer of transgressive sands, indicates this shelf region is one of long-term erosion.

Mercury Bay

Sub-bottom profiles within Mercury Bay show subsurface sediments ranging in thickness from > 50 m off the two main beaches (Buffalo and Cooks), to < 5 m where basement rock rises to the surface. The seismic data obtained here were of poorer quality than in the other surveyed areas, thus making interpretations of records difficult, particularly for Pleistocene deposits.

Holocene sediments form a relatively thick sequence and occur over most of the bay (Figure 8.22). The nearshore accretionary wedge (Unit 5E) is very thick (up to 15 m) and extensive within the inner bay area off Whitianga Harbour, but elsewhere is significantly narrower and thinner (~ 10 m-thick).

The Holocene transgressive sand sheet (Unit 5B) appears to underlie nearshore deposits, and extends out across the bay as a relatively thick unit (up to 10 m; Figures 8.23, 8.24). The deposits have surface exposure at the nearshore-inner shelf boundary (20 m water depth), and continue across the shelf surface from 23 to 28 m water depth. Areas of exposure generally coincide

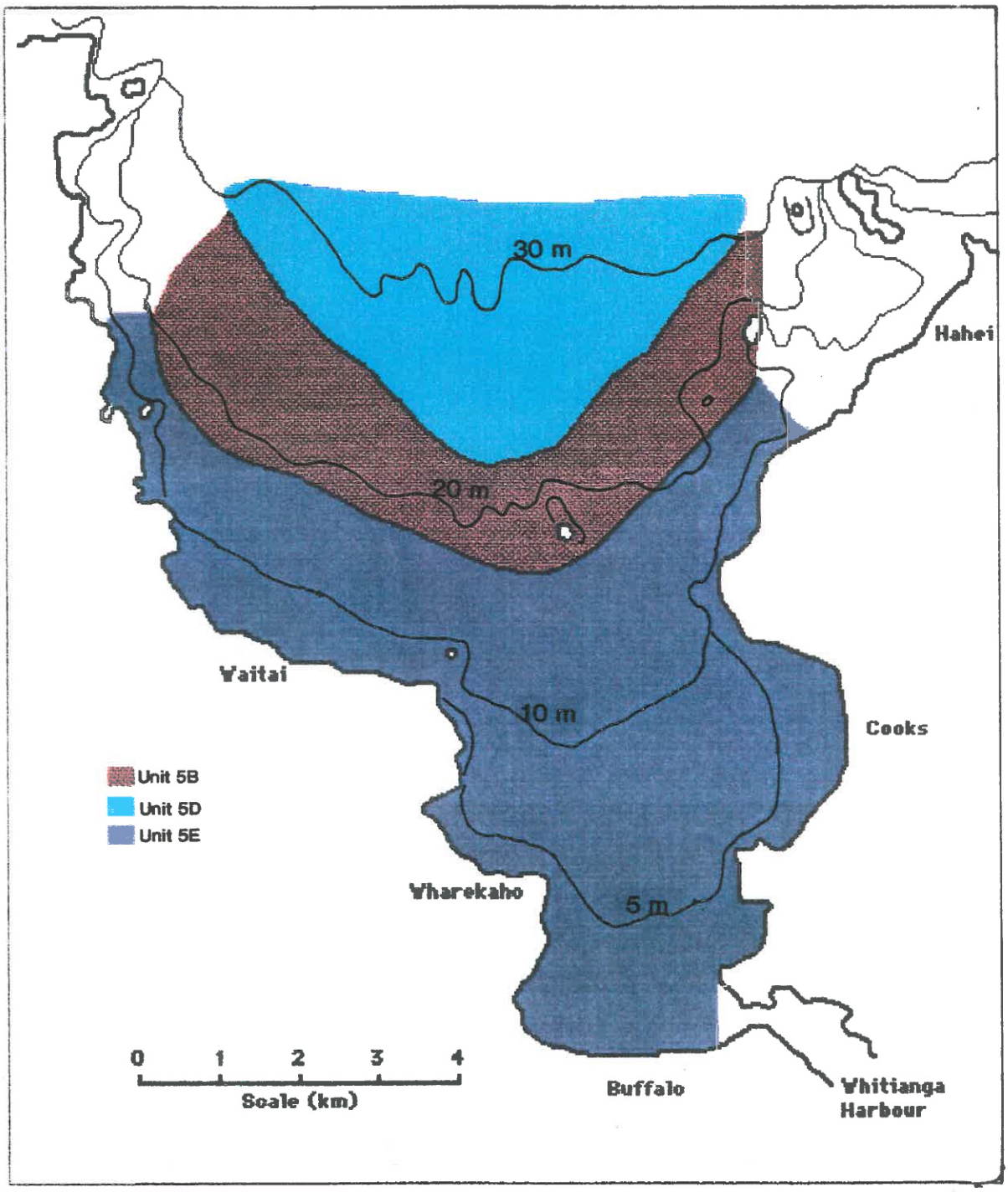

Figure 8.22. Surface distribution of seismic stratigraphic units within Mercury Bay.

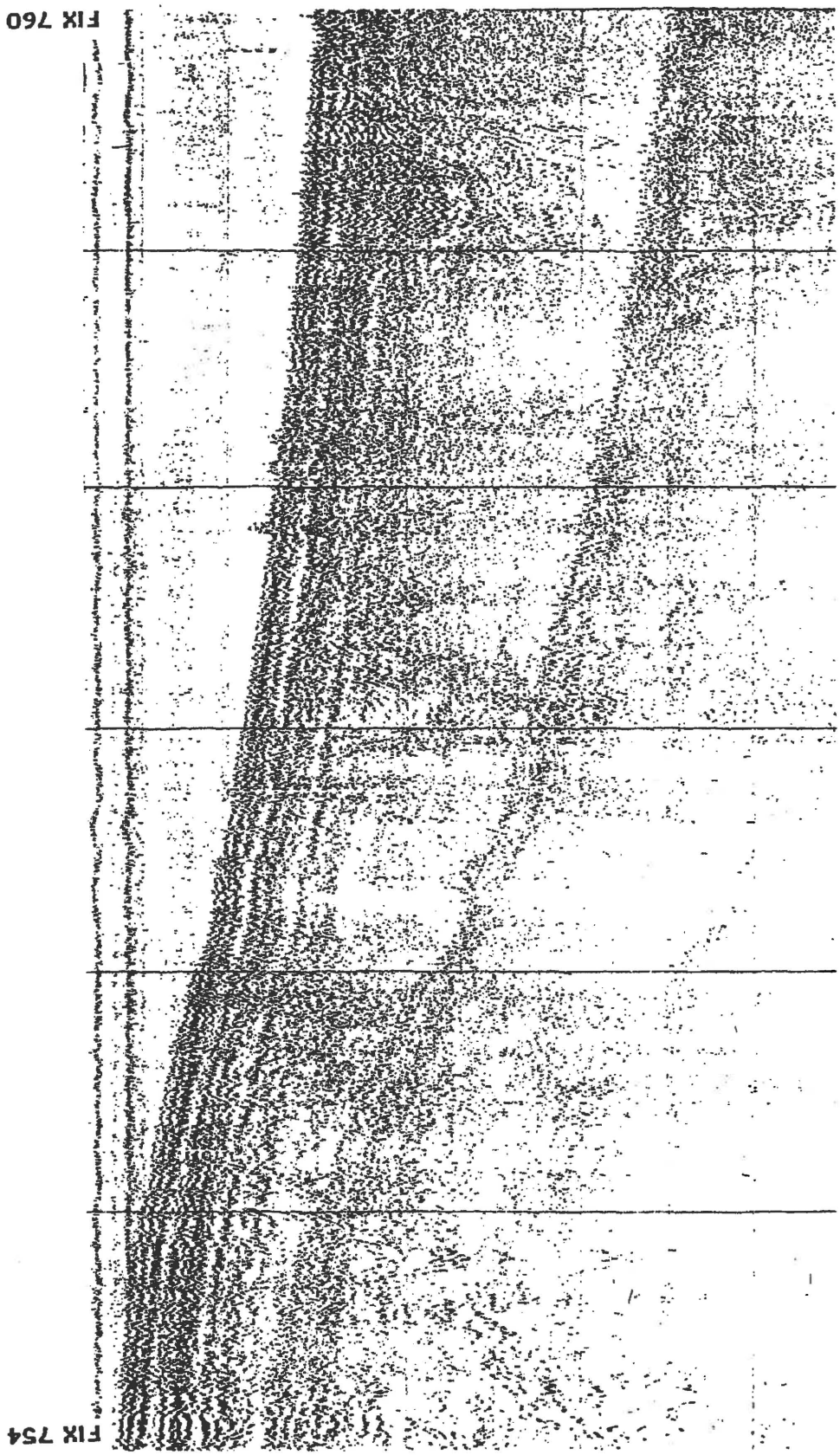

Figure 8.23 a. Raw seismic profile data off Buffalo Beach.

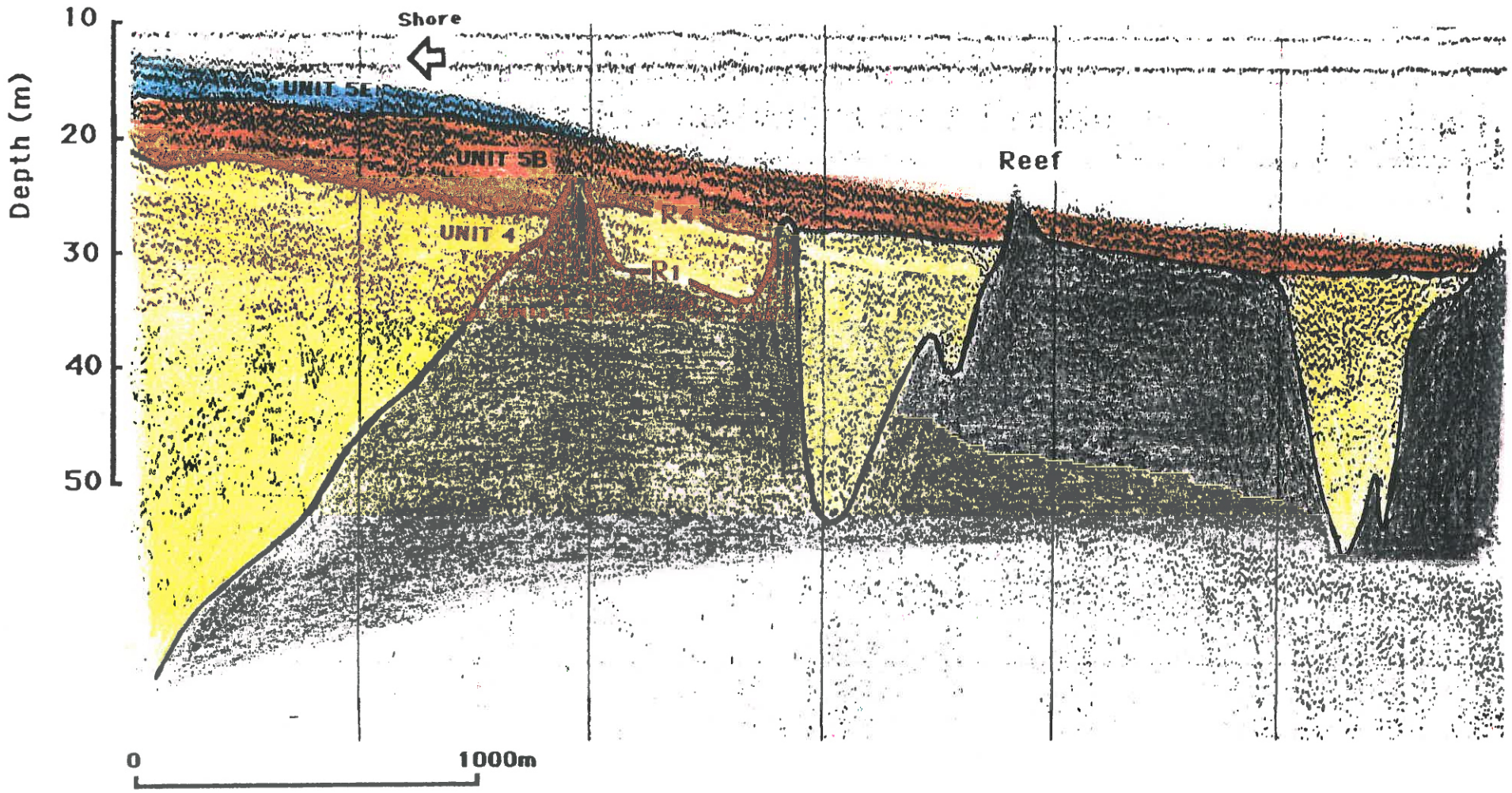

Figure 8.23 b. Interpreted seismic stratigraphy offshore from Buffalo Beach. Holocene nearshore sands (Unit 5E) extend offshore as a thin wedge over relatively thick basal transgressive deposits (Unit 5B). Basement rock (Unit 1) generally rises close to the sea-bed, although its surface has been deeply incised and infilled with thick alluvial deposits (Unit 4).

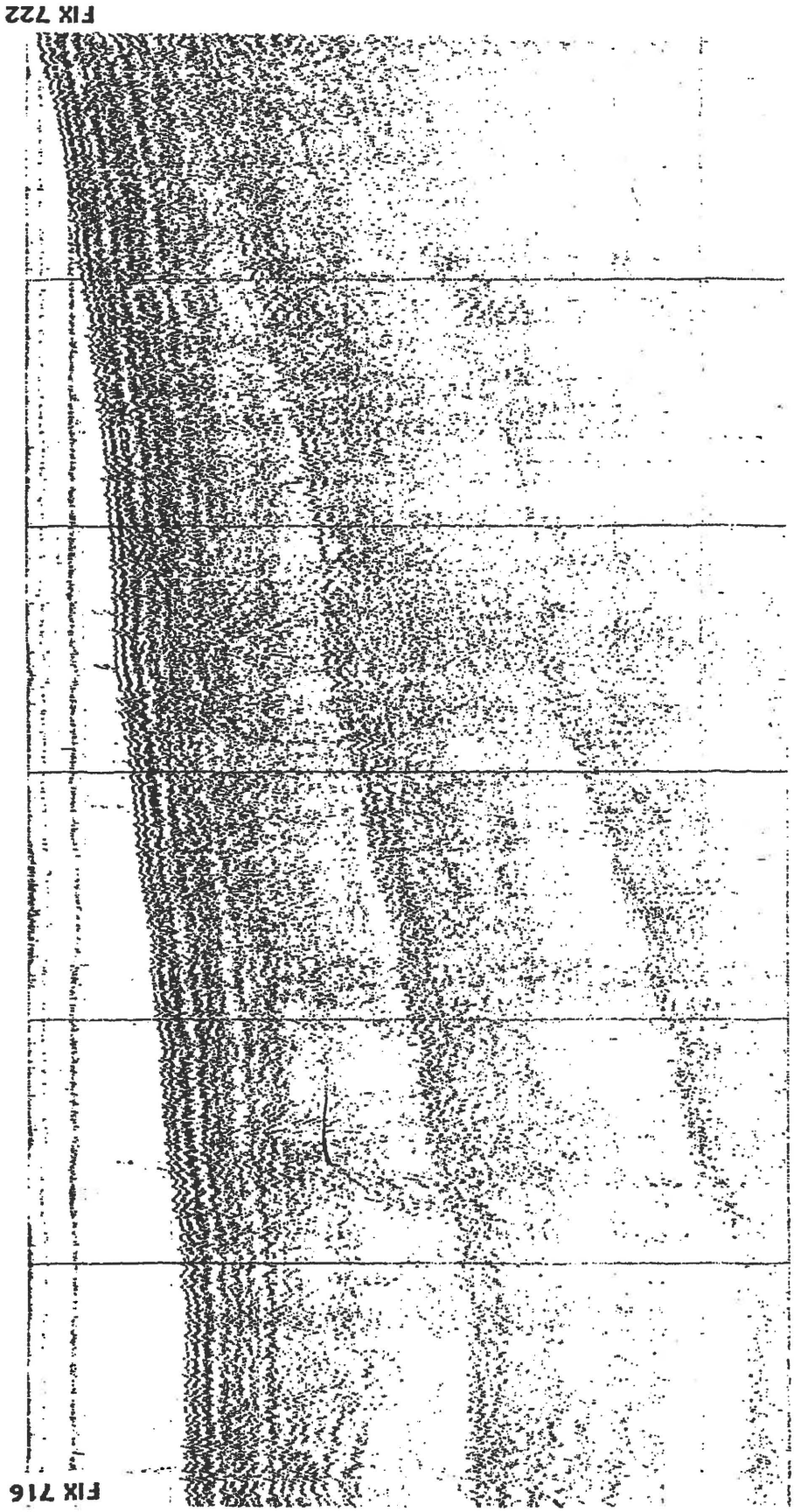

Figure 8.24 a. Raw seismic profile data off Waitaia Beach.

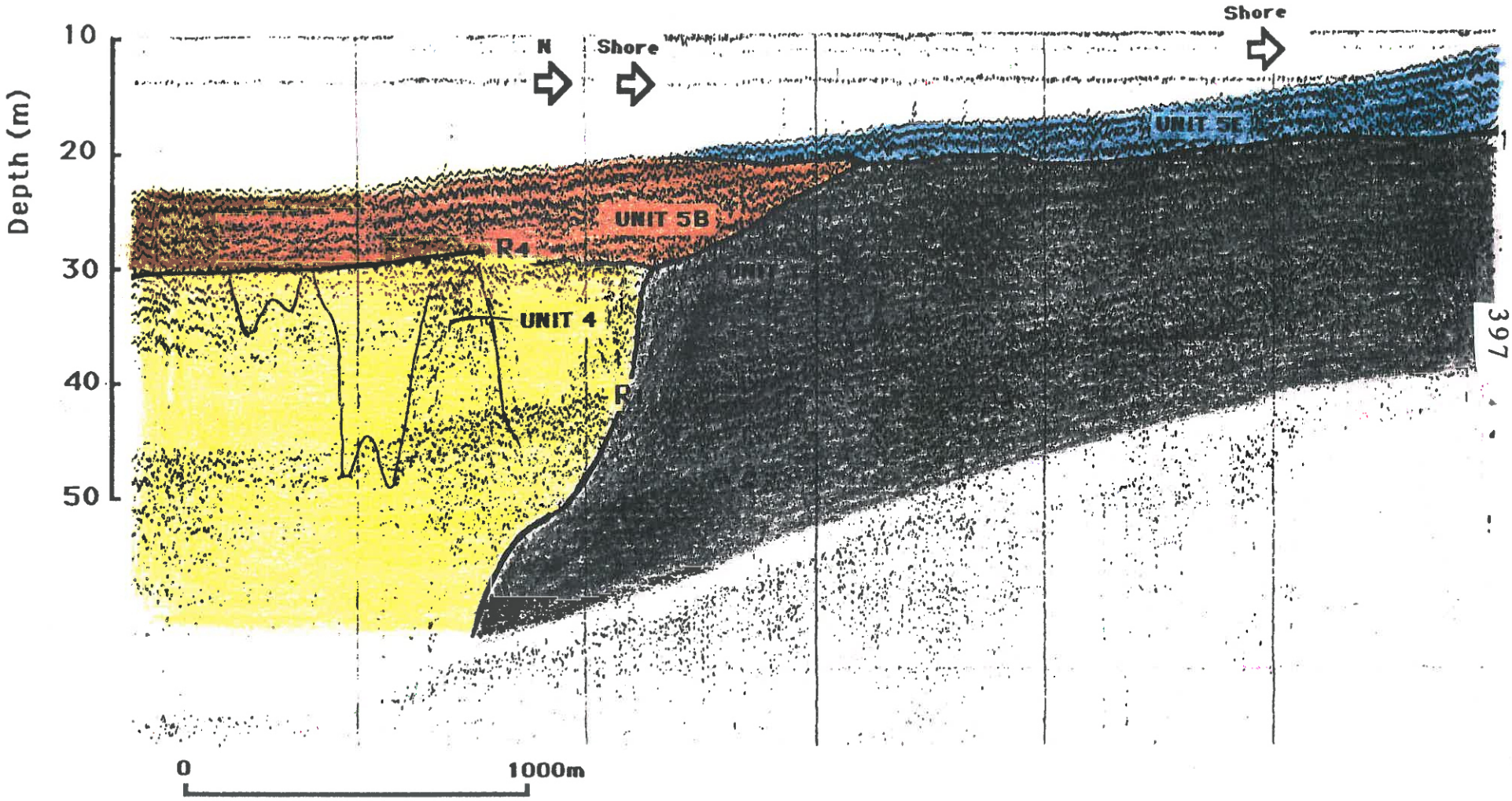

Figure 8.24 b. Interpreted seismic stratigraphy offshore from Waitaia Beach. Holocene nearshore sands (Unit 5E) have formed extensively offshore over basement rock (Unit 1) and basal transgressive deposits (Unit 5B). Thick alluvial deposits (Unit 4) occur beneath the transgressive sands over eroded basement rock.

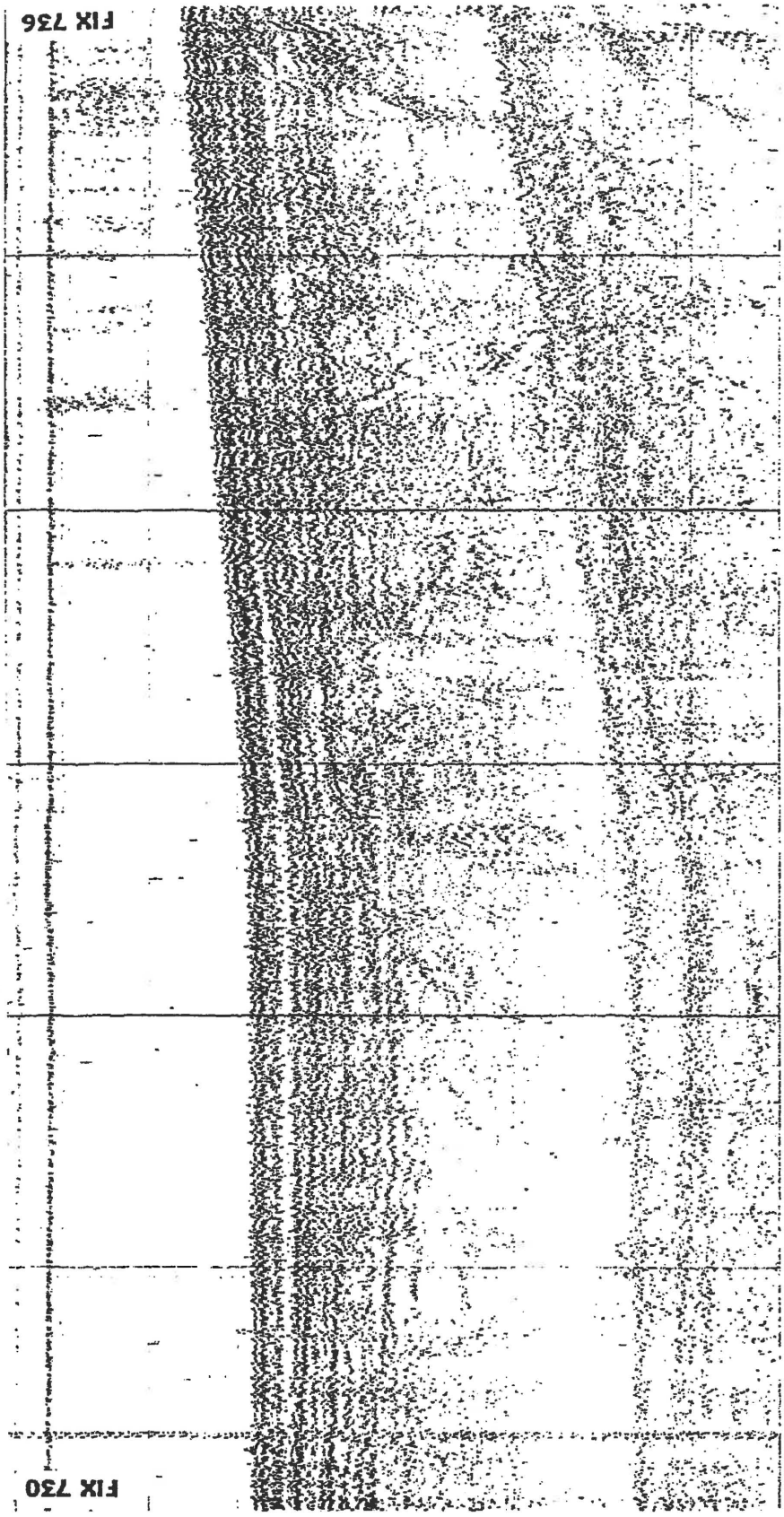

Figure 8.25 a. Raw seismic profile data from the Mercury Bay inner shelf.

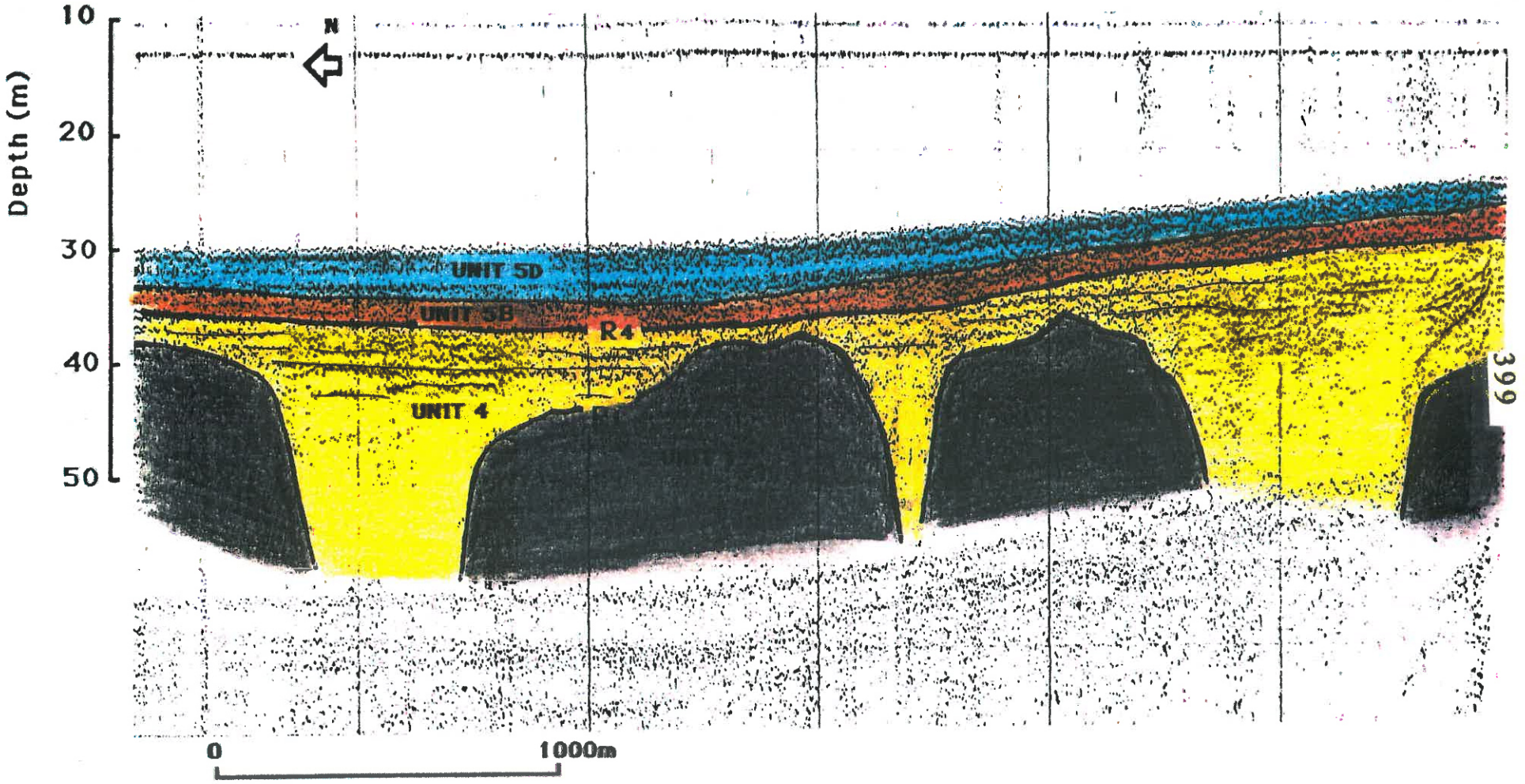

Figure 8.25 b. Interpreted shore-parallel seismic stratigraphy on the Mercury Bay inner shelf. Holocene fine grained surficial fine sands (Unit 5D) form a thick blanket over basal transgressive sands (Unit 5B). Pleistocene alluvial deposits (Unit 4) have formed over the eroded basement rock surface (Unit 1).

with locations of extensive CMR bands from the side-scan surveys. Thus, the transgressive sands are probably covered by a thin veneer of fine sediments (too thin to be detected on sub-bottom profiles), and become locally exposed as coarse megarippled deposits by wave or current scouring.

Further offshore, fine grained surficial sediments (Unit 5D) blanket transgressive deposits (Figure 8.25). These are up to 6 m-thick, and are the dominant surficial inner shelf deposit. Their presence on the inner shelf coincides with the extensive very fine grained sands found in surface sediment samples and side-scan sonar surveys, and indicates modern accretion is occurring on the inner shelf surface.

In many areas, Pleistocene alluvial deposits occupy deep broad channels (up to 50 m deep and 2500 m wide) beneath the Holocene deposits (Figures 8.22, 8.23, and 8.24). It is uncertain whether any older Pleistocene units are present due to the poor quality of records. These ancient river deposits occur within channels eroded into basement rock (Unit 1), which extend offshore from the modern harbour systems (Whitianga and Cooks). Where the channels are absent or poorly developed, particularly in the southern bay area off Hahei Beach, the basement rock rises to the surface and is often exposed on the sea-bed as reefs (Figure 8.23).

Seismic sub-bottom stratigraphic patterns from Mercury Bay therefore indicate an area dominated by modern nearshore and inner shelf accretion in most parts, particularly offshore from Whitianga Harbour. However, a zone of sea-bed scouring appears to extend along the bay across the nearshore-inner shelf boundary, resulting in the exposure of underlying basal transgressive deposits. Modern accretion also appears to be limited on the southern side of Mercury Bay, where Holocene sediments form only a thin veneer over basement rock.

8.3. BOX CORE DATA

Box cores provide additional information on the lithological nature of the upper surface of shelf stratigraphic units. They also provide important information on the modern depth of reworking for surface deposits. Representative photographs of box cores collected from surface exposures of stratigraphic units are shown in Figure 8.26, and their original characteristics described in Appendix 6. These cores were obtained prior to the seismic sub-bottom surveys, and thus were collected in a fairly random fashion. Their association with seismic stratigraphic units has been made by plotting core positions on the seismic stratigraphic outcrop maps (see Figures 8.8, 8.12 and 8.16).

Because exposures of Pleistocene sediments are fairly rare, these were not generally sampled by cores. However, surface exposures of the Pleistocene alluvial deposits (Unit 4) off the northern end of Waihi Beach appear to have been penetrated by one core (Figure 8.26 A). This contains very coarse grained, pale yellow to dark brown sands, analogous to the inner shelf storm lag deposits (Chapter 5.7). As the sands are very well sorted, and have a subsurface layer (-0.20 m)

Figure 8.26. Photographs of representative box cores, with their upper surfaces shown at the top of each photo: A) Pleistocene alluvial deposits (Unit 4) off Waihi Beach (WB 246); B) Holocene basal transgressive sands (Unit 5B) off Waihi Beach (WB 243); C) Holocene basal transgressive marine sands (Unit 5B) interfingering with fine grained surficial sands (Unit 5D) on the Onemana lower nearshore surface (ON 167); D) Holocene basal transgressive sands (Unit 5B) overlying mid shelf muddy sands (Unit 5C) on the Waihi inner-mid shelf boundary (WB 252); E) Mid shelf muddy coarse sands (Unit 5C) off Waihi Beach (WB 253); F) Mid-outer shelf muddy fine sands (unit 5C) off Waihi Beach (WB 256); G) Fine grained surficial sands (Unit 5D) off Whangapoua showing upper bioturbated aerobic layer (5 cm) over darker anaerobic sands (KB 147); H) Fine grained surficial fine sands (Unit 5D) showing aerobic conditions throughout off Mataora Beach (M 236); I) Fine grained nearshore accretionary wedge sands (Unit 5A) off Waihi Beach (WB 247).

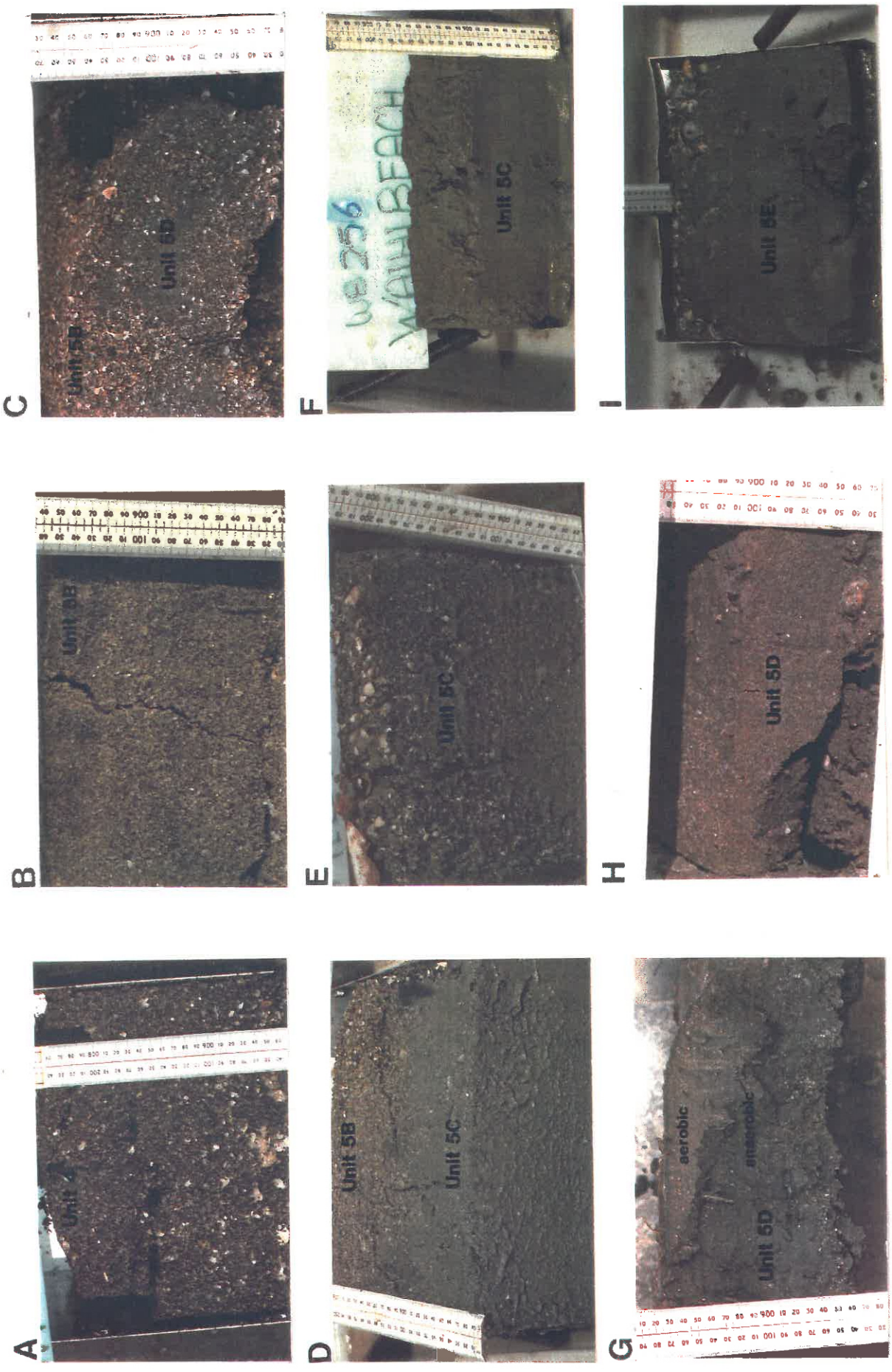
A
Unit 4
B
Unit 5B
C
Unit 5B
Unit 5D
D
Unit 5B
Unit 5C
E
Unit 5C
F
WB 256
MOUNT BEACH
Unit 5C
G
aerobic
anaerobic
Unit 5D
H
Unit 5D
I
Unit 5E

which contains relatively high quantities of shell fragments (13%), the upper surface of the Pleistocene alluvial deposits would appear to have been reworked during the Holocene, and they thus represent palimpsest rather than true relict deposits.

Surface exposures of the Undifferentiated Pleistocene (Unit 2) were sampled in a box core from Whiritoa. The core is dominated by coarse grained, light grey sands, also analogous to the inner shelf storm lag deposits. These contain a high shell content (21%), including whole pectens, indicating that the upper surface has been reworked during the Holocene.

Deposits from the Holocene transgressive sand sheet (Unit 5B) were frequently sampled, particularly off Waihi and Whangamata Beaches. They are characterised by coarse to medium grained, light gray to pale yellow coloured sands, again analogous to inner shelf storm lag deposits (Figure 8.26 B). Shell fragments are commonly present (*Tawera spissa* and pectens), ranging from 10 to 20%, and are often coated with pink coralline algae on their surfaces. This latter feature has been suggested by BLACK *et al.* (1989) to indicate only limited sediment transport is occurring. However, the general oxidised nature of sands throughout cores shows evidence of active sediment reworking to subsurface depths of at least 0.20 m. This minimum depth of reworking is very similar to the size range of megaripple crest heights (see Figure 7.4). As megaripples were observed to respond to storm wave conditions (see Chapter 7.2.2.), this gives further evidence that transgressive surface deposits are intermittently reworked during short-lived storm events each year. Cores through transgressive sands generally show uniform sediment characteristics. However, in one sample from a CMR band off Onemana, fine sand interfingers with coarser material (Figure 8.26 C). This sample was taken from the lower nearshore surface, where fine grained surficial sands overlie transgressive deposits in seismic profiles. It thus supports deductions that CMR bands in these areas form from exposure of the transgressive surface, through erosion of lower nearshore deposits.

Mid shelf deposits (Unit 5 C) were extensively penetrated by box cores off Waihi Beach, and in one instance off Whangamata. Off Waihi Beach, these are first encountered beneath Holocene transgressive sands in 51 m water depth (Figure 8.26 D), indicating the offshore boundary between these two stratigraphic units. The nature of mid shelf deposits varies from medium to coarse sands off Waihi Beach in 51 to 81 m water depth (Figure 8.26 E), to fine grained sands in > 100 m off Waihi, and 50 m off Whangamata (Figures 8.26 F). They are consistently characterised by the presence of greyish olive muddy sands (10 to 15% mud), with moderate amounts of shell fragments (12 to 20%). The mid shelf unit is therefore formed by either the mixing of older coarse Pleistocene or Holocene deposits with modern muddy material, or the modern deposition of fine sands and muds.

Fine surficial sediments (Unit 5D) were extensively sampled by box cores at Whiritoa, Whangamata, Onemana and Whangapoua. They are generally composed of fine grained, grey brown sands, analogous to the lower nearshore and inner shelf fine sands. Shell fragments are of

low abundance in most areas (3 to 12%). In many instances, the cores show a thin grey brown zone with extensive biological activity in the upper 5 cm, changing to greyish olive sands and anaerobic conditions in the lower core (Figure 8.26 G). Areas in which this pattern occurs (lower nearshore deposits off Mataora and Whangapoua; inner shelf deposits off Whiritoa, Whangamata, Onemana, and Whangapoua) are interpreted to be characterised by either the abundant modern deposition of fine sands, or limited reworking of surface deposits by waves and currents. This limited depth of reworking is generally consistent with observations from depth of activity rod surveys in Chapter 7.2.2. Surficial fine sands from many other shelf areas (lower nearshore deposits off Whiritoa, Whangamata, and Onemana; inner shelf deposits off Mataora) show aerobic conditions throughout the box cores (Figure 8.26 H), interpreted to indicate extensive reworking by waves and currents.

Cores obtained in the nearshore accretionary wedge show fine to very fine grained, light grey to light yellow sands, analogous to the very fine upper nearshore deposits (Figure 8.26 I). At Whiritoa, Onemana, and Whangapoua, a greyish olive anaerobic layer was often present beneath the upper 5 cm. This shows a lower depth of reworking for upper nearshore sands than was indicated in the depth of activity rod surveys. As the cores were collected in 1984, and the surveys undertaken in 1985, it is possible that calm conditions and hence upper nearshore accretion occurred in the former, while erosion under frequent storm waves occurred in the latter. Shell fragments are rare within this unit, but live *Tawera spissa* and *Dosinia anus* shells were frequently noted.

8.4. RADIOCARBON DATES AND IMPLICATIONS FOR SHELF SEDIMENTATION

As a final part of the stratigraphic analysis, radiocarbon dates obtained by Paul Dell in 1985 are presented. These are derived from three shell-rich surface deposits from the Holocene transgressive sand sheet at Whiritoa (33 m), Whangamata (34 m) and Onemana (23 m; see Appendix 7 for more details). These data are of limited use, as it cannot be certain whether the shells represent the true age of the transgressive sheet surface. The main problem is whether the shells are autochthonous in origin, and thus in situ surface deposits, or whether they represent allochthonous material derived from either younger or older shell-rich deposits.

However, the data are used here to gain some initial feeling for the age of these transgressive deposits, and the approximate sedimentation rates of the fine surficial sediment which often blankets their surface. For the latter, it is necessary to assume that the radiocarbon dates are representative of the transgressive sand sheet surface age across the inner shelf at each location.

Results are given in Table 8.2, and indicate similar ages for transgressive surfaces at Whiritoa and Onemana (~ 3800 y.B.P.), but a younger age at Whangamata (3000 y. B.P.). An approximate indication of the sedimentation rates for the transgressive sheet deposits is shown in Table 8.2, by

Table 8.2. Radiocarbon ages of transgressive sheet surface deposits (Unit 5B), and approximate sedimentation rates for deposition of transgressive sand sheet and surficial fine sands (Unit 5D).

Location	Unit 5B Radiocarbon Age	Unit 5B Thickness	Unit 5B Rate	Unit 5D Thickness	Unit 5D Rate
Whiritoa-33 m	3840±60 yrs.B.P.	5 m	0.75 mm/y	5 m	1.30 mm/y
Whangamata-34 m	3000±50 yrs.B.P.	7 m	0.93 mm/y	2 m	0.67 mm/y
Onemana-23 m	3800±60 yrs.B.P.	3 m	0.52 mm/y	1 m	0.26 mm/y

observing the depth below present sea level of the marine planation surface (R_4), and obtaining an approximate date of this from Holocene sea level curves by THOM and ROY (1983) and GIBB (1986). This indicates that sedimentation rates were probably higher off Whangamata (~ 0.95 $mm.y^{-1}$) than at Whiritoa and Onemana (~ 0.75 $mm.y^{-1}$ and 0.5 $mm.y^{-1}$ respectively). This in turn indicates that a greater amount of sediment was reworked landwards from the shelf surface at Whangamata during the Holocene marine transgression, compared to Whiritoa and Onemana. These sediments were probably derived from extensive alluvial deposits found within the deeply incised Whangamata palaeo-river channels.

When these dates are integrated with information on the thickness of fine surficial sands, some interesting variations in approximate sedimentation rates are apparent (Table 8.2). These indicate an increase southwards, from a minimum of 0.26 $mm.yr^{-1}$ at Onemana, to 0.67 $mm.yr^{-1}$ at Whangamata, and to a maximum of 1.3 $mm.yr^{-1}$ at Whiritoa. The sedimentation rates of fine surficial sands appear to almost double between each region. This indicates that Whiritoa is an offshore area dominated by presently high sedimentation rates, whilst Whangamata and Onemana are characterised more by inner shelf erosion.

These dates are obviously very open to interpretation, and the sedimentation rates are by no means conclusive. An accurate impression of present and overall sedimentation rates can better be gained through deep coring of the stratigraphic units and dating of appropriate stratigraphic horizons. Such resources were not available in this study, but could be undertaken in the future using the seismic stratigraphic information from this study.

8.5. CONCLUSIONS

The presence of several shallow subsurface seismic stratigraphic units on the east Coromandel coast has been inferred by applying the principles of seismic and sequence stratigraphic analysis, and correlating these data with information on the lithological characteristics of surface unit outcrops from box cores. This has allowed modern shelf sedimentation patterns to be associated with shallow sub-bottom stratigraphic units, and has helped determine the possible controls on these patterns by past environments of deposition. At least five major seismic stratigraphic units are inferred to be present, separated by unconformities representing either major erosional events or hiatuses in the deposition of sediments, formed during global eustatic sea level oscillations.

Modern surface sedimentation patterns along the east Coromandel coast generally coincide with relatively extensive Holocene seismic stratigraphic units beneath the shelf floor. This indicates that the present sedimentation patterns, and hence the modern hydrodynamic processes, have probably occurred throughout most of the Holocene stillstand period (i.e. the past 6500 y.). However, there is no clear evidence in the seismic stratigraphy of short-term oscillations in sea level during the Holocene stillstand, as proposed by RILEY *et al.* (1985) for the northeast coast of New Zealand. On the southern exposed coast between Waihi Beach and Onemana, the association

between modern sedimentation patterns and inferred seismic stratigraphic units can be summarised as follows:

1. Fine to very fine grained, upper nearshore terrigenous sands coincide with an inferred Holocene accretionary wedge in water depths of < 20 m. This wedge is generally up to 10 m-thick, and ranges from 7 m off Onemana Beach, to 11 m off Otahu Harbour. As the latter area is associated with an infilling estuary system, this supports deductions that the upper nearshore sands are derived from local catchments. Box cores from their upper surface show upper nearshore sands in some locations to be less extensively reworked than indicated in the depth of activity rod surveys (Chapter 7.2.2.). This may result from their upper surface actively accreting during periods of relatively calm sea conditions, but subject to extensive reworking during short phases of intense storm wave activity.

2. Fine grained shelf sands coincide with a 5 to 7 m-thick lower nearshore wedge from 20 to 30 m water depth, and a surficial sheet from 30 to 50 m depth. The latter varies in extent from isolated 1 to 5 m-thick lobes (associated with sand ridges) off Waihi and Whangamata, to an extensive 5 m-thick sheet off Whiritoa and Mataora. Inferred sedimentation rates of these fine sands increase southwards from Onemana to Whiritoa. Seismic profiles off Whangamata Beach show the changes in sedimentation patterns observed following Cyclone Bola (see Chapter 6.4.) to be associated with the deposition of a 2 m-thick sheet of fine surficial sands over the Mar-84 inner shelf surface. This supports earlier deductions from morphological observations that lower nearshore sands are eroded and redeposited on the inner shelf surface during extreme storm events. Some supporting evidence for this comes from the box core data, which generally indicate extensive reworking of lower nearshore deposits (except at Mataora), and limited reworking (< 5 cm) of inner shelf fine sands.

3. Medium to coarse grained inner shelf storm lag deposits generally coincide with basal Holocene transgressive sands. These vary from a 1 to 2 m-thick veneer off Onemana, to a 5 m-thick sheet off Waihi and Whiritoa, and a 10 m-thick sheet off Whangamata. Surficial transgressive sand deposits date between 3000 and 4000 y. B.P., and appear to have accumulated at different rates between various locations, with the highest rates off Whangamata Beach, and the lowest at Onemana. This is inferred to result from a larger amount of sediment present on the Whangamata shelf during the Holocene marine transgression, which was derived from the reworking of Pleistocene alluvial deposits beneath the Holocene marine planation surface. In some instances, storm lag deposits appear to be derived from the modern surficial reworking of older Pleistocene deposits. Thus, the inner shelf storm lag deposits are essentially palimpsest sands. Box cores indicate that the modern storm lag deposits are intermittently reworked to depths equivalent to the present range of megaripple crests heights, and possibly deeper. This is consistent with the previous depth of activity rod surveys (Chapter 7.2.2.), which showed megaripples to be active under storm wave conditions.

4. Fine to very fine grained muddy mid shelf sands off Whiritoa and Whangamata form part of a 7 to 8 m-thick unit of mid shelf deposits. This is inferred to indicate the active accumulation of mid shelf deposits in these locations. However, the coarse textured nature of Waihi Beach mid shelf deposits may result from only a thin veneer of modern muds intermixing with older transgressive or Pleistocene sands.

Within Mercury Bay, very fine grained sands coincide with a relatively thick nearshore accretionary wedge offshore from Whitianga Harbour (15 m-thick), and a thinner surficial sediment blanket on the inner shelf (6 m-thick). This supports deductions that the shelf surface off Mercury Bay is actively accreting, with modern terrigenous sands derived from the local major harbour systems (Whitianga and Cooks). Holocene transgressive sands form a 10 m-thick sheet, which as at Whangamata, are interpreted to have formed from the onshore reworking of extensive pre-existing alluvial deposits during the Holocene marine transgression. Transgressive deposits are exposed along the nearshore-inner shelf boundary, which coincides with the area of most extensive reworking of shelf sediments in Mercury Bay (see Chapter 6.2.2.). Modern sediments within Mercury Bay are very limited along the southern shoreline, where transgressive and fine surficial sands form only a thin veneer over rock basement.

Box cores off Whangapoua Harbour support deductions in previous chapters for active sediment reworking only in the nearshore surface in < 20 m water depth. The anaerobic nature of sediments beneath the inner and mid shelf surfaces indicates that the flat sea-bed here is due to limited sediment reworking, and is not associated with sheet flow conditions during storms.

Pre-Holocene seismic stratigraphic units are inferred to directly influence modern sedimentation patterns in some areas, particularly where they are exposed on the sea floor at Waihi and Whiritoa. However, their greatest impact on modern sedimentation patterns is through the influence their upper surfaces have on the broad shelf morphology, which in turn affects modern hydrodynamic processes. Off Waihi Beach, a thick progradational marine sequence is identified, which is characterised by a flat upper surface. This results in a broad and flat inner shelf surface, which is inferred to favour the generation of infragravity waves, and thus the formation of extensive sand ridges across the shelf (see Chapter 7.3.3.). However, this unit is absent in more northern shelf locations, where instead either a steeper dipping Undifferentiated Pleistocene or extensive bedrock outcrops occur. This results in a narrower and steeper shelf surface, which does not favour the generation of sand ridges.

The presence of this progradational marine sequence (Unit 3B) beneath Holocene deposits at Waihi Beach requires further consideration. Although the facies present cannot be positively identified without core data, the seismic information suggests a prograded barrier and shelf sequence is present (WALKER, 1984). Analysis by sequence stratigraphic principles suggests this formed during isotope stage 3 (25 000 to 60 000 y. B.P.), when sea level fluctuated between 30 to 60 m below present. This age is also supported by the presence of beach and river deposits of this time

range within the Tauranga Basin (HARMSWORTH, 1983). Similarly dated prograded barrier and shelf sequences have also been identified in other studies, from Australia (ROY and HUDSON, 1987), North America (CHIN *et al.*, 1988), and Japan (SAITO, 1989). Their presence here off Waihi Beach shows a complete contrast to the present shelf stratigraphic patterns (i.e. depositional vs. erosional), and thus a change in the conditions of shelf sedimentation during the late Quaternary.

It is possible that when sea level was lower, the present Matakana Island barrier system was located further offshore, and extended along the coast to include the area offshore from Waihi Beach (Figure 8.27). This expansion of barrier deposits may have resulted from higher sediment discharges into river systems as their catchments expanded, and incorporation of previous marine and fluvial deposits from within the Tauranga Basin. Other environmental factors could also have been important, such as:

- the presence of different wave and/or current conditions, which may have favoured the accumulation of shelf sediments in this region;

- the presence of a significant regional littoral drift system, resulting in the northwestward transport of sediments from rivers draining the extensive Bay of Plenty coastal plains;

- geological factors such as increased volcanism and hence larger supplies of unconsolidated pyroclastic deposits to the coast, and the affects of local faulting;

The absence of a Pleistocene progradational marine unit north of Waihi also requires explanation. Between Whiritoa and Whangamata, the steep Undifferentiated Pleistocene surface identified from seismic interpretations, suggests that during a lower sea level event, the coastline here would be located only a few kilometres seawards of its present position. Fluvial sediment discharge would have increased only slightly, with some additions from previous harbour and Undifferentiated Pleistocene deposits. Offshore from Onemana, the basement rock would be exposed to form a similar rocky coastline as presently found. It is likely that the shelf north of Waihi had a similar physiography to that presently found, and was probably characterised by similar nearshore and inner shelf sedimentation patterns, although a more southerly wind and hence wave climate may have been present (HARRAY and HEALY, 1978).

Environmental conditions present on the east Coromandel coast during the lower sea level conditions of isotope stage 3 were probably of high shelf sedimentation in the northern (and possibly southern) Bay of Plenty, with extensive barrier deposits prograding out over the present shelf, and contrasting erosional conditions further north. This can be accounted for by the presence of both a significant sediment source and accommodation for these sediments in the Waihi-Bay of Plenty area, but the absence of either of these conditions further north. Accommodation for deposits occurs within subsiding sedimentary basins, evident both south

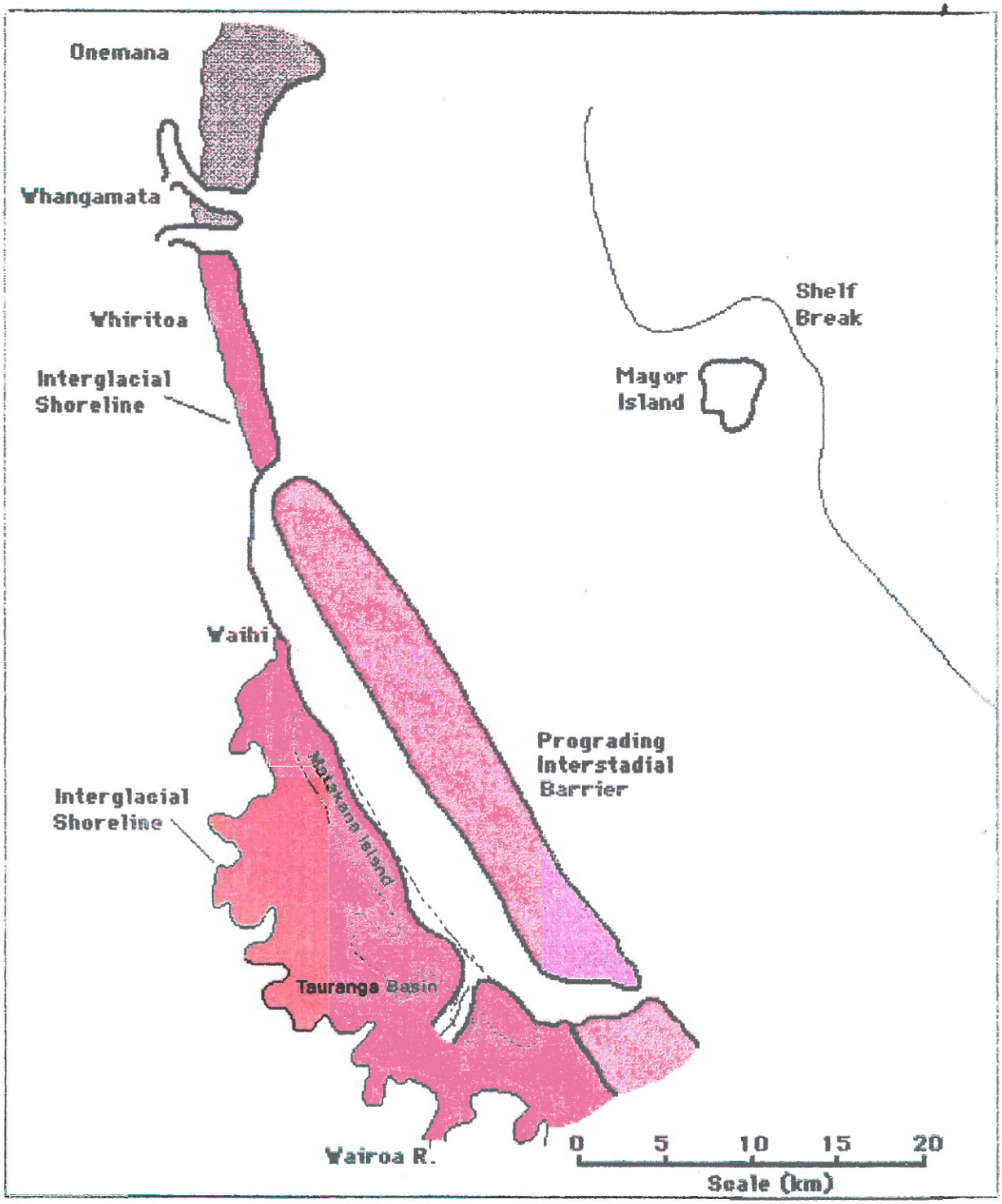

Figure 8.27. Inferred environmental conditions present on the east Coromandel coast during the lower sea level conditions of isotope stage 3 (25 000 to 60 000 y.B.P.). This shows a large prograded barrier system offshore from the present Waihi Beach, formed from reworking of older marine and fluvial deposits within the Tauranga Basin. Further north, limited exposures of older Pleistocene sediments and basement rock would have resulted in similar environmental shelf conditions to the present.

and east of Whangamata, as identified in seismic surveys by THRASHER (1986; see Figure 2.18). However, north of Mayor Island, THRASHER (1986) identified only a relatively thin sediment veneer over an igneous platform on the continental shelf. In this study, basement rock was also found to rise close to the sea-bed in this region, with only a thin Holocene mantle present. During lower sea level periods, this mantle would be eroded and the bedrock exposed. Thus, the northern shelf area cannot provide the same accommodation for shelf sediments as areas further south, except in embayed locations such as Mercury Bay (and probably Whangapoua), where relatively large incised river valleys provide some accommodation for local terrestrial sediments.

In summary, variations in east Coromandel shelf physiography and modern sedimentation patterns can largely be attributed to the geological character of different sections of the coast. Areas south of Whangamata are capable of accumulating thick sedimentary sequences within subsiding sedimentary basins, but more northern areas are generally incapable of doing this, even where large sediment sources are available, due to the presence of an extensive rock platform across the shelf.

CHAPTER NINE

SEDIMENT COMPOSITION

9.0. INTRODUCTION

The textural data in Chapter 5 allowed some initial interpretations to be made concerning the interactions between different sedimentary environments along the east Coromandel coast, as well as possible sources of various beach/barrier and shelf deposits. These included:

1. All barrier spit beach systems, and most northern pocket beaches, appear to be diabathically coupled with the upper nearshore zone, while southern pocket beaches are isolated sedimentary systems;

2. Fine grained modern barrier spit beach sands appear to be supplied to some extent from their adjacent river catchments;

3. Coarse inner shelf storm lag deposits, and fine grained lower nearshore and inner shelf sands, are possibly derived from the same offshore source;

4. Very fine grained shelf sands are derived from a modern onshore terrigenous source;

5. Medium to coarse grained pocket barrier sediments have been derived from reworking of either older Pleistocene barrier deposits, or Holocene transgressive sands;

6. Fine grained barrier spit deposits were derived from the onshore reworking of fine lower nearshore and inner shelf sands.

However, the textural evidence alone is only one indicator, and requires substantiating information on the sediment composition to allow more confidence in subsequent conceptual sedimentation models. This chapter therefore aims to ascertain the degree of interaction between different environments within the study area (rivers, beaches, barriers, and continental shelf) from an investigation of the mineralogical properties of each morphodynamic environment, and to also ascertain the likely provenance of coastal and shelf sediments.

9.1. METHODS

As the mineralogical analysis represents only a small part of the east Coromandel inner shelf study and is very time consuming, it was necessary to restrict the number of samples. In total 141 samples have been selected from all of the major sites within the study area(Figures 9.1. and 9.2). Fluvial samples were collected by hand from river beds as far downstream as possible, but above tidal influence to avoid possible 'contamination' by marine sediments. However, access difficulties in some areas meant that samples had to be collected from the tidal sections of rivers (northern Hotwater Beach, Hahei, Tarapatiki Str., Otama R., Kuaotunu R., and Rings Beach), and so mineralogical results from these areas may not be definitive (i.e. 'contaminated' samples

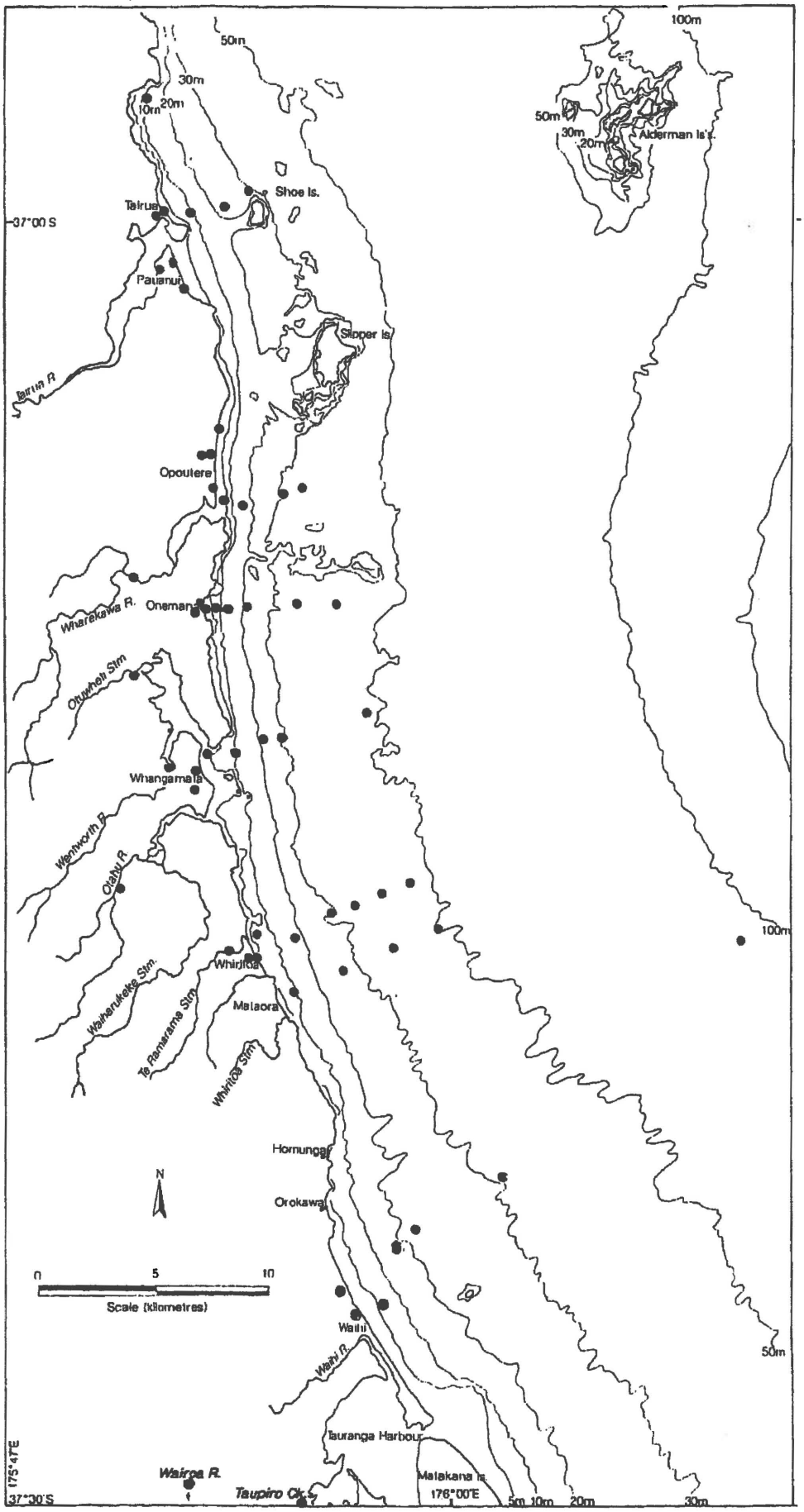

Figure 9.1. Location sites of samples used in the mineralogical analysis along the southern exposed coast (see Appendix 2 for more detailed sample locations).

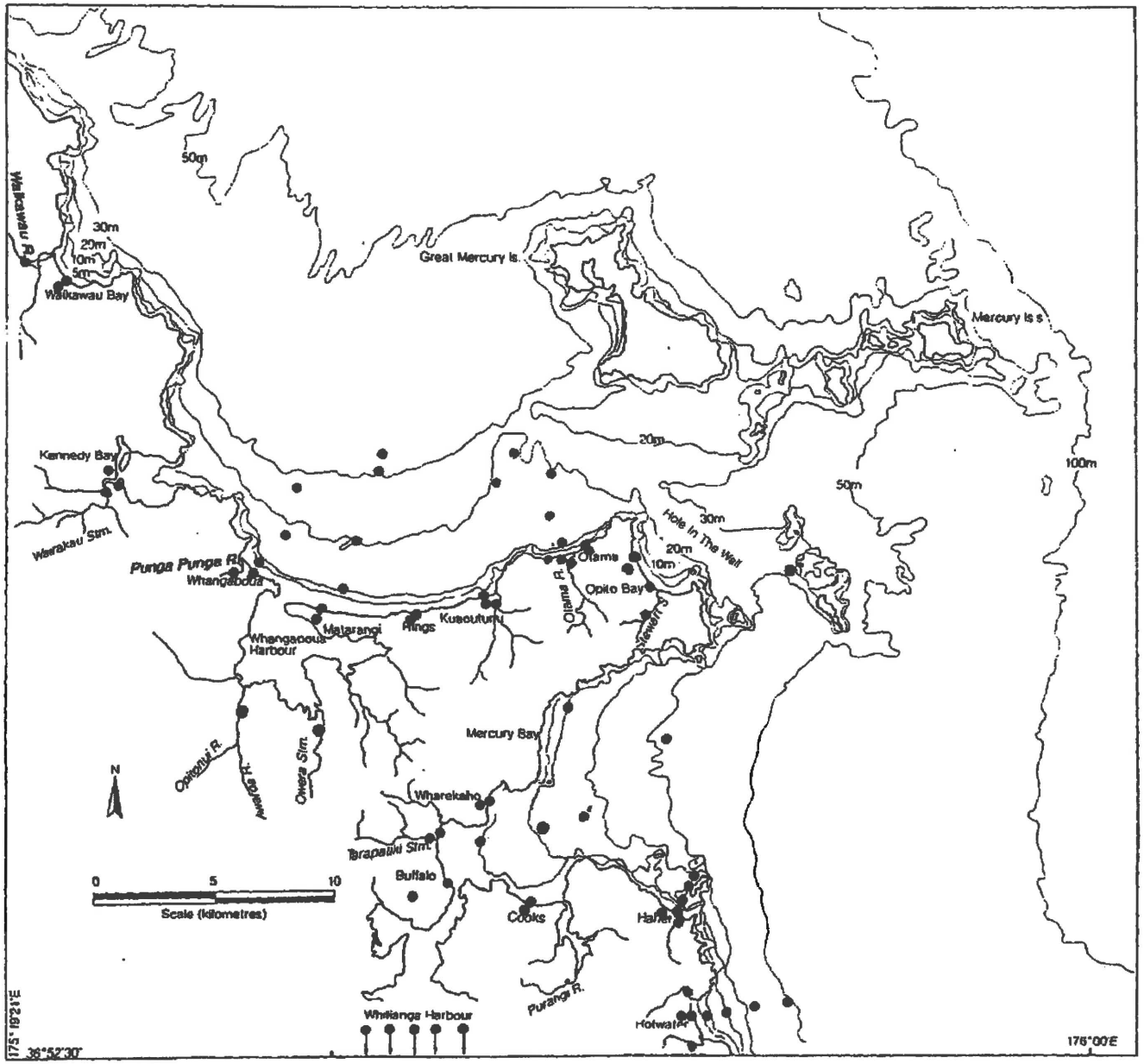

Figure 9.2. Location sites of samples used in the mineralogical analysis on the northern embayed coastline (see Appendix 2 for more detailed sample locations).

may be present). Beach samples were gathered from the high tide swash zone, and dune samples by auger from ~ 1 m below the Holocene or Pleistocene barrier surface. The shelf samples analysed are from water depths of 5 to 50 m, although at Waihi a mid shelf (81 m) and outer shelf (200 m) sample have also been examined.

Standard laboratory methods for sample preparation were used before the analysis (see LEWIS, 1984 for details), with each sample washed, dried, then mechanically split by sieves to retain the 'fine sand' fraction (2 to 4ϕ). This restricted grain size was used in the analysis for several reasons, including:

1. GRIFFITH (1967) has shown that mineral proportions can be strongly dependent on grain size, and hence use of a non-restricted grain size can generate problems in sediment provenance studies.

2. Heavy minerals are most abundant within this 'fine sand' fraction.

3. The 2 to 4 ϕ sand fraction is most representative of east Coromandel shelf deposits, with the mean grain size of ~ 65% of samples occurring within this range, and most coarser samples moderately well sorted and fine skewed, and thus containing a significant proportion of 'fine sands' within their sediment population (see Chapter 5.6.).

It should be noted though that this method may not show the true compositional character of very coarse grained samples. However, examples in which a significant 2 to 4 ϕ split was not obtained were very rare, and generally restricted to coarse grained, very well sorted beach samples (e.g. Whiritoa and Onemana Beach). The 'fine sand' split was also treated with HCL acid to remove the carbonate component from samples so that the clastic compositional character and hence provenance of sediments could be determined (see Chapter 5 and Appendix 3A for details on carbonate concentrations and type).

Fine sand splits were impregnated with araldite resin and prepared as thin sections. When these were initially examined under a standard petrographic microscope, problems were encountered in differentiating quartz from feldspar when twinning was absent in the feldspar grains. In view of the time consuming nature of standard feldspar staining techniques, it was decided to use a cathodoluminescence (CL) microscope to help determine the light mineralogy of selected samples. Details regarding operation of the CL microscope are found in MARSHALL (1988). The CL microscope works by bombarding samples with energetic electrons, which cause different minerals to produce a characteristic visible radiation. Thus, it provides a very quick and accurate means of differentiating various minerals. This technique proved very successful for differentiation of feldspar from quartz. However, one disadvantage of the CL microscope is that the slide cannot be rotated, and so it is not possible to determine extinction angles of minerals. In some cases, particularly in very fine samples, this made the distinction of quartz and volcanic glass hard, and

necessitated use of a standard petrographic microscope for differentiation of these minerals. Another problem is that the slides are often damaged through overheating if they remain stationary for too long, which can limit their subsequent use. Additional preparation of slides for the CL microscope involves polishing their surface with 0.3 micron alpha alumina powder. For each slide, an average of 300 grains was examined and counted. Results of this analysis are listed in Appendix 8A.

Heavy minerals were extracted from the fine sand split with tetrabromoethane and mounted in araldite resin. A standard petrographic microscope was then used to identify the heavy minerals present, with ~ 300 grains being examined and counted from each sample. Details of results from the heavy mineralogical analysis are found in Appendix 8B.

9.2. RESULTS OF MINERALOGICAL ANALYSIS

9.2.1. Characteristics of Major Minerals Identified

As the CL microscope represents a relatively new innovation in petrographic analysis, it is pertinent to briefly describe the characteristic properties of major minerals identified using this equipment. A thorough inventory of the CL properties of various minerals can be found in MARSHALL (1988). Major minerals identified in the east Coromandel study are as follows.

Quartz: The CL intensity of quartz is dull compared to that of many other minerals. Several different colours are often found, ranging from blue, violet, and gray to red and brown. However, it is believed that quartz with blue CL is formed at high temperatures, whereas red-luminescing quartz is of low temperature origin (MARSHALL, 1988). In this study, quartz had a characteristically violet CL (Figure 9.3), which is consistent with a volcanic origin. Quartz grains were always monocrystalline, and occasionally attached to either groundmass or plagioclase fragments. No evidence for low temperature quartz of a sedimentary origin was found in the analysis.

Feldspar: Different feldspars are often observed to have contrasting CL properties, which is useful in quickly differentiating K-feldspar from plagioclase. Feldspars in igneous and metamorphic rocks often exhibit either a yellowish-green CL, due to Mn^{2+}- or Fe^{2+}- activated plagioclase, or a bright blue-luminescing, Ti-activated K-feldspar (MARSHALL, 1988). In this study, a bright yellow CL characteristic of plagioclase was dominantly found (Figures 9.3 and 9.4), with bright blue K-feldspar very rare (usually < 1% of the sample). No attempt was made to distinguish different plagioclase species based on extinction angles. Feldspar grains were always monocrystalline, and occasionally attached to either groundmass or quartz fragments.

Lithic fragments: Weathered lithic fragments were detected by the CL microscope, and generally characterised by either bright blue, bright orange, or non-luminescing grains (Figures 9.3 and 9.4).

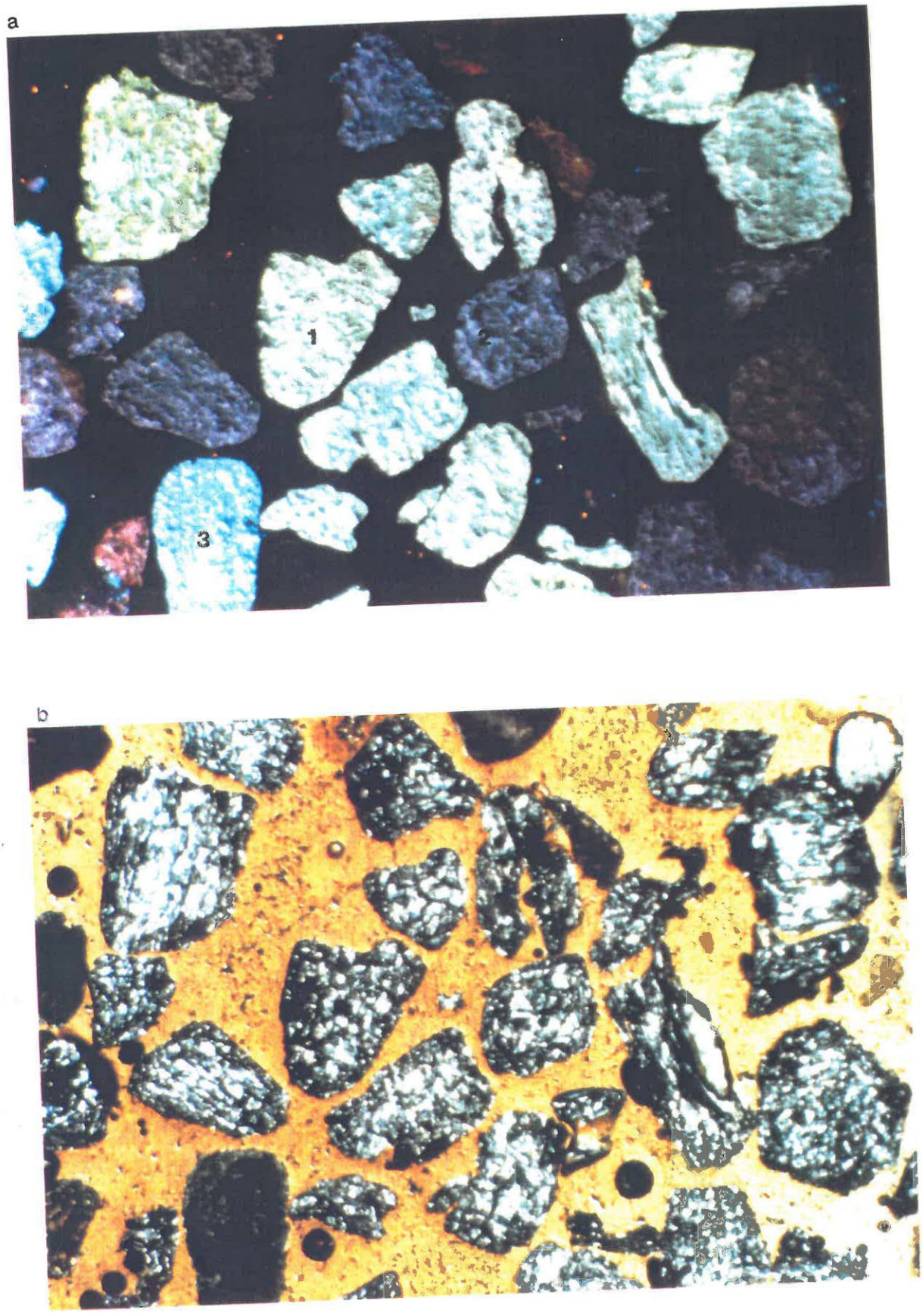

Figure 9.3. a) CL photo-micrograph showing yellow-luminescing plagioclase feldspar (1), dull violet-luminescing volcanic quartz (2), and bright blue-luminescing volcanic rock fragment (3). b) Photo-micrograph of same sample under polarised light. Note the 'cooked' nature of slide due to over exposure to CL microscope.

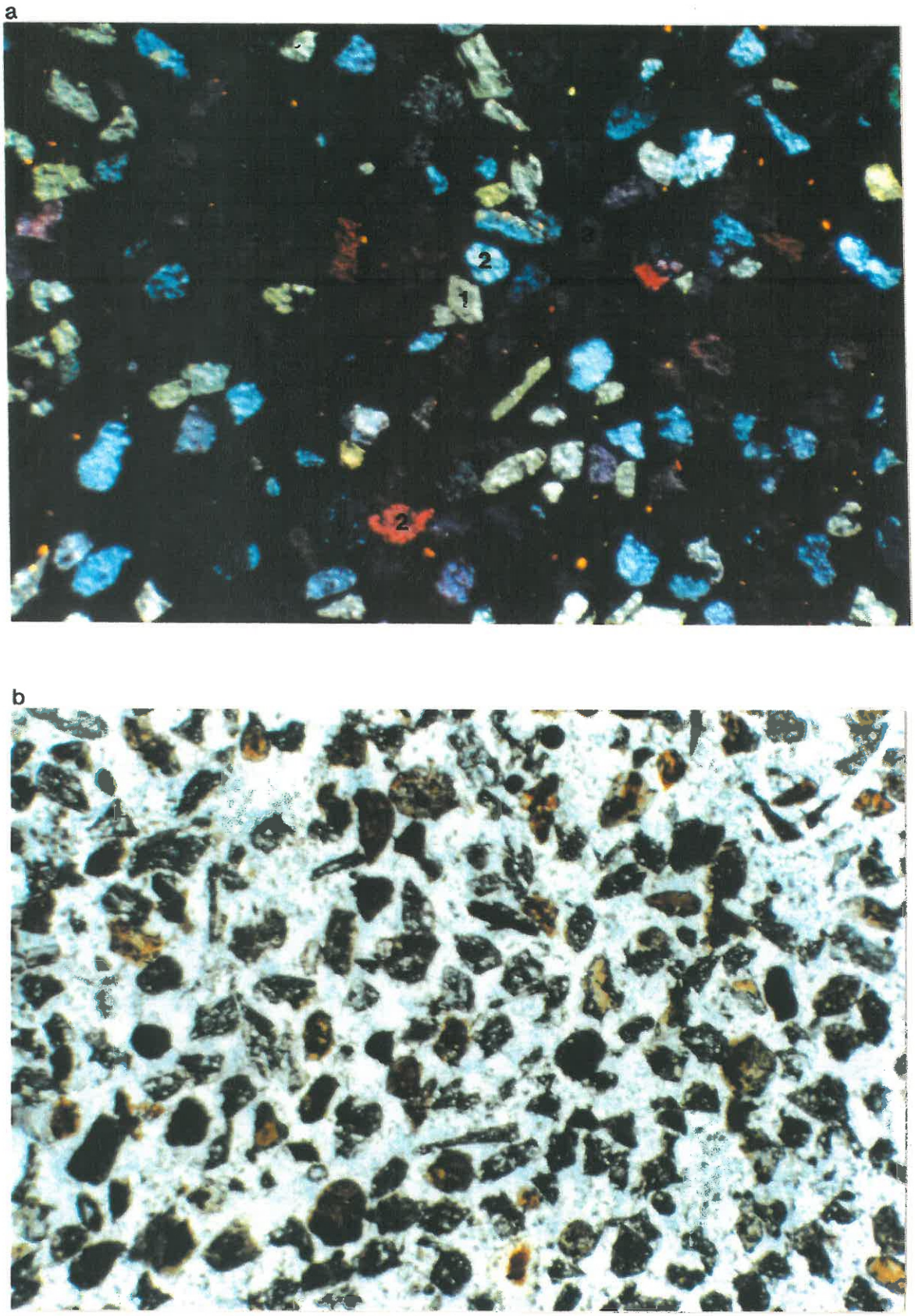

Figure 9.4. a) CL photo-micrograph showing yellow-luminescing plagioclase (1), bright blue- and red-luminescing lithic fragments (2), and dull-luminescing volcanic glass (3). b) Photo-micrograph of the same sample under polarised light.

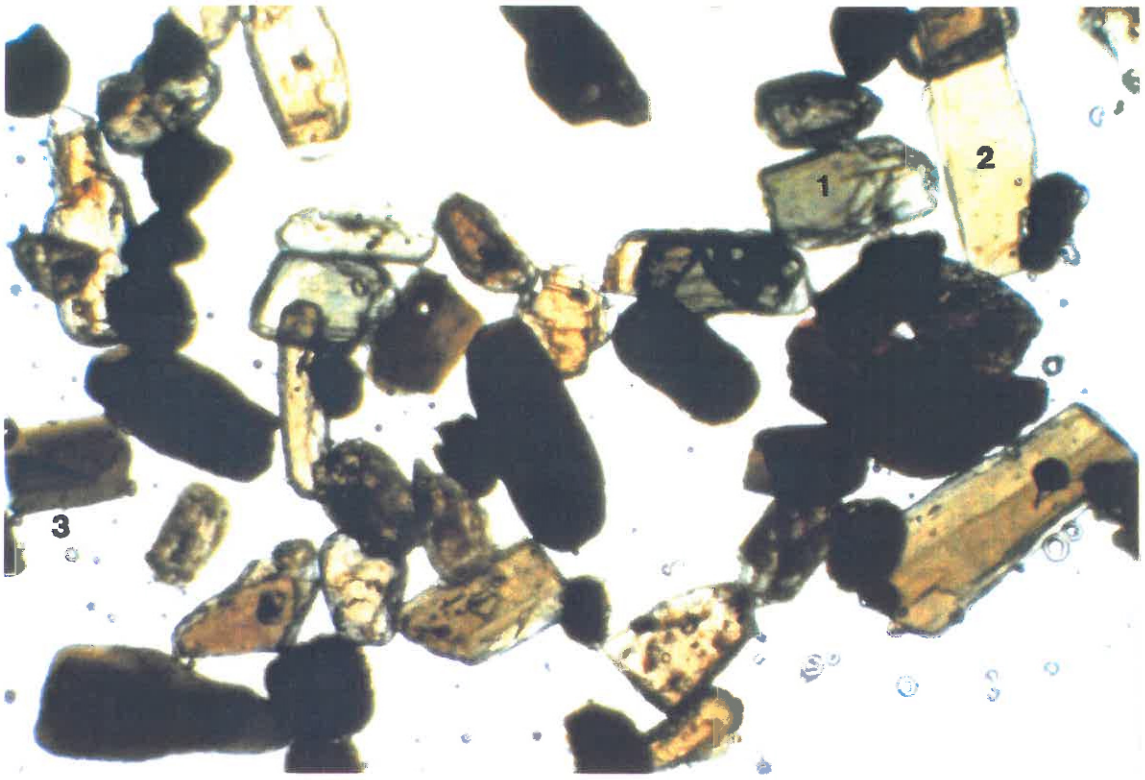

Figure 9.5. Photo-micrograph of a heavy mineral grain mount under polarised light, showing the presence of hypersthene (1), cummingtonite (2), green hornblende (3), and opaques (4).

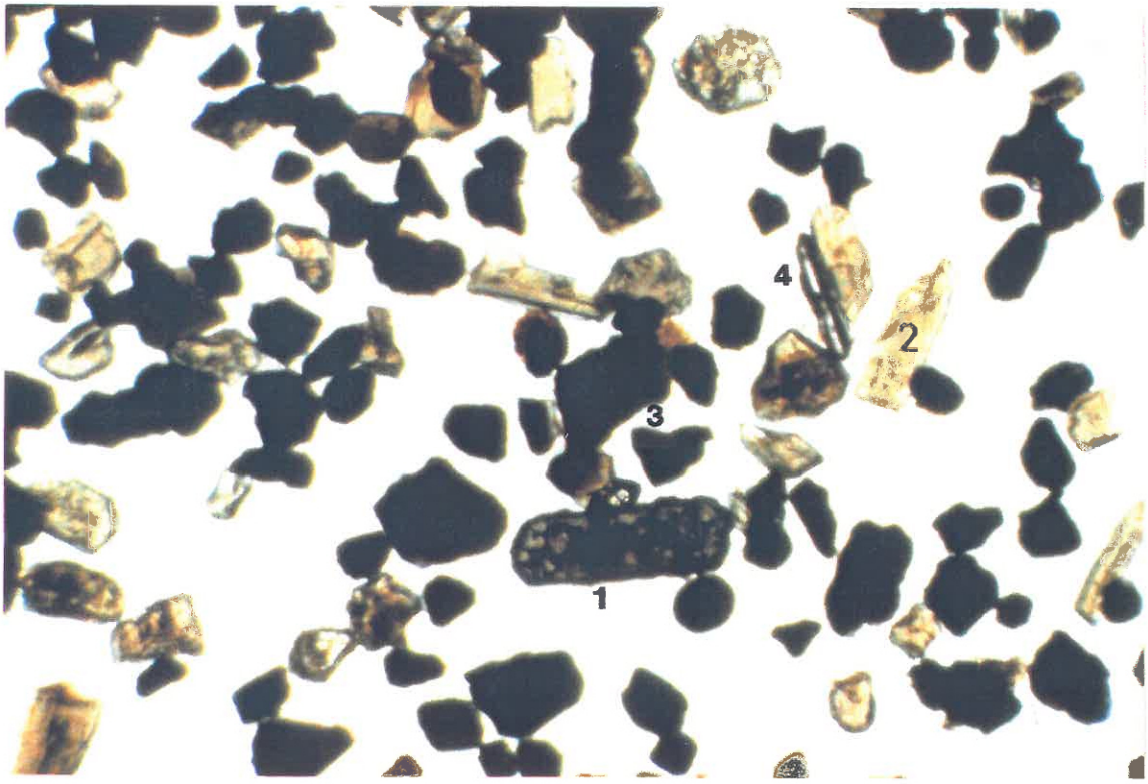

Figure 9.6. Photo-micrograph of heavy mineral grain mount under polarised light, showing hypersthene (1), cummingtonite (2), opaques (3), and zircon (4).

Due to the small size of sand grains examined (2 to 4ϕ), it was not possible to determine the exact lithology each lithic fragment was derived from. However, they are generally poly-crystalline fragments, which appear to have been derived from the groundmass of various volcanic rocks.

Volcanic glass: Fragments of volcanic glass were difficult to detect under the CL microscope, due to their dull-luminescing character (Figure 9.4). However, they could be distinguished under a petrographic microscope by their irregular, jagged (or shard-like) outline, and isotropic character.

Heavy minerals: Various heavy minerals are present in the analysed samples, but are generally indistinguishable under the CL microscope due to their non-luminescing character. One heavy mineral which was detected is zircon, which produces a characteristically bright yellow to white CL. Heavy mineral analysis therefore required use of a standard petrographic microscope. The major heavy minerals identified include: opaques, hypersthene, augite, green and brown hornblendes, cummingtonite, biotite, zircon, apatite and aegerine (Figures 9.5 and 9.6). Optical properties of these minerals are well documented (see HOGG, 1979, ABRAHAMSON, 1987), and thus not presented in this text. No attempt was made to distinguish the various opaque heavy minerals, although ABRAHAMSON (1987) showed these were dominated by titanomagnetite and ilmenite.

9.2.2. Fluvial Sand Mineralogy

The composition of sands from major river systems along the east Coromandel Peninsula are shown in Figures 9.7 and 9.8. The 2 to 4 ϕ composition of river sands varies along the peninsula, with rivers north of Wharekawa Harbour (Opoutere) containing abundant lithics (30 to 85%), while other light minerals are generally less common (quartz 1 to 10%, plagioclase and glass shards 1 to 15% each). South of Wharekawa Harbour, lithics decrease in abundance (10 to 30%), while glass shards and plagioclase are more common (10 to 20% and 15 to 30% respectively).

Heavy minerals vary from 1 to 50% of the bulk mineralogy for river sands. This heavy mineral fraction is dominantly composed of opaques (15 to 75%), and hypersthene (10 to 60%), with no regional variations apparent in the occurrence of either (Figure 9.3). Green and brown hornblendes vary in occurrence, from generally scarce in rivers south of Mercury Bay (0 to 10%), to more common in northern rivers (10 to 30%). Augite ranges between 1% and 28%, with no regional trends in its occurrence. Cummingtonite tends to be more common in rivers south of Wharekawa Harbour (5 to 20%), but is scarce north of here (0 to 12%), and generally only present in catchments associated with the major harbour systems (Cooks, Whitianga, and Whangapoua). Other heavy minerals are generally rare in river deposits, although some significant traces (1 to 2%) of biotite are found in catchments associated with Whitianga Harbour, Whangapoua Harbour, and Kennedy Bay. Zircon and apatite are of similar quantities in these same locations, as well as at Whangamata Harbour, Wharekawa Harbour, and Opito.

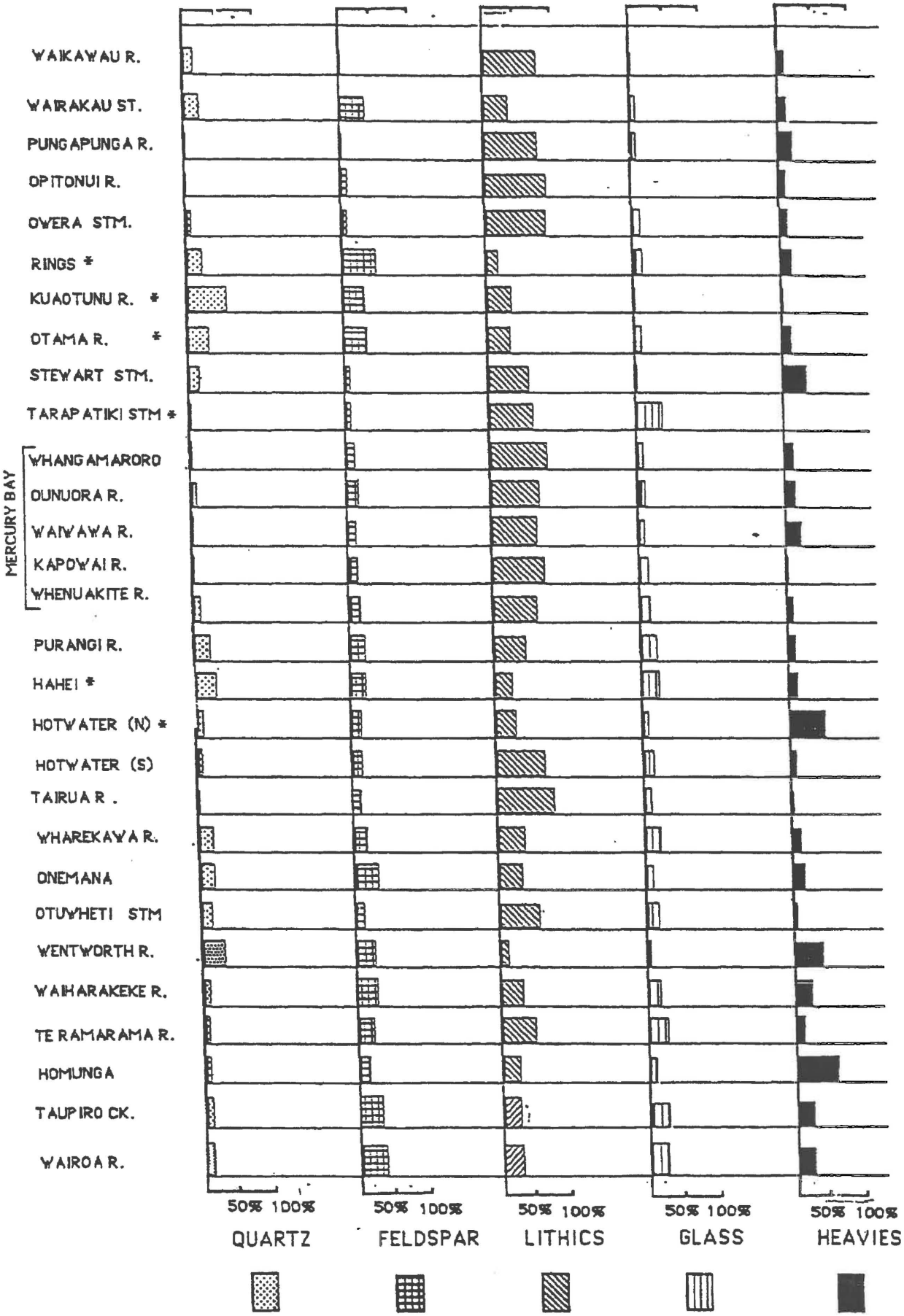

Figure 9.7. Mineralogy of the 2 to 4 ϕ fraction of river sands along the east Coromandel Peninsula (* denotes samples suspected of being contaminated with marine sands; see Appendix 8A for more detailed information on % occurrence of each mineral).

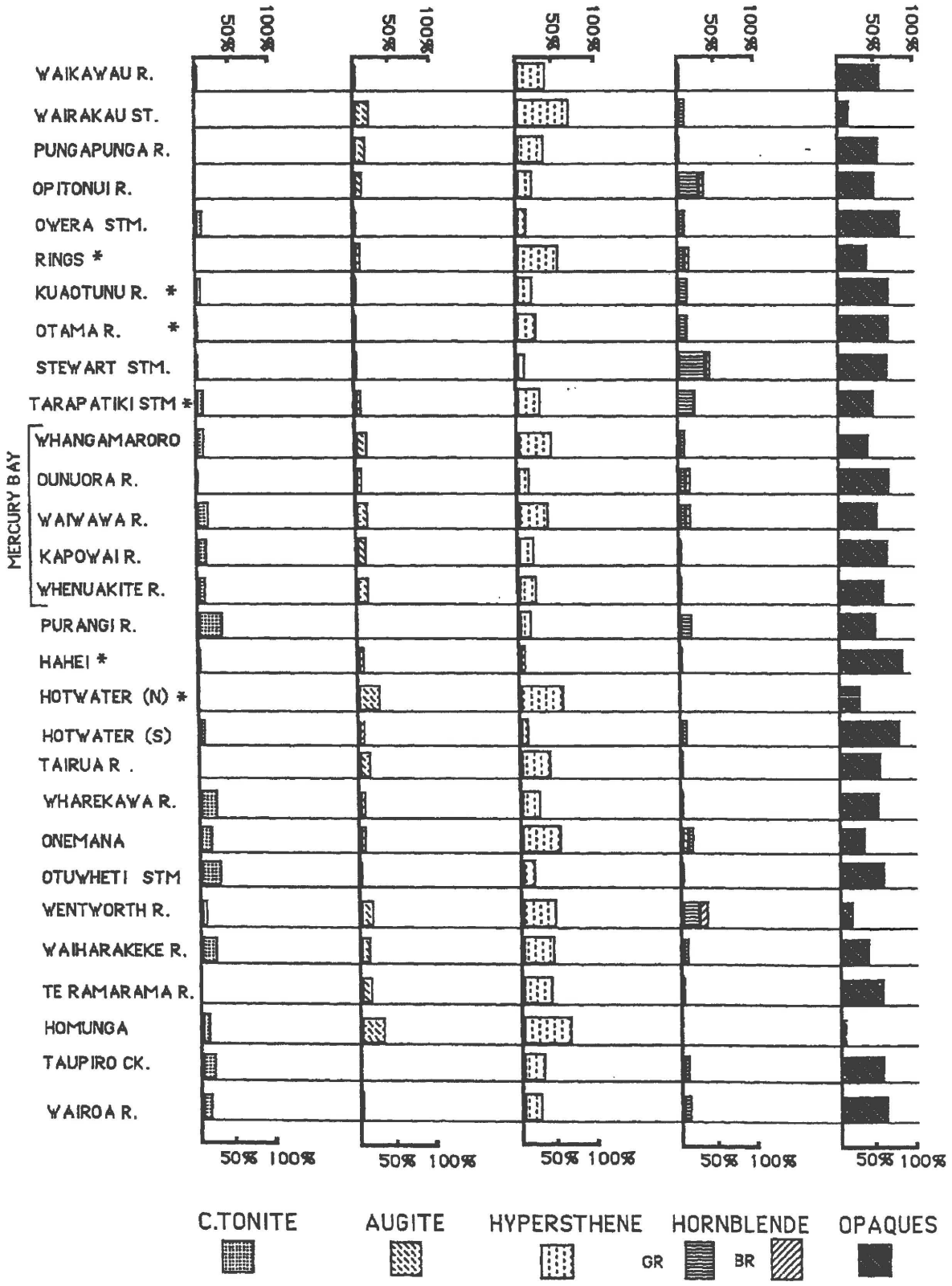

Figure 9.8. Heavy mineral components of the 2 to 4 ϕ fraction of river sands along the east Coromandel Peninsula (* denotes samples suspected of being contaminated with marine sands; see Appendix 8B for more detailed information on the % occurrence of various heavy minerals).

Therefore, river sands are generally characterised by abundant lithic fragments, opaque heavy minerals, and hypersthene. Regional variations in mineralogy patterns includes: south of Wharekawa Harbour more plagioclase, volcanic glass, and cummingtonite; and north of Mercury Bay more lithics, hornblende, and biotite. These variations in river mineralogy are not generally associated with variations in catchment geology along the peninsula. However, they do relate to variations in the extent of late Quaternary tephras mantling Tertiary volcanic rocks. These range in thickness from 2 m near Waihi, to about 0.8 m at Whangapoua, and almost halve in thickness between Whangamata and Whitianga (HOGG and McCRAW, 1983). Therefore, it is possible that late Quaternary ash deposits are a major source of river sediments in catchments south of Wharekawa Harbour. This would account for the relatively high amount of plagioclase, volcanic glass, and cummingtonite found in the southern rivers, as these minerals are all abundant components of the late Quaternary ashes (HOGG, 1979). In areas further north, weathered volcanic rock is probably the primary source of fluvial sands, thus resulting in abundant lithic fragments, and common occurrences of hornblende and biotite. It is only in the largest catchment areas north of Mercury Bay, that ash deposits are weathered in sufficient quantities for cummingtonite to be incorporated into river deposits.

9.2.3. Barrier Mineralogy

The composition of Holocene (and some Pleistocene) barrier deposits along the east Coromandel coast are shown in Figures 9.9 and 9.10. Within the 2 to 4 ϕ sand fraction (Figure 9.10), quartz and glass are of relatively uniform occurrence along the coast, with quartz generally common (10 to 30%), and volcanic glass scarce (1 to 15%). The occurrence of plagioclase in barrier samples shows some noticeable trends, being relatively abundant between Waihi Beach and Pauanui (15 to 60%) and Opito Bay to Whangapoua (40 to 55%), but less common between Tairua and Mercury Bay (10 to 30%) and Kennedy Bay to Waikawau (20 to 25%). Lithic fragments are generally scarce to common in most barrier sands (5 to 20%), with more common occurrences in Mercury Bay (30%),Kennedy Bay (50%), and Waikawau (45%).

Concentrations of heavy minerals in barrier sands are generally scarce at Waihi, Whangamata, Opoutere, Buffalo, and from Opito Bay to Waikawau (1 to 15%), but relatively abundant at Orokawa, Whiritoa, Onemana, and from Pauanui to Wharekaho (30 to 80%). This heavy mineral fraction of barrier sands is dominantly composed of hypersthene (10 to 50%), and opaques (10 to 90%), with no regional trends apparent in either (Figure 9.10). Green and brown hornblendes are common in barrier spit sands from Waihi Beach to Opoutere (30 to 35%), and Buffalo Beach to Waikawau (18 to 38%), but less common (1 to 6%) in most pocket barrier sands (except Onemana and Otama), and in barrier spits at Pauanui and Cooks Beach. Augite is generally scarce (< 10%), with no regional trends apparent. Cummingtonite is scarce in most pocket barrier sands (< 5%; except Onemana), but more common in barrier spits along the coast (5 to 15%; except Buffalo). Other heavy minerals are generally rare in barrier deposits (< 1%), although zircon and apatite occur in more significant traces (1 to 3%) in pocket barriers north of Hahei,

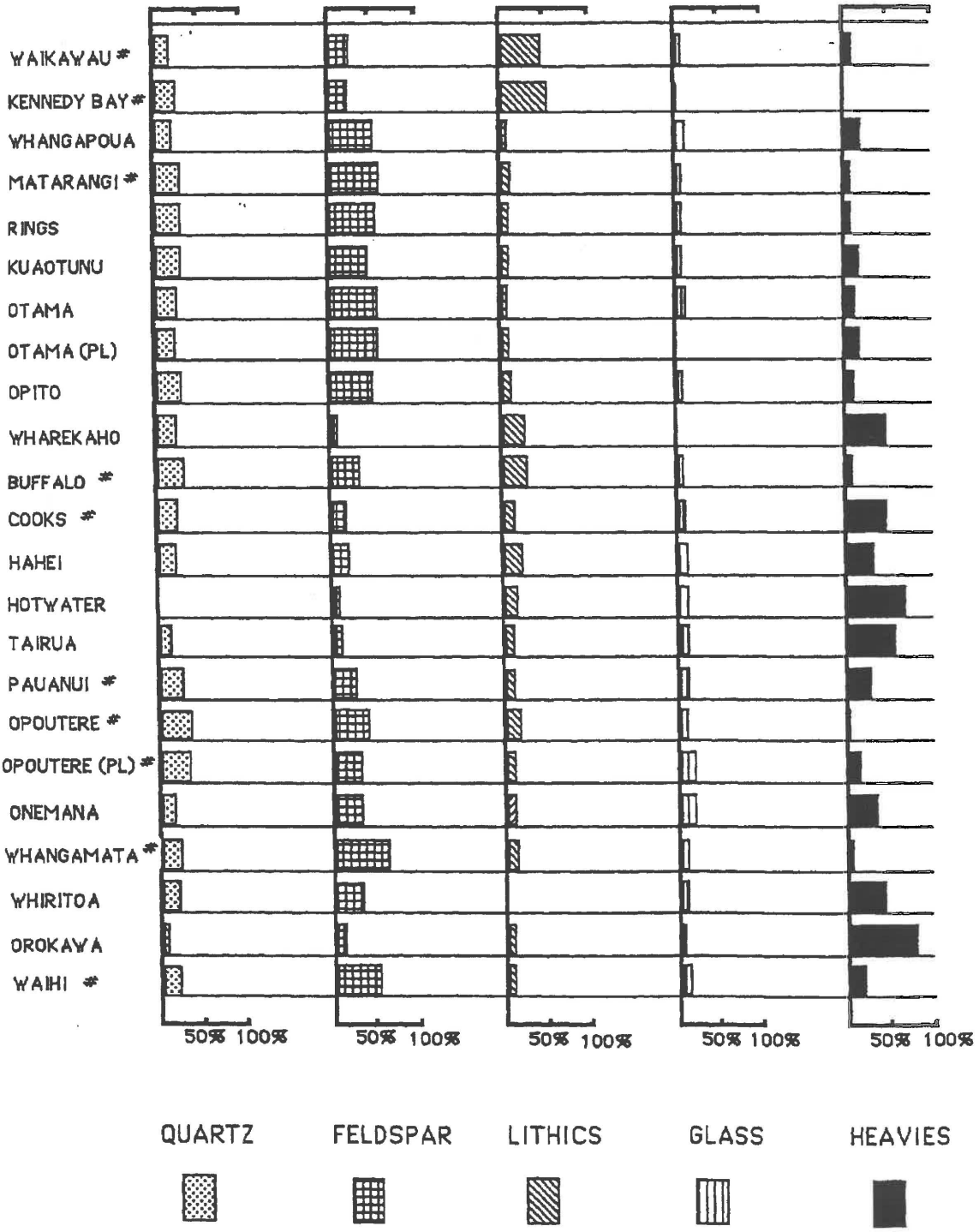

Figure 9.9. Mineralogy of the 2 to 4 ϕ fraction of barrier sands along the east Coromandel Peninsula (# denotes barrier spit system; see Appendix 8A for more detailed information on % occurrence of each mineral).

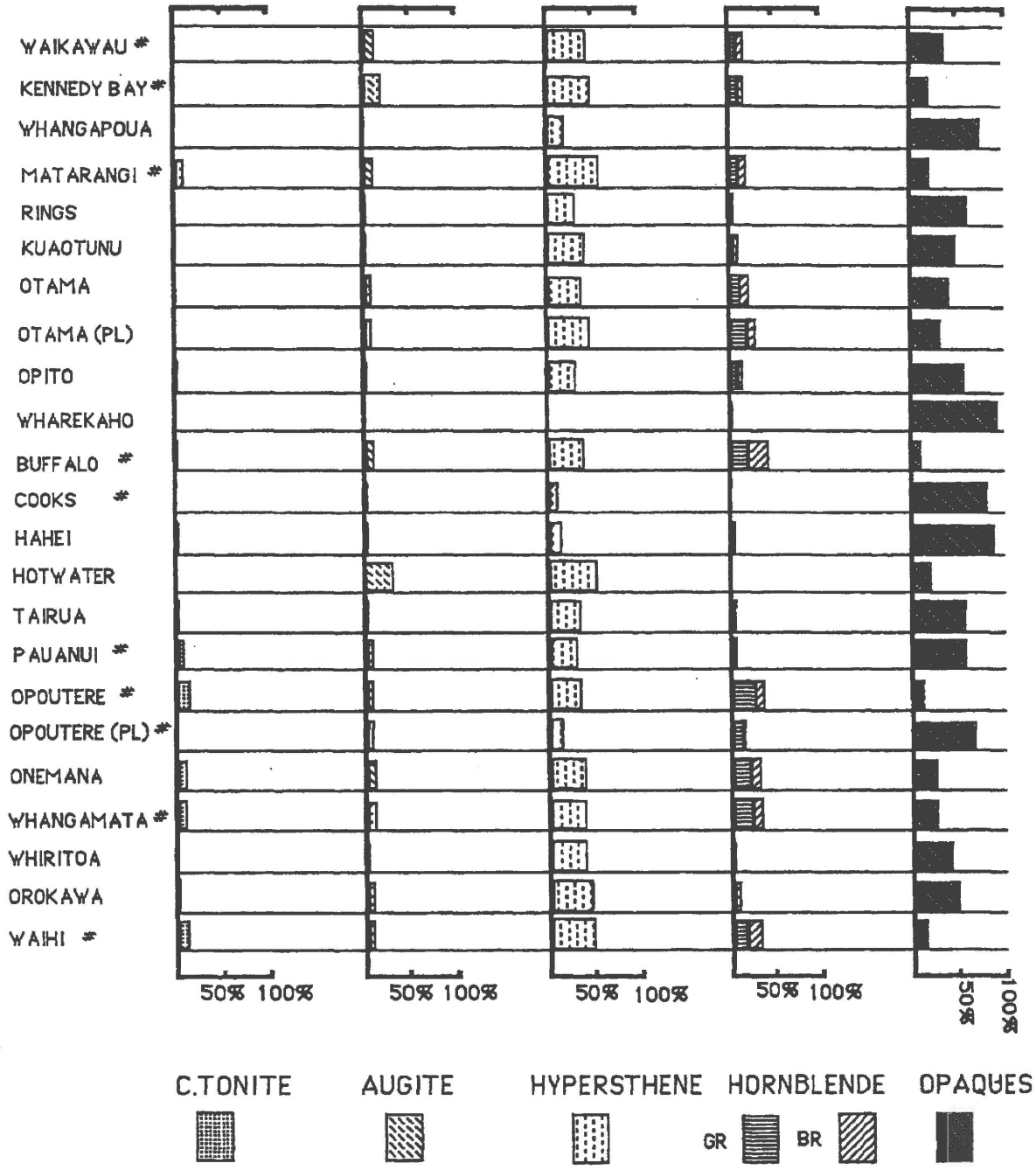

Figure 9.10. Heavy mineral components of the 2 to 4 ϕ fraction of barrier sands along the east Coromandel Peninsula (# denotes barrier spit system; see Appendix 8B for more detailed information on the % occurrence of various heavy minerals).

and in barrier spits sands at Opoutere and Cooks Beach. Biotite also occurs in significant traces in barrier deposits at Buffalo (4.0%) and Kennedy Bay (1.3%).

In comparison to fluvial sands, barrier deposits are generally characterised by more common occurrences of quartz, plagioclase and heavy minerals, and less lithic fragments and volcanic glass. This may indicate that either the barrier sands have not been derived from the local catchments, or that they have undergone greater physical and chemical erosion than the river sands, but are still ultimately derived from these. Observations of the mineral composition for barriers along the coast, and comparison with the river sand mineralogy, allows some broad interpretations to be made regarding their provenance. Significant traces of cummingtonite and hornblende in barrier spit deposits between Waihi Beach and Opoutere indicate a similar provenance for these, with cummingtonite possibly derived from local catchments. Likewise, the occurrence of cummingtonite in barrier sands at Matarangi indicates a possible source from the adjacent catchment area. A local provenance for pocket barrier sands between Opito Bay and Whangapoua is suggested by the consistent occurrences of abundant plagioclase, scarce heavy minerals, common green and brown hornblende, and significant traces of zircon and apatite. The presence of abundant lithic fragments and significant traces of biotite at Buffalo and Kennedy Bay, and abundant lithics at Waikawau, indicates a possible source from their associated catchments. In other locations, the provenance of barrier sands is harder to interpret, due to the dominance of heavy minerals, specifically opaques.

9.2.4. Beach Sand Mineralogy

The composition of beach sands along the east Coromandel coast is shown in Figures 9.11 and 9.12. The 2 to 4 ϕ composition of beach sands tends to vary along the coast (Figure 9.11). Quartz is generally scarce from Waihi Beach to Whiritoa (1 to 15%), and Hotwater to Cooks Beach (3 to 13%), but common from Whangamata to Tairua (25 to 30%), and Buffalo Beach to Waikawau (10 to 33%). Plagioclase follows a similar trend, with abundant concentrations in beach sands between Waihi Beach and Pauanui (40 to 66%; except Whiritoa), and Buffalo Beach to Waikawau (35 to 70%), but is less common from Tairua to Cooks Beach (12 to 27%). The amount of lithic fragments in beach sands shows the reverse trend to quartz and plagioclase, with very common to abundant occurrences from Tairua to Buffalo Beach (35 to 68%), and Kennedy Bay to Waikawau (35 to 45%), but less common between Waihi Beach and Pauanui (0 to 20%), and from Wharekaho to Whangapoua (5 to 25%). Volcanic glass is generally scarce in beach sands (0 to 10%), with some common occurrences found at Cooks Beach (30%) and Opito south (24%).

Heavy minerals are generally a rare to common component of the beach sand mineralogy (0 to 35%) although abundant concentrations occur at Whiritoa (92%; note that this is only the 'fine sand composition, and that previous studies of the bulk mineralogy by CHRISTOPHERSON, 1977, have shown Whiritoa Beach sands to be more quartz- and plagioclase-enriched). This heavy mineral fraction of beach sands is dominated by abundant hypersthene (20 to 73%), with no

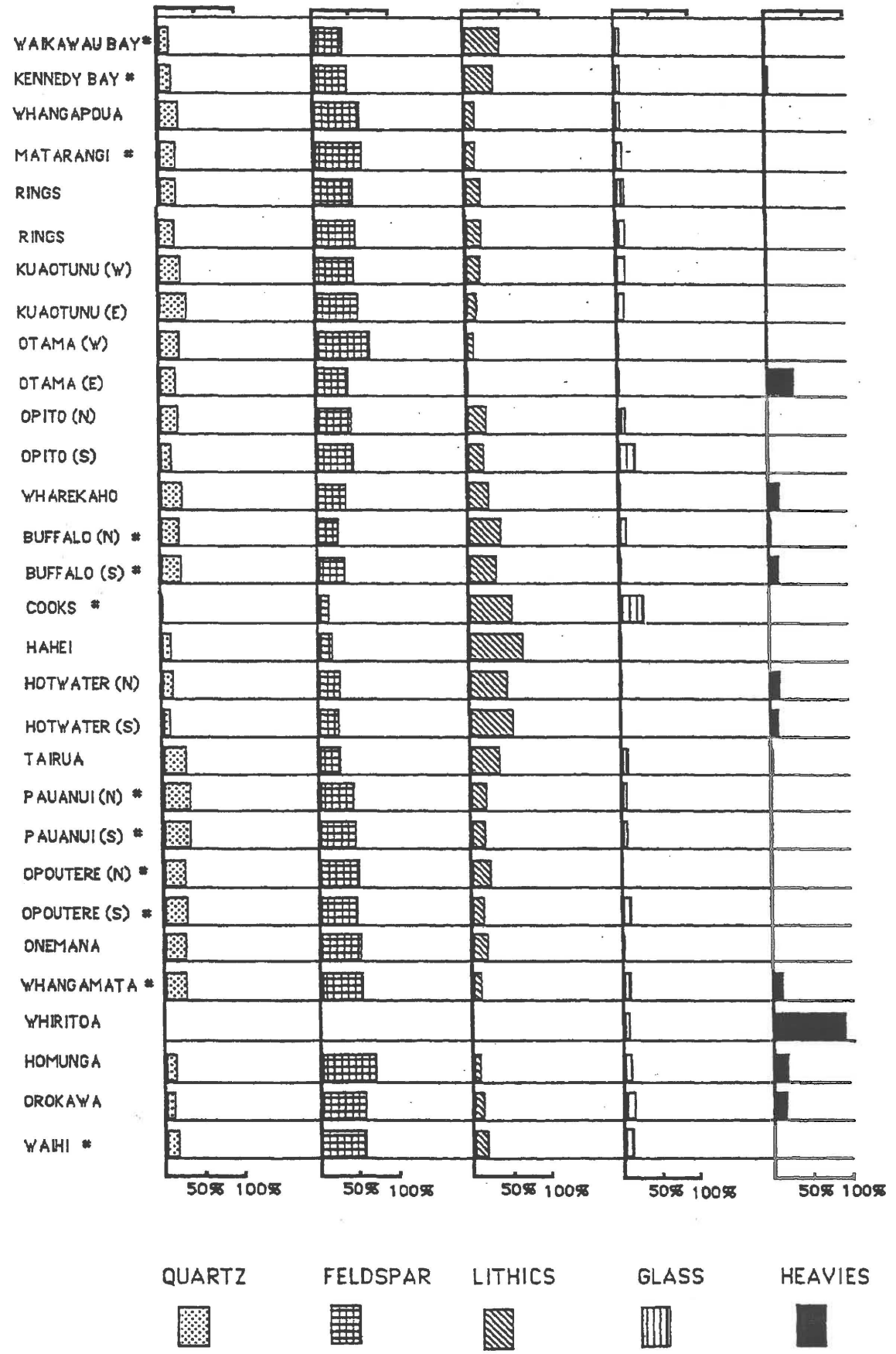

Figure 9.11. Mineralogy of the 2 to 4 ϕ fraction of beach sands along the east Coromandel Peninsula (# denotes barrier spit system; see Appendix 8A for more detailed information on % occurrence of each mineral).

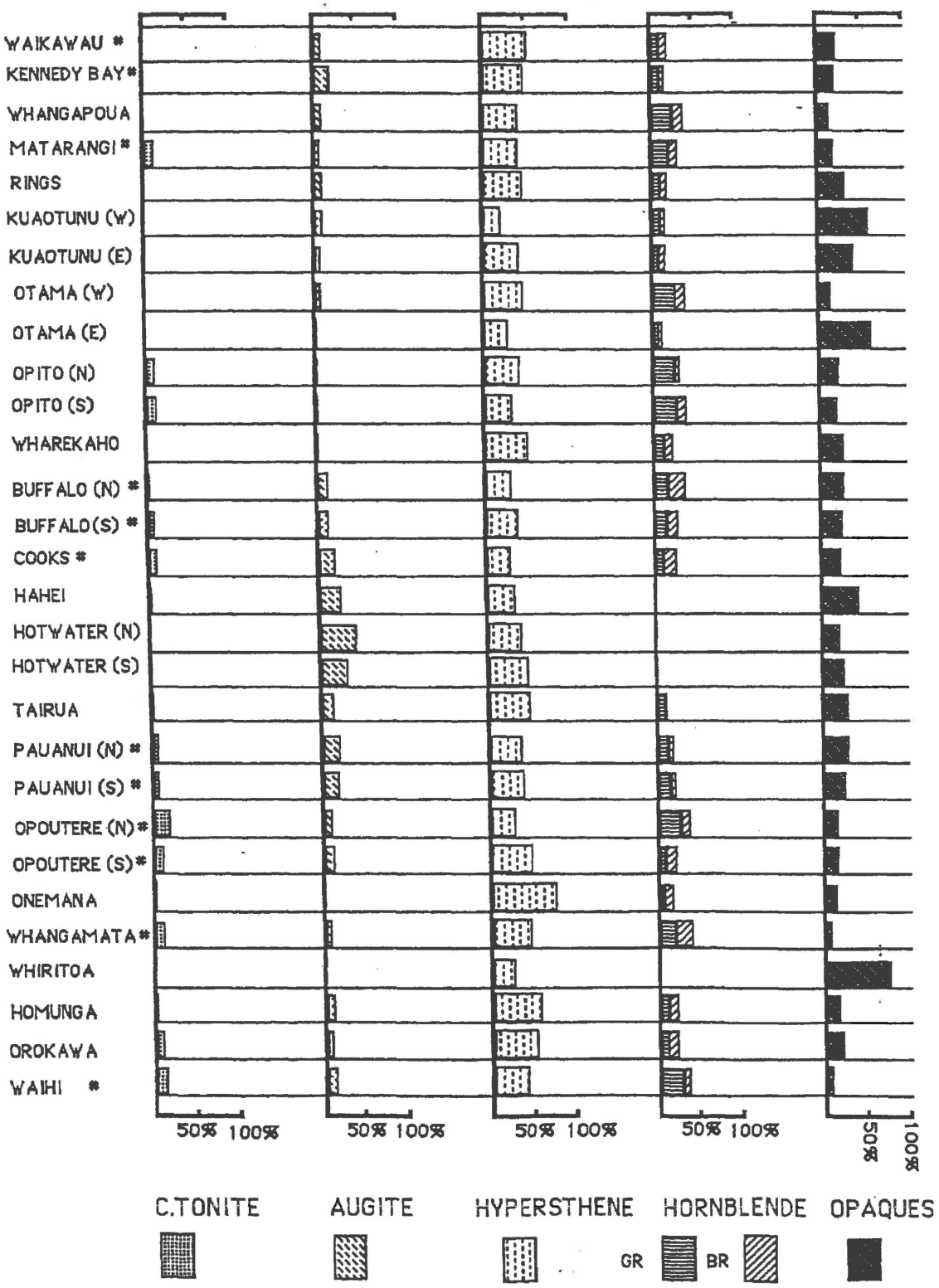

Figure 9.12. Heavy mineral components of the 2 to 4 ϕ fraction of beach sands along the east Coromandel Peninsula (# denotes barrier spit system; see Appendix 8B for more detailed information on the % occurrence of various heavy minerals).

regional trends in its occurrence (Figure 9.12). Opaques are common in most beach sands (5 to 30%), with abundant concentrations (30 to 75%) found in some pocket beaches (Whiritoa, Hahei, Otama, Kuaotunu). Hornblende is common in most beach deposits (10 to 30%), but is generally rare (< 1%) between Hotwater Beach and Hahei. Augite shows a similar trend to lithic fragments, with only scarce quantities (1 to 10%) generally occurring, but common occurrences (10 to 42%) in sands from Pauanui to Cooks Beach. Cummingtonite is generally scarce in pocket beach deposits (< 5%; except Orokawa and Opito), but common in most barrier spit beaches (5 to 20%; except Kennedy Bay and Waikawau). Other heavy minerals generally occur in trace quantities (<1%), although biotite is significant (1 to 5%) in beach sands from most areas north of Cooks Beach (except Otama, Rings and Waikawau).

Therefore, the composition of beach sands shows some important trends along the east Coromandel coast. These generally vary from: plagioclase-enriched sands from Waihi Beach to Homunga; heavy mineral-enriched (in the 'fine sand' fraction) at Whiritoa (and from ABRAHAMSON, 1987, at Wharekaho north); plagioclase- and quartz-enriched from Whangamata to Pauanui, and Opito to Whangapoua; and lithic-enriched from Tairua to Buffalo Beach, and Kennedy Bay to Waikawau. This may indicate different provenances for these beach deposits, with lithic-enriched sands possibly derived from local river systems. Alternatively, lithic-enriched beach deposits between Tairua and Cooks Beach may be influenced by the hydrothermal alteration of plagioclase to clay, as noted in rhyolite outcrops from this region by SCHOFIELD (1970). Heavy minerals are generally only a small component of beach sands, and are dominated by hypersthene. Significant regional trends in the occurrence of other less abundant heavy minerals are apparent. Cummingtonite occurs in most barrier spit beach sands along the coast (except Kennedy Bay and Waikawau), and thus indicates a possible source for these from local catchments. Augite is generally scarce, but more common from Pauanui to Cooks Beach, while hornblende is generally common, but scarce in this same region. This indicates that beach deposits in this region are either derived from a similar augite-enriched and hornblende-depleted source material, or that they have been affected by similar degrees of hydrothermal alteration. Biotite is a small but significant component of beach sands from Cooks Beach to Kennedy Bay (except Otama and Rings), which coincides with the same area where biotite occurs in river sands. Thus, local rivers may supply significant quantities of sediments to these northern beaches.

In comparison to dune mineralogy, beach sands show more noticeable trends in their composition, which may indicate a stronger influence on beach mineralogy from local catchments. Beach sands are characterised by less heavy minerals in their bulk composition, and less opaques, but more cummingtonite, hornblende, and augite. This indicates either different sources for beach and barrier sands, different degrees of post-depositional alteration, or different processes of transport and deposition.

9.2.5. Shelf Sand Mineralogy

The composition of shelf sands off the east Coromandel coast is shown in Figures 9.13 and 9.14. The 2 to 4 ϕ sand mineralogy shows important variations, both along the coast and across the shelf (Figure 9.13). Quartz is generally of moderate concentration (5 to 25%). Plagioclase is common to abundant in shelf sands between Waihi Beach and Tairua (15 to 60%), and from Otama to Whangapoua (20 to 67%), but less common between Hotwater Beach and Mercury Bay (10 to 40%). Lithic fragments are scarce to common in shelf sands from Waihi Beach to Tairua (10 to 25%; except on Waihi mid and outer shelf), and between Otama and Whangapoua (3 to 22%), but are abundant in shelf deposits from Hotwater Beach to Mercury Bay (30 to 60%; except on the Hotwater mid shelf). Volcanic glass varies considerably in concentration. It generally occurs in scarce concentrations (< 10%) in inner shelf deposits between Waihi Beach and Opoutere, and nearshore and inner shelf sands at both Hotwater Beach and from Otama to Whangapoua. Some common occurrences are found in mid shelf deposits from Whiritoa and Whangamata (15 to 20%). However, volcanic glass is very common (20 to 50%) in depths of 6 to 26 m between Waihi Beach and Tairua, in 10 to 32 m water depth at Mercury Bay, and in mid shelf deposits off Hotwater Beach and Whangapoua. Abundant volcanic glass (45 to 80%) only occurs in 6 to 20 m water depth off Mataora and Whiritoa Beaches.

Heavy minerals occur in scarce concentrations for most shelf sands (0 to 10%), but are common to abundant (15 to 70%) in inner shelf deposits off Waihi, Whangamata, and Onemana, and nearshore deposits at Hahei and Otama. This heavy mineral fraction of beach sands is dominated by common to abundant hypersthene (15 to 70%), and opaques (5 to 80%), with no regional trends apparent in either (Figure 9.14). Hornblende is common in most locations (10 to 40%), but scarce in nearshore and inner shelf deposits at Hotwater and Hahei (< 5%). Augite is scarce in most areas (< 5%), but common in nearshore sands at Hotwater and Hahei (15 to 30%). Cummingtonite is scarce in most shelf sands (< 10%), but more common in shelf deposits between Waihi Beach and Whiritoa (10 to 35%). Biotite is generally only present in trace quantities (< 1%), but is more common in: nearshore deposits from Waihi Beach to Tairua (1 to 2%); inner shelf deposits off Whiritoa (1 to 2.6%); Mercury Bay and Hahei shelf sands (2.3 to 3.6%); and Whangapoua mid shelf deposits (2.3 to 2.6%). Zircon and apatite show a similar pattern to biotite, with significant quantities found in: nearshore deposits between Waihi Beach and Tairua (1.0 to 2.3%); Hotwater Beach mid shelf deposits (1.3%); Mercury Bay and Hahei shelf sands (1.0 to 2.3%), and Whangapoua mid shelf sands (2.3 to 2.9%). Aegerine is only a significant component in shelf sands on the mid and outer shelf off Waihi Beach (7.6 to 34.2%).

Overall, the mineralogical nature of shelf deposits is highly variable off the east Coromandel coast. The amount of quartz and heavy minerals in shelf sands is relatively consistent, the latter characterised by abundant hypersthene and opaques. However, areas between Waihi Beach and

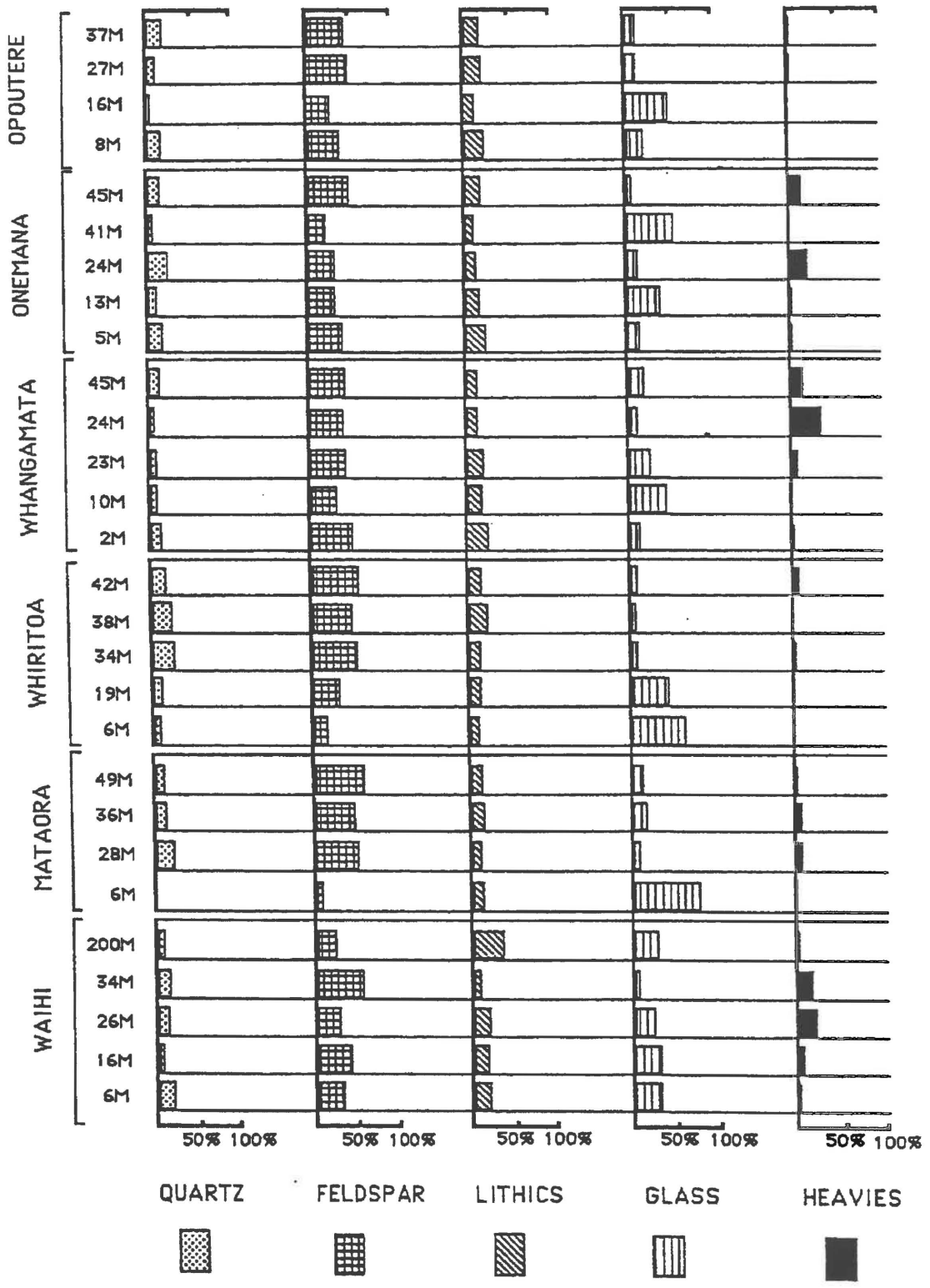

Figure 9.13. Mineralogy of the 2 to 4 ϕ fraction of shelf sands along the east Coromandel Peninsula (see Appendix 8A for more detailed information on % occurrence of each mineral).

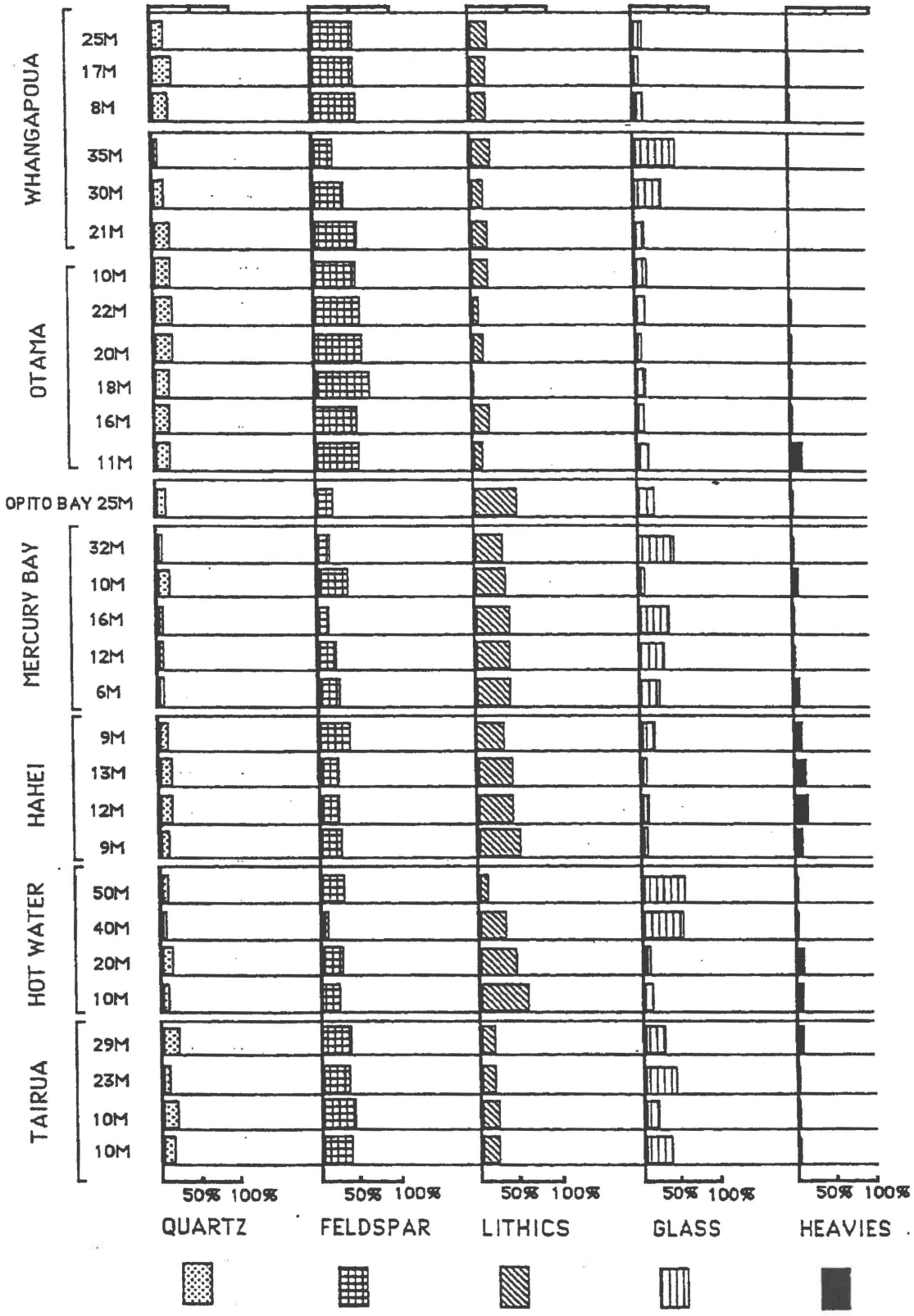
WHANGAPOUA
25M
17M
8M
35M
30M
21M
OTAMA
10M
22M
20M
18M
16M
11M
OPITO BAY 25M
MERCURY BAY
32M
10M
16M
12M
6M
HAHEI
9M
13M
12M
9M
HOT WATER
50M
40M
20M
10M
TAIRUA
29M
23M
10M
10M
50% 100%
QUARTZ
FELDSPAR
LITHICS
GLASS
HEAVIES

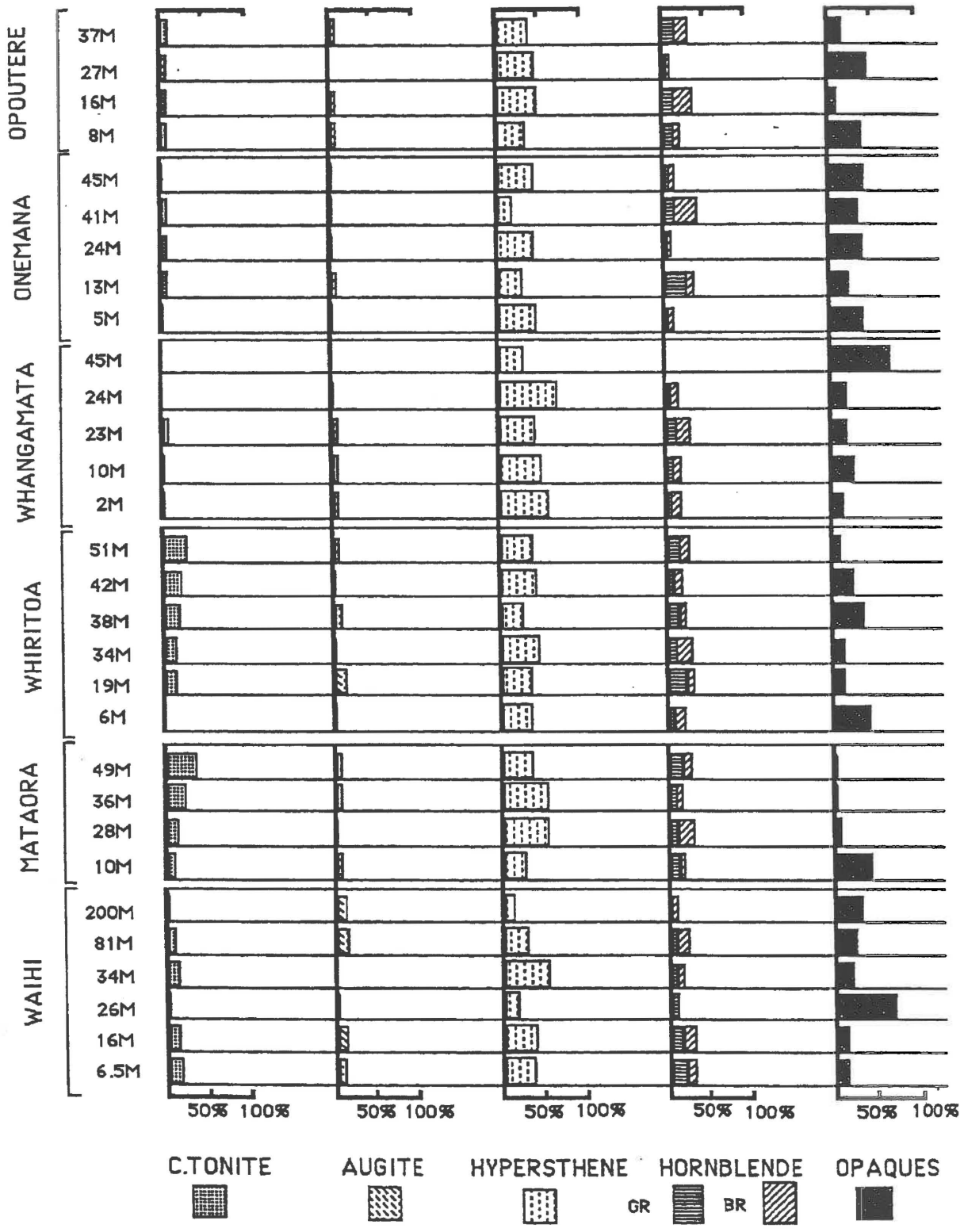
OPOUTERE
37M
27M
16M
8M
ONEMANA
45M
41M
24M
13M
5M
WHANGAMATA
45M
24M
23M
10M
2M
WHIRITOA
51M
42M
38M
34M
19M
6M
MATAORA
49M
36M
28M
10M
WAIHI
200M
81M
34M
26M
16M
6.5M
50% 100%
50% 100%
50% 100%
50% 100%
50% 100%
C.TONITE
AUGITE
HYPERSTHENE
HORNBLENDE
GR
BR
OPAQUES

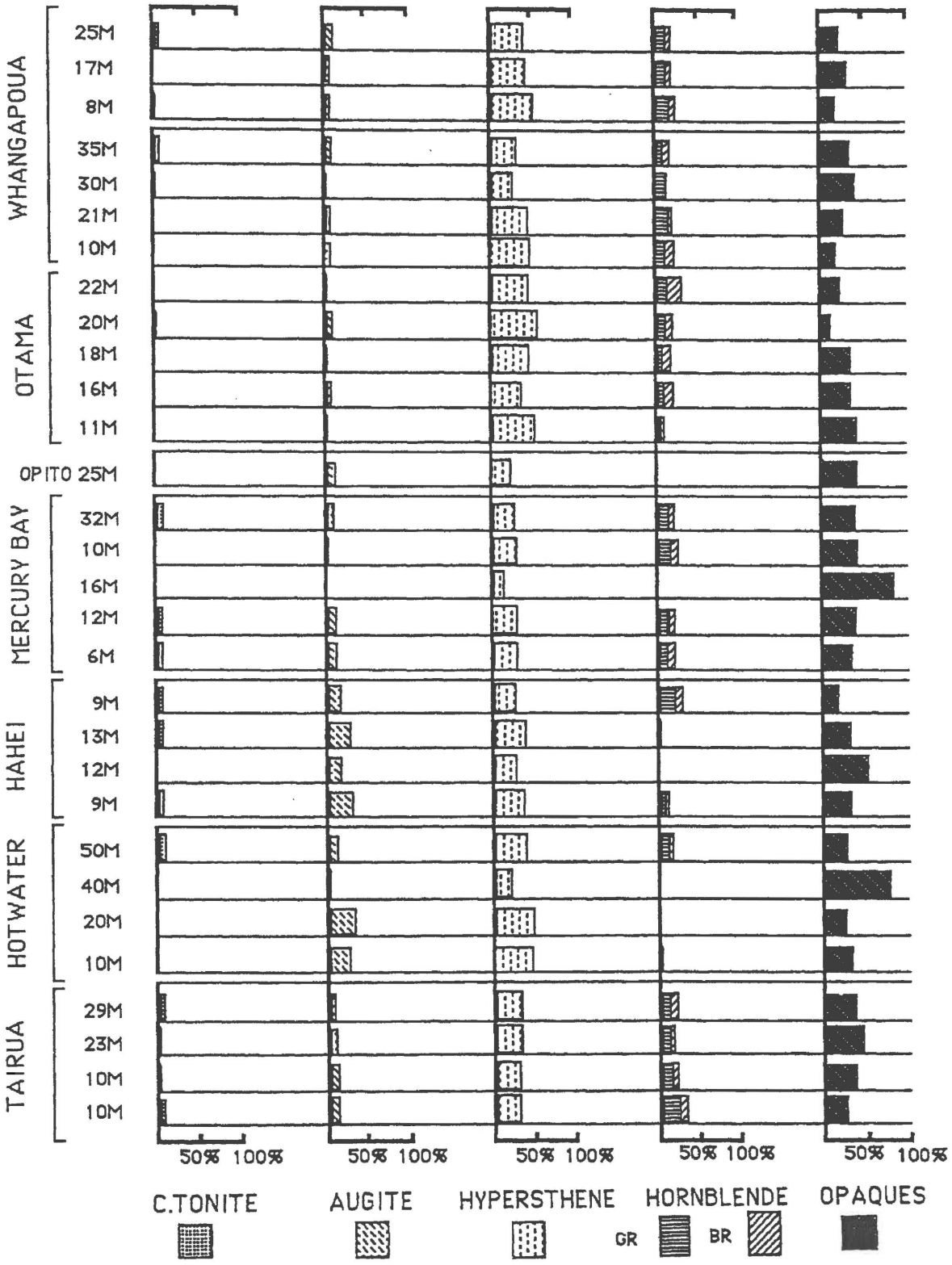

Figure 9.14. Heavy mineral components of the 2 to 4 ϕ fraction of shelf sands along the east Coromandel Peninsula (see Appendix 8B for more detailed information on the % occurrence of various heavy minerals).

Tairua, and from Otama to Whangapoua are characterised by relatively abundant plagioclase, but scarce lithics. In contrast, shelf deposits between Hotwater Beach and Mercury Bay are generally lithic-enriched, but depleted in plagioclase. Shelf sediments at Hotwater Beach and Hahei are also characterised by common augite, but scarce hornblende. This is very similar to trends found in beach sand mineralogy, and may likewise indicate either a lithic- and augite-enriched, and plagioclase- and hornblende-depleted source material, or the hydrothermal alteration of shelf sediments in the Hotwater Beach-Hahei area. The presence of relatively abundant volcanic glass in some shelf samples, as well as small but significant amounts of biotite, zircon and apatite, may indicate a modern terrigenous origin. These deposits include: upper nearshore sands from Waihi Beach to Tairua; Mercury Bay shelf sands; and mid shelf deposits from Whiritoa to Whangamata, Hotwater Beach, and off Whangapoua. The common occurrence of cummingtonite in shelf deposits between Waihi Beach and Whiritoa, but its scarcity north of here, indicates a local cummingtonite-enriched source, possibly from the Bay of Plenty region further south. It also indicates restricted intermixing of shelf deposits north of Whiritoa. The abundant aegerine found in outer shelf deposits off Waihi Beach is consistent with a local source from the adjacent Mayor Island peralkaline tephras.

9.3. CLAY COMPOSITION

The composition of the mud fraction in a limited number of mid shelf deposits (6 in total) was analysed to determine the nature of their clay fraction. Samples were prepared by stirring them in a beaker, then decanting the fine clays from coarser silts. This clay fraction was placed on a glass slide, and allowed to dry at room temperature. The clay composition was then determined by X-ray diffraction (XRD) analysis (for details of XRD technique see: HUME and NELSON, 1982; LOWE and NELSON, 1983). Results from the XRD analysis consistently show diffraction peaks corresponding to the following minerals: calcite; aragonite; halite; feldspar; quartz; halloysite; kaolinite; and illite. The latter three are of most importance to the clay composition, and indicate that the mid shelf muds are of terrestrial origin (as opposed to a marine in-situ origin). Halloysite or illite corresponds to the 10°A peak, and kaolinite or dehydrated halloysite to the 7°A peak. Halloysite is probably the dominant clay mineral at both peaks, being derived from weathering of volcanic lithologies, whereas illite and kaolinite are probably derived from weathering of less extensively exposed Mesozoic basement rocks (NELSON, pers. comm.).

9.4. STATISTICAL CLASSIFICATION OF MINERALOGICAL DATA

As a final part of the sediment composition analysis, statistical grouping of the mineralogical data (for sands) is undertaken, using the same ENTROPY program as was successfully applied to the sediment textural data (see Chapter 5). The statistical grouping was undertaken because the analysis so far has shown some very complex trends in the mineralogical data, which may be simplified and thus easier to interpret if the information is placed into groups of similar

compositional characteristics. This grouping will also assist in the later delineation of various shelf lithofacies along the east Coromandel coast (see Chapter 10.1.).

Compositional data were applied to the ENTROPY program by entering results from both the bulk and heavy mineralogical analysis. Results are shown in Figure 9.15, from which a classification of 10 groups (or entropy classes) explaining 65% of the matrix variability is obtained. Further inspection of the 10 classes indicated strong similarities between four of these, and so 7 major mineralogical classes are used, with one of these broken down into four sub-classes (A to D). Plots of the average values for minerals within each class are illustrated in Figure 9.16. The distribution of various classes in each major environment in the study area (river, barrier, beach, and shelf) is summarised in Table 9.1, and maps of the class distributions along both the southern exposed and northern embayed shelves presented in Figures 9.17 and 9.18 respectively.

9.4.1. Entropy Class Descriptions and Interpretations.

Class 1 (Felsic sands) Entropy Class 1 was originally classified into 4 separate classes. However, these were placed into the one class due to their obvious compositional similarities. All 4 sub-classes are characterised by abundant plagioclase feldspar (mean 42 to 53%), and common quartz (mean 13 to 22%), with only scarce to common amounts of lithics (mean 8 to 25%), volcanic glass (mean 7 to 9%), and heavy minerals (mean 3 to 18%). Hence these are termed 'felsic sands'. The heavy mineral fraction is characterised by relatively abundant hypersthene (mean 35 to 45%) and opaques (mean 11 to 44%), common brown and green hornblendes (mean 14 to 27%), and scarce amounts of augite (mean 4 to 8%).

Sub-class divisions are based on several criteria. In sub-classes 1A and 1D, heavy minerals are relatively scarce, but are more common in 1B and 1C. Sub-class 1D also contains common lithics. Within the heavy mineral fraction, cummingtonite occurs commonly in sub-classes 1A and 1B, but 1A contains more hornblende and less opaques than 1B. Sub-classes 1C and 1D both contain scarce cummingtonite, but 1C is characterised by more opaques and less hornblende than 1D.

Of these four sub-classes, 1A and 1B dominate the inner shelf and beach/barrier deposits south of Opoutere. Sub-classes 1C and 1D dominate beaches from Buffalo to Waikawau, and nearshore deposits between Otama and Whangapoua. However, beach deposits at Whangapoua and Otama, and beach/barrier deposits from Matarangi are characterised by the more cummingtonite-rich sub-class 1A. Class 1C also occurs in several river systems, however only one of these (at Whiritoa) could be considered non-contaminated by marine sands.

Class 2 (Glass-enriched): Entropy class 2 is distinguished by large amounts of volcanic glass (mean 43%), with common plagioclase (mean 31%), and scarce quartz (mean 9%), lithics (mean 15%), and heavy minerals (mean 2%). Hence, these are termed 'glass-enriched sands'. The

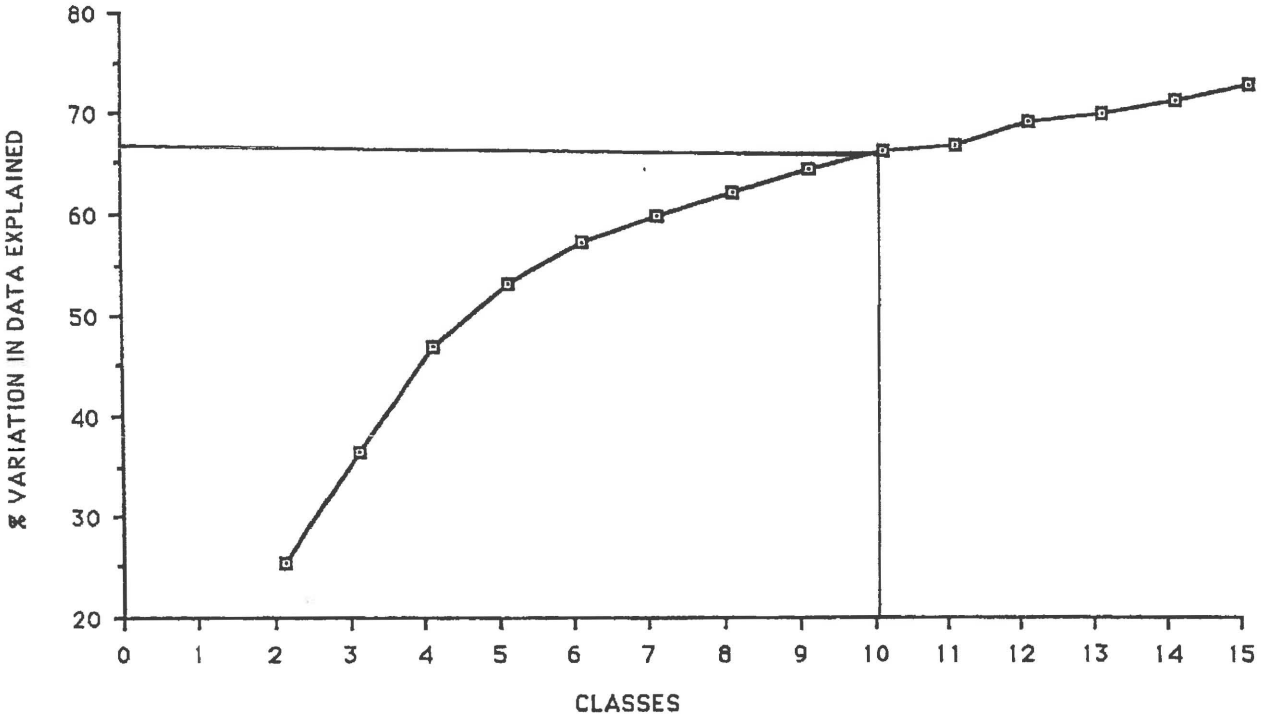

Figure 9.15. Plot showing the number of entropy classes into which the mineralogical data can be classified, and the amount of variation in the data matrix that each classification will explain. From this analysis, a 10 entropy class classification was used, as this is the point on the graph where additional entropy classes do not result in any significant increase in the amount of data variation that is explained.

Table 9.1. Summary of the distribution of entropy classes in different environments along the coast (* denotes river samples suspected of being contaminated by marine sands).

Location	River	Dune	Beach	5 m	10 m	20 m	30 m	40 m	50 m
Waikawau	7	4	1D	—	—	—	—	—	—
Kennedy	7	4	1D	—	—	—	—	—	—
Whangapoua	7	1A	1A	—	1D	1D	—	—	—
Matarangi	7	1A	1A	—	1D	1D	2	—	—
Rings	*1C	1C	1D	—	—	—	—	—	—
Kuaotunu	* 5	1C	1D	—	—	—	—	—	—
Otama	* 8	1C	1D	—	1C	1A	—	—	—
Opito	7	1C	1D	—	—	4	—	—	—
Wharekaho	* 3	5	1D	—	—	—	—	—	—
Buffalo	7	1D	1D	3	3	3	3	—	—
Cooks	7	5	3	—	—	—	—	—	—
Hahei	* 5	5	4	4	4	—	—	—	—
Hotwater	5	6	4	—	4	4	—	3	2
Tairua	7	6	1A	—	2	2	1D	—	—
Pauanui	7	—	1D	—	—	—	—	—	—
Opoutere	7	1A	1A	—	1D	2	1A	1A	—
Onemana	1B	5	1A	1D	2	1C	—	1C	—
Whangamata	7	1A	1A	1D	2	2	1B	5	
Whiritoa	7	1C	6	—	2	2	1A	1B	1A
Homunga	6	—	1A	—	—	—	—	—	—
Orokawa	—	6	1A	—	—	—	—	—	—
Waihi	5	1B	1A	2	—	2	1B	—	—


100%
50%
Felsic (1A)


100%
50%
Felsic (1A)


100%
50%
Felsic (1B)


100%
50%
Felsic (1B)


100%
50%
Felsic (1C)


100%
50%
Felsic (1C)


100%
50%
Felsic (1D)


100%
50%
Felsic (1D)


100%
50%
Glass-enriched (2)

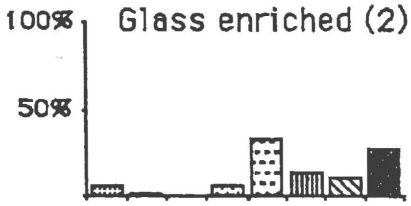
100%
50%
Glass enriched (2)


100%
50%
Lithic&glass enriched (3)


100%
50%
Lithic & glass enriched (3)

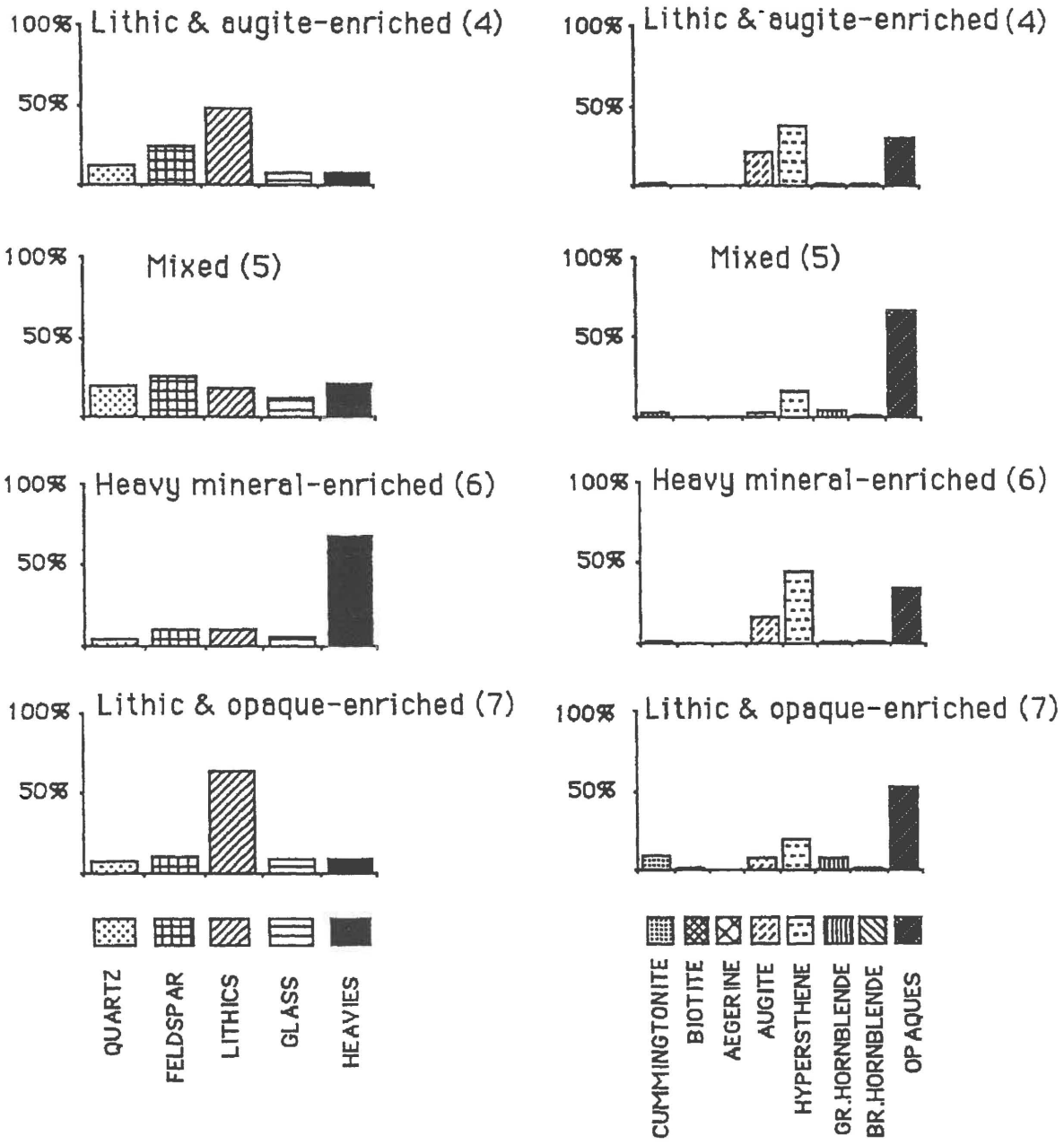

Figure 9.16. Plots of the average occurrence of both light and heavy minerals within each entropy class.

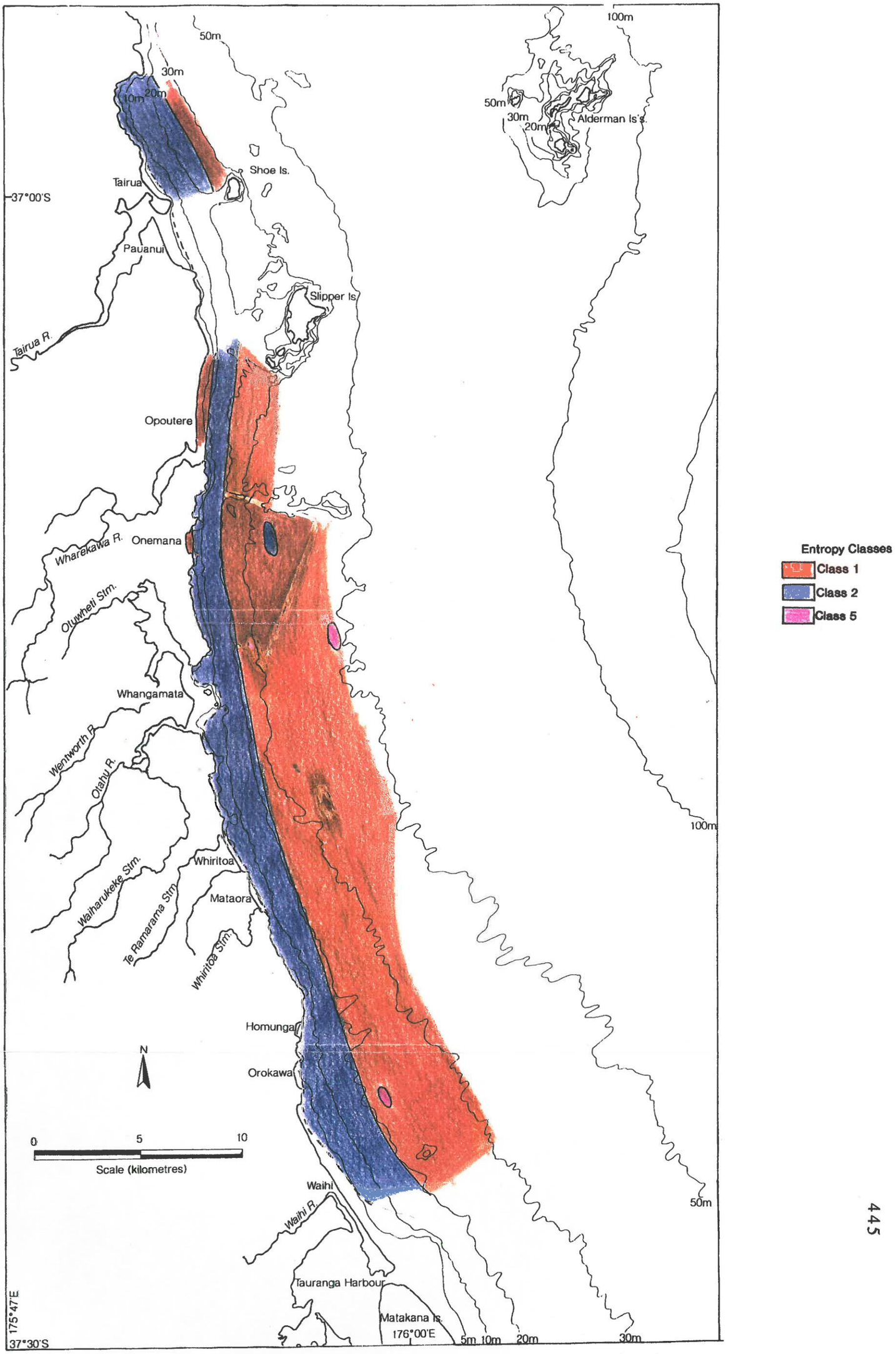

Figure 9.17. Distribution of the 2 to 4 ϕ sand mineralogy entropy classes across the continental shelf (5 to 50 m depth) on the southern exposed coastline.

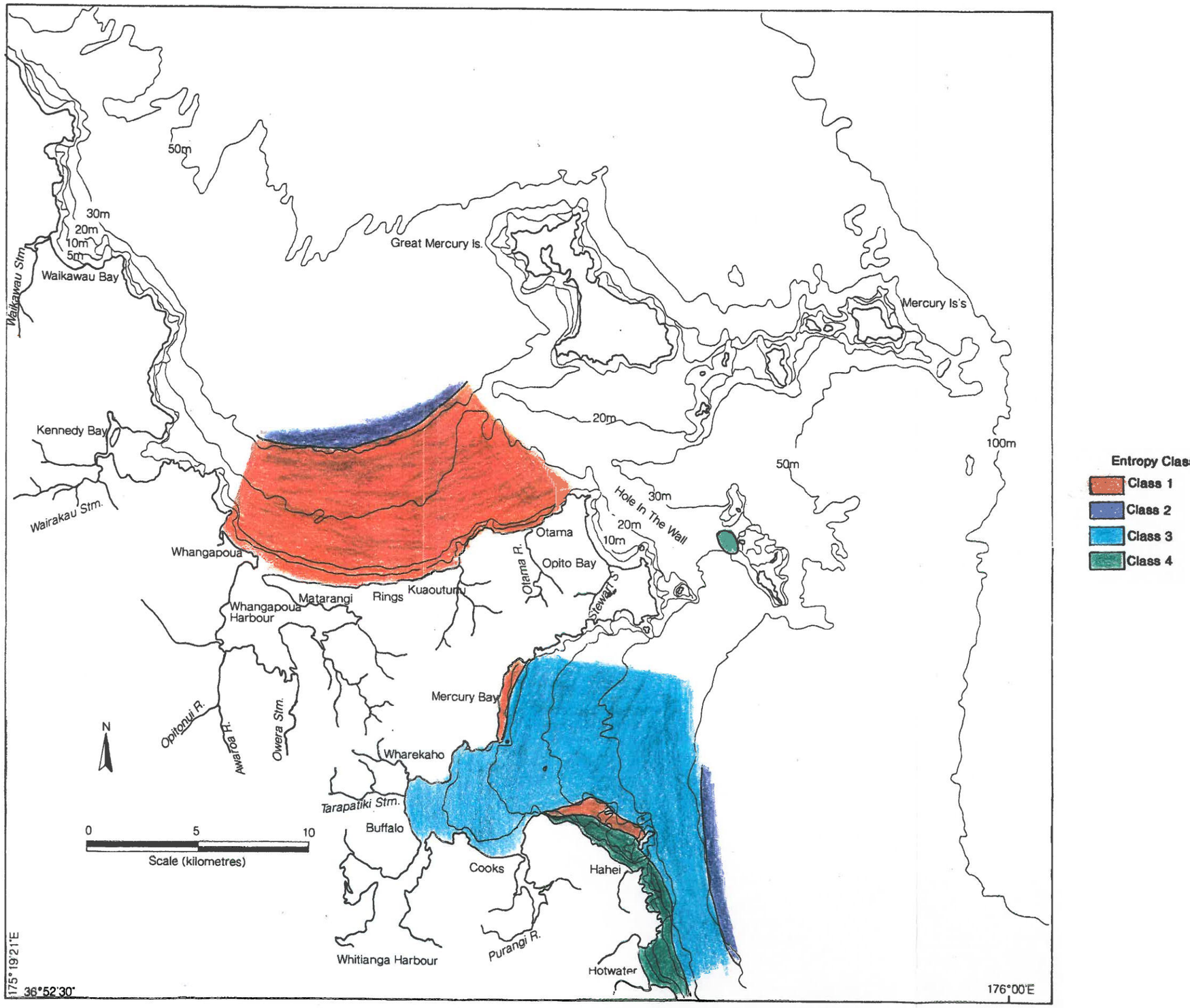

Figure 9.18. Distribution of the 2 to 4 ϕ sand mineralogy entropy classes across the continental shelf (5 to 50 m depth) on the northern embayed coastline.

heavy mineral fraction for this class is very similar to the felsic sands, with common hypersthene (mean33%), green and brown hornblende (mean 23%), and opaques (mean 28%). It also contains scarce amounts of cummingtonite (mean 7%).

The glass-enriched sands are restricted almost exclusively to offshore sands, with only one beach sample at the southern end of Opito Bay. Offshore glass-enriched sands are found extending from Waihi Beach to Tairua in depths of 5 to 25 m, and in a weathered ignimbrite sample from the sea bed at Onemana (41 m depth). They are also found in deeper mid shelf waters at Hotwater Beach (50 m) and Kuaotunu (30 to 35 m).

Class 3 (Lithic- and glass-enriched sands): Entropy class 3 is characterised by common to large amounts of lithic fragments (mean 41%), and volcanic glass (mean 37%), with only scarce quantities of quartz (mean 5%), plagioclase (mean 15%), and heavy minerals (mean 3%). These are termed 'lithic- and glass-enriched sands'. The heavy mineral fraction is dominated by abundant opaques (mean 41%), with other heavy minerals relatively sub-dominant.

Lithic- and glass-enriched sands are mainly found on the nearshore and inner shelf around Mercury Bay, with other locations including Cooks Beach, Hotwater mid shelf (40 m water depth), and on the mid to outer shelf around Mayor Island (this latter area distinguished by abundant aegerine).

Class 4 (Lithic- and augite-enriched sands): Entropy class 4 is characterised by abundant concentrations of lithic fragments (mean 48%), with common plagioclase (mean 23%), and scarce quartz (mean 13%), glass (mean 8%), and heavy minerals (mean 8%). In the heavy mineral fraction, the common occurrence of augite (mean 20%) is a distinguishing feature, as well as hypersthene (mean 38%), and opaques (mean 30%). Hence, these are termed 'lithic- and augite-enriched sands'.

Lithic- and augite-enriched sands are found in beach and nearshore deposits between Hotwater Beach and Hahei, inner shelf deposits off Opito Bay, and in barrier sands at Kennedy Bay and Waikawau. They are also found in river deposits at Hotwater (north) and Kennedy Bay.

Class 5 (Mixed mineralogy sands): Entropy class 5 is characterised by common occurrences of all the bulk minerals (means 15 to 20%). These are termed 'mixed mineralogy sands'. In the heavy mineral fraction, very abundant opaques (mean 68%) is the most prominent feature.

This class is found in shelf deposits at Waihi and Whangamata, in rivers south of Waihi, and in barrier deposits at Onemana, Opoutere (Pleistocene), Pauanui, Hahei, Cooks, Wharekaho, and Kuaotunu.

Class 6 (Heavy mineral-enriched sands): Entropy class 6 is distinguished by very abundant heavy minerals (mean 68%), with all other bulk minerals scarce (< 10%). Hence, these are termed

'heavy mineral-enriched sands'. In the heavy mineral fraction, the only significant occurrences are augite (mean 16%), hypersthene (mean 44%), and opaques (mean 33%).

Heavy mineral-enriched sands occur in beach deposits at Waihi (storm lag deposit), Whiritoa and Otama (Pleistocene), and in dune deposits at Orokawa (Pleistocene), Tairua, and Hotwater.

Class 7 (Lithic- and opaque-enriched sands): Entropy class 7 is characterised by very abundant lithic fragments (mean 65%), with only scarce (means < 10%) quartz, feldspar, volcanic glass, and heavy minerals. In the heavy mineral fraction, abundant opaques (mean 52%) are the dominant feature, with common hypersthene (mean 20%), scarce (means < 10%) cummingtonite, augite, and hornblende. Hence, these are termed 'lithic- and opaque-enriched sands'. These are restricted to river samples which extend north of Whangamata (except those suspected of being contaminated by marine sands, and Hotwater and Kennedy Bay river deposits).

9.5. PROVENANCE FOR EAST COROMANDEL COASTAL AND SHELF SEDIMENTS

The provenance for east Coromandel coastal and shelf sands is difficult to ascertain due to their highly variable composition. Modern river sediments along the eastern peninsula tend to be characterised by abundant lithic fragments, hypersthene, and opaques. As lithic fragments are mainly the weathered groundmass from Tertiary volcanic rocks, they are likely to breakdown fairly rapidly when extensively reworked or subaerially exposed. Thus, the presence of abundant lithic fragments in coastal and shelf sands is a useful indicator of recently derived terrigenous sediments. Volcanic glass and cummingtonite both occur in significant concentrations where river sediments have been derived from the weathering of late Quaternary ash deposits, particularly in catchments south of Wharekawa, and can therefore also be used to indicate a fluvial source for coastal and shelf sediments. Other trace minerals which are inferred to indicate a modern terrigenous sediment source include biotite, and zircon and apatite (the latter two both probably derived from ignimbrite formations; Roger Briggs, pers. comm.).

In general, barrier deposits along the coast are characterised by more quartz and plagioclase, and less volcanic glass and lithic fragments than river sediments. Thus, it is unlikely that local river systems provided a direct source for east Coromandel barriers during their formation. Some indication of the provenance for barrier deposits along different parts of the coast is shown by trends in their composition, with similarities occurring between: Waihi Beach and Pauanui; Tairua and Hahei; Opito and Whangapoua; Kennedy Bay and Waikawau. The ratio of plagioclase feldspar to quartz in coastal sediments has been used by DELL and HEALY (1982) to determine the degree to which local catchment geology influences coastal sand mineralogy. Plots for data obtained from this study in Figure 9.19 show some association between dune F:Q ratios and the local catchment geology, with ratios < 2 associated with Minden Rhyolites and Whitianga Group Volcanics, and ratios > 2 with Beesons Island Andesites. When compared to results from other studies, these data show similar trends in F:Q ratios to DELL and HEALY (1982), SCHOFIELD

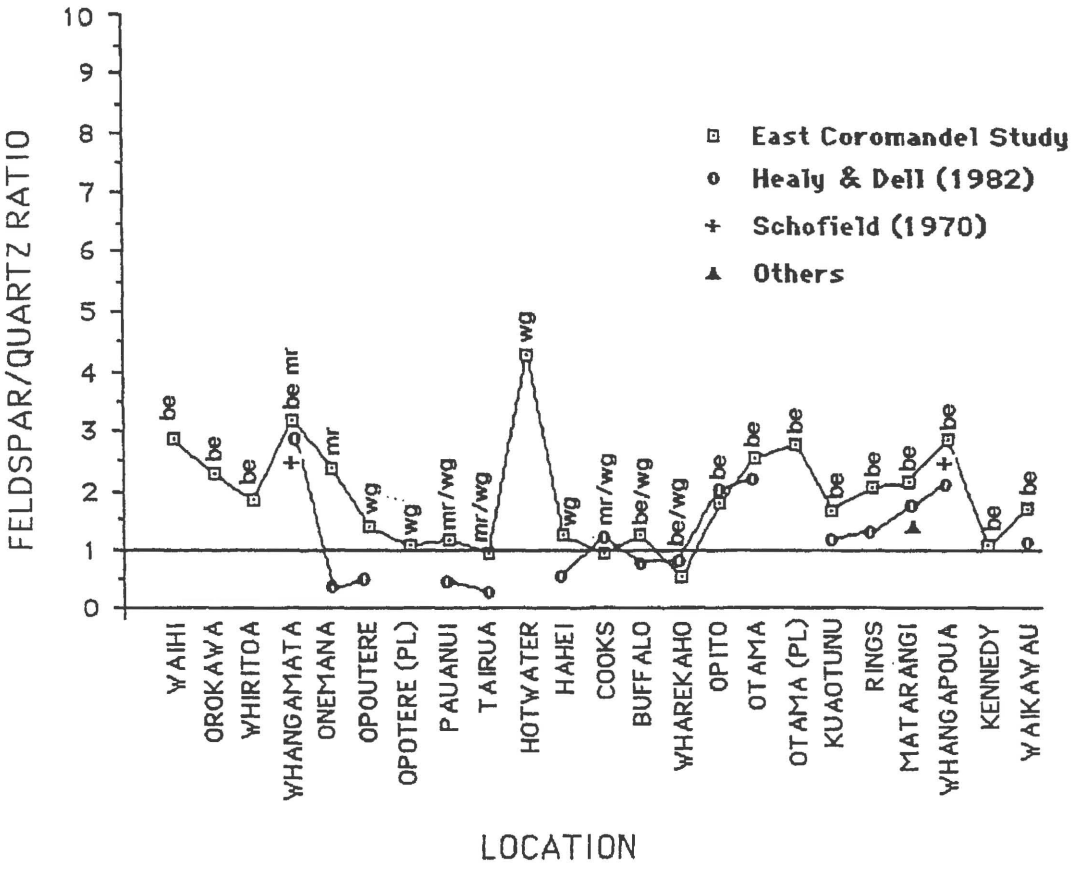

Figure 9.19. F:Q ratios of barrier deposits along the east Coromandel coast. Note how ratios of < 2 are associated with catchments dominated by Minden Rhyolite (mr) and Whitianga Group Volcanics (wg), while higher ratios occur in Beesons Island Andesite (be) dominated catchment areas.

(1970), HARRAY (1978) and MARKS (1975), but different trends to ABRAHAMSON (1987) and CHRISTOPHERSON (1977). Results from this study also show consistently higher ratios than found by other investigators. This is attributed to two factors. Firstly, only SCHOFIELD (1970) used staining to positively identify detrital feldspar, while other workers used bulk XRD, except ABRAHAMSON (1987) who examined standard thinsections. Thus, only SCHOFIELD (1970)also used a recognised technique for positive feldspar identification. Secondly, in none of these studies was a restricted size range used. As SCHOFIELD (1970) found lower F:Q ratios in coarser grained sands along the east Coromandel coast, this should be an important factor.

Further examination of the barrier mineralogy provides additional information on their provenance. Barrier spits at Buffalo, Kennedy Bay, and Waikawau contain large quantities of lithics, and traces of biotite. This is inferred to indicate a major source for these barrier systems from their local catchments. Other barrier spits contain significant traces of cummingtonite, which indicates some contribution from their adjacent catchments. Most pocket barrier systems, however, show very few similarities with adjacent river deposits, and are generally characterised by abundant heavy minerals, particularly opaques. This probably indicates that they are derived from an older, more extensively weathered source than the barrier spit systems.

In general, beach deposits are characterised by felsic sands (except between Hotwater and Cooks Beach). These differ slightly in composition from their associated barrier deposits, as they tend to contain less heavy minerals, but more cummingtonite, hornblende, and augite. In many cases, modern beach sands appear to be in part derived from modern terrigenous sources. Most barrier spit beaches (except at Kennedy Bay and Waikawau) contain significant traces of cummingtonite, which is inferred to indicate some contribution from their adjacent river systems. The presence of large amounts of lithics at Buffalo Beach, Kennedy Bay, and Waikawau, probably reflects a large input of fluvial sediments into these beaches, as is inferred for their associated barrier systems. Several pocket beach systems also appear to be characterised by some modern inputs of terrestrial sediments, as shown by the presence of lithic- and augite-enriched sands at Hotwater and Hahei Beach, and traces of biotite in pocket beach sands north of Wharekaho (except Otama and Rings).

F:Q ratios for beach deposits in this study are shown in Figure 9.20. These tend to be higher than those found in barrier sediments, ranging from 1.0 to 5.6. This indicates either a modern terrigenous source for many beach deposits, or large amounts of quartz present in barrier deposits due to the extensive subaerial weathering of other, less stable minerals. There appears to be little association between these ratios and the local catchment geology. However, the local cliff geology shows some association, with ratios of < 2 found in areas where Minden Rhyolite and Whitianga Group Volcanics occur, and ratios > 2 where Beesons Island Andesite dominates. Thus, much of the sands which comprise modern beach deposits are possibly derived from local headland erosion.

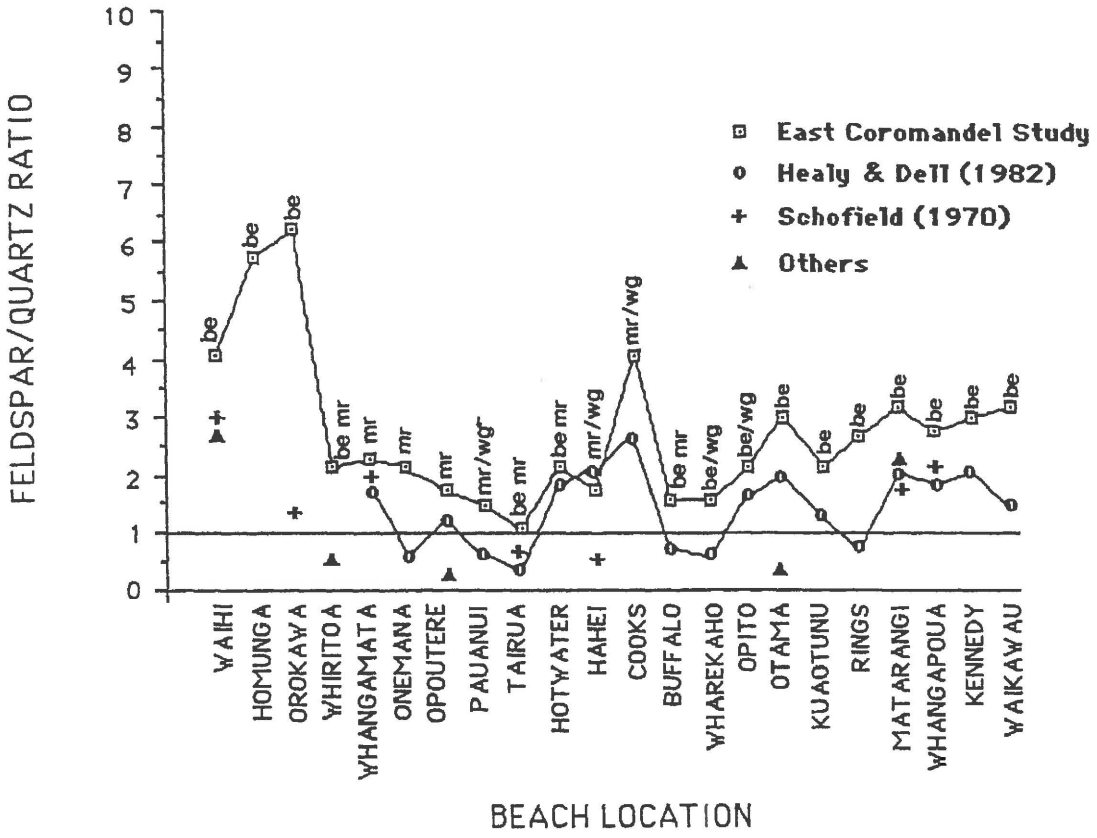

Figure 9.20. F:Q ratios of beach deposits along the east Coromandel coast. Note how ratios of < 2 are associated with headlands dominated by Minden Rhyolite (mr) and Whitianga Group Volcanics (wg), while higher ratios occur in Beesons Island Andesite (be) dominated headlands.

The composition, and hence provenance of shelf sands varies considerably, both across the shelf surface and along the coast. On the southern exposed coast between Waihi Beach and Tairua, felsic sands dominate lower nearshore and inner shelf deposits. The mineralogical similarities between these and adjacent barrier spit systems suggests that the latter were formed by the onshore reworking of these shelf sands, with significant contributions also made from local rivers. Pocket barrier systems from the southern coast are slightly different in composition, containing more heavy minerals than these shelf sands. Thus, they may have been derived by the reworking of older Pleistocene sediments.

Upper nearshore sands in the southern shelf region are characterised by the abundance of volcanic glass. This, along with traces of biotite, zircon, and apatite, is inferred to indicate a modern terrigenous source for these upper nearshore sands. Two possible provenances may exist. Firstly, as mineralogical studies by SHEFFIELD (1991) have shown similar amounts of glass-enriched sands (15 to 47% glass) in the upper and mid reaches of Whangamata Harbour, it is possible that they are derived from the offshore transport of local estuarine sediments. Alternatively, upper nearshore deposits off Mount Manganui Beach, south of the east Coromandel coast, are characterised by very large quantities of glass-enriched sands (65 to 80% glass; DAHM and HEALY, 1980), which may be transported along the shelf by northerly-directed wind-generated currents. Thus, it is possible that glass-enriched upper nearshore sands are derived from either local east Coromandel harbour systems, or from the northward transport of sediments deposited by rivers draining from the Taupo Volcanic Zone into the Bay of Plenty.

Another major area of modern terrigenous shelf sedimentation appears to be present in Mercury Bay on the northern embayed coast, as shown by the presence of abundant lithics and volcanic glass, and traces of biotite in shelf sands. This is consistent with a local source from Whitianga Harbour, which has the largest catchment area of all east Coromandel harbours, and is thus the greatest potential source of modern terrigenous shelf sediments.

The shelf region just south of Mercury Bay, between Hotwater Beach and Hahei, appears to be influenced by a local source for beach and nearshore sediments, as shown by the presence of lithic- and augite-enriched sands. These will be derived from the weathering of two-pyroxene (augite and hypersthene) andesites which dominate the coastline from Tairua to Hahei (Jeremy Adams, pers. comm.). Further offshore across the inner and mid shelf surfaces, terrigenous sediments from Mercury Bay appear to have been deposited, as shown by the increasing abundance of volcanic glass.

North of Mercury Bay off the Kuaotunu Peninsula, nearshore and inner shelf sediments are characterised by felsic sands. These are very similar in composition to the pocket barrier deposits, and so shelf sands in this region may have been the original source for these local pocket barrier systems. However, barrier spit deposits at Matarangi are characterised by significant

traces of cummingtonite, which indicates some contribution from the adjacent catchment area during barrier formation. Mid shelf deposits in this region differ significantly in composition from these shallower shelf deposits, as they contain large amounts of volcanic glass, and traces of biotite. Thus, it is possible these have been derived from reworking of the terrigenous sediments within Mercury Bay. An onshore origin for these mid shelf deposits from Whangapoua Harbour is unlikely, as significant amounts of volcanic glass should be present in nearshore sands off Matarangi if a local provenance was present.

Thus, the provenance of east Coromandel shelf sands is highly variable, and in some parts of the coast uncertain. ABRAHAMSON (1987) proposed that east Coromandel coastal deposits are primarily derived from erosion of local volcanic rocks. Secondary sources were attributed to volcanic sediments derived from the Taupo Volcanic Zone, or erosion of local ash deposits. Results from this study show that these deductions by ABRAHAMSON are quite reasonable for the shelf area between Hotwater Beach and Mercury Bay, with deposits from Whitianga Harbour forming a major source of modern shelf deposits, and a secondary source also produced from erosion of local andesite formations at Hotwater Beach. However, the sources of shelf deposits along the southern coastline between Waihi Beach and Tairua, and nearshore and inner shelf sediments off the Kuaotunu Peninsula, are less definitive.

The mineralogy of some local volcanic rock formations is shown in Table 9.2, based on the work of HAYWARD (1974) from Table Mountain, and FULTON (1988) from Whangamata and Whiritoa.

Table 9.2. Characteristic mineralogy of various east Coromandel volcanic lithologies, based on results of HAYWARD (1974) from Table Top Mountain (Tairua), and FULTON (1988) from Whiritoa and Whangamata.

	HAYWARD (1974)		FULTON (1988)		
	COROMANDEL GR	WHITIANGA GR	ANDESITE	RHYOLITE	DACITE
PLAGIOCLASE	11.8-33.2	2.9-12.3	44-64	1.3-27.6	26-36.4
QUARTZ	0-0.4	0.1-1.4	0	0-18	0-1
ORTHOPYROXENE	1.4-10.4	0-0.8	8.6-1.5	0-0.4	5-8
CLINOPYROXENE	0.2-5.9	0	0	0	0-6.7
AMPHIBOLE	0-2.1	0-0.8	0	0-6.4	0-2.8
BIOTITE	0	0-2	0.2	0.4-12.6	0-2.8
OPAQUES	0.4-1.2	0.3-1.1	11.5-15.0	0-5.6	1.4-9.8
GROUNDMASS	59.6-75.3	72.3-94.3	15.4-26.0	54-80.6	41.8-55.6

More generalised information on the mineral assemblages for various east Coromandel volcanics from SKINNER (1986) is shown in Tables 9.3 and 9.4. Coromandel Group lithologies range in composition from basic andesite to rhyodacite, most being porphyritic, plagioclase phyric, hypersthene dominant pyroxene or pyroxene-hornblende andesites to dacites (Table 9.3; SKINNER, 1986). Rhyolites from the Whitianga Group have a wide range of mineralogical compositions (Table 9.4), plagioclase being the dominant phenocryst type, with pyroxene, pyroxene-hornblende, hornblende, hornblende-biotite, and quartz-biotite associations (SCHOFIELD, 1986). Although plagioclase and hypersthene occur in comparable quantities, quartz would appear to be of too low a concentration in these local volcanic rocks to produce the moderate concentrations found in marine sediments.

The mineralogy of late Quaternary tephras as determined by HOGG (1979) is shown in Table 9.5. These show a more comparable range in quartz concentration than the local volcanic rocks, as well as similar occurrences of plagioclase and hypersthene. Pleistocene inner barrier sands of Last Interglacial age in the study area have a very similar felsic sediment composition to Holocene barriers, and are therefore most probably derived from the same provenance. However, the oldest late Quaternary tephra on the east Coromandel (Rotoehu Ash) has been dated between 50 000 and 55 000 years B.P. (FROGATT and LOWE, 1990), and was thus emplaced after the inner barrier sands. This, and the relatively small volume of tephra deposits on the peninsula, would rule out local ash deposits as a primary source of east Coromandel marine sands.

However, most late Quaternary tephras on the east Coromandel coast are ultimately derived from the Taupo Volcanic Zone. This is an extensive area of Quaternary volcanism to the south of the study area, containing about 6500 km^2 of dominantly rhyolitic material, with only minor amounts of basalt and andesite (CHALLIS, 1978). Phenocryst assemblages of these rhyolites are plagioclase (andesine), hypersthene, titanomagnetite, ilmenite, quartz, hornblende, and biotite. The mineralogy of Taupo Volcanic Zone and associated river deposits was shown by HAMILL and BALLANCE (1985) to comprise major plagioclase, quartz, titanomagnetite, and hypersthene phenocrysts. Comparisons of their data in Table 9.6 with results from this study show a strong association between the mineralogy of Taupo Volcanic Zone rivers and east Coromandel marine sands. Rivers draining into the Bay of Plenty from the Taupo Volcanic Zone have already been proposed as a possible source for volcanic glass-enriched upper nearshore deposits from Waihi Beach to Tairua. Thus, it is also possible that large quantities of quartz-enriched sands are transported northwards from the Bay of Plenty coastline by northerly wind-generated currents, but mainly during lower sea level periods when a large increase in shelf sedimentation for the northern (and probably southern) Bay of Plenty region was inferred to occur in Chapter 8.5.

Alternatively, the larger quantities of quartz in coastal and shelf sands, compared to local river deposits, may result from the gradual breakdown of more unstable mineral components, particularly lithic fragments, as these fluvial sediments experience several phases of subaerial and submarine weathering and erosion.

Table 9.3. Mineral assemblages for Coromandel Group volcanics, as reported by SKINNER (1986).

subgroup	formation	composition
Ōmahine	Tauranikau Andesite	2px ± ol
Kaimai	Pukepenga, Uretara	mixed dacitic and andesitic 2px: hn–hy: px–hn–bi
	Waipupu	andesitic 2px
Kiwitahi	—	2px ± ol: hn
Waiwawa	Tapuaetahi Andesite	2px ± hn
	Taurahuehue Andesite	2px
	Maumaupaki	andesitic-dacitic hy–hn ± bi
Kuaotunu	Cook Intrusives	basic andesitic aug ± hy ± ol
	Huruhi Andesite	hn–hy
	Maunganui Basaltic Andesite	2px ± ol
	Mahinapua Andesite	dacitic hn–hy ± aug ± bi
	Waitaia Sinter	silica
	Rauporoa Basaltic Andesite	2px
	Te Tutu Andesite	2px ± ol
	Parakete	dacitic hn–hy
	Materangi Andesite	dacitic hn ± 2px
	Whangapoua Andesite	2px
	Beesons Island Volcanics	andesitic-dacitic hn–hy ±aug ± bi
	Tuateawa Andesite	2px ± hn
	Te Karaka Andesite	2px
	Kai-iti Porphyrites	andesitic-dacitic intrusives
	Kokumata Dacite	andesitic hn–px: bi–hn
	Omoho Formation	rhyodacite bi ± hy ± hn ± musc
	Port Charles Andesite	hn–2px: 2px
	Paritu Plutonics	2px–hn–bi
	Cuvier Plutonics	2px ± hn ± bi

px = pyroxene; hy = hypersthene; aug = augite; ol = olivine; hn = hornblende; bi = biotite; musc = muscovite.

Table 9.4. Mineral assemblages for Whitianga Group volcanics, as reported by SKINNER (1986).

subgroup	formation	composition
Minden Rhyolite	Ohena Rhyolite	bi-plag ± hn
	Ahu Ahu Rhyolite	bi-hn-san-qu-olig
	Rangihau	hy-plag ± aug
	Ruahine	bi-qu-plag- ± hn
	informal	bi-qu-plag
		hn-hy-plag
		bi-hn-plag
		hn-plag
		bi-san-qu-plag
	Te Weraiti	hn-bi-plag-qu
Coroglen Ignimbrite	Coralie Breccia	plag ± san ± qu ± hn ± aug ± bi
	Te Koru Ignimbrite	qu-olig ± bi
	Whakapenui Ignimbrite	plag-hy-hn ± aug ± qu ± bi
	Hot Water Beach Ignimbrite	plag
	Wharepapa Ignimbrite	plag-hy-lithic ± aug ± bi
	"Owharoite"	plag-qu-hy-bi
	"Tridymite rhyolite"	plag-hy ± qu ± bi

plag = plagioclase; olig = oligoclase; san = sanidine; bi = biotite; hn = hornblende; hy = hypersthene; aug = augite; qu = quartz

Table 9.5. Mineralogy of late Quaternary tephras along the Coromandel Peninsula, as reported by HOGG (1979).

	CLASS1	CLASS2	CLASS3	CLASS4
PLAGIOCLASE	18-37	20-25	14-15	14-16
ANORTHOCLASE	0	0	7-9	5-6
QUARTZ	5-21	9	9	9-13
GLASS	34-67	49-65	65-67	64-69
HEAVIES	4-17	6-17	2-3	2
HYPERTHENE	7-14	21-33	32-47	23-49
AUGITE	0	0-2	2-8	0-24
HORNBLENDE	1-7	4-16	8-24	8-34
CUMMINGTONITE	50-72	50-72	25-52	14-32
AEGERINE	0	0	0	7-36

Table 9.6. Comparison between phenocryst mineralogy from Taupo Volcanic Zone and Waikato River deposits, as reported by HAMILL and BALLANCE (1985), and east Coromandel marine sand mineralogy.

	HAMILL & BALLANCE	EAST COROMANDEL
MAJOR MINERALS	PLAGIOCLASE	PLAGIOCLASE
	QUARTZ	QUARTZ
	TITANOMAGNETITE	LITHICS
	HYPERSTHENE	GLASS
		HYPERSTHENE
MINOR	GR.HORNBLENDE	OPAQUES
	K FELDSPAR	GR.HORNBLENDE
	AUGITE	BR.HORNBLENDE
	EPIDOTE	AUGITE
	BIOTITE	CUMMINGTONITE
	ILMENITE	
RARE/ACCESSORIES	ZIRCON	BIOTITE
	APATITE	ZIRCON
	ACTINOLITE	APATITE
	MUSCOVITE	AEGERINE
	HEMATITE	K FELDSPAR
		OLIVINE
		PUMPELLYITE

Thus, two possibilities exist for the ultimate provenance of east Coromandel marine and shelf sands. Firstly, rivers draining extensive coastal plains within the Taupo Volcanic Zone may form the primary source of both felsic and glass-enriched sands, with secondary but important contributions made by local rivers, particularly those associated with barrier spit systems. Alternatively, local rivers may have been the primary source of marine deposits, with differences in composition between modern river and marine sands attributed to the increased weathering and breakdown of unstable minerals through time. It is possible that both scenarios apply to different parts of the east Coromandel coast, the former to the southern exposed coast where late Quaternary sediments extend deep beneath the modern shelf surface south of Whangamata, and the latter in more northern areas, particularly within Mercury Bay, where significant areas of modern terrigenous shelf sedimentation appear to be present.

9.6. CONCLUSIONS

A preliminary assessment of sediment composition (for the 2 to 4ϕ sand fraction) from various environments along the east Coromandel coast (rivers, barriers, beaches, and shelf), allows additional deductions to be made regarding the degree of interaction between these different environments, and the likely provenance of coastal and shelf sediments. These can be summarised as follows:

1. There is some evidence of interactions occurring between beach, surfzone, and nearshore sands in many barrier spit systems (Waihi, Opoutere, Buffalo, Otama, and Matarangi), as well as several pocket beaches (Hotwater, Hahei, Otama), by the tendency for sediment mineralogy to gradually change offshore in these locations. However, a lack of interaction outside of the beach-surfzone system (< 5 m water depth) in southern pocket beaches (Whiritoa, Onemana and Tairua), is indicated by their more sudden offshore changes in mineralogy. Supporting evidence for the latter comes from previous mineralogical studies at Mataora Beach by HEALY (1981; see Chapter 2.4.), in which sudden changes in sediment composition outside of the surfzone were also found.

2. Some modern barrier spit beach deposits (Waihi, Whangamata, Opoutere, Pauanui, and Matarangi) appear to be derived from local catchments, as shown by the presence of cummingtonite in their beach sands and associated catchment areas. A general absence of cummingtonite in adjacent shelf sands (except off Waihi Beach) rules out an offshore source for these modern beach deposits. Other barrier spit systems (Buffalo, Kennedy Bay, and Waikawau) appear to be supplied by relatively large quantities of river sands, as shown by the presence of abundant lithic fragments in their beach deposits, as well as significant traces of biotite in the former two areas.

3. Several modern pocket beach deposits may be derived from the weathering of adjacent headlands. At Hahei and Hotwater Beach, this is shown by the presence of abundant lithics and

significant augite in their beach deposits, which appear to be derived from weathering of local two-pyroxene andesites. Between Opito Bay and Whangapoua Beach, this is shown by the presence of significant traces of biotite in their beach deposits.

4. The presence of cummingtonite in most barrier spit deposits south of Pauanui, and also at Matarangi, indicates that local river systems may have supplied some sediments during barrier formation. However, the compositional similarity of these barrier spit deposits and adjacent lower nearshore-inner shelf fine sands, indicates that the majority of barrier sediments were supplied by the onshore reworking of shelf deposits. The presence of large quantities of lithics and significant traces of biotite at Buffalo, Kennedy Bay, and Waikawau, indicates that in these areas, local rivers may have supplied the majority of sediments during barrier development.

5. The presence of abundant heavy minerals, particularly opaques, in several pocket barrier systems (Onemana, Tairua, Hotwater, Wharekaho), indicates that these are possibly derived from the reworking of older Pleistocene deposits. However, pocket barrier systems along the Kuaotunu Peninsula are of similar felsic composition to adjacent shelf deposits, and so may have been derived from the onshore reworking of Holocene transgressive sands.

6. Similarities in the composition of coarse grained inner shelf, and fine grained lower nearshore-inner shelf sands between Waihi Beach and Tairua, and from Otama to Whangapoua, indicates that these were derived from the same offshore source. In the former area, these deposits may ultimately be derived from the northerly transport of more quartz-enriched Bay of Plenty shelf sediments, particularly during lower sea level events when shelf sedimentation is inferred to increase in the northern Bay of Plenty-Waihi Beach region (see Chapter 8.5.), while deposits from the latter area are probably locally derived from weathering of the Kuaotunu Peninsula. Medium and coarse grained lithic- and augite-enriched shelf sediments at Hotwater and Hahei seem to be presently derived from an onshore two-pyroxene andesite source.

7. The composition of very fine grained shelf sands suggests a modern terrigenous origin, as shown by their large quantities of volcanic glass (which give these deposits their characteristic very angular texture), as well as traces of biotite, zircon, and apatite. These sands appear to be derived from local rivers (Whitianga Harbour) on the northern embayed coastline, and from either local harbours, or the northerly transport of Bay of Plenty shelf sediments on the southern exposed coastline.

CHAPTER TEN

CONCEPTUAL MODELS FOR SHELF SEDIMENTATION AND EVOLUTION

10.0. INTRODUCTION.

In preceding chapters, data have been presented on the nature of east Coromandel shelf dynamics, sediment texture, mineralogy, morphology and stratigraphy. The purpose of this chaptēr is to integrate the data and interpretations presented in previous chapters, and put forward a series of conceptual models of nearshore and inner shelf sedimentation processes for the study area.

Firstly, various shelf lithofacies are defined, and their surface distributions across shelf morphological provinces examined. Secondly, information on the nature of shelf hydrodynamics, as presented in Chapters 4, 6, and 7, is integrated with the identified lithofacies, to interpret possible sediment transport pathways and sedimentation processes. Following this, the possible diabathic links between local beach systems and the shelf are interpreted, through integrating observations of beach/barrier morphodynamics with interpretations of shelf lithofacies and sedimentation processes. Finally, the late Quaternary development of the east Coromandel shelf is addressed in an effort to ascertain the geological scale processes responsible for present shelf sedimentation patterns.

10.1 EAST COROMANDEL SHELF LITHOFACIES

Earlier in Chapter 3, a review of shelf sedimentation processes was presented, which introduced the concept of dividing continental shelf surfaces into morphological provinces. These are defined by their morphological characteristics, and are generally associated with various shelf lithofacies and distinct zones of hydraulic activity. Commonly defined shelf lithofacies include, nearshore (or shoreface), inner shelf, and mid shelf lithofacies (e.g. ROY and STEPHENS, 1980; LIU and ZARILLO, 1989; HILTON, 1990). The overall characteristics of these morphological provinces and shelf lithofacies are determined by the rate and character of sediment supply, the fluid power expenditure, and relative sea level rises (SWIFT *et al.*, 1985).

Morphological characteristics of the east Coromandel continental shelf have already been described in Chapter 6. The distribution of various lithofacies across these morphological provinces is now presented, in an effort to ascertain the degree to which shelf sedimentation patterns are dependent on factors such as local sediment sources and supply, modern oceanographic conditions, and the local Holocene sea level history.

10.1.1. Delineation of Shelf Lithofacies

In other studies in which shelf lithofacies have been delineated, this has often been based on the textural nature of surface sediments. Sediment textural groups presented in Chapter 5 for the east Coromandel coast are placed into two broad categories, 'modern detrital' sands and 'palimpsest' sands. Modern detrital sands correspond to textural groups 6 and 7, and are characterised by fine to very fine grained, moderately well to very well sorted, relatively angular

sands, with only low to moderate quantities of carbonate and iron oxide stained grains. These represent either allochthonous terrigenous, or reworked autochthonous shelf sediments that are presently depositing on the sea-bed. Palimpsest sands correspond to textural groups 1, 2, 3, and 4, and are characterised by medium to very coarse grained, poorly to well sorted, relatively rounded sands, with moderate to high amounts of carbonate and iron stained grains present. These are essentially in situ sediments, which are intermittently reworked under storm conditions, but do not appear to be presently accreting on the shelf.

These two broad categories of shelf sediments can be further broken down into lithofacies, by including considerations of information on sediment composition from Chapter 9.4. This leads to the classification of 5 modern detrital and 3 palimpsest sediment facies, namely:

1A - very fine grained, volcanic glass-enriched, modern detrital sand facies;

1B - fine grained, felsic, modern detrital sand facies;

1C - very fine grained, lithic- and volcanic glass-enriched, modern detrital sand facies;

1D - fine grained, lithic- and augite-enriched, modern detrital shelly sand facies;

1E - very fine grained, volcanic glass-enriched, modern detrital muddy sand facies;

2A - medium to coarse grained, felsic, palimpsest sand facies;

2B - medium to coarse grained, felsic, mixed recent shell and palimpsest sand facies;

2C - coarse grained, lithic- and volcanic glass-enriched, palimpsest sand facies.

Each lithofacies is fully characterised by integrating additional information on their morphological and stratigraphic characteristics, which are summarised in Table 10.1. This is in accord with the traditional approach to lithofacies delineation, based on descriptions of a particular suite of grain types, sediment sizes, sedimentary structures, and sediment geometry (LEEDER, 1982). The distribution of each lithofacies within the study area is presented for both the southern exposed and northern embayed coastlines. Information is also presented on their offshore distributions over the various shelf morphological provinces.

10.1.2. Lithofacies Distribution on the Southern Coast

The distribution of shelf lithofacies off the southern exposed coastline is shown in Figure 10.1, and related to shelf morphological provinces in Figure 10.2. In the southern study region, similar

Table 10.1. Characteristic features associated with each east Coromandel shelf lithofacies. Textural abbreviations include: v.f.s. = very fine sand, f.s. = fine sand, m.s. = medium sand, c.s. = coarse sand; p.sor. = poorly sorted, m.sor. = moderately sorted, m.w.sor. = moderately well sorted, w.s. = well sorted, v.w.sor. = very well sorted; CO3 = % carbonate; FeO = % iron oxide staining; V.A. = very angular, A. = angular, S.A. = subangular, S.R. = subrounded, R. = rounded, W.R. = well rounded.

Facies	Locations	Depth Range	Sediment Texture	Bedforms	Stratigraphy	Composition
1A	Waihi-Tairua	5-20 m	Class 7: f.s.-v.f.s.; w.-v.w.sor.; 10% CO3; 10% FeO; V.A.-A.	Actively reworked ripples	Unit 5E/8-11 m thick wedge	Class 2 - Glass-enriched.
1B	Waihi-Tairua; Whangapoua	20-50 m; 0-30 m.	Class 6: f.s.; m.w-w.sor. 10-40% CO3; 10-40% FeO; A-R.	Rippled-flat, sand ridges	Unit 5D/Sheet 5-6 m thick, ribbons 1-5 m thick.	Class 1- Felsic sands
1C	Hotwater; Mercury Bay	40-50 m; 0-50 m	Class 7: v.f.s.; w.-v.w.sor.; 10%-20% CO3; 10-30% FeO.; V.A.-W.R.	Sand waves	Unit 5E/15 m thick wedge, Unit 5D/6 m thick sheet.	Class 3 - Glass- & lithic-enriched
1D	Hotwater; Hahei	10-30 m; 10 m.	Classes 5 & 6: f.s; w-v.w.sor.; 20-60% CO3; 50-60% FeO; A-R.	Actively reworked ripples.	Unknown.	Class 4 - Lithic- & augite enriched
1E	Whiritoa- Hotwater; Whangapoua	> 45 m > 30 m	Class 7: v.f.s.; 5-35% mud; m.w.sor.; 10-30% CO3; 0% FeO; V.A.-S.R.	Flat-megarippled, sand ridges	Unit 5C/7-8 m thick sheet.	Class 2-Glass-enriched.
2A	Waihi-Tairua	20-50 m.	Classes 1-4: m.s-c.s.; m.w.-w.sor.; 10-40% CO3; 20-70% FeO; S.A.-R.	Megarippled, sand ridges	Units 2, 3, 4 and 5B/(5-10 m thick).	Class 1- Felsic sands.
2B	Otama-Whangapoua	0-30 m.	Classes 1-4: m.s-c.s.; p-w.sor.; 40-80% CO3; 10-40% FeO; A-R.	Rippled, sand ridges.	Unknown.	Class 1 - Felsic sands.
2C	Hotwater; Mercury Bay.	30-50 m; 10-30 m.	Classes 1-2: c.s.; p-w.sor.; 20-40% CO3; 40-80% FeO; A-R.	Megarippled.	Unit 5B/10 m thick.	Class 3 - Glass- & lithic enriched.

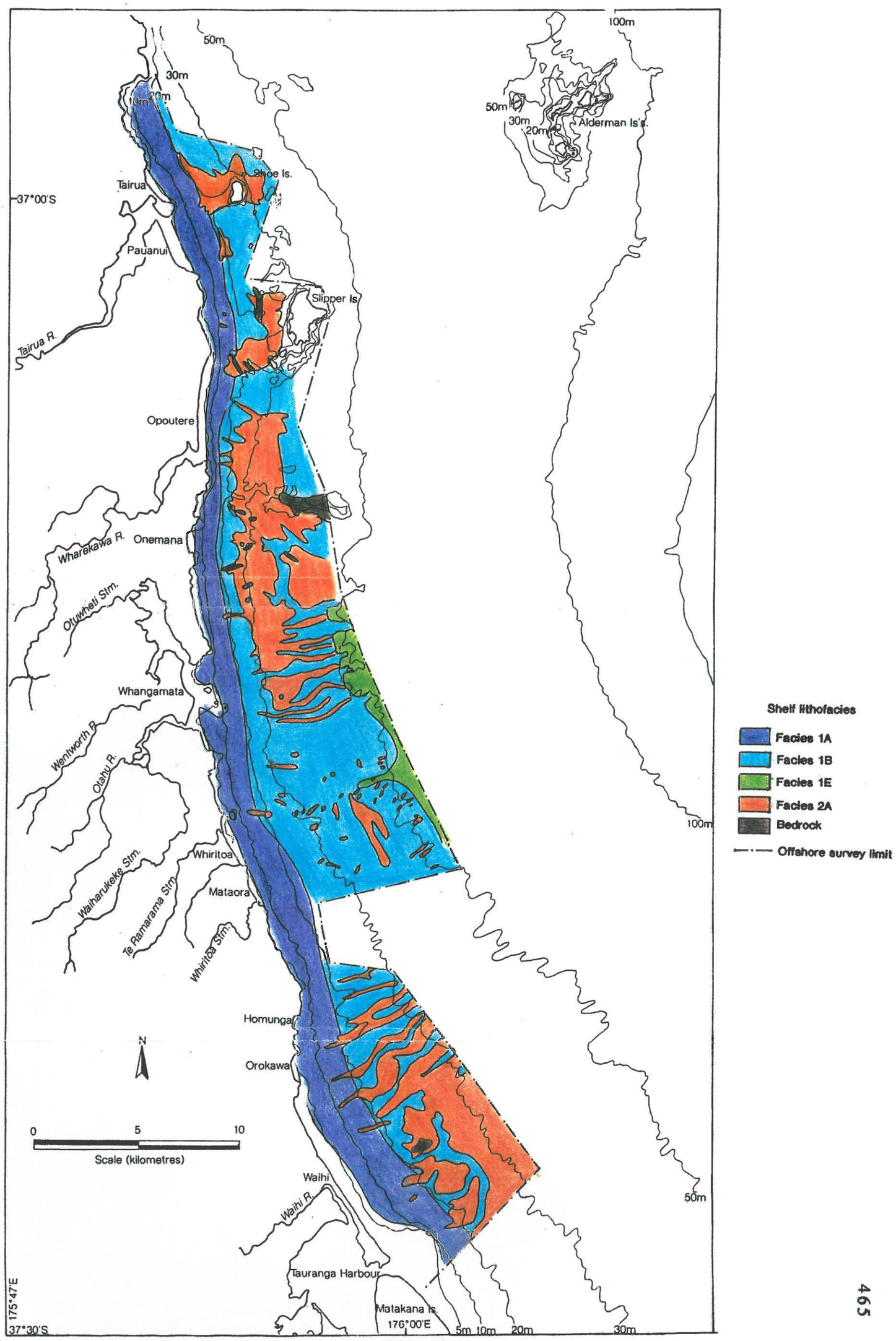

Figure 10.1. Distribution of shelf sediment lithofacies (5 to 50 m water depth) for the southern, exposed coastline.

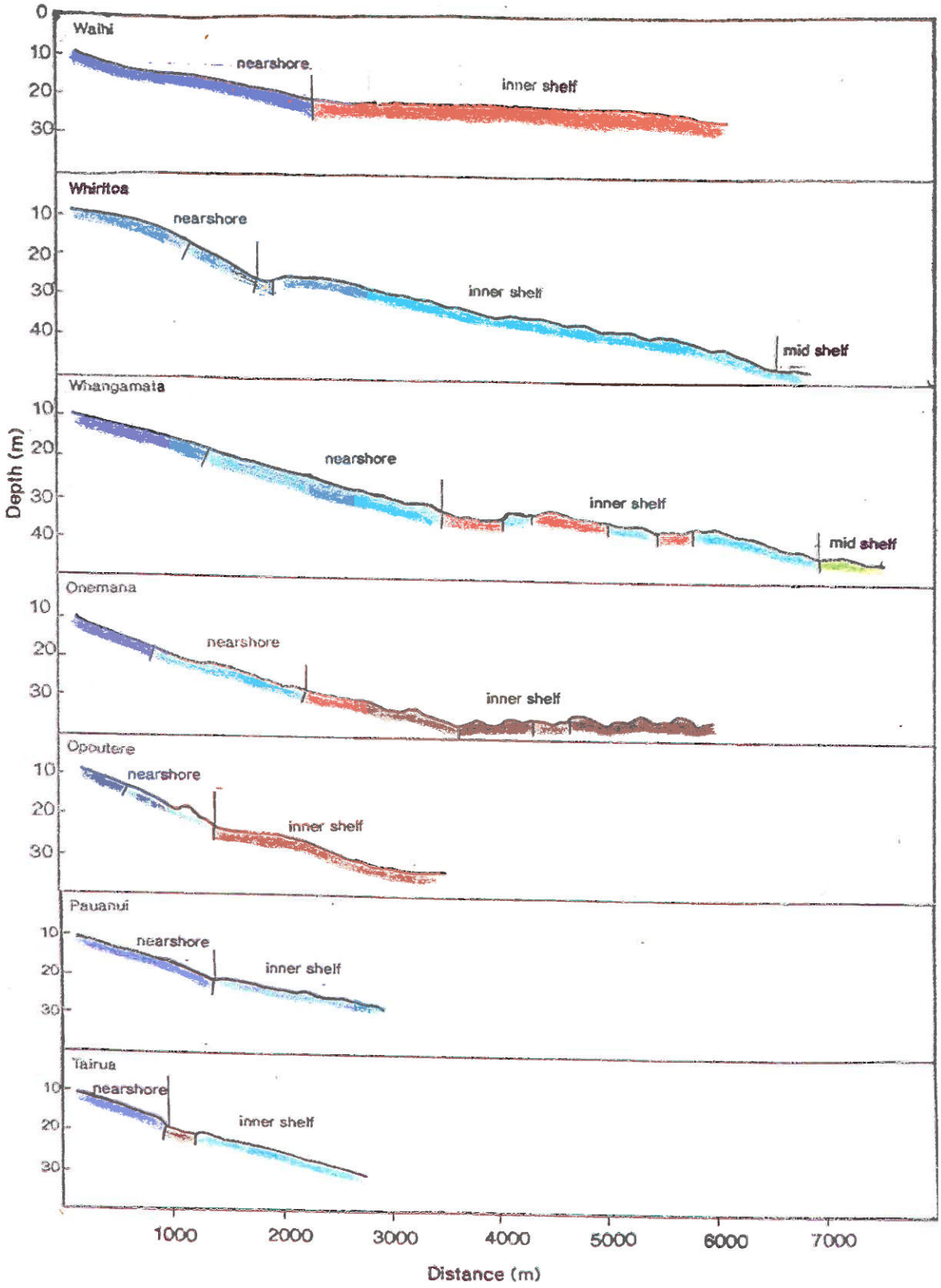

Figure 10.2. Occurrence of east Coromandel sediment lithofacies across shelf morphological provinces on the southern exposed coastline.

sediment facies occur over 60 km of coastline between Waihi Beach and Tairua, although their spatial distributions vary considerably. The very fine grained glass-enriched lithofacies 1A occurs as a relatively continuous band in the upper nearshore zone along the coast, which forms a convex- to concave-up surface in 5 to 20 m water depth, and is generally characterised by the presence of active, irregularly-crested ripples. Diver and depth of activity rod surveys indicate that this lithofacies is extensively reworked by wave-orbital currents. The textural and mineralogical characteristics of abundant angular, non-iron stained, volcanic glass deposits, and the general lack of carbonate material, indicates an environment of relatively abundant modern clastic sedimentation of allochthonous terrestrial material. Seismic stratigraphic data presented in Chapter 8 show that this facies may form part of an 8 to 11 m thick wedge of upper nearshore deposits.

The fine grained felsic lithofacies 1B occurs further offshore on the lower nearshore surface, where it usually extends relatively discontinuously to at least 50 m water depth. On its landward boundary with lithofacies 1A, the textural and mineralogical characteristics seem to grade offshore, with sand increasing in size and glass decreasing in abundance. However, on the inner shelf surface, lithofacies 1B contains only very low amounts of volcanic glass, and greater quantities of quartz. The association of these deposits with rippled bedforms and current-lineated sand ridges indicates that they are reworked by modern oceanographic processes. The occurrence of facies 1B across a wide range of water depths presents some problems for delineating shelf zones based on sediment lithofacies, particularly off Whiritoa Beach. As the facies forms a relatively thick (5 to 6 m) sheet of surficial sands on the lower nearshore surface, but thinner (1 to 5 m) and less continuous lenses over the inner and mid shelf surfaces, it probably represents sediments which were originally emplaced at the base of the nearshore zone, that have since been redeposited further offshore, in some areas quite extensively, and often outside of the immediate shelf region.

A third modern clastic group of sediments found in the southern study region is the very fine grained glass enriched muddy lithofacies 1E. This occurs at depths > 45 m, and represents sediments formed on the relatively flat mid shelf plain. The lateral continuity of this facies is uncertain, as most offshore regions were not sampled beyond the inner shelf surface. The nature of mid shelf deposits varies considerably in texture between Waihi Beach and Whiritoa-Whangamata, with both medium and very fine sands dominating the former area, but only very fine sands in the latter regions. Characteristic features of this lithofacies are the presence of muddy, very fine grained, angular sands, containing moderate amounts of volcanic glass. It thus shows lithological similarities with the upper nearshore lithofacies 1A, and is possibly derived from the offshore reworking of these. The surface of mid shelf deposits is either flat, or reworked into isolated bands of megaripples, the latter associated with the flanks of current-lineated sand ridges. Thus, these are at least occasionally reworked by storm waves and currents. This lithofacies occurs on the surface of what appears in seismic records to be a 7 to 8 m thick stratigraphic unit, and thus represent an area characterised by active shelf sedimentation.

Sediments corresponding to the coarse grained felsic palimpsest lithofacies 2A occur discontinuously along the shelf in the southern study region, at depths usually ranging from 20 to 50 m, but in some instances as shallow as 10 m (Waihi, Onemana, Opoutere). The lithological nature of deposits (i.e. coarse grained, rounded, iron oxide stained, carbonate, quartz and feldspar grains), shows that these are reworked from either older Holocene, or relict Pleistocene deposits. This is supported by radiocarbon dates of surficial shell material, and their association with older basal Holocene and Pleistocene stratigraphic units. Their surfaces are actively reworked under storm conditions, as shown by the presence of extensive megarippling, and their association with the flanks of current-lineated sand ridges. Deposits are mainly found on the inner shelf surface, but in many instances form isolated bands on the nearshore slope. There appears to be a strong similarity between the composition of these palimpsest sands, and the actively depositing lithofacies 1B. It is therefore likely that both lithofacies were derived from the same parent source, and that lithofacies 1B represents a winnowed, actively reworking product, with the palimpsest lithofacies 2A forming a residual erosional lag.

10.1.3. Lithofacies Distribution on the Northern Coast

The distribution of shelf lithofacies off the northern embayed coastline is shown in Figure 10.3, and related to shelf morphological provinces in Figure 10.4. Sediment lithofacies found in the northern part of the study area show greater regional variations than those described from further south. A major shelf lithofacies from this region is the lithic- and volcanic glass-enriched, very fine grained sands within Mercury Bay (facies 1C). These appear to represent locally derived allochthonous shelf deposits. The extensive lateral distribution of this lithofacies, both across the bay and south onto the Hotwater Beach shelf area, indicates it represents a very significant sediment lithofacies in terms of local shelf sedimentation. Within Mercury Bay, it is hard to associate the occurrence of this lithofacies with offshore zones, as it extends over both the relatively low gradient nearshore and inner shelf slopes. However, it appears to be associated with a thick (15 m) accretionary wedge across the nearshore zone, and a thinner (6 m) sediment blanket on the inner shelf. If stratigraphic interpretations from seismic records are correct, then it could be deduced that modern clastic deposits within Mercury Bay are prograding offshore over the nearshore surface, where they are subsequently reworked further seawards onto the inner shelf.

In mid shelf deposits both north and south of Mercury Bay (Hotwater Beach and Whangapoua), a very fine grained, muddy, glass-enriched lithofacies occurs (facies 1E). As neither area is characterised by an onshore glass-enriched source, this lithofacies appears to be derived from the offshore and along-shelf reworking of volcanic glass deposits (facies 1C) in Mercury Bay. In both areas, the amount of mud within deposits varies, from 35% off Hotwater Beach, to 5% off Whangapoua. Thus, different sedimentation conditions probably occur within each shelf region.

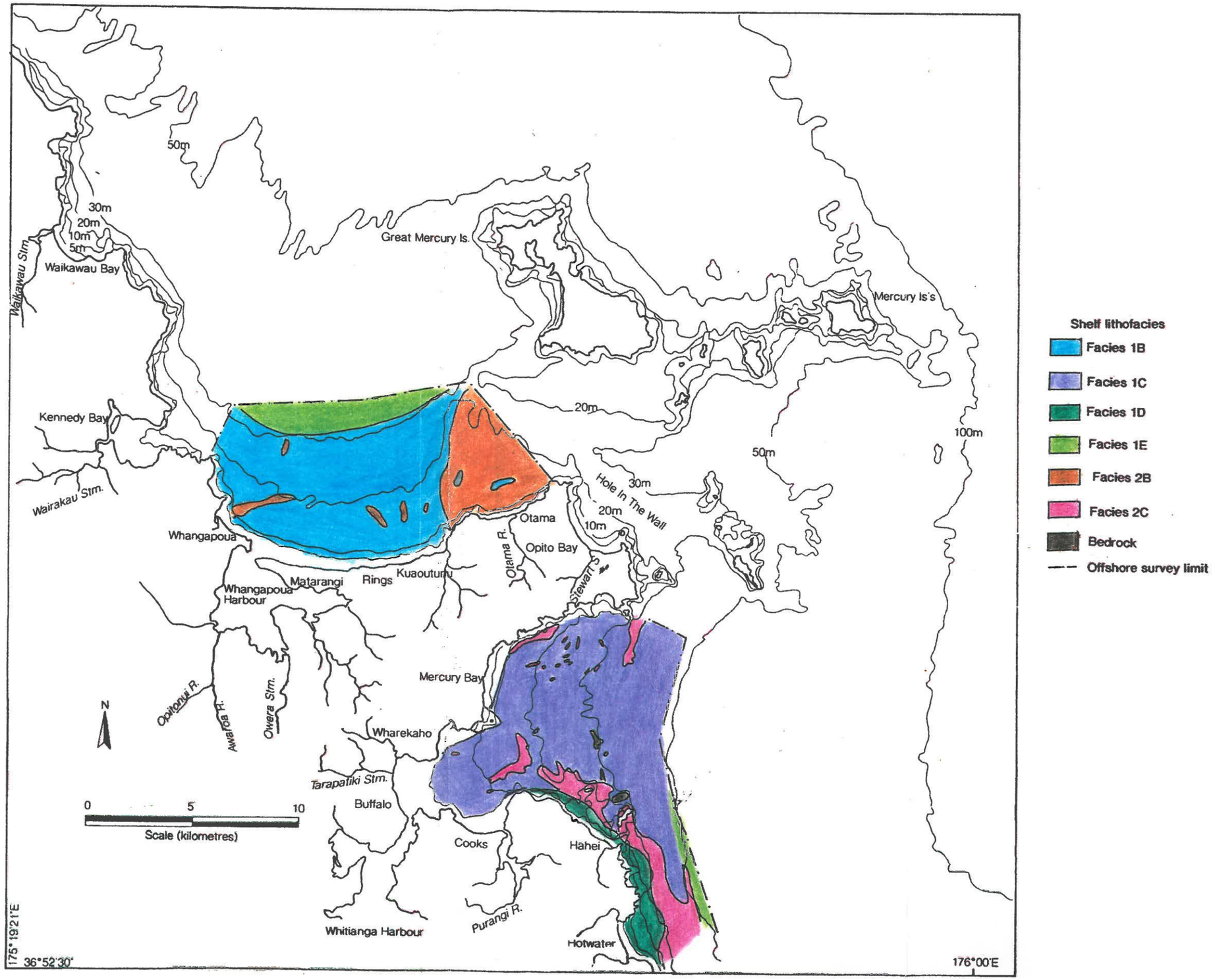

Figure 10.3. Distribution of shelf sediment lithofacies (5 to 50 m water depth) for the northern embayed coastline.

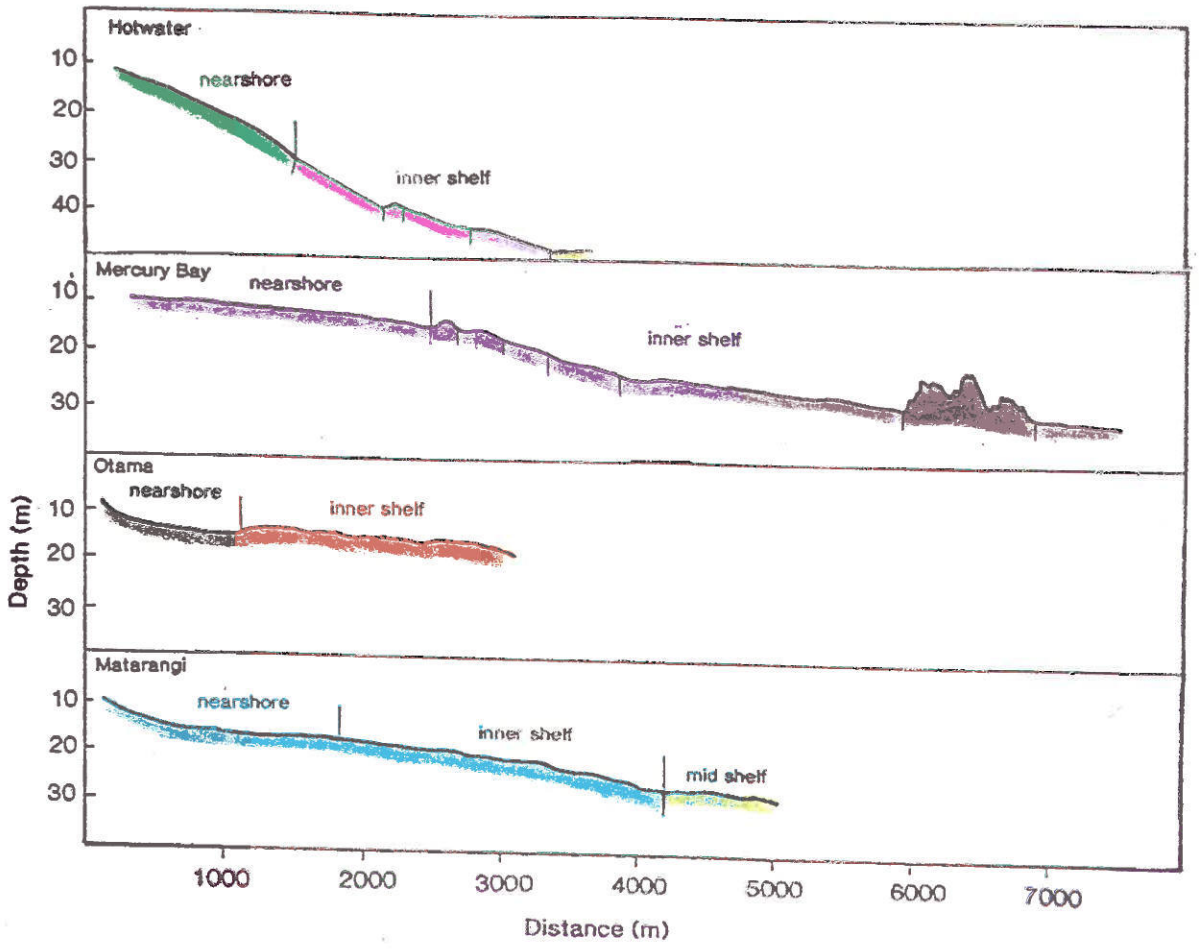

Figure 10.4. Occurrence of east Coromandel sediment lithofacies across shelf morphological provinces on the northern embayed coastline.

At Hotwater Beach, a relatively narrow band of fine grained, lithic- and pyroxene-enriched sands (Facies 1D) extends across a convex nearshore slope (out to 30 m water depth), and continues a short distance north to Hahei. The sediment mineralogy indicates a local source from two-pyroxene andesite outcrops along the coast. Thus, the facies represents a locally derived allochthonous shelf deposit.

Offshore of Whangapoua Harbour on the Kuaotunu Peninsula, modern clastic sediments equivalent to lithofacies 1B extend seawards from 5 to 30 m water depth. Deposits here differ slightly in being more enriched in feldspar and carbonate material (mainly microfauna), and only being associated with small morphological features (irregular active ripples). Thus it is uncertain whether these are locally derived terrigenous sediments from Whangapoua Harbour, or reworked autochthonous shelf sediments from Otama. Their association with offshore zones is also obscure, as they commence on a concave nearshore surface, and then extend offshore across a convex inner shelf. The only differentiation possible is from the presence of ripples in nearshore deposits, and a flat bed over the inner shelf.

Palimpsest sands with similar compositional (i.e. abundant lithic fragments), but different textural characteristics to lithofacies 1C are found in 30 to 50 m water depth off Hotwater Beach, and 10 to 30 m within Mercury Bay (facies 2C). As in areas further south, their occurrence coincides mainly with the inner shelf surface. However, deposits within Mercury Bay also extend onto the nearshore slope. This lithofacies probably represents erosional lag deposits from the basal Holocene transgressive sand sheet, as indicated in seismic profiles from this region. Modern reworking of this lithofacies is indicated by the occurrence of megaripple bedforms, and small current-lineated sand waves.

Offshore from Otama Beach, palimpsest sands (facies 2B) are of similar lithology to 2A in the southern region, but are characterised here by a large amount of recently derived bioclastic material. This lithofacies extends from 5 to 30 m water depth, and occurs across both a concave-up nearshore, and flatter convex-up inner shelf surface. Some differentiation of deposits over each zone is possible by the presence of ripples on the nearshore surface, and a flat sea-bed on the inner shelf surface. The large carbonate concentration reflects locally favourable conditions for bioclastic sediments to develop, and low modern detrital sediment inputs. Similarities in composition between this lithofacies and the adjacent fine felsic sediments off Whangapoua (facies 1 B), suggest that the latter may have been (and still are) derived from winnowing of finer material by wind- and tide- generated currents off Otama.

10.1.4. Interpretations of Shelf Lithofacies Distributions

In comparison to other studies in which shelf zones and lithofacies have been examined, the east Coromandel coast shows some similarities, in that along the more open and exposed shelf regions distinct offshore morphological provinces appear to be present. However, these morphological

provinces are not always associated with a distinct lithofacies, particularly on the nearshore and inner shelf surfaces, where one sediment lithofacies may show extensive spatial variations. Also, studies from many other shelf regions (e.g. U.S. Atlantic coast, and eastern Australia) show a seaward fining trend in sediment texture across the nearshore zone, while an offshore coarsening trend is found in this study. HILTON (1990) likewise describes a coarsening of sands on the lower nearshore zone at Pakiri, to the north of the Coromandel Peninsula. However, offshore patterns differ on the east Coromandel from Pakiri, in that upper nearshore sediments are finer grained, and shelf lithofacies generally have a patchier distribution.

Factors responsible for this set of shelf characteristics within the study area are inferred to relate to local sediment inputs from terrigenous sources, and variations in the regional oceanographic climate. The presence of very fine grained, angular, glass-enriched sands on the upper nearshore and mid shelf surfaces, and in Mercury Bay across the entire shelf surface, shows the study area is influenced to some degree by modern allochthonous shelf sedimentation. Therefore, lithofacies distributions within the study area probably result to some degree from the dominant influence of local terrigenous sediment sources over offshore variations in bottom boundary layer processes.

Local variations in shelf sediment patterns could also result from the oceanographic conditions on the northeast New Zealand coast. In particular, the lower wave energy environment of the east Coromandel coast compared to high wave energy shelves such as the east Australian coast probably results in wind-generated currents dominating sediment transport seaward of the upper nearshore zone. JAGO and BARUSSEAU (1981) found that when tidal currents dominate shelf flows, an offshore coarsening trend develops. Thus, the presence of offshore coarsening trends in lower nearshore deposits on the east Coromandel coast may result from the effects of wind-generated currents dominating over wave-induced flows seaward of the upper nearshore zone. This is supported by the extensive development of sand ridges in depths of 20 to 80 m on the southern coast.

In summary, sediment lithofacies on the east Coromandel have modal zones of accumulation which tend to occur within morphological provinces across the shelf. However, sediments within the nearshore zone appear to extend seawards in most areas, where they are deposited as either sand ridges or a sheet of fine sediments over the inner and mid shelf surfaces. This therefore makes delineation of shelf zones in the study area difficult when based on the occurrence of different sediment lithofacies. The seaward extension of nearshore deposits is either due to different oceanographic conditions within the study area which do not favour the confinement of fine sands to the nearshore zone, and/or modern allochthonous terrigenous sediment inputs causing nearshore deposits to prograde seawards over inner and mid shelf sediments.

10.2. NEARSHORE AND INNER SHELF SEDIMENTATION PROCESSES

Having defined and mapped the distribution of east Coromandel shelf lithofacies, it is now possible to integrate this information with other data on shelf dynamics and morphology to deduce the sediment transport pathways along the coast, and sedimentation patterns in the nearshore and inner shelf zones under different oceanographic conditions.

10.2.1. Regional Sediment Transport Pathways

Some information on the transport pathways for east Coromandel shelf sediments has been deduced in previous chapters through direct measurements of currents patterns (Chapter 4.3. and 4.5.), and indirect evidence from textural and morphological data (Chapters 5.3., 6.2.3., and 7.3.). This information is integrated with the distribution of shelf lithofacies to determine sediment transport pathways along the east Coromandel coast. The contrasting lithofacies found on the southern exposed and northern embayed coastlines suggests that these represent two isolated sediment compartments. Hence, two major sediment transport pathways are inferred to be present on the east Coromandel coast (Figure 10.5).

On the southern exposed coast, a northerly-directed transport pathway appears to extend from Waihi Beach to Tairua, as indicated by the presence of similar nearshore, inner shelf, and mid shelf lithofacies along the shelf. From the morphology of sand ridges between Waihi Beach and Opoutere, as well as current measurements off Onemana, this transport system is related to the interaction of northerly-directed wind-generated currents and large waves during storm conditions. This transport pathway on the southern shelf appears to diminish north of Opoutere Beach, as shown by the decreasing presence of current-generated bedforms. Instead, shelf sedimentation patterns appear to be associated with the refraction of storm waves around offshore islands and reefs, to produce areas of concentrated wave energy and hence sea-bed scouring. The continuity of this transport system on the southern coast breaks down between Whiritoa and Whangamata, where a reverse southerly-directed transport of shelf sands occurs on the inner and mid shelf zones. This results in the deposition of fine sands off Whiritoa and Mataora, and their erosion from adjacent shelf areas both north and south. The cause of this reverse transport of shelf sediments is attributed to the sharp indentation in the shelf surface at Whiritoa and Whangamata, which allows the East Auckland Current to intrude over the shelf surface from deeper oceanic waters, and attain sufficient speeds to transport shelf sediments to the south.

Along the northern embayed coastline, a second transport pathway appears to extend from Hotwater Beach to the shelf area offshore of Otama. This transport pathway is inferred to be driven by a clockwise downwelling circulation pattern generated within Mercury Bay during easterly storms, as found for less intense tidal-driven flows in the same area by

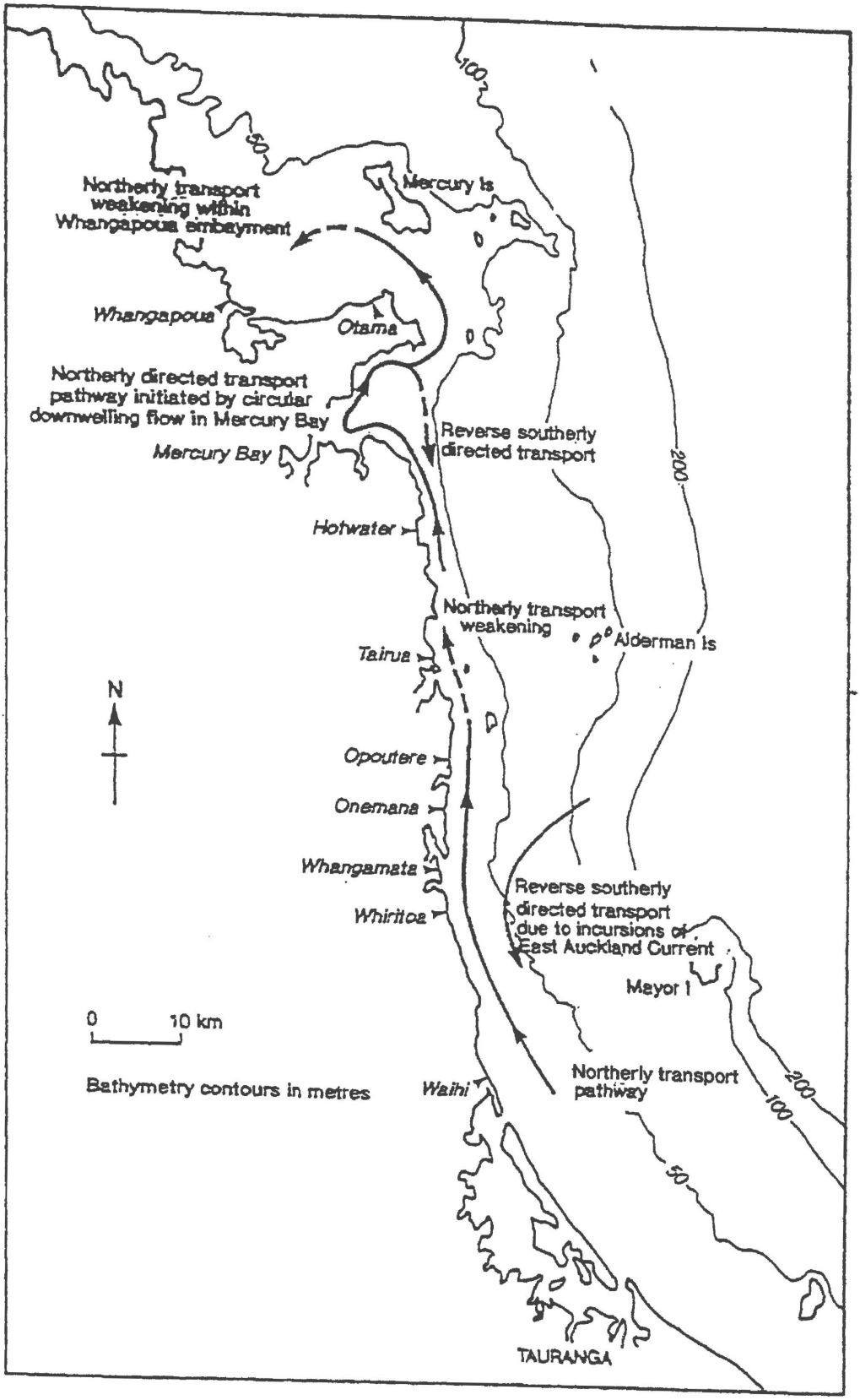

Figure 10.5. Conceptual model of the two along-shelf northerly-directed, and smaller reverse southerly-directed sediment transport pathways found on the east Coromandel shelf. These are driven by strong wind-generated currents during storm events on the east coast, and are also inferred to be influenced by intrusions of the East Auckland Current in the shelf region between Whiritoa and Whangamata.

SMITH (1980). From the distribution of lithofacies, as well as information obtained from current meters and morphological features, it appears that this pathway begins on the nearshore zone off Hotwater Beach, then continues around the southern and northern periphery of Mercury Bay, through the Hole in the Wall to Otama Beach, offshore of which it is retarded by the relatively tranquil waters off Whangapoua. A small reversal in transport direction may occur between Mercury Bay and Hotwater Beach, as shown by the presence of volcanic glass fragments in inner and mid shelf deposits from Hotwater. Such a reversal may be accounted for by the northerly flow being diverted to the south by the northern promontory in Mercury Bay. This northern transport pathway seems to be much weaker than that found on the southern coast, as shown by the general lack of current-generated sand ridges, except off Otama Beach. However, it does appear to be sufficiently intense to transport very fine grained, glass-enriched sediments from Mercury Bay to the mid shelf surface off Hotwater Beach and Whangapoua, as well as fine felsic sands from Otama to Whangapoua.

10.2.2. Nearshore and Inner Shelf Sedimentation Processes

To account for nearshore and inner shelf sedimentation patterns on the east Coromandel coast, a conceptual model is presented for the transport of these deposits as observed under different oceanographic conditions. This is based on observations from the region between Whiritoa and Whangamata, as this is the most extensively examined shelf region from the east Coromandel study, and also because it shows aspects of sedimentation patterns observed from most parts of the open coastline within the study area. From consideration of the oceanographic conditions which occurred in the course of the study, the model is broken down into three elements: fair weather processes; storm processes; and extreme storm processes.

An important factor to consider in this model is the mode of sediment transport. Other studies have generally found that shelf sediment transport, particularly during storms, involves the entrainment of sediments by agitation from wave oscillatory currents (WRIGHT, 1987). Once entrained in this way, the sediments may be diffused upwards above the wave-induced boundary layer, where they are then transported by mean flows. This usually applies for material less than fine sand in size, and is referred to as the suspended sediment load. Coarser material is usually only entrained temporarily, seldom rising far above the bed, and thus incorporated into a bed load mode of transport (COWELL and NIELSON, 1984; SHI and LARSON, 1984). Other studies have found that the suspended sediment load is transported over the greatest distances during storms, and thus leads to the most significant changes in shelf sedimentation patterns (e.g. WRIGHT *et al.*, 1986; GAGAN *et al.*, 1990; LYNE *et al.*, 1990). In order to gain some idea of the potential for different scale events to entrain shelf sediments on the east Coromandel coast, a 'wave mobilisation of sand beds' program published by COWELL and NIELSON (1984) was utilised to calculate the concentrations of mobile suspended sand. Results of the program for selected areas from both the southern and northern coastlines are shown in Figure 10.6.

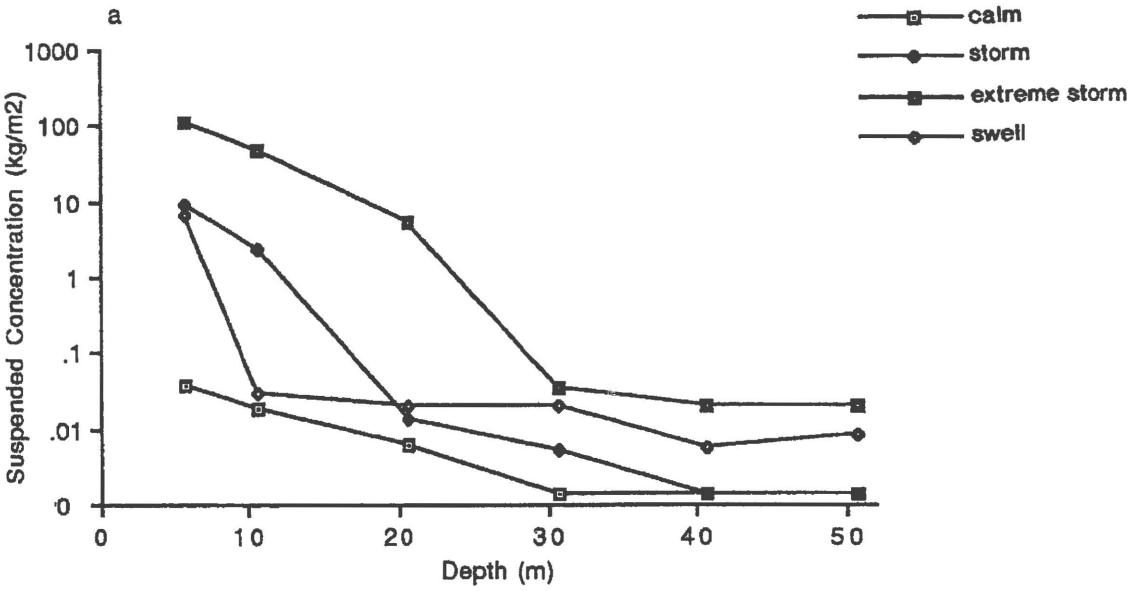
a
calm
storm
extreme storm
swell
Suspended Concentration (kg/m2)
1000
100
10
1
.1
.01
0
0
10
20
30
40
50
Depth (m)

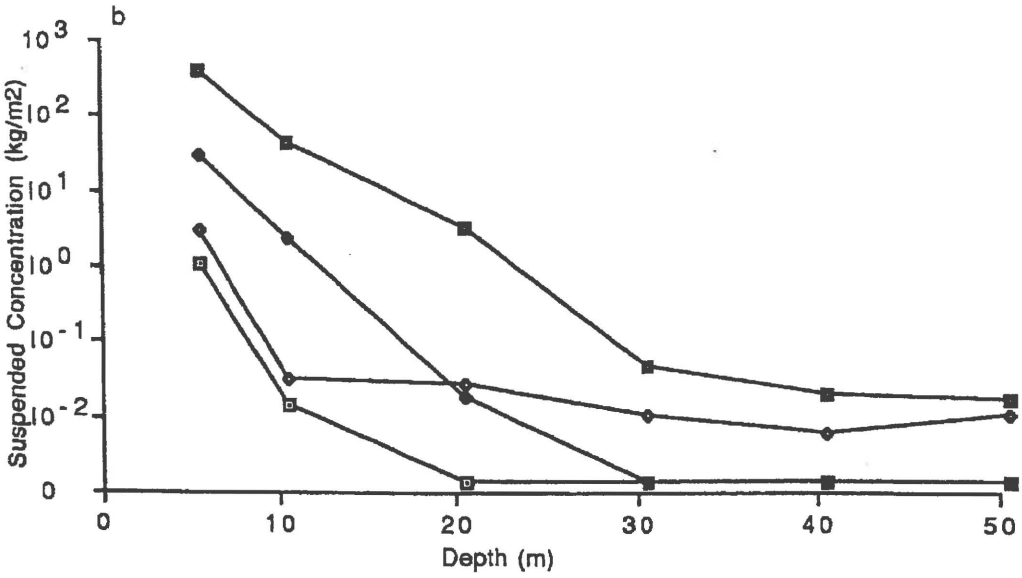
b
Suspended Concentration (kg/m2)
10^3
10^2
10^1
10^0
10^-1
10^-2
0
0
10
20
30
40
50
Depth (m)

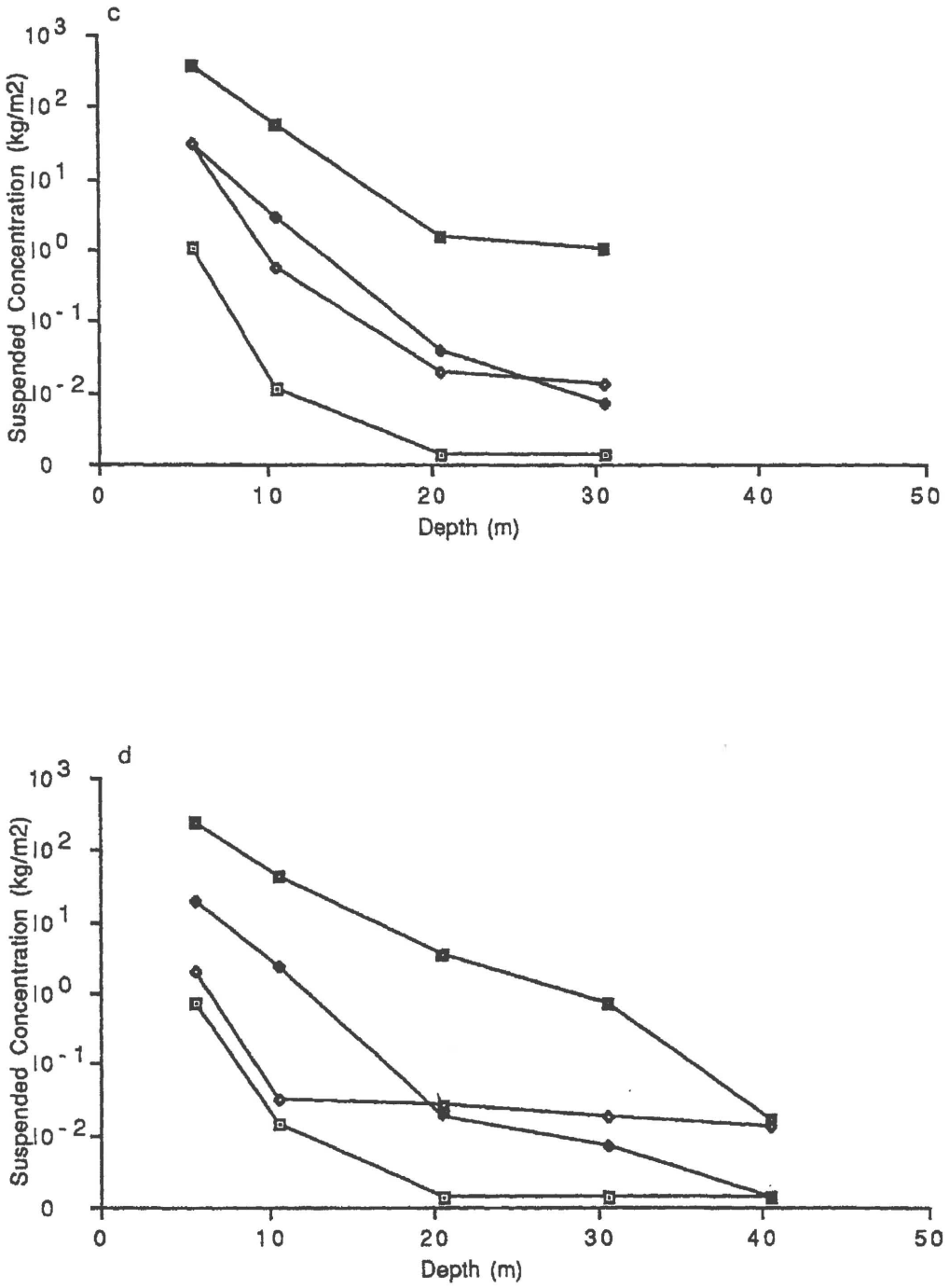

Figure 10.6. Suspended concentrations of shelf sediments during calm weather, storm and extreme storm events at: a) Whiritoa; b) Whangamata; c) Whangapoua; d) Mercury Bay; based on predictions from COWELL and NIELSON (1984) wave mobilisation of sand beds program.

The amount of fine sand entrained into suspension is a complex process, with two important parameters influencing this. Firstly, ripple crests create a bed roughness which increases the skin friction produced over sediments, thus enhancing their entrainment. As flow intensity increases during a storm event, ripples over fine sand may reach a break off point and decrease in size to a flat bed. This decrease in bedform size may lead to the lowest suspended sediment concentrations occurring during the peak of a storm event (VINCENT *et al.*, 1991). Secondly, when a mixture of sediment grain sizes occurs, surficial sediments during a storm will become progressively coarser as finer material is entrained and selectively removed. This armouring of the sea-bed by coarse lag deposits will then retard the further resuspension of fine sand (LYNE *et al.*, 1990). Thus, the suspended sediment concentrations illustrated in Figure 10.6 will only give a relative indication of values associated with different events, and cases of very high values probably represent an overestimation.

Fair Weather Conditions

During fair weather periods which prevail within the study area, waves are typically small (H< 1.5 m, T< 6 s.), and sediment transport appears to be limited to the upper nearshore zone (< 20 m), where wave-orbital currents interact with the sea-bed to entrain low quantities of very fine sand into suspension (10^{-1} to 10^{-2} $kg.m^{-2}$; Figure 10.6). This is inferred to result in a slow onshore movement of very fine sands by asymmetrical wave-orbital flows (Figure 10.7). Evidence supporting this deduction comes from the sea-bed drifter experiments in Chapter 4.2.2., which showed that relatively large numbers of drifters were transported onshore under calm weather conditions from depths of 10 to 24 m. Further evidence comes from studies by HARMS (1989) and HEALY *et al.* (1991) on the Tauranga shelf south of the study area, where fine sand from dredge spoil mounds in 11 to 17 m water depth were observed to be reworked onshore within a few years of their emplacement (see Figure 3.19). Some reverse offshore-directed sediment transport may also occur due to the presence of amplitude-modulated waves (SHI and LARSON, 1984; WRIGHT *et al.*, 1991), or the complex interactions of wave-orbital currents with rippled bedforms (NIELSON, 1979). However, no direct evidence for these was found in the course of this study. Diver observations during such calm weather periods show that sediment entrainment by waves is limited to depths of < 20 m, which is also predicted by the wave mobilisation program (Figure 10.6). This depth coincides with the offshore limit of very fine upper nearshore sands, and thus indicates that their offshore extent is probably controlled by the depth of reworking by modal wave conditions. In shallow nearshore waters adjacent to local harbours (< 10 m), tidal currents may develop flows of sufficient speed to transport the entrained very fine sands, as found at Tairua Harbour by DELL (1983). Tidal currents may also be important for the transport of very fine grained glass-enriched sands from the upper reaches of harbours, and their subsequent deposition on the upper nearshore surface. Thus, calm weather periods are probably characterised by the accumulation of 'very fine sands' on the upper nearshore surface.

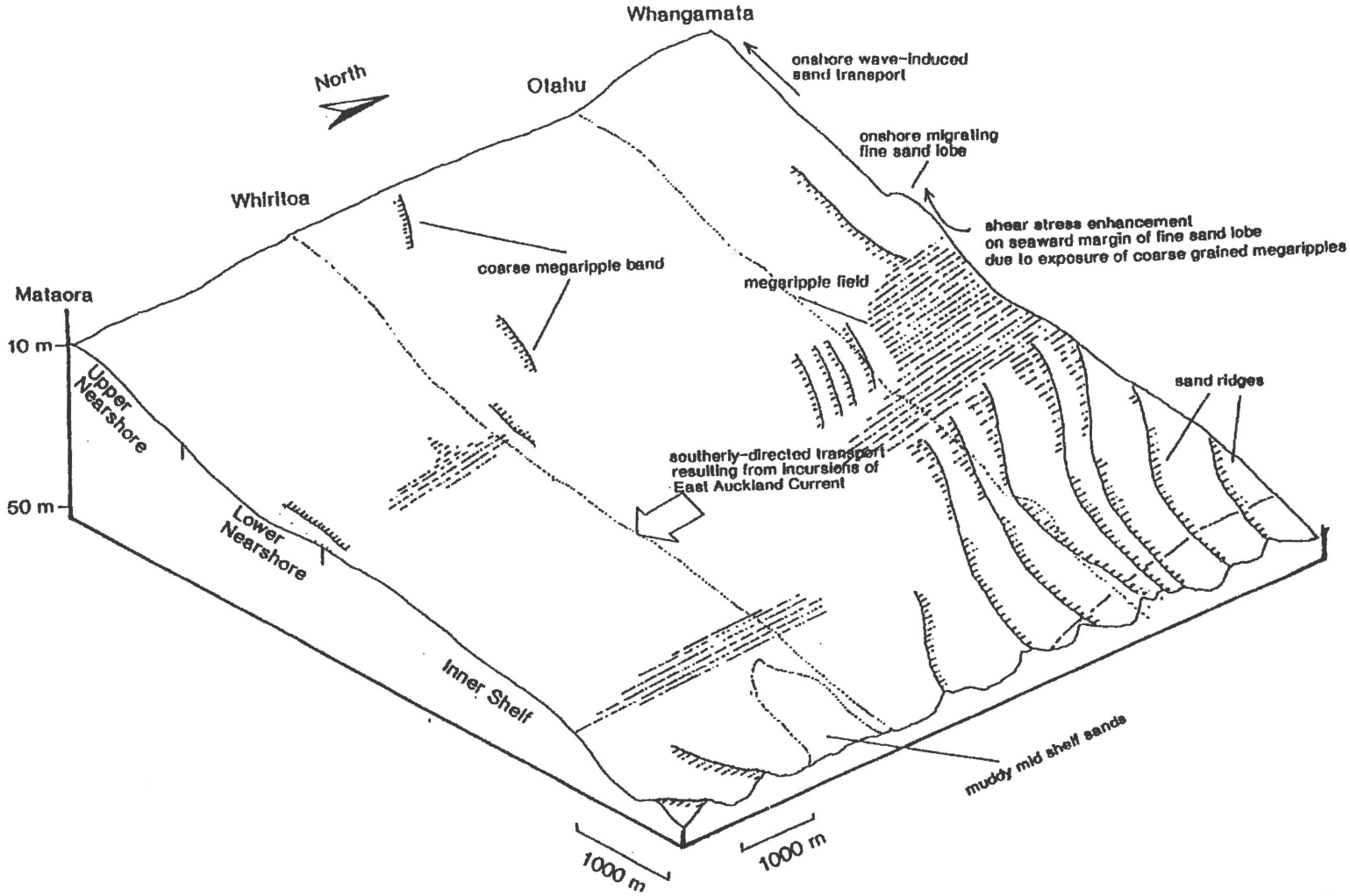

Figure 10.7. Shelf transport processes occurring during calm weather periods based on side-scan sonar and bathymetric surveys from Mar-84 between Mataora and Whangamata. Important features are the onshore movement of very fine sands on the upper nearshore profile by shoaling short period waves (H=1.5 m, T=6 s), onshore transport of fine sand from the lower nearshore-inner shelf boundary by longer period swell waves (H = 0.91 to 1.73 m; T = 8.3 to 13.0 s), and the southerly transport of mid shelf and inner shelf fine sediments by incursions of the East Auckland Current.

Beyond the upper nearshore surface, the above wave conditions are not predicted to entrain sediments (Figure 10.6). However, the presence of a fine sand lobe in 30 m water depth off Whangamata during Mar-84, suggests an onshore reworking of fine sands from the inner shelf surface during calm periods. This may be due to upwelling currents produced by the prevailing offshore westerly winds within the study area. Current records from Onemana though show that upwelling flows are not present during even high speed offshore wind events. An alternative explanation may come from recent wave rider data at Tauranga (see Figure 2.7), where long period swell waves (H = 0.91 to 1.73 m, T = 8.3 to 13.0 s) have been recorded during relatively calm periods. These would be sufficient to entrain small quantities of fine sand across the inner shelf surface (10^{-1} to 10^{-2} $kg.m^{-2}$; Figure 10.6), and over longer periods of time slowly transport them onshore. This process is possibly enhanced by the exposure of coarse megarippled sands when the fine sediments move onshore, as the higher surface roughness of megarippled bedforms was shown in Chapter 7.3. to produce an enhanced shear stress effect, which should also cause higher shear stresses to be excerted on the seaward margin of the fine sands, thus accentuating their onshore movement. Sediment entrainment on the Whiritoa-Whangamata shelf region during calm periods may also result from incursions of the East Auckland Current over the narrow shelf surface, thus resulting in a southerly-directed transport of fine sands, and their deposition on the Mataora-Whiritoa shelf region.

Storm Conditions

About twice each year, relatively small-scale storm events occur on the east Coromandel coast, and produce variable periods of strong onshore winds (wind force 6 to 7 Beaufort Scale, speed 12 to 15 ms^{-1}, and 5 to 65 hours duration; HAY, 1991). Current and wind measurements in this study show that high speed shore-parallel currents (0.3 to 0.4 ms^{-1}), and high waves (up to H=3 m, T=7 s) develop during such storm conditions. The along-shelf current direction is to the north over the shelf surface, with an offshore downwelling component also likely (Figure 10.8). Depth of activity rod observations in this study show that sediments are reworked to significant levels (0.1 to 0.2 m) on the upper nearshore surface, resulting in high suspended sediment concentrations (10 to 100 $kg.m^{-2}$; Figure 10.6). Some additional suspended load (mud and very fine sand) is also expected from rivers and harbours along the coast, as a result of catchment erosion and flooding induced by torrential rainfall associated with these easterly storms. This suspended terrigenous material would then be transported offshore by strong downwelling flows. As these storms are of only moderate strength, any very fine sand is probably deposited over the nearshore surface, and only the colloidal mud fraction transported further offshore to be deposited on the mid shelf plain, as observed on the Banks Peninsula by GIBB (1982).

Over the lower nearshore surface (20 to 30 m water depth), fine sediments are reworked down to a few centimetres depth, and thus suspended sediment concentrations will be low (10^{-1} to 10^{-2} $kg.m^{-2}$). Therefore, only limited transport of fine grained lower nearshore sands is expected during these storm events, although over longer periods of time (several years) the cumulative

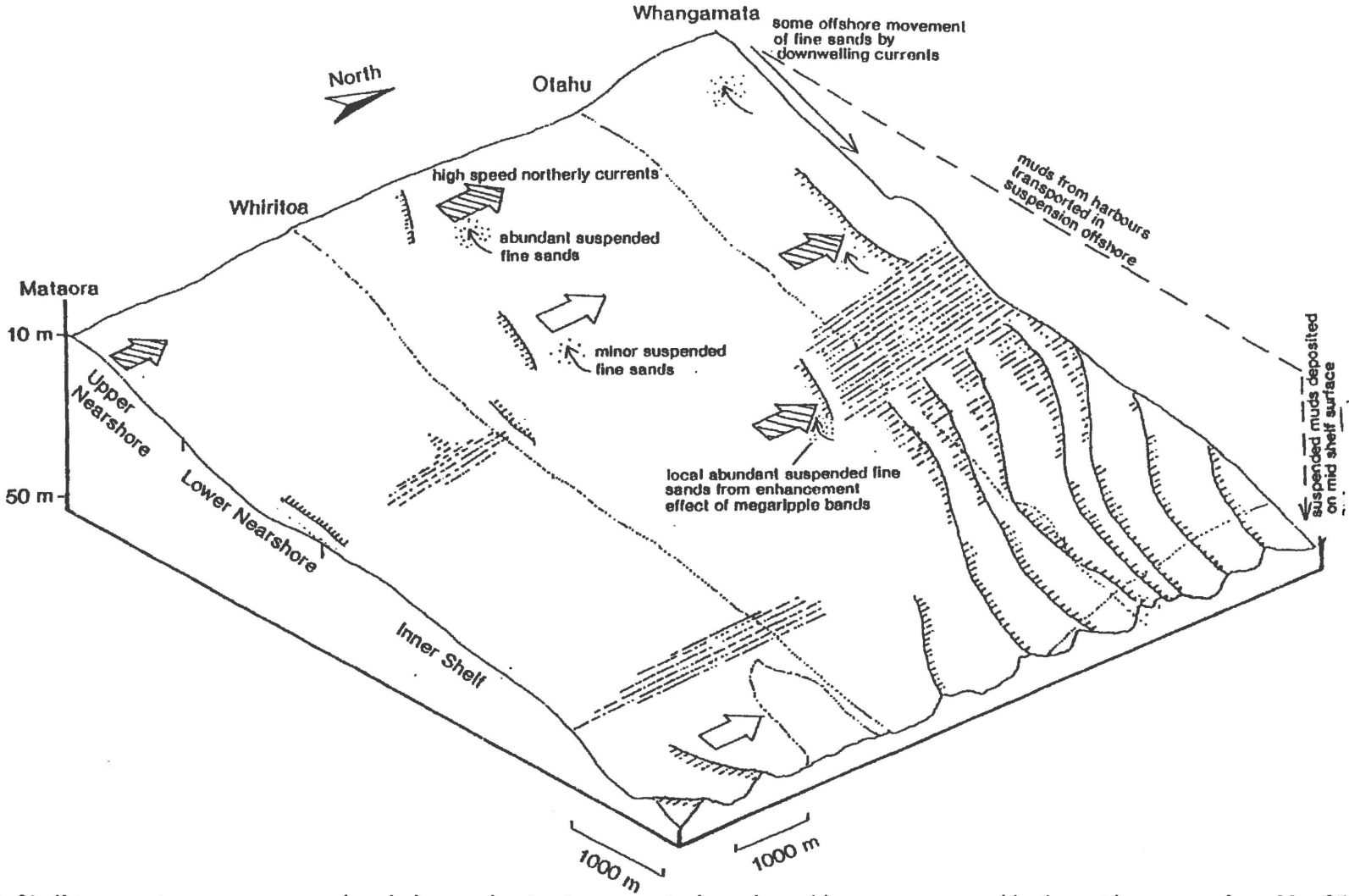

Figure 10.8. Shelf transport processes occurring during moderate storm events, based on side-scan sonar and bathymetric surveys from Mar-85 between Mataora and Whangamata. Important features are: abundant entrainment of very fine upper nearshore sands by storm waves, and their transport by strong northerly-directed wind-generated currents; offshore transport of terrigenous muds and their deposition on the mid shelf surface; the localised entrainment of moderate amounts of fine sand on the lower nearshore and inner shelf due to the presence of coarse megaripple deposits, which are subsequently transported along the shelf in strong wind-generated currents.

transport of fine sands may be more significant. Depth of activity rod surveys show that coarse megarippled sediments are more extensively reworked than adjacent rippled fine sands during such storm events. This is inferred to result from a shear stress enhancement occurring over the coarse megaripple deposits (see Chapter 7.2.3.). Any fine sand which has accumulated in the troughs of the megaripples during calm periods will be readily transported out of these due to the latter factor (COWELL and NIELSON, 1984). This would explain the large increase in size of coarse megaripple bedforms during depth of activity rod surveys. On the inner shelf surface (30 to 45 m water depth), these wave conditions are not predicted to result in the entrainment of sediments. This is supported by the depth of activity rod surveys, which show insignificant surface erosion during storms. However, megaripple bedforms in areas of coarse sand are reworked during these events, which indicates that some bedload transport occurs. Again, this is probably related to lower wave orbital currents required for initiation of sediment movement due to the enhanced shear stresses formed over megaripples. Thus, significant erosion of fine sand across the inner shelf may only occur adjacent to megaripple bands during these events. This is consistent with observations from the side-scan sonar surveys, which show a southern increase in extent of the megaripple field at Whangamata between Mar-84 and Mar-85, in an area previously characterised by fine sand and coarse megaripple bands.

On the mid shelf surface (> 45 m water depth), the wave mobilisation program predicts that no wave-induced entrainment of sediments should occur (Figure 10.6). This is supported by the consistently different orientation of megaripples in sonographs on the mid shelf surface compared to inner shelf bedforms. Under these storm conditions, deposition of muds out of suspension would be possible as the storm wanes. These could be derived either from flood deposits transported offshore by downwelling currents, or mid shelf muds reworked from areas further south.

Extreme Storm Events

Observations made 2 years after the occurrence of an extreme storm event (Cyclone Bola), indicate significant changes in shelf sedimentation between Whiritoa and Whangamata, with erosion of the lower nearshore fine sands, and their deposition further offshore on the inner shelf. It is concluded that the most intense transport of shelf sediments occurs during relatively infrequent but intense storm events (1 every 14 to 30 years, wind force 8 to 10 Beaufort Scale or 17 to 25 ms^{-1}; HAY; 1991). No data have been published on the wave conditions associated with Cyclone Bola in 1988, but a similar extreme storm event in Jul-78 produced waves with a maximum height of 9 m and peak period of 12 s (PEEK, 1979). HARRIS *et al.* (1983) note that waves exceeding 3 m height do not persist for more than 36 hours, and greater than 4 m for no more than 12 hours. Such conditions will be sufficient to entrain sediments out to mid shelf depths (45 m), and thus produce very high suspended sediment concentrations for short durations (10 to 1000 $kg.m^{-2}$ across the nearshore, and 10^{-2} $kg.m^{-3}$ on the inner and mid shelf; Figure 10.6).

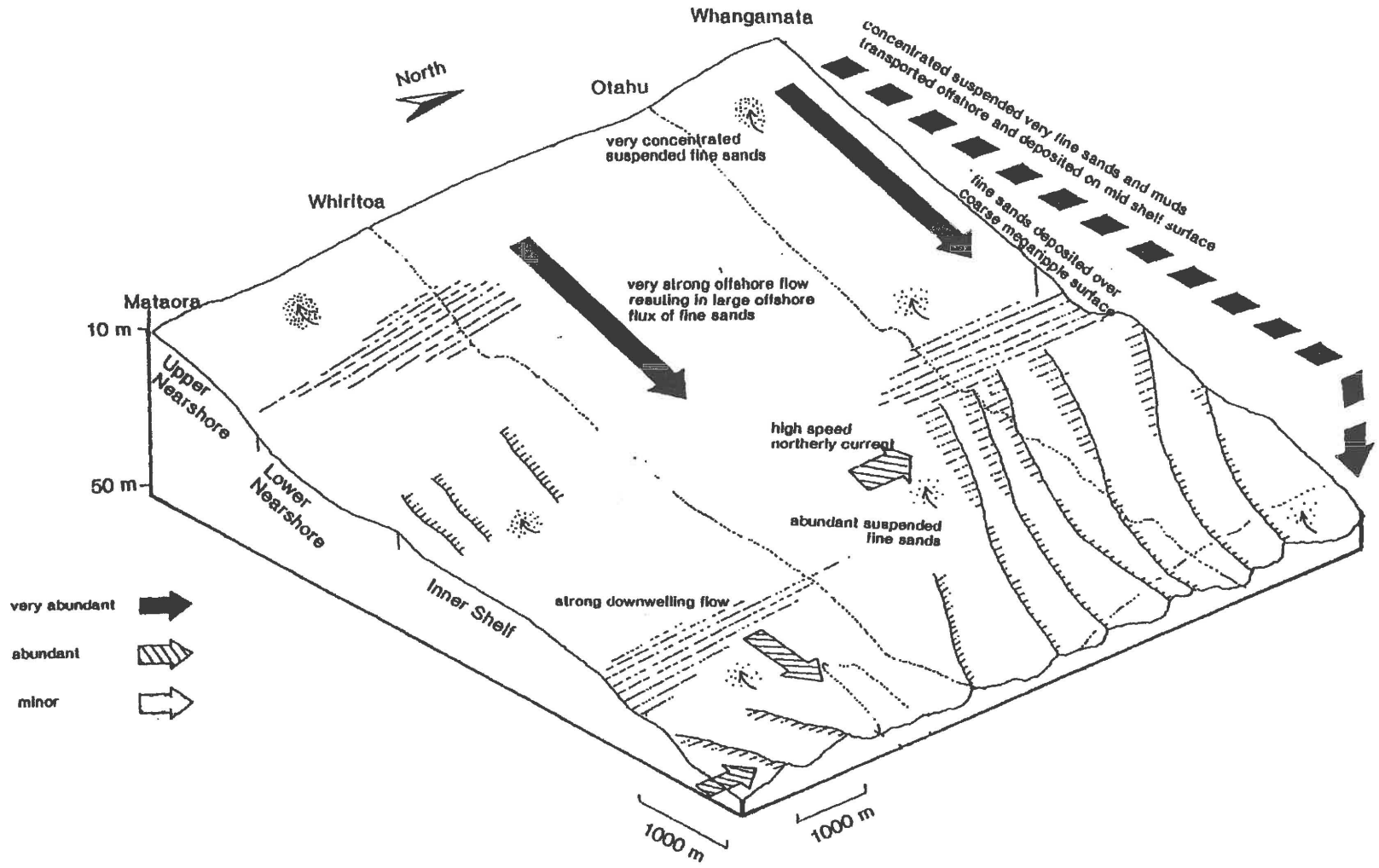

Figure 10.9. Shelf transport processes occurring during an extreme storm event (Cyclone Bola 1988), based on side-scan sonar and bathymetric surveys from Jun-90 between Mataora and Whangamata. Important features are the very high entrainment of fine sediments over the nearshore surface by storm waves, their offshore transport by strong seaward flowing currents to the inner and mid shelf surfaces, and their along-shelf transport by strong wind-generated currents.

Depending on the wind direction associated with these infrequent events, a similar current pattern is expected to develop as during the less intense storms (Figure 10.9).The extensive erosion of lower nearshore deposits and very high suspended sediment concentrations could lead to the development of gravity-induced hyperpycnal plumes, which retain and transport fine material in suspension across the nearshore slope. Such flows have been observed under similar conditions by WRIGHT *et al.* (1986) on the southern mid Atlantic Bight when abundant fine sands are entrained into suspension. This would account for the observed morphological changes following Cyclone Bola. Alternatively, the very strong onshore winds associated with these extreme events could develop a more intense downwelling flows than occur in moderate storms, and thus result in a large offshore flux of fine sediments. Whatever the cause, the very high suspended sediment concentrations and strong offshore flows result in large quantities of fine material transported offshore, with fine sand deposited across the inner shelf surface, and very fine sands probably deposited further offshore over the mid shelf plain.

One important observation is that even two years after Cyclone Bola, fine grained sediments had not returned to their original Mar-84 location at Whangamata and Whiritoa. Thus, the onshore return of lower nearshore fine sands is probably a very slow process, particularly within the first few years when a flat inner shelf surface dominates, and no megaripples are exposed to enhance the entrainment of fine sands. This onshore reworking may therefore only commence once coarse megarippled sands are extensively exposed through scouring by storm waves and currents. Observations in this study show numerous, small, shore-parallel, elongate coarse megaripple bands present two years after Cyclone Bola. This may indicate that the onshore reworking of fine sands has begun, and will continue at an increasing rate as more megaripples are exposed. If the Jul-78 storm produced a similar offshore transport of nearshore sands at Whangamata, then a period of at least 6 years may be necessary before these will return to their original Mar-84 location.

Sedimentation Patterns Between Mercury Bay and Whangapoua

Embayments between Mercury Bay and Whangapoua on the northern east Coromandel coastline are expected to show some important variations from this conceptual model for shelf sedimentation on the southern exposed coastline. These differences include:

1. Mercury Bay and Whangapoua will be less frequently reworked by waves and currents during calm periods, due to their sheltered physiography. This is supported by the occurrence of extensive live shell fish beds on the inner shelf from both areas (Chapter 6.2.2.).

2. Shelf sediments off Opito Bay and Otama Beach will be frequently reworked under all conditions due to the presence of strong tidal- and wind-generated currents through the adjacent Hole in the Wall channel. This is supported by current measurements from Opito Bay (Chapter 4.5.1.), the textural patterns of Otama shelf sands (Chapter 5.3.2.), and the presence of current-generated bedforms off Otama Beach (Chapter 6.2.2).

3. Mercury Bay inner shelf sediments will have higher suspended sediment concentrations than other shelf areas during storms from an easterly direction, due to the very fine texture of shelf sediments, as predicted by the wave mobilisation program (Figure 10.6).

4. The set-up of coastal waters and hence formation of downwelling currents may be important for shelf sedimentation in Mercury Bay during easterly storm events when strong winds blow onshore. This is shown by the apparent formation of sand waves at Wharekaho Beach following Cyclone Bola in Mar-88 (Chapter 6.2.2.).

5. Due to the northerly exposure of the Kuaotunu Peninsula, and the presence of the Mercury Islands further offshore, sediment transport off Whangapoua is expected to be low, and dominated by wave-induced sediment transport through the refraction of storm waves around the Mercury Islands. This deduction is supported by: box cores from Whangapoua (Chapter 8.3.), which show anaerobic fine sands dominating inner and mid shelf surface deposits; diver observations which show bedforms restricted to small ripples in depths of < 20 m (Chapter 6.3.); and current measurements which show that only very weak flows (< 0.10 $m.s^{-1}$) occur over the shelf (Chapter 4.5.1.).

10.3. DIABATHIC BEACH-SHELF INTERACTIONS

Having modelled the processes of nearshore and inner shelf sedimentation along the east Coromandel shelf, it is now pertinent to expand on these and consider the diabathic links of shelf sediments with the local beach and barrier systems. This is undertaken through incorporating data on the texture and mineralogy of beach, barrier, surfzone, nearshore and fluvial sands (see Chapter 5 and 9), with field observations of beach morphodynamics under calm weather conditions, and during one moderate storm event. Pocket and barrier spit beach systems have continually shown different morphological and sedimentological characteristics in this study, and are thus modelled separately in terms of their diabathic interactions with the shelf surface.

10.3.1. Pocket Barrier-Beach Systems

Results in this study support the earlier conclusions of HEALY (1981), that pocket beaches such as Mataora and Whiritoa generally represent isolated systems, with no sediment exchange occurring either along-shore or offshore beyond the surfzone. This is shown by the lack of textural and mineralogical overlap between beach and upper nearshore deposits. However, pocket systems on the northern coast at Hotwater and Otama do show a strong textural and

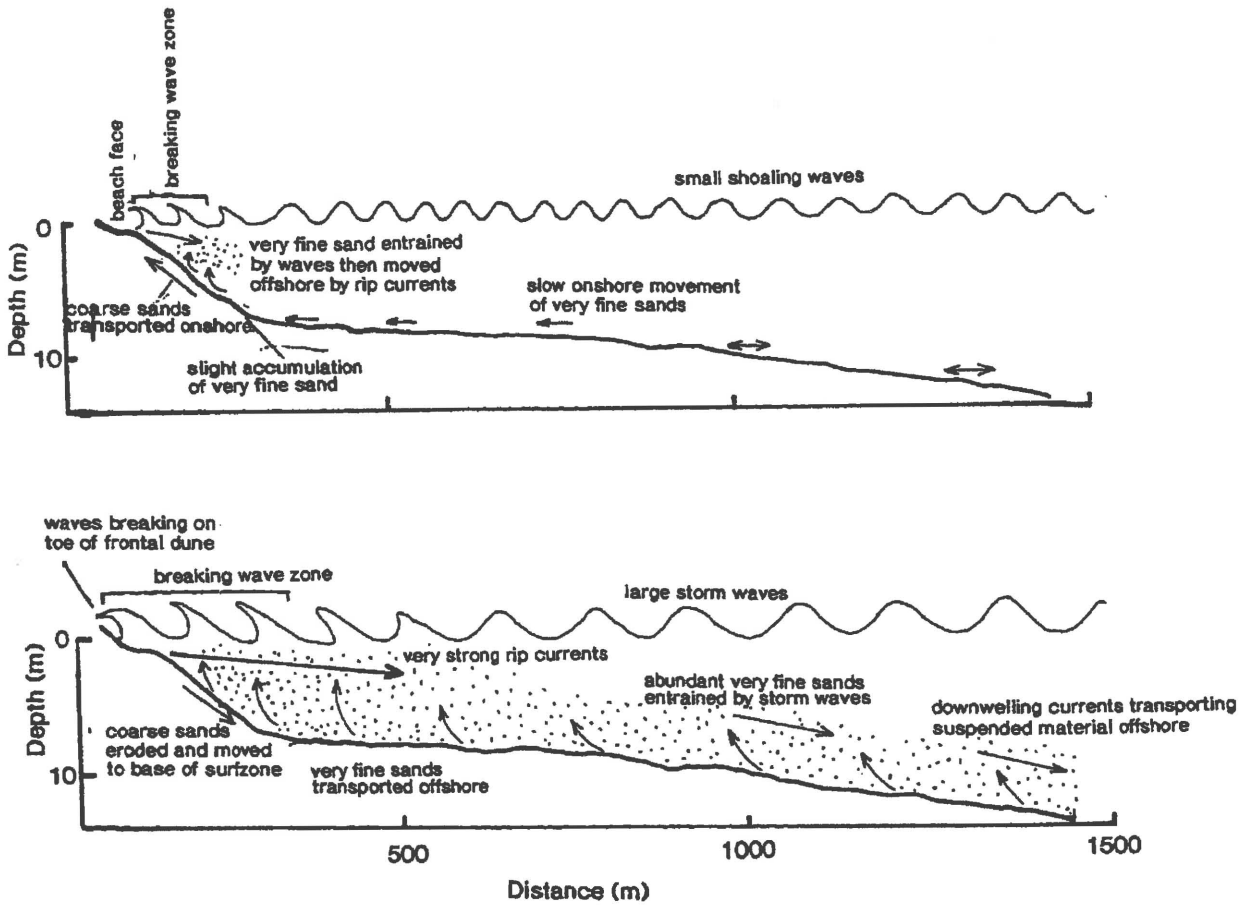

Figure 10.10. Conceptual model showing the response of pocket beach systems to fair and storm weather conditions (offshore profile based on published data in HEALY, 1981): a) fair weather periods (H = 1.5 m, T = 6 s) characterised by the onshore transport of coarse sands by shoaling waves, but very fine upper nearshore sands unable to enter the surfzone due to the presence of turbulent, high energy conditions, and offshore flowing rip currents; b) Storm conditions (H = 3 to 5 m, T = 7 to 10 s) with coarse sands eroded from the beach face and surfzone, then transported offshore by strong rip currents, and very fine upper nearshore sands entrained and transported offshore by rip and downwelling currents.

mineralogical overlap between beach and nearshore deposits, which suggests a diabathic beach-shelf coupling may be present in these northern locations.

A conceptual model for sediment transport processes within southern pocket beach systems is shown in Figure 10.10, based on short-term field observations in this study, and previously published data from Whiritoa Beach (HEALY, 1981). An important aspect of pocket beaches is the sharp increase in slope at the nearshore-surfzone boundary. This should produce a relatively high wave energy surfzone, due to only minor frictional dissipation of incident wave energy across a narrow and steep offshore surface. This is consistent with field observations of transverse bar and rip morphologies dominating during calm weather conditions (see Chapter 2.4.3.). Thus, very fine grained upper nearshore sands will not be transported across the surfzones of pocket beaches during calm weather periods, as these would be entrained by breaking waves and transported offshore by rip currents if they were to enter the surfzone (Figure 10.10 a). The apparent diabathic couplings between beach and nearshore deposits at Otama and Hotwater Beach may result from the presence of coarser nearshore deposits in these northern regions, which can be transported onshore across such steep and high energy surfzones.

During storm conditions, pocket beaches were observed to develop relatively wide surfzones (~ 200 m), with large rip currents eroding into the beach face, and then flowing several hundred metres offshore (Figures 10.10 b and 10.11). The presence of both high breaking waves (~ 3 m in Aug-89) and strong rip currents causes extensive erosion of beach sands within rip embayments, which may be transported offshore onto the lower surfzone surface. Further offshore on the upper nearshore surface, fine material will be entrained in very high suspension by these storm waves (Figure 10.6), and subsequently transported offshore by the strong rip currents, or further seawards by downwelling flows generated by strong onshore winds.

Thus, the main impact of storm events on pocket systems is to excavate deep rip channels into the beach face, possibly extending onto the backshore and frontal dune, and to transport coarse sands offshore across the surfzone. The coarse sands will then be reworked back onshore by shoaling waves during subsequent calm periods. This cycle of episodic cut and fill was observed in the field at Whiritoa Beach during this study, when several moderate storms forced beach sands to retreat behind the southern headland in winter 1989, which subsequently prograded seawards beyond the headland during prolonged calm conditions in autumn 1990. Therefore, in the absence of unnatural losses such as sand extraction, pocket beach systems should remain relatively stable, with only minor onshore losses into dune blowouts, which are possibly balanced by gains from cliff erosion and local streams.

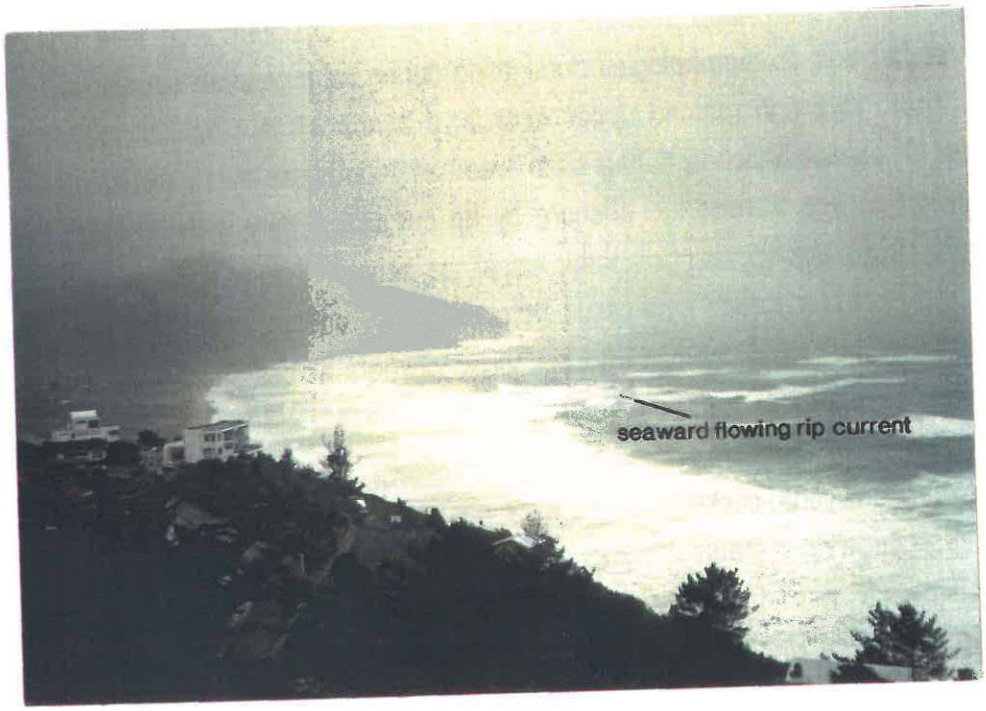

Figure 10.11. Typical observed response of a pocket beach system to storm wave conditions (Tairua Beach, 7-Sep-89), with a wide breaking wave zone present and strong rip currents flowing several hundred metres seawards of the outer breaker zone.

10.3.2. Barrier Spit Systems

The fine grained sands which dominate barrier spit beach and surfzone deposits, show textural and mineralogical overlaps with adjacent upper nearshore sands on both the southern and northern coastline (see Chapters 5.4. and 9.2.). Thus, there is positive evidence that barrier spit beaches are diabathically coupled to their adjacent upper nearshore surfaces, and form open sedimentary systems with the continental shelf.

An important characteristic of barrier spit beach systems is that offshore gradients appear to gradually decrease seawards from the beach face to the surfzone and nearshore zone. Thus, wave energy will be dissipated across a wide and flat surfzone. Under fair weather conditions, shoaling waves can therefore transport fine sands onshore from the upper nearshore zone, where they are attached to the beach face as a series of ridge-runnels or low tide terraces (Figures 10.12, 10.13, and 10.14). Another important feature is that ebb tide deltas are formed at the mouth of adjacent harbour inlets, and appear to be skewed into the surfzone to form an offshore bar during calm conditions. Textual and mineralogical analysis of beach samples in this study has shown good evidence for modern barrier spit deposits being derived from onshore terrigenous sources. Thus, reworking of these ebb tide delta deposits onto the beach face may be the process by which such terrigenous sands are incorporated into barrier spit systems, as proposed for Pauanui Beach by GIBB and ABURN (1986). Further evidence also comes from beach erosion surveys by HEALY *et al.* (1981), which showed the distal end of some barrier spit systems (Matarangi, Cooks, Pauanui, and Whangamata) to be characterised by accretion at the point of ebb tide delta attachment.

During storm conditions, two slightly different responses for barrier spit beaches were observed on the southern exposed and northern embayed coastline. During storm conditions on the southern coast, waves begin dissipating over multiple bars about 500 to 800 m offshore, and then developed a rhythmic erosion pattern on the beach face. At Waihi, large rips were observed forming in these embayments, which flowed several hundred metres offshore beyond the outer breaking wave zone. As barrier spit beach deposits are fine grained sands, these rips provide a potential mechanism for the offshore transport of beach and surfzone deposits onto the upper nearshore surface. This offshore transport is presumably most severe during extreme storm events, such as in July 1978, when extensive beach and frontal dune erosion occurred along the east Coromandel coast (HEALY *et al.*, 1981). Rip embayment erosion into the frontal dune also provides the potential for onshore loss of beach sediments into dune blowout systems.

On deeply embayed barrier spit beaches, storm conditions produce a very distinctive dissipative character, with waves first breaking 500 m offshore, where they then progressively spill and decay landwards across the surfzone (Figures 10.12 b and 10.15). Standing waves were apparent during storms, as shown by observations of the water line moving in the order of 100 m across the beach face onto the back shore area. These standing waves allow the surfzone to be

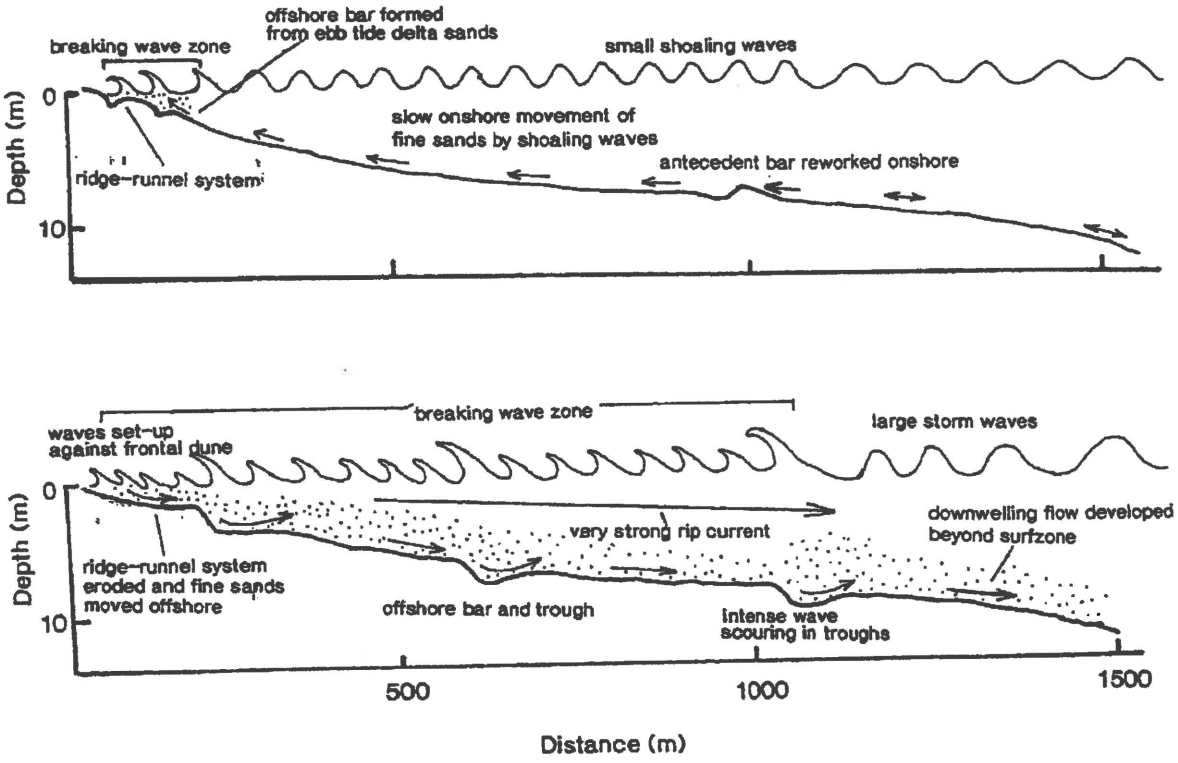

Figure 10.12. Conceptual model showing the response of barrier spit beaches to fair and storm weather conditions (profile based on bathymetric data from Pauanui Beach, as published in GIBB and ABURN, 1986): a) fair conditions (H=1.5 m, T=6 s) characterised by waves shoaling across the upper nearshore and surfzone, resulting in a slow onshore movement of fine sands, and their attachment on the beach face as ridge-runnel systems; b) storm conditions (H=3 to 5 m, T=6 s) with waves breaking about 1000 m offshore and dissipating across the wide surfzone. Standing waves are developed within the surfzone, which cause waves to be set-up against the frontal dune, and erosion of beach and foredune sands. Further seawards, waves scour surfzone sands and form numerous offshore bars. Fine sands are then transported offshore by either strong seaward flowing rip currents, or bottom return flows.



Figure 10.13. Waihi Beach during calm weather conditions (4-Sep-89), showing numerous ridge-runnel systems attached to the beach face. Note the scarped embayment on the frontal dune, which indicates erosion by strong rip currents during the last major storm event.

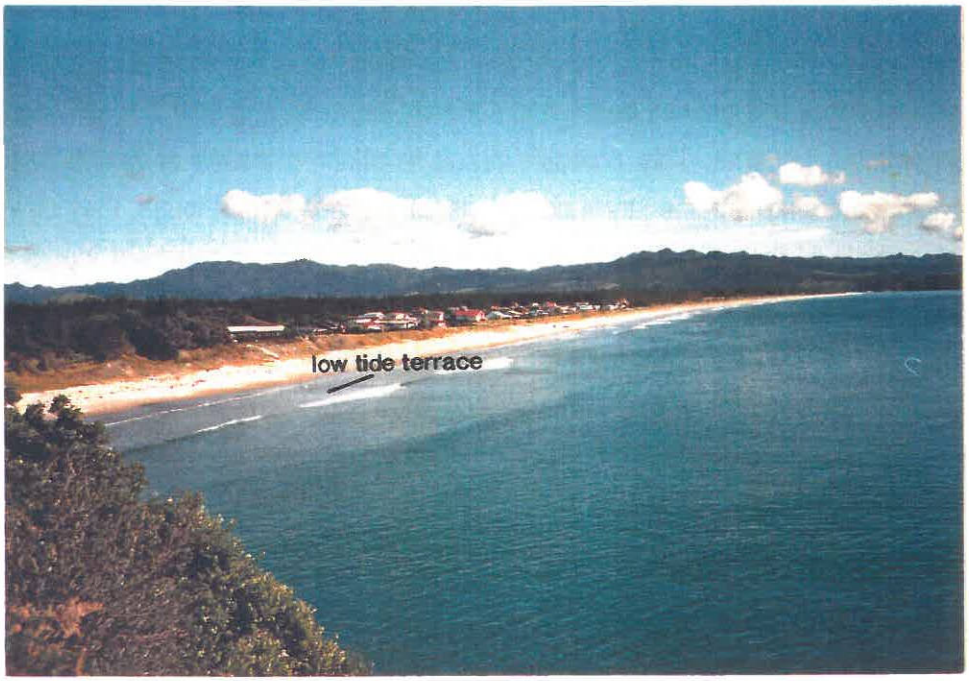

Figure 10.14. Matarangi Beach during calm weather conditions (11-May-89), showing a continuous low tide terrace feature along the beach face.



Figure 10.15. Matarangi Beach under storm conditions (7-Sep-89), showing a very wide and dissipative surfzone, with wave bores penetrating and eroding the back dune area.

set-up against the frontal dune, which could cause severe erosion and back dune flooding along the beach. They will also produce a strong seaward flow across the sea floor, resulting in the offshore transport of beach and surfzone sands, possibly onto the upper nearshore surface (e.g. SHORT and WRIGHT, 1984).

Thus, barrier spit systems are inferred to be relatively unstable in the short-term, due to the very dynamic nature of their fine grained beach and surfzone deposits, and their diabathic coupling with shelf sedimentation patterns. This probably result in offshore losses of beach sands to the nearshore surface during extreme storm conditions. In the long-term, though, they may have the potential to accrete at their distal ends, due to modern terrigenous sediment inputs from local infilling harbours. However, it is hard to account for the large volumes of sand presently found on most barrier spit systems as derived from reworking of terrigenous harbour sediments (exceptions possibly found at Buffalo Beach, Kennedy Bay and Waikawau). The lithology of barrier sands is strongly affiliated with those found on the lower nearshore and inner shelf surfaces in most barrier spit systems. Thus, it is possible that in earlier Holocene times, the shelf was a major source for barrier spit deposits. In most locations, however, this pattern may have been been reversed, with the shelf now acting as a temporary repository for eroded beach sands during storm conditions.

10.3.3. Summary of Beach-Shelf Interactions

The diabathic links between local beach systems and the shelf is important in understanding sedimentation processes along the east Coromandel coast. At present, coarse grained pocket beach systems on the southern coast are isolated from the shelf, with no gains or losses from adjacent nearshore sediments. Barrier spit beaches, and some northern pocket beaches (Hotwater and Otama), do appear to be diabathically linked to the upper nearshore surface, with sands eroded from their beach and surfzones and transported offshore during storms. Barrier spits also appear to be linked to sedimentation patterns within adjacent harbours, with some terrigenous sediments from infilling harbours incorporated into ebb tide deltas, and later welded onto the beach face. The main factors which cause these differences in sedimentation patterns between pocket and barrier spit systems are inferred to include the contrast or similarity in texture between beach and upper nearshore deposits, the presence of infilling harbour systems adjacent to barrier spits, and the presence of either a steep high energy, or broad dissipative surfzone.

Variations in these factors between pocket and barrier spit beaches is difficult to explain by present sedimentation processes along the coast. It is therefore likely that they are inherent characteristics, associated with the particular late Quaternary sedimentation history of pocket and barrier spit beach systems. The composition and texture of barrier and beach sands may assist in these interpretations, with pocket barriers composed of similar deposits to both Pleistocene inner barriers and Holocene transgressive sands, thus suggesting their formation

from reworking of these sediments. Barrier spit systems, however, show textural and compositional affiliations with fine grained nearshore sands, and may thus have formed from the onshore reworking of these deposits. Thus, the two types of beach-barrier systems along the east Coromandel coast were probably established very early in the Holocene, when shelf sediments were reworked by the marine transgression. This final, but important aspect of coastal sedimentation for the study area, i.e. Holocene evolution, is examined in the following section.

10.4 HOLOCENE EVOLUTION

In preceding sections of this chapter, various conceptual models have been proposed to account for the morphology and distribution of shelf deposits along the east Coromandel coast in terms of contemporary hydrodynamic processes. While these may help to explain the present surficial sedimentation patterns, they cannot completely account for their initial establishment. For instance: why did fine sands develop into a steep nearshore slope, and coarse sands a flatter inner shelf surface ?; or why did coarse grained pocket embayments form closed sedimentary systems, while fine grained barrier spits developed into an integral part of the shelf sediment transport system? In an attempt to address such open questions, a conceptual model is presented which infers the response of the east Coromandel coast to three important stages during the late Quaternary period: the Last Glacial lowstand; the Holocene marine transgression; and the Holocene stillstand.

Much of the basis for this model comes from interpretations of the shallow sub-bottom seismic stratigraphy in Chapter 8. These interpretations include:

1. Present surface sedimentation patterns generally coincide with extensive Holocene seismic stratigraphic units, which implies that similar sedimentation processes have occurred throughout most of the Holocene stillstand.

2. Very fine grained upper nearshore terrigenous sands coincide with a thick accretionary wedge (7 to 20 m thick) in water depths of < 20 m.

3. Fine grained shelf sands form a thick lower nearshore wedge (5 to 7 m thick) in depths of 20 to 30 m, and either a continuous sheet (5 m thick), or discontinuous lobes (1 to 5 m thick) over the inner and mid shelf surfaces.

4. Medium to coarse grained inner shelf storm lag deposits generally coincide with an extensive basal Holocene transgressive sheet, which ranges in thickness from 5 m off Waihi Beach, Whiritoa, and Onemana, to 10 m off Whangamata and Whitianga.

5. Extensive Pleistocene alluvial deposits occur within deep and broad palaeo-river channels beneath the shelf surface off barrier spit beaches (Waihi north, Whangamata, Mercury Bay), but are generally absent off pocket beach systems (Whiritoa and Onemana).

6. Extensive subsurface deposits occur below the shelf south of Whangamata, but north of here basement rock rises close to the sea-bed, thus limiting thick subsurface sequences to areas such as Mercury Bay where deep river valleys have been incised.

In addition, the model incorporates results from similar storm-dominated shelf settings, with the North American mid-Atlantic shelf providing a basis for conditions during the Holocene marine transgression, and models from the east Australian coast used to infer processes during the Holocene stillstand.

10.4.1. Last Glacial Low Stand (25 000 to 12 000 y. B.P.)

During the latter stages of the Glacial period, sea level fell to a minimum of 120 m below present about 17 000 y. B.P. (CHAPPELL, 1983). Interstadial conditions prior to this fall in sea level were examined in Chapter 8.5., and are inferred to have been characterised by extensive barrier progradation in the region offshore from Waihi Beach (and further south in the Bay of Plenty), while the coastline to the north was under similar shelf sedimentation conditions to those presently found (see Figure 8.27).

As the present continental shelf break varies in depth from 125 m off Waihi Beach, to 200 m north of the Alderman Islands, a 120 m fall in sea level would dramatically change the east Coromandel coastline physiography. In the area south and immediately north of Mayor Island, the coastline would be found on the continental slope, whereas further north, the coast should occur about 10 km from the shelf break.

Through integrating this physical setting with stratigraphic interpretations from Chapter 8, a conceptual image of the coastline is generated in Figure 10.16. It is inferred that previous shelf deposits off Waihi Beach (and south in the Bay of Plenty) were reworked offshore by the ancestral Wairoa, Kaituna, and Tarawera River systems. As the coastline was located on the shelf break, much of these deposits would have been lost over the continental slope, thus restricting the development of barriers along the coastline.

Further north at Whiritoa, abundant pre-existing Pleistocene sediments would be exposed over the shelf surface. However, as no major river systems are present in this area, sediment reworking was probably limited to transgressive dune deposits. Such aeolian features may still be preserved on the shelf surface, as shown by the presence of a hummocky Pleistocene surface on the present sea-bed in seismic profiles.

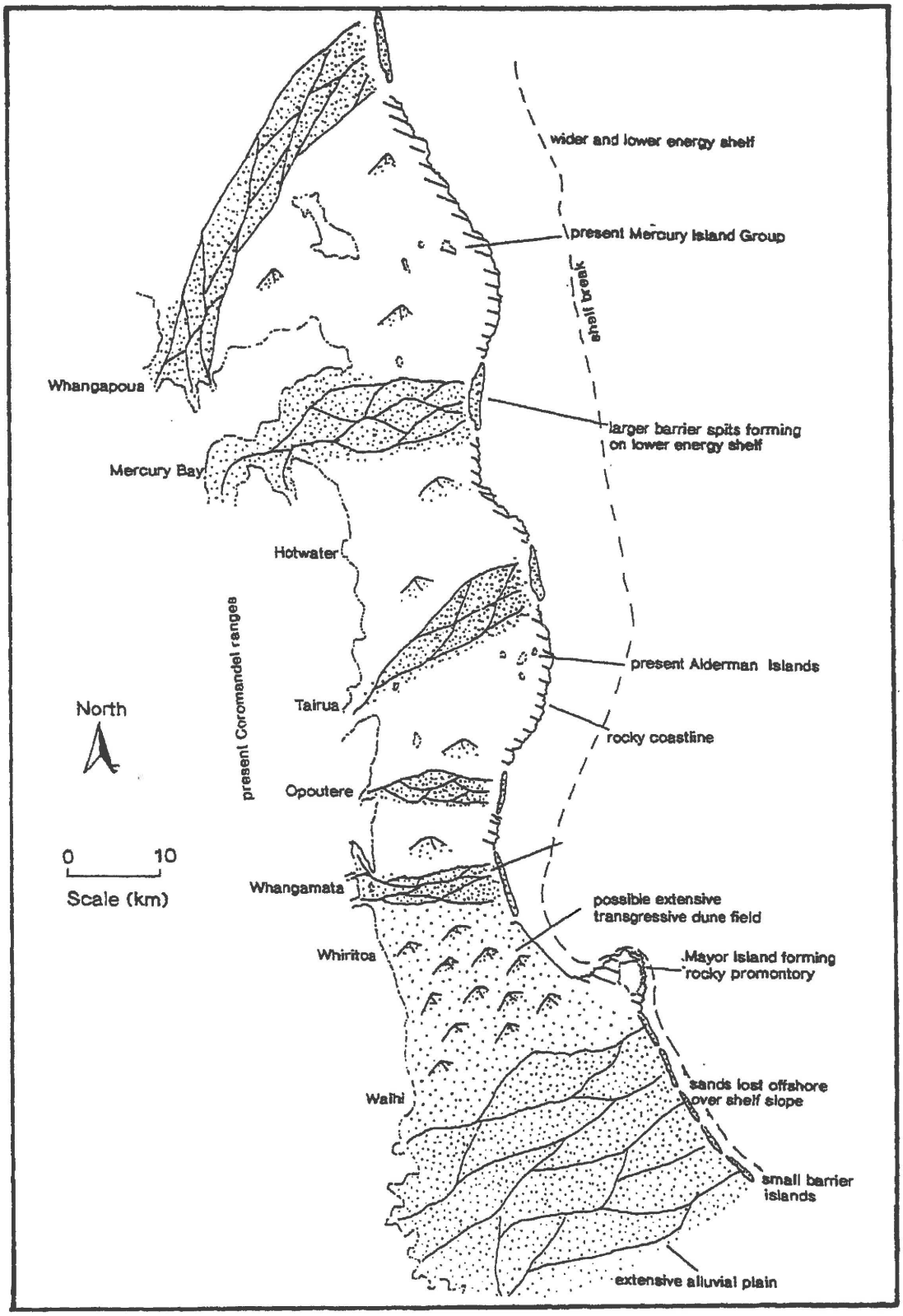

Figure 10.16. Inferred physiography of the east Coromandel coastline during the last Glacial period (17 000 years B.P.) when sea level was 120 m below present. Important features include: an extremely narrow shelf and high energy coastline south and immediately north of Mayor Island, but a broader and lower energy shelf north of here; extensive alluvial deposits south of Mayor Island delivering large quantities of sand to the coast, which are subsequently lost offshore to the continental slope; extensive aeolian dune deposits east of Whiritoa; a dominantly rocky coastline north of Mayor Island, and intervening areas of extensive alluvial deposits delivering large quantities of sand to the coast to form extensive barrier spits.

North of Whangamata, pre-Holocene sediment units appear to be very limited in seismic profiles, and thus a rocky coastline was probably found offshore from small pocket embayments (e.g. Onemana). However, off present barrier spit systems at Whangamata and Mercury Bay, thick alluvial deposits are evident in seismic profiles, and thus extensive river systems may have supplied large quantities of sediment to the coast. As this coastline would be of lower energy than that south of Mayor Island, conditions may have favoured the development of extensive barrier spits from these fluvial deltaic deposits.

Thus, the setting prior to the Holocene marine transgression is inferred to be characterised by relatively large quantities of non-cohesive sand at the mouths of relatively large river systems north of Mayor Island. Off Waihi and Whiritoa, significant areas of non-cohesive sands were presumably located landwards of the coastline in extensive unconsolidated alluvial and aeolian deposits. However, off pocket embayments north of Whangamata, a very rocky subaerial surface with only a thin veneer of unconsolidated sediments is likely to have been present.

10.4.2. Holocene Marine Transgression (12 000 to 6500 y.B.P.)

At the end of the Glacial low stand, sea level began to rise rapidly at a rate of approximately 10 to 15 $mm.y^{-1}$ (THOM and ROY, 1983). Under these transgressive marine conditions, the coastline is inferred to have been subject to similar processes of barrier retreat and shoreface erosion as occurs on the present North American mid-Atlantic shelf (see Figure 3.10), with coastal deposits literally 'buldosed' landwards by processes of aeolian, washover, and tidal delta formation, and the incorporation of underlying pre-Holocene substrates into transgressive sand sheets. Therefore, the size and composition of transgressive deposits would have been determined by the characteristics of their pre-Holocene substrates.

Off present barrier spit systems, transgressive deposits are inferred to have been derived from the reworking of extensive alluvial deposits, as transgressive barriers were driven landwards along the palaeo-river valleys identified in seismic records (Figure 10.17). However, off pocket barrier systems the development of transgressive deposits was more restricted, as these could only be derived from either the reworking of thin underlying substrates (except of Whiritoa), or from longshore reworking of the larger transgressive barrier deposits. This would account for the contrast in thickness of transgressive sand sheets off pocket barriers and barrier spits respectively.

10.4.3. Holocene Stillstand (6500 y.B.P to present)

Present variations in the morphology and deposits found in barrier spit and pocket barrier systems are inferred to result from the different responses of each embayment type during the stable sea level conditions which have occurred for the past 6500 years (i.e. the Holocene stillstand). These responses are presumed to have been very similar to those described for the east

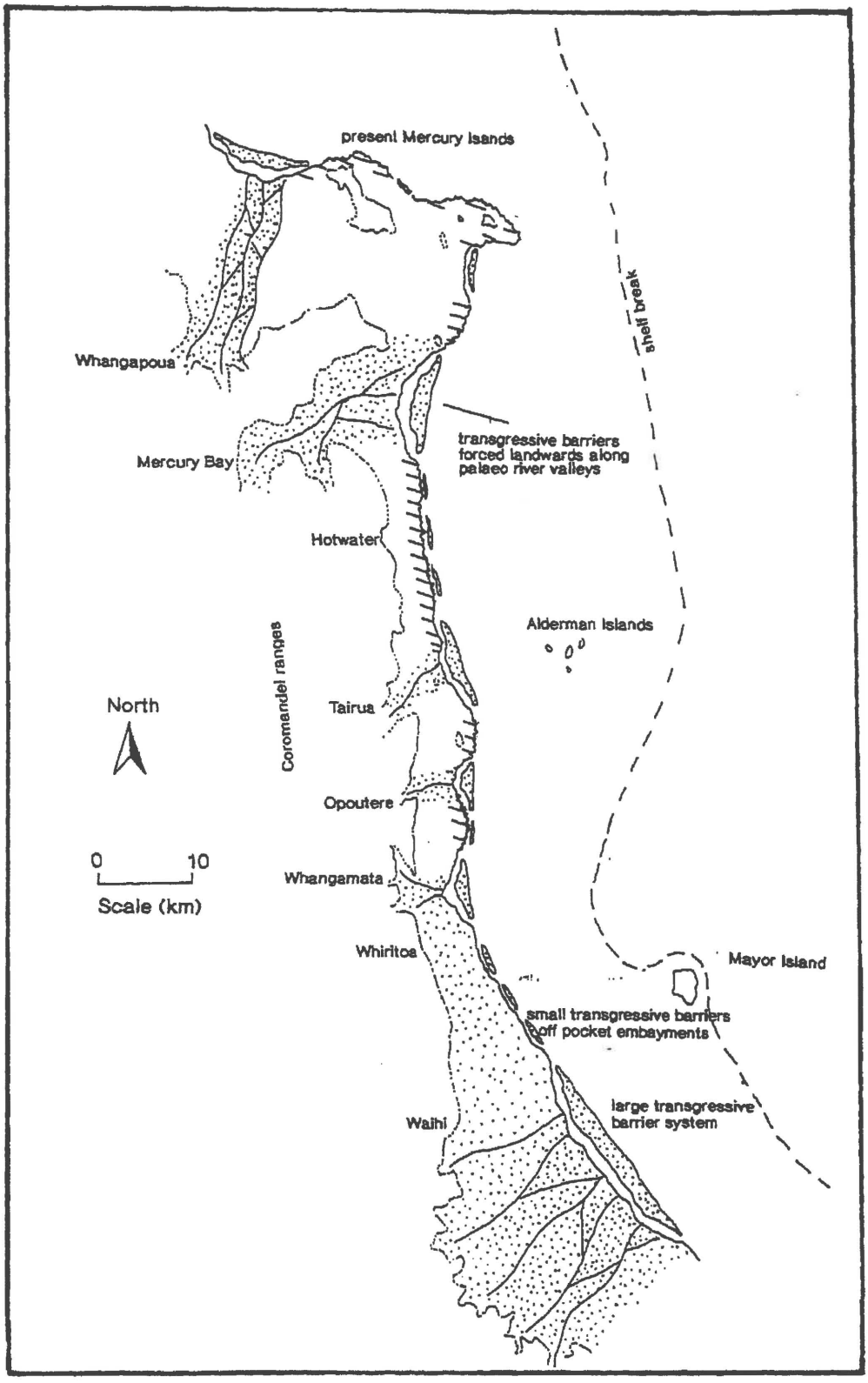

Figure 10.17. Inferred coastal physiography during Holocene marine transgression (~ 10 000 y.B.P.). Important features include: extensive transgressive barrier deposits east of Tauranga formed of reworked alluvial deposits (note that much of the surface shown would have been submarine deposits, with only a narrow subaerial surface present); large transgressive barriers off major river systems along the east Coromandel coast; and only limited transgressive deposits off pocket embayments.

Australian coast by ROY and THOM (1981), as east Australia is characterised by an analogous Holocene sea level history to the east Coromandel coast (see Table 3.1).

Barrier Spit Development

Barrier spit genesis is inferred to have begun during the latter stages of the marine transgression, when sea level rose over the steep coastal boundary zone (< 50 m water depth), and the landward rate of shoreline retreat exceeded the capabilities of onshore sediment transfer (BOYD and PENLAND, 1984). This would result in the development of an over-steepened offshore profile, in disequilibrium with the oceanographic climate (ROY and THOM, 1981; Figure 10.18 a).

The transgressive sands are presumed to have been composed of a mixture of coarse and fine material. Thus, if similar conditions were present when sea level stabilised to those presently occurring on the shelf, equilibrium may have been established by storm waves and currents winnowing fine sand from coarse sediments, with the fine sand subsequently transported onshore under calm weather conditions. The coarse inner shelf deposits developed by this winnowing process would not just simply form a residual lag, but should have accentuated the onshore transport of fine sands during calm conditions, as presently occurs on the inner shelf surface. As large transgressive sand sheets are inferred to have developed from the reworking of extensive alluvial deposits, a large onshore flux of fine sand would occur, resulting in the development of extensive prograded barrier systems, and associated with this a steep concave nearshore surface (Figure 10.18 b). Evidence supporting this comes from the similarities in texture and composition of barrier spit and lower nearshore sediments, and the initial rapid growth of prograded barrier systems in the early Holocene, as found at Matarangi by MARKS and NELSON (1979), and Pauanui by GIBB and ABURN (1986).

Once the original transgressive deposits had been reworked into equilibrium, fine sands would no longer be supplied from offshore, and thus the seaward transport of sediments during storm conditions would begin to balance their landward movement during subsequent calm conditions (Figure 10.18 c). In locations such as Waihi and Whangamata where a significant along-shelf loss of fine sands appears to occur, this may have resulted in the erosion of some beach and nearshore deposits. Dates of barrier deposits from Matarangi (MARKS and NELSON, 1979) and Pauanui (GIBB and ABURN, 1986) show that this stage of stationary or erosional coastal development probably occurred between 3000 to 4000 y. B.P., when barrier progradation rates were significantly reduced.

At some stage during the Holocene stillstand, large amounts of very fine terrigenous sediments have deposited on the upper nearshore (and probably mid shelf) surface (Figure 10.18 d). The offshore accumulation of these terrigenous sediments on the upper nearshore surface would counteract the previous seaward loss of fine sands, and in some locations have even caused

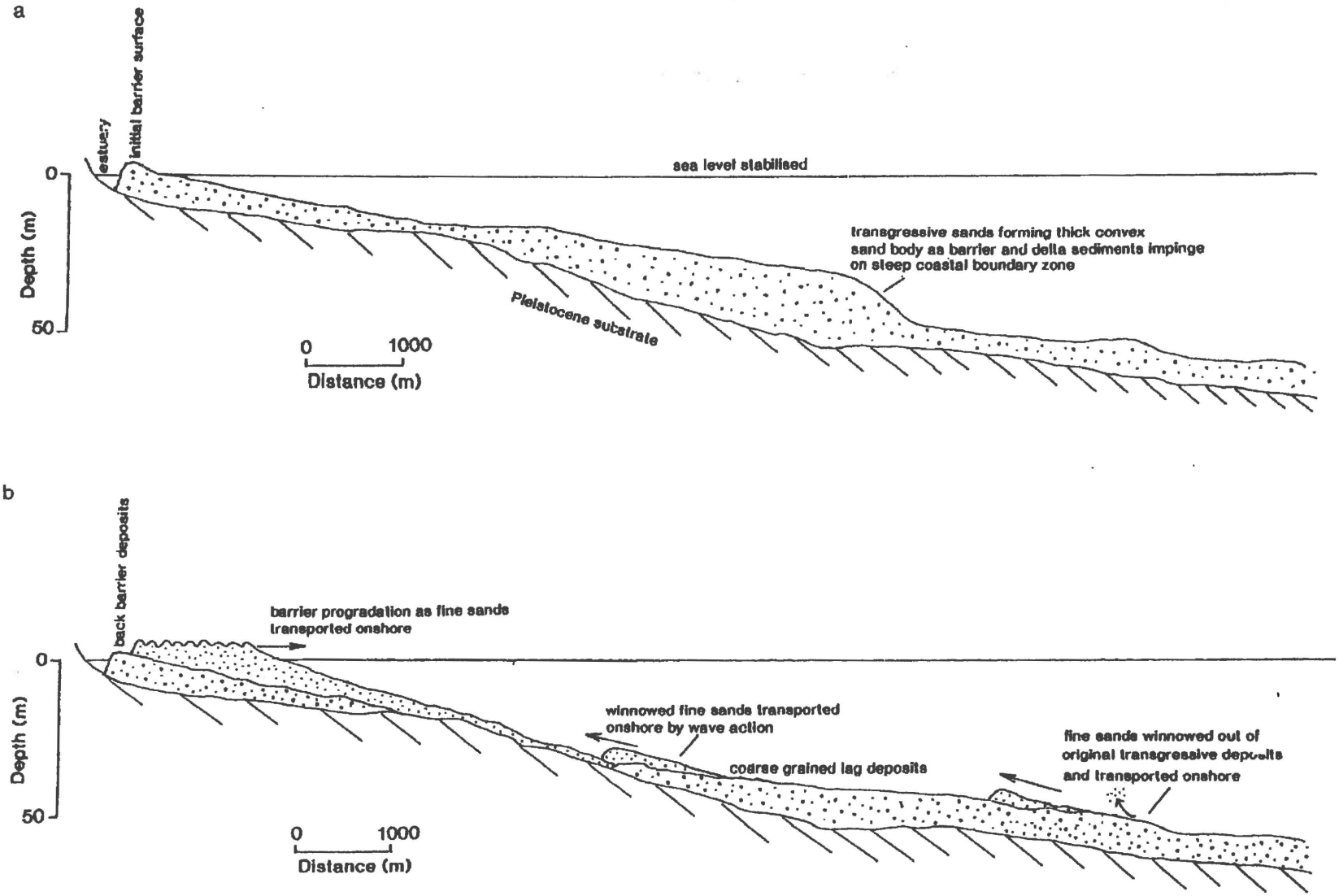
a
estuary
initial barrier surface
sea level stabilised
0
Depth (m)
50
transgressive sands forming thick convex
sand body as barrier and delta sediments impinge
on steep coastal boundary zone
Pleistocene substrate
0
1000
Distance (m)
b
back barrier deposits
barrier progradation as fine sands
transported onshore
0
Depth (m)
50
winnowed fine sands transported
onshore by wave action
coarse grained lag deposits
fine sands winnowed out of
original transgressive deposits
and transported onshore
0
1000
Distance (m)

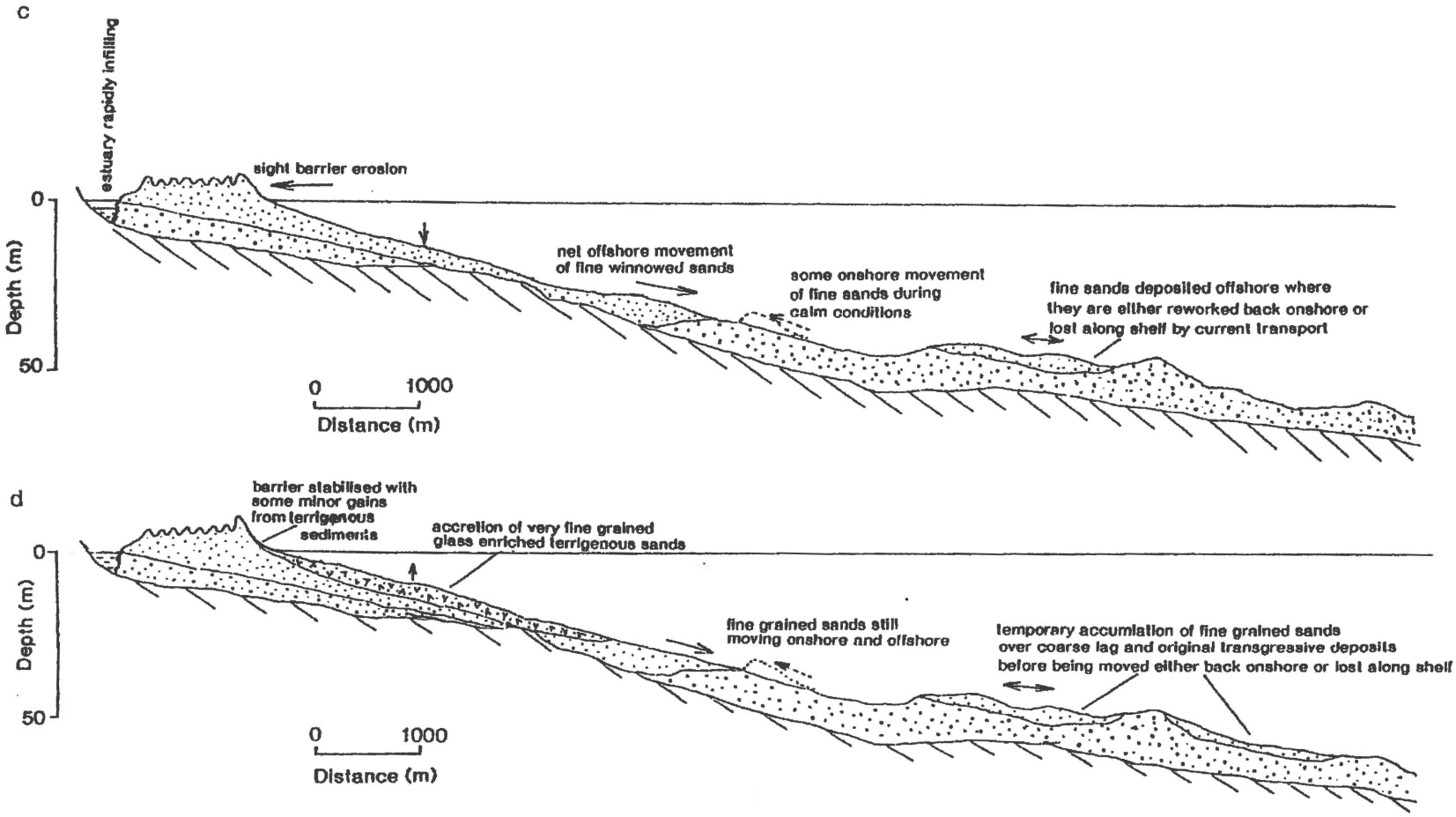

Figure 10.18. Evolutionary model for barrier spit systems (based on seismic stratigraphic patterns at Whangamata): a) convex bulge of sediments formed as transgressive deposits encounter steep coastal boundary zone, with head of transgressive sand body developing into an initial subaerial barrier spit (~ 6500 y. B.P.); b) fine sands winnowed out of original transgressive deposits by storm waves, which were transported onshore during calm conditions as lobes over coarser 'lag' deposits, resulting in development of the nearshore and inner shelf surfaces and barrier progradation (~ 4000 to 5000 y. B.P.); c) erosional phase as offshore fine sand source is depleted, and the seaward removal of these sediments either balances or exceeds their onshore reworking (~ 2000-4000 y. B.P.); d) deposition of terrigenous sediments, resulting in accretion of very fine sands on upper nearshore and mid shelf surfaces (latter not shown), and some fine sands on the beach face.

slight barrier progradation (e.g. 0.06 $m.yr^{-1}$ at Pauanui; GIBB and ABURN, 1986). At Buffalo Beach, this offshore supply of terrigenous sands appears to have resulted in extensive barrier progradation, with a rate of 0.5 $m.y^{-1}$ for the last 1800 years estimated by ABRAHAMSON (1987). This may also have been responsible for the phases of dune deposition in stationary barriers over the last 2000 years, as identified by ABRAHAMSON (1987).

Pocket Barrier Development

In smaller pocket embayments, a similar disequilibrium offshore surface is inferred to have formed as sea level stabilised (Figure 10.19 a). However, as transgressive sand sheets in these locations contained much lower amounts of sediment, it is inferred that insufficient quantities of fine sand were winnowed and transported onshore for subaerial barrier deposits to form (Figure 10.19 b). Instead, small stationary barriers developed from either the erosion and offshore reworking of coarse Pleistocene inner barrier deposits, or from the initial onshore reworking of coarse transgressive sands. In the southern pocket barrier systems, the former is believed to apply, as supported by the following evidence:

1. The presence of Pleistocene inner barrier sediments, and limited Holocene barrier deposits in most pocket embayments;

2. Textural similarities between Pleistocene and Holocene barrier deposits;

3. Abundant heavy minerals (particularly opaques) in the fine sand fraction of many Holocene pocket beach and barrier sediments;

4. The presence of undifferentiated Pleistocene deposits in seismic records off Whiritoa Beach, which appear to rise steeply landwards and link-up with surfzone and beach deposits.

This would account for the development of closed sedimentary systems within southern pocket systems. The source of northern pocket barrier sands is less certain. However, these may be supplied to some degree from the nearshore surface, as shown by the textural and compositional similarities of beach and nearshore deposits at Hotwater and Otama.

As for the barrier spit systems, a steep concave nearshore surface had probably developed about 3000 to 4000 y.B.P., after which similar amounts of fine sands were reworked onshore during calm conditions, and offshore during storms. At Whiritoa though, a net influx of fine sands has occurred from both southern and northern shelf areas, resulting in the development of a thick surficial blanket of fine sands over older lag deposits (Figure 10.19 c). However, as shelf sedimentation patterns are not linked to the beach system here at Whiritoa, this has not resulted in onshore barrier accretion. Modern terrigenous sediments have also deposited on the upper

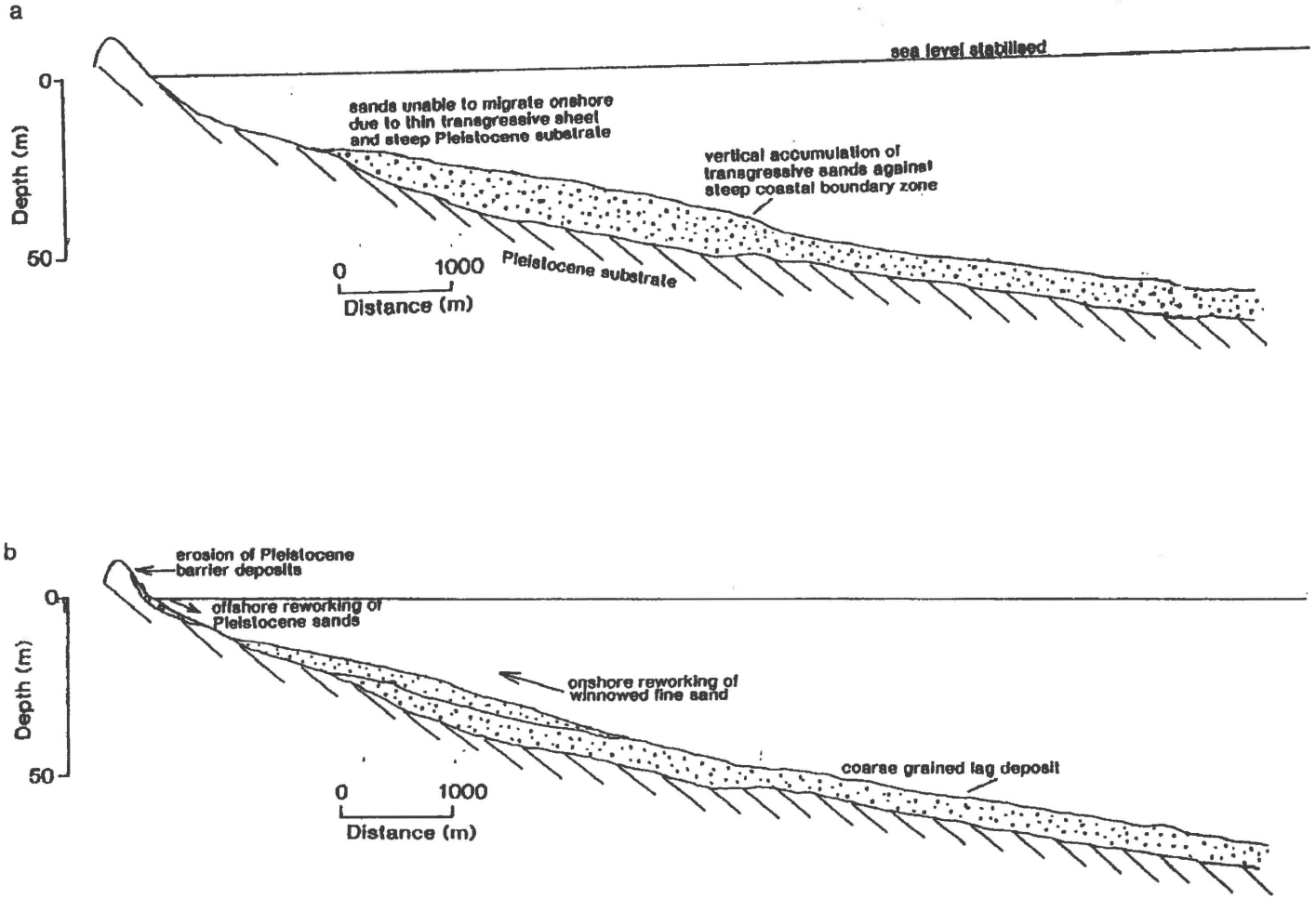
a
sea level stabilised
0
Depth (m)
50
sands unable to migrate onshore
due to thin transgressive sheet
and steep Pleistocene substrate
vertical accumulation of
transgressive sands against
steep coastal boundary zone
0
1000
Distance (m)
Pleistocene substrate
b
erosion of Pleistocene
barrier deposits
0
offshore reworking of
Pleistocene sands
Depth (m)
50
onshore reworking of
winnowed fine sand
coarse grained lag deposit
0
1000
Distance (m)

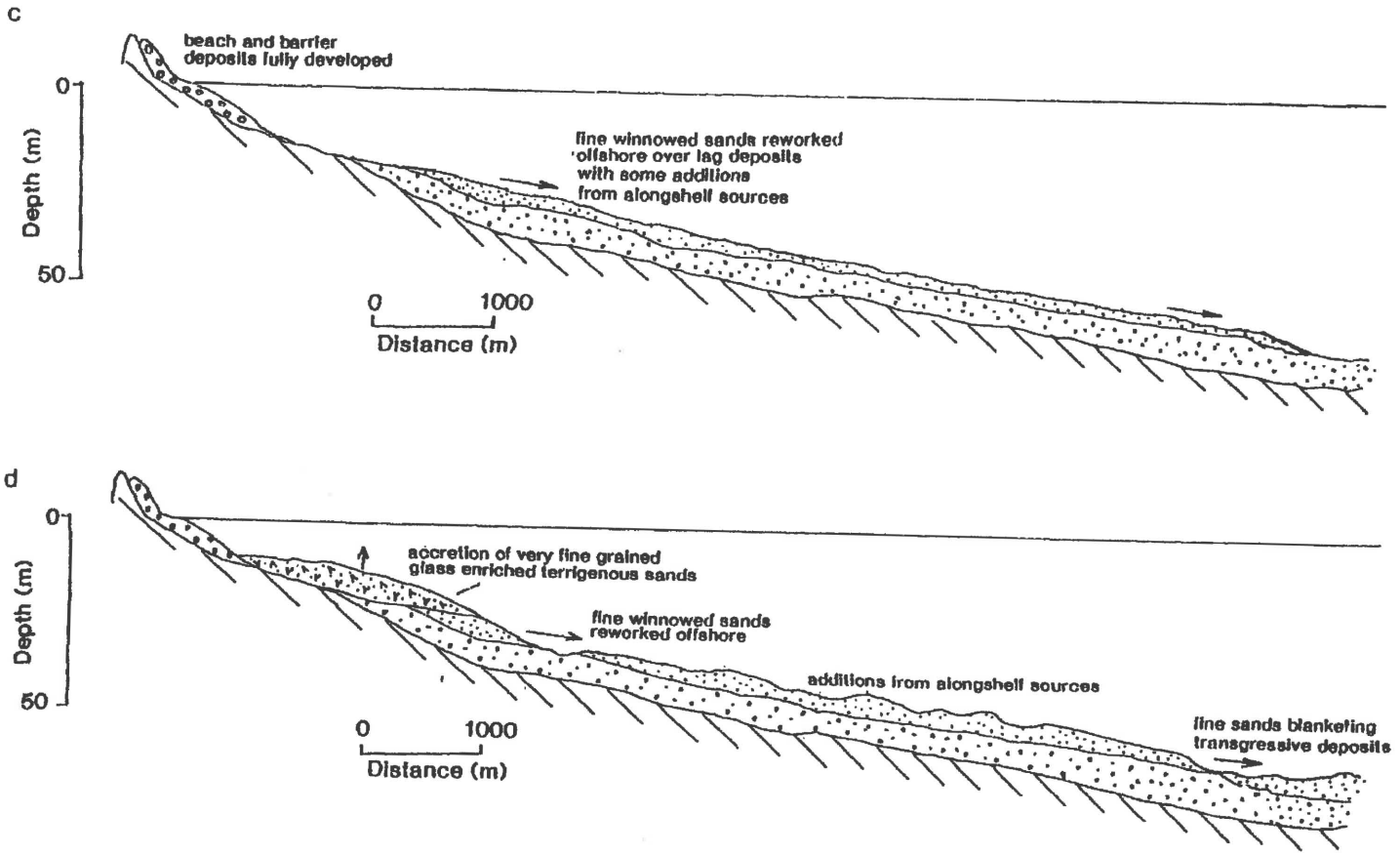

Figure 10.19. Evolutionary model for pocket barriers (based on seismic stratigraphic interpretations from Whiritoa): a) slight convex bulge of sediments formed as transgressive deposits encounter steep coastal boundary zone, however insufficient volume for onshore barrier formation (~ 6500 y. B.P.); b) fine sands winnowed out of original transgressive deposits and transported onshore as lobes over coarser lag deposits, resulting in the development of nearshore and inner shelf surfaces. Barrier deposits formed separately from offshore reworking of older Pleistocene deposits (~ 4000 to 5000 y. B.P.); c) offshore fine sand source depleted, and seaward removal of these sediments either balancing or exceeding their onshore reworking. Here at Whiritoa though, an influx of sediments from adjacent regions results in the formation of an extensive fine sand blanket over coarser inner shelf deposits (~ 2000 to 4000 y. B.P.); d) addition of modern terrigenous sediments.

nearshore surface of pocket barriers, but have been of insufficient quantity to encroach over the steep high energy surfzones into their beach systems (Figure 10.19 d).

Thus, it is proposed that the present shelf morphology and sedimentation patterns on the east Coromandel coast are not simply the result of contemporary oceanographic processes, but to some degree controlled by larger scale events which occurred during and following the Holocene marine transgression. The influence of past depositional environments may trace back even beyond events within the Holocene period, as the nature of pre-Holocene substrates has already been shown in Chapter 8.5 to strongly influence the present shelf morphology.

10.5. CONCLUSIONS

Through integrating data gathered on ocean dynamics, sediment texture, mineralogy, shelf morphology, and stratigraphy, it has been possible to achieve the first major aim of this study, namely to conceptually model the past and present processes controlling the modern distribution of nearshore and inner shelf sediments along the east Coromandel coast. Major findings regarding the patterns of shelf sedimentation in the study area include:

1. Shelf deposits (nearshore, inner shelf, and mid shelf) can be categorised into eight different sediment lithofacies based on texture and mineralogy, of which five are actively depositing, and three are in situ palimpsest deposits. However, two generic groups of deposits are essentially present, with autochthonous deposits derived from the reworking of previous shelf sediments in early Holocene times, and modern allochthonous sediments derived from onshore terrestrial sources.

2. A mixed oceanographic climate characterises the study area, which results in spatially variable shelf sedimentation patterns. Transport of shelf sediments along the coast is dominated by northerly-directed wind-generated flows associated with the intermittent presence of strong onshore winds during annual and extreme storm events. Wind-generated current transport on the east Coromandel coast is complex, however, due to the highly changeable shelf and coastal physiography. This results in the development of two separate along-shelf transport systems, with smaller reverse southerly-directed flows formed in areas of changing coastal and shelf physiography.

3. Nearshore and inner shelf sedimentation in the study area occurs under three different scales of oceanographic conditions. The inferred pattern is for large quantities of fine sediments to be eroded and transported offshore during extreme storm events. This results in very fine sands deposited on the mid shelf surface where they are inter-mixed with terrigenous muddy material, while fine lower nearshore sands deposited over coarse megarippled sands on the inner shelf surface. The latter are subsequently reworked along the shelf by either wind-generated currents during annual storm events, or oceanographic currents at Whangamata and Whiritoa during calm

weather periods. Their onshore return to the lower nearshore surface is inferred to result from entrainment and transport by long-period swell waves during calm weather conditions, with this process assisted by the enhanced shear stress exerted on the fine sands as coarse megaripple deposits become increasingly exposed.

4. Beach-barrier systems along the coast fall into two important groups. Pocket embayments occur along the steeper rocky sections of coastline, and appear to be completely isolated from the shelf transport system, with offshore sediment exchanges confined to their steep and narrow surfzones during calm and storm weather periods. This lack of interaction with the shelf has resulted in the development of stationary depositional systems, with sediment losses confined to dune blowouts of varying sizes on their associated barrier systems, this loss probably balanced in most locations through additions from cliff erosion and local streams.

Barrier spit beaches within larger embayments at the mouth of local harbours are inferred to form an onshore extension of the shelf transport system, and are thus open to diabathic sediment exchanges with the shelf during both calm and storm weather periods. This results from their characteristically fine grained and thus mobile beach and surfzone sediments, and relatively low gradient surfzone profiles. During calm conditions, fine nearshore sediments are transported onshore by shoaling waves, and attached to the beach face as ridge-runnel and low tide terrace features. It also appears that some terrigenous sediments are deposited on barrier spit beaches during calm conditions, presumably through the welding of ebb tide deltas from their enclosed estuary systems onto the beach face. However, beach and surfzone sands are eroded during storm conditions and transported offshore, possibly onto the upper nearshore surface. Thus, barrier spit systems are directly influenced by shelf sedimentation processes, and are therefore more inherently unstable features than pocket systems. However, their beach deposits also appear to be renourished to some extent by sediments from local catchments, and consequently have some potential to accrete in the long-term.

5. Shelf sedimentation patterns within each embayment along the coast are inferred to have been primarily established by processes occurring at about the time sea level stabilised, 6500 y. B.P. At this stage, transgressive shelf sediments were reworked into equilibrium with the regional oceanographic conditions, by the winnowing of fine sand from transgressive deposits during storms, which were subsequently transported onshore by wave-induced currents under calm weather conditions. Depending on the local volumes of sediments incorporated into transgressive sand bodies during the marine transgression, each embayment developed into either an integral onshore extension of the shelf transport system, with fine shelf sands moving onshore and forming wide barrier spits, or a closed system unaffected by shelf sedimentation patterns (pocket embayments), with small barriers simply composed of reworked subaerial Pleistocene inner barrier deposits. Shelf equilibrium was attained by the fine sands developing a steep seaward dipping concave-up nearshore profile, and coarse sands forming a flatter inner

shelf profile. Very fine grained terrigenous sands later deposited over these fine nearshore sands to form a relatively thick upper nearshore accretionary wedge.

These conceptual models for nearshore and inner shelf sedimentation in the study area can also be used to achieve the second important aim of the study, i.e. to compare and contrast findings to some overseas studies in which shelf sedimentation has been extensively modelled. Aspects of the east Coromandel coast which compare and contrast to other investigations include:

1.Nearshore and inner shelf sedimentation within the study area is primarily controlled by the interaction of wave oscillatory and wind-driven currents during storm conditions. This is similar to most other 'storm-dominated' shelves, where high waves and isobath-parallel wind-generated currents interact during storms, and result in the most significant advection of shelf sediments (see Chapter 3.4). However, the east Coromandel differs from most other storm-dominated shelf settings, in that it shows aspects of tide-dominated conditions between Opito Bay and Otama, and an oceanographic current-dominated shelf between Whangamata and Whiritoa. Sediment transport also varies along the shelf from being current-dominated between Waihi Beach and Opoutere, to more wave-dominated north of here (except between Opito Bay and Otama). These changeable hydrodynamic conditions result in highly variable sediment textural patterns and morphological characteristics along the shelf. This distinctive aspect of the east Coromandel coast is a consequence of its collision shelf setting, with offshore volcanic islands modifying local current and wave refraction patterns, and the presence of local up- or down-faulted blocks producing a physiographically highly variable coast and shelf, characterised by open ocean embayments to the south, but deeply indented embayments only semi-exposed to the ocean climate in the north.

2. Shelf sedimentation is inferred to occur in the study area under three different scale events, fair weather, storm, and extreme storm events. This is very similar to the mid-Atlantic and Texas-Louisiana North American coastlines, where oceanographic conditions are dominantly low energy, but occasionally interrupted by higher energy storm conditions. The shelf sedimentation model proposed for the east Coromandel coast under these oceanographic conditions is very similar to previous models from the mid-Atlantic North American shelf (e.g. NIEDORODA *et al.*, 1985 b), and Pakiri Bay on the northeast coast of New Zealand by HILTON (1990), in that extreme storms are seen to transport large quantities of fine nearshore sands offshore onto the inner shelf surface, where they are slowly reworked back onshore under fair weather conditions. However, in this study the onshore return of fine nearshore sands is proposed to result from an enhanced shear stress effect of long-period swell wave orbital currents over the coarse megarippled inner shelf sands. This differs from previous interpretations of the role played by coarse inner shelf sands of simply developing a storm lag deposit (e.g. SWIFT, 1976 a), although a similar enhancement process has previously been proposed by COWELL and NIELSON (1984) as occurring in channels of coarse sand formed across the surface of inner shelf sand bodies on the east Australian coast (see Chapter 3.3.2).

3. An autochthonous mode of shelf sedimentation characterised the east Coromandel coast in early Holocene times, and is still evident under present conditions in most areas by the cyclical reworking of fine sands between the lower nearshore and inner shelf surfaces. Most east Coromandel embayments are, however, presently characterised by varying degrees of an allochthonous mode of shelf sedimentation. This involves the deposition of very fine terrigenous sands, which are derived from either local catchments or Bay of Plenty river systems. In other storm-dominated shelf settings where an allochthonous mode of sedimentation presently dominates (e.g. Western Cook Strait and Otago-Canterbury, New Zealand; Oregon-Washington and Texas-Louisiana, North America), fine to very fine sands and silts often extend from river mouths across the nearshore surface, then mix with or mantle inner shelf and mid shelf sediments. The east Coromandel coast generally differs from most allochthonous shelf environments, in that on the exposed southern coastline, the supply of terrigenous sediments has not as yet been sufficient to blanket the lower nearshore and inner shelf surfaces. Thus, two separate modes of shelf sedimentation occur at present, with a nearshore inner shelf recycling of fine allochthonous shelf sands, and an open exchange of terrestrial autochthonous deposits from the upper nearshore surface to the mid shelf plain. This sedimentation pattern can also be related to the physiographic setting of the coastline seaward of the very steep and young Coromandel Ranges. As the local catchments are geologically very recent features, they have not existed for sufficient time to form deep and large coastal embayments. This, along with the relatively unstable nature of local lithologies to weathering, has meant that only small river valleys were drowned by the Holocene marine transgression, which are presently infilling and possibly acting as significant sources for allochthonous shelf sediments.

Therefore, the east Coromandel coast represents a very distinct setting for continental shelf sedimentation, in that it shows aspects of both autochthonous and allochthonous shelf environments formed under presently stable sea level conditions, and subject to a highly variable though generally storm-dominated oceanographic climate. As such, it tends to be characterised by elements of shelf sedimentation found in numerous different shelf settings throughout the world (see Table 3.1), and may therefore offer some potential for an improved understanding of our present knowledge of shelf sedimentation processes.

CHAPTER ELEVEN

IMPLICATIONS AND CONCLUSIONS OF STUDY

11.0. INTRODUCTION

Present nearshore and inner shelf sedimentation patterns within the east Coromandel study area have been described in detail and accounted for in a series of conceptual models. These results are now applied to important local resource management issues, specifically those relating to beach erosion and coastal set-back, the dispersion of dredge and mining wastes on the shelf, and the possibility of the shelf as a source for either aggregate or mineral deposits. Recommendations are also made for future, more detailed investigations which should be undertaken on the east Coromandel shelf, in order to improve and possibly quantify the proposed conceptual models. The chapter is then concluded with a resume´ of the major findings of the study.

11.1. IMPLICATIONS FOR COASTAL RESOURCE MANAGEMENT

11.1.1. *Beach and Dune Erosion*

Most beaches along the east Coromandel coast have been developed into moderately populated townships since the 1960's, with only a few locations presently at or near their natural state of integrity (e.g. Orokawa Bay and Opoutere; Figure 11.1), or remaining as undeveloped pastoral lands (Hotwater Beach, Otama). Unfortunately, most coastal townships were developed with little regard for the dynamic nature of the beach and dune systems (HEALY and DELL, 1987). As a consequence, they have experienced episodic problems with storm erosion, dune blowouts and coastal flooding.

Many of the beach systems identified by HEALY *et al.* (1981) as showing present trends in coastal erosion are the developed barrier spit beaches (Whangapoua, Matarangi East, Buffalo, Cooks, Pauanui and Waihi; see Figure 1.2). However, this same beach-barrier system at Opoutere has remained undeveloped, and shown by HEALY *et al.* (1981) to be naturally accreting. In contrast, pocket beach systems regardless of their level of development, show few signs of long-term beach erosion, being subject only to episodic cut and fill and some onshore losses through dune blowouts.

These trends in coastal erosion can be accounted for by the conceptual models presented in Figures 10.10 and 10.12. In these, most pocket beaches form closed sedimentary systems from the continental shelf, and are thus not susceptible to offshore losses to the nearshore surface. Barrier spit beaches, though, are seen to be an onshore extension of the shelf transport system, and thus susceptible to long-tem erosion through losses of beach and dune sands to the nearshore surface. However, they also appear to be supplied to some degree by sediments from local catchments, and thus have the potential to accrete. In most cases, barrier spit systems appear to have been either naturally stable or slowly prograding features prior to development. This can still be seen to occur at Opoutere where the barrier system has remained in its natural state of integrity. Recent trends in erosion in most cases are therefore believed to result from interference to the natural systems, which have broken down the elements that promote accretion, and accentuated those that cause erosion.



Figure 11.1. Example of a beach system preserved in its natural state, at the Orokawa Bay Nature Reserve, just north of Waihi Beach (Apr-90).



Figure 11.2. Stable frontal dune system at Matarangi Beach (west), with an incipient foredune formed just above the high tide swash zone fronting a well vegetated established foredune (May-89). The latter, though, has been modified by removal of its original natural vegetation cover and replacement with exotic grasses. Further east in the background of the photo, the frontal dune system was removed by bulldozers during development, resulting in episodic storm erosion and flooding problems.

Processes which will naturally lead to beach accretion will relate to supply of sediment from catchments, their transport onshore from the nearshore surface following storms, and their subsequent stabilisation on the beach through incorporation into natural reserves within the frontal dune. Coastal subdivision does not appear to have interfered with the supply of beach sands, as both harbour and nearshore sediments have not as yet been removed through dredging or diverted by engineering structures (groynes, breakwalls etc.). Development has, however, greatly retarded the ability of the beach systems to stabilise sands due to the stress placed on frontal dune systems. Coastal erosion problems along the east Coromandel coast have therefore largely arisen due to a basic ignorance of the role played by the frontal dune system. In their eagerness to obtain the best site, developers have often removed the natural protective vegetation cover to be replaced with less dense exotic species, and in many cases completely destroyed the frontal dune. The adverse effects of this are shown at Matarangi Beach, where the eastern dune system was bulldosed for development and has continued to suffer beach erosion and coastal flooding problems, whereas the western end retained its natural frontal dune and has shown signs of slow progradation (HEALY *et al.*, 1981; Figure 11.2).

Destabilisation of the frontal dune system has two major detrimental effects in terms of coastal erosion. Firstly, the beaches natural reservoir of sand used to protect it from storm wave erosion is lost from the system, consequently making it prone to more severe erosion than would naturally occur, and thus endangering properties located behind the frontal dune. This was vividly shown in many embayments along the coast during an extreme storm event in Jul-78, when houses were undercut at Waihi, Hahei and Cooks Beaches (HEALY *et al.*, 1981). Secondly, the absence of a vegetated dune surface behind the beach will allow loose sheets of sand to transgress landwards and encroach over properties located within the dune system. This is a problem which characterises many beaches along the coast, with dune erosion particularly concentrated along walkways placed through the frontal dune (DELL and VINE, 1988). A good example of this coastal erosion problem is shown at Tairua Beach, where mobile dune sands pose some danger to houses located within the dune system (Figure 11.3).

Protection of beaches from coastal erosion can therefore only be effective where the frontal dune system occurs in its natural state of integrity. Ideally, a buffer zone should be allowed to extend landwards from the incipient foredune, to a position outside of the natural prism of sediment reworking expected from the most severe storm event within a 50 to 100 year period (CHAPMAN *et al.*, 1982; Figure 11.4). Within this buffer zone, activities and installations detrimental to the stability of the dune system should be avoided, including: roads, permanent buildings, destruction of natural vegetation, dune levelling, permanent grazing of stock, storm water discharge, certain types of intense recreation (especially offroad vehicles), access pathways, and adverse engineering structures such as groynes and seawalls. This buffer zone should also allow for the effects of rising sea level predicted to occur due to the effects of global atmospheric warming by 'greenhouse gases'. For Pauanui Beach, GIBB and ABURN (1986) determined a 54 to 116 m wide buffer zone was required, including a 30 to 70 m wide extreme risk zone that allows for short-term storm erosion, a further 20 to 40 m wide high risk zone which allows for wind deflation, and another 23 to 31 m to allow for an expected 7 $mm.y^{-1}$ rise in sea level.

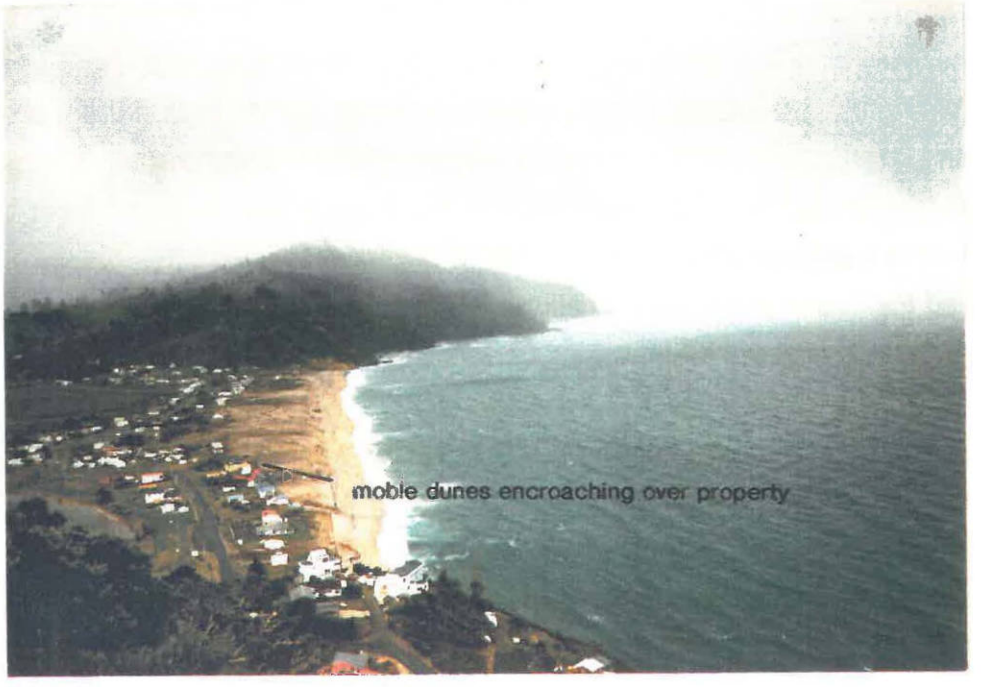

Figure 11.3. Unstable dune blowouts threatening property at the southern end of Tairua Beach (Aug-89). Wind fences have been erected on the frontal dune, but would be more effective at stabilising the blowouts if seedlings were to be planted and a dense vegetation canopy encouraged to grow over the bare dune sands.

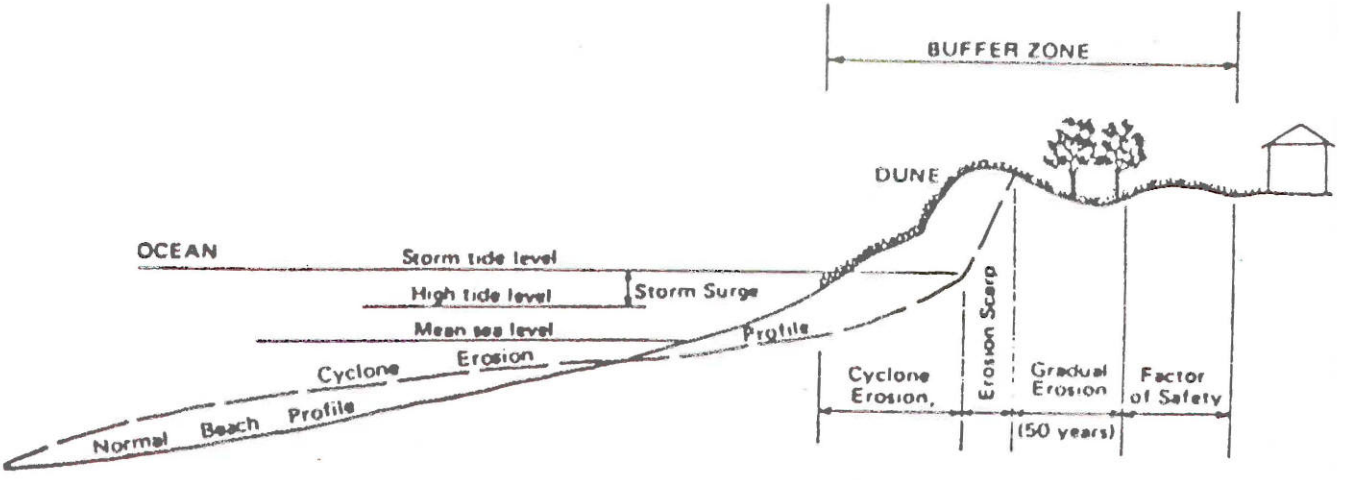

Figure 11.4. Example of the requirements for an adequate buffer zone, with space allowed for the natural reworking of beach and dune sands during storms, as well as allowing for future erosional trends from effects of predicted global rises in sea level (from CHAPMAN *et al.*, 1982).

This approach to coastal zone management thus adopts a 'prevention is better than cure' philosophy to erosion problems, and is a relatively easy and inexpensive approach to coastal management within previously undeveloped regions. However, most subdivision along the east Coromandel coast has already occurred within the zone of natural reworking of beach and dune sediments, particularly in barrier spit beach systems, as shown by the extent of erosion and property damage along the east Coromandel coast during the Jul-78 storm. Only in a few rare examples of recent development, as at Pauanui, has an undeveloped buffer zone been emplaced within the frontal dune system, although this still suffers from the lack of a natural, dense vegetation canopy (Figure 11.5). This leaves a range of other, though less effective options available to decision makers, which can only be determined through consideration of the benefits desired and funding available.

An approach of leaving the coastline as it is could be adopted, thus placing the burden of dealing with future erosion problems on individual property owners. In areas of only minor development (e.g. Orokawa, Opoutere, and Hotwater Beach) this may be the most viable option. As pointed out by DELL and VINE (1988), some natural areas of bare sand along the coast are important ecologically, e.g. for nesting and roosting sites of New Zealand dotterels and oystercatchers. In general though, a large amount of property investment is tied up within local foreshore developments ($15 000 000 at Pauanui, GIBB and ABURN, 1986), thus justifying some preventative action to be undertaken. Exactly what is required depends on each individual setting, however some generalisations are made for both pocket barrier and barrier spit systems.

Management of Pocket Beach Systems

For most of the developed pocket beach systems, only minor preventative maintenance is required in the form of stabilising present blowout systems, with the long-term goal of developing a natural vegetation canopy to prevent further breaches. As the barriers associated with pocket beaches are stationary systems which tend to develop high vertical dunes (ABRAHAMSON, 1987), they will form good buffers to future extreme storm events and rises in sea level if left in their natural state of integrity. Future erosion problems could be averted by encouraging the development of an incipient foredune in front of the established frontal dune. This can be achieved by implacing wind fences to build up wind blown sand, then planting pioneer plant species to stabilise these deposits and encourage further accretion, as has successfully been implemented at Hotwater Beach (DELL and VINE, 1988; Figure 11.6).

An important aspect of pocket beach systems is that because they form closed sedimentary systems, any long-term extraction of sand, as occurs at Whiritoa, will inevitably lead to long-term erosion problems. The textural nature of pocket beach sediments means that replenishment of any lost beach sands would be costly, requiring coarse material to be imported either from elsewhere in New Zealand, or from far offshore. Therefore, extraction of these sands will only encourage an irreversibly unstable



Figure 11.5. Example of a developed barrier system at Pauanui Beach which has allowed an adequate buffer zone between the frontal dune and properties (May-89). Note however that the stability of this buffer zone would be improved by developing a natural, dense vegetation canopy over its surface and restricting pedestrian traffic to walkways.



Figure 11.6. Successful stabilisation of the frontal dune system at Hotwater Beach through initial use of wind trapping fences and subsequent planting of colonising grasses (Aug-89). Dune erosion here originally began following the Jul-78 storms (DELL and VINE, 1988).

system to develop, which is particularly undesirable considering the likelihood of predicted future global rises in sea level.

Management of Barrier Spit Beach Systems

In most cases, barrier spit beach systems require some work to redevelop a stable frontal dune system. This is particularly important in the light of the mobile nature of their fine beach sands, and their characteristic morphodynamic response to storms. The dissipative character that these beach systems tend to take on during storms makes them highly susceptible to continuous frontal dune scarping, as a result of the generation of standing waves within their surfzones which enable wave bores to be set-up against the frontal dune system. If this frontal dune is unstable, then fine sands will be eroded and transported offshore, and possibly lost to the upper nearshore surface. Also, the developed back dune area will be vulnerable to overtopping and thus coastal flooding. This latter problem appears to be particularly severe in deeply embayed beaches such as Buffalo, Wharekaho and Matarangi (Figure 11.7), where the frontal dunes have been destabilised, and storm surges tend to be amplified by their broad embayments (HEALY *et al.*, 1981). In other more open barrier spit beaches, scarping of the frontal dune appears to be concentrated in rip embayments during storms, which will make beaches with an unstable frontal dune system susceptible to offshore losses through rip fallout onto the nearshore surface, and onshore losses through landward migrating dune blowouts.

Barrier spit beaches therefore require a much wider buffer zone than the pocket beach systems. An adequate buffer zone would not be possible to develop in most areas at present, due to the location of permanent constructions within safe limits. However, these beaches appear to be naturally renourished to some extent by modern terrigenous sands from their local catchments (see Chapters 5.5. and 9.5.), and so may be naturally prograding features. As with the pocket beaches, natural barrier accretion can probably be accomplished through establishing a stable frontal dune system, particularly by encouraging the continual presence of a stable incipient foredune above the high tide swash zone. This may mean making sections of the beach inaccessible to recreational users that were previously available. However, new dune growth and hence progradation requires protection of this ecologically sensitive area from destabilising influences.

Progradation could be further encouraged at most sites through beach and profile renourishing within the surfzone, using sand presently found within adjacent infilling harbours. In many cases, this would create an additional benefit of deepening these harbours and thus allowing greater boat navigation. However, such renourishment would need to be carefully planned so that the material selected was as close to, and possibly slightly coarser than, the natural beach sands (DEAN, 1991), and to ensure that the resulting changes in harbour configuration do not cause adverse erosion within and adjacent to their inlets. The dispersal of this renourishment material would also need to be carefully planned to ensure that it formed a surface as close as possible to the natural beach equilibrium profile (BRUUN, 1988 b, 1990), and was not dispersed where it could be reworked back into the harbour system. The best proven method is to disperse fill over the beach face and offshore to a depth equal to about twice the



PENINSULA RESORT TOWN MOPS UP AFTER STORMS HIGH SEAS

25/8/89

JOSEPH Barlow, 14, Danis Hammond, 13, and Cheris Dorreen, 14, make their way through the flooded road near Totara.

Sea at doorstep no joke for them

FLOODING on the Kauaeranga Valley Rd.

JAMES Archibald adjusting the sandbags outside his motel yesterday.

By John Macdonald

Whitianga's Anchorage Motel offers guests a short walk across the road to the sea — except yesterday the sea crossed the road to the guests.

The two owners James Archibald and Julie Haddy knew of their grounds being awash was when one guest started knocking on the door of their upstairs flat on Tuesday night.

"He had a downstairs unit. He came up thinking the water was going to come right in at the door," said Julie Haddy.

The scare sparked a sandbagging operation involving more than 100 Whitianga residents and the fire service to keep the Mercury Bay waters back below the sea wall across The Esplanade during yesterday's high spring tide at midday.

One man served seafood soup to the sandbaggers who worked for more than an hour to clear the rocks and debris from the road and motel grounds, said Mr Archibald.

The couple were planning to lease the motel out, but yesterday's flooding made them have second thoughts, he says.

"I would like to give it away if someone would take it. We wouldn't be doing much business with this happening."

Storms destroyed an attractive seafront promenade two years ago and the rock retaining wall built by the Thames-Coromandel District Council had little to lure visitors, he said.

Council chief engineer Ross Vincent said civil defence, fire service and council workers met in Whitianga yesterday afternoon to discuss a possible civil defence problem on the beachfront during last night's high tide.

But as winds were changing to southerlies and the rain was easing, workers decided to leave the area as it was, he said.

All of the roads closed yesterday — including State Highway 25 south of Thames and south of Whitianga — were open late night, but council workers were still clearing slips, he said.

"All the roads on the Peninsula have minor slipping here and there and drivers will have to take care."

A slip last night on State Highway 2 in the Karangahake Gorge cut the traffic to one lane and Works Consultancy Services workers were trying to clear it.

More than [illegible] on the Kauaeranga River catchment behind Thames over the last [illegible] the only river to flow [illegible] close State Highway 25 at [illegible] Thames and the Kauaeranga Valley Rd.

Hauraki Catchment Board [illegible] Peter Mora said the rain was not enough to cause surface flooding in some areas.

"The total amount of rain was a little bit extra, but because it fell over a long period we were able to accommodate it," said Mr Mora.

Figure 11.7. Problems experienced with coastal flooding at Buffalo Beach during only a moderate storm event in Aug-89. This can be attributed to an inadequate frontal dune system which is unable to protect property against wave bores and storm surges.



Figure 11.8. Example of an ineffective management strategy to prevent further beach erosion, at Buffalo Beach (south). The rip rap placed here does not absorb the wave energy as had originally been hoped, but simply concentrates it onto the beach face and thus undermines the structure. The rip rap is also totally ineffective for prevention of coastal flooding, which is the greatest present hazard for property owners behind the beach.

modal breaking wave height, as the sand will then be moved onshore by wave action, and form an offshore shoaling surface to dissipate storm waves (BRUUN, 1988 a, b, 1990; HOUSTON, 1991). Therefore, in most densely developed barrier spit beach systems, future coastal erosion problems could be averted by encouraging the natural seaward progradation of beach and dune deposits. In some locations, however, more drastic action is probably required due to the present extreme risk for properties located on the frontal dune system (Waihi Beach, Cooks Beach, and Buffalo Beach; Figure 11.8). These areas presently have little potential to withstand even moderate storm events, due to the virtual absence of a frontal dune to buffer the beach against storm waves and surges. Measures used so far to prevent further erosion have included various engineering structures such as semi-permeable sea-walls, rock back-filling and gabion baskets (HARRAY and HEALY, 1978; Figure 11.8). Such options have proven to be ineffective and even harmful, as they simply divert erosion problems onto other sections of the beach, and have little effect in increasing accretion. Future approaches to controlling beach erosion in these areas should probably follow similar strategies to those used in North America and by the Dutch, of either standing by, giving way or letting nature take its course (BRUUN, 1988 a).

A stand by approach would involve trying to restore the beach to a more stable volume of sand by nourishing it with sediment fill. A suitable fill source at Waihi Beach might be from the sand ridges found in this study offshore from Orokawa and Homunga Bay. At present, fine sand appears to be transported northwards over the shelf sand ridges, and deposited on the shelf offshore from Mataora and Whiritoa. As shelf sands evidently do not interact with any of these pocket beach systems, its removal should not theoretically be translated onshore into beach erosion. However, it is not certain whether destabilisation of the sand ridges would accelerate nearshore and thus beach erosion at Waihi. Also, a reduction in size of the ridges would alter offshore wave refraction patterns (as found in Chapter 7.4), and possibly cause adverse wave focussing effects on the beach. An alternative source for both Waihi Beach and other areas may be from their adjacent infilling harbours, as outlined above.

A second standby approach would be the construction of a hard artificial dune surface that prevents further beach and dune erosion (BRUUN, 1988 a). Previous efforts on these beaches to construct such structures have failed as they have not been designed in harmony with the natural beach system. A 'Dutch type' high energy absorbing rock revetment could be of benefit though, as these have proved to be excellent wave absorbers in overseas case studies where they have been designed in accord with the natural beach and dune geometry (e.g. Figure 11.9; BRUUN, 1988 a). If a suitably designed revetment were to be constructed, and the offshore profile nourished with an appropriate fill, then it is conceivable that properties presently threatened by coastal erosion could be protected, as evidenced by overseas successes using this same approach (see BRUUN, 1988 a). However, NAKASHIMA (1989) found on the mid-Atlantic North American coastline, that beaches with either natural or modified dune surfaces recovered more rapidly following storms than those backed by revetments. Therefore, revetments should only be looked upon as a short-term option, with the ultimate goal being to establish a vegetated dune surface over such features.

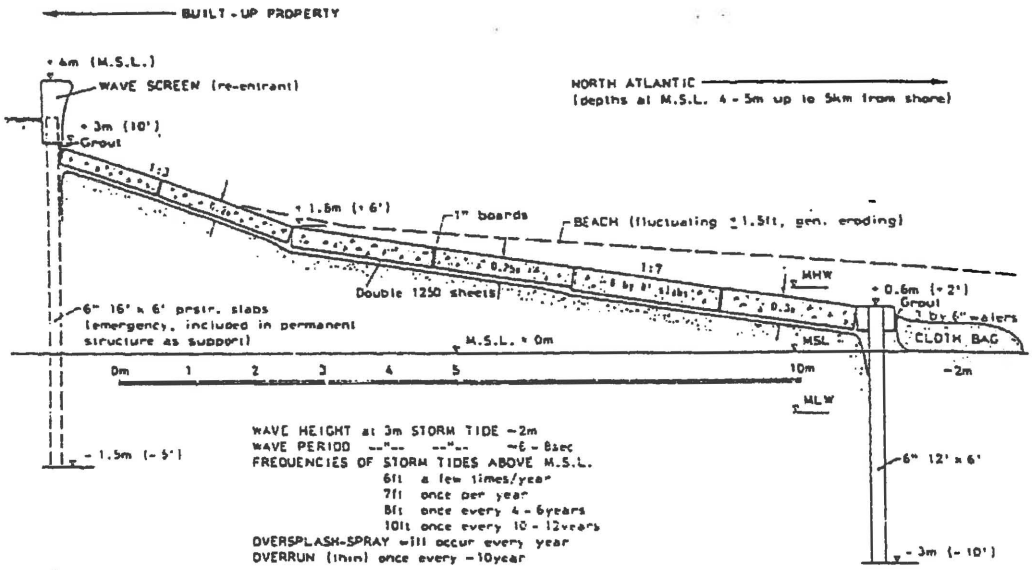

Figure 11.9. Example of a revetment which has been designed in harmony with the dynamics of the natural beach system, at Hilton Head Island, South Carolina, North America (from BRUUN, 1988 a).

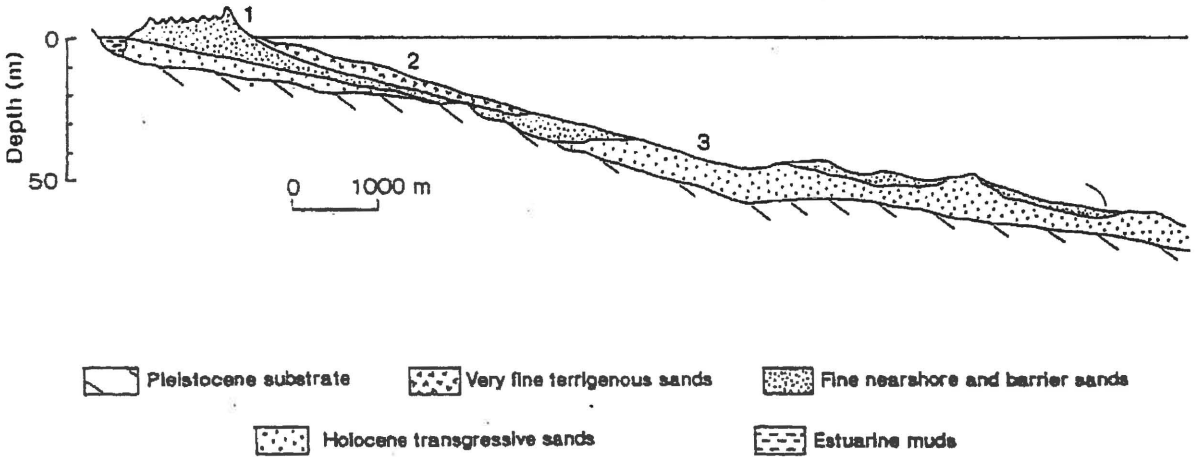

Figure 11.10. Important offshore zones for shelf resource management off barrier spit beaches: 1. Ideal location for dispersion of fine sand from dredge spoil or mining tailings over the beach and surfzone; 2. Suitable location for dispersion of very fine grained sands, which will help build up the nearshore surface. This is also the proposed location for mineral extraction by Max Resources N.Z. Ltd., which is considered unsuitable as it will directly lead to beach erosion problems; 3. Possible location for dispersion of muddy material, where it will be reworked both along the shelf and offshore onto the mid shelf surface during storm conditions. This is also the best alternative site for commercial aggregate sand and mineral extraction, as sufficiently deep not to directly cause beach erosion.

Coastal Erosion-Summary

Beach front property along the east Coromandel coast is presently at varying degrees of risk, due to poor development planning and the implementation of often bad management strategies to overcome the resulting erosion problems. As a consequence, decision makers must now face the choice of either ignoring these problems and thus possibly allowing them to escalate, particularly if predicted global sea level rises continue, or adopting sensible management strategies that allow for and possibly avert future coastal erosion problems. The degree of action that needs to be taken varies for each individual location, from minor in undeveloped areas such as Opoutere, to extreme remedial measures in locations such as Waihi Beach. In all cases, it is felt that the minimum action required is to follow the recommendations of DELL and VINE (1988) and stabilise all frontal dune systems in developed regions. If coast-wide action is not possible due to financial constraints, then a priority should be set for each location based on its extent of development (and hence value of assets at risk), and degree of degradation in the beach and dune systems. Before any remedial action is to be undertaken, a thorough examination of the natural dynamics of each system must be made so that these will not be adversely altered.

11.1.2. Disposal of Dredge and Mining Tailings on the Shelf

The east Coromandel continental shelf has so far not been used for any large-scale dispersion of either dredge spoil from harbour mouths or tailings from mining operations. However, the increasing rates of sedimentation in estuaries since European settlement (see Table 2.2), means that the nearshore and inner shelf may in future be looked upon as a potential economic location for the dumping of materials dredged from local harbours. Dredge spoil dispersion on the nearshore and inner shelf has in fact proceeded for the past 22 years at Tauranga Harbour, just south of the study area HEALY *et al.* (1991). North of the study area at Waitemata Harbour, Auckland, the uncontrolled dumping of such material on snapper spawning grounds has led to a significant reduction in abundance and diversity of marine life (GRACE, 1988). This has resulted in a tightening of legislative procedures for obtaining dredge permits, with applications now requiring an environmental impact assessment. Results from the E.C.S.S., and consideration of findings at Tauranga by HARMS (1989) and HEALY *et al.* (1991 a), allow some preliminary deductions to be made regarding the sedimentological response to disposal on various parts of the east Coromandel shelf.

Exactly where deposits should be dumped (from a sedimentological perspective) depends largely on the textural nature of sediments and dynamics of the local beach, nearshore and inner shelf systems (Figure 11.10). Obviously, the option chosen should be one which incurs the minimum financial costs, but with the greatest potential gain to the environment. The optimum location, provided the material is no less than fine sand in size, would be on barrier spit beaches and surfzones. This material, however, should not be dispersed in a random haphazard manner, but be carefully controlled and dispersed over

the entire offshore profile so that the beach equilibrium profile is maintained (BRUUN, 1988 a, b). Thus, the environmental benefits to the coast would be maximised (provided there are no adverse ecological effects) by helping the local beach equilibrium profile to aggrade on barrier spit systems, which generally suffer the greatest erosion problems along the coast. This approach has been successfully implemented at Pilot Bay in Tauranga Harbour, where spoil obtained from maintenance dredging was used to stabilise a severely eroding beach system (DE LANGE and HEALY, 1990). A similar approach has also been used recently at Mount Manganui Beach, where dredge spoil from Tauranga Harbour has been dumped in 6 to 8 m water depth and reworked into the beach equilibrium profile (FOSTER, 1991; HEALY *et al.*, 1991 b).

If the material was to be composed of very fine sand, then greater benefits could probably be gained by dispersing it over the upper nearshore surface (10 to 20 m water depth) where it could accelerate the natural accretion of these deposits, and thus indirectly help stabilise beaches by dissipating wave energy further offshore than would naturally have occurred. Such material should probably be avoided in the beach and surfzone, as it is too fine to remain in these systems and could cause an adverse increase in water turbidity. Again, this material should if possible be dispersed over a wide area rather than concentrated in mounds, as such features will interact with wave refraction patterns and possibly cause adverse wave focussing effects further onshore.

Material containing large quantities of silt and mud should be dispersed outside of the depth of modal wave reworking (> 20 m), as continual wave entrainment of these sediments would cause high turbidity and have possible adverse effects on marine plants and animals. Material of this size appears to be presently accreting over the mid shelf surface (> 50 m water depth), which would thus be the ideal location for its ultimate deposition. However, in most areas this would probably be too far offshore for the material to be economically transported from harbours, and it would also take considerable time to be reworked on the mid shelf due to the low energy environment found here. In this case, the coarse megaripple sand deposits found on the inner shelf surface in many regions may prove a better site for their dispersal. Here, they would only be entrained into large suspended sediment concentrations during storm events (when concentrations are naturally high anyway), and transported both along the shelf by intense storm-generated currents, and offshore by strong downwelling flows to be deposited on the mid shelf surface. Their reworking would probably be accelerated if the sediments were deposited in small mounds over the coarse megaripple sands rather than as an extensive sheet blanketing them, as the megaripples will enhance the shear stress exerted on the material and thus accelerate its reworking. Any resulting ecological problems, particularly during dispersion of the material when water clarity would be reduced by high suspended plumes of mud and silt, would be a contention requiring separate consideration.

Dispersion of dredge spoil on the northern embayed coastline would be more restrictive, due to the abundant commercial shell fish beds in this region, and the lower current and wave energy environment. To avoid adverse impacts on marine life, only sand sized material within Mercury Bay or at Whangapoua should be disposed of in shallow nearshore water depths (< 20 m) where sediments are

frequently reworked under natural conditions. No material should be disposed of over the inner shelf surface, due to its low energy characteristics on the northern coast (except of Otama and Opito), and the presence of abundant live shell fish beds.

11.1.3. Potential Offshore Aggregate and Mineral Resources

Sands along the east Coromandel coast have already been sought as a source of both commercial aggregates and mineral deposits. Beach sediments at Whiritoa have been extracted for commercial use since the 1930's, and continue to be exploited despite fears of beach erosion from local residents. As yet, few signs of such adverse effects have been evident, probably because the present volume of deposits removed is small compared to the total volume of beach and surfzone sands. There is, however, strong evidence from this and several studies (CHRISTOPHERSON, 1977; HEALY, 1981; WILLOUGHBY, 1981,) that Whiritoa Beach is a closed sedimentary system, with a finite volume of sands present. Thus, continued extraction of these sands will ultimately result in erosion of beach and dune deposits. The only other site for commercial beach sand extraction on the coast, at Kuaotunu Beach, was recently abandoned due to such considerations of adverse erosion effects. A question which has thus been addressed in this study is whether similar commercial aggregate sources are present on the continental shelf at depths where they could be extracted without causing adverse environmental problems?

Suitable alternative offshore sources for aggregate sands must be based on considerations of the lithological nature of deposits, and avoiding perturbations to the shelf sediment equilibrium which could be translated into onshore erosion problems. ANCTIL and OUELLET (1990) studied commercial nearshore dredging operations in the Gulf of St. Lawrence Canada, and present a set of criteria to avoid onshore erosion as including:

1. The site must exclude any bars or dunes which are an integral part of the coastal system;

2. The dredging site must be sufficiently deep to prevent direct shore erosion from beach draw down or interference with sediment transport to shore;

3. The excavation produced must not modify wave refraction patterns sufficiently to affect local littoral drift.

Suitable alternative shelf deposits would need to be of similar textural properties to those on Whiritoa Beach, which are coarse grained, well to very well sorted sands containing moderate amounts of shell fragments. From examinations of the textural properties of offshore sands, similar sized sands are present on the inner shelf surface off most beaches (Table 11.1). Only in a few locations, however, are these of similar sorting and shell concentration, namely on the inner shelf surface at Waihi, Whangamata, Onemana, and Hotwater Beach. The latter area though is enriched in lithic fragments and so may be unsuitable. Also, coarse grained inner shelf sands at Onemana form only a thin veneer

Table 11.1. Textural characteristics of Whiritoa Beach sands presently extracted as commercial aggregates, and their comparison with possible alternative inner shelf deposits.

LOCATION	DEPTH (m)	MEAN (0)	SORTING (O)	% CARBONATE
Whiritoa	Beach	0.92	0.37	11.42
Waihi	26.5	-0.05	0.35	13.42
Mataora	41	0.29	0.54	8.68
Whiritoa	44	0.57	0.43	22.3
Whangamata	30	0.53	0.5	22.5
Whangamata	31	0.85	0.44	6.49
Whangamata	32	0.92	0.49	9.3
Whangamata	34	0.52	0.3	10.67
Onemana	31	0.38	0.4	20
Hotwater	35	0.49	0.41	11.7
Hotwater	40	0.38	0.4	21.11
Hotwater	43	0.25	0.32	8.1
Mercury Bay	27	0.12	0.53	4.91

over basement rock (see Chapter 8.2.3), and so maybe too thin to be extracted. However, Waihi and Whangamata are of similar composition, although they do not contain the same very high concentrations of heavy minerals as Whiritoa Beach sands, and are characterised by relatively thick subsurface deposits. They may therefore prove to be suitable alternative sources.

Results from this study, however, have shown that the coarse inner shelf sands are not simply relict or lag deposits as has previously been suggested in many overseas investigations, but are in fact an important integral part of the shelf transport system. The uncontrolled extraction of inner shelf sands in other areas would result in several adverse reactions in the shelf transport system (Figure 11.10). Firstly, the loss of coarse megaripple deposits will retard the ability of the shelf system to rework fine grained nearshore sands back onshore following extreme storm events. Secondly, if the coarse sands are removed and large holes left on the shelf surface, then fine sands will infill these during extreme storms and thus be lost from the nearshore surface, which would then be translated onshore as coastal erosion. Thirdly, the shelf would loose its 'armoured surface' which prevents excessive erosion occurring from storm waves. Finally, a deepened shelf surface would be less effective at dissipating storm wave energy and thus cause higher than normal waves to be present during storms on the coastline.

Therefore, certain guideline's would need to be established before any coarse sand extraction were to proceed.

1. Extraction should only occur in areas where coarse sands are sufficiently thick to guarantee that the depth removed will not prevent them continuing in their role of armouring the shelf surface and enhancing the reworking of fine nearshore sands. This can be determined by obtaining cores and observing the present depth of reworking for these sediments.

2. The thickness of sand extracted should not be allowed to cause a significant lowering of the shelf surface, which may lead to either infilling by fine nearshore sands and/or increased wave energy through reduced frictional dissipation. MOTYKA and WILLIS (1974) found that the distance from shore and depth of excavation in North Sea deposits had the most significant impact on sediment responses, whereas the length and width of dredge excavation was less important. Further studies would need to be conducted to determine these limits for the east Coromandel. However, ANCTILL and OUELLET (1990) used an excavation depth of only 10 cm with a suction hopper dredge in no less than 20 m water depth over a wide shelf area in order to avoid impacts on the local bathymetry.

3. Extraction of coarse sands should not be permitted in ecologically sensitive areas.

Interest in the commercial prospects of east Coromandel sediments has recently included their potential as mineral resources. This has followed Max Resources N.Z. Ltd. application in 1989 to the Minister of Energy for an exploration licence, both inland at Opoutere, Whitianga, and Wharekaho, and offshore between Tauranga and Otama (M.H.W.M to 20 m water depth). The minerals sought after by Max Resources are ilmenite and zircon, which were estimated by that company at quantities representing a

value of approximately $1 Billion. Since 1989, Max Resources have dropped the original onshore applications, but their persistence in seeking the offshore sands as a potential mineral resource has caused considerable controversy, with fears of impending damages to local fisheries and coastal erosion should such mining operations proceed (Figure 11.11).

The application area for exploration by Max Resources is mostly covered by the present study area (Figure 11.12), and thus the results can be used to assess the viability of this proposed exploration region. Results of this investigation show several major problems in the area proposed by Max Resources. Firstly, the exploration region proposed coincides with the very dynamic nearshore zone along the coast. While sedimentation patterns in this zone do not appear to interact with local pocket beach systems, they do appear to be diabathically coupled with the barrier spit beach systems. Therefore, the extraction of these nearshore sands off barrier spits will inevitably lead to coastal erosion problems. Also, results from HILTON (1990) at Pakiri Bay, north of the east Coromandel coast, have shown that the nearshore zone is the area of highest modern shell production, and thus an ecologically sensitive area.

This does not necessarily mean that prospects of shelf mineral resources should be abandoned along the coast, but rather that more suitable deposits be explored, where higher economic concentrations can be expected in less environmentally sensitive areas. Our understanding of shelf sands as a potential mineral resource is inhibited to some degree by a lack of geological theories explaining how and where these deposits will be concentrated by shelf processes (ROY and HUDSON, 1987). In eastern Australia, ROY and HUDSON (1987) have proposed that they may occur in economic concentrations within four commonly occurring sediment units along this coast, as either concentrated heavy minerals in narrow zones of accumulation (lag deposits, drowned barriers, and buried valleys) or in low concentrations of disseminated heavy minerals within large sand bodies (Figure 11.13).

The minerals sought after by Max Resources were examined to some degree within the compositional analysis of this investigation (Chapter 9), the amount of zircon being observed directly, but ilmenite incorporated into overall estimates of opaque heavy minerals. In terms of the bulk sediment sample, the most abundant heavy mineral concentrations occur in Pleistocene and Holocene barrier deposits (up to 17% at Wharekaho; Figure 11.14 a). As for placer minerals along the east Australian coast, this is because during storms light minerals are winnowed out of beach and surfzone sediments and transported offshore, leaving behind a heavy mineral-rich lag deposit. As the barrier systems develop, seams of placer deposits are formed during storm events, emplaced between thicker accumulations of light sands as the barrier prograded in subsequent calm periods (ROY, 1989; Figure 11.15).

Coromandel fisheries, beaches under threat

Wellington (PA) — Recreational fisheries, snapper, scallop beds, micro organisms and eroding beaches, could be badly affected if dredge mining in the Coromondel goes ahead, marine biologist Stella Penny says.

Auckland-based gold explorer Max Resources NL has applied for exploration licences over more than 500 square kilometres in the Wharekawa, Whitianga and Mercury Bay districts to search for ilmenite and zircon.

The company estimates the area to contain more than 23 million tonnes of heavy mineral concentrate on and off-shore with a potential value of close to $1 billion.

The company said the Mercury Bay area — home of the America's Cup-challenging yacht club — contained a potential world class resource of mineral sands.

Ilmenite is a key ingredient in the production of titanium dioxide, a high value industrial chemical used extensively as a pigment in paint, paper, paper board and plastics.

The annual world usage of titanium dioxide is valued at $7 billion.

Dr Penny, Coromandel representative on the Auckland Harbour Board, said she needed to know more details about what amount of sand would be taken out and how.

Harmful effects depended on where the company dredged. There were valuable scallop beds off the coast. Currents also brought a great variety of micro organisms which were vulnerable to sedimentation and reduced water clarity.

Snapper fed near the sea bed and the area was important for recreational fishing. Beaches were already eroding. If they started taking out sand erosion would increase. There was the sceptre of rising sea levels because of global warming. The Coromandel and Northland were seen as being the most vulnerable. If they started taking sand out their vulnerability would increase.

"We need to start thinking about these things now to avoid problems later," she said. A preventative attitude was needed.

The Conservation Department and the local Catchment Board told her they had not had applications from the company.

There was no talk of consultation with local people, she said.

The company was trying to impress the Government with how much money the project could bring in but Dr Penny said she could not see any benefit for the Coromandel region. The proposed smelter was to be in Tauranga.

Max has applied for two onshore prospecting licences, one near Wharekawa consisting of 2.48 million tonnes of heavy mineral concentrate averaging 73 per cent ilmenite and 1.3 per cent zircon, and a second near Whitianga consisting of 1.2 million tonnes of heavy mineral concentrate averaging 83 per cent ilmenite and 1.8 per cent zircon.

The report values the onshore deposits at $A269.7 million ($NZ348 million).

A submission to the Government is being prepared on the proposed development covering dredging activities, environmental impact studies and refining facilities at Tauranga.

The report says funding of the project would be in two phases.

The initial stage would involved a capital raising programme through a share issue to carry out a detailed exploration programme through to mine feasibility, while the second stage would involve project finance to fund development to production.

Max Resources has entered into an agreement with an Australian public listed company, Dry Creek Mining NL, based in Perth, whereby Dry Creek would acquire 30 per cent of the project.

The transaction will be subject to an independent geologist's valuation and approval by both companies' shareholders, the Foreign Investment Review Board of Australia and the Overseas Investment Commission of New Zealand.

New bill may help mining

Wellington (PA) — The Opposition plans to introduce a new bill that will give mining a "fair go and remove the prejudice built into the Conservation Act".

National's Energy spokesman Merv Wellington said the Mining Ministerial Consent Amendment Bill was a direct result of the mismanagement over the Spectrum Resources mining application at Monowai, near Thames.

Months of procrastination by Conservation Minister Philip Woollaston and predecessor Helen Clark showed the determination of the "greenies" in Cabinet to frustrate genuine mining activity.

A review of Spectrum's mining application was ordered last year by Mr Justice Heron in the High Court when he quashed Ms Clark's veto on a proposal to develop an abandoned mine at Monowai.

The judge found the minister should have considered the policy of the Mining Act alongside the Conservation Act before deciding on the veto.

The review is expected to be completed by July and today Spectrum's executive director Peter Roberts was reported in the National Business Review to be "absolutely aghast" that the company was going to have to pay for it.

Mr Wellington said the new bill was based on the belief that the powers vested in the Conservation Minister were excessive and that decision on applications should give equal weight to environmental and mining interests.

Figure 11.11. The proposal in 1989 by Max Resources N.Z. Ltd. has caused considerable controversy amongst east Coromandel residents, who are particularly concerned about the likely adverse effects of coastal erosion should mining proceed.

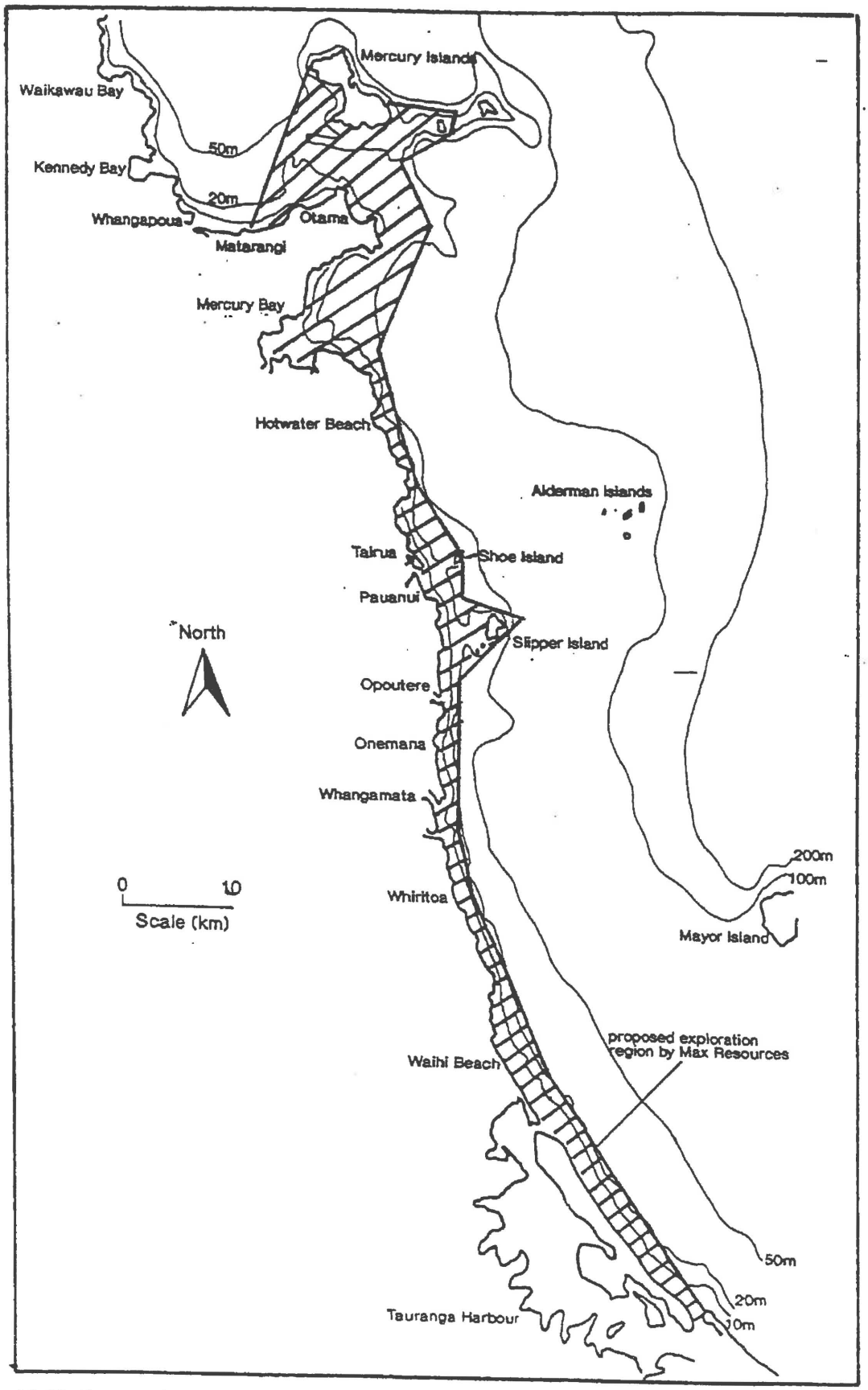

Figure 11.12. Proposed exploration area for offshore mineral deposits by Max Resources N.Z. Ltd. This coincides with the nearshore zone along the east Coromandel coast, which is the most dynamic shelf zone on the shelf and thus the most likely to lead to beach erosion problems should a long-term loss of sediments occur.

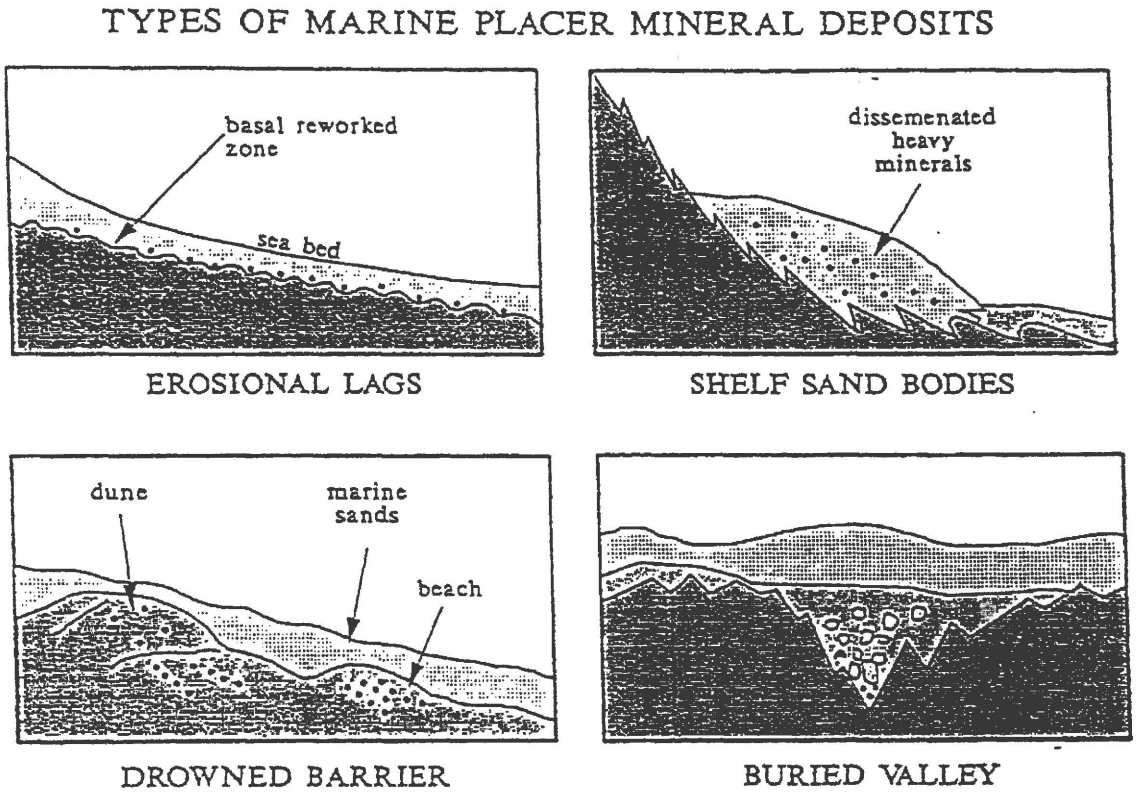

Figure 11.13. Potential sites of placer mineral concentrations in continental shelf deposits on the east Australian coast, as proposed by ROY and HUDSON (1987).

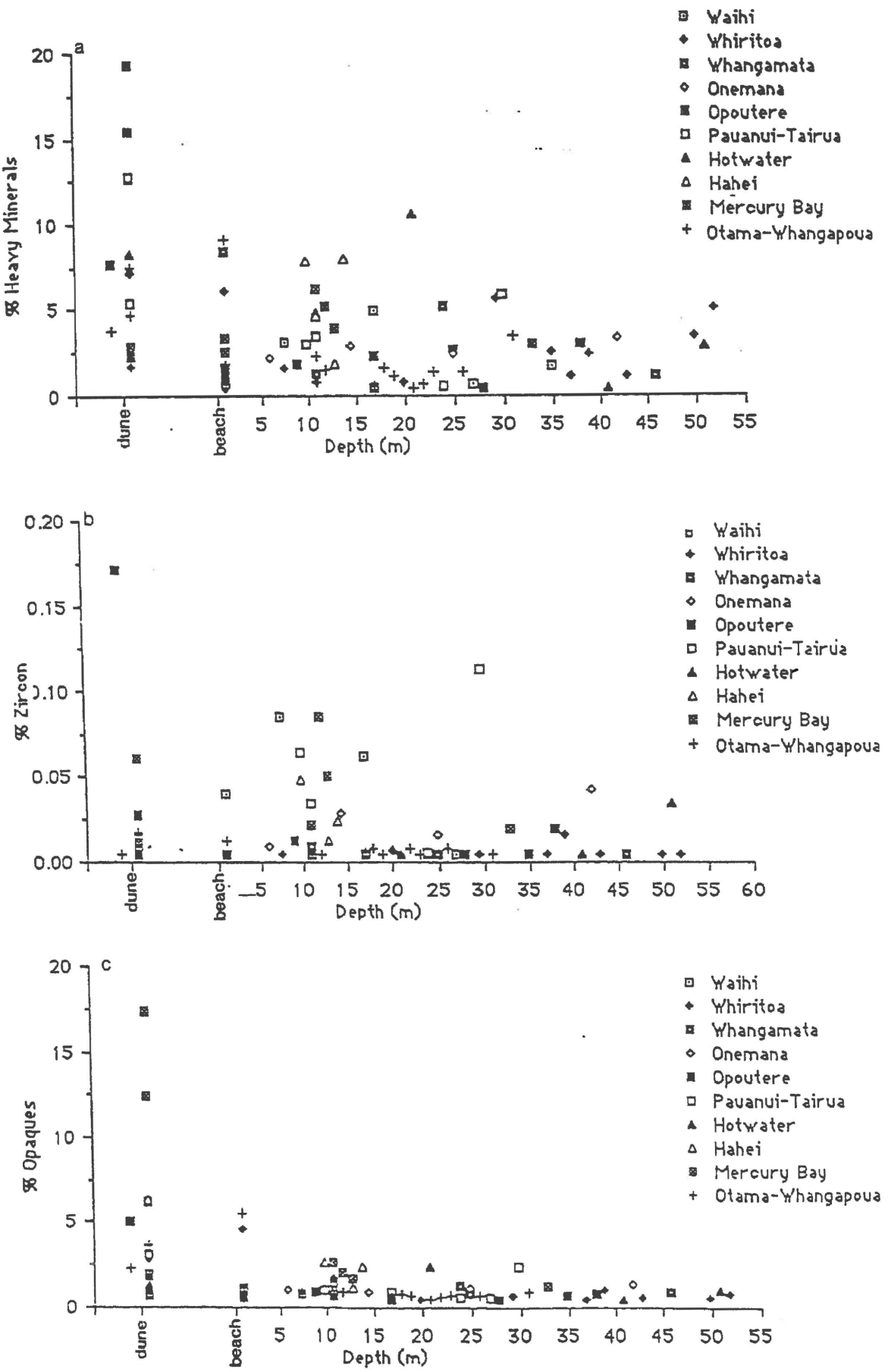

Figure 11.14. Concentrations of: a) heavy minerals; b) zircon; c) opaque heavy minerals (mainly titanomagnetite and ilmenite); in bulk sediment samples.

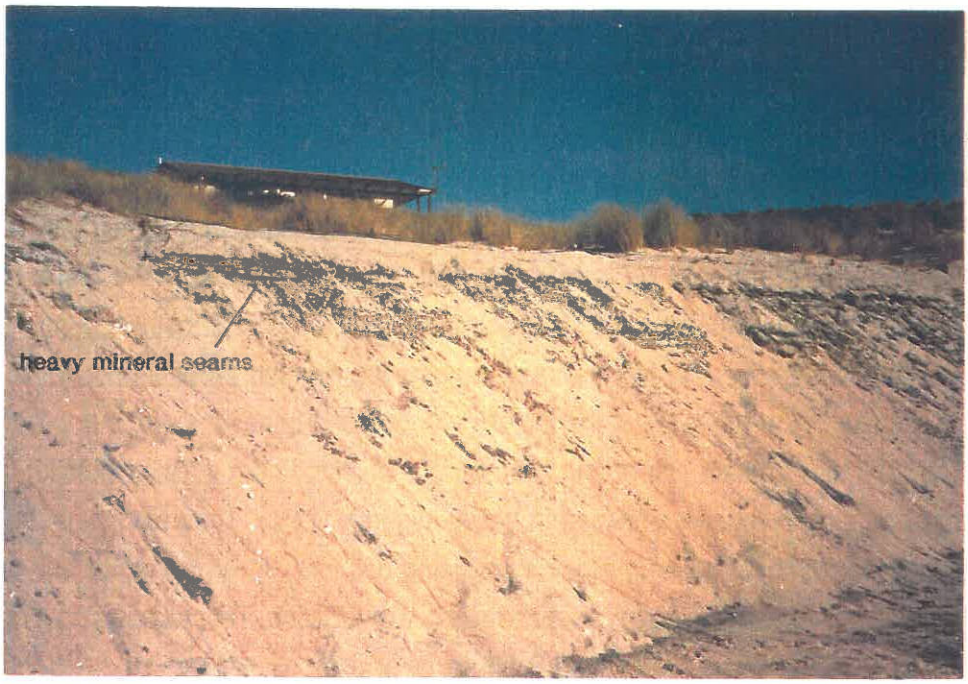

Figure 11.15. Heavy mineral seams exposed in the frontal dune system at Whiritoa Beach. Such deposits appear to contain the richest economic placer mineral deposits along the coast, but are largely inaccessible for extraction due to extensive property development over barrier systems. Similar concentrations however may be present in older Pleistocene barrier deposits presently found beneath the shelf surface offshore from Waihi Beach.

Across the shelf, deposits have much lower concentrations of heavy minerals (<10 %), these tending to decrease offshore. In terms of economic minerals from samples analysed in this study, zircon is of low concentration in all sediments (max. 0.17% at Opoutere Pleistocene inner barrier), tending to be most abundant in upper nearshore and mid shelf samples (Figure 11.14 b), while opaques are more abundant (up to 17% at Wharekaho), particularly in barrier deposits (Figure 11.14 c). Therefore, of the placer mineral deposits sought after by Max Resources, only ilmenite would appear to occur in economic concentrations in east Coromandel sediments, particularly within Pleistocene and Holocene barrier sands along the coast. Unfortunately though, these are the most intensively developed parts of the coastline, and could not be mined in most areas without threatening properties.

However, if it were possible to easily remove the fine sand fraction from coarse grained inner shelf deposits, then they may contain more economically viable concentrations of heavy minerals, as shown in Figure 11.16. These coarse inner shelf sands are found along the coast from 30 to 50 m water depth, and in most cases are interpreted as 'storm lag' deposits formed during the Holocene marine transgression. Any extraction of these sands though would have to follow the strict guideline's outlined above to avoid detrimental effects in terms of coastal erosion. Another potential economic source of heavy minerals may lie in the Pleistocene marine sediments found beneath surface deposits off Waihi Beach, particularly if these contain barrier sands. A sample obtained from surface exposures indicates that these deposits may be relatively enriched in heavy minerals (21%). Their extraction though would be difficult to undertake without causing erosion problems onshore, which is particularly undesirable considering the problems already being experienced along Waihi Beach. These deposits were, however, traced out to at least 30 m water depth, and if future investigations show them to continue further offshore beyond depths where they can interact with the coastline, then this may prove to be the most viable region for mineral exploitation. Also, as only the fine sand fraction would be used to extract ilmenite (and zircon if it occurs in greater concentrations beneath the surface), then the coarse sand tailings could either be extracted onboard by dredging and later pumped back to fill in the excavation hole, or retained for use as commercial aggregate sands.

Thus, shelf deposits along the east Coromandel coast in inner shelf water depths or greater may represent an economically viable source for aggregate and mineral deposits. In particular, Pleistocene marine deposits found near the shelf surface at Waihi may in future prove to be the most economic source for the simultaneous extraction of both heavy minerals and commercial sands. Any future extraction though must be in harmony with the dynamics of local shelf sediment transport systems in order to avoid future problems in coastal erosion.

11.2. FUTURE RESEARCH

The conceptual models and recommendations for resource management presented for the east Coromandel coast in this study have been based on a wide range of field data collected over an

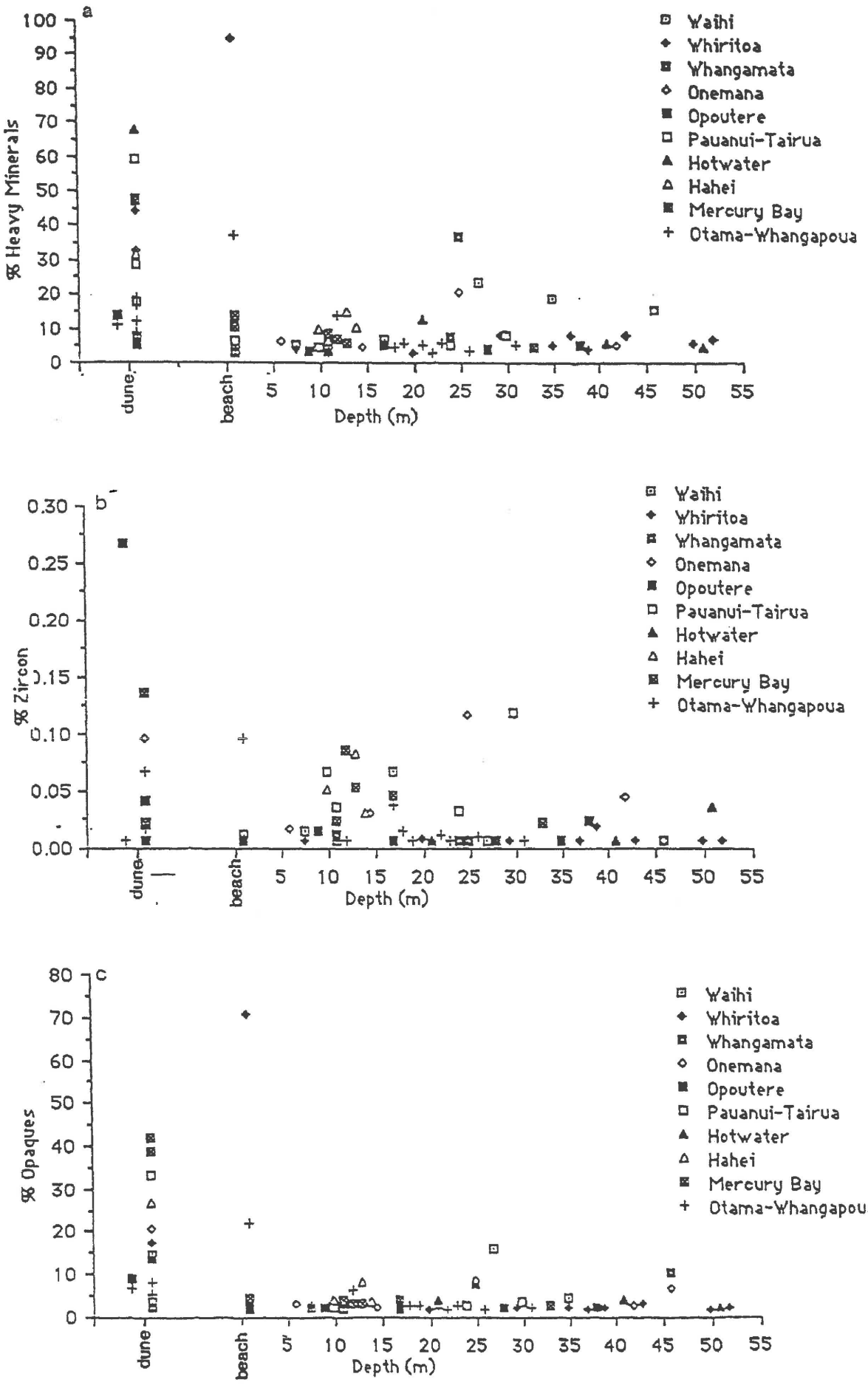

Figure 11.16. Concentrations of: a) heavy minerals; b) zircon; and c) opaque heavy minerals (mainly titanomagnetite and ilmenite) in the fine sand fraction (2-4ϕ only) of deposits.

ensive study area. As such, there is an obvious need for future more detailed investigations to nprove and quantify these ideas.

An initial examination of regional current patterns in this study has shown them to be highly variable along the coast. However, in only a few specific areas (Onemana, Waihi-Whiritoa, and Opito-Whangapoua) were direct recordings obtained. This, along with a lack of calibration data on the local wave climate, and measurements of the amount of sediment entrained by different wave conditions, makes it presently difficult to produce a suitable numerical model for sediment transport along the coast. Such information is essential for any future use of the continental shelf as either a commercial source or sink for sediments. If the appropriate resources become available in future, then the ideal equipment to use would be an instrument tripod system within the benthic boundary layer, as utilised in overseas investigations such as WRIGHT *et al.* (1991), with sensors of long recording duration for simultaneous measurements of currents, waves, suspended sediments and water pressure. These measurements should if possible be taken over a wide shelf area, to determine changes in current patterns and sediment transport with depth, as well as their variations along the coast. One of the main areas of interest is the shelf region extending from Waihi to Whangamata, which from initial results has proven to be the most highly variable part of the open coastline in terms of sediment transport.

The textural and mineralogical nature of shelf sediments was comprehensively examined in most parts of the study area. However, sediment sampling was sparse in the region extending from Opoutere to Opito Bay, and probably warrants further investigation to determine in more detail the textural and mineralogical nature of shelf samples in this region. Future investigations of sediment composition may also add to the results from this study, by investigating the bulk mineralogy outside of the 2 to 4 ϕ sand fraction for coarse grained shelf samples.

The shelf morphology and its association with different sediment textures was comprehensively examined with the numerous sonograph and echosounding surveys. Repeated surveys using these systems provided some of the most important data on the response of shelf sediments and morphological features to different sea conditions, particularly within the region extending from Waihi to Onemana. Surveys from this important region should therefore be continued in future, particularly during periods when instruments are deployed to measure sediment transport under different sea conditions. In addition to this, further surveys of shelf deposits using depth of activity rods should be undertaken on the margins of fine rippled and coarse megarippled sands, to determine exactly how important the proposed shear stress enhancement associated with coarse megaripple deposits is for the onshore and along-shelf transport of fine sands.

Perhaps the greatest potential area for future research along the east Coromandel is studies dealing with the stratigraphic nature of coastal and shelf deposits. This aspect has only just been touched upon in this investigation through gathering continuous seismic sub-bottom profiles. However, even this limited data revealed the very unique and diverse characteristics of shelf stratigraphy along the east

Coromandel coast. Future stratigraphic investigations should probably focus on a few type localities, such as Whiritoa, Whangamata and Mercury Bay, where cores could be obtained through seismic units identified in this study and dated to determine their age of emplacement. The associated barrier systems should also be cored and dated to determine the degree of synchroneity between emplacement of barrier and shelf deposits.

Data that were not collected in this study, but which should be obtained to assist in future management of the coast, would be the dynamics of local beach and dune deposits over a range of different conditions. This would involve repeated surveying of beaches from inland of the frontal dune to the offshore depth of closure, so that the active sediment prism for each location can be determined and adequate buffer zones then set aside. As development has often completely altered the original integrity of the frontal dune system, undeveloped areas such as Orokawa Bay and Opoutere would make excellent control sites to determine the degree of degradation similar barrier systems have suffered in other locations, and thus the measures that may be required to restore them to a more stable form.

11.3. SUMMARY OF MAJOR FINDINGS IN THE EAST COROMANDEL SHELF STUDY

In concluding this investigation of nearshore and inner shelf sedimentation on the east Coromandel coast, it is pertinent to reiterate the major findings from each of the chapters in which interpretations of data have been presented.

Chapter 4 examined shelf current patterns through Aanderaa current meter and sea-bed drifter data. Long-term recordings from the Onemana inner shelf indicate that two mutually exclusive currents dominate most of the east Coromandel shelf, with a relatively weak (< 0.2 $m.s^{-1}$) southerly-directed flow present during periods of offshore westerly winds (possibly generated by incursions of the East Auckland Current), and a strong (up to 0.4 $m.s^{-1}$) northery-directed current generated by strong onshore winds during cyclonic storms. This information shows some potential for a northerly-directed transport of shelf sediments to occur under storm conditions. Additional short-term current measurements show regional variations to this pattern, with both tidal- and wind-generated flows important for sediment transport on the inner shelf off Opito Bay, but no apparent current transport occurring further west off Whangapoua. Variations in the intensity of currents under fair weather conditions were also observed between Whiritoa and Waihi, with stronger flows in the former region indicating that this is possibly significantly affected by incursions of the East Auckland Current.

Chapter 5 examined the surface sediment textural patterns for shelf deposits. These data indicate highly variable sediment textural patterns occur, both along the coast and over the shelf surface, which are inferred to result from changeable hydrodynamic conditions and sediment sources within the study area. The southern exposed coastline from Waihi Beach to Tairua is consistently characterised by: a continuous belt of fine to very fine grained, well sorted, very angular upper nearshore sands from 5 to 20 m water depth; fine grained, well to moderately well sorted, iron stained, sub-rounded sands with

a very patchy distribution across the lower nearshore and inner shelf surface (20 to 50 m water depth); medium to coarse grained, well to moderately sorted, shelly, iron stained, rounded inner shelf storm lag deposits (30 to 50 m water depth); and fine to very fine grained, moderately sorted, very angular muddy mid shelf sands (> 50 m). On the northern embayed coast from Mercury Bay to Whangapoua, textural patterns are very localised, with fine and very fine grained sands dominating shelf deposits off Whangapoua and Mercury Bay respectively, and coarse shelly sands dominating the Otama shelf region.

Textural data also provide important information on the diabathic links between local beaches and the shelf, with barrier spit and northern pocket beaches showing textural overlap with upper nearshore sands, thus indicating an open sediment exchange between these environments, while southern pocket beach systems show no textural overlap, and are therefore isolated from the shelf.

Chapter 6 presents a detailed analysis of shelf morphology, based on extensive side-scan sonar, echosounder, and diver surveys. These indicate that variations in textural patterns in the study area result in part from changing hydrodynamic conditions. For the southern coast, the very fine grained upper nearshore sands are dominated by active ripples, thus indicating transport by fair weather waves, while lower nearshore, inner shelf and mid shelf deposits are characterised by large ripples, megaripples, and sand ridges, and are therefore less frequently reworked by combined storm wave-current flows. Within Mercury Bay, the occurrence of megaripples in coarse sands indicates transport by storm waves, while the presence of small sand waves on the nearshore surface shows some current-induced transport also occurs during storms. At Otama, the presence of large sand ridges and an absence of megaripples across the inner shelf surface indicates this is a region dominated by tidal- and wind-generated current transport, while further west off Whangapoua, sediment transport is restricted to the nearshore surface where active ripples are present during fair weather conditions.

An important observation from the morphological surveys is that following the occurrence of an extreme storm event (Cyclone Bola, Mar-88), lower nearshore deposits on the southern exposed coast were transported offshore and deposited over coarse megaripple deposits on the inner shelf surface. However, in Mercury Bay very few changes were apparent, with only some localised areas of wave- or current-scouring on the sea-bed.

Chapter 7 investigates the morphodynamic interactions between hydrodynamic processes and morphological features. Theoretical considerations suggest that upper nearshore sands are actively reworked under all wave conditions, that reworking of lower nearshore and inner shelf sands should occur under storm wave conditions, and mid shelf deposits will only be transported under extreme storm conditions. Depth of activity rod surveys at Whiritoa, Whangamata, and Onemana support theoretical deductions for the conditions required for sheet flow of fine sands, but indicate that present theories overestimate conditions required for reworking of coarse megarippled deposits. This is attributed to the variable texture of deposits on megaripple crests and troughs, and to the important shear stress enhancement effect these bedforms create due to their high surface roughness.

The morphology of shelf sand ridges indicates that current-dominated transport to the north characterises the shelf between Waihi Beach and Opoutere, and is attributed to the interaction of coastally-trapped topographic waves, wind-generated currents, and storm waves, all of which form during storm conditions. However, current transport is reversed in direction between Whangamata and Whiritoa, presumably due to incursions of the East Auckland Current during fair weather conditions. Morphodynamic interactions also occur between storm waves and sand ridges, reefs, and offshore islands, which produce localised areas of sea-bed scouring and hence coarse megaripple band formation.

Chapter 8 investigates the shallow sub-bottom stratigraphy through seismic profile and box core data. This shows that various shelf deposits are associated with relatively thick sub-bottom Holocene units, with: a thick upper nearshore accretionary wedge (10 m thick) present in < 20 m water depth; fine grained shelf sands associated with a 5 m thick wedge on the nearshore surface (20 to 30 m), and 1 to 5 m thick lobes and sheets over the inner shelf surface (30 to 50 m); coarse grained inner shelf sands generally coinciding with a 5 to 10 m thick basal Holocene transgressive sand sheet; and the occurrence of a 7 to 8 m thick mid shelf unit.

Pre-Holocene units are also inferred to influence the shelf morphology (and hence morphodynamics), with thick sedimentary sequences present beneath the shelf off Waihi influencing the very flat and broad shelf surface here, while the presence of a basement rock platform beneath Holocene deposits north of Whangamata produces a steep, rocky shelf surface in this region.

Chapter 9 examines the mineralogical composition of the fine sand fraction (2 to 4ϕ) for sediments from different environments within the study area (river, beach, barrier, and shelf). This indicates that: modern barrier spit beach and some pocket beach deposits are partially derived from their local catchments, particularly at Buffalo Beach, Kennedy Bay, and Waikawau; the bulk of barrier spit deposits were derived from the onshore transport of fine grained shelf sands during the Holocene stillstand, with some contributions also made by their local catchments; pocket barriers deposits were possibly derived from reworking of older Pleistocene inner barrier sands; coarse and fine grained shelf sands appear to have been derived from a similar offshore parent source; and very fine grained upper nearshore and mid shelf sands, and Mercury Bay shelf sediments, appear to have a modern terrigenous origin. In addition, the sediment composition also indicates two possible provinces for east Coromandel shelf sands, either from weathering of local catchment rocks, or the northerly along-shelf transport of Bay of Plenty sands, each possibly applying to different parts of the study area.

Chapter 10 proposes a series of conceptual models which account for these modern nearshore and inner shelf sedimentation patterns. In this, textural and mineralogical data are integrated to define eight different lithofacies within the study area, with five actively depositing, and three essentially 'in situ' palimpsest sands. Two major sediment transport pathways are inferred to occur along the coast, these driven by wind-generated currents, and modified by variations in the shelf and coastal physiography. Nearshore and inner shelf sedimentation is proposed to presently occur under three

different scale events, with extreme storms transporting fine sands offshore, annual storms reworking sediments along the shelf, and fair weather conditions characterised by the onshore return of fine sands by the interaction of long period swell waves with coarse megaripple deposits, as well as some along-shelf transport between Whiritoa and Whangamata by oceanic currents. Diabathic exchanges between local beaches and the shelf is only seen to occur off barrier spit beaches and some northern pocket beaches (Otama and Hotwater), while southern pocket beaches appear to be isolated sedimentary systems. These sedimentation patterns which presently characterise the east Coromandel coast are inferred to have been primarily established by processes occurring during both the Holocene marine transgression, and as shelf sediments adjusted into equilibrium with the subsequent stable sea level conditions.

The east Coromandel coast is thus characterised by a storm-dominated shelf setting, but with aspects of a tide-dominated shelf off Opito Bay and Otama, and oceanic current-dominated shelf off Whangamata and Whiritoa. The hydrodynamic conditions of the study area are similar to those found in North American locations on the mid-Atlantic and Gulf of Mexico coasts. Also, the autochthonous sedimentation patterns which characterise lower nearshore and inner shelf deposits in most parts of the study area shows similarities to regions such as the mid Atlantic U.S., east Australian, and north east New Zealand coasts. However, an allochthonous sedimentation pattern also occurs on the upper nearshore and inner shelf surface, thus showing similarities to regions such as the Washington-Oregon, western Cook Strait, and Canterbury-Otago coasts. This highly variable character of shelf sedimentation within the study area is inferred to result from its collision plate setting, in a mid-latitude lee-shelf environment.

Chapter 11 concludes the study by applying the results to resource management issues. This has shown that coastal erosion problems can largely be resolved by establishing stable incipient and frontal dune systems along the coast, and encouraging accretion on barrier spits by renourishment from adjacent infilling harbour deposits. Sediments from dredge and mine tailings (provided these are not contaminated with toxic substances) have the potential to provide benefits to the east Coromandel coastline in terms of promoting beach accretion, and thus reversing present coastal erosion trends which characterise much of the study area. Decisions on where this material is to be disposed should be based on: the textural nature of these sediments; the energy and thus ability of the offshore environment to rework them; and likely impacts on offshore biological communities. Coarse sands on the inner shelf surface may represent an economic source for extraction of both aggregate and mineral deposits without causing any detrimental erosion problems onshore, provided that guideline's are followed which minimise alteration to the shelf transport system. It is not recommended, however, to allow Max Resources N.Z. Ltd. to extract minerals from their proposed exploration region, which coincides with the very dynamic nearshore zone.

REFERENCES

REFRENCES

ABRAHAMSON, L. (1987). Aspects of Late Quaternary stratigraphy and evolution on the Coromandel Peninsula - New Zealand. Unpublished M.Sc. Thesis, University of Waikato, Hamilton, New Zealand, 250 p..

ANCTILL, F. and OULLET, Y. (1990). Preliminary evaluations of impacts of sand extraction near Iles-des-la-Madeleine Archipelago, Quebec, Canada. *Journal of Coastal Research*, 6, 37-51.

BAGNOLD, R.A. (1963). Mechanics of marine sedimentation. *In*: M.N. HILL (ed.), *The Sea*. Willey-Interscience, New York, Vol.3, 507-528.

BARKER, P.H, and KIBBLEWHITE, A.C., (1965). Physical oceanographic data from the TUI cruise 1962. *New Zealand Journal of Science*, 8, 604-634.

BARKER, R.W. (1960). Taxonomic notes on the species figured H.B. BRADY in his report on the foraminiferal dredged by H.M.S. Challenger during the years 1873-1876. *Society of Economic Palaeontologists and Mineralogists*, Special Publication 9.

BARTOLINI, C and PRANZINI, E. (1977). Tracing nearshore bottom currents with sea-bed drifters. *Marine Geology*, 23, 275-284.

BELDERSON, R.H., JOHNSON, M.A., and KENYON, N.H. (1982). Bedforms. In STRIDE, A.H. (ed), *Offshore Tidal Sands*, Chapman and Hall, New York, 222 p.

BELDERSON, R.R, KENYON, N.H., STRIDE, A.H., and STUBBS, A.R. (1972). *Sonographs of the sea floor. A picture atlas*. Elsevier, 185 p.

BELL. R.G., OLDMAN, J.W., and HUME, T.M., 1988. A handbook on the use of moored current meters in coastal waters. *Water and Soil Miscellaneous Publication No 117*, Water Quality Centre, Ministry of Works and Development, Hamilton, New Zealand, 64 p.

BLACK, K.P. (1983). Sediment transport and tidal inlet hydraulics. Unpublished D.Phil thesis, University of Waikato, Hamilton, New Zealand, 331 p.

BLACK, K.P. and HEALY, T.R. (1981). Computer programs for waves for wave analysis, wind generation, wave refraction diagrams, and Fast Fourier analysis: Occasional Report No.6, Department of Earth Sciences, University of Waikato, New Zealand.

BLACK, K.P. and HEALY, T.R. (1983). Northland forestry port Marsden Point, side scan survey. Northland Harbour Board, 88 p.

BLACK, K.P. and HEALY, T.R. (1988). Formation of ripple bands in a wave-convergence zone. *Journal of Sedimentary Petrology*, 58, 195-207.

BLACK, K.P., HEALY, T.R., and HUNTER, M.G. (1989). Sediment dynamics in the lower section of a mixed sand shell-lagged tidal estuary, New Zealand. *Journal of Coastal Research*, 5, 503-521.

BLACK, K.P., NELSON., C.S., and HENDY, C.H. (1988). A spectral analysis procedure for dating Quaternary deep-sea cores and its application to high-resolution Bruhnes record from the southwest Pacific. *Marine Geology*, 83, 21-30.

BOCZAR-KARAKIEWICZ, B., ALMOS, C.L. and DRAPEAU, G. (1990). The origin and stability of sand ridges on Sable Island Bank, Scotian Shelf. *Continental Shelf Research*, 10, 683-704.

BOCZAR-KARAKIEWICZ, B., BONA, J.L. and PELCHAT, B. (1991). Sand ridges and internal waves on continental shelves. *Coastal Sediments '91'*, ASCE Vol. 1, 527-542.

BOGGS, S. (1987). *Principles of Sedimentology and Stratigraphy*. Merrill, Columbus, 784 p.

BOOTHROYD, J.C. (1978). Mesotidal inlets and estuaries. In R.A. DAVIS Jr. (ed), *Coastal Sedimentary Environments*, Springer, New York, 287-360.

BOWDEN, K.F. (1983). *Physical Oceanography of Coastal Waters*. Halsted Press, New York, 302 p.

BOYD, R. and PENLAND, S. (1984). Shoreface translation and the Holocene stratigraphic record: Examples from Nova Scotia, the Mississippi Delta and eastern Australia. *Marine Geology*, 60, 391-412.

BRADSHAW, B.E., HEALY, T.R., DELL, P.M. and BOLSTAD, W.M. (1991). Inner shelf dynamics on a storm-dominated coast, east Coromandel, New Zealand. *Journal of Coastal Research*, 7, 11-30.

BRADSHAW, B.E., HEALY, T.R., and DELL, P.M. (in press). Shelf sedimentation on the East Coromandel coast, New Zealand: Implications for resource management. Submitted

to the *Australasian Coastal Conference on Coastal and Ocean Engineering*, Auckland, 1991.

BRODIE, J.W. (1960). Coastal surface currents around New Zealand. *New Zealand Journal of Geology and Geophysics*, 3, 235-252.

BRUNN, P. (1988a). Rationalities of coastal erosion and protection: an example from Hilton Head Island, South Carolina. *Journal of Coastal Research*, 4, 129-138.

BRUUN, P. (1988b). Profile nourishment, its background and economic advantages. *Journal of Coastal Research*, 4, 219-228.

BRUNN, P. (1990). Beach nourishment, improved economy through better profiling and back passing from offshore sources. *Journal of Coastal Research*, 6, 265-278.

CACCHIONE, D.A., DRAKE, D.E., GRANT, W.D., and TATE, G.B. (1984). Rippled scour depressions on the inner continental shelf off central California: *Journal of Sedimentary Petrology*, 54, 1280-1291.

CARTER, L. (1986). A budget for modern Holocene sediment on the South Otago continental shelf. *New Zealand Journal of Marine and Freshwater Research*, 20, 665-676.

CARTER, L., and CARTER, R.M. (1986). Holocene evolution of the nearshore sand wedge, South Otago continental shelf, New Zealand. *New Zealand Journal of Geology and Geophysics*, 29, 413-424.

CARTER, L., and HEATH, R.A. (1975). Roles of mean circulation, tides, and waves in transport of bottom sediment on the New Zealand continental shelf. *New Zealand Journal of Marine and Freshwater Research*, 9, 423-48.

CARTER, R.M., CARTER, L., WILLIAMS, J.J., and LANDIS, C.A. (1985). Modern and relict sedimentation on the South Otago continental shelf, New Zealand. *New Zealand Oceanographic Institute Memoir*, 93, 43 p.

CHALLIS, G.A. (1978). [Tertiary-Quaternary] Volcanism, p 632-633. *In* SUGGATE, R.P; STEVENS, G.R.; TePUNGA, M.T. (eds), *The Geology of New Zealand*. Government Printer, Wellington, 2 Vols., 820 p.

CHAPMAN, D., GEARY, M., ROY, P.S., and THOM, B.G. (1982). *Coastal evolution and erosion in N.S.W.* A report prepared for the Coastal Council of N.S.W., 341 p.

CHAPPELL, J. (1983). A revised sea-level record for the last 300 000 years from Papua New Guinea. *Search*, 14, 99-101.

CHIN, J.L., CLIFTON, H.E., and MULLINS, H.T. (1988). Seismic stratigraphy and late Quaternary shelf history, south-central Monteray Bay, California. *Marine Geology*, 81, 137-157.

CHRISTIE-BLICK, N. (1991). Onlap. offlap, and the origin of unconformity-bound depositional sequences. *Marine Geology*, 97, 35-56.

CHRISTOPHERSON, M.J. (1977). The effect of sand mining on the erosion potential of Whiritoa Beach. Unpublished M.Sc. thesis, University of Waikato, Hamilton New Zealand, 120 p.

CLIFTON, H.E. (1976). Wave generated structures-a conceptual model. In R.A. DAVIS and R.A. ETHINGTON (eds), *Beach and Nearshore Processes, Society of Economic Palaeontologists and Mineralogists*, Special Publication, 24, 126148.

CLIFTON, H.E., and DINGLER, J.R. (1984). Wave-formed sedimentary structures and palaeoenvironmental reconstruction. *Marine Geology*, 60, 165-198.

COOK, D.O. (1982). Discussion: Nearshore bedform patterns along Rhode Island from side-scan sonar surveys. Journal of Sedimentary Petrology, 52, 677-678.

COOK, D.O. and GORSLINE, D.S. (1972). Field observations of sand transport by shoaling waves. *Marine Geology*, 13, 31-55.

CORNISH, V. (1898). On sea beach and sand banks. *Geographical Journal*, 11, 628-651.

COWELL, P.J. and NIELSON, P. (1984). Prediction of sand movement on the south Sydney inner continental shelf, south-east Australia. University of Sydney, Coastal Studies Unit, Technical Report 84/2.

DAHM, J. and HEALY, T.R. (1980). A study of dredge spoil dispersion off the entrance to Tauranga Harbour. Report submitted to the Bay of Plenty Harbour Board, 64 p.

DAVIES-COLLEY, R.J. and HEALY, T.R. (1978). Sediment transport near the entrance to Tauranga Harbour. *New Zealand Journal of Marine and Freshwater Research*, 12, 237-243.

DAVIS, R.A. Jr. and HAYES, M.O. (1984). What is a wave-dominated coast? *Marine Geology*, 60, 313-329.

DEAN, R.G. (1991). Equilibrium beach profiles: characteristics and applications. *Journal of Coastal Research*, 7, 53-84.

de LANGE, W.P. (1988). Wave climate and sediment transport within Tauranga Harbour. Unpublished D.Phil. thesis, University of Waikato, Hamilton, New Zealand.

de LANGE W.P. and HEALY, T.R. (1990). Renourishment of a flood-tide delta adjacent beach, Tauranga Harbour, New Zealand. *Journal of Coastal Research*, 6, 627-640.

DELL, P.M. (1983). The offshore and nearshore current circulation patterns at Pauanui and Tairua. Unpublished report to the Hauraki Catchment Board, Te Aroha New Zealand, No. 142, 30 p.

DELL, P.M. , HEALY, T.R. and NELSON, C.S. (1985). A preliminary investigation of the sediments on the eastern Coromandel inner shelf and implications for across-shelf sediment transport. *Australasian Conference on Coastal and Ocean Engineering, Christchurch*, 489-99.

DELL. P.M. and VINE, M. (1988). Sand dune erosion and stabilisation eastern Coromandel. Unpublished report to the Hauraki Catchment board, Te Aroha, New Zealand, 31 pp.

DENHAM, R.N., BANNISTER, R.W., GUTHRIE, K.M., and CROOK, F.G. (1984). Surveys of the East Auckland and East Cape Currents, New Zealand. *Australian Journal of Marine and Freshwater Research*, 35, 491-504.

DINGLER, J.R. (1974). Wave-formed megaripples in nearshore sands. Unpublished D.Phil. dissertation, University of California, San Diego, 133 p.

DINGLER, J.R. (1979). The threshold of grain motion under oscillatory flow in a laboratory wave channel. *Journal of Sedimentary Petrology*, 49, 287-294.

DINGLER, J.R. and INMAN, D.L. (1977). Wave-formed ripples in nearshore sands. *Proceedings of the 15th Conference on Coastal Engineering*, Honolulu, Hawaii, 2109-2126.

D'OLIER, B. (1979). Side-scan sonar and reflection seismic profiling. In DYER, K.R. (ed.), *Estuarine Hydrography and Sedimentation, a Handbook*, Cambridge University Press.

DOYLE, A.C., CARTER, L., GLASBY, G.P., and LEWIS, K.B. (1979). *Bay of Plenty Sediments.* N.Z. Oceanographic Institute Chart, Coastal Series, 1:200 000.

EAGLESON, P.S. and DEAN, R.C. (1961). Wave-induced motions of bottom sediment particles. *Transactions ASCE*, 126, 1162-1189.

EASDALE, S. and JACOMB, C. (1982). A study of archaeological sites on the beaches of the Coromandel Peninsula. Unpublished Report Submitted to the Hauraki Catchment Board, Te Aroha New Zealand, No. 121, 98 p.

EMERY, K.O. (1952). Continental shelf sediments off southern California. *Geological Society of America Bulletin*, 63, 1105-1108.

EMERY, K.O. (1968). Relict sediments on continental shelves of the world. *The American Society of Petroleum Geologist*, 52, 445-464.

EWANS, K.C. and KIBBLEWHITE, A.C. (1981). Ocean wave measurements near Great Barrier Island: an interim report. Unpublished Report Submitted to Shell B.P. and Todd Oil Services Ltd.

FIELD. M.E. and ROY, P.S. (1984). Offshore transport and sand-body formation: evidence from a steep, high energy shoreface, southeastern Australia. *Journal of Sedimentary Petrology*, 54, 1292-1302.

FLEMMING, B.W. (1978). Underwater sand dunes along the southeast African continental margin-observations and implications. *Marine Geology*, 26, 177-198.

FLEMMING, B.W. (1980). Sand transport and bedform patterns on the continental shelf between Durban and Port Elizabeth (south-east African continental margin). *Journal of Sedimentary Geology*, 26, 179-205.

FORBES, D.L. and BOYD, R. (1987). Gravel ripples on the inner Scotian shelf. *Journal of Sedimentary Petrology*, 57, 46-54.

FOSTER, G.A. (1991). Beach nourishment from a nearshore dredge spoil dump at Mount Manganui Beach. Unpublished M.Sc. thesis, University of Waikato, Hamilton, New Zealand, 156p.

FRIEDMAN, G.M. and SANDERS, J.E. (1978). *Principles of Sedimentology.* John Wiley and Sons, New York, 792 p.

FROGGATT, P.C. and LOWE. D.J. (1990). A review of Quaternary silicic and some other tephra formations from New Zealand: their stratigraphy, nomenclature, distribution, volume and age. *New Zealand Journal of Geology and Geophysics*, 33, 89-109.

FULTON, W.J. (1988). The volcanic geology of the Whiritoa area. Unpublished Msc. thesis, University of Waikato, Hamilton New Zealand, 172 p.

GADD, P.E, LAVELLE, J.W., SWIFT, D.J.P., 1978. Estimates of sand transport on the New York shelf using near-bottom current meter observations. *Journal of Sedimentary Petrology*, 48, 239-252.

GARY, M, Mc CAFEE, R, Jr., and CAROL, C.L. (1972). *Glossary of Geology*. American Geological Institute, Washington D.C., 805 p.

GIBB, J.G. (1983). Geology and sedimentology of the Tairua-Pauanui area, Coromandel Peninsula, and provenance of the sediments. Unpublished report to Water and Soil Directorate, Ministry of Works and Development, Wellington, 46 p.

GIBB, J.G. (1986). A New Zealand regional Holocene eustatic sea-level curve and its application to determination of vertical tectonic movements. A contribution to IGCP-project 200. Proceedings of International Symposium on Recent Crustal movements from the Pacific Region, Wellington New Zealand, *Royal Society of New Zealand, Bulletin* , 24; 377-395.

GIBB, J.G. and ABURN .J.H. (1986). Shoreline fluctuations and an assessment of a Coastal Hazard Zone along Pauanui Beach, eastern Coromandel Peninsula, New Zealand. *Water and Soil Technical Publication,* No.27, 48 p.

GIBB, J.G. and ADAMS, J. (1982). A sediment budget for the east coast between Oamaru and Banks Peninsula, South Island, New Zealand. *New Zealand Journal of Geology and Geophysics*, 25, 335-352.

GILLIE, R.D. (1979). Sand and gravel deposits on the coast and inner shelf, east coast, Northland Peninsula, New Zealand. Unpublished D.Phil thesis, University of Canterbury, Christchurch, New Zealand, 331 p.

GORDON, A.D. and HOFFMAN, J.G. (1986). Sediment features and processes of the Sydney continental shelf . In FRANKEL, E., KEENE, J.B. and WALTHO, A.E. (eds), *Recent sediments in Eastern Australia - Marine Through Terrestrial.* Publication of the Geological society of Australia, N.S.W. Division , No.2, 29-51.

GRACE, R. (1988). Ecological investigations of the Auckland Harbour Board's alternative dredge spoil site off Browns Island, Waitemata Harbour. Unpublished report to the Auckland *Harbour Board.*

GRANT, W.D. and MADSEN, O.S. (1979). Combined wave and current interaction with a rough bottom. *Journal of Geophysical Research*, 84, 1797-1808.

GREGORY, M.R. (1979). Movement of sea-bed drifters near Oaonui. University of Auckland, Maui Development Environmental Study Phase II, 10 p.

GRIFFITH, J.C. (1967). *Scientific Methods in Analysis of Sediments.* McGraw Hill, New York, 508 p.

HAMILL, P.F. and BALLANCE, P.F. (1985). Heavy mineral rich sands of the Waitakere coast, Auckland, New Zealand. *New Zealand Journal of Geology and Geophysics*, 28, 503-511.

HAMMOND, R.R., and WALLACE, W.J. (1982). Seabed drifter movements in the San Diego Bay and adjacent waters. *Estuarine Coastal and Shelf Science.* 14, 623-634.

HARMS, C. (1989). Dredge spoil dispersion from an inner shelf dump-mound. Unpublished M.Phil. Thesis, University of Waikato, Hamilton New Zealand, 177 p.

HARMS, J.C., SOUTHARD, J.B., SPEARLING, P.R, and WALKER, R.G. (1975). Depositional environments as interpreted from primary sedimentary structures and stratigraphic sequences. *Lecture Notes, SEPM Short Course No. 2*, Dallas Texas, 161 p.

HARMSWORTH, G.R. (1983). Quaternary stratigraphy of the Tauranga Basin. Unpublished M.Sc. Thesis, University of Waikato, Hamilton New Zealand, 342 pp.

HARRAY, K.G. (1977). Beach erosion and sediments at Waihi Beach. Unpublished Msc.Thesis, University of Waikato, Hamilton New Zealand, 94 p.

HARRAY, K.G. and HEALY, T.R. (1978). Beach erosion at Waihi Beach, Bay of Plenty. *New Zealand Journal of Marine and Freshwater Research*, 12, 99-107.

HARRIS, T.F.W. (1985). North Cape to East Cape: aspects of the physical oceanography. University of Auckland Department of Physics and Marine Laboratory, Leigh, 178 p.

HARRIS, T.F.W. , HUGHES, T.S. and VALENTINE, E.M. (1983). Deep waves off Hicks Bay and the north-east coast, North Island. *Water and Soils Miscellaneous Publications*, No. 56, 83 p.

HAY, D.N. (1991). Storm and oceanographic databases for the Western Bay of Plenty. Unpublished M.Sc. thesis, University of Waikato, Hamilton New Zealand, 209 pp.

HAYES, J.D., IMBRIE, J., and SHACKLETON, N.S. (1976). Variations in the Earths orbit: Parameter of the ice ages. *Science*, 194, 1121-1132.

HAYES, M.O. (1967). Hurricanes as geological agents: Case studies of Hurricane Carla and Cindy, 1963. *Report of the Investigation Bureau of Economic Geology*, 61, Austin, Texas.

HAYWARD, B.W. (1974). Geology and eruptive history of Table Top Mountain area, Coromandel Peninsula. *New Zealand Journal of Geology and Geophysics*, 17, 403-422.

HEALY, T.R. (1981). Impact of proposed sand mining on an isolated unspoiled beach system - the case of Mataora, east Coromandel, N.Z. *Proceedings from the 11th. New Zealand Geography Conference*, 167-172.

HEALY, T.R. (1985). Tauranga Harbour study, part v, morphological study. A Report for the Bay of Plenty Harbour Board.

HEALY, T.R. and DELL, P.M. (1982). The Coromandel coastal survey volume 2, beach sediment textural and mineralogical data. Unpublished Report to the Hauraki Catchment Board, No. 115, 31 p.

HEALY, T.R. and DELL, P.M. (1987). Baseline data beach surveys for management of an embayed coastline, east Coromandel, New Zealand. *Journal of Shoreline Management*, 3, 129-157.

HEALY, T.R. and KIRK, R.M. (1982). Coasts . In SOONS, J.M. and SELBY, M.J. (eds.), *Landforms of New Zealand*, Longman Paul, Auckland, 81-104.

HEALY, T.R., BLACK, K.P., and de LANGE, W.P., (1987). Field investigations required for numerical modelling studies of port developments in large tidal inlet harbours. *International Geomorphology*, 1, 1099-1112.

HEALY, T.R. , DELL, P.M. and WILLOUGHBY, A.J. (1981). Coromandel coastal survey vol. 1 basic survey data. Unpublished Report to the Hauraki Catchment Board, No. 114, 233 p.

HEALY, T.R., HARMS, C., de LANGE, W.P. (1991a). Dredge spoil and inner shelf investigations off Tauranga Harbour, Bay of Plenty, New Zealand. *Coastal Sediments 91'*. ASCE, Vol. 2, 2037-2057.

HEALY, T.R., Mc CABE, B., and THOMPSON, G. (1991b). Port of Tauranga Ltd. Channel Deepening and Widening Program, 1991-1992 Environmental Impact Assessment. 122 p.

HEATH, R.A., (1978). Atmospherically induced water motions off the west coast of New Zealand. *New Zealand Journal of Marine and Freshwater Research*, 12, 381-390.

HEATH, R.A., (1979). Edge waves on the New Zealand east coast. *Marine Geodesy*, 4, 337-350.

HEATH, R.A., (1980). East oceanic flow past northern New Zealand. *New Zealand Journal of Marine and Freshwater Research*, 14, 169-182.

HEATH, R.A., (1982). Generation of 2-3 hour oscillations on the east coast of New Zealand. *New Zealand Journal of Marine and Freshwater Research*, 16, 111-117.

HEATH, A. (1985). Large scale influence of the New Zealand seafloor topography on western boundary currents of the South Pacific Ocean. *Australian Journal of Marine and Freshwater Research* 36, 1-14.

HILTON, M.J. (1990). Processes of sedimentation in the shoreface and continental shelf and the development of facies, Pakiri, New Zealand. Unpublished D.Phil thesis, University of Auckland, Auckland New Zealand, 263 p.

HOCHSTEIN, M.P. and NIXON, I.M. (1979). Geophysical study of the Hauraki Depression, North Island, New Zealand. *New Zealand Journal of Geology and Geophysics*, 22(1), 1-19.

HOGG, A.G. (1979). Identification and correlation of thinly bedded Late Quaternary tephras of Coromandel Peninsula, New Zealand. Unpublished D.Phil thesis, University of Waikato, Hamilton New Zealand, 333 p.

HOGG, A.G. and McCRAW, J.D. (1983). Late Quaternary tephras of Coromandel Peninsula, a mixed peralkaline and calcalkaline tephra sequence. *New Zealand Journal of Geology and Geophysics*, 26, 163-187.

HOUSTON, J.R. (1991). Rejoinder to : discussion of PILLEY and LEONARD (1990) and HOUSTON (1990). *Journal of Coastal Research*, 7, 565-577.

HUDSON, J.P. (1985). Geology and depositional history of Late Quaternary marine sediments on the south Sydney inner continental shelf, southeast Australia. University of Sydney, Coastal Studies Unit ,Technical Report No.85/2 .

HUME, T.M. and GIBB. J.G. (1987). The 'wooden floor' marker bed - a new method of determining historical sedimentation rates in some New Zealand estuaries. *Journal of the Royal Society of New Zealand*, 17, 1-7.

HUME, T.M. and DAHM, J. (1991). An investigation of the effects of Polynesian and European land use on sedimentation in Coromandel estuaries. Department of Conservation Consultancy Report, No. 7106:3, 47 p.

HUME, T.M. and NELSON, C.S. (1982). X-Ray diffraction analytical procedures and some mineralogical characteristics for south Auckland region sediments and sedimentary rocks, with special reference to their clay fraction. Ocassional Report No. 10, University of Waikato, Hamilton New Zealand, 33 p.

INMAN, D.L., and NORDSTROM, C.E. (1971). On the tectonic and morphologic classification of coasts. *Journal of Geology*, 79, 1-21.

JAGO, C.F. and BARUSSEAU, J.P. (1981). Sediment entrainment on a wave graded shelf, Rousillon, France. *Marine Geology*, 42, 279-299.

JOHNSON, D.W. (1919). *Shoreline processes and shoreline development*, John Wiley and Sons, New York, 584 p.

JOHNSTON, R.J. and SEMPLE, R.K. (1983). Classification using information statistics. *CATMOG*, 37., 43 p.

KAPDASLI and DYER (1986). Threshold conditions for sand movement on a rippled bed. *Geo-marine Letters*, 6, 161-164.

KIBBLEWHITE, A.C, BERGQUIST, P.R., FOSTER, B.A., and GREGORY, M.R., 1982. Maui development environmental study, report on phase 2. Report Prepared at the University of Auckland, New Zealand, for Shell B.P. and Todd Oil Services Limited, 174 p.

KOMAR, P.D. (1976). *Beach Processes and Sedimentation*. Prentice-Hall, New Jersey.

KOMAR, P.D. and MILLER, M.C. (1973). The threshold of movement under oscillatory water waves. *Journal of Sedimentary Petrology*, 43, 1101-1110.

KOMAR, P.D. and MILLER, M.C. (1975). Sediment threshold under oscillatory waves. *Proceedings, 14th Conference on Coastal Engineering*, 756-775.

KOOPMANS, L.H., (1974). *Spectral Analysis of Time Series*. Academic Press, New York and London, 366 p.

KOS'YAN, R.D. (1988). On the dimensions of passive ripple marks in the nearshore zone. *Marine Geology*, 80, 149-153.

KULM, L.D., ROUSH, J.G., HARTLETT, R.H., NEUDECK, D.M., CHAMBERS, D.M., and RUNGE, E.J. (1975). Oregon continental shelf sedimentation: Interrelationships of facies distribution and sedimentation processes. *Journal of Geology*, 83, 145-175.

LAVELLE, J.M., GADD, P.E, HAN, G.C., MAYER, W.L., STUBBLEFIELD, W.L., and SWIFT, D.J.P. (1976). Preliminary results of coincident current meter and sediment transport observations for winter time conditions of the Long Island inner shelf. *In* SWIFT, D.J. and PALMER, H.D. (eds), *Coastal Sedimentation, Bench mark papers in Geology* V42, 326-329.

LEATHERMAN, S.P. (1985). Geomorphic and stratigraphic analysis of Fire Island, New York. Marine Geology, 63, 173-195.

LEE YOUNG, J.S. and SLEATH, J.F.A. (1990). Ripple formation in combined transdirectory and steady flow. *Sedimentology*, 37, 509-516.

LEEDER, M.R. (1982). *Sedimentology, Process and Product*. George Allen and Unwin, London, 344 p.

Le MEHAUTE, B., DIVOKY, D., and LIN, A. (1969). Shallow water waves: a comparison of theories and experiments. *Proceedings of the 11th. Conference on Coastal Engineering, London*, 86-96.

LEWIS, D.W. (1984). *Practical Sedimentology*. Hutchinson Ross, Stroudsburg Pennsylvania, 229 p.

LEWIS, K.B. (1979). A storm-dominated inner shelf, western Cook Strait, New Zealand. *Marine Geology*, 31, 31-43.

LIU, J.T. and ZARILLO, G.A. (1989). Distribution of grain sizes across a transgressive shoreface. *Marine Geology*, 87, p 121-136..

LOWE, D.J. and NELSON, C.S. (1983). Guide to the nature and methods of analysis of the clay fraction of tephras from the south Auckland region, New Zealand. Ocassional Report No.11, University of Waikato, Hamilton New Zealand, 69p.

LYNE, V.D., BUTMAN, B. and GRANT, W.D. (1991a). Sediment movement along the U.S. east continental shelf - I. Estimates of bottom stress using the GRANT-MADSEN model and near-bottom wave and current measurements. *Journal of Continental Shelf Research*, 10, 397-428.

LYNE, V.D., BUTMAN, B. and GRANT, W.D. (1991b). Sediment movement along the U.S. east continental shelf - II. Modelling suspended sediment concentration transport rate during storms. *Continental Shelf Research*, 10, 429-460.

Mc CABE, P. (1985). Stratigraphy and sedimentology of late Neogene coastal deposits at Taharoa, S.W.Auckland. Unpublished M.Sc. Thesis, University of Waikato, Hamilton New Zealand, 216 p.

Mc LEAN, R.F. (1979). Dimensions of the Whiritoa sand system and implications for sand mining and shore erosion. Unpublished report to the Hauraki Catchment Board, Te Aroha, New Zealand.

McKINNEY, T.F., STUBBLEFIELD, W.L., SWIFT, D.J.P., (1974). Large-scale current lineations on the central New Jersey shelf: investigations by side-scan sonar. *Marine Geology*, 17, 79-102.

McQUILLEN, R.M. and ARDOS, D.A. (1977). *Exploring the Geology of Shelf seas.* Graham and Trotman Ltd., London, 243 pp.

MARKS, G.P. (1975). Sedimentology of Omaro barrier spit Whangapoua Harbour Coromandel Peninsula. Unpublished Msc. thesis, University of Waikato, Hamilton New Zealand, 105 p.

MARKS, G.P. and NELSON, C.S. (1979). Sedimentology and evolution of Omaro spit, Coromandel Peninsula. *New Zealand Journal of Marine and Freshwater Research, 13, 347-372.*

MARSDEN, M.A.H. (1979). Circulation patterns from sea-bed drifter studies, Western Port and inner Bass Strait, Australia. *Marine Geology*, 30, 85-99.

MARSHALL, D.J. (1988). *Cathodoluminescence of Geological Materials*. Unwin Hyman, Boston, 146 p.

MAZZULLO, J. (1986). Sources and provinces of late Quaternary sand on the east Texas-Louisianna continental shelf. *Geological Society of America Bulletin*, 97, 638-647.

MEHTA, A.J., LEE, J. and CHRISTENSEN, B.A. (1980). Fall velocity of shells as coastal sediments. *American Society of Civil Engineers, Hydraulic Division*, 106, HY11, 1727-1744.

MICHE, R. (1954). Undulatory motions of the sea in constant and decreasing depth. Ann de Ponts et Chausses, May-June, July-August, p 25-68, 131-164, 369-406.

MILLER, M.C. and KOMAR, P.D. (1980a). A field investigation of the relationship between oscillation ripple spacing and the near-bottom water orbital motions. *Journal of Sedimentary Petrology*, 50, 183-191.

MILLER, M.C. and KOMAR, P.D. (1980b). Oscillation sand ripples generated by laboratory experiments. *Journal of Sedimentary Petrology*, 50, 173-182.

MORANG, A. and McMASTER, R.L. (1980). Nearshore bedform patterns along Rhode Island from side-scan sonar surveys. *Journal of Sedimentary Petrology*, 50, 831-840.

MURRAY, S.P. (1970). Bottom currents near the coast during Hurricane Camille. *Journal of Geophysical Research*, 75, 612-634.

MUTYKA, J.M. and WILLIS, D.H. (1974). The effect of wave refraction over dredge holes. *14th. Conference on Coastal Engineering, American Society of Civil Engineers*, Copenhagen, 615-625.

NAKASHIMA, L.D. (1989). Shoreline responses to Hurricane Bonnie in southwest Louisiana. *Journal of Coastal Research*, 5, 127-136.

NELSON, C.S. and HEALY, T.R. (1982). Side-scan sonar survey of the sea floor of Northern Poverty Bay in the vicinity of the Port of Gisborne. Occasional Report No.9, Earth Sciences Department University of Waikato, Hamilton New Zealand, 38 p.

NIEDORODA, A.W. , SWIFT, D.J. and HOPKINS, T.S. (1985a). The shoreface. *In* DAVIS, R.A. Jr. (ed), *Coastal Sedimentary Environments*, New York, Springer-Verlag, 533-624.

NIEDORODA, A.W., SWIFT, D.J.P., FIGUEIREDO, A.G., and FREELAND, G.L. (1985b). Barrier island evolution, Mid Atlantic Shelf, U.S.A. part II: evidence from the shelf floor. *Marine Geology*, 63, 363-396.

NIEDORODA, A.W., SWIFT, D.J., HOPKINS, T.S., and CHEN-MEAN, M.A. (1984). Shoreface morphodynamics on wave-dominated coasts. *Marine Geology*, 60, 331-354.

NIELSON, P. (1979). Some basic concepts of wave sediment transport. *Series paper 20, I.S.V.A.*, Technical Report, University of Denmark.

NITTROUER, C.A. and STERNBERG, R.W. (1981). The formation of sedimentary strata in an allochthonous shelf environment: the Washington continental shelf. *Marine Geology*, 42, 202-232.

NODA, E.K. (1972). Wave-induced circulation and longshore current patterns in the coastal zone: Tetra Tech. Report No. TC-149-3, California, 120 p.

PANOFSKY and BRIER (1968). *Some Applications of Statistics to Meteorology*. Pennsylvania State University Publication, 224 p.

PEEK, S.M. (1979). A comparative study of beach morphodynamics on the east and west coasts of the North Island, New Zealand. Unpublished M.A. thesis , University of Auckland, Auckland New Zealand.

PHILLIPS, A.W. (1970). The use of the Woodhead seabed drifter. *British Geomorphological Research Group*, Technical Bulletin, 4, 29 p.

PICKARD, G.L. and EMERY, W.J. (1984). *Descriptive Physical Oceanography - an Introduction*. 4th. edition, Pergamon Press, 249 p.

PICKRILL, R.A. and MITCHELL, J.S. (1979). Ocean wave characteristics around New Zealand. *New Zealand Journal of Marine and Freshwater Research*, 13, 501-520.

POND, S. and PICKARD, G.L. (1983). *Introductory Dynamic Oceanography*. 2nd edition, Pergamon Press, 329 p.

POSAMENTIER, H.W. and VAIL, P.R. (1988). Eustatic controls on clastic deposition II-Sequence and systems tract models. In C.K. WILGUS, B.. HASTINGS, C.G.St.C. KENDALL, H.W. POSAMANTIER, C.A. ROSS, and J.C. VAN WAGONER (eds), *Sea Level Changes: An Integrated Approach*. Society of Economic Paleontologists and Mineralogists, Special Publication, 42, 187-202 p.

POWELL, A.W.B. (1979). *New Zealand Mollusca, Marine, Land and Freshwater.* Collins, London, 500 p.

RIGLER, J.K. and COLLINS, M.B. (1984). Initial grain motion under oscillatory flow: a comparison of some threshold criteria. *Geo-marine Letters*, 3, 43-48.

RILEY, P.B., MONRO, I.S. and SCHOFIELD, J.C. (1985). Late Holocene sedimentation in Omaha Bay, North Island, New Zealand. *New Zealand Journal of Geology and Geophysics*, 28, 299-312.

ROY, P.S. (1985) . Marine sand bodies on the south Sydney shelf , S.E. Australia . University of Sydney , Coastal Studies Unit Tech. Report No.85/1 .

ROY, P.S. (1989). Offshore mineral exploration in the Gulf of Thailand. Quaternary geology: a methodology of marine exploration using lithofacies concepts. *Unpublished report to the Department of Mineral Resources, Thailand*, THA/86/018, 92 p.

ROY, P.S. and HUDSON, J.P. (1987). The marine placer mineral project-seismic results from the continental shelf, southern New South Wales: Narooma-Montague Island-Bermagui area. *Geological Survey of New South Wales*, Report No. G.S. 1987/094.

ROY, P.S. and STEPHENS, A.W. (1980). geological controls on process-response, S.E. Australia. *Proceedings of the 17th. International Coastal Engineering Conference*, Sydney, 913-933.

ROY, P.S. and THOM, B.G. (1981) Late Quaternary marine deposition in N.S.W. and southern Queensland, an evolutionary model. *Journal of the Geological Society of Australia*, 28, 471-489.

ROY, P.S. , THOM, B.G. and WRIGHT, L.D. (1980). Holocene sequences of an embayed high-energy coast: an evolutionary model. *Sedimentary Geology*, 26, 1-19.

RYAN, S.G. (1989). Investigations of the sedimentological impact of dredge spoil in the Purakau Channel, Manakau harbour. Unpublished M.S.c. Thesis, University of Waikato, Hamilton New Zealand.

SAITO, Y. (1989). Late Pleistocene coastal sediments, drainage patterns and sand ridge systems on the shelf of Sendai, northeast Japan. *Marine Geology*, 89, 229-244.

SALLENGER, A.H., Jr. and RICHMOND, B.M. (1984). High frequency sediment level oscillations in the surfzone. *Marine Geology*, 60, 155-164.

SANDERSON, B.G. (1979). A study of ocean circulation using radio drogues. Unpublished M.Sc. thesis, University of Auckland, Auckland New Zealand.

SAS/ETS *User's Guide, Version 5 Edition.* Cary, NC: SAS Institute Inc., 1984. 738 p.

SCHOFIELD, J.C. (1970). Coastal sands of Northland and Auckland. *New Zealand Journal of Geology and Geophysics*, 13, 767-824.

SCHOFIELD, J.C. (1978). Sea-floor sediments and sea-level change, Omaha Bay, New Zealand. *4th Australian Conference on Coastal and Ocean Engineering*, Adelaide, Institute of Engineers Australia National Conference, Publication 78/11: 30-33

SCHOFIELD, J.C. (1985). Coastal change at Omaha Bay and Great Barrier Island. *New Zealand Journal of Geology and Geophysics*, 28, 313-322.

SELLEY, R.C. (1982). *An Introduction to Sedimentology.* Academic Press, 2nd edition, 417 p.

SEYMOUR, R.J., THOMAS, J.O., CASTEL, D., WOODS. A.E., and SESSIONS, M.H. (1982). Coastal Data Information Program: Sixth Annual Report January-December 1981, IMR Ref. 81-3, U.S. Army Corps of Engineers and California Department of Boating and Waterways, 190 p.

SHACKLETON, N.S. and OPDYKE, N.D. (1973). Oxygen isotope and palaeomagnetic stratigraphy of equitorial Pacific core V28-238: Oxygen isotope temperatures and ice volumes on a 10^5 and 10^6 year scale. *Quaternary Research*, 3, 39-55.

SHEFFIELD, A.T. (in prep.). Sediments and hydrodynamics of Whangamata Harbour. Unpublished M.Sc thesis, University of Waikato, Hamilton New Zealand., 190 p.

SHEPARD, F.P. (1932). Sediments on the continental shelves. *Geological Society of America Bulletin*, 43, 1017-1039.

SHEPARD, F.P. (1973). *Submarine Geology.* 3rd Edition, Harper and Row, New York, 517 p.

SHI, N.C. and LARSEN, L.H. (1984). Reverse sediment transport induced by amplitude modulated waves. *Marine Geology*, 54, 181-200.

SHIPP, R.C., BELKNAP, D.F., and KELLEY, J.T. (1991). Seismic-stratigraphic and geomorphic evidence for a post-glacial sea-level low stand in the Northern Gulf of Maine. *Journal of Coastal Research*, 7, 341-364.

SHORT, A.D. (1987). Modes of Holocene coastal dune formation in southern Australia: a case study. *Sedimentary Geology*, 55, 121-142.

SHORT, A.D. (in press). Beach systems of the central Netherlands coast. I. Processes and morphology. Submitted to *Marine Geology*, 1991.

SHORT, A.D. (in press). Beach systems of the central Netherlands coast. 2. Morphodynamics of a storm-driven, multi bar system. Submitted to *Marine Geology*, 1991.

SHORT, A.D. and WIGHT, L.D. (1984). Morphodynamics of high energy beaches: an Australian perspective. In THOM, B.G. (ed), *Coastal Geomorphology in Australia, Academic Press*, 43-68.

SKINNER, D.N.B. (1967). Geology of the Coromandel region with emphasis on some economic aspects. Unpublished D.Phil Thesis, University of Auckland, Auckland New Zealand.

SKINNER, D.N.B. (1976). Sheet N40 and pts N35, N36, N39 Northern Coromandel (1st ed.). Geological map of New Zealand 1:63 360. Department of Scientific and Industrial Research, Wellington, New Zealand.

SKINNER, D.N.B. (1986). Neogene volcanism of the Hauraki volcanic region. In SMITH, I.E.M. *Late Cenozoic Volcanism in New Zealand*, The Royal Society of New Zealand, Bulletin 23, 19-47.

SMITH, D.B. (1980). Sea level oscillations, hydrology and sedimentology of Mercury Bay. Unpublished M.Sc. thesis, University of Waikato, Hamilton, New Zealand, 235 p.

SNEDDEN, J.W., NUMMEDAL, D., and AMOS, A.F., (1988). Storm and fair-weather combined flow on the central Texas continental shelf. *Journal of Sedimentary Petrology*, 58, No.4, 580-595.

SOUTHARD, J.B. and DINGLER, J.R. (1971). Flume study of ripple progradation behind mounds of flat sand beds. *Sedimentology*, 16, 251-263.

SWIFT, D.J.P. (1976a). Shelf sedimentation. In D.J. STANLEY and D.J. SWIFT (eds), *Marine Sediment transport and environmental management*, Wiley New York, 602 pp.

SWIFT, D.J.P. (1976b). Coastal sedimentation. In D.J. STANLEY and D.J. SWIFT (eds), *Marine Sediment transport and environmental management*, Wiley New York, 602 pp.

SWIFT, D.J.P., and FIELD, M.E. (1981). Evolution of a classic sand ridge field: Maryland sector, North America inner shelf. *Sedimentology*, 28, 461-482.

SWIFT, D.J.P. and FREELAND, G.L. (1978). Current lineations and sand waves on the inner shelf, middle Atlantic Bight of North America. *Journal of Sedimentary Petrology*, 48, 1257-1266.

SWIFT, D.J.P. and NUMMEDAL, D. (1987). Hummock cross-stratification, tropical hurricanes and intense winter storms. *Sedimentology*, 34, 338-344.

SWIFT, D.J.P., FIGUEIREDO, A.G., FREELAND, G.L., and OERTEL, G.F. (1983). Hummocky cross-stratification and megaripples: a geological double standard? *Journal of Sedimentary Petrology*, 53, 1295-1317.

SWIFT, D.J.P., STANLEY, D.J., and CURRAY, J.R. (1971). Relict sediments on continental shelves: a reconsideration. *Journal of Geology*, 79, 322-346.

SWIFT, D.J.P., NIEDORODA, A.W., VINCENT, C.E. and HOPKINS, T.S. (1985). Barrier island evolution, middle Atlantic shelf, U.S.A. Part 1. shoreface dynamics. *Marine Geology*, 63, 331-361.

THOM, B.G. (1984). Sand barriers of eastern Australia - a case study. *In* B.G. THOM (ed), *Coastal Geomorphology in Australia*, Academic Press, 232-261.

THOM, B.G. and ROY, P.S. (1984). sea level changes in New South Wales over the last 15 000 years. In D. HOPLEY (ed) *Australian Sea Levels in the Last 15 000 Years: a Review*. Department of Geography, James Cook University, Monograph Series, Occasional Paper No.3, 64-84.

THOM, B.G., POLACH, H.A., and BOWMAN, G.M. (1978). Holocene age structure of coastal sand barriers in New South Wales, Australia. Department of Geography, University of N.S.W., Duntroon, A.C.T.

THRASHER, G.P. (1986) . Basement structure and sediment thickness beneath the continental shelf of the Hauraki Gulf and offshore Coromandel region, New Zealand. *New Zealand Journal of Geology and Geophysics*, 29, 41-50.

TWICHELL, D. C. (1983). Bedform distribution and inferred sand transport on Georges Banks, United States Atlantic continental shelf. *Sedimentology*, 30, 695-710.

VAIL, P.R. (1987). Seismic stratigraphy interpretations using sequence stratigraphy. Part I: Seismic stratigraphy interpretation procedure. In: A.W. BALLY (ed), *Atlas of Seismic Stratigraphy*. American Association of Petroleum Geologists Studies in Geology, 27, 1-10.

VAIL, P.R., MITCHUM, R.M., TODD, R.G., WIDMIER, J.M., THOMPSON, S., SANGREE, J.B., BUBB, J.N., and HATLELID, W.G. (1977). Seismic stratigraphy and global changes of sea level. In C.E. PAYTON (ed.), *Seismic Stratigraphy-Applications to Hydrocarbon Exploration*: American Association of Petroleum Geologists Memoirs, 26, 49-212.

VAN WAGONER, J.C., MITCHUM, R.M., CAMPION, K.M., and RAHMANIAN, V.D. (1990). Siliclastic sequence stratigraphy in well logs, cores, and outcrops: Concepts for high resolution correlation of time and facies. *American Society of Petroleum Geologists.* Methods Explor. Ser., 7, 55 p.

VINCENT, C.E., HANES, D.M. and BOWEN, A.J. (1991). Acoustic measurements of suspended sand on the shoreface and the control of concentration by bed roughness. *Marine Geology*, 96, 1-18.

VINCENT, C.E., SWIFT, D.J.P., and HILLARD, B., (1981). Sediment transport in the New York Bight, North American Atlantic shelf. *Marine Geology*, 42, 369-398.

VINE, M.H. (1981). Report on the flood of April 1981, Vol. 2 erosion, deposition, and costs. Unpublished Report to the Hauraki Catchment Board, Te Aroha New Zealand, 53 p.

WALKER, R.G. (1984). *Facies Models*. Ainsworth Press Ltd., Ontario, 317 p.

WIEGEL, R.L. (1954). Gravity wave, tables of functions. Council on Wave Research, Engineering Foundation, University of California, Berkeley California, 30 p.

WILLOUGHBY, A.J. (1981). Nearshore sediments off Whiritoa Beach, Coromandel Peninsula, New Zealand. Unpublished M.Sc. thesis, University of Waikato, Hamilton New Zealand, 123 p.

WRIGHT, I.L. (1989). *Bay of Plenty Bathymetry, 2nd. ed.* New Zealand Oceanographic Instititute Chart, Coastal Series, 1-200 000.

WRIGHT, L.D. (1976). Nearshore wave power dissipation and the coastal energy regime of the Sydney-Jervis Bay region, N.S.W: A comparison. *Australian Journal of Marine and Freshwater Research*, 27, 633-640.

WRIGHT, L.D. (1987). Shelf-surfzone coupling: Diabathic shoreface transport. *In* N.C. KRAUS (ed), *Coastal Sediments '87*, 26-40.

WRIGHT, L.D. and COLEMAN, J.M. (1972). River delta morphology: wave climate and the role of the subaqeous profile. *Science*, 176, 282-284.

WRIGHT, L.D. and SHORT, A.D. (1984). Morphodynamic variability of surfzones and beaches , a synthesis. *Marine Geology*, 56, 93-118.

WRIGHT, L.D. and THOM, B.G. (1977). Coastal depositional landforms, a morphodynamic approach. *Progress in Physical Geography*, 2, 412-459.

WRIGHT, L.D., BOON, J.D., GREEN, M.O. and LIST, J.H. (1986). Response of the mid-shoreface of the southern mid-Atlantic Bight to a "northeaster". *Geomarine Letters*, 6, 153-160.

WRIGHT, L.D., BOON, J.D., KIM, S.C. and LIST, J.H. (1991). Modes of cross-shore sediment transport on the shoreface of the middle Atlantic Bight. *Marine Geology*, 96, 19-51.

WOODHEAD, P.M.J. and LEE, A.J. (1960). A new instrument for measuring residual currents near the seabed. *International Council for Exploration of the Sea C.M. 1960 Hydrographic Committee*, No.12.

YALIN, M.S. (1977). *Mechanics of Sediment Transport*. 2nd. edition. Permagon Press Inc., London, 298 p.

APPENDICES

APPENDIX 1

CURRENT MEASUREMENT INFORMATION

Appendix 1A

Equipment Specifications & Deployment

Sea bed Drifters.

An example of the Woodhead sea bed drifter used in this study is shown in Figure A.1. The head on this is pierced by four equidistant holes, each of 2 cm diameter and a distance of 3 cm from the center. These are necessary in preventing back pressure from developing and slowing the drifter down, allowing the drifter to sink back relatively rapidly when lifted by turbulence, and to prevent air pockets from forming under the saucer (PHILLIPS, 1970)

The copper weight is required to give the drifter a slight negative buoyancy so that it will move with the current. WOODHOUSE and LEE (1960) found that with an attached weight of between 5 and 8 g, when the current dropped below 0.17 $m.s^{-1}$ the drifters will begin to move at a speed less than the true water speed. The above authors have suggested a 7 g weight as appropriate for use at sea.

One disadvantage with the Woodhead drifters is that they are not readily available in New Zealand, and must therefore be obtained by overseas mail order. This can involve undesirable postage expenses. In order to minimise the costs involved for future local studies, an analogous sea-bed drifter has since been designed at the Earth Sciences Department, University of Waikato, and has since been successfully applied for Langrangian current measurements at Gisborne Harbour by KENSINGTON (1990).

Aanderaa Current Meters.

Current meters used in this study were non-vector averaging RCM-4 Aanderaa systems. Details regarding the design, deployment and limitations of this current meter system for New Zealand coastal conditions are described comprehensively by BELL *et al.* (1988), and briefly outlined here for East Coromandel conditions. The current meters were programmed to record an average speed taken over a fifteen minute interval, but could only measure direction at the end of this interval. Thus some uncertainties will be present as to the true nature of the velocity vector components. One of the main problems found with this system related to biological fouling of the the meters. This potential source of error was reduced to some degree by coating most of the current meter in anti-fouling paint. Despite this, the speed and salinity recordings usually showed evidence of interference after periods of about 6 weeks. Common fouling organisms found were hydroids and squid eggs (Figure A1.2). Although BELL *et al* . (1988) note wave pumping of the savonious rotor as a general source of error in current measurements around New Zealand, evidence presented in Chapter 4 did not show this as a probable short comming for the East

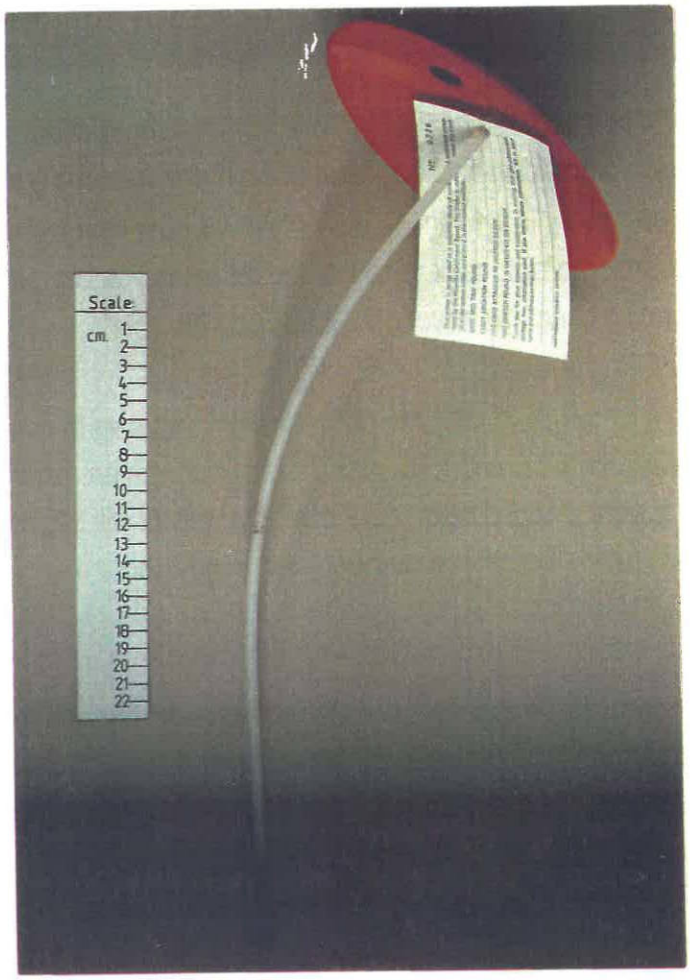

Figure A1.1. Example of the Woodhead sea-bed drifter used for the east Coromandel study.

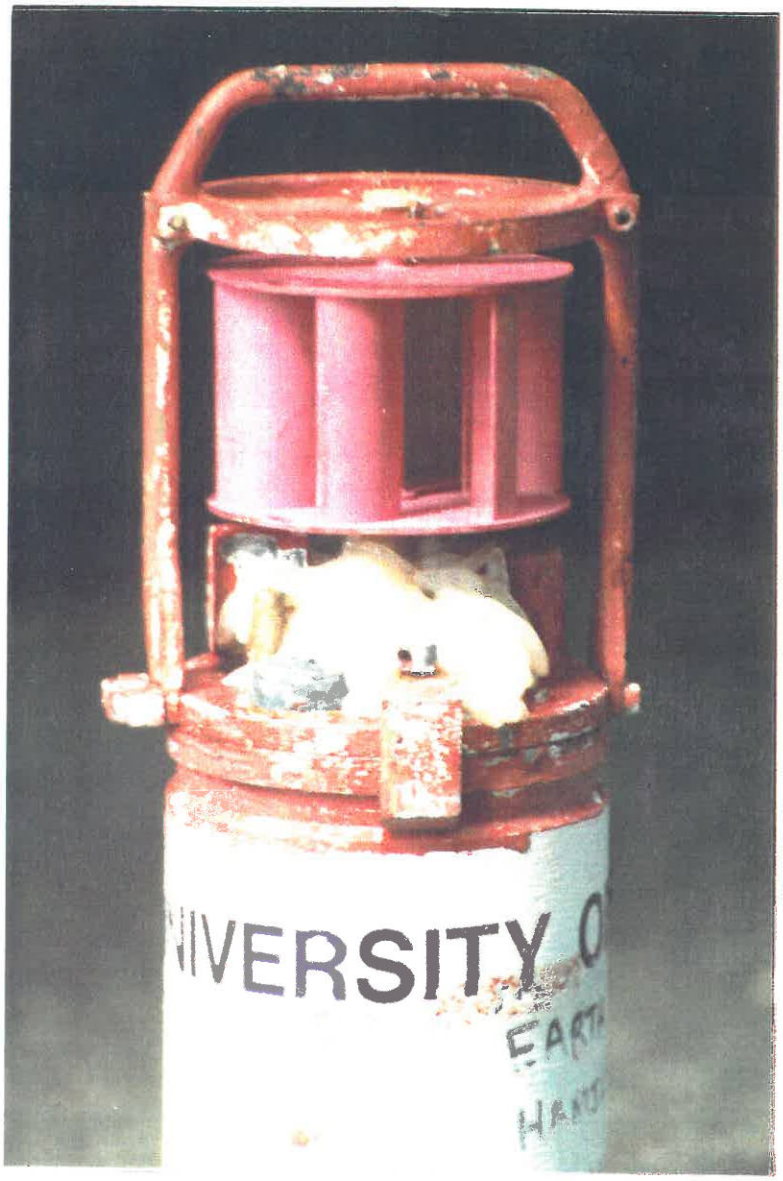

Figure A1.2. Example of bio-fouling (squid eggs) impeding movements of the savonious rotor (non-shrouded), from a current meter deployed for c.2 months at Whiritoa.

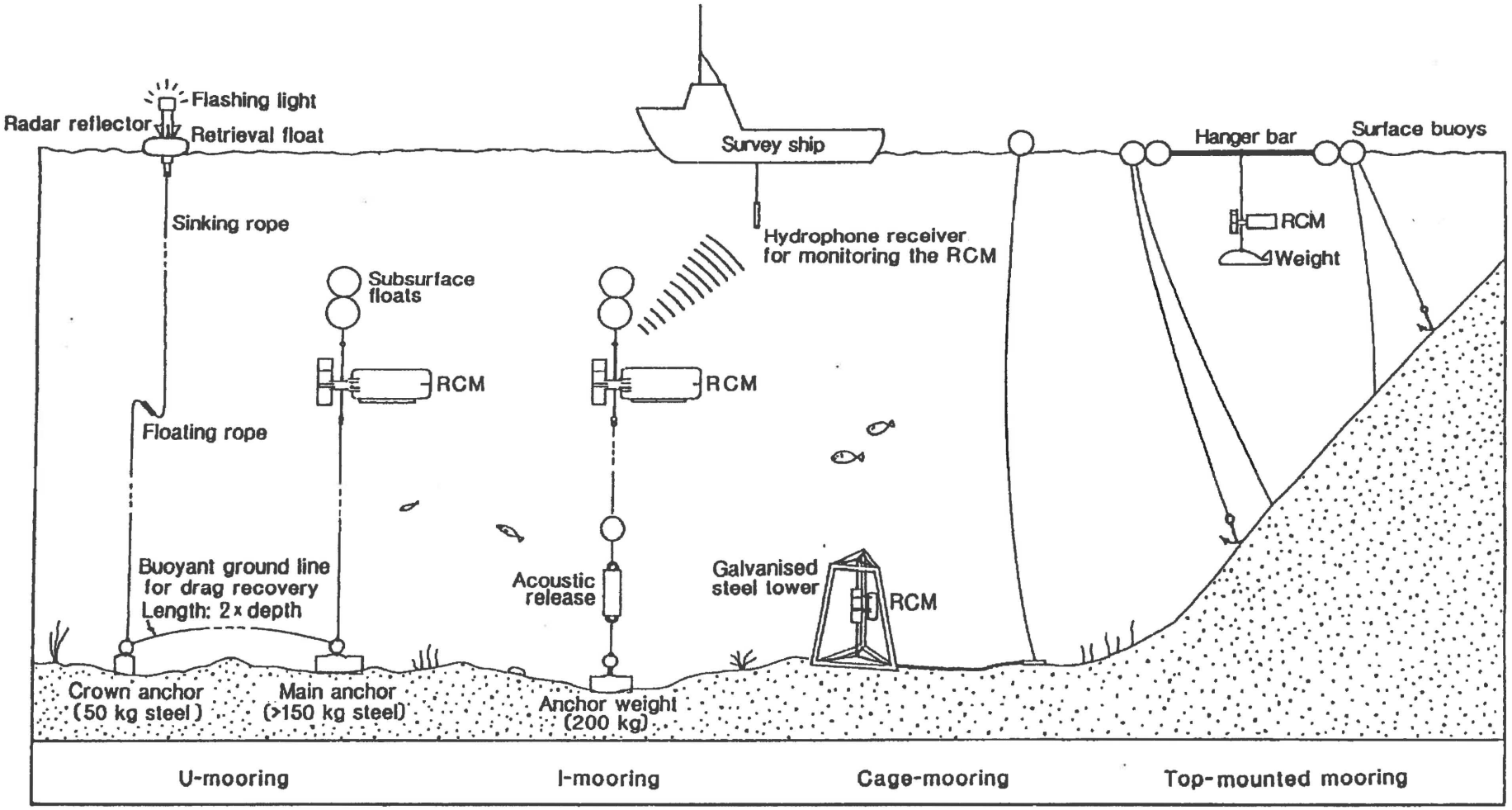

Figure A1.3. Different methods for mooring current meters in coastal waters (from BELL *et al.*, 1988). For the east Coromandel study, a U-mooring system was utilised.

Coromandel current measurements. This potential error source was also further reduced by using a flat bladed "paddle" rotor shielded around half it's circumference by a metal shroud, for experiments conducted latter in the study at Opito Bay, Whangapoua and Waihi.

The current meters were deployed at each site with a "U-mooring" system as described by BELL *et al.* (1988; Figure A1.3). Here the current meter is anchored to the sea-bed by c.150-200 kg. of metal chain, and stabilised with a pair of sub-surface buoys. A surface buoy is necessary for location of the current meter, and is attached to the mooring by a separate "crown" anchor to minimise the effects of wave-induced surface buoy motions on the meter. The system was first set-up on the ship deck, then lowered overboard by mechanical winch . Problems encountered in previous studies using this system include: fouling of the current meter by the mooring ropes; shifting of the mooring away from the original site during storms; and theft/loss of the mooring by fishing vessels. These risks were minimised by: sending divers down to the mooring after deployment overboard to check that all lines are free; placing radar beacons on the current meters so that they could be relocated if lost; and attaching an additional anchor line to the surface buoy with a steel cable and welded shackle to discourage local fisherman from acquiring the buoy. Fortunately, in the course of all 7 current meter deployments, no problems were encountered in loss or movement of the current meter moorings.

Anemographs

Anemographs used to record wind velocity vector components were an integral part of the regional current pattern analysis. To be comparable with similar oceanographic studies, these needed to be positioned c. 10 m above sea level, and as close as possible to the frontal dune of each beach system (away from any structures which might interfere with wind recordings e.g trees, high buildings). Locations used included: the Bowentown Boat Club at Waihi; the Whiritoa Surf Club; and a fence post on the western end of Matarangi Beach.

Two recording systems were used in the course of the study. For most areas (except Whiritoa in the Sep-90 study), a Woeffler Anemograph was used (Figure A1.4). This contains an enclosed graphic trace recording system, with a wind vane and wind cups mounted to its upper surface. The graphic trace gives a continuous record of wind direction and the wind run, which must latter be converted to wind speed. One of the main disadvantages of this system is that for any long-term deployment, a high degree of maintenance is required (about once monthly) in terms of re-winding the mechanical trace rolls, and replacing the trace paper. Analysis of results is also very time consuming and cumbersome.

An improved computerised wind recording system was available in Sep-90 at Whiritoa. The main components of this system are a "Vector" brand pair of detached wind cups and vane, which are connected by cable to a digital recording "Starlog" unit (Figure A1.5). Before operation, it is first

necessary to program the system by computer for the recording specifications to be used. In this study, the same specifications were used as for current meter recordings, i.e. speed averaged over 15 min. intervals and direction measured instantaneously at the end of this. Upon completion of measurements, the recorder is again connected to the computer and the data read onto an appropriate analytical program. Advantages of this system are that it is a low maintenance unit, which only requires attendance initially and upon completion of recordings. The data is also readily available for analysis upon completion of recordings, and can be directly compared with current meter recordings. Some disadvantages are that for long-term recordings, an external power source is required (although a rechargeable battery can be used over shorter periods), and the electronic parts of the system need to be contained within some sheltered area.



Figure A1.4. The Woeffler Anemograph used throughout most of the study to collect information on wind velocity vector components. In this example, the recorder has been placed on a fence post at Matarangi Beach c.10 m above sea level. The system works by recording wind run and direction on a continuous graphic trace, contained within a protected metal casing.



Figure A1.5. Computerised wind recording system used at Whiritoa Surf Club in SEP-90. Here, a separate "Vector" wind cup and vane are connected by cable to a digital recording "Starlog" unit, contained within the surf club premises.

Appendix 1B

Analysis of Semi-Diurnal Tidal Component in Current Records

As no computer programs were readily available to separate the semi-diurnal M_2 tidal component from current records, the importance of this factor in influencing current patterns could only be assessed through very simple means. This was done by plotting various sections of the current records over 48 hr. periods of calm weather conditions.

Data from the initial recordings at Onemana showed no obvious semi-diurnal variations in any of the recorded properties (i.e. current direction and speed, water temperature and salinity; Figure A1.6). As progressive vector plots showed this to be a reasonably representative period of current recordings, it is assumed that tidal currents were not responsible for fair weather current patterns at Onemana.

Recordings from Opito Bay were analysed over two 48 hr. periods, at the beginning of data collection (Figure A1.7), and two weeks latter when the pronounced temperature variations described in Chapter 4 were apparent (Figure A1.8). The data shows that pronounced semi-diurnal variations occur for current direction and speed at Opito, with northwesterly ebbing and northeasterly flooding tidal flows present initially, but the opposite association present a fortnight latter. Current speed during both periods tends to peak either at mid-tide or just prior to low tide. Water temperature and salinity values show only minor semi-diurnal variations initially, but temperature fluctuations increase noticeably a fortnight latter, with maximum temperatures and minimum salinities tending to occur at low tide. Thus the semi-diurnal M_2 tide has a strong influence on fair weather water circulation off Opito Bay.

Data obtained offshore from Whangapoua Harbour was analysed over the same 48 hr. periods as Opito Bay (Figures A1.9, A1.10). Current direction showed the most pronounced semi-diurnal variations, with northeasterly ebbing and northwesterly flooding tidal flows present initially, and a southeasterly ebbing and westerly flooding tidal flow present 2 weeks latter. Speed fluctuations were less pronounced, although peak flows tend to occur again at mid tide or just prior to low tide, and fluctuations in water temperature and salinity showed no obvious semi-diurnal patterns. Thus the M_2 tidal wave still appears to affect waters off Whangapoua, however its influence is far less pronounced than off Opito Bay.

Records obtained from Whiritoa were only analysed for the first 48 hrs.. of current meter recordings (Figure A1.11). This shows no apparent cyclic fluctuations in either current speed, or water temperature and salinity. As this area showed similar variations in these properties to

Waihi, it is assumed that tidal flows form an insignificant component to current patterns during calm conditions.

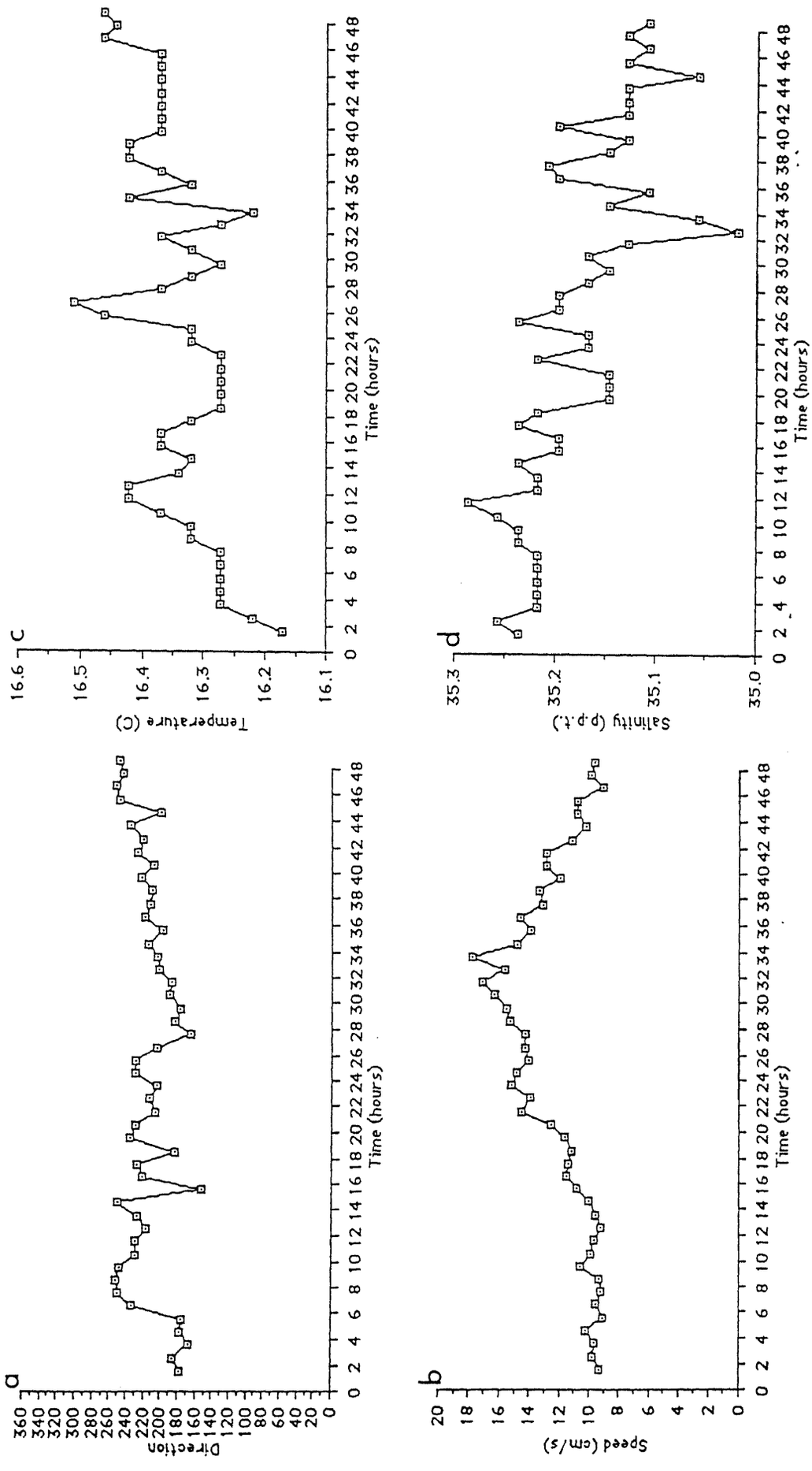

Figure A1.6. 48 hour current measurements from Onemana (7-8-JUN-85): a) current direction; b) current speed; c) water temperature; d) water salinity. Note that no obvious semi-diurnal trends can be seen in any of these records.

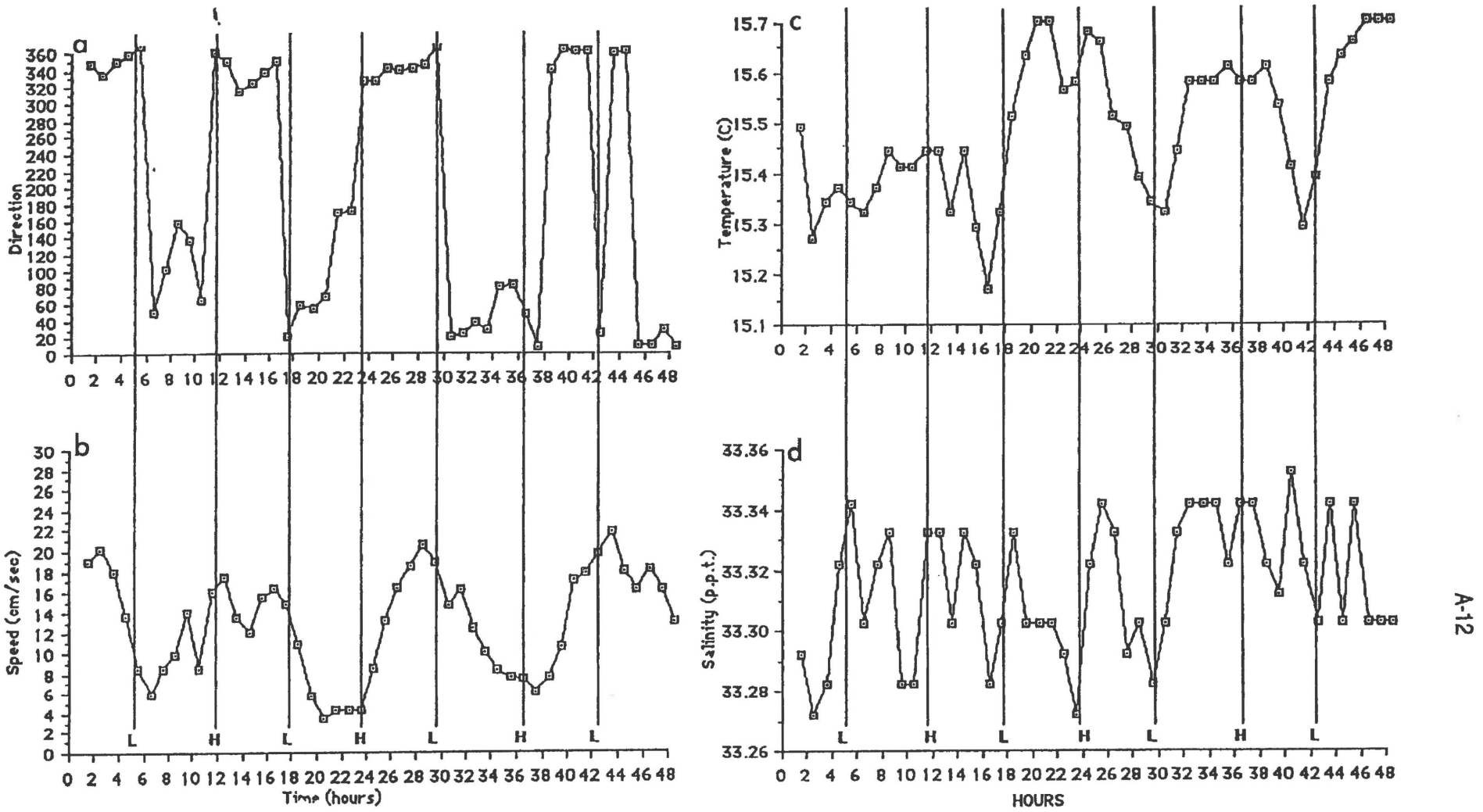

Figure A1.7. 48 hour current recordings from Opito Bay (20-21-OCT-89): a) current direction; b) current speed; c) water temperature; d) water salinity. Note that significant fluctuations in the data tend to coincide with periods of high (H) and low water (L) along the coast.

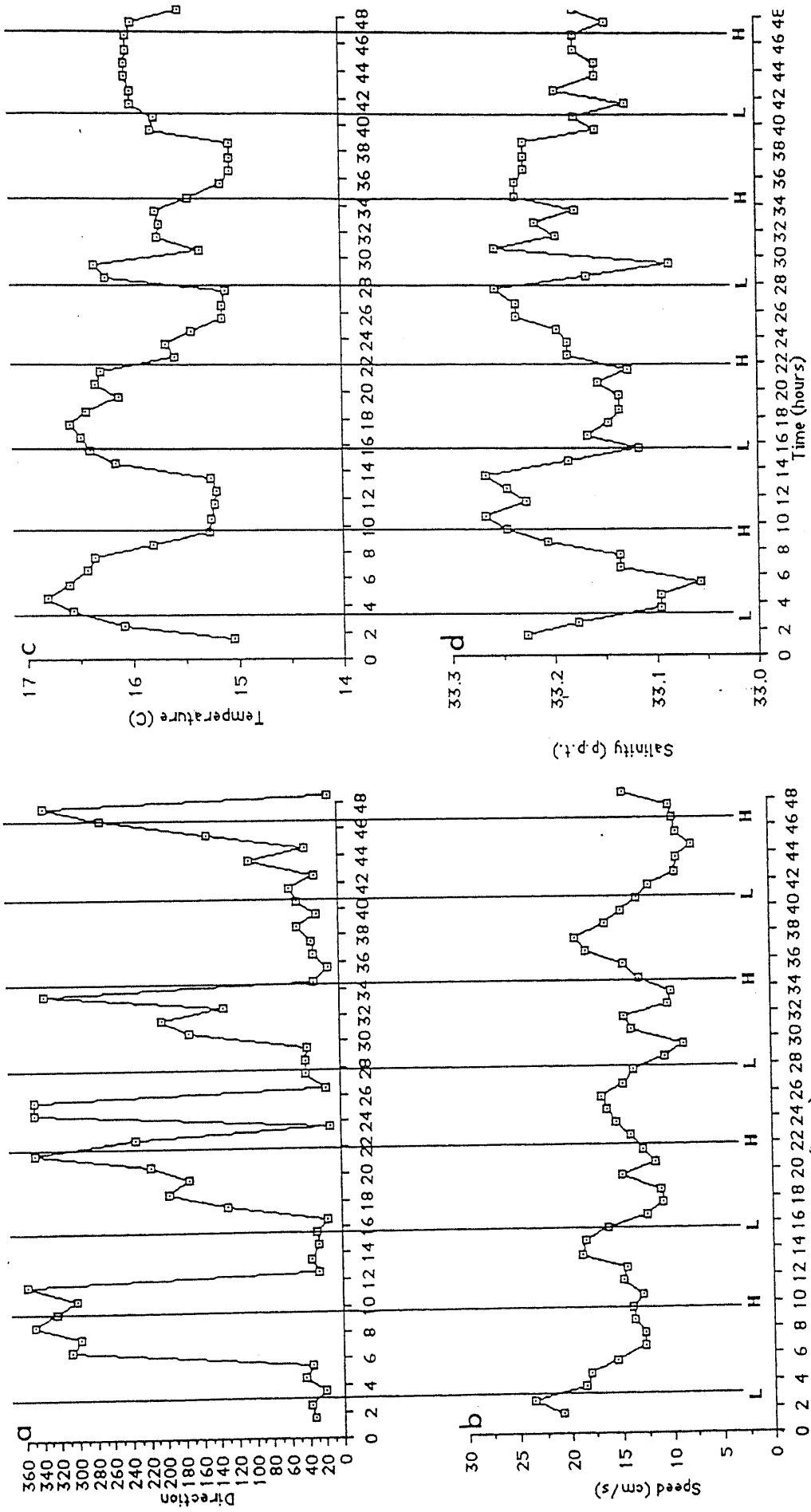

Figure A1.8. 48 hour current recordings from Opito Bay (2-3-SEP-89): a) current direction; b) current speed; c) water temperature; d) water salinity. Note that semi-diurnal direction and speed fluctuations are less pronounced here than before, but water temperature and salinity variations are more synchronous with the local tidal wave.

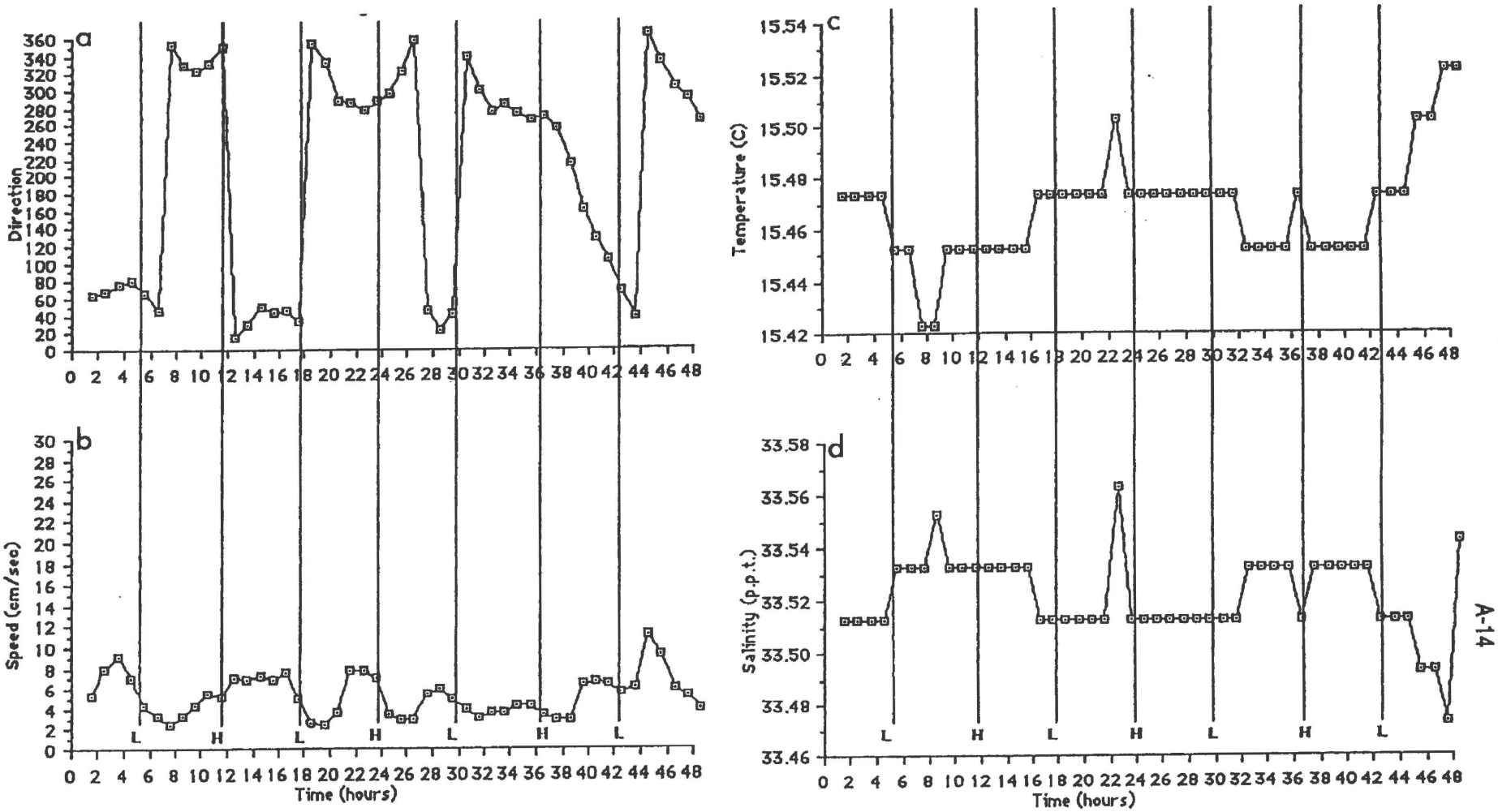

Figure A1.9. 48 hour current recordings from Matarangi (20-21-OCT-89): a) current direction; b) current speed; c) water temperature; d) water salinity. Note that significant fluctuations in the current direction and speed data tend to coincide with periods of high (H) and low water (L) along the coast, but similar variations are not apparent in the temperature and salinity records.

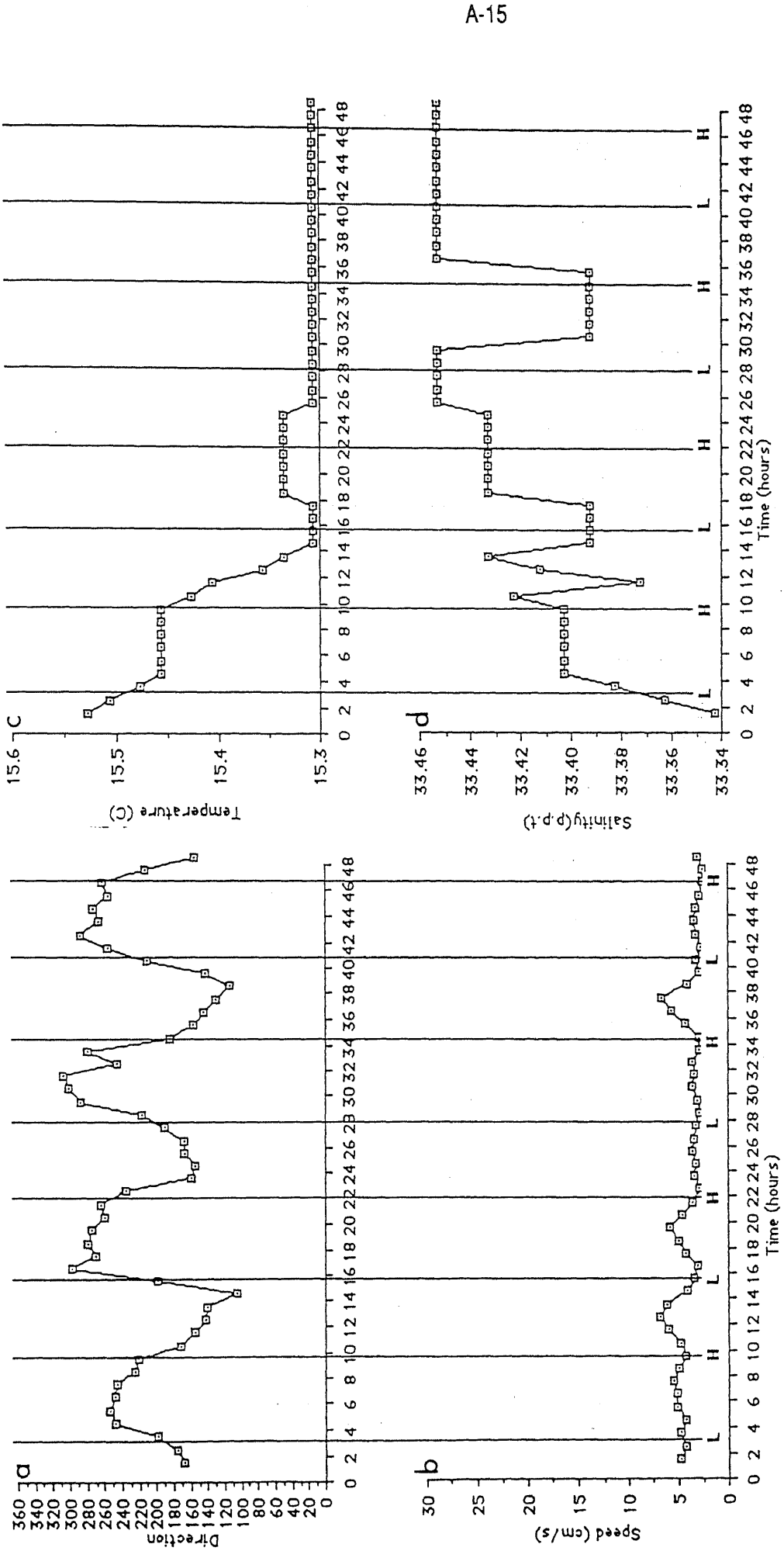

Figure A1.10. 48 hour current recordings from Matarangi (2-3-SEP-89): a) current direction; b) current speed; c) water temperature; d) water salinity. Note that significant fluctuations in the current direction and speed data tend to coincide with periods of high (H) and low water (L) along the coast, but variations in the temperature and salinity records have only a slight association with the tidal component.

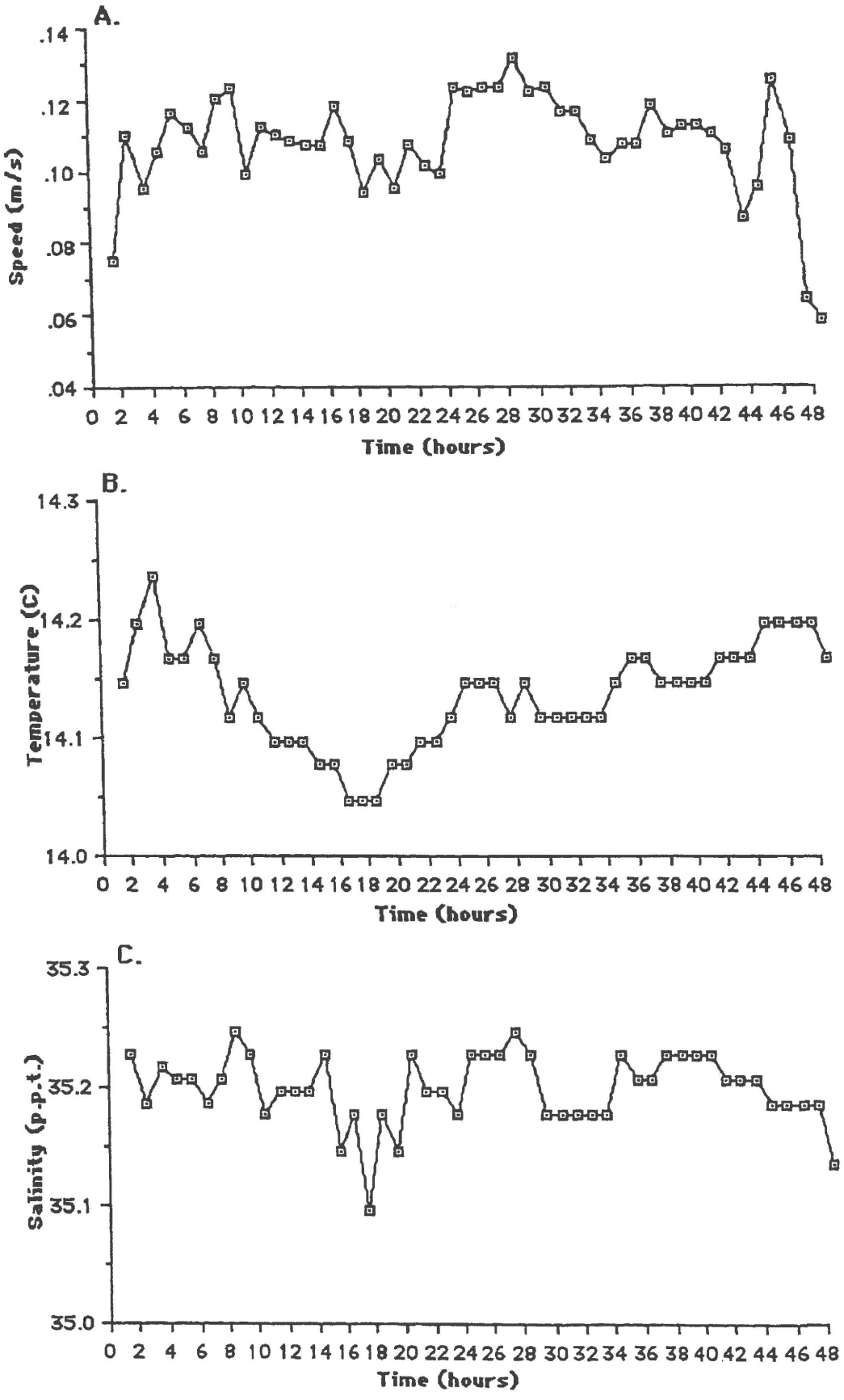

Figure A1.11. 48 hour current measurements from Waihi (11-12-SEP-90): a) current speed; b) water temperature; c) water salinity. Note that no obvious semi-diurnal trends can be seen in any of these records.

APPENDIX 2

SEDIMENT SAMPLE LOCATIONS

A-17

WAIHI BEACH

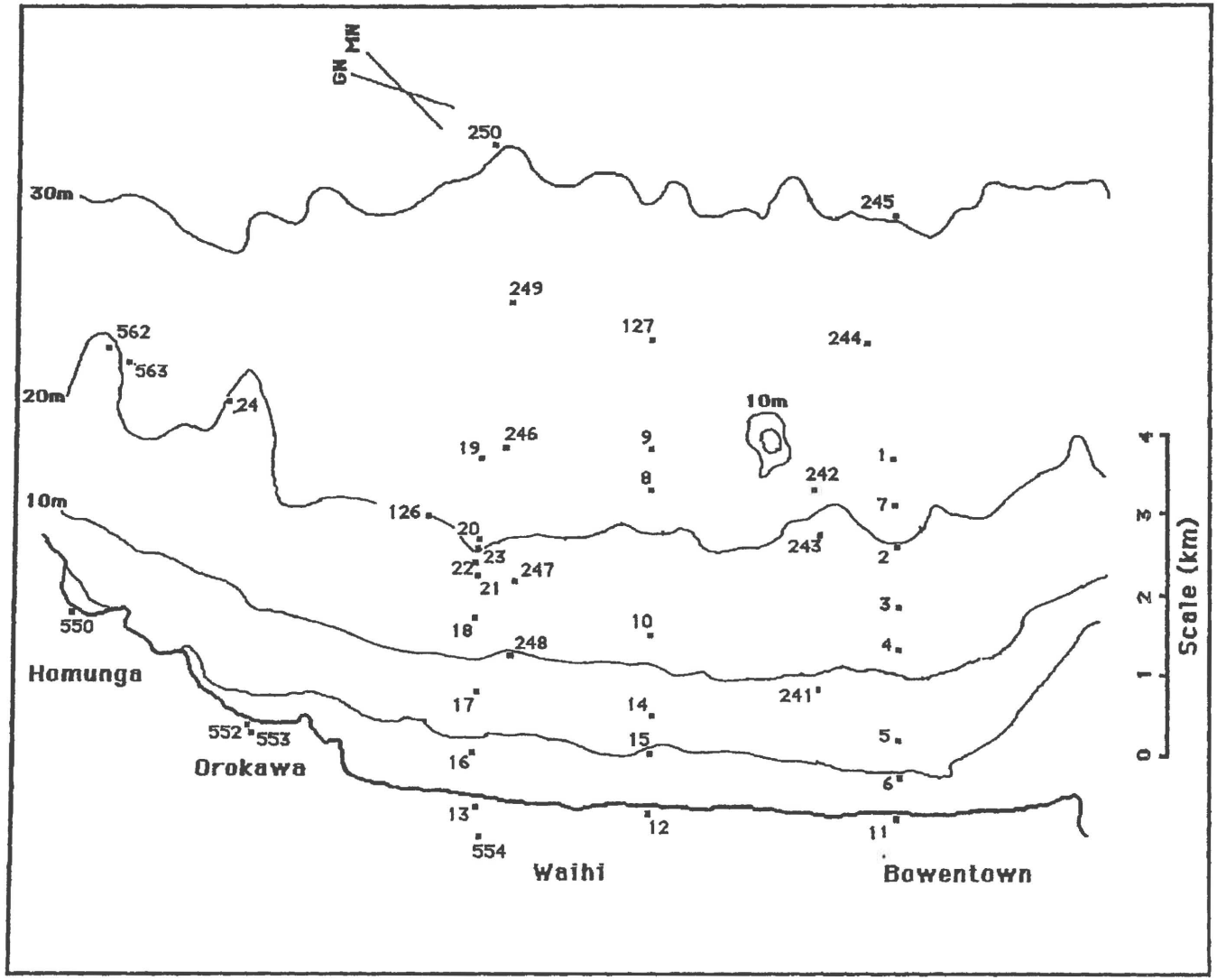

WAIHI-MAYOR ISLAND

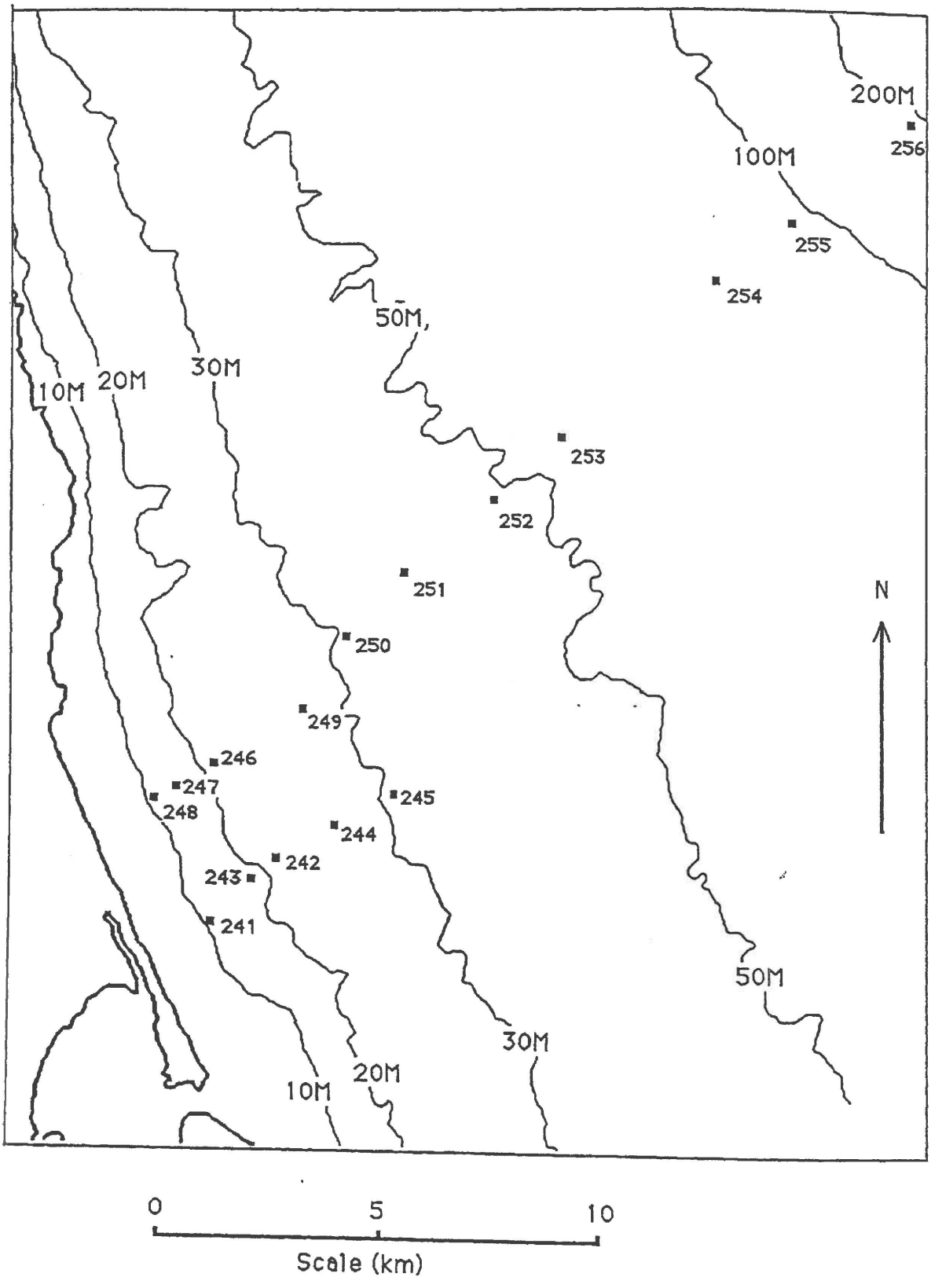

WHIRITOA

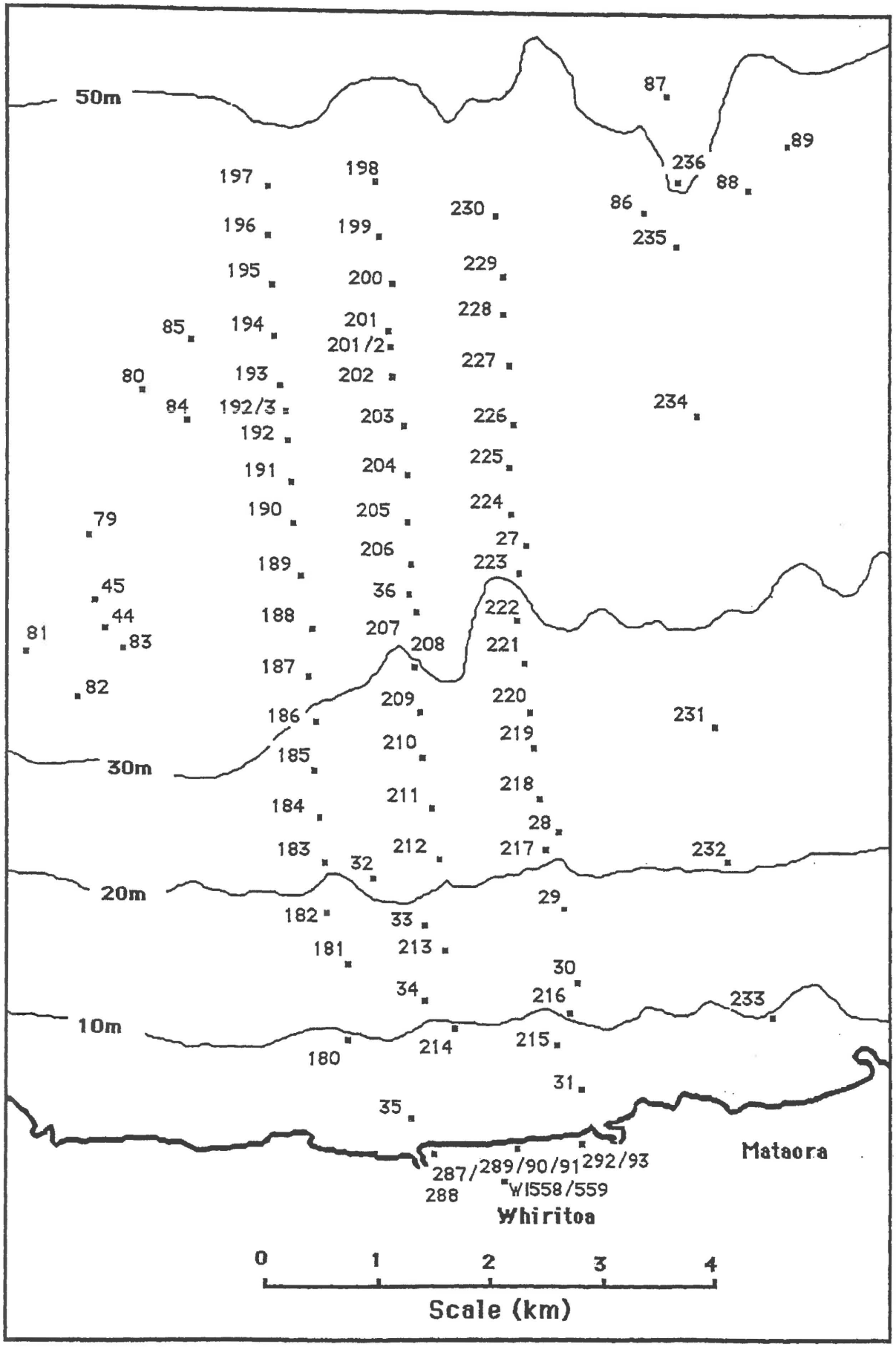
50m
30m
20m
10m
87
89
236
88
86
235
230
197
198
196
199
195
200
229
228
85
194
201
201/2
227
80
193
202
84
192/3
203
226
234
192
191
204
225
190
205
224
79
27
206
189
223
45
36
188
222
44
207
81
83
208
221
187
82
209
220
231
186
219
210
185
218
211
184
28
183
212
217
232
32
29
182
33
181
213
30
34
216
233
214
215
180
31
35
Mataora
287/
288
289/90/91
292/93
W1558/559
Whiritoa
0
1
2
3
4
Scale (km)

WHANGAMATA

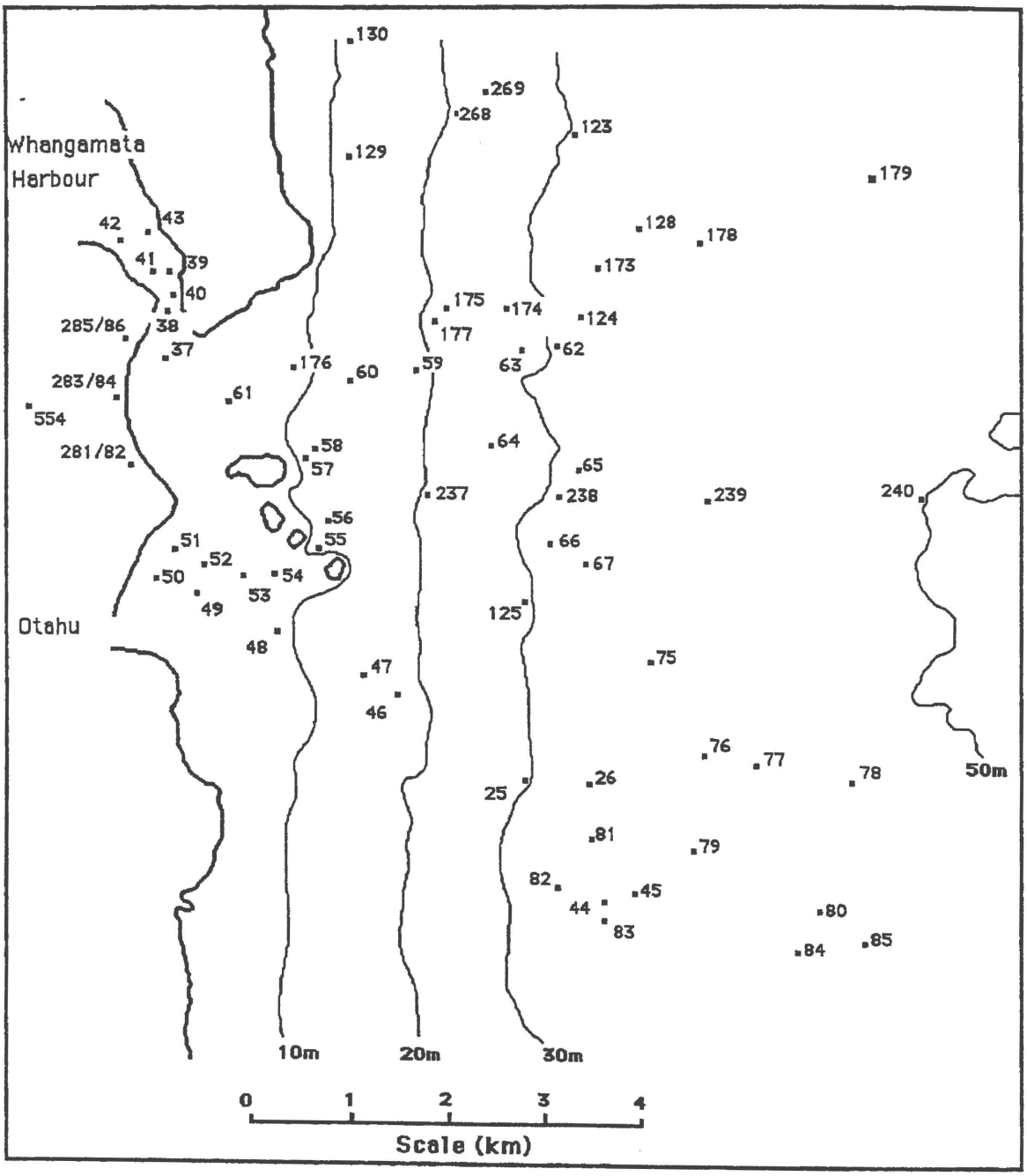
Whangamata
Harbour
Otahu
130
269
268
123
129
179
128
178
173
42
43
41
39
40
175
174
124
177
285/86
38
37
62
63
176
60
59
283/84
61
554
64
58
65
281/82
57
237
238
239
240
56
66
51
55
52
67
50
54
53
125
49
48
75
47
46
76
77
78
50m
26
25
81
79
82
45
44
80
83
84
85
10m
20m
30m
0
1
2
3
4
Scale (km)

A-21

ONEMANA

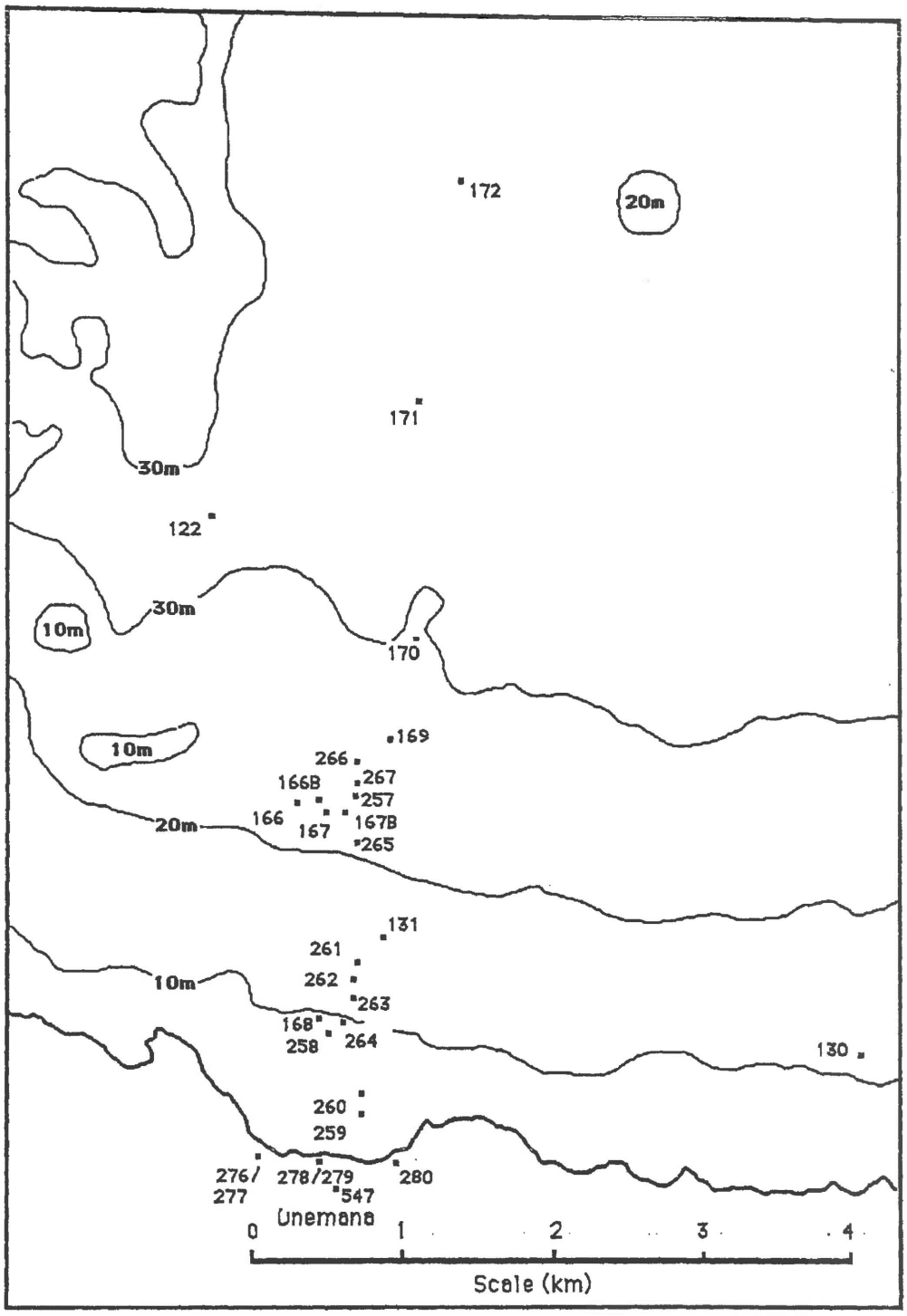
172
20m
171
30m
122
30m
10m
170
169
10m
266
166B
267
257
166
167
167B
265
20m
131
261
262
10m
263
168
258
264
130
260
259
276/
277
278/279
547
280
Onemana
0
1
2
3
4
Scale (km)

OPOUTERE

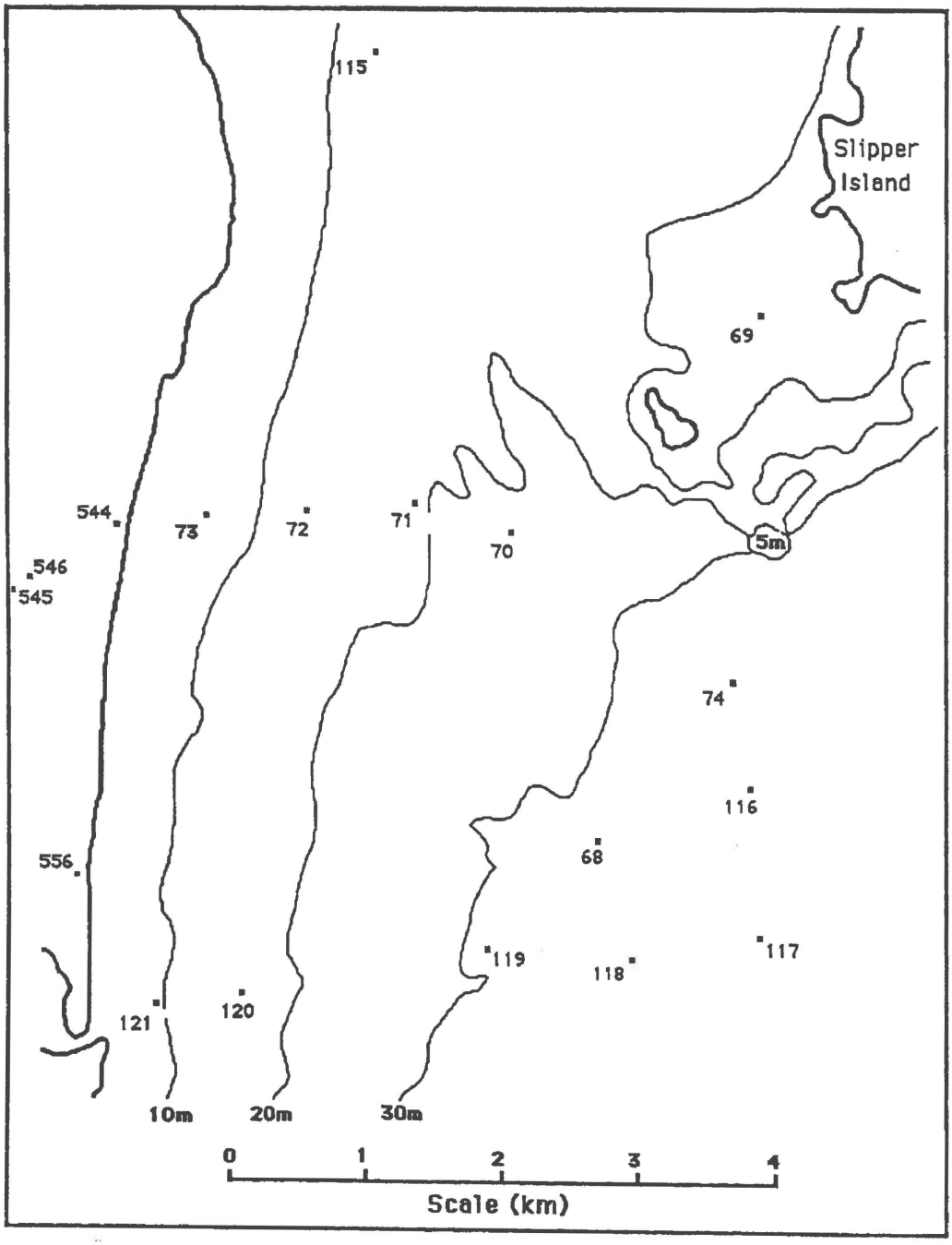
115
Slipper
Island
69
544
73
72
71
70
5m
546
545
74
116
556
68
119
118
117
121
120
10m
20m
30m
0
1
2
3
4
Scale (km)

A-23

HOTWATER

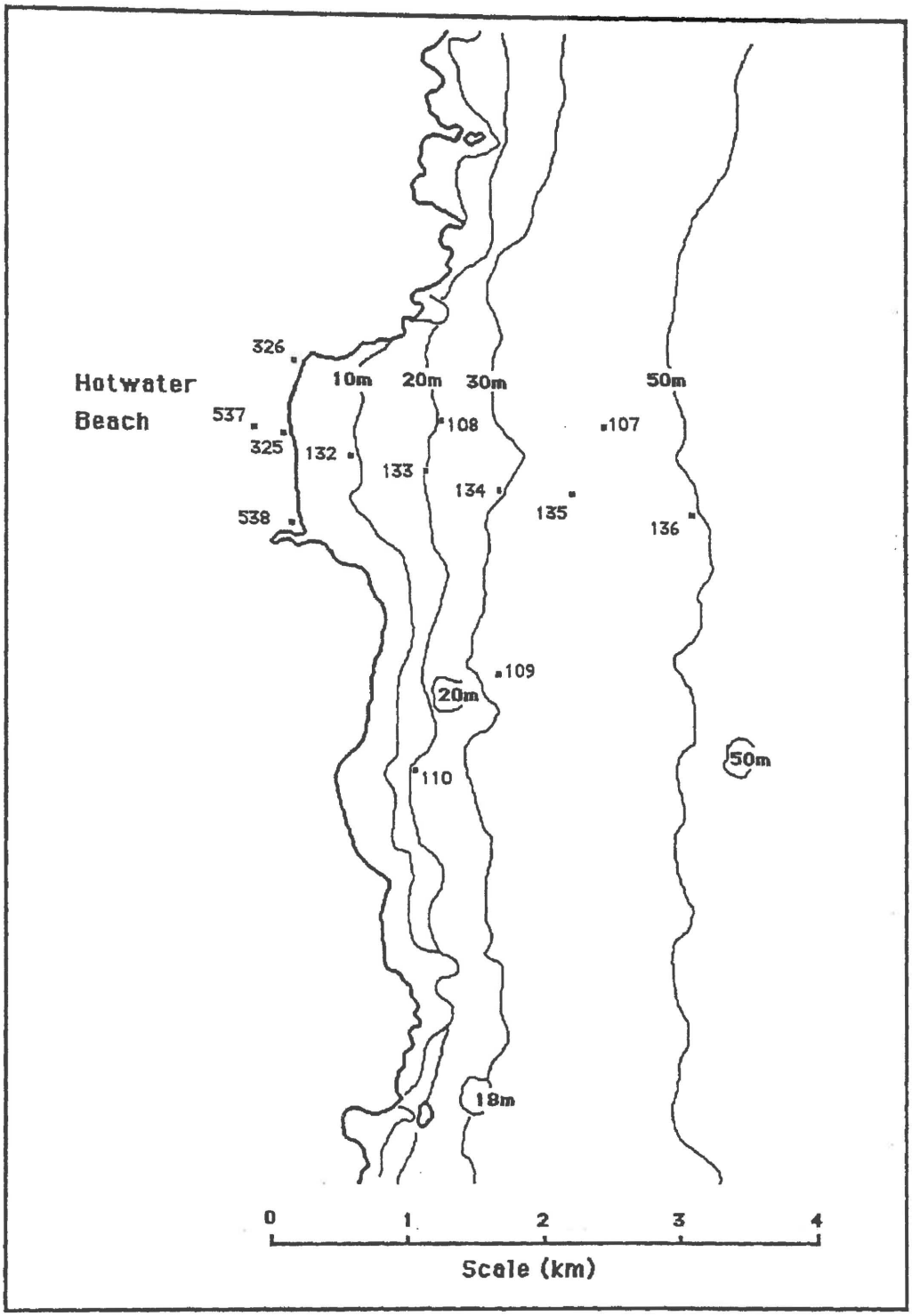

MERCURY BAY

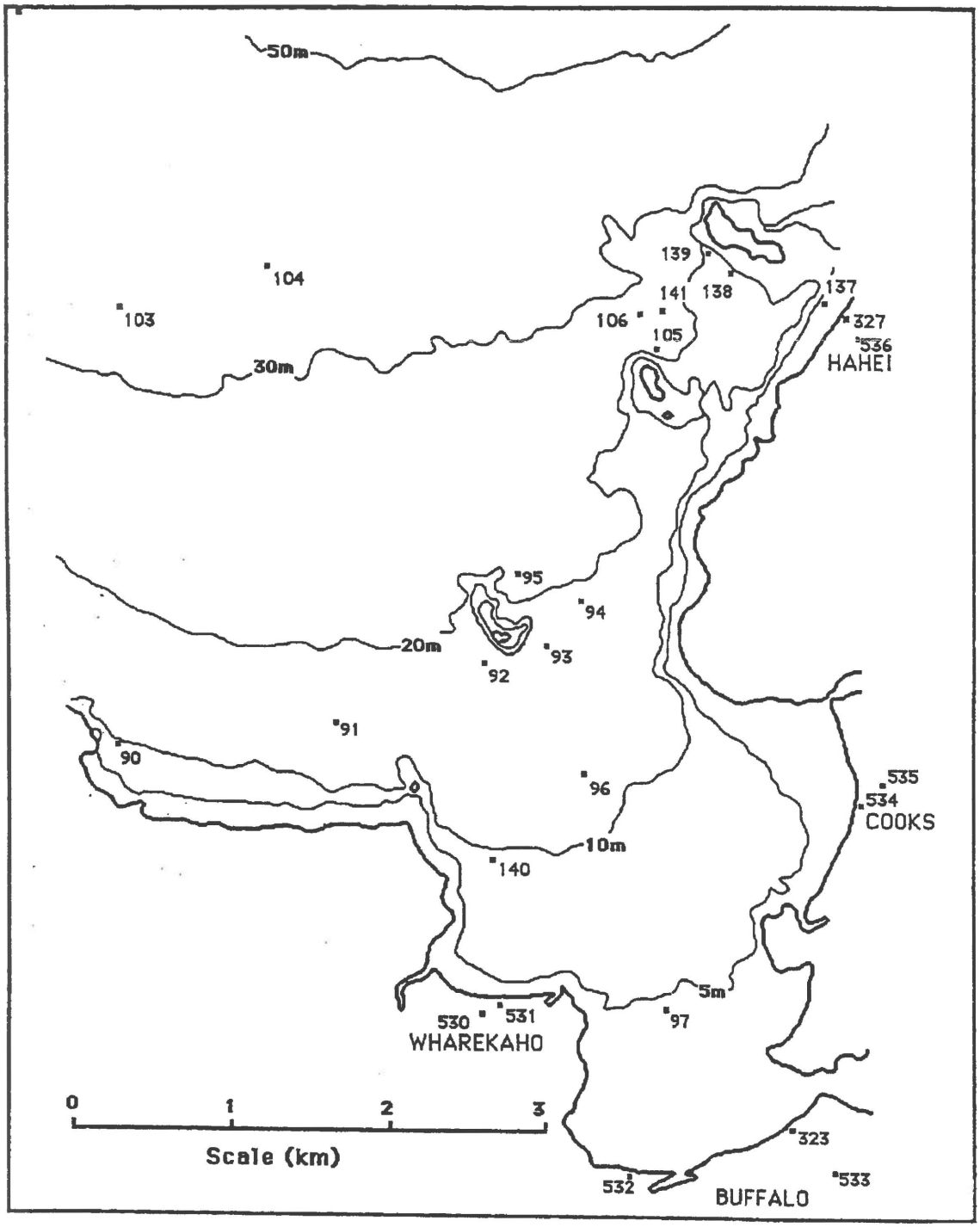
50m
104
103
30m
139
141
138
137
106
105
327
536
HAHEI
95
94
20m
93
92
91
90
96
535
534
COOKS
10m
140
5m
530
531
WHAREKAHO
97
0
1
2
3
Scale (km)
323
533
532
BUFFALO

A-25

OTAMA

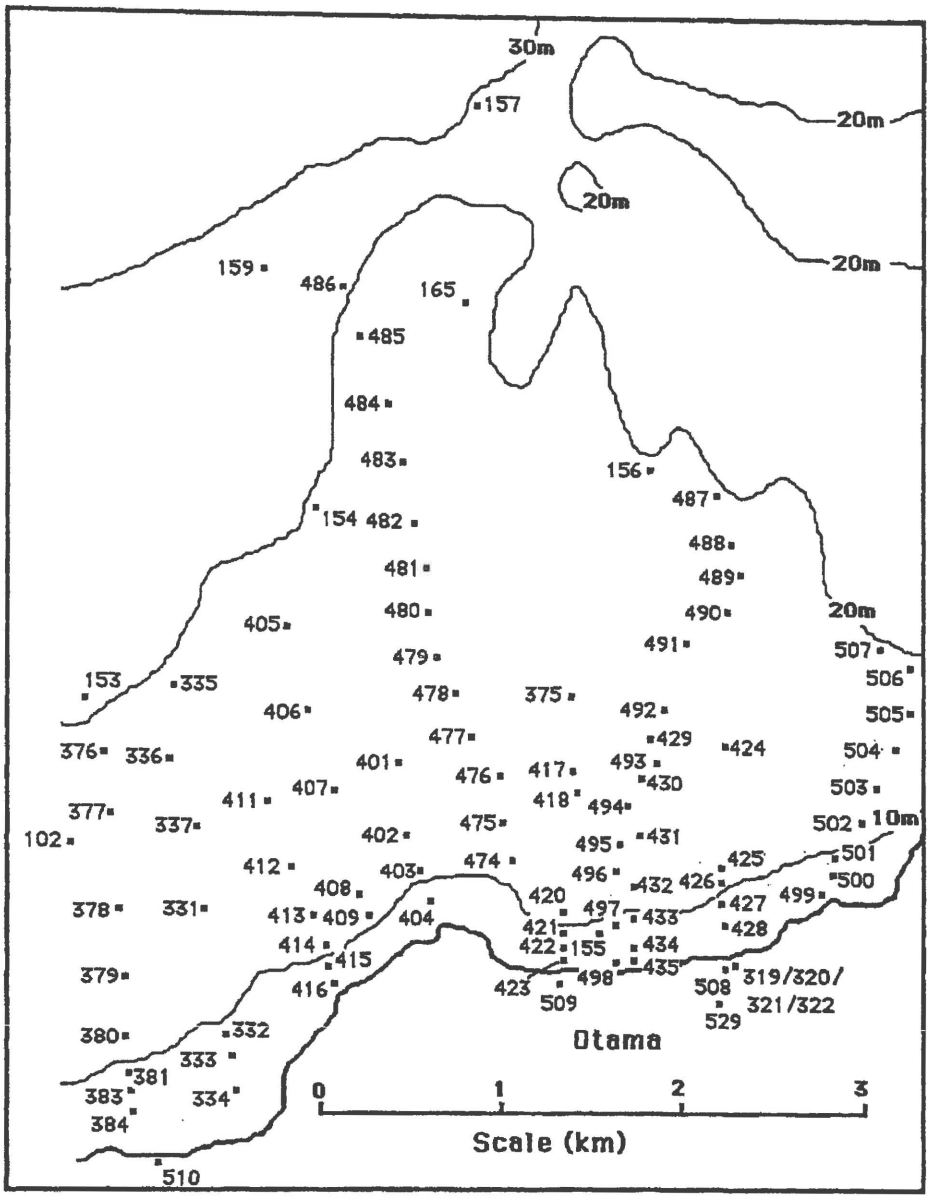
30m
20m
20m
20m
20m
10m
157
159
486
165
485
484
483
156
487
154
482
488
481
489
480
490
405
491
507
479
506
153
335
478
375
492
505
406
477
429
424
504
376
336
401
476
417
493
430
503
411
407
418
494
377
337
475
502
102
402
495
431
501
412
474
425
403
496
432
426
500
408
420
427
499
378
331
413
409
404
497
433
421
428
414
422
155
434
415
435
379
416
423
498
508
319/320/
321/322
509
529
380
332
Otama
333
381
383
334
384
0
1
2
3
Scale (km)
510

MATARANGI

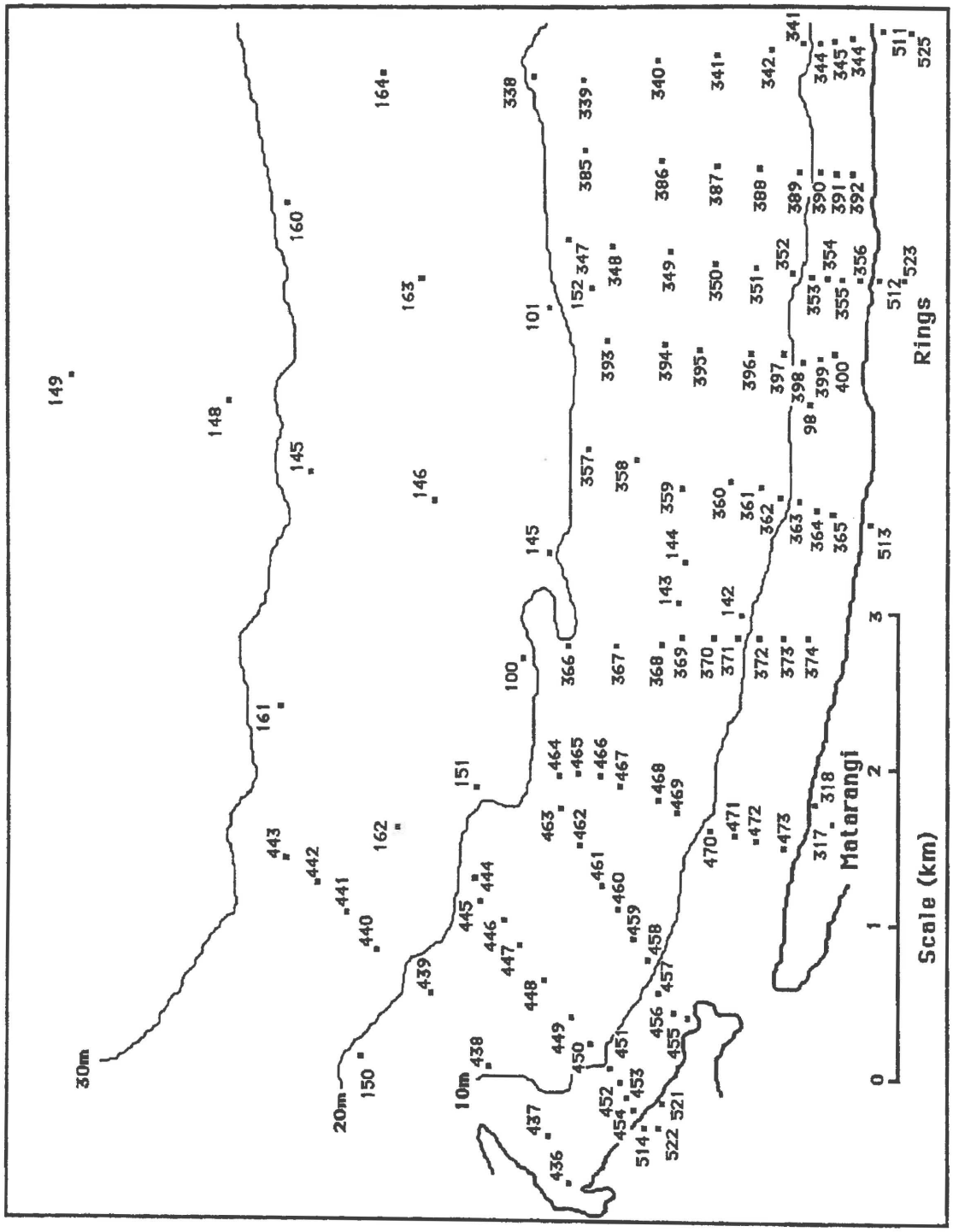

APPENDIX 3

SEDIMENT TEXTURE RESULTS

Appendix 3A

Sediment Texture Data

SAMPLE NO	SAMPLE TYPE	DEPTH (m)	MEAN	MODE	SORTING	SKEWNESS	KURTOSIS	CO3 (%)	FeO (%)	ANGULARITY	COLOUR	WT NUMBER
WB1	Grab	23.00	0.16	-0.25, 1.25	1.05	0.10	2.62	10.85	70.00	SA-SR	P-L YELLOW	28724
WB2	Grab	21.00	2.63	3.00	0.60	-0.23	3.46	3.86	2.00	V.A-S.A	OLIVE-YELLOW	28725
WB3	Grab	15.00	2.59	3.00	0.65	-1.06	6.96	6.50	5.00	V.A-A	GRY-OLIVE	28726
WB4	Grab	10.00	2.43	2.75	0.54	-1.28	9.95	10.11	5.00	V.A-A	L.GRY-GRY.ORANGE	28727
WB5	Grab	5.50	2.16	2.50	0.54	-0.86	6.80	4.64	2.00	V.A-A	GRY.OLIVE	28728
WB6	Grab	3.00	2.14	2.50	0.62	-3.21	22.82	7.34	7.50	V.A-S.A	L.GRAY	28729
WB7	Grab	23.00	1.50	1.50	0.47	0.51	6.52	7.83	15.00	S.A-S.R	L.YELLOW	28730
WB8	Grab	22.00	1.92	1.75	0.54	-1.11	13.82	13.43	15.00	S.A-S.R	L.YELLOW	28731
WB9	Grab	23.00	1.06	1.00	0.55	1.20	5.57	18.74	60.00	S.A-S.R	GRY.YELL-L.YELL	28732
WB10	Grab	12.00	2.58	3.00	0.72	-2.75	17.23	12.95	5.00	V.A-S.R	GRY-OLIVE	28733
WB11	Hand	0.00	1.71	1.75	0.75	-2.71	15.57	5.87	5.00	A-SR	L.GRAY	28734
WB12	Hand	0.00	1.95	1.75	0.42	-0.32	7.39	6.48	5.00	A-S.R	GRY.YELLOW	28735
WB13	Hand	0.00	1.98	2.00	0.54	-3.67	29.93	6.06	10.00	A-S.R	L.GRAY-GR.YELL	28736
WB14	Grab	6.50	2.61	3.00	0.51	-3.58	24.63	3.39	2.00	V.A-S.A	YELL.GRAY	28737
WB15	Grab	3.00	2.38	2.75	0.64	-4.20	27.62	6.00	15.00	A.A-S.A	GRY.YELLOW	28738
WB16	Grab	3.00	2.58	2.75	0.65	-4.12	30.36	8.68	5.00	V.A-A	YELL.GRAY	28739
WB17	Grab	8.00	2.67	3.00	0.50	-4.30	40.91	13.18	1.00	V.A-S.A	GRY.YELLOW	28740
WB18	Grab	14.50	2.66	3.00	0.62	-2.64	22.22	15.23	5.00	V.A-A	GRY.OLIVE	28741
WB19	Grab	25.00	-0.04	0.25	0.43	-0.06	5.97	28.63	70.00	S.A-S.R	L.GRY-D.BROWN	28742
WB20	Grab	20.00	0.19	0.25	0.64	0.70	5.28	32.57	30.00	S.A-S.R	P.YELL-YELL.BRWN	28743
WB21	Grab	18.00	2.37	2.50	0.72	-0.66	4.83	25.55	5.00	V.A-A	GRY.YELLOW	28744
WB22	Grab	19.50	2.99	3.00	0.46	-0.06	2.47	10.77	0.00	V.A-A	GRY.YELLOW	28745
WB23	Grab	20.00	0.81	1.00	0.68	0.71	6.54	31.37	40.00	S.A-R	L.GRAY-D.BRWN	28746
WB24	Grab	20.00	1.81	1.75	0.44	-0.20	11.00	4.38	30.00	A-S.R	L.GRAY-P.YELLOW	28747
WH25	Grab	20.00	2.14	2.00	0.50	0.70	4.01	8.49	40.00	S.A-S.R	L.YELLOW	28748
WH26	Grab	24.00	1.99	2.00	0.39	-0.17	7.80	11.93	10.00	A-S.R	L.GRY-P.YELLOW	28749
WI27	Dredge	33.50	2.11	2.00	0.46	-0.28	5.39	7.83	40.00	A-S.R	L.YELLOW	28750
WI28	Grab	24.00	2.13	2.25	0.54	-1.93	15.05	8.83	60.00	A-S.R	DULL.YELLOW	28751
WI29	Grab	18.00	2.94	3.00	0.46	-4.10	35.37	10.52	5.00	V.A-A	L.GRAY	28752
WI30	Grab	12.00	2.68	3.00	0.58	-4.46	37.72	8.02	5.00	A.A-A	L.GRAY	28753
WI31	Grab	7.00	1.40	1.50	0.40	-0.26	10.79	10.94	30.00	S.R-W.R	L.BRW.GRAY	28754
WI32	Grab	24.00	2.35	2.25	0.48	0.03	5.62	9.70	5.00	A-S.R	GRY.OLIVE	28755
WI33	Grab	18.00	2.83	3.00	0.43	-1.96	21.41	7.19	0.00	V.A-A	GRY.OLIVE	28756
WI34	Grab	12.00	2.79	2.75	0.41	-1.63	17.93	8.41	5.00	V.A-S.A	YELL.GRAY	28757
WI35	Grab	6.00	2.07	1.75	0.61	0.43	2.25	11.52	7.00	V.A-R	L.GRY-GRY.YELL	28758
WI36	Dredge	30.00	2.21	2.25	0.44	-0.65	7.82	8.71	15.00	A-S.R	L.YELLOW	28759
WH37	Grab	2.00	1.32	1.25	0.36	0.85	7.42	20.76	25.00	S.A-W.R	L.YELL.ORANGE	28760
WH38	Grab	0.00	1.24	1.25	0.38	0.79	4.48	27.22	40.00	S.A-S.R	GRY.YELL-YELLOW	28761
WH39	Grab	0.00	1.20	1.25	0.31	0.19	8.11	24.62	70.00	S.A-S.R	L.GRY-YELLOW	28762
WH40	Grab	2.00	1.32	1.25	0.41	-1.34	19.94	31.18	30.00	S.R-R	L.GRAY-YELL	28763
WH41	Grab	0.00	1.50	0.25, 1.75	0.78	-0.92	3.55	42.56	40.00	V.A-S.R	GRY.YELL-L.YELL	28764
WH42	Grab	2.00	0.23	1.00	0.90	0.33	2.58	31.65	60.00	S.A-R	GRY.YELLOW	28765
WH43	Grab	0.00	1.62	1.50	0.36	0.97	4.15	-	60.00	S.A-S.R	P.YELLOW	28766
WH44	Dredge	35.00	1.87	2.00	0.55	-0.44	6.37	14.35	30.00	A-S.R	L.YELLOW	28767
WH45	Dredge	38.00	2.18	2.25	0.50	-0.32	4.89	12.87	20.00	A-S.A	OLIVE-YELL.	28768
WH46	Grab	18.00	2.48	2.25	0.56	0.06	2.60	29.97	7.00	V.A-S.R	GRY.OLIVE	28769
WH47	Grab	15.00	2.73	3.00	0.47	-1.26	10.04	8.89	5.00			28770

SAMPLE NO	SAMPLE TYPE	DEPTH (m)	MEAN	MODE	SORTING	SKEWNESS	KURTOSIS	CO3 (%)	FeO (%)	ANGULARITY	COLOUR	
WH48	Grab	9.00	2.83	3.00	0.41	-0.62	5.60	15.50	5.00	V.A-A	GRY.YELLOW	28771
WH49	Grab	6.00	2.79	3.00	0.41	0.07	3.17	8.74	5.00	V.A-S.A	L.GRAY	28772
WH50	Grab	3.00	1.95	2.00	0.45	-0.08	3.09	19.33	40.00	V.A-S.A	L.GRAY-P.YELLOW	28773
WH51	Grab	3.00	2.56	2.50	0.49	-2.08	17.68	12.17	10.00	V.A-S.A	GRY.OLIVE	28774
WH52	Grab	3.50	2.62	2.50	0.46	-1.58	13.15	8.70	7.00	V.A-S.A	GRY.OLIVE	28775
WH53	Grab	6.00	0.50	0.75	0.27	-0.29	3.55	76.18	10.00	A-S.R	GRY.YELL-YELLOW	28776
WH54	Grab	9.00	0.94	1.00	0.59	1.66	5.75	52.11	25.00	S.A-S.R	GRY.YELL-YELL	28777
WH55	Grab		BEDROCK				BEDROCK					28778
WH56	Grab	13.00	2.86	3.00	0.39	-0.23	4.92	8.95	5.00	V.A-S.A	GRY.OLIVE	28779
WH57	Grab		BEDROCK				BEDROCK					28780
WH58	Grab	12.00	2.50	2.75	0.62	-0.24	2.62	7.79	10.00	V.A-S.R	GRY.OLIVE	28781
WH59	Grab	18.00	2.34	2.25	0.55	-0.04	3.88	15.49	30.00	A-S.R	GRY.OLIVE	28782
WH60	Grab	12.00	2.69	2.50	0.51	-0.68	9.67	10.33	20.00	A-S.R	GRY.YELLOW	28783
WH61	Grab	6.00	2.88	2.75	0.31	0.65	3.33	17.26	2.00	V.A-A	GRY.YELLOW	28784
WH62	Grab	30.00	1.12	1.00	0.49	1.50	7.94	8.15	40.00	S.A-S.R	L.YELL-BRW.BLK	28785
WH63	Dredge	24.00	1.13	1.25	0.42	0.32	5.96	8.15	40.00	S.A-S.R	L.YELL-BRW.BLK	28786
WH64	Dredge	24.00	2.13	2.25	0.50	0.57	5.24	3.30	25.00	S.A-R	PALE-L.YELL.	28787
WH65	Dredge	32.00	0.92	1.00	0.49	1.66	7.04	9.30	30.00	S.R-R	L.GRAY-P.YELLOW	28788
WH66	Dredge	27.00	1.89	2.00	0.35	0.17	4.44	3.70	25.00	A-S.R	P.YELLOW	28789
WH67	Dredge	32.00	1.06	1.00	0.38	1.86	7.50	6.55	30.00	S.A-R	P.YELL-D.BRW	28790
OP68	Dredge	30.00	2.03	2.25	0.81	-1.05	4.19	16.95	7.00	A-S.R	GRY.YELLOW	28791
OP69	Grab	8.00	0.54	0.75	0.44	0.96	9.37	73.19	15.00	S.A-R	L.GRAY	28792
OP70	Grab	24.00	2.88	3.00	0.53	-1.70	13.21	14.40	5.00	V.A-S.A	L.YELLOW	28793
OP71	Grab	20.00	3.00	3.00	0.49	-1.85	19.51	18.70	5.00	V.A-S.A	GRY.OLIVE	28794
OP72	Grab	12.00	2.77	2.75	0.47	-1.08	10.42	13.40	20.00	V.A-S.R	GRY.YELLOW	28795
OP73	Grab	6.00	2.35	2.50	0.38	0.14	3.48	12.35	10.00	A-S.A	P.YELL-L.GRAY	28796
OP74	Dredge	34.00	2.34	2.25	0.49	0.21	3.21	15.46	7.00	A-S.R	GRY.YELLOW	28797
WH75	Dredge	34.00	0.52	0.75	0.30	0.04	5.69	10.67	60.00	S.A-R	P.YELL.BRN	28798
WH76	Dredge	40.00	2.69	2.75	0.50	-2.08	22.68	8.30	30.00	A-S.R	OLIVE.YELL	28799
WH77	Dredge	40.00	2.47	2.50	0.43	-0.38	4.49	10.80	15.00	V.A-S.R	L.YELLOW	28800
WH78	Dredge	43.00	2.60	2.50	0.34	0.18	3.87	10.46	0.00	A-S.R	OLIVE.YELL	28801
WI79	Dredge	40.00	2.49	2.50	0.35	0.15	5.19	8.69	7.00	A-S.A	OLIVE.YELL	28802
WI80	Dredge	45.00	2.24	2.25	0.40	0.13	7.28	6.72	5.00	A-S.R	OLIVE.YELL	28803
WI81	Dredge	37.00	1.67	1.50	0.43	0.60	4.36	8.22	40.00	S.A-S.R	L.GRY-P.YELL	28804
WI82	Dredge	32.00	2.10	2.25	0.33	-0.44	11.76	7.20	7.00	S.A-S.R	L.YELLOW	28805
WI83	Dredge	34.00	2.18	2.25	0.33	-1.30	22.93	4.90	20.00	A-S.R	L.YELLOW	28806
WI84	Dredge	42.00	2.09	2.25	0.78	-1.30	5.83	18.10	7.00	S.A-S.R	L.YELL-ORANGE.YELL	28807
WI85	Dredge	46.00	2.06	2.00	0.51	0.38	3.09	9.38	5.00	A-S.R	OLIVE.YELLOW	28808
M86	Dredge	41.00	0.29	0.50	0.54	1.66	8.22	8.68	20.00	S.A-S.R	L.GRY-YELL.BRWN	28809
M87	Dredge	44.00	2.37	2.50	0.50	-2.37	18.31	9.60	5.00	A-S.R	OLIVE.YELLOW	28810
M88	Dredge	38.00	2.02	2.25	0.55	-1.63	13.61	10.40	5.00	S.A-S.R	OLIVE.YELLOW	28811
M89	Dredge	41.00	0.63	0.75	0.51	1.39	6.72	14.70	20.00	S.A-S.R	L.GRY-P.YELL	28812
MB90	Dredge	10.00	2.23	2.25	0.35	0.21	3.18	17.30	30.00	A-S.A	OLIVE.YELL-YELL.BRWN	28813
MB91	Dredge	15.00	2.83		0.59	-1.51	7.91	12.69	5.00	V.A-S.A	YELL.GRY-GRY.YELL	28814
MB92	Dredge	18.00	0.25	0.50	0.46	-0.05	3.19	92.60	70.00	S.A-S.R	L.YELL.ORANGE	28815
MB93	Dredge	16.00	0.27	0.50	0.37	1.81	7.66	77.24	100.00	S.R-R	L.YELL.ORANGE	28816
MB94	Dredge	18.00	1.21	0.50	1.05	1.01	2.77	76.19	50.00	S.R		28817

SAMPLE NO	SAMPLE TYPE	DEPTH (m)	MEAN	MODE	SORTING	SKEWNESS	KURTOSIS	CO3 (%)	FeO (%)	ANGULARITY	COLOUR	
MB95	Dredge	22.00	3.17	3.50	0.43	0.62	2.61	9.14	5.00	V.A-S.A	GRY.OLIVE	28818
MB96	Dredge	12.00	3.21	3.50	0.34	0.27	2.75	5.06	30.00	V.A-S.A	D.YELLOW	28819
MB97	Dredge	11.00	3.03	3.00	0.36	0.88	3.09	9.37	25.00	V.A-A	YELL.BRWN	28820
K98	Dredge	7.00	2.66	2.50	0.32	0.86	3.21	8.20	10.00	V.A-S.A	GRY.YELLOW	28821
K99	Dredge	11.00	2.69	2.75	0.34	0.89	3.54	5.39	20.00	S.A	P.YELL-L.BRWN	28822
K100	Dredge	21.00	2.19	2.25	0.50	-1.81	20.63	5.90	5.00	A-S A	L.YELLOW	28823
K101	Dredge	20.00	2.00	2.00	0.56	-1.74	16.26	11.40	7.00	S.A-S.R	L.GRAY	28824
K102	Dredge	15.00	1.98	2.00	0.71	-0.53	3.20	41.50	20.00	A-S.R	L.YELLOW	28825
MB103	Dredge	33.00	1.21	0.75, 1.50	0.89	0.35	2.49	14.00	15.00	S.A-W.R	GRY-BRWN.BLK	28826
MB104	Dredge	32.00	3.26	3.50	0.38	-1.07	5.01	5.71	5.00	V.A-S.A	GRY.OLIVE	28827
MB105	Dredge	27.00	0.12	0.25	0.53	0.86	5.82	4.91	30.00	S.A-R	L.YELL.ORANGE	28828
MB106	Dredge	26.00	2.46	2.25	0.66	-0.39	3.82	16.88	10.00	A-S.A	GRY.OLIVE	28829
HW107	Dredge	43.00	0.25	0.25	0.32	0.43	2.37	8.10	0.00	S.A-S.R	BRWN-BRWN.BLK	28830
HW108	Dredge	22.00	1.90	1.75	0.32	0.92	3.40	82.40	25.00	A-R	D.GRY.YELLOW	28831
HW109	Dredge	35.00	0.49	0.50	0.41	0.95	5.07	11.70	0.00	A-S.R	OLIVE.BLK.BRWN	28832
HW110	Dredge	18.00	1.08	1.25	0.72	0.70	4.72	20.30	40.00	V.A-R	BLK.BRWN-B.YELL.BRWN	28833
TP111	Dredge							11.39	3.00	V.A-S.A	GRY.OLIVE	28834
TP112	Dredge	10.00	2.56	2.50	0.42	-0.75	7.32	9.08	10.00	V.A-A	GRY.OLIVE	28835
TP113	Dredge	23.00	0.35	0.75	0.42	-0.24	3.48	88.13	70.00	S.A-R	D.YELL.ORANGE	28836
TP114	Dredge	29.00	2.74	2.50	0.57	0.08	3.00	19.68	5.00	V.A-A	GRY.OLIVE	28837
OP115	Dredge	12.00	2.70	2.75	0.49	0.01	3.35	29.17	5.00	V.A	GRY.OLIVE	28838
OP116	Dredge	37.00	2.10	2.00	0.43	-0.07	5.15	12.60	5.00	S.A-S.R	L.GRAY	28839
OP117	Dredge	37.00	2.23	2.25	0.42	-0.05	3.85	11.73	20.00	S.A-S.R	GRY.OLIVE	28840
O P118	Dredge	35.00	0.24	0.25	0.58	0.62	6.72	25.59	20.00	S.A-R	L.GRY-D.YELL.BRWN	28841
OP119	Dredge	27.00	0.20	0.00	0.58	-0.38	4.64	43.75	50.00	S.A-W.R	D.YELL.ORANGE	28842
OP120	Dredge	16.00	1.98	2.00	0.45	0.27	2.94	22.41	25.00	A-S.R	GRY.YELL	28843
OP121	Dredge	8.00	2.61	2.75	0.34	-0.29	8.16	7.02	10.00	V.A-S.A	GRY.YELLOW	28844
OP122	Dredge	32.00	0.35	0.25	0.69	1.24	4.94	9.60	40.00	S.R-R	BRWN.BLK-L.YELL	28845
WH123	Dredge	30.00	0.53	0.50	0.50	1.58	6.17	22.50	25.00	S.R-R	L.GRY-YELL	28846
WH134	Dredge	31.00	0.85	0.75	0.44	1.48	6.61	6.49	40.00	S.A-R	L.YELL.BRWN	28847
WH125	Dredge	31.00	1.12	1.00	0.43	1.55	6.21	3.10	40.00	R	P.YELLOW	28848
WB126	Dredge	20.00	2.90	3.00	0.61	-2.06	18.41	5.95	0.00	V.A-A	GRY.YELL	28849
WB127	Dredge	25.00	2.03	2.00	0.59	-0.13	4.80	8.30	10.00	S.A-S.R	L.GRAY	28850
WH28	Dive	38.00	0.66	0.75	0.38	1.22	8.52	27.63	50.00	S.A-R	P.YELL-D.BRWN	28851
WH128	Dredge	38.00	0.82	1.00	0.40	1.89	7.87					28852
WH129	Grab	10.00	2.53	2.50	0.61	-2.13	15.29	8.44	5.00	V.A-S.A	P.YELL-L.GRY	28853
WH130	Grab	10.00	2.59	2.50	0.42	-1.12	16.60	7.30	5.00	V.A-S.R	GRY.OLIVE	28854
WH131	Grab	15.00	2.70	2.75	0.63	-2.86	19.48	9.27	10.00	A-S.A	YELL.GRAY	28855
HW132	Dredge	10.00	2.05	2.00	0.44	0.94	5.07	27.40	70.00	A-R	YELL.BRWN	28856
HW133	Dredge	20.00	2.14	2.00	0.46	-1.38	20.28	14.52	50.00	S.A-S.R	D.YELL.BRWN	28857
HW134	Dredge	30.00	0.44	0.50	0.42	1.08	7.69	56.51	70.00	S.A-W.R	L.YELL.OR-D.BRWN	28858
HW135	Dredge	40.00	0.38	0.50	0.40	0.27	6.46	21.11	70.00	A-R	YELL.BRWN-D.BRWN	28859
HW136	Dredge	50.00	3.35	3.25	0.52	-2.81	25.28	18.50	0.00	V.A-A	OLIVE-YELLOW	28860
HA137	Dredge	9.00	2.55	2.50	0.40	-2.31	33.61	19.15	20.00	A-S.A	D.GRY.YELL	28861
HA138	Dredge	12.00	0.79	0.50	0.71	1.12	3.90	41.24	25.00	A-S.A	GRY.YELLOW	28862
HA138	Diver	12.00	1.62	0.75, 2.0	0.88	0.00	2.01	73.19	10.00	A-S.A	L.GRY-D.YELL.ORANGE	28863
HA139	Dredge	13.00	2.77	2.50	0.62	-0.98	5.28	20.53	30.00	A-S.A		28864

SAMPLE NO	SAMPLE TYPE	DEPTH (m)	MEAN	MODE	SORTING	SKEWNESS	KURTOSIS	CO3 (%)	FeO (%)	ANGULARITY	COLOUR	
HA139	Diver	13.00	2.73	2.50	0.49	0.12	2.55					28865
HA140	Dredge	9.00	2.93	3.00	0.50	-1.08	5.82	10.78	40.00	A-S.A	YELL.BROWN	28866
HA141	Grab	21.00	0.48	0.75	0.67	0.49	4.97	70.74	50.00	S.A-R	LGRY-LYELLOR	28867
K142	Box Core	10.00	2.41	2.75	0.58	-4.14	33.75	2.81	10.00	A-S.A	LYELLOW	28868
K142	Grab	10.00	2.52	2.25	0.63	-2.99	22.22					28869
K143	Grab	15.00	2.53	2.75	0.50	0.99	4.21	6.70	30.00	A-S.A	LYELLOW	28870
K144	Grab	20.00	2.43	2.25	0.83	-3.47	19.17	5.70	7.00	S.A	LGRAY	28871
K145	Box Core	21.00	2.28	2.25	0.45	0.74	3.43	6.96	10.00	S.A-S.R	LYELLOW	28872
K146	Grab	25.00	2.12	1.75	0.62	0.65	2.79	13.50	0.00	S.R-W.R	LGRAY	28873
K147	Box Core	30.00	2.78	3.00	0.54	-0.36	3.11	21.13	0.00	V.A-A	OLIVE.YELL	28874
K148	Grab	35.00	2.81	3.00	0.89	-2.89	15.89					28875
K149	Box Core	40.00	3.05	3.50	0.57	-0.52	3.01	27.38	0.00	V.A-A	LYELLOW	28876
K150	Grab	21.00	2.14	2.00	0.45	0.97	4.95	4.22	15.00	A-S.R	LYELLOW	28877
K151	Grab	22.00	2.03	2.00	0.52	0.47	4.66	5.80	7.00	S.A-S.R	LGRAY	28878
K152	Grab	20.00	2.12	2.00	0.51	0.21	2.18	17.80	5.00	S.R	LGRAY-P.YELLOW	28879
K153	Grab	23.00	1.90	2.75	0.85	-0.25	2.10	42.20	5.00	S.R-R	LGRAY-P.YELLOW	28880
K154	Grab	18.00	1.50	1.50	0.44	-0.54	4.94	17.58	3.00	S.A-R	P.YELLOW	28881
K155	Box Core	10.00	1.35	1.25	0.50	-0.37	4.17					28882
K156	Box Core	20.00	0.53	0.75	0.50	-0.30	3.73					28883
K157	Box Core	30.00	1.82	1.50	0.56	0.24	3.70					28884
K158	Box Core	40.00	2.61	3.00	0.81	-1.09	4.11					28885
K159	Grab	30.50	2.34	2.75	0.41	0.75	3.58	34.10	5.00	A-S.A	LYELLOW	28886
K160	Grab	32.50	2.90	3.00	0.42	0.35	3.18	27.10	0.00	V.A-A	OLIVE.YELLOW	28887
K161	Grab	31.00	0.93	0.75	0.74	1.52	6.33	25.10	60.00	S.R-R	LGRY-P.YELLOW	28888
K162	Grab	27.00	2.42	2.25	0.56	0.07	3.27	7.70	15.00	S.A-S.R	LYELL.GRAY	28889
K163	Grab	28.00	2.71	3.00	0.45	-0.14	2.88	21.24	10.00	S.A-S.R	LGRAY	28890
K164	Grab	28.00	2.44	2.75	0.73	-0.90	3.64	31.15	10.00	A-S.A	P.YELLOW	28891
K165	Grab	22.00	1.83	1.75	0.50	-3.38	28.65	9.37	2.00	A-S.R	P.YELLOW	28892
ON166	Box Core	23.00	2.60	2.75	0.55	0.23	2.76	7.90	5.00	V.A-S.R	LGRAY	28893
ON166B	Diver	23.50	1.45	0.75	0.86	0.67	2.46	19.11	5.00	V.A-S.R	GRY.YELLOW	28894
ON167	Box Core	23.50	0.93	0.75	0.69	2.09	6.84	7.67	30.00	S.R-R	P.YELL-D.BRWN	28895
ON167B	Diver	23.50	1.01	0.75	0.53	0.78	3.58	7.10	40.00	S.R-R	P.YELLOW	28896
ON168	Box Core	10.00	2.43	2.50	0.61	-0.75	6.59					28897
ON169	Box Core	31.00	0.38	0.25	0.40	0.93	4.28					28898
ON170	Box Core	34.00				BEDROCK						28899
ON171	Box Core	41.00				BEDROCK						28900
ON172	Box Core	45.00	1.84	2.00	0.61	0.32	4.20					28901
WH173	Box Core	32.00	1.11	1.25	0.47	1.84	8.61	7.99	30.00	S.A-S.R	LYELLOW	28902
W174	Box Core	29.00	1.31	1.25	0.45	1.12	6.91	6.13	70.00	S.A-R	P.YELLOW	28903
WH175	Box Core	26.00	2.17	2.00	0.47	0.29	4.11	WHOLE SHELL				28904
WH176	Box Core	10.00	2.65	2.75	0.70	-1.79	11.59	28.18	0.00	V.A-S.R	LGRAY	28905
WH177	Box Core	23.00	2.31	2.00	0.59	-0.86	10.90	10.65	10.00	A-S.A	GRY.OLIVE	28906
WH178	Box Core	39.00	2.32	2.25	0.49	-0.66	7.27	3.55	5.00	S.A-R	GRY.OLIVE	28907
WH179	Box Core	45.00	0.14	0.25	0.74	0.99	5.41	17.32	20.00	S.A-R	P.YELL-D.BRWN	28908
WI180	Grab	12.00	2.77	3.00	0.51	0.26	3.28	5.10	0.00	A	LGRAY	28909
WI181	Grab	19.00	2.88	3.00	0.48	-2.66	28.86	3.03	0.00	V.A-A	GRY.OLIVE	28910
WI182	Grab	21.00	2.08	1.75	0.58	-0.07	3.83	6.97	15.00	V.A.-S.R.		28911

SAMPLE NO	SAMPLE TYPE	DEPTH (m)	MEAN	MODE	SORTING	SKEWNESS	KURTOSIS	CO3 (%)	FeO (%)	ANGULARITY	COLOUR	
WI183	Grab	26.00	2.27	2.25	0.71	-2.02	15.44	6.00	10.00	V.A-R	GRY.YELLOW	28912
WI184	Grab	30.00	2.32	2.25	0.46	0.76	4.37	8.44	20.00	V.A-S.R	GRY.YELLOW	28913
WI185	Grab	32.00	2.21	2.25	0.52	-1.34	19.64	5.89	15.00	SA-SR	L.YELLOW	28914
WI186	Grab	34.00	2.15	2.00	0.48	0.81	4.09	5.55	25.00	S.A-S.R	P.YELLOW	28915
WI187	Grab	36.00	2.21	2.00	0.48	-0.48	6.41	6.46	70.00	S.A-S.R	L.YELLOW	28916
WI188	Grab	37.00	2.26	2.25	0.71	-3.11	20.08	6.29	10.00	A-S.R	L.YELLOW	28917
WI189	Grab	39.00	2.17	2.00	0.38	0.53	3.02	6.70	20.00	S.A-S.R	L.GRAY	28918
WI190	Grab	40.00	2.14	2.00	0.51	1.20	5.95	6.65	10.00	S.A-S.R	L.YELLOW	28919
WI191	Grab	42.00	2.29	2.25	0.54	0.99	4.64	8.24	25.00	S.A-S.R	OLIVE.YELLOW	28920
WI192	Grab	43.00	0.77	0.75	0.57	1.23	5.09	33.00	10.00	A-S.R	L.GRAY	28921
WI192-193	Box Core	43.00	2.24	2.00	0.43	0.30	3.74	5.97	10.00	SA-SR	GRY.OLIVE	28922
WI193	Grab	44.00	0.57	0.75	0.43	1.66	8.03	22.30	5.00	S.R	L.GRAY	28923
WI194	Grab	47.50	2.45	2.25	0.40	0.24	2.89	6.32	5.00	A-S.R	OLIVE.YELLOW	28924
WI195	Grab	50.50	2.52	2.25	0.75	-3.28	23.22	7.40	1.00	A-S.R	GRY.OLIVE	28925
WI196	Grab	54.00	2.49	2.75	0.54	0.47	3.49	10.99	0.00	A-S.A	OLIVE.YELLOW	28926
WI197	Grab	54.00	2.64	2.75	0.41	0.55	3.00	13.88	0.00	A-S.A	GRY.OLIVE	28927
WI198	Grab	50.00	2.20	2.00	0.50	0.39	5.89	7.76	0.00	S.A-S.R	OLIVE.YELLOW	28928
WI199	Grab	51.00	2.30	2.25	0.39	0.46	2.85	6.13	0.00	A-S.R.	GRY.OLIVE	28929
WI200	Grab	50.00	1.73	1.75	1.05	-0.38	3.68	28.79	1.00	S.A-S.R	OLIVE.YELLOW	28930
WI201	Grab	50.00	2.35	18.46, 18.55	0.65	-0.19	2.22	13.58	0.00	A-S.R	GRY.OLIVE	28931
WI201	Box Core	50.00	1.93	1.50	0.85	-0.27	3.82	13.60	5.00	A-S.A	GRY.OLIVE	28932
WI201-202	Box Core	46.00	0.95	0.50	0.98	0.98	4.23	20.50	5.00	S.R-R	L.GRAY	28933
WI202	Grab	47.50	2.35	2.25	0.94	-0.93	3.34	28.35	0.00	A-S.R	GRY.OLIVE	28934
WI202A	Grab	47.50	0.13	0.00	0.83	1.55	4.62	40.90	0.00	V.A-R	GRY.OLIVE	28935
WI203	Grab	42.00	0.91	0.75	0.62	1.46	4.35	32.40	15.00	S.A-R	P.YELLOW	28936
WI204	Grab	40.00	1.99	2.25	0.33	0.91	4.09	3.60	15.00	S.R	P.YELLOW	28937
WI205	Grab	38.00	2.17	2.00	0.34	1.08	3.59	6.15	10.00	S.A-S.R	L.YELLOW	28938
WI206	Grab	38.00	2.12	2.00	0.38	1.64	7.75	4.16	10.00	S.A-S.R	L.YELLOW	28939
WI206B	Grab	38.00	2.18	2.25	0.68	-2.68	22.61	3.92	10.00	A-S.R.	GRY.OLIVE	28940
WI207	Grab	35.00	1.77	1.75	0.43	1.32	5.29	4.50	10.00	A-S.R.	L.GRAY	28941
WI208	Grab	34.00	2.00	2.00	0.91	-2.86	14.88	5.74	5.00	S.A-S.R	L.GRAY	28942
WI209	Grab	33.00	2.19	2.25	0.46	-0.17	6.39	4.90	5.00	S.A-S.R	L.GRAY	28943
WI210	Grab	32.00	1.67	2.00	0.69	0.30	4.54	6.02	10.00	S.A-S.R	L.GRAY	28944
WI211	Grab	32.00	2.32	2.25	0.36	1.11	5.03	7.41	25.00	A-S.A	L.YELLOW	28945
WI212	Grab	27.00	2.74	2.75	0.30	0.35	3.86	11.96	5.00	V.A-A	GRY.OLIVE	28946
WI213	Grab	19.00	2.68	2.75	0.42	0.78	3.75	5.14	2.00	V.A-A	L.GRAY	28947
WI214	Grab	13.00	2.85	2.75	0.31	0.33	2.80	7.90	0.00	V.A-A	L.GRAY	28948
WI215	Grab	15.00	2.71	2.75	0.37	-0.56	4.94	7.93	1.00	V.A-A	L.GRAY	28949
WI216	Grab	11.00	2.90	2.75	0.37	-0.33	2.66	7.90	0.00	V.A	GRY.OLIVE	28950
WI217	Box Core	24.00	2.22	2.00	0.48	-0.07	3.51	12.50	15.00	A-S.A	P.YELL-L.GRAY	28951
WI218	Grab	29.50	2.18	2.25	0.43	0.62	3.91	5.50	50.00	S.R-R	L.YELLOW	28952
WI219	Grab	28.50	2.11	2.00	0.47	-3.13	30.11	3.50	40.00	S.R	L.YELLOW	28953
WI220	Grab	29.00	2.10	2.00	0.35	-0.04	4.34	2.90	40.00	S.R	P-L.YELLOW	28954
WI220	Box Core	29.00	2.10	2.00	0.60	-4.88	34.34	2.90	25.00	S.A-S.R	L.YELLOW	28955
WI220	Diver	29.00	2.17	2.25	0.65	-5.03	33.13					28956
WI221	Grab	31.00	1.68	1.75	0.55	-1.61	12.34	6.90	40.00	S.A-S.R	L.GRAY	28957
WI222	Grab	32.50	2.53	2.50	0.59	-5.47	44.31	6.70	10.00	S.A.		28958

SAMPLE NO	SAMPLE TYPE	DEPTH (m)	MEAN	MODE	SORTING	SKEWNESS	KURTOSIS	CO3 (%)	FeO (%)	ANGULARITY	COLOUR	
WI223	Grab	33.00	2.27	2.25	0.49	1.20	6.08	10.17	10.00	A-S.R	OLIVE.YELL	28959
WI224	Grab	34.00	2.14	2.00	0.44	0.46	3.96	6.00	20.00	S.R-R	L.GRAY	28960
WI225	Grab	36.00	1.89	2.00	0.35	0.24	5.47	9.60	30.00	S.A-S.R	L.GRAY	28961
WI226	Grab	38.00	1.68	1.75	0.39	-2.45	32.47	6.10	40.00	S.R-R	P.YELLOW	28962
WI227	Grab	40.50	1.85	1.75	0.36	0.58	4.01	4.60	40.00	S.R	L.GRAY	28963
WI228	Grab	42.00	2.29	2.25	0.43	0.26	4.24	6.01	1.00	A-S.R	GRY.OLIVE	28964
WI229	Grab	44.00	1.72	1.75	0.44	0.91	5.76	7.34	5.00	S.A-R	L.GRY-P.YELLOW	28965
WI230A	Grab	48.50	2.50	2.50	0.50	0.43	6.46	8.41	0.00	A-R	OLIVE.YELLOW	28966
WI230B	Grab	48.50	2.38	2.50	0.56	-0.21	5.35	9.90	0.00	S.A-S.R	GRY.OLIVE	28967
M231	Box Core	28.50	2.21	2.00	0.47	-0.26	5.38	6.29	5.00	S.A-S.R	L.YELLOW	28968
M232	Box Core	25.00	2.49	2.50	0.40	0.84	3.54	7.80	5.00	A-S.R	L.GRAY	28969
M233	Box Core	10.00	2.90	2.75	0.44	-1.49	14.15	4.05	0.00	V.A-A	L.GRAY	28970
M234	Box Core	36.50	1.47	1.50	0.46	0.82	4.43	8.88	10.00	A-S.R	L.GRAY	28971
M235	Box Core	44.00	2.29	2.25	0.48	-0.74	9.82	10.88	0.00	A-S.A	OLIVE.YELLOW	28972
M236	Box Core	49.00	2.11	2.25	0.34	1.06	4.98	3.98	5.00	A-S.R	GRY.OLIVE	28973
WH237	Box Core	20.50	2.79	2.75	0.72	-4.25	29.94	8.15	5.00	V.A-S.R	L.GRAY	28974
WH238	Box Core	33.00	0.12	0.00	0.88	1.28	4.88	45.15	7.00	V.A-S.R	L.GRAY	28975
WH239	Box Core	41.50	1.00	0.25, 1.50	0.85	0.32	2.51	11.53	25.00	A-R	GRY.YELLOW	28976
WH239A	Box Core	41.50	1.98	2.00	0.70	-0.27	4.27	11.74	5.00	A-S.R	L.GRAY	28977
WH240	Box Core	50.50	2.75	3.00	0.55	0.12	2.97	13.15	0.00	A-S.R	GRY.OLIVE	28978
WB241	Box Core	10.00	2.77	2.75	0.37	0.07	3.45	4.61	5.00	V.A-A	L.GRAY	28979
WB242	Box Core	24.00	1.03	1.00	0.73	0.58	5.20	11.58	20.00	S.A-R	L.GRY-P.YELLOW	28980
WB243	Box Core	20.50	1.04	1.00	0.33	0.85	3.38	8.75	20.00	S.A-S.R	L.GRY-P.YELLOW	28981
WB244	Box Core	26.00	1.04	1.00	0.68	-0.19	5.81	11.88	25.00	S.A-R	L.GRY-P.YELLOW	28982
WB245	Box Core	32.00	0.92	1.25	0.72	-0.54	7.38	17.67	30.00	S.A-S.R	YELL-D.BRWN	28983
WB246	Box Core	26.50	-0.05	0.00	0.35	1.32	6.37	13.42	30.00	S.R-W.R	P.YELL-D.BRWN	28984
WB247	Box Core	17.00	2.75	3.00	0.49	-0.10	2.36	13.68	5.00	V.A-A	ORANGE.YELLOW	28985
WB248	Box Core	11.00	2.78	3.00	0.33	0.31	2.76	7.51	0.00	V.A-A	L.GRAY	28986
WB249	Box Core	26.00	1.16	1.25	0.58	0.99	5.03	11.89	20.00	A-R	P.YELLOW	28987
WB250	Box Core	34.00	0.89	0.75	0.61	0.98	4.58	35.60	30.00	S.R-W.R	P.YELLOW	28988
WB251	Box Core	45.00	0.94	0.75	0.52	0.72	2.87	21.50	20.00	S.A-R	P.YELLOW	28989
WB251A	Box Core	45.00						3.49	30.00	S.A-R	P.YELLOW	28990
WB251B	Box Core	45.00						12.09	50.00	S.A-R	GRY.YELLOW-P.YELLOW	28991
WB252	Box Core	51.50	0.93	0.50, 1.50	0.86	0.45	2.46	20.20	7.00	S.A-S.R	L.GRAY	28992
WB252A	Box Core	51.50	0.35	-0.25	1.01	1.04	4.35	12.86	10.00	S.A-S.R	P.YELLOW	28993
WB252B	Box Core	51.50	1.43	2.00	0.95	-0.40	4.22	27.97	0.00	S.A-R	GRY.OLIVE	28994
WB253A	Box Core	63.00	0.70	1.00	0.73	-0.02	2.78	18.84	0.00	A-S.R	GRY.OLIVE	28995
WB253B	Box Core	63.00	0.37	-0.25	1.20	0.39	2.36	12.36	0.00	A-R	L.GRY-GRY.OLIVE	28996
WB253C	Box Core	63.00	0.26	-0.50, 0.75	0.93	0.58	2.83					28997
WB254	Box Core	81.00	1.49	1.50	0.96	-0.13	2.65	15.87	0.00	A-S.A	GRY.OLIVE	28998
WB255	Box Core	100.00	1.68	2.00	0.98	-0.11	2.21	10.26	0.00	A-R	GRY.OLIVE	28999
WB256	Box Core	190.00	2.80	3.00	0.27	0.02	2.35	11.19	0.00	V.A-A	GRY.OLIVE	29000
WB256A	Box Core	190.00	2.78	3.00	0.33	0.17	2.61					29001
WB256B	Box Core	190.00	3.01	2.75	0.31	0.43	2.20	15.66	0.00	V.A-A	GRY.OLIVE	29002
WB56C	Box Core	190.00	2.88	2.75	0.38	0.50	2.37	19.26	0.00	V.A-A	GRY.OLIVE	29003
ON257	Grab	24.00	0.74	0.75	0.57	1.78	6.48	19.41	60.00	S.R-R	L.YELL.BROWN	29004
ON258	Grab	9.50	2.68	2.50	0.41	0.11	3.53	11.65	5.00	A-S.A.		29005

SAMPLE NO	SAMPLE TYPE	DEPTH (m)	MEAN	MODE	SORTING	SKEWNESS	KURTOSIS	CO3 (%)	FeO (%)	ANGULARITY	COLOUR	
ON259	Grab	5.00	1.72	1.25	0.51	0.56	2.52	15.58	20.00	A-R	L.GRY-L.YELL.ORANGE	29006
ON260	Grab	7.00	1.90	2.00	0.49	-0.07	2.54	13.88	25.00	A-S.R	GRY.YELLOW	29007
ON261	Grab	18.00	2.73	2.50	0.47	-0.35	4.04	9.52	5.00	V.A-S.A	L.YELLOW	29008
ON262	Grab	15.00	2.83	2.75	0.36	0.28	2.80	10.60	0.00	A-S.A	GRY.OLIVE	29009
ON263	Grab	13.50	2.64	2.75	0.42	0.23	2.66	6.37	10.00	V.A-A	L.GRAY	29010
ON264	Grab	11.00	2.60	2.75	0.46	-0.60	6.95	12.00	10.00	V.A-S.A	GRY.YELLOW	29011
ON265	Grab	23.00	2.71	2.50	0.50	0.24	2.62	11.61	10.00	V.A-S.A	L.YELLOW	29012
ON266	Grab	28.00	2.45	2.25	0.53	6.48	1.08	3.15	10.00	A-S.R	GRY.OLIVE	29013
ON267	Grab	24.50	1.01	0.75	0.57	1.02	3.86	12.82	10.00	S.R-W.R	L.YELLOW	29014
ON268	Grab	22.00	2.27	2.50	0.71	-2.40	15.84	6.75	25.00	A-S.R	GRY.YELLOW	29015
WH269	Grab	26.00	2.00	2.00	0.37	0.66	4.49	2.79	30.00	A-S.R	P.YELLOW	29016
WH270	Grab	32.00	1.98	2.00	0.50	-0.98	7.96	28.62	10.00	A-R	P.YELLOW	29017
WI271	Grab	33.00	1.45	1.25	0.50	0.74	3.07	5.37	15.00	S.A-R	L.GRY-P.YELLOW	29018
WH272	Grab	34.00	0.92	1.00	0.43	0.41	13.96	28.34	60.00	S.A-S.R	YELLOW-ORANGE	29019
WH274	Grab	22.00										29020
WH275	Grab	27.00										29021
ON276	Hand	-2.00	1.12	1.25	0.27	0.94	3.89	18.89	70.00	S.A-R	L.GRY-L.YELL.ORANGE	29022
ON277	Hand	0.00	0.94	1.00	0.34	-0.82	10.36					29023
ON278	Hand	-2.00	0.94	1.00	0.31	-1.99	18.68	23.80	20.00	S.A-W.R	L.YELL.OR-D.BRWN	29024
ON279	Hand	0.00	-0.25	0.00	0.15	-0.57	2.44	47.46	60.00	S.A-R	L.GRY-B.YELL.BRWN	29025
ON280	Hand	-2.00	1.00	1.00	0.26	-0.08	4.49	16.65	25.00	S.A-R	L.GRY-L.YELL.ORANGE	29026
WH281	Hand	-2.00	2.17	2.25	0.32	0.50	3.51	15.78	20.00	V.A-R	L.YELLOW	29027
WH282	Hand	0.00	2.15	2.25	0.33	-0.05	2.67	17.24	70.00	A-S.R	P.YELLOW	29028
WH283	Hand	-2.00	2.09	2.00	0.33	-0.65	5.83	8.18	20.00	S.A-S.R	P.YELL-GRY.YELL	29029
WH284	Hand	0.00	2.06	2.00	0.35	0.55	2.85	17.79	60.00	A-R	L.GRY-P.YELLOW	29030
WH285	Hand	-2.00	1.83	1.75	0.33	0.26	3.24	13.44	30.00	S.A-S.R	P.YELLOW	29031
WI286	Hand	0.00	1.93	2.00	0.46	-0.18	3.74	26.25	50.00	S.A-S.R	GRY.YELL-P.YELL	29032
WI287	Hand	-2.00	0.98	1.00	0.34	-0.23	5.52					29033
WI288	Hand	0.00	0.69	0.75	0.37	-0.21	4.00	16.14	30.00	R-W.R	L.GRY.YELLOW	29034
WI289	Hand	-3.00	1.26	1.25	0.26	0.77	3.45	3.49	7.00	S.R-W.R	P.YELL.BLK	29035
WI290	Hand	-2.00	1.07	1.25	0.24	0.69	3.99	8.34	5.00	S.R-W.R	L.GRY-P.YELL	29036
WI291	Hand	0.00	0.80	0.75	0.43	0.13	2.76	13.76	30.00	R-W.R	L.GRY-P.YELL.ORANGE	29037
WI292	Hand	-2.00	0.92	1.00	0.37	0.23	3.93	11.42	5.00	S.R-W.R	L.GRY-P.YELLOW	29038
WI293	Hand	0.00	0.55	0.50	0.33	2.35	12.16	17.24	30.00	S.R-W.R	L.GRY-L.YELL.ORANGE	29039
WAIROA 294	Hand	RIVER	1.24	1.25	0.64	0.09	4.35	0.00	10.00	A-S.R	L.YELLOW	29040
TAUPIRO 295	Hand	RIVER	1.48	1.25	0.66	0.55	3.91	0.00	30.00	A-S.A	BROWN	29041
TERAMA. 296	Hand	RIVER	0.84	0.75	0.99	0.96	3.67	0.00	20.00	A-S.R	D.YELLOW	29042
WHARA. 297	Hand	RIVER	1.20	1.50	0.92	-0.03	2.78	0.00	20.00	A-S.A	D.YELL.BRWN	29043
MOANOA.298	Hand	RIVER	1.42	2.00	0.84	-0.68	3.47	0.00				29044
OTUWHETI 299	Hand	RIVER	0.92	0.75	0.91	0.24	1.99	0.00	50.00	V.A-S.A	YELL.BROWN	29045
WHARE.300	Hand	RIVER	1.87	2.00	0.53	0.53	2.87	0.00	30.00	V.A-S.A	D.YELL.ORANGE	29046
TAIRUA. 301	Hand	RIVER	1.62	1.25	0.56	0.57	4.76	0.00	50.00	V.A-S.A	D.YELL.ORANGE	29047
HW 302	Hand	RIVER	1.58	1.25	0.56	0.69	3.13	0.00	30.00	V.A-R	GRY.YELL.BRWN	29048
WIGMORE 303	Hand	RIVER	1.70	1.75	0.57	-1.02	6.24	0.00	0.00	S.A-W.R	BRWN.GRAY	29049
PURANGI 304	Hand	RIVER	1.08	0.75	0.82	0.53	2.70	0.00	30.00	V.A-S.A	YELL.BROWN	29050
WHENU. 305	Hand	RIVER	0.44	0.50	1.05	0.25	2.65	0.00	5.00	A-S.A	GRY.YELLOW	29051
KAPUWAI. 306	Hand	RIVER	1.78	1.50	0.84	-0.87	4.17	0.00	30.00	A-S.A.		29052

SAMPLE NO	SAMPLE TYPE	DEPTH (m)	MEAN	MODE	SORTING	SKEWNESS	KURTOSIS	CO3 (%)	FeO (%)	ANGULARITY	COLOUR	
WAIWAUA. 306B	Hand	RIVER	1.14	1.00	0.61	0.46	3.18	0.00	30.00	A-S.A	D.YELL.BRWN	29053
ONUORA. 307	Hand	RIVER	1.46	POLYMODAL	1.16	-0.15	1.87	0.00	50.00	V.A-S.R	D.YELL.BROWN	29054
WHANGA. 308	Hand	RIVER	1.56	1.75	0.62	0.81	4.41	0.00	50.00	A-S.A	YELL.BROWN	29055
TARA. 309	Hand	RIVER	1.92	1.50	0.46	0.54	2.59	0.00	30.00	V.A-S.R	D.YELL.BROWN	29056
STEWART 310	Hand	RIVER	2.11	2.00	0.62	0.75	4.56	0.00	10.00	A-S.A	GRY.YELL.BROWN	29057
OTAMA 311	Hand	RIVER	1.65	1.50	0.59	1.17	4.60	0.00	5.00	S.A-R	L.YELLOW	29058
KUAOT. 312	Hand	RIVER						0.00	5.00	A-S.R	GRY.YELL.BROWN	29059
OTANGURU 313	Hand	RIVER						0.00	50.00	A-R	YELL.BROWN	29060
OWERA 314	Hand	RIVER	1.35	1.25	0.53	0.48	3.16	0.00	50.00	V.A-S.A	YELL.BROWN	29061
OPITO 315	Hand	RIVER	2.15	2.00	0.50	0.97	3.72	0.00	50.00	V.A-S.A	YELL.BROWN	29062
PUNGA. 316	Hand	RIVER	0.58	0.25	0.76	0.72	3.23	0.00	50.00	A-S.A	D.BROWN	29063
KB317	Hand	H.BARRIER	1.75	1.75	0.42	-1.94	19.65	0.00	10.00	S.A-S.R	P.YELLOW	29064
KB318	Hand	-2.00	2.24	2.25	0.49	0.29	3.33	7.26	2.00	S.A-S.R	L.GRAY	29065
KB319	Hand	P.BARRIER	1.67	1.50	0.44	-0.11	10.39	0.00	50.00	A-S.R	YELL.ORANGE	29066
KB320	Hand	P.BARRIER	1.48	1.25	0.43	0.84	3.56	0.00	2.00	S.A-R	P.YELLOW	29067
KB321	Hand	P.BEACH	1.46	1.25	0.39	0.96	3.54	0.00	30.00	S.A-S.R	YELLOW	29068
KB322	Hand	H.BEACH	1.49	1.25	0.38	-0.12	7.01	1.94	5.00	S.A-R	L.GRY-BLACK	29069
MB323	Hand	-2.00	1.63	1.50	0.57	0.36	2.50	21.37	30.00	V.A-S.A	GRY.YELLOW	29070
WB324	Hand	-2.00	1.62	1.25	0.51	-0.42	9.30	0.00	10.00	S.A-R	BLACK	29071
HW325	Hand	-2.00	1.11	1.00	0.58	0.71	9.67	22.22	50.00	A-R	D.YELL.BROWN	29072
HW326	Hand	-2.00	1.17	1.00	0.44	1.79	8.08	16.67	50.00	A-R	D.YELLORANGE	29073
HA327	Hand	-2.00	1.96	2.00	0.53	-1.15	11.63	25.22	5.00	A-S.A	D.YELLORANGE	29074
OPIB328	Hand	-2.00	1.01	0.75	0.59	0.64	4.26	38.68	10.00	A-R	L.YELLOR-D.YELL.BRWI	29075
OPIB329	Diver	27.40	0.80	0.75	0.91	1.64	5.97	89.64	30.00	S.A-S.R	L.YELLORANGE	29076
K330	Diver	35.00	2.87	3.00	0.55	0.02	0.98	28.30	0.00	V.A-A	OLIVE.YELLOW	29077
K331		13.00	2.61		0.41	0.10	2.23	83.67	20.00	A-S.R	L.YELLOW	29078
K332		9.00	1.59	1.75	0.31	0.10	2.11	37.74	15.00	S.A-S.R	L.YELLOW	29079
K333		8.00	3.06	3.50	0.64	-1.12	4.13	26.85	50.00	V.A-S.A	L.YELLOW	29080
K334		4.00	2.79	3.00	0.52	-1.05	5.11	13.90	20.00	A-S.A	L.YELLOW	29081
K335		20.00	2.16	2.25	0.79	-1.14	4.44	10.45	10.00	A-R	L.YELLOW	29082
K336		18.00	2.17	2.25, 3.00	0.87	-0.65	4.23	49.47	2.00	A-S.R	OLIVE.YELLOW	29083
K337		16.00	0.19	-0.25	1.24	0.76	2.78	82.63	20.00	A-S.R	L.YELLOW	29084
K338		20.00	2.87	3.00	0.34	0.41	2.48	47.12	5.00	A-S.A	L.YELLOW	29085
K339		18.00	SAMPLE MISSING					SAMPLE MISSING				29086
K340		16.00	2.31	2.00	0.82	-0.35	2.80	WHOLE SHELL				29087
K341		14.00	2.48	2.50	0.35	-0.27	1.76	29.62	15.00	A-S.R	L.YELLOW	29088
K342		12.00	2.87	3.25	0.25	-0.46	2.04	11.35	2.00	A-S.R	L.YELLOW	29089
K343		10.00	2.44	2.75	0.53	-0.03	3.04	12.78	10.00	A-S.R	L.YELLOW	29090
K344		8.00	2.52	2.50	0.44	0.18	2.80	13.52	5.00	A-S.A	L.YELLOW	29091
K345		6.00	SAMPLE MISSING					SAMPLE MISSING				29092
K346		4.00	2.51	2.25	0.59	0.39	3.07	13.06	15.00	S.A-R	L.YELLOW	29093
K347		20.00	2.48	2.75	0.53	0.65	3.08	17.82	5.00	A-S.R	L.YELLOW	29094
K348		16.00	2.16	2.25	0.44	0.21	4.28	30.33	5.00	A-S.A	L.YELLOW	29095
K349		16.00	SAMPLE MISSING					SAMPLE MISSING				29096
K350		14.00	2.49	2.50	0.43	-1.68	14.45	24.94	10.00	A-S.A	L.YELLOW	29097
K351		12.00	1.86	2.75	0.98	-0.40	2.31	47.74	5.00	A-S.A	L.YELLOW	29098
K352		10.00	2.65	2.75	0.68	-4.37	28.03	54.92	7.00	A-R		29099
												29100

SAMPLE NO	SAMPLE TYPE	DEPTH (m)	MEAN	MODE	SORTING	SKEWNESS	KURTOSIS	CO3 (%)	FeO (%)	ANGULARITY	COLOUR	
K353		8.00	1.70	1.50	0.47	0.49	2.94	12.11	10.00	A-S.A	LYELLOW	291002
K354		6.00	2.61	2.75	0.47	-2.75	23.81	12.08	10.00	A-S.A	LYELLOW	291003
K355		4.00	2.72	2.75	0.39	-0.04	4.07	10.45	10.00	A-R	LYELLOW	291004
K356		2.00	2.25	2.25	0.50	-0.65	5.05	10.91	15.00	A-S.R	GRY.YELLOW	291005
K357		20.00	1.79	1.75	0.56	0.51	3.44	17.91	5.00	A-S.R	LYELLOW	291006
K358		18.00	2.52	2.50	0.44	0.45	2.83					291007
K359		16.00	2.41	2.25	0.38	0.57	2.76	10.00	5.00	A-S.A	LYELLOW	291008
K360		14.00	2.55	2.50	0.42	-0.57	6.90	13.26	20.00	A-S.A	LYELLOW	291009
K361		12.00	2.54	2.75	0.32	0.59	3.02	21.48	15.00	A-S.A	P.YELLOW	291010
K362		10.00	2.48	2.75	0.34	0.02	2.93	30.54	5.00	A-S.A	LYELLOW	291011
K363		8.00	2.26	2.50	0.48	-0.08	4.55	7.69	15.00	A-S.A	LYELLOW	291012
K364		6.00	2.39	2.50	0.35	0.55	4.03	15.40	15.00	V.A-S.A	LYELLOW	291013
K365		4.00	SAMPLE MISSING					SAMPLE MISSING				291014
K366		20.00	2.24	2.00	0.54	-1.20	13.10	18.56	15.00	A-S.R	LYELLOW	291015
K367		18.00	2.16	2.25	0.67	-0.18	2.85	WHOLE SHELL				291016
K368		16.00	2.59	2.50	0.48	-2.14	18.66	8.91	25.00	A-S.A	LYELLOW	291017
K369		14.00	2.57	2.50	0.34	0.77	3.79	2.97	10.00	A-S.A	LYELLOW	291018
K370		12.00	2.31	2.00	0.46	-0.18	5.08					291019
K371		10.00	2.64	2.75	0.33	0.61	4.14	7.88	5.00	A-S.A	LYELLOW	291020
K372		8.00	2.59	2.50	0.40	0.87	3.41	6.43	7.00	A-S.A	LYELLOW	291021
K373		6.00	2.36	2.25	0.50	0.29	3.47	13.42	2.00	S.A-S.R	LYELLOW	291022
K374		4.00	2.43	2.25	0.44	0.05	2.85	13.70	5.00	A-S.R	GRY.YELLOW	291023
K375		16.00	1.01	1.00	0.33	0.46	2.44	51.27	10.00	S.A-W.R	P.YELLOW	291024
K376		19.00	1.99	2.00, 2.75	0.86	-0.08	2.38	57.13	30.00	A-R	LYELLOW	291025
K377		17.00	2.60	2.50	0.57	-0.34	3.13	60.76	10.00	A-S.R	LYELLOW	291026
K378		15.00	2.09	2.00	0.80	-0.19	4.17	24.80	30.00	V.A-S.R	LYELLOW	291027
K379		13.00	2.29	2.50	0.64	-0.26	2.98	27.85	5.00	A-S.R	LYELLOW	291028
K380		11.00	2.26	2.25	0.61	-0.73	4.23	0.24	15.00	A-S.R	LYELLOW	291029
K381		9.00	SAMPLE MISSING					SAMPLE MISSING				291030
K382		9.00	SAMPLE MISSING					SAMPLE MISSING				291031
K383		7.00	2.22	2.00, 2.50	0.68	-0.53	3.36	15.34	20.00	A-S.R	LYELLOW	291032
K384		5.00	SAMPLE MISSING					SAMPLE MISSING				291033
K385		18.00	2.46	2.50	0.46	-1.02	8.79	20.51	10.00	A-S.A	LGRAY	291034
K386		16.00	1.97	1.50	0.66	0.37	2.65	68.28	5.00	A-S.R	LYELLOW	291035
K387		14.00	SAMPLE MISSING					SAMPLE MISSING				291036
K388		12.00	2.11	2.00	0.64	-0.81	6.99	14.92	5.00	S.A-S.R	LYELLOW	291037
K389		10.00	2.45	2.50	0.37	0.38	2.41	10.78	5.00	A-S.A	LYELLOW	291038
K390		8.00	2.66	2.50	0.41	0.33	2.55	8.97	20.00	A-S.R	LYELLOW	291039
K391		6.00	2.39	2.75				15.43	10.00	A-S.A	P.YELLOW	291040
K392		4.00	2.41	2.50	0.37	0.60	3.00	12.15	10.00	A-S.A	GRY.YELLOW	291041
K393		18.00	2.14	2.00	0.73	-0.66	3.90	11.35	10.00	S.A-S.R	P.YELLOW	291042
K394		16.00	SAMPLE MISSING					SAMPLE MISSING				291043
K395		14.00	2.13	2.25	0.63	-1.03	6.63	39.31	10.00	A-S.A	LYELLOW	291044
K396		12.00	2.49	2.50	0.39	0.00	2.49	7.15	10.00	A-S.A	LYELLOW	291045
K397		10.00	2.37	2.50	0.55	-1.85	14.17					291046
K398		8.00	2.50	2.75	0.54	-2.65	18.02	23.55	10.00	A-S.A	LYELLOW	291047
K399		6.00	2.53	0.33	-1.22	5.44						291048

SAMPLE NO	SAMPLE TYPE	DEPTH (m)	MEAN	MODE	SORTING	SKEWNESS	KURTOSIS	CO3 (%)	FeO (%)	ANGULARITY	COLOUR	
K400		4.00	2.43	2.75	0.62	-1.71	10.18	13.08	15.00	A-S.R	GRY.YELLOW	291049
K401		18.00	2.19		0.47	0.45	3.20	57.57	20.00	A-S.A	P.YELLOW	291050
K402		16.00	1.03	1.25	0.50	0.32	2.64	29.09	2.00	S.A-R	P.YELLOW	291051
K403		13.00	1.43	1.25	0.49	0.54	3.32	44.25	10.00	S.A-S.R	P.YELLOW	291052
K404		10.00	SAMPLE MISSING					SAMPLE MISSING				291053
K405		19.00	1.78	1.25	0.81	0.98	2.98	43.11	2.00	A-S.R	L.YELLOW	291054
K406		17.00	1.81	1.75	0.75	0.16	3.61	WHOLE SHELL				291055
K407		15.00	SAMPLE MISSING					48.54	5.00	S.A-S.R	L.YELLOW	291056
K408		13.00	1.16	1.00	0.74	0.66	3.64	41.88	30.00	S.R-R	P.YELLOW	291057
K409		11.00	1.15	1.00	0.34	1.02	4.48	58.32	50.00	S.A-S.R	P.YELLOW	291058
K410		18.00	SAMPLE MISSING					SAMPLE MISSING				291059
K411		16.00	1.92	2.25	0.74	-0.26	2.99					291060
K412		14.00	1.38	1.50	0.56	1.01	3.76	38.56	20.00	S.S-R	L.YELLOW	291061
K413		12.00	1.21	1.25	0.43	1.14	5.48	30.91	15.00	S.A-R	L.YELLOW	291062
K414		10.00	1.05	1.00	0.39	0.07	4.56	34.15	10.00	S.A-S.R	P.YELL.-OR.BRWN	291063
K415		8.00	1.13	1.00	0.34	0.52	2.60	23.57	30.00	S.A-S.R	P.YELL.-OR.BRWN	291064
K416		6.00	1.73	1.75	0.47	0.72	3.38	22.00	30.00	A-S.R	YELLOW	291065
K417		12.50	SAMPLE MISSING					SAMPLE MISSING				291066
K418		11.50	SAMPLE MISSING					SAMPLE MISSING				291067
K419		11.50	SAMPLE MISSING					SAMPLE MISSING				291068
K420		9.00	SAMPLE MISSING					SAMPLE MISSING				291069
K421		7.30	SAMPLE MISSING					SAMPLE MISSING				291070
K422		5.20	SAMPLE MISSING					SAMPLE MISSING				291071
K423		3.50	SAMPLE MISSING					SAMPLE MISSING				291072
K424		14.00	2.23	2.50	0.42	-0.35	4.28					291073
K425		12.00	SAMPLE MISSING					SAMPLE MISSING				291074
K426		10.00	1.90	1.75	0.46	0.06	3.45	37.00	5.00	S.A-S.R	P.YELLOW	291075
K427		8.00	1.69	1.50	0.49	0.74	3.05	5.19	5.00	S.A-R	P.YELLOW	291076
K428		6.00	1.87	2.00	0.32	0.87	4.21	10.67	10.00	S.A-S.R	P.YELLOW	291077
K429		16.00	SAMPLE MISSING					SAMPLE MISSING				291078
K430		14.00	1.24	1.00, 1.50	0.66	0.21	3.68	41.38	20.00	S.A-R	P.YELLOW	291079
K431		12.00	SAMPLE MISSING					SAMPLE MISSING				291080
K432		10.00	1.89	2.00	0.39	1.36	5.79	7.42	5.00	S.A-S.R	P.YELLOW	291081
K433		8.00	1.86	1.75	0.41	1.38	5.90	9.23	5.00	S.A-R	P.YELLOW	291082
K434		6.00	1.77	1.75	0.36	0.51	4.24	9.97	10.00	S.A-R	P.YELLOW	291083
K435		4.00	SAMPLE MISSING					SAMPLE MISSING				291084
K436		1.00	2.04	2.25	0.40	0.17	3.47	9.70	10.00	A-S.R	GRY.YELLOW	291085
K437		5.00	2.46	2.50	0.74	-3.01	16.27	5.87	5.00	A-S.A	GRY.YELLOW	291086
K438		10.00	SAMPLE MISSING					SAMPLE MISSING				291087
K439		18.00	2.47	2.75	0.44	-1.00	5.96	8.32	5.00	A-S.A	L.YELLOW	291088
K440		22.00	1.44	0.50, 2.75	1.26	-0.44	2.05	66.32	10.00	A-S.R	L.GRAY	291089
K441		24.00	2.40	2.50	0.44	-1.53	8.43	9.67	2.00	S.A-S.R	L.GRAY	291090
K442		26.00	2.31	2.25	0.37	0.18	0.93	39.99	20.00	A-S.A	L.YELLOW	291091
K443		28.00	SAMPLE MISSING					SAMPLE MISSING				291092
K444		19.00	2.28	2.25	0.43	0.11	3.74	39.99	20.00	A-S.A	L.YELLOW	291093
K445		18.00	2.18	2.00	0.83	-1.24	5.11	57.93	10.00	A-S.R	L.YELLOW	291094
K466		17.00	SAMPLE MISSING					SAMPLE MISSING				291095

SAMPLE NO	SAMPLE TYPE	DEPTH (m)	MEAN	MODE	SORTING	SKEWNESS	KURTOSIS	CO3 (%)	FeO (%)	ANGULARITY	COLOUR	
K447		16.00	1.77	1.75	0.65	-1.75	13.06	12.20	5.00	S.A-S.R	L.YELLOW	291096
K448		15.00	2.48	2.50	0.63	-2.46	16.02	18.07	25.00	A-S.A	P.YELLOW	291097
K449		13.00	2.26	2.50	0.72	-1.39	7.13	41.00	20.00	A-S.R	L.YELLOW	291098
K450		11.00	2.53	2.50	0.43	-0.37	3.68	8.82	10.00	A-R	L.YELLOW	291099
K451		10.00	2.43	2.50	0.46	-0.44	4.02	9.25	2.00	A-S.R	L.YELLOW	291100
K452		8.00	2.40	2.25	0.41	0.27	2.85	0.00	5.00	A-S.A	GRY.YELLOW	291101
K453		5.00	2.06	2.25	0.49	0.18	3.21	0.00	5.00	A-S.R	L.GRAY	291102
K454		2.00	SAMPLE MISSING						SAMPLE MISSING			291103
K455		2.00	1.75	1.75	0.48	0.22	3.08	5.17	5.00	A-S.R	GRY.YELLOW	291104
K456		2.00	2.02	2.25	0.46	-0.06	3.43	6.38	5.00	S.A-S.R	L.GRAY	291105
K457		9.00	2.25	2.50	0.45	0.39	2.74	6.62	10.00	A-S.A	L.YELLOW	291106
K458		11.00	2.35	2.75	0.59	-1.27	12.39	6.77	5.00	A-S.A	GRY.YELLOW	291107
K459		14.00	SAMPLE MISSING						SAMPLE MISSING			291108
K460		10.00	2.26	2.50	0.73	-1.32	5.96	43.24	20.00	A-S.R	L.YELLOW	291109
K461		17.00	2.16	2.50	0.65	-1.29	4.35	22.19	30.00	A-S.R	L.YELLOW	291110
K462		18.00	SAMPLE MISSING						SAMPLE MISSING			291111
K463		19.00	1.61	1.75	0.44	1.41	5.47	12.63	10.00	S.A-R	P.YELLOW	291112
K464		19.50	2.11	2.00	0.69	-0.07	3.96	22.43	15.00	A-S.R	L.YELLOW	291113
K465		19.00	2.14	1.75, 2.5	0.65	-0.06	2.56	16.46	25.00	V.A-S.A	L.YELLOW	291114
K466		18.00	2.39	2.50	0.45	-0.50	4.05	8.52	20.00	A-S.A	L.YELLOW	291115
K467		17.00	2.27	2.00	0.59	-0.34	5.11	43.88	2.00	S.A-R	L.YELLOW	291116
K468		15.00	SAMPLE MISSING						SAMPLE MISSING			291117
K469		13.00	2.21	2.25	0.57	-1.43	7.00	45.03	5.00	A-S.R	L.YELLOW	291118
K470		10.00	2.59	2.50	0.31	0.43	2.80	15.02	10.00	A-S.A	L.YELLOW	291119
K471		8.00	2.37	2.25	0.42	0.26	2.36	7.21	5.00	A-S.A	L.YELLOW	291120
K472		7.00	2.08	2.00	0.35	0.43	4.78	4.96	5.00	A-S.A	P.YELLOW	291121
K473		2.00	2.06	2.00	0.43	-0.38	11.07	9.38	5.00	S.A-R	P.YELLOW	291122
K474		11.00	2.09	1.75	0.61	0.48	2.56	13.47	20.00	A-S.R	P.YELLOW	291123
K475		13.00	0.69	0.75	0.34	0.21	3.38	63.20	25.00	S.A-S.R	L.YELL.ORANGE	291124
K476		14.00	0.51	0.50	0.63	0.48	3.90	47.55	15.00	S.A-S.R	P.YELLOW	291125
K477		15.00	-0.11	-0.75, 1.00	1.20	0.83	3.00	92.12	20.00	A-R	P.YELLOW	291126
K478		16.00	1.89	2.00	0.49	-0.14	3.45	35.77	10.00	A-R	P.YELLOW	291127
K479		16.50	2.32	2.25	0.44	0.45	2.92	34.26	5.00	A-S.A	P.YELLOW	291128
K480		17.00	1.75	1.75	0.62	-0.65	4.42	34.64	2.00	S.A-S.R	P.YELLOW	291129
K481		17.50	1.40	1.75, 2.25	0.85	-0.17	2.40	30.58	40.00	A-S.A	L.YELLOW	291130
K482		18.00	1.55	1.50	0.48	0.90	4.78	75.68	50.00	S.A-S.R	P.YELLOW	291131
K483		18.50	1.45	1.50	0.58	0.10	3.43	62.32	30.00	S.A-S.R	P.YELLOW	291132
K484		19.00	1.19	1.50	0.69	0.19	4.16	69.63	5.00	S.A-R	P.YELLOW	291133
K485		19.50	1.01	1.25	0.68	0.00	2.64	68.75	30.00	A-S.A	P.YELL.-YELLOW	291134
K486		20.00	0.74	1.75	1.00	-0.03	2.08	66.53	25.00	A-R	P.YELLOW	291135
K487		20.00	0.70	-0.25, .75	0.73	0.24	4.63					291136
K488		19.00	1.11	1.25	0.41	0.02	4.62	85.00	50.00	S.A-S.R	P.YELL.-P.YELL BROWN	291137
K489		18.00	0.76	1.00	0.67	-0.09	3.59	89.78	10.00	S.A-R	P.YELLOW	291138
K490		17.50	-0.39	-1.00, -0.25	0.96	0.59	3.01	WHOLE SHELL				291139
K491		17.00	-0.70	-1.00, -0.25	0.96	0.96	3.31	WHOLE SHELL				291140
K492		15.00	1.45	1.50	0.70	0.33	2.81	77.88	25.00	A-R	P.YELLOW	291141
K493		14.00	1.98	2.00	0.86	-1.11	3.80					291142

SAMPLE NO	SAMPLE TYPE	DEPTH (m)	MEAN	MODE	SORTING	SKEWNESS	KURTOSIS	CO3 (%)	FeO (%)	ANGULARITY	COLOUR	
K494		13.00	2.29	2.50	0.44	-0.06	2.85	61.75	5.00	A-S.R	P.YELLOW	291143
K495		12.00	1.71	1.75	0.43	0.59	3.44	42.55	25.00	A-R	P.YELL.BRWN	291144
K496		11.00	1.12	1.25	0.48	0.26	3.40	14.74	20.00	S.A-R	P.YELL-YELLOW	291145
K497		10.00	SAMPLE MISSING						SAMPLE MISSING			291146
K498		2.00	1.72	1.75	0.36	0.24	4.22	6.32	5.00	S.A-R	L.GRAY	291147
K499		2.00	1.85	1.75	0.30	-0.96	5.48	6.11	5.00	S.A-R	L.GRAY	291148
K500		5.00	1.77	1.75	0.44	0.03	2.96	7.40	5.00	S.A-R	L.GRAY	291149
K501		9.00	2.13	2.00	0.30	0.96	3.61	9.68	10.00	S.A-S.R	P.YELLOW	291150
K502		11.00	1.82	1.50	0.64	-0.10	3.18	46.92	5.00	A-S.R	P.YELLOW	291151
K503		13.00	1.66	1.75	0.49	-0.09	4.91	28.65	2.00	S.A-R	P.YELLOW	291152
K504		15.00	1.29	1.50	0.64	-0.82	5.22	45.33	10.00	S.A-R	P.YELLOW	291153
K505		17.00	1.26	1.25	0.23	0.52	3.77	44.82	5.00	S.R-W.R	P.YELLOW	291154
K506		19.00	0.85	0.75	0.52	-0.03	3.16	38.85	15.00	S.A-R	P.YELLOW	291155
K507		20.00	0.54	0.75	0.49	-0.81	3.36	83.34	5.00	S.A-S.R	P.YELLOW	291156
K508	Hand	-2.00	1.64	1.75	0.30	0.04	4.05	4.90	2.00	SR	P.YELLOW	291157
K509	Hand	-2.00	1.84	1.75	0.34	1.56	5.36	10.57	2.00	S.A-R	L.GRAY	291158
K510	Hand	-2.00	2.03	2.00	0.38	0.64	4.22	10.53	5.00	S.A-R	P.YELLOW	291159
K511	Hand	-2.00	1.48	1.75	0.58	0.10	2.39	26.95	10.00	A-R	P.YELL-YELL.ORANGE	291160
K512	Hand	-2.00	0.93	0.50	0.60	0.79	3.00	34.71	5.00	S.R-W.R	P.YELL.-BLACK	291161
K513	Hand	-2.00	1.77	1.50	0.42	-0.43	4.84	4.71	2.00	S.A-R	L.GRAY	291162
K514	Hand	-2.00	2.20	2.50	0.37	-0.04	2.95	5.46	5.00	A-S.R	L.GRAY	291163
WAIB515	Hand	RIVER	0.48	0.75	0.69	0.43	2.74	0.00	50.00	A-S.A	YELL.BRWN	291164
WAIB516	Hand	-2.00	1.56	1.50	0.42	0.07	2.12	13.43	30.00	S.A-R	D.YELL.ORANGE	291165
WAIB517	Hand	H.BARRIER	1.44	1.50	0.40	-0.10	3.21	0.00	70.00	S.A-R	D.YELL.BRWN	291166
KENB518	Hand	H.BARRIER	1.95	1.75, 2.25	0.43	0.23	2.42	0.00	70.00	A-S.R	BROWN	291167
KENB519	Hand	-2.00	2.52	2.50	0.42	0.12	2.74	5.47	10.00	A-S.A	D.YELLOW	291168
KENB520	Hand	RIVER	2.20	2.25	0.41	0.52	2.92	0.00	50.00	A-S.A	D.YELL.BROWN	291169
K521	Hand	H.BARRIER	1.53	1.50	0.46	1.28	5.18	0.00	70.00	S.A-R	D.YELL.ORANGE	291170
K522	Hand	-2.00	1.55		0.57	-1.21	8.90	7.92	2.00	A-R	P.YELL-GRY.YELL	291171
K523	Hand	RIVER	1.74	1.75	0.52	0.15	3.06	0.00	2.00	S.A-R	L.GRAY	291172
K524	Hand	H.BARRIER	1.39	1.50	0.45	0.71	3.41	0.00	0.00	S.A-R	D.BROWN	291173
K525	Hand	H.BARRIER	1.74	1.75	0.45	0.35	3.07	0.00	70.00	S.A-R	YELL.BROWN	291174
OPIB526	Hand	H.BARRIER	2.06	2.50	0.49	-0.59	4.01	0.00	0.00	S.A-S.R	D.YELL.BROWN	291175
OPIB527	Hand	RIVER	0.53	POLYMODAL	0.86	-0.09	2.72	0.00	50.00	A-S.A	D.YELL.ORANGE	291176
OPIB528	Hand	-2.00	1.62	1.75	0.42	0.18	2.57	22.47	20.00	A-S.R	D.YELL.OR.-D.YELL.BRWN	291177
K529	Hand	H.BARRIER	1.50	1.50	0.29	0.88	3.67	0.00	5.00	S.R-R	D.YELL.BRWN	291178
MB530	Hand	H.BARRIER	1.69	1.50	0.57	0.55	3.59	0.00	50.00	S.A-R	B.YELL.BRWN	291179
MB531	Hand	-2.00	1.27	1.25	0.52	0.82	5.26	20.91	15.00	S.A-R	D.YELL.ORANGE	291180
MB532	Hand	-2.00	2.35	2.25	0.49	-0.10	6.03	5.73	20.00	A-S.R	D.GRY.YELLOW	291181
MB533	Hand	H.BARRIER	1.77	1.50	0.41	0.76	3.75	0.00	50.00	A-S.R	B.YELL.BROWN	291182
MB534	Hand	-2.00	2.29	2.25	0.69	-3.13	18.20	14.11	0.00	V.A-S.A	L.GRAY	291183
MB535	Hand	H.BARRIER	1.66	1.75	0.41	1.42	6.17	0.00	20.00	A-S.R	D.YELL.ORANGE	291184
HA536	Hand	H.BARRIER	1.46	1.25	0.42	0.21	3.41	0.00	0.00	S.A-W.R	D.GRY.YELLOW	291185
HW537	Hand	H.BARRIER	1.31		0.43	-0.57	11.55					291186
HW538	Hand	-2.00	1.22	1.25	0.48	0.79	11.73	19.35	50.00	S.A-R	D.YELL.BROWN	291187
TP539	Hand	-2.00	1.00	1.00	0.40	0.51	2.69	25.65	20.00	S.A-R	D.YELL.ORANGE	291188
TP540	Hand	H.BARRIER	1.09	1.00	0.37	0.51	2.74	0.00	10.00	S.A.-W.R.		291189

SAMPLE NO	SAMPLE TYPE	DEPTH (m)	MEAN	MODE	SORTING	SKEWNESS	KURTOSIS	CO3 (%)	FeO (%)	ANGULARITY	COLOUR	
TP541	Hand	-2.00	1.26	1.50	0.49	-0.17	2.87	12.60	15.00	A-R	GRY.YELLOW	291190
TP542	Hand	-2.00	1.82	1.75	0.48	-2.08	19.21	5.60	15.00	A-S.A	GRY.YELLOW	291191
TP543	Hand	H.BARRIER	1.76	1.75	0.37	0.70	4.87	0.00	10.00	S.A-S.R	D.YELLORANGE	291192
OP544	Hand	-2.00	1.83	1.75	0.44	-1.66	20.63	12.30	10.00	A-S.A	GRY.YELLOW	291193
OP545	Hand	P.BARRIER	1.93	1.75	0.37	0.33	2.81	0.00	5.00	S.A-S.R	P.YELLOW	291194
OP546	Hand	H.BARRIER	1.95	2.00	0.38	0.54	3.05	0.00	5.00	A-S.R	P.YELLOW	291195
ON547	Hand	H.BARRIER	0.91	0.75	0.40	0.71	3.04	0.00	15.00	S.A-R	D.YELLORANGE	291196
WH548	Hand	H.BARRIER	1.98	1.75	0.42	0.54	2.80	0.00	30.00	S.A-S.R	D.YELLORANGE	291197
WB550	Hand	-2.00	0.81	0.75	0.55	0.23	3.13	27.27	5.00	S.A-R	P.YELLOW	291198
WB551	Hand	RIVER	0.35	0.25	0.93	0.13	2.68	0.00	0.00	S.A-R	GRY.YELLBROWN	291199
WB552	Hand	-2.00	1.04	1.25	0.48	-0.26	4.68	22.88	5.00	S.A-R	L.YELLOW	291200
WB553	Hand	P.BARRIER	1.27	1.50	0.34	0.04	2.72	0.00	20.00	S.A-R	P.YELL.BLACK	291201
WB554	Hand	H.BARRIER	2.04	2.00	0.44	0.37	6.48	0.00	5.00	A-S.R	YELLBROWN	291202
WH555	Hand	P.BARRIER	1.96	2.00	0.53	-1.11	10.90	0.00				291203
OP556	Hand	-2.00	1.28	1.25	0.44	0.65	3.22	19.62	10.00	A-S.R	D.YELLORANGE	291204
MB557	Hand	RIVER	1.65		0.54	-0.05	3.51					
W1558	Hand	H.BARRIER	1.57		0.29	0.97	4.82					
W1559	Hand	P.BARRIER										
ON560	Hand	RIVER										
HW562	Hand	RIVER										
WB562	Diver	20.00	1.87		0.32	0.02	6.49					
WB563	Diver	20.00	2.38		0.49	0.74	2.53					

Appendix 3B

Mean Grain Size Maps

WAIHI BEACH

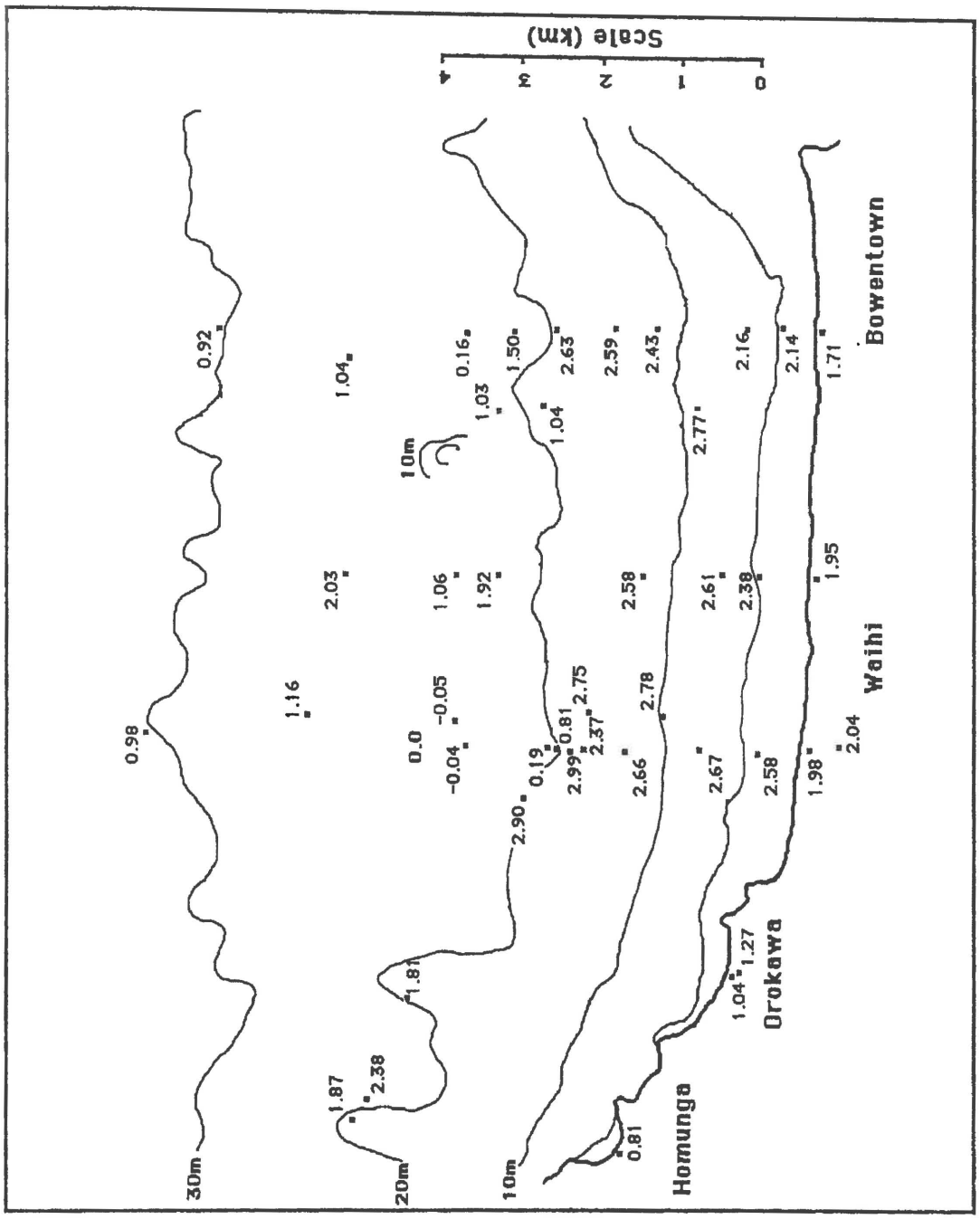
Scale (km)
0
1
2
3
4
30m
20m
10m
10m
Homunga
Orokawa
Waihi
Bowentown
0.98
0.92
1.16
2.03
1.04
0.16
1.03
1.50
2.63
1.06
1.92
0.0
-0.04
-0.05
0.19
0.81
2.75
2.37
2.99
2.90
1.81
1.87
2.38
2.66
2.78
2.58
2.59
2.43
1.04
2.77
2.61
2.67
2.38
2.16
1.04
1.27
2.58
2.14
1.98
1.95
1.71
2.04
0.81

WHIRITOA

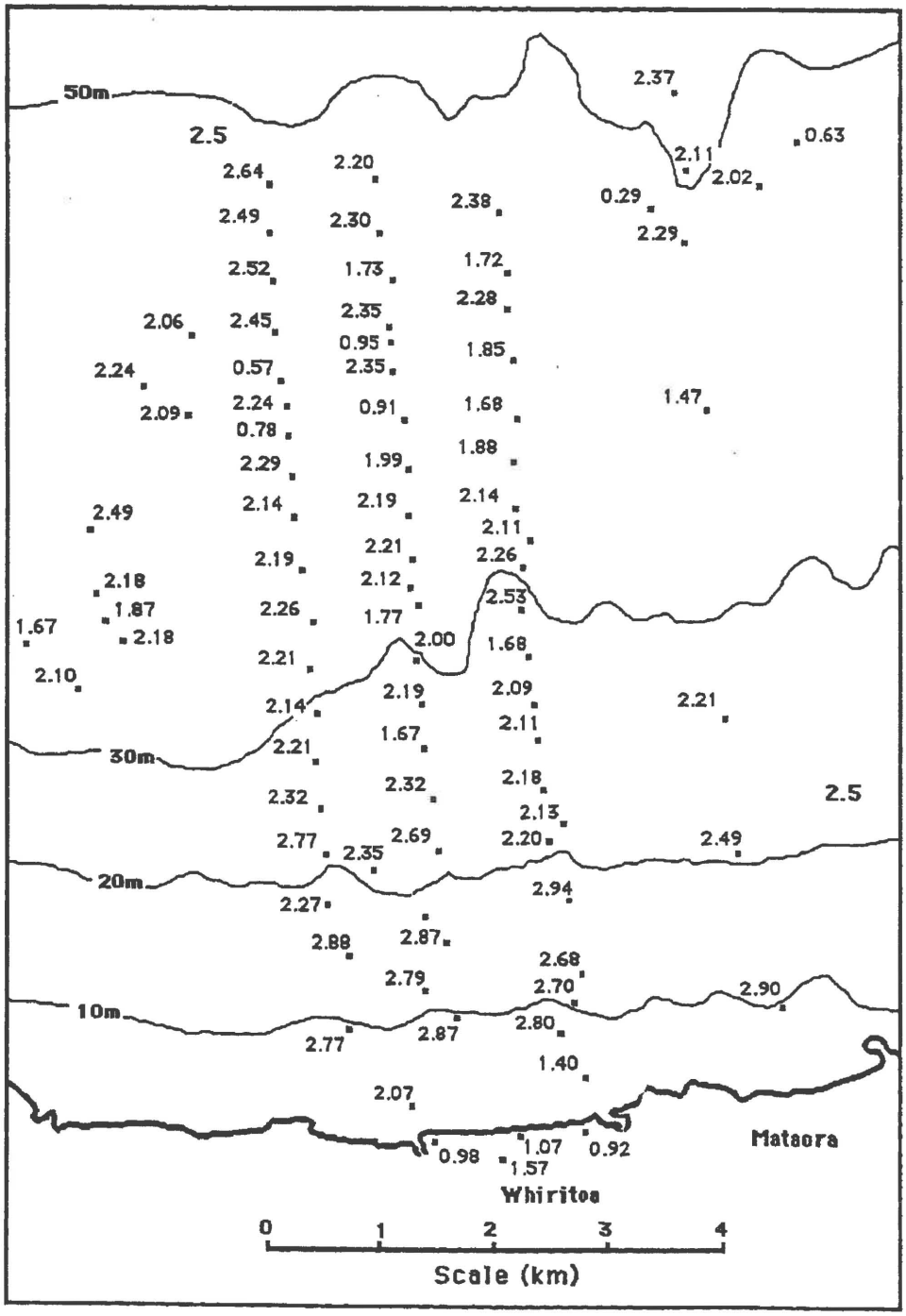
50m
30m
20m
10m
2.5
2.37
0.63
2.11
2.02
0.29
2.29
2.64
2.20
2.38
2.49
2.30
2.52
1.73
1.72
2.28
2.06
2.45
2.35
0.95
1.85
2.24
0.57
2.35
2.09
2.24
0.91
1.68
1.47
0.78
2.29
1.99
1.88
2.49
2.14
2.19
2.14
2.11
2.19
2.21
2.26
2.18
2.12
2.53
1.87
2.26
1.77
1.67
2.18
2.00
1.68
2.21
2.10
2.19
2.09
2.21
2.14
2.11
1.67
2.21
2.32
2.32
2.18
2.5
2.13
2.77
2.35
2.69
2.20
2.49
2.94
2.27
2.88
2.87
2.68
2.79
2.70
2.90
2.77
2.87
2.80
1.40
2.07
0.98
1.07
0.92
1.57
Mataora
Whiritoa
0
1
2
3
4
Scale (km)

WHANGAMATA

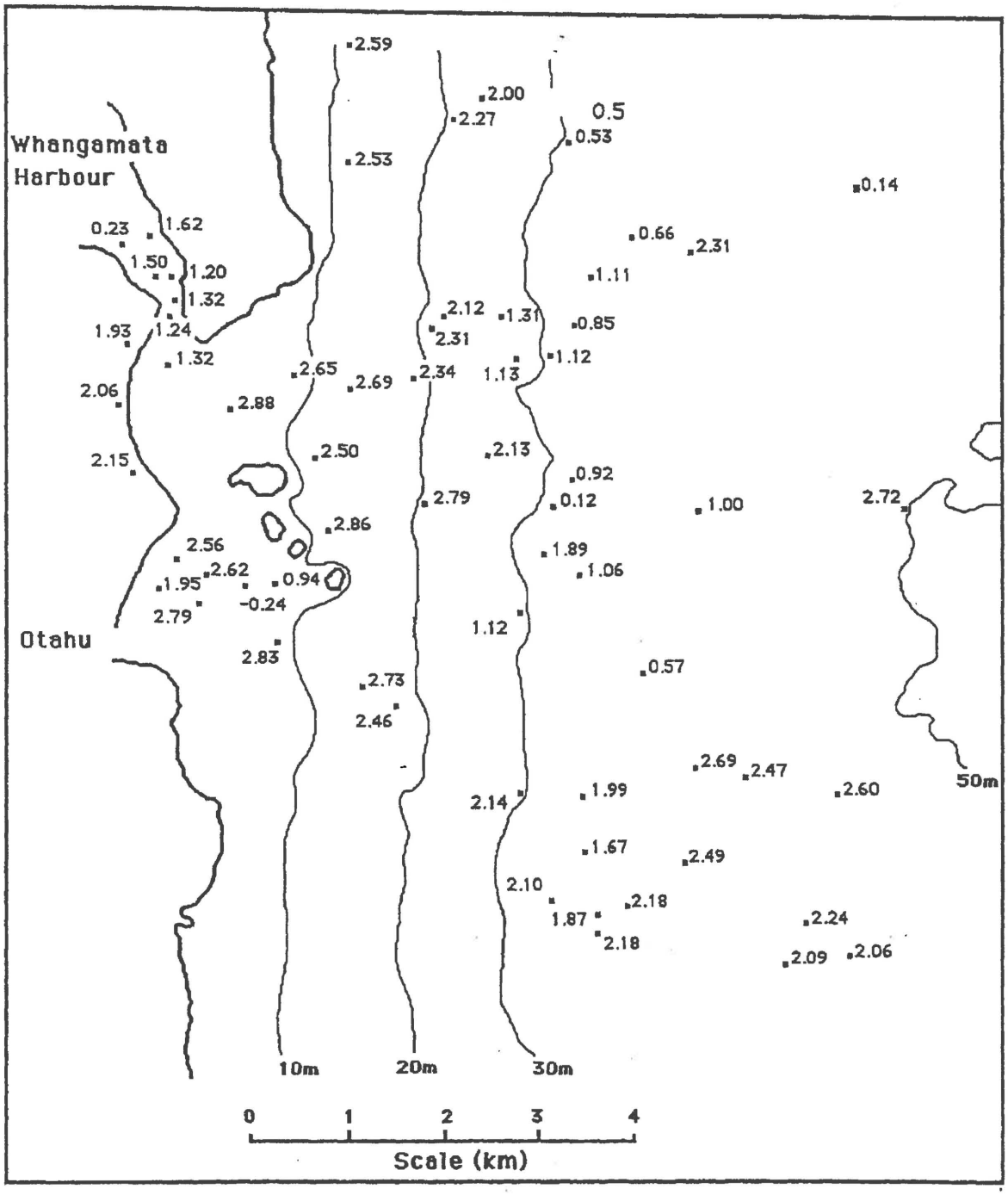
Whangamata
Harbour
Otahu
0.5
50m
10m
20m
30m
0
1
2
3
4
Scale (km)
2.59
2.00
2.27
0.53
2.53
0.14
0.23
1.62
0.66
2.31
1.50
1.20
1.11
1.32
2.12
1.31
0.85
1.93
1.24
2.31
1.32
1.12
2.65
2.69
2.34
1.13
2.06
2.88
2.50
2.13
2.15
0.92
2.79
0.12
1.00
2.72
2.86
2.56
1.89
2.62
1.06
1.95
0.94
-0.24
2.79
1.12
2.83
0.57
2.73
2.46
2.69
2.47
2.14
1.99
2.60
1.67
2.49
2.10
2.18
1.87
2.24
2.18
2.09
2.06

ONEMANA

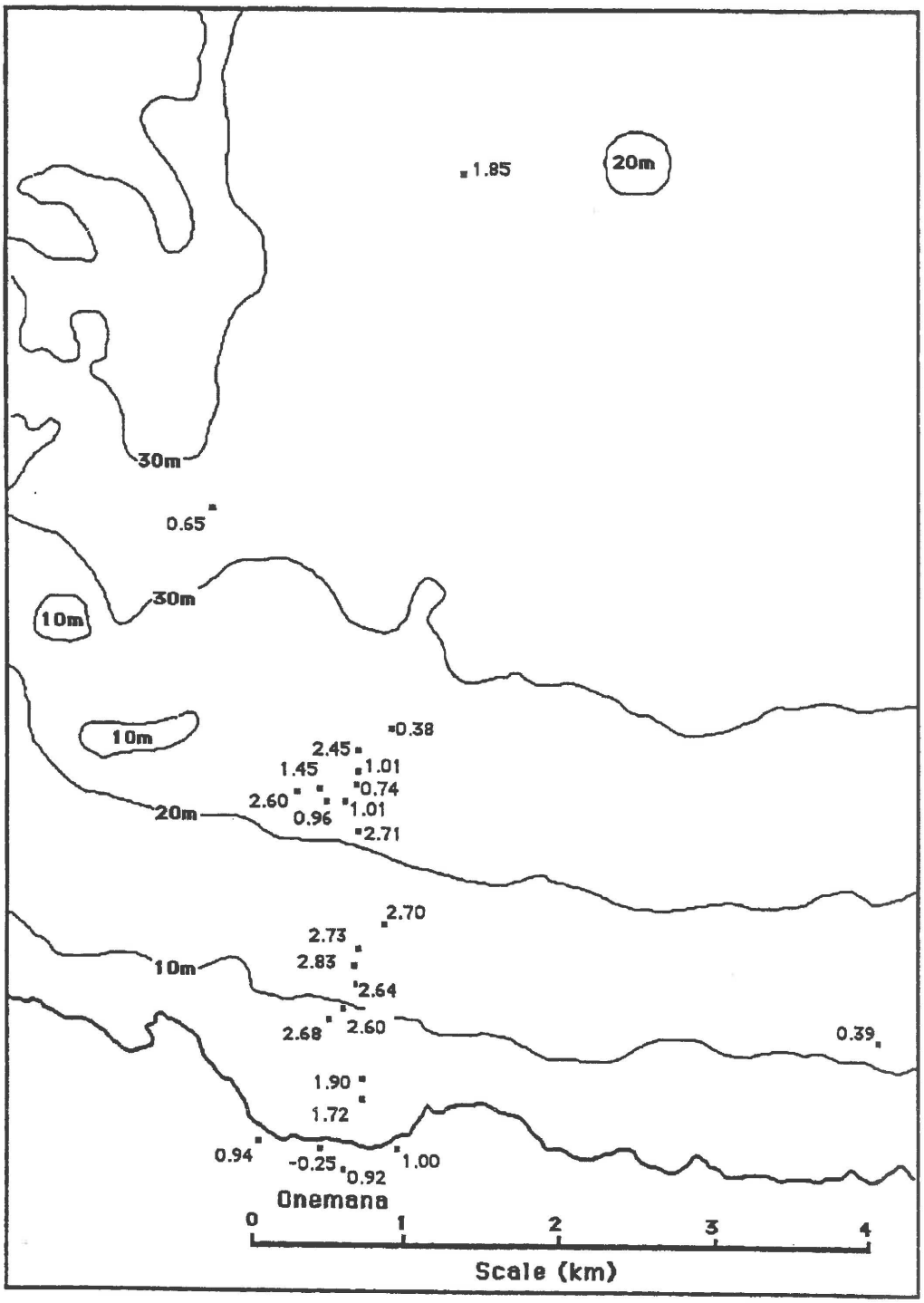
1.85
20m
30m
0.65
30m
10m
10m
0.38
2.45
1.45
1.01
0.74
2.60
1.01
0.96
2.71
20m
2.70
2.73
2.83
10m
2.64
2.68
2.60
0.39
1.90
1.72
0.94
-0.25
0.92
1.00
Onemana
0
1
2
3
4
Scale (km)

A-45

OPOUTERE

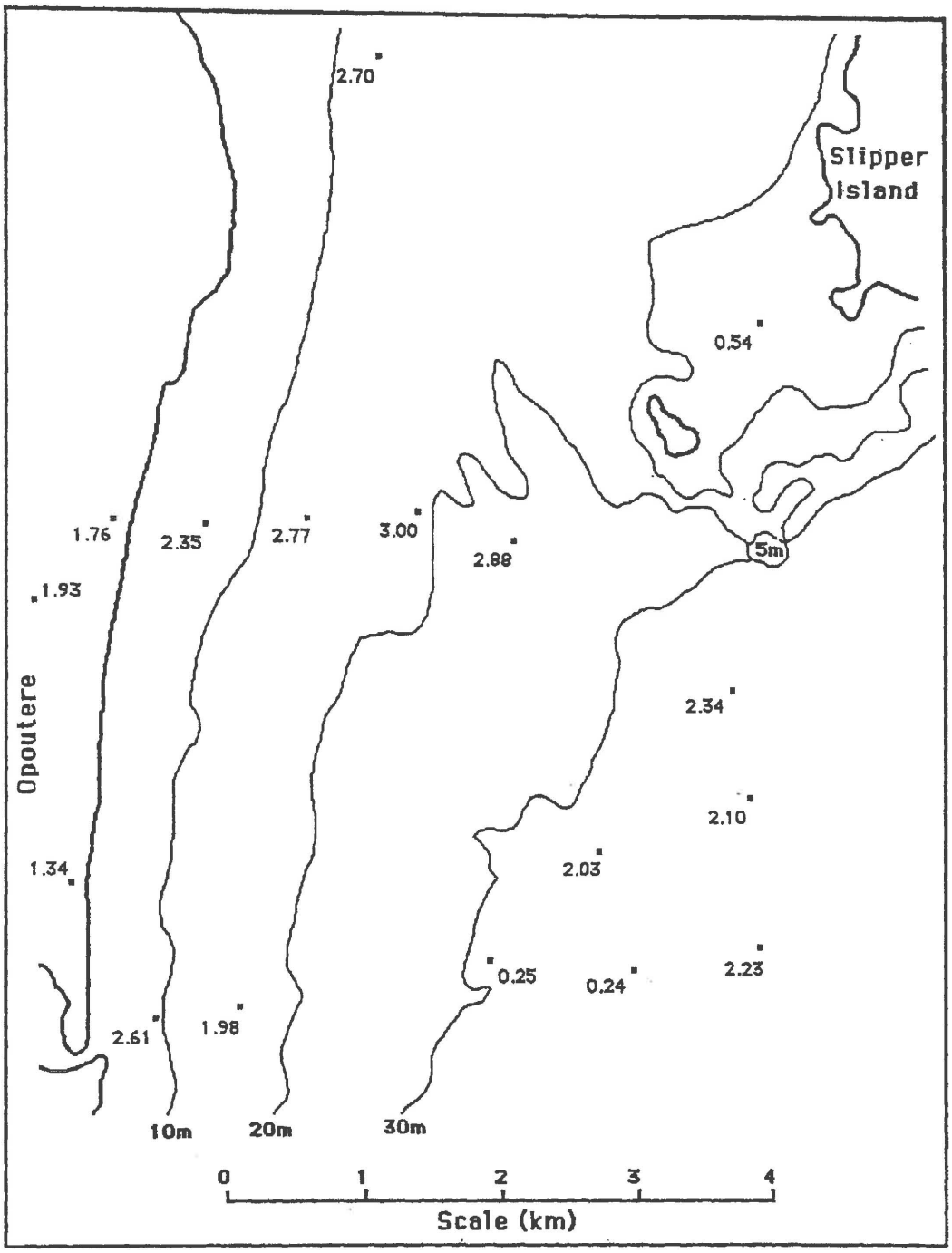

HOTWATER

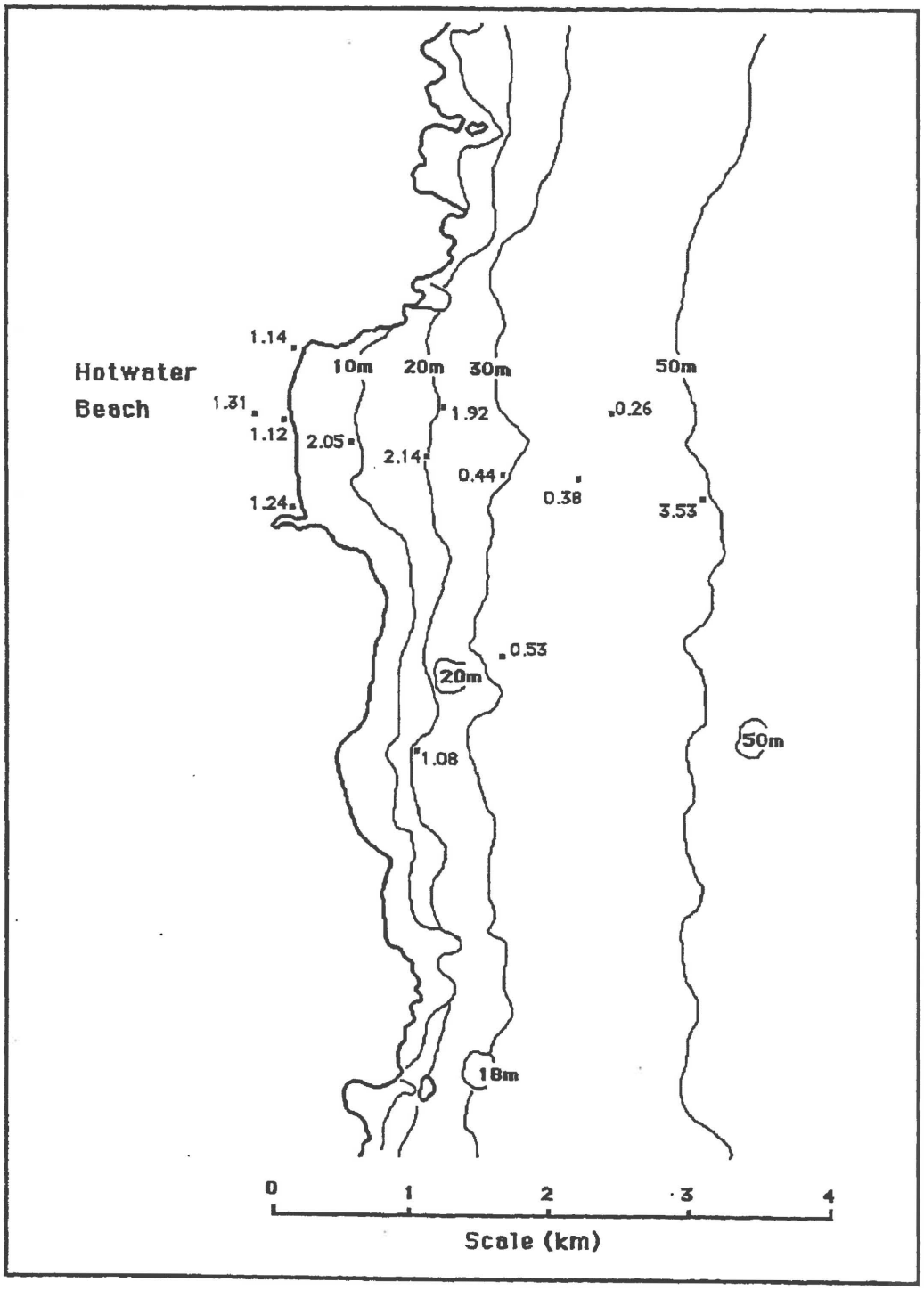
Hotwater
Beach
1.14
1.31
1.12
2.05
1.24
10m
20m
30m
50m
1.92
2.14
0.44
0.38
0.26
3.53
0.53
20m
1.08
50m
18m
0
1
2
3
4
Scale (km)

MERCURY BAY

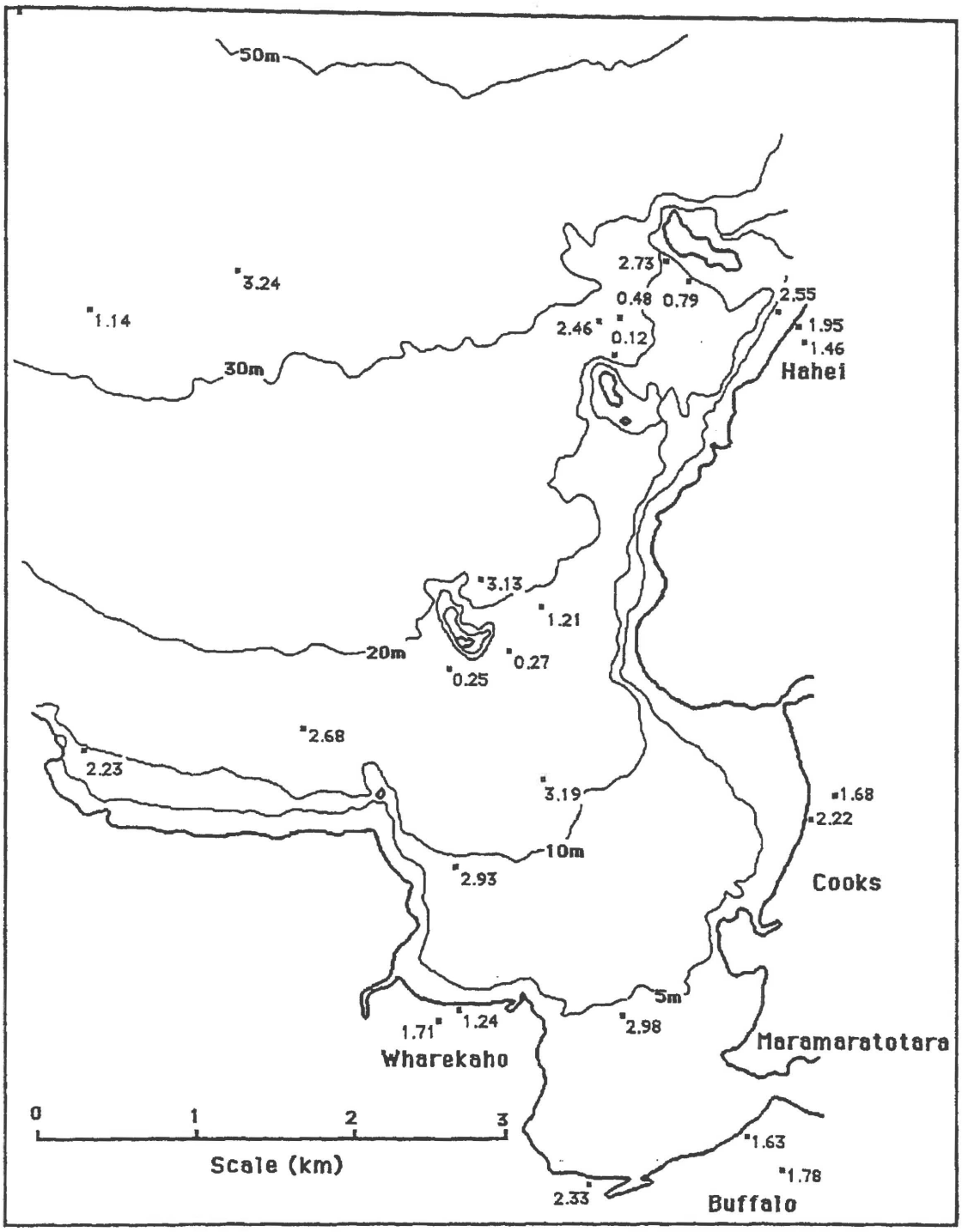
50m
30m
20m
10m
5m
3.24
1.14
2.73
0.48
0.79
2.46
0.12
2.55
1.95
1.46
Hahei
3.13
1.21
0.27
0.25
2.68
2.23
3.19
1.68
2.22
2.93
Cooks
1.71
1.24
2.98
Whareakaho
Maramaratotara
0
1
2
3
Scale (km)
1.63
1.78
2.33
Buffalo

A-48

OTAMA

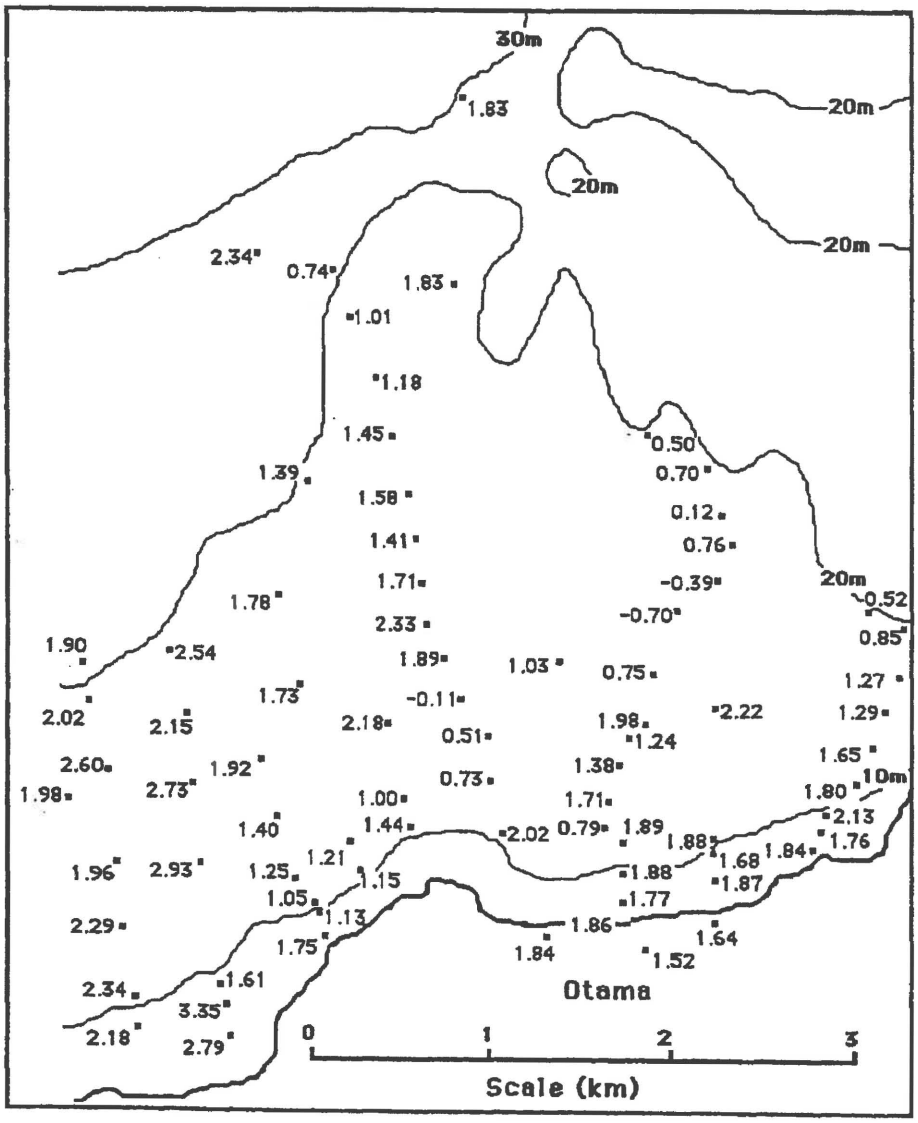
30m
20m
20m
20m
20m
1.83
2.34
0.74
1.83
1.01
1.18
1.45
1.39
1.58
1.41
1.71
1.78
2.33
1.90
2.54
1.89
1.03
0.75
1.73
-0.11
2.02
2.15
2.18
0.51
1.98
1.24
2.22
1.29
2.60
1.92
0.73
1.38
1.65
1.98
2.73
1.00
1.71
1.80
10m
1.40
1.44
2.02
0.79
1.89
1.88
2.13
1.96
2.93
1.25
1.21
1.15
1.68
1.84
1.76
1.88
1.87
1.05
1.13
1.77
2.29
1.86
1.64
1.75
1.84
1.52
2.34
1.61
Otama
3.35
2.18
2.79
0
1
2
3
Scale (km)
0.50
0.70
0.12
0.76
-0.39
-0.70
0.52
0.85
1.27
1.29
1.65

WHANGAPOUA

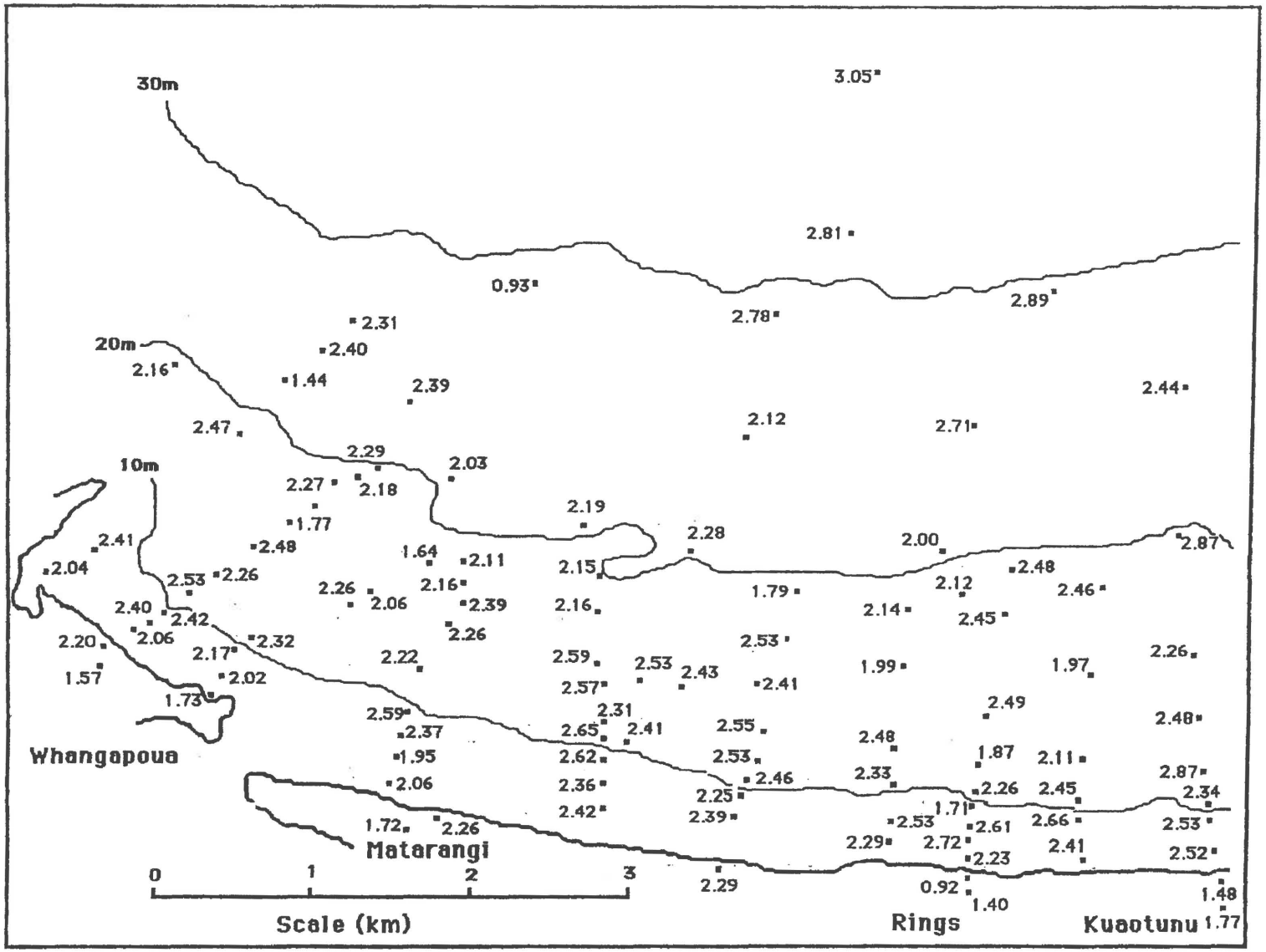
30m
20m
10m
3.05
2.81
0.93
2.78
2.89
2.31
2.40
2.16
1.44
2.39
2.44
2.47
2.12
2.71
2.29
2.03
2.27
2.18
2.19
1.77
2.28
2.00
2.87
2.41
2.48
1.64
2.11
2.15
2.04
2.53
2.26
2.26
2.16
2.12
2.48
2.46
2.06
2.39
2.16
1.79
2.14
2.45
2.40
2.42
2.26
2.20
2.06
2.32
2.53
2.17
2.22
2.59
2.53
2.43
1.99
1.97
2.26
1.57
2.02
2.57
2.41
1.73
2.49
2.59
2.31
2.48
2.37
2.65
2.41
2.55
2.48
Whangapoua
1.95
2.62
2.53
1.87
2.11
2.87
2.06
2.36
2.46
2.33
2.26
2.45
2.34
2.25
1.71
2.42
2.39
2.53
2.61
2.66
2.53
1.72
2.26
2.29
2.72
2.41
2.52
Matarangi
2.23
0
1
2
3
2.29
0.92
1.48
1.40
Scale (km)
Rings
Kuaotunu
1.77

Appendix 3C

Sediment Sorting Size Maps

A-51

WAIHI BEACH

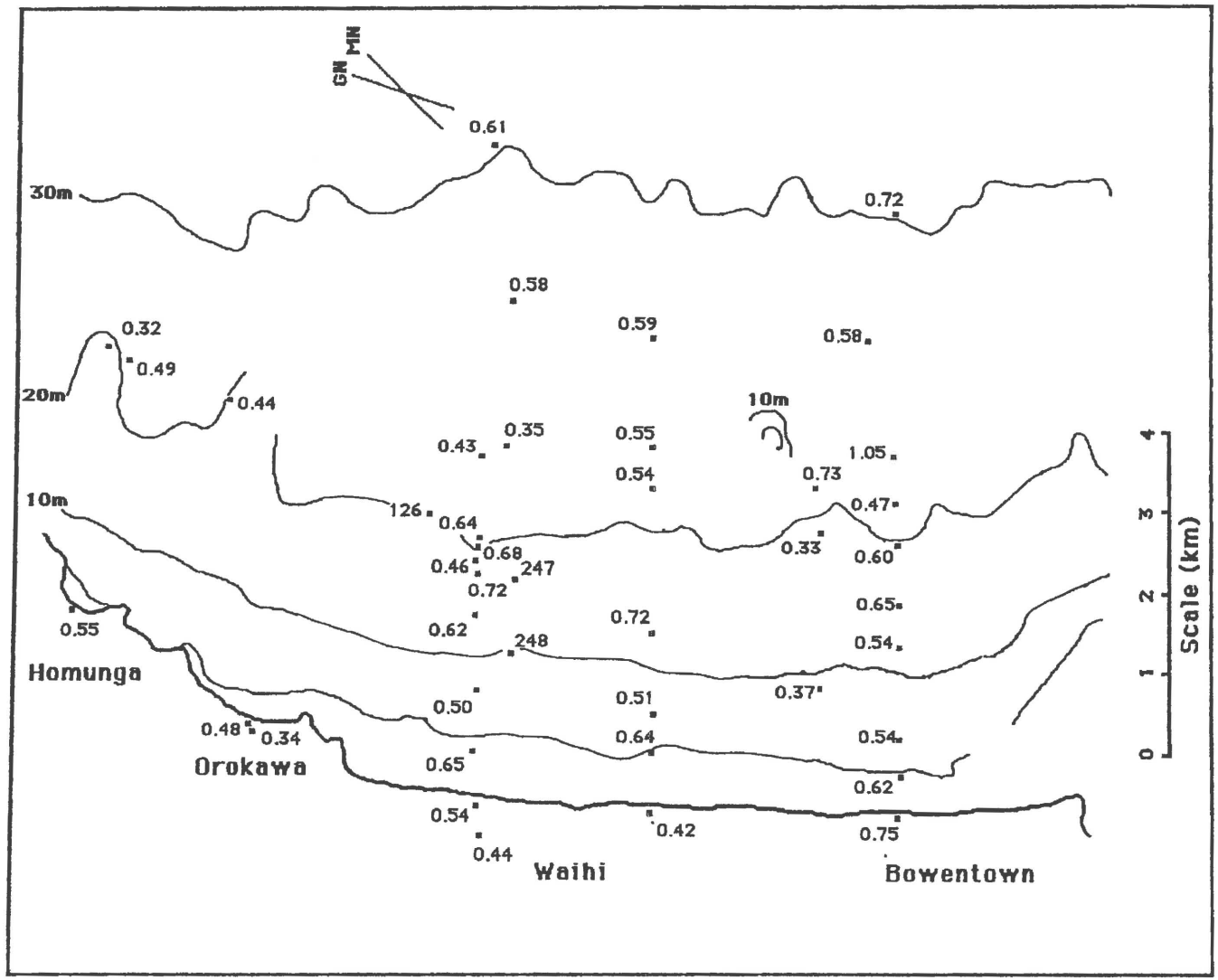

WHIRITOA

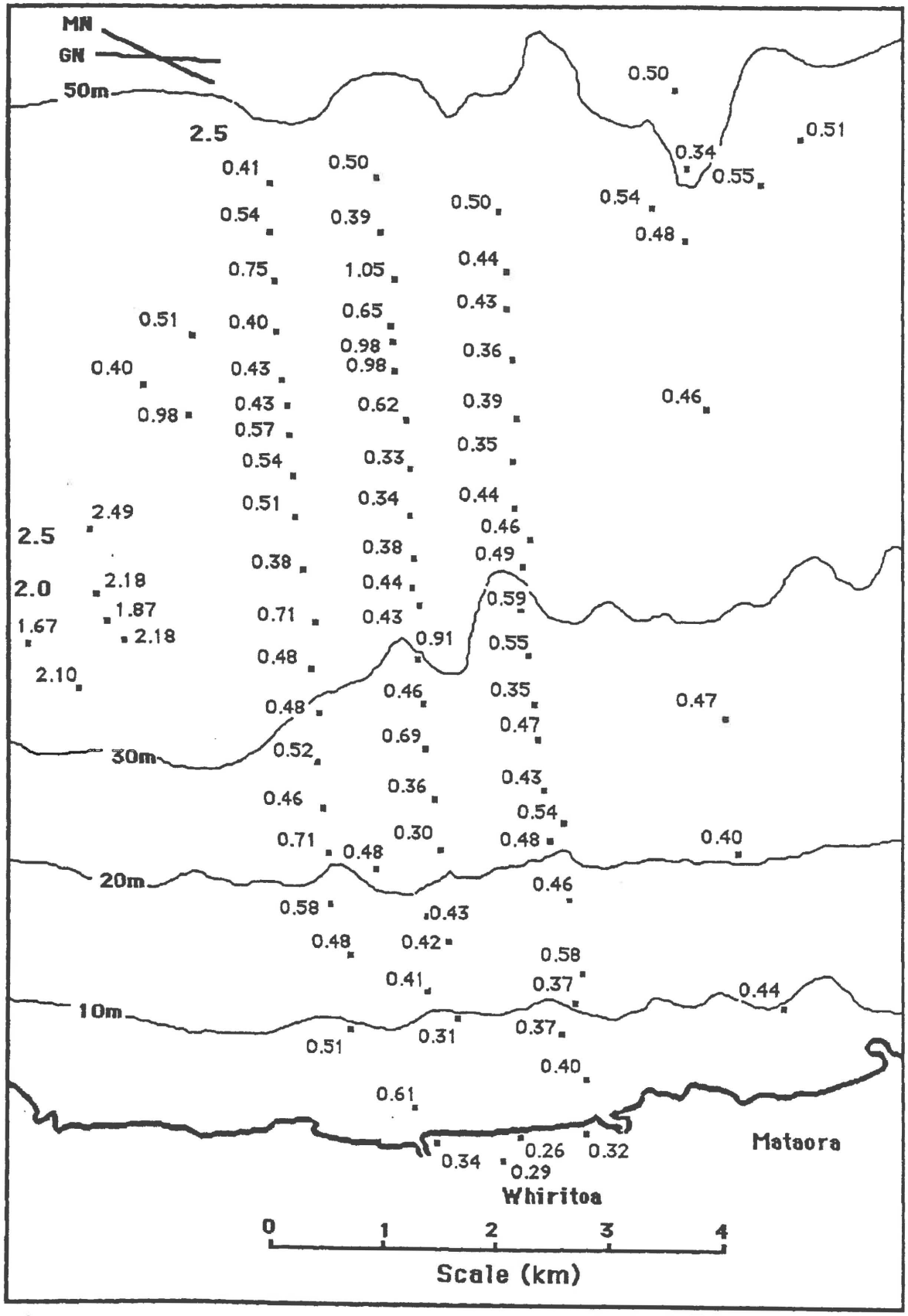
MN
GN
50m
2.5
0.41
0.50
0.54
0.39
0.50
0.54
0.48
0.50
0.34
0.55
0.51
0.75
1.05
0.44
0.51
0.40
0.65
0.43
0.98
0.36
0.40
0.43
0.98
0.98
0.43
0.62
0.39
0.46
0.57
0.54
0.33
0.35
0.51
0.34
0.44
2.49
0.46
2.5
0.38
0.38
0.49
2.0
2.18
0.44
0.59
1.87
0.71
0.43
1.67
2.18
0.91
0.55
0.48
2.10
0.46
0.35
0.47
0.48
0.47
30m
0.69
0.52
0.43
0.36
0.46
0.54
0.71
0.30
0.48
0.40
0.48
20m
0.46
0.58
0.43
0.48
0.42
0.58
0.41
0.37
0.44
10m
0.51
0.31
0.37
0.40
0.61
Mataora
0.34
0.26
0.32
0.29
Whiritoa
0
1
2
3
4
Scale (km)

WHANGAMATA

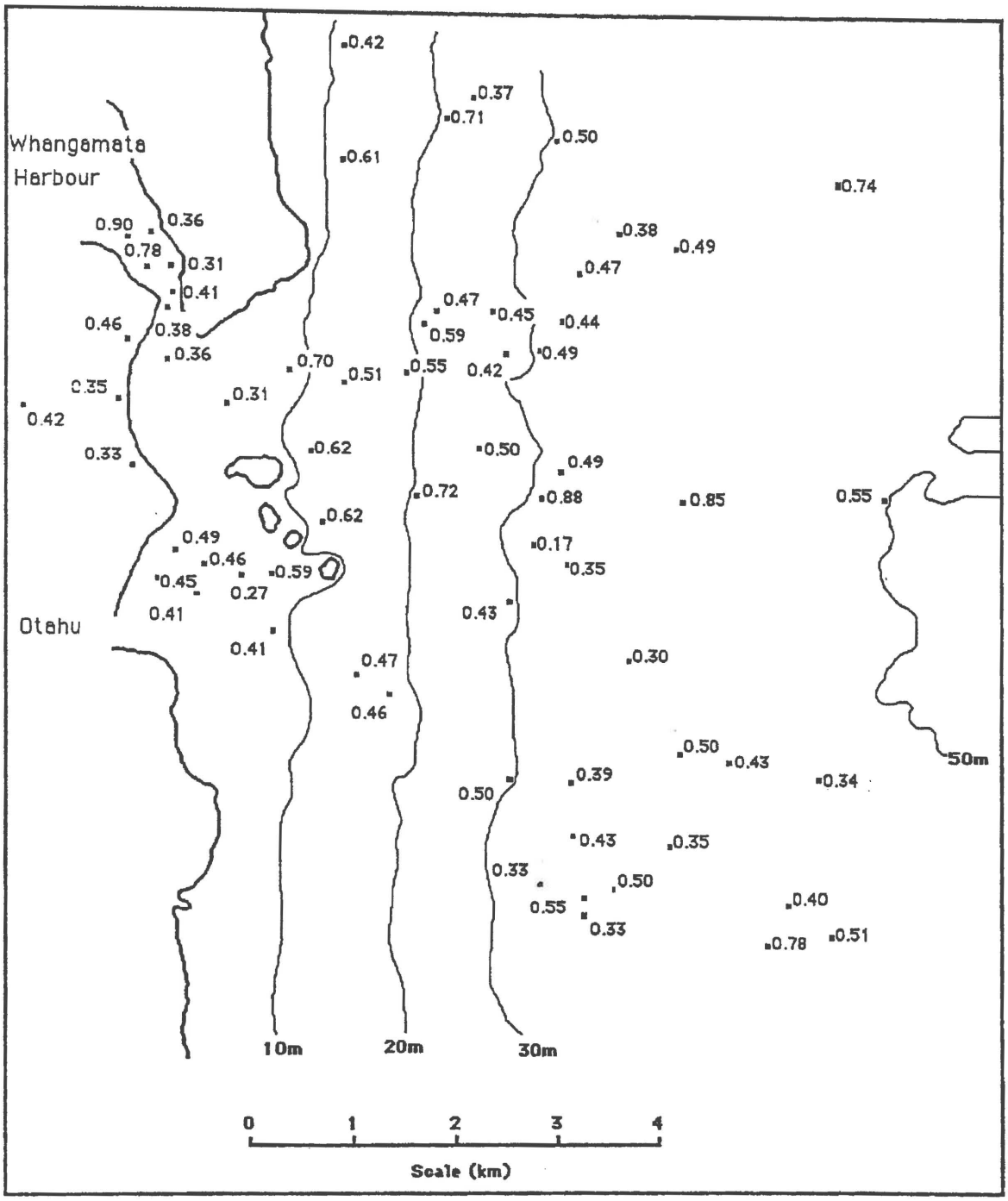
Whangamata
Harbour
Otahu
0.42
0.37
0.71
0.50
0.61
0.74
0.90
0.36
0.78
0.31
0.41
0.38
0.49
0.47
0.46
0.38
0.47
0.45
0.44
0.59
0.36
0.49
0.70
0.51
0.55
0.42
0.35
0.31
0.42
0.33
0.62
0.50
0.49
0.72
0.88
0.85
0.55
0.62
0.49
0.46
0.17
0.59
0.35
0.45
0.27
0.43
0.41
0.41
0.30
0.47
0.46
0.50
0.43
50m
0.39
0.34
0.50
0.43
0.35
0.33
0.50
0.40
0.55
0.33
0.78
0.51
10m
20m
30m
0
1
2
3
4
Scale (km)

ONEMANA

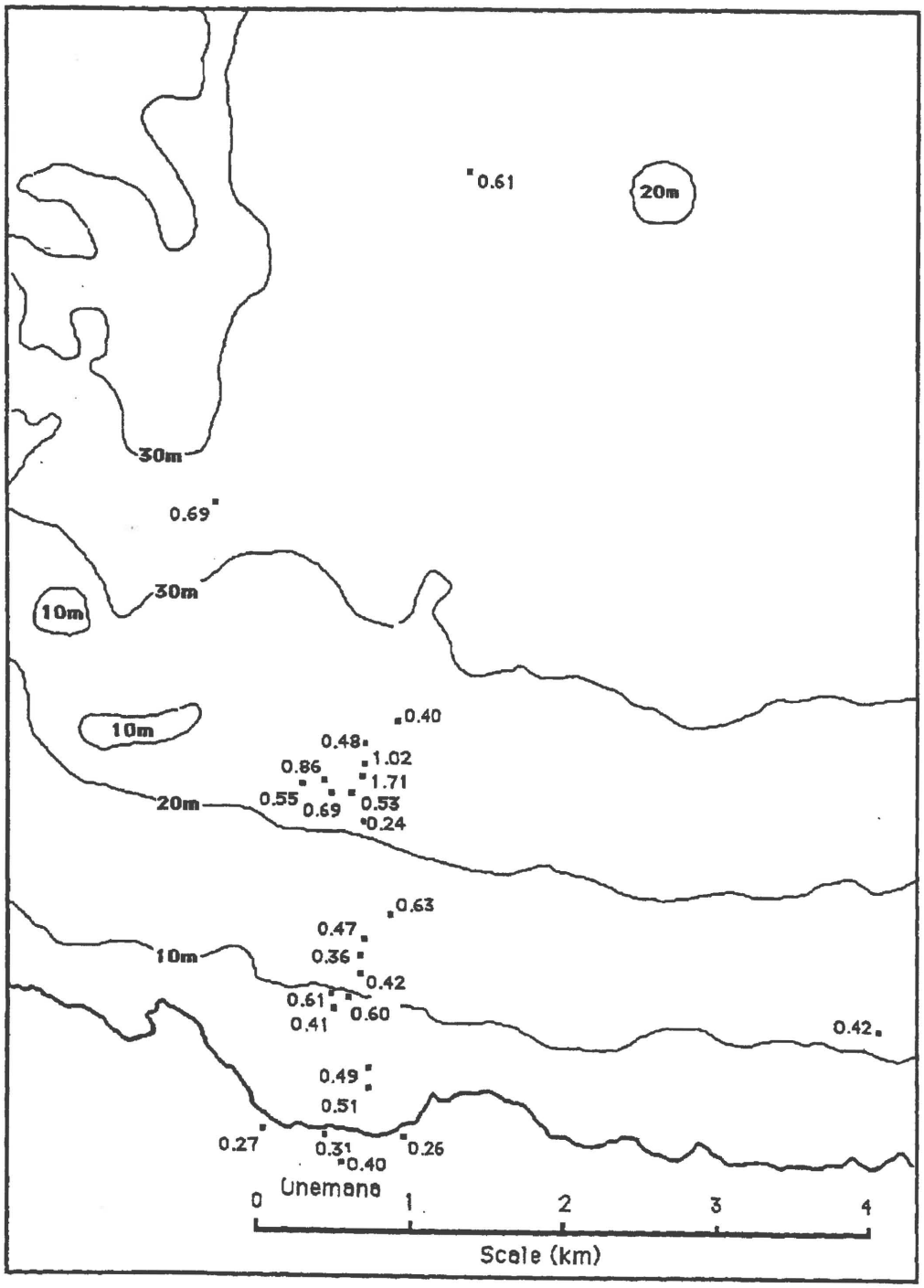
0.61
20m
30m
0.69
30m
10m
10m
0.40
0.48
0.86
1.02
1.71
0.55
0.69
0.53
0.24
20m
0.63
0.47
10m
0.36
0.42
0.61
0.60
0.41
0.42
0.49
0.51
0.27
0.31
0.40
0.26
Onemana
0
1
2
3
4
Scale (km)

A-55

OPOUTERE

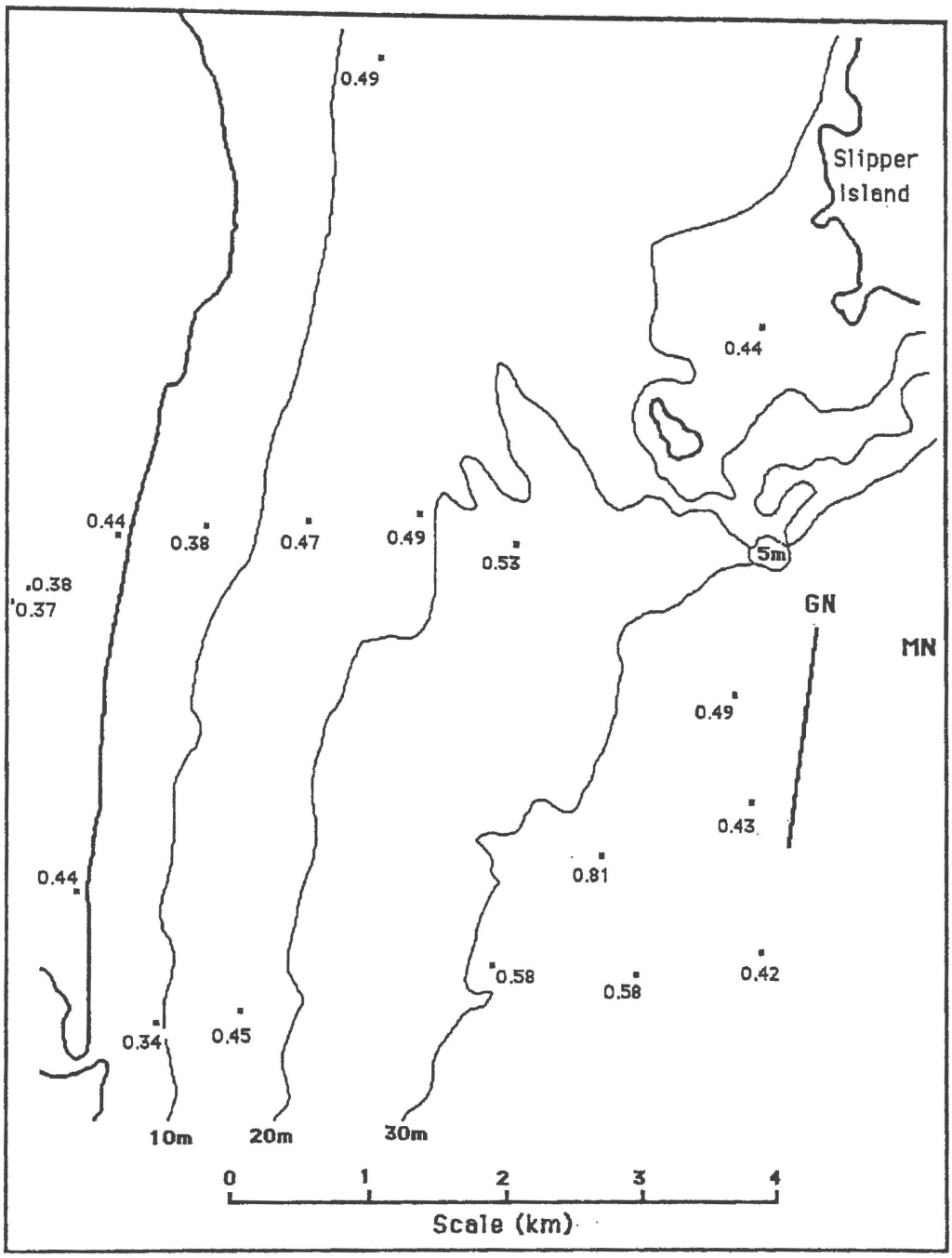

HOTWATER

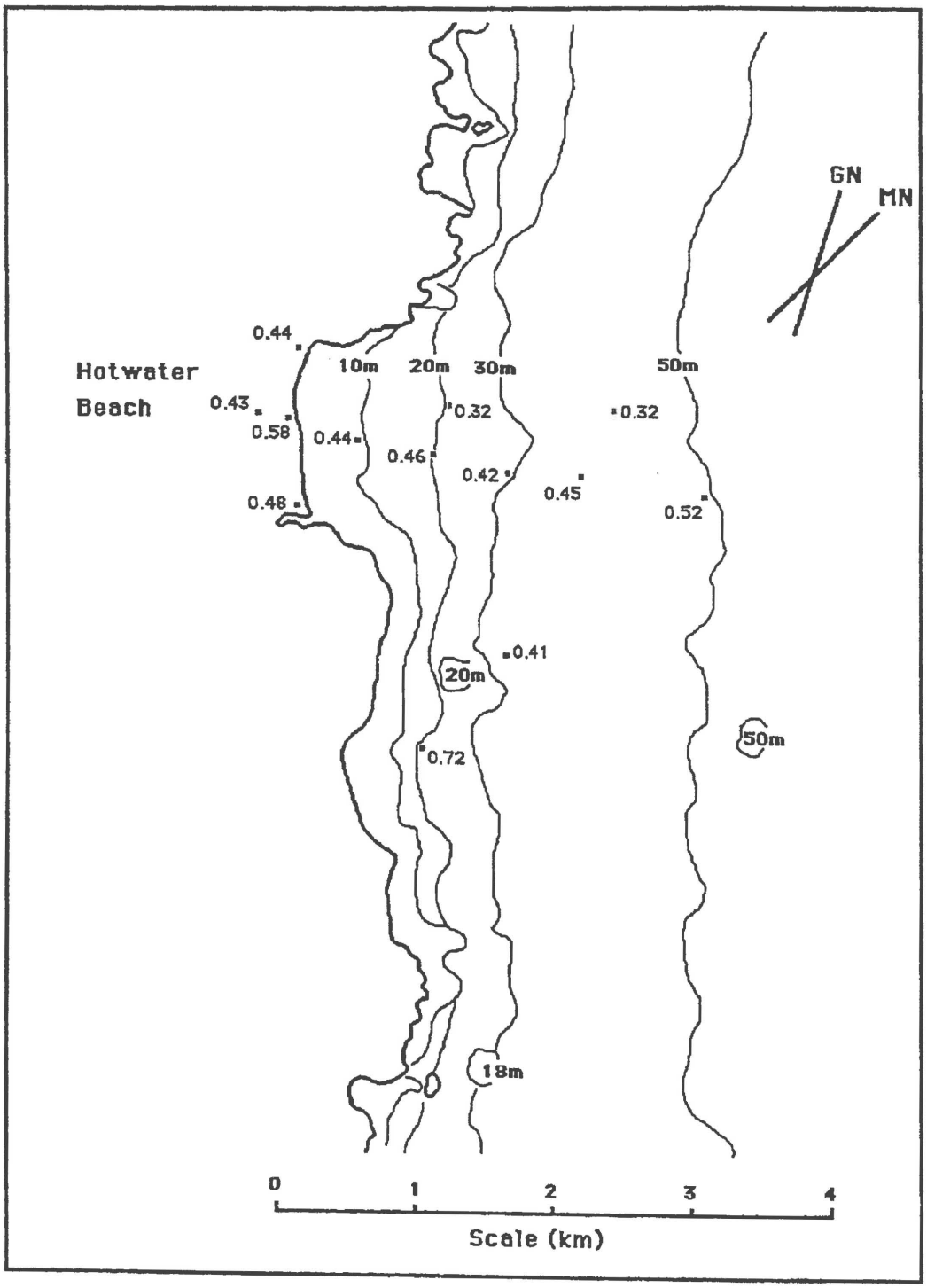
GN
MN
Hotwater
Beach
0.44
0.43
0.58
0.44
0.48
10m
20m
30m
0.32
0.46
0.42
0.45
0.41
20m
0.72
18m
50m
0.32
0.52
50m
0
1
2
3
4
Scale (km)

MERCURY BAY

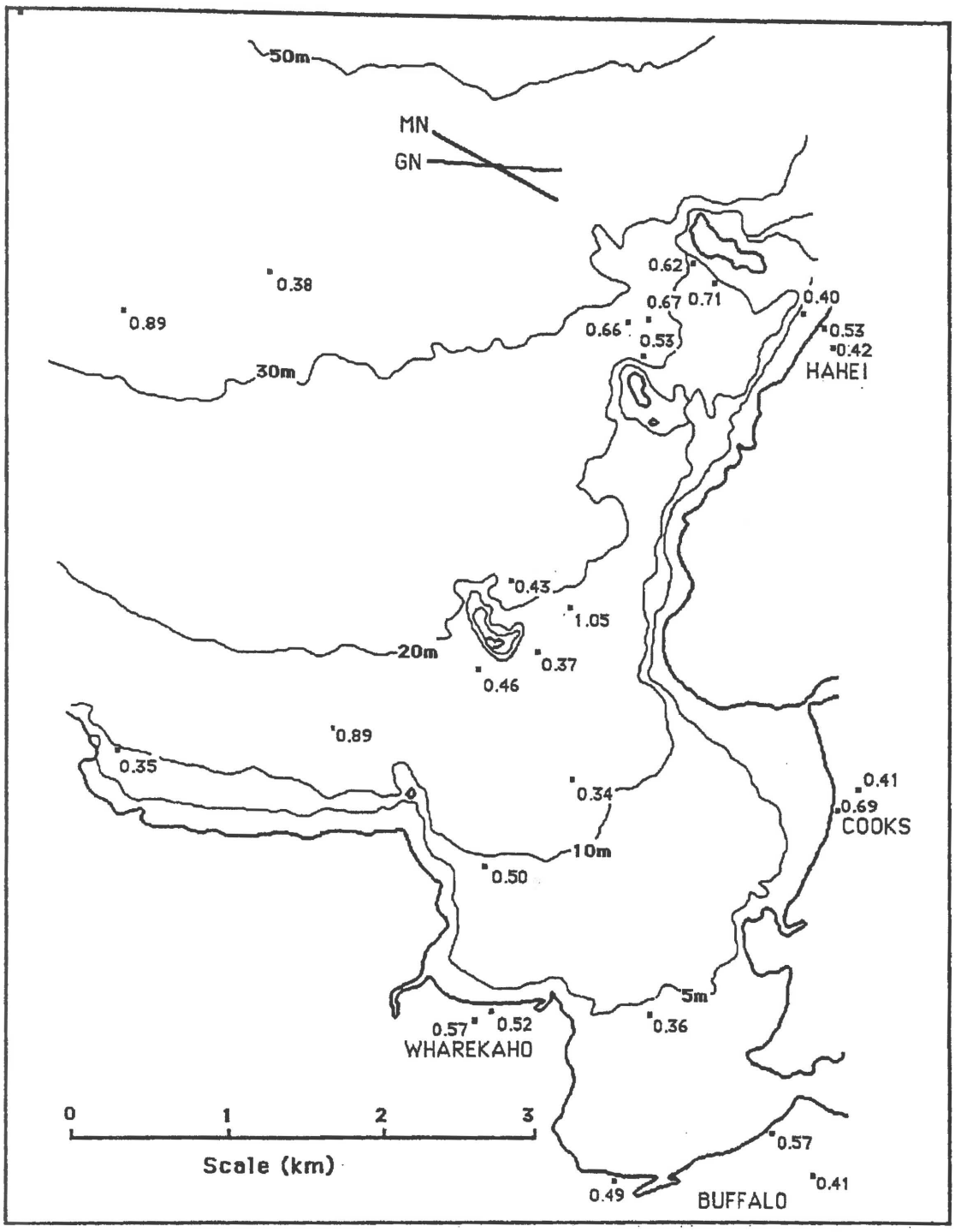
50m
MN
GN
0.38
0.89
30m
0.62
0.67
0.71
0.66
0.53
0.40
0.53
0.42
HAHEI
0.43
1.05
20m
0.37
0.46
0.89
0.35
0.34
0.41
0.69
COOKS
10m
0.50
5m
0.57
0.52
WHAREKAHO
0.36
0
1
2
3
Scale (km)
0.57
0.41
0.49
BUFFALO

OTAMA

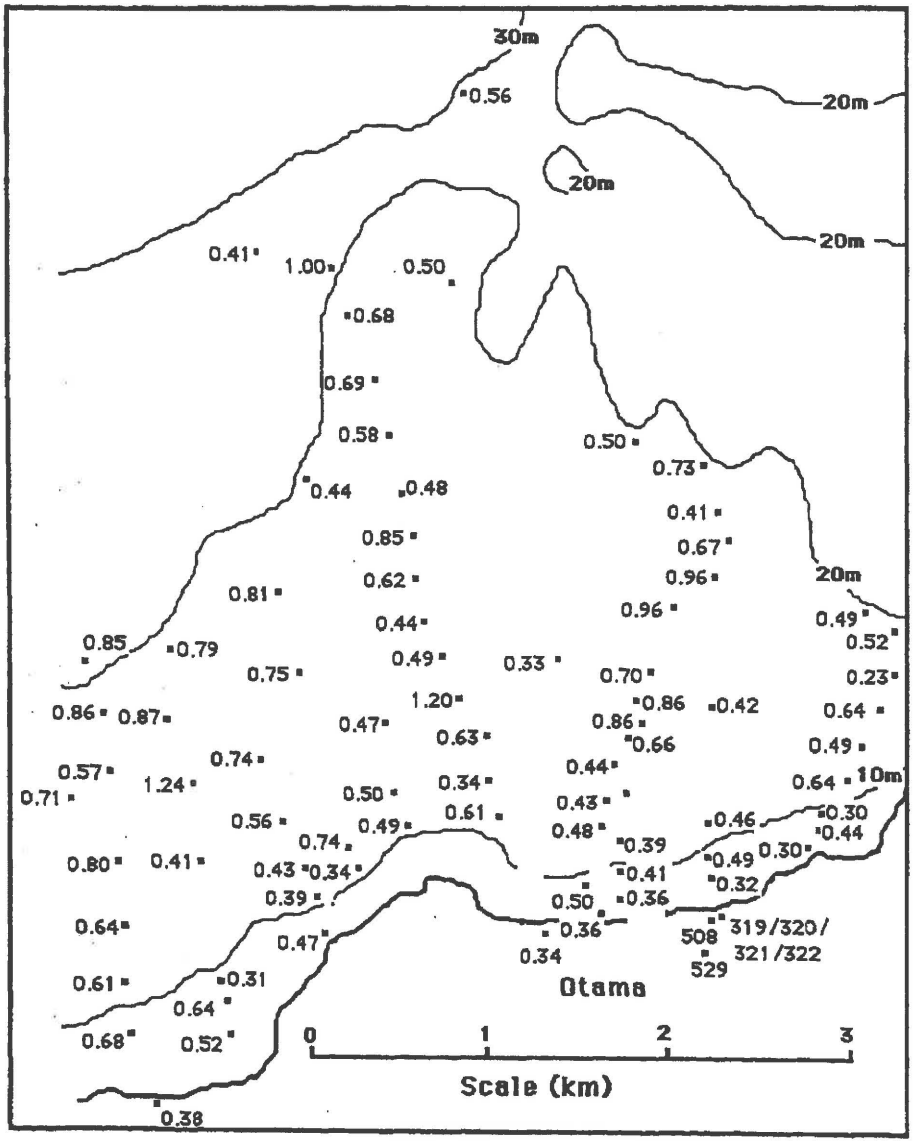
30m
20m
20m
20m
20m
10m
0.56
0.41
1.00
0.50
0.68
0.69
0.58
0.50
0.73
0.44
0.48
0.41
0.85
0.67
0.62
0.96
0.81
0.96
0.44
0.49
0.85
0.79
0.52
0.49
0.33
0.75
0.70
0.23
1.20
0.86
0.42
0.86
0.87
0.64
0.47
0.86
0.63
0.66
0.74
0.49
0.57
0.44
0.64
1.24
0.34
0.71
0.50
0.43
0.56
0.61
0.46
0.30
0.74
0.49
0.48
0.44
0.80
0.41
0.43
0.34
0.39
0.41
0.49
0.30
0.39
0.32
0.50
0.36
0.64
0.36
508
319/320/
0.47
0.34
321/322
529
0.61
0.31
Otama
0.64
0.68
0.52
0
1
2
3
Scale (km)
0.38

WHANGAPOUA

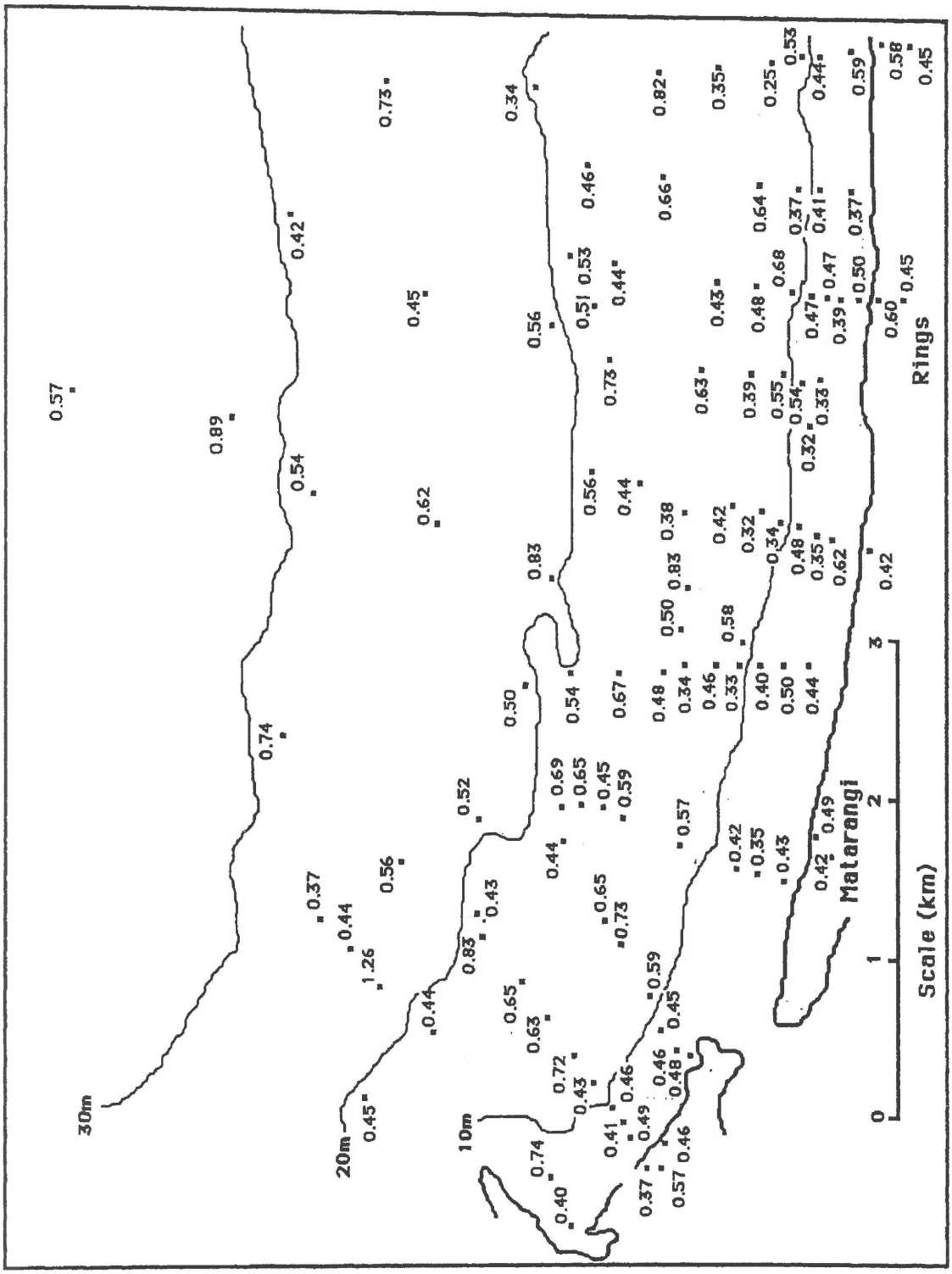

Appendix 3D

Sediment Skewness Maps

A-61

WAIHI BEACH

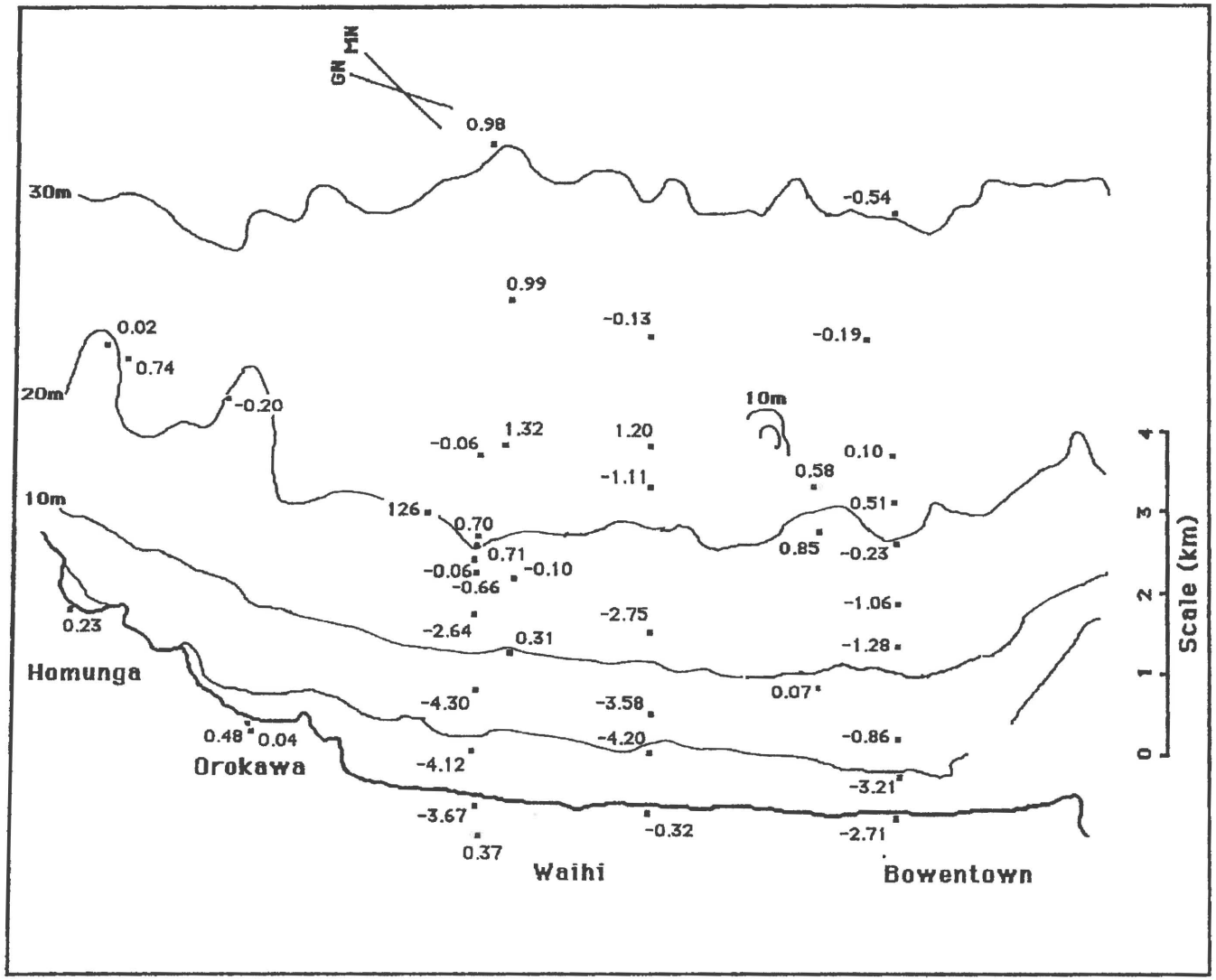

WHIRITOA

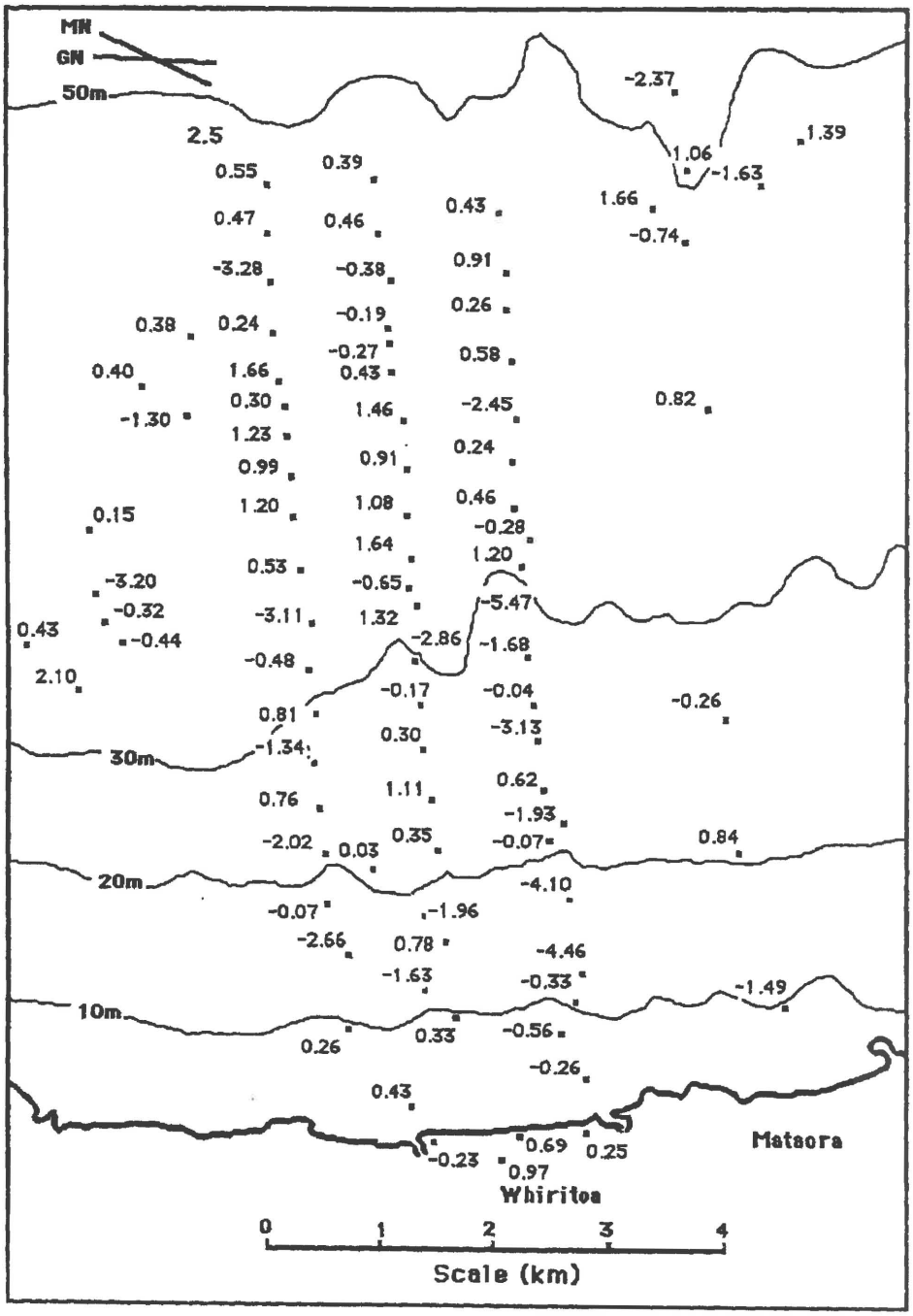
MN
GN
50m
30m
20m
10m
2.5
0.55
0.39
0.47
0.46
0.43
-3.28
-0.38
0.91
0.38
0.24
-0.19
0.26
-0.27
0.58
0.40
1.66
0.43
0.30
1.46
-2.45
-1.30
1.23
0.99
0.91
0.24
0.15
1.20
1.08
0.46
-0.28
1.64
1.20
0.53
-0.65
-3.20
-5.47
-0.32
-3.11
1.32
0.43
-2.86
-1.68
-0.44
-0.48
2.10
-0.17
-0.04
0.81
-3.13
0.30
-1.34
0.62
0.76
1.11
-1.93
-2.02
0.03
0.35
-0.07
-4.10
-0.07
-1.96
-2.66
0.78
-4.46
-1.63
-0.33
-0.56
0.26
0.33
-0.26
0.43
0.69
0.25
-0.23
0.97
-2.37
1.06
-1.63
1.39
1.66
-0.74
0.82
-0.26
0.84
-1.49
Matacra
Whiritoa
0
1
2
3
4
Scale (km)

WHANGAMATA

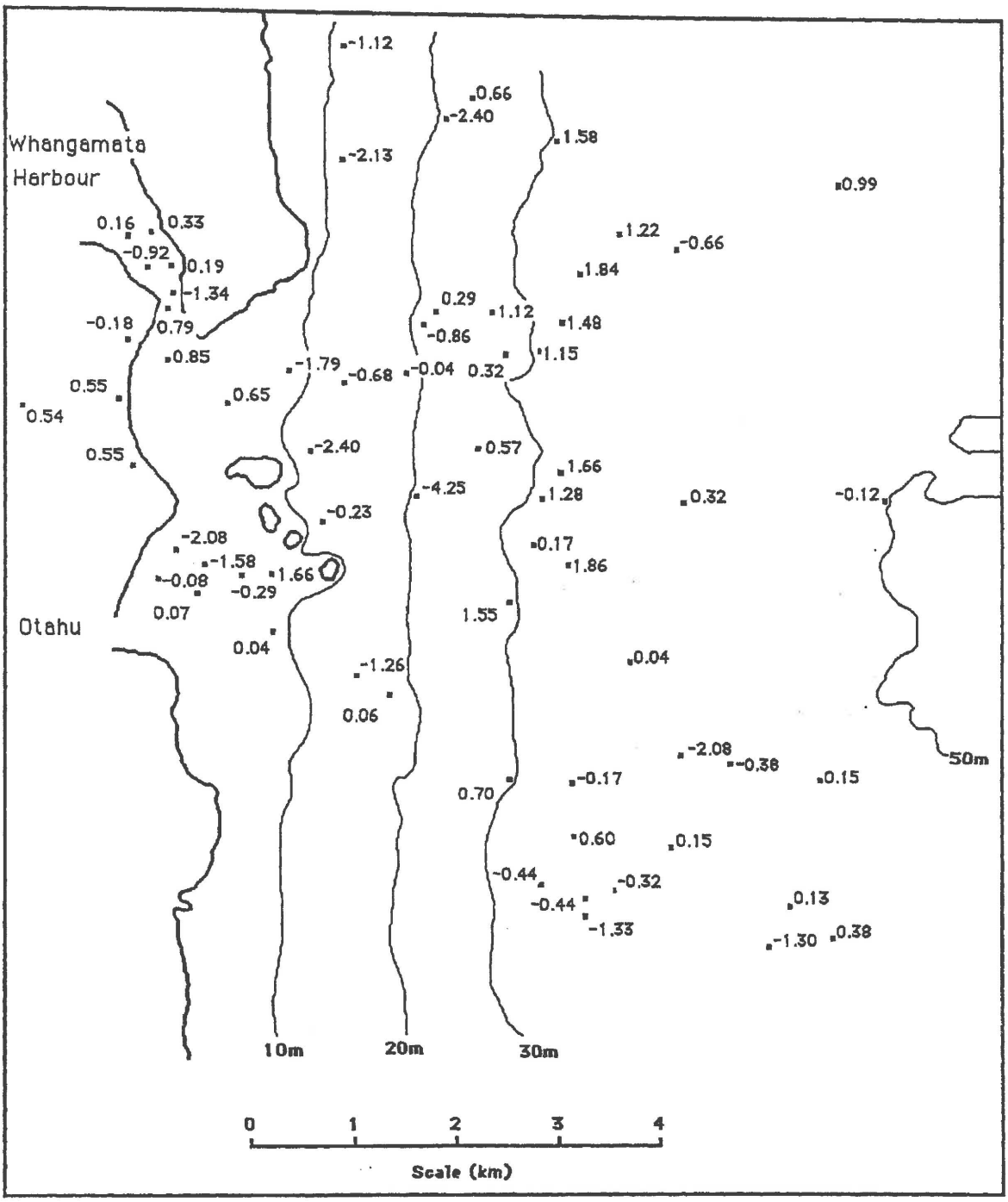
Whangamata
Harbour
Otahu
-1.12
0.66
-2.40
1.58
-2.13
0.99
1.22
-0.66
1.84
0.16
0.33
-0.92
0.19
-1.34
0.29
1.12
1.48
-0.18
0.79
-0.86
1.15
0.85
-1.79
-0.68
-0.04
0.32
0.55
0.65
0.54
0.55
-2.40
0.57
1.66
-4.25
1.28
0.32
-0.12
-0.23
-2.08
0.17
-1.58
1.66
1.86
-0.08
-0.29
0.07
1.55
0.04
0.04
-1.26
0.06
-2.08
-0.38
50m
0.15
-0.17
0.70
0.60
0.15
-0.44
-0.32
0.13
-0.44
-1.33
-1.30
0.38
10m
20m
30m
0
1
2
3
4
Scale (km)

ONEMANA

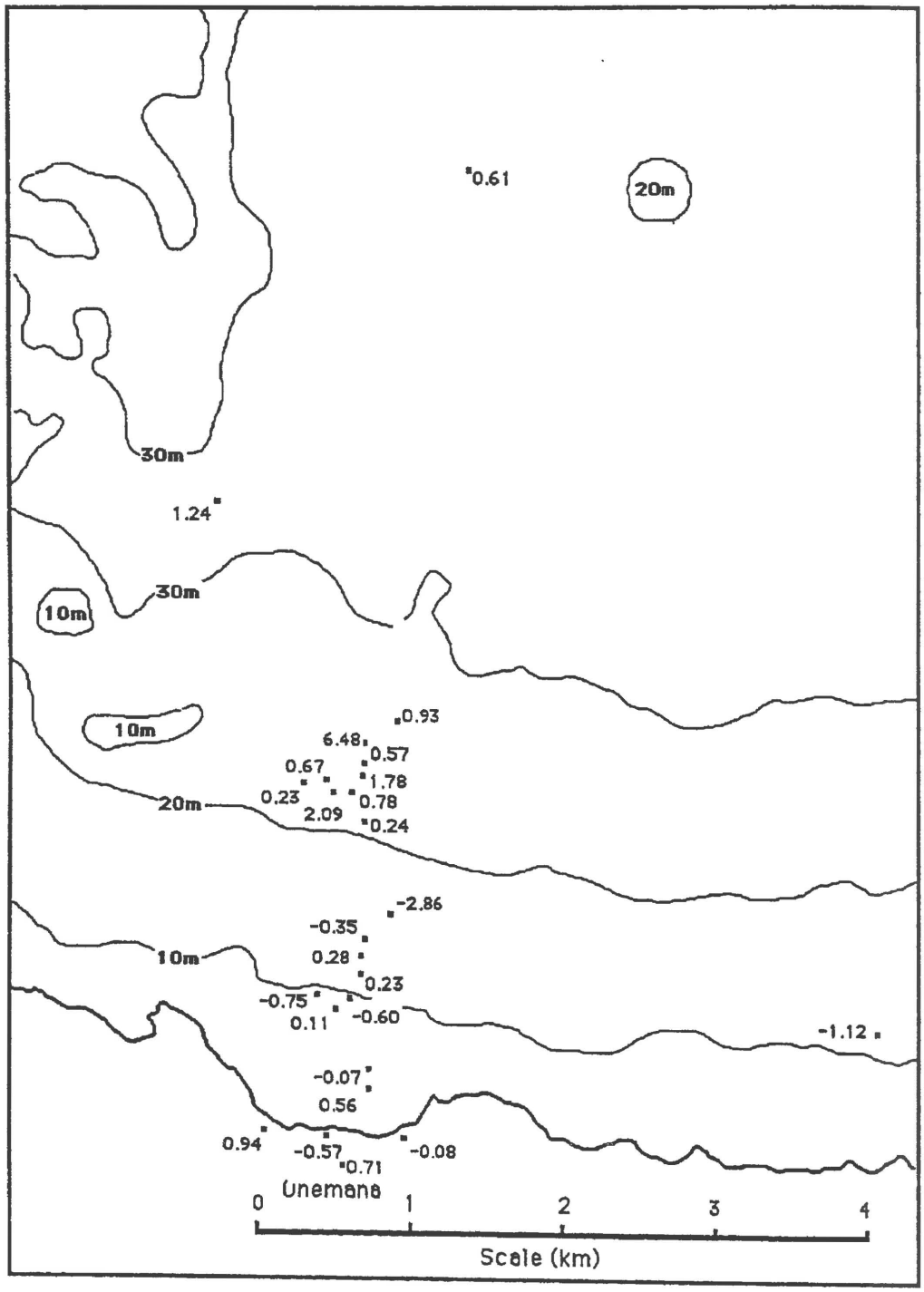
0.61
20m
30m
1.24
30m
10m
10m
0.93
6.48
0.57
0.67
1.78
0.23
0.78
2.09
0.24
20m
-2.86
-0.35
10m
0.28
0.23
-0.75
0.11
-0.60
-1.12
-0.07
0.56
0.94
-0.57
-0.08
0.71
Onemana
0
1
2
3
4
Scale (km)

OPOUTERE

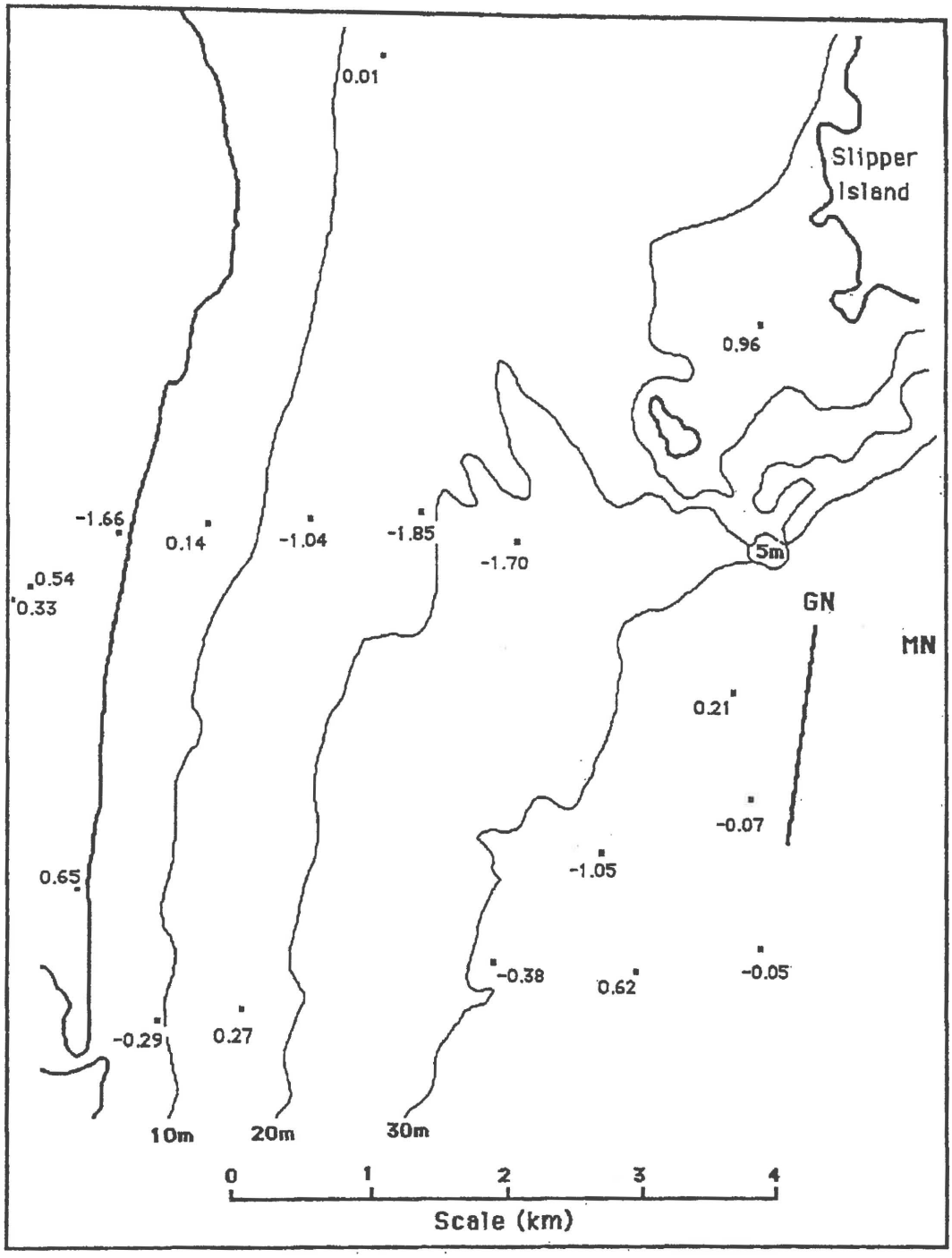
0.01
Slipper
Island
0.96
-1.66
0.14
-1.04
-1.85
-1.70
5m
0.54
0.33
GN
MN
0.21
-0.07
0.65
-1.05
-0.38
0.62
-0.05
-0.29
0.27
10m
20m
30m
0
1
2
3
4
Scale (km)

HOTWATER

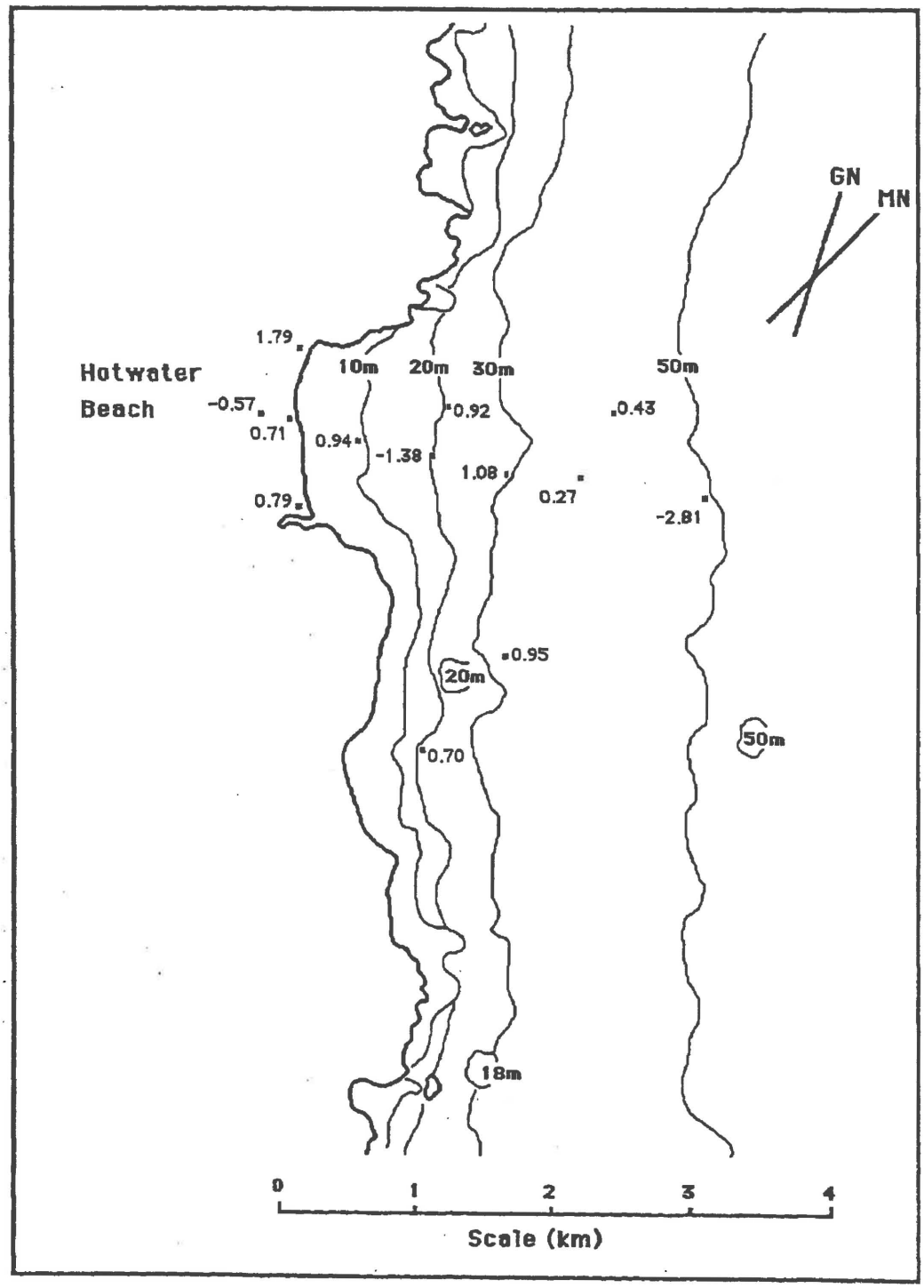
GN
MN
Hotwater
Beach
1.79
10m
20m
30m
50m
-0.57
0.71
0.94
-1.38
0.92
0.43
1.08
0.27
-2.81
0.79
0.95
20m
50m
0.70
18m
0
1
2
3
4
Scale (km)

MERCURY BAY

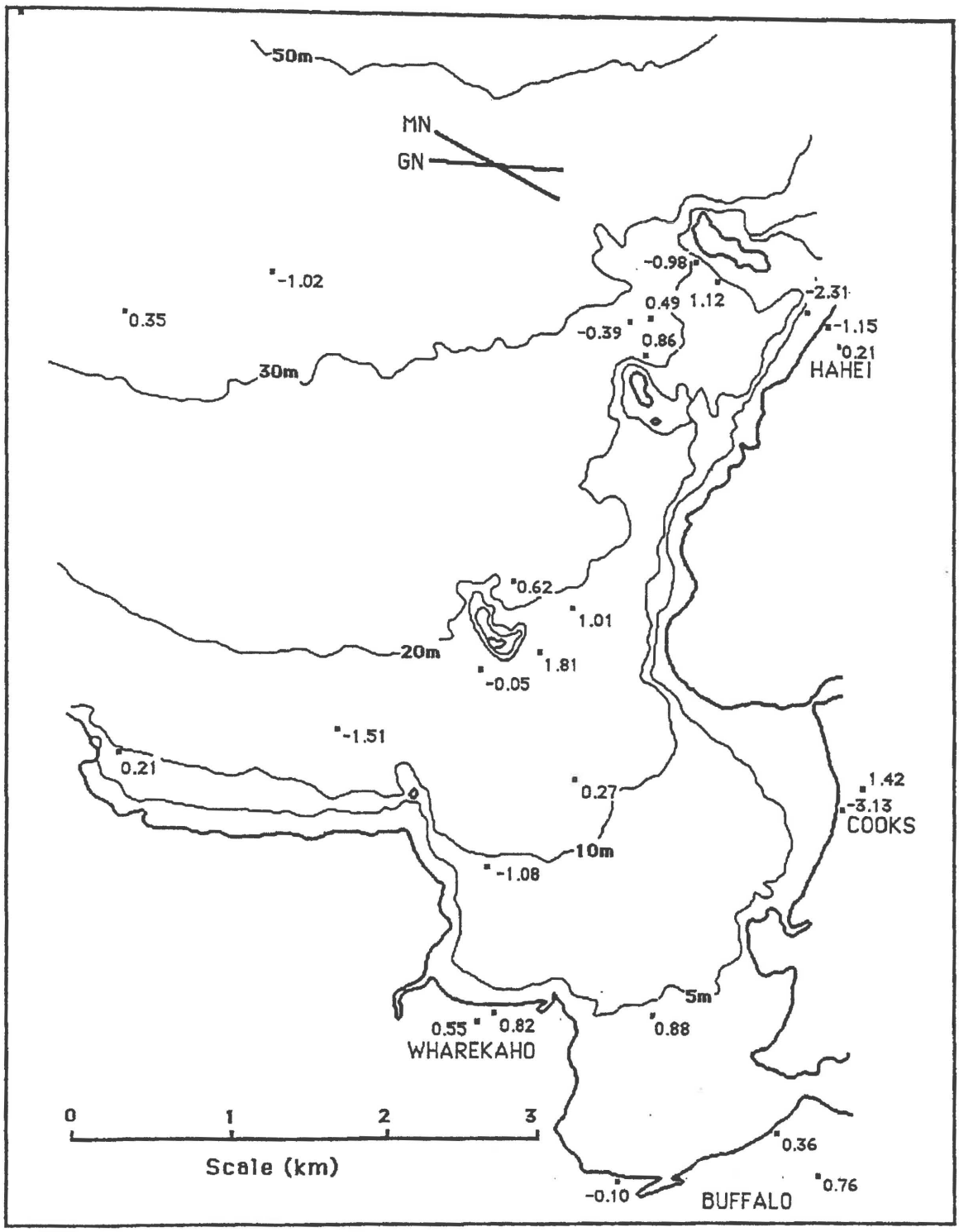
50m
MN
GN
-1.02
0.35
30m
-0.98
0.49
1.12
-2.31
-0.39
0.86
-1.15
0.21
HAHEI
0.62
1.01
20m
1.81
-0.05
-1.51
0.21
0.27
1.42
-3.13
COOKS
10m
-1.08
5m
0.55
0.82
0.88
WHAREKAHO
0
1
2
3
Scale (km)
0.36
0.76
-0.10
BUFFALO

OTAMA

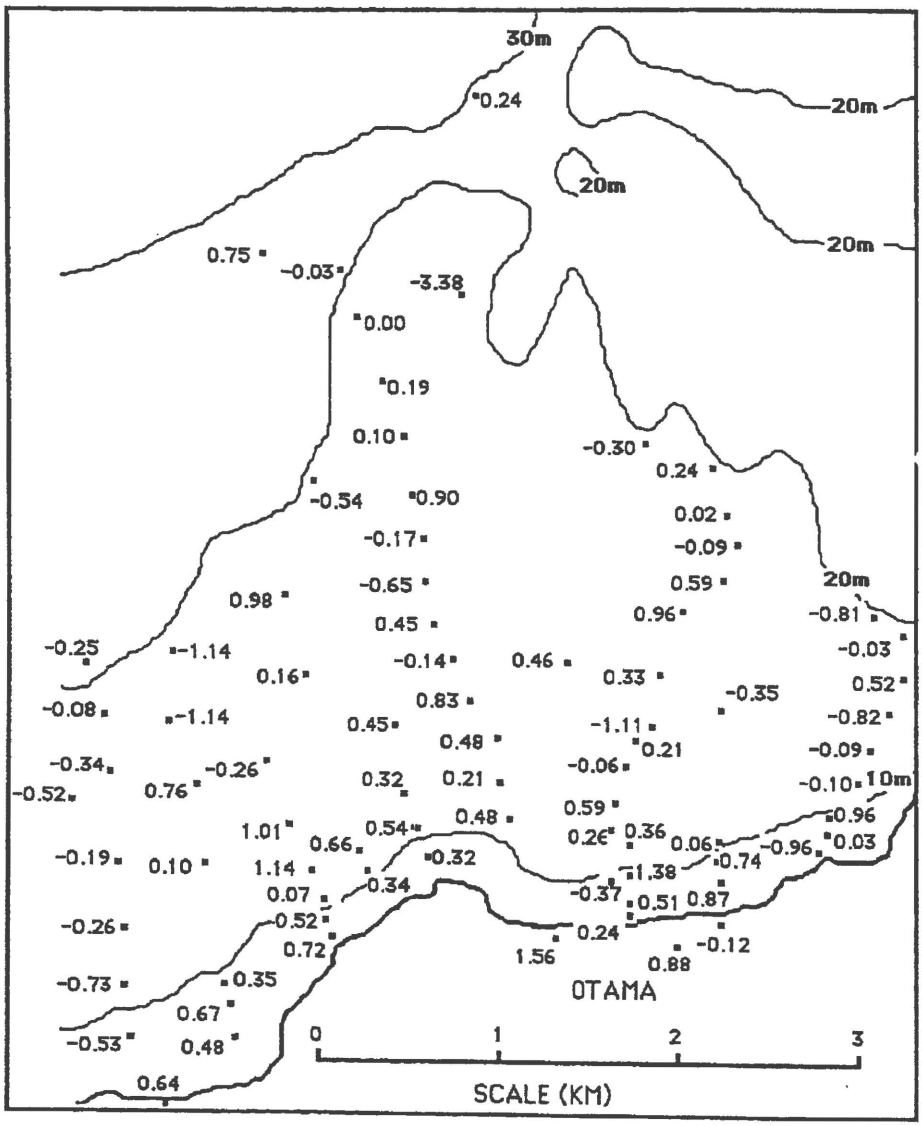
30m
20m
20m
20m
20m
10m
0.24
0.75
-0.03
-3.38
0.00
0.19
0.10
-0.30
0.24
-0.54
0.90
0.02
-0.17
-0.09
-0.65
0.59
0.98
0.96
-0.81
0.45
-0.25
-1.14
-0.14
0.46
0.33
-0.03
0.16
-0.35
0.52
0.83
-0.08
-1.14
-0.82
0.45
-1.11
0.48
0.21
-0.09
-0.34
-0.26
-0.06
-0.10
-0.52
0.76
0.32
0.21
0.59
0.96
1.01
0.54
0.48
0.26
0.36
0.06
0.03
0.66
-0.19
0.10
1.14
0.32
1.38
0.74
-0.96
0.07
0.34
-0.37
0.51
0.87
-0.26
0.52
0.24
0.72
1.56
-0.12
0.88
-0.73
0.35
OTAMA
0.67
-0.53
0.48
0
1
2
3
0.64
SCALE (KM)

WHANGAPOUA

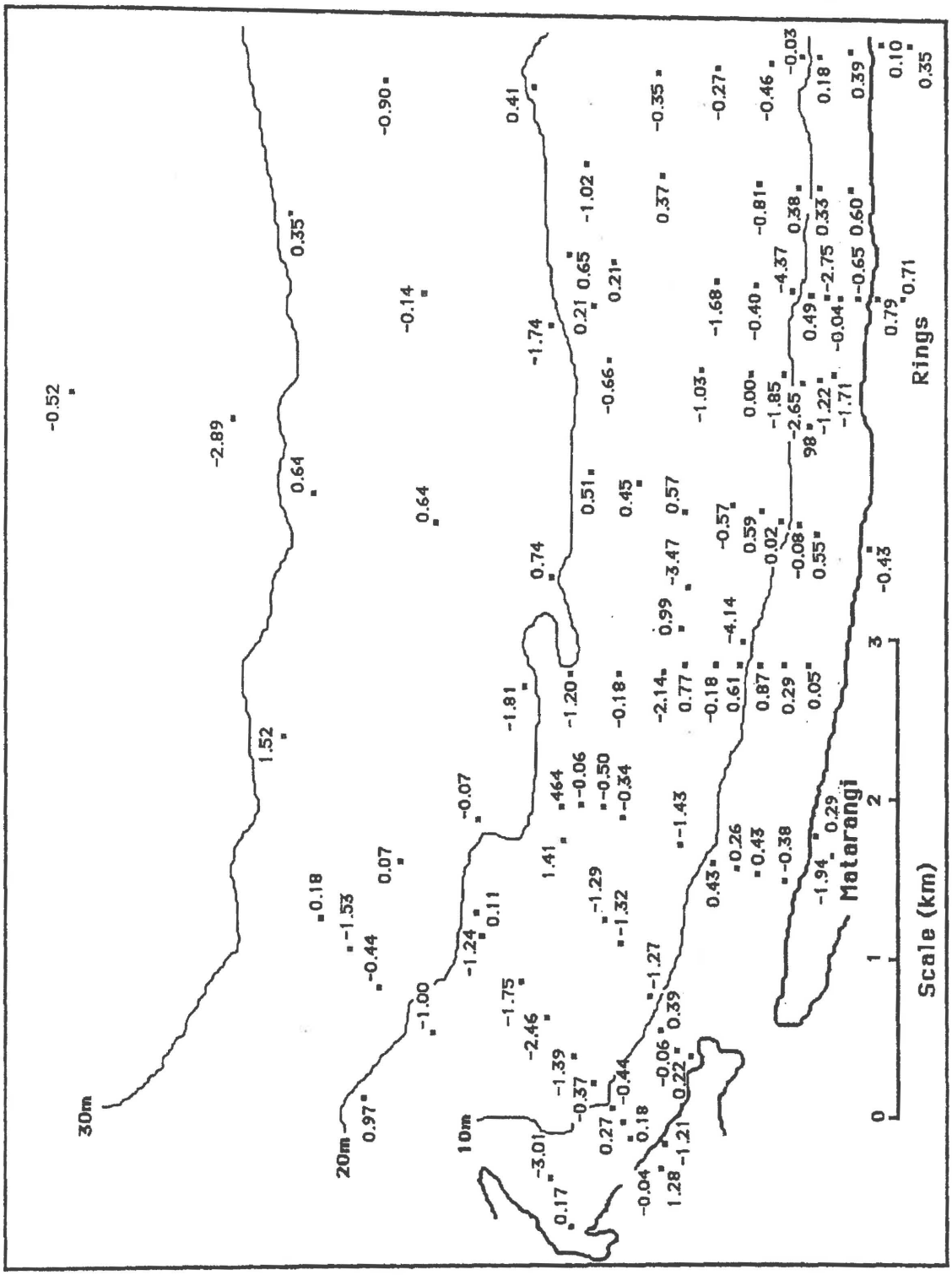

APPENDIX 4

SIDE-SCAN SONAR AND SUB-BOTTOM FIX POSITIONS

WAIHI
MAR-84

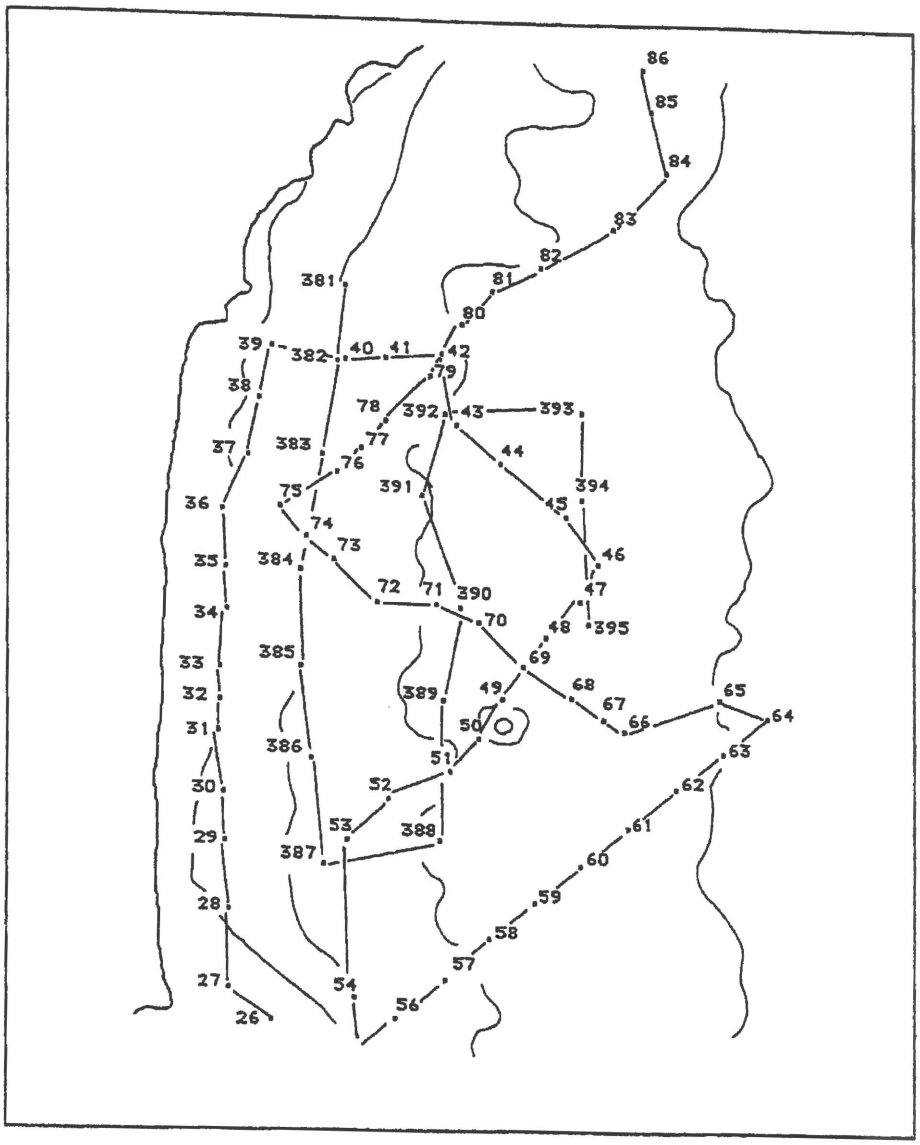
86
85
84
83
82
81
80
381
39
382
40
41
42
79
38
78
392
43
393
37
383
77
44
76
391
394
36
75
45
74
46
35
384
73
72
71
390
47
34
70
48
395
385
69
33
68
65
32
389
49
67
64
31
50
66
386
63
51
30
52
62
53
388
61
29
387
60
59
28
58
57
27
54
56
26

WAIHI
JUN-90

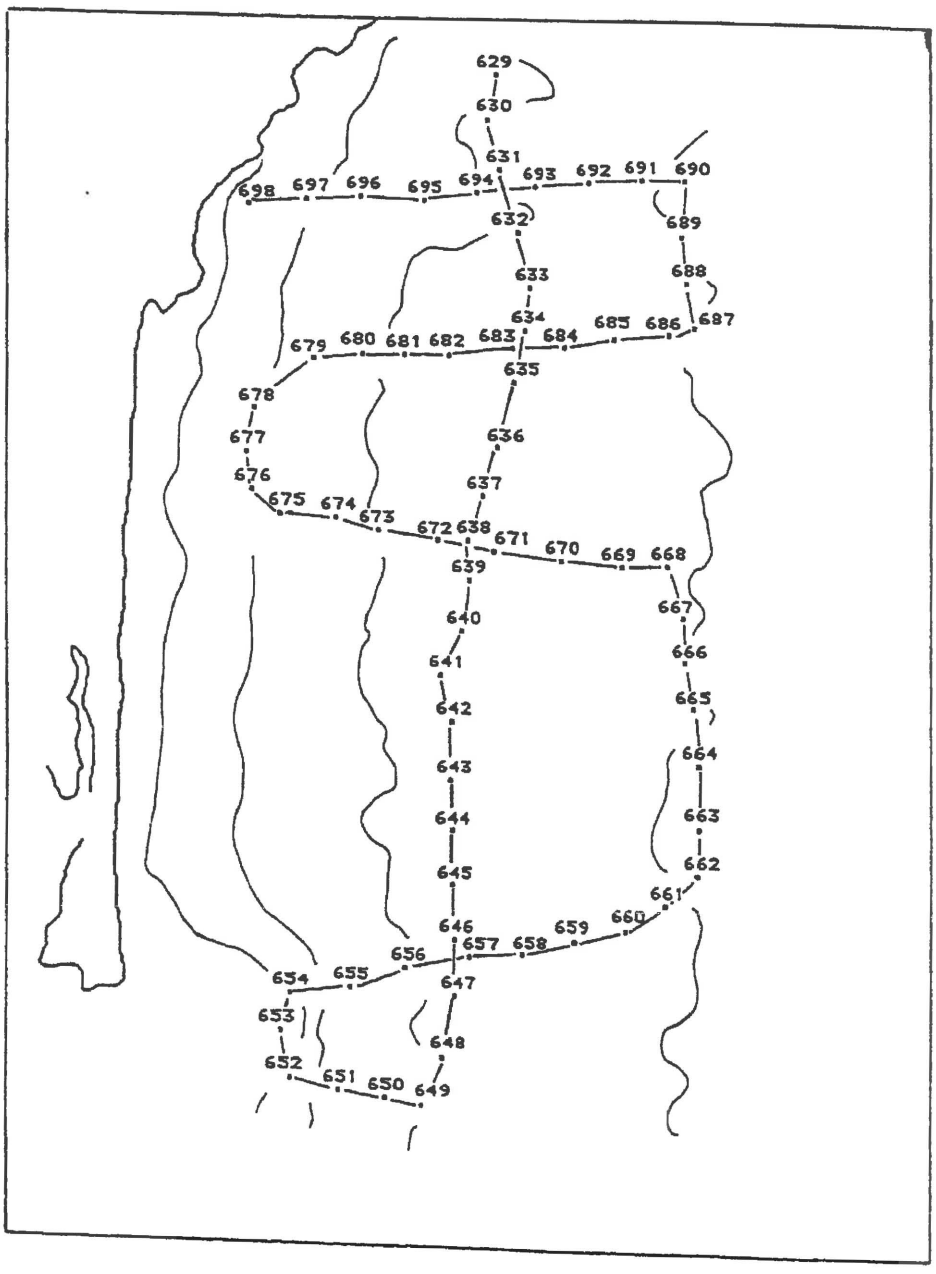
629
630
631
698 697 696 695 694 693 692 691 690
632
689
633
688
634
679 680 681 682 683 684 685 686 687
635
678
677
636
676
637
675 674 673 672 638 671 670 669 668
639
667
640
666
641
665
642
664
643
663
644
662
645
661
646
659 660
656 657 658
654 655
647
653
648
652 651 650 649

WHIRITOA
MAR-84

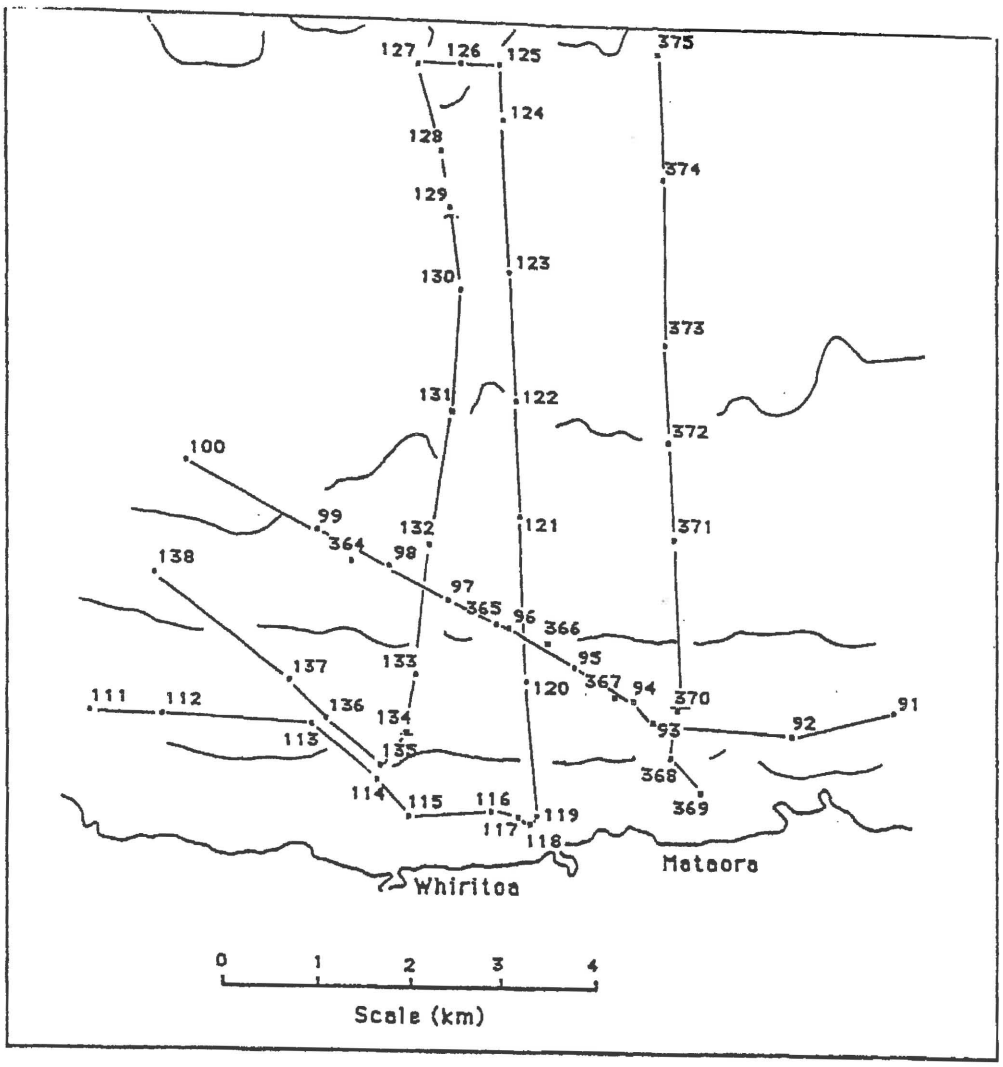

WHIRITOA
JUN-90

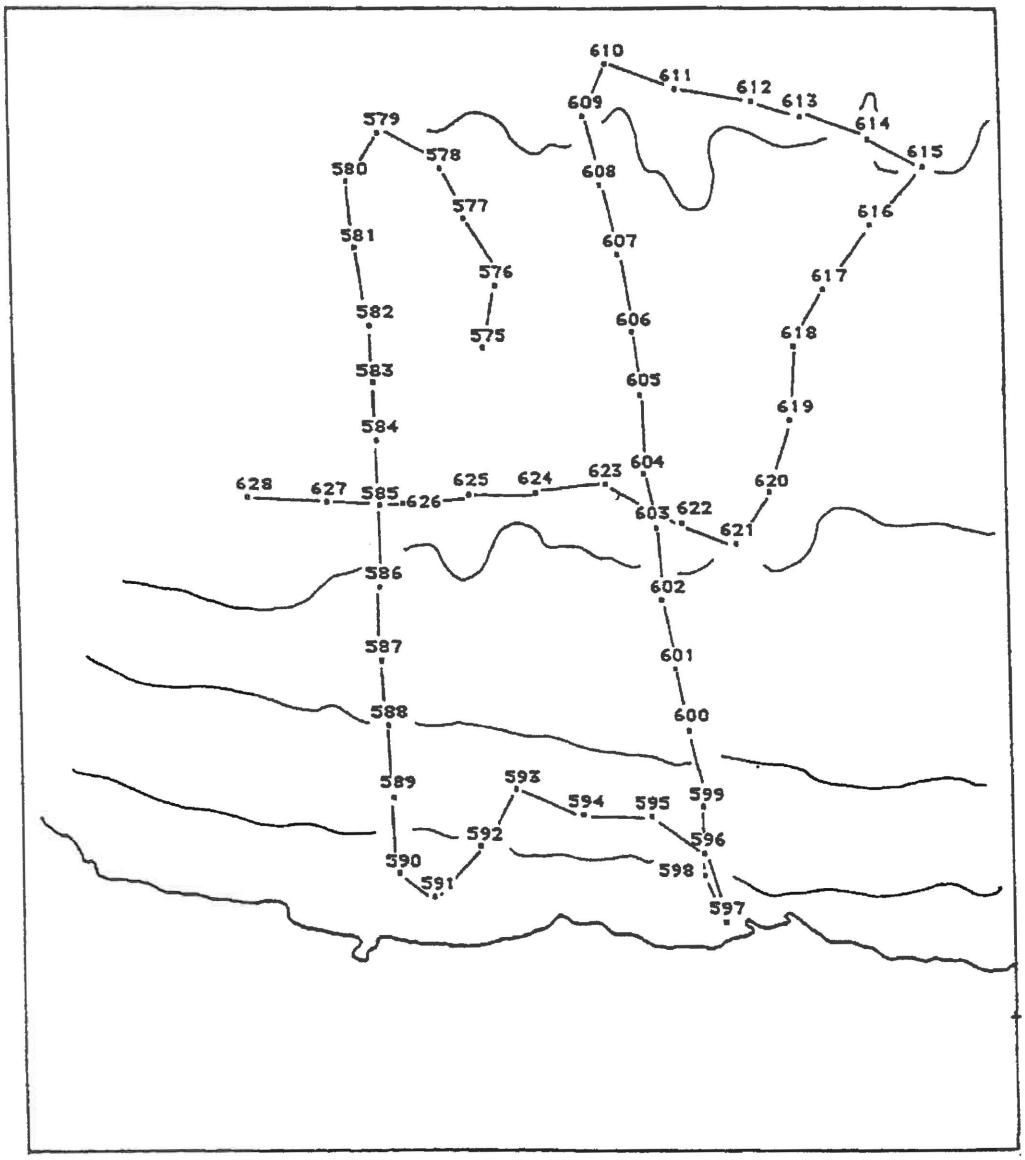

A-75

WHANGAMATA
MAR-84

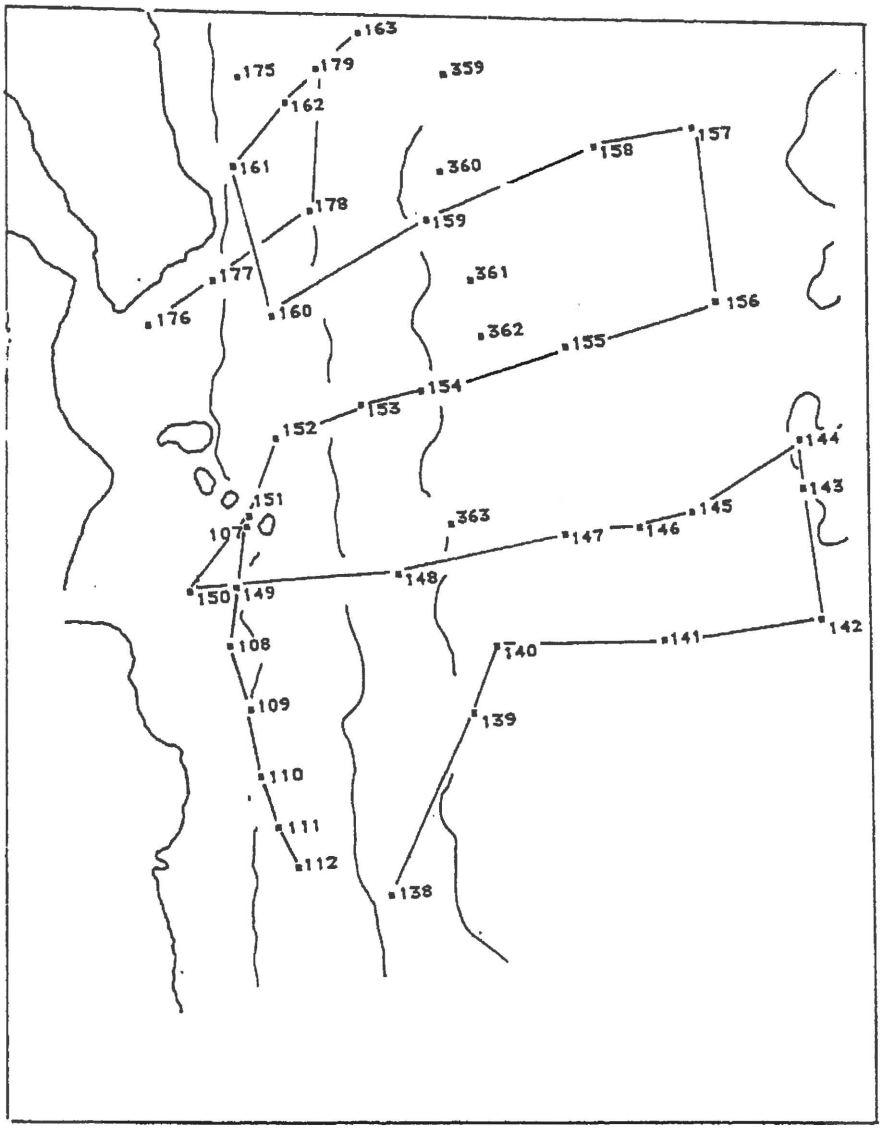

WHANGAMATA
MAR-85

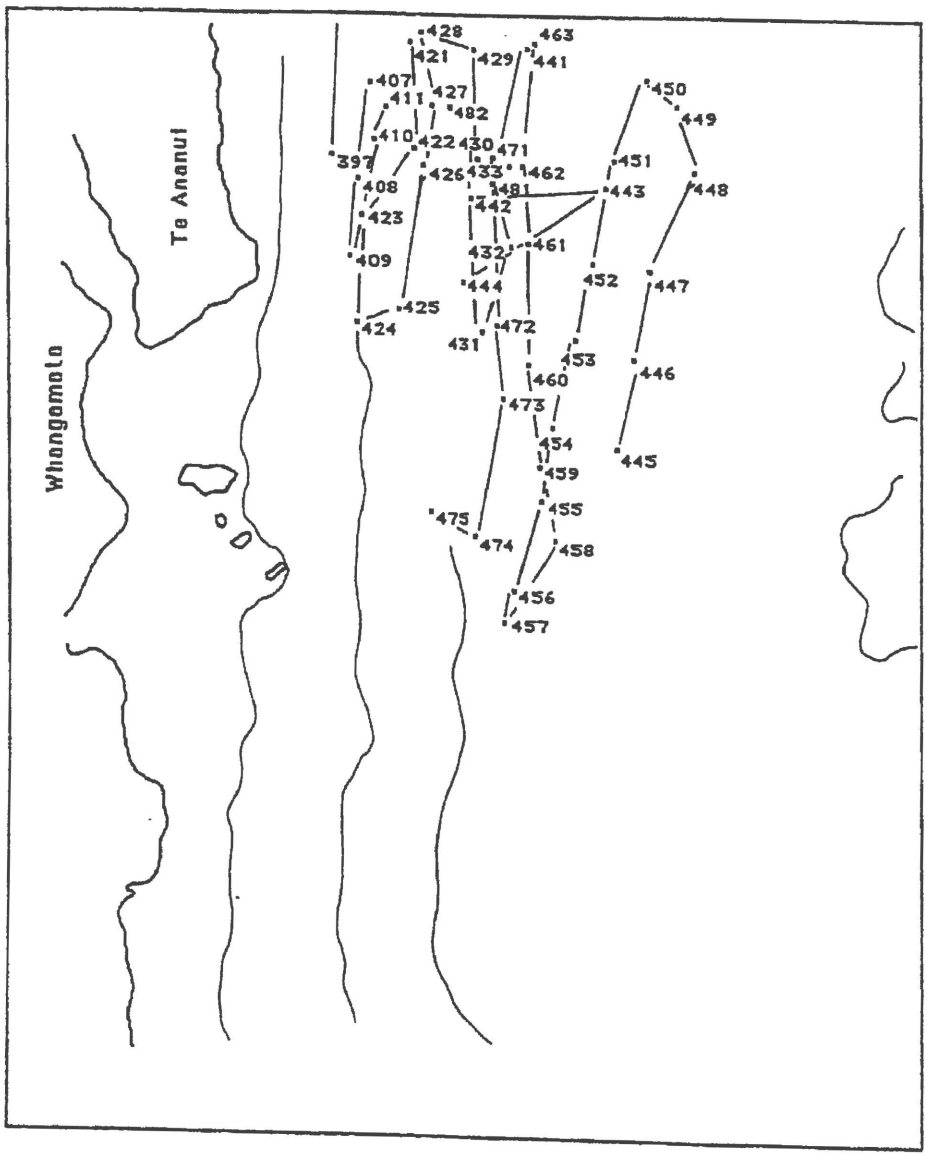

WHANGAMATA
JUN-90

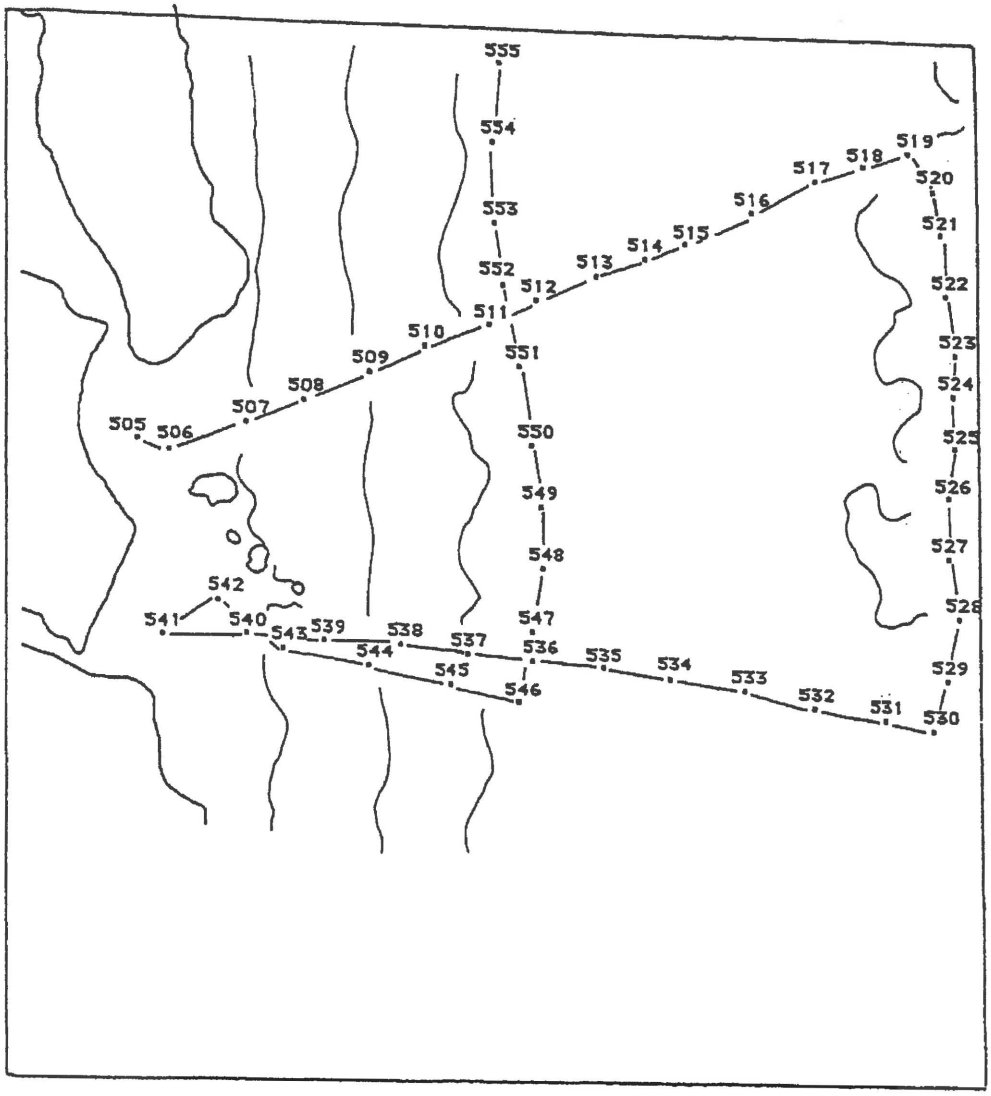

ONEMANA
MAR-84

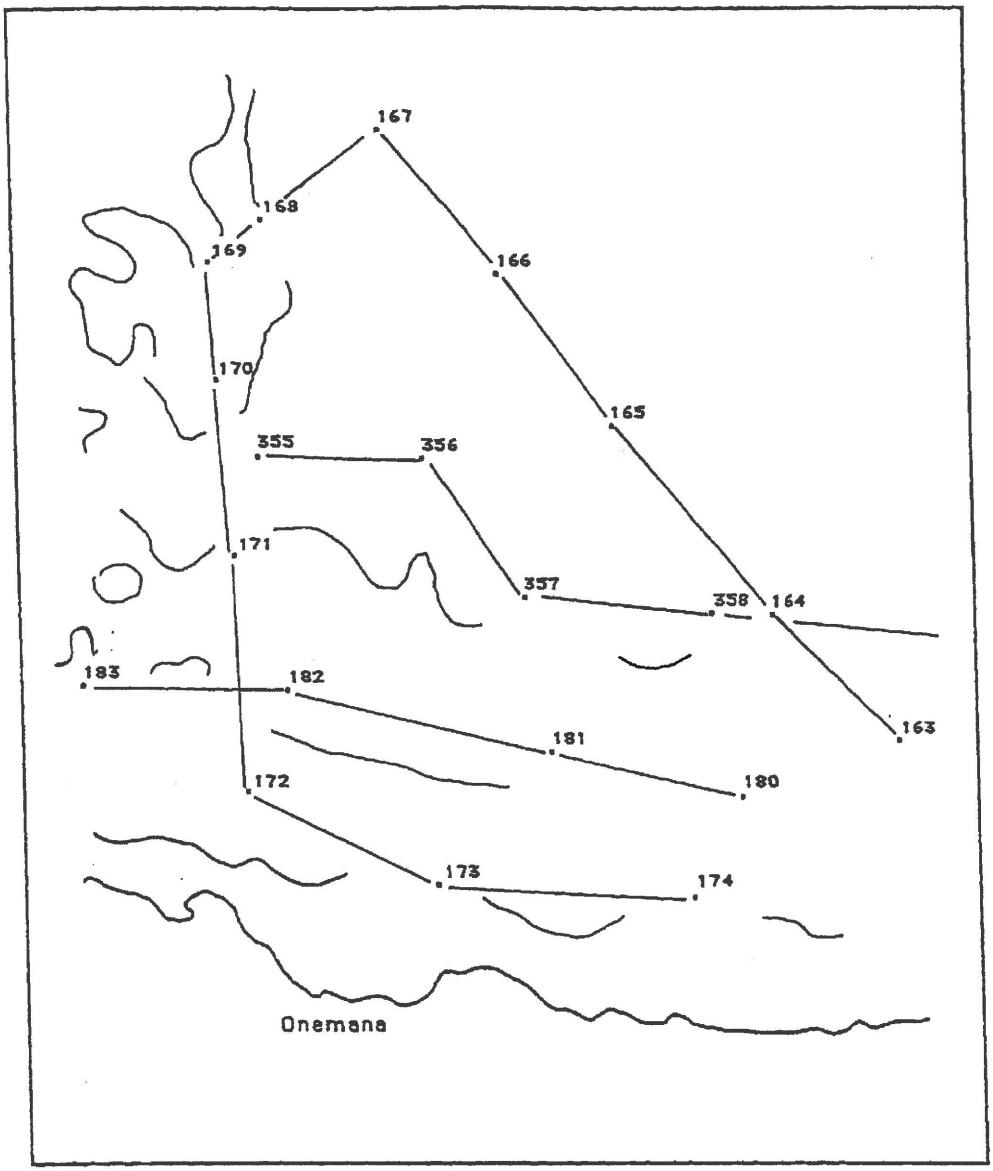

ONEMANA
MAR-85

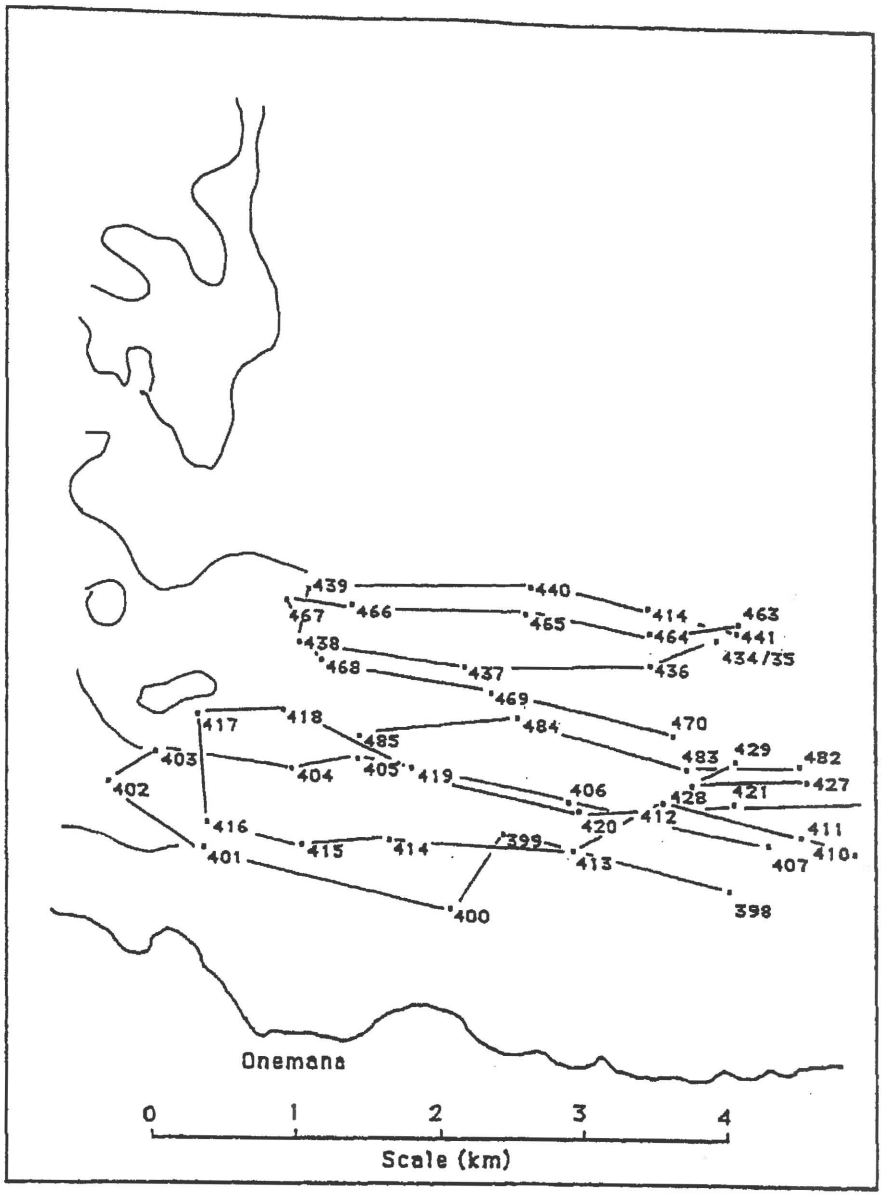

A-80

ONEMANA
JUN-90

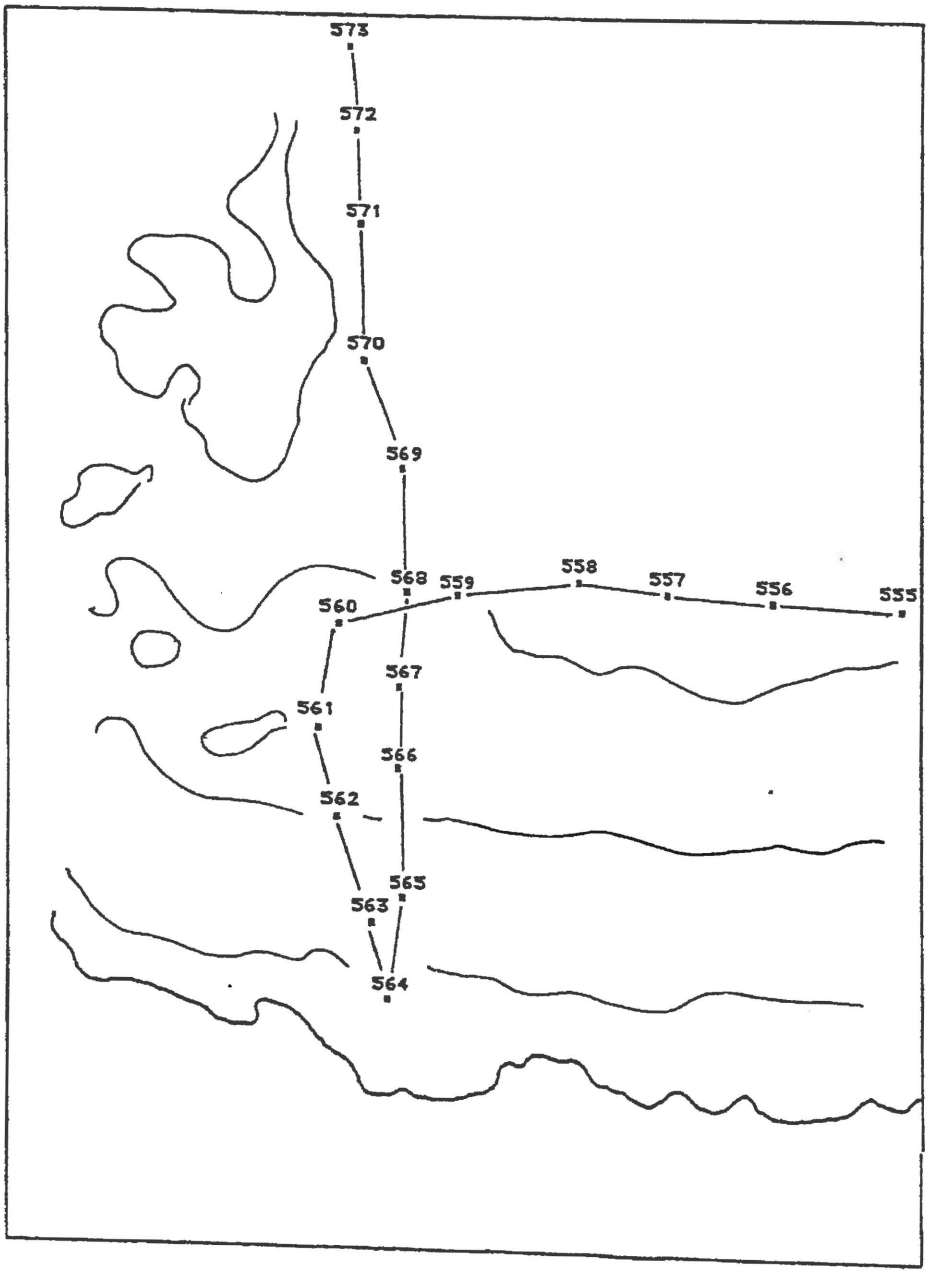

A-81

OPOUTERE
MAR-84

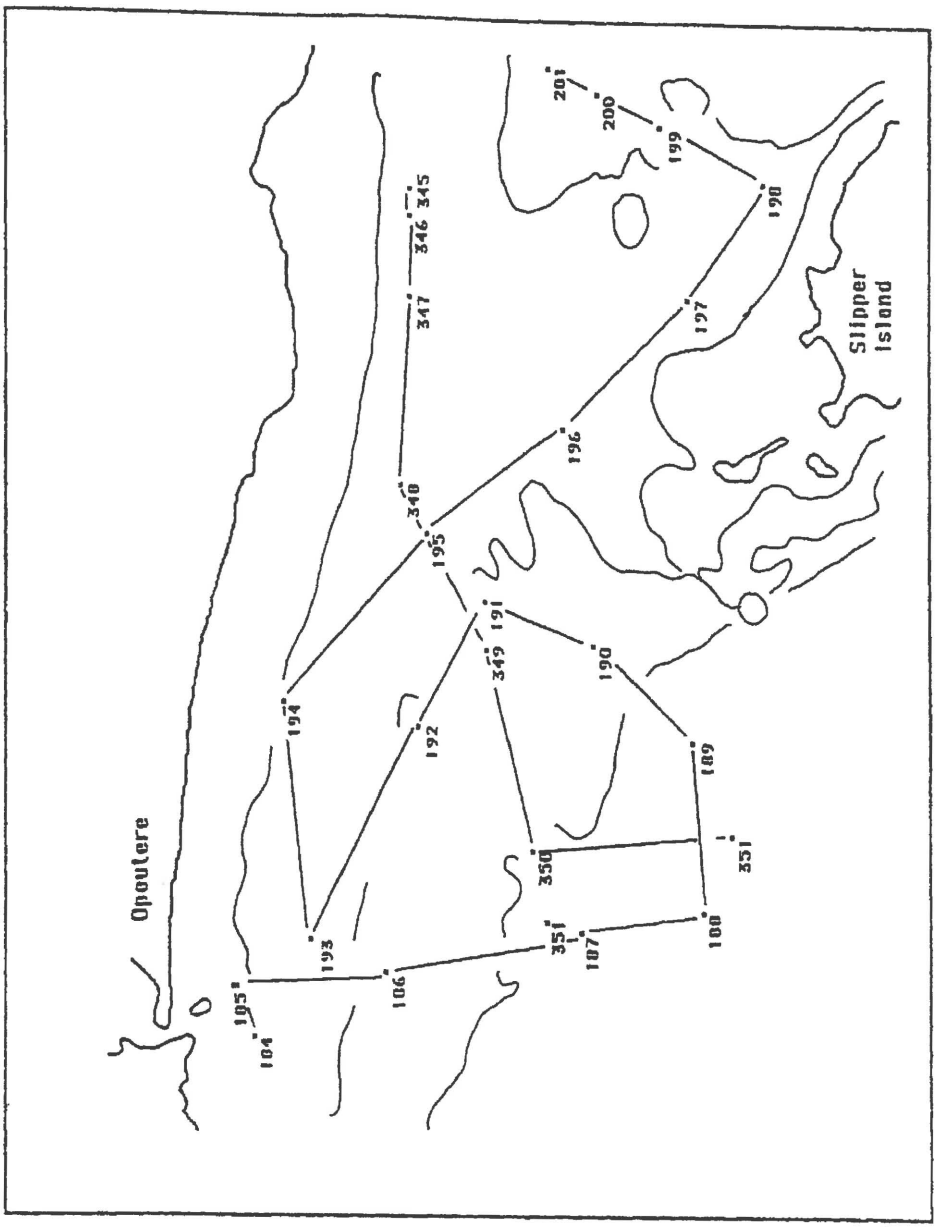

A-82

PAUANUI
MAR-84

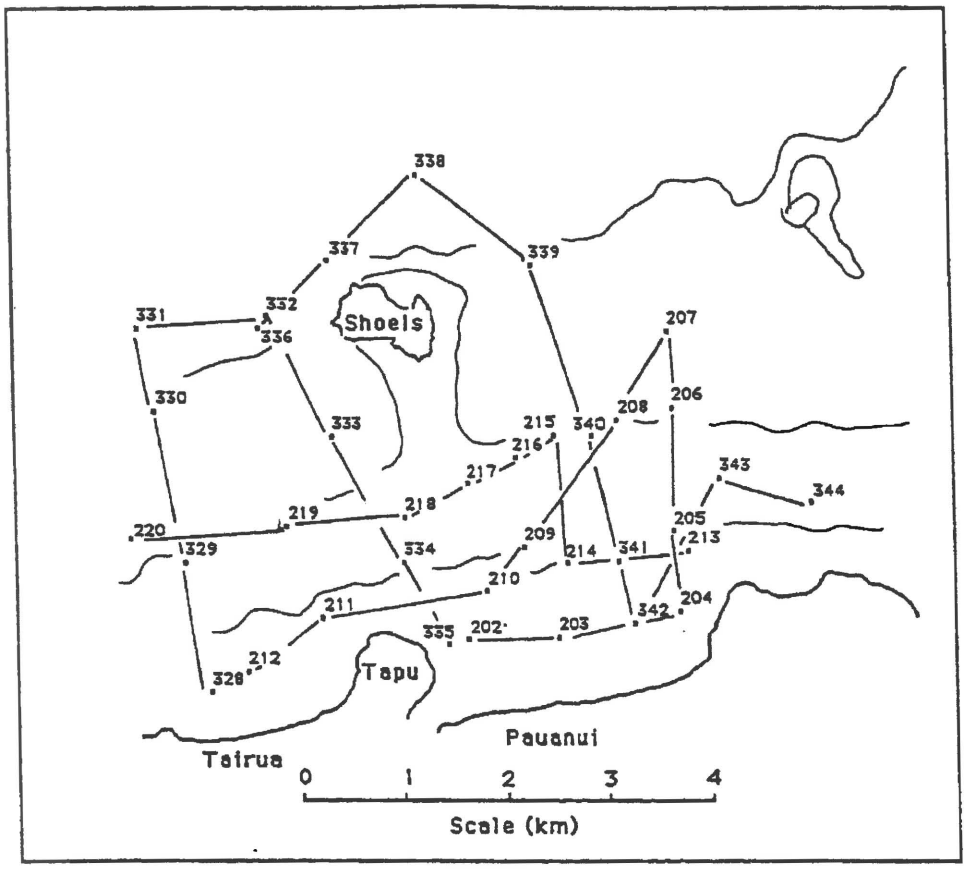

A-83

HOTWATER
MAR-84

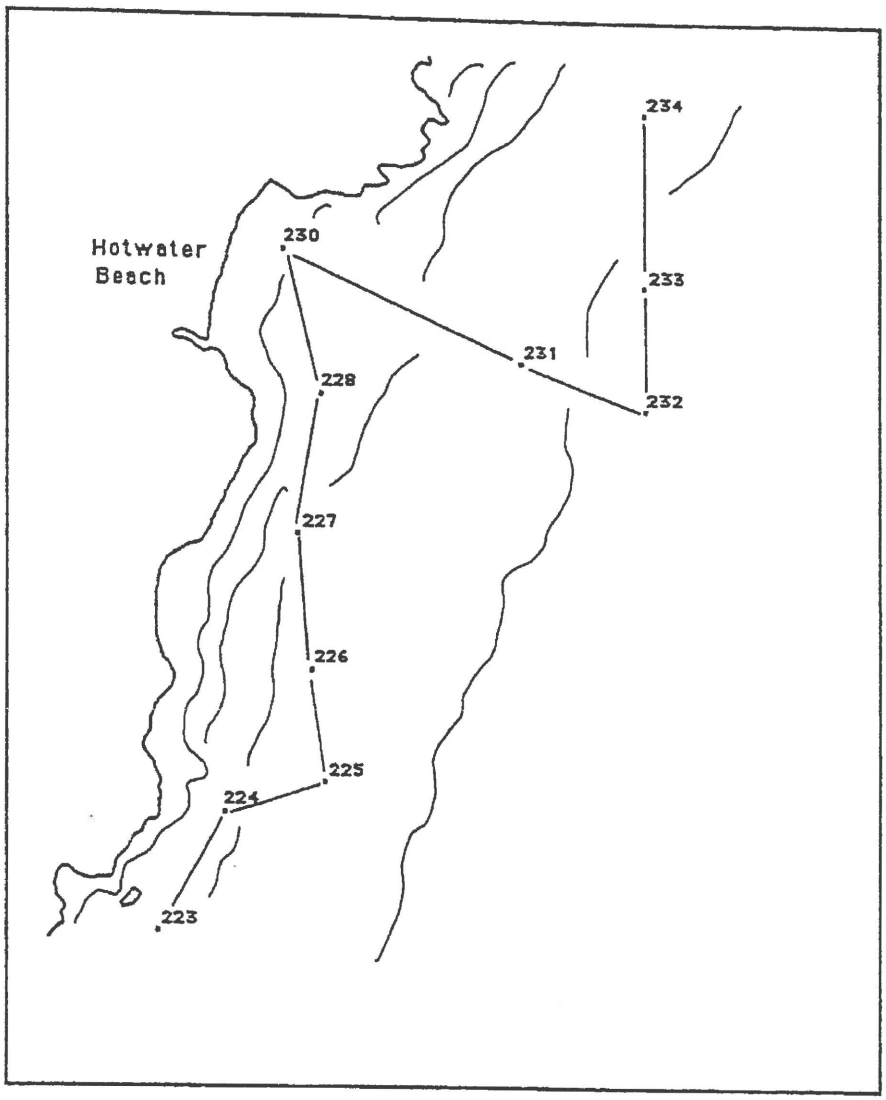

MERCURY BAY
MAR-84

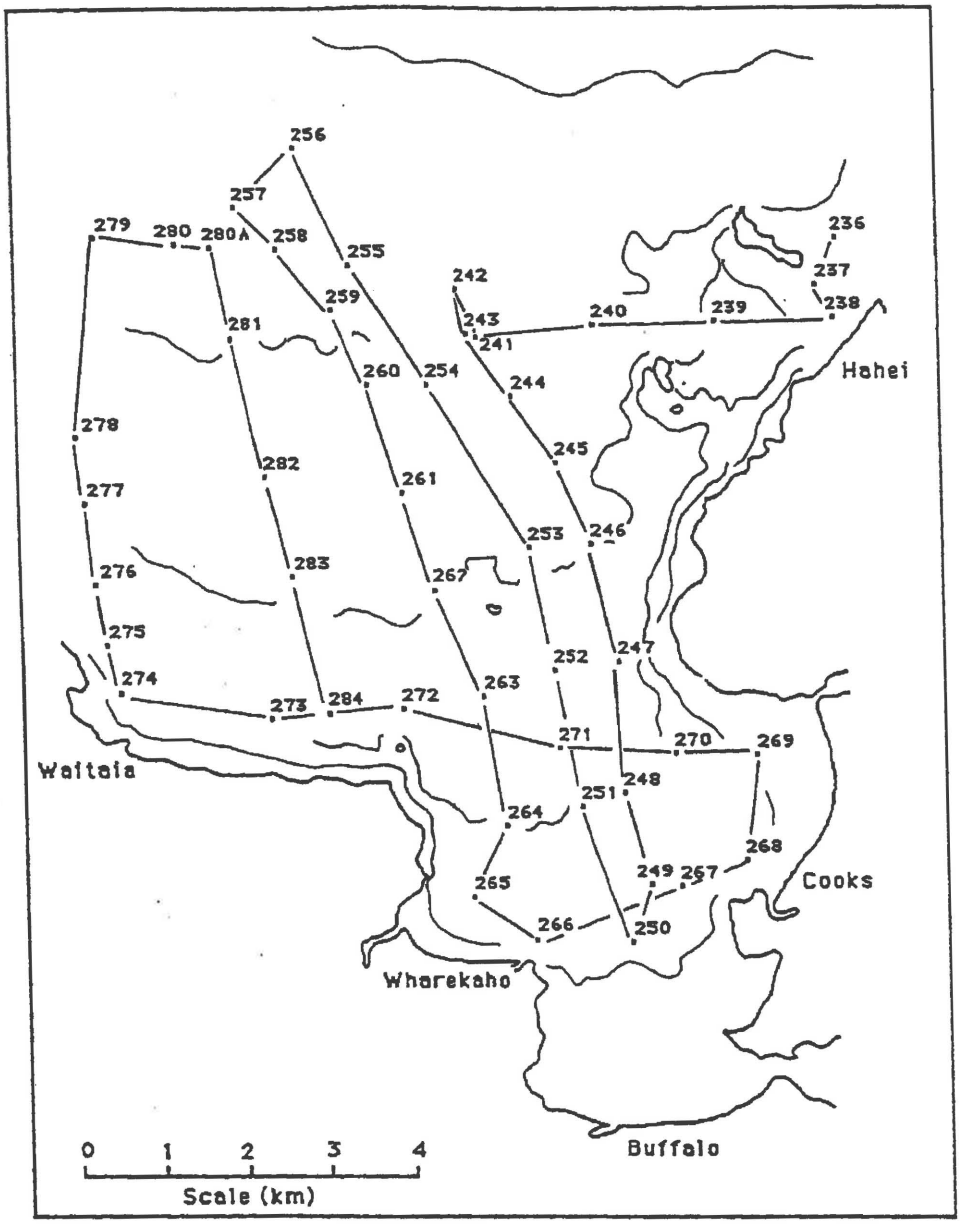

MERCURY BAY
JUN-90

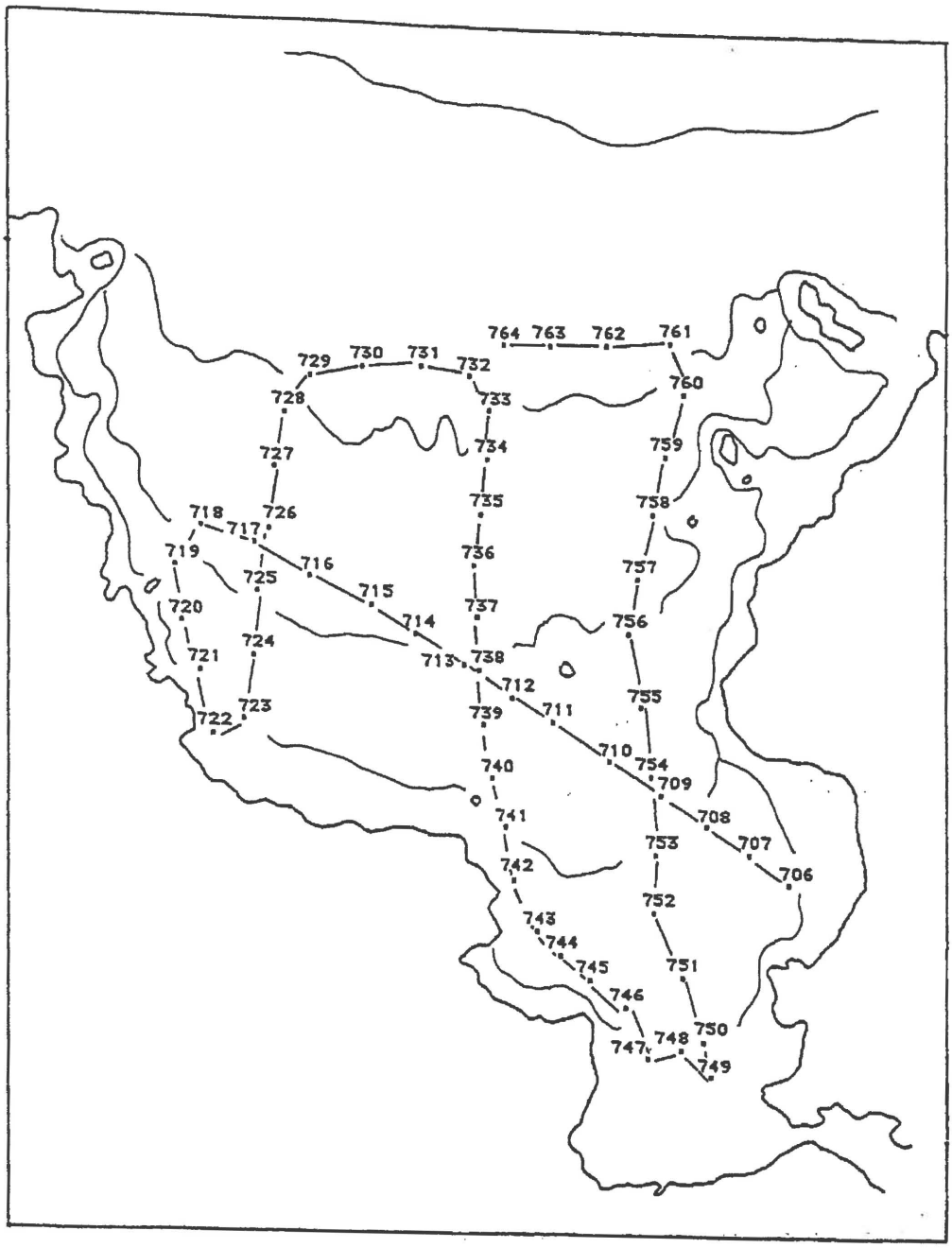

WHANGAPOUA
MAR-84

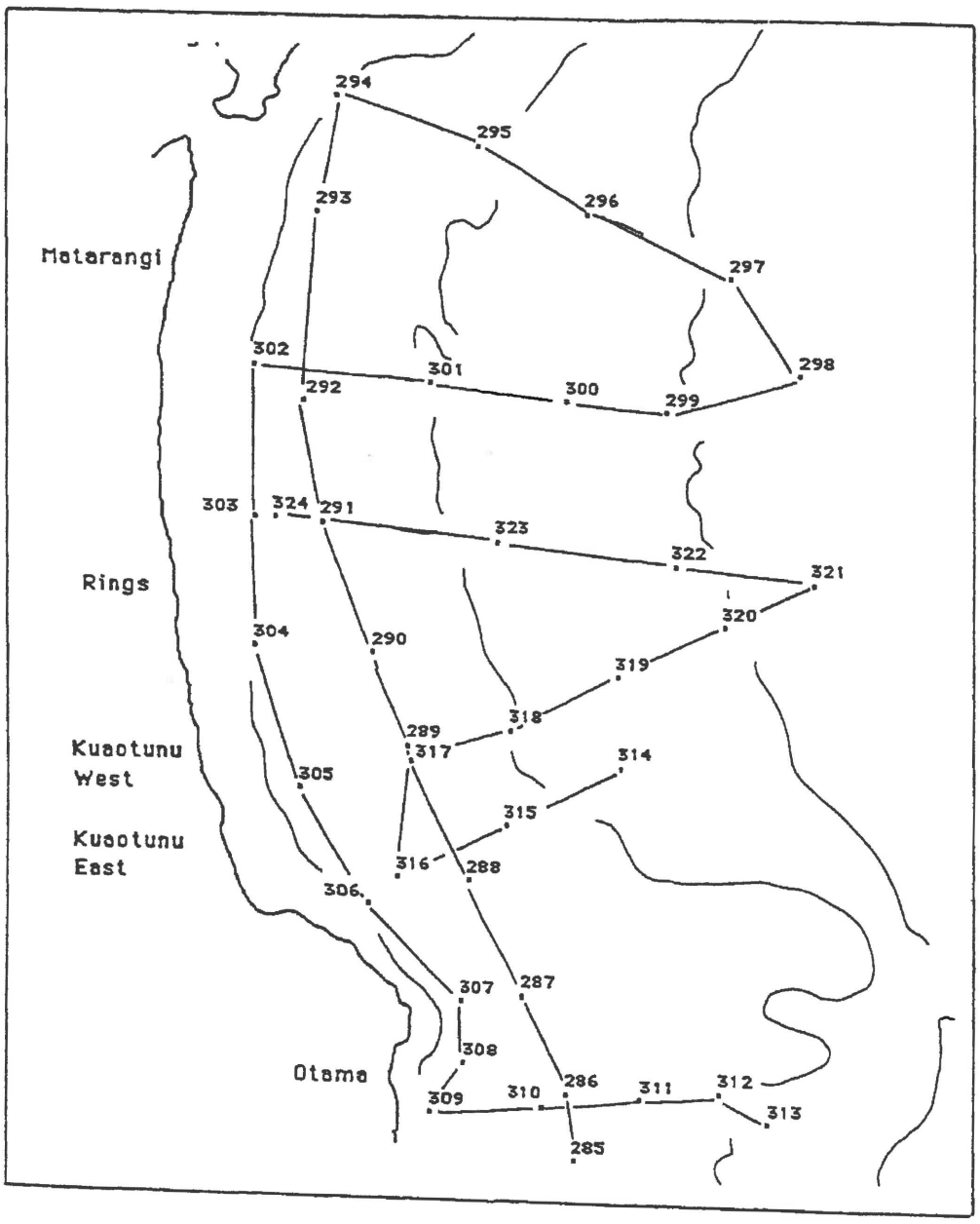

APPENDIX 5

BEDFORM SURVEYS

Appendix 5A

Original Diver Observations

WAIHI BEACH DIVER OBSERVATIONS

NO	DATE	h	MEAN	λ(M)	η(M)	SYMM	θ	OBSERVATIONS
1	15-FEB-84	23	0.16	0.50	0.08	A	-	Coarse crests, shelly troughs
2	15-FEB-84	21	2.63	0.20	0.05	A	70	
3	15-FEB-84	15	2.59	0.10	0.02	S	60	
4	15-FEB-84	10	2.43	0.23	0.06	S	60	Slight movement of sand
5	15-FEB-84	5.5	2.16	-	-	-	-	Very turbid no meas. possible
6	15-FEB-84	3	2.14	-	-	-	-	Very turbid
8	16-FEB-84	22	1.92	0.25	0.03	S	50	To & fro movement of sediment
9	16-FEB-84	23	1.06	0.60	0.07	-	70	No sediment movement
10	16-FEB-84	12	2.58	0.10	0.03	S	50	Sediment very mobile
14	17-FEB-84	6.5	2.61	0.05	0.01	A	55	Sediment very mobile
17	17-FEB-84	8	2.67	0.10	0.01	-	35	
18	17-FEB-84	14	2.66	0.10	0.02	-	30	To & fro movement of sediment
19	17-FEB-84	25	-0.04	1.20	0.08	S	35	Coarse crests, shelly troughs
20	17-FEB-84	20	0.19	0.86	0.17	S	25	Coarse crests, shelly troughs
22	17-FEB-84	19	2.99	0.10	0.02	S	-	
24	17-FEB-84	20	1.81	0.10	0.03	S	35	
243	15-NOV-84	21	1.04	0.50	0.05	S	-	
246	15-NOV-84	27	-0.05	0.75	0.10	S	30	Mafic grans on crests, coarse sand and shell in troughs.
247	15-NOV-84	17	2.75	-	-	-	-	

WHIRITOA DIVER OBSERVATIONS

No	Date	h	Mean	λ (m)	η (m)	Symm	θ	Observations
28	18-Feb-84	24	2.13	0.20	0.04	-	60	No movement of sediment observed.
29	18-Feb-84	18	2.94	0.10	0.05	S	45	Hummocky shaped bedforms.
30	18-Feb-84	12	2.68	0.10	0.05	S	-	To & fro movement of sediment.
31	18-Feb-84	7	1.40	-	-	-	-	Bottom completely disturbed.
32	18-Feb-84	24	2.35	0.15	0.03	S	-	Slight to & fro movement.
33	18-Feb-84	18	2.83	0.10	0.02	S	-	To & fro movement of sediment.
34	18-Feb-84	12	2.79	0.07	0.01	S	40	Lots of sediment movement.
35	18-Feb-84	6	2.07	0.10	0.05	-	-	Lots of mov. bedforms v.disturbed
217	14-Nov-84	24	2.22	-	-	-	-	Slightly hummocky, no obs. b.f.
232	14-Nov-84	25	2.49	-	-	-	-	V.lightly rippled, horse mussels and silt on surface.

WHANGAMATA DIVER OBSERVATIONS

No	Date	h	Mean	λ(m)	η(m)	SYMM	θ	Observations
25	17-FEB-84	20	2.14	0.22	0.04	S	38	Sandy crests & shelly troughs.
26	17-FEB-84	24	1.99	0.10	0.03	S	40	Sinuous shaped crests.
46	19-FEB-84	18	2.48	0.10	0.02	S	-	Sinuous shaped crests.
47	19-FEB-84	15	2.73	0.10	0.02	S	35	To & fro movement of sediment.
48	19-FEB-84	9	2.83	0.10	0.01	S	-	To & fro movement of sediment.
49	19-FEB-84	6	2.79	-	-	-	-	Ripples rapidly form & deform.
50	19-FEB-84	3	1.95	-	-	-	-	Very disturbed, no bedforms.
52	19-FEB-84	4	2.62	0.10	0.02	-	-	Variable strike of ripples.
53	19-FEB-84	6	0.50	0.70	0.10	S	20	Sinuous crests, little movement
54	19-FEB-84	9	0.94	0.80	0.15	S	-	Ripple crests parallel.
56	19-FEB-84	13	2.86	0.08	0.02	S	57	To & fro movement of sediment.
58	19-FEB-84	12	2.50	0.08	0.02	-	40	To & fro movement of sediment.
59	19-FEB-84	18	2.34	0.09	0.03	S	45	
60	19-FEB-84	12	2.69	0.10	0.02	S	30	To & fro movement of sediment.
61	19-FEB-84	6	2.88	0.10	0.01	-	-	Form & deform with to & fro movement of sediment.
173	13-NOV-84	32	1.11	1.00	0.15	S	-	Shell in troughs.
174	13-NOV-84	29	1.31	0.50	0.04	-	30	Irregular sinuous crests.

Onemana - Diver Observations

No	Date	h	Mean	λ(m)	η(m)	Symm	θ	Observations
131	10-Jul-84	15	2.70	0.20	0.04	S	40	
166	13-Nov-84	23	2.60	0.10	0.02	-	-	Sinuous crested ripples.
167	13-Nov-84	24	0.93	0.75	0.10	-	25	Linear-slightly sinuous crests. Shell in troughs over c.sand.
257	6-Jul-85	24	0.74	0.80	0.13	-	-	Ripple crests straight-offset.

Opoutere Diver Observations

No	Date	h	Mean	λ(m)	η(m)	Symm	θ	Observations
69	20-Feb-84	8	0.54	-	-	-	-	Scattered boulders on a flat sea bed, no sediment movement.
70	20-Feb-84	24	2.88	0.10	0.04	-	40	Slight to & fro movement.
71	20-Feb-84	20	3.00	0.09	0.03	-	30	
72	20-Feb-84	12	2.77	0.09	0.04	-	20	To & fro sediment movement.
73	20-Feb-84	6	2.35	0.09	0.02	-	20	Ripples form & deform with to & fro movement of sediments.

Otama Beach - Diver Observations

No	Date	h	Mean	λ(m)	η(m)	Sym	θ	Observations
417	14-APR-85	14	1.47	0.2	0.02	S	60	
418	14-APR-85	13	1.53	0.8	0.18	-	60	
419	14-APR-85	13	-	0.25	0.05	-	60	
420	14-APR-85	9	1.83	0.25	0.05	S	70	Sinuous crested bedforms.
421	14-APR-85	7	1.74	0.25	0.05	S	65	
422	14-APR-85	5	1.84	0.20	0.05	S	-	
430	14-APR-85	14	1.24	0.50	0.06	-	-	Shell hash in troughs.
432	14-APR-85	10	1.89	0.12	0.03	-	-	Coarse shell debris on flanks of crests.
433	14-APR-85	8	-	0.11	0.03	-	-	Sharp crests and flat troughs.
434	14-APR-85	6	1.77	0.15	0.03	-	-	Linear crests on bedforms.

Matarangi-Otama Diver Observations

		h		λ(M)	η(M)	SYM	θ	OBSERVATIONS
142		10	2.52	0.2	-	-		To & fro motion, sinuous crests.
145	12-NOV-84	21	2.43	-	-	-		V.small hummocky bedforms. Horse mussels & starfish present.
147	12-NOV-84	30	2.78	-	-	-		Irregular, small bedforms. Plant growth on surface.
331	9-APR-85	13	2.61	-	-	-		Flat & featurless. Abundant cockles.
332	9-APR-85	9	1.59	0.4	0.03	-		Megarripples next to small ripples. Horse mussels on bed.
338	10-APR-85	20	2.87	0.1	0.02	-	240	Irregular crests. Cockles, scallops & horse mussels found.
340	10-APR-85	16	2.31	0.1	0.02	-	130	Irregular crested bedforms.
342	10-APR-85	12	2.87	0.1	0.03	S	-	Sediment in suspension due to wave action.
345	10-APR-85	6	2.47	0.08	0.02	S	-	Stones found in troughs.
346	10-APR-85	4	2.51	0.06	0.01	A	-	Stones in troughs. Net shoreward movement of sediment.
347	10-APR-85	20	2.48	0.05	0.02	-	60	Lots of cockles and horse mussels present.
349	10-APR-85	16	2.51	0.05	0.01	-	-	Cockles present. Very murcky.
352	10-APR-85	10	2.65	0.12	0.02	S	60	Shells in troughs. Some movement of sediment by waves.
354	10-APR-85	6	2.61	0.12	0.02	S	120	Net shoreward movement of sand. Discontinuous crests c.60cm long
355	10-APR-85	4	2.72	0.12	0.02	S	-	Net shoreward movement of sand. Discontinuous crests.
357	11-APR-85	20	1.79	0.12	0.03	-	90	Horse mussels & shell frags on sea bed.
359	11-APR-85	16	2.41	0.06	0.02	S	90	Shell frags on seaward trough faces.
362	11-APR-85	10	2.48	0.11	0.02	-	90	Some movement of sediment by waves. Lots of shell frags.
364	11-APR-85	6	2.39	0.06	0.01	-	90	Hummocky dimpled appearance to bedforms. Some movement of sand.
367	11-APR-85	18	2.16	0.06	0.01	S	90	Cockles present.
369	11-APR-85	14	2.57	0.08	0.01	-	90	Sinuous crested ripples. Some movement of sediment, v.murcky.
372	11-APR-85	8	2.59	0.1	0.03	S	-	To & fro movement of sediment on crests.
375	12-APR-85	16	1.01	0.06	0.02	-	60	Hummocky shaped ripples.

Appendix 5B

Bedform Measurement Maps

WAIHI

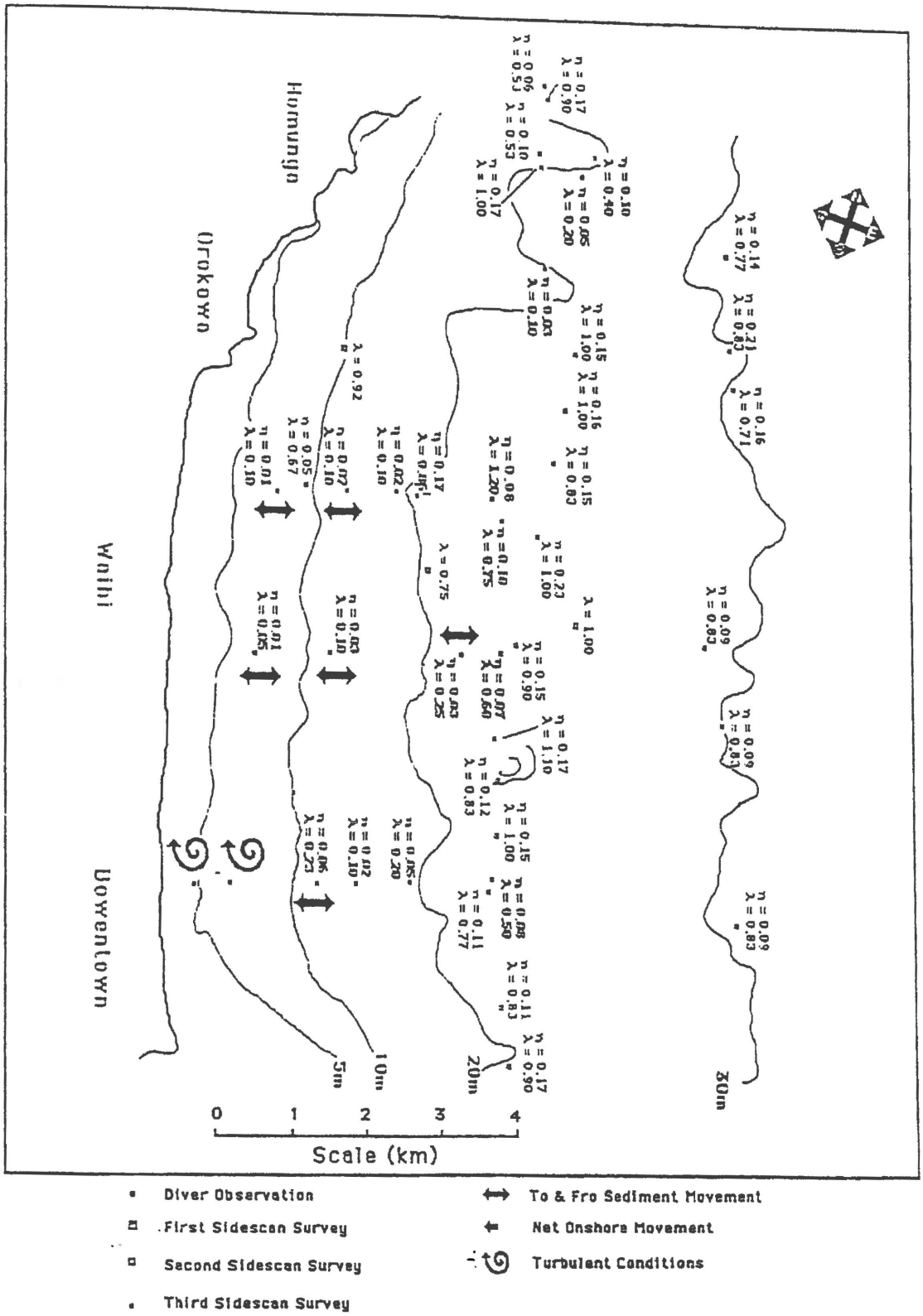

Bedform measurements from diver observations and side-scan sonographs at Waihi. Overlay shows bedform patterns and orientation.

WHIRITOA

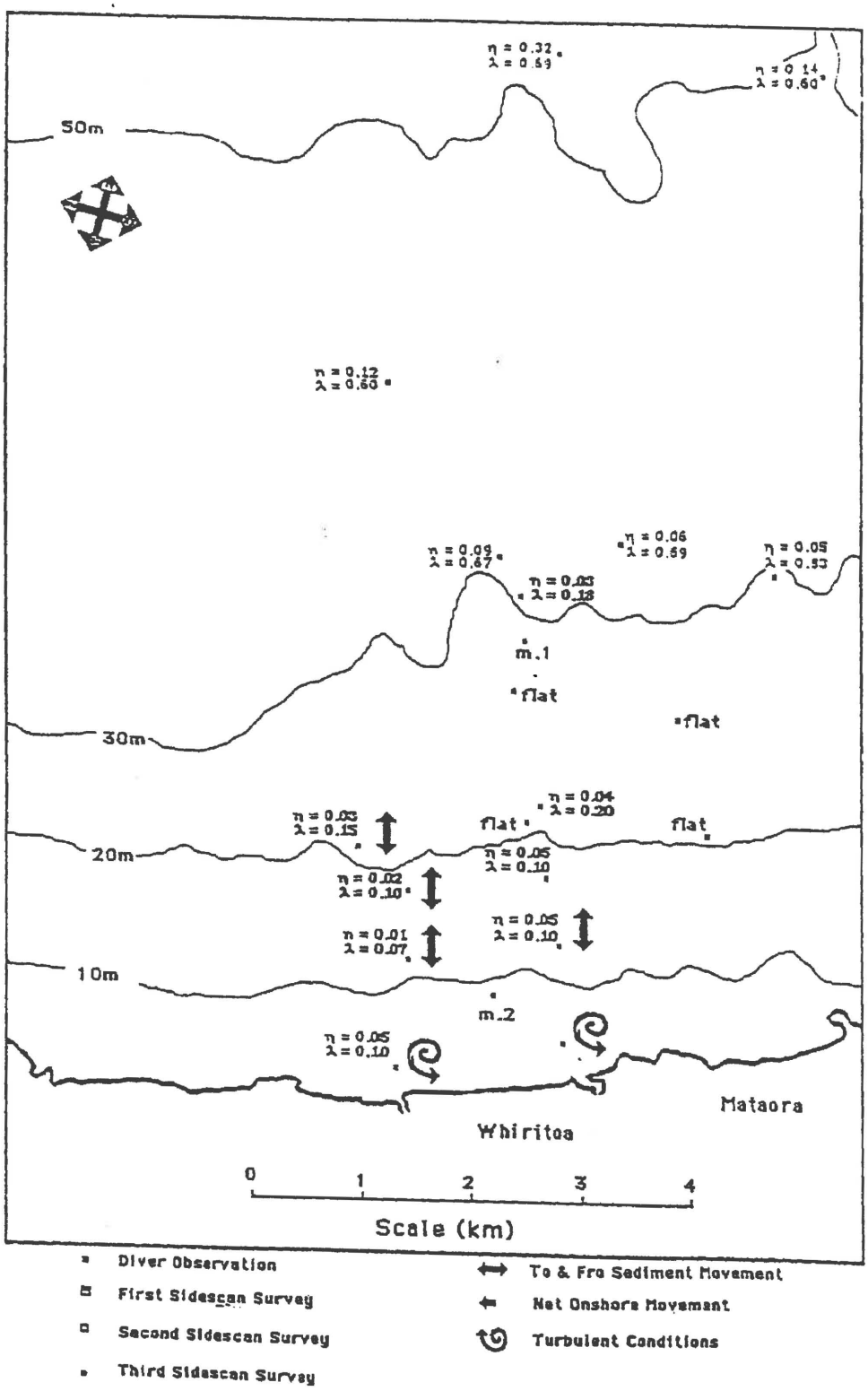

Bedform measurements from diver observations and side-scan sonographs at Whiritoa. Overlay shows bedform patterns and orientation.

WHANGAMATA

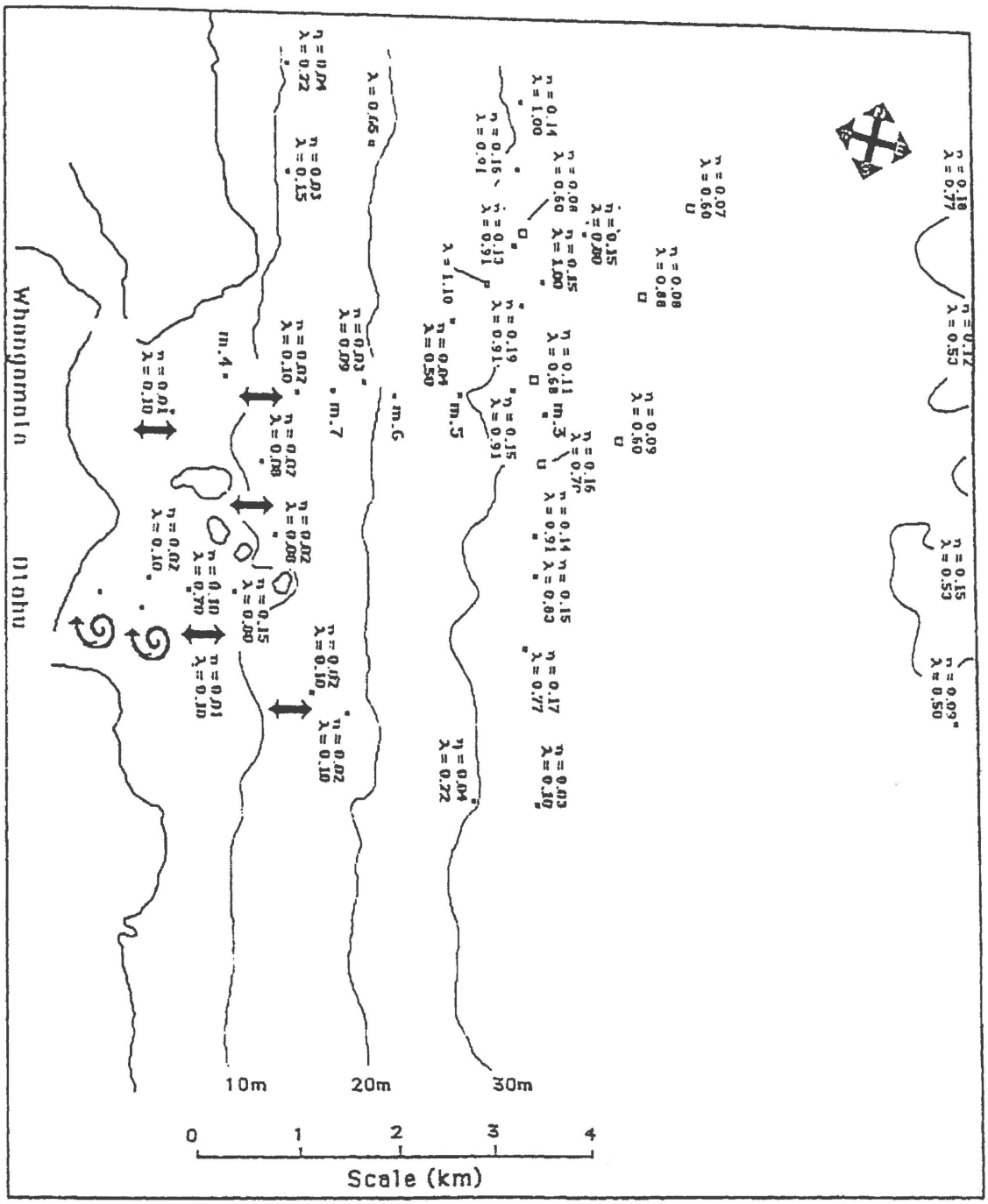

Bedform measurements from diver observations and side-scan sonographs at Whangamata. Overlay shows bedform patterns and orientation.

ONEMANA

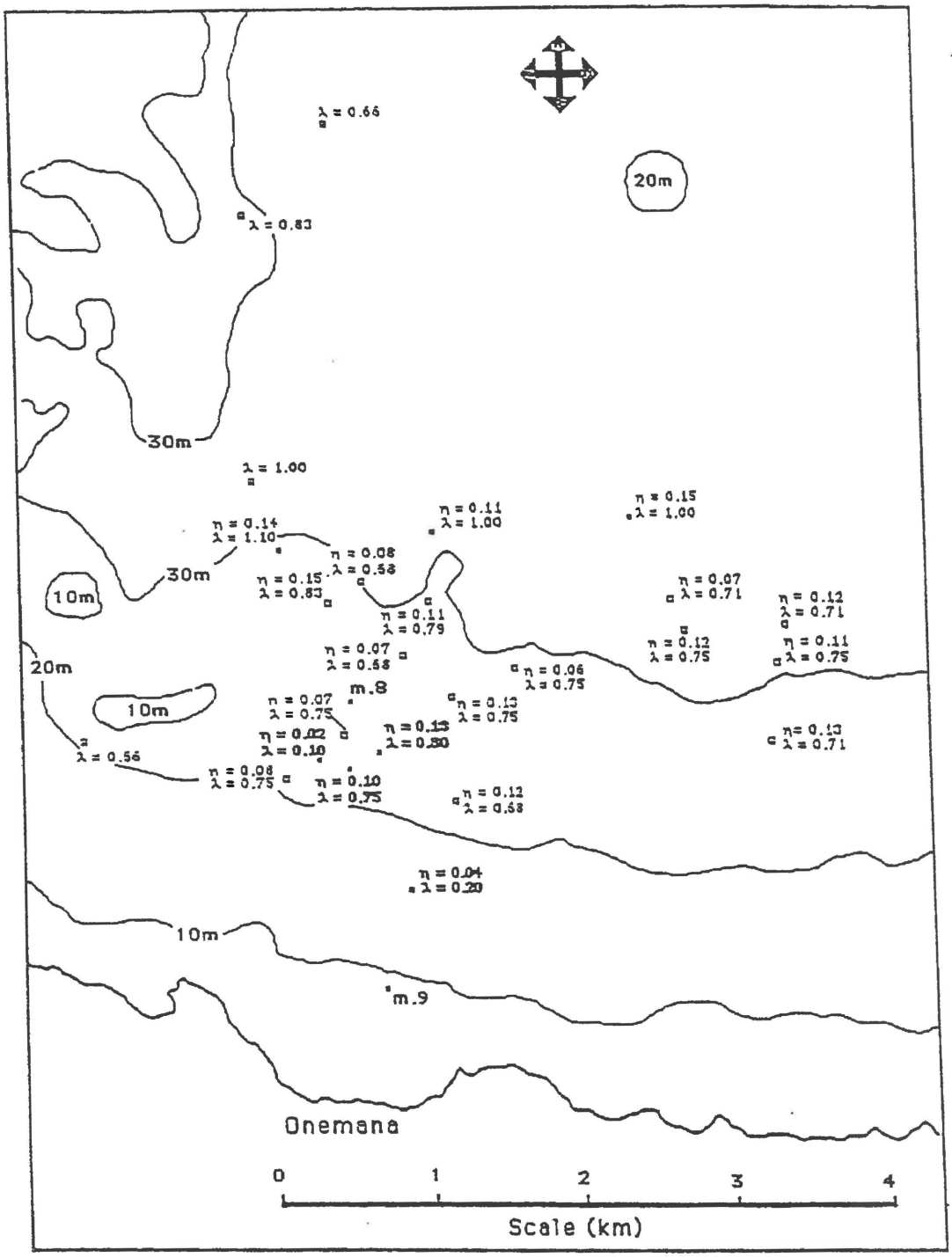

Bedform measurements from diver observations and side-scan sonographs at Onemana. Overlay shows bedform patterns and orientation.

OPOUTERE

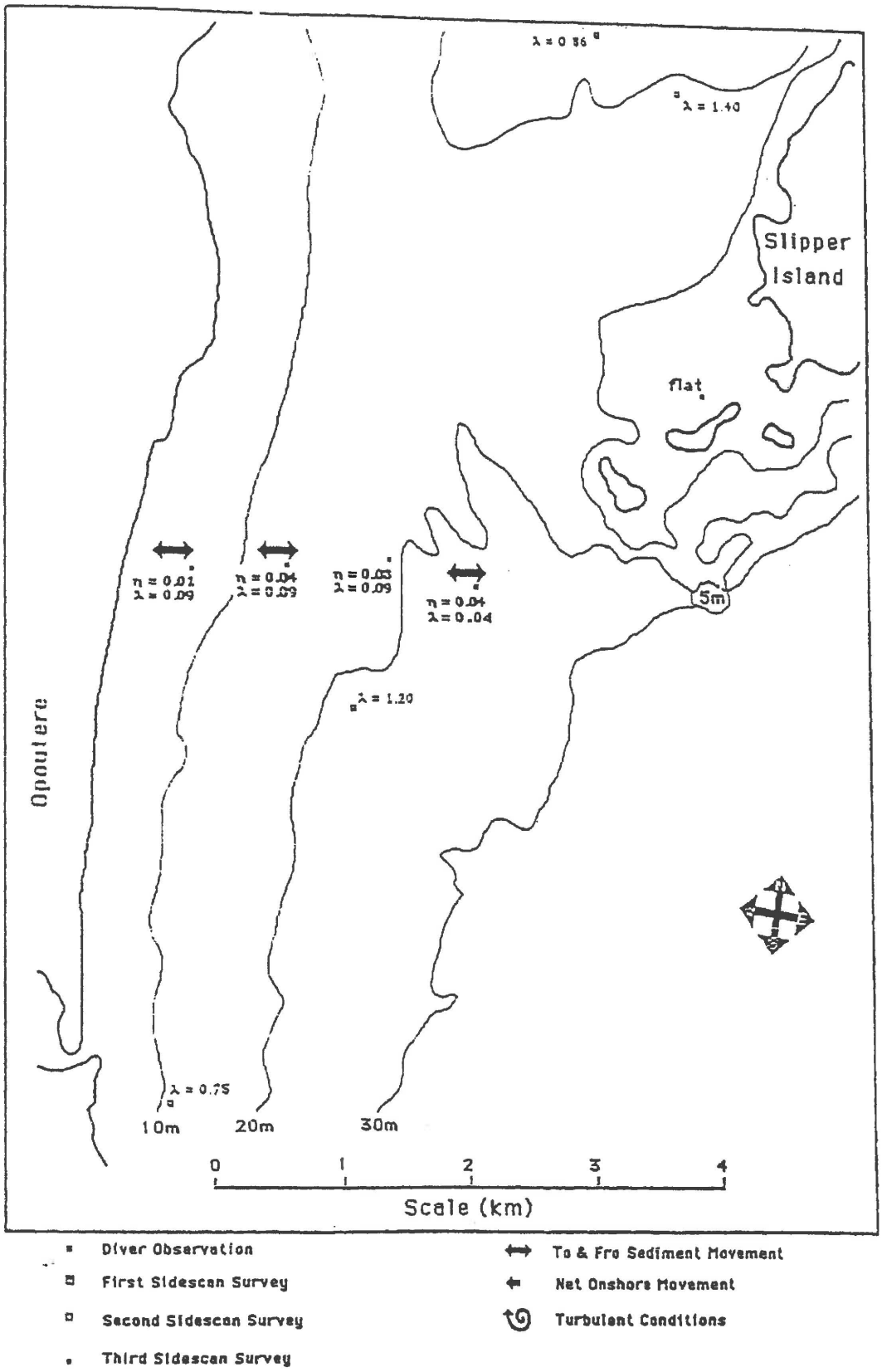

Figure 7.11. Bedform measurements from diver observations and side-scan sonographs at Opoutere. Overlay shows bedform patterns and orientation.

MERCURY BAY

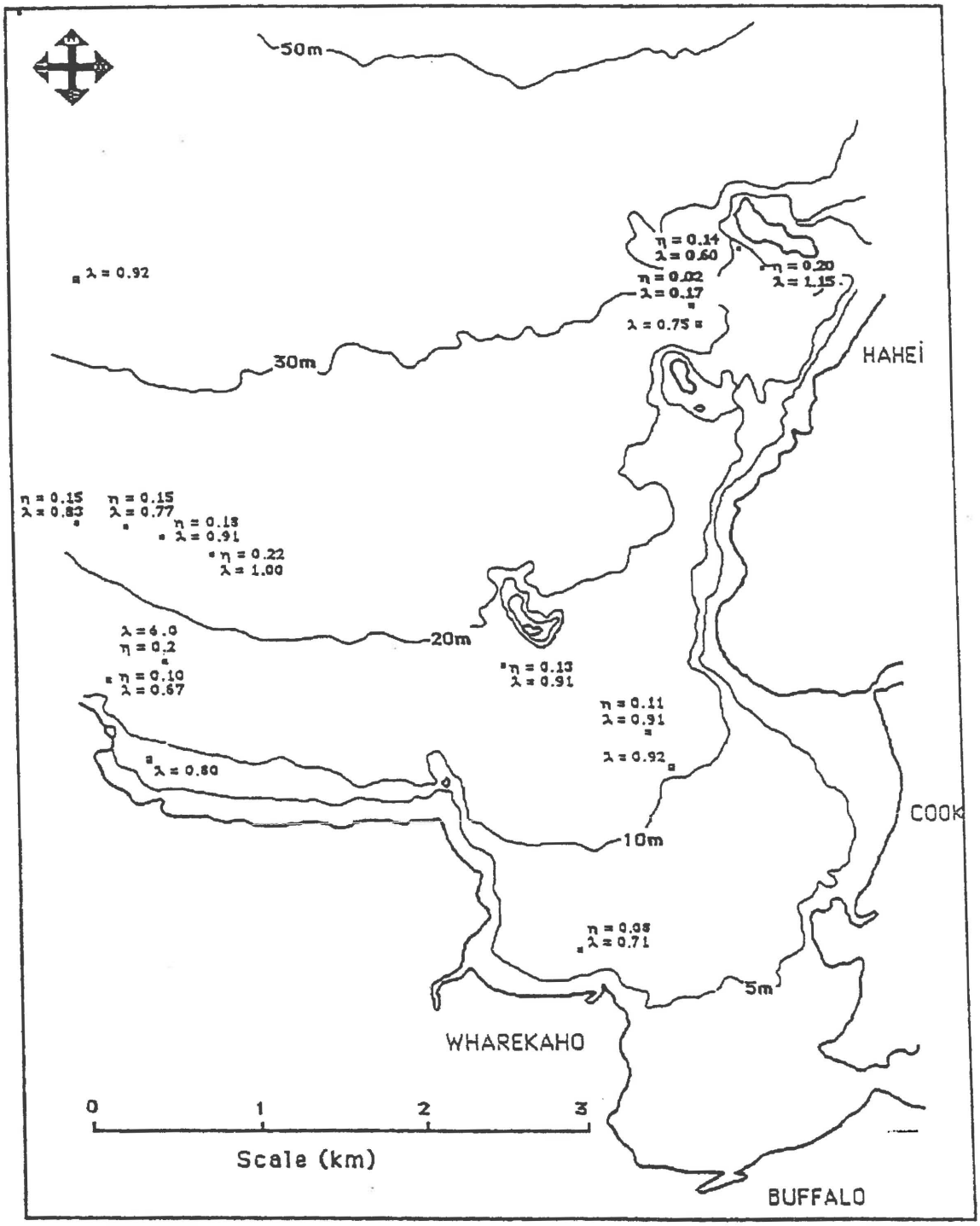

Bedform measurements from diver observations and side-scan sonographs at Mercury Bay. Overlay shows bedform patterns and orientation.

OTAMA

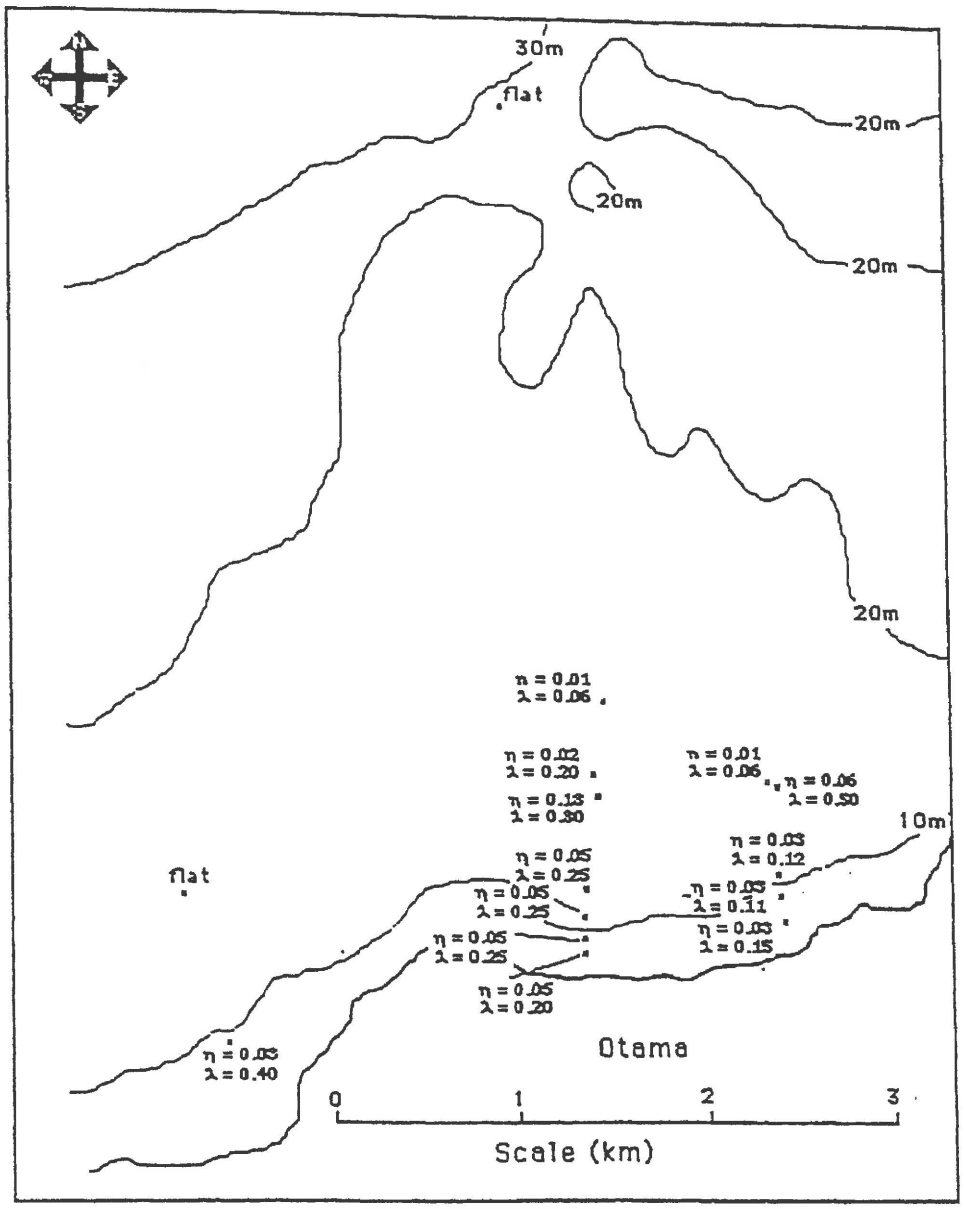

Bedform measurements from diver observations and side-scan sonographs at Otama. Overlay shows bedform patterns and orientation.

WHANGAPOUA

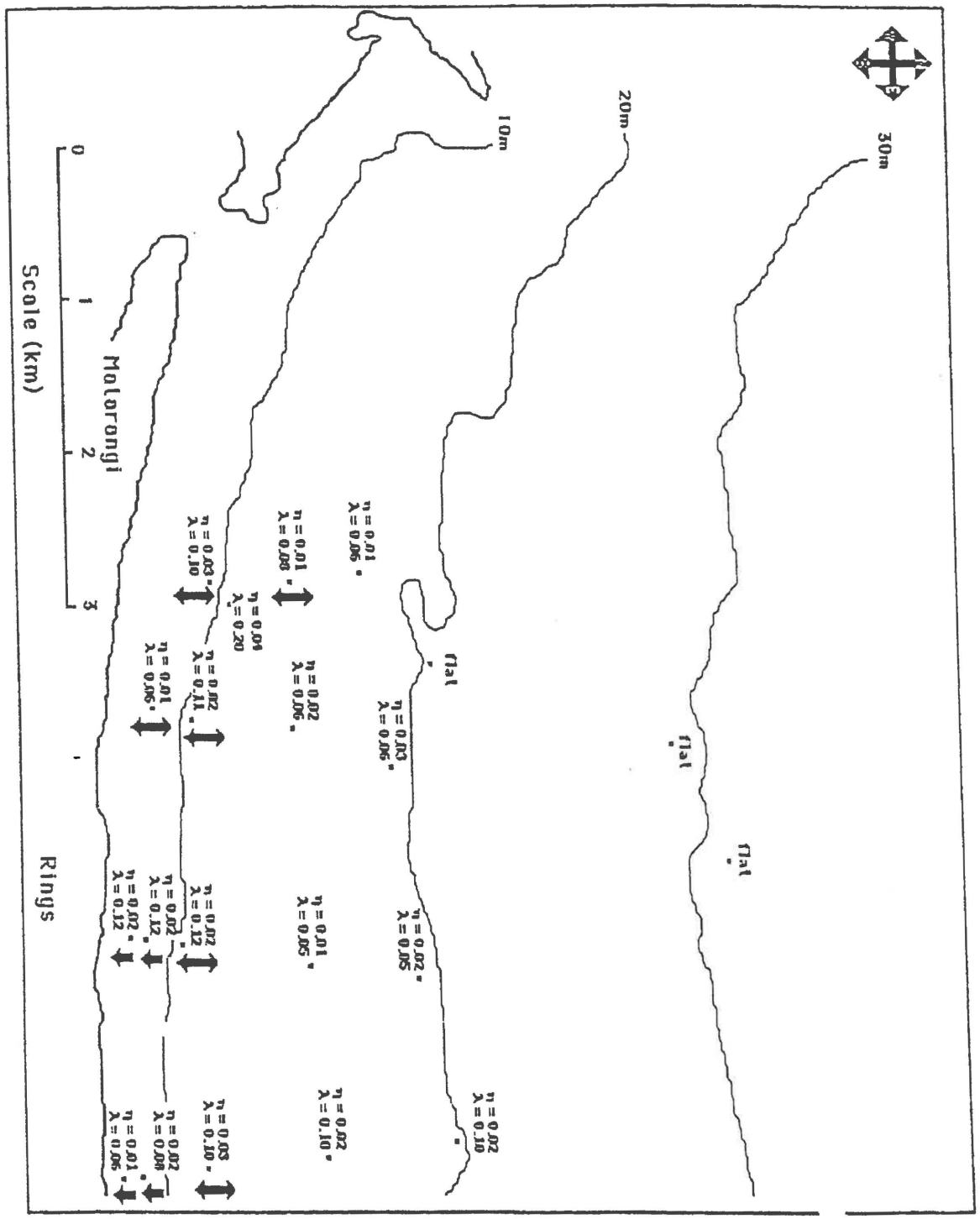

- Diver Observation
- First Sidescan Survey
- Second Sidescan Survey
- Third Sidescan Survey
- To & Fro Sediment Movement
- Net Onshore Movement
- Turbulent Conditions

Bedform measurements from diver observations and side-scan sonographs at Matarangi. Overlay shows bedform patterns and orientation.

APPENDIX 6

BOX CORE DATA

A-101

WAIHI BEACH

No	h	Length	Mean	Sorting	Core Description
241	10m	6cm	2.77	0.37	Homogeneous fine grained sand throughout. Brownish black sand, rare shells, bioturb.
242	24m	12cm	1.03	0.73	Contains c.15% lithic frags. and 25% shell frags., mainly at bottom. Anaerobic appearance below 10cm. Brown gray color.
243	20m	17cm	1.04	0.33	Abundant fine broken shell (c.40%), with some large frags and whole shells. Sand has yellowish brown appearance.
244	26m	14cm	1.04	0.58	Contains c.20% broken shell and 20% whole cockle shells. No stratification. Yellow brown color, pink algae on some shells.
245	32m	13cm	0.92	0.72	Contains c.20% lith. frags., 25% shell frags. and 10% whole cockles and pectens. No strat, y.brown color, algae on shells.
246	27m	28cm	-0.05	0.35	Brown sand with FeO staining on granules. Slight strat. below 20cm of whole cockles and pectens. Slightly muddy below 25cm.
247	17m	-	2.75	0.49	Homogeneous fine sand. Some broken fine shell frags overlying 4-5cm layer of whole cockle shells. Brownish black appearance.
248	11m	5.5cm	2.78	0.33	Homogeneous fine sand. No stratification. Few whole cockles present. Brownish black appearance.
249	28m	12cm	1.16	0.58	Homogeneous medium sand. Abundant lithic frags. and disarticulated cockle shells. Yellowish gray appearance.
250	34m	13cm	0.89	0.61	Homogeneous coarse sand. Numerous broken shell fragments present. Brownish gray appearance.
251 251A 251B	45m - -	15cm - -	0.94 1.43 0.97	0.52 0.95 0.93	Two layers present; top 8cm medium snad, bottom layer coarse sand. Shell frags. and whole pectens present. Osidian in lower layer. Brownish gray appearance.
252 252A 252B	51m - -	23cm - -	0.93 0.35 1.43	0.86 1.01 0.95	Two distinct layers. Top 10 cm coarse clean brownish gray sand, with numerous shell frags and obsidian. Sharp contact with medium gray muddy (10%) sand layer.

WAIHI BEACH

No	h	Length	Mean	Sorting	Box Core Description
253A 253B 253C	63m - -	20cm - -	0.67 0.37 0.26	0.73 1.20 0.93	Top 4cm mod.sorted, 5.1% mud with abundant lithic grans. and whole pecten shells. Next 7cm poorly sorted, 4.9% mud. Remainder mod.sorted 9.1% mud. Gray color.
254	81m	8cm	1.49	1.96	Poorly sorted medium muddy (8.9%) sand with gravel clasts. Olive brown color.
255	100	20cm	1.68	0.98	Poorly sorted medium muddy (7%) sand. Layers of lithic frags., pumice and shells in bottom 2cm layer. Olive brown color.
256A 256B 256C	190 - -	12cm - -	2.78 3.01 2.88	0.33 0.31 0.38	Upper 3cm fine poorly sorted muddy (11.2%) sand. Next 7cm medium very poorly sorted muddy (12%) sand. Rest fine well sorted muddy (11%) sand. Olive brown color.

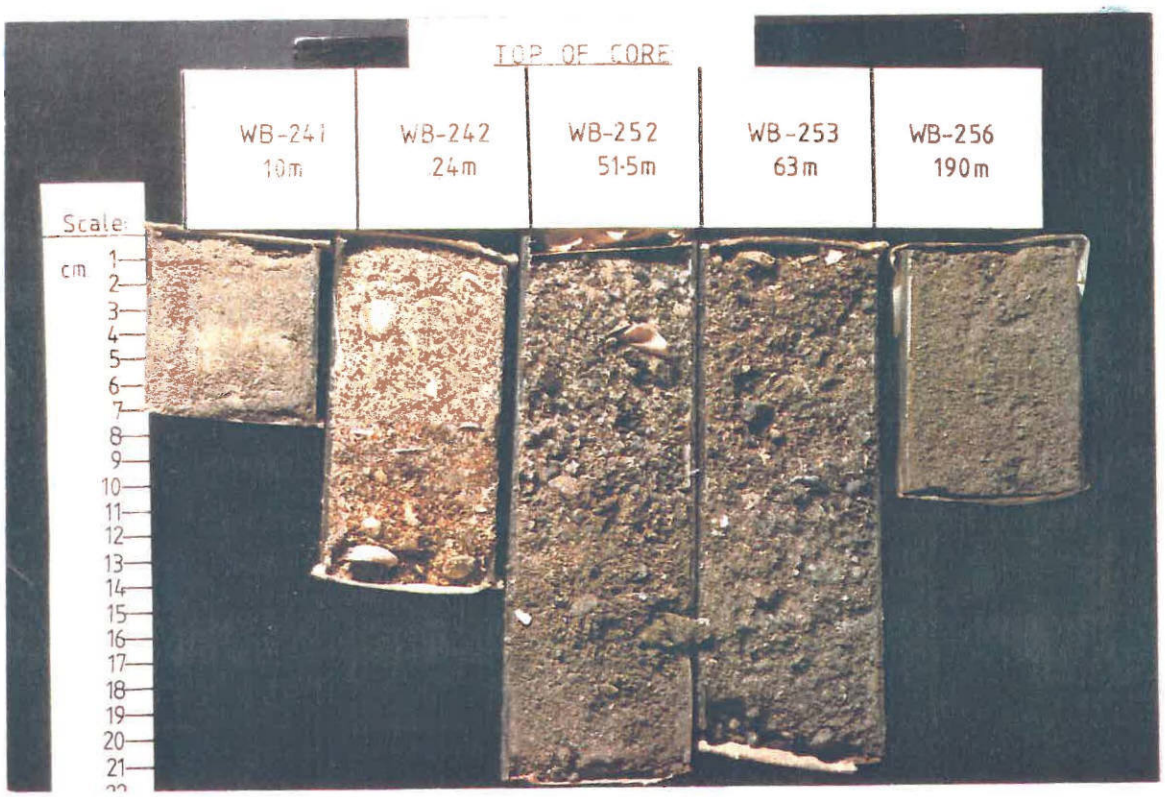

A-103

WHIRITOA

No	h	Length	Mean	Sorting	Box Core Description
192/ 193	40m	10cm	2.24	0.43	Homogeneous fine clean sand. Large shell fragments and some whole shells present.
201/ 202	43m	10cm	0.95	0.98	Mixture of shell hash and coarse sand. Thin wedge of fine sand overlying coarse on surface. Whole pectens and lith.grans.
217	24m	10cm	2.22	0.48	Two layers present. Top 8cm brown colored sand with numerous worm casts. Beneath unit of broken cockle shells and gray sand.
220	29m	12cm	2.10	0.60	Fine gray colored clean sand. No strat. Worm casts and live cockles present on surface.
231	29m	12cm	2.21	0.47	Two layers. Top 7cm fine brown colored sand , cockles present. Lower 5cm gray green colored muddy anaerobic sand, no cockles.
232	25m	9cm	2.49	0.40	Two layers. Top 3cm fine brown colored , dead cockles and worm casts. Bottom gray green anaerobic, no cockles, organic traces
233	10m	10cm	2.10	0.44	From 0-3cm brownish colored sand with live Dosinia. Below changes to gray green colored sand. Few shell frags (c.2%).
234	37m	15cm	1.47	0.46	Homogeneous medium grained sand containing c.1-2% shell fragments.
235	44m	11cm	2.29	0.48	Homogeneous fine grained sand. Worm tubes present on surface.
236	49m	11cm	2.11	0.34	Homogeneous fine grained sand. Few organics and very few shell fragments present.

WHIRITOA

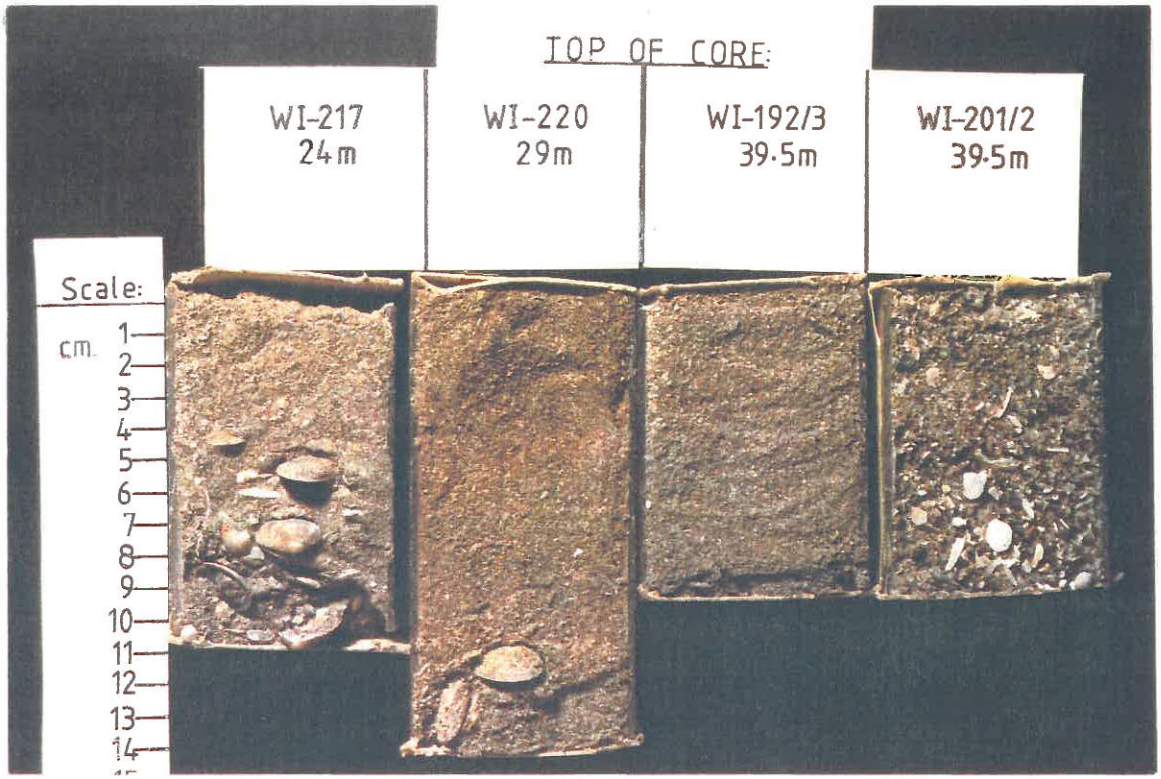
TOP OF CORE:
WI-217
24m
WI-220
29m
WI-192/3
39.5m
WI-201/2
39.5m
Scale:
cm.
1
2
3
4
5
6
7
8
9
10
11
12
13
14

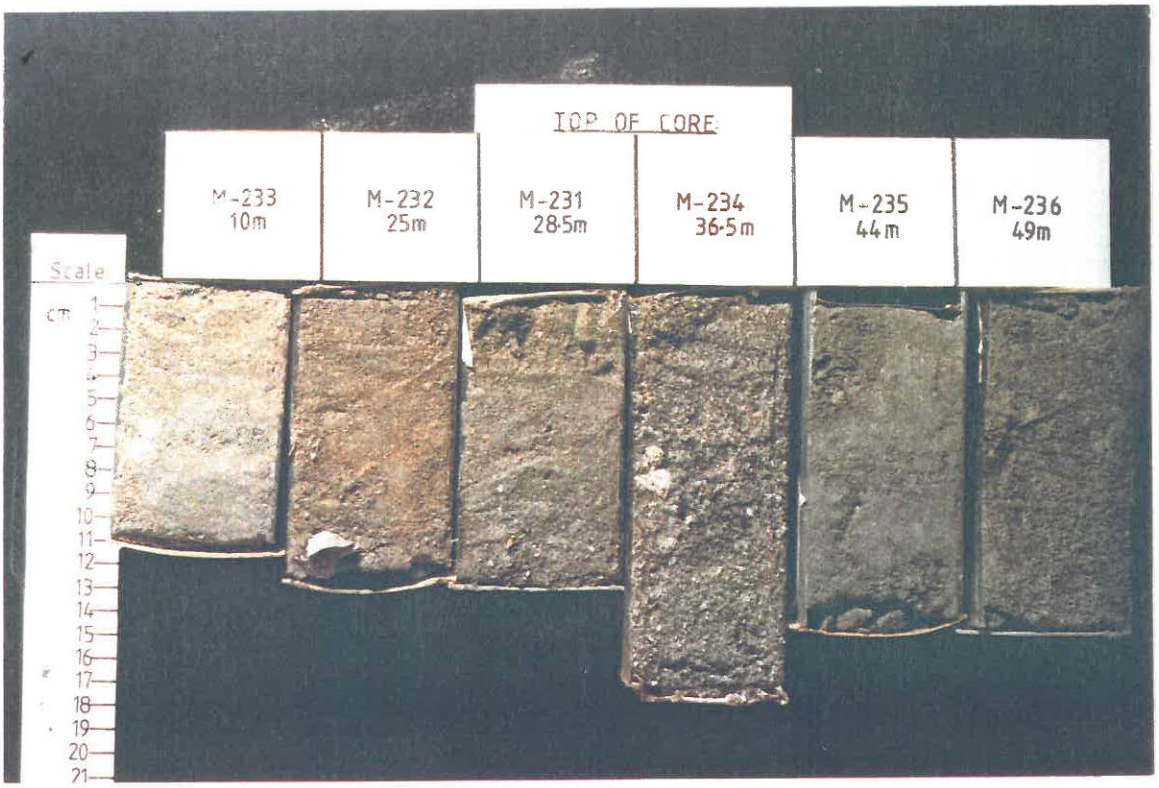
TOP OF CORE:
M-233
10m
M-232
25m
M-231
28.5m
M-234
36.5m
M-235
44m
M-236
49m
Scale
cm
1
2
3
4
5
6
7
8
9
10
11
12
13
14
15
16
17
18
19
20
21

WHANGAMATA

No	h	Length	Mean	Sorting	Core Description
173	32m	-	1.11	0.47	Uniform medium sand containing mainly shell frags & qtz grans. Core through seaward side of coarse-fine sand boundary
174	29m	10cm	1.31	0.45	Two layers, upper 5cm contains some shell frags., lower layer contains more shell frags with some whole pectens.
175	26m	12cm	2.17	0.47	Two layers, upper 10cm brown-gray colored sand & rare shell frags., lower 2cm grey-green sand with whole cockle shells.
176	10m	6cm	2.65	0.70	Massive gray-green compacted fine sand. Shell fragments common throughout and extensively biouturbated.
177	23m	8.5cm	2.31	0.59	Homogeneous fine sand. Slight layering of blue colored sediments just below surface . Occassional shell fragments.
178	39m	12cm	2.32	0.49	Uniform bioturbated fine sand throughout. Rare shell fragments present.
179	45m	15cm	0.14	0.74	Uniform coarse sand and granules throughout. Large pecten and cockle shell fragments in upper 8cm, mainly on surface
237	21m	7cm	2.79	0.72	Uniform fine gray-brown colored sand. No shell fragments present. Some mud present in sample (5%).
238	33m	-	0.12	0.88	Coarse sand and gravel throughout. Both whole and broken shell fragments present. Some mud in sample (3.8%).
239	42m	10cm	1.00	0.85	Large amount of coarse shell fragments and lithic granules. Small amount of mud present in sample (1.3%).
240	51m	-	2.75	0.55	Sample contains high percentage of mud (14.6%) and organic traces.

A-106

WHANGAMATA

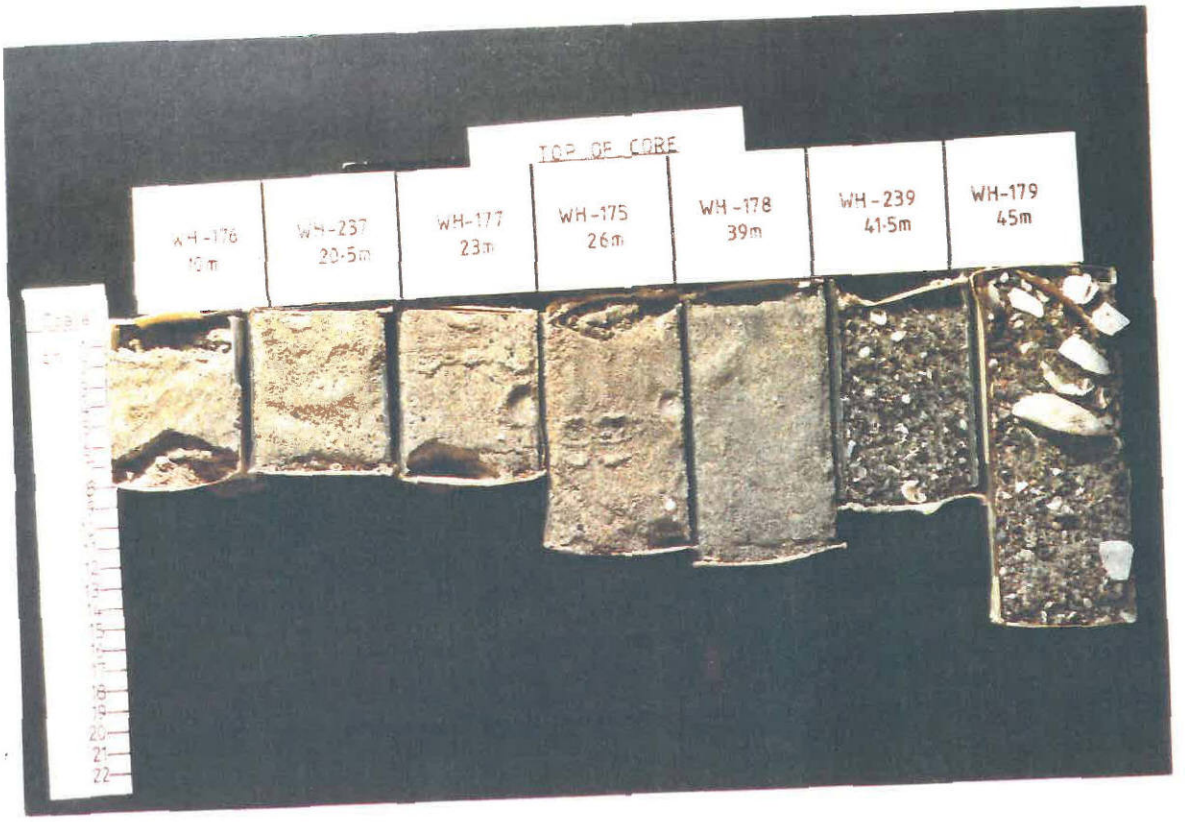

A-107

ONEMANA

No	h	Length	Mean	Sorting	Core Description
166	23m	-	2.60	0.55	Mainly fine gray sand with worm casts & some broken live shells on surface. Thin anaerobic layer evident in core.
167	24m	19cm	0.93	0.69	Sample taken through large finger of coarse sand surrounded by fine. Fine/ coarse sand laminations evident in core.
168	10m	15cm	2.43	0.61	Two zones evident. Upper 9cm fine brown colored sand with c.5% shell. Lower 6cm blue-gray anaerobic sand & whole shells.
169	31m	16cm	0.38	0.41	Core composed of coarse sand and shell hash with some whole scallop shells present.
170	34m	-	-	-	Box core returned bent. Echo sounding trace showed evidence of reef.
171	41m	-	-	-	Box core returned with thin veneer of sand overlying bedrock. Trace showed evidence of reef.
172	45m	15cm	1.84	0.61	Core composed of fine-medium sand and broken shell throughout.

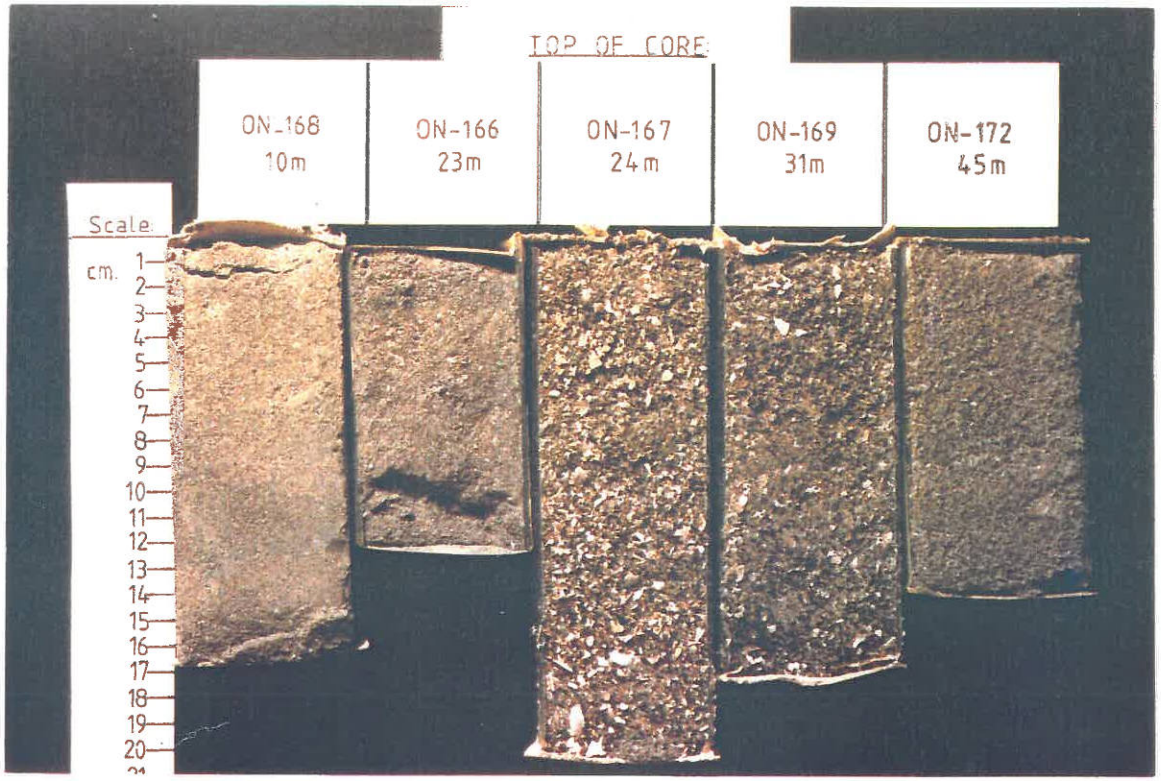

OTAMA-WHANGAPOUA

No	h	Length	Mean	Sorting	Box Core Description
142	10	8cm	2.41	0.58	Mostly composed of non-cohesive, brownish colored sand with very few shell fragments present.
145	21	10cm	2.28	0.45	Two layers present. First 0-5cm brown aerobic sand. Next 5cm gray-green anaerobic sand with layer of cockles.
147	30	15cm	2.78	0.54	Two layers present. First 5cm brown aerobic sand with worm casts present. Next 10cm anaerobic sand with abundant shell frags.
149	40	20cm	3.05	0.57	Very fine, slightly muddy (1.6%) sand with sparse shell fragments throughout.
155	10	9cm	1.35	0.50	Two layers. First 5cm light brown sand and shell frags. Next 4cm finer black anaerobic sand with shell increasing down (5-50%).
156	20	12cm	0.53	0.50	Surface covered in layer of dog cockles, wich overlies a shell lag deposit & then a shell hash layer.
157	30	10cm	1.82	0.56	Two layers. First 4cm medium grained very compact shell hash layer, mainly worm tubes . Next 6cm darkens, to anaerobic conditions
158	40	30cm	2.61	0.81	Two layers. First 4cm fine silty sand. Next 26cm finer gray-green anaerobic sand layer containing some shell.

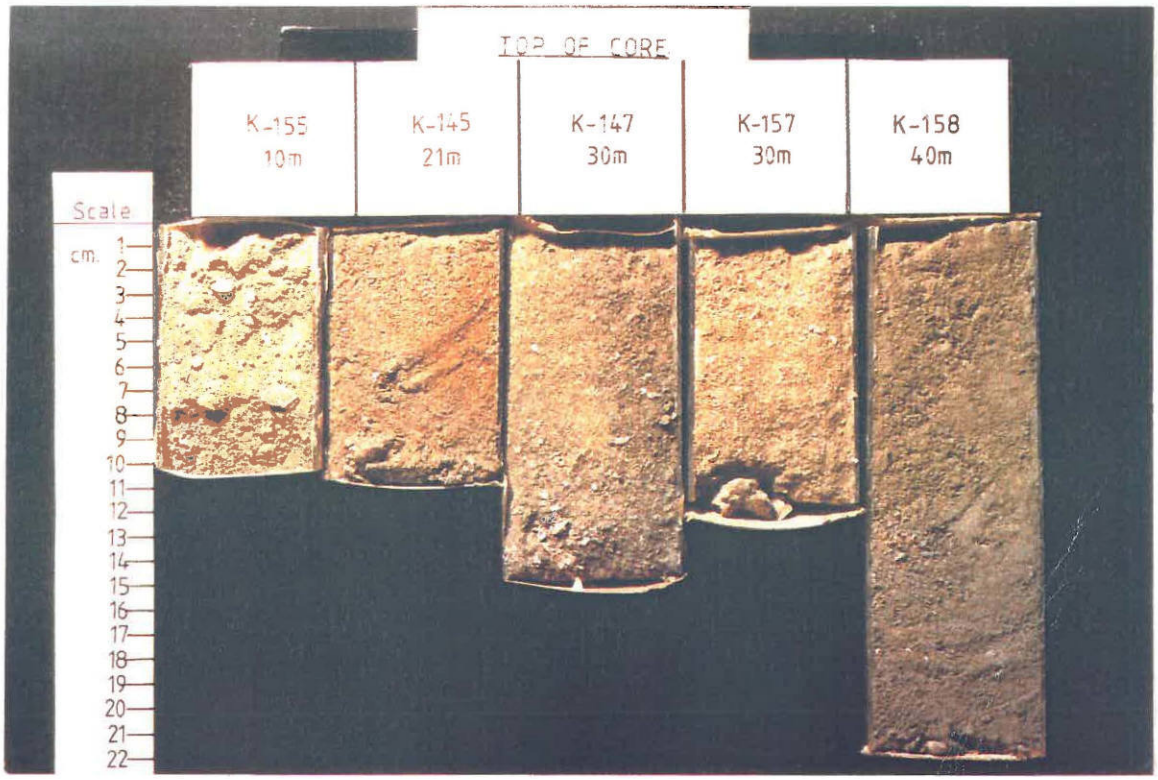

APPENDIX 7

RADIOCARBON DATES

Wk-: 843 ONC1

Conv Age (SE): 3700 ± 60
True Age (SE): 3800 ± 60
$\delta^{13}C$: +1.4

Nature of sample: Shell hash (80% biv,15% barn,2% gastro,2% rock frags,1% bryo)
Collected by: P.Dell 1985
Submitted by: P.Dell
Earth Sciences,Univ.of Waikato,PB,Hamilton,NZ
Geographic location: From 23m depth off Onemana Beach, E.Coromandel,NZ
Lat.& Long.or G.R.: 37°8'36"S;175°54'E
Comments: *SITE ON-257*
Sig:

Wk-: 844 WHC1

Conv Age (SE): 2910 ± 50
True Age (SE): 3000 ± 50
$\delta^{13}C$: +3.0

Nature of sample: Shell hash (75% biv,10% gastro,10% bryo,2% rock frags)
Collected by: P.Dell 1985
Submitted by: P.Dell
Earth Sciences,Univ.of Waikato,PB,Hamilton,NZ
Geographic location: From 33-35m depth off Whangamata Beach, E.Coromandel,N
Lat.& Long.or G.R.: 37°12'6"S;175°55'18"E
Comments: *SITE WH-272*
Sig:

Wk-: 845 WIC1

Conv Age (SE): 3730 ± 60
True Age (SE): 3840 ± 60
$\delta^{13}C$: +2.4

Nature of sample: Shell hash (90% biv,7% barn,2% gastro,1% rock frags)
Collected by: P.Dell 1985
Submitted by: P.Dell
Earth Sciences,Univ.of Waikato,PB,Hamilton,NZ
Geographic location: From 33m depth off Whiritoa Beach, E.Coromandel,NZ
Lat.& Long.or G.R.: 37°16'30"S;175°56'50"E
Comments: *SITE WI-271.*
Sig:

WHIRITOA RADIOCARBON SAMPLE

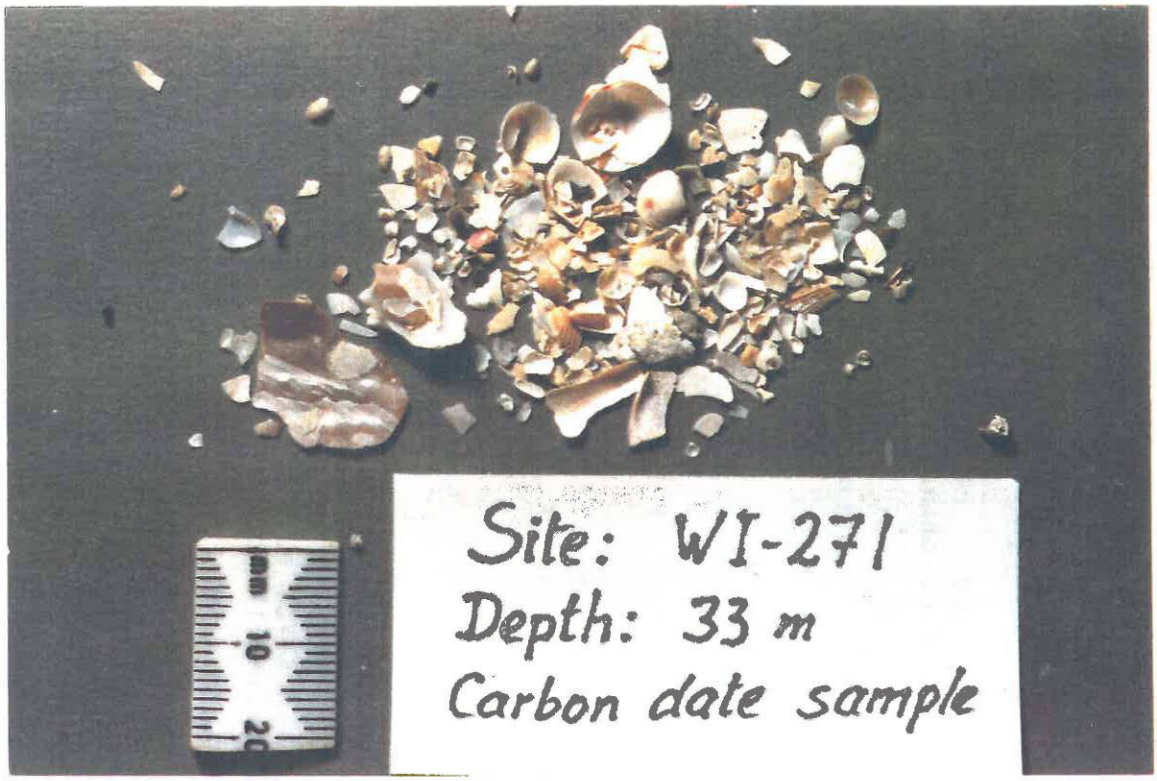

WHANGAMATA RADIOCARBON SAMPLE

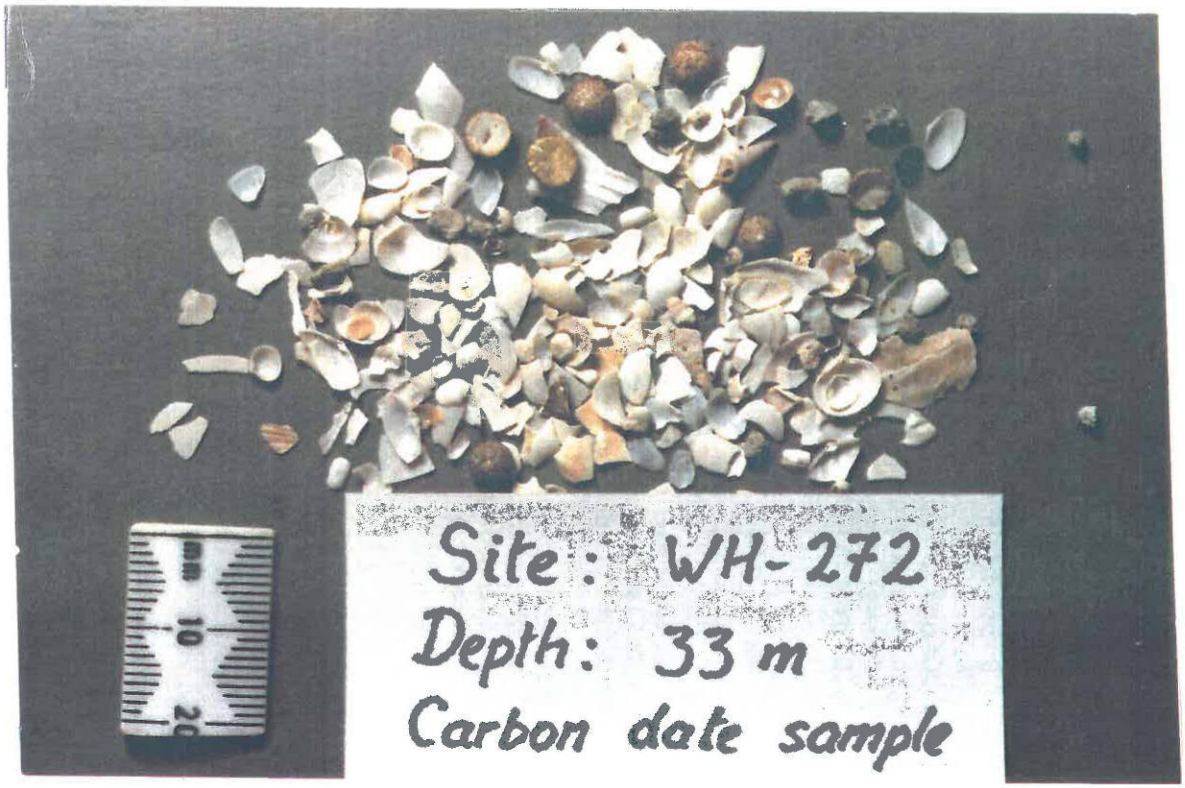

A-111

ONEMANA RADIOCARBON SAMPLE



APPENDIX 8

SEDIMENT MINERALOGY

Appendix 8A

2-4 ϕ Sand Fraction

SAMPLE	ENVIRONMENT	QUARTZ	PLAGIOCLASE	K FELDSPAR	LITHICS	GLASS	HEAVIES
WB294	RIVER	6.4	27.7	0	22.8	22.5	20.6
WB295	RIVER	6.3	13.6	0	31.1	19.4	29.6
WB324	BEACH	1.5	1.9	0	0	6.3	90.3
WB554	BARRIER	18.5	49.7	0.3	6.8	9.4	15.6
WB12	BEACH	14.7	57	0	15.4	11	1.8
WB14	SHELF(6.5M)	19.1	31.4	0	17.8	30.7	2.7
WB247	SHELF(16M)	4.7	41.9	0.3	15.9	32.9	4.7
WB246	SHELF(26M)	10.8	28.9	0	17.1	22.2	21
WB250	SHELF(34M)	13	56.3	1.2	8.7	5.6	16.4
WB254	SHELF(81M)	8.7	22.3	0	36.4	28.9	3.8
WB256	SHELF(200M)	5.4	9.7	0	30	53.1	1.8
WB551	RIVER	3	12.7	0	24.2	5.8	54.2
WB552	BEACH	9.7	54.4	0.7	10.8	11.4	13.7
WB550	BEACH	10.8	66	0	7.6	7.3	15
WB553	PL.BARRIER	4.5	9.4	0	6.7	2.7	76.7
WI296	RIVER	4.7	15.8	0	45.5	20.2	10.4
WI558	BARRIER	17.9	30	0.3	0.7	8.6	42.1
WI289	BEACH	0.7	1.4	0	0	5	92.4
WI35	SHELF(6.5M)	7.6	16.4	0	9.1	65.2	1.8
WI213	SHELF(19M)	10.8	31.2	0	12.9	44.8	0.4
WI208	SHELF(34M)	24.9	54.5	0	12.5	5.4	2.7
WI206	SHELF(38M)	24.2	47.5	0.3	20.2	6.1	2
WI203	SHELF(42M)	16.5	57.4	1.4	13.7	6.9	5.5
WI199	SHELF(51M)	25.2	39.6	0.3	20.8	9.6	4.8
M233	SHELF(10M)	1.4	8.1	0	11.6	78.6	0.4
M231	SHELF(28.5M)	21.4	55.2	0.7	10.7	7.1	5.7
M234	SHELF(36M)	12.3	48.1	0	14	16.9	5.5
M236	SHELF(49M)	10.1	60.7	1.3	12.9	13.2	3.3
WH297	RIVER	7	28.5	0	29.1	14.5	20.9
WH298	RIVER	28.5	23.1	0	9.5	4.1	35.5
WH299	RIVER	12.5	12.5	0	54.9	16.3	3.8
WH548	BARRIER	19.5	58.8	1.6	12.3	6.6	2.8
WH283	BEACH	24.7	51.3	0	8.5	6.7	8.7
WH37	ETD	12.3	49.2	0.6	26.5	12.3	2.8
WH176	SHELF(10M)	8.6	30.9	0	16.3	43.3	0.9
WH177	SHELF(23M)	7	44	0	18.3	25.4	5.3
WH63	SHELF(24M)	5.5	40	1.5	11.3	9.1	34.2
WH179	SHELF(45M)	12.7	43.3	0.3	12.7	18.2	13
ON560	RIVER	16.7	29.4	0	31.3	7.7	14.9
ON547	BARRIER	13.2	29.4	0.3	10.6	16.5	30.4
ON278	BEACH	26.5	51.6	0	17.7	3.5	0.7
ON259	SHELF(5M)	15.6	42.4	0.3	24	14.3	3.8
ON263	SHELF(13.5M)	10.9	32.4	1.2	16.2	38.2	2.4
ON267	SHELF(24M)	22.3	34.4	0.3	13.4	11.5	18.5
ON171	SHELF(41M)	6.5	21.7	2.6	10.3	58.7	2.9
ON172	SHELF(45M)	14.2	48.8	1	17.8	6.3	13.2
OP300	RIVER	17.3	16.9	0.3	37.4	19.4	9
OP545	PL.BARRIER	32.4	30.4	0	9.4	16.2	11.5
OP546	BARRIER	32.4	39.5	0	16.2	8.5	3.4
OP556	BEACH	28.2	44.7	0	14.12	11.2	1.7
OP544	BEACH	25	49.7	0.7	23.6	0.4	1.4
OP121	SHELF(8M)	15.7	37.7	0	23.8	21.4	1.4
OP120	SHELF(16M)	9.6	51.6	0.6	21.8	14.4	2.6
OP119	SHELF(27M)	5.3	29.5	0	14.3	51.2	1.6
OP117	SHELF(37M)	18.3	46.6	0	19.3	13.1	2.8
TP301	RIVER	1.9	11.7	0	75.9	9.4	1.1
TP543	BARRIER	25.8	26.7	0.9	10.4	10.7	26.4
TP540	BARRIER	12.7	9.9	0	10.6	9.9	57
TP542	BEACH	31	43.2	0.6	17.2	6.6	2
TP541	BEACH	31.5	41.3	1	19.8	5.4	2
TP539	BEACH	27.4	26	0	37	6.1	3.8
TP111	SHELF(10M)	12.9	33.3	0.3	22	32.4	2.6
TP112	SHELF(10M)	17.2	41.7	0.3	21	16.9	3.1

SAMPLE	ENVIRONMENT	QUARTZ	PLAGIOCLASE	K FELDSPAR	LITHICS	GLASS	HEAVIES
TP113	SHELF(23M)	8.2	32	1.3	17.1	39.5	2.6
TP114	SHELF(29M)	17.6	35.4	0.9	16.3	25.1	5.6
HW302	RIVER	5.7	13	0.8	64.4	12.1	5.3
HW561	RIVER	7.2	12.7	0	28.8	6.2	45.1
HW537	BARRIER	1.9	7.8	0	14.8	9.8	65.6
HW538	BEACH	8.3	26.6	0	53.2	2.2	9.7
HW325	BEACH	12.7	25.4	0	48.1	3.1	10.8
HW132	SHELF(10M)	6.8	21.7	0	57.4	8.5	5.5
HW133	SHELF(20M)	11.8	25	0.7	46.3	6.8	10.1
HW135	SHELF(40M)	5.3	8.7	0	32.7	50	3.3
HW136	SHELF(50M)	8.1	27.8	0	9.3	52.4	2.4
HA303	RIVER	25.2	19	0.3	24.2	21.8	9.8
HA536	BARRIER	19.7	21.6	0.3	20.3	9.2	29.2
HA327	BEACH	11	17.5	0	67.5	2.9	1
HA137	SHELF(9M)	10	24.9	0.3	51.4	6.4	7.5
HA138	SHELF(12M)	15	22.4	0	42.5	7.4	12.7
HA139	SHELF(13M)	17.8	25.3	0.3	35.3	13.7	7.9
HA140	SHELF(9M)	8.6	39.4	0.3	33.3	14.4	4.3
MB304	RIVER	17.5	16.7	0.3	43.2	17.5	5
MB557	RIVER	8.7	60.6	0	8.7	13.9	8
MB305	RIVER	8.7	14.6	0	58.7	13.4	4.7
MB306	RIVER	1.5	13.4	0	70.3	11.2	3.7
MB306B	RIVER	3.4	10.7	0	61.1	5	19.8
MB307	RIVER	4.9	13.3	0	64.2	7.7	11.4
MB308	RIVER	3.4	7.2	0	76.4	4.8	8.2
MB309	RIVER	3.5	6.6	0.3	58	31.1	0.7
MB535	BARRIER	21.1	16.2	0.6	12.1	5.2	45.4
MB533	BARRIER	29.7	31.8	0.6	28.2	5	5.3
MB530	BARRIER	19.9	8.9	0	25	1.6	44.6
MB534	BEACH	3	11.6	0	54.9	29.9	0.6
MB323	BEACH	22.6	31.4	0	34.8	3.4	7.8
MB532	BEACH	20.6	27	0.6	42.1	6.8	3.5
MB531	BEACH	24.8	34.7	0.3	25.4	3.6	11.6
MB97	SHELF(11M)	5.8	25.1	0.7	40.7	23.7	4.7
MB96	SHELF(12M)	4.5	19.9	0	41.6	30.4	3.5
MB93	SHELF(16M)	4.5	13.8	0.3	41.2	37.5	3.1
MB90	SHELF(10M)	14.3	36.3	1	36.9	6.4	6.1
MB104	SHELF(32M)	4.4	15.6	0	32.1	45.4	2.5
OP527	RIVER	11.3	5.3	0.3	53.3	2.7	27.3
OPB526	BARRIER	28.7	47.3	0.3	10.4	4.7	8.9
OPB528	BEACH	21.7	44.2	1.4	24.2	8.2	1.6
OPB328	BEACH	11.8	45.3	0.3	18.9	23.6	2
OPB329	SHELF(25M)	11.2	19.1	0.3	50.9	18.1	2.5
KB311	RIVER	25.9	30.7	1	30.4	5.5	7.4
KB312	RIVER	45.3	23.3	0.3	28	1.3	2
KB523	RIVER	19.1	42.7	0.6	16.2	9.7	12.3
KB314	RIVER	5.3	4.6	0	79	5	6
KB315	RIVER	3.1	6.9	0	84.7	0.4	5
KB319	PLBARRIER	25.3	60.9	0	0.86	4.3	8.6
KB320	PLBARRIER	21.5	55.3	0.3	7	1.7	14.6
KB529	BARRIER	22.5	54.2	0.9	5.7	10.8	10
KB525	BARRIER	28.4	43.6	0	8.7	4.9	14.4
KB524	BARRIER	27	51.5	0.6	8.5	6.6	6.3
KB317	BARRIER	27.3	55.5	0.3	8.9	4.5	3.9
KB322	BEACH	19.2	39.5	0.7	3.5	2.8	35
KB509	BEACH	24.2	68.3	0.7	4.6	2.1	0.7
KB321	PLBEACH	9.1	25.9	0	1.8	2.6	60.6
KB511	BEACH	24.5	47.8	0.6	14.8	11.9	0.9
KB510	BEACH	32.3	50.6	0.3	11.3	4.4	1.5
KB512	BEACH	19.8	50.1	0.9	18	10.8	0.6
KB318	BEACH	19.7	59.1	1.8	12.9	7.2	1.1
KB496	SHELF(11M)	15.5	50.9	1.2	9.6	12.4	11.5
KB375	SHELF(16M)	17.8	53.1	1.4	18.2	7.9	3.1

KB154	SHELF(18M)	16.2	66.7	1.3	3.6	9.9	3.6
KB142	SHELF(10M)	17.8	49.3	0	18.1	12.8	1.9
KB145	SHELF(21M)	18.2	52.7	0.6	19.4	9.4	0.3
KB330	SHELF(30M)	13	36.4	0	14.2	35.1	1.3
KB156	SHELF(20M)	20.6	58.8	0.3	12.2	5.7	2.7
KB165	SHELF(22M)	21.6	57.2	1.1	8.6	9.3	3.3
KB148	SHELF(35M)	6.3	22.4	0.3	22.4	49.2	0
WP316	RIVER	4.1	4.1	0	71	5	16.1
WP521	BARRIER	18.3	49.1	0.3	6.6	9.3	16.6
WP522	BEACH	22.2	57	1.1	11.9	7.4	1.5
WP452	SHELF(8M)	17.8	50.7	0.6	18.4	10.2	3
WP446	SHELF(17M)	23.5	49.5	1.4	18.6	6	2.5
WP442	SHELF(25M)	14.4	53	0	21.1	10.5	1
KDB520	RIVER	18.7	32.6	0.8	31.3	6.4	11
KDB518	BARRIER	22.9	21.2	0.7	52.6	2.7	0.7
KDB519	BEACH	14.6	40.3	0.9	35.8	6	3.3
WAB515	RIVER	11.7	3.8	0.3	73.2	3.2	8.2
WAB517	BARRIER	16.7	25.1	0.3	45.3	5.2	7.7
WAB516	BEACH	12.2	36.1	0.6	45.6	4.6	1.5

Appendix 8B

Heavy Mineral Fraction

SAMPLE	ENVIRONMENT	CUMMINGTONI	BIOTITE	ZIRCON	APATITE	AEGERINE	AUGITE	HYPERSTHENE	G.H.BLENDE	B.H.BLENDE	OPAQUES
WB294	RIVER	9.6	0.3	0.6	0	0	4	20	8.7	1.9	54.6
WB295	RIVER	14	0	0	0	0	1.6	26.3	6.16	0.84	51
WB324	BEACH	1.1	0	0.3	0	0	29.6	50.6	0.3	0.6	18
WB554	BARRIER	9.6	0.3	0	0	0	5	46	12.3	14	12.6
WB12	BEACH	12.3	0.3	0.3	0	0	10	38.6	23.3	9.3	5.6
WB14	SHELF(6.5M)	15	0	0.3	0	0.3	8.6	35	16.3	11	13.3
WB247	SHELF(16M)	12.6	0.3	1.3	0	0.3	9	37.6	13.3	14	11.3
WB246	SHELF(26M)	3.1	0	0	0.4	0	2.2	17.1	6.7	1.8	68.3
WB250	SHELF(34M)	12	0	0	0	0	3.6	52.6	6.6	7	18
WB254	SHELF(81M)	8	0.3	0.3	0	7.6	12.6	29	5.3	13.6	23
WB256	SHELF(200M)	2.2	0.4	0.8	0	34.2	10.1	11.8	1.3	7.9	29.9
WB551	RIVER	7.3	0	0	0	0	28	57	1.6	0	6
WB552	BEACH	7.3	0.6	0	0.3	0	6	49.3	7	12	17.3
WB550	BEACH	3.6	0.6	0	0	0	7	55.3	8.6	10.6	14
WB553	PL.BARRIER	2.6	0.3	0	0.3	0	5	40	1.3	4.6	45.6
WI296	RIVER	1.6	0.3	0	0	0	12	33.6	2.3	2	48
WI558	BARRIER	0.6	0	0	0	0	2.3	35.3	1.6	3	37
WI289	BEACH	0	0	0	0	0	0.3	23.3	0.3	1.3	74.6
WI35	SHELF(6.5M)	1	1	0	0.3	0	2.6	34.6	6.3	13	41
WI213	SHELF(19M)	11.3	1	0.6	0	0.6	11.3	34.3	21	8	11.6
WI208	SHELF(34M)	12.6	1.3	0	0.6	0	3	42.6	10.6	17.6	11.3
WI206	SHELF(38M)	15.6	2.6	0.6	0.3	0.3	8.6	26.6	12.3	7.6	33.3
WI203	SHELF(42M)	18	0	0	0	0.3	4.3	41	5	9	22.3
WI199	SHELF(51M)	26	0.3	0	0	0	5.3	36	13.6	11.3	7.3
M233	SHELF(10M)	8	1.6	0.3	0.3	0	6	26	10.6	6.6	40.3
M231	SHELF(28.5M)	11.6	0	0	0.3	0	4.3	51	8.6	18.6	5.3
M234	SHELF(36M)	22	0	0	0	0.3	5.3	52	8.6	8.3	3.3
M236	SHELF(49M)	33.6	0	0	0	0	6.3	34	14	9.3	2.6
WH297	RIVER	16	1	0	0	0	9	37.6	4.4	0.2	31.6
WH298	RIVER	5.3	0	0.3	0	0	13.6	39.6	19.3	10	11.6
WH299	RIVER	24	0.3	2	1	0.7	2.3	13.6	4	1	51
WH548	BARRIER	7	0.3	0	0	0	7	36.3	17.3	9	23
WH283	BEACH	9.6	0.6	0	0.6	0	6	42.6	17	18	5.3
WH37	ETD	2.4	0	0	0	0.4	4.4	57.6	6.4	13.3	14.7
WH176	SHELF(10M)	4.3	0	0.6	0	0	4.6	47	8.6	10.3	24.3
WH177	SHELF(23M)	6	0.6	0	0.3	0	5.6	41	11.3	17	18
WH63	SHELF(24M)	1	0	0	0	0	2.6	67	2.3	9.3	17.3
WH179	SHELF(45M)	1.3	0	0	0	0	1.6	27.6	0.6	1.6	67
ON560	RIVER	12.3	0	0	0.3	1	5	45	4.6	4.6	27
ON547	BARRIER	4	0.3	0.3	0.3	0	3.3	25	2.6	2.3	61.6

SAMPLE	ENVIRONMENT	CUMMINGTONI	BIOTITE	ZIRCON	APATITE	AEGERINE	AUGITE	HYPERSTHENE	G.H.BLENDE	B.H.BLENDE	OPAQUES
ON278	BEACH	2.3	0	0	0	0	1	72.6	2.3	10	11.6
ON259	SHELF(5M)	3.6	0	0.3	0	0	3.3	42.3	4.3	8.6	37.3
ON263	SHELF(13.5M)	5.6	1.6	1	0.3	0.3	5.6	28.6	24.6	11	21
ON267	SHELF(24M)	4.6	0.3	0.6	0	0	3.3	44.3	3.6	6.3	36.4
ON171	SHELF(41M)	5	0.6	1.3	0	0.3	3.3	16.3	12.6	27.3	33
ON172	SHELF(45M)	2.3	0	0	0.3	0.3	3	42	5	8.3	38.6
OP300	RIVER	18	1	0.6	1	0.3	6.6	21.6	3.7	1.1	45.3
OP545	PL.BARRIER	1.3	0.3	2.3	0.6	0	4.6	13.3	9.6	3.3	64.3
OP546	BARRIER	13	0.3	1	0	0	5.3	32.6	23	11	13
OP556	BEACH	9.3	0.3	0	0	0	10	46.3	6.6	12.3	15
OP544	BEACH	19	0	0	0	0	7	26.3	22.3	10.3	15
OP121	SHELF(8M)	4.6	0.3	0.6	0	0	6.6	33	12.6	8	34
OP120	SHELF(16M)	6.1	0.4	0	0	0	4.6	44.6	13.6	22.5	7.9
OP119	SHELF(27M)	1.6	0	0	0	0	4.6	42.6	3.3	6.3	41.3
OP117	SHELF(37M)	8.6	0.6	0.6	0.3	0.3	5.3	36.3	17.3	16.6	13.6
TP301	RIVER	1.6	0.3	0	0	0	12	33.6	2.3	2	48
TP543	BARRIER	5.3	0	0	0.3	0	5.6	28	4	2.3	54.3
TP540	BARRIER	2.6	0	0	0.6	0	4	32	2.6	3.3	54.6
TP542	BEACH	6.3	0	0	0	0	15.6	36.6	12.6	6.3	22.3
TP541	BEACH	4.6	0	0	0	0	18.6	33.3	9	5.3	29
TP539	BEACH	2.6	0	0	0	0	11.3	46.6	7.6	4.3	27.3
TP111	SHELF(10M)	6	0.6	2.3	0	0	10	28.3	21.3	9	22.3
TP112	SHELF(10M)	3	1	1	0	0	9.6	28	13.3	7.3	36.6
TP113	SHELF(23M)	3.3	0.3	1	0.6	0	8.6	30	9	4.6	42.3
TP114	SHELF(29M)	6	0.3	2	0	0	6.6	30	10	9.3	35.6
HW302	RIVER	5	0.2	0	0.6	0	6.3	8.3	5.5	0.6	73
HW561	RIVER	0.6	0	0	0.3	0	25	48.6	0.3	0.3	24
HW537	BARRIER	0.3	0.3	0	0	0	29.6	50.6	0.3	0.6	18
HW538	BEACH	0	0	0	0	0	30.3	44.3	0	1.6	23.6
HW325	BEACH	0.3	0	0	0	0	42	35.6	1	1.3	19.6
HW132	SHELF(10M)	0.6	0	0	0	0	23	44.3	0	2.3	29.6
HW133	SHELF(20M)	0.6	0	0	0	0	29	45	1	2	22.3
HW135	SHELF(40M)	0.6	0	0	0.3	0	4	18.6	0	0	76.3
HW136	SHELF(50M)	8.6	0.6	1.3	0	0.3	10	36	11	6	26
HA303	RIVER	4	0	2	4	0	4.5	6.5	2.4	0.8	77.4
HA536	BARRIER	0.6	0	0	1.6	0	1	10	1	0.3	85.3
HA327	BEACH	2.6	0.3	0	0	0	23.3	30.6	1.3	1.6	40
HA137	SHELF(9M)	3.6	0.6	0.6	1	1.3	25	32.3	3	3.3	29
HA138	SHELF(12M)	2	1.3	0.6	0.6	0.3	13.6	26.3	1.6	1.3	52
HA139	SHELF(13M)	6	0	0.3	0	0	26	36	2.3	1.6	27

SAMPLE	ENVIRONMENT	CUMMINGTONI	BIOTITE	ZIRCON	APATITE	AEGERINE	AUGITE	HYPERSTHENE	G.H.BLENDE	B.H.BLENDE	OPAQUES
HA140	SHELF(9M)	5.6	8.6	0	0	0	15	26	19	11	14
MB304	RIVER	27.3	0	0.6	0.3	0.3	2	12.6	11.7	0.8	44
MB557	RIVER	39	0	0.3	0	0	0.3	20	1.3	1	38
MB305	RIVER	8	0.6	0	0	0	13	18.6	3.7	0.6	55
MB306	RIVER	9	0	0	0.6	0	11	17	3.2	1	58
MB306B	RIVER	12.3	2.3	0	0	0	12.3	33.6	2.2	2.6	42.6
MB307	RIVER	4	4.6	0.3	0.3	0	6.6	12.6	5.6	4.6	61
MB308	RIVER	8	0.6	0	0	0	12	39	5.6	1	33.6
MB309	RIVER	6.6	0.8	1	0	0	6.6	25.3	16.1	2.4	40.6
MB535	BARRIER	2	0	0	3	0	3.3	8.3	1.6	1	80.6
MB533	BARRIER	2.6	4	0.3	0.3	0	8.3	37.6	17	21	8.6
MB530	BARRIER	0.6	0	0.3	2.3	0	1	0	3.6	2	90
MB534	BEACH	7	5.3	0	0	1	16	26.6	8.3	14.6	20.3
MB323	BEACH	5.6	3	0	0.3	0	9	35.3	12.3	12	22.3
MB532	BEACH	2.3	3.3	0	0	0	10	27.3	14	17.6	25.3
MB531	BEACH	0.6	2.3	0	0	0	4	48.3	10.6	9.3	24.6
MB97	SHELF(11M)	4.6	3.6	1.6	0	0	9.6	27	10	9.6	33.3
MB96	SHELF(12M)	4	3.6	1.3	0	0.3	10	29	9	7.3	35.3
MB93	SHELF(16M)	0	0.3	1.3	1	0	1.6	12.6	1	1.3	80.6
MB90	SHELF(10M)	0.6	2.3	0.3	0.3	0	3.6	28.6	13.6	11	39.3
MB104	SHELF(32M)	7.3	2.6	0.6	0.3	0.3	8.6	26.6	12.3	7.6	33.3
OP527	RIVER	2.3	0	0.3	1	0	2	5	29.3	2.6	57.3
OPB526	BARRIER	3	0.3	0	1.3	0	2.6	28.6	6.3	5	52.6
OPB528	BEACH	7.6	1.6	0	0	0	3.3	38	22.3	6	21
OPB328	BEACH	9.6	3.3	0.3	0	0	3.3	29.3	25.3	10	18.6
OPB329	SHELF(25M)	1.6	0	0	0.6	0.3	9	24.3	1.3	1	3.8
KB311	RIVER	2	0	0	0	0	2.6	21	8	4	62.3
KB312	RIVER	5	0.3	2	0.6	0	2.6	17.3	9.5	1.1	61
KB523	RIVER	1.3	0.3	0	0.6	0	5	47.6	6	4	35
KB314	RIVER	6.3	1	0.6	1.6	0	2	9	4.1	0.3	74.3
KB315	RIVER	1.6	1.9	0	0	0	7	16.3	23.6	6.4	43
KB319	PL.BARRIER	0.3	0	0	1.3	0	1	0.3	36	4.3	56.6
KB320	PL.BARRIER	1	0.3	0	1.3	0	4	41.6	16	6.6	29
KB529	BARRIER	1	0	0.6	0.3	0	4.6	35.3	9.3	9.3	39.3
KB525	BARRIER	0.3	0	0	1.6	0	3.3	39.3	3.3	6	46
KB524	BARRIER	0.6	0	1	0.6	0	4.3	28.6	2.6	3.6	58.3
KB317	BARRIER	6.6	0.6	0.3	0	0	7.3	52.3	7.6	7	18
KB322	BEACH	0	0.3	0	0.3	0	4	25.6	5.6	5.6	58.3
KB509	BEACH	1.8	0	0.9	0	0	5.6	42.6	25.1	11.3	11.3
KB321	PL.BEACH	2	0	0	0.3	0	9.6	50.3	3.3	6	28.3

SAMPLE	ENVIRONMENT	CUMMINGTONI	BIOTITE	ZIRCON	APATITE	AEGERINE	AUGITE	HYPERSTHENE	G.H.BLENDE	B.H.BLENDE	OPAQUES
KB511	BEACH	2	2	0	0	0	6.7	19.4	7.3	5.3	55.7
KB510	BEACH	1.3	0.3	0.6	0.3	0	6	39.3	5.6	7	39
KB512	BEACH	1.3	0.3	0.6	0.3	0	8	43.6	8.6	7.6	29.3
KB318	BEACH	9.3	1.6	0	0	0	5.6	38.3	18.6	9.3	16.3
KB496	SHELF(11M)	0	0	0	0	0	3	48.6	3	6.3	39
KB375	SHELF(16M)	1	2.6	1	0.3	0.3	5.3	37.6	8.6	11.6	31.6
KB154	SHELF(18M)	1	0	0	0	0	3.6	44	7.6	12.6	31
KB142	SHELF(10M)	3	1.3	0	0	0	7.6	47.3	12.3	12.6	15.3
KB145	SHELF(21M)	2.3	0.6	1.6	0	0	5	42.3	16.6	6	25.3
KB330	SHELF(30M)	10.6	2.3	1.3	1	0	4.3	26.3	12.3	1	40.6
KB156	SHELF(20M)	2.6	1	0	0	0	8.6	57.3	11	9.3	9.3
KB165	SHELF(22M)	0.6	0	0	1	0	4.3	43	11.6	18	21
KB148	SHELF(35M)	6.3	2.6	2.3	0.6	0	8.3	30	8	9	32.6
WP316	RIVER	2	2.3	0	0.6	0.3	11.6	30	2	3	47.3
WP521	BARRIER	0	2	0	2	0	1.6	17.3	1.3	1.3	74.3
WP522	BEACH	3.6	1.3	0	0	0	7	39.6	22.3	13	13
WP452	SHELF(8M)	3	1.6	0	0	0.3	5.6	49	16	7.6	16.6
WP446	SHELF(17M)	1.6	0.3	0.3	0	0	4.6	42	12.3	8.3	30.3
WP442	SHELF(25M)	6.3	1	0.3	0.3	0.3	9.6	39.3	13.3	8.6	20.3
KDB520	RIVER	0	1.1	0.3	0	0	16	62.1	5.2	1.7	13.2
KDB518	BARRIER	0.3	1.3	0	0	0	5.6	38.2	1.1	3.6	49.6
KDB519	BEACH	1	4	0.3	0	0	16.3	46.6	7.3	5.6	18.6
WAB515	RIVER	2.3	0	0	0	0	2.3	31.3	2.6	0.3	52.6
WAB517	BARRIER	2	0	0	0.6	0	10.6	39.6	6	7.6	33.3
WAB516	BEACH	1	0	0	0	0.3	7.6	50.6	7.3	11	22

APPENDIX 9

ENTROPY PROGRAM RESULTS

Appendix 9B

Textural Entropy Classification

CLASS 1							
SAMPLE NO	DEPTH (m)	MEAN (PHI)	SORTING (PHI)	SKEWNESS	CARBONATE (%	IRON STAINING (%)	ANGULARITY
WB1	23	0.16	1.05	0.1	11	70	SA-SR
WB19	25	-0.04	0.43	-0.06	28	70	SA-SR
WB20	20	0.19	0.64	0.7	33	30	SA-SR
WB246	27	-0.05	0.35	1.32	13	30	SR-WR
MB6	41	0.34	0.54	1.66	9	20	SA-SR
WH42	2	0.27	0.9	0.33	32	60	SA-R
WH53	6	0.49	0.27	-0.29	76	10	A-SR
WH238	32	0.12	0.88	1.28	95	7	VA-SR
WH179	45	0.2	0.74	0.99	17	20	SA-R
ON169	31	0.36	0.4	0.93			
ON122	32	0.38	0.69	1.24	10	40	SR-R
ON279	-2	-0.25	0.15	-0.57	47	60	SA-R
OP116	35	0.25	0.58	0.62	26	20	SA-R
OP119	27	0.17	0.58	-0.38	44	50	SA-WR
HW135	40	0.39	0.4	0.27	21	70	A-R
HW107	43	0.24	0.32	0.43	8	0	SA-SR
MB92	18	0.26	0.46	-0.05	93	70	SA-SR
MB93	16	0.33	0.37	1.81	77	100	SR-R
HA141	12	0.5	0.67	0.49	70	50	SA-R
KB507	20	0.52	0.49	-0.81	83	5	SA-SR
KB490	18	-0.38	0.96	0.59			
KB156	18	0.5	0.5	-0.3			
KB337	16	0.17	1.24	0.76	83	20	A-SR
KB477	15	-0.04	1.2	0.83	92	20	A-R
KB491	17	-0.66	0.96	0.96			
MEANS	23.54	0.19	0.63	0.51	44	39	
CLASS 2							
SAMPLE NO	DEPTH (m)	MEAN (PHI)	SORTING (PHI)	SKEWNESS	CARBONATE (%	IRON STAINING (%)	ANGULARITY
WB253	63	0.7	0.73	-0.02	19	0	A-SR
WB252	52	0.93	0.86	0.45	20	7	SA-R
WB251	45	0.94	0.52	0.72	22	20	SA-R
WB250	34	0.88	0.61	0.98	36	30	SR-WR
WB245	32	0.92	0.72	-0.54	18	30	SA-SR
WB23	20	0.81	0.68	0.71	31	40	SA-R
WB244	26	1.04	0.58	-0.19	12	25	SA-R
WI89	41	0.68	0.51	1.39	15	20	SA-SR
WI292	-2	0.85	0.57	1.23	11	5	SR-WR
WI293	0	0.56	0.24	0.56	17	30	SR-WR
WI291	0	0.79	0.43	0.13	14	30	R-WR
WI288	0	0.68	0.37	-0.21	16	30	R-WR
WI201/202	48	0.94	0.98	0.98	21	5	SR-WR
WI203	42	0.97	0.62	1.46	32	15	SA-R
WI192	43	0.85	0.57	1.23	8	25	SA-SR
WI193	44	0.6	0.43	1.66	6	10	SA-SR
WH75	34	0.52	0.3	0.04	11	60	SA-R
WH54	9	1	0.59	1.66	52	25	SA-SR
WH239	42	1.02	0.85	0.32	12	5	A-SR
WH65	32	0.98	0.49	1.66	9	30	SR-R
WH124	31	0.88	0.44	1.48	6	40	SA-R
WH128	38	0.68	0.38	1.22	27	50	SA-R
WH123	30	0.56	0.5	1.58	23	25	SR-R
ON167	23	1.02	0.69	2.09	8	30	SR-R
ON257	24	0.79	0.57	1.78	19	60	SR-R
ON267	25	1.01	0.57	1.02	13	10	SR-WR
ON547	-10	0.92	0.4	0.71	0	15	SA-R
OP69	--	8	0.55	0.44	0.96	73	15	SA-R
HW134	30	0.46	0.42	1.08	57	70	SA-WR
HW109	35	0.51	0.41	0.95	12	0	A-SR
HW110	18	1.09	0.72	0.7	20	40	VA-R
HA138	12	0.8	0.71	1.12	41	25	A-SA
HA141	21	0.5	0.67	0.49	71	50	SA-R
MB94	18	1.14	1.05	1.01	76	50	SR
MB103	33	1.21	0.89	0.35	14	15	SA-WR
KB506	19	0.85	0.52	-0.03	39	15	SA-R
KB488	19	1.09	0.41	0.02	85	50	SA-SR

KB475	13	0.7	0.34	0.21	63	25	SA-SR
KB484	19	1.18	0.69	0.19	70	5	SA-R
KB486	20	0.78	1	-0.03	67	25	A-R
KB402	16	1	0.5	0.32	29	2	SA-R
KB408	13	1.21	0.74	0.66	42	30	SR-R
KB476	14	0.52	0.63	0.48	48	15	SA-SR
KB485	19	1.05	0.68	0	69	30	A-SA
KB486	20	0.78	1	-0.03	67	25	A-R
KB487	20	0.7	0.73	0.24			
KB511	-2	1.48	0.58	0.1	27	10	A-R
KB512	-2	0.97	0.6	0.79	35	5	SR-WR
KB489	18	0.81	0.55	0.23	27	5	SA-R
WB	-2	0.81	0.55	0.23	27	5	SA-R
TP539	-2	1.01	0.4	0.51	26	20	SA-R
OPB328	-2	1.01	0.59	0.64	39	10	A-R
OPB329	27	0.88	0.91	1.64	90	30	SA-SR
KB161	31	0.97	0.74	1.52	25	60	SR-R
MEANS	22.2	0.86	0.61	0.7	29.6	24.7	
CLASS 3							
SAMPLE NO	DEPTH (m)	MEAN (PHI)	SORTING (PHI)	SKEWNESS	CARBONATE (%)	IRON STAINING (%)	ANGULARITY
WB242	24	1.03	0.73	0.58	12	20	SA-R
WB243	21	1.04	0.33	0.85	9	20	SA-SR
WB9	23	1.06	0.55	1.2	19	60	SA-SR
WB249	28	1.16	0.58	0.99	12	20	A-R
WB	-2	1.04	0.48	-0.26	23	5	SA-R
WB	-10	1.27	0.34	0.04	0	20	SA-R
WI289	-3	1.27	0.26	0.77	3	7	SR-WR
WI290	-2	1.09	0.24	0.69	8	5	SR-WR
WH125	31	1.15	0.43	1.55	3	40	R
WH67	32	1.1	0.38	1.86	7	30	SA-R
WH62	30	1.16	0.49	1.5	8	40	SA-SR
WH38	0	1.26	0.38	0.79	27	40	SA-SR
WH63	24	1.13	0.42	0.32	8	40	SA-SR
WH173	32	1.16	0.47	1.84	8	30	SA-SR
WH40	2	1.32	0.41	-1.34	31	30	SR-R
WH39	0	1.22	0.31	0.19	25	70	SA-SR
WH174	29	1.33	0.45	1.12	6	70	SA-R
ON276	-2	1.14	0.27	0.94	19	70	SA-R
ON277	0	0.94	0.34	-0.82			
ON278	-2	0.92	0.31	-1.99	24	20	SA-WR
ON280	-2	1	0.26	-0.08	17	25	SA-R
ON167B	23	1.23	0.53	0.78	7	40	SR-R
OP556	-2	1.34	0.35	0.14	20	10	A-SR
HW325	-2	1.12	0.58	0.71	22	50	A-R
HW326	-2	1.14	0.44	1.79	17	50	A-R
HW538	-2	1.28	0.48	0.79	19	50	SA-R
HW537	-10	1.31	0.43	-0.57			
MB531	-2	1.24	0.52	0.82	21	15	SA-R
KB430	14	1.25	0.66	0.21	41	20	SA-R
KB416	6	1.75	0.47	0.72	22	30	A-SR
KB414	10	1.05	0.39	0.07	34	10	SA-SR
KB409	11	1.18	0.34	1.02	58	50	SA-SR
KB413	12	1.25	0.43	1.14	31	15	SA-R
KB496	11	1.13	0.48	0.26	15	20	SA-R
KB524	-10	1.4	0.45	0.71	0	0	SA-R
TP541	-2	1.25	0.49	-0.17	13	15	A-R
TP540	-10	1.1	0.37	0.51	0	10	SA-WR
KB505	17	1.27	0.23	0.52	45	5	SR-R
MEANS	8.2	1.19	0.42	0.53	17.6	29	
CLASS 4							
SAMPLE NO	DEPTH (m)	MEAN (PHI)	SORTING (PHI)	SKEWNESS	CARBONATE (%)	IRON STAINING (%)	ANGULARITY
WB254	81	1.49	0.96	-0.13	16	0	A-SA
WB255	100	1.68	0.98	-0.11	11	0	A-R
WB7	23	1.5	0.47	0.51	8	15	SA-SR
M88	38	1.98	0.55	-1.63	10	5	SA-SR

M34	12	2.76	0.41	-1.63	8	5	VA-SA
WI31	7	1.41	0.4	-0.26	11	30	SR-WR
WI239	44	1.75	0.44	0.91	7	5	SA-R
WI200	50	1.72	1.05	-0.38	29	1	SA-SR
WI558	-10	1.57	0.29	0.97	0		
WI81	37	1.67	0.43	0.6	8	40	SA-SR
WH41	0	1.53	0.78	-0.92	43	40	VA-SR
WH81	37	1.67	0.43	0.6	8	40	SA-SR
ON172	45	1.65	0.61	0.32	10	5	A-SA
ON259	5	1.74	0.51	0.56	16	20	A-R
HA536	-10	1.47	0.42	0.21	0	0	SA-WR
MB535	-10	1.65	0.41	1.42	0	20	A-SR
MB323	-2	1.63	0.57	0.36	21	30	VA-SA
KB500	5	1.76	0.44	0.03	7.4	5	SA-R
KB502	11	1.8	0.64	-0.1	47	5	A-SR
KB503	13	1.65	0.49	-0.09	29	2	SA-R
KB427	8	1.68	0.49	0.74	5	5	SA-R
KB508	-2	1.64	0.3	0.04	5	2	SA-R
KB498	2	1.72	0.36	0.24	6	5	SA-R
KB135	10	1.35	0.5	-0.37			
KB495	12	1.72	0.43	0.59	43	25	A-R
KB480	17	1.71	0.62	-0.65	35	2	SA-SR
KB482	18	1.58	0.46	0.9	76	50	SA-SR
KB405	19	1.78	0.81	0.98	43	2	A-SR
KB406	17	1.73	0.75	0.16			
KB403	13	1.43	0.49	0.54	44	10	SA-SR
KB416	6	1.75	0.47	0.72	22	30	A-SR
KB412	14	1.4	0.56	1.01	39	20	SA-R
KB411	16	1.91	0.74	-0.26			
KB322	9	1.59	0.31	0.1	38	15	SA-SR
KB319	-10	1.66	0.44	-0.11	0	50	A-SR
KB320	-10	1.55	0.43	0.84	0	2	SA-R
KB321	-10	1.48	0.39	0.96	0	30	SA-SR
KB153	23	1.92	0.85	-0.25	42	5	SR-R
KB481	18	1.41	0.85	-0.17	31	40	A-SA
KB483	19	1.44	0.58	0.1	62	30	SA-SR
KB492	15	1.46	0.7	0.33	78	25	A-R
KB504	15	1.26	0.64	-0.82	45	10	SA-R
KB525	-10	1.77	0.45	0.35	0	70	SA-R
KB353	8	1.71	0.47	0.49	12	10	A-SA
KB351	12	1.87	0.98	-0.4	40	5	A-SA
KB393	18	2.08	0.73	-0.66	11	10	SA-SR
KB513	-2	1.75	0.42	-0.43	5	2	SA-R
KB357	20	1.8	0.56	0.51	18	5	A-SR
KB455	2	1.73	0.48	0.22	5	5	A-SR
KB463	19	1.64	0.44	1.41	13	10	SA-R
KB521	-10	1.57	0.46	1.28	0	70	SA-R
KB522	-2	1.55	0.57	-1.21	8	2	A-R
KB440	22	1.4	1.26	-0.44	66	10	A-SR
KB447	16	1.73	0.65	-1.75	12	5	A-SR
MEANS	14.6	1.67	0.57	0.12	22.3	16	
CLASSS							
SAMPLE NO	DEPTH (m)	MEAN (PHI)	SORTING (PHI)	SKEWNESS	CARBONATE (%)	IRON STAINING (%)	ANGULARITY
WB11	0	1.71	0.75	-2.71	6	5	A-SR
WB12	0	1.95	0.42	-0.32	6	5	A-SR
WB13	0	1.98	0.54	-3.67	6	10	A-SR
WB127	25	2.03	0.59	-0.13	8	10	SA-SR
WB8	22	1.92	0.54	-1.11	13	15	SA-SR
WB24	20	1.81	0.44	-0.2	4	30	A-SR
WI219	29	2.09	0.47	-3.13	4	40	SR
WI220	29	2.09	0.35	-0.04	3	40	SR
WI27	34	2.09	0.46	-0.28	8	40	A-SR
WI224	34	2.15	0.44	0.46	6	20	SR-R
WI225	36	1.9	0.35	0.24	10	30	SA-SR
WI226	38	1.68	0.39	-2.45	6	40	SR-R
WI227	41	1.85	0.36	0.58	5	40	SR
WI35	6	2.06	0.61	0.43	12	7	VA-R
WI204	40	2.01	0.33	0.91	4	15	SR

WI207	35	1.8	0.43	1.32	5	10	SR-R
WI37	7	1.41	0.4	-0.26	11	30	SR-WR
WI182	21	2.06	0.58	-0.07	7	15	VA-SR
WI85	46	2.05	0.51	0.38	9	5	A-SR
WI45	38	2.13	0.5	-0.32	14	30	A-SR
WI44	35	1.86	0.55	-0.44	13	20	A-SA
WI82	32	2.09	0.33	-0.44	7	7	SA-SR
WI208	34	1.92	0.91	-2.86	5	5	SA-SR
WH25	20	2.14	0.5	0.7	8	40	SA-SR
WH37	2	1.34	0.36	0.85	21	25	SA-WR
WH66	27	1.9	0.35	0.17	4	25	A-SR
WH26	24	1.99	0.39	-0.17	12	10	A-SR
WH44	35	1.86	0.55	-0.44	14	30	A-SR
WH50	3	1.93	0.45	-0.08	19	40	VA-SA
WH85	46	2.05	0.51	0.38	9	5	A-SR
WH269	26	2.01	0.37	0.66	3	30	A-SR
WH283	-2	2.07	0.33	-0.65	8	20	SA-SR
WH284	0	2.06	0.35	0.55	18	60	A-R
WH285	-2	1.83	0.33	0.26	13	30	SA-SR
WH546	-10	1.98	0.42	0.54	0	30	SA-SR
ON260	7	1.9	0.49	-0.07	14	25	A-SR
OP120	16	1.98	0.45	0.27	22	25	A-SR
OP116	37	2.09	0.43	-0.07	13	5	SA-SR
OP544	-2	1.76	0.44	-1.66	12	10	A-SA
OP545	-10	1.93	0.37	0.33	0	5	SA-SR
OP546	-10	1.95	0.38	0.54	0	5	A-SR
HW108	22	1.93	0.32	0.92	82	25	A-R
HA327	-2	1.95	0.53	-1.15	25	5	A-SA
KB426	10	1.88	0.46	0.06	37	5	SA-SR
KB434	6	1.78	0.36	0.51	10	10	SA-R
KB433	8	1.88	0.41	1.38	9	5	SA-R
KB432	10	1.93	0.39	1.36	7	5	SA-SR
KB478	16	1.87	0.49	-0.14	36	10	A-R
KB474	11	2.02	0.61	0.48	13	20	A-SR
KB102	15	1.94	0.71	-0.53	42	20	A-SR
KB428	6	1.88	0.32	0.87	11	10	SA-SR
KB386	16	1.97	0.66	0.37	68	5	A-SR
KB388	12	2.07	0.64	-0.81	15	5	SA-SR
KB395	14	1.99	0.63	-1.03	39	10	A-SA
KB366	20	2.15	0.54	-1.2	19	15	A-SR
KB464	20	2.09	0.69	-0.07	22	15	A-SR
KB472	7	2.09	0.35	0.43	5	5	A-SA
KB473	2	2.06	0.43	-0.38	9	5	SA-R
KB456	2	2.02	0.46	-0.06	6	5	SA-SR
KB461	17	2.06	0.65	-1.29	22	30	A-SR
KB151	22	2.05	0.52	0.47	6	7	SA-SR
KB436	1	2.05	0.4	0.17	10	10	A-SR
KB434	6	1.78	0.36	0.51	10	10	SA-R
KB499	2	1.83	0.3	-0.96	6	5	SA-R
TP542	-2	1.79	0.48	-2.08	6	15	A-SA
TP543	-10	1.77	0.37	0.7	0	10	SA-SR
HW132	10	2.08	0.44	0.94	27	70	A-R
KB146	25	2.13	0.62	0.65	14	0	SR-WR
KB356	2	2.23	0.5	-0.65	11	15	A-SR
KB453	5	2.06	0.49	0.18	0	5	A-SR
MEANS	15.5	1.95	0.47	-0.18	13.3	17	
CLASS6							
SAMPLE NO	DEPTH (m)	MEAN (PHI)	SORTING (PHI)	SKEWNESS	CARBONATE (%	IRON STAINING (%)	ANGULARITY
WB4	10	2.43	0.54	-1.28	10	5	VA-A
WB5	6	2.16	0.54	-0.86	5	2	VA-A
WB3	15	2.59	0.65	-1.06	7	5	VA-A
WB15	3	2.38	0.64	-4.2	6	15	VA-SA
WB21	3	2.4	0.62	-3.21	7	7	VA-SA
WB563	20	2.38	0.49	0.74			
M87	44	2.32	0.5	-2.37	10	5	A-SR
M231	29	2.2	0.47	-0.26	6	5	A-SR
M232	25	2.51	0.4	0.84	8	5	A-SR
M235	44	2.31	0.48	-0.74	11	0	A-SA

M236	49	2.13	0.34	1.96	4	5	A-SR
WI217	24	2.2	0.48	-0.07	13	15	A-SA
WI28	24	2.11	0.54	-1.93	9	60	A-SR
WI218	30	2.19	0.43	0.62	6	50	SR-R
WI222	33	2.48	0.59	-5.47	7	10	SA
WI223	33	2.32	0.49	1.2	10	10	A-SR
WI226	38	1.68	0.39	-2.45	6	40	SR-R
WI230	49	2.53	0.5	0.43	6	0	A-R
WI198	50	2.21	0.5	0.39	6	0	SA-SR
WI199	51	2.32	0.39	0.46	6	0	A-SR
WI201	50	2.31	0.65	-0.19	14	0	A-SR
WI202	48	2.22	0.94	-0.93	28	0	A-SR
WI205	38	2.19	0.34	1.08	6	10	SA-SR
WI206	38	2.14	0.38	1.54	4	10	SA-SR
WI36	30	2.18	0.44	-0.65	8	15	A-SR
WI209	33	2.18	0.46	-0.17	5	5	A-SR
WI211	32	2.34	0.36	1.11	7	25	A-SA
WI32	24	2.35	0.48	0.03	10	5	A-SR
WI183	26	2.26	0.71	-2.02	6	10	VA-R
WI184	30	2.35	0.46	0.76	6	20	VA-SR
WI185	32	2.23	0.52	-1.34	6	15	SA-SR
WI186	34	2.17	0.48	0.81	6	25	SA-SR
WI187	36	2.21	0.48	-0.48	6	70	SA-SR
WI188	37	2.21	0.71	-3.11	6	10	A-SR
WI189	39	2.17	0.38	0.53	7	20	SA-SR
WI190	40	2.17	0.51	1.2	7	10	SA-SR
WI192.193	43	2.25	0.43	0.3	6	10	SA-SR
WI194	48	2.45	0.4	0.24	6	5	A-SR
WI195	51	2.48	0.75	-3.28	7	1	A-SR
WI196	54	2.53	0.54	0.47	11	0	A-SA
WI83	34	2.18	0.33	-1.3	5	20	A-SR
WI79	40	2.44	0.35	0.15	9	7	A-SA
WI84	42	2.02	0.78	-1.3	18	7	SA-SR
WI80	45	2.22	0.4	0.13	7	5	A-SR
WH45	38	2.13	0.5	-0.32	13	20	A-SA
WH78	43	2.57	0.34	0.18	11	0	A-SR
WH77	40	2.39	0.43	-0.38	11	15	VA-SR
WH178	39	2.3	0.49	-0.66	4	5	SA-R
WH46	18	2.46	0.56	0.06	30	7	VA-SR
WH177	23	2.3	0.59	-0.86	11	10	A-SA
WH59	18	2.32	0.55	-0.04	16	30	A-SR
WH64	24	2.17	0.5	0.57	24	25	SA-R
WH80	45	2.22	0.4	0.13	7	5	A-SR
WH175	26	2.18	0.47	0.29			
WH266	22	2.22	0.71	-2.4	7	25	A-SR
WH129	10	2.49	0.61	-2.13	8	5	VA-SA
WH58	12	2.46	0.62	-0.24	8	10	VA-SR
WH281	-2	2.18	0.32	0.3	16	20	VA-R
WH282	0	2.15	0.33	-0.05	17	70	A-SR
ON266	28	2.41	0.53	-1.02	3	10	A-SR
OP68	30	1.97	0.81	-1.05	17	7	A-SR
OP73	6	2.34	0.38	0.14	17	70	A-SA
OP74	34	2.34	0.49	0.21	16	7	A-SR
HW133	20	2.14	0.46	-1.38	15	50	SA-SR
HA106	26	2.44	0.66	-0.39	17	10	A-SA
M8534	-2	2.22	0.69	-3.13	14	0	VA-SA
M8532	-2	2.33	0.49	-0.1	5	20	A-SR
M890	5	2.22	0.35	0.21	17	30	A-SA
KB424	14	2.22	0.42	-0.35			
KB401	18	2.19	0.47	0.45	58	20	A-SA
KB335	20	2.11	0.79	-1.14	11	10	A-R
KB336	18	2.15	0.87	-0.65	50	2	A-SR
KB376	19	2.02	0.86	-0.06	57	30	A-R
KB378	15	1.96	0.8	-0.19	25	30	VA-SR
KB379	13	2.29	0.64	-0.26	28	5	A-SR
KB380	11	2.34	0.61	-0.73	0	15	A-SR
KB383	7	2.18	0.68	-0.53	15	20	A-SR
KB159	31	2.38	0.41	0.75	34	5	A-SA
KB479	17	2.33	0.44	0.45	34	5	A-SA
KB493	14	1.94	0.86	-1.11			
KB494	13	2.3	0.44	-0.06	62	5	A-SR

KB346	4	2.52	0.59	0.39	13	15	SA-R
KB344	8	2.53	0.44	0.18	14	5	A-SA
KB343	10	2.34	0.53	-0.03	13	10	A-SR
KB341	14	2.49	0.35	-0.27	30	15	A-SR
KB164	28	2.41	0.73	-0.9	31	10	A-SA
KB385	18	2.45	0.46	-1.02	21	10	A-SA
KB389	10	2.45	0.37	0.38	11	5	A-SA
KB392	4	2.41	0.37	0.6	13	10	A-SA
KB350	14	2.47	0.43	-1.68	25	10	A-SA
KB348	18	2.16	0.44	0.21	30	5	A-SA
KB347	20	2.51	0.53	0.65	18	5	A-SR
KB152	20	2.12	0.51	0.21	18	5	SR
KB396	12	2.48	0.39	0	7	10	A-SA
KB397	10	2.33	0.55	-1.85			
KB398	8	2.46	0.54	-2.65	24	10	A-SA
KB394	6	2.53	0.33	-1.22			
KB400	4	2.29	0.62	-1.71	13	15	A-SR
KB364	6	2.4	0.35	0.55	15	15	VA-SA
KB363	8	2.25	0.48	-0.08	8	15	A-SA
KB362	10	2.48	0.35	0.02	31	5	A-SA
KB361	12	2.55	0.32	0.59	21	15	A-SA
KB360	14	2.54	0.42	-0.57	13	20	A-SA
KB359	16	2.42	0.38	0.57	10	5	A-SA
KB358	18	2.53	0.44	0.45			
KB350	14	2.47	0.43	-1.68	25	10	A-SA
KB144	20	2.34	0.83	-3.47	20	7	SA
KB374	4	2.42	0.44	0.05	14	5	A-SR
KB373	6	2.35	0.5	0.29	13	2	SA-SR
KB370	12	2.31	0.46	-0.18			
KB367	18	2.16	0.67	-0.18			
KB100	21	2.19	0.5	-1.81	6	5	A-SA
KB460	10	2.19	0.73	-1.32	43	20	A-SR
KB458	11	2.32	0.59	-1.27	7	5	A-SA
KB457	9	2.17	0.45	0.39	6	10	A-SA
KB452	8	2.4	0.41	0.27	0	5	A-SA
KB451	10	2.4	0.46	-0.44	9	2	A-SR
KB450	11	2.5	0.43	-0.37	9	10	A-R
KB449	13	2.21	0.72	-1.39	41	20	A-SR
KB448	15	2.41	0.63	-2.46	18	20	A-SR
KB449	13	2.21	0.72	-1.39	41	20	A-SR
KB445	18	2.06	0.83	-1.24	58	10	A-SR
KB501	9	2.15	0.3	0.96	10	10	SA-SR
KB437	5	2.36	0.74	-3.01	6	5	A-SA
KB439	18	2.44	0.44	-1	6	5	A-SA
KB441	24	2.36	0.44	-1.53	10	2	SA-SR
KB442	26	2.3	0.41	-0.66	40	20	A-SA
KB145	21	2.31	0.45	0.74	9	10	A-SR
KB162	27	2.41	0.56	0.07	8	15	SA-SR
MEANS	21.8	2.28	0.52	-0.53	14.9	12.6	
CLASS 7							
SAMPLE NO	DEPTH (m)	MEAN (PHI)	SORTING (PHI)	SKEWNESS	CARBONATE (%	IRON STAINING (%)	ANGULARITY
WB2	21	2.63	0.6	-0.23	4	2	VA-SA
WB16	3	2.58	0.65	-4.12	9	5	VA-A
WB14	7	2.61	0.51	-3.58	4	2	VA-SA
WB10	12	2.58	0.72	-2.75	13	5	VA-SR
WB18	15	2.66	0.62	-2.64	15	5	VA-A
WB17	8	2.67	0.5	-4.3	13	1	VA-SA
WB241	10	2.77	0.37	0.07	4	15	VA-SA
WB15	3	2.38	0.64	-4.2	6	15	VA-SA
WB22	20	2.99	0.46	-0.06	11	0	VA-A
WB126	20	2.9	0.61	-2.06	6	0	VA-A
WB256	190	2.8	0.27	0.02	11	0	VA-A
W1233	10	2.9	0.44	-1.49	4	0	VA-A
W1215	15	2.69	0.37	-0.56	8	1	VA-A
W1216	11	2.89	0.37	-0.33	8	1	VA-A
W130	12	2.61	0.58	-4.46	8	5	VA-A
W129	18	2.9	0.46	-4.1	11	5	VA-A
W1212	27	2.75	0.3	0.35	12	5	VA-A

	A	B	C	D	E	F	G	H
421	WI233	10	2.9	0 44	-1.49	4	0	VA-A
422	WI215	15	2.69	0.37	-0.56	8	1	VA-A
423	WI216	11	2.89	0.37	-0.33	8	1	VA-A
424	WI30	12	2.61	0.58	-4.46	8	5	VA-A
425	WI29	18	2.9	0.46	-4.1	11	5	VA-A
426	WI212	27	2.75	0.3	0.35	12	5	VA-A
427	WI34	12	2.78	0.41	-1.63	8	5	VA-SA
428	WI213	19	2.9	0.42	0.78	5	2	VA-A
429	WI33	18	2.8	0.43	-1.96	7	0	VA-A
430	WI214	13	2.84	0.31	0.33	8	0	VA-A
431	WI180	12	2.79	0.51	0.26	5	0	A
432	WI181	19	2.88	0.48	-2.66	3	0	VA-A
433	WI197	54	2.67	0.41	0.55	14	0	A-SA
434	WH240	51	2.73	0.55	0.12	14	0	A-SR
435	WH237	21	2.72	0.72	-4.25	8	5	VA-SR
436	WH47	15	2.69	0.47	-1.26	9	5	VA-A
437	WH48	9	2.82	0.41	-0.62	16	5	VA-A
438	WH49	6	2.79	0.41	0.07	9	5	VA-SA
439	WH52	4	2.59	0.46	-1.58	9	7	VA-SA
440	WH51	3	2.53	0.49	-2.08	12	10	VA-SA
441	WH56	13	2.84	0.39	-0.23	9	5	VA-SA
442	WH130	10	2.58	0.42	-1.12	7	5	VA-SR
443	WH60	12	2.64	0.51	-0.68	10	20	A-SR
444	WH61	6	2.86	0.31	0.65	17	2	VA-A
445	WH176	10	2.61	0.7	-1.79	28	0	VA-SR
446	ON131	15	2.63	0.63	-2.86	9	10	A-SA
447	ON258	10	2.67	0.41	0.11	12	5	A-SA
448	ON263	14	2.65	0.42	0.23	6	10	VA-A
449	ON262	15	2.83	0.36	0.28	6	0	A-SA
450	ON264	11	2.6	0.46	-0.6	12	10	VA-SA
	ON261	18	2.7	0.47	-0.35	11	5	VA-SA
	ON265	23	2.7	0.5	0.24	12	10	VA-SA
	OP70	24	2.81	0.53	-1.7	14	5	VA-SA
	OP71	20	2.96	0.49	-1.85	19	5	VA-SA
	OP72	12	2.68	0.47	-1.08	13	20	VA-SR
	OP121	8	2.57	0.34	-0.29	7	10	VA-SA
	OP115	12	2.6	0.49	0.01	29	5	VA
	HW136	50	3.32	0.52	-2.81	19	0	VA-A
	MB97	11	3.03	0.36	0.88	9	25	VA-A
	MB140	9	2.88	0.5	-1.08	11	40	A-SA
	MB96	12	3.22	0.34	0.27	5	30	VA-SA
	MB95	22	3.05	0.4	0.62	9	5	VA-SA
	MB91	15	2.83	0.59	-1.51	13	5	VA-SA
	MB104	32	3.24	0.38	-1.07	6	5	VA-SA
	HA137	9	2.54	0.4	-2.31	19	20	A-SA
	HA139	13	2.72	0.62	-0.98	21	30	A-SA
	KB331	13	2.61	0.41	0.1	84	20	A-SR
	KB333	8	2.98	0.64	-1.12	27	50	VA-SA
	KB334	4	2.75	0.52	-1.05	14	20	A-SA
	KB377	17	2.58	0.57	-0.34	61	10	A-SR
	KB342	12	2.86	0.25	-0.46	11	2	A-SR
	KB338	20	2.86	0.34	0.41	47	5	A-SA
	KB390	8	2.66	0.41	0.33	9	20	S-SR
	KB101	20	1.98	0.56	-1.74	11	7	SA-SR
	KB147	30	2.79	0.54	-0.36	21	0	VA-A
	KB148	35	2.73	0.89	-2.89			
	KB149	40	3.03	0.57	-0.52	27	0	VA-A
	KB354	6	2.56	0.47	-2.75	12	10	A-SA
	KB160	33	2.91	0.42	0.35	27	0	VA-A
	KB98	7	2.68	0.32	0.86	8	10	VA-SA
	KB163	28	2.72	0.45	-0.14	21	10	SA-SR
	KB352	10	2.59	0.68	-4.37	55	7	A-R
	KB355	4	2.72	0.39	-0.04	11	10	A-R
	KB309	14	2.58	0.34	0.77	3	10	A-SA
	KB371	10	2.65	0.33	0.61	8	5	A-SA
	KB372	8	2.62	0.4	0.87	6	7	A-SA
	KB142	10	2.37	0.58	-4.14	3	10	A-SA
	KB368	16	2.58	0.48	-2.14	9	25	A-SA
	KB367	18	2.16	0.67	-0.18			
	KB143	15	2.57	0.5	0.99	7	30	A-SA
	KB470	10	2.59	0.31	0.43	15	10	A-SA
	WB247	17	2.75	0.49	-0.1	14	5	VA-A
	WB248	11	2.78	0.33	0.31	8	0	VA-A
	WB256	190	2.8	0.27	0.02	11	0	VA-A
	TP112	10	2.56	0.42	-0.75	10	10	VA-A
	TP114	29	2.69	0.57	0.08	20	5	VA-A
	HA140	9	2.88	0.5	-1.08	11	40	A-SA
	MEANS	15.5	2.68	0.48	-0.98	13.6	9	

Appendix 9B

Textural Entropy Maps

WAIHI

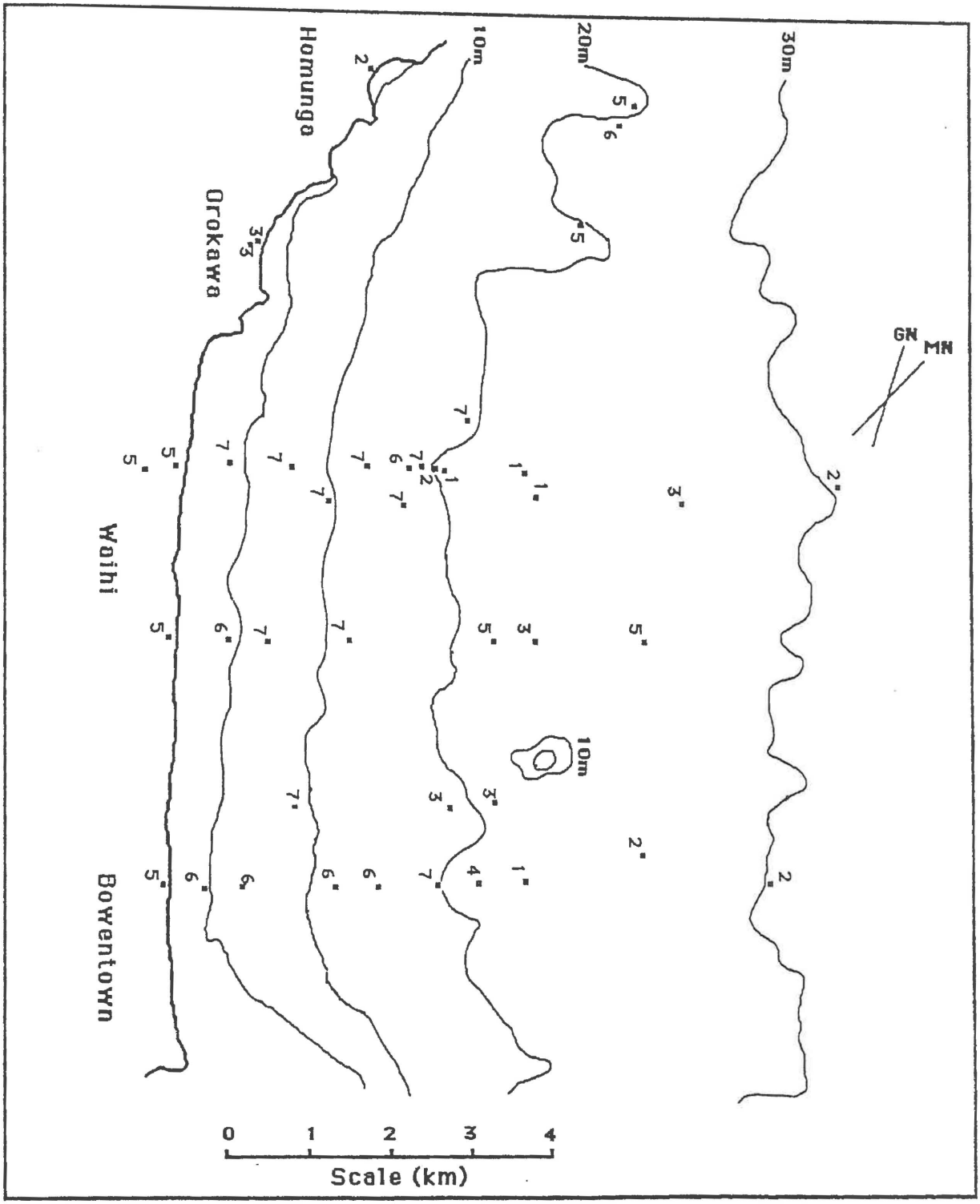
Homunga
Orokawa
Waihi
Bowentown
10m
20m
30m
GN
MN
0 1 2 3 4
Scale (km)

A-130

WHIRITOA

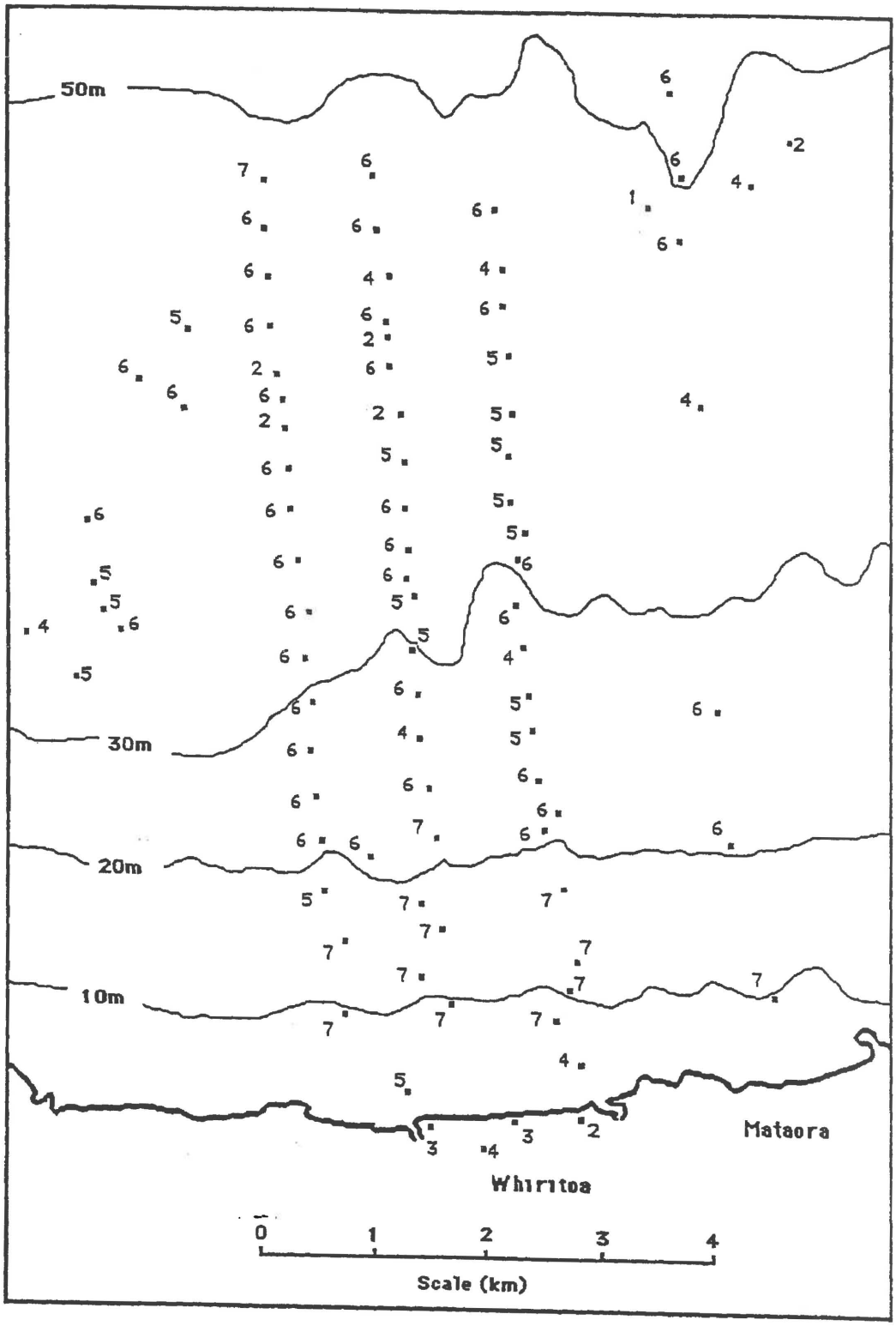

A-131

WHANGAMATA

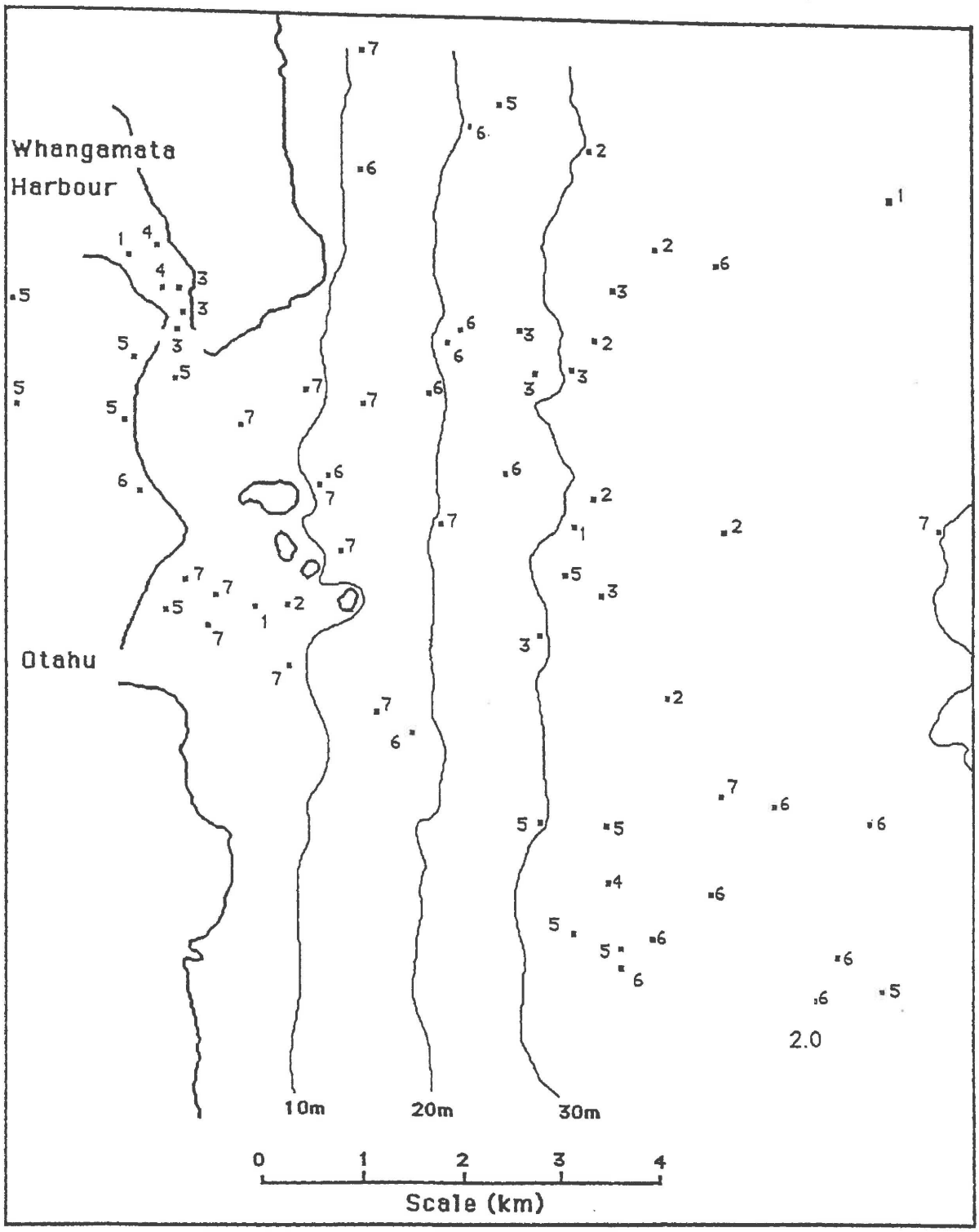

A-132

ONEMANA

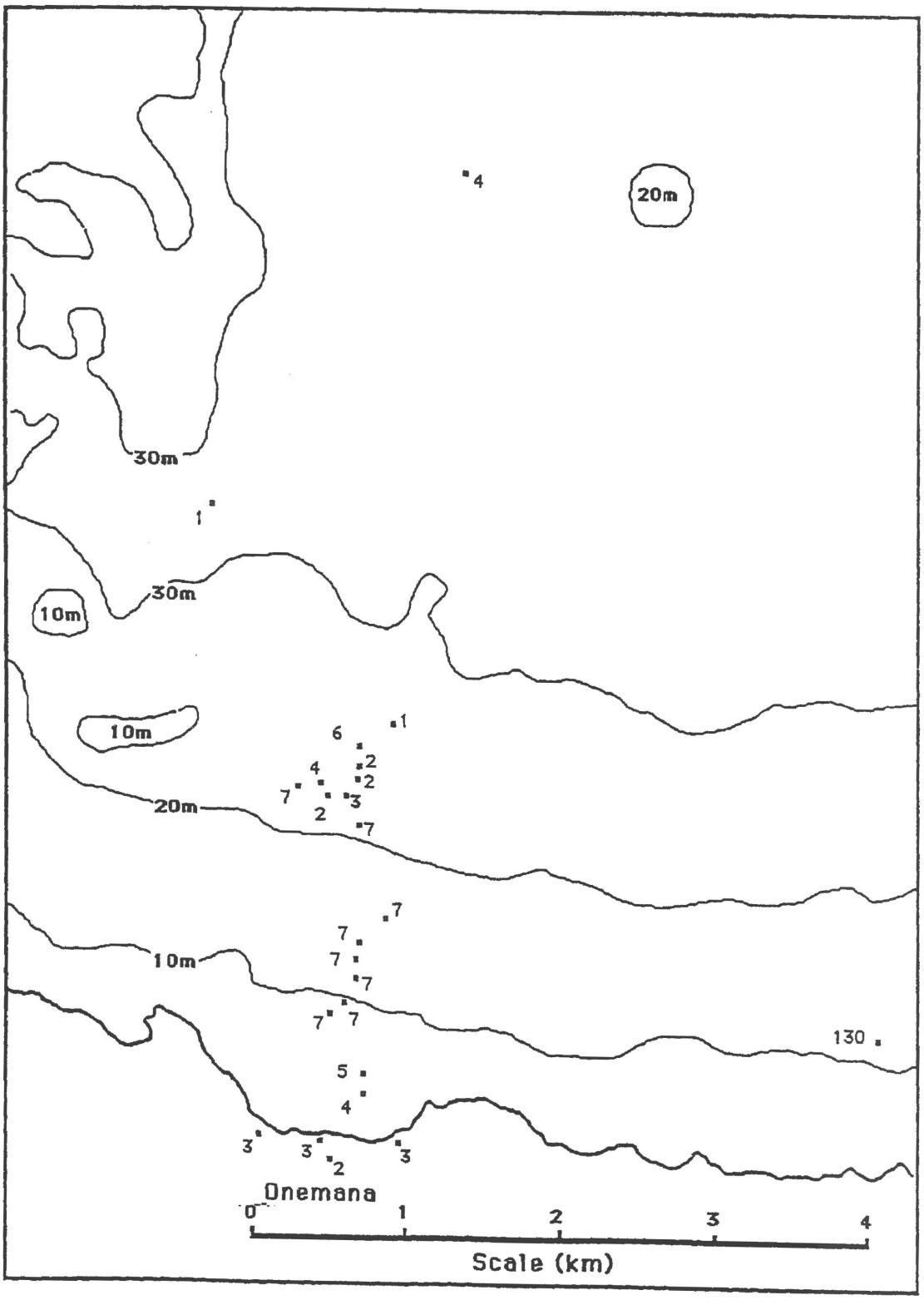

A-133

OPOUTERE

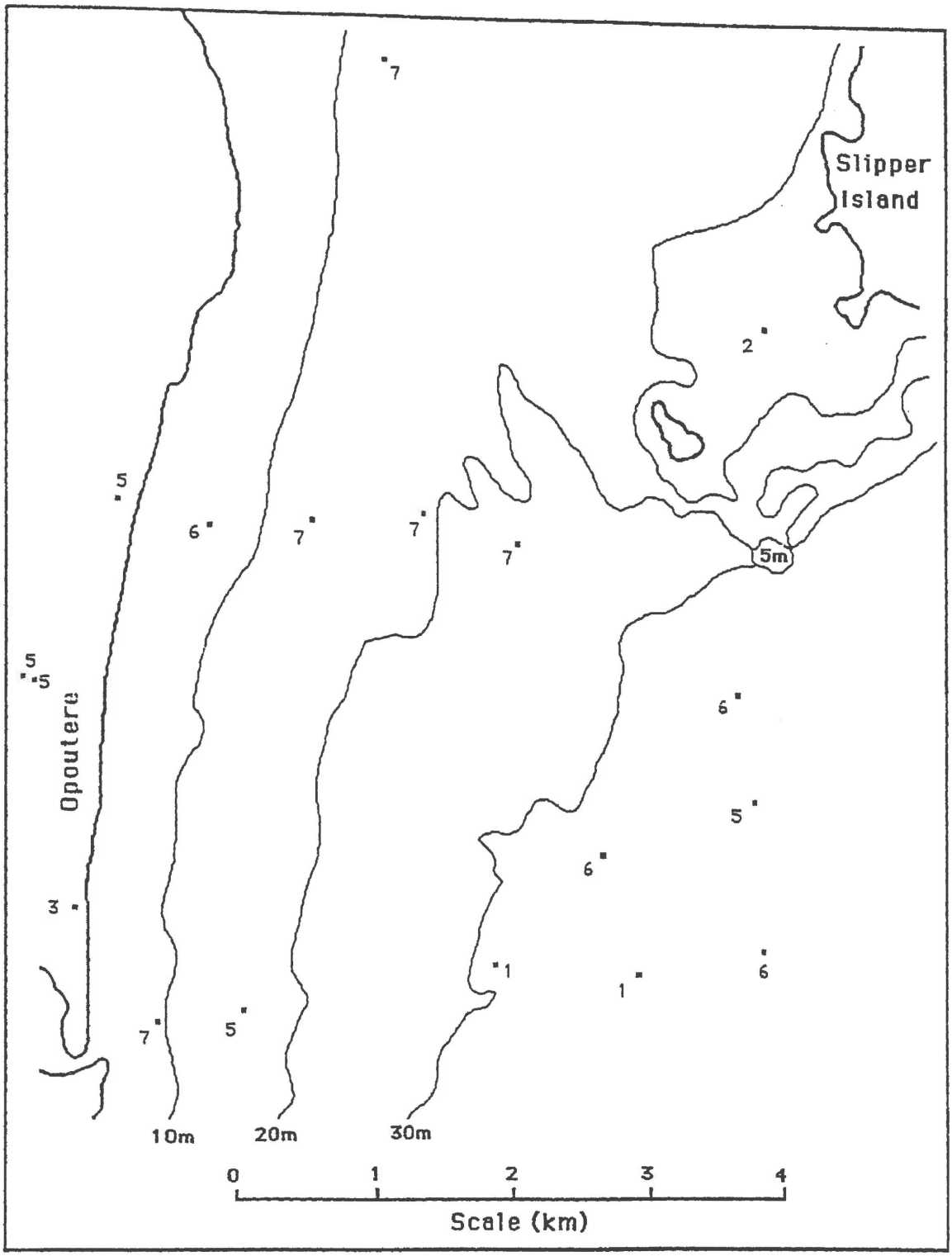

A-134

HOTWATER

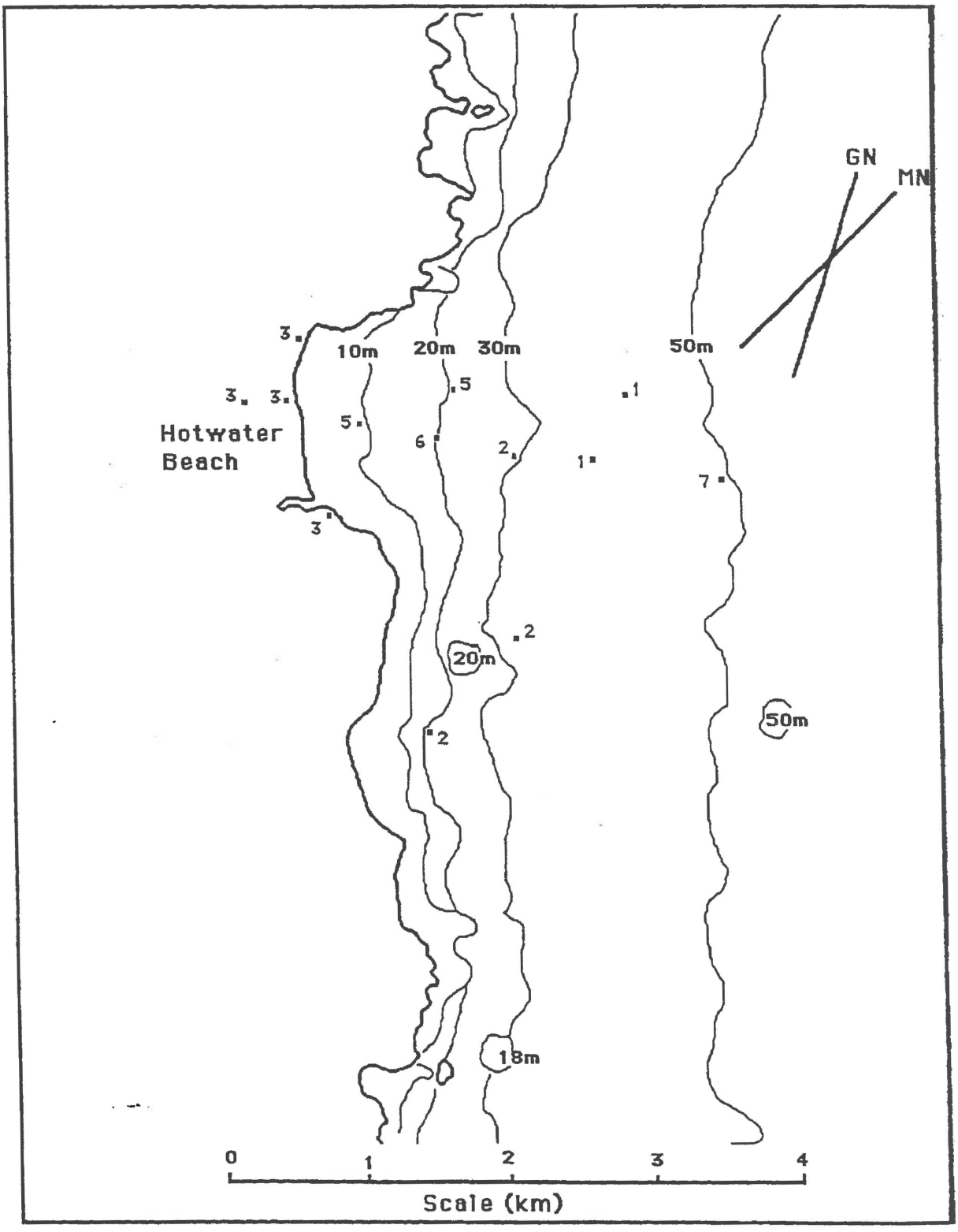

MERCURY BAY

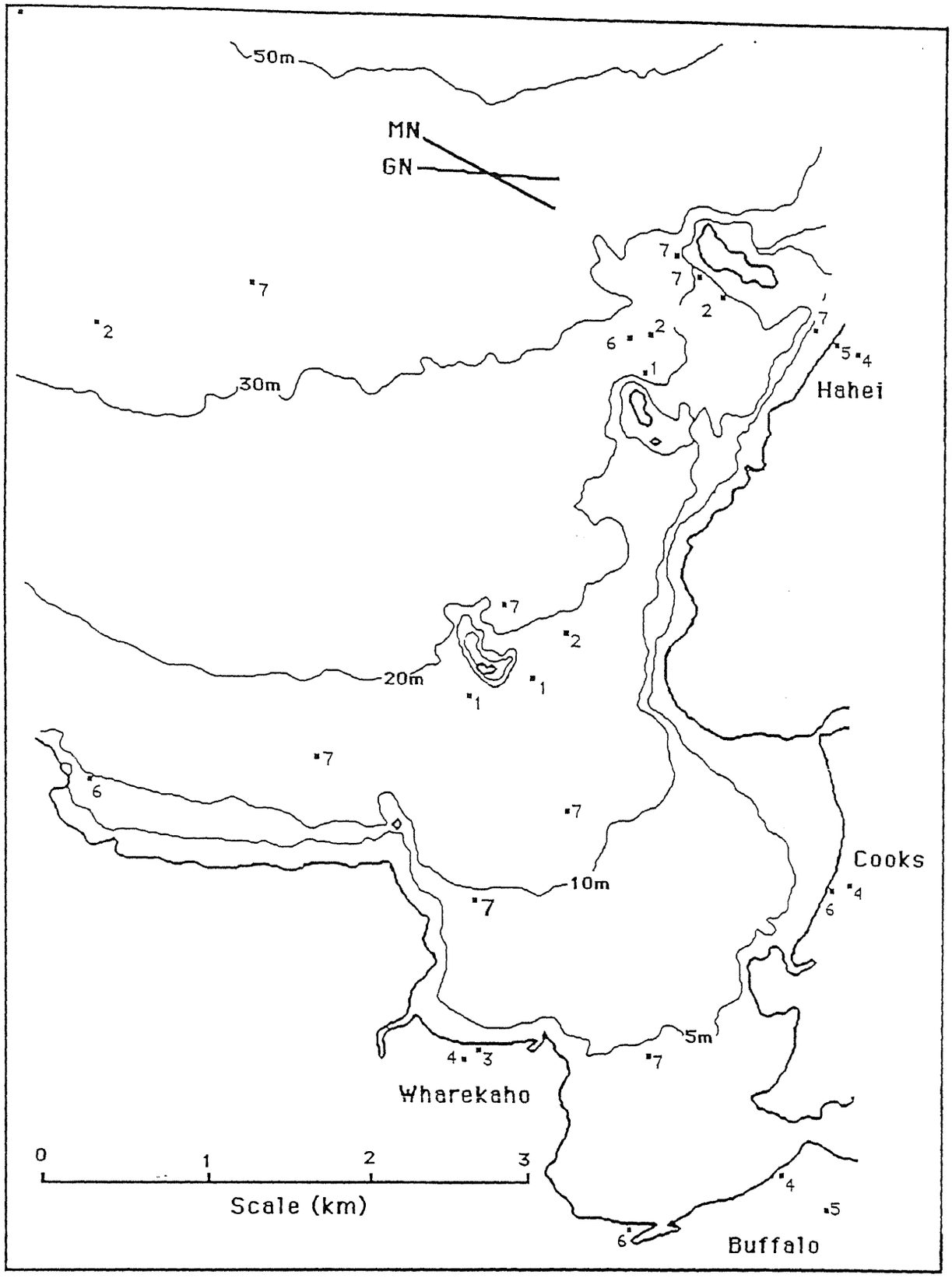
50m
MN
GN
30m
20m
10m
5m
Hahei
Cooks
Whareakaho
Buffalo
0
1
2
3
Scale (km)

A-136

OTAMA

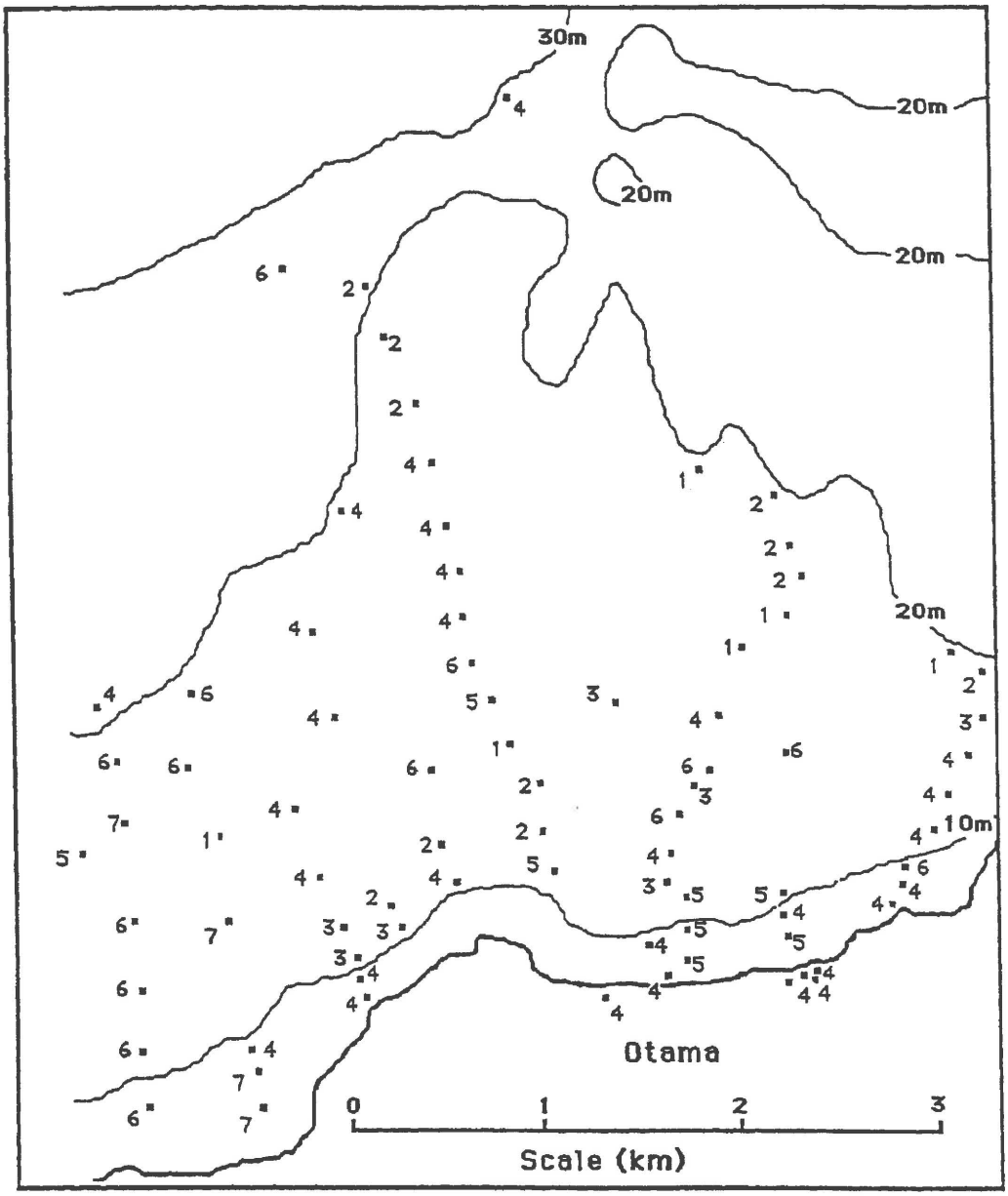

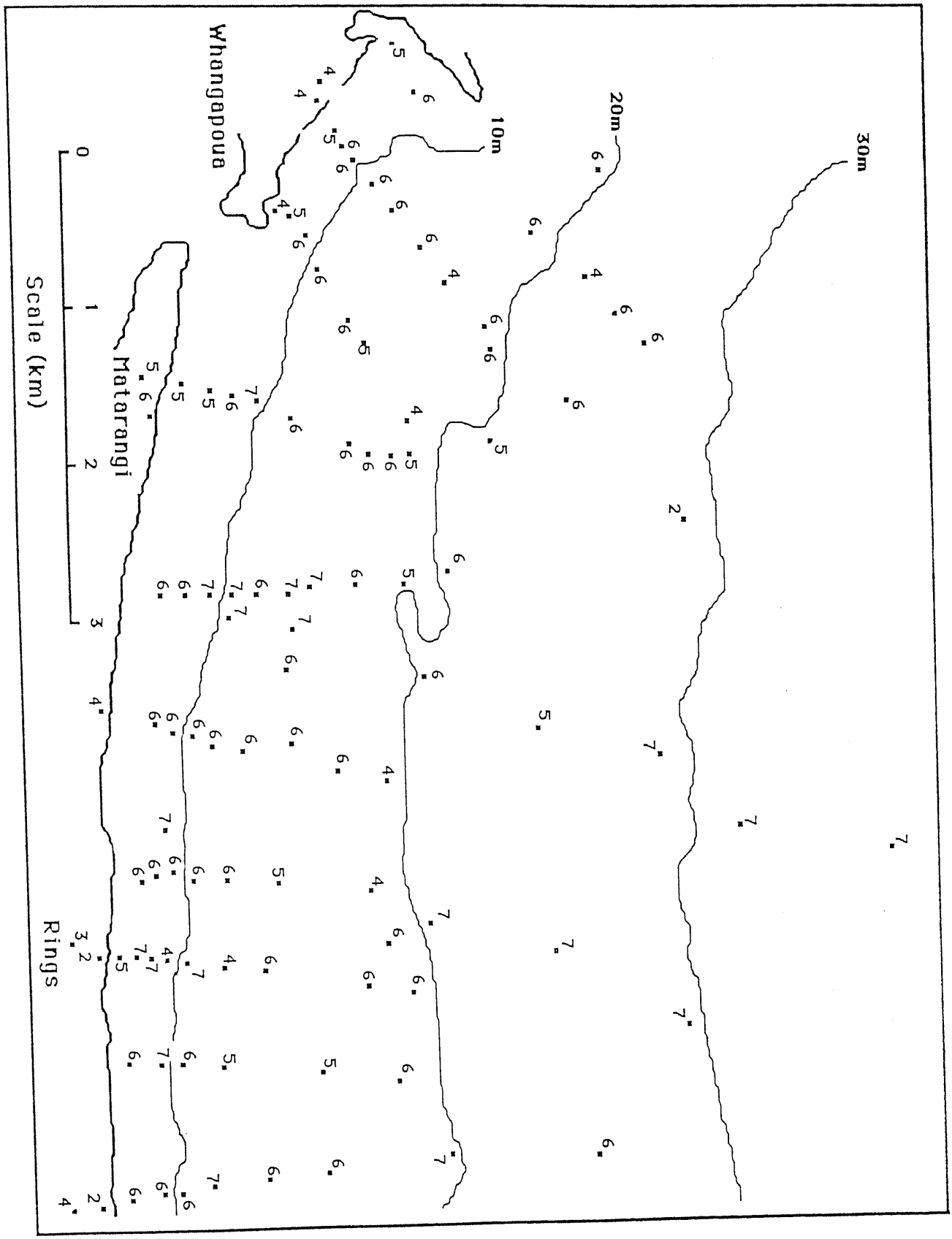
Whangapoua
10m
20m
30m
Matarangi
Scale (km)
0
1
2
3
Rings

Appendix 9C

Mineralogical Entropy Classification

CLASS 1A

SAMPLE NO	ENVIRONMENT	QUARTZ	FELDSPAR	LITHICS	GLASS	HEAVIES	CUMMINGTONITE	BIOTITE	AEGERINE	AUGITE	HYPERSTHENE	GR.HORNBLENDE	BR.HORNBLENDE	OPAQUES
WB12	BEACH	14.70	57.00	15.40	11.00	1.80	12.30	0.30	0.01	10.00	38.60	23.30	9.30	5.60
WI208	SHELF (34M)	24.90	54.50	12.50	5.40	2.70	12.60	1.30	0.01	3.00	42.60	10.60	17.60	11.30
WI199	SHELF (51M)	25.20	39.60	20.80	9.60	4.80	26.00	0.30	0.01	5.30	36.00	13.60	11.30	7.30
M234	SHELF (36M)	12.30	48.10	14.00	16.90	5.50	22.00	0.01	0.30	5.30	52.00	8.60	8.30	3.30
M236	SHELF (49M)	10.10	60.70	12.90	13.20	3.30	33.60	0.01	0.01	6.30	34.00	14.00	9.30	2.60
WH548	HOL.DUNE	19.50	58.80	12.30	6.60	2.80	7.00	0.30	0.01	7.00	36.30	17.30	9.00	23.00
WH283	BEACH	24.70	51.30	8.50	6.70	8.70	9.60	0.60	0.01	6.00	42.60	17.00	18.00	5.30
ON278	BEACH	26.50	51.60	17.70	3.50	0.70	2.30	0.01	0.01	1.00	72.60	2.30	10.00	11.60
OP546	HOL.DUNE	32.40	39.50	16.20	8.50	3.40	13.00	0.30	0.01	5.30	32.60	23.00	11.00	13.00
OP556	BEACH	28.20	44.70	14.12	11.20	1.70	9.30	0.30	0.01	10.00	46.30	6.60	12.30	15.00
OP544	BEACH	25.00	49.70	23.60	0.40	1.40	19.00	0.01	0.01	7.00	26.30	22.30	10.30	15.00
OP120	SHELF (16M)	9.60	51.60	21.80	14.40	2.60	6.10	0.40	0.01	4.60	44.60	13.60	22.50	7.90
OP117	SHELF (37M)	18.30	46.60	19.30	13.10	2.80	8.60	0.60	0.30	5.30	36.30	17.30	16.60	13.60
KB317	HOL.DUNE	27.30	55.50	8.90	4.50	3.90	6.60	0.60	0.01	7.30	52.30	7.60	7.00	18.00
KB509	BEACH	24.20	68.30	4.60	2.10	0.70	1.80	0.01	0.01	5.60	42.60	25.10	11.30	11.30
KB318	BEACH	19.70	59.10	12.90	7.20	1.10	9.30	1.60	0.01	5.60	38.30	18.60	9.30	16.30
KB156	SHELF (20M)	20.60	58.80	12.20	5.70	2.70	2.60	1.00	0.01	8.60	57.30	11.00	9.30	9.30
KB165	SHELF (22M)	21.60	57.20	8.60	9.30	3.30	0.60	0.01	0.01	4.30	43.00	11.60	18.00	21.00
WP522	BEACH	22.20	57.00	11.90	7.40	1.50	3.60	1.30	0.01	7.00	39.60	22.30	13.00	13.00
MEANS		21.42	53.24	13.95	8.19	3.06	10.88	0.45	0.04	5.94	43.24	14.72	12.60	11.44
Z TEST		3.30	5.21	-2.74	-1.99	-2.26	3.49	-1.22	-0.52	-1.35	3.16	3.76	4.91	-5.09

CLASS 1B

SAMPLE NO	ENVIRONMENT	QUARTZ	FELDSPAR	LITHICS	GLASS	HEAVIES	CUMMINGTONITE	BIOTITE	AEGERINE	AUGITE	HYPERSTHENE	GR.HORNBLENDE	BR.HORNBLENDE	OPAQUES
WB554	HOL.DUNE	18.50	49.70	6.80	9.40	15.60	9.60	0.30	0.01	5.00	46.00	12.30	14.00	12.60
WB250	SHELF (34M)	13.00	56.30	8.70	5.60	16.40	12.00	0.01	0.01	3.60	52.60	6.60	7.00	18.00
WB552	BEACH	9.70	54.40	10.80	11.40	13.70	7.30	0.60	0.01	6.00	49.30	7.00	12.00	17.30
WB550	BEACH	10.80	66.00	7.60	7.30	15.00	3.60	0.60	0.01	7.00	55.30	8.60	10.60	14.00
WI203	SHELF (42M)	16.50	57.40	13.70	6.90	5.50	18.00	0.01	0.30	4.30	41.00	5.00	9.00	22.30
WH297	RIVER	7.00	28.50	29.10	14.50	20.90	16.00	1.00	0.01	9.00	37.60	4.40	0.20	31.60
WH298	RIVER	28.50	23.10	9.50	4.10	35.50	5.30	0.01	0.01	13.60	39.60	19.30	10.00	11.60
WH63	SHELF (24M)	5.50	40.00	11.30	9.10	34.20	1.00	0.01	0.01	2.60	67.00	2.30	9.30	17.30
ON560	RIVER	16.70	29.40	31.30	7.70	14.90	12.30	0.01	1.00	5.00	45.00	4.60	4.60	27.00
MEANS		13.49	46.54	13.75	8.99	17.97	12.41	0.26	0.14	5.64	45.34	7.14	7.77	20.97
Z TEST		-0.57	2.45	-1.97	-1.23	1.20	3.21	-1.35	-0.26	-1.09	2.73	-0.73	0.59	-2.09

CLASS 1C

SAMPLE NO	ENVIRONMENT	QUARTZ	FELDSPAR	LITHICS	GLASS	HEAVIES	CUMMINGTONITE	BIOTITE	AEGERINE	AUGITE	HYPERSTHENE	GR.HORNBLENDE	BR.HORNBLENDE	OPAQUES
WI558	HOL.DUNE	17.90	30.00	0.70	8.60	42.10	0.60	0.01	0.01	2.30	35.30	1.60	3.00	37.00
ON267	SHELF (24M)	22.30	34.40	13.40	11.50	18.50	4.60	0.30	0.01	3.30	44.30	3.60	6.30	36.40

ON172	SHELF (45M)	14.20	48.60	17.80	6.30	13.20	2.30	0.01	0.30	3.00	42.00	5.00	8.30	38.60
OP526	HOL.DUNE	28.70	47.30	10.40	4.70	8.90	3.00	0.30	0.01	2.60	28.60	6.30	5.00	52.60
KB523	RIVER	19.10	42.70	16.20	9.70	12.30	1.30	0.30	0.01	5.00	47.60	6.00	4.00	35.00
KB319	PL.DUNE	25.30	60.90	0.86	4.30	8.60	0.30	0.01	0.01	1.00	0.30	36.00	4.30	56.60
KB320	PL.DUNE	21.50	55.30	7.00	1.70	14.60	1.00	0.30	0.01	4.00	41.60	16.00	6.60	29.00
KB529	HOL.DUNE	22.50	54.20	5.70	10.80	10.00	1.00	0.01	0.01	4.60	35.30	9.30	9.30	39.30
KB525	HOL.DUNE	28.40	43.60	8.70	4.90	14.40	0.30	0.01	0.01	3.30	39.30	3.30	6.00	46.00
KB524	HOL.DUNE	27.00	51.50	8.50	6.60	6.30	0.60	0.01	0.01	4.30	28.60	2.60	3.60	58.30
KB322	BEACH	19.20	39.50	3.50	2.80	35.00	0.01	0.30	0.01	4.00	25.60	5.60	5.60	58.30
KB511	BEACH	24.50	47.80	14.80	11.90	0.90	2.00	2.00	0.01	6.70	19.40	7.30	5.30	55.70
KB510	BEACH	32.30	50.60	11.30	4.40	1.50	1.30	0.30	0.01	6.00	39.30	5.60	7.00	39.00
KB496	SHELF (11M)	15.50	50.90	9.60	12.40	11.50	0.01	0.01	0.01	3.00	48.60	3.00	6.30	39.00
KB154	SHELF (18M)	16.20	66.70	3.60	9.90	3.60	1.00	0.01	0.01	3.60	44.00	7.60	12.60	31.00
MEANS		22.31	48.28	8.80	7.37	13.43	1.29	0.26	0.03	3.78	34.65	7.92	6.21	43.95
Z TEST		3.26	3.39	-3.41	-1.95	0.43	-2.66	-1.65	-0.46	-2.36	0.24	-0.46	-0.42	1.80

CLASS ID

SAMPLE NO	ENVIRONMENT	QUARTZ	FELDSPAR	LITHICS	GLASS	HEAVIES	CUMMINGTONITE	BIOTITE	AEGERINE	AUGITE	HYPERSTHENE	GR.HORNBLENDE	BR.HORNBLENDE	OPAQUES
WI206	SHELF (28M)	24.20	47.50	20.20	6.10	2.00	15.60	2.60	0.30	8.60	26.60	12.30	7.60	33.30
WN37	SHELF (2M)	12.30	49.20	26.50	12.30	2.80	2.40	0.01	0.40	4.40	57.60	6.40	13.30	14.70
ON259	SHELF (5M)	15.60	42.40	24.00	14.30	3.80	3.60	0.01	0.01	3.30	42.30	4.30	8.60	37.30
OP121	SHELF (8M)	15.70	37.70	23.80	21.40	1.40	4.60	0.30	0.01	6.60	33.00	12.60	8.00	34.00
TP542	BEACH	31.00	43.20	17.20	6.60	2.00	6.30	0.01	0.01	15.60	36.60	12.60	6.30	22.30
TP541	BEACH	31.50	41.30	19.80	5.40	2.00	4.60	0.01	0.01	18.60	33.30	9.00	5.30	29.00
TP534	BEACH	27.40	26.00	37.00	6.10	3.80	2.60	0.01	0.01	11.30	46.60	7.60	4.30	27.30
TP112	SHELF (10M)	17.20	41.70	21.00	16.90	3.10	3.00	1.00	0.01	9.60	28.00	13.30	7.30	36.60
HA140	SHELF (9M)	8.60	39.40	33.30	14.40	4.30	5.60	8.60	0.01	15.00	26.00	19.00	11.00	14.00
MB533	HOL.DUNE	29.70	31.80	28.20	5.00	5.30	2.60	4.00	0.01	8.30	37.60	17.00	21.00	8.60
MB323	BEACH	22.60	31.40	34.80	3.40	7.80	5.60	3.00	0.01	9.00	35.30	12.30	12.00	22.30
MB532	BEACH	20.60	27.00	42.10	6.80	3.50	2.30	3.30	0.01	10.00	27.30	14.00	17.60	25.30
MB531	BEACH	24.80	34.70	25.40	3.60	11.60	0.60	2.30	0.01	4.00	48.30	10.60	9.30	24.60
MB90	SHELF (10M)	14.30	36.30	36.90	6.40	6.10	0.60	2.30	0.01	3.60	28.60	13.60	11.00	39.30
OPB528	BEACH	21.70	44.20	24.20	8.20	1.60	7.60	1.60	0.01	3.30	38.00	22.30	6.00	21.00
KB512	BEACH	19.60	50.10	18.00	10.80	0.60	1.30	0.30	0.01	6.00	39.30	5.60	7.00	39.30
KB375	SHELF (16M)	17.80	53.10	18.20	7.90	3.10	1.00	2.60	0.30	5.30	37.60	8.60	11.60	31.60
KB142	SHELF (10M)	17.80	49.30	18.10	12.80	1.90	3.00	1.30	0.01	7.60	47.30	12.30	12.60	15.30
KB145	SHELF (21M)	18.20	52.70	19.40	9.40	0.30	2.30	0.60	0.01	5.00	42.30	16.60	6.00	25.30
WP452	SHELF (8M)	17.80	50.70	18.40	10.20	3.00	3.00	1.60	0.30	5.60	49.00	16.00	7.60	16.60
WP446	SHELF (17M)	23.50	49.50	18.60	6.00	2.50	1.60	0.30	0.01	4.60	42.00	12.30	8.30	30.30
WP442	SHELF (25M)	14.40	53.00	21.10	10.50	1.00	6.30	1.00	0.30	9.60	39.30	13.30	8.60	20.30
KD8519	BEACH	14.60	40.30	35.80	6.00	3.30	1.00	4.00	0.01	16.30	46.60	7.30	5.60	18.60
MEANS		20.05	42.28	25.30	9.15	3.34	3.79	1.77	0.08	8.31	38.63	12.13	9.39	25.52
Z TEST		2.78	2.53	-0.10	-1.81	-2.34	-1.46	3.76	-0.49	0.18	1.73	2.28	2.36	-2.08

CLASS 2

SAMPLE NO	ENVIRONMENT	QUARTZ	FELDSPAR	LITHICS	GLASS	HEAVIES	CUMMINGTONITE	BIOTITE	AEGERINE	AUGITE	HYPERSTHENE	GR.HORNBLENDE	BR.HORNBLENDE	OPAQUES
WB14	SHELF (6.5M)	19.10	31.40	17.80	30.70	2.70	15.00	0.01	0.30	8.60	35.00	16.30	11.00	13.30
WB247	SHELF (16M)	4.70	41.90	15.90	32.90	4.70	12.60	0.30	0.30	9.00	37.60	13.30	14.00	11.30
WI35	SHELF (6.5M)	7.60	16.40	9.10	65.20	1.80	1.00	1.00	0.01	2.60	34.60	6.30	13.00	41.00
WI213	SHELF (19M)	10.80	31.20	12.90	44.80	0.40	11.30	1.00	0.60	11.30	34.30	21.00	8.00	11.60
M233	SHELF (10M)	1.40	8.10	11.60	78.60	0.40	8.00	1.60	0.01	6.00	26.00	10.60	6.60	40.30
WH176	SHELF (10M)	8.60	30.90	16.30	43.30	0.90	4.30	0.01	0.01	4.60	47.00	8.60	10.30	24.30
WH177	SHELF (23M)	7.00	44.00	18.30	25.40	5.30	6.00	0.60	0.01	5.60	41.00	11.30	17.00	18.00
ON263	SHELF (13.5M)	10.90	32.40	16.20	38.20	2.40	5.60	1.60	0.30	5.60	28.60	24.60	11.00	21.00
ON267	SHELF (24M)	6.50	21.70	10.30	58.70	2.90	5.00	0.60	0.30	3.30	16.30	12.60	27.30	33.00
[illegible]119	SHELF (27M)	5.30	29.50	14.30	51.20	1.60	1.60	0.01	0.01	4.60	42.60	3.30	6.30	41.30
[illegible]111	SHELF (10M)	12.90	33.30	22.00	32.40	2.60	6.00	0.60	0.01	10.00	28.30	21.30	9.00	22.30
[illegible]P112	SHELF (10M)	8.20	32.00	17.10	39.50	2.60	3.30	0.30	0.01	8.60	30.00	9.00	4.60	42.30
TP113	SHELF (23M)	17.60	35.40	16.30	25.10	5.60	6.00	0.30	0.01	6.60	30.00	10.00	9.30	35.60
HW136	SHELF (50M)	8.10	27.80	9.30	52.40	2.40	8.60	0.60	0.30	10.00	36.00	11.00	6.00	26.00
OPB328	BEACH	11.80	45.30	18.90	23.60	2.00	9.60	3.30	0.01	3.30	29.30	25.30	10.00	18.60
KB330	SHELF (30M)	13.00	36.40	14.20	35.10	1.30	10.60	2.30	0.01	4.30	26.30	12.30	1.00	40.60
KB148	SHELF (35M)	6.30	22.40	22.40	49.20	0.01	6.30	2.60	0.01	8.30	30.00	8.00	9.00	32.60
MEANS		9.40	30.59	15.46	42.72	2.33	7.11	0.98	0.13	6.61	32.52	13.22	10.20	27.83
Z TEST		-2.70	-0.64	-2.20	8.12	-2.26	0.84	0.64	-0.35	-0.85	-0.40	2.60	2.66	-1.31

CLASS 3

SAMPLE NO	ENVIRONMENT	QUARTZ	FELDSPAR	LITHICS	GLASS	HEAVIES	CUMMINGTONITE	BIOTITE	AEGERINE	AUGITE	HYPERSTHENE	GR.HORNBLENDE	BR.HORNBLENDE	OPAQUES
WB254	SHELF (81M)	8.70	22.30	36.40	28.90	3.80	8.00	0.30	7.60	12.60	29.00	5.30	13.60	23.00
WH256	SHELF (200M)	5.40	9.70	30.00	53.10	1.80	2.20	0.40	34.20	10.10	11.80	1.30	7.90	29.90
HW135	SHELF (40M)	5.30	8.70	32.70	50.00	3.30	0.60	0.01	0.01	4.00	18.60	0.01	0.01	76.30
MB309	RIVER	3.50	6.60	58.00	31.10	0.70	6.60	0.80	0.01	6.60	25.30	16.10	2.40	40.60
MB534	BEACH	3.00	11.60	54.90	29.90	0.60	7.00	5.30	1.00	16.00	26.60	8.30	14.60	20.30
MB97	SHELF (1[illegible]M)	5.80	25.10	40.70	23.70	4.70	4.60	3.60	0.01	9.60	27.00	10.00	9.60	33.30
MB96	SHELF (12M)	4.50	19.90	41.60	30.40	3.50	4.00	3.60	0.30	10.00	29.00	9.00	7.30	35.30
MB93	SHELF (16M)	4.50	13.80	41.20	37.50	3.10	0.01	0.30	0.01	1.60	12.60	1.00	1.30	80.60
MB104	SHELF (32M)	4.40	15.60	32.10	45.40	2.50	7.30	2.60	0.30	8.60	26.60	12.30	7.60	33.30
MEANS		5.01	14.81	40.84	36.67	2.67	4.48	1.88	4.83	8.79	22.94	7.03	7.15	41.40
Z TEST		-3.49	-3.23	2.36	4.64	-1.58	-0.59	2.61	4.60	0.32	-2.45	-0.74	0.21	1.08

CLASS 4

SAMPLE NO	ENVIRONMENT	QUARTZ	FELDSPAR	LITHICS	GLASS	HEAVIES	CUMMINGTONITE	BIOTITE	AEGERINE	AUGITE	HYPERSTHENE	GR.HORNBLENDE	BR.HORNBLENDE	OPAQUES
WI296	RIVER	4.70	15.80	45.50	20.20	10.40	1.60	0.30	0.01	12.00	33.60	2.30	2.00	48.00
HW538	BEACH	8.30	26.60	53.20	2.20	9.70	0.01	0.01	0.01	30.30	44.30	0.01	1.60	23.60
HW325	BEACH	12.70	25.40	48.10	3.10	10.80	0.30	0.01	0.01	42.00	35.60	1.00	1.30	19.60
HW132	SHELF (10M)	6.80	21.70	57.40	8.50	5.50	0.60	0.01	0.01	23.00	44.30	0.01	2.30	29.60

HW133	SHELF (20M)	11.80	25.00	46.30	6.80	10.10	0.60	0.01	0.01	29.00	45.00	1.00	2.00	22.30
HA327	BEACH	11.00	17.50	67.50	2.90	1.00	2.60	0.30	0.01	23.30	30.60	1.30	1.60	40.00
HA137	SHELF (9M)	10.00	24.90	51.40	6.40	7.50	3.60	0.60	1.30	25.00	32.30	3.00	3.30	29.00
HA138	SHELF (12M)	15.00	22.40	42.50	7.40	12.70	2.00	1.30	0.30	13.60	26.30	1.60	1.30	52.00
HA139	SHELF (13M)	17.80	25.30	35.30	13.70	7.90	6.00	0.01	0.01	26.00	36.00	2.30	1.60	27.00
OP329	SHELF (25M)	11.20	19.10	50.90	18.10	2.50	1.60	0.01	0.30	9.00	24.30	1.30	1.00	3.80
KD8520	RIVER	18.70	32.60	31.30	6.40	11.00	0.01	1.10	0.01	16.00	62.10	5.20	1.70	13.20
KD8518	HOL.DUNE	22.90	21.20	52.60	2.70	0.70	0.30	1.30	0.01	5.60	38.20	1.10	3.60	49.60
WAB517	HOL.DUNE	16.70	25.10	45.30	5.20	7.70	2.00	0.01	0.01	10.60	39.60	6.00	7.60	33.30
MEANS		12.89	23.28	46.25	7.97	7.50	1.63	0.38	0.15	20.42	37.86	2.01	2.38	30.08
Z TEST		-0.90	-2.10	4.23	-1.66	-0.87	-2.29	-1.18	-0.27	6.36	1.09	-3.45	-2.99	-0.74

CLASS 5

SAMPLE NO	ENVIRONMENT	QUARTZ	FELDSPAR	LITHICS	GLASS	HEAVIES	CUMMINGTONITE	BIOTITE	AEGERINE	AUGITE	HYPERSTHENE	GR.HORNBLENDE	BR.HORNBLENDE	OPAQUES
WB294	RIVER	6.40	27.70	22.80	22.50	20.60	9.60	0.30	0.01	4.00	20.00	8.70	1.90	54.60
WB295	RIVER	6.30	13.60	31.10	19.40	29.60	14.00	0.01	0.01	1.60	26.30	6.16	0.84	51.00
WB246	SHELF (24M)	10.80	26.90	17.10	22.20	21.00	3.10	0.01	0.01	2.20	17.10	6.70	1.80	68.30
WH179	SHELF (45M)	12.70	43.30	12.70	18.20	13.00	1.30	0.01	0.01	1.60	27.60	0.60	1.60	67.00
ON547	HOL.DUNE	13.20	29.40	10.60	16.50	30.40	4.00	0.30	0.01	3.30	25.00	2.60	2.30	61.60
OP545	PL.DUNE	32.40	30.40	9.40	16.20	11.50	1.30	0.30	0.01	4.60	13.30	9.60	3.30	64.30
TP543	HOL.DUNE	25.80	26.70	10.40	10.70	26.40	5.30	0.01	0.01	5.60	28.00	4.00	2.30	54.30
HA303	RIVER	25.20	19.00	24.20	21.80	9.80	4.00	0.01	0.01	4.50	6.50	2.40	0.80	77.40
HA536	HOL.DUNE	19.70	21.60	20.30	9.20	29.20	0.60	0.01	0.01	1.00	10.00	1.00	0.30	85.30
MB535	HOL.DUNE	21.10	16.20	12.10	5.20	45.40	2.00	0.01	0.01	3.30	8.30	1.60	1.00	80.60
MB530	HOL.DUNE	19.90	8.90	25.00	1.60	44.60	0.60	0.01	0.01	1.00	0.01	3.60	2.00	90.00
KB311	RIVER	25.90	30.70	30.40	5.50	7.40	2.00	0.01	0.01	2.60	21.00	8.00	4.00	62.30
KB312	RIVER	45.30	23.30	28.00	1.30	2.00	5.00	0.30	0.01	2.60	17.30	9.50	1.10	61.00
WP521	HOL.DUNE	18.30	49.10	6.60	9.30	16.60	0.01	2.00	0.01	1.60	17.30	1.30	1.30	74.30
MEANS		20.21	26.34	18.62	12.83	21.96	3.77	0.23	0.01	2.82	16.98	4.70	1.75	68.00
Z TEST		2.24	-1.51	-1.38	-0.45	2.31	-1.15	-1.66	-0.47	-2.79	-4.73	-2.16	-3.55	6.33

CLASS 6

SAMPLE NO	ENVIRONMENT	QUARTZ	FELDSPAR	LITHICS	GLASS	HEAVIES	CUMMINGTONITE	BIOTITE	AEGERINE	AUGITE	HYPERSTHENE	GR.HORNBLENDE	BR.HORNBLENDE	OPAQUES
WB324	BEACH	1.50	1.90	0.01	6.30	90.30	1.10	0.01	0.01	29.60	50.60	0.30	0.60	18.00
WB551	RIVER	3.00	12.70	24.20	5.80	54.20	7.30	0.01	0.01	28.00	57.00	1.60	0.01	6.00
WB553	PL.DUNE	4.50	9.40	6.70	2.70	76.70	2.60	0.30	0.01	5.00	40.00	1.30	4.60	45.60
WI289	BEACH	0.70	1.40	0.01	5.00	92.40	0.01	0.01	0.01	0.30	23.30	0.30	1.30	74.60
TP540	BEACH	12.70	9.90	10.60	9.90	57.00	2.60	0.01	0.01	4.00	32.00	2.60	3.30	54.60
HW561	RIVER	7.20	12.70	28.80	6.20	45.10	0.60	0.01	0.01	25.00	48.60	0.30	0.30	24.00
HW537	HOL.DUNE	1.90	7.80	14.80	9.80	65.60	0.30	0.30	0.01	29.60	50.60	0.30	0.60	18.00
KB321	PL.BEACH	9.10	25.90	1.80	2.60	60.60	2.00	0.01	0.01	9.60	50.30	3.30	6.00	28.30
MEANS		5.08	10.21	10.87	6.04	67.74	2.06	0.08	0.01	16.39	44.05	1.25	2.09	33.64

Z TEST		-3.27	-3.80	-2.19	-1.68	9.43	-1.61	-1.60	-0.36	3.36	2.17	-3.01	-2.50	-0.08
CLASS 7														
SAMPLE NO	ENVIRONMENT	QUARTZ	FELDSPAR	LITHICS	GLASS	HEAVIES	CUMMINGTONITE	BIOTITE	AEGERINE	AUGITE	HYPERSTHENE	GR.HORNBLENDE	BR.HORNBLENDE	OPAQUES
WH299	RIVER	12.50	12.50	54.90	16.30	3.80	24.00	0.30	0.70	2.30	13.60	4.00	1.00	51.00
OP300	RIVER	17.30	16.90	37.40	19.40	9.00	18.00	1.00	0.30	6.60	21.60	3.70	1.10	45.30
TP301	RIVER	1.90	11.70	75.90	9.40	1.10	1.60	0.30	0.01	12.00	33.60	2.30	2.00	48.00
HW302	RIVER	5.70	13.00	64.40	12.10	5.30	5.00	0.20	0.01	6.30	8.30	5.50	0.60	73.00
MB304	RIVER	17.50	16.70	43.20	17.50	5.00	27.30	0.01	0.30	2.00	12.60	11.70	0.80	44.00
MB306	RIVER	8.70	14.60	58.70	13.40	4.70	8.00	0.60	0.01	13.00	18.60	3.70	0.60	55.00
MB306	RIVER	1.50	13.40	70.30	11.20	3.70	9.00	0.01	0.01	11.00	17.00	3.20	1.00	58.00
MB3068	RIVER	3.40	10.70	61.10	5.00	19.80	12.30	2.30	0.01	12.30	33.60	2.20	2.60	42.60
MB307	RIVER	4.90	13.30	64.20	7.70	11.40	4.00	4.60	0.01	6.60	12.60	5.60	4.60	61.00
MB308	RIVER	3.40	7.20	76.40	4.80	8.20	8.00	0.60	0.01	12.00	39.00	5.60	1.00	33.60
OPB527	RIVER	11.30	5.30	53.30	2.70	27.30	2.30	0.01	0.01	2.00	5.00	29.30	2.60	57.30
KB314	RIVER	5.30	4.60	79.00	5.00	6.00	6.30	1.00	0.01	2.00	9.00	4.10	0.30	74.30
KB315	RIVER	3.10	6.90	84.70	0.40	5.00	1.60	1.90	0.01	7.00	16.30	23.60	6.40	43.00
WP316	RIVER	4.10	4.10	71.00	5.00	16.10	2.00	2.30	0.30	11.60	30.00	2.00	3.00	47.30
WAI515	RIVER	11.70	3.80	73.20	3.20	8.20	2.30	0.01	0.01	2.30	31.30	2.60	0.30	52.60
MEANS		7.49	10.31	64.51	8.87	8.97	8.78	1.01	0.11	7.27	20.14	7.27	1.86	52.40
Z TEST		-3.40	-5.18	7.82	-1.54	-0.59	1.78	0.68	-0.35	-0.43	-3.98	-0.82	-3.59	3.53
10 CLASSES	65%	EXPLAINED												